Rare Earth Elements in Ultramafic and Mafic Rocks and their Minerals

Main types of rocks. Rock-forming minerals.

F.P. Lesnov

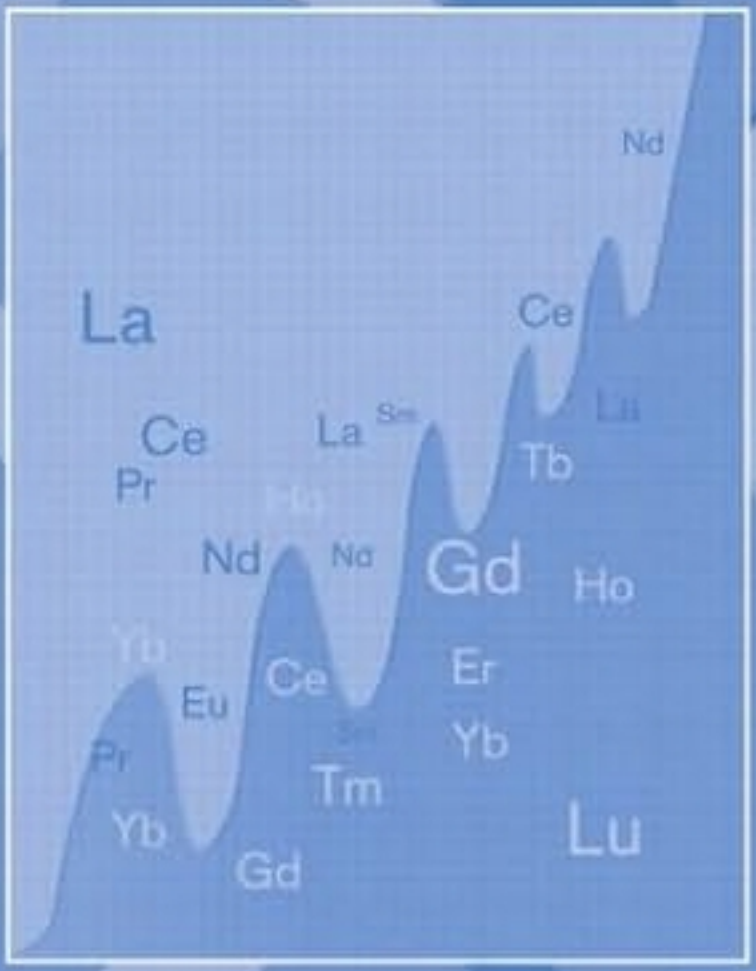

CRC Press

Rare Earth Elements in Ultramafic and Mafic Rocks and their Minerals

Rare Earth Elements in Ultramafic and Mafic Rocks and their Minerals

Main types of rocks. Rock-forming minerals

F.P. Lesnov

Institute of Geology and Mineralogy, Novosibirsk, Russia

Russian Academy of Sciences Siberian Branch Sobolev Institute of Geology and Mineralogy

Scientific editors:
Corresponding Member of Russian Academy of Sciences
G.V. Polyakov & Professor G.N. Anoshin

CRC Press
Taylor & Francis Group
Boca Raton London New York Leiden

CRC Press is an imprint of the
Taylor & Francis Group, an **informa** business

A BALKEMA BOOK

Originally published in Russian under the title: “Редкоземельные элементы в ультрамафитовых и мафитовых породах и их минералах.”

CRC Press/Balkema is an imprint of the Taylor & Francis Group, an informa business

Typeset by MPS Limited (A Macmillan Company), Chennai, India
Printed and bound in Great Britain by Antony Rowe (a CPI Group Company), Chippenham, Wiltshire

British Library Cataloguing in Publication Data
A catalogue record for this book is available from the British Library

Library of Congress Cataloging-in-Publication Data

Lesnov, F. P. (Feliks Petrovich)
[Redkozemel'nye elementy v ul'tramafitovykh i mafitovykh porodakh i ikh mineralakh. English]
Rare earth elements in ultramafic and mafic rocks and their minerals : main types of rocks : rock-forming minerals / F.P. Lesnov.
p. cm.
Includes bibliographical references and index.
ISBN 978-0-415-57890-5 (hard cover : alk. paper)
1. Rocks, Ultrabasic. 2. Rare earth metals. I. Title.
QE462.U4L4713 2010
552'.1–dc22

2010027607

Published by: CRC Press/Balkema
P.O. Box 447, 2300 AK Leiden, The Netherlands
e-mail: Pub.NL@taylorandfrancis.com
www.crcpress.com – www.taylorandfrancis.co.uk – www.balkema.nl

ISBN: 978-0-415-57890-5 (Hbk)
ISBN: 978-0-203-83031-4 (eBook)

Dedicated to my wife, Emma, of blessed memory

Contents

Introduction to the English Edition

Nowadays lanthanides or rare earths are recognized as a group of elements of the periodic table with unique chemical properties and extremely important for science. Although these elements were discovered long ago and their chemistry is well studied, their application in geology was made difficult due to their extremely low concentrations in most natural media and to difficulties in obtaining correct data on their contents in particular samples. In the latter half of last century these difficulties were overcome mostly due to the development and introduction of new devices and methods which provided a rather high level of sensibility and precision for determining the low concentrations of rare earth elements (REE) not only in rocks but in individual mineral crystals as well. At present, REE are widely used for solving many geological problems, including reconstructions of the geochemical evolution of the Earth and other planets of the solar system.

In recent years a great volume of geochemical information has been accumulated on the distribution of REE in various rocks and their minerals both enriched and strongly depleted. A number of earlier unknown regularities have also been revealed concerning the interrock and interphase distribution of REE at different physico-chemical parameters of geological processes. All this was a major contribution to the knowledge of the evolution of cosmic matter, which proceeded for many millions of years and was accompanied by the generation and crystallization of various magmatic melts and formation of the whole variety of rocks and ore bodies and mineral species.

In studying properties and ways of formation of magmatic rocks, particular attention in geochemistry was and is focused on the products of mantle origin, such as ultramafic and mafic rocks which are strongly depleted both in REE and some other chemical elements. Starting in the last quarter of the past century, the volume of information on the geochemistry of rare earth elements in mafic and ultramafic rocks, whose genesis is the subject of hot debates, has increased. After the period of intense accumulation of analytical information about ultramafic and mafic rocks, which was promptly published in international journals, there came a period of its systematization, generalization and theoretical conception. The thesis of Frey (1966) and the monograph of Balashov (1976) can be referred to as the first generalizing works on the geochemistry of REE in ultramafic and mafic rocks. A particularly important event in the geochemistry of REE was the publication of the monograph "Rare Earth Element Geochemistry" edited by P. Henderson. The data on the geochemistry of REE in ultramafic and mafic rocks were also summarized in the monograph "Magmatic rocks" (volumes 4 and 5) edited by Sharkov and Laz'ko and published between 1985–1988.

However, because of the rapid accumulation of new information on the geochemistry of REE in various types of rocks and other natural environment, which was observed during the last decade, there was a need for new generalizing works on this subject, this time, concerning a narrower class of natural objects. Among these works are the monograph of Dubinin "Geochemistry of rare earth elements in the ocean" (2006) and the present monograph of Lesnov. The monograph of Lesnov in Russian, published in 2007, marks the next stage of generalization and theoretical interpretation of the main results of researches in the geochemistry of REE in ultramafic and mafic rocks and their major minerals, which were carried out in the last decades in different laboratories of the world. The authors collected, systematized and interpreted the material both borrowed from literature and his own data on the distribution of REE in a few thousands of samples of major petrographic types of ultramafic rocks (dunites, harzburgites, lhezolites, wehrlites, websterites, clinopyroxenes, etc.), hypabyssal rocks with a high magnesian contents (kimberlites, komatiites, meimechites, picrites, and lamproites), gabbros (gabbro, gabbronorites, norites, olivine gabbro, troctolites, and anorthosites), and their minerals (olivines, orthiopyroxenes, clinopyroxenes, plagioclases, and amphiboles). An important feature of this work is that, unlike most of preceding works, it includes a large volume of primary data obtained in different laboratories, by different procedures and from individual objects from different regions of the world. Due to this, the monograph can be, in addition, used as a reference guide on the geochemistry of ultramafic and mafic rocks and their minerals.

We also want to draw the readers' attention to the very important, to our opinion, methodological aspect discussed in Lesnov's monograph. It shows, in particular, that the analyzed rocks along with the structural impurity of rare-earth elements, which are isomorphously incorporated directly into the crystal lattice of minerals, contain some amounts of nonstructural admixture. The latter is typically localized in intra- and inter-grain microcracks and is genetically related to the percolation of epigenetic fluids. Especially distinctly this phenomenon is manifested in ultramafic restites from deep xenoliths in basalts and kimberlites that are in most cases abnormally enriched in the nonstructural admixture of light rare earth elements. The nonstructural form of REE admixture in rocks and minerals is sui generis "information noise" not directly related to the endogenic processes of rock- and mineral formation, which must be taken into account in genetic interpretation of analytical data. Considerable attention in the work is focused on the generalization of available data on the coefficients of REE distribution between coexisting phases, including minerals and their parental melts. The correctness of these data is responsible for the reliability of numerical modeling of generation and crystallization processes of magmatic melts leading to the formation of various types of rocks. After being published, the monograph of Lesnov was in demand among Russian petrologists and geochemists and has found its "information niche". We believe that this monograph will also be welcomed by an international audience of researchers.

Academician of the Russian Academy of Natural Sciences,
Professor of the Department of Geochemistry in Moscow
State University

A.A. Yaroshevsky
Moscow.
April 15, 2010

Preface

The best way to become acquainted with a subject is to write a book about it.
Disraeli

The idea to write this book occurred to me more than 20 years ago. That time was marked by an increasing number of publications both in international and Russian literature on the geochemistry of rare earth elements (REE) in different types of magmatic rocks and their minerals. However, data on ultramafic and mafic rocks and especially their minerals of this type were less abundant than on other types of rocks. This was mainly due, on the one hand, to extremely low contents of REE in these magmatic formations and, on the other, to rather high thresholds of detectability of these trace elements, attainable with the help of analytical techniques which had been developed by that time. With time the number of papers dealing with the problem of REE partitioning in ultramafic and mafic rocks and their minerals grew. Because of the great interest to this topical information, which was new in many respects, it was published mainly in scientific journals. At the same time, works of generalizing and reference character including a considerable amount of analytical data on particular massifs, rocks, and minerals, required for researchers in practical work, were scarce. This led me to a decision to emphasize, as far as possible, the general principles oriented on the consideration of general regularities of REE partitioning, first of all, in plutonic ultramafic and mafic rocks and similar rocks, whose geology, petrology and mineralogy have been the subject of my studies for many years.

I hope that this book will be of use to the researchers in the field of petrology and geochemistry of ultramafic and mafic magmatism and will, probably, inspire some of them to more detailed studies in this promising field of geosciences.

F.P. Lesnov
felix@uiggm.nsc.ru
lesnovfp@list.ru

Acknowledgments

I am especially indebted to editors of this book: Corresponding member of the RAS G.V. Polyakov and Prof. G.N. Anoshin for their helpful advice and recommendations in the preparation of this manuscript. Sincere thanks go to the following reviewers: Prof. L.P. Rikhvanov, Prof. O.M. Glazunov, Dr. A.S Mekhonoshin, anonymous experts of the RFBR for their support of the Russian edition of this book and also to Russian and foreign scientists, who recommended this book to be published in English—Academician V.V. Reverdatto, Prof. A.A. Yaroshevsky, Prof. G.B. Fershtater, Prof. G.N. Savelyeva, Dr. V.G. Batanova, Dr. N.A. Krivolutskaya, Prof. S. Karipi, and Prof. A. Beard.

From the editors

The monograph "Rare earth elements in ultramafic and mafic rocks and their minerals" by F.P. Lesnov is devoted to an important problem of modern geochemisrty and mineralogy, *rare earth elements* (REE), which has for many years been some of the most "enigmatic" chemical elements of Mendeleyev's Periodic System. As the well-known French chemist Urbain wrote on the history of the discovery of REE, "It was a sea of mistakes, and the truth was sinking in it."

Hundred and twenty years have passed between the discovery of yttrium, the first of the elements later referred to as a rare earth element, and *lutetium*, the last one. In 1787, Carl Arrhenius, a lieutenant of the Swedish army, who, while on leave, was doing some mineralogical research in an abandoned quarry near the settlement of Ytterby, discovered an unknown black mineral and named it *ytterbite* after the place of discovery. Later the mineral was renamed *gadolinite* after the Finnish chemist Gadolin who 7 years later carried out the first analyses of the mineral and discovered, along with the oxides of silicon, calcium, magnesium, and iron, about 38% of the oxide of an unknown element, "new earth." He named this element *yttrium*. Hence, 1794 is considered to be the year of discovering the first of the REE. But yttrium was separated in a chemically individual form by the Swedish chemist Mosander only 50 years later. The discovery of many other REE abounds in various entertaining incidents and represents a particularly bright page in the history of chemistry.

The specific physicochemical, geochemical, and mineralogical properties of REE reflecting their surprising similarities are known to be determined by the peculiarities of the electronic configuration of their atoms. In accordance with the recommendations of the International Union of Pure and Applied Chemistry (IUPAC), the group of REE includes ^{21}Sc, ^{39}Y, ^{57}La, and *lanthanides* involving 14 elements from ^{58}Ce to ^{71}Lu. Their common distinguishing feature is that their electrons fill the inner 4f-sublevel, which predetermined referring them all to *f-elements*. The same circumstances account for the so-called *effect of lanthanide contraction* discovered by Goldshmidt, which, as a consequence of an increase in the charge of the nucleus and in the number of electrons at the 4f-sublevel, consists in a decrease of the atomic and ionic radii, which leads to smooth changes in the properties of the elements from ^{57}La to ^{71}Lu. This effect accounts for many geochemical peculiarities of the behavior of lanthanides in natural processes. As for the similarity in filling the valence sublevels (5d and 6f) with electrons, it results in the similarity of chemical properties of lanthanides for equal oxidation degrees.

Taken together, the REE amount to about 1/5 of the chemical elements available in nature. Due to their very close chemical properties they frequently occur in minerals and ores together, and the separation of their mixtures into component elements has turned out to be a very complicated problem. It has also been found that the occurrence of REE in the Earth's crust is not so rare since a significant part of them have higher Clarks than, for instance, germanium, arsenic, selenium, to say nothing of gold, silver, and the platinum group elements.

The research on some minerals of REE in the 1950s has clearly shown that these elements can be used as sensitive geochemical indicators in studying different natural processes. When speaking at a conference held at the Geochemical Institute of the Academy of Sciences of the USSR in December 1957 on the topic "Geochemistry of rare elements in connection with the problems of petrogenesis" the leading Soviet geochemist, academician A.P. Vinogradov formulated the most important tasks in the problems of the geochemistry of REE. He paid particular attention to the topicality of the research on the distribution of REE in ultramafic rocks and meteorites for the purpose of creating the theory of the origin of chemical elements. It should be emphasized that it is in ultramafic rocks that the lowest contents of REE have been observed, and the very identification of REE in these rocks has always been a difficult analytical problem. In this connection it should be noted that the progress in the field of the chemistry of REE has always been greatly dependent on the development of analytical, primarily physical methods of identifying them in different geological formations.

The outstanding scientists Goldshmidt and Hevesi, who used mainly semiquantitative techniques of X-ray spectrum analyses, carried out the first systematic investigations on the geochemistry of REE in the 1920s. For a long time the difficulties met with in the course of analytical separation and identification of REE gave rise to the wrong conclusion about their poor fractionation under natural conditions, which was believed to be feasible only under exceptional circumstances. Later on, a significant progress in the geochemistry of REE was achieved, thanks to the development and application of the neutron activation analysis used in instrumental and radiochemical variants. The latter variant made it possible to essentially reduce the limits of discovering REE by permitting for the first time their identification in ultramafic rocks and in some of their minerals. One of the techniques of the radiochemical neutron activation analysis was developed at the laboratory of analytical geochemistry of the Joint Institute of Geology, Geophysics and Mineralogy (JIGGM) of the SB RAS (Novosibirsk) (Kovaliova & Anoshin, 1996) and was successfully applied in practical investigations including those carried out by F. Lesnov. In the mid-1990s another method became one of the leading methods of identifying REE in geochemical investigations on most various objects: mass-spectroscopy with inductively coupled plasma (ICP-MS) including the use of laser ablation (LA ICP-MS). Starting from 1999 at the laboratory of analytical geochemistry of the JIGGM SB RAS and using a high-resolution mass-spectrometer "Element" of the firm Finnigan (Germany), different versions of techniques were developed for analyzing REE and other rare elements in different media by the methods ICP-MS and LA ICP-MS. The last few years these techniques have been used to perform hundreds of analyses of REE in various rocks and minerals as well as in a number of international and national geological standards. All this has made it possible to essentially expand the geochemical component in the mineral-petrologic investigations carried out at the JIGGM SB RAS. To this it should

be added that similar investigations in the field of geochemistry of REE with the use of ICP-MS and some other methods are now carried on in many other geological-type institutes of the RAS, including the GEOKHI and IGEM (Moscow), Institute of Geology and Geochronology of Precambrian (St. Petersburg), Institute of Geology and Geochemistry of the UB RAS (Ekaterinburg), and Institute of Geochemistry of the SB RAS (Irkutsk).

In using and interpreting analytical data on REE distribution in the course of geochemical research, much importance is now attached to the procedure of the graphic expression of these data based on the method of the so-called "normalization" with respect to chondrite meteorites, to "average" sedimentary rock, to the clarke of REE in the Earth's crust or to any other entities. This method was first proposed by (Coryell *et al.*, 1963; Masuda, 1982), so sometimes diagrams created on the basis of this method are referred to as Masuda–Coryell diagrams. From that time on, diagrams of this kind became an integral component not only of geochemical and petrological, but also geodynamical works. Data on the distribution of REE along with other rare elements (spider-diagrams, etc.) did prove to be very effective geochemical indicators in diagnosing different geological processes and reconstructing paleogeodynamic environments.

In Lesnov's monograph the author has carefully systematized and generalized the Russian and International data accumulated within recent decades on the distribution of REE in ultramafic and mafic rocks of various geneses as well as in their main rock-forming minerals. This work is undoubtedly very timely and necessary not only for geochemists and petrologists, but also for geologists of another directions because it contains a sufficiently full body of evidence available to date on the contents of REE in different types of ultramafic and mafic rocks and minerals forming them including the data obtained in studying the author's collections. An indubitable merit of this work is the fact that it contains a significant amount of original results of the analyses of rocks and minerals, and indicates, wherever possible, the analytical methods used in identifying REE. All of this will allow the readers to effectively compare their own data with those already available in the geochemistry of REE in ultramafic and mafic rocks and their minerals, and to solve, all by themselves, the problems of reliability of the presented geochemical characteristics and of the ensuing geochemical and geological interpretation.

G.V. Polyakov and G.N. Anoshin

Introduction

We will collect facts for ideas to appear.

Pasteur

Before one can arrive at substantiated conclusions, one should collect significantly more data on the distribution of the rare earth group elements both in basalts and in ultrabasic rocks.

Green, Ringwood

The lower the content, the more interesting the element.

Shaw

This monograph is the generalization of up-to-date data and theoretical ideas on the problems of the geochemistry of rare earth elements (REE) in ultramafic and mafic rocks as well as in their minerals. As is the convention in the Russian, URSS literature, by the term "rare earth elements" or REE, we mean, after Henderson (*Rare Earth Element Geochemistry*, 1984), the chemical elements of Group IIIA of the Periodic Table of Elements from lanthanum to lutetium with atomic numbers from 57 to 71: La, Ce, Pr, Nd, Pm, Sm, Eu, Gd, Tb, Dy, Ho, Er, Tm, Yb, and Lu. For brevity, this group of elements is sometimes referred to as "lanthanides" (Solodov *et al.*, 1998). In 1968, in accordance with the decision of the International Union of Pure and Applied Chemistry (IUPAC), Sc and Y were also included in the REE, but this usage has not become generally accepted. Despite the similarity of their chemical properties, among them the fact that the charge of their ions is predominantly 3^+, the REE differ in the sizes of their ion radii, which decrease from La^{3+} (1.032 Å) to Lu^{3+} (0.861 Å) (Shannon, 1976]. This served as the basis for dividing the REE into groups, first into ceric and yttric elements, and later, into light (La ... Eu) and heavy (Gd ... Lu) ones (this division is followed in the present work). Somewhat less frequently the REE are divided into three groups: light (La ... Nd), middle (Pm ... Ho), and heavy (Er ... Lu) elements (*Rare Earth Element Geochemistry*, 1984). All the REE, except Eu^{2+}, just as a number of other trace elements, are included among the high-field strength elements (HFSE) (Rollinson, 1993; Sklyarov, 2001).

In modern petrology the REE are considered to be important and rather informative geochemical indicators of magmatic, metamorphic, and some other processes. The systematic research into the regularities of their distribution in different types of magmatic rocks that has been carried on for over half a century already has in recent decades been accompanied by an ever-increasing interest in the geochemistry of

these elements in rock-forming, secondary, accessory, and ore minerals. This interest is mainly due to the fact that the estimates of the general REE concentration level as well as of the correlations between their contents are very sensitive indicators in studying the processes of mineral and rock formation.

As distinct from many other types of magmatic rocks, mafic rocks, and particularly ultramafic ones as well as nearly all of their minerals are considerably depleted of REE, which for a long time imposed certain restrictions on using most of the analytical methods to study these rocks and minerals since they did not secure the necessary lower limits of detecting these elements. The new methods that have been developed and brought into use, especially those based on the principles of the local analysis of incompatible elements in rocks and minerals, have provided much lower detection levels, which has made it possible to make considerable progress in studying the distribution of REE in the REE-depleted products of ultramafic and mafic magmatism.

Most of the published data on the geochemistry of REE in rocks of many mafic–ultramafic complexes belong to different rocks of mafic composition relatively rich in these impurities. The REE chemistry has been less investigated in the rocks of the ultramafic row. Most publications on the REE geochemistry in minerals are devoted to clinopyroxenes, fewer analyses have been carried out on orthopyroxene, olivine, plagioclase, garnet, amphiboles, chromespinel, and other accessory minerals. Among those explored in more detail are minerals from garnet and spinel lherzolites, proper and harzburgites represented in abyssal xenoliths as well as in samples dredged in mid-oceanic ridges. Much less is known about minerals from rocks forming mafic and ultramafic complexes widespread in folded and platform regions.

Systematic investigations on the geochemistry of the REE in magmatic formations were started only in 1964–1965, and they concerned mainly the problems of the REE content of rocks. The study of the REE distribution in mafic and ultramafic rock minerals were started only in the late 1960s. At that time some evidence was obtained on the REE content in isolated samples of olivines, pyroxenes, plagioclases from ultramafites, represented in abyssal xenoliths dredged in mid-oceanic ridges as well as from meteorites. Published somewhat later were much more representative data on the distribution of REE in different rocks and minerals from mafic and ultramafic massifs of many regions. At present the investigation of the regularities of the REE distribution in olivine, orthopyroxene, clinopyroxene, plagioclase, amphibole, and other minerals of mafic and ultramafic rocks remains an important problem, and the theoretical generalization of these data extremely topical. These investigations contribute to the revelation of the cause-and-effect relations between the distribution of REE and the genesis of rocks and minerals, to the discovery of new typomorphic indicators of minerals, they are an important basis for a more detailed geochemical and petrogenetical systematics of mafic and ultramafic rocks and complexes formed by them, and, in the final analysis, contribute to the creation of less contradictory and better-founded petrological–geochemical models of abyssal magma formation and subsequent mineral formation under various physical and chemical conditions.

In the development of research on the geochemistry of REE in magmatic and other rocks and minerals several periods are conventionally singled out differing in the applied analytical methods as well as in the number of publications. Even early in the 1970s the problems of REE differentiation in magmatic processes were discussed

(Balashov, 1963), the data available at the time on the regularities in REE distribution in basic and ultrabasic rocks were generalized (Frey, 1966), and the first data on the geochemistry of REE in Precambrian gabbroid and other towns from the Barberton province in South Africa were presented (Goles, 1968). At the same time the first generalization of the results obtained in studying the distribution of REE in different natural objects was published (Haskin, Frey, 1966). Somewhat later, Balashov (1976) published a summary on the geochemistry of REE, the most complete one for the time, where he summarized the data on the crystalline properties of REE, on the peculiarities of their distribution in different rocks starting with meteorites and the most important types of magmatic properties, and finishing with sedimentary rocks, waters of the World ocean, and other objects. It should be noted, however, that the initial analytical data on the content of REE in different types of rocks and particularly in their minerals, that are necessary to the investigators for comparing them with the objects under investigation, were presented in very small amounts. Balashov distinguished two periods of research in the field of REE geochemistry: initial (1924–1952) and modern (1953–1976). It is obvious that at the present time it is appropriate to single out the following, the newest period in the development of research on the geochemistry of REE in rocks and minerals of magmatic rocks (starting with 1977).

In recent years, owing to the progress in the development of the local methods of REE analysis, to a significant reduction of the lower limits of discovering them in natural objects as well as to an increase in the number of analytic centers where these investigations were carried on, a marked rise has been observed in the number of publications on this topical problem. The researchers have been paying particular attention to the problems of intragranular and intermineral distribution of REE, to the estimation of the coefficients of REE distribution between phases, and to the estimation of the coefficients of REE distribution in model parental fusions, which is considered particularly important in the modern geochemistry of magmatic rocks (Zharikov & Yaroshevsky, 2003). Among the works generalizing the later groundwork in the field of REE geochemistry in magmatic rocks of different composition, a special place is occupied by the collective monograph edited by Henderson (*Rare Earth Element Geochemistry*, 1984), but it contains very few original analyses that are necessary in studying new objects. Original analyses of this kind on many varieties of ultramafic and mafic rocks in limited amounts are represented in fundamental summaries on ultramafic and mafic magmatism (Magmatic Rocks, 1985, 1988). In 1989 a large generalization on a wide range of problems of the geochemistry and mineralogy of REE including their cosmic distribution, isotopic geochemistry, distribution among melts and minerals, etc. was published (Lipin & McKey, 1989). One of the papers included in this book is devoted to the problems of the geochemistry of REE in outer mantle and ultramafic rocks from peridotite massifs and abyssal xenoliths (McDonough & Frey, 1989). It should be noted, however, that, unfortunately, in this work, no original analytical data are cited on the geochemistry of REE in ultramafic rocks from particular manifestations. The works by McKay (1986, 1989), McKay *et al.* (1986), McDonough *et al.* (1992), and Green (1994) contains generalized results of experimental investigations on estimating the coefficients of distribution of trace elements, including the REE, among many minerals (olivine, clinopyroxene, garnet, amphibole, spinel, feldspar, phlogopite, apatite, sphene, rutile, ilmenite, perovskite, and zircon) and melts. Worthy of attention is also the summary by Skublov (2005)

Table In.1 Methods of REE analysis.

Method	Abbreviations
Chromatography analysis	CHR
Mass-spectrometry analysis	MS
Autoradiography analysis	ARG
Optical emission-spectrometry analysis	OES
Photon-activation analysis	PAT
Absorption-spectrometry analysis	AAS
Liquid-chromatography analysis	LCHR
Laser microanalysis	LMA
X-ray-fluorescence analysis	XRF
Neutron-activation analysis	NAA
Instrumental neutron-activation analysis	INAA
X-ray chemical neutron-activation analysis	RNAA
Ion-microprobe mass-spectrometry analysis	IPMA
Isotope dissolution mass-spectrometry analysis	IDMS
Second-ion mass-spectrometry analysis	SIMS
Inductive-couple plasma mass-spectrometry analysis (from liquids)	ICP-MS
Laser ablation inductive-couple plasma mass-spectrometry analysis (in solid phase)	LA ICP-MS
Atom-emission spectrometry with inductive-couple plasma	ICP-AES

presenting the first generalization of the available materials on the geochemistry of REE in the main minerals from metamorphic rocks.

It is known that chemical elements, both in the composition of the Earth and in space, are characterized by their different occurrence (Voytkevich *et al.*, 1970). Among them there are the main elements (more than 1 wt%), trace elements (from 1 wt% to 0.1 wt%), and microelements (from 0.1 wt%, or 1000 ppm and less) (Shaw, 1969). Earlier it was suggested that the nonstructure-forming elements for minerals should be called oligoelements (Jedwab, 1953). According to the cited classifications, the elements conventionally referred to as lanthanides and usually contained in magmatic rocks in amounts less than 1 wt% are referred either to admixture elements or to microelements. To name them in the literature published in English, use is made of the general term "trace elements" or "microelements." Following Sklyarov *et al.* (2001) we denote rare earth and other microelements using the term "trace elements."

Depending on the type of rocks and minerals, on the character of problems to be solved and on the technical possibilities in studying REE geochemistry problems, researchers use different analytical methods which are constantly improved (Table In.1). Over a long period of time the methods most generally used were those based on the analysis of rock samples or mineral monofractions with the use of neutron REE activation technologies. The instrumental version of this method (INAA) provides the discovery of the REE in the interval of 5 ppm (Nd) to 0.05 ppm (Sm, Lu), which is quite acceptable in studying relatively REE-enriched mafic rocks and minerals such as clinopyroxene. However, these conditions did not make it possible to investigate the distribution of the REE in rocks and minerals bearing their lower concentrations. Later, to solve these problems, methods were developed and mastered for the radiochemical preparation of samples with the subsequent analysis of them by the instrumental method (RNAA). This provided the detection limit from 0.05 ppm

Table In.2 Bottom boundaries of finding REE by some analytical methods (ppm).

	Types of analyses					
Element	1	2	3	4	5	6
La	0.5	5.0×10^{-3}	2.1×10^{-7}	1.3×10^{-3}	7.0×10^{-3}	0.32
Ce	0.8	5.0×10^{-2}	3.0×10^{-7}	1.9×10^{-3}	1.0×10^{-2}	0.32
Pr	N.d.	N.d.	3.8×10^{-8}	2.4×10^{-4}	3.0×10^{-3}	0.28
Nd	2.0	5.0×10^{-3}	9.5×10^{-8}	5.9×10^{-4}	1.8×10^{-2}	1.6
Sm	0.05	1.0×10^{-4}	2.3×10^{-8}	1.4×10^{-4}	3.0×10^{-3}	1.9
Eu	0.01	1.0×10^{-3}	6.1×10^{-9}	3.8×10^{-5}	1.0×10^{-2}	0.54
Gd	0.2	1.0×10^{-2}	2.0×10^{-8}	1.2×10^{-4}	1.9×10^{-2}	1.7
Tb	0.05	1.0×10^{-3}	4.5×10^{-9}	2.8×10^{-5}	1.0×10^{-3}	N.d.
Dy	N.d.	N.d.	2.0×10^{-8}	1.2×10^{-4}	2.0×10^{-3}	1.5
Ho	N.d.	N.d.	4.9×10^{-9}	3.1×10^{-5}	1.0×10^{-3}	0.30
Er	N.d.	N.d.	1.1×10^{-8}	7.1×10^{-5}	4.0×10^{-3}	1.3
Tm	0.1	1.0×10^{-3}	1.7×10^{-8}	1.1×10^{-4}	2.0×10^{-3}	0.49
Yb	0.1	5.0×10^{-3}	3.6×10^{-8}	2.2×10^{-4}	5.0×10^{-3}	0.95
Lu	0.05	1.0×10^{-4}	3.3×10^{-9}	2.1×10^{-5}	2.0×10^{-3}	0.30

1, 2: unpublished data of the Laboratory of neutron-activation analysis of Analytical Centre of IGM SB RAS: 1—INAA, 2—RNAA; 3–5: unpublished data Laboratory of mass-spectrometry analysis of Analytical Centre of IGM SB RAS: 3—ICP-MS, 4—the same, on solid sample basis; 5: LA ICP-MS; 6: data Laboratory GEMOS, University Macquarie (Australia) (Belousova *et al.*, 2002), LA ICP-MS. N.d.: no data.

(Ce, Nd) to 0.0001 ppm (Sm, Lu) (Table In.2). At the same time, these methods of detecting the REE in *bulk* samples of minerals cannot prevent errors in analyses caused by the contamination of samples with foreign submicroscopic matter, since it is practically impossible to obtain a perfectly pure mineral fraction not only by mechanical but also by manual separation. In recent years it has become possible to overcome these difficulties by adopting local (microprobe) techniques of identifying REE in minerals to study individual grains of minerals in thin-section preparations without rock decomposition. Among these methods is the mass-spectrometric analysis with inductively coupled plasma (LA ICP-MS) (Norman *et al.*, 1996). Nevertheless, in using even these methods there may emerge difficulties connected with some distortions of the real REE contents due to the possible presence of submicroscopic solid or gas–liquid microinclusions, fine concretions (structures of solid solution disintegration), and of microcrack epigenetic contaminations in the mineral grains.

The reliability of determining REE contents provided by various methods depends both on the method itself and on the concentration of elements: the lower the element concentration, the higher the number of errors. Presented in Table In.3 are examples of average estimates of standard errors in determining the REE in the geochemical gabbro and granodiorite standards of the Geochemical Service of Japan, which were analyzed at many laboratories of the world using different analytical methods (Itoh *et al.*, 1993). It follows from them that the scatter of standard errors for the REE as a whole varies from 5.2% to 47.7% with the average values 17.7% for granodiorite and 15.4% for gabbro. Here it is pertinent to quote an extract from the monograph by Shaw (1969), who emphasized that "any analytical technique yields good results only in the laboratory where it has been developed."

Table In.3 Average contents, values of standard deviations and errors of determining the REE in the Japan geochemical standards of granodiorite and gabbro by the most widespread analytical methods.

	Granodiorite JG-3		Gabbro JGb-1	
Element	Average contents, (ppm)	Errors of determining (%)	Average contents (ppm)	Errors of determining (%)
La	20.7 ± 2.3 (14)	±11.1	3.7 ± 0.4 (23)	±10.8
Ce	40.1 ± 2.9(14)	±7.2	7.9 ± 1.7(24)	±21.5
Pr	4.7 ± 1.4(6)	±29.8	1.1 ± 0.1(9)	±9.1
Nd	16.8 ± 0.88(11)	±5.2	5.7 ± 0.7(15)	±12.3
Sm	3.4 ± 0.5(14)	±14.7	1.5 ± 0.2(20)	±13.3
Eu	0.91 ± 0.08(12)	±8.8	0.63 ± 0.05(20)	±7.9
Gd	2.9 ± 0.3(5)	±10.3	1.6 ± 0.2(10)	±12.5
Tb	0.46 ± 0.05(8)	±9.2	0.31 ± 0.07(13)	±22.6
Dy	2.6 ± 0.6(8)	±23.1	1.5 ± 0.4(14)	±26.7
Ho	0.36 ± 0.15(5)	±47.7	0.32 ± 0.05(10)	±15.6
Er	1.4 ± 0.4(6)	±28.6	1.1 ± 0.2(11)	±18.2
Tm	0.2 ± 0.27(3)	N.d.	0.15 ± 0.03(8)	±20.0
Yb	1.9 ± 0.3(11)	±15.8	0.97 ± 0.12(18)	±12.4
Lu	0.27 ± 0.05(11)	±18.5	0.15 ± 0.02(19)	±13.1
Average	–	±17.7	–	±15.4

Data Itoh *et al.* (1992). In the parentheses, numbers of analyses geochemical standards made in different laboratories of the World. Values of errors of determining separate elements (in %) were calculated as ratios of standard deviations to average contents of each elements.

In various natural objects it has become a routine to normalize them by the Masuda–Coryell method (*Rare Earth Element Geochemistry*, 1984) with the use of the average contents of each element in carbonaceous chondrites or in the primitive mantle (PM). The average estimates of the REE contents in carbonaceous chondrite C1 were repeatedly made more exact starting with earlier works (Haskin *et al.*, 1966) and finishing by modern computations (Table In.4, Fig. In.1). For the normalization in the present work, the average REE content in chondrite C1 according to Evensen *et al.* (1978) was used. In giving a graphical interpretation to the results of analyzing the REE and other admixtures in some cases, the normalization was performed according to the average content of the elements in the PM, in the normal (N-MORB) and enriched (E-MORB) basalts of the mid-oceanic ridges, and in the basalts of oceanic islands (OIB) according to Sun and McDonough (1989) (Table In.5).

By now the overwhelming part of the new information on the geochemistry of REE in rocks and minerals from mafic and ultramafic complexes has been published in periodicals. Generalizing publications in this field of petrology and geochemistry are practically lacking. This circumstance has induced the present author to create a bank of analytic information on the geochemistry of the REE in rocks and minerals of mafic and ultramafic complexes in order to reveal new regularities in the distribution of REE depending on the petrographical type of rocks, their geological position, and alleged origin. The author has systematized and generalized the available world data on the geochemistry of the REE in the objects under investigation. This monograph includes the published results of several thousand analyses of ultramafic and mafic rocks as well as over 2000 analyses of their minerals: olivine, orthopyroxene,

Table In.4 Average REE composition of carbonaceous chondrites (from different references) (ppm).

Element	Haskin *et al.* (1968)	Wakita *et al.* (1971)	Masuda *et al.* (1973)	Nakamura (1974)	Boynton (1984)	Taylor & McLennan, (1985)	Anders & Grevesse (1989)	Evensen *et al.* (1978)
La	0.330	0.340	0.378	0.329	0.310	0.367	0.238	**0.2446**
Ce	0.880	0.910	0.976	0.865	0.808	0.957	0.603	**0.6379**
Pr	0.112	0.121	N.d.	N.d.	0.122	0.137	0.089	**0.0964**
Nd	0.600	0.640	0.716	0.630	0.600	0.711	0.452	**0.4738**
Sm	0.181	0.195	0.230	0.203	0.195	0.231	0.147	**0.1540**
Eu	0.069	0.073	0.087	0.077	0.074	0.087	0.056	**0.0580**
Gd	0.249	0.260	0.311	0.276	0.259	0.306	0.197	**0.2043**
Tb	0.047	0.047	N.d.	N.d.	0.047	0.058	0.036	**0.0375**
Dy	N.d.	0.300	0.390	0.343	0.322	0.381	0.243	**0.2541**
Ho	0.070	0.078	N.d.	N.d.	0.072	0.085	0.056	**0.0567**
Er	0.200	0.020	0.255	0.225	0.210	0.249	0.159	**0.1660**
Tm	0.030	0.032	N.d.	N.d.	0.032	0.036	0.024	**0.0256**
Yb	0.200	0.220	0.249	0.220	0.209	0.248	0.163	**0.1651**
Lu	0.034	0.034	0.039	0.034	0.032	0.038	0.024	**0.0254**

Bold type—REE amounts in the chondrite C1 (Evensen *et al.*, 1978), used for normalization in this work. In the other cases their values have been rounded to the decimal digit after the point.

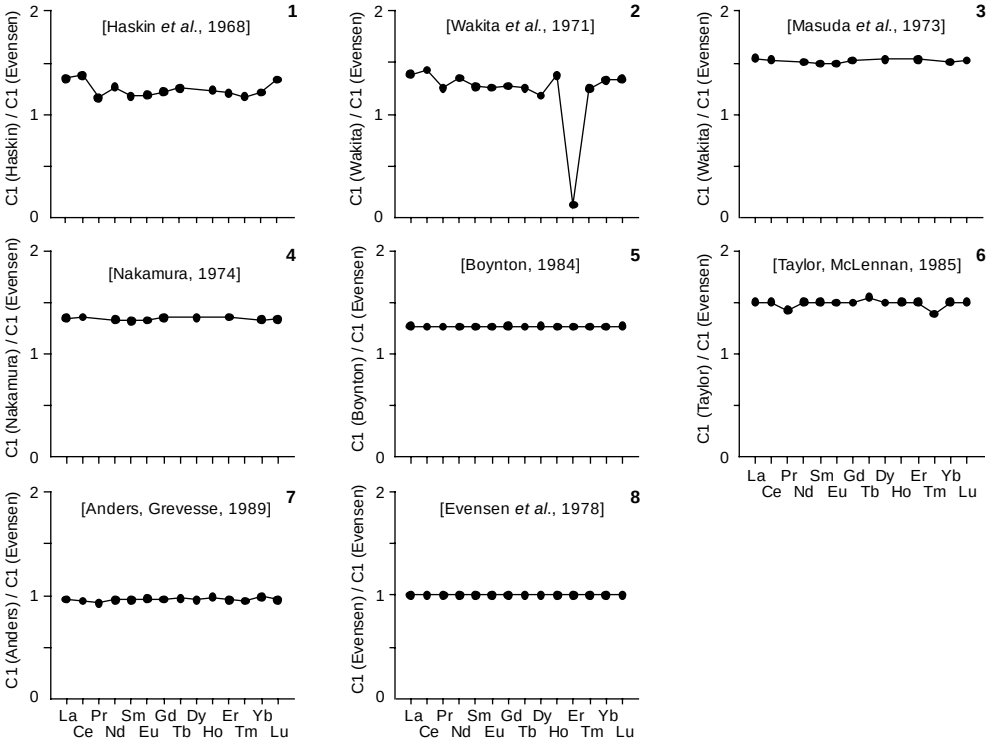

Figure In.1 Patterns of average REE compositions of carbonaceous chondrites (C1) (data Table In.4).

Table In.5 Average REE composition of primitive mantle and different types of oceanic basalts (ppm).

Element	PM	N-MORB	E-MORB	OIB
La	0.687	2.50	6.30	37.0
Ce	1.775	7.50	0.15	80.0
Pr	0.276	1.32	2.05	9.70
Nd	1.354	7.30	9.00	38.5
Sm	0.444	2.63	2.60	10.0
Eu	0.168	1.02	0.91	3.00
Gd	0.596	3.680	2.970	7.620
Tb	0.108	0.670	0.530	1.050
Dy	0.737	4.550	3.550	5.600
Ho	0.164	1.01	0.790	1.06
Er	0.480	2.97	2.31	2.62
Tm	0.074	0.456	0.356	0.350
Yb	0.493	3.05	2.37	2.16
Lu	0.074	0.455	0.354	0.300

PM—primitive mantle; N-MORB and E–MORB—normal and enriched basalts from mid-oceanic ridges, respectively; OIB—basalts from oceanic islands (Sun & McDonough, 1989).

clinopyroxene, plagioclase, and amphibole, which are supplemented with the results of analyses performed by the author as he studied his own stone collections of rocks and minerals. The REE analyses in rocks and minerals represented in the database had been performed by different methods, at different laboratories, and are unequal in their portliness and reliability as well as in the number of identified elements. In most cases the samples were analyzed for 10–14 elements, more rarely for 7–9 elements, still more rarely for 2–4 ones. A significant part of the analyses has been performed by instrumental or radiochemical versions of the neutron-activation method, and, a much smaller number, by the modern microprobe techniques.

This monograph consists of six chapters, introduction, and afterword. It presents the materials on the regularities of REE distribution in different petrographical types of plutonic and subvolcanic rocks of ultramafic and mafic composition, which form massifs different in structure, composition, and conditions of their formation, and located in continental folded regions and mid-oceanic ridges as well as within the platforms. This book discusses the regularities of the REE distribution in the main minerals of ultramafic and mafic rocks as well as some aspects of using REE as geochemical indicators in studying the processes of magma, rock, and mineral formation.

Chapter 1 considers the peculiarities of REE distribution in the rocks of ultramafic and similar composition that are represented in different types of mafic and ultramafic massifs cropping out within folded belts as well as in mid-oceanic ridges. Apart from the ultramafic restites (dunites, harzburgites, and lherzolites) this chapter also characterizes the rocks of the wehrlite–pyroxenites series (wehrlites, clinopyroxenites, websterites, and their olivine- and plagioclase-bearing varieties), which in the author's view were formed as a result of active interaction of mafic melts with ultramafic restites, and, hence, are hybrid formations. These regularities are discussed on the basis of more than 250 analyses of samples of 30 separate massifs. Chapter 2 is devoted to the discussion of the problems of REE geochemistry in ultramafic rocks (dunites,

harzburgites, and lherzolites), which are usually represented as forming parts of mantle xenoliths from subalkaline basalts of many provinces. Ultramafic rocks of this kind also occur in the form of xenoliths among kimberlites. However, they are not dealt with in the present work. This chapter is based on the generalization of over 180 analyses of samples from 30 massifs. Chapter 3 generalizes the materials on the geochemistry of REE in the most widespread varieties of hypabyssal, subvolcanogenic, and volcanogenic rocks possessing increased $Mg^{\#} = 100 \cdot Mg/(Mg + FeO_{tot})$: kimberlites (320 analyses from 80 provinces and separate pipes), komatiites (over 130 analyses from 10 provinces), meimechites (12 analyses from 1 province), picrites (28 analyses from 6 provinces), and lamproites (56 analyses from 16 provinces). Chapter 4 discusses the regularities of the REE distribution in the most widespread varieties of plutonic rocks of mafic composition represented in polytypic mafic and ultramafic massifs. Characterized among them are gabbros (more than 100 analyses from 18 massifs and provinces), gabbro-norites (50 analyses from 10 massifs), norites (12 analyses from 2 massifs), olivine-bearing gabbros (40 analyses from 18 massifs), troctolites (19 analyses from 8 massifs), anorthosites (24 analyses from 7 massifs), and, finally, eclogites as mafic rocks formed at increased pressures and forming part of some high-pressure metamorphic complexes and frequently present in abyssal xenoliths in alkali basalts and kimberlites (90 analyses from 21 manifestations). Chapter 5 presents materials on the regularities of REE distribution in rock-forming minerals of ultramafic and mafic rocks: olivine, orthopyroxene, clinopyroxene, plagioclase, and amphibole. Chapter 6 discusses, on the basis of the generalizations of the presented material, the main indicatory properties of the REE, which can to a greater or lesser extent be used in systematizing the ultramafic and mafic rocks and their main minerals as well as in constructing their genetic models.

The overwhelming part of the results obtained from the analyses of the REE in ultramafic and mafic rocks and their minerals and used for generalization is presented in the tables. In the author's opinion, they may be requested both by petrologists as well as geochemists for their studies on theoretical problems of mafic–ultramafic magmatism, and by geologists doing practical work, for example, studying and systematizing mafic–ultramafic complexes at the regional level. The references contained in this monograph, the author believes, are the most significant works on the problem under consideration published from the mid-1960s to 2009.

Chapter 1

Rare earth elements in ultramafic rocks from mafic–ultramafic massifs of folded regions

He who wants to cognize
must be able to doubt.
Aristotle

This chapter discusses the general characteristics of rare earth element (REE) distribution in the most common varieties of ultramafic rock (alpine-type, or "metamorphic" peridotites): dunites, harzburgites, and lherzolites). These rocks form numerous mafic–ultramafic massifs within folded belts on the continents and mid-oceanic ridges. These formations are usually considered to be mantle restites that have undergone some degree of REE depletion in the process of partial melting of the mantle. We define these rocks as orthomagmatic ultramafites to underline their primarily magmatogenic nature. By contrast, complex mafic–ultramafic massifs contain paramagmatic ultramafic rocks, including wehrlites, clinopyroxenites, websterites, and orthopyroxenites, all of which formation is connected with the magmatic and metasomatic interactions of mantle mafic melts with orthomagmatic ultramafic restites and their serpentinous varieties (Lesnov, 1986). A common feature of ultramafites that differs from most other types of magmatogenic rocks is that ultramafites contain relatively low total concentrations of all REE, especially light ones. For a long time this characteristic was the main obstacle to geochemical investigations of the REE composition of ultramafites. Another feature of ultramafic rocks is that their REE are weakly fractionated. At the same time, monotypic petrographical varieties of ultramafites from different massifs can differ from one another both in total REE content and in extent of fractionation. Not infrequently, however, the latter is due not so much to the primary processes involved in ultramafite restite formation, as to the later redistribution of light REE under the influence of metamorphic and hydrothermal processes. As a result, variable amounts of REE, especially light ones, were added to the initial rocks by epigenetic fluids circulating through microcracks, thus creating a false effect of REE fractionation. These REE are not part of the mineral structure and, thus, represent a non-structural admixture sometimes referred to as a "contaminant" (Kovalenko *et al.*, 1989). Note that, as will be shown later (see Chapter 2), the presence of such a "contaminant" is very characteristic of ultramafic restites brought up to the Earth's surface by basaltic or kimberlitic melts in the form of deep xenoliths. Relatively little analytical data have been obtained on the geochemistry of REE in ultramafic restites from mafic–ultramafic massifs that are widespread both within the folded regions of the continents and in the mid-oceanic ridges. Particularly scarce are data on paramagmatic ultramafites such as

plagioclase-bearing peridotites, plagioclase-bearing wehrlites and plagioclase-bearing pyroxenites. (Frey, 1984; Laz'ko, 1988b; Lesnov, 2003c,d).

1.1 DUNITES

Dunites are one of the most common varieties of ultramafic rock and are found in many structural matter types of proper ultramafic massifs as well as in complicated mafic–ultramafic massifs that involve different magmatic formations, including massifs that form ophiolitic associations. In a majority of these massifs, dunites are in a close positional connection with two other common ultramafic varieties—harzburgites and lherzolites. Dunites usually play a secondary role with respect to harzburgites and lherzolites. However, in some massifs, these three varieties of ultramafic rock are present in comparable amounts, while in the concentrically zonal massifs of the Ural–Alaskan type, dunites are frequently predominant. Besides olivine dunites sometimes contain, orthopyroxene, clinopyroxene, or, more rarely, plagioclase as secondary phases, and the rocks usually contain accessory chrome-spinel. In nearly all massifs, dunites have to some extent been subjected to serpentinization, with the result that olivine was replaced by serpentine to varying degrees, up to and including a total transformation of these rocks into serpentinites.

On the basis of about 200 chemical analyses, the concentrations of both the main and secondary components of dunites vary within a relatively narrow range. The mean concentrations of these components vary within the following cofidence intervals (wt% based on a dry analysis): MgO (46.4–47.4), SiO_2 (40.9–42.0), FeO_{tot} (8.6–9.5), and CaO (0.6–0.9). The concentration of the leading component, MgO, is inversely related to the concentrations of other petrogenic components in these rocks. The mean values of petrochemical parameters of dunites have the following cofidential intervals CaO/Al_2O_3 (0.59–0.91), MgO/CaO (44000–48000), Al_2O_3/MgO (0.27–0.33), and $100 \cdot FeO_{tot}/(FeO_{tot} + MgO)$ (15.5–16.9) (Lesnov, 1986). According to modern conceptions, alpine-type ultramafites (metamorphic peridotites), which include dunites, harzburgites, and lherzolites, are by their nature mantle rocks formed as refractory remains (restites) upon partial melting of the upper mantle. As a result of this process, ultramafic restites are considerably depleted of easily fusible components, including incompatible trace elements such as REE. For a long time, the very low concentrations of REE in ultramafic restites was the main reason for a lack of analytical data on these rocks.

We studied the main characteristics of REE distribution in dunites on the basis of 40 samples of these rocks from 19 separate massifs that include uneven-aged ophiolite associations located in Canada, the US, Colombia, Greece, Bulgaria, Norway, Oman, New Caledonia, New Guinea, and Russia (Table 1.1, Fig. 1.1).

The total concentration of REE in dunites varies within a wide range of more than two orders of magnitude (0.03–9.3 ppm). The mean total concentration of REE in dunites from individual massifs vary within a range of 0.04–5.96 ppm (Table 1.2, Fig. 1.2). The mean total concentration of REE computed over all samples is about 1.6 ppm, which is much less than the values of 3.36 ppm reported by Lutts (1975) and 7.1 ppm reported by Wedepohl and Muramatsu (1979) for mantle ultramafites as a whole. The highest maximum–minimum ratio is observed for Eu (~1900), and

Table 1.1 Rare earth element composition of dunites from some massifs and manifestations (ppm).

	Massifs and manifestations													
	Ural, Russia			Paramskiy, Russia			Dobromirsky, Bulgaria	Pindos, Greece	Japan	Canada	Samail, Oman			
	(Sav., 2000)	(Fershtater *et al.*, 1998), ICP-MS		(Gladkikh *et al.*, 1988), NAA			(Alexiev & Zheliazk, 1971)	(Montigny *et al.*, 1973)	(Frey *et al.*, 1971), NAA	(Suen *et al.*, 1979)	(Godard *et al.*, 2000), ICP-MS			
Element	Sav-D-2	FU4	FU11	B-85-12	B-85-22	B-85-35/1	281	K1	AK-29	195	MA5AL	94MA5	95OD78	96OF59
La	0.220	1.310	0.690	0.150	0.140	0.310	0.100	N.d.	0.039	0.0023	N.d.	N.d.	N.d.	0.0041
Ce	0.560	1.190	1.400	0.320	0.420	0.800	0.700	0.043	N.d.	N.d.	0.0062	0.0045	0.0031	0.0078
Pr	0.080	0.340	0.190	N.d.	N.d.	N.d.	N.d.	N.d.	0.011	N.d.	N.d.	N.d.	N.d.	N.d.
Nd	0.420	1.070	0.690	N.d.	N.d.	N.d.	0.300	0.021	N.d.	N.d.	0.0063	0.0051	0.0045	0.0081
Sm	0.150	0.330	0.140	0.022	0.029	0.100	0.100	0.006	0.009	0.0004	0.0033	N.d.	N.d.	N.d.
Eu	0.040	0.060	0.020	0.008	0.009	0.030	N.d.	0.005	0.002	0.0001	0.0014	0.0014	N.d.	N.d.
Gd	0.240	0.200	0.100	N.d.	N.d.	N.d.	0.150	0.012	0.008	0.0011	0.0051	0.0050	N.d.	0.0066
Tb	0.040	0.030	0.010	0.010	0.010	0.022	N.d.	N.d.	N.d.	N.d.	0.001	0.0011	0.0008	0.00107
Dy	0.280	0.160	0.070	N.d.	N.d.	N.d.	0.300	0.029	N.d.	N.d.	0.0109	0.0124	0.0077	0.0112
Ho	0.070	0.030	0.020	N.d.	N.d.	N.d.	N.d.	N.d.	0.002	0.0016	0.00363	0.0039	0.0027	0.00308
Er	0.210	0.100	0.050	N.d.	N.d.	N.d.	N.d.	0.028	0.006	N.d.	0.015	0.0166	0.0118	0.0116
Tm	0.030	0.010	0.010	N.d.	N.d.	N.d.	N.d.	N.d.	0.003	N.d.	0.00383	0.0042	0.0023	0.00257
Yb	0.200	0.050	0.040	0.044	0.032	0.075	0.350	N.d.	0.014	0.0077	0.0353	0.0407	0.0199	0.0232
Lu	0.040	0.010	0.010	0.0095	0.006	0.013	N.d.	N.d.	0.005	0.0033	0.0088	0.0096	0.0048	0.0056
Total	2.58	4.89	3.44	0.56	0.65	1.35	2.00	0.14	0.10	0.02	0.10	0.11	0.06	0.09
$(La/Yb)_n$	0.74	17.68	11.64	2.30	2.95	2.79	0.19	N.d.	1.88	0.20	N.d.	N.d.	N.d.	0.12

(*Continued*)

Table 1.1 Continued

	Massifs and manifestations													
	Samail, Oman		Gorgona, Columbia.			Twin Sisters, USA			Thetford Mines, Canada.					
	(Godard *et al.*, 2000), ICP-MS		(Revillon *et al.*, 2000), ICP-MS			(Frey *et al.*, 1971), NAA			(Harnois *et al.*, 1990, RNAA					
Element	OMB32	OMB33	GOR 503	GOR 505	GOR 542	DTS-1	DTSMIT	PCNA-1	MC-81-2	MC-81-3	VR-80-1	VR-80-4	LF-81-5	LF-81-6
La	0.0037	0.0016	0.150	0.130	0.230	0.057	0.0225	0.047	N.d.	N.d.	N.d.	N.d.	N.d.	0.011
Ce	0.0107	0.0042	0.430	0.390	0.720	N.d.	0.056	0.131	0.024	0.072	0.048	0.102	0.021	0.034
Pr	0.002	N.d.	0.090	0.090	0.150	0.013	0.0063	0.014	N.d.	N.d.	N.d.	N.d.	N.d.	N.d.
Nd	0.0091	0.0048	0.590	0.570	1.000	0.06	0.0267	0.062	N.d.	N.d.	N.d.	N.d.	N.d.	N.d.
Sm	0.0049	N.d.	0.340	0.340	0.530	0.008	0.0044	0.012	0.002	0.007	0.005	0.008	0.003	0.02
Eu	0.0019	0.0008	0.160	0.170	0.250	0.0013	0.00092	0.003	0.002	0.004	0.002	0.002	0.002	0.009
Gd	0.0065	0.003	0.670	0.690	1.000	N.d.	0.0043	0.012	N.d.	N.d.	N.d.	N.d.	N.d.	N.d.
Tb	0.0015	0.00077	0.130	0.140	0.200	0.002	0.00088	0.0021	N.d.	N.d.	N.d.	N.d.	N.d.	N.d.
Dy	0.0136	0.006	0.960	1.000	1.440	N.d.	N.d.	N.d.	N.d.	N.d.	N.d.	N.d.	N.d.	N.d.
Ho	0.00374	0.00175	0.210	0.220	0.310	0.0019	0.00127	0.0022	N.d.	N.d.	N.d.	N.d.	N.d.	N.d.
Er	0.0145	0.007	0.590	0.590	0.900	N.d.	0.0055	0.0087	N.d.	N.d.	N.d.	N.d.	N.d.	N.d.
Tm	0.00282	0.00165	0.090	0.090	0.130	0.0015	0.0012	0.0017	N.d.	N.d.	N.d.	N.d.	N.d.	N.d.
Yb	0.0227	0.0145	0.530	0.540	0.820	0.013	0.0073	0.009	0.007	0.006	0.007	0.014	0.007	0.029
Lu	0.0048	0.0036	0.090	0.090	0.130	0.0038	0.0034	0.0033	0.002	0.004	0.002	0.003	0.002	0.005
Total	0.10	0.05	5.03	5.05	7.81	0.16	0.14	0.31	0.04	0.09	0.06	0.13	0.04	0.11
$(La/Yb)_n$	0.11	0.08	0.19	0.16	0.19	2.96	2.08	3.53	N.d.	N.d.	N.d.	N.d.	N.d.	0.26

	Massifs and manifestations													
	Blashke Islands, Canada		Can Peak, Alaska, USA			Union Bay, USA		Marinkin, Russia		Lukinda, Russia		*Romanche trough, Atlantic ocean		
	(Himmelberg & Loney. 1995)							(Mekhonoshin *et al.*, 1986), INAA				(Nikol'skaya & Kogarko, 1995)		
Element	80BI10	80BI37	81KP7A	81SK045	81SK048	87GH27A	87GH27B	Б2638	Б2645	П1502	П1609	D9-10	D9-12	D9-16
La	0.045	0.0254	0.286	0.0929	0.0597	0.0233	0.0257	0.290	0.160	0.450	0.370	1.070	0.840	0.470
Ce	0.14	0.058	0.593	0.32	0.13	0.045	0.05	0.310	0.300	0.550	0.620	2.170	1.760	1.980
Pr	N.d.	N.d.	N.d.	N.d.	N.d.	N.d.	N.d.	N.d.	N.d.	N.d.	N.d.	0.293	0.270	0.297
Nd	0.12	0.029	0.37	0.25	0.065	0.02	0.037	0.230	0.200	0.400	0.250	1.430	1.500	1.700
Sm	0.0503	0.0079	0.112	0.0829	0.0188	0.0062	0.0133	0.070	0.070	0.067	0.060	0.390	0.440	0.280
Eu	0.0191	0.0042	0.0414	0.0315	0.0089	0.0021	0.0049	0.037	0.100	0.081	0.050	0.132	0.190	0.130
Gd	0.074	N.d.	0.13	0.12	N.d.	N.d.	N.d.	0.120	0.180	0.150	0.140	0.500	0.590	0.430
Tb	0.0149	0.005	0.021	0.018	0.0047	0.001	0.0033	0.023	0.034	0.030	0.024	0.110	0.110	0.080
Dy	N.d.	N.d.	N.d.	N.d.	N.d.	N.d.	N.d.	N.d.	N.d.	N.d.	N.d.	0.641	0.670	0.530
Ho	N.d.	N.d.	N.d.	N.d.	N.d.	N.d.	N.d.	N.d.	N.d.	N.d.	N.d.	0.126	0.149	0.121
Er	N.d.	N.d.	N.d.	N.d.	N.d.	N.d.	N.d.	N.d.	N.d.	N.d.	N.d.	0.380	0.420	0.400
Tm	N.d.	0.0059	N.d.	N.d.	N.d.	N.d.	N.d.	0.010	0.021	0.030	0.015	0.048	0.057	0.057
Yb	0.0782	0.0444	0.0543	0.0769	0.023	0.0088	0.013	0.110	0.120	0.180	0.130	0.360	0.430	0.450
Lu	0.0124	0.0063	0.0074	0.0117	0.0033	0.0015	0.0021	N.d.	N.d.	N.d.	N.d.	0.060	0.078	0.046
Total	N.d.	N.d.	N.d.	N.d.	N.d.	N.d.	N.d.	N.d.	N.d.	N.d.	N.d.	7.71	7.50	6.97
$(La/Yb)_n$	0.39	0.39	3.56	0.82	1.75	1.79	1.33	N.d.	N.d.	N.d.	N.d.	2.01	1.32	0.71

(*Continued*)

Table 1.1 Continued

	Massifs and manifestations															
	*Romanche trough, Atlantic ocean					Mount Orford, Canada		Koryakia, Russia	Chukotka, Russia		New Caledonia			Norway	Oman	New Guinea
	(Nikol'skaya & Kogarko, 1995)					(Harnois & Morency, 95)		(Laz'ko, 1988)								
Element	D9-2	D9-3	D9-6	D9-7	D9-8	E -0	E-1	Laz-1	P-131	P-12-78	Laz-2	Pr-6	Pr-7	Laz-3	Laz -4	Laz -5
La	0.580	0.730	0.310	0.470	0.280	0.008	0.01	0.047	0.041	0.053	N.d.	N.d.	N.d.	0.013	0.097	N.d.
Ce	1.300	2.350	0.740	1.860	0.900	0.024	0.034	0.14	0.16	0.13	0.014	0.022	0.005	0.1	0.55	0.011
Pr	0.210	0.320	0.113	0.198	0.131	N.d.	N.d.	N.d.	N.d.	N.d.	N.d.	N.d.	N.d.	N.d.	N.d.	N.d.
Nd	1.300	1.450	0.600	0.850	0.740	N.d.	N.d.	0.11	0.14	0.11	0.0063	0.011	0.0025	N.d.	0.45	0.0033
Sm	0.270	0.380	0.150	0.280	0.170	0.006	0.008	0.04	0.055	0.037	0.0014	0.0025	0.00056	0.096	0.017	0.00079
Eu	0.119	0.143	0.070	0.132	0.090	0.002	0.004	0.016	0.021	0.014	0.00032	0.00056	0.00016	0.02	0.005	0.00025
Gd	0.390	0.570	0.245	0.380	0.245	N.d.	N.d.	0.052	0.08	0.05	N.d.	N.d.	0.001	N.d.	N.d.	0.0014
Tb	0.070	0.120	0.050	0.110	0.050	0.002	0.003	0.011	0.017	0.011	N.d.	N.d.	N.d.	0.01	0.009	N.d.
Dy	0.480	0.730	0.330	0.436	0.290	N.d.	N.d.	N.d.	N.d.	N.d.	N.d.	0.0034	0.0023	N.d.	N.d.	N.d.
Ho	0.110	0.150	0.070	0.100	0.062	N.d.	N.d.	N.d.	N.d.	N.d.	N.d.	N.d.	N.d.	N.d.	N.d.	N.d.
Er	0.340	0.420	0.200	0.300	0.170	N.d.	N.d.	N.d.	N.d.	N.d.	N.d.	0.0032	0.0038	N.d.	N.d.	N.d.
Tm	0.048	0.055	0.026	0.043	0.022	N.d.	N.d.	N.d.	N.d.	N.d.	N.d.	N.d.	N.d.	N.d.	N.d.	N.d.
Yb	0.350	0.363	0.190	0.350	0.170	0.007	0.014	0.047	0.01	0.036	0.0094	0.0082	0.011	0.02	0.085	0.013
Lu	0.060	0.070	0.023	0.040	0.030	0.002	0.002	0.008	0.017	0.008	0.0027	0.0019	0.0036	0.004	0.02	0.0035
Total	5.63	7.85	3.12	5.55	3.35	N.d.	N.d.	N.d.	N.d.	N.d.	N.d.	N.d.	N.d.	N.d.	N.d.	N.d.
$(La/Yb)_n$	1.12	1.36	1.10	0.91	1.11	0.77	0.48	0.68	2.77	0.99	N.d.	N.d.	N.d.	0.44	0.77	N.d.

	Massifs and manifestations															
	Sugomaksky, Ural, R.		Ufaleysky, Ural, Russia					Nuraly, Ur.	Khabarninsky (Ural), Russia				Khalilov, R	Kosvin.	Sakhar.	Khabar.
	(Saveliev *et al.*, 2008), RNAA													(Fershtater *et al.*, 2009)		
Element	4229-1	4236-2	**Uf-04-2	**Uf-09-3	**Uf-10-2	**Uf-01-2	**Uf-02-2	Nr-6	Kh-9-2	Kh -27-3	Kh -29-3	Kh -73	Khal-4-1	Kt355	K1836	K1832
La	0.150	0.120	0.21	0.29	0.12	0.055	0.14	0.82	0.091	0.028	0.022	0.29	0.096	0.13	0.34	0.19
Ce	0.330	0.290	0.44	0.72	0.18	0.089	0.26	1.65	0.2	0.063	0.04	0.61	0.23	0.37	0.73	0.48
Pr	0.042	0.042	0.058	0.11	0.017	0.008	0.029	0.19	0.025	0.008	0.005	0.074	0.033	0.06	0.09	0.07
Nd	0.180	0.200	0.26	0.55	0.053	0.024	0.11	0.79	0.11	0.036	0.019	0.32	0.16	0.30	0.30	0.37
Sm	0.052	0.066	0.075	0.18	0.011	0.005	0.026	0.21	0.031	0.011	0.005	0.093	0.05	0.12	0.14	0.11
Eu	0.320	0.011	0.032	0.28	0.063	0.12	0.014	0.044	0.018	0.023	0.034	0.055	0.003	0.03	0.02	0.03
Gd	0.093	0.140	0.12	0.33	0.053	0.04	0.052	0.39	0.067	0.046	0.047	0.15	0.094	0.13	0.10	0.14
Tb	0.017	0.025	0.023	0.059	0.012	0.01	0.01	0.076	0.013	0.009	0.009	0.025	0.017	0.02	0.01	0.03
Dy	0.120	0.190	0.16	0.41	0.11	0.074	0.073	0.55	0.1	0.058	0.068	0.16	0.12	0.12	0.10	0.17
Ho	0.031	0.051	0.042	0.11	0.033	0.022	0.019	0.16	0.028	0.015	0.018	0.04	0.032	0.03	0.02	0.04
Er	0.100	0.170	0.13	0.3	0.13	0.08	0.066	0.54	0.098	0.05	0.06	0.12	0.11	0.07	0.05	0.11
Tm	0.018	0.033	0.023	0.055	0.029	0.016	0.012	0.1	0.018	0.008	0.011	0.02	0.018	0.012	0.01	0.02
Yb	0.120	0.220	0.14	0.36	0.24	0.11	0.081	0.69	0.13	0.053	0.071	0.12	0.12	0.079	0.04	0.11
Lu	0.023	0.045	0.028	0.065	0.055	0.025	0.017	0.14	0.027	0.01	0.015	0.022	0.024	0.015	0.01	0.02
Total	1.596	1.603	1.741	3.819	1.106	0.678	0.909	6.350	0.956	0.418	0.424	2.099	1.107	1.486	1.960	1.890
$(La/Yb)_n$	0.844	0.368	1.012	0.544	0.337	0.337	1.167	0.802	0.472	0.357	0.209	1.631	0.540	0.111	5.737	1.168

Note: Here and further in the columns "References" or "Subject" note names of analytical methods are give in conformity with the abreviations in Table In.1. N.d. – no data. *Dunites have admixture of amphibole. ** Serpentinised dunites.

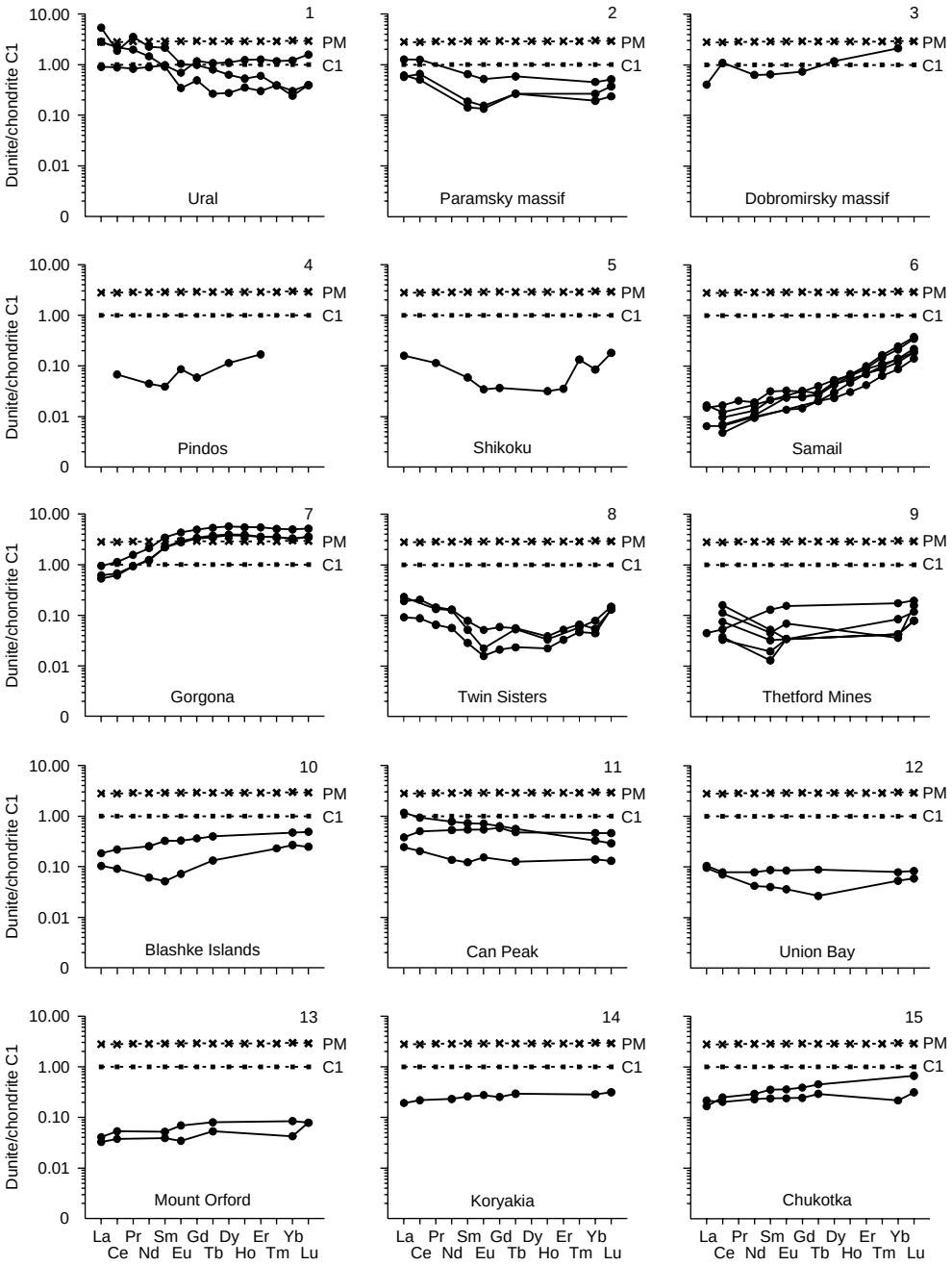

Figure 1.1 Chondrite-normalized REE patterns for dunites from different massifs (data Table 1.1). Here, and in all figures, normalization was based on chondrite C1 (Evensen *et al.*, 1978). PM—primitive mantle (Sun & McDonough, 1989).

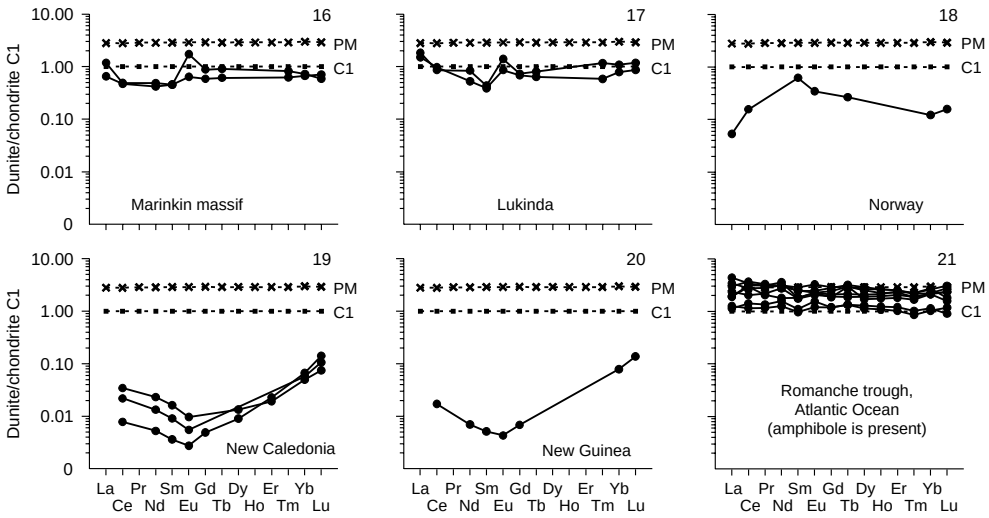

Figure 1.1 Continued

the lowest is observed for Lu (<70). According to their total REE content and to their distribution patterns on REE diagrams, dunites are conventionally divided into two groups. The first group includes REE-depleted varieties in which REE concentrations are within a range of about 0.1–0.4 times their concentration in chondrite C1 (t. ch.). Dunites of this type are represented in the Pindos, Shikoku Island, Twin Sisters, Thetford mine, Mount Orford, Bay of Islands, Blashke Islands, Union Bay, Samail, and New Caledonia massifs. The second group encompasses dunites that are somewhat enriched with REE. The levels of most REE in this type of dunite are at about 1.0 t. ch. Dunites of the second group are represented in the Sredny Kraka, Nuralinsky, Paramsky, Dobromirsky, and Gorgona Island massifs, as well as in the Romanche Trough in the equatorial Atlantic Ocean. Differences in REE accumulation in dunites, expressed through chondrite normalization, reflect both epigenetic transformations that occurred in these rocks as well as primary endogenic geochemical peculiarities that were caused by variable degrees of mantle protolith depletion. On the basis of available data, one can assume that the most intensive depletion of mantle protoliths occurred in dunite formations in the Mount Orford, Thetford Mines, Union Bay, Samail, and New Caledonia massifs. Dunites also differ in their intensity of REE fractionation. In most cases, $(La/Yb)_n$ values are less than unity. For example, dunites from the Gorgona Islands, Samail, Ufaleysky, and Khabarninsky massifs have $(La/Yb)_n$ values in the range of 0.07–0.8, and, therefore, the REE in these rocks are fractionated intensively. On the other hand, dunites from the Paramsky, Nuralinsky, Shikoku Island, Twin Sisters, and Kosvinsky massifs are enriched with light REE and are characterized by $(La/Yb)_n$ values greater than unit. Some dunite samples reveal relatively increased or decreased content of Eu, which accounts for the positive or negative anomalies of this element in dunite REE patterns. The relative enrichment of some dunites with light REE is assumed to be due to epigenetic redistribution under the action of different fluids, resulting in different intensities of lixiviation, transportation,

Table 1.2 Average REE composition of dunites from some massifs (ppm).

	Massifs												
Element	Ural (2)	Paramskiy (3)	Chukotka (2)	Mount Orford (2)	Thetford Mines (7)	Blashke Islands (2)	Can Peak (3)	Union Bay (2)	Twin Sisters (3)	Samail (6)	Gorgona (3)	New Caledonia (3)	Romanche trough (8)
La	1.000	0.200	0.047	0.009	0.011	0.035	0.146	0.025	0.042	0.003	0.170	N.d.	0.594
Ce	1.295	0.513	0.145	0.029	0.051	0.099	0.348	0.048	0.094	0.006	0.513	0.014	1.633
Pr	0.265	N.d.	N.d.	N.d.	N.d.	N.d.	N.d.	N.d.	0.011	0.002	0.110	N.d.	0.229
Nd	0.880	N.d.	0.125	N.d.	N.d.	0.075	0.228	0.029	0.050	0.006	0.720	0.007	1.196
Sm	0.235	0.050	0.046	0.007	0.020	0.029	0.071	0.010	0.008	0.004	0.403	0.002	0.295
Eu	0.040	0.016	0.018	0.003	0.007	0.012	0.027	0.004	0.002	0.001	0.193	0.0003	0.126
Gd	0.150	N.d.	0.065	N.d.	N.d.	0.074	0.125	N.d.	0.008	0.005	0.787	0.001	0.419
Tb	0.020	0.014	0.014	0.003	N.d.	0.010	0.015	0.002	0.002	0.001	0.157	N.d.	0.088
Dy	0.115	N.d.	N.d.	N.d.	N.d.	N.d.	N.d.	N.d.	N.d.	0.010	1.133	0.003	0.513
Ho	0.025	N.d.	N.d.	N.d.	N.d.	N.d.	N.d.	N.d.	0.002	0.003	0.247	N.d.	0.111
Er	0.075	N.d.	N.d.	N.d.	N.d.	N.d.	N.d.	N.d.	0.007	0.013	0.693	0.004	0.329
Tm	0.010	N.d.	N.d.	N.d.	N.d.	0.006	N.d.	N.d.	0.002	0.003	0.103	N.d.	0.045
Yb	0.045	0.050	0.023	0.011	0.022	0.061	0.051	0.011	0.010	0.026	0.630	0.010	0.333
Lu	0.010	0.010	0.013	0.002	0.004	0.009	0.017	0.002	0.004	0.006	0.103	0.003	0.051
Total	4.17	N.d.	N.d.	N.d.	N.d.	N.d.	N.d.	N.d.	0.20	0.08	5.96	N.d.	5.96
$(La/Yb)_n$	14.66	2.68	1.88	0.63	0.26	0.39	2.04	1.56	2.85	0.10	0.18	N.d.	1.20

Note: Data Table 1.1. Here and further in parentheses—numbers of analysis used for calculation.

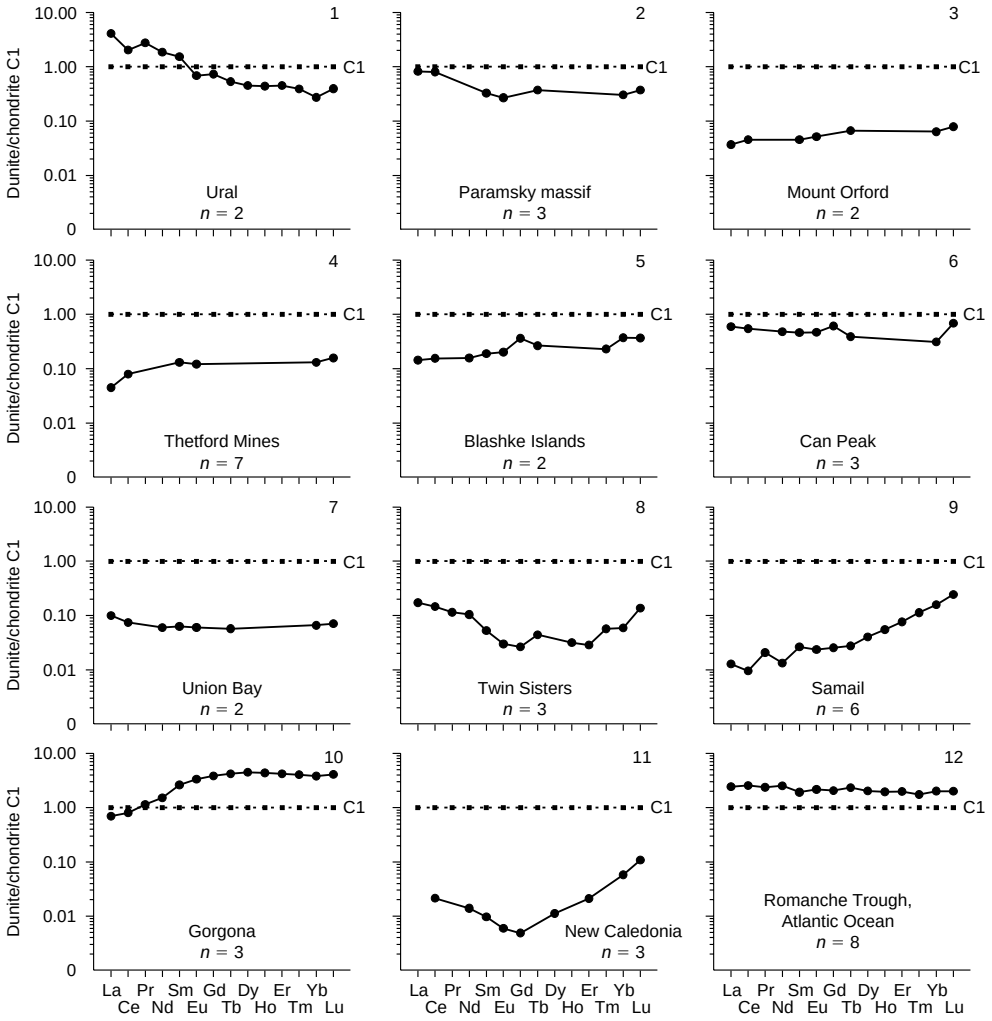

Figure 1.2 Chondrite-normalized REE patterns for the average composition of dunites from different massifs (data Table 1.2).

and subsequent sedimentation of mobile elements in the microcracks and intergranular spaces of the rocks. This kind of redistribution of light REE appears to have occurred in dunites from the Paramsky, Dobromirsky, Pindos, Shikoku Island, Bay of Islands, Twin Sisters, and Thetford Mines massifs. In addition, some dunites might have been enriched with light REE in the course of their hydrothermal and metasomatic transformations accompanied by the neogenesis of amphibole, as, for example, has been recorded in dunites from the Romanche Trough (Nikol'skaya & Kogarko, 1995). Fershtater *et al.* (2009) reported REE concentrations in individual samples of dunites from the Kosvinsky, Sakharinsky, and East Khabarninsky mafic–ultramafic massifs, all of which are part of the platinum-bearing belt of the Ural Mountains.

According to the researchers, these dunites were typically characterized by very low total REE concentrations, very weak fractionation, and minimal Eu deficiency. The REE distribution in dunites should be considered together with the peculiarities of the distribution of these impurities in olivines, which differ from other minerals that form magmatic rocks by having the lowest "lanthanophility", that is, the ability to accumulate REE in their structure (Lesnov *et al.*, 1995; Lesnov, 2000a). For example, according to available data, (see Section 5.1), the REE concentration in olivines from different types of rock is usually about 0.01 t. ch. or somewhat higher.

* * *

Thus, dunites from most mafic–ultramafic massifs represent an intensively depleted product of the partial melting of mantle protoliths. These rocks are characterized by a very low level of REE accumulation, at about one order of magnitude lower than that in chondrite C1. Dunites can be enriched with REE, particularly light ones, as a result of epigenetic processes, including dynamo-metamorphic recrystallization, serpentinization, and other hydrothermal transformations connected with the circulation of fluids. In some cases, dunites are abnormally enriched with, or depleted of, Eu.

1.2 HARZBURGITES

Harzburgites, together with dunites and lherzolites, occur in numerous ultramafic and mafic–ultramafic massifs that mainly involve uneven-aged ophiolitic associations and are located in the folded regions of the continents as well as within the limits of mid-oceanic ridges. In addition, abyssal xenoliths composed of harzburgites can be found in alkali basalts and kimberlites. Harzburgites are generally agreed to be refractory residual products formed during substantial partial melting of mantle sources. Within the upper levels of the Earth's crust, these rocks penetrated along the zone of deep-seated faults in the form of steeply dipping tabular tectonic block protrusions. In some cases, however, harzburgites contained in mafic–ultramafic massifs are considered to be cumulates, that is, the product of intrachamber gravity crystallization of mantle mafic melts. In particular, the cumulative model of harzburgite formation is assumed for the Bushweld complex (Wager & Brown, 1970; Sharkov & Bogatikov, 1985) and Monchegorsky massif (Laz'ko *et al.*, 1988).

Harzburgites contain variable amounts of olivine (40–90%) and orthopyroxene (10–60%); besides these minerals, the less-depleted varieties quite often contain clinopyroxene as a secondary mineral in amounts of up to 10%. Some harzburgites contain admixtures of garnet, plagioclase, and amphibole. Accessory minerals are often represented by chrome-spinels, in addition to which, judging by some geochemical and mineralogical data, a uniformly distributed, submicroscopic disaggregating of minerals with platinum group elements may take place. The chemical composition of harzburgites is defined by the following ranges (wt%): SiO_2 (36–42), Al_2O_3 (0.2–2.5), FeO_{tot} (5–10), CaO (0.2–2.0), and MgO (34–42) (Bogatikov *et al.*, 1981). These rocks are distinguished by their narrow confidence intervals for the mean values of petrochemical parameters (wt%): CaO/Al_2O_3 (0.9–1.4), Al_2O_3/MgO (0.04–0.06), and $100 \cdot FeO_{tot}/(FeO_{tot} + MgO)$ (18–20) (Lesnov, 1986).

As with other ultramafic restites, harzburgites are characterized by considerable REE depletion, which was established as early 1976 when the first samples to be analyzed were dragged from mid-oceanic ridges (Balashov, 1976) and obtained from the Josephine massif (Oregon, USA) (Frey, 1984). Over the past 20 years, a significant body of analytical data has been published on the geochemistry of REE in harzburgites. Their representative composition is presented in Table 1.3 and Figure 1.3. These analyses characterize samples of harzburgites from more than 20 ultramafic and mafic–ultramafic massifs and were tested with a variable degree of detail. In most massifs, only isolated samples of harzburgites were analyzed for REE and in only a few cases were ten or more samples studied. Among the massifs in which the REE geochemistry of harzburgites were studied in particular detail are the Samail (Pallister & Knight, 1981; Godard *et al.*, 2000), Lherz (Bodinier *et al.*, 1990), and Ivrea Verbano (Hartmann & Wedepohl, 1993) massifs. Some of the harzburgite samples from these studies, those from Ivrea Verbano for example, demonstrate a low degree of REE fractionation, while other samples show increased fractionation because they are enriched with light REE. For this reason, the histograms of light REE distribution in the harzburgites from these massifs have a bimodal or complicated form. The REE patterns of harzburgites enriched with light REE usually demonstrate a smoothed minimum in the region of middle elements. This pattern is sometimes complicated by an anomaly of Eu, in which case the graph has a general negative slope. The U-shaped REE pattern is typical of rocks from the Sredny Kraka, Paramsky, Ivrea Verbano, Thetford Mines, Sud, and Tiebugy massifs, among others.

The harzburgites of each massif are distinguished by certain specific features of REE distribution, as is evident from data on the average contents of the elements (Table 1.4). The average total REE content in the harzburgites of individual massifs varies within a wide range. The highest average total REE concentrations were recorded in the harzburgite samples from the Kokchetavsky and Harzburg massifs, while the lowest ones were recorded in those from the Samail, Sud, Ronda, and Kempirsaisky massifs. The average total REE concentration over all harzburgite samples is about 1.8 ppm, which is somewhat lower than that in chondrite C1 (2.60 ppm) and substantially less than that in the primitive mantle (~7.43 ppm). The $(La/Yb)_n$ values calculated over all the analyses vary in the range of 0.03–17 and average to about 0.3. The lowest average value of this parameter was found in harzburgites from the Samail massif, and the highest was found in isolated samples from the Ivrea Verbano and Lherz massifs. The peculiarities of REE distribution in harzburgites from individual massifs can be observed in their REE patterns (see Fig. 1.3). One should pay attention to the fact that in the massifs from which a large number of samples were analyzed, the REE patterns usually resemble one another in configuration and slope, but differ in position. This can be most distinctly illustrated by the samples from the Samail and Sud massifs.

Available data on REE geochemistry make it possible to divide harzburgites, similarly to dunites, into two geochemically different types. The first type is represented by varieties that are significantly depleted of light REE, and, accordingly, their REE patterns have a general positive slope. This type includes harzburgites from the Ivrea Verbano, Lherz, and Ronda massifs, among others. Harzburgites of the second type are to a certain extent enriched with light REE, and their patterns have a general negative slope. These varieties are widespread in the Sud, Thetford Mines, Trinity, and

Table 1.3 Rare earth element composition of harzburgites from massifs (ppm).

	Massifs													
	Khabarninsky, Russia	Nuralinsky, Russia	Sredny Kraka, Russia	Voykar-Sin'insky, Russia		Krasnogorsky, Russia	Paramsky, Russia					Kokchetavsky, Kazakhstan		
	(Fershtater *et al.*, 1998)		(Savel'ev *et al.*, 2000)	(Laz'ko, 1988b)		(Laz'ko, 1988b)	(Gladkikh *et al.*, 1998), NAA					(Reverdatto *et al.*, 2000), INAA		
Element	FU1	FU10	Sav-2	Laz-118	Laz-139	L-131-2	V8513	V8534	V8535	V8538	V8554	R118	R118A	9-L-2
La	0.010	0.270	0.650	0.004	0.020	0.022	0.120	0.120	0.110	0.120	0.220	1.700	2.100	1.300
Ce	0.030	0.440	0.950	0.010	0.044	0.180	0.280	0.300	0.270	0.260	0.580	4.100	6.300	3.400
Pr	0.010	0.080	0.080	N.d.	N.d.	N.d.	N.d.	N.d.	N.d.	N.d.	N.d.	N.d.	N.d.	N.d.
Nd	0.030	0.290	0.220	N.d.	0.023	0.090	N.d.	N.d.	N.d.	N.d.	N.d.	2.400	4.100	2.500
Sm	0.010	0.070	0.050	0.087	0.064	0.040	0.031	0.019	0.026	0.020	0.034	0.690	1.300	0.800
Eu	0.010	0.010	0.090	0.042	0.001	0.006	0.009	0.007	0.006	0.012	0.010	0.370	0.310	0.380
Gd	0.020	0.050	0.080	0.022	0.010	0.030	N.d.	N.d.	N.d.	N.d.	N.d.	1.100	2.000	1.200
Tb	0.010	0.010	0.010	N.d.	N.d.	0.010	0.010	0.010	0.010	0.010	0.010	0.200	0.370	0.240
Dy	0.040	0.040	0.100	0.049	0.018	N.d.	N.d.	N.d.	N.d.	N.d.	N.d.	N.d.	N.d.	N.d.
Ho	0.010	0.010	0.030	N.d.	N.d.	N.d.	N.d.	N.d.	N.d.	N.d.	N.d.	N.d.	N.d.	N.d.
Er	0.040	0.020	0.100	0.050	0.020	N.d.	N.d.	N.d.	N.d.	N.d.	N.d.	N.d.	N.d.	N.d.
Tm	0.010	0.010	0.020	N.d.	N.d.	N.d.	N.d.	N.d.	N.d.	N.d.	N.d.	N.d.	N.d.	N.d.
Yb	0.070	0.030	0.140	0.071	0.032	0.050	0.038	0.035	0.032	0.050	0.030	1.100	2.200	1.400
Lu	0.010	N.d.	0.030	0.014	0.001	0.006	0.007	0.008	0.007	0.010	0.006	0.180	0.320	0.230
Total	0.31	1.33	2.55	0.25	0.18	N.d.	N.d.	N.d.	N.d.	N.d.	N.d.	N.d.	N.d.	N.d.
$(La/Yb)_n$	0.10	6.07	3.13	0.03	0.42	0.30	2.13	2.31	2.32	1.62	4.95	1.04	0.64	0.63

	Massifs													
	Bulgaria	Troodos, Cyprus	Otris, Greece			Ivrea Verbano, Italy								
	(Alexsiev & Zheliazkova, 1971)	(Menzies, 1976), NAA				(Hartmann & Wedepohl, 1993), INAA								
Element	1111a	T9	O6	O7	O8	FIN-1	FIN-11	FIN-12	FIN-2	FIN-3A	FIN-3B	FIN-4	FIN-5	FIN-6
La	0.520	0.020	N.d.	0.610	N.d.	0.070	0.670	3.480	0.050	0.020	0.020	0.700	0.670	0.540
Ce	1.400	0.040	0.530	0.340	N.d.	0.230	1.230	7.870	0.150	0.050	0.040	1.720	1.530	1.150
Pr	N.d.	N.d.	N.d.	N.d.	N.d.	N.d.	N.d.	N.d.	N.d.	N.d.	N.d.	N.d.	N.d.	N.d.
Nd	0.650	0.030	N.d.	N.d.	0.040	0.170	0.500	2.530	0.120	0.040	0.040	0.610	0.650	0.530
Sm	0.180	0.010	0.040	0.080	0.010	0.070	0.120	0.500	0.040	0.010	0.010	0.110	0.110	0.100
Eu	N.d.	0.010	N.d.	0.020	N.d.	N.d.	0.037	0.120	0.015	N.d.	N.d.	0.032	0.034	0.031
Gd	0.200	0.010	0.060	0.240	N.d.	0.100	0.120	0.290	0.060	0.030	0.030	0.090	0.090	0.090
Tb	N.d.	N.d.	0.020	0.050	N.d.	N.d.	0.020	0.040	0.010	N.d.	N.d.	0.020	0.010	0.010
Dy	0.160	N.d.	N.d.	N.d.	N.d.	0.120	0.100	0.250	0.080	0.060	0.060	0.090	0.070	0.080
Ho	N.d.	N.d.	0.040	0.100	0.020	N.d.	N.d.	N.d.	N.d.	N.d.	N.d.	N.d.	N.d.	N.d.
Er	N.d.	N.d.	N.d.	N.d.	N.d.	0.090	0.070	0.150	0.070	0.050	N.d.	0.030	0.040	0.040
Tm	N.d.	N.d.	N.d.	N.d.	N.d.	N.d.	N.d.	N.d.	N.d.	N.d.	N.d.	N.d.	N.d.	N.d.
Yb	0.130	0.020	0.160	N.d.	N.d.	0.090	0.060	0.140	0.070	0.050	0.050	0.030	0.030	0.040
Lu	N.d.	N.d.	0.030	0.030	N.d.	0.015	0.010	0.025	0.012	0.008	0.008	0.005	0.005	0.006
Total	N.d.	N.d.	N.d.	N.d.	N.d.	0.96	2.93	15.40	0.68	0.32	N.d.	3.44	3.24	2.62
$(La/Yb)_n$	2.70	0.68	N.d.	N.d.	N.d.	0.53	7.54	16.78	0.48	0.27	0.27	15.75	15.07	9.11

(*Continued*)

Table 1.3 Continued

	Massifs													
	Ivrea Verbano, Italy		Mediterrya	Ronda, Spain						Lherz, France				
	(Hartmann & Wedepohl, 1993)		(Laz'ko, 1988b)	(Garvella & Remaidi, 1993)	(Van der Wal & Bodinier, 1996)					(Bodinier *et al.*, 1988)		(Bodinier *et al.*, 1990), RNAA		
Element	FIN-7	FIN-8	Л1а3-1	RO130	V-28	V-39	V-11	V-13	V-2	71-325	73-104	Bod 1	Bod 2	Bod 3
La	0.960	0.590	0.310	0.037	0.062	0.226	0.023	N.d.	0.070	0.021	0.054	0.120	0.1500	0.300
Ce	2.110	1.230	0.210	0.166	0.116	0.487	0.074	0.077	0.181	0.081	0.062	0.349	0.4400	0.699
Pr	N.d.	N.d.	N.d.	N.d.	0.016	0.049	0.016	0.012	0.026	N.d.	N.d.	N.d.	N.d.	N.d.
Nd	0.920	0.460	0.047	0.074	0.071	0.144	0.105	0.060	0.118	N.d.	N.d.	0.340	0.360	0.530
Sm	0.200	0.090	0.023	0.019	0.019	0.019	0.045	0.020	0.031	0.018	0.030	0.113	0.118	0.146
Eu	0.055	0.026	0.007	0.009	0.006	0.007	0.020	0.007	0.012	0.007	0.014	0.038	0.039	0.048
Gd	0.150	0.070	0.059	N.d.	0.029	0.023	0.065	0.027	0.040	N.d.	N.d.	N.d.	N.d.	N.d.
Tb	0.020	0.010	0.035	0.012	0.006	0.004	0.013	0.005	0.006	0.005	0.010	0.025	0.024	0.025
Dy	0.090	0.070	N.d.	N.d.	0.043	0.032	0.085	0.037	0.047	N.d.	N.d.	N.d.	N.d.	N.d.
Ho	N.d.	N.d.	N.d.	0.027	0.011	0.008	0.020	0.009	0.011	N.d.	N.d.	N.d.	N.d.	N.d.
Er	0.050	0.040	N.d.	N.d.	0.041	0.029	0.060	0.030	0.036	N.d.	N.d.	N.d.	N.d.	N.d.
Tm	N.d.	N.d.	N.d.	N.d.	0.008	0.006	0.010	0.006	0.006	N.d.	N.d.	N.d.	N.d.	N.d.
Yb	0.040	0.030	0.067	0.130	0.060	0.040	0.066	0.045	0.046	0.026	0.065	0.100	0.136	0.125
Lu	0.007	0.006	0.021	0.022	0.012	0.009	0.013	0.009	0.010	0.005	0.011	0.017	0.024	0.022
Total	4.60	2.62	N.d.	N.d.	1.08	0.62	0.34	0.64	0.50	N.d.	N.d.	N.d.	N.d.	N.d.
$(La/Yb)_n$	16.20	13.27	3.12	0.19	0.70	3.81	0.24	N.d.	1.03	0.55	0.56	0.81	0.74	1.62

	Massifs													
	Lherz, France													
	(Bodinier *et al.*, 1990), RNAA													
Element	Bod 8	Bod 12	Bod 15	Bod 16	Bod 18	Bod 21	Bod 22	Bod 25	Bod 28	Bod 33	Bod 39	Bod 49	Bod 65	Fr-1
La	0.085	0.209	0.080	0.161	0.157	0.105	0.106	0.130	0.190	0.250	0.340	0.349	0.422	0.366
Ce	0.229	0.640	0.170	0.270	0.290	0.160	0.280	0.340	0.500	0.669	0.979	1.080	1.089	1.200
Pr	N.d.	N.d.	N.d.	N.d.	N.d.	N.d.	N.d.	N.d.	N.d.	N.d.	N.d.	N.d.	N.d.	0.205
Nd	0.220	0.550	0.140	0.160	N.d.	0.100	0.140	0.140	0.150	0.240	0.500	0.649	0.659	1.000
Sm	0.070	0.179	0.046	0.046	0.048	0.027	0.043	0.025	0.020	0.029	0.068	0.096	0.120	0.410
Eu	0.024	0.056	0.016	0.015	0.017	0.010	0.015	0.008	0.007	0.007	0.016	0.024	0.030	0.083
Gd	N.d.	N.d.	N.d.	N.d.	N.d.	N.d.	N.d.	N.d.	N.d.	N.d.	N.d.	N.d.	N.d.	0.600
Tb	0.012	0.029	0.008	0.010	0.007	0.004	0.008	0.004	0.002	0.003	0.004	0.007	0.012	0.117
Dy	N.d.	N.d.	N.d.	N.d.	N.d.	N.d.	N.d.	N.d.	N.d.	N.d.	N.d.	N.d.	N.d.	N.d.
Ho	N.d.	N.d.	N.d.	N.d.	N.d.	N.d.	N.d.	N.d.	N.d.	N.d.	N.d.	N.d.	N.d.	0.183
Er	N.d.	N.d.	N.d.	N.d.	N.d.	N.d.	N.d.	N.d.	N.d.	N.d.	N.d.	N.d.	N.d.	0.538
Tm	N.d.	N.d.	N.d.	N.d.	N.d.	N.d.	N.d.	N.d.	N.d.	N.d.	N.d.	N.d.	N.d.	0.078
Yb	0.071	0.014	0.051	0.070	0.052	0.040	0.052	0.030	0.015	0.012	0.016	0.017	0.035	0.550
Lu	0.012	0.020	0.010	0.014	0.010	0.008	0.010	0.006	0.004	0.003	0.003	0.004	0.006	0.080
Total	N.d.	N.d.	N.d.	N.d.	N.d.	N.d.	N.d.	N.d.	N.d.	N.d.	N.d.	N.d.	N.d.	5.41
$(La/Yb)_n$	0.81	10.08	1.06	1.55	2.04	1.77	1.38	2.92	8.55	14.06	14.34	13.86	8.14	0.45

(*Continued*)

Table 1.3 Continued

	Massifs													
	Horoman, Japan		Bay of Island, Canada	Thetford Mines, Canada					Trinity, California, USA				Samail, Oman	
	(Frey *et al.*, 1991)		(Suen *et al.*, 1979)	(Harnois & Morency, 1989), RNAA					(Gruau *et al.*, 1998)				(Godard *et al.*, 2000), ICP-MS	
Element	62128	62127	183	LC81-1	MC81-1	MC81-4	MP81-3	VR80-6	CH-2	CH6	KO92	TL42	93OA09	96OF59B
La	0.036	0.033	0.001	N.d.	N.d.	N.d.	N.d.	N.d.	N.d.	0.231	0.200	0.014	0.004	0.003
Ce	N.d.	N.d.	N.d.	0.031	0.112	0.056	0.112	0.145	0.013	0.471	0.342	0.030	0.009	0.008
Pr	N.d.	N.d.	N.d.	N.d.	N.d.	N.d.	N.d.	N.d.	N.d.	N.d.	N.d.	N.d.	0.002	N.d.
Nd	N.d.	N.d.	N.d.	N.d.	N.d.	N.d.	N.d.	N.d.	0.037	0.119	0.092	0.020	0.007	0.008
Sm	0.012	0.019	0.0001	0.004	0.013	0.005	0.009	0.005	0.010	0.029	0.021	0.008	0.005	N.d.
Eu	0.0076	0.0100	0.0001	0.002	0.002	0.001	0.003	0.002	0.003	0.007	0.039	0.002	N.d.	0.002
Gd	N.d.	N.d.	0.001	N.d.	N.d.	N.d.	N.d.	N.d.	0.017	0.034	0.024	0.016	0.006	0.007
Tb	N.d.	N.d.	N.d.	0.001	0.002	0.002	0.002	0.001	N.d.	N.d.	N.d.	N.d.	0.001	0.001
Dy	N.d.	N.d.	N.d.	N.d.	N.d.	N.d.	N.d.	N.d.	0.037	0.038	0.031	0.036	0.010	0.009
Ho	N.d.	N.d.	N.d.	N.d.	N.d.	N.d.	N.d.	N.d.	N.d.	N.d.	N.d.	N.d.	0.003	0.002
Er	N.d.	N.d.	N.d.	N.d.	N.d.	N.d.	N.d.	N.d.	0.037	0.028	0.025	0.031	0.013	0.010
Tm	N.d.	N.d.	N.d.	N.d.	N.d.	N.d.	N.d.	N.d.	N.d.	N.d.	N.d.	N.d.	0.003	0.002
Yb	0.027	0.022	0.029	0.017	0.009	0.066	0.108	0.066	0.057	0.038	0.039	0.053	0.026	0.020
Lu	0.006	0.005	0.005	0.004	0.004	0.015	0.023	0.011	N.d.	0.007	0.007	0.011	0.006	0.005
Total	N.d.	N.d.	N.d.	N.d.	N.d.	N.d.	N.d.	N.d.	0.21	0.33	1.00	0.82	0.09	0.08
$(La/Yb)_n$	0.90	1.01	0.03	N.d.	N.d.	N.d.	N.d.	N.d.	N.d.	4.10	3.46	0.18	0.09	0.11

	Massifs													
	Samail, Oman													
	(Godard *et al.*, 2000), ICP-MS													
Element	5OD92	5OD191	5OD131	5OD153	5OD107	5OD174	3OF22	3OF23	4MA6T	5OD84	5OF21	1OA29	4OE23	4OE27
La	N.d.	0.004	0.003	0.002	0.003	N.d.	N.d.	N.d.	0.003	0.001	N.d.	0.003	N.d.	0.0060
Ce	0.008	0.009	0.006	0.004	0.005	0.002	0.003	N.d.	0.002	0.007	N.d.	0.013	0.010	0.0221
Pr	N.d.	N.d.	N.d.	0.001	N.d.	N.d.	N.d.	N.d.	N.d.	N.d.	N.d.	N.d.	N.d.	N.d.
Nd	0.005	0.007	0.005	0.003	0.004	0.002	0.003	N.d.	0.003	0.005	N.d.	0.018	0.012	0.0251
Sm	N.d.	N.d.	0.002	N.d.	N.d.	N.d.	N.d.	0.001	N.d.	0.003	N.d.	0.008	N.d.	0.0151
Eu	N.d.	N.d.	0.001	0.001	N.d.	0.001	N.d.	0.001	0.001	0.002	0.001	0.003	N.d.	0.0058
Gd	0.004	N.d.	N.d.	N.d.	0.002	0.003	0.002	0.002	0.002	0.005	0.002	0.011	0.010	0.0211
Tb	0.001	0.001	0.001	0.001	0.001	0.001	0.001	0.001	0.0004	0.001	0.001	0.002	0.002	0.0045
Dy	0.009	0.006	0.007	0.007	0.007	0.007	0.009	0.007	0.007	0.010	0.009	0.017	0.017	0.0360
Ho	0.003	0.003	0.003	0.003	0.002	0.003	0.003	0.003	0.003	0.003	0.003	0.005	0.005	0.0098
Er	0.015	0.014	0.013	0.011	0.011	0.014	0.015	0.012	0.012	0.014	0.013	0.018	0.017	0.0340
Tm	0.003	0.004	0.003	0.003	0.003	0.003	0.003	0.003	0.003	0.004	0.003	0.004	0.004	0.0069
Yb	0.030	0.028	0.028	0.026	0.024	0.027	0.032	0.026	0.029	0.029	0.025	0.032	0.030	0.0512
Lu	0.006	0.006	0.006	0.006	0.005	0.006	0.007	0.006	0.007	0.007	0.006	0.007	0.007	0.0104
Total	N.d.	N.d.	N.d.	0.07	0.07	0.07	N.d.	N.d.	0.07	0.09	N.d.	0.14	N.d.	0.25
$(La/Yb)_n$	N.d.	0.10	0.07	0.04	0.19	N.d.	N.d.	N.d.	0.068	0.03	N.d.	0.07	N.d.	0.08

(*Continued*)

Table 1.3 Continued

	Massifs													
	Samail, Oman									Sud, New Caledonia				
	(Godard *et al.*, 2000). ICP-MS						(Pallister & Knight, 1981)			(Prinzhofer & Allegre, 1985)				
Element	OMB23	OMB27	5OA77	3OF101	0OA38	0OA37A	K21-pl	K22-pl	P568-2	AP-28	AP-405	AP-507	AP509	AP512
La	0.003	0.006	N.d.	0.004	0.004	0.006	0.130	0.100	0.0830	N.d.	N.d.	N.d.	N.d.	N.d.
Ce	0.005	0.011	0.005	0.011	0.012	0.019	1.300	1.000	0.7300	0.009	0.059	0.014	0.007	0.009
Pr	N.d.	N.d.	N.d.	N.d.	N.d.	N.d.	N.d.	N.d.	N.d.	N.d.	N.d.	N.d.	N.d.	N.d.
Nd	0.005	0.009	0.003	0.008	0.010	0.025	N.d.	N.d.	N.d.	0.006	0.025	0.008	0.003	0.003
Sm	0.005	0.007	N.d.	0.003	0.005	0.014	0.020	0.011	0.017	0.002	0.004	0.002	0.001	0.001
Eu	0.002	0.003	0.001	0.001	0.002	0.005	0.004	N.d.	0.004	0.001	0.001	0.001	0.0002	0.0001
Gd	0.018	0.019	0.003	0.003	0.007	0.018	N.d.	N.d.	N.d.	0.002	0.005	N.d.	0.001	0.001
Tb	0.005	0.005	0.001	0.001	0.002	0.003	0.007	0.002	0.001	N.d.	N.d.	N.d.	N.d.	N.d.
Dy	0.055	0.050	0.005	0.007	0.015	0.029	N.d.	N.d.	N.d.	0.003	0.008	0.003	0.002	0.001
Ho	0.016	0.014	0.002	0.002	0.005	0.008	N.d.	N.d.	N.d.	N.d.	N.d.	N.d.	N.d.	N.d.
Er	0.052	0.048	0.008	0.010	0.020	0.030	N.d.	N.d.	N.d.	0.003	0.006	0.003	0.002	0.001
Tm	0.010	0.009	0.002	0.002	0.005	0.006	N.d.	N.d.	N.d.	N.d.	N.d.	N.d.	N.d.	N.d.
Yb	0.077	0.065	0.019	0.022	0.036	0.049	0.059	0.041	0.096	0.014	0.009	0.010	0.006	0.006
Lu	0.015	0.013	0.005	0.005	0.008	0.011	0.015	0.017	0.023	0.004	0.002	0.002	0.002	0.002
Total	0.27	0.26	0.05	0.08	0.13	0.22	N.d.	N.d.	N.d.	0.04	0.12	0.04	0.03	0.03
$(La/Yb)_n$	0.03	0.06	N.d.	0.13	0.08	0.08	1.49	1.65	0.58	N.d.	N.d.	N.d.	N.d.	N.d.

	Massifs														
	Sud, New Caledonia			Tiebugy, New Caledonia		Japan	Khutulsky, Mongolia		Harzburg, Germany		Kempirsaysky, Kazakhstan				Pindos, Greece
	(Prinzhofer & Allegre, 1985)					(Itoh *et al.*, 1992)	(Erkushev, 1985)		(Sano *et al.*, 2002), ICP		(Chaschukhin *et al.*, 2003), ICP-MS				(Saccani *et al.*, 2004)
Element	AP513	AP514	AP515	TU4	TU5	PCC-1	M-233A	M-220B	H-16	87-9	Ch-8078	Ch-8095	Ch-8123	Ch-8156	ER6
La	N.d.	N.d.	N.d.	N.d.	N.d.	0.052	4.280	5.627	1.280	1.660	0.038	0.027	0.032	0.165	0.02
Ce	0.009	0.003	0.004	0.007	0.008	0.100	6.370	9.060	2.840	3.970	0.118	0.049	0.063	0.387	0.04
Pr	N.d.	N.d.	N.d.	N.d.	N.d.	0.013	1.000	1.018	0.380	0.550	0.014	0.007	0.009	0.052	0.01
Nd	0.004	0.001	0.002	0.003	0.004	0.042	6.720	2.237	1.610	2.340	0.072	0.035	0.047	0.229	0.02
Sm	0.001	0.0004	0.001	0.001	0.002	0.007	N.d.	0.284	0.440	0.660	0.019	0.01	0.011	0.062	0.01
Eu	0.0002	0.0001	0.0001	0.0003	0.001	0.002	0.420	0.106	0.160	0.180	0.006	0.003	0.003	0.011	N.d.
Gd	0.002	0.001	0.001	N.d.	N.d.	0.014	0.360	0.930	0.620	0.910	0.018	0.008	0.01	0.067	0.01
Tb	N.d.	N.d.	N.d.	N.d.	N.d.	0.002	0.084	0.200	0.110	0.160	0.002	0.001	0.001	0.012	N.d.
Dy	0.0003	0.002	0.001	0.006	0.010	0.010	1.130	1.010	0.740	1.090	0.016	0.01	0.016	0.086	0.02
Ho	N.d.	N.d.	N.d.	N.d.	N.d.	0.003	0.270	0.230	0.160	0.230	0.004	0.003	0.004	0.021	0.01
Er	0.003	0.003	0.001	0.010	0.0139	0.012	0.930	0.730	0.510	0.710	0.015	0.011	0.015	0.066	0.02
Tm	N.d.	N.d.	N.d.	N.d.	N.d.	0.003	0.043	0.122	0.070	0.100	0.003	0.002	0.003	0.011	N.d.
Yb	0.009	0.088	N.d.	0.023	0.027	0.024	0.260	1.490	0.510	0.690	0.027	0.022	0.027	0.08	0.03
Lu	0.003	0.002	0.001	0.005	0.005	0.006	0.055	0.350	0.080	0.110	0.005	0.004	0.005	0.014	0.01
Total	0.02	0.10	0.004	N.d.	N.d.	0.07	3.13	5.06	9.51	13.36	0.36	0.19	0.25	1.26	0.02
$(La/Yb)_n$	N.d.	N.d.	N.d.	N.d.	N.d.	1.46	11.11	2.55	1.69	1.62	0.95	0.83	0.80	1.39	0.45

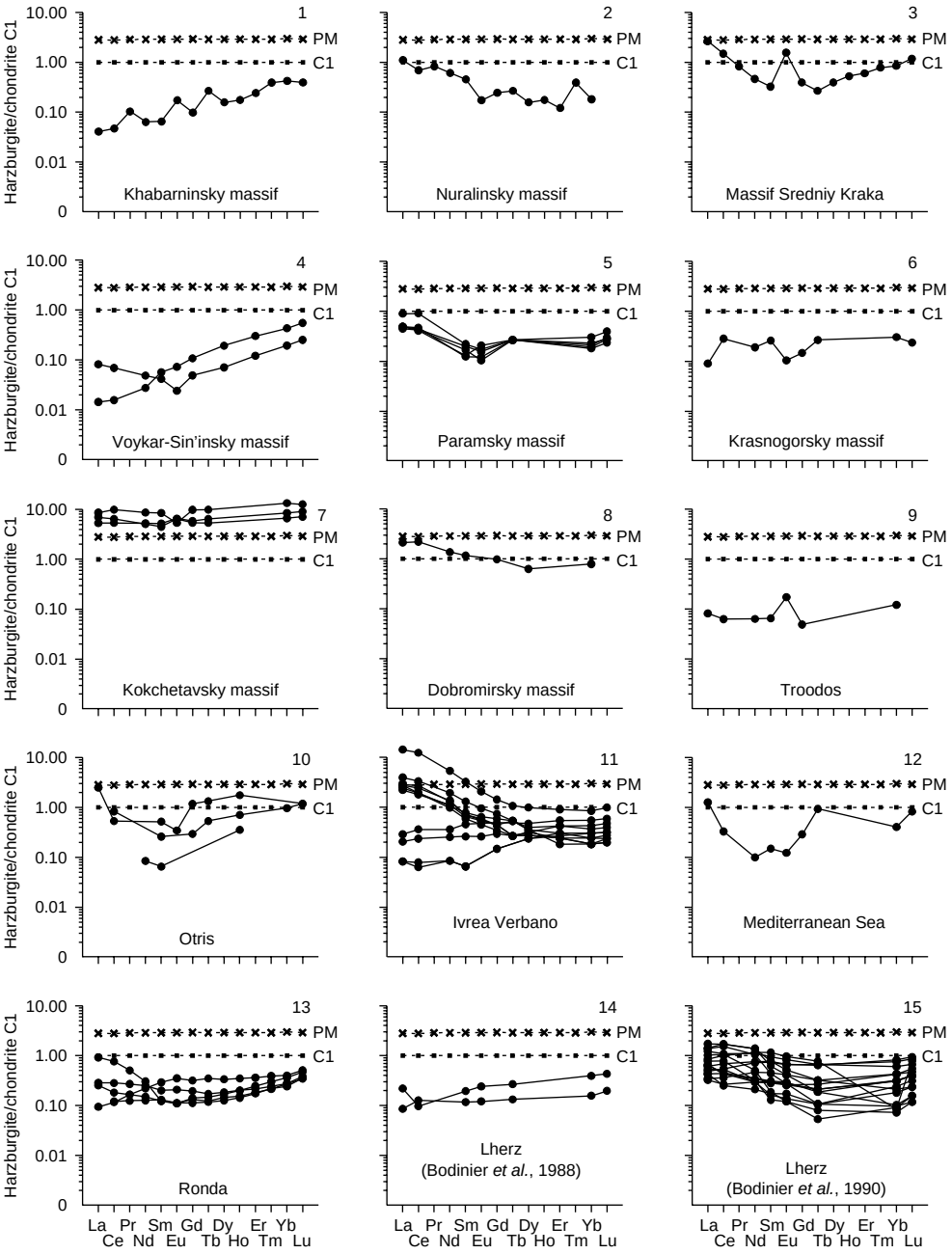

Figure 1.3 Chondrite-normalized REE patterns for harzburgites from different massifs (data Table 1.3).

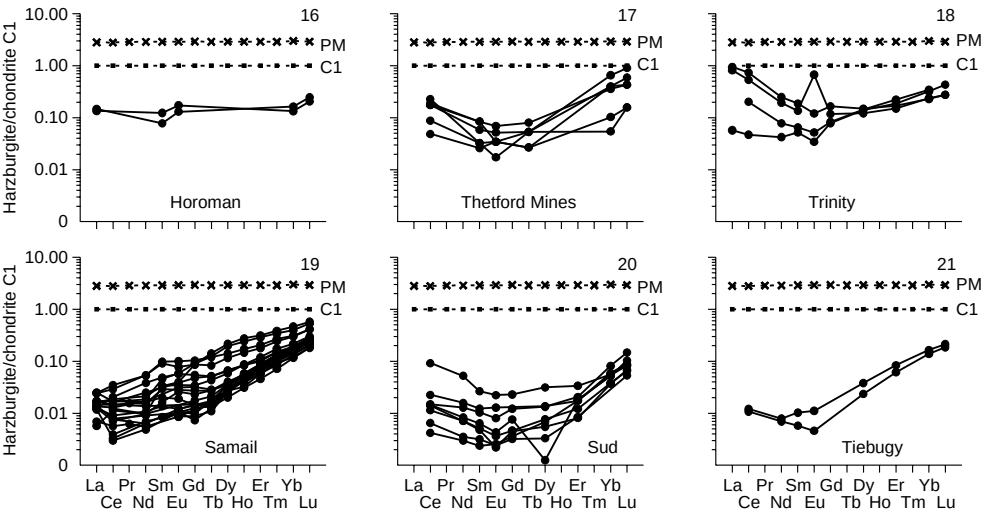

Figure 1.3 Continued

Kempirsaisky massifs, among others. The REE patterns of this type of harzburgites are usually U-shaped and convex downwards. Sometimes these patterns display negative and positive anomalies of Eu of insignificant intensity.

Notably, samples of ultramafites from the Kokchetavsky (Reverdatto *et al.*, 2000) and Harzburg (Sano *et al.*, 2002) massifs have been described by the authors as harzburgites, but the abnormally high level of REE accumulation in these rocks and the nearly "flat" pattern of distribution do not correspond to either geochemical type of harzburgite. These unusual properties do not conform to the accepted model of mantle restite formation, so it is reasonable to assume that these rocks have some other origin. Investigations have shown that the "harzburgites" from the Kokchetav massif were most probably formed as a result of a high-pressure metamorphism resulting in a chemical composition similar to that of chloritized basalts, which conforms in particular with the unusually low $Mg^{\#}$ of olivine in these samples (Reverdatto & Selyatitsky, 2004). Petrographical and mineralogical data on the "harzburgites" from the Harzburg massif show that these rocks are products of the differentiation of mafic melts (Sano *et al.*, 2002). At the same time, the geological position of the rocks as isolated lentiform separations among olivine-deficient gabbros suggests that these formations are xenoliths of earlier ultramafic restites that were subjected to magmatic and metasomatic transformations under the action of mafic melts and fluids enriched with light REE. This process manifested itself in a significant enrichment of these rocks with both easily fusible petrogenic components (CaO, Al_2O_3, FeO for example) and light REE.

The content of REE in harzburgites, similarly to other mantle restites, is to a certain extent dependent on the petrochemical properties of the rocks, including the depletion of easily fusible petrogenic components (CaO, Al_2O_3, TiO_2 for example) as a result of the partial melting of mantle protoliths (Frey, 1984). The concentration of these components is directly proportional to the concentration of REE in these ultramafic rocks, and this correlation manifests itself more distinctly for heavy elements.

Table 1.4 Average REE composition of harzburgites from some massifs (ppm).

	Massifs															
Element	Voykar-Sin'insky (2)	Kempirsaysky (4)	Paramsky (5)	Kokchetavsky (3)	Othris (3)	Ivrea Verbano (11)	Ronda (5)	Lherz (18)	Thetford Mines (5)	Trinity (4)	Samail (22)	Sud (8)	Horoman (2)	Tiebugy (2)	Khutulsky (2)	Harzburg (2)
La	0.012	0.084	0.138	1.700	0.610	0.706	0.095	0.179	N.d.	0.148	0.004	N.d.	0.035	N.d.	4.954	1.470
Ce	0.027	0.198	0.338	4.600	0.435	1.574	0.187	0.463	0.096	0.243	0.009	0.014	N.d.	0.007	7.715	3.405
Pr	N.d.	0.027	N.d.	N.d.	N.d.	N.d.	0.024	N.d.	N.d.	N.d.	0.001	N.d.	N.d.	N.d.	1.009	0.465
Nd	0.018	0.119	N.d.	3.000	0.040	0.597	0.010	0.325	N.d.	0.067	0.008	0.007	N.d.	0.004	4.479	1.975
Sm	0.008	0.033	0.026	0.930	0.043	0.124	0.027	0.069	0.008	0.017	0.006	0.001	0.016	0.001	0.282	0.550
Eu	0.003	0.007	0.009	0.353	0.020	0.044	0.011	0.022	0.002	0.013	0.002	0.0004	0.009	0.001	0.263	0.170
Gd	0.016	0.037	N.d.	1.433	0.150	0.102	0.037	N.d.	N.d.	0.023	0.008	0.002	N.d.	N.d.	0.645	0.765
Tb	N.d.	0.006	0.010	0.270	0.035	0.018	0.007	0.011	0.002	N.d.	0.002	N.d.	N.d.	N.d.	0.142	0.135
Dy	0.034	0.048	N.d.	N.d.	N.d.	0.097	0.049	N.d.	N.d.	0.034	0.015	0.007	N.d.	0.008	1.070	0.915
Ho	N.d.	0.012	N.d.	N.d.	0.053	N.d.	0.012	N.d.	N.d.	N.d.	0.005	N.d.	N.d.	N.d.	0.250	0.195
Er	0.035	0.037	N.d.	N.d.	N.d.	0.063	0.039	N.d.	N.d.	0.030	0.018	0.003	N.d.	0.012	0.830	0.610
Tm	N.d.	0.007	N.d.	N.d.	N.d.	N.d.	0.007	N.d.	N.d.	N.d.	0.004	N.d.	N.d.	N.d.	0.083	0.085
Yb	0.052	0.050	0.037	1.567	0.160	0.057	0.051	0.052	0.054	0.047	0.033	0.009	0.025	0.025	0.875	0.600
Lu	0.010	0.009	0.008	0.243	0.030	0.010	0.011	0.012	0.011	0.008	0.007	0.002	0.006	0.005	0.203	0.095
Total	0.21	0.67	N.d.	N.d.	N.d.	N.d.	0.64	N.d.	N.d.	N.d.	0.12	N.d.	N.d.	N.d.	22.80	11.44
$(La/Yb)_n$	0.15	1.14	2.52	0.73	2.57	8.32	1.25	2.35	N.d.	2.14	0.08	N.d.	0.95	N.d.	3.82	1.65

Note: Data Table 1.3.

On the other hand, the concentration of refractory components (MgO, NiO for example) is inversely proportional to REE concentration (Van der Wal & Bodinier, 1996).

The observed differences among harzburgites from different massifs with respect to REE accumulation and fractionation are satisfactorily accounted for by the model for depletion of ultramafic substances from mantle sources in the process of partial melting. This mechanism provides for various degrees of melting of the upper mantle substratum as well as for corresponding differences in the extent of upper mantle depletion of incompatible elements. Meanwhile, the U-shaped REE pattern frequently observed in harzburgites has not yet been unambiguously interpreted. From one point of view, this pattern is the most characteristic feature of harzburgites, as well as of dunites, from basal zones of ophiolite associations (Frey, 1984); from another point of view, this pattern is indicative of primordial geochemical characteristics of ultramafic restites determined by the specific conditions during melting of mantle protoliths (Prinzhofer & Allegre, 1985). In the latter case, the authors propose their own version of the model, according to which the partial melting of mantle sources during the formation of ultramafic restites started under conditions of garnet lherzolite facies, and then continued and ended under conditions of plagioclase facies.

Some researchers have tried to explain the nature of the U-shaped patterns of REE distribution in ultramafites by the magma generation mechanism with participation of fluids or melts, separated from the subducted oceanic lithosphere. The U-shaped patterns may also have been caused by the enrichment of ultramafites with light REE after the process of mantle source melting was completed (McDonough & Frey, 1989). Let us enumerate a few more possible explanations of the geochemical "paradox" in question: (1) the interaction of ultramafites with melts enriched with light REE; (2) differential REE transfer rates during melt–ultramafic rock interactions; (3) selective depletion of ultramafites of their middle REE during the process of serpentinization (Agafonov & Erkushev, 1985; Savel'ev *et al.*, 2000; Chaschukhin *et al.*, 2003); (4) and low-temperature enrichment of ultramafites with light REE during the serpentinization process under the action of oceanic or meteoric waters (Gruau *et al.*, 1998). U-shaped patterns of REE distribution are indeed most frequently observed in ultramafites that were in some measure subjected to serpentinization. The depletion of middle REE from the initial ultramafic restites would account for the U-shaped form, but this is an unlikely mechanism. A more plausible mechanism entails the addition of light REE to these rocks. The U-shaped REE distribution observed in harzburgites was most probably caused by their epigenetic enrichment with light REE while the concentration of heavy and middle ones remained stable. Sources of light REE include oceanic and meteoric waters, as well as fluids that were separated from later mafic or granitic melts and introduced into ultramafic protrusions. The enrichment of these rocks with light REE is confirmed by data obtained on the chemistry of REE in ultramafic restites from abyssal xenoliths represented in alkali basalts. The U-shaped distribution curve will be dealt with in greater detail below. Importantly, abnormal enrichment with light REE at slightly different intensities can always be observed in ultramafic restites from deep xenoliths, as a result of which the REE patterns of these rocks also become U-shaped. The present author inclines to the opinion that the enrichment with light REE of ultramafic restites from deep xenoliths represented in alkaline basalts is first and foremost due to the fact that the REE were brought to the restites by fluids separating from

Table 1.5 REE composition of fluid inclusions in minerals from rocks, generated by crystallization of andesite melts (ppm) (Norman *et al.* (1989, 1990)).

	Number of samples				
Element	CF4	CF6	CF8a	CF8b	CF17
La	2.8	67	71	65	23
Ce	2.8	89	46	42	40
Nd	1.5	44	26	23	17
Sm	0.39	8.3	3.8	3.4	3.2
Eu	0.08	1.3	0.51	0.48	0.90
Tb	0.05	0.99	0.35	0.29	0.26
Yb	0.12	2.7	0.85	0.80	0.42
Lu	0.02	0.44	0.13	0.11	0.04
Total	7.8	214	149	135	84.8

basalts in the process of transporting the xenoliths to the upper layers of the Earth's crust. The REE brought up in this way concentrate in the intragranular and intergranular microcracks of the rocks in the form of non-structural admixtures (Lesnov, 2003a).

The form in which the increased amounts of light REE are found in harzburgites is of principal significance since these rocks are chiefly made up of olivine and orthopyroxene, both of which have crystalline structures that can accumulate only limited amounts of REE. Probably, abnormally increased amounts of admixtures are localized either in the structural microdefects of these minerals or in the intragranular and intergranular microcracks. The former assumption is corroborated by results of research into the fluid microinclusions in olivines and orthopyroxenes from samples of ultramafites that were found to contain abnormally increased contents of light REE compared with middle and heavy elements (Stosch, 1982; Lesnov *et al.*, 1998b; Lesnov, 2000a). The latter assumption is corroborated by Kovalenko *et al.* (1989) who leached mineral samples from ultramafic restites present in xenoliths from alkaline basalts with strongly diluted hydrochloric acid solutions and established the presence of easily solvable compounds of REE, mainly of the light elements, localized in the microcracks of mineral grains. According to Norman and Leeman (1990) (Table 1.5), the fluids discovered in minerals from subvolcanic andesitic rocks also contain significantly predominant amounts of light REE compared with heavy ones.

Thus, one can assume that a direct dependence exists between the U-shaped REE patterns observed in harzburgites and the postmagmatic changes, serpentinization in particular, undergone by these rocks. In addition, some researchers believe that the serpentinization of ultramafites has in many cases been brought about by the action of seawater, that is, halmyrolysis.

In light of the above statement, we turn to data obtained by studying the distribution of REE in the waters of modern oceans. On the whole, oceanic waters contain rather low REE concentrations, by about 5–6 orders of magnitude lower than in chondrite C1 (Table 1.6, Fig. 1.4). The total content of REE in the waters of the Pacific and Atlantic Ocean ranges from $4.6–9.1 \cdot 10^{-6}$ ppm in the near-surface layers to $16–19 \cdot 10^{-6}$ ppm at depths of 2500 m. Light elements (La, Ce, Nd) prevail markedly over

Table 1.6 REE composition of water from the Pacific and Atlantic Oceans at different depths ($n \cdot 10^{-6}$, ppm).

	Pacific Ocean (north-west)				Atlantic Ocean			
	Surface		2500 m		100 m		2500 m	
Element	$n \cdot 10^{-6}$ (ppm)	Relative %	$n \cdot 10^{-6}$ (ppm)	Relative %	$n \cdot 10^{-6}$ (ppm)	Relative %	$n \cdot 10^{-6}$ (ppm)	Relative %
La	1.2	26.1	6.5	34.3	1.81	19.9	4.08	**25.4**
Ce	1.4	30.6	1.3	6.8	2.35	25.7	3.68	**23.0**
Nd	0.74	16.1	4.3	22.6	1.85	20.3	3.61	**22.5**
Sm	0.15	3.3	0.80	4.2	0.401	4.4	0.714	**4.5**
Eu	0.050	1.1	0.21	1.1	0.0979	1.1	0.136	**0.8**
Gd	0.25	5.4	1.3	6.8	0.536	5.9	1.13	**7.1**
Dy	0.33	7.2	1.6	8.4	0.777	8.5	0.991	**6.2**
Er	0.28	6.1	1.6	8.4	0.681	7.5	0.851	**5.3**
Yb	0.19	4.1	1.4	7.4	0.614	6.7	0.829	**5.2**
Total	4.59	100.0	19.01	100.0	9.12	100.0	16.03	**100.0**

Note: Data from Brookins (1989). Bold type—percentage correlation of REE weight quantity in water samples from the Atlantic Ocean at depth 2500 m which was used in numerical experiment (see Table 1.7).

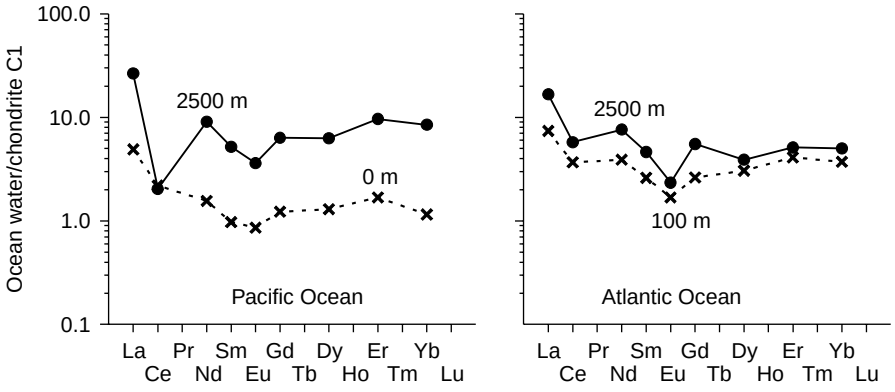

Figure 1.4 Chondrite-normalized REE patterns for oceanic water: 1—Pacific Ocean, depth 0 m and 2500 m; 2—Atlantic Ocean, depth 100 m and 2500 m. The REE composition of water was multiplied by 10^6 (data Table 1.6).

middle and heavy ones, for they amount to more than 60% of the total REE content in oceanic waters. Convincing data regarding a significant increase in the concentration of light REE in the waters of the Atlantic, Pacific, and Indian Oceans at depths of 0–6000 m have been presented by Dubinin (2006). All these observations conform with the assumption that as oceanic waters infiltrate ultramafic restites through microcracks, light REE are introduced at greater proportions than heavy ones (Humphris, 1984). Note also that, according to the available data, the igneous rocks forming the ocean bed, basalts in particular, interact with oceanic waters and are enriched (as a result of halmyrolysis) with such mobile elements as U, Cs, Rb, B, Li, P, and K (Henderson, 1985).

Table 1.7 REE composition of harzburgites sample which was subjected to infiltration by seawater (data of numeric experiment).

Element	Contents in initial sample of harzburgite (ppm)	Composition of seawater on depth 2500 m		REE contents in harzburgite after addition of different amounts of seawater due to infiltration (calculated per 1 tonne of rock) (ppm)					
		$n \cdot 10^{-6}$ (ppm)	Relative %	+0.01	+0.05	+0.1	+0.25	+0.5	+1.0
La	0.006	4.08	25.4	0.009	0.019	0.031	0.070	0.133	0.260
Ce	0.022	3.68	23.0	0.024	0.034	0.045	0.080	0.137	0.252
Nd	0.025	3.61	22.5	0.027	0.036	0.048	0.081	0.138	0.250
Sm	0.015	0.714	4.5	0.016	0.017	0.020	0.026	0.038	0.060
Eu	0.006	0.136	0.8	0.006	0.006	0.007	0.008	0.010	0.014
Gd	0.021	1.13	7.1	0.022	0.025	0.028	0.039	0.057	0.092
Dy	0.036	0.991	6.2	0.037	0.039	0.042	0.052	0.067	0.098
Er	0.034	0.851	5.3	0.035	0.037	0.039	0.047	0.061	0.087
Yb	0.051	0.829	5.2	0.052	0.054	0.056	0.064	0.077	0.103
Total	0.22	16.0	100.0	0.23	0.23	0.32	0.47	0.72	1.22
$(La/Yb)_n$	0.08	3.32	–	0.11	0.31	0.38	0.73	1.16	1.70

Note: Depleted harzburgite from Samail massif (sample 94OE27) (see Table 1.2) was taken as initial sample for numerical experiment. Weight quantity correlation of every element for Atlantic Ocean seawater at depth 2500 m (see Table 1.6. bold type) was taken for calculation.

To determine, at least to a first approximation, the scope and tendencies of the possible changes of REE distribution in ultramafic restites as a result of infiltration through microcracks of oceanic waters, we performed the following simplified numerical experiment. A sample of harzburgite from the Samail massif (see Table 1.3, sample 96OF59B) was taken as the initial rock for this experiment. Analysis of this sample shows that it is considerably depleted of all REE, particularly of the light elements, and its REE pattern has the form of nearly a straight line with a steep positive slope, which, by definition, is typical of ultramafic restites (see Fig. 1.3, 19). In these calculations we proceeded from the assumption that this sample of harzburgite stayed at the bottom of the equatorial part of the Atlantic Ocean at a depth of about 2500 m and was for a long time subjected to infiltration by the seawater through microcracks. The infiltration was accompanied by the introduction of some REE into the rock; therefore, data on REE content in the water of the Atlantic Ocean at the indicated depth was used for the numerical modeling (see Table 1.6). To assess the dynamics of variable REE concentrations during the process of seawater infiltration into the harzburgite, calculations were made for six different concentrations: 0.01, 0.05, 0.1, 0.25, 0.5 and 1.0 ppm (Table 1.7, Fig. 1.5). The results obtained testify to the leading accumulation of light REE with respect to middle and heavy elements. At the same time, one can see in the figure that the REE patterns show a systematic anomaly of Ce, Sm, and Eu. The origins of this anomaly remain unclarified. The deficit of elements revealed in the graphs, however, might be false and due to analytical errors made in determining the REE balance in oceanic waters. On the whole, the results of our numerical experiment do not contradict the assumption that as seawaters infiltrate harzburgites through microcracks, accompanied by serpentinization, the ultramafites must be enriched predominantly with non-structural admixtures of light REE. Obviously, this process is precisely what

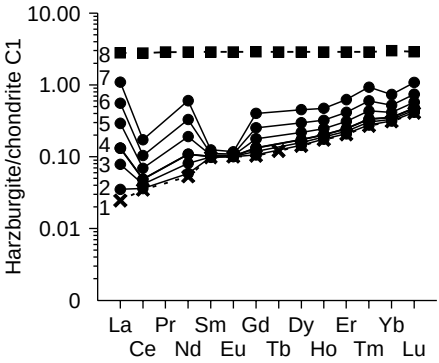

Figure 1.5 Chondrite-normalized REE patterns for harzburgites that were infiltrated by oceanic water in a numerical experiment: 1—initial sample. 2–7—patterns of harzburgites after addition of different amounts of REE through infiltration of ocean water: 2—0.01 ppm; 3—0.05 ppm; 4—0.1 ppm; 5—0.25 ppm; 6—0.5 ppm; 7—1.0 ppm; 8—REE composition of the primitive mantle (Sun & McDonough, 1989) (data Table 1.7).

accounts for the seeming minima in the region of middle elements observed in REE patterns of serpentinized harzburgites. Thus, the main reasons for the variation in REE content of harzburgites appear to be: (1) distinctions among these rocks in the modal concentrations of olivine, orthopyroxene, and secondary clinopyroxene, and the presence of structural admixtures of REE as a result of the partial melting of mantle protoliths, to various extents, in forming the restites; (2) distinctions among harzburgites in the intensity of their enrichment with non-structural admixtures of REE localized in intragranular and intergranular microcracks, as well as in secondary fluid inclusions, as a result of different epigenetic processes.

One more point of view concerning the abnormal enrichment of ultramafic restites with light REE and other incompatible elements is worthwhile to mention. This additional viewpoint is based on the results of an investigation into the geochemistry of REE in 130 samples of ultramafic restites that were selected in the process of dragging at many sites of the Pacific and Indian mid-oceanic ridges (Niu, 2004). The mass of most of these peridotite samples varied from 20 to 200 g, and nearly all of them were serpentinized by more than 60%. Analyses made by the ICP-MS method showed that all these peridotites were abnormally enriched with light REE to varying degrees; however, the clinopyroxenes within the peridotites were depleted of light REE compared with heavy ones. Niu discovered that the concentrations of Dy and Lu in peridotites have an inversely proportional dependence on the MgO concentration, while the concentration of La is independent of MgO. He also found that significant positive connections exist in peridotites between the concentrations of La, Ce, Pr, and Nd and the concentrations of the more inert Nb and Zr. Based on these facts, Niu came to the opinion that the enrichment of peridotites with these trace elements is due to a single magmatic process. He assumed that the enrichment occurred in the intergranular space of the rocks and in the edge zones of clinopyroxene grains, while no inner zones of the grains were enriched. The author also believes that submarine weathering did not cause any changes in the "magmatic" relations among the contents of chemical elements except

for Rb, Cs, K, Sr, and U. This concept should be taken into account along with the other views regarding the abnormal enrichment of restites with light REE. Nevertheless, it should be stressed that, firstly, this concept does not touch on the problem of the nature of the hypothetic melts, which are assumed to have acted on the peridotites of the oceanic bed, nor does it indicate any direct signs of the existence of such melts; secondly, no account is taken of the presence of excess amounts of incompatible admixtures in the composition of fluid microinclusions that are frequently contained in olivine grains (which is to be discussed later), as well as of the possible accumulation of light REE and other admixtures in the layered structure of serpentines.

Importantly, in the opinion of most investigators, harzburgites originated as restites at sufficiently high but different degrees of partial melting of mantle sources. If one assumes that the mineral composition of mantle protoliths corresponds to that of pyrolite (lherzolite), in which the content of clinopyroxene, the main source of basaltoid melts, varies within a range of 10–50%, then harzburgites, which are fully or nearly fully depleted of clinopyroxene, must contain REE concentrations that are decreased by about the same proportions. Harzburgites often contain clinopyroxene as a second phase, and, therefore, one can conclude that this mineral did not always pass completely into a mafic melt. Hence, when harzburgites were formed as restites, the degree of mantle protolite melting was usually below 50%. Researchers have suggested that in the process of harzburgite formation the extent of melting of mantle sources probably lies within a range of 10–30%. According to published data, harzburgites from the Othris and Lherz massifs were formed from a partial protolite melting of 10–30% (Menzies, 1976), harzburgites from the Samail massif were formed from a partial melting of 15% (Godard *et al.*, 2000), and those from the New Caledonia massifs were formed from a partial melting of 20% (Prinzhofer & Allegre, 1985).

If we assume that the total content of REE in harzburgites is inversely proportional to the degree of partial melting of mantle protolite, then mafic–ultramafic massifs can be arranged in order of increasing degrees of partial melting as follows: Ivrea Verbano → Othris → Lherz → Kempirsaisky → Ronda → Trinity → Paramsky → Thetford Mines → Samail → Sud. However, the average total REE concentrations used in this scheme are rather approximate because, firstly, the necessary data on the contents of all REE are not always available and, secondly, the concentration of the structural admixture of light REE in these samples is frequently distorted by the presence of a non-structural admixture of these elements. An analysis using the average concentrations of only less–mobile, heavy REE can provide a more correct arrangement, in which case the same massifs will form the following sequence: Othris → Ivrea Verbano → Thetford Mines → Ronda → Kempirsaisky → Trinity → Paramsky → Samail → Sud.

* * *

Harzburgites are generally considered to be mantle restites and are depleted of REE to different extents. The structural admixture of REE in these rocks is mainly concentrated in orthopyroxenes and, to a small extent, in olivines. These elements are also present in clinopyroxenes contained in the rocks as secondary phases. Harzburgites from separate massifs differ somewhat in their REE content, which is due to different modal concentrations of olivine, orthopyroxene, and clinopyroxene, as well

as to variations in the content of non-structural trace elements. The average total REE concentration in harzburgites from individual massifs varies in the range of 0.01–23 ppm. The overall average total REE content in these rocks is about 1.8 ppm, which is less than their content in chondrite C1. The $(La/Yb)_n$ values of harzburgites vary in the range of 0.30–17 with an average value of about 3 over all samples. The REE patterns of harzburgites, particularly those subjected to considerable serpentinization, are U-shaped, and different authors have different explanations for the origin of this shape. The present author holds to the idea that patterns of this kind are due to a more recent enrichment of rocks with light REE mated with the infiltration of heterogeneous epigenetic fluids and seawater.

1.3 LHERZOLITES

Lherzolites, along with harzburgites and dunites, are included in the composition of many ultramafic and mafic–ultramafic massifs that are widespread within continental folded regions. These rocks are represented to a lesser degree in the massifs of mid-oceanic ridges. They are also often represented in abyssal xenoliths, but these structures will be discussed later (see Chapter 2). Lherzolites are slightly less abundant than harzburgites, from which they differ mainly in a higher (>10%) content of clinopyroxene, and lherzolites are generally regarded to be a less-depleted variety of mantle restites compared to harzburgites. Lherzolites were formed as refractory residues at a relatively low degree of partial melting of upper mantle sources, which were later tectonically shifted in the solid–plastic state to different levels of the Earth's crust. In mafic–ultramafic massifs, which some researchers consider to be stratiform, lherzolites are considered to be the products of differentiation of high magnesium mafic melts. The quantitative mineral composition of lherzolites varies within the following ranges (wt%): olivine (40–80), orthopyroxene (10–50), and clinopyroxene (10–50) (Bogatikov *et al.*, 1981). Garnets, plagioclase, and amphibole are sometimes represented in these rocks as secondary phases. Chrome-spinel can be present as an accessory mineral. In some cases, lherzolites can contain submicroscopic mineral isolations of platinum group elements. The chemical composition of lherzolites varies within a wide confidence intervals and, compared with harzburgites and dunites, they are distinguished by increased contents of SiO_2 (44.5–45.9 wt%), Al_2O_3 (2.3–3.2 wt%), CaO (3.5–5.1 wt%), and TiO_2 (0.20–0.34 wt%), and a decreased content of MgO (34–38 wt%). The average values of the petrochemical parameters of lherzolites have the following confidence intervas (wt%): CaO/Al_2O_3 (1.45–2.23), MgO/CaO (13.5–35.8), Al_2O_3/MgO (0.04–0.06), and $100 \cdot FeO_{tot}/(FeO_{tot} + MgO)$ (21.9–25.7) (Lesnov, 1986).

The first data on REE distribution in lherzolites were obtained by analyzing samples taken from the Lizard (England), Tinaquillo (Venezuela), and Mount Albert (Canada) (Haskin *et al.*, 1966) massifs. The analyses showed these samples to be more depleted of REE admixtures compared to chondrite C1. Subsequently, the REE distribution in lherzolites from the mafic–ultramafic massifs located in the folded structures of Liguria, Morocco, Canada, Greece, Cyprus, the Alps, the Pyrenees, and the British Isles were studied. Lherzolites from the Bay of Islands massif were found to be distinct from the others in that they were somewhat enriched with light REE (~0.7–5.0

t. ch.) (Suen *et al.*, 1979). The accumulation level of light REE in these samples was higher than that of heavy elements, similarly to what is frequently observed in deep xenoliths of ultramafites from alkali basalts. When the rare earth content of spinel lherzolites from the Baldissero and Balmuccia massifs in the western Alps were later studied (Ottonello *et al.*, 1984), lherzolites from both massifs were found to be significantly depleted of light REE, especially of La. In addition, lherzolite samples from the Baldissero massif were characterized by decreased concentrations of heavy REE and very gentle slopes in the corresponding part of REE patterns, while lherzolites from the Balmuccia massif had a somewhat increased level of REE accumulation, and their patterns were characterized by a distinctly positive slope. Note that one of the first reviews on the geochemistry of REE in ultramafic rocks, lherzolites among them, was published in 1984 (Frey, 1984).

Study of the lherzolites from the Ronda massif in the south of Spain, which bear relatively small amounts of clinopyroxene (<15%), has revealed that these rocks are depleted of light REE, primarily of La, and have a nearly "flat" form in the region of heavy elements in the REE pattern (Frey *et al.*, 1985). Lherzolites from this massif also show an inversely proportional dependence between Yb and MgO concentrations. Frey *et al.* concluded that lherzolites from the Ronda massif, similarly to harzburgites from this massif, were formed as restites as a result of mantle resource melting to an extent of 0–30%. Lherzolites from some of the eastern Pyrenees massifs were discovered to be somewhat enriched with light REE, which was attributed to the action of subsequent basalt melts and their fluids on these rocks (Bodinier *et al.*, 1988).

On the whole, the REE content of lherzolites has been studied on the basis of samples taken from more than 30 mafic–ultramafic massifs of many regions. A meaningful body of information exists on the REE distribution in lherzolites present in abyssal xenoliths, which will be discussed later. Most of the analyses characterized the spinel-bearing varieties of lherzolites, and far less evidence exists on the garnet-, plagioclase-, and amphibole-bearing varieties (Table 1.8).

The average total REE concentrations in lherzolites of mafic–ultramafic massifs vary within a relatively narrow interval (1.4–4.3 ppm). The average total REE concentration in spinel lherzolites calculated over all analyses is about 2.3 ppm, which is comparable with the values calculated for chondrite C1: 2.60 ppm (Evensen *et al.*, 1978); 2.50 ppm (Anders & Grevesse, 1989); and 2.40 ppm (Nakamura, 1974). The present author calculated the average total REE concentration in spinel lherzolites to be somewhat higher than that for dunites (1.6 ppm) (Lesnov, 2002b), and for harzburgites it amounts to 1.7 ppm (Lesnov, 2002). Overall, the differences in the average concentrations of REE in these rocks are in agreement with a decreased partial melting of mantle protoliths during the process of lherzolite formation compared with that of harzburgite and dunite formation. The geochemical differences among the three varieties of ultramafic restites conform with their modal mineral composition since the content of the main REE carrier mineral, clinopyroxene, increases from dunites to harzburgites to lherzolites. An estimate of the average total REE concentration in spinel lherzolites obtained by the present author is one-third of that in the primitive mantle (7.4 ppm) (Sun & McDonough, 1989).

Varieties of lherzolites that contain modal amphibole always have somewhat increased total content of REE compared with amphibole-free spinel and spinel-free

Table 1.8 REE composition of lherzolites from massifs (ppm).

	Massifs													
	Baldissero, Italy													
	(Hartmann & Wedepohl, 1993), ICP-MS, INAA													
	BAD-1A	BAD-1B	BAD-2	BAD-3A	BAD-3B	BAD-3C	BAD-4	BAD-5	BAD-7A	BAD-7B	BAD-8	BAD-9	BAD-10	BAD-11
Element	*Spinel lherzolites*													
La	0.040	0.040	0.050	0.080	0.070	0.080	0.040	0.030	0.030	0.030	0.030	0.020	0.010	0.010
Ce	0.130	0.130	0.170	0.350	0.330	0.360	0.170	0.090	0.130	0.130	0.110	0.090	0.080	0.080
Pr	N.d.	N.d.	N.d.	N.d.	N.d.	N.d.	N.d.	N.d.	N.d.	N.d.	N.d.	N.d.	N.d.	N.d.
Nd	0.180	0.180	0.330	0.330	0.310	0.320	0.170	0.170	0.190	0.190	0.210	0.140	0.170	0.140
Sm	0.180	0.130	0.180	0.140	0.140	0.140	0.120	0.120	0.150	0.140	0.120	0.120	0.090	0.120
Eu	0.070	N.d.	0.070	N.d.	N.d.	N.d.	0.070	0.060	N.d.	0.070	0.063	0.055	0.051	N.d.
Gd	0.270	0.270	0.350	0.270	0.260	0.270	0.270	0.250	0.270	0.280	0.250	0.240	0.250	0.200
Tb	0.050	N.d.	0.070	N.d.	N.d.	N.d.	0.050	0.050	N.d.	0.070	0.050	0.060	0.060	N.d.
Dy	0.410	0.390	0.500	0.390	0.390	0.390	0.390	0.390	0.400	0.400	0.390	0.400	0.390	0.280
Ho	N.d.	N.d.	N.d.	N.d.	N.d.	N.d.	N.d.	N.d.	N.d.	N.d.	N.d.	N.d.	N.d.	N.d.
Er	0.290	0.290	0.350	0.290	0.280	0.280	0.280	0.270	0.290	0.280	0.290	0.310	0.310	0.220
Tm	N.d.	N.d.	N.d.	N.d.	N.d.	N.d.	N.d.	N.d.	N.d.	N.d.	N.d.	N.d.	N.d.	N.d.
Yb	0.310	0.300	0.320	0.300	0.300	0.300	0.320	0.300	0.320	0.310	0.290	0.290	0.290	0.260
Lu	0.053	0.051	0.056	0.052	0.052	0.051	0.056	0.052	0.053	0.055	0.048	0.048	0.049	0.044
Total	1.98	1.78	2.45	2.20	2.13	2.19	1.94	1.78	1.83	1.96	1.85	1.77	1.75	1.35
$(La/Yb)_n$	0.09	0.09	0.11	0.18	0.16	0.18	0.08	0.07	0.06	0.07	0.07	0.05	0.02	0.03

(*Continued*)

Table 1.8 Continued

	Massifs													
	Baldissero, Italy					Balmuccia, Italy								
	(Ottonello *et al.*, 1984), RNAA					(Hartmann & Wedepohl, 1993), ICP-MS, INAA								
	BA-4a	F-63a	F-64	BA-1b	BA-3b	BAM-10	BAM-11	BAM-12A	BAM-12B	BAM-13A	BAM-13B	BAM-1A	BAM-1B	BAM-2A
Element	*Spinel lherzolites*													
La	0.260	0.038	0.011	0.113	0.177	0.200	0.020	0.090	0.080	0.070	0.070	0.020	0.020	0.380
Ce	0.865	0.246	0.168	0.231	0.396	0.080	0.090	0.350	0.310	0.350	0.350	0.090	0.090	1.520
Pr	N.d.	N.d.	N.d.	N.d.	N.d.	N.d.	N.d.	N.d.	N.d.	N.d.	N.d.	N.d.	N.d.	N.d.
Nd	1.340	N.d.	N.d.	0.270	0.870	0.190	0.150	0.400	0.270	0.360	0.540	0.120	0.150	1.750
Sm	0.512	0.079	0.135	0.100	0.434	0.120	0.080	0.140	0.110	0.180	0.180	0.080	0.080	0.590
Eu	0.230	0.043	0.061	0.045	0.191	0.048	N.d.	0.060	N.d.	0.070	N.d.	N.d.	N.d.	0.223
Gd	N.d.	N.d.	N.d.	N.d.	N.d.	0.230	0.190	0.260	0.180	0.350	0.350	0.150	0.150	0.870
Tb	0.152	0.030	0.049	0.035	0.130	0.050	N.d.	0.050	N.d.	0.080	N.d.	N.d.	N.d.	0.150
Dy	N.d.	N.d.	N.d.	N.d.	N.d.	0.390	0.420	0.350	0.230	0.530	0.530	0.190	0.190	0.960
Ho	N.d.	N.d.	N.d.	N.d.	N.d.	N.d.	N.d.	N.d.	N.d.	N.d.	N.d.	N.d.	N.d.	N.d.
Er	N.d.	N.d.	N.d.	N.d.	N.d.	0.310	0.320	0.250	0.180	0.380	0.380	0.140	0.150	0.660
Tm	N.d.	N.d.	N.d.	N.d.	N.d.	N.d.	N.d.	N.d.	N.d.	N.d.	N.d.	N.d.	N.d.	N.d.
Yb	0.600	0.201	0.205	0.160	0.429	0.280	0.290	0.230	0.170	0.360	0.360	0.130	0.140	0.590
Lu	0.109	0.037	0.038	0.029	0.075	0.047	0.050	0.038	0.030	0.060	0.060	0.023	0.023	0.100
Total	4.07	0.67	0.67	0.98	1.92	1.95	1.61	2.22	1.56	2.79	2.82	0.94	0.99	7.79
$(La/Yb)_n$	0.29	0.13	0.04	0.48	0.28	0.48	0.05	0.26	0.32	0.13	0.13	0.10	0.10	0.44

	Massifs													
	Balmuccia, Italy													
	(Hartmann & Wedepohl, 1993), ICP-MS, INAA									(Ottonello *et al.*, 1984), RNAA				
	BAM-2B	BAM-3	BAM-4	BAM-5	BAM-6	BAM-7A	BAM-7B	BAM-8	BAM-9	B-3b	F-59b	F-62	B-1b	B-3c
Element	*Spinel lherzolites*													
La	0.500	0.040	0.090	0.170	0.200	0.090	0.090	0.050	0.020	0.041	0.021	0.064	0.024	0.046
Ce	1.610	0.150	0.330	0.180	0.650	0.310	0.310	0.250	0.100	0.257	0.125	0.239	0.205	0.181
Pr	N.d.	N.d.	N.d.	N.d.	N.d.	N.d.	N.d.	N.d.	N.d.	N.d.	N.d.	N.d.	N.d.	N.d.
Nd	1.760	0.160	0.340	0.200	0.580	0.350	0.350	0.310	0.140	N.d.	0.210	N.d.	N.d.	N.d.
Sm	0.600	0.090	0.150	0.120	0.290	0.180	0.180	0.170	0.070	0.120	0.104	0.110	0.099	0.162
Eu	0.230	0.059	0.068	0.060	0.110	0.070	N.d.	0.070	0.039	0.053	0.046	0.052	0.045	0.069
Gd	0.870	0.270	0.310	0.160	0.450	0.310	0.310	0.320	0.200	N.d.	0.180	N.d.	0.180	N.d.
Tb	0.150	0.060	0.060	0.060	0.090	0.060	N.d.	0.060	0.050	0.049	0.042	0.046	0.041	0.064
Dy	0.950	0.390	0.440	0.330	0.630	0.410	0.410	0.450	0.350	N.d.	N.d.	N.d.	N.d.	N.d.
Ho	N.d.	N.d.	N.d.	N.d.	N.d.	N.d.	N.d.	N.d.	N.d.	N.d.	N.d.	N.d.	N.d.	N.d.
Er	0.650	0.290	0.330	0.250	0.440	0.290	0.290	0.320	0.250	N.d.	N.d.	N.d.	N.d.	N.d.
Tm	N.d.	N.d.	N.d.	N.d.	N.d.	N.d.	N.d.	N.d.	N.d.	N.d.	0.040	N.d.	0.030	N.d.
Yb	0.500	0.300	0.300	0.270	0.380	0.270	0.270	0.320	0.280	0.330	0.224	0.253	0.236	0.315
Lu	0.100	0.049	0.050	0.046	0.065	0.046	0.047	0.055	0.048	0.070	0.042	0.050	0.046	0.059
Total	7.92	1.86	2.47	1.85	3.89	2.39	2.26	2.38	1.55	N.d.	N.d.	N.d.	N.d.	N.d.
$(La/Yb)_n$	0.68	0.09	0.20	0.43	0.36	0.23	0.23	0.11	0.05	0.84	0.06	0.171	0.07	0.10

(*Continued*)

Table 1.8 Continued

	Massifs													
	Lherz, France												Freychinede, France	
	(Bodinier *et al.*, 1988), RNAA													
	69-356	70-321	71-367	71-324	71-326	72-282	72-443a	72-443b	73-114	70-249	73-2	73-3	71-335	71-336
Element	*Spinel lherzolites*					*Spinel lherzolites, clinopyroxene rich*				*Amphibole-bearing lherzolites*			*Spinel lherzolites*	
La	0.100	0.170	0.230	0.150	0.180	0.030	0.200	0.200	0.140	0.170	0.550	0.730	0.130	0.120
Ce	0.630	0.680	0.910	0.450	0.690	0.160	0.660	0.820	0.720	0.650	1.780	2.570	0.470	0.550
Pr	N.d.	N.d.	N.d.	N.d.	N.d.	N.d.	N.d.	N.d.	N.d.	N.d.	N.d.	N.d.	N.d.	N.d.
Nd	0.830	N.d.	N.d.	0.470	N.d.	N.d.	N.d.	0.770	N.d.	0.580	1.340	2.210	N.d.	0.550
Sm	0.330	0.270	0.280	0.190	0.250	0.220	0.280	0.320	0.520	0.180	0.470	0.660	0.170	0.250
Eu	0.120	0.110	0.110	0.075	0.100	0.100	0.110	0.120	0.200	0.061	0.150	0.200	0.070	0.100
Gd	N.d.	N.d.	N.d.	N.d.	N.d.	N.d.	N.d.	N.d.	N.d.	N.d.	N.d.	N.d.	N.d.	N.d.
Tb	0.084	0.070	0.075	0.054	0.080	0.080	0.090	0.080	0.160	0.035	0.075	0.093	0.048	0.072
Dy	N.d.	N.d.	N.d.	N.d.	N.d.	N.d.	N.d.	N.d.	N.d.	N.d.	N.d.	N.d.	N.d.	N.d.
Ho	N.d.	N.d.	N.d.	N.d.	N.d.	N.d.	N.d.	N.d.	N.d.	N.d.	0.110	N.d.	N.d.	N.d.
Er	N.d.	N.d.	N.d.	N.d.	N.d.	N.d.	N.d.	N.d.	N.d.	N.d.	N.d.	N.d.	N.d.	N.d.
Tm	N.d.	N.d.	N.d.	N.d.	N.d.	N.d.	N.d.	N.d.	N.d.	N.d.	N.d.	N.d.	N.d.	N.d.
Yb	0.510	0.290	0.370	0.320	0.400	0.620	0.490	0.470	0.780	0.170	0.310	0.320	0.330	0.340
Lu	0.086	0.043	0.060	0.052	0.062	0.120	0.075	0.076	0.120	0.027	0.049	0.050	0.057	0.050
Total	N.d.	N.d.	N.d.	N.d.	N.d.	N.d.	N.d.	N.d.	N.d.	N.d.	N.d.	N.d.	N.d.	N.d.
$(La/Yb)_n$	0.13	0.40	0.42	0.32	0.30	0.03	0.28	0.29	0.12	0.68	1.20	1.54	0.27	0.24

	Massifs													
	Freychinede, France								Caussou, France					
	(Bodinier *et al.*, 1988), RNAA													
	72-425	71-339	72-357	72-108b	73-1-1	73-1-2	73-1-3	73-1a	70-122	70-192	70-195	70-5	CAU-3	70-120
Element	*Spinel lherzolites*			*Amphibole-bearing lherzolites*										*Spinel lherzolites*
La	0.350	0.140	0.230	0.550	0.620	0.480	0.500	0.580	0.530	1.200	1.400	1.500	2.150	0.330
Ce	0.680	0.660	0.440	1.560	1.820	1.420	1.720	1.690	1.200	4.300	5.000	5.300	9.300	1.100
Pr	N.d.	N.d.	N.d.	N.d.	N.d.	N.d.	N.d.	N.d.	N.d.	N.d.	N.d.	N.d.	N.d.	N.d.
Nd	N.d.	0.790	N.d.	1.200	1.320	1.070	1.450	1.330	1.100	5.300	6.100	7.100	9.900	1.050
Sm	0.230	0.310	0.140	0.350	0.410	0.360	0.470	0.430	0.360	1.900	2.100	2.350	2.880	0.390
Eu	0.100	0.110	0.063	0.120	0.140	0.120	0.160	0.140	0.120	0.590	0.660	0.740	0.880	0.150
Gd	N.d.	N.d.	N.d.	N.d.	N.d.	N.d.	N.d.	N.d.	N.d.	N.d.	N.d.	N.d.	N.d.	N.d.
Tb	0.080	0.080	0.055	0.065	0.077	0.064	0.085	0.073	0.073	0.320	0.350	0.360	0.410	0.099
Dy	N.d.	N.d.	N.d.	N.d.	N.d.	N.d.	N.d.	N.d.	N.d.	N.d.	N.d.	N.d.	N.d.	N.d.
Ho	N.d.	N.d.	N.d.	N.d.	0.090	0.110	N.d.	0.060	0.095	0.270	0.320	0.320	N.d.	0.150
Er	N.d.	N.d.	N.d.	N.d.	N.d.	N.d.	N.d.	N.d.	N.d.	N.d.	N.d.	N.d.	N.d.	N.d.
Tm	N.d.	N.d.	N.d.	N.d.	N.d.	N.d.	N.d.	N.d.	N.d.	N.d.	N.d.	N.d.	N.d.	N.d.
Yb	0.380	0.390	0.320	0.230	0.220	0.190	0.270	0.180	0.160	0.560	0.600	0.650	0.740	0.400
Lu	0.060	0.067	0.048	0.032	0.030	0.027	0.040	0.025	0.029	0.079	0.079	0.084	0.120	0.063
Total	N.d.	N.d.	N.d.	N.d.	N.d.	N.d.	N.d.	N.d.	N.d.	N.d.	N.d.	N.d.	N.d.	N.d.
$(La/Yb)_n$	0.62	0.24	0.49	1.61	1.90	1.71	1.25	2.18	2.24	1.45	1.58	1.56	1.96	0.56

(*Continued*)

Table 1.8 Continued

	Massifs													
	Caussou, France		Porteteny, France			Sem, France		Pic de Geral, France				Peak Couder, France		
	(Bodinier *et al.*, 1988), RNAA													
	70-118	70-189	POR-1	POR-2	POR-3	SEM-1	SEM-2	71-264	PGER-1	PGER-2	PGER-3	PCOU-1	PCOU-2	PCOU-3
Element	*Lherzolites, clinopyroxene rich*		*Spinel lherzolites*					*Spinel lherzolites, clinopyroxene poor*				*Spinel lherzolites*		
La	0.840	0.880	0.089	0.240	0.112	0.520	0.390	0.160	0.160	0.080	0.140	0.300	0.190	0.420
Ce	3.000	3.400	0.370	0.710	0.400	1.020	0.870	0.510	0.430	0.330	0.470	0.640	0.530	0.890
Pr	N.d.	N.d.	N.d.	N.d.	N.d.	N.d.	N.d.	N.d.	N.d.	N.d.	N.d.	N.d.	N.d.	N.d.
Nd	3.000	4.000	0.300	0.580	0.260	0.980	0.860	0.340	0.350	N.d.	0.330	0.420	0.400	0.490
Sm	0.930	1.210	0.150	0.220	0.146	0.330	0.280	0.110	0.110	0.078	0.080	0.200	0.170	0.170
Eu	0.290	0.410	0.065	0.086	0.061	0.115	0.101	0.046	0.041	0.034	0.029	0.076	0.075	0.065
Gd	N.d.	N.d.	N.d.	N.d.	N.d.	N.d.	N.d.	N.d.	N.d.	N.d.	N.d.	N.d.	N.d.	N.d.
Tb	0.140	0.210	0.050	0.055	0.040	0.073	0.065	0.030	0.025	0.022	0.020	0.056	0.048	0.046
Dy	N.d.	N.d.	N.d.	N.d.	N.d.	N.d.	N.d.	N.d.	N.d.	N.d.	N.d.	N.d.	N.d.	N.d.
Ho	N.d.	0.250	0.081	0.097	0.086	0.121	0.107	N.d.	0.055	0.052	0.032	0.103	0.081	0.075
Er	N.d.	N.d.	N.d.	N.d.	N.d.	N.d.	N.d.	N.d.	N.d.	N.d.	N.d.	N.d.	N.d.	N.d.
Tm	N.d.	N.d.	N.d.	N.d.	N.d.	N.d.	N.d.	N.d.	N.d.	N.d.	N.d.	N.d.	N.d.	N.d.
Yb	0.390	0.450	0.300	0.410	0.340	0.420	0.420	0.150	0.200	0.190	0.118	0.350	0.300	0.330
Lu	0.060	0.069	0.050	0.070	0.060	0.072	0.075	0.023	0.035	0.032	0.020	0.059	0.052	0.056
Total	N.d.	10.88	1.46	2.47	1.51	3.65	3.17	N.d.	1.41	0.82	1.24	2.20	1.85	2.54
$(La/Yb)_n$	1.45	1.32	0.20	0.39	0.22	0.84	0.63	0.72	0.54	0.28	0.80	0.58	0.43	0.86

	Massifs													
	Bestiac, France						Fonte, France	Alpe Aramy, Italy					Lanzo, Italy	
	(Bodinier *et al.*, 1988), RNAA							(Ottonello *et al.*, 1984). RNAA						
	72-451	BES-5	72-280	72-452	72-267	72-268	72-228	F-16c	F-16b	F-56	F-16a	F-52c	F-72	F-73b
Element	*Spinel lherzolites, clinopyroxene rich*		Spinel *lherzolites*	*Kelyphitic lherzolites*			*Spinel lherzolites*	*Garnet-spinel lherzolites*					*Spinel lherzolites*	
La	0.270	0.510	0.190	0.290	0.330	0.200	0.140	0.155	0.215	0.113	0.241	0.175	0.089	0.061
Ce	0.900	1.400	0.710	0.770	1.200	0.640	0.220	0.503	0.750	0.445	0.743	0.602	0.507	0.310
Pr	N.d.	N.d.	N.d.	N.d.	N.d.	N.d.	N.d.	N.d.	N.d.	N.d.	N.d.	N.d.	N.d.	N.d.
Nd	0.950	1.940	N.d.	N.d.	1.780	0.610	0.160	0.510	0.460	N.d.	0.530	0.070	0.500	0.455
Sm	0.500	0.700	0.290	0.320	0.740	0.210	0.067	0.222	0.130	0.171	0.155	0.249	0.225	0.202
Eu	0.210	0.250	0.110	0.110	0.280	0.091	0.028	0.119	0.049	0.080	0.057	0.119	0.096	0.102
Gd	N.d.	N.d.	N.d.	N.d.	N.d.	N.d.	N.d.	N.d.	0.166	N.d.	0.208	N.d.	0.350	0.330
Tb	0.130	0.140	0.075	0.090	0.230	0.077	0.019	0.077	0.023	0.050	0.039	0.072	0.068	0.072
Dy	N.d.	N.d.	N.d.	N.d.	N.d.	N.d.	N.d.	N.d.	N.d.	N.d.	N.d.	N.d.	N.d.	N.d.
Ho	N.d.	0.200	0.130	0.120	N.d.	0.130	N.d.	N.d.	N.d.	N.d.	N.d.	N.d.	N.d.	N.d.
Er	N.d.	N.d.	N.d.	N.d.	N.d.	N.d.	N.d.	N.d.	N.d.	N.d.	N.d.	N.d.	N.d.	N.d.
Tm	N.d.	N.d.	N.d.	N.d.	N.d.	N.d.	N.d.	N.d.	0.014	N.d.	0.028	N.d.	N.d.	0.047
Yb	0.690	0.620	0.360	0.160	0.840	0.340	0.150	0.370	0.150	0.210	0.210	0.330	0.251	0.238
Lu	0.110	0.110	0.058	0.022	0.130	0.046	0.028	0.070	0.030	0.040	0.040	0.060	0.039	0.041
Total	N.d.	5.87	1.92	1.88	N.d.	2.34	N.d.	N.d.	N.d.	N.d.	2.25	1.68	2.13	1.86
$(La/Yb)_n$	0.26	0.56	0.36	1.22	0.27	0.40	0.63	0.28	0.97	0.36	0.78	0.36	0.24	0.17

(*Continued*)

Table 1.8 Continued

	Massifs													
	Ronda, Spain							Alps						Beni Bouch.
	(Frey *et al.*, 1985)							(Loubet *et al.*, 1975)						
	R255	R238	R243	R717	Rond 4	R123	R131	Alp4	Alp5	Alp6	Alp7	Alp8	Alp9	1BenBu
Element	*Spinel lherzolites*					*Grt. lhrzol.*	*Pl. lherzol.*	*Spinel lherzolites*						
La	0.300	0.160	0.190	0.220	0.218	0.400	0.056	N.d.	N.d.	N.d.	N.d.	N.d.	N.d.	N.d.
Ce	0.780	0.600	N.d.	0.830	0.737	1.200	0.470	0.464	0.124	0.130	0.360	0.029	0.101	0.610
Pr	N.d.	N.d.	N.d.	N.d.	N.d.	N.d.	N.d.	N.d.	N.d.	N.d.	N.d.	N.d.	N.d.	N.d.
Nd	0.690	0.690	0.720	0.880	0.745	1.200	0.960	0.461	0.278	0.271	0.537	0.271	0.165	0.590
Sm	0.260	0.270	0.300	0.330	0.290	0.530	0.370	0.172	0.144	0.144	0.225	0.131	0.105	0.239
Eu	0.120	0.130	0.120	0.140	0.128	0.230	0.150	0.074	0.067	0.066	0.095	0.057	0.048	0.099
Gd	N.d.	N.d.	N.d.	N.d.	N.d.	N.d.	N.d.	0.272	0.326	0.271	0.375	0.269	0.216	0.386
Tb	0.072	0.100	0.080	0.100	0.088	0.140	0.085	N.d.	N.d.	N.d.	N.d.	N.d.	N.d.	N.d.
Dy	N.d.	N.d.	N.d.	N.d.	N.d.	N.d.	N.d.	0.382	0.407	0.398	0.492	0.355	0.345	0.537
Ho	N.d.	N.d.	N.d.	N.d.	N.d.	N.d.	N.d.	N.d.	N.d.	N.d.	N.d.	N.d.	N.d.	N.d.
Er	N.d.	N.d.	N.d.	N.d.	N.d.	N.d.	N.d.	0.242	0.263	0.270	0.309	0.224	0.240	0.342
Tm	N.d.	N.d.	N.d.	N.d.	N.d.	N.d.	N.d.	N.d.	N.d.	N.d.	N.d.	N.d.	N.d.	N.d.
Yb	0.380	0.430	0.400	0.420	0.408	0.540	0.270	0.248	0.285	0.290	0.327	0.258	0.266	0.337
Lu	0.065	0.072	0.064	0.070	0.068	0.089	0.040	N.d.	N.d.	N.d.	N.d.	N.d.	N.d.	N.d.
Total	N.d.	N.d.	N.d.	N.d.	N.d.	N.d.	N.d.	2.32	1.89	1.84	2.72	1.59	1.49	3.14
$(La/Yb)_n$	0.53	0.25	0.32	0.35	0.36	0.50	0.14	N.d.	N.d.	N.d.	N.d.	N.d.	N.d.	N.d.

	Massifs													
	Beni Boushera, Morocco		Bay of Islands, Canada		Otris, Greece		Troodos, Cyprus	Lizard, England		Naransky, Mongolia		Beriozovsky, Russia	Orford Mount, Canada	Dobromirsky, Bulgaria
	(Loubet *et al.*, 1975)		(Suen *et al.*, 1979)		(Menzies, 1976)			(Frey, 1969)		(Author's data)			(Harnois & Morency, 1989)	(Alexsiev & Zheliazkova, 1971)
	2BenBu	3BenBu	V-13	V-14	O1	O2	T5	90681r	90683r	1133v	705b	154	E-32	1720-67
Element	*Spinel lherzolites*				*Llherzolites*									
La	N.d.	N.d.	1.600	0.210	N.d.	N.d.	0.290	0.009	0.010	1.480	0.600	0.125	0.062	1.300
Ce	0.520	0.480	6.200	1.100	0.530	0.800	0.150	N.d.	0.020	2.660	0.440	2.000	0.245	1.700
Pr	N.d.	N.d.	N.d.	N.d.	N.d.	N.d.	N.d.	0.005	0.014	0.490	0.096	N.d.	N.d.	N.d.
Nd	0.650	0.383	3.600	0.860	0.720	0.550	N.d.	0.047	0.130	3.770	0.740	N.d.	0.278	1.500
Sm	0.257	0.140	0.860	0.330	0.180	0.170	0.030	0.052	0.110	0.150	0.315	0.025	0.130	0.200
Eu	0.110	0.062	0.340	0.140	0.060	0.090	0.010	0.024	0.045	0.077	0.113	0.190	0.047	N.d.
Gd	0.423	0.218	0.870	0.560	0.180	0.350	N.d.	0.132	0.250	0.245	0.510	N.d.	N.d.	0.250
Tb	N.d.	N.d.	0.170	0.090	0.050	0.050	0.010	0.046	N.d.	0.018	0.107	N.d.	0.026	N.d.
Dy	0.584	0.313	N.d.	N.d.	N.d.	N.d.	N.d.	N.d.	N.d.	0.170	0.740	N.d.	N.d.	0.150
Ho	N.d.	N.d.	N.d.	N.d.	0.080	0.080	0.040	0.069	0.090	0.210	0.120	N.d.	N.d.	N.d.
Er	0.383	N.d.	N.d.	N.d.	N.d.	N.d.	N.d.	0.213	0.302	0.780	0.320	N.d.	N.d.	N.d.
Tm	N.d.	N.d.	N.d.	N.d.	N.d.	N.d.	N.d.	0.038	0.050	0.096	0.049	N.d.	N.d.	N.d.
Yb	0.400	0.270	0.230	0.420	0.300	0.280	0.190	0.280	0.330	0.950	0.540	0.200	0.130	0.550
Lu	N.d.	N.d.	0.040	0.060	0.070	0.030	0.010	0.037	0.045	0.158	0.096	0.040	0.020	N.d.
Total	N.d.	N.d.	N.d.	N.d.	2.17	2.40	0.73	0.95	1.40	11.25	4.79	N.d.	N.d.	N.d.
$(La/Yb)_n$	N.d.	N.d.	4.70	0.34	N.d.	N.d.	1.03	0.02	0.02	1.05	0.75	0.42	0.32	1.60

varieties. This observation is connected to the ability of amphiboles to accumulate significant amounts of REE in their structure compared with clinopyroxene. The total REE concentration in amphibole-bearing lherzolites varies in the range of 5–20 ppm with an average value of 9 ppm.

The estimates of average REE content in spinel- and amphibole-bearing lherzolites (Table 1.9) has revealed some peculiarities in the massifs that were explored in greater detail. According to estimates of the average total REE concentration, spinel lherzolites and the massifs folded by them can be divided into three groups: (1) those with a low total REE content (1.2–1.9 ppm), including the Pic de Geral, Freychinede, Porteteny, Alpe Aramy, Lherz, and Baldissero massifs; (2) those with a moderate total REE content (2.2–3.9 ppm), including the Peak Couder, Balmuccia, and Bestiac massifs; (3) and those with an increased total REE content (7.8 ppm), including the Caussou massif. When comparing lherzolites from separate massifs, the ratios between the maximum and minimum concentrations of La and Yb may be a required supplementary criteria. The ratio between the maximum and minimum concentrations of La increases from the Alpe Aramy massif (2) to the Balmuccia massif (25) (Table 1.10). A similar comparison using the ratio between the maximum and minimum concentrations of Yb makes it possible to outline the following sequence of massifs in order of increasing values of this ratio: Baldissero → Caussou → Peak Couder → Lherz. Amphibole-bearing lherzolites with the highest average total REE content are found in the Caussou massif (15.9 ppm); REE content is markedly less in the Lherz (6.8 ppm) and Freychinede massifs (4.4 ppm). However, when the ratios between the maximum and minimum concentrations of La (1.3–4.3 ppm) and Yb (1.5–4.6 ppm) are analyzed, the amphibole-bearing lherzolites from these massifs do not reveal essential differences.

The frequency histograms we built on the basis of available analyses of spinel lherzolites show that the statistical distribution of Yb and Lu content in these rocks corresponds, to a first approximation, to the normal law, while the distribution of La, Ce, Nd, Sm, Eu, and Tb content obeys the lognormal law. On the other hand, the contents of Gd, Tb, and Ho have a polymodal distribution. Hence, the calculated concentrations of Yb and Lu in lherzolites are closer to their real values than are those of other elements.

Some characteristics of REE distribution in lherzolites from individual massifs can be judged by the character of their REE patterns (Fig. 1.6). Spinel lherzolites from the Baldissero, Balmuccia, Lherz, Freychinede, Porteteny, Lanzo, and Ronda massifs have patterns that are very similar to each other. Their steep positive slope points to an intensive fractionation of REE at the expense of light element depletion, which is strongest in samples from the Lizard massif. The REE patterns of lherzolites from the Peak Couder, Sem, Pic de Geral, Mount Orford, and Beni Bouchera massifs have an almost flat form, which testifies to the fact that the REE in these rocks have undergone almost no fractionation. The differences in the geochemistry of REE contained in spinel lherzolites from individual massifs are reflected in differences in the average content of REE (see Table 1.9) and in the configuration of the REE patterns (Fig. 1.7). The amphibole-enriched lherzolites from the Lherz, Freychinede, and Caussou massifs differ from the previously mentioned ones by having a slightly convex upwards pattern in the left-hand part of the REE diagrams, which is a result of their relative enrichment with light REE. Spinel lherzolites in all the massifs under consideration are characterized by low average values of $(La/Yb)_n$, which vary in the range of

Table 1.9 Average REE composition of spinel lherzolites from some massifs (ppm).

	Massifs											
	Baldissero, (Hartmann *et al.*, 1993) (14)	Baldissero (Ottonello *et al.*, 1984) (5)	Balmuccia (Hartmann *et al.*, 1993) (18)	Balmuccia (Ottonello *et al.*, 1984) (5)	Lherz (5)	Lherz (clinopyroxene rich) (4)	Freychinede (6)	Caussou (3)	Porteteny (3)	Sem (2)	Pic de Geral (4)	Peak Couder (3)
Element	*Spinel lherzolites*											
La	0.040	0.120	0.122	0.052	0.168	0.143	0.175	0.683	0.147	0.455	0.135	0.303
Ce	0.168	0.381	0.396	0.284	0.577	0.590	0.535	2.500	0.493	0.945	0.435	0.687
Pr	N.d.	N.d.	N.d.	N.d.	N.d.	N.d.	N.d.	N.d.	N.d.	N.d.	N.d.	N.d.
Nd	0.216	0.827	0.451	0.139	0.650	0.770	0.670	2.683	0.380	0.920	0.340	0.437
Sm	0.135	0.252	0.189	0.149	0.212	0.335	0.217	0.843	0.172	0.305	0.095	0.180
Eu	0.064	0.114	0.092	0.068	0.119	0.133	0.090	0.283	0.071	0.108	0.038	0.072
Gd	0.264	N.d.	0.329	0.180	N.d.	N.d.	N.d.	N.d.	N.d.	N.d.	N.d.	N.d.
Tb	N.d.	0.079	0.077	0.055	0.057	0.103	0.068	0.150	0.048	0.069	0.024	0.050
Dy	0.394	N.d.	0.453	N.d.	N.d.	N.d.	N.d.	N.d.	N.d.	N.d.	N.d.	N.d.
Ho	N.d.	N.d.	N.d.	N.d.	N.d.	N.d.	N.d.	0.200	0.088	0.114	0.046	0.086
Er	0.288	N.d.	0.327	N.d.	N.d.	N.d.	N.d.	N.d.	N.d.	N.d.	N.d.	N.d.
Tm	N.d.	N.d.	N.d.	0.035	N.d.	N.d.	N.d.	N.d.	N.d.	N.d.	N.d.	N.d.
Yb	0.301	0.319	0.302	0.234	0.299	0.590	0.378	0.413	0.350	0.420	0.165	0.327
Lu	0.051	0.058	0.052	0.058	0.049	0.098	0.061	0.064	0.060	0.074	0.028	0.056
Total	1.92	N.d.	2.73	N.d.	N.d.	N.d.	N.d.	7.75	1.81	3.41	1.21	2.20
$(La/Yb)_n$	0.09	0.25	0.24	0.15	0.54	0.18	0.31	1.1	0.27	0.73	0.59	0.62

(*Continued*)

Table 1.9 Continued

	Massifs												
	Bestiac (2)	Alpe Aramy, (garnet-b.) (4)	Lanzo (2)	Lizard (2)	Bay of Island (2)	Otris (2)	Beni Bouchera (3)	Ronda (5)	Alps (21)	Naransky (2)	Lherz (3)	Freychinede (5)	Caussou (5)
Element	*Spinel lherzolites*										*Amphibole-bearing lherzolites*		
La	0.323	0.180	0.075	0.010	0.905	N.d.	N.d.	0.218	N.d.	1.040	0.483	0.546	1.356
Ce	1.003	0.609	0.409	0.020	3.650	0.665	0.537	0.737	0.201	1.550	1.667	1.642	5.020
Pr	N.d.	N.d.	N.d.	0.009	N.d.	N.d.	N.d.	N.d.	N.d.	0.293	N.d.	N.d.	N.d.
Nd	1.445	0.550	0.478	0.089	2.230	0.635	0.541	0.745	0.331	2.255	1.377	1.274	5.900
Sm	0.497	0.185	0.214	0.081	0.595	0.175	0.212	0.290	0.154	0.233	0.437	0.404	1.918
Eu	0.190	0.085	0.099	0.034	0.240	0.075	0.090	0.128	0.068	0.095	0.137	0.136	0.598
Gd	N.d.	0.187	0.340	0.191	0.715	0.265	0.342	N.d.	0.288	0.378	N.d.	N.d.	N.d.
Tb	0.115	0.052	0.070	0.046	0.130	0.050	N.d.	0.088	N.d.	0.063	0.068	0.073	0.303
Dy	N.d.	N.d.	N.d.	N.d.	N.d.	N.d.	0.478	N.d.	0.397	0.455	N.d.	N.d.	N.d.
Ho	0.165	N.d.	N.d.	0.080	N.d.	0.080	N.d.	N.d.	N.d.	0.165	0.110	0.087	0.251
Er	N.d.	N.d.	N.d.	0.258	N.d.	N.d.	0.363	N.d.	0.258	0.550	N.d.	N.d.	N.d.
Tm	N.d.	0.021	0.047	0.044	N.d.	N.d.	N.d.	N.d.	N.d.	0.073	N.d.	N.d.	N.d.
Yb	0.557	0.254	0.245	0.305	0.325	0.290	0.336	0.408	0.279	0.745	0.267	0.218	0.542
Lu	0.093	0.048	0.040	0.041	0.050	0.050	N.d.	0.068	N.d.	0.127	0.042	0.031	0.078
Total	3.85	1.81	N.d.	1.17	N.d.	N.d.	2.90	N.d.	1.98	8.02	4.51	4.38	15.9
$(La/Yb)_n$	0.39	0.55	0.21	0.02	2.5	0.60	N.d.	0.36	N.d.	0.94	1.1	1.7	1.8

Note: Data Table 1.8.

Table 1.10 Average value of $(La/Yb)_n$ in spinel- and amphibole-bearing lherzolites from massifs.

Massif	Value of $(La/Yb)_n$			Number of determinations
	Average	Minimum	Maximum	
Spinel lherzolites				
Lizad	0.02	–	–	2
Baldissero (Hartmann *et al.*)	0.09	0.02	0.18	14
Lanzo	0.21	–	–	2
Baldissero (Ottonello *et al.*)	0.24	0.04	0.48	5
Balmuccia (Hartmann *et al.*)	0.24	0.05	0.68	18
Porteteny	0.27	0.20	0.40	3
Freychinede	0.31	0.17	0.46	6
Bestiac	0.39	0.26	0.56	3
Lherz	0.40	0.03	1.72	11
Balmuccia (Ottonello *et al.*)	0.50	0.06	1.76	6
Alpe Aramy	0.55	0.28	0.97	5
Pic de Geral	0.59	0.28	0.80	4
Peak Couder	0.62	0.43	0.86	3
Sem	0.73	–	–	2
Amphibole-bearing lherzolites				
Lherz	1.1	0.68	1.5	3
Freychinede	1.7	1.3	2.2	5
Caussou	1.8	1.5	2.2	5

0.02–0.73 (Table 1.10). Relatively low average values of this parameter (0.1–0.5) are seen in samples from the Lizard, Baldissero, Balmuccia, and Freychinede massifs, among others. Spinel lherzolites from the Sem, Peak Couder, Pic de Geral, and Alpe Aramy massifs show higher average $(La/Yb)_n$ values (0.5–0.73), and the average value over the whole set of analyses is about 0.5. In amphibole-bearing lherzolites from the Lherz, Freychinede, and Caussou massifs, all of which are enriched with light REE. The average values of $(La/Yb)_n$ vary in the range of 1.14–1.76. Notably, in the spinel lherzolites present in mafic–ultramafic massifs, anomalous enrichment with light REE is less often observed than in the harzburgites, dunites, and ultramafites present in abyssal xenoliths, which were usually subjected to the action of fluids coming from alkaline basalts bringing them to the Earth's surface.

Despite the non-equivalence of the available analyses for REE, it is possible to compare the order of magnitude of the average contents of these admixtures in dunites, harzburgites, and lherzolites from the mafic–ultramafic massifs that have been studied most comprehensively (Table 1.11). Thus, the average total content of REE increase from dunites (0.89 ppm) to harzburgites (1.80 ppm) to lherzolites (~2.45 ppm). Calculations have also shown that the average value of $(La/Yb)_n$ for lherzolites is less than unity, while for harzburgites and dunites this value is greater than unity because they have been enriched with light elements. The REE patterns shown in Figure 1.8 represent the average levels of element accumulation in separate varieties of ultramafic restites: dunites, harzburgites, and lherzolites. In conclusion, we should stress again that the estimates of the average content of REE in the whole set of ultramafic

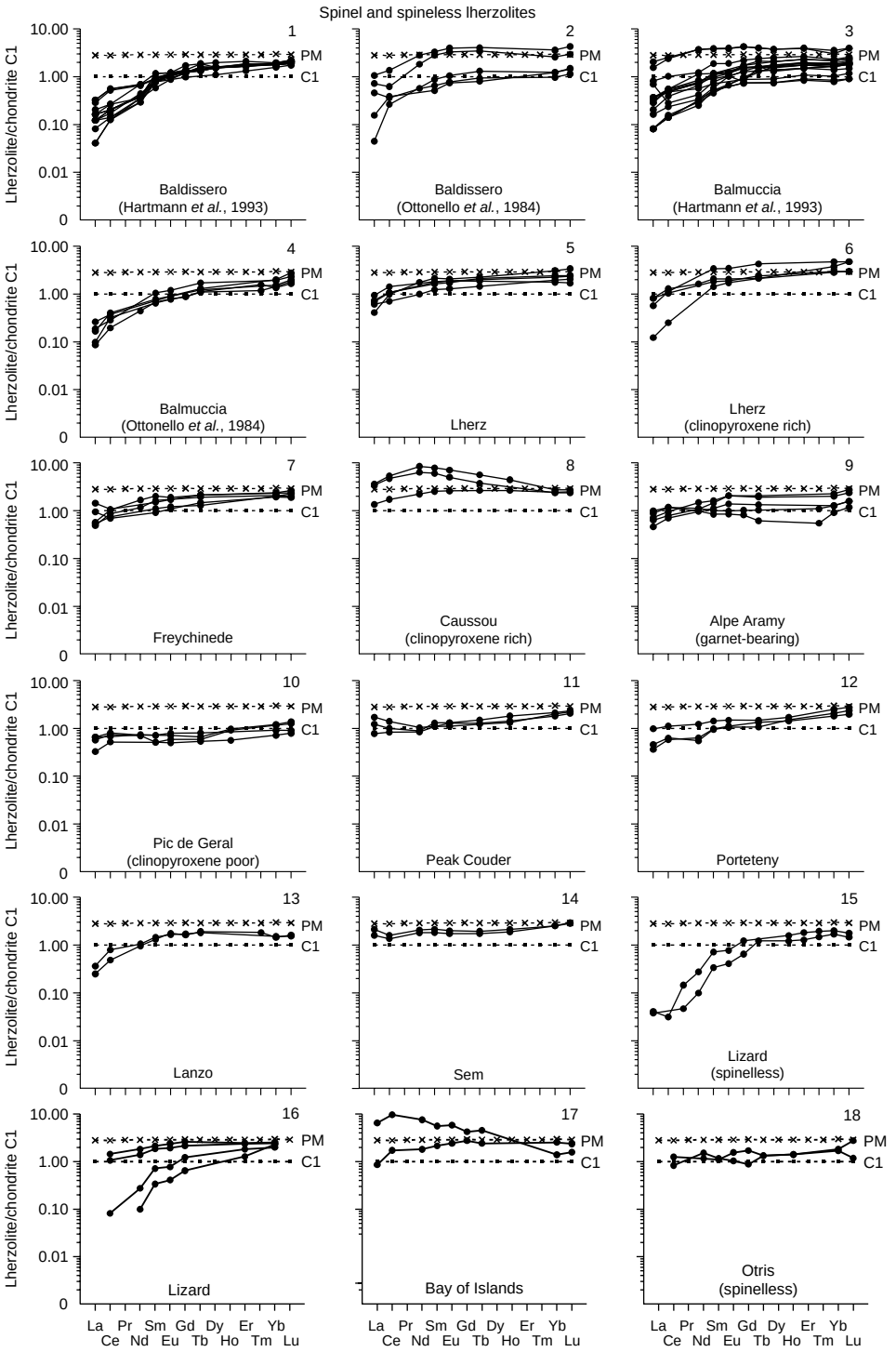

Figure 1.6 Chondrite-normalized REE patterns for spinel and spineless lherzolites from different massifs (data Table 1.8).

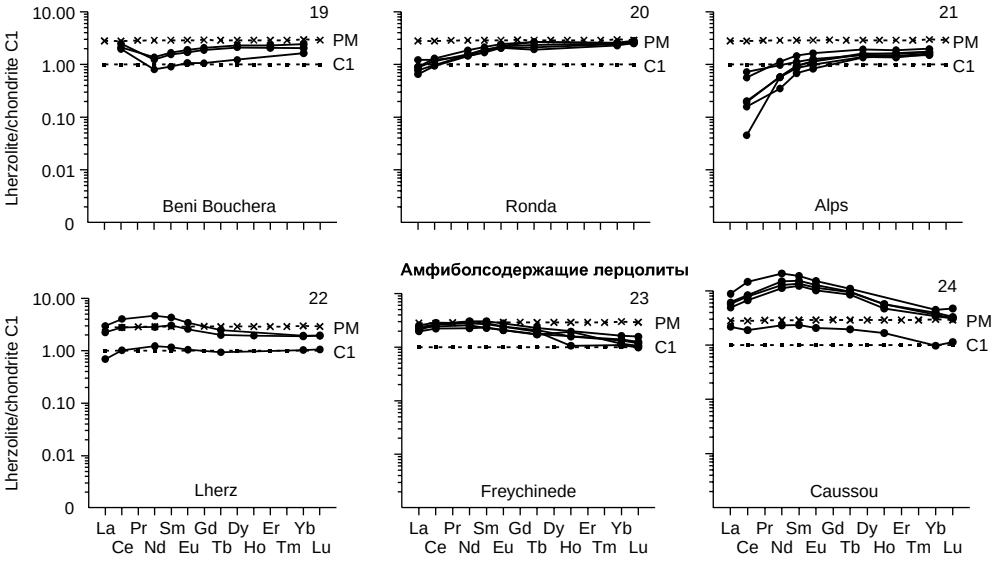

Figure 1.6 Continued

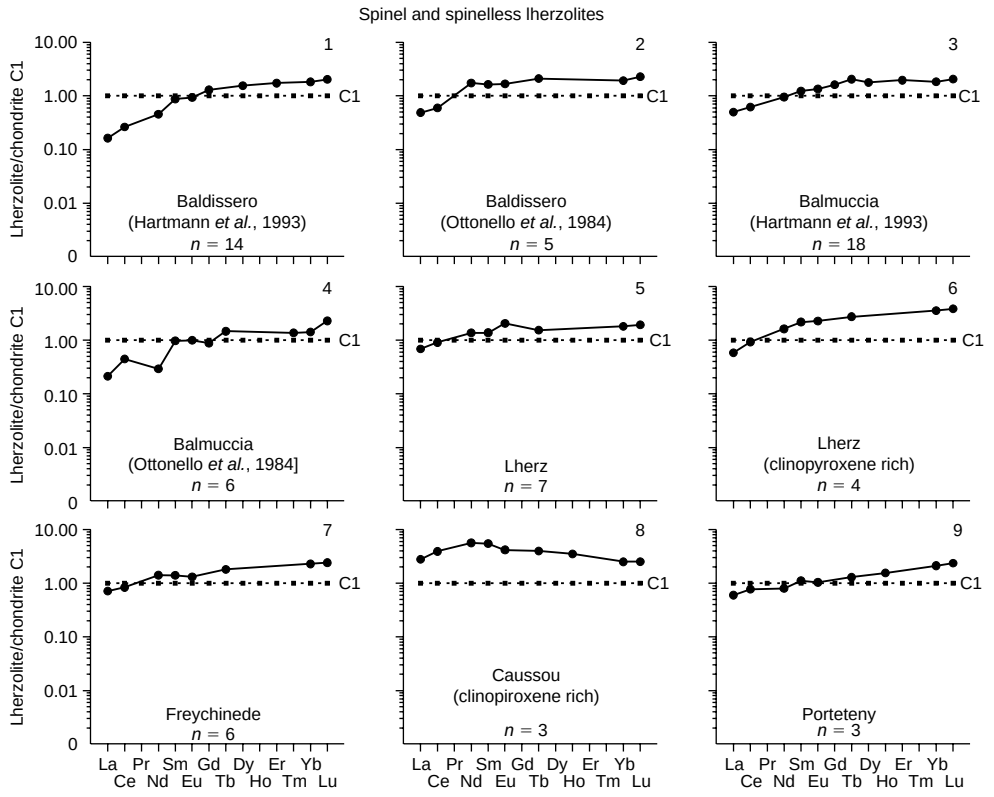

Figure 1.7 Chondrite-normalized REE patterns for the average composition of lherzolites from different massifs (data Table 1.9).

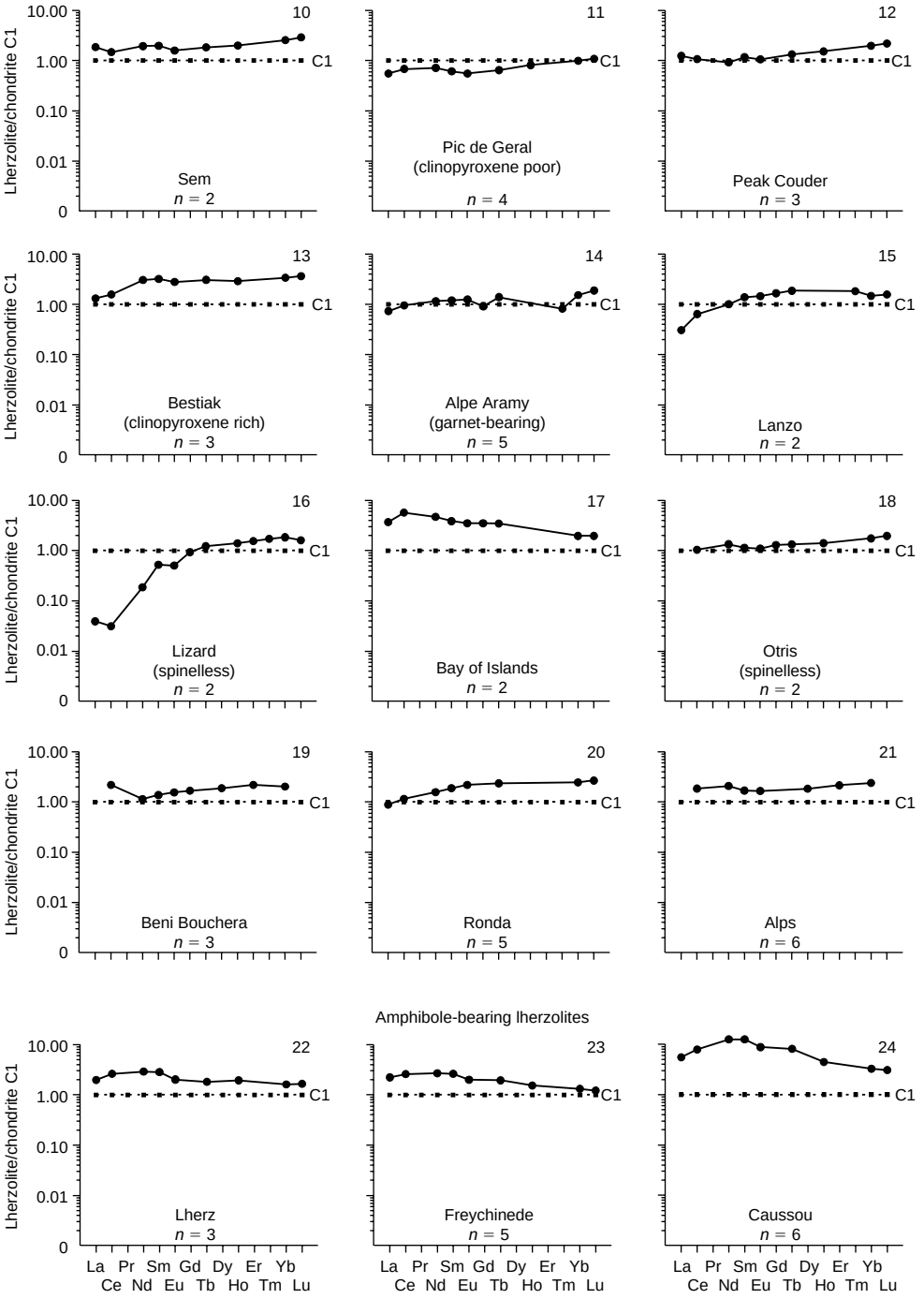

Figure 1.7 Continued

Table 1.11 Average REE composition of dunites, harzburgites, and lherzolites from massifs (ppm).

Element	Dunites (data Table 1.1)	Harzburgites (data Table 1.3)	Lherzolites (data Table 1.8)	All ultramafites (Lutts, 1975)	All ultramafites (Wedepohl & Muramatsu, 1979)	Chondrite C1 (Evensen *et al.*, 1978)	Primitive mantle (Sun & McDonough, 1989)
La	0.132	0.393	0.687	0.199	0.920	0.2446	0.687
Ce	0.227	0.702	1.775	0.589	1.930	0.6379	1.775
Pr	0.091	0.171	0.276	0.151	0.320	0.0964	0.276
Nd	0.205	0.417	1.3540	0.624	1.440	0.4738	1.3540
Sm	0.065	0.085	0.444	0.221	0.400	0.1540	0.444
Eu	0.023	0.032	0.168	0.099	0.160	0.05802	0.168
Gd	0.141	0.142	0.596	0.314	0.740	0.2043	0.596
Tb	0.022	0.024	0.108	0.070	0.120	0.03745	0.108
Dy	0.268	0.095	0.737	0.425	N.d.	0.2541	0.737
Ho	0.051	0.034	0.164	0.105	0.160	0.0567	0.164
Er	0.139	0.078	0.480	0.313	0.400	0.1660	0.480
Tm	0.023	0.015	0.074	0.044	0.070	0.0256	0.074
Yb	0.076	0.117	0.493	0.329	0.380	0.1651	0.493
Lu	0.014	0.022	0.074	0.056	0.060	0.02539	0.074
Total	0.89	1.80	7.43	2.45	7.10	2.60	7.43
$(La/Yb)_n$	2.2	3.0	0.94	0.46	1.6	–	0.94
n	45	114	N.d.	127	N.d.	N.d.	N.d.

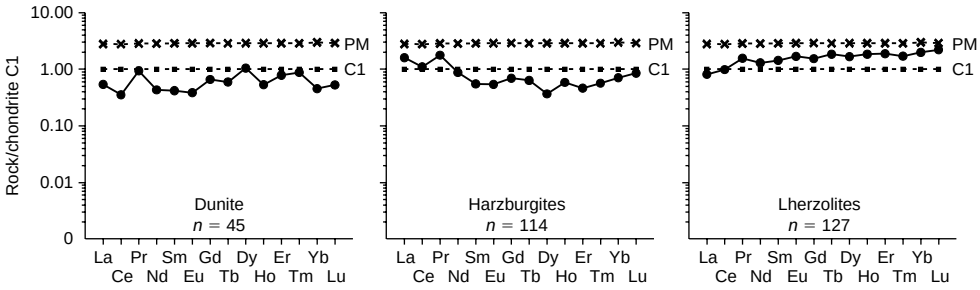

Figure 1.8 Chondrite-normalized REE patterns for the average composition of dunites, harzburgites, and lherzolites from different massifs (data Table 1.11). C1—chondrite (Evensen *et al.*, 1978), PM—primitive mantle (Sun & McDonough, 1989).

rocks—dunites, harzburgites, and lherzolites—that the present author obtained is somewhat lower than previously calculated estimates: 7.10 ppm (Lutts, 1975); and 3.6 ppm (Wedepohl & Muramatsu, 1979). In addition, a significantly higher average total concentration of REE in the primitive mantle has been suggested: 743 ppm (Sun & McDonough, 1989).

* * *

Lherzolites, thus, represent a variety of ultramafic restites that is less depleted than harzburgites and dunites, and they were formed under conditions of decreased partial melting of mantle protoliths. Within individual mafic–ultramafic massifs, the average content of REE in lherzolites varies within a range of 1.4–4.3 ppm. For the entire set of available analyses, the average content of REE is about 2.3 ppm, which is comparable with their total content in chondrite C1. The average total REE concentration decreases from spinel lherzolites to harzburgites to dunites. Amphibole-bearing lherzolites contain a higher REE content than do spinel lherzolites. The statistical distribution of the contents of Yb and Lu is close to the normal law while the distribution of other elements either corresponds to the lognormal law or has a polymodal character. The average values of $(La/Yb)_n$ for spinel lherzolites from individual massifs vary within a comparatively narrow interval (0.02–0.73). In amphibole-bearing lherzolites, these values are higher (1.14–1.76) since the rocks are to a certain degree enriched with light REE.

1.4 WEHRLITES

Wehrlites are included in the composition of many complex mafic–ultramafic massifs and do not usually form autonomous bodies. In almost all of these massifs, wehrlites play a subordinate role. Usually, they are significantly exceeded in abundance by lherzolites and rocks of gabbroic composition. In many mafic–ultramafic massifs, wehrlites form band- and lens-shaped bodies in so-called banded complexes and alternate without any apparent regularity, and with both gradual and contrasting transitions, with similar bodies of clinopyroxenites, websterites, troctolites, and olivine gabbros. Wehrlites often form vein-shaped bodies in dunites, harzburgites, lherzolites, and their serpentinized varieties. They are also present in the form of

schlieren-shaped or angular xenoliths among gabbroic rocks within transition zones of varying thickness and along gabbroic intrusions with protrusions of ultramafic restites. Wehrlites are present at more substantial amounts in some concentrically zonal clinopyroxenite–dunite massifs of the Ural–Alaska type.

The texture of wehrlites varies from fine- and medium-grained to porphyroblastic, coarse-grained, and gigantic-grained; many of these rocks have a taxitic texture due to the random distribution of rock-forming minerals. The mineral composition of these rocks is determined by the predominance of olivine and clinopyroxene in their varying quantitative correlations over secondary minerals such as orthopyroxene, plagioclase, amphibole, and, in some cases, garnet. Chrome-spinel, sulfides of iron, nickel, and copper, as well as compounds of the platinum group elements are often present in wehrlites as accessory minerals. Compared to dunites, harzburgites, and lherzolites, wehrlites are enriched with components such as SiO_2 (40–45 wt%), Al_2O_3 (0.4–7.0 wt%), CaO (6–12 wt%), and FeO_{tot} (6–13 wt%), but depleted of MgO (23–30 wt%) (Bogatikov *et al.*, 1981). Wehrlites differ from other rocks of mafic–ultramafic massifs by wide confidence intervals of average values of petrochemical parameters such as CaO/Al_2O_3, MgO/CaO, and $100 \cdot FeO_{tot}/(FeO_{tot} + MgO)$, with a relatively narrow confidence interval of the average value of Al_2O_3/MgO (Lesnov, 1986).

Data on the REE content of wehrlites are more limited than those available for lherzolites, harzburgites, and dunites. The published analyses characterize individual samples from only a few massifs (Table 1.12). Judging by these assessments, the total content of REE in wehrlites are seldom more than 10 ppm. The level of REE accumulation in most wehrlite samples exceeds the level found in chondrite C1 and is comparable with that in the primitive mantle (Fig. 1.9). Wehrlites from the Thetford Mines massif are an exception in that the level of REE accumulation is lower than that in chondrite C1. The main REE-concentrating mineral in wehrlites is clinopyroxene, and, therefore, the total level of accumulation of these admixtures depends directly on the modal content of this mineral in the rocks. In some varieties of wehrlites, a certain contribution to the REE content may be made by secondary minerals such as amphibole, plagioclase, and garnet.

The configurations of the REE patterns of wehrlites testify to a relatively weak fractionation of these elements. Wehrlites from the Gorgona Island, De Cura, Thetford Mines, and Seinavsky massifs have a general gentle slope in their patterns, which is due to an insignificant depletion of light REE compared to heavy and middle elements. This observation is confirmed by the $(La/Yb)_n$ values of these samples, which vary in the range of 0.15–0.94. Some samples of wehrlites from the Mazhaliksky and Seinavsky massifs manifest somewhat increased contents of light elements. These wehrlites have $(La/Yb)_n$ values of greater than unity. The enrichment of these samples with light REE may be due to the presence of some amount of non-structural impurities concentrated in microcracks. The REE patterns of wehrlites from the Kalbakdagsky, Mazhaliksky, and Niurundukansky massifs have a nearly "flat" form, that is, the elements in them are practically unfractionated. Note that wehrlites from the Gorgona Island, De Cura, Seinavsky, Dugdinsky, and Niurundukansky massifs have comparable average REE content and have a higher total level of element accumulation than do wehrlites from the Thetford Mines massif (Table 1.13).

* * *

Table 1.12 REE composition of wehrlites and plagioclase-bearing (*) wehrlites from massifs (ppm).

	Massifs							
	Gorgona, Columbia		Thetfotd Mines, Canada		Venezuela	Seynavsky, Koryakia, Russia		
	(Revillon *et al.*, 2000)		(Harnois & Morency, 1989)		(Giunta *et al.*, 2002)	(Ledniova, 2001), ICP-MS		
Element	GOR 506	GOR 507	LF-81-7	LF-81-8	VNZ-190	111	104	103
La	0.73	0.15	0.03	0.04	0.79	0.78	0.66	0.60
Ce	2.48	0.48	0.10	0.10	2.51	2.71	2.31	2.11
Pr	0.48	0.11	N.d.	N.d.	0.45	0.55	0.45	0.42
Nd	3.07	0.74	0.20	0.11	2.94	3.36	2.63	2.60
Sm	1.28	0.43	0.08	0.06	1.12	0.97	0.73	0.81
Eu	0.53	0.22	0.03	0.02	0.37	0.30	0.23	0.27
Gd	1.90	0.86	0.14	0.08	1.25	0.95	0.75	0.92
Tb	0.33	0.17	0.02	0.01	0.20	0.15	0.12	0.16
Dy	2.24	1.25	N.d.	N.d.	1.28	0.84	0.78	0.99
Ho	0.46	0.27	N.d.	N.d.	0.28	0.16	0.16	0.20
Er	1.24	0.75	N.d.	N.d.	0.68	0.42	0.43	0.51
Tm	0.18	0.11	N.d.	N.d.	0.11	0.06	0.06	0.07
Yb	1.08	0.67	0.10	0.08	0.71	0.36	0.38	0.43
Lu	0.17	0.11	0.02	0.01	0.10	0.05	0.06	0.06
Total	16.2	6.32	N.d.	N.d.	12.8	11.7	9.75	10.2
$(La/Yb)_n$	0.46	0.15	0.23	0.33	0.75	1.5	1.2	0.94

	Massifs								
	Niurundukansky, Russia			Dugdinsky, Russia, INAA			Mazhaliksky Russia		
	(Tsigankov *et al.*, 2002)			(Mekhonoshin *et al.*, 1986), INAA			(Author's data: Lesnov *et al.*, 2001), INAA		
Element	Ts-3	Ts-5	Ts-7	Mekh-1	Mekh-2	Mekh-3	Mazh-35-5*	L-104a*	Mazh-35-4 (ICP-MS)
La	0.87	0.64	0.61	0.40	0.70	2.60	1.00	0.89	18.00
Ce	2.20	2.50	1.80	2.50	4.50	13.90	3.30	3.60	48.00
Pr	N.d.	N.d.	N.d.	N.d.	N.d.	N.d.	N.d.	N.d.	8.70
Nd	1.40	1.60	1.30	5.00	8.60	13.50	3.10	3.00	42.00
Sm	0.40	0.92	0.43	0.30	0.50	2.70	1.10	1.27	12.00
Eu	0.10	0.34	0.19	0.12	0.19	0.87	0.32	0.44	v 4.20
Gd	N.d.	N.d.	N.d.	N.d.	N.d.	N.d.	0.80	1.39	13.00
Tb	0.06	0.17	0.08	0.07	0.14	0.42	0.16	0.21	2.40
Dy	N.d.	N.d.	N.d.	N.d.	N.d.	N.d.	N.d.	N.d.	15.00
Ho	N.d.	N.d.	N.d.	N.d.	N.d.	N.d.	N.d.	N.d.	2.90
Er	N.d.	N.d.	N.d.	N.d.	N.d.	N.d.	N.d.	N.d.	7.80
Tm	N.d.	N.d.	N.d.	N.d.	N.d.	N.d.	0.08	0.12	1.10
Yb	0.23	0.41	0.22	0.18	0.23	1.08	0.51	0.64	6.90
Lu	0.04	0.07	0.036	N.d.	N.d.	N.d.	0.07	0.10	0.92
Total	N.d.	N.d.	N.d.	N.d.	N.d.	N.d.	N.d.	N.d.	183
$(La/Yb)_n$	2.6	1.1	1.9	1.5	2.1	1.6	1.3	0.94	1.8

(*Continued*)

Table 1.12 Continued

	Massifs							
	Mazhaliksky, Russia		Karaossky, Russia	Kalbakdagsky, Russia				
	(Author's data: Lesnov *et al.*, 2001), INAA							
Element	L-101a	L-106	M-30-98	Kal-5-2*	Kal-3-3	Kal-6-3	Kal-8-1	Kal-9-2
La	0.12	0.45	7.90	0.90	0.77	0.64	0.97	1.54
Ce	0.40	1.20	17	2.50	2.00	1.30	2.20	4.10
Pr	N.d.	N.d.	2.80	N.d.	N.d.	N.d.	N.d.	N.d.
Nd	0.40	1.00	12.00	2.00	1.20	0.80	1.90	2.80
Sm	0.10	0.29	3.40	0.68	0.35	0.32	0.49	1.00
Eu	0.04	0.14	1.40	0.25	0.16	0.15	0.22	0.39
Gd	0.15	0.44	3.90	0.80	1.29	0.50	0.61	1.66
Tb	0.02	0.06	0.68	0.14	0.11	0.06	0.13	0.24
Dy	N.d.	N.d.	4.2	N.d.	N.d.	N.d.	N.d.	N.d.
Ho	N.d.	N.d.	0.90	N.d.	N.d.	N.d.	N.d.	N.d.
Er	N.d.	N.d.	2.30	N.d.	N.d.	N.d.	N.d.	N.d.
Tm	0.02	0.04	0.34	0.10	0.06	0.04	0.08	0.16
Yb	0.10	0.20	2.4	0.69	0.36	0.29	0.56	1.00
Lu	0.02	0.04	0.39	0.11	0.06	0.05	0.09	0.16
Total	N.d.	N.d.	61	N.d.	N.d.	N.d.	N.d.	N.d.
$(La/Yb)_n$	0.81	1.5	2.2	0.88	1.1	1.5	1.2	1.0

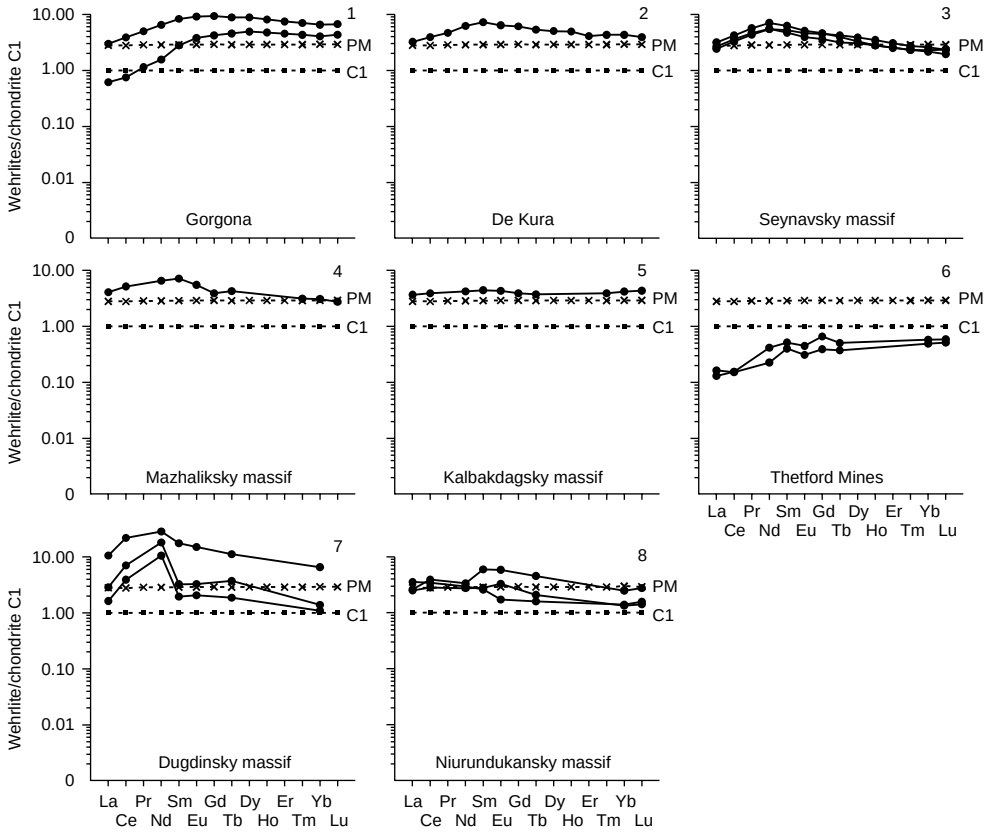

Figure 1.9 Chondrite-normalized REE patterns for wehrlites from different massifs (data Table 1.12).

Table 1.13 Average REE composition of wehrlites from some massifs (ppm).

	Massif					
Element	Gorgona (2)	Seynavsky (3)	Thetford Mines (2)	Dugdinsky (3)	Niurundukansky (3)	Average content in wehrlites (16)
La	0.440	0.680	0.036	1.233	0.707	0.72
Ce	1.480	2.377	0.098	6.967	2.167	2.87
Pr	0.295	0.473	N.d.	N.d.	N.d.	0.41
Nd	1.905	2.863	0.152	9.033	1.433	3.26
Sm	0.855	0.837	0.071	1.167	0.583	0.78
Eu	0.375	0.267	0.022	0.393	0.210	0.27
Gd	1.380	0.873	0.108	N.d.	N.d.	0.84
Tb	0.250	0.143	0.017	0.210	0.103	0.15
Dy	1.745	0.870	N.d.	N.d.	N.d.	1.23
Ho	0.365	0.173	N.d.	N.d.	N.d.	0.26
Er	0.995	0.453	N.d.	N.d.	N.d.	0.67
Tm	0.145	0.063	N.d.	N.d.	N.d.	0.10
Yb	0.875	0.390	0.088	0.497	0.287	0.46
Lu	0.140	0.057	0.014	N.d.	0.049	0.07
Total	11.3	10.5	N.d.	N.d.	N.d.	7.94
$(La/Yb)_n$	0.30	1.2	0.28	1.7	1.8	1.1

Note: Data Table 1.12.

The accumulation level of REE in wehrlites is close to their level in the primitive mantle, and these elements are only slightly fractionated. The content of REE is directly dependent on the modal amount of clinopyroxene in the sample. Some wehrlites are somewhat depleted of light elements. Different points of view exist with regard to the genesis of wehrlites. The most widespread theory is that these rocks were formed as a result of the crystallization differentiation of mafic melts (Harnois *et al.*, 1990; Revillon *et al.*, 2000). Less common is the view that wehrlites represent hybrid rock associations formed from magmatic and metasomatic interactions of ultramafic restites with mafic melts, which penetrated the bodies of the restites (Lesnov, 1986). The latter viewpoint is supported, in particular, by such facts as the absence of wittingly autonomous intrusive massifs formed by wehrlites, the abundance of wehrlites vein bodies among ultramafic restites, and the presence of wehrlite xenoliths among gabbroid intrusives. The increased level of REE accumulation in wehrlites compared to ultramafic restites and the decreased level of these elements compared with the associating gabbroic rocks is also in good agreement with the view that wehrlites were formed as hybridization products.

1.5 CLINOPYROXENITES

In most mafic–ultramafic massifs of folded regions, clinopyroxenites, in conjunction with wehrlites, websterites, troctolites, and olivine gabbros, are included in the composition of so-called banded complexes or transition zones. In addition, clinopyroxenites frequently form single or serial veined and dike bodies lying among dunites, harzburgites, and lherzolites. These rocks are sometimes present in the form of xenoliths of different size and shape that lie within the limits of gabbros intrusives breaking through ultramafites. In some cases, these xenoliths have gradual contacts with surrounding gabbros and are described as "schlieren-shaped bodies". Together with wehrlites and websterites, clinopyroxenites often form "zalbands" along the periphery of small-thickness gabbroid bodies that inject ultramafic rocks. As these gabbroid injections are tapered, the clinopyroxenite zones draw together to gradually pass into the clinopyroxenite vein bodies proper. Many xenoliths of ultramafic restites represented among gabbroic rocks are surrounded by margins consisting of clinopyroxenites, websterites, and wehrlites.

Clinopyroxenites are most widespread in concentrically zoned clinopyroxenite–dunite massifs of the Ural–Alaska type (Ivanov, 1997). The inner zones of these massifs represent dunite "cores" of different sizes surrounded by wehrlite–clinopyroxenite zones, thus separating the "core" from the more-recent, ring-shaped gabbroic intrusions. The thickness of these clinopyroxenite zones vary from a few meters to many hundreds of meters and sometimes exceed 1 km. In these zonal massifs, the quantitative ratios among dunites, clinopyroxenites, and gabbros are largely determined by the level of erosional truncation. Apart from the main phase, clinopyroxene, clinopyroxenites can contain secondary minerals such as olivine, orthopyroxene, and plagioclase, as well as accessories, such as magnetite, titanomagnetite, ilmenite, and minerals of the platinum group elements. In some cases, the content of such accessories may be high.

The concentrations of the main chemical components of clinopyroxenites vary within the following ranges (wt%): SiO_2 (44–53), CaO (12–18), and MgO (12–22) (Bogatikov *et al.*, 1981). The average values of the most important petrochemical parameters of clinopyroxenites have the following confidence intervals CaO/Al_2O_3 (5.4–10.9); MgO/CaO (0.9–1.4); Al_2O_3/MgO (0.19–0.23); and $100 \cdot FeO_{tot}/(FeO_{tot} + MgO)$ (22–33) (Lesnov, 1986).

The REE composition of clinopyroxenites has so far been insufficiently investigated. We have characterized clinopyroxenites using a limited number of analyses of samples from a few massifs, most of which are located in the Ural province (Table 1.14). The REE accumulation level in clinopyroxenites is determined by the quantitative correlations of clinopyroxene and secondary minerals as well as by the content of these admixtures in clinopyroxene itself. The total content of REE in clinopyroxenites varies within a wide range (1–100 ppm). Taking into account the character of the REE patterns of clinopyroxenites, one can conclude that the REE accumulation in these rocks usually exceeds not only the REE level in chondrite C1, but also that in the primitive mantle (Fig 1.10).

The configuration and position of REE patterns reveal differences between clinopyroxenites from separate massifs. Rocks from the Klyuchevskoy, Sredny Kraka, and Mount Orford massifs testify to a certain depletion of light REE and have $(La/Yb)_n$ values that are less than unity. On the other hand, clinopyroxenites from the Khabarinsky, Uktussky, Voykar-Syn'insky, and Surinamsky massifs demonstrate an enrichment of light elements, with $(La/Yb)_n$ values of greater than unity. The patterns of a majority of the analyzed clinopyroxenites have an almost "flat" shape in the fields of middle and heavy elements.

Panina and Usol'tseva (2009) investigated the mineralogy (diopsidic and fassaitic clinopyroxene, perovskite, titanomagnetite, micas, calsilite, apatite, pectolite) and geochemical features of clinopyroxenites from the Krestovsky alcali–ultramafic massif (Meimecha–Kotuy region) and determined the REE distribution in the minerals and microinclusions of these rocks. The authors concluded that these rocks crystallized from two types of melts that were generated from mantle sources at different depths.

An analysis of garnet clinopyroxenites from xenoliths present among the basalts of the Salt Lake crater (Hawaii, USA) and the Kilbourne Holl crater (New Mexico, USA) revealed that the rocks, as well as the clinopyroxene contained in them, have an increased accumulation of light REE (8–20 t. ch.) compared with heavy elements (2–8 t. ch.) (Reid & Frey, 1971). The REE patterns of these clinopyroxenites show smoothed maxima in the region between Pr and Gd. According to the researchers, the clinopyroxenites from xenoliths were not subjected to contamination under the influence of the basalts that were transporting them. They also believe that the pyroxenites from xenoliths were crystallized from the same melts that intruded the upper mantle lherzolites, which are also present in the abyssal xenoliths of the studied manifestations.

* * *

Various views exit regarding the origin of clinopyroxenites within the composition of complex mafic–ultramafic massifs, including concentrically zonal massifs. Without going into a detailed discussion, we hold to the idea that clinopyroxenites, similarly to wehrlites and other varieties of hybrid rocks contained in polygenic mafic–ultramafic

Table 1.14 REE composition of clinopyroxenites from massifs (ppm).

	Massifs								
	Klyuchevskoy, Russia	Gora Kirpichnaya, Russia	Platinum belt, Ural, Russia	Khabarninsky, Russia	Surinamsky, Russia	Uktussky, Russia	Sredny Kraka, Russia	Voykar-Syn'insky, Russia	
	(Fershtater *et al.*, 1998), ICP-MS						(Savel'ev *et al.*, 2000), INAA	(Savel'ev *et al.*, 1999)	
Element	FU2	FU 3	FU 5	FU 6	FU 7	FU 8	Kr -5	587-3	588
La	0.130	0.160	2.310	1.150	18.580	1.910	0.600	0.020	N.d.
Ce	0.240	0.640	5.240	1.910	37.660	4.760	1.920	0.110	0.070
Pr	0.050	0.130	1.150	0.460	5.350	0.760	0.300	0.030	0.020
Nd	0.320	0.820	6.360	2.830	25.390	3.080	1.700	0.230	0.160
Sm	0.120	0.330	2.170	0.830	6.070	1.180	0.700	0.150	0.110
Eu	0.050	0.140	0.630	0.250	1.750	0.330	0.190	0.100	0.050
Gd	0.230	0.570	1.690	0.860	4.360	1.070	1.040	0.380	0.210
Tb	0.040	0.110	0.270	0.150	0.610	0.170	0.170	0.070	0.040
Dy	0.320	0.740	1.870	0.920	2.880	1.030	1.040	0.510	0.320
Ho	0.070	0.160	0.360	0.190	0.560	0.230	0.240	0.110	0.070
Er	0.210	0.470	0.940	0.510	1.370	0.580	0.710	0.340	0.190
Tm	0.030	0.070	0.120	0.060	0.180	0.070	0.110	0.050	0.030
Yb	0.200	0.430	0.700	0.420	1.190	0.460	0.650	0.290	0.170
Lu	0.030	0.060	0.110	0.080	0.180	0.080	0.110	0.040	0.020
Total	2.04	4.83	23.9	10.6	106	15.7	9.40	2.43	1.46
$(La/Yb)_n$	0.44	0.25	2.2	1.9	10.5	2.8	0.62	0.05	N.d.

	Massifs								
	Mount Orford, Canada		Karaossky, Russia	Kalbagdagsky, Russia	Karashatsky, Russia	Khobseksky, Russia			
	(Harnois & Morency, 1989), RNAA		(Lesnov *et al.*, 2001), RNAA			(Author's and A. Mongush data) RNAA			
Element	E-36	E-4	M-35-97	Kal-3-2 (with Ol)	L-48	L-69	L-70	L-78	L-84
La	0.034	0.140	2.300	0.700	0.560	0.140	0.960	0.240	0.240
Ce	0.176	0.499	7.300	1.900	1.400	0.400	2.800	0.600	0.400
Pr	N.d.	N.d.	N.d.	N.d.	N.d.	N.d.	N.d.	N.d.	N.d.
Nd	0.586	0.678	7.700	2.100	1.000	0.400	2.000	0.600	0.200
Sm	0.216	0.296	2.970	0.820	0.300	0.140	0.790	0.150	0.090
Eu	0.070	0.107	0.880	0.310	0.100	0.05	0.290	0.110	0.040
Gd	0.358	0.349	3.000	1.100	0.440	0.330	0.950	0.290	0.330
Tb	0.060	0.060	0.490	0.170	0.080	0.040	0.140	0.040	0.020
Dy	N.d.	N.d.	N.d.	N.d.	N.d.	N.d.	N.d.	N.d.	N.d.
Ho	N.d.	N.d.	N.d.	N.d.	N.d.	N.d.	N.d.	N.d.	N.d.
Er	N.d.	N.d.	N.d.	N.d.	N.d.	N.d.	N.d.	N.d.	N.d.
Tm	N.d.	N.d.	0.210	0.110	0.050	0.030	0.080	0.040	0.020
Yb	0.318	0.352	1.370	0.700	0.350	0.180	0.430	0.270	0.090
Lu	0.052	0.055	0.210	0.100	0.060	0.030	0.050	0.050	0.020
Total	N.d.	N.d.	N.d.	N.d.	N.d.	N.d.	N.d.	N.d.	N.d.
$(La/Yb)_n$	0.07	0.27	1.1	0. 67	1.1	0.52	1.5	0.60	1.8

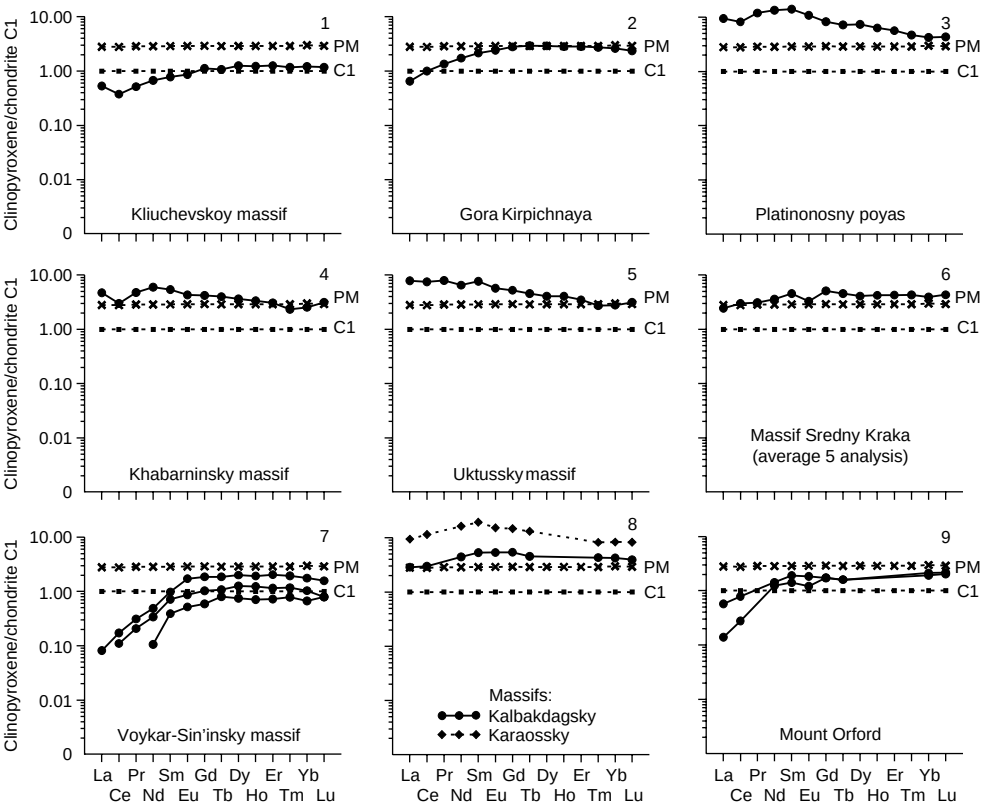

Figure 1.10 Chondrite-normalized REE patterns for clinopyroxenites from different massifs (data Table 1.14).

massifs, were formed as a result of complicated magmatic and metasomatic transformations of ultramafic restites under the action of gabbroic intrusions. The REE composition of clinopyroxenites, similarly to their general chemical composition, is determined by the intensity of the mixing (integrating) between the components of ultramafic restites and those of mafic melts and fluids. Variations in the proportions of components during the mixing of solid restites and melts appear to be the main cause for heterogeneities in the chemical composition of clinopyroxenites. For this reason, clinopyroxenites from different massifs manifest different levels of REE accumulation and frequently exceed REE levels of the primitive mantle. Some clinopyroxenites are depleted of light REE while others are somewhat enriched with them. The limited data on the REE composition of clinopyroxenites make it difficult to reach a substantiated conclusion to the question of the genesis of these rocks.

1.6 WEBSTERITES

Websterites, along with clinopyroxenites and wehrlites, are included in the composition of banded complexes of mafic–ultramafic massifs, many of which include ophiolitic

associations. These rocks generally form band- and lens-shaped bodies of various length and thickness that alternate in a complicated manner with similar bodies of wehrlites, clinopyroxenites, troctolites, and olivine gabbros and gabbro-norites. Websterites often form series of subparallel non-unidirectional veins of various thicknesses that distinctly cut the bodies of ultramafic restites in endomorphic zones of gabbroic intrusions. Websterites are often characterized by a taxitic texture caused by changes in their structure from fine-grained to medium-, coarse-, and giant-grained. In the author's opinion, websterites, similarly to clinopyroxenites and wehrlites, represent hybrid (paramagmatic) rocks formed during the process of magmatic and metasomatic transformations of ultramafic restites under the action of basaltic melts.

The mineral composition of websterites is determined by the varying concentrations of two main minerals: clinopyroxene and orthopyroxene. Some websterites contain olivine, plagioclase, or amphibole as secondary phases. Compared to clinopyroxenites, websterites are somewhat enriched with MgO (15–30 wt%), while at the same time are depleted of CaO (6–20%) (Bogatikov *et al.*, 1981). The average values of the main petrochemical parameters of websterites have the following confidence intervals CaO/Al_2O_3 (3.1–7.5); MgO/CaO (1.2–10.8); Al_2O_3/MgO (0.1–0.2); $100 \cdot FeO_{tot}/(FeO_{tot} + MgO)$ (22–30) (Lesnov, 1986).

The REE composition of websterites has been characterized from a limited number of samples from six mafic–ultramafic massifs (Table 1.15). The main concentrator of REE in these rocks is clinopyroxene, as is also true in wehrlites and clinopyroxenites. The modal amount of clinopyroxene in websterites determines the total level of REE accumulation in these rocks. The total REE content in websterites varies in the range of 1–26 ppm. Increased total concentrations of REE were recorded in websterites from the Balmuccia massif (9–26 ppm), and decreased REE concentrations were found in samples from the Lherz and Freychinede massifs (2.7–7.4 ppm). Even lower values of this indicator were recorded in samples from the Mount Orford, Beriozovsky, and Naransky massifs (0.8–2.6 ppm). Differences in the REE composition of websterites from separate massifs are clearly displayed by the position and configuration of their REE patterns (Fig. 1.11). The patterns of the rocks from the Balmuccia, Lherz, Freychinede, and Mount Orford massifs have a general positive slope resulting from a depletion of light elements relative to heavy ones. The websterites from these massifs have relatively low values of $(La/Yb)_n$ that vary in the range of 0.06–0.66. In the region of heavy and middle elements these patterns assume a "flat" shape. The level of REE accumulation in websterites from the Beriozovsky and Naransky massifs is lower than that in chondrite C1, with the exception of La, with which these rocks are enriched. The $(La/Yb)_n$ values in these websterites are somewhat increased (0.9–1.5). In the sample from the Carolina massif, the concentrations of middle and heavy elements are lower than those in chondrite C1, while websterites from the Chaysky massif have a heavy element concentration that is comparable with that of the primitive mantle. Judging by the negative anomalies in their REE patterns, the previous two samples are characterized by a deficit in Eu, which is possibly due to the leading crystallization of the secondary plagioclase. Differences in the REE composition of websterites from individual massifs can also be seen by the estimated concentrations of their average contents (Table 1.16, Fig. 1.12).

* * *

Table 1.15 REE composition of websterites and plagioclase-bearing (*) websterites from massifs (ppm).

	Massifs									
	Beriozovsky, Russia		Naransky, Mongolia	Balmuccia, Italy						
	(Author's data, RNAA), RNAA			(Rivalenti *et al.*, 1995), SIMS						
Element	134	137	266	TS2	TS4	TS32	BM90-11	BM90-17	BM90-19	BM90-36
La	0.390	0.180	0.250	0.399	1.510	0.890	0.390	0.600	0.630	N.d.
Ce	0.240	0.250	0.330	1.710	5.900	4.760	3.420	1.510	1.960	2.310
Pr	N.d.	N.d.	N.d.	N.d.	N.d.	N.d.	N.d.	N.d.	N.d.	N.d.
Nd	0.180	0.200	0.230	2.200	5.730	5.290	3.670	1.970	2.910	2.710
Sm	0.056	0.047	0.064	1.025	2.520	1.740	1.190	0.820	1.020	1.020
Eu	0.024	0.019	0.027	0.352	1.050	0.560	0.470	0.320	0.370	0.440
Gd	0.098	0.083	0.120	1.170	2.440	1.710	1.340	1.030	1.220	1.320
Tb	0.019	0.016	0.024	N.d.	N.d.	N.d.	N.d.	N.d.	N.d.	N.d.
Dy	N.d.	N.d.	N.d.	1.770	2.870	1.580	1.470	1.230	1.270	1.620
Ho	N.d.	N.d.	N.d.	N.d.	N.d.	N.d.	N.d.	N.d.	N.d.	N.d.
Er	N.d.	N.d.	N.d.	1.290	2.280	0.810	0.830	0.710	0.750	0.870
Tm	0.026	0.021	0.027	N.d.	N.d.	N.d.	N.d.	N.d.	N.d.	N.d.
Yb	0.180	0.130	0.150	1.080	2.040	0.910	0.780	0.730	0.740	0.940
Lu	0.029	0.019	0.025	N.d.	N.d.	N.d.	N.d.	N.d.	N.d.	N.d.
Total	N.d.	N.d.	N.d.	11.0	26.3	18.3	13.6	8.92	10.9	11.2
$(La/Yb)_n$	1.5	0.93	1.1	0.25	0.50	0.66	0.34	0.55	0.57	N.d.

	Massifs											
	Mount Orford, Canada				Lherz, France				Freychinede, France			
	(Harnois & Morency, 1989), RNAA				(Bodinier *et al.*, 1987), RNAA							
Element	E-3	E-35	E-2	E-37	E-6	70-379b	70-379d	70-379a	72-445	70-385c	72-364	72-357
La	0.039	0.047	0.070	0.152	0.108	0.370	0.390	0.670	0.330	0.520	0.270	0.050
Ce	0.126	0.223	0.207	0.357	0.496	1.430	1.650	2.180	1.260	2.080	1.130	2.980
Pr	N.d.	N.d.	N.d.	N.d.	N.d.	N.d.	N.d.	N.d.	N.d.	N.d.	N.d.	N.d.
Nd	0.242	N.d.	0.496	0.383	0.716	N.d.	N.d.	N.d.	N.d.	N.d.	N.d.	N.d.
Sm	0.120	0.198	0.224	0.167	0.299	0.650	0.830	0.640	0.650	0.970	0.560	0.750
Eu	0.039	0.072	0.075	0.082	0.092	0.290	0.290	0.240	0.290	0.390	0.260	0.340
Gd	N.d.	0.291	0.323	0.249	0.334	N.d.	N.d.	N.d.	N.d.	N.d.	N.d.	N.d.
Tb	0.024	0.055	0.051	0.040	0.071	0.380	0.310	0.170	0.270	0.280	0.180	0.250
Dy	N.d.	N.d.	N.d.	N.d.	N.d.	N.d.	N.d.	N.d.	N.d.	N.d.	N.d.	N.d.
Ho	N.d.	N.d.	N.d.	N.d.	N.d.	N.d.	N.d.	N.d.	N.d.	N.d.	N.d.	N.d.
Er	N.d.	N.d.	N.d.	N.d.	N.d.	N.d.	N.d.	N.d.	N.d.	N.d.	N.d.	N.d.
Tm	N.d.	N.d.	N.d.	N.d.	N.d.	N.d.	N.d.	N.d.	N.d.	N.d.	N.d.	N.d.
Yb	0.143	0.306	0.258	0.295	0.400	3.740	1.740	0.660	1.970	1.600	1.000	1.360
Lu	0.023	0.050	0.041	0.047	0.066	0.580	0.270	0.110	0.290	0.250	0.17	0.220
Total	N.d.	N.d.	N.d.	N.d.	N.d.	N.d.	N.d.	N.d.	N.d.	N.d.	N.d.	N.d.
$(La/Yb)_n$	0.18	0.10	0.18	0.35	0.18	0.07	0.15	0.69	0.11	0.22	0.18	0.02

(*Continued*)

Table 1.15 Continued

	Massifs										
	Freychinede, France				Carolina, USA	Chaysky, Russia	Karaossky, Russia				Karashatsky, Russia
	(Bodinier *et al.*, 1987), RNAA				(Philpotts *et al.*, 1972)	(Amelin *et al.*, 1997)	(Author's and A. Mongush's data), RNAA				
Element	72-361	72-427a	72-202	72-212	174	Ch-5	M-26-98*	M-36-98*	M-27-98	L-50	L-37*
La	0.270	0.200	0.180	0.200	N.d.	0.222	2.90	1.60	3.9	0.46	0.30
Ce	0.900	0.800	0.760	1.150	0.203	0.828	7.94	5.00	11.8	1.40	0.70
Pr	N.d.	N.d.	N.d.	N.d.	N.d.	N.d.	N.d.	N.d.	2.2	N.d.	N.d.
Nd	N.d.	N.d.	N.d.	N.d.	0.288	0.973	7.40	4.50	11.3	1.10	0.40
Sm	0.720	0.370	0.570	0.690	0.109	0.372	2.60	1.34	3.2	0.47	0.10
Eu	0.330	0.180	0.270	0.330	0.038	0.116	0.62	0.47	0.91	0.22	0.06
Gd	N.d.	N.d.	N.d.	N.d.	0.154	0.507	2.60	1.60	3.7	0.89	0.15
Tb	0.230	0.130	0.280	0.220	N.d.	N.d.	0.37	0.21	0.65	0.15	0.03
Dy	N.d.	N.d.	N.d.	N.d.	0.196	0.659	N.d.	N.d.	3.8	N.d.	N.d.
Ho	N.d.	N.d.	N.d.	N.d.	N.d.	N.d.	N.d.	N.d.	0.74	N.d.	N.d.
Er	N.d.	N.d.	N.d.	N.d.	0.111	0.461	N.d.	N.d.	2.1	N.d.	N.d.
Tm	N.d.	N.d.	N.d.	N.d.	N.d.	N.d.	0.20	0.12	0.31	0.10	0.02
Yb	1.000	0.860	1.900	1.040	0.141	0.515	1.16	0.78	1.8	0.72	0.09
Lu	0.160	0.150	0.320	0.170	N.d.	N.d.	0.18	0.12	0.25	0.12	0.02
Total	N.d.	N.d.	N.d.	N.d.	N.d.	N.d.	N.d.	N.d.	46.6	N.d.	N.d.
$(La/Yb)_n$	0.18	0.16	0.06	0.13	N.d.	0.29	1.7	1.4	1.5	0.43	2.3

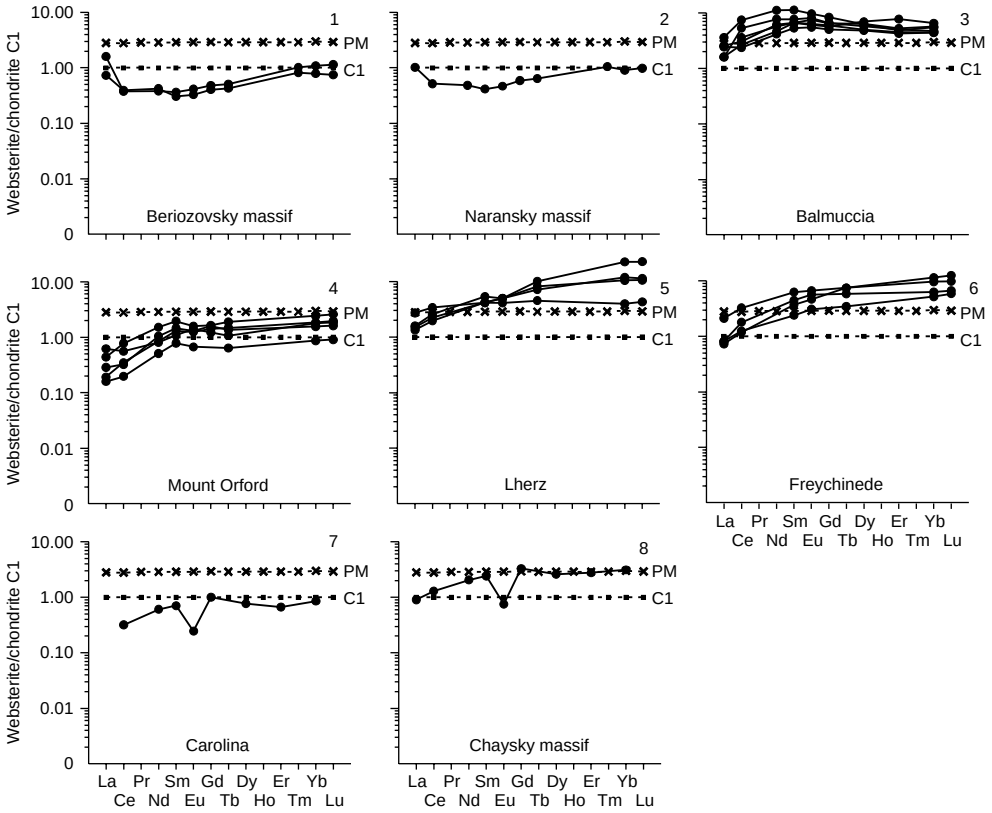

Figure 1.11 Chondrite-normalized REE patterns for websterites from different massifs (data Table 1.15).

Table 1.16 Average REE composition of websterites from some massifs (ppm).

Element	Massifs					Average content in websterites (27)
	Beriozovsky (2)	Balmuccia (6)	Mount Orford (5)	Lherz (4)	Freychinede (7)	
La	0.285	0.582	0.083	0.440	0.241	0.313
Ce	0.245	2.612	0.282	1.630	1.400	1.306
Pr	N.d.	N.d.	N.d.	N.d.	N.d.	N.d.
Nd	0.190	3.125	0.459	N.d.	N.d.	1.497
Sm	0.052	1.136	0.202	0.693	0.661	0.588
Eu	0.022	0.419	0.072	0.278	0.300	0.234
Gd	0.091	1.298	0.299	N.d.	N.d.	0.663
Tb	0.018	N.d.	0.048	0.283	0.224	0.158
Dy	N.d.	1.490	N.d.	N.d.	N.d.	1.224
Ho	N.d.	N.d.	N.d.	N.d.	N.d.	N.d.
Er	N.d.	0.877	N.d.	N.d.	N.d.	0.729
Tm	0.024	N.d.	N.d.	N.d.	N.d.	0.025
Yb	0.155	0.863	0.280	2.028	1.251	0.910
Lu	0.024	N.d.	0.045	0.313	0.206	0.157
Total	N.d.	12.3	N.d.	N.d.	N.d.	5.33
$(La/Yb)_n$	1.20	0.48	0.20	0.25	0.14	0.37

Note: Data Table 1.15.

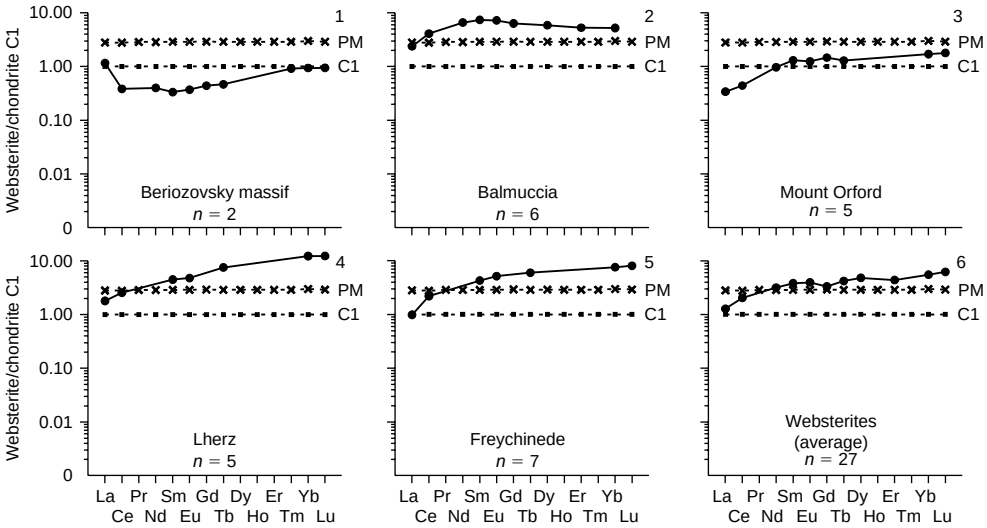

Figure 1.12 Chondrite-normalized REE patterns for the average composition of websterites from different massifs (data Table 1.16).

We consider websterites, similarly to clinopyroxenites and wehrlites, to be hybrid rocks that resulted from the transformation of ultramafic restites under the action of basalts melts. The REE concentration in websterites is usually less than that in clinopyroxenites, which is a result of the lower modal contents of clinopyroxene in websterites. Available data on the REE composition of websterites, along with their petrographical and petrochemical characteristics, make it possible to systematize these rocks in more detail according to their material constitution. According to their average REE content, websterites can be divided into enriched (Balmuccia massif), moderately depleted (Lherz and Freychinede massifs), and significantly depleted (Beriozovsky and Naransky massifs) varieties.

1.7 SUMMARY

The depleted content of REE, especially light ones, in a vast majority of ultramafic rocks that form the polytypic mafic–ultramafic massifs that are widespread in the folded regions of the continents and in the mid-oceanic ridges is an essential geochemical feature that is of great significance in establishing a good understanding of the genesis of these rocks.

Dunites are incorporated in many mafic–ultramafic massifs with various quantitative and structural correlations with other varieties of ultramafic restites and are highly depleted of REE, as well as of other incompatible admixtures. The average total content of REE in dunites is about 0.9 ppm. The accumulation levels of separate REE in dunites is significantly lower than those in chondrite C1. The geochemical properties of dunites are due to the fact that these rocks are almost completely barren of minerals capable of accumulating REE. In addition, the structure of olivine, a

mineral dramatically predominant in dunites, is highly unfavorable for the isomorphic entrance of these elements. At the same time, certain samples of dunites show increased contents of light REE. The assumption, therefore, can be made that, apart from an insignificant amount of a structural admixture of REE present in olivine, these rocks contain some amount of a non-structural admixture of light elements. These light REE were localized in the form of readily soluble compounds in intergranular and intragranular microcracks as well as in secondary fluid microinclusions during epigenetic processes.

Harzburgites are also significantly depleted of REE, which accumulates at low levels in the structures of olivines and orthopyroxenes, and, at somewhat greater amounts, in secondary clinopyroxene. The differences in the quantitative correlations among these minerals account for the heterogeneity in REE composition of harzburgites from different massifs. The REE concentration in harzburgites is usually lower than that in chondrite C1, and the average total concentration is about 1.80 ppm. REE patterns of many harzburgite samples, particularly of those subjected to considerable serpentinization, have a specific U-shaped form. In the author's opinion, this form is due to enrichment of the rocks with non-structural impurities of light REE during infiltration of epigenetic fluids and seawater.

Lherzolites represent the least REE-depleted variety of ultramafic restites. Their REE composition is believed to be the closest to that of the undepleted mantle. Samples of lherzolites from different massifs, and sometimes from the same one, differ in their REE composition. This variation is due to quantitative differences in the mineral composition of these rocks, primarily in the content of clinopyroxene as the main concentrator of REE, which, in turn, can testify to variations in the degree of mantle protolite melting. The average total content of REE in spinel varieties of lherzolites is about 2.45 ppm. Lherzolites sometimes contain amphibole as a secondary mineral formed during the course of epigenetic processes. The presence of amphibole accounts for an increase in the total content of REE in these varieties of lherzolites, which on average equals about 9 ppm. In the spinel varieties of lherzolites, the $(La/Yb)_n$ values vary in the range of 0.02–0.73, while in amphibole-bearing varieties, which are usually enriched with light elements, this indicator is increased to 1.1–1.8.

Wehrlites are hybrid formations that arose as a result of the magmatic and metasomatic interactions of basalts melts with ultramafic restites and are generally serpentinized. In these rocks, the total REE content is frequently within a range of 3–10 ppm, but it can be higher. REE accumulation in wehrlites varies depending on the quantitative correlations between olivine and clinopyroxene. Some varieties of these rocks that are enriched with clinopyroxene manifest a comparatively low level of light element accumulation.

Clinopyroxenites also represent hybrid formations that arose from the interaction of basalts melts with ultramafic restites. Their REE composition is largely determined by the degree of mixing of REE-depleted ultramafic restites with REE-enriched basalt melts. Clinopyroxenites are, therefore, rather heterogeneous in their REE accumulation level, but this level is usually higher in clinopyroxenites than in chondrite C1. In some mafic–ultramafic massifs, these rocks are depleted of light REE, while in others, the rocks are enriched with these elements. Certain varieties of clinopyroxenites have REE concentrations that are comparable with those in the primitive mantle. The REE patterns of many clinopyroxenite samples have a "flat" shape in the region of middle and heavy elements.

Websterites resemble clinopyroxenites in their character of REE distribution, but the level of REE accumulation is somewhat lower in websterites, which is consistent with their decreased clinopyroxene content.

To conclude the discussion of the main characteristics of REE distribution in ultramafic restites as well as in hybrid ultramafic rocks from the zones of gabbros contact, we draw the reader's attention to new data obtained from petrological and geochemical explorations of the southern part of the long studied Lanzo massif, which belongs to the ophiolite association of the West Alps (Piccardo *et al*., 2005). These authors have shown that the considerable structural, quantitative-mineral, and geochemical heterogeneity of ultramafic rocks of the Lanzo massif, which include harzburgites, dunites, plagioclase-bearing peridotites, and various pyroxenites, results from the infiltration of mafic melts and their active interaction with preliminarily dynamo-metamorphosed ultramafic restites. These processes led to the formation of porphyroblastic crystals of orthopyroxene, olivine, and clinopyroxene, all of which are unevenly distributed and are of different size and morphology. As a result, the ultramafic rocks have acquired a fine- and coarse-banded texture. The authors emphasized the idea that the heterogeneity in distribution of new-forming clinopyroxene crystals led to the considerable heterogeneity of REE distribution in the transformed ultramafic restites. In addition, on the basis of data on rocks from mafic–ultramafic massifs of the southern Ural Mountains, Savel'ev *et al*. (2008) concluded that light REE are less informative then heavy elements, that is caused by later processes of redistribution.

Chapter 2

Rare earth elements in ultramafites from deep xenoliths in alkali basalts

A special ultramafic rock group includes ultramafites that are part of deep xenoliths in alkali basalts, kimberlites, and some subvolcanic rocks of increasing alkalinity. Geological, petrographical, petrochemical, mineralogical, and geochemical investigations of ultramafic rocks from deep xenoliths have been carried out for 150 years. Results from these investigations suggest the exclusive role of these rocks in studying the composition and evolution of the upper mantle substrata (Frey, 1984; Ionov, 1988a,b; Ryabchikov *et al.*, 1988; McDonough & Frey, 1989). Late in the 1960s, when more-sensitive and more-precise analytical methods were developed that enabled determination of REE in depleted ultramafic rocks, ultramafic xenoliths were among the first samples to be analyzed. Since that time, the number of REE analyses in ultramafites from deep xenoliths has been progressively increasing. Accumulated data reveal some petrogenetically important peculiarities of REE distribution in ultramafic xenoliths, which are different from analogous rocks that are contained in ultramafic and mafic–ultramafic massifs. By now, more than 120 occurrences of deep xenoliths of ultramafic rocks are found in different regions of the world. The majority of these are represented by so-called inclusions, or nodules, within the subalkali and alkali basalts, as well as kimberlites. McDonough and Frey (1989) published a general review of analytical data on REE geochemistry in ultramafic xenoliths from alkaline basalts and kimberlites that had been accumulated in the geological literature up to 1989, and the major problems of their interpretation. In this review, three groups of ultramafic xenoliths (spinel peridotites, garnet peridotites, and pyroxenites) and some other rocks were characterized. McDonough and Frey (1989) also considered petrogenetic models based on REE distributions in ultramafic xenoliths and summarized data on REE distributions in megacrystals and minerals that composed xenoliths, as well as in mineral inclusions in diamonds. They conducted a comparative analysis of REE geochemistry in ultramafites from deep xenoliths and in ultramafic rocks that are contained in massifs. Note that any original analyses of REE content in ultramafic xenoliths are absent in this review.

Ultramafites from deep xenoliths are considered to be upper mantle restites. They are represented mainly by lherzolites, and rarely by harzburgites and dunites. High-pressure varieties of these rocks usually contain spinel and garnet (McDonough & Frey, 1989). Some low-pressure ultramafic xenoliths contain plagioclase, amphibole, and mica as minor phases and in some cases, small basalt inclusions (Varne & Graham, 1971; Ionov *et al.*, 1994, 1995a).

Together with ultramafic rocks, which are regarded as upper mantle restites, alkaline basalts in some provinces contain xenoliths of wehrlites, pyroxenites, gabbros, and

also metamorphic and sedimentary rocks. Compared to analogous rocks from massifs, which are exposed in folded areas of the continents and within mid-oceanic ridges, ultramafite from deep xenoliths, as a rule, are almost never affected by serpentinization processes. This is an important feature of this type of ultramafic rocks from the point of view of studying their geochemical characteristics. The size of ultramafic xenoliths varies from a few centimeters to 10–15 cm, and are rarely more than 30 cm. Some xenoliths are disintegrated, resulting in the appearance of xenogenic grains of olivine or pyroxenes in hosted basalt. Usually, ultramafic xenoliths are of a rounded shaped.

We shall consider the major trends of REE distribution in ultramafic rocks from deep xenoliths that are present in alkaline basalts only, and we will present as many original analyses of REE in major petrographical varieties of these xenoliths as possible. We considered published analyses on REE compositions of about 180 samples of deep-seated ultramafic xenoliths, collected in 30 alkaline basalt provinces. The majority of these analyses studied ultramafic xenoliths from continental provinces: Dreiser Weiher, Western Germany (Stosch & Seck, 1980); Shavaryn Tsaram (Stosch *et al.*, 1986, 1995; Kovalenko *et al.*, 1989; Lesnov *et al.*, 2007, 2009a,b) and Dariganga (Wiechert *et al.*, 1997), Mongolia; British Columbia, Canada (Sun & Kerrich, 1995); Wangqing (Xu *et al.*, 1998) and Hannuoba (Song & Frey, 1989), China; Tell-Danun, Syria (Sharkov *et al.*, 1996); Assab, Ethiopia (Ottonello, 1980); Austria (Kurat *et al.*, 1980); Victoria, Australia (Frey & Green, 1974); San Carlos, Arizona, USA (Frey & Prinz, 1978); Ile Bizard, Canada (Harnois *et al.*, 1990b); and Khamar Daban (Ionov *et al.*, 1995a) and Sikhote-Alin', Russia (Ionov *et al.*, 1995b). Analyses of ultramafic xenoliths from alkaline basalts provinces of oceanic islands, such as Spitsbergen Island (Shubina *et al.*, 1997), Hawaii (Sen *et al.*, 1993), and Kerguelen (Mattielli *et al.*, 1996) are used to a smaller extent. In most of these studies, no more than five samples were analyzed; in rare cases about twenty samples were studied. Various analytical methods were used to determine REE content in ultramafic xenoliths (% of all analyses): INAA (39%), RNAA (24%), IPMA (6%), ICP-MS (4%), and ICP-AES (31%). Representative analyses of REE content in ultramafites from xenoliths of the above-mentioned provinces and occurrences are listed in Table 2.1 and shown in Figure 2.1.

Ultramafites from deep xenoliths of various provinces differ to some extent in their petrographical and petrochemical characteristics. As noted above, these rocks are predominately composed of lherzolites, while harzburgites are less common, and even less common are dunites, wehrlites, pyroxenites, and other varieties. The chemical composition and geochemical properties of the considered ultramafic xenoliths are significantly influenced by the modal proportions of clinopyroxene, which is a main concentrator of REE, and other phases. Values of the parameter Mg# ($MgO/(MgO + FeO_{tot})$) in lherzolites vary within a wide range (0.78–0.86 mol%) in comparison with harzburgites (0.83–0.85 mol%). Lherzolites and harzburgites differ somewhat in their CaO content (0.71–3.68 wt% and 0.40–1.65 wt%, respectively) and also in their Al_2O_3 content (0.62–4.60 wt% and 0.66–1.95 wt%, respectively). In addition, harzburgites contain less Na_2O (0.05–0.11 wt%) than lherzolites do (0.11–0.38 wt%). Higher contents of Na_2O are detected in ultramafic xenoliths from Wangqing province. In some cases, anomalous enrichment of ultramafic xenoliths with K and P is observed.

Ultramafic rocks from deep-seated xenoliths of different alkaline basalts provinces differ in their REE composition, with especially wide variations in light REE content.

Table 2.1 Rare earth element composition of dunites, harzburgites, and lherzolites from deep xenoliths in alkaline basalts (ppm).

	Provinces													
	Kerguelen, Indian ocean			San Carlos, USA	Kerguelen, Indian ocean					Spitsbergen				
	(Mattielli *et al.*, 1996), ICP-MS			(Frey & Prinz, 1978)	(Mattielli *et al.*, 1996), ICP-MS					(Shubina *et al.*, 1997), INAA				
	M-92-286	G-91-114	G-91-40	PA-10	M-92-509	G-91-38	G-91-42	G-91-8	M-92-502	2sv	4pavl	5pavl	6pavl	11pavl
Element	*Dunites*				*Harzburgites*									
La	1.340	0.960	0.120	0.980	1.250	0.100	0.390	0.420	2.780	0.180	2.100	2.090	2.380	2.364
Ce	1.740	1.410	0.260	1.700	3.060	0.160	0.690	0.770	4.560	0.440	4.950	4.980	5.300	5.200
Pr	0.160	0.130	0.040	0.250	0.420	0.020	0.080	0.080	0.490	N.d.	N.d.	N.d.	N.d.	N.d.
Nd	0.490	0.350	0.200	0.880	1.810	0.070	0.280	0.290	1.760	0.340	3.000	3.050	3.140	3.330
Sm	0.070	0.040	0.060	0.163	0.340	0.010	0.050	0.050	0.310	0.080	0.700	0.780	0.710	0.850
Eu	0.030	0.010	0.030	0.056	0.110	0.004	0.020	0.020	0.100	0.040	0.210	0.220	0.240	0.270
Gd	0.070	0.040	0.090	0.170	0.320	0.010	0.060	0.040	0.350	N.d.	N.d.	N.d.	N.d.	N.d.
Tb	N.d.	N.d.	N.d.	0.022	N.d.	N.d.	N.d.	N.d.	N.d.	0.030	0.100	0.140	0.150	0.150
Dy	0.070	0.040	0.110	N.d.	0.180	0.010	0.050	0.040	0.190	N.d.	N.d.	N.d.	N.d.	N.d.
Ho	0.010	0.010	0.020	0.028	0.030	0.003	0.010	0.010	0.030	N.d.	N.d.	N.d.	N.d.	N.d.
Er	0.040	0.030	0.070	0.082	0.080	0.010	0.030	0.020	0.080	N.d.	N.d.	N.d.	N.d.	N.d.
Tm	N.d.	N.d.	N.d.	0.011	N.d.	N.d.	N.d.	N.d.	N.d.	N.d.	N.d.	N.d.	N.d.	N.d.
Yb	0.040	0.050	0.070	0.083	0.070	0.020	0.040	0.030	0.070	0.100	0.300	0.340	0.320	0.390
Lu	N.d.	N.d.	N.d.	0.016	N.d.	N.d.	N.d.	N.d.	N.d.	0.020	0.040	0.044	0.041	0.055
Total	4.06	3.07	1.07	4.44	7.67	0.42	1.70	1.77	10.7	N.d.	N.d.	N.d.	N.d.	N.d.
$(La/Yb)_n$	22.6	13.0	1.16	7.97	12.1	3.38	6.58	9.45	26.8	1.22	4.73	4.15	5.02	4.09

(*Continued*)

Table 2.1 Continued

	Provinces													
	Hawaii, USA				The Komory Islands		Ile Bizard, Canada				Dariganga, Mongolia			
	(Balashov, 1976)						(Harnois *et al.*, 1990), INAA				(Wiechert *et al.*, 1997), ICP-AES			
	bal10	bal9	bal11	bal8	bal12	bal13	75-IB-3	75-IB-8	75-IB-13	75-IB-20	8520-5	8520-06	8520-30	8520-41
Element	*Harzburgites*													
La	N.d.	0.490	0.925	0.530	0.730	0.490	0.730	0.700	0.820	1.400	0.900	1.940	10.100	7.080
Ce	1.020	0.480	N.d.	1.100	1.350	0.880	2.000	1.420	1.100	3.150	1.700	4.650	15.310	15.820
Pr	N.d.	0.140	0.277	N.d.	0.490	0.350	N.d.	N.d.	N.d.	N.d.	N.d.	N.d.	N.d.	N.d.
Nd	0.611	0.850	1.360	N.d.	1.930	1.510	0.820	1.050	0.000	2.500	0.540	3.070	4.890	9.100
Sm	0.153	0.200	0.336	0.130	0.860	0.820	0.340	0.140	0.050	0.820	0.120	0.850	0.720	1.910
Eu	0.049	0.067	0.103	0.048	0.350	0.250	0.110	0.050	0.030	0.320	0.036	0.278	0.203	0.528
Gd	N.d.	0.210	N.d.	N.d.	1.240	1.500	N.d.	N.d.	N.d.	N.d.	0.100	0.790	0.480	1.220
Tb	N.d.	0.037	0.060	0.022	0.200	0.280	0.020	0.020	0.010	0.090	N.d.	N.d.	N.d.	N.d.
Dy	0.104	N.d.	0.318	N.d.	1.330	1.860	N.d.	N.d.	N.d.	N.d.	0.110	0.600	0.300	0.810
Ho	N.d.	0.038	0.048	N.d.	0.280	0.370	N.d.	N.d.	N.d.	N.d.	N.d.	N.d.	N.d.	N.d.
Er	0.052	N.d.	N.d.	N.d.	1.010	1.050	N.d.	N.d.	N.d.	N.d.	0.070	0.210	0.140	0.280
Tm	N.d.	N.d.	N.d.	N.d.	N.d.	N.d.	N.d.	N.d.	N.d.	N.d.	N.d.	N.d.	N.d.	N.d.
Yb	N.d.	N.d.	0.112	0.074	0.560	0.990	0.120	0.200	0.030	0.130	0.070	0.130	0.130	0.170
Lu	0.012	N.d.	0.020	0.012	0.100	0.150	0.014	0.056	0.006	0.020	0.016	0.020	0.019	0.022
Total	N.d.	N.d.	N.d.	N.d.	10.4	10.5	N.d.	N.d.	N.d.	N.d.	3.66	12.5	32.3	36.9
$(La/Yb)_n$	N.d.	N.d.	5.58	4.83	0.88	0.33	4.11	2.36	18.5	7.27	8.68	10.1	52.4	28.1

	Provinces													
	Wangqing, China			Assab, Ethiopia									Austria	
	(Xu *et al.*, 1998), ICP-MS			(Ottonello *et al.*, 1978), RNAA									(Kurat *et al.*, 1980), INAA	
	W91-5	W91-13	W91-22	3G9	3G12	3G15	3G16	3G17	3G18	3G19	3G28	3G51	Ka 167	Ka 125
Element	*Harzburgites*													*Lherzolites*
La	0.330	0.530	0.910	0.285	0.240	0.445	0.730	0.610	0.500	0.590	0.340	0.960	0.190	0.250
Ce	0.700	0.980	1.690	0.625	0.490	1.225	1.050	1.270	1.100	1.220	0.700	1.770	N.d.	N.d.
Pr	0.100	0.100	0.220	N.d.	N.d.	N.d.	N.d.	N.d.	N.d.	N.d.	N.d.	N.d.	N.d.	N.d.
Nd	0.460	0.490	0.920	0.300	0.220	0.840	0.390	0.690	0.420	0.640	0.370	0.680	N.d.	N.d.
Sm	0.150	0.150	0.240	0.063	0.052	0.235	0.087	0.164	0.074	0.011	0.058	0.130	0.033	0.088
Eu	0.050	0.050	0.070	0.025	0.019	0.073	0.032	0.060	0.026	0.032	0.016	0.049	0.017	0.037
Gd	0.180	0.180	0.140	N.d.	0.061	0.241	0.102	0.190	0.056	N.d.	N.d.	0.153	N.d.	N.d.
Tb	N.d.	N.d.	N.d.	0.018	0.013	0.046	0.021	0.035	0.010	0.017	0.010	0.023	N.d.	N.d.
Dy	0.130	0.130	0.120	N.d.	N.d.	N.d.	N.d.	N.d.	N.d.	N.d.	N.d.	N.d.	N.d.	N.d.
Ho	N.d.	N.d.	N.d.	N.d.	N.d.	N.d.	N.d.	N.d.	N.d.	N.d.	N.d.	N.d.	N.d.	N.d.
Er	0.080	0.080	0.080	N.d.	N.d.	N.d.	N.d.	N.d.	N.d.	N.d.	N.d.	N.d.	N.d.	N.d.
Tm	N.d.	N.d.	N.d.	N.d.	N.d.	0.027	N.d.	N.d.	N.d.	N.d.	N.d.	0.017	N.d.	N.d.
Yb	0.080	0.080	0.120	0.080	0.018	0.167	0.087	0.127	0.041	0.065	0.080	0.100	0.090	0.160
Lu	0.010	0.010	0.010	0.015	0.004	0.030	0.019	0.025	0.010	0.015	0.020	0.024	0.015	N.d.
Total	2.27	2.78	4.52	N.d.	N.d.	N.d.	N.d.	N.d.	N.d.	N.d.	N.d.	N.d.	N.d.	N.d.
$(La/Yb)_n$	2.78	4.47	5.12	2.41	9.00	1.80	5.66	3.24	8.23	6.13	2.87	6.48	1.43	1.06

(*Continued*)

Table 2.1 Continued

	Provinces													
	Austria				British Columbia, Canada									
	(Kurat *et al.*, 1980), INAA				(Sun & Kerrich, 1995), ICP-MS									
	Ka168	Ka105	Ka111	Ka155	BM-16	BM-55	KR-35	JL-14	JL-15	BM-11	KR-1	KR-2	LL-1	JL-18
Element	*Lherzolites*													
La	0.180	0.780	0.340	0.110	0.165	0.209	0.181	0.250	0.112	1.430	0.261	1.110	1.820	2.970
Ce	0.690	2.500	N.d.	N.d.	0.340	0.567	0.616	0.638	0.424	2.620	0.300	3.490	3.380	6.080
Pr	N.d.	N.d.	N.d.	N.d.	0.063	0.107	0.128	0.103	0.083	0.298	0.064	0.184	0.425	0.703
Nd	N.d.	N.d.	N.d.	N.d.	0.370	0.860	0.790	0.670	0.520	1.120	0.280	0.740	1.880	3.060
Sm	0.270	0.280	0.240	0.180	0.209	0.409	0.341	0.261	0.230	0.285	0.057	0.121	0.456	0.585
Eu	0.100	0.110	0.093	0.060	0.084	0.174	0.134	0.123	0.090	0.101	0.021	0.031	0.125	0.189
Gd	N.d.	N.d.	N.d.	N.d.	0.375	0.687	0.514	0.486	0.346	0.372	0.080	0.152	0.474	0.593
Tb	0.075	N.d.	0.060	0.060	0.070	0.132	0.096	0.091	0.066	0.068	0.014	0.022	0.080	0.081
Dy	0.540	0.480	N.d.	N.d.	0.567	1.030	0.764	0.617	0.493	0.537	0.114	0.204	0.572	0.522
Ho	N.d.	N.d.	N.d.	N.d.	0.125	0.231	0.163	0.146	0.098	0.112	0.027	0.045	0.113	0.102
Er	N.d.	N.d.	N.d.	N.d.	0.408	0.675	0.467	0.459	0.312	0.352	0.065	0.152	0.355	0.271
Tm	N.d.	N.d.	N.d.	N.d.	0.065	0.106	0.069	0.062	0.056	0.051	0.017	0.028	0.053	0.042
Yb	0.370	0.250	0.350	0.250	0.468	0.705	0.475	0.452	0.329	0.358	0.088	0.191	0.366	0.285
Lu	0.056	0.036	0.053	0.037	0.063	0.101	0.080	0.077	0.061	0.056	0.013	0.029	0.053	0.045
Total	N.d.	N.d.	N.d.	N.d.	3.37	5.99	4.82	4.44	3.22	7.76	1.40	6.50	10.2	15.5
$(La/Yb)_n$	0.33	2.11	0.66	0.30	0.24	0.20	0.26	0.37	0.23	2.70	2.00	3.92	3.36	7.03

	Provinces												
	British Columbia	Spitsbergen											
	(Sun & Kerrich, 1995)	(Shubina *et al.*, 1997), INAA											
	LL-14	1si	3sv	4sv	5ha	6ha	7ha	8sv	9sv	10si	12sv	13sv	14si	1pavl
Element	*Lherzolites*													
La	5.530	0.560	0.270	0.110	1.600	1.540	0.309	0.370	0.190	0.880	2.900	0.400	3.970	2.450
Ce	2.840	2.070	0.680	0.420	1.300	3.900	0.760	1.150	N.d.	N.d.	5.300	0.940	6.000	5.200
Pr	1.150	N.d.	N.d.	N.d.	N.d.	N.d.	N.d.	N.d.	N.d.	N.d.	N.d.	N.d.	N.d.	N.d.
Nd	4.810	1.180	0.440	0.560	0.790	1.700	0.860	0.590	N.d.	N.d.	3.300	0.620	3.200	2.100
Sm	0.775	0.390	0.120	0.150	0.210	0.390	0.190	0.180	0.130	0.209	0.720	0.190	0.720	0.320
Eu	0.161	0.130	0.040	0.060	0.090	0.140	0.060	0.058	0.045	0.068	0.200	0.071	0.260	0.100
Gd	0.674	N.d.	N.d.	N.d.	N.d.	N.d.	N.d.	N.d.	N.d.	N.d.	N.d.	N.d.	N.d.	N.d.
Tb	0.074	0.090	0.023	0.060	0.056	0.080	0.050	0.055	0.034	0.039	0.110	0.055	0.140	0.079
Dy	0.408	N.d.	N.d.	N.d.	N.d.	N.d.	N.d.	N.d.	N.d.	N.d.	N.d.	N.d.	N.d.	N.d.
Ho	0.082	N.d.	N.d.	N.d.	N.d.	N.d.	N.d.	N.d.	N.d.	N.d.	N.d.	N.d.	N.d.	N.d.
Er	0.218	N.d.	N.d.	N.d.	N.d.	N.d.	N.d.	N.d.	N.d.	N.d.	N.d.	N.d.	N.d.	N.d.
Tm	0.027	N.d.	N.d.	N.d.	N.d.	N.d.	N.d.	N.d.	N.d.	N.d.	N.d.	N.d.	N.d.	N.d.
Yb	0.180	0.460	0.087	0.130	0.240	0.260	0.190	0.210	0.150	0.205	0.240	0.186	0.380	0.370
Lu	0.031	0.060	0.012	0.021	0.033	0.030	0.030	0.030	0.027	0.035	0.030	0.025	0.054	0.049
Total	1.96	N.d.	N.d.	N.d.	N.d.	N.d.	N.d.	N.d.	N.d.	N.d.	N.d.	N.d.	N.d.	N.d.
$(La/Yb)_n$	20.7	0.82	2.10	0.57	4.5	4.0	1.1	1.2	0.86	2.9	8.2	1.5	7.1	4.5

(*Continued*)

Table 2.1 Continued

	Provinces													
	Spitsbergen									Sikhote-Alin', Russia				
	(Shubina *et al.*, 1997), INAA									(Ionov *et al.*, 1995b), ICP-MS				
	2pavl	3pavl	7pavl	8pavl	10pavl	16pavl	17pavl	18pavl	19pavl	8701-4	8802-1	8802-2	8803-1	8803-3
Element	*Lherzolites*													
La	1.100	3.900	2.140	6.120	2.990	1.860	0.110	0.210	0.197	0.160	0.660	0.882	4.500	1.070
Ce	2.360	8.980	5.130	13.600	6.500	3.960	0.360	0.750	0.560	0.086	0.920	1.020	11.400	2.760
Pr	N.d.	N.d.	N.d.	N.d.	N.d.	N.d.	N.d.	N.d.	N.d.	0.049	0.175	0.246	1.410	0.355
Nd	1.060	4.600	2.900	7.000	3.740	1.920	0.260	0.740	0.390	0.326	0.817	1.140	5.690	1.590
Sm	0.207	0.930	0.730	1.570	0.820	0.450	0.090	0.270	0.140	0.208	0.240	0.341	0.882	0.346
Eu	0.060	0.320	0.240	0.470	0.280	0.140	0.035	0.110	0.056	0.094	0.098	0.135	0.244	0.116
Gd	N.d.	N.d.	N.d.	N.d.	N.d.	N.d.	N.d.	N.d.	N.d.	0.386	0.347	0.501	0.591	0.311
Tb	0.037	0.140	0.140	0.250	0.140	0.090	0.025	0.086	0.058	0.075	0.061	0.090	0.066	0.041
Dy	N.d.	N.d.	N.d.	N.d.	N.d.	N.d.	N.d.	N.d.	N.d.	0.559	0.417	0.616	0.300	0.221
Ho	N.d.	N.d.	N.d.	N.d.	N.d.	N.d.	N.d.	N.d.	N.d.	0.128	0.093	0.137	0.049	0.038
Er	N.d.	N.d.	N.d.	N.d.	N.d.	N.d.	N.d.	N.d.	N.d.	0.401	0.271	0.394	0.113	0.095
Tm	N.d.	N.d.	N.d.	N.d.	N.d.	N.d.	N.d.	N.d.	N.d.	0.061	0.042	0.059	0.016	0.013
Yb	0.066	0.240	0.330	0.530	0.390	0.380	0.110	0.370	0.156	0.396	0.271	0.378	0.092	0.082
Lu	0.008	0.030	0.040	0.063	0.044	0.490	0.015	0.060	0.022	0.068	0.046	0.066	0.015	0.013
Total	N.d.	N.d.	N.d.	N.d.	N.d.	N.d.	N.d.	N.d.	N.d.	3.00	4.46	6.01	25.4	7.05
$(La/Yb)_n$	11.3	11.0	4.38	7.79	5.18	3.30	0.68	0.38	0.85	0.27	1.64	1.58	33.0	8.8

	Provinces													
	Sikhote-Alin'	Ile Bizard, Canada			Hawaii, USA					Dariganga, Mongolia				
	(Ionov *et al.*, 1995b)	(Harnois *et al.*, 1990), INAA			(Sen *et al.*, 1993), IPMA					(Wiechert *et al.*, 1997), ICP-AES				
	8805-1	78-IB-2	77-IB-15	78-IB-1	Vein1	Wall1	Wall2	Wall3	Wall4	8520-07	8520-09	8520-11	8520-12	8520-15
Element		*Spinele lherzolites*												
La	0.465	9.910	6.100	1.840	N.d.	N.d.	N.d.	N.d.	N.d.	0.150	0.260	0.440	1.670	0.260
Ce	1.010	16.800	10.800	2.590	8.980	10.500	6.930	8.980	4.460	0.440	0.790	0.980	2.860	0.640
Pr	0.179	N.d.	N.d.	N.d.	N.d.	N.d.	N.d.	N.d.	N.d.	N.d.	N.d.	N.d.	N.d.	N.d.
Nd	0.923	4.280	4.100	1.770	5.670	6.040	4.050	5.670	2.730	0.350	0.600	0.720	0.940	0.520
Sm	0.302	1.600	0.500	0.490	1.750	1.640	1.160	1.750	1.000	0.130	0.230	0.230	0.190	0.190
Eu	0.129	0.400	0.190	0.280	0.620	0.550	0.390	0.620	0.400	0.051	0.091	0.088	0.055	0.077
Gd	0.433	N.d.	N.d.	N.d.	N.d.	N.d.	N.d.	N.d.	N.d.	0.190	0.360	0.330	0.180	0.310
Tb	0.080	0.090	0.030	0.060	N.d.	N.d.	N.d.	N.d.	N.d.	N.d.	N.d.	N.d.	N.d.	N.d.
Dy	0.540	N.d.	N.d.	N.d.	1.810	1.260	1.160	1.810	1.010	0.260	0.460	0.430	0.170	0.400
Ho	0.012	N.d.	N.d.	N.d.	N.d.	N.d.	N.d.	N.d.	N.d.	N.d.	N.d.	N.d.	N.d.	N.d.
Er	0.372	N.d.	N.d.	N.d.	0.870	0.740	0.540	0.870	0.520	0.190	0.320	0.290	0.120	0.300
Tm	0.056	N.d.	N.d.	N.d.	N.d.	N.d.	N.d.	N.d.	N.d.	N.d.	N.d.	N.d.	N.d.	N.d.
Yb	0.359	0.200	0.090	0.130	0.870	0.790	0.580	0.870	0.480	0.200	0.320	0.300	0.140	0.290
Lu	0.063	0.033	0.016	0.023	N.d.	N.d.	N.d.	N.d.	N.d.	0.032	0.048	0.047	0.025	0.045
Total	4.92	N.d.	N.d.	N.d.	N.d.	N.d.	N.d.	N.d.	N.d.	1.99	3.48	3.86	6.35	3.03
$(La/Yb)_n$	0.87	33.5	45.8	9.55	N.d.	N.d.	N.d.	N.d.	N.d.	0.51	0.55	0.99	8.05	0.61

(*Continued*)

Table 2.1 Continued

	Provinces													
	Dariganga, Mongolia						Shavaryn Tsaram, Mongolia							
	(Wiechert *et al.*, 1997), ICP-AES						(Stosch *et al.*, 1986), RNAA							
	8520-17	8520-19	8520-20	8520-22	8520-28	8520-35	MHP 1	MHP 79/1	MHP 79/2	MHP 79/3	MHP 79/4	Mo22	Mo101	Mo102
Element	*Spinele lherzolites*													
La	4.910	0.240	0.140	0.320	2.590	0.340	0.210	0.230	0.760	0.560	0.255	0.360	0.340	0.210
Ce	8.690	0.600	0.520	0.830	6.130	0.870	0.840	0.950	1.550	1.210	0.790	0.880	1.340	0.840
Pr	N.d.	N.d.	N.d.	N.d.	N.d.	N.d.	N.d.	N.d.	N.d.	N.d.	N.d.	N.d.	N.d.	N.d.
Nd	3.210	0.470	0.490	0.790	2.500	0.660	N.d.	N.d.	1.350	0.950	N.d.	0.710	N.d.	N.d.
Sm	0.650	0.190	0.210	0.270	0.530	0.240	0.280	0.295	0.360	0.245	0.195	0.243	0.380	0.280
Eu	0.172	0.088	0.080	0.114	0.155	0.096	0.113	0.109	0.138	0.099	0.084	0.081	0.154	0.113
Gd	0.500	0.300	0.290	0.410	0.450	0.370	N.d.	N.d.	N.d.	N.d.	N.d.	N.d.	N.d.	N.d.
Tb	N.d.	N.d.	N.d.	N.d.	N.d.	N.d.	0.080	0.072	0.107	0.065	0.067	0.066	0.104	0.080
Dy	0.410	0.400	0.400	0.560	0.320	0.470	N.d.	N.d.	N.d.	N.d.	N.d.	N.d.	N.d.	N.d.
Ho	N.d.	N.d.	N.d.	N.d.	N.d.	N.d.	N.d.	N.d.	N.d.	N.d.	N.d.	N.d.	N.d.	N.d.
Er	0.190	0.280	0.280	0.380	0.160	0.340	N.d.	N.d.	N.d.	N.d.	N.d.	N.d.	N.d.	N.d.
Tm	N.d.	N.d.	N.d.	N.d.	N.d.	N.d.	0.074	0.069	0.077	0.055	0.045	0.036	0.094	0.074
Yb	0.180	0.280	0.290	0.400	0.120	0.360	0.360	0.400	0.420	0.300	0.300	0.280	0.510	0.360
Lu	0.032	0.042	0.045	0.062	0.016	0.054	0.068	0.077	0.073	0.049	0.047	0.045	0.093	0.068
Total	18.9	2.89	2.75	4.14	13.0	3.80	N.d.	N.d.	N.d.	N.d.	N.d.	N.d.	N.d.	N.d.
$(La/Yb)_n$	18.4	0.58	0.33	0.54	14.6	0.64	0.39	0.39	1.22	1.26	0.57	0.87	0.45	0.39

	Provinces													
	Shavaryn Tsaram, Mongolia								Hannuoba, China					
	(Stosch *et al.*, 1986), RNAA					(Ionov *et al.*, 1994)			(Song & Frey, 1989), RNAA					
	M103	M104	M105	M-Z1	4230/16	8530-5b/1	8530-5b/3	8530-5b/5	DM1-4	DM1-9	DM1-5	DM1-2	DM1-3	DM1-7
Element	*Spinele lherzolites*													
La	0.800	4.100	0.380	2.340	1.250	0.940	4.000	6.560	0.082	0.116	0.239	0.290	0.505	0.400
Ce	1.770	7.400	1.350	4.300	4.250	1.740	8.280	13.900	N.d.	0.319	0.717	0.475	0.876	0.954
Pr	N.d.	N.d.	N.d.	N.d.	N.d.	0.190	0.980	1.660	N.d.	N.d.	N.d.	N.d.	N.d.	N.d.
Nd	0.700	2.550	1.100	2.200	3.500	0.590	3.610	6.590	0.224	0.287	0.587	0.350	0.523	N.d.
Sm	0.143	0.490	0.440	0.600	0.770	0.149	0.639	1.290	0.105	0.116	0.210	0.117	0.124	0.100
Eu	0.052	0.156	0.186	0.210	0.265	0.047	0.179	0.360	0.048	0.052	0.083	N.d.	0.046	0.035
Gd	N.d.	N.d.	N.d.	N.d.	N.d.	0.141	0.457	1.010	N.d.	N.d.	N.d.	N.d.	N.d.	N.d.
Tb	0.032	0.081	0.115	0.128	0.127	0.025	0.065	0.138	0.037	0.030	0.520	N.d.	0.021	0.009
Dy	N.d.	N.d.	N.d.	N.d.	N.d.	0.193	0.379	0.720	N.d.	N.d.	N.d.	N.d.	N.d.	N.d.
Ho	N.d.	N.d.	N.d.	N.d.	N.d.	0.043	0.075	0.129	N.d.	N.d.	N.d.	N.d.	N.d.	N.d.
Er	N.d.	N.d.	N.d.	N.d.	N.d.	0.133	0.215	0.340	N.d.	N.d.	N.d.	N.d.	N.d.	N.d.
Tm	0.022	0.048	0.077	0.080	0.073	0.019	0.030	0.042	N.d.	N.d.	N.d.	N.d.	N.d.	N.d.
Yb	0.132	0.290	0.550	0.480	0.440	0.125	0.195	0.260	0.207	0.176	0.250	0.169	0.130	0.081
Lu	0.026	0.050	0.090	0.069	0.076	0.022	0.032	0.040	0.045	0.038	0.043	0.033	0.027	0.020
Total	N.d.	N.d.	N.d.	N.d.	N.d.	4.36	19.14	33.04	N.d.	N.d.	N.d.	N.d.	2.25	1.60
$(La/Yb)_n$	4.09	9.54	0.47	3.29	1.92	5.08	13.9	17.0	0.27	0.45	0.65	1.16	2.62	3.33

(*Continued*)

Table 2.1 Continued

	Provinces													
	Wangqing, China							Massif Central, France		Tell-Danun, Syria				
	(Xu *et al.*, 1998), ICP-MS							(Downes & Dupuy, 1987), INAA		(Sharkov *et al.*, 1996), INAA				
	WQ91-1	WQ91-37	WQ91-6	WQ91-11	WQ91-77	WQ91-20	WQ91-21	Ms17	RP70	149/3	149/3-2	149/3-4	149/5	217/18
Element	*Spinele lherzolites*													
La	0.230	0.750	0.500	0.180	0.440	0.610	0.170	0.700	1.600	0.320	1.040	0.560	0.440	0.340
Ce	0.520	1.180	1.000	0.320	0.760	1.000	0.290	1.000	2.700	0.550	2.240	1.300	0.940	N.d.
Pr	0.090	0.170	0.150	0.050	0.120	0.130	0.050	N.d.	N.d.	N.d.	N.d.	N.d.	N.d.	N.d.
Nd	0.470	0.980	0.800	0.270	0.510	0.540	0.280	N.d.	N.d.	N.d.	0.840	0.790	0.570	N.d.
Sm	0.260	0.330	0.300	0.150	0.210	0.180	0.100	0.330	0.290	0.072	0.222	0.128	0.134	0.067
Eu	0.100	0.130	0.120	0.060	0.080	0.060	0.040	0.120	0.110	0.021	0.084	0.043	0.049	0.022
Gd	0.360	0.510	0.430	0.190	0.290	0.180	0.150	N.d.	N.d.	N.d.	N.d.	N.d.	N.d.	N.d.
Tb	N.d.	N.d.	N.d.	N.d.	N.d.	N.d.	N.d.	0.070	0.080	N.d.	0.360	0.140	0.050	N.d.
Dy	0.420	0.610	0.560	0.220	0.410	0.200	0.180	N.d.	N.d.	N.d.	N.d.	N.d.	N.d.	N.d.
Ho	N.d.	N.d.	N.d.	N.d.	N.d.	N.d.	N.d.	N.d.	N.d.	N.d.	N.d.	N.d.	N.d.	N.d.
Er	0.270	0.410	0.400	0.180	0.290	0.120	0.110	N.d.	N.d.	N.d.	N.d.	N.d.	N.d.	N.d.
Tm	N.d.	N.d.	N.d.	N.d.	N.d.	N.d.	N.d.	N.d.	N.d.	N.d.	N.d.	N.d.	N.d.	N.d.
Yb	0.300	0.390	0.390	0.220	0.290	0.120	0.120	0.350	0.310	0.093	0.133	0.078	0.108	0.203
Lu	0.040	0.060	0.060	0.050	0.040	0.020	0.020	0.060	0.050	0.014	0.024	0.010	0.025	0.028
Total	3.06	5.52	4.71	1.89	3.44	3.16	1.51	N.d.	N.d.	N.d.	N.d.	N.d.	N.d.	N.d.
$(La/Yb)_n$	0.52	1.30	0.87	0.55	1.02	3.43	0.96	1.35	3.48	2.32	5.28	4.85	2.75	1.13

	Provinces												
	Tell-Danun	San Carlos, Arizona, USA				Khamar Daban, Russia				West Germany			
	(Sharkov *et al.*, 1996)	(Frey & Prinz, 1978), RNAA				(Ionov *et al.*, 1995a), INAA				(Stosch & Seck, 1980), RNAA			
	217/22	PA-6	PA-65G	PA-15A	PA-51	83-36	83-50	83-69	98-13	D-58	Ia/105	Ia/110	Ia/171	Ia/211
Element	*Plagioclase-bearing lherzolites*													
La	0.190	0.850	0.840	0.210	1.360	0.437	0.236	0.186	0.538	0.195	2.200	3.100	2.400	1.690
Ce	0.260	1.500	2.000	0.790	0.990	1.260	0.727	0.551	1.300	0.520	6.000	8.000	5.700	4.400
Pr	N.d.	0.210	0.360	0.180	0.340	0.181	0.131	0.104	0.179	0.075	0.840	1.000	0.950	0.520
Nd	N.d.	0.810	1.500	1.200	1.500	0.932	0.752	0.582	0.872	0.470	2.000	N.d.	3.000	2.100
Sm	0.021	0.171	0.342	0.461	0.314	0.322	0.285	0.222	0.288	0.163	0.380	0.880	0.540	0.450
Eu	0.005	0.061	0.119	0.228	0.101	0.136	0.120	0.090	0.116	0.067	0.087	0.280	0.175	0.097
Gd	N.d.	0.200	0.390	0.890	0.360	0.499	0.457	0.335	0.425	0.260	N.d.	N.d.	N.d.	0.260
Tb	0.400	0.032	0.060	0.160	0.055	0.090	0.083	0.060	0.077	0.047	0.032	0.080	0.043	0.031
Dy	N.d.	N.d.	N.d.	N.d.	N.d.	0.620	0.589	0.416	0.533	0.340	0.220	0.450	0.270	0.200
Ho	N.d.	0.033	0.096	0.230	0.076	0.139	0.133	0.093	0.118	0.071	N.d.	N.d.	N.d.	0.044
Er	N.d.	0.093	0.240	0.620	0.270	0.413	0.404	0.279	0.355	N.d.	0.150	0.220	0.091	N.d.
Tm	N.d.	0.015	0.038	0.092	0.041	0.062	0.060	0.043	0.053	0.035	N.d.	N.d.	N.d.	0.016
Yb	0.029	0.098	0.270	0.540	0.270	0.405	0.394	0.281	0.349	0.270	0.130	0.180	0.098	0.114
Lu	0.011	0.020	0.041	0.098	0.070	0.067	0.065	0.048	0.057	0.047	0.021	0.041	0.015	0.020
Total	N.d.	4.09	6.30	5.70	5.75	5.56	4.44	3.29	5.26	2.56	N.d.	N.d.	N.d.	9.94
$(La/Yb)_n$	4.42	5.85	2.10	0.26	3.40	0.73	0.40	0.45	1.04	0.49	11.4	11.6	16.5	10.0

(*Continued*)

Table 2.1 Continued

	Provinces													
	West Germany											Victoria, Australia		
	(Stosch & Seck, 1980), RNAA											(Frey & Green, 1974), RNAA		
	Ia/236	Ia/249	Ia/412	Ia/415	Ib/2	Ib/24	Ib/3	Ib/5	Ib/6	Ib/8	Ib/K1	V2604	V2669	V2640
Element	*Spinel peridotites*													
La	1.620	2.200	4.200	2.400	0.189	0.142	0.730	0.079	0.265	0.880	0.160	0.878	1.740	0.259
Ce	1.760	4.400	8.000	6.400	0.350	0.310	1.520	0.205	0.760	2.200	0.590	1.970	2.630	0.590
Pr	0.098	N.d.	0.760	0.810	0.048	N.d.	0.113	0.026	N.d.	0.250	0.075	0.222	0.556	0.101
Nd	0.380	2.200	3.500	2.700	0.166	0.182	N.d.	0.161	0.590	1.590	0.600	0.820	2.190	0.500
Sm	0.082	0.400	0.700	0.400	0.041	0.035	0.098	0.070	0.225	0.470	0.225	0.133	0.346	0.115
Eu	0.025	0.080	0.186	0.117	0.012	0.012	N.d.	0.028	0.086	0.176	0.089	0.033	0.099	0.039
Gd	0.091	N.d.	0.460	0.290	0.042	0.035	N.d.	0.094	0.320	0.610	0.310	0.094	0.250	0.140
Tb	0.023	0.020	0.060	0.042	0.007	0.006	0.012	0.027	0.053	0.114	0.056	0.013	0.032	0.023
Dy	0.210	N.d.	0.390	0.320	0.035	0.043	0.091	0.197	0.350	0.740	0.380	N.d.	N.d.	N.d.
Ho	0.052	N.d.	0.070	0.063	0.008	0.013	0.023	0.050	N.d.	0.163	0.096	0.011	0.027	0.029
Er	N.d.	N.d.	N.d.	N.d.	N.d.	N.d.	0.076	N.d.	N.d.	N.d.	N.d.	0.039	0.066	0.084
Tm	0.026	N.d.	0.015	0.025	0.005	0.007	N.d.	0.025	0.035	0.069	0.043	0.005	0.009	0.014
Yb	0.191	0.068	0.124	0.182	0.040	0.056	0.091	0.172	0.230	0.490	0.330	0.024	0.056	0.092
Lu	0.034	0.011	0.021	0.030	0.008	0.011	0.022	0.031	0.042	0.077	0.054	0.006	0.009	0.016
Total	4.59	N.d.	18.5	13. 8	0.95	0.85	N.d.	1.17	N.d.	7.83	3.01	4.25	8.01	2.00
$(La/Yb)_n$	5.73	21.8	22.9	8.90	3.19	1.71	5.42	0.31	0.78	1.21	0.33	24.7	21.0	1.90

	Provinces															
	Victoria, Australia			Fidra, Scotland				South Yemen	Kakanui, Hawaii	Camperdaun	Cape Navarin	Otago	Salt Lake, USA	Carolina	Eifel	Massif Central, France
	(Frey & Green, 1974), RNAA			(Downes *et al.*, 2001)				(Varne & Graham, 1971)	(Philpotts *et al.*, 1972), IPMA		(Fedorov *et al.*, 1993), INAA	(Philpotts *et al.*, 1972), IPMA				(Menzies, 1976)
	V2728	V2700	V2642	Fd65	Fd124	Fd127	Fd260	VG	26	20	Nav2	137	58	DR3	57	M4
Element	*Spinel lherzolites*							*Lherzolites*								
La	0.271	3.370	0.361	0.54	0.60	2.02	1.57	4.000	N.d.	N.d.	2.000	N.d.	N.d.	N.d.	0.928	1.580
Ce	0.580	2.880	0.550	1.09	1.20	4.42	3.63	4.500	0.369	2.510	3.300	0.102	1.020	0.114	N.d.	3.050
Pr	0.094	0.477	0.088	0.15	0.16	0.54	0.49	0.630	N.d.	N.d.	N.d.	N.d.	N.d.	N.d.	0.527	N.d.
Nd	0.480	1.700	0.458	0.79	0.80	2.31	2.20	2.300	0.506	1.540	N.d.	0.099	0.611	0.047	0.132	2.190
Sm	0.165	0.300	0.187	0.264	0.300	0.52	0.51	N.d.	0.238	0.302	0.420	0.069	0.153	N.d.	0.047	0.500
Eu	0.068	0.099	0.083	0.109	0.122	0.204	0.183	N.d.	0.098	N.d.	0.120	0.030	0.049	N.d.	N.d.	0.160
Gd	0.280	0.290	0.300	0.401	0.468	0.63	0.60	N.d.	0.390	0.320	N.d.	0.164	N.d.	N.d.	N.d.	0.450
Tb	0.048	0.038	0.061	0.075	0.088	0.110	0.104	N.d.	N.d.	N.d.	0.080	N.d.	N.d.	N.d.	0.228	0.080
Dy	N.d.	N.d.	N.d.	0.55	0.64	0.77	0.69	N.d.	0.526	0.346	N.d.	0.298	0.104	0.029	N.d.	N.d.
Ho	0.074	0.050	0.110	0.121	0.138	0.160	0.149	N.d.	N.d.	N.d.	N.d.	N.d.	N.d.	N.d.	0.148	0.120
Er	0.220	0.146	0.330	0.362	0.415	0.474	0.436	N.d.	0.332	0.177	N.d.	0.205	0.052	0.038	N.d.	N.d.
Tm	0.029	0.021	0.050	0.054	0.063	0.069	0.065	N.d.	N.d.	N.d.	N.d.	N.d.	N.d.	N.d.	N.d.	N.d.
Yb	0.207	0.117	0.310	0.347	0.406	0.455	0.417	N.d.	0.358	0.233	0.220	0.227	N.d.	0.072	N.d.	0.360
Lu	0.032	0.021	0.055	0.059	0.067	0.076	0.069	N.d.	N.d.	N.d.	0.030	0.040	0.012	0.012	2.010	0.060
Total	2.55	9.51	2.94	N.d.	N.d.	N.d.	N.d.	N.d.	N.d.	N.d.	N.d.	N.d.	N.d.	N.d.	N.d.	N.d.
$(La/Yb)_n$	0.88	19.4	0.79	N.d.	N.d.	N.d.	N.d.	N.d.	N.d.	N.d.	6.14	N.d.	N.d.	N.d.	N.d.	2.96

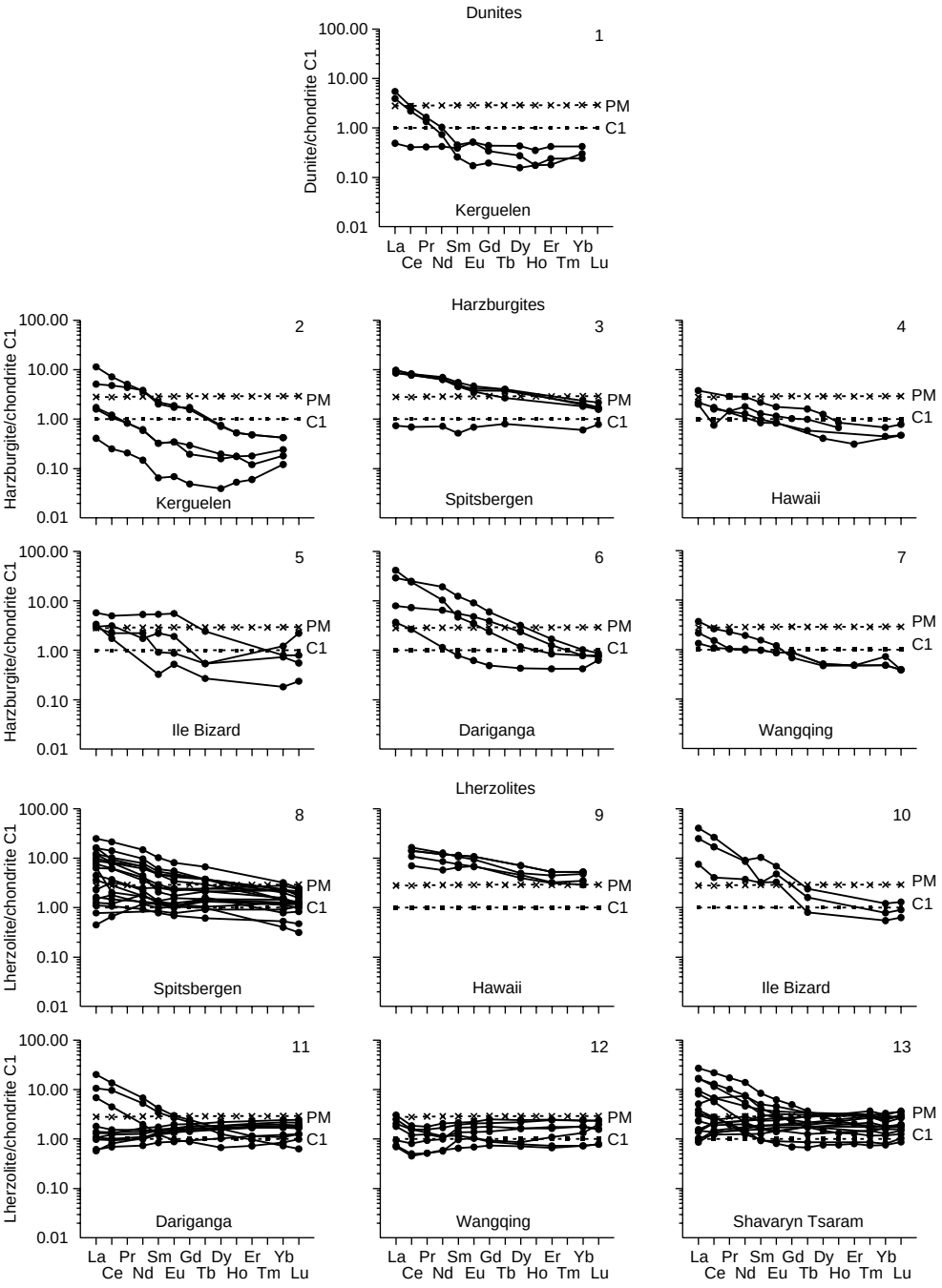

Figure 2.1 Chondrite-normalized REE patterns for dunites, harzburgites, and lherzolites from deep xenoliths from some alkaline basalt provinces (data Table 2.1).

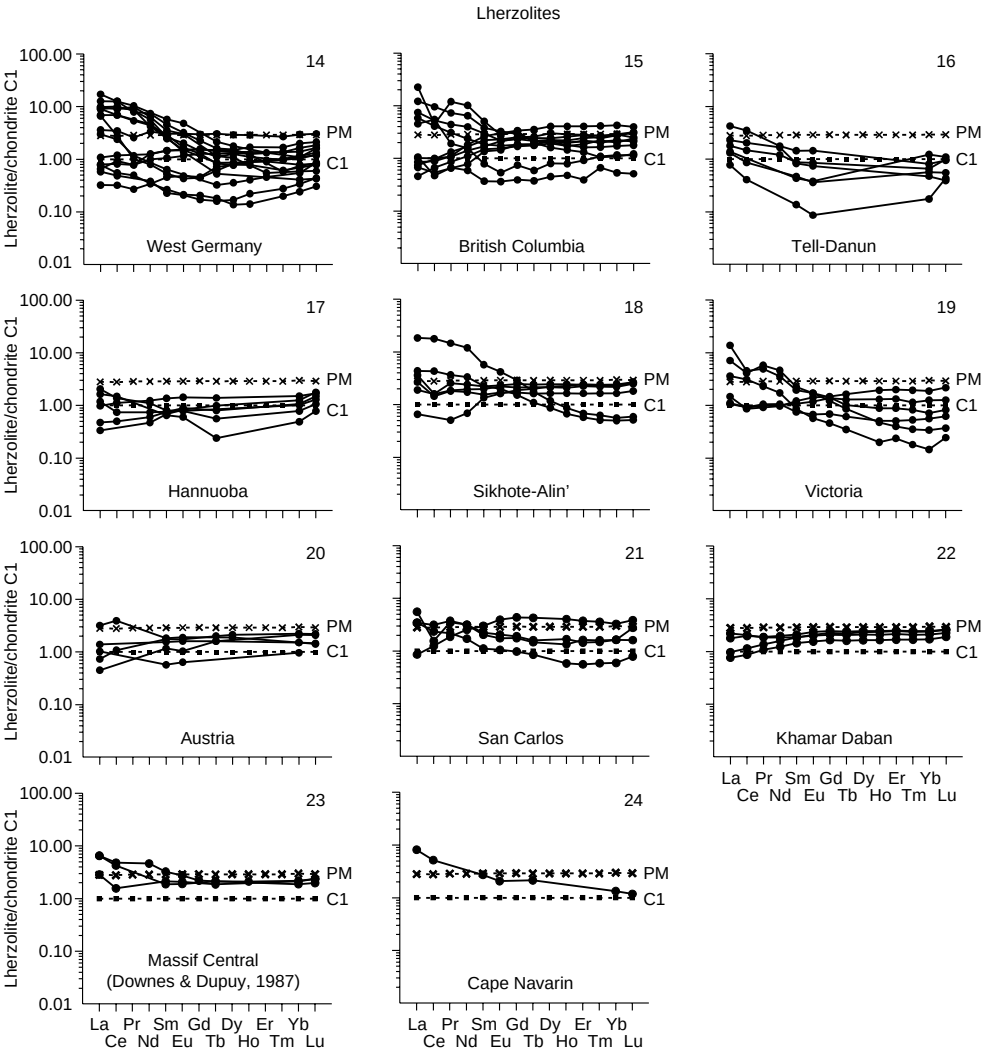

Figure 2.1 Continued

In this respect, these rocks differ from ultramafic rocks from massifs in that the REE composition of the latter is more consistent. Dissimilar REE distributions are observed not only between samples from different provinces, but often between samples from the same province and even within the same xenolith. According to calculations, the average total REE content in harzburgite xenoliths of different provinces ranges from 2.4 ppm (Assab, Ethiopia) to 21 ppm (Dariganga, Mongolia). In lherzolite xenoliths, this parameter varies from 1.6 ppm (Hawaii, USA) to 20.9 ppm (Ile Bizard, Canada) (Table 2.2, Fig. 2.2).

Geochemical inhomogeneity of ultramafites is manifested when comparing the REE patterns of lherzolite, harzburgite, and dunite xenoliths from different provinces.

Table 2.2 Average REE composition of lherzolites and harzburgites from deep xenoliths from some alkaline basalt provinces (ppm).

	Provinces							
	Austria (5)	British Columbia (11)	Spitsbergen (22)	Sikhote-Alin' (6)	Ile Bizard (3)	Hawaii (5)	Dariganga (11)	Shavaryn Tsaram (16)
Element	*Lherzolites*							
La	0.332	1.276	1.553	1.290	5.950	N.d.	1.029	1.567
Ce	1.595	1.936	3.496	2.866	10.06	7.970	2.123	3.384
Pr	N.d.	0.301	N.d.	0.402	N.d.	N.d.	N.d.	0.943
Nd	N.d.	1.373	1.898	1.748	3.383	4.832	1.023	2.073
Sm	0.212	0.339	0.415	0.387	0.863	1.460	0.278	0.423
Eu	0.080	0.112	0.138	0.136	0.290	0.516	0.097	0.145
Gd	N.d.	0.432	N.d.	0.428	N.d.	N.d.	0.335	0.536
Tb	0.065	0.072	0.084	0.069	0.060	N.d.	N.d.	0.082
Dy	0.510	0.530	N.d.	0.442	N.d.	1.410	0.389	0.431
Ho	N.d.	0.113	N.d.	0.076	N.d.	N.d.	N.d.	0.082
Er	N.d.	0.339	N.d.	0.274	N.d.	0.708	0.259	0.229
Tm	N.d.	0.052	N.d.	0.041	N.d.	N.d.	N.d.	0.055
Yb	0.276	0.354	0.258	0.263	0.140	0.718	0.262	0.328
Lu	0.046	0.055	0.055	0.045	0.024	N.d.	0.041	0.056
Total	1.82	7.29	7.41	8.47	21.0	17.6	5.84	8.01
$(La/Yb)_n$	0.89	3.73	3.82	7.70	29.6	N.d.	4.16	4.17

	Provinces							
	Hannuoba (6)	Wangqing (7)	Massif Central (2)	Tell-Danun (6)	San Carlos (4)	Khamar Daban (4)	West Germany (16)	Victoria (6)
Element	*Lherzolites*							
La	0.272	0.411	1.150	0.482	0.815	0.349	1.403	1.147
Ce	0.668	0.724	1.850	1.058	1.320	0.960	3.195	1.533
Pr	N.d.	0.109	N.d.	N.d.	0.273	0.149	0.428	0.256
Nd	0.394	0.550	N.d.	0.733	1.253	0.785	1.403	1.025
Sm	0.129	0.219	0.310	0.107	0.322	0.279	0.322	0.208
Eu	0.053	0.084	0.115	0.037	0.127	0.116	0.101	0.070
Gd	N.d.	0.301	N.d.	N.d.	0.460	0.429	0.252	0.226
Tb	0.123	N.d.	0.075	0.238	0.077	0.078	0.041	0.036
Dy	N.d.	0.371	N.d.	N.d.	N.d.	0.540	0.282	N.d.
Ho	N.d.	N.d.	N.d.	N.d.	0.109	0.121	0.059	0.050
Er	N.d.	0.254	N.d.	N.d.	0.306	0.363	0.134	0.148
Tm	N.d.	N.d.	N.d.	N.d.	0.047	0.055	0.027	0.021
Yb	0.169	0.261	0.330	0.107	0.295	0.357	0.173	0.134
Lu	0.034	0.041	0.055	0.019	0.057	0.059	0.030	0.023
Total	1.64	3.33	3.89	2.16	5.46	4.64	7.37	4.88
$(La/Yb)_n$	1.41	1.24	2.42	3.46	2.90	0.66	7.65	11.5

(*Continued*)

Table 2.2 Continued

	Provinces							
	Kerguelen (5)	Spitsbergen (5)	Hawaii (4)	The Komory Islands (2)	Ile Bizard (4)	Dariganga (4)	Wangqing (3)	Assab (9)
Element	*Harzburgites*							
La	0.988	1.823	0.648	0.610	0.913	5.005	0.590	0.522
Ce	1.848	4.174	0.790	1.115	1.918	9.370	1.123	1.050
Pr	0.218	N.d.	0.209	0.420	N.d.	N.d.	0.140	N.d.
Nd	0.842	2.572	1.105	1.720	1.093	4.400	0.623	0.506
Sm	0.152	0.624	0.222	0.840	0.338	0.900	0.180	0.097
Eu	0.051	0.196	0.073	0.300	0.128	0.261	0.057	0.037
Gd	0.156	N.d.	0.210	1.370	N.d.	0.648	0.167	0.134
Tb	N.d.	0.114	0.040	0.240	0.035	N.d.	N.d.	0.021
Dy	0.094	N.d.	0.318	1.595	N.d.	0.455	0.127	N.d.
Ho	0.017	N.d.	0.043	0.325	N.d.	N.d.	N.d.	N.d.
Er	0.044	N.d.	N.d.	1.030	N.d.	0.175	0.080	N.d.
Tm	N.d.	N.d.	N.d.	N.d.	N.d.	N.d.	N.d.	0.022
Yb	0.046	0.290	0.093	0.775	0.120	0.125	0.093	0.085
Lu	N.d.	0.040	0.016	0.125	0.024	0.019	0.010	0.018
Total	4.46	N.d.	N.d.	10.5	N.d.	21.36	3.19	N.d.
$(La/Yb)_n$	11.7	3.84	5.20	0.61	8.05	24.8	4.13	5.09

Data Table 2.1.

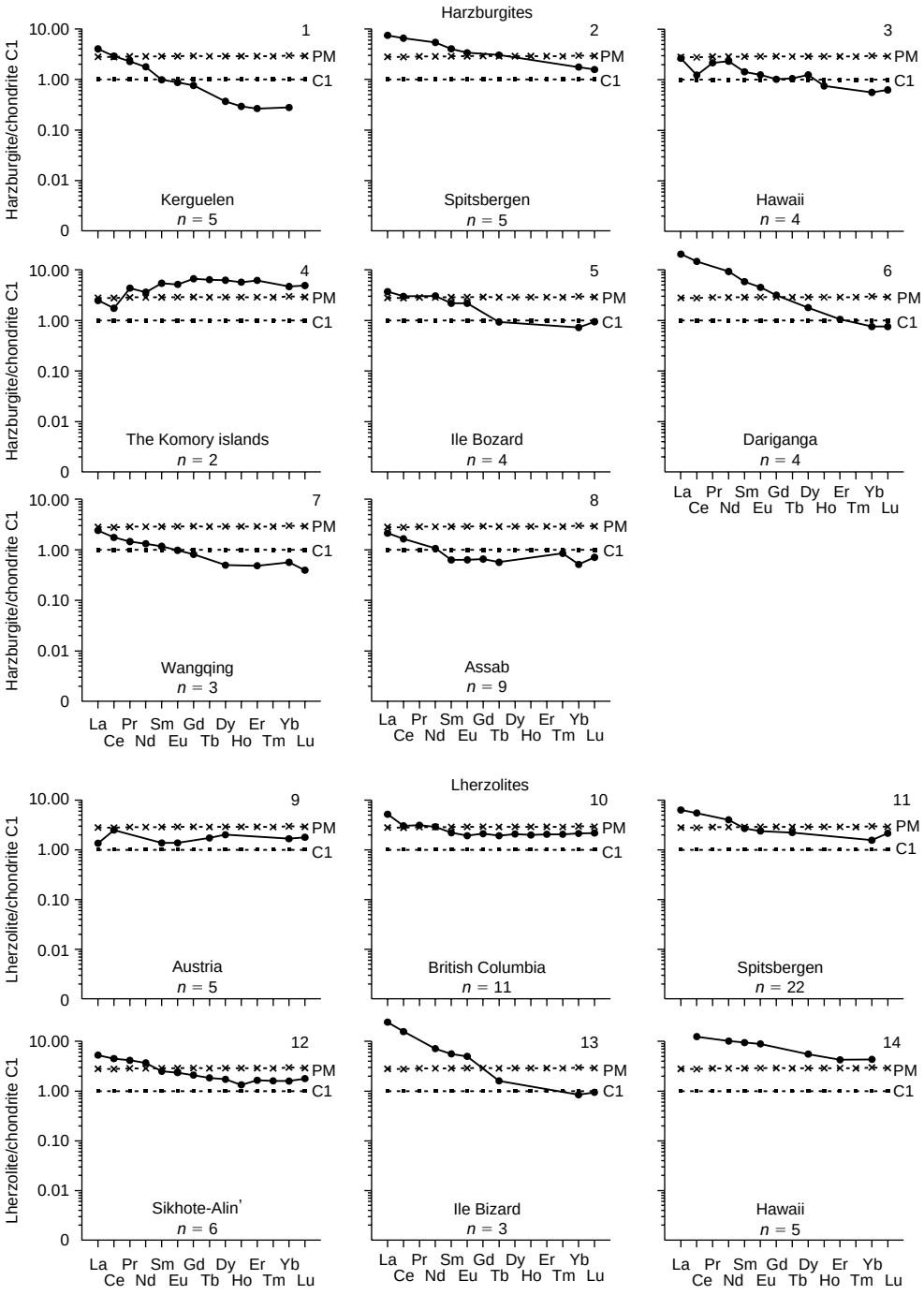

Figure 2.2 Chondrite-normalized REE patterns for average compositions of harzburgites, and lherzolites from deep xenoliths from some alkaline basalt provinces (data Table 2.2).

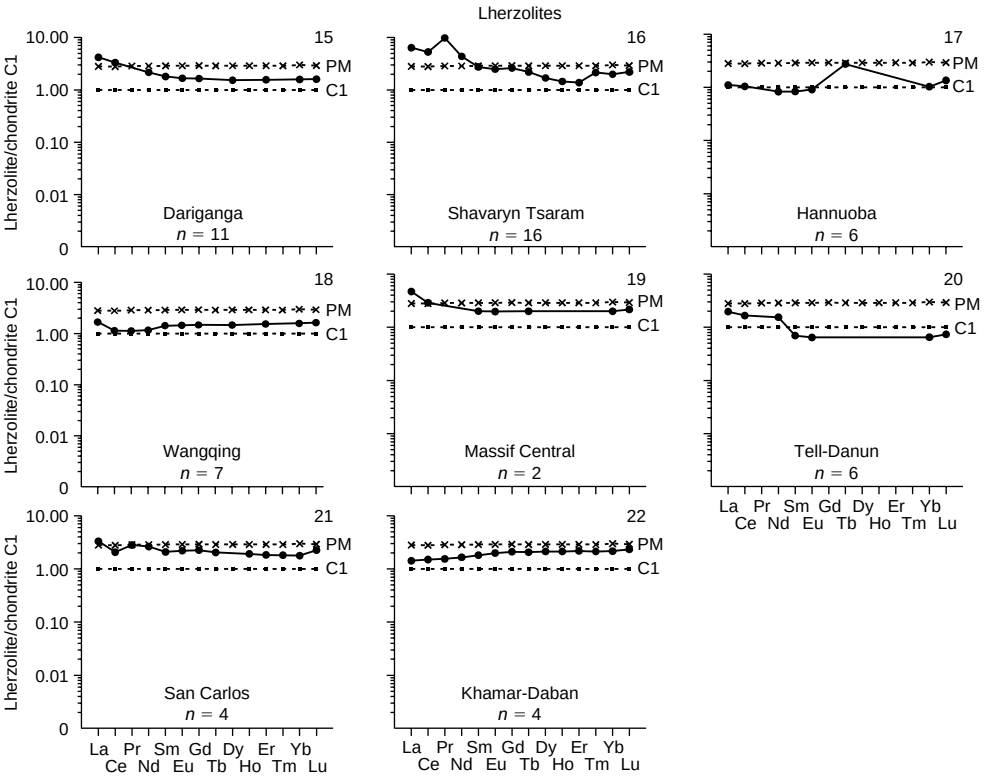

Figure 2.2 Continued

Most distinctly, this inconsistency is seen in those provinces where detailed geochemical studies of xenoliths were conducted, for example, in British Columbia (Sun & Kerrich, 1995), Spitsbergen (Shubina *et al.*, 1997), Dariganga (Wiechert *et al.*, 1997), Shavaryn Tsaram (Stosch *et al.*, 1986), and Dreiser Weiher (Stosch & Seck, 1980). These ultramafic xenoliths are enriched to a variable degree by light REE, and, therefore, the REE patterns often demonstrate a negative slope, that is, $(La/Yb)_n$ is greater than unity. At the same time, along with xenoliths enriched in light REE, some provinces contain a few ultramafic xenoliths that are appreciably depleted of, or very poorly enriched with, light REE, and these rocks have REE patterns that are almost flat shaped.

On the basis of representative data about the chemical composition and geochemical properties of deformed lherzolites from xenoliths present in the kimberlitic Udachnaya pipe (Yakutia), Agashev *et al.* (2008) showed that in these ultramafic rocks, the contents of the most incompatible element impurities (Rb, Th, Nb, light REE) are 2–10 times above those in a model of the primitive mantle, while contents of heavy REE are much lower than those in the primitive mantle. Calculations of the conditions of partial melting of mantle sources together with the use of data on the composition of deformed lherzolites show that kimberlites from the Udachnaya pipe are identical in composition to melts generated at a degree of partial melting of about 1%.

Lesnov *et al.* (2008, 2009a,b) used the ICP-MS method to investigate the distribution of incompatible elements (REE, Ba, Sr, Rb, Zr, Hf, Nb, Ta, Th, U) within large

xenoliths of spinel lherzolites. Irregular enrichment by light REE was found in bulk samples of lherzolite from various zones of xenoliths. Results of experiments on leaching lherzolite samples in a subacidic environment show that the rock contains easily soluble compounds in which the content of La (in particular) can reach 50%. The relation $(La/Yb)_n$ in these compounds appears to be sharply raised (100–130). The authors concluded that for geochemical systematization of mantle ultramafic restites, as well as for reconstruction of the processes proceeding in the top mantle, it is necessary to "subtract" irregularly distributed non-structural impurities of incompatible elements which are usually concentrated at borders of mineral grains, in the microcracks, and also in microinclusions.

Lesnov *et al.* (2009c,d) used data obtained by the ICP-MS and LA ICP-MS methods and from results of microprobe analyses and established that the real distribution of incompatible element impurities, in particular light REE, in lherzolites from large xenoliths and in its minerals, differs from the modeled microelement composition. The products of weak acid leaching of lherzolite samples included, besides the raised contents of light REE and other large ionic elements, appreciable quantities of Ca and P. The authors concluded that besides a structural impurity of incompatible elements in minerals of lherzolite, this rock contains a non-structural impurity that is non-uniformly distributed in their microfractures. The most probable mechanism of accumulation of this non-structural impurity in lherzolite and its minerals is considered to be infiltration of fluids rich with such elements separating from basalts, and the main concentrator of light REE in the microfractures is the apatite microphase.

Over all analyses of ultramafic xenoliths, the maximum light REE content is almost two orders of magnitude higher than the minimum light REE content. This difference is many times more than the parameter for heavy REE. According to our calculations, the average total REE content in all considered ultramafic xenoliths is about 7 ppm, which is close to their average total content in the primitive mantle—7.4 ppm (Sun & McDonough, 1989). In comparison with the primitive mantle, almost all ultramafites from deep-seated xenoliths are considerably depleted of heavy and middle REE, but are enriched with light REE to various extents. Note, that REE patterns of ultramafic xenoliths are similar to patterns of alkaline basalts of oceanic islands (OIB), but OIB rocks differ in total level of REE concentration.

Lherzolites, harzburgites, and dunites from deep xenoliths differ in the average content of individual REE (Table 2.3, Fig. 2.3). Thus, dunites are depleted of middle and heavy REE, concentrations of which are much lower than those in chondrite C1, but La and Ce concentrations in dunites, on the contrary, are higher than those in chondrite. The average total content of REE in dunites (3.2 ppm) is almost twice as low as this parameter in harzburgites (6.7 ppm) and lherzolites (5.6 ppm). The last estimation can be regarded as more exact than the other values, taking into account the high number of analyses used to calculate this value. Patterns of average REE content in harzburgites and lherzolites occupy an intermediate position between the patterns for chondrite and the primitive mantle, but La and Ce concentrations in both rocks are higher than those in the primitive mantle.

To a first approximation, the available analytical data on REE distributions have allowed researchers to subdivide ultramafites from deep-seated xenoliths in alkaline basalts into three geochemical types. The first type includes about 20% of all analyzed samples of rocks. These rocks are essentially depleted in light REE, and, as a result,

Table 2.3 Average REE composition of dunites, harzburgites, and lherzolites from deep xenoliths from some alkaline basalt provinces (ppm).

Element	Dunites (4)	Harzburgites (37)	Lherzolites (140)
La	0.850	1.352	1.028
Ce	1.278	2.615	2.138
Pr	0.145	0.240	0.340
Nd	0.480	1.434	1.166
Sm	0.083	0.341	0.334
Eu	0.032	0.110	0.100
Gd	0.093	0.428	0.335
Tb	0.022	0.052	0.082
Dy	0.073	0.571	0.368
Ho	0.017	0.184	0.078
Er	0.056	0.333	0.244
Tm	0.011	0.022	0.042
Yb	0.061	0.164	0.244
Lu	0.016	0.028	0.041
Total	3.16	6.68	5.56
$(La/Yb)_n$	11.2	8.01	4.60

Data Table 2.3.

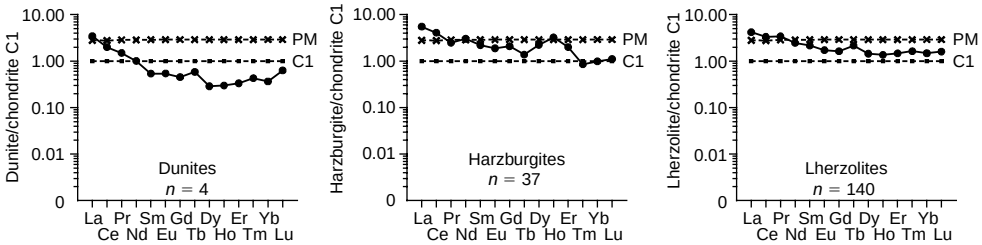

Figure 2.3 Chondrite-normalized REE patterns for average compositions of dunites, harzburgites, and lherzolites from deep xenoliths from all alkaline basalt provinces (data Table 2.3).

their REE patterns have a general positive slope and are described by values of the parameter $(La/Yb)_n$ less than unity. This geochemical type is represented, in particular, by lherzolite samples from Spitsbergen Island, Dariganga, Shavaryn Tsaram, and British Columbia. Ultramafites that are related to this geochemical type are comparable in all parameters of REE distribution to ultramafic rocks, which are contained in massifs that developed in folded areas on the continents and in mid-oceanic ridges and enter into ophiolitic associations.

The second geochemical type includes about 40% of the whole collection of analyzed xenoliths. These samples are slightly enriched in light REE in comparison with ultramafites of the first type; many of them have almost flat REE patterns, and values of the parameter $(La/Yb)_n$ are often close to unity. Ultramafites of this geochemical type occur more often among xenoliths from Khamar Daban, Wangqing, Austria, Dariganga, Shavaryn Tsaram, and Spitsbergen.

The amount of analyzed samples of ultramafic xenoliths that are related to the third type is also about 40%. These rocks are the most specific in their geochemical characteristics. All of these are considerably enriched with light REE, so, as a consequence, their

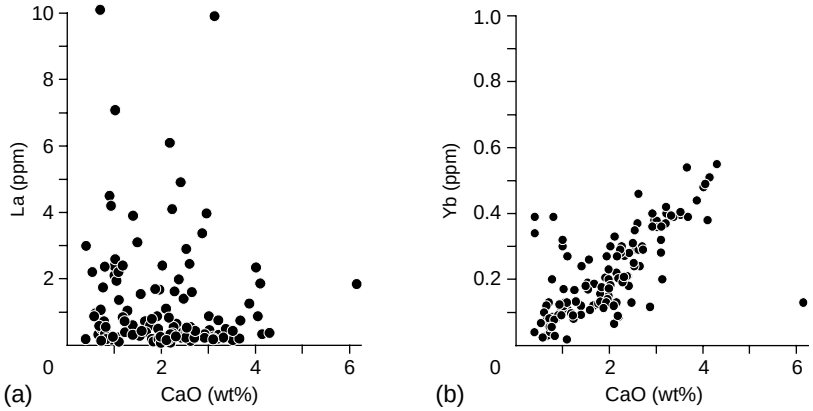

Figure 2.4 Correlation between CaO–La (a), and CaO–Yb (b) compositions of harzburgites and lherzolites from deep xenoliths from some alkaline basalt provinces.

REE patterns are usually characterized by a strong negative slope and are described by very high values of the parameter $(La/Yb)_n$, which vary from 10 to 52. Ultramafites of this type often occur among xenoliths from Ile Bizard, Tell-Danun, Kerguelen Island, Dariganga, Shavaryn Tsaram, British Columbia, Dreiser Weiher, and Spitsbergen Island. As shown from observations, their anomalous enrichment in light REE does not depend on modal composition. In many alkaline basalt provinces, ultramafites of this type occur along xenoliths, indistinguishable in petrographical features, but relating to the previous two geochemical types.

The important distinctive feature of ultramafites from deep-seated xenoliths is that their light REE content, including La, does not correlate with CaO content (Fig. 2.4, a), while Yb content directly depends on CaO content (see Fig. 2.4, b). At the same time, the relationship between La and CaO contents in separate sets of analyses of harzburgite and lherzolite xenoliths, along with similitude signs, testify to some specificity of composition of samples from Spitsbergen and Wangqing (Fig. 2.5). So, in diagrams for both these provinces, figurative points of harzburgite and lherzolite xenoliths reveal signs of discreteness in distribution of CaO content. Lherzolite and harzburgite xenoliths from Spitsbergen differ in their CaO content, but are similar in their La content. The same rocks from xenoliths of Wangqing province differ in La content (see Fig. 2.5).

As the La content in lherzolites and harzburgites increases, the contents of other mobile rare elements, for example Th, U, and K_2O, also increase. In addition, Yb content in harzburgite and lherzolite samples increases with increasing Ti content (Fig. 2.6). Probably, this relation is caused by the fact that the main mineral concentrator of both the elements in this case is clinopyroxene. It should be noted that on the basis of the analyses of ultramafic xenoliths from different provinces, the trend of inverse dependence between values of the parameter $(La/Yb)_n$ and CaO content in the rocks (Fig. 2.7) is revealed.

Using the data on REE composition of ultramafic xenoliths, it is possible to conditionally subdivide alkaline basalt provinces into two categories. The provinces of Wangqing, Tell-Danun, Hannuoba, San Carlos, and Khamar Daban, the majority

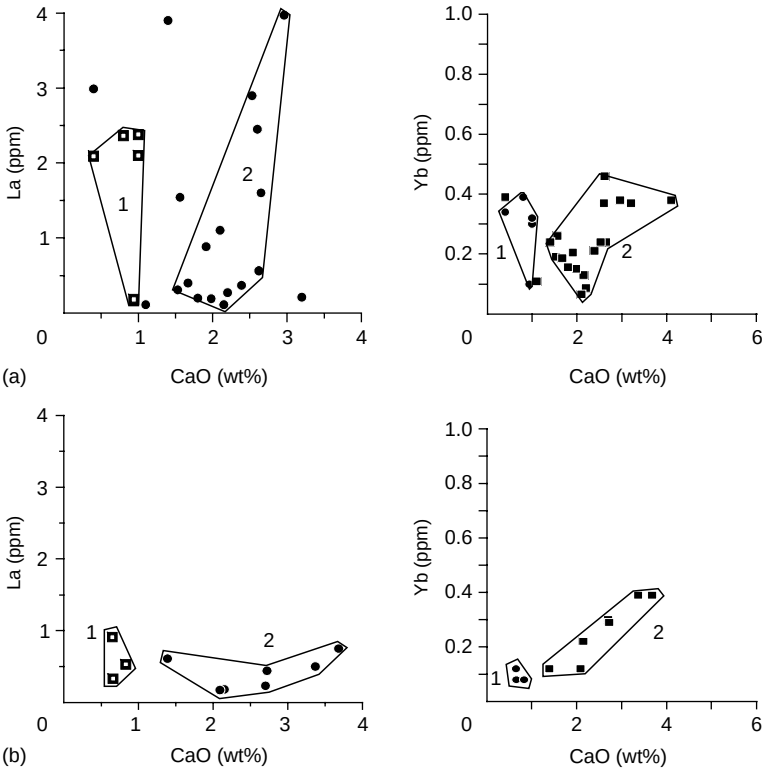

Figure 2.5 Correlation between CaO–La and CaO–Yb composition of harzburgites (1) and lherzolites (2) from deep xenoliths from Spitsbergen (a) and Wangqing (b) alkaline basalt provinces.

of xenoliths from which show unimodal distributions of both heavy and light REE, are related to the first category. REE patterns for xenoliths from these provinces are arranged compactly and are in many respects similar in their configuration, that is, they are concordant (see Fig. 2.1, 12, 16, 17, 21, 22).

The second category is represented by alkaline basalt provinces with xenoliths that are characterized by a close to unimodal distribution of heavy REE, while light REE display a clearly expressed bimodal distribution (see Fig. 2.1, 3, 4, 9, 10, 13, 14, 15, 18, 19). The last feature is caused by the fact that in these provinces, for example, Spitsbergen, Dariganga, Shavaryn Tsaram, Western Germany, British Columbia, Sikhote-Alin', and Victoria, xenoliths that are variably enriched in light REE are alongside ultramafic xenoliths that are variably depleted in light REE. We suppose that in a detailed geochemical study of ultramafic xenoliths in an individual province, the bimodal distribution of light REE will probably not be so apparent because of the presence of xenoliths that have intermediate contents of these elements between, on the one hand, depleted samples, and on the other hand, strongly enriched samples. One example of such distribution of REE in ultramafic xenoliths is the Spitsbergen province (see Fig. 2.1, 8).

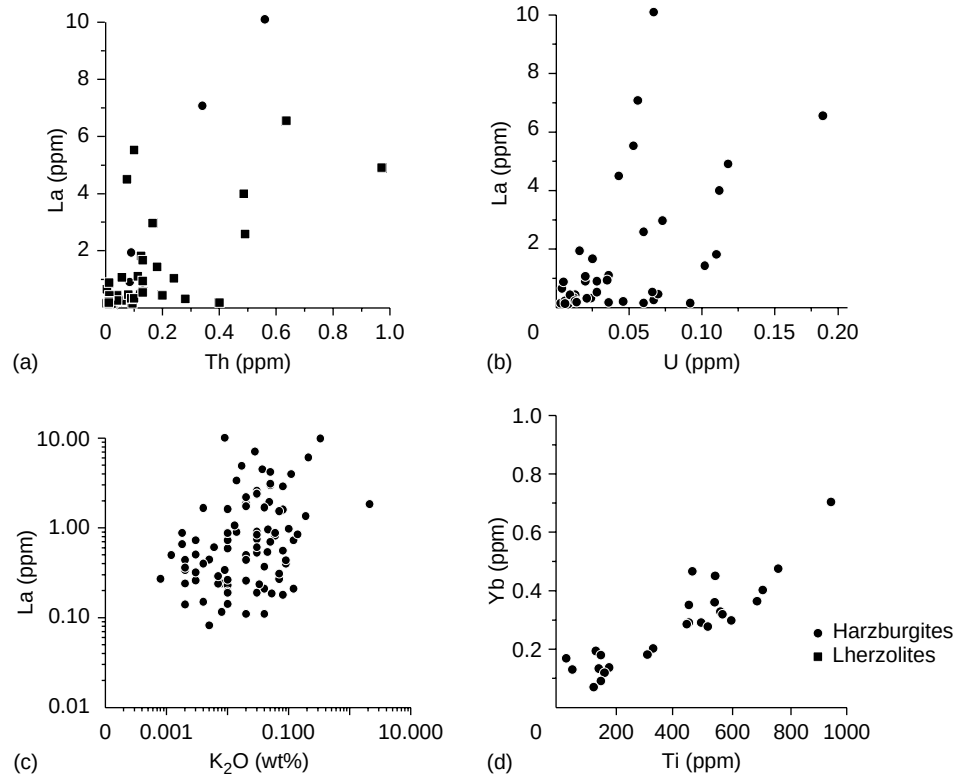

Figure 2.6 Correlation between La compositions and Th (a), U (b), K_2O (c), Yb, and Ti (d) compositions of harzburgites and lherzolites from deep xenoliths from some alkaline basalt provinces.

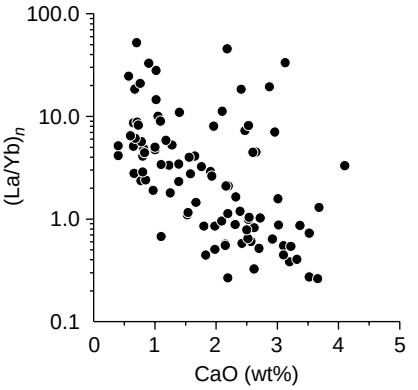

Figure 2.7 Correlation between CaO composition and parameter $(La/Yb)_n$ of ultramafic rocks from deep xenoliths from different alkaline basalt provinces.

In some provinces, such non-uniform enrichment of ultramafic xenoliths by light REE, accompanied by bimodal distribution, is also observed at the mineral level. In particular, this fact was established based on the results of REE analyses in clinopyroxenes from ultramafic xenoliths of a province located in Canadian Cordillera (Shi *et al.*, 1998). By contrast, in clinopyroxenes from lherzolite xenoliths sampled in a province located in Poland, practically all analyzed samples displayed anomalous enrichment with light REE, which is responsible for the unimodal form of the frequency histograms of La and Ce content (Blusztajn & Shimizu, 1994). Furthermore, there is some evidence for enrichment of clinopyroxenes from ultramafic xenoliths by light REE only in narrow (about 1.5 mm) rim zones of their grains (Yang *et al.*, 1998).

Apart from REE, the considered ultramafites from deep-seated xenoliths of many provinces were analyzed for other rare elements, including Rb, Th, U, Pb, Y, Ti, K, Hf, Li, Sr, Zr, Nb, and Ba. In this respect, xenoliths in Dariganga (Wiechert *et al.*, 1997), Sikhote-Alin' (Ionov *et al.*, 1995b), and Tell-Danun (Sharkov *et al.*, 1996) are characterized in more detail. Contents of the majority of the aforenamed elements vary over very wide limits. Estimations of their average contents show that lherzolite, harzburgite, and dunite xenoliths are slightly enriched in Rb, Th, U, and Pb, but are depleted in Y, Ti, K, and Hf in comparison with the primordial mantle (Sun & McDonough, 1989). However, the contents of certain rare elements, such as Li, Sr, Zr, Nb, Ba, and Ta, do not differ between ultramafites from deep-seated xenoliths and the primitive mantle. The contents of Th, U, and K in ultramafic xenoliths are in direct proportion to La content. The same dependence is observed between Yb and Ti contents.

All available data on distributions of REE and other rare elements in deep-seated ultramafic xenoliths from alkaline basalts suggest that these rocks have some geochemical features that should not be observed in essentially depleted mantle restites, as is evident from the model of partial melting. Many investigators (Nagasawa *et al.*, 1969; Philpotts *et al.*, 1972; Frey & Green, 1974) long ago paid attention to this geochemical specificity of ultramafic xenoliths. Further investigations have confirmed the early observations (Frey, 1984; Ionov, 1988a,b). In these works, it was noted that, in spite of significant inhomogeneity and frequently observable anomalous enrichment of the ultramafites by light REE and other mobile rare elements, these rocks are characterized by a rather stable distribution of heavy REE. Some researchers proposed that the distribution of REE and other incompatible elements in ultramafites from deep-seated xenoliths are caused by the fact that these elements occur not only as a structural impurities in rock-forming minerals, but also as a non-structural impurities localized in intergranular and intragranular microcracks, and also in new-formed phases.

At the first stages of the geochemical study of ultramafic deep-seated xenoliths, researchers supposed that the composition of these rocks is characterized by the presence of two genetically not connected associations of chemical elements called "components" A and B (Frey & Green, 1974). Frey and Green supposed that "component" A includes the major elements and some compatible elements (Sc, V, Cr, Co, Ni, and heavy REE) that were concentrated in minerals during mantle restite formation, that is, at extraction of basalts melts from mantle pyrolite. Incompatible elements, such as K, Ti, P, Th, U, as well as light REE were included in "component" B. Later while studying ultramafic xenoliths from the Dreiser Weiher province, Stosch and Seck (1980) proposed to distinguish two geochemical types of ultramafic xenoliths. According to these authors, rocks belonging to the first type are characterized by a light REE

content at a level similar to that of chondrite C1 or slightly higher, and by an absence of amphibole. Ultramafites of the second type are to some extent enriched with light REE and usually contain a minor quantity of amphibole. Moreover, enrichment with light REE was established in rock-forming minerals from ultramafites of the second type: olivine, orthopyroxene, and clinopyroxene. The enrichment with light REE of the ultramafic rocks relating to the second type, as well as the presence of amphibole in them, are supposed to be due to the same process, namely, a later affect of fluids enriched with REE on ultramafites related to the first type. A similar affect of fluids and introduction of mobile elements could take place at all stages of transportation of deep-seated ultramafic xenoliths to the day surface.

McDonough and Frey (1989) generalized a significant amount of REE analyses and data on their distribution in xenoliths of spinel peridotites from many alkaline basalt provinces and paid attention to the following conditions. Firstly, rather wide variations of $(La)_n$ and the parameter $(La/Yb)_n$ in these peridotites were established. Secondly, it was shown that anhydrous xenoliths, that is, xenoliths not containing amphibole and/or phlogopites, usually have low contents of $(La)_n$ (<1) and low values of the parameter $(La/Yb)_n$ (<1), and these parameters show an inverse dependence with CaO and Al_2O_3 contents in the rocks. These features are distinct from previously studied hydrous peridotites from xenoliths, in which amphibole and/or phlogopites are present, in that hydrous peridotites usually have high values of $(La)_n$ (>1) and $(La/Yb)_n$ (>1), and these parameters do not show a distinct inverse relationship with CaO content. For pyroxenite xenoliths, McDonough and Frey (1989) also revealed very wide variations of light REE concentration, so many of them have a negative slope in their REE pattern. Noting, that the peridotites from xenoliths often have higher values of the parameter $(La/Yb)_n$ in comparison with clinopyroxenes from xenoliths, these authors came to the opinion that light REE can concentrate in significant amounts at boundaries of mineral grains as well as in fluid inclusions.

According to data by Kovalenko *et al.* (1989), ultramafites from deep-seated xenoliths usually contain a so-called "contaminant" presenting in variable quantities, that is, a substance that has been introduced to these rocks at later stages of their evolution. These authors considered that similar "contaminant" should be concentrated mainly in intergranular space. A microscopic study of xenoliths revealed that it is represented by a mat thin coating on the surface of mineral grains. After the crushed samples of ultramafic rocks were subjected to leaching by a strongly diluted solution of hydrochloric acid, the mat thin coating on grains disappeared. The analysis of samples after leaching and careful washing showed that the contents of light REE decreased by one to two orders of magnitude in comparison with their initial quantities (before leaching), while the contents of heavy REE were retained at their original level.

The results of an investigation by Kovalenko *et al.* (1989) show that in ultramafic xenoliths the contents of heavy REE and CaO are in a direct relationship, while light REE content directly depends on CaO content in only those xenoliths where any "contaminant" is absent. Detected "contaminant," which is the concentrator of a significant amount of light REE, is not connected genetically with primary substance of ultramafites. Heavy REE as an isomorphous impurity enter mainly in the composition of clinopyroxene, which occurs in variable quantities in ultramafic xenoliths. The results of the investigation by Kovalenko *et al.* coincide with the data described above on anomalous enrichment with light REE of clinopyroxenes from peridotite

xenoliths occurring among alkaline basalts in Poland (Blusztajn & Shimizu, 1994). In addition, it should be noted that, in some cases, the anomalous enrichment of olivines and orthopyroxenes in ultramafic rocks with light REE is supposed to be caused by the presence of secondary fluid inclusions in the minerals (Stosch, 1982; Lesnov *et al.*, 1998b,c; Lesnov, 2000a). Having considered the possibilities of using the Sm–Nd isotopic system to determine the model age of ultramafites from mantle xenoliths, Pushkariov *et al.* (2004) came to a conclusion that such dating is impossible; in the process of transportation to the crust the mantle xenoliths of ultramafites were practically always subjected to contamination by REE from the carrying magmatic melt. Simon *et al.* (2008) generalized the representative data on chemical composition and geochemical features ultramafic xenoliths from basalts of a series of oceanic islands—Azores, Canary, Madeira, Kerguelen. The researchers established that these xenoliths are mainly represented by harzburgites which can be divided into two types. The first type concerns ultradepleted harzburgites, while the second type concerns their enriched varieties. The first type of harzburgite differs from the second in the absence of primary clinopyroxenes, lower contents of Al_2O_3 and CaO, lower values of FeO/MgO, lower contents of heavy REE, lower content of Al_2O_3 in orthopyroxenes, and also higher content of chromous spinel. In orthopyroxenes and clinopyroxenes from harzburgite xenoliths from basalts of the Canary and other islands, the irregular enrichment with light REE and relatively heavy elements is observed.

Thus, the presented data allow suggesting that a distinctive feature of ultramafites from the majority of deep-seated xenoliths is their anomalous enrichment with light REE and other mobile elements. Similar enrichment with light REE is stipulated by their accumulation, firstly, as non-structural impurities in intergrain and intragrain microcracks, secondly, in the composition of secondary fluid inclusions in rock-forming minerals and, thirdly, as a structural impurity in new-formed minerals, in particular in amphiboles and micas. At the same time, it is impossible to consider the regarded problem as being solved, as there is no consensus concerning the origins of the geochemical features of ultramafites from deep-seated xenoliths. Let's consider this question in more details. During some time, investigators discussed a hypothesis supposing that the enrichment of ultramafites from deep-seated xenoliths with light REE and other mobile elements is connected with deep-seated processes, named "mantle metasomatism" (Frey & Prinz, 1978; Roden *et al.*, 1984). Two varieties of such metasomatism were recognized: evident and latent. An evident "mantle metasomatism" means a process in which enrichment of ultramafic xenoliths with light REE is accompanied by the appearance of water-bearing phases, such as amphibole and mica. Latent "mantle metasomatism" means that enrichment of ultramafites with light REE proceeds without formation of water-bearing phases. In the opinion of these investigators, the enrichment of ultramafic rocks of xenoliths in light REE takes place as a result of seepage through the rocks of mantle fluids, which are rich in light REE, CO_2, and Sr, but poor in Zr, Hf, Nb, and Ti. According to another idea, a source of fluids, stipulated "mantle metasomatism" of ultramafic xenoliths, were carbonatite melts (Dupuy *et al.*, 1992; Ionov *et al.*, 1993b).

Available published data and original observations (see Sections 5.1–5.3, and also (Lesnov *et al.*, 2007)) allow us to offer another point of view concerning the considered problem. We believed that the source of fluids that introduced mobile elements into ultramafic xenoliths can be not only the upper mantle itself, but also those alkaline

basalts which carried the xenoliths to the surface. A priori it is possible to assume that a heterogenic system "*xenolith of ultramafic restite—alkaline basalt melt*," which formed in upper mantle chambers at the certain stages, was initially not in chemical equilibrium. We proceed from the assumption that alkaline basalt melts uplifting from a melting chamber have higher temperatures than those of earlier generated and, in part, already cooled ultramafic restites. In addition, the contents of incompatible and volatile components in basalts melts was incomparably higher than those injected by them into ultramafic restites, xenoliths of which were then trapped by basalts. For these reasons, one can assume that from the moment of its origination an evolution of the regarded non-equilibrium system "*xenolith of ultramafic restite—melt of alkaline basalt*" was directed towards achievement of thermal and chemical equilibrium, that is, leveling of the temperature and concentration of mobile components. As basalts with xenoliths uplifted to the surface, the pressure and temperature in the system decreased. Then, the fluids enriched with mobile components filtered from the melt into ultramafic xenoliths along the macrocracks and microcracks, and deposited soluble compounds that were rich in incompatible elements, including light REE, into the rocks. During the short-term rise of basaltic melts to the surface, obviously, almost complete balance in fluid pressures in the melt and in rather small xenoliths was attained; the xenoliths were saturated by fluids and, accordingly, mobile components were uniformly introduced over the whole volume. In larger xenoliths, equilibrium distribution of fluid and enrichment with mobile elements could come only in their external zones that resulted in geochemical zonality of such xenoliths, including in relation to light REE distribution. Apart from the deposition of light REE-enriched "contaminant" in microcracks, some quantities of light REE could remain in fluid inclusions in minerals such as olivine, orthopyroxene, and clinopyroxene.

In some cases, under the effect of fluids that emanated by basaltic melt and containing essential quantities of water, the primary minerals of ultramafites were subjected to hydration, while being replaced by amphibole or micas. As a result of these processes, the REE that represent non-structural impurities were added to the REE that occur as a structural impurity in primary minerals of the restites. In these ultramafic xenoliths, which were not subjected to fluid infiltration or to enrichment of light REE for various reasons, the light REE content did not change, that is, the light REE content is directly dependent on the amount of modal clinopyroxene and, accordingly, on the calcium content in the rocks. In those xenoliths which were subjected to intensive infiltration of fluids and anomalous enrichment by light REE, the direct dependence of light REE content on the modal amount of clinopyroxene and, accordingly, on CaO content, was disturbed. At the same time, heavy REE, which were not introduced by fluids and are completely concentrated in the clinopyroxene structure, a similar direct dependence was maintained. Note that the fluids that emanated from basalts introduced, along with light REE, incompatible elements such as U, Th, K, and other elements to ultramafic xenoliths. The enrichment of ultramafic xenoliths by these large ion elements as a result of so-called "mantle metasomatism," as believed by some researchers, looks problematic.

Let's consider several aspects of interpretation of anomalous accumulation of light REE in ultramafites from deep-seated xenoliths. As is known, for a long time the determination of REE in various rocks was carried out mainly by the instrumental or radiochemical neutron activation methods, in which rather light specimens of bulk

rock samples are used. Quite clearly, the contribution of non-structural impurities of REE to the total content of REE in the samples is impossible to estimate using these methods. Apparently, without preliminary leaching of samples, or without ICP-MS with application of laser ablation, it is impossible to determine precisely the contents of REE as isomorphic impurities in minerals.

As noted above, ultramafites from deep xenoliths are anomalously enriched in light REE very in a non-uniform way, and this variability is seen in comparisons of xenoliths from various provinces as well as between samples from a single province. The certain gradients of light REE concentrations are observed in limits of large xenoliths, and even in individual mineral grains. It does not coincide with the hypothesis of "mantle metasomatism," which is supposed to proceed at large depths under high pressure and temperature conditions, and for a significant time. It is obvious that at such conditions the probability of appearance of the raised irregularity of light REE distributions, which is observed in ultramafic xenoliths, is very low. The hypothesis that suggests that this geochemical feature is caused by the introduction of rare elements by fluids, which were separated from basaltic melts during their transportation from the upper mantle to a day surface, is believed by us to be a more valid theory.

The non-structural impurity of light REE in ultramafic xenoliths can occur not only as a "contaminant" in microcracks, but also in the composition of fluid inclusions, conserved in mineral grains. Apparently, such fluid inclusions, being specific microdefects of crystal structure of minerals, could essentially decrease the physical strength of this structure. It is improbable that such microdefects in mineral structures appeared at a level of the upper mantle under conditions of high pressures at which basaltic melts captured ultramafic xenoliths. Therefore light REE-enriched fluid inclusions in minerals of ultramafic xenoliths most likely were formed at rather low pressures as a result of the infiltration of fluids, separated from basaltic melts, transporting xenoliths.

* * *

According to widespread petrological notions, ultramafites contained in deep-seated xenoliths in alkaline basalts are upper mantle restites. Among these ultramafites, lherzolites are predominant, while harzburgites and dunites occur rarely. In many structural, petrochemical, and petrographical features, restites from deep xenoliths do not differ from ultramafic restites, which are contained in numerous ultramafic and mafic–ultramafic massifs in continental folded areas and mid-oceanic ridges. To tell the truth, sometimes they can contain high-pressure minerals (garnet, spinel) or new-formed phases (plagioclase, amphibole, mica), and in some cases, small inclusions of weakly crystallized basalt. Distinctly from ultramafites from massifs, their analogs in deep xenoliths, as a rule, are characterized by a variably anomalous and usually non-uniform enrichment with light REE and other incompatible elements. Such enrichment is caused by the wide presence of various quantities of non-structural impurities of light REE in these rocks. Light REE as soluble compounds are concentrated in intergrain and intragrain microcracks, as well as in fluid inclusions in minerals. The total content of REE in harzburgite xenoliths from different provinces varies from 2.4 to 21.0 ppm. Approximately the same interval of variations of total REE content (1.6–20.9 ppm) is observed in lherzolites. REE patterns of the majority of studied ultramafites from

deep-seated xenoliths are characterized by a negative slope owing to their anomalous enrichment in light REE.

During its appearance at the upper mantle level, the system of "xenolith of ultramafic restite—alkali basalt melt" was in non-equilibrium conditions in relation to both temperature and geochemical features, including the contents of incompatible elements. During uplifting of basaltic melts with ultramafic xenoliths to the surface, this system developed towards the achievement of equilibrium in relation to contents of mobile components, by which ultramafites were enriched under the effect of basaltic melts and their fluids. As a result of this process, light REE and other mobile elements non-uniformly accumulated in microcracks of ultramafic xenoliths, as well as in fluid inclusions in minerals. For a rather short-timed uplifting of melts, the fluids are capable "of filtering" within the whole volume of relatively small xenoliths. During the same time interval, these fluids could penetrate larger xenoliths only in their rim zones, which caused a rather non-uniform distribution of impurities in such xenoliths.

Chapter 3

Rare earth elements in hypabyssal and subvolcanic rocks with high in magnesium composition

This chapter deals with the characteristics of REE distribution in kimberlites, komatiites, meimechites, picrites, and lamproites. All these rocks are characterized, on the one hand, by relatively increased contents of refractory components including magnesium, and, on the other, by more or less increased contents of incompatible elements including REE, particularly light ones. According to the commonly held view, all these rocks crystallized at relatively moderate depths or under surface conditions (Bogatikov *et al.*, 1981). At the same time, many mineralogical, petrographical, geochemical, metallogenic, and genetic aspects of the rocks in question as well as the mechanisms of their mother melt generation remain the subject of ever more-detailed explorations and discussions. Special attention is paid to kimberlites and lamproites, which are genetically connected to diamondiferous deposits, and to komatiites, which are often associated with different-sized deposits of nickel, copper, and platinum metals. In summarizing the available data on the rare earth composition of the said varieties of small-depth rocks, use was made of the results, both borrowed from the literature and obtained with the author's participation, of about 300 original analyses of samples from a great number of manifestations.

3.1 KIMBERLITES

Kimberlites make up different-sized bodies shaped like pipes, dikes, or sills and are characterized by the diversity of their structures, textures, modal mineral content, and petrochemical composition. They often have a breccias structure; they contain megacrysts and xenocrysts of different minerals, as well as xenoliths of peridotites, eclogites, different crust rocks, and products of their transformation. All these components vary in amounts and sizes. All kimberlites are also characterized by an increased content of MgO and relatively a decreased content of SiO_2. There are different approaches to the systematic classification of kimberlites, in which, besides the structural and textural features, use is made of mineralogical and petrochemical criteria. In some cases, kimberlites are classified into kimberlite tuffs, breccias, varieties with a porphyric texture, as well as those enriched with olivine or mica. Sometimes kimberlites are divided into micaceous (containing more than 5% mica) and basaltic varieties. Vladimirov *et al.* (1990) proposed a mineralogical classification of kimberlites according to which they isolated olivine, calcite, monticellite–melilite, pyroxene,

and amphibole varieties of kimberlites. Vasilenko *et al.* (1997) developed a petrochemical classification of kimberlites based on dividing them into several material populations. Frequently used as distinctive features in the systematization of kimberlites are the contents of TiO_2, K_2O, and a number of other components, as well as such a criterion as the ilmenite index (Ilm. I. $= (FeO + TiO_2)/(2K_2O + MgO)$). To classify kimberlites according to the degree of their contamination by the enclosing rock, the C.I. index $((SiO_2 + Al_2O_3 + Na_2O)/(2K_2O + MgO))$ is usually used. The parameter Mg# $(100 \cdot MgO/(Mg + FeO_{tot}))$, which is used to systemize kimberlites from most of the explored regions, varies in the range of 64–84%. When studying the petrochemical and geochemical, as well as isotopic, characteristics of kimberlites from pipes of the Yakutian province, Bogatikov *et al.* (2004) proposed to divide these rocks according to TiO_2 content: low-titaniferous (<1 wt%), moderate-titaniferous (1.0–2.7 wt%), and high-titaniferous (>2.5 wt%). It has been observed that kimberlites from diamond pipes are characterized by moderate total contents of heavy REE (from Er to Lu), which vary in a narrow range—from 1.2 to 2.1 ppm.

3.1.1 A brief history of research on the geochemistry of REE in kimberlites

The peculiarities of the geological position, petrography, mineralogy, and geochemistry of kimberlites as well as the conditions of their formation have been intensively studied for over 150 years. Within this time interval, in addition to the kimberlite manifestations that were known earlier, new kimberlite pipes and whole regions have been revealed in different regions of the world. For a long period, the prevailing trends in studying these rocks have been geologo-structural, petrographical, petrochemical, mineralogical, and geochronological ones. At the same time, considerable attention has been paid to the ever more-detailed investigation of ultramafic abyssal xenoliths that are nearly always present in kimberlite pipes. The regularities of distribution in kimberlites of incompatible elements, including REE, have been studied to a lesser extent. However, at the very beginning of research into the geochemistry of kimberlites, it was established that these rocks are characteristically significantly enriched with light REE, and to a lesser degree, with middle ones, as well as with a number of other incompatible admixture elements. Later on, the results of geochemical investigations, which were obtained in ever-increasing amounts, began to find application in classifying both the kimberlites proper and the pipes formed by them, as well as in prognosticating the diamond content of the kimberlite provinces and in constructing petrogenetic models. Owing to this, the rare earth composition of kimberlites from many provinces has by now been studied in much greater detail than that of other magmatogenic rocks.

Dawson (1962) was the first to call attention to the fact that the accumulation level of some REE in kimberlites was abnormally high for magnesian magmatic rocks. Somewhat later, Burkov and Podporina (1966) were the first to determine the contents of nearly all REE in several samples from the Yakutian province. On further studying the geochemistry of kimberlites, these rocks were found to be second only to carbonatites, among magmatic rocks, in REE content. The extremely high contents of REE in kimberlites were assumed to be due to their enrichment with perovskite, which can contain up to 5 wt% REE, predominantly light ones (Frey *et al.*, 1971). In these

authors' opinion, the significant enrichment of kimberlites with light REE is an important genetic feature that should be taken into account when studying the conditions under which peridotite, and the eclogite xenoliths contained in them (which are also frequently enriched with light REE), are formed.

While studying the kimberlites from the Yakutian province, Ilupin *et al.* (1974) were the first to discover in them a directly proportional dependence between the contents of REE and those of CaO. Similar observations led Lutts and Frantsesson (1976) to the conclusion that the significant enrichment of kimberlites with REE is conditioned by the acid leaching of mantle substance under the action of fluids rich in the reduced volatile components H_2 and CO. In his first summary on the results of the complex investigation of kimberlites, Dawson (1983) noted that the investigations confirmed his initial conclusion that all kimberlites are abnormally enriched with REE, mainly light ones. He also noted that the REE patterns usually have a steep negative slope and are in the vast majority of cases characterized by an almost rectilinear form. Nevertheless, the patterns of some kimberlites from the Yakutian and the South African provinces exhibit negative Eu anomalies. Dawson assumed the reason for the occurrence of these anomalies to consist in the large amounts of perovskite and/or phlogopite, which rank among the main concentrator minerals of REE, in these rocks, along with diopside, garnet, and apatite. A belief has also been stated that the unusually high contents of heavy REE in some kimberlites of the South African provinces result from the presence of significant amounts of xenogenic grains of garnet, which occurred in the matrix of kimberlites due to the disintegration of the xenoliths of garnetferous ultramafites (Fieremans *et al.*, 1984). The linear forms of the kimberlite REE patterns as well as the presence of Eu anomalies on some of them were also noted by other explorers (Cullers & Graf, 1984a). Ilmenites and phosphates, apart from perovskite, are referred to as concentrator minerals in some kimberlites; these minerals are also capable of accumulating appreciable amounts of the REE (Chakhmouradian & Mitchell, 1999).

Limited data on the contents of some REE in the kimberlites from the Yakutian province were cited by Marshintsev (1986). According to his observations, the kimberlites of the so-called "pipe" type are characterized by higher values of the parameter $(La/Yb)_n$ than kimberlites from intrusive facies. He pointed to the presence in the kimberlites of the direct dependence between the total content of REE and the contents of CaO and P_2O_5. Marshintsev assigns apatites, perovskites, and, presumably, calcites to the main concentrators of REE in kimberlites.

Laz'ko (1988a) gave a brief generalized overview of the REE composition of kimberlites up to the corresponding period in his detailed review on their petrology. He noted that kimberlites differ from many magmatic rocks not only by their significant enrichment with REE, but also by sharply increased contents of other admixture elements, among them K, Ti, P, Rb, Sr, Ba, Zr, Y, Nb, Ta, Th, and U. While studying the geochemistry of the crusts of weathering on kimberlite pipes, Burkov (1990) discovered that their formation had been accompanied by REE fractionation, due to which the primary correlations between the admixture element contents had been subjected to transformation, with a tendency towards accumulation of the REE from Sm to Ho and simultaneous depletion of La and Ce.

Larsen and Rex (1992) drew attention to certain differences in the REE distribution in kimberlites from provinces occupying different structural and tectonic positions.

Nevertheless, they believe that the conditions of the formation of kimberlites were determined not only by structural and tectonic factors, including lithosphere composition, but also by the character of magmatic differentiation, to which their primary and residual melts were subjected. Ilupin *et al.* (1978) established that in the kimberlites from the African and Indian provinces, the amount of REE is 20–30% higher than that in the rocks from the Yakutian and South American provinces. On this ground they recognized two kimberlitic superprovinces: Gondwanian and Laurasian.

In recent years, considerable bodies of geological, petrographical, and geochemical information have been obtained on the kimberlites from the northwestern provinces of Russia. The studies carried out have shown, in particular, that the kimberlites from diatremes and sills of the Arkhangelsk province are characterized by a low common level of REE accumulation compared to the rocks from many other kimberlite provinces of the world (Parsadanian *et al.*, 1996). Evidence has also been obtained that indicates that kimberlites from the Terskiy Coast province (Kola Peninsula) are distinguished by higher contents of light REE than the rocks from the Kandalaksha province (Beard *et al.*, 1998). The authors state that kimberlites of the Terskiy Coast province crystallized from the melts formed at a very low degree of the partial melting of a carbonate-bearing mantle source; the SiO_2 content and the Nb/Y ratio in these melts were also determined by the degree of the partial melting of the source. According to the data of Bogatikov *et al.* (2003), kimberlites of the northern margins of the Russian plate, represented mainly by micaless varieties, have been depleted of REE to a greater extent than the typical kimberlites from many other provinces of the world (Mitchell, 1986).

Studies of kimberlites from Canada show that their heavy REE fractionation intensity, which is assessed by the value of the parameter $(Tb/Lu)_n$, varies within the range 4.6–5.9 and is somewhat lower than that of the light elements ($(La/Sm)_n = 9.9–12.1$) (Price *et al.*, 2000). In his comparative study on the rare earth composition of kimberlites and meimechites Arndt showed the former to be characterized by higher contents of La (Arndt, 2003). A significant amount of new research has recently been carried out on the geochemistry of REE and other admixture elements, and isotopic characteristics have been obtained for kimberlites from the Yakutian province using the ICP-MS method (Bogatikov *et al.*, 2004), and Egorov (2006) obtained, by use of the same method, new data on the distribution of the REE and other admixtures in kimberlites from some pipes in the northeastern regions of Angola province. Kargin *et al.* (2008) showed that complicatedly constructed, and also spatially draw together, kimberlitic pipes consisting of several petrographical varieties, could be formed both as a result of single phase, and as a result of two and more phase injections of portions magmatic melts. Thus, $(La/Yb)_n$ is considered one of the main geochemical informative criteria for assigning different phases of injection. It has been established that in kimberlites, one measure of injection correlation (light REE/heavy REE) remains stable.

Concluding therewith the brief review of the geochemical investigations on kimberlites one should emphasize that, according to the calculations made by Girnis and Ryabchikov (2005), kimberlite mantles could have been formed at low degrees of the partial melting of mantle peridotite in the garnet stability field with CO_2 participation. These authors also assumed that in the process of kimberlite formation proceeding at a pressure of about 6 GPa, magnesite-bearing harzburgites were probably subjected to partial melting. As for the assumed significant rates of the rise of the kimberlite melt to the upper crust levels, these appear to have been promoted by the emission of

significant amounts of CO_2. The said authors believe that the fast ascent of kimberlite mantles are one of the factors determining the preservation in the kimberlites of high-pressure minerals, diamonds among them.

3.1.2 Comparative characteristics of the REE composition of kimberlites from major provinces

Consider the most essential peculiarities of the REE distribution in kimberlites from the best known and minutely investigated provinces and superprovinces located in the territory of Australia, China, Canada, India, Finland, USA, South Africa (including Angola), Brazil, and Russia (Timan, Kola peninsula, Arkhangelsk, and Yakutian kimberlite provinces) (Table 3.1). A considerable number of the analyses of samples from the Yakutian province and from other manifestations, results of which are presented in this table, have recently been carried out at the Analytic Centre of the Joint Institute of Geology, Geophysics and Mineralogy (JIGGM) of the Siberian Branch of the Russian Academy of Sciences (SB RAS) using the INAA method (weighed portion is 100 mg). The samples to be analyzed were previously rayed in the Tomsk Research Reactor with an integrated flux of $5 \cdot 10^{17}$ neut/cm^2. The element contents were determined in the course of three measurement cycles after 7-, 14-, and 60-day "cooling-down" periods of the samples. The element contents were calculated from measured values in the standard rock samples: BIL-1, ZUK-1, ST-1A, BIR-1, DNC-2, W-2, BHVO-1, and AGV-1. The reproducibility of the analysis for most elements amounted to no worse than 10%, and for Gd and Tm, no worse than 15%.

Figure 3.1 shows the REE patterns of all the kimberlite samples, which analyses are presented in Table 3.1. For comparison, Figure 3.2 presents some analyses of kimberlites from the Yakutian province, which were made at an earlier stage of research using less-than-perfect analytical methods, as evidenced by the form of their patterns abounding in fractures (Fig. 3.2).

It is customary to think that the contents of REE and the character of REE distribution in kimberlites, just as their petrochemical and mineralogical characteristics, were conditioned by many factors, among them the structural and tectonic position of kimberlite provinces, geodynamic conditions of kimberlite formation, physical and chemical parameters of the generation, and crystallization of their parent melts. At the same time, REE distribution in kimberlites correlates with their modal mineral content, above all with the modal quantity of the concentrator minerals of these admixtures, among which are diopside, calcite, apatite, perovskite, monazite, phlogopite, ilmenite, zircon, as well as xenogenic pyrope.

The contents of separate REE in kimberlites from different provinces vary in a very broad range (see Table 3.1). These differences become particularly distinct when comparing average element content estimates and the patterns obtained from them in separate provinces (Tables 3.2, 3.3, Fig. 3.3). The known kimberlite provinces have been characterized by analyses with different degrees of minuteness, and far from all the elements have been covered by the available data. The calculated average estimate of the total REE content in kimberlites, despite a certain conventionality of this geochemical characteristic, makes it possible to arrange the kimberlite provinces in the following descending series (ppm): Australia (744), China (676), Canada (565), India (544), Finland (522), USA (508), South Africa (without Angola) (450), Timan (291), Kola

Table 3.1 Rare earth element composition of kimberlites (ppm).

	Provinces									
	Australia		De Beers, Africa			Kundelungu, Zaire, Africa				
	(Edwards *et al.*, 1992), INAA		(Philpotts *et al.*, 1972), IDMS			(Fieremans *et al.*, 1984), INAA				
Element	AP5/93	AP2/6776	156	154	153	Kun1	Kun2	Kun15C	KunM1	KunM2
La	268	234	N.d.	N.d.	N.d.	114	35.4	104	133	104
Ce	433	340	147	68.1	207	205	63	194	241	185
Pr	N.d.	N.d.	N.d.	N.d.	N.d.	N.d.	N.d.	N.d.	N.d.	N.d.
Nd	103	82	85.6	110	91.8	66	24	65	79	63
Sm	9.94	8.59	12.5	15.6	13.5	7.1	3.15	7.1	9.1	7.1
Eu	2.09	1.91	3.67	3.92	3.61	1.74	0.84	1.75	2.33	1.82
Gd	N.d.	N.d.	N.d.	9.48	N.d.	N.d.	N.d.	N.d.	N.d.	N.d.
Tb	0.5	0.5	N.d.	N.d.	N.d.	0.44	0.23	0.42	0.61	0.49
Dy	N.d.	N.d.	3.77	4.51	4.27	N.d.	N.d.	N.d.	N.d.	N.d.
Ho	0.91	0.94	N.d.	N.d.	N.d.	N.d.	N.d.	N.d.	N.d.	N.d.
Er	N.d.	N.d.	1.15	1.45	1.36	N.d.	N.d.	N.d.	N.d.	N.d.
Tm	N.d.	N.d.	N.d.	N.d.	N.d.	N.d.	N.d.	N.d.	N.d.	N.d.
Yb	1.04	1.09	0.707	0.874	0.842	0.48	0.34	0.32	0.49	0.5
Lu	0.15	0.16	0.148	0.124	0.146	N.d.	N.d.	N.d.	N.d.	N.d.
Total	819	669	255	214	323	N.d.	N.d.	N.d.	N.d.	N.d.
$(La/Yb)_n$	174	145	N.d.	N.d.	N.d.	160	70.3	219	183	140

	Provinces									
	Mbuji-Mayi, Zaire, Africa									
	(Fieremans *et al.*, 1984), INAA									
Element	Nod1	Nod2	Nod4	Nod5	Nod7	Nod11C	Nod11R	Nod12	Nod13	Nod14
La	54.9	41.3	206	143	33.5	135	128	77	44	114
Ce	100	83	440	261	52	239	224	127	92	217
Pr	N.d.	N.d.	N.d.	N.d.	N.d.	N.d.	N.d.	N.d.	N.d.	N.d.
Nd	36.4	32.1	168	103	19.4	87	82	42	31	83
Sm	5.13	4.31	21.5	14.6	3.02	11	10.4	5.56	3.87	12.2
Eu	1.34	1.09	5.29	4.19	0.96	2.86	2.71	1.46	0.89	3.41
Gd	N.d.	N.d.	N.d.	N.d.	N.d.	N.d.	N.d.	N.d.	N.d.	N.d.
Tb	0.38	0.33	1.19	1.15	0.37	0.68	0.65	0.43	0.22	0.95
Dy	N.d.	N.d.	N.d.	N.d.	N.d.	N.d.	N.d.	N.d.	N.d.	N.d.
Ho	N.d.	N.d.	N.d.	N.d.	N.d.	N.d.	N.d.	N.d.	N.d.	N.d.
Er	N.d.	N.d.	N.d.	N.d.	N.d.	N.d.	N.d.	N.d.	N.d.	N.d.
Tm	N.d.	N.d.	N.d.	N.d.	N.d.	N.d.	N.d.	N.d.	N.d.	N.d.
Yb	0.43	0.34	0.47	0.82	0.98	0.66	0.69	0.6	0.23	0.84
Lu	N.d.	N.d.	N.d.	N.d.	N.d.	N.d.	N.d.	N.d.	N.d.	N.d.
Total	N.d.	N.d.	N.d.	N.d.	N.d.	N.d.	N.d.	N.d.	N.d.	N.d.
$(La/Yb)_n$	86.2	82.0	296	118	23.1	138	125	86.6	129	91.6

(*Continued*)

Table 3.1 Continued

	Provinces									
	Koidu, Sierra Leone, Africa									
	(Taylor *et al.*, 1994), INAA									
Element	79-ZB-1	79-ZB-3	80-1	80-7	80-9	80-14-1	80-14-2	81-DP-1	81-BS-1	81-DP-2
La	82	198	201	141	219	126	128	146	207	141
Ce	154	390	376	276	444	235	241	277	430	264
Pr	N.d.	N.d.	N.d.	N.d.	N.d.	N.d.	N.d.	N.d.	N.d.	N.d.
Nd	52	123	125	92.7	137	76.5	80.2	107	161	97.1
Sm	7.32	13.9	16.5	12.8	14.6	10.6	11.1	12.7	18.5	11.5
Eu	1.73	2.94	4.08	3	2.88	2.42	2.59	3.02	4.12	2.7
Gd	N.d.	N.d.	N.d.	N.d.	N.d.	N.d.	N.d.	N.d.	N.d.	N.d.
Tb	0.56	0.81	0.79	0.7	0.75	0.52	0.41	0.73	0.85	0.6
Dy	N.d.	N.d.	N.d.	N.d.	N.d.	N.d.	N.d.	N.d.	N.d.	N.d.
Ho	0.32	0.44	0.6	0.46	0.42	0.37	0.28	0.48	0.54	0.48
Er	N.d.	N.d.	N.d.	N.d.	N.d.	N.d.	N.d.	N.d.	N.d.	N.d.
Tm	N.d.	N.d.	N.d.	N.d.	N.d.	N.d.	N.d.	N.d.	N.d.	N.d.
Yb	0.48	0.57	1.01	0.65	0.61	0.5	0.47	0.6	0.7	0.6
Lu	0.07	0.07	0.13	0.09	0.07	0.06	0.07	0.07	0.07	0.08
Total	298	730	725	527	819	452	464	548	823	518
$(La/Yb)_n$	115	234	134	146	242	170	184	164	200	159

	Provinces									
	India									
	(Paul *et al.*, 1975), INAA									
Element	HV-1/3	HV-4/2	UG 191	HV-4/6	UG 11a	MG 50	MG 6	LM-4/9	WK-2/7	LM-4/6
La	71	139	161	192	179	188	156	68	117	60
Ce	138.1	381.3	332.3	468.5	472.7	508.8	371.8	122.5	249.4	124.9
Pr	N.d.	N.d.	N.d.	N.d.	N.d.	N.d.	N.d.	N.d.	N.d.	N.d.
Nd	78.7	193.6	140.5	220.8	225.9	241.9	159	46.4	95.3	47.4
Sm	24.2	39.7	22.2	32.2	33.3	31.9	22.5	N.d.	16.6	N.d.
Eu	5.8	9.1	5.2	7.2	6.5	6.5	5	2	4.4	2
Gd	11.1	17.6	9.8	14.6	17.8	16.8	8	4.8	7.8	3.7
Tb	2.11	2.68	1.81	2.12	2.07	1.85	1.32	0.82	1.79	0.81
Dy	N.d.	N.d.	N.d.	N.d.	N.d.	N.d.	N.d.	N.d.	N.d.	N.d.
Ho	N.d.	N.d.	N.d.	N.d.	N.d.	N.d.	N.d.	N.d.	N.d.	N.d.
Er	N.d.	N.d.	N.d.	N.d.	N.d.	N.d.	N.d.	N.d.	N.d.	N.d.
Tm	N.d.	N.d.	N.d.	N.d.	N.d.	N.d.	N.d.	N.d.	N.d.	N.d.
Yb	1.79	2.21	1.98	1.75	1.33	1.3	0.98	0.95	1.38	0.69
Lu	0.01	0.24	0.29	0.24	0.13	0.12	0.11	0.13	0.15	0.07
Total	N.d.	N.d.	N.d.	N.d.	N.d.	N.d.	N.d.	N.d.	N.d.	N.d.
$(La/Yb)_n$	26.8	42.5	54.9	74.1	90.8	97.6	108	48.3	57.2	58.7

(*Continued*)

Table 3.1 Continued

	Provinces									
	India					Jerico, Canada,				
	(Paul *et al.*, 1975), INAA		(Balashov, 1976)			(Price *et al.*, 2000), ICP-MS				
Element	WK-2/9	LM-3/5	Bal-5	Bal-6a	Bal-6b	JD51	JD69-1	JD69-2	JD69-3	JD82-1
La	143	100	106	43	26	218.7	154.5	161.5	182.5	146.2
Ce	218.2	156.2	196	66	72	353.8	236.9	238.1	263.2	230.6
Pr	N.d.	N.d.	22	8.3	6.6	34.81	22.81	22.4	24.69	22.2
Nd	79.5	53.1	78	31	40	109.48	72.26	70.51	78.32	70.6
Sm	N.d.	N.d.	10.6	3.76	5.6	12.59	8.58	8.56	9.53	8.32
Eu	3.7	2.3	2.8	0.86	1.39	2.95	2.08	2.05	2.34	2.11
Gd	7.3	3.9	7.7	2.34	8.9	8.03	5.61	5.69	6.53	5.46
Tb	1.62	0.9	0.83	0.185	N.d.	0.56	0.42	0.45	0.49	0.42
Dy	N.d.	N.d.	N.d.	N.d.	N.d.	2.76	2.13	2.19	2.51	2.09
Ho	N.d.	N.d.	0.503	0.322	N.d.	0.4	0.31	0.33	0.36	0.29
Er	N.d.	N.d.	1.34	2.05	N.d.	0.83	0.65	0.73	0.78	0.62
Tm	N.d.	N.d.	0.14	0.327	0.22	0.09	0.07	0.08	0.1	0.07
Yb	1.16	0.6	0.71	3.75	1.18	0.43	0.38	0.47	0.52	0.38
Lu	0.11	N.d.	0.087	0.545	0.19	0.07	0.05	0.06	0.07	0.05
Total	N.d.	N.d.	427	162	N.d.	745	507	513	572	489
$(La/Yb)_n$	83.2	113	101	7.7	14.9	343	274	232	237	260

	Provinces									
	Paranatinga, Brazil									
	(Greenwood *et al.*, 1999), ICP-MS									
Element	G-92	G-93	G-96	G-97	G-118b	G-139	G-140	G-141	G-143	G-125
La	23.2	23.3	12.5	14.1	29	14.4	16.7	23.6	20.5	13.7
Ce	42.8	41.9	22.4	26.2	52.6	25.4	28.5	43.3	41.2	23.9
Pr	4.7	4.5	2.5	2.9	5.7	2.9	3.1	5	4.7	2.5
Nd	17.2	16.1	9.4	10.5	19.9	10.6	11.5	19	18	8.8
Sm	2.74	2.36	1.53	1.72	2.94	1.79	1.9	3.32	2.87	1.37
Eu	0.71	0.6	0.41	0.48	0.66	0.49	0.6	0.76	0.74	0.38
Gd	2.36	1.86	1.29	1.57	2.21	1.55	1.8	2.83	2.58	1.36
Tb	0.32	0.23	0.19	0.22	0.27	0.21	0.24	0.4	0.37	0.17
Dy	1.72	1.14	1.06	1.21	1.33	1.15	1.32	2.19	2.08	0.94
Ho	0.33	0.21	0.19	0.23	0.24	0.22	0.25	0.42	0.38	0.19
Er	0.89	0.53	0.52	0.62	0.65	0.59	0.97	1.09	0.98	0.53
Tm	0.14	0.08	0.08	0.1	0.1	0.09	0.1	0.17	0.15	0.08
Yb	0.86	0.51	0.49	0.58	0.64	0.53	0.67	0.99	0.92	0.55
Lu	0.13	0.08	0.07	0.09	0.09	0.08	0.1	0.14	0.14	0.09
Total	98.1	93.4	52.6	60.5	116	60	67.8	103	95.6	54.6
$(La/Yb)_n$	18.2	30.8	17.2	16.4	30.6	18.3	16.8	16.1	15.0	16.8

(*Continued*)

Table 3.1 Continued

	Provinces									
	Finland								Mengin, China	
	(O'Brien & Tyni, 1999), ICP-MS								(Tompkins *et al.*, 1999)	
Element	F-1	F-2	F-3	F-4	F-5	F-6	F-9	F-10	54022	54023
La	189	174	186	107	141	130	158	111	138	136
Ce	304	287	304	182	237	226	260	190	263	233
Pr	29.5	26.7	28.4	17.2	23.5	22.4	26.8	19.6	23	22
Nd	88.5	83.3	87.8	54	76.1	72.5	86.5	64.8	78	71
Sm	9.23	8.92	9.23	5.78	9.45	8.92	11.1	8.56	10	9
Eu	1.87	1.67	1.74	1.14	2.16	2.09	2.52	1.92	2.6	2.6
Gd	6.37	5.56	5.84	4.19	6.37	6.14	7.7	6.56	N.d.	N.d.
Tb	0.68	0.61	0.63	0.45	0.74	0.72	0.88	0.79	0.8	0.6
Dy	2.19	1.91	2.15	1.64	2.89	2.81	3.41	3.43	3	2.3
Ho	0.37	0.29	0.33	0.27	0.47	0.45	0.57	0.59	0.4	0.3
Er	0.87	0.77	0.74	0.61	1.15	1.14	1.28	1.68	N.d.	N.d.
Tm	0.1	0.09	0.1	0.08	0.17	0.14	0.15	0.2	0.1	0.1
Yb	0.58	0.53	0.58	0.46	0.92	0.87	0.98	1.33	0.7	0.5
Lu	0.1	0.07	0.08	0.09	0.13	0.012	0.14	0.21	0.1	0.1
Total	633	591	628	375	502	474	560	411	520	478
$(La/Yb)_n$	220	222	216	157	103	101	109	56.3	133	184

	Provinces									
	Mengin, China						Fuxian, China			
	(Tompkins *et al.*, 1999), ICP-MS									
Element	54025	54026	54027	54028	54029	54030	54031	54032	54017	54018
La	216	154	196	129	133	241	314	125	262	385
Ce	352	242	308	211	198	394	449	245	491	571
Pr	44	31	39	28	27	51	52	36	46	60
Nd	113	74	96	69	66	132	125	90	142	161
Sm	14	9	12	10	9	18	14	12	21	20
Eu	3.4	2.2	3.1	2.5	2.4	4.6	3.3	3.3	5.3	4.9
Gd	N.d.	N.d.	N.d.	N.d.	N.d.	N.d.	N.d.	N.d.	N.d.	N.d.
Tb	1.1	0.7	0.9	0.8	0.8	1.5	1.1	0.9	1.6	1.4
Dy	2.9	2.1	2.6	2.6	2.5	4.7	2.9	2.7	5.8	4.7
Ho	0.4	0.3	0.3	0.4	0.3	0.6	0.4	0.3	0.8	0.6
Er	N.d.	N.d.	N.d.	N.d.	N.d.	N.d.	N.d.	N.d.	N.d.	N.d.
Tm	0.1	0.1	0.1	0.1	0.1	0.2	0.1	0.1	0.2	0.1
Yb	0.5	0.4	0.5	0.7	0.6	1	0.6	0.5	2	1.2
Lu	0.1	0.1	0.1	0.1	0.1	0.2	0.1	0.1	0.4	0.2
Total	748	516	659	454	440	849	963	516	978	1210
$(La/Yb)_n$	292	260	265	124	150	163	353	169	88.4	217

(*Continued*)

Table 3.1 Continued

	Provinces									
	Fuxian, China									
	(Tompkins *et al.*, 1999), ICP-MS									
Element	54019	54080	54081	54015	54016	54012	54013	54014	54009	54008
La	359	395	401	128	69	125	114	120	116	67
Ce	554	552	548	233	87	299	207	214	202	115
Pr	60	50	50	21	10	33	30	30	27	18
Nd	164	136	134	64	30	161	116	100	92	58
Sm	20	16	16	8	4	24	16	13	12	9
Eu	5	3.6	3.7	2	1	5.7	3.3	3.2	2.8	2.4
Gd	N.d.	N.d.	N.d.	N.d.	N.d.	N.d.	N.d.	N.d.	N.d.	N.d.
Tb	1.4	1.2	1.3	0.7	0.4	1.7	1.2	1.1	0.9	0.8
Dy	5	3.9	4	3	1.9	6.9	4.5	4.4	3.4	3.9
Ho	0.6	0.4	0.4	0.4	0.3	0.8	0.5	0.6	0.4	0.5
Er	N.d.	N.d.	N.d.	N.d.	N.d.	N.d.	N.d.	N.d.	N.d.	N.d.
Tm	0.1	0.1	0.1	0.1	0.1	0.2	0.1	0.2	0.1	0.2
Yb	1.2	1.1	1.1	1.1	0.8	1.7	1.2	1.4	1	1.2
Lu	0.2	0.2	0.2	0.2	0.2	0.2	0.2	0.2	0.1	0.2
Total	1171	1160	1160	462	205	659	494	488	458	276
$(La/Yb)_n$	202	242	246	78.5	58.2	49.6	64.1	57.9	78.3	37.7

	Provinces									
	Arkhangelsk, Russia									
	(Makhotkin *et al.*, 2000), ICP-MS									
Element	1017	942	987	146.3	172.7	247.3	395	400	11/27.2	13(6)-1
La	44.40	32.30	27.20	30.30	38.10	41.60	50.40	27.10	104.0	111.0
Ce	79.90	58.80	43.00	58.50	66.60	76.60	86.10	54.70	151.0	194.0
Pr	8.91	6.59	N.d.	6.80	7.34	8.74	N.d.	N.d.	N.d.	N.d.
Nd	32.90	24.70	18.90	24.70	27.00	32.70	37.70	27.60	57.50	49.90
Sm	5.11	3.75	2.84	4.28	4.22	5.12	5.90	4.19	8.60	9.30
Eu	1.45	1.00	0.77	1.28	1.14	1.40	1.46	1.00	2.00	1.87
Gd	3.85	2.62	N.d.	3.36	3.09	3.77	N.d.	N.d.	N.d.	N.d.
Tb	0.49	0.34	0.45	0.47	0.40	0.49	0.66	0.48	N.d.	N.d.
Dy	2.29	1.55	N.d.	2.37	1.91	2.32	N.d.	N.d.	N.d.	N.d.
Ho	0.38	0.27	0.52	0.42	0.33	0.41	0.45	0.57	N.d.	N.d.
Er	0.91	0.65	N.d.	0.96	0.78	0.98	N.d.	N.d.	N.d.	N.d.
Tm	0.12	0.09	N.d.	0.13	0.11	0.15	N.d.	N.d.	N.d.	N.d.
Yb	0.72	0.53	0.88	0.65	0.64	0.84	1.04	1.02	1.44	0.50
Lu	0.10	0.08	0.09	0.09	0.09	0.12	0.12	0.12	0.10	0.10
Total	182	133	N.d.	134	152	175	N.d.	N.d.	N.d.	N.d.
$(La/Yb)_n$	41.6	41.1	20.9	31.5	40.2	33.4	32.7	17.9	48.8	150

(*Continued*)

Table 3.1 Continued

	Provinces									
	Arkhangelsk, Russia									
	(Beard *et al.*, 2000), ICP-AES									
Element	Z1-2-1	Z1-2-2	Z1-2-3	Z1-2-4	Z1-3-2	Z1-3-3	Z1-4-1	Z3-8-1	Z3-8-2	Z8-15-1
La	54.90	36.40	21.80	19.80	16.80	21.60	28.50	30.70	82.20	94.30
Ce	77.30	66.80	41.50	37.90	34.30	43.50	63.00	59.00	170.8	236.0
Pr	N.d.	N.d.	N.d.	N.d.	N.d.	N.d.	N.d.	N.d.	N.d.	N.d.
Nd	21.20	25.90	15.70	14.30	13.40	14.70	25.20	23.80	66.30	101.20
Sm	3.13	4.01	2.82	2.41	2.15	2.51	4.92	4.29	10.86	18.30
Eu	0.75	1.13	0.73	0.60	0.57	0.68	1.27	1.38	2.98	4.92
Gd	2.32	2.87	2.24	1.80	1.85	2.06	4.15	4.23	8.71	13.59
Tb	N.d.	N.d.	N.d.	N.d.	N.d.	N.d.	N.d.	N.d.	N.d.	N.d.
Dy	1.36	1.66	1.50	1.12	1.38	1.30	2.75	3.01	3.98	6.26
Ho	N.d.	N.d.	N.d.	N.d.	N.d.	N.d.	N.d.	N.d.	N.d.	N.d.
Er	0.68	0.63	0.73	0.53	0.64	0.63	1.08	1.16	1.41	2.33
Tm	N.d.	N.d.	N.d.	N.d.	N.d.	N.d.	N.d.	N.d.	N.d.	N.d.
Yb	0.54	0.48	0.64	0.51	0.59	0.56	0.74	0.75	0.83	1.69
Lu	0.09	0.07	0.10	0.09	0.09	0.10	0.16	0.10	0.12	0.26
Total	162	140	87.8	79.1	71.8	87.6	132	128	348	479
$(La/Yb)_n$	68.6	51.2	23.0	26.2	19.2	26.0	26.0	27.6	66.9	37.7

	Provinces									
	Arkhangelsk, Russia									
	(Beard *et al.*, 2000), ICP-AES			(Bogatikov *et al.*, 2003), INAA						
Element	Z9-18-1	Z9-20-1	Z9-21-1	64-AP	65-AP	40-AP	41-AP	47-AP	58-AP	105-AP
La	120.4	119.6	142.3	145.8	154.7	85.50	120.5	34.00	37.60	31.50
Ce	260.2	248.7	309.1	243.1	246.9	124.0	220.0	51.20	58.10	55.50
Pr	N.d.	N.d.	N.d.	N.d.	25.20	N.d.	21.70	N.d.	N.d.	5.80
Nd	82.30	81.30	96.70	140.0	91.20	49.00	77.50	25.00	38.00	22.90
Sm	10.80	10.70	12.20	18.70	12.58	5.00	9.67	3.90	4.00	3.64
Eu	2.67	2.75	3.03	2.70	3.26	2.20	2.51	1.20	1.20	1.09
Gd	6.52	6.60	7.15	N.d.	9.54	N.d.	6.93	N.d.	N.d.	3.20
Tb	N.d.	N.d.	N.d.	0.70	1.40	0.50	0.98	0.60	0.50	0.47
Dy	3.10	3.10	3.31	N.d.	6.40	N.d.	4.21	N.d.	N.d.	2.33
Ho	N.d.	N.d.	N.d.	N.d.	0.910	N.d.	0.500	N.d.	N.d.	0.36
Er	0.96	1.06	1.08	N.d.	2.26	N.d.	1.140	N.d.	N.d.	0.91
Tm	N.d.	N.d.	N.d.	N.d.	0.27	N.d.	0.16	N.d.	N.d.	0.13
Yb	0.82	0.88	0.91	5.20	1.65	1.60	0.85	1.10	0.80	0.63
Lu	0.16	0.13	0.14	0.09	0.25	0.15	0.13	0.13	0.12	0.10
Total	488	475	576	N.d.	557	N.d.	467	N.d.	N.d.	129
$(La/Yb)_n$	99.1	91.7	106	18.9	63.3	36.1	95.7	20.9	31.7	33.8

(*Continued*)

Table 3.1 Continued

	Provinces									
	Arkhangelsk, Russia		Kola Peninsula, Russia							
	(Bogatikov *et al.*, 2003), INAA		(Beard *et al.*, 1998), ICP-AES			(Parsadanian *et al.*, 1996), INAA				
Element	56-AP	107/302	K25-1	T1-28-1	T1-28-2	P-687	P-Zv-1	P-Zv-2	P-Ml-1	P-Ml-2
La	19.40	19.40	77.09	119.8	201.2	146.0	86.00	124.0	152.0	137.0
Ce	35.20	35.50	153.9	202.7	246.2	243.0	124.0	175.0	217.0	189.0
Pr	N.d.	3.60	N.d.	N.d.	N.d.	N.d.	N.d.	N.d.	N.d.	N.d.
Nd	23.00	13.70	52.08	56.70	89.10	140.00	49.00	74.00	81.00	62.00
Sm	2.40	2.09	6.68	7.51	10.96	18.70	5.00	9.30	11.90	8.60
Eu	0.60	0.48	1.62	2.05	2.91	2.70	2.20	2.40	3.10	2.50
Gd	N.d.	1.64	4.09	5.33	6.77	N.d.	N.d.	N.d.	N.d.	N.d.
Tb	0.50	0.24	N.d.	N.d.	N.d.	0.70	0.50	0.60	1.20	0.80
Dy	N.d.	1.13	2.56	2.91	3.49	N.d.	N.d.	N.d.	N.d.	N.d.
Ho	N.d.	0.17	N.d.	N.d.	N.d.	N.d.	N.d.	N.d.	N.d.	N.d.
Er	N.d.	0.41	0.96	1.07	1.15	N.d.	N.d.	N.d.	N.d.	N.d.
Tm	N.d.	0.05	N.d.	N.d.	N.d.	N.d.	N.d.	N.d.	N.d.	N.d.
Yb	0.80	0.32	0.74	0.89	1.04	5.20	1.60	2.30	1.90	1.40
Lu	0.10	0.05	0.10	0.14	0.16	0.09	0.15	0.09	0.23	0.20
Total	N.d.	78.8	300	399	563	N.d.	N.d.	N.d.	468	402
$(La/Yb)_n$	16.4	40.9	70.3	90.9	131	19.0	36.3	36.4	54.0	66.1

	Provinces									
	Kola Peninsula, Russia									
	(Parsadanian *et al.*, 1996), INAA									
Element	PKl-1	P-734	PLom-1	PLom-2	Kar-21	Kar-22	PKar-1	PPi-1	PPi-2	PPi-3
La	88.00	79.00	25.00	23.00	34.00	26.00	41.00	38.00	37.00	35.00
Ce	140.0	117.0	41.00	40.00	51.00	43.00	73.00	58.00	62.00	62.00
Pr	N.d.	N.d.	N.d.	N.d.	N.d.	N.d.	N.d.	N.d.	N.d.	N.d.
Nd	76.00	55.00	28.00	22.00	25.00	18.00	39.00	38.00	26.00	22.00
Sm	10.20	5.70	3.00	2.50	3.90	2.90	5.20	4.00	4.20	3.90
Eu	2.60	1.70	0.80	0.80	1.20	0.80	1.50	1.20	1.20	1.10
Gd	N.d.	N.d.	N.d.	N.d.	N.d.	N.d.	N.d.	N.d.	N.d.	N.d.
Tb	0.80	0.60	0.30	0.40	0.60	0.30	0.50	0.50	0.50	0.50
Dy	N.d.	N.d.	N.d.	N.d.	N.d.	N.d.	N.d.	N.d.	N.d.	N.d.
Ho	N.d.	N.d.	N.d.	N.d.	N.d.	N.d.	N.d.	N.d.	N.d.	N.d.
Er	N.d.	N.d.	N.d.	N.d.	N.d.	N.d.	N.d.	N.d.	N.d.	N.d.
Tm	N.d.	N.d.	N.d.	N.d.	N.d.	N.d.	N.d.	N.d.	N.d.	N.d.
Yb	2.20	3.90	0.80	0.90	1.10	0.90	1.10	0.80	0.80	0.80
Lu	0.01	0.01	0.13	0.11	0.13	0.08	0.12	0.12	0.09	0.12
Total	N.d.	N.d.	N.d.	N.d.	N.d.	N.d.	N.d.	N.d.	N.d.	N.d.
$(La/Yb)_n$	27.0	13.7	21.1	17.3	20.9	19.5	25.2	32.1	31.2	29.5

(*Continued*)

Table 3.1 Continued

	Provinces									
	Timan, Russia									
	(Malakhov, 1984)									
Element	35/55	35/93	37/533	37/151	37/231	47/110	52/140	56/127	62/126	68/99
La	92.1	87	117.3	79.3	81	51.6	53.7	45.2	55.1	62.1
Ce	143.3	124.6	164.4	122.1	128.6	94.4	81.1	70.7	80.4	86.8
Pr	20.1	19.3	23	17	17.4	10.2	10.7	9.8	11.85	9.5
Nd	79	77.9	90.5	66.9	67.9	36.7	41.2	38.2	47.2	34.6
Sm	11.5	10.3	14.7	10.6	12.8	6.9	7.8	6.7	9.1	6.3
Eu	3	2.9	4.4	3.3	3.6	2.1	1.9	1.9	2.3	1.8
Gd	7.5	6.9	9.7	6.8	7.1	4.8	6.1	5.6	5.6	4.1
Tb	1.1	0.74	1.33	0.94	1.08	0.78	0.56	0.62	0.56	0.85
Dy	7.5	6.7	8.4	6.3	6.4	7.2	6.4	6.4	5.9	5.7
Ho	1.22	1.13	1.13	1.22	1.05	0.7	1.05	0.87	0.79	0.7
Er	2.2	2.4	2.3	1.75	1.9	2.01	1.8	2.4	1.8	1.66
Tm	0.26	0.35	0.26	0.26	0.26	0.26	0.26	0.35	0.26	0.26
Yb	1.41	1.59	1.59	1.23	1.32	1.5	1.7	2.03	1.32	1.14
Lu	N.d.	N.d.	N.d.	N.d.	N.d.	N.d.	N.d.	N.d.	N.d.	N.d.
Total	369	342	439	318	330	219	214	191	222	216
$(La/Yb)_n$	44.1	36.9	49.8	43.5	41.4	23.2	21.3	15.0	28.2	36.8

	Provinces									
	Timan, Russia				Kansas, USA					
	(Bogatikov *et al.*, 2003), INAA				(Alibert & Albarede, 1988), ICP-MS					
Element	427/157	436/231	615/103	425/331	Prai-1	Cross-1	Leon-1	Bal-1	Bach-1	Bizard-1
La	105.0	100.3	34.50	38.10	140.0	N.d.	105.0	N.d.	N.d.	108.0
Ce	211.0	180.1	73.10	75.40	305.0	223.0	123.0	442.0	394.0	222.0
Pr	23.20	18.70	8.30	8.10	N.d.	N.d.	N.d.	N.d.	N.d.	N.d.
Nd	87.10	70.10	32.90	33.70	108.0	71.80	40.60	149.00	167.00	99.00
Sm	13.11	11.57	5.85	6.53	12.70	8.67	6.23	19.00	26.80	16.80
Eu	3.36	2.81	1.35	1.81	3.00	1.89	1.66	4.36	7.44	4.25
Gd	9.70	8.70	5.11	5.58	6.43	4.45	3.97	10.70	19.20	11.30
Tb	1.32	1.28	0.81	0.94	N.d.	N.d.	N.d.	N.d.	N.d.	N.d.
Dy	6.15	5.72	4.80	4.86	3.05	2.16	2.47	5.04	10.60	5.76
Ho	0.83	0.76	0.82	0.80	N.d.	N.d.	N.d.	N.d.	N.d.	N.d.
Er	1.87	1.64	2.20	2.15	1.05	0.79	1.06	1.81	3.54	2.20
Tm	0.21	0.21	0.33	0.28	N.d.	N.d.	N.d.	N.d.	N.d.	N.d.
Yb	1.29	1.20	1.99	1.68	0.69	0.60	0.80	1.36	2.30	1.40
Lu	0.18	0.17	0.31	0.26	N.d.	N.d.	N.d.	N.d.	N.d.	N.d.
Total	464	403	172	180	N.d.	N.d.	N.d.	N.d.	N.d.	N.d.
$(La/Yb)_n$	54.9	56.4	11.7	15.3	137	N.d.	88.6	N.d.	N.d.	52.1

(*Continued*)

Table 3.1 Continued

	Provinces									
	Kentucky, USA		Colorado and Wyoming, USA					Pennsylvania, USA		
	(Alibert & Albarede, 1988), ICP-MS									
Element	Creek 1	Ising-1	Nix 2	Nix 4	Her-1	GM2	Rad-1	M70-54	M65-69	Dixon-1
La	83.00	87.60	205.0	N.d.	N.d.	116.0	N.d.	136.0	144.0	N.d.
Ce	150.0	153.0	341.0	342.0	218.0	195.0	147.0	243.0	250.0	222.0
Pr	N.d.	N.d.	N.d.	N.d.	N.d.	N.d.	N.d.	N.d.	N.d.	N.d.
Nd	52.50	53.10	99.30	92.50	73.80	66.80	49.70	91.80	93.80	69.70
Sm	7.16	8.26	10.90	9.64	9.36	9.69	6.89	14.10	14.50	8.20
Eu	1.84	1.94	2.55	2.15	2.32	2.20	1.90	3.42	3.58	2.05
Gd	4.84	5.62	5.89	4.71	5.35	6.32	4.32	9.15	9.32	4.68
Tb	N.d.	N.d.	N.d.	N.d.	N.d.	N.d.	N.d.	N.d.	N.d.	N.d.
Dy	2.63	2.57	2.65	2.18	2.48	2.39	2.38	4.19	4.55	2.13
Ho	N.d.	N.d.	N.d.	N.d.	N.d.	N.d.	N.d.	N.d.	N.d.	N.d.
Er	1.04	1.08	0.95	0.78	0.78	0.88	0.84	1.62	1.87	0.71
Tm	N.d.	N.d.	N.d.	N.d.	N.d.	N.d.	N.d.	N.d.	N.d.	N.d.
Yb	0.76	0.66	0.66	0.57	0.46	0.50	0.56	0.95	1.23	0.43
Lu	N.d.	N.d.	N.d.	N.d.	N.d.	N.d.	N.d.	N.d.	N.d.	N.d.
Total	N.d.	N.d.	N.d.	N.d.	N.d.	N.d.	N.d.	N.d.	N.d.	N.d.
$(La/Yb)_n$	73.7	89.6	210	N.d.	N.d.	157	N.d.	96.6	79.0	N.d.

	Provinces									
	Kansas, USA									
	(Cullers *et al.*, 1982)									
Element	19(6)	27(9)	50(7)	75(3)	94	113	137(8)	Rand-1	Rand-2	Leo-1
La	301	301	298	314	293	297	309	231	230	178
Ce	529	537	502	534	508	504	500	397	364	235
Pr	N.d.	N.d.	N.d.	N.d.	N.d.	N.d.	N.d.	N.d.	N.d.	N.d.
Nd	N.d.	N.d.	N.d.	N.d.	N.d.	N.d.	N.d.	N.d.	N.d.	N.d.
Sm	18.5	18.5	17.5	18.9	18.1	17.3	19.5	15.5	15	12.2
Eu	5.2	4.9	4.1	5.05	4.6	3.86	4.2	3.9	3.54	3.3
Gd	N.d.	N.d.	N.d.	N.d.	N.d.	N.d.	N.d.	N.d.	N.d.	N.d.
Tb	1.19	1.09	0.97	1.24	0.98	1.05	0.96	0.92	0.88	0.86
Dy	N.d.	N.d.	N.d.	N.d.	N.d.	N.d.	N.d.	N.d.	N.d.	N.d.
Ho	N.d.	N.d.	N.d.	N.d.	N.d.	N.d.	N.d.	N.d.	N.d.	N.d.
Er	N.d.	N.d.	N.d.	N.d.	N.d.	N.d.	N.d.	N.d.	N.d.	N.d.
Tm	N.d.	N.d.	N.d.	N.d.	N.d.	N.d.	N.d.	N.d.	N.d.	N.d.
Yb	1.38	1.45	1.27	1.23	1.03	1.23	1.1	1.55	N.d.	1.26
Lu	0.3	0.34	0.28	0.3	0.27	0.15	0.16	0.22	0.23	0.2
Total	N.d.	N.d.	N.d.	N.d.	N.d.	N.d.	N.d.	N.d.	N.d.	N.d.
$(La/Yb)_n$	147	140	158	172	192	163	190	101	N.d.	95

(*Continued*)

Table 3.1 Continued

	Provinces								Pipes	
	Kansas, USA								Botuobinskaya, Yakutia	
	Cullers *et al.*, 1982								(Golubeva *et al.*, 2004)	
Element	Leo-22	Leo-68	Leo-120	Leo213	Leo-273	Stoc-1	Stoc-2	Stoc-3	B-5-89	B-5-101
La	156	161	150	129	140	89.2	83.7	95	12.9	9.3
Ce	262	256	251	219	235	133	148	145	28.2	21.2
Pr	N.d.	N.d.	N.d.	N.d.	N.d.	N.d.	N.d.	N.d.	3.5	2.7
Nd	N.d.	N.d.	N.d.	N.d.	N.d.	N.d.	N.d.	N.d.	14.7	11.7
Sm	11.8	10.4	10.9	9.91	10.3	7.08	6.4	6.75	3	2.5
Eu	2.74	3.08	3.16	2.66	2.58	1.82	1.76	1.66	0.86	0.66
Gd	N.d.	N.d.	N.d.	N.d.	N.d.	N.d.	N.d.	N.d.	2.79	2.24
Tb	0.77	0.79	0.83	0.71	0.74	0.55	0.5	0.44	0.38	0.31
Dy	N.d.	N.d.	N.d.	N.d.	N.d.	N.d.	N.d.	N.d.	2.03	1.59
Ho	N.d.	N.d.	N.d.	N.d.	N.d.	N.d.	N.d.	N.d.	0.41	0.31
Er	N.d.	N.d.	N.d.	N.d.	N.d.	N.d.	N.d.	N.d.	1	0.76
Tm	N.d.	N.d.	N.d.	N.d.	N.d.	N.d.	N.d.	N.d.	0.13	0.1
Yb	0.8	0.63	0.99	0.7	0.73	0.97	0.8	0.7	0.79	0.57
Lu	0.19	0.14	0.15	0.14	0.16	0.13	0.13	0.11	0.12	0.08
Total	N.d.	N.d.	N.d.	N.d.	N.d.	N.d.	N.d.	N.d.	70.8	54.0
$(La/Yb)_n$	132	172	102	124	129	62.1	70.6	91.6	11.0	11.0

	Pipes of Yakutian province									
	Botuobinskaya				Niurbinskaya		Mir	Internatsionaln.	Niurbinskaya	Aykhal
	(Golubeva *et al.*, 2004), ICP-MS						(Serov *et al.*, 2001), ICP-MS			
Element	B-415	B-210	B-270	B-350	N-440	N-266	M-1	I-1	N-1	A-1
La	16.6	13.4	14.1	20.8	20.6	13.6	41.84	114.08	16.61	31.87
Ce	33.2	28.9	29.6	60.7	44.1	28.8	78.47	200.69	35.48	57.38
Pr	4.2	3.8	3.8	8.7	5.5	3.6	8.52	21.06	4.30	5.70
Nd	17.5	16.7	15.7	39.5	22.8	15	30.34	73.21	19.12	21.81
Sm	3.4	3.3	3.1	7	4.6	2.9	4.21	9.83	3.91	3.01
Eu	0.97	0.95	0.72	1.71	1.33	0.76	1.14	2.52	1.16	0.86
Gd	2.98	3.14	2.78	5.36	3.69	2.44	2.61	5.04	3.37	2.63
Tb	0.37	0.4	0.37	0.59	0.47	0.32	0.38	0.73	0.49	0.39
Dy	1.89	1.99	1.96	2.35	2.29	1.6	1.73	3.06	2.23	1.86
Ho	0.34	0.36	0.33	0.39	0.38	0.27	0.29	0.46	0.35	0.30
Er	0.84	0.84	0.8	0.91	0.88	0.66	0.68	0.92	0.90	0.73
Tm	0.11	0.1	0.1	0.09	0.1	0.09	0.10	0.12	0.10	0.10
Yb	0.67	0.61	0.61	0.52	0.57	0.49	0.57	0.66	0.69	0.60
Lu	0.1	0.09	0.09	0.08	0.08	0.07	0.09	0.09	0.09	0.7
Total	83.2	74.6	74.1	149	107	70.6	171	432	88.8	128
$(La/Yb)_n$	16.7	14.8	15.6	27.0	24.4	18.7	49.6	117	16.3	35.9

(*Continued*)

Table 3.1 Continued

	Pipes of Yakutian province									
	Internatsionalnaya			Amakinskaya	Krasnopresnenskaya	Radiovolnovaya	Dolgozhdannaya	Imeni 23 s'ezda	Sputnik	
	(Data of V.P. Afanasiev, F.P. Lesnov, N.M. Podgorhnikh), INAA									
Element	M-1R	M-2R	M-3R	M-4R	M-5R	M-6R	M-7R	M-8R	M-9R	M-10M
La	104	101	94	46	137	76	45	127	175	133.26
Ce	170	165	155	74	238	123	68	194	295	233.2
Pr	N.d.	N.d.	N.d.	N.d.	N.d.	N.d.	N.d.	N.d.	N.d.	N.d.
Nd	61	60	60	24	91	39	25	67	104	86.50
Sm	8.9	8.9	8.7	4.1	13.2	5.9	3.58	11	18.1	12.99
Eu	2.24	2.21	2.2	1.11	2.94	1.53	0.85	2.82	4.29	3.32
Gd	6.3	5.8	5.6	2.8	6.8	3.9	2.3	6.9	10.7	8.10
Tb	0.65	0.706	0.67	0.418	0.888	0.498	0.35	0.91	1.34	1.02
Dy	N.d.	N.d.	N.d.	N.d.	N.d.	N.d.	N.d.	N.d.	N.d.	N.d.
Ho	N.d.	N.d.	N.d.	N.d.	N.d.	N.d.	N.d.	N.d.	N.d.	N.d.
Er	N.d.	N.d.	N.d.	N.d.	N.d.	N.d.	N.d.	N.d.	N.d.	N.d.
Tm	N.d.	N.d.	N.d.	N.d.	N.d.	N.d.	N.d.	N.d.	N.d.	0.22
Yb	0.7	0.75	0.67	0.54	0.82	0.55	0.5	0.89	1.17	1.14
Lu	0.075	0.088	0.085	0.053	0.092	0.063	0.058	0.099	0.126	0.16
Total	N.d.	N.d.	N.d.	N.d.	N.d.	N.d.	N.d.	N.d.	N.d.	N.d.
$(La/Yb)_n$	100	90.9	94.7	57.5	113	93.3	60.8	96.3	101	78.7

	Pipes of Yakutian province									
	Sputnik	Molodezhnaya	Yakutskaya		Ivushka	Leningradskaya	Ukrainskaya	Sytykanskaya		
	(Data of V.P. Afanasiev, F.P. Lesnov, N.M. Podgorhnikh), INAA									
Element	M-10R	M-11R	M-12R	M-13R	M-14R	M-15R	M-16R	M-17R	M-18R	M-19R
La	132	110	43	38	76.00	48.00	54.00	61.00	46.00	47.00
Ce	218	175	73	65	140.0	72.00	80.00	97.00	72.00	70.00
Pr	N.d.	N.d.	N.d.	N.d.	N.d.	N.d.	N.d.	N.d.	N.d.	N.d.
Nd	80	61	28	22.7	58.00	28.00	30.00	34.00	27.00	25.00
Sm	12.6	8.2	4.43	3.37	9.80	4.47	4.58	4.80	4.09	4.03
Eu	3.32	2.11	1.09	0.83	2.20	1.04	0.82	1.31	0.98	0.90
Gd	7.9	4.7	3	2.1	5.50	2.70	2.50	2.80	2.60	2.00
Tb	1.14	0.651	0.402	0.28	0.79	0.40	0.37	0.42	0.37	0.31
Dy	N.d.	N.d.	N.d.	N.d.	N.d.	N.d.	N.d.	N.d.	N.d.	N.d.
Ho	N.d.	N.d.	N.d.	N.d.	N.d.	N.d.	N.d.	N.d.	N.d.	N.d.
Er	N.d.	N.d.	N.d.	N.d.	N.d.	N.d.	N.d.	N.d.	N.d.	N.d.
Tm	N.d.	N.d.	N.d.	N.d.	N.d.	N.d.	N.d.	N.d.	N.d.	N.d.
Yb	1.21	0.69	0.58	0.4	1.05	0.65	0.49	0.51	0.41	0.34
Lu	0.14	0.08	0.067	0.053	0.14	0.09	0.06	0.06	0.05	0.04
Total	N.d.	N.d.	N.d.	N.d.	N.d.	N.d.	N.d.	N.d.	N.d.	N.d.
$(La/Yb)_n$	73.6	108	50.0	64.1	48.9	49.8	74.4	80.7	75.7	93.3

(*Continued*)

Table 3.1 Continued

	Pipes of Yakutian province									
	Sytykanskaya	Tayozhnaya		Radiovolnovaya	Zarnitsa	Aykhal	Faynshteynovskaya	Komsomol'skaya		Snezhinka
	(Data of V.P. Afanasiev, F.P. Lesnov, N.M. Podgorhnikh), INAA									
Element	M-20R	M-21M	M-21R	M-22R	M-23R	M-24R	M-25R	M-26R	M-27R	M-28R
La	33.00	224.1	205.0	78.00	116.0	162.0	103.0	39.00	36.00	97.00
Ce	54.00	319.6	279.0	128.0	189.0	248.0	168.0	62.00	61.00	146.0
Pr	N.d.	N.d.	N.d.	N.d.	N.d.	N.d.	N.d.	N.d.	N.d.	N.d.
Nd	18.00	88.98	83.00	46.00	80.00	97.00	62.00	24.00	24.00	50.00
Sm	3.08	12.98	11.50	6.68	10.90	13.20	9.20	4.12	4.11	7.30
Eu	0.81	3.03	2.80	1.62	2.46	2.92	2.01	1.11	0.95	1.70
Gd	1.90	7.38	6.50	3.90	6.50	6.40	6.50	2.60	2.40	3.60
Tb	0.27	0.99	0.91	0.56	0.84	0.92	0.76	0.36	0.34	0.50
Dy	N.d.	N.d.	N.d.	N.d.	N.d.	N.d.	N.d.	N.d.	N.d.	N.d.
Ho	N.d.	N.d.	N.d.	N.d.	N.d.	N.d.	N.d.	N.d.	N.d.	N.d.
Er	N.d.	N.d.	N.d.	N.d.	N.d.	N.d.	N.d.	N.d.	N.d.	N.d.
Tm	N.d.	0.18	N.d.	N.d.	N.d.	N.d.	N.d.	N.d.	N.d.	N.d.
Yb	0.36	0.91	0.93	0.59	0.95	0.84	0.82	0.51	0.43	0.53
Lu	0.05	0.15	0.11	0.07	0.09	0.11	0.09	0.07	0.06	0.08
Total	N.d.	N.d.	N.d.	N.d.	N.d.	N.d.	N.d.	N.d.	N.d.	N.d.
$(La/Yb)_n$	61.9	165	149	89.2	82.4	130	84.8	51.6	56.5	124

	Pipes of Yakutian province									
	Zarnitsa		Aykhal			Markoka	Irelyakhskaya	Yubileynaya		
	(Data of V.P. Afanasiev, F.P. Lesnov, N.M. Podgorhnikh), INAA									
Element	M-29R	M-30R	M-31R	M-32R	M-33R	M-34R	M-35R	M-36M	M-36R	M-37R
La	71.00	64.00	57.00	185.0	96.00	65.00	84.00	55.44	54.00	75.00
Ce	114.0	110.0	87.00	307.0	171.0	104.0	132.0	80.80	76.50	117.0
Pr	N.d.	N.d.	N.d.	N.d.	N.d.	N.d.	N.d.	N.d.	N.d.	N.d.
Nd	44.00	41.00	30.00	105.0	60.00	35.00	46.00	25.77	23.00	38.00
Sm	6.60	6.15	4.32	15.10	9.50	4.70	6.45	4.29	4.00	6.30
Eu	1.58	1.50	0.66	3.78	2.46	1.05	1.68	1.07	1.07	1.40
Gd	3.70	3.40	2.50	7.90	5.70	2.50	4.30	2.62	2.90	3.00
Tb	0.54	0.51	0.37	1.02	0.76	0.33	0.51	0.37	0.38	0.45
Dy	N.d.	N.d.	N.d.	N.d.	N.d.	N.d.	N.d.	N.d.	N.d.	N.d.
Ho	N.d.	N.d.	N.d.	N.d.	N.d.	N.d.	N.d.	N.d.	N.d.	N.d.
Er	N.d.	N.d.	N.d.	N.d.	N.d.	N.d.	N.d.	N.d.	N.d.	N.d.
Tm	N.d.	N.d.	N.d.	N.d.	N.d.	N.d.	N.d.	0.10	N.d.	N.d.
Yb	0.70	0.70	0.43	1.04	0.96	0.38	0.58	0.52	0.71	0.28
Lu	0.09	0.10	0.05	0.13	0.11	0.05	0.07	0.07	0.09	0.03
Total	N.d.	N.d.	N.d.	N.d.	N.d.	N.d.	N.d.	N.d.	N.d.	N.d.
$(La/Yb)_n$	68.5	61.7	89.5	120	67.5	115	97.8	72.0	51.3	181

(*Continued*)

Table 3.1 Continued

	Pipes of Yakutian province									
	Yubileynaya	Botuobinskaya			Malo-Kuonamskaya	Ruslovaya	Obnazhonnaya		Dal'niaya	Zarnitsa
	(Data of V.P. Afanasiev, F.P. Lesnov, N.M. Podgorhnikh), INAA									
Element	M-39R	M-40R	M-41R	M-42R	M-43R	M-44R	M-45R	M-46R	M-47R	M-48R
La	50.00	14.50	9.70	8.40	118.0	37.00	139.0	152.0	76.00	91.00
Ce	77.00	27.00	18.00	17.00	205.0	63.00	216.0	232.0	126.0	147.0
Pr	N.d.	N.d.	N.d.	N.d.	N.d.	N.d.	N.d.	N.d.	N.d.	N.d.
Nd	27.00	12.00	8.80	9.00	75.00	24.00	70.00	84.00	48.00	54.00
Sm	4.00	2.60	2.05	2.30	12.00	3.60	10.80	12.90	7.30	8.00
Eu	0.96	0.58	0.54	0.66	2.62	0.89	2.97	3.01	1.68	2.13
Gd	2.10	1.84	1.76	1.75	5.50	1.70	6.60	7.20	4.00	4.40
Tb	0.34	0.27	0.27	0.28	0.80	0.27	0.88	0.97	0.48	0.59
Dy	N.d.	N.d.	N.d.	N.d.	N.d.	N.d.	N.d.	N.d.	N.d.	N.d.
Ho	N.d.	N.d.	N.d.	N.d.	N.d.	N.d.	N.d.	N.d.	N.d.	N.d.
Er	N.d.	N.d.	N.d.	N.d.	N.d.	N.d.	N.d.	N.d.	N.d.	N.d.
Tm	N.d.	N.d.	N.d.	N.d.	N.d.	N.d.	N.d.	N.d.	N.d.	N.d.
Yb	0.38	0.32	0.63	0.44	0.71	0.34	0.82	1.03	0.51	0.59
Lu	0.05	0.04	0.09	0.06	0.08	0.04	0.09	0.12	0.07	0.07
Total	N.d.	N.d.	N.d.	N.d.	N.d.	N.d.	N.d.	N.d.	N.d.	N.d.
$(La/Yb)_n$	88.8	30.6	10.4	12.9	112	73.5	114	99.6	101	104

	Pipes of Yakutian province									
	Zarnitsa	Chomur	Mir							Udachnaya
	(Data of V.P. Afanasiev, F.P. Lesnov, N.M. Podgorhnikh), INAA									
Element	M-49R	M-50R	M-51R	M-52M	M-53M	M-54M	M-55M	M-56M	M-57M	M-58R
La	43.00	140.0	102.3	85.62	84.75	57.07	92.61	39.04	35.34	58.00
Ce	59.00	245.0	176.9	143.7	132.8	99.00	160.8	66.44	60.09	87.00
Pr	N.d.	N.d.	N.d.	N.d.	N.d.	N.d.	N.d.	N.d.	N.d.	N.d.
Nd	22.00	105.0	68.51	56.80	40.90	34.91	53.91	24.67	21.88	27.00
Sm	3.66	18.90	10.58	9.76	6.16	5.22	8.00	3.94	3.32	4.26
Eu	0.82	4.84	3.16	2.57	1.46	1.27	2.31	0.96	0.88	0.84
Gd	2.00	11.10	7.22	6.59	3.97	3.66	5.48	2.51	2.30	2.40
Tb	0.35	1.51	0.89	0.81	0.53	0.44	0.70	0.35	0.31	0.32
Dy	N.d.	N.d.	N.d.	N.d.	N.d.	N.d.	N.d.	N.d.	N.d.	N.d.
Ho	N.d.	N.d.	N.d.	N.d.	N.d.	N.d.	N.d.	N.d.	N.d.	N.d.
Er	N.d.	N.d.	N.d.	N.d.	N.d.	N.d.	N.d.	N.d.	N.d.	N.d.
Tm	N.d.	N.d.	0.17	0.18	0.14	0.10	0.13	0.10	0.10	N.d.
Yb	0.47	1.74	0.81	0.90	0.77	0.52	0.59	0.51	0.59	0.42
Lu	0.06	0.20	0.11	0.13	0.11	0.07	0.07	0.08	0.08	0.05
Total	N.d.	N.d.	N.d.	N.d.	N.d.	N.d.	N.d.	N.d.	N.d.	N.d.
$(La/Yb)_n$	61.8	54.3	85.1	64.3	74.5	73.9	106	52.0	40.5	93.2

(*Continued*)

Table 3.1 Continued

	Pipes of Yakutian province									
	Udachnaya									
	(Data of V.P. Afanasiev, F.P. Lesnov, N.M. Podgorhnikh), INAA									
Element	M-59M	M-59R	M-60R	M-61R	M-62R	M-63R	M-64M	M-65M	M-66M	M-67M
La	46.94	45.00	50.00	17.10	47.00	38.00	7.28	39.28	64.07	60.94
Ce	81.08	70.00	77.00	27.00	75.00	64.00	15.14	66.17	116.2	105.0
Pr	N.d.	N.d.	N.d.	N.d.	N.d.	N.d.	N.d.	N.d.	N.d.	N.d.
Nd	28.05	23.00	28.00	11.50	25.00	24.00	6.25	24.18	40.46	37.00
Sm	4.26	3.96	4.37	2.10	3.98	3.94	1.01	3.90	5.37	5.01
Eu	0.83	0.81	0.82	0.48	0.94	0.92	0.38	0.96	1.51	1.38
Gd	3.02	2.60	2.80	1.50	2.10	2.20	0.95	2.31	3.54	3.13
Tb	0.37	0.39	0.38	0.24	0.33	0.32	0.13	0.35	0.46	0.40
Dy	N.d.	N.d.	N.d.	N.d.	N.d.	N.d.	N.d.	N.d.	N.d.	N.d.
Ho	N.d.	N.d.	N.d.	N.d.	N.d.	N.d.	N.d.	N.d.	N.d.	N.d.
Er	N.d.	N.d.	N.d.	N.d.	N.d.	N.d.	N.d.	N.d.	N.d.	N.d.
Tm	0.10	N.d.	N.d.	N.d.	N.d.	N.d.	0.04	0.10	0.09	0.09
Yb	0.50	0.41	0.44	0.50	0.43	0.40	0.20	0.54	0.47	0.42
Lu	0.06	0.04	0.04	0.07	0.05	0.05	0.02	0.07	0.06	0.06
Total	N.d.	N.d.	N.d.	N.d.	N.d.	N.d.	N.d.	N.d.	N.d.	N.d.
$(La/Yb)_n$	63.8	74.1	76.7	23.1	73.8	64.1	24.7	48.7	93.0	97.7

	Pipes of Yakutian province									
	Udachnaya									
	(Data of V.P. Afanasiev, F.P. Lesnov, N.M. Podgorhnikh), INAA									
Element	M-68M	M-69M	M-70M	M-71M	M-72M	M-73M	M-74M	M-75M	M-76M	M-77M
La	76.25	74.56	75.81	81.43	77.44	51.52	50.86	24.38	31.88	35.22
Ce	128.5	123.8	127.9	142.2	136.8	87.46	83.73	41.53	54.04	58.74
Pr	N.d.	N.d.	N.d.	N.d.	N.d.	N.d.	N.d.	N.d.	N.d.	N.d.
Nd	44.16	44.88	42.85	48.17	45.30	31.10	28.31	13.02	18.37	19.32
Sm	6.63	6.12	5.75	6.86	6.90	5.22	3.94	2.16	3.13	3.32
Eu	1.63	1.58	1.45	1.78	1.74	1.17	1.03	0.59	0.84	0.86
Gd	3.73	3.88	3.50	4.16	4.42	3.13	2.72	1.39	1.95	2.35
Tb	0.51	0.49	0.43	0.54	0.58	0.45	0.36	0.21	0.27	0.31
Dy	N.d.	N.d.	N.d.	N.d.	N.d.	N.d.	N.d.	N.d.	N.d.	N.d.
Ho	N.d.	N.d.	N.d.	N.d.	N.d.	N.d.	N.d.	N.d.	N.d.	N.d.
Er	N.d.	N.d.	N.d.	N.d.	N.d.	N.d.	N.d.	N.d.	N.d.	N.d.
Tm	0.09	0.09	0.10	0.11	0.11	0.13	0.09	0.06	0.08	0.09
Yb	0.42	0.44	0.50	0.53	0.57	0.67	0.47	0.35	0.43	0.50
Lu	0.07	0.06	0.07	0.07	0.09	0.08	0.07	0.05	0.07	0.07
Total	N.d.	N.d.	N.d.	N.d.	N.d.	N.d.	N.d.	N.d.	N.d.	N.d.
$(La/Yb)_n$	123	113	102	104	91.8	52.0	73.5	46.8	50.4	47.9

(*Continued*)

Table 3.1 Continued

	Pipes of Yakutian province									
	Udachnaya									
	(Data of V.P. Afanasiev, F.P. Lesnov, N.M. Podgorhnikh), INAA									
Element	M-78M	M-79M	M-80M	M-81M	M-82M	M-83M	M-84M	M-85M	M-86M	M-87M
La	32.32	46.35	64.54	69.35	45.07	37.20	37.66	38.84	17.87	30.39
Ce	53.08	79.37	117.22	113.26	82.13	65.72	64.27	70.90	30.90	52.16
Pr	N.d.	N.d.	N.d.	N.d.	N.d.	N.d.	N.d.	N.d.	N.d.	N.d.
Nd	19.48	27.02	41.36	40.29	30.01	23.96	23.79	26.41	14.68	18.87
Sm	3.03	3.53	5.92	5.56	4.32	3.89	3.62	3.82	3.08	3.10
Eu	0.80	0.91	1.58	1.42	1.00	0.88	0.93	0.92	0.75	0.81
Gd	2.00	1.96	3.72	3.46	2.59	2.36	2.22	2.37	2.73	2.13
Tb	0.30	0.25	0.49	0.43	0.32	0.31	0.31	0.29	0.43	0.28
Dy	N.d.	N.d.	N.d.	N.d.	N.d.	N.d.	N.d.	N.d.	N.d.	N.d.
Ho	N.d.	N.d.	N.d.	N.d.	N.d.	N.d.	N.d.	N.d.	N.d.	N.d.
Er	N.d.	N.d.	N.d.	N.d.	N.d.	N.d.	N.d.	N.d.	N.d.	N.d.
Tm	0.08	0.07	0.10	0.08	0.08	0.08	0.09	0.08	0.22	0.08
Yb	0.47	0.37	0.50	0.41	0.39	0.42	0.46	0.42	1.28	0.45
Lu	0.07	0.06	0.06	0.06	0.05	0.05	0.07	0.05	0.18	0.07
Total	N.d.	N.d.	N.d.	N.d.	N.d.	N.d.	N.d.	N.d.	N.d.	N.d.
$(La/Yb)_n$	46.6	84.1	86.7	113	78.3	59.9	55.7	62.8	9.4	45.9

	Province								
	Udachnaya	25-Finland		7-Finland	Snake Lake, Canada	Africa		Venezuela	
	(Data of V.P. Afanasiev, F.P. Lesnov, N.M. Podgorhnikh), INAA								
Element	M-110M	M-88R	M-89R	M-90R	M-91R	M-93M	M-93R	M-94R	M-95R
La	28.92	39.00	83.00	85.00	100.0	116.7	115.0	181.0	130.0
Ce	49.73	59.00	130.0	130.0	155.0	207.4	212.0	205.0	145.0
Pr	N.d.	N.d.	N.d.	N.d.	N.d.	N.d.	N.d.	N.d.	N.d.
Nd	17.81	20.00	46.00	44.00	45.00	82.91	91.00	47.00	30.00
Sm	2.71	3.24	7.20	6.00	6.20	13.83	15.00	4.70	3.10
Eu	0.77	0.74	1.65	1.45	1.45	3.70	3.94	0.94	0.69
Gd	2.01	2.10	3.50	3.30	3.20	8.86	10.10	2.10	1.50
Tb	0.25	0.32	0.52	0.44	0.44	1.12	1.28	0.27	0.22
Dy	N.d.	N.d.	N.d.	N.d.	N.d.	N.d.	N.d.	N.d.	N.d.
Ho	N.d.	N.d.	N.d.	N.d.	N.d.	N.d.	N.d.	N.d.	N.d.
Er	N.d.	N.d.	N.d.	N.d.	N.d.	N.d.	N.d.	N.d.	N.d.
Tm	0.07	N.d.	N.d.	N.d.	N.d.	0.18	N.d.	N.d.	N.d.
Yb	0.41	0.71	0.60	0.46	0.42	0.86	1.14	0.30	0.32
Lu	0.06	0.09	0.08	0.06	0.05	0.13	0.13	0.04	0.04
Total	N.d.	N.d.	N.d.	N.d.	N.d.	N.d.	N.d.	N.d.	N.d.
$(La/Yb)_n$	47.2	37.1	93.4	125	161	91.2	68.1	407	274

(*Continued*)

Table 3.1 Continued

	Province								
	Katoka, Angola				Kamitonga, Angola				Kakale, Angola
	(Egorov, 2006), ICP-MS								
Element	Ang-1	Ang -2	Ang -3	Ang -4	Ang -5	Ang -6	Ang -7	Ang -8	Ang -9
La	86.78	54.4	41.97	98.78	152.5	45.31	41.67	132.09	35.33
Ce	138.4	92.1	70.81	182.2	331.2	66.95	70.53	213.9	60.10
Pr	13.73	9.72	7.5	17.89	31.02	8.25	7.55	24.54	7.14
Nd	48.66	35.64	25.47	64.91	103.61	30.2	26.79	82.41	24.48
Sm	6.94	5.72	4.19	13.09	13.63	5.13	3.78	11.93	3.85
Eu	1.64	1.39	0.98	3.48	3.1	1.27	1.09	3.08	1.15
Gd	6.9	5.33	4.17	13.48	17.15	5.87	3.92	12.21	4.10
Tb	0.95	0.73	0.48	1.7	1.95	0.71	0.6	1.8	0.58
Dy	2.27	2.09	1.83	5.32	3.68	2.31	1.39	3.78	1.73
Ho	0.38	0.35	0.31	0.86	0.61	0.42	0.23	0.58	0.31
Er	1.77	1.43	1.06	3.18	3.64	1.49	1.1	3.06	1.25
Tm	0.13	0.12	0.11	0.37	0.23	0.16	0.07	0.16	0.12
Yb	0.84	0.73	0.71	2.4	1.63	0.92	0.49	1.08	0.73
Lu	0.14	0.12	0.1	0.35	0.23	0.13	0.07	0.14	0.11
Total	309	210	160	408	664	169	159	491	141
$(La/Yb)_n$	69.7	50.3	39.9	27.8	63.2	33.2	57.4	82.6	32.7

	Province							
	Kakele, Angola			Anomalia 1. Angola		Anomalia 2. Angola	Anomalia 3. Angola	Anomalia 5. Angola
	(Egorov, 2006), ICP-MS							
Element	Ang -10	Ang -11	Ang -12	Ang -13	Ang -14	Ang -15	Ang -16	Ang -17
La	27.98	24.28	28.98	40.10	35.87	64.94	40.83	34.73
Ce	51.90	43.15	50.74	67.81	66.99	128.16	70.85	67.47
Pr	5.07	5.26	5.55	6.98	6.89	12.47	7.37	7.28
Nd	17.96	17.90	19.06	24.33	23.44	45.52	25.70	27.15
Sm	3.02	2.80	3.05	3.97	3.92	7.94	4.26	4.51
Eu	0.82	1.05	1.24	1.15	0.97	2.15	1.07	1.26
Gd	3.28	2.88	3.19	4.76	4.11	8.38	4.55	4.95
Tb	0.39	0.42	0.43	0.52	0.50	1.04	0.56	0.66
Dy	1.51	1.22	1.33	1.78	1.60	2.78	1.63	1.88
Ho	0.27	0.21	0.23	0.36	0.26	0.44	0.27	0.31
Er	0.87	0.83	0.86	1.22	0.96	1.75	1.15	1.17
Tm	0.11	0.07	0.08	0.12	0.10	0.14	0.10	0.10
Yb	0.65	0.47	0.54	0.62	0.60	0.81	0.61	0.69
Lu	0.09	0.07	0.07	0.11	0.10	0.10	0.09	0.10
Total	114	101	115	154	146	277	159	152
$(La/Yb)_n$	29.1	34.9	36.2	43.7	40.4	54.1	45.2	34.0

(*Continued*)

Table 3.1 Continued

	Province							
	Anomalia 8. Angola		Luante, Angola			Angola		
	(Egorov, 2006), ICP-MS							
Element	Ang-18	Ang-19	Ang-20	Ang-21	Ang-22	Min.	Max.	Average ($n = 22$)
La	114.99	65.17	203.36	32.68	47.30	24.28	203.36	65.91
Ce	221.4	128.4	246.4	35.31	53.38	35.31	331.2	111.7
Pr	22.25	12.70	38.22	5.21	7.48	5.07	38.22	12.28
Nd	77.89	46.79	152.22	20.13	27.80	17.90	152.22	44.00
Sm	12.62	7.41	24.21	3.19	4.44	2.80	24.21	6.98
Eu	3.20	1.84	6.08	0.87	1.32	0.82	6.08	1.83
Gd	12.80	7.59	30.68	3.66	5.07	2.88	30.68	7.68
Tb	1.43	1.12	2.72	0.35	0.51	0.35	2.72	0.92
Dy	3.96	2.90	7.03	1.27	1.75	1.22	7.03	2.50
Ho	0.60	0.48	1.10	0.21	0.29	0.21	1.10	0.41
Er	2.49	1.70	2.14	0.50	0.64	0.50	3.64	1.56
Tm	0.16	0.17	0.24	0.07	0.09	0.07	0.37	0.14
Yb	1.19	1.05	2.06	0.48	0.63	0.47	2.40	0.91
Lu	0.13	0.15	0.18	0.06	0.08	0.06	0.35	0.12
Total	475	277	717	104	151	101	717	257
$(La/Yb)_n$	65.2	41.9	66.6	46.0	50.7	34.9	57.2	49.1

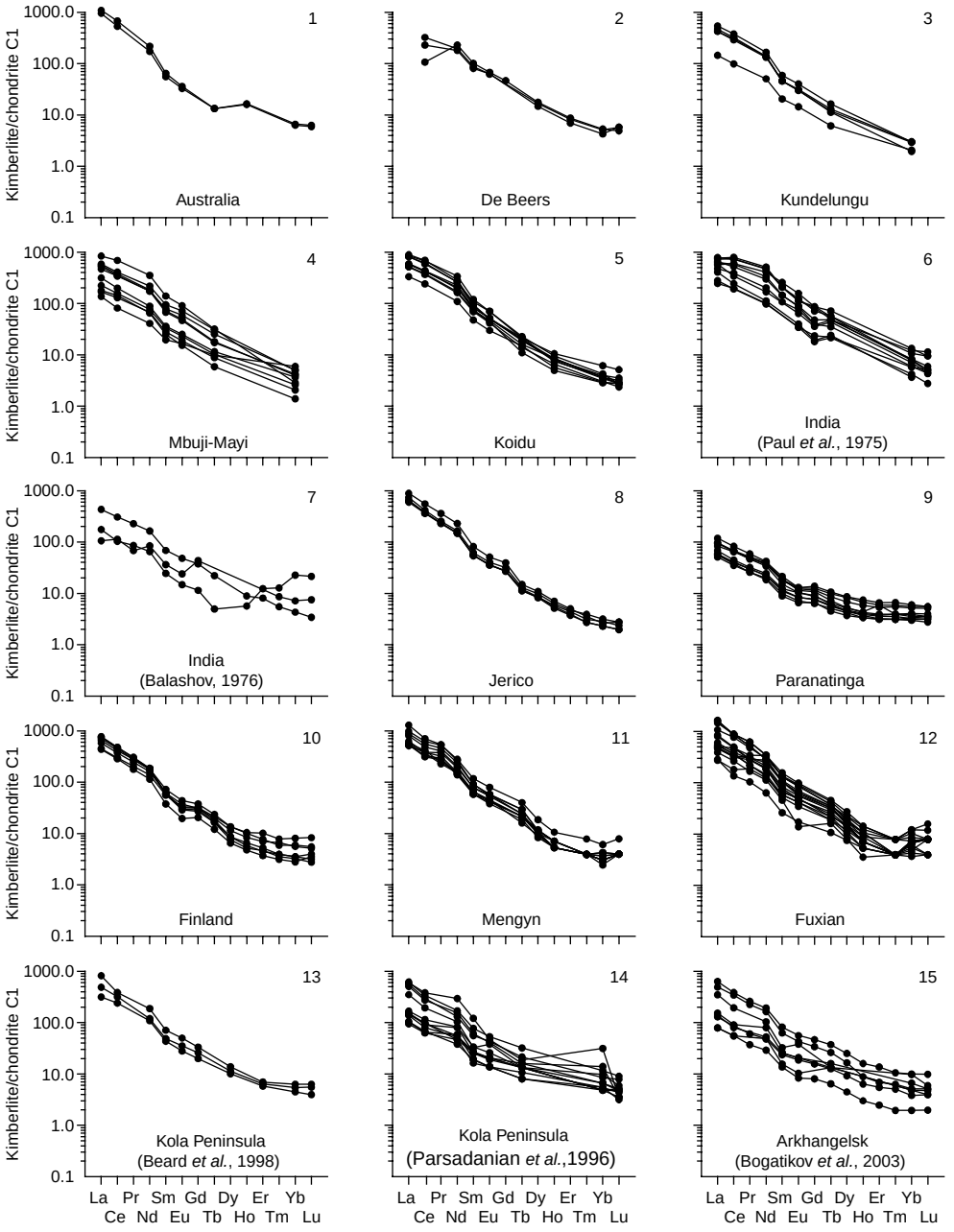

Figure 3.1 Chondrite-normalized REE patterns for kimberlites (data Table 3.1).

Peninsula (279), Angola (257), Arkhangelsk (235), Yakutian (229), and Brazil (80). The average total REE content in kimberlites calculated according to 313 analyses from all the said provinces amounts to 342 ppm (the standard deviation is 240 ppm). On the basis of the estimated average values of the parameter $(La/Yb)_n$, the provinces are

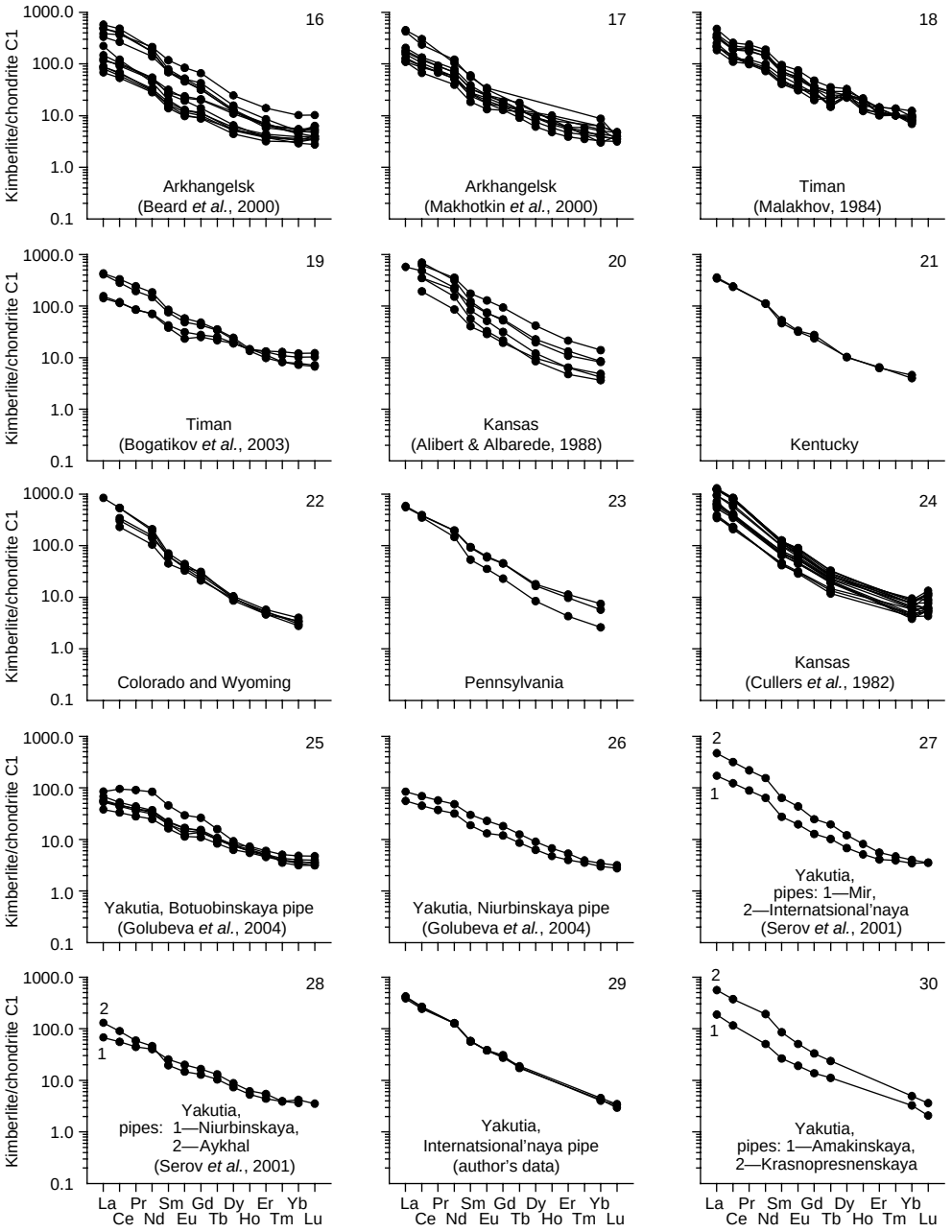

Figure 3.1 Continued

conventionally divided into two types. The first type is represented by the provinces in which the kimberlites are characterized by increased REE fractionation intensity (provinces of Canada, Australia, China, Finland, Africa, and the USA). In the second type of province, kimberlites are distinguished by a less intensively fractionated

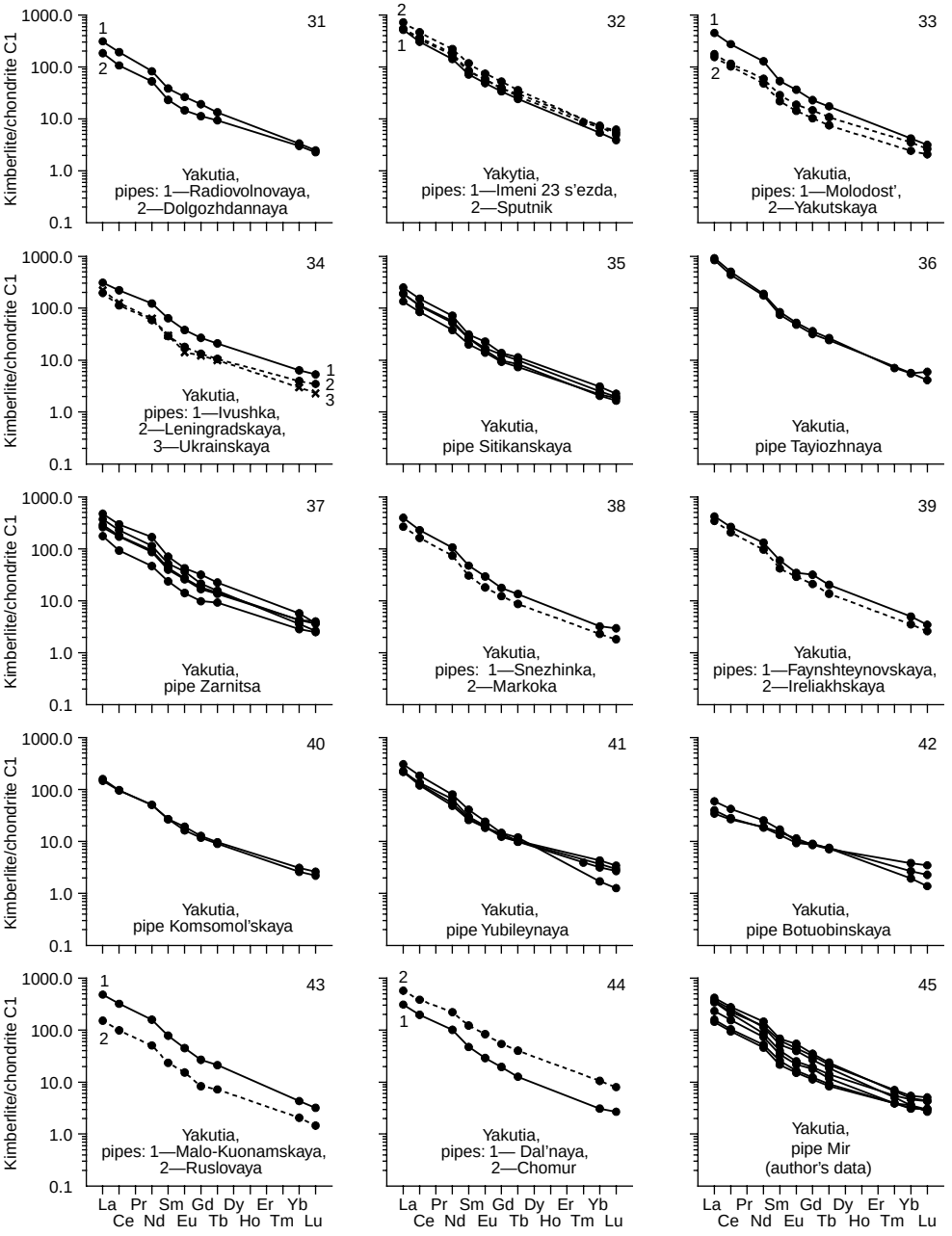

Figure 3.1 Continued

REE distribution (provinces of Yakutia, India, Angola, Archangelsk, Kola Peninsula, Timan, Brazil). The average value of the parameter $(La/Yb)_n$ calculated from the data on 313 analyses of the kimberlite samples from all the above-listed provinces amounts to 85 (the standard deviation is 64).

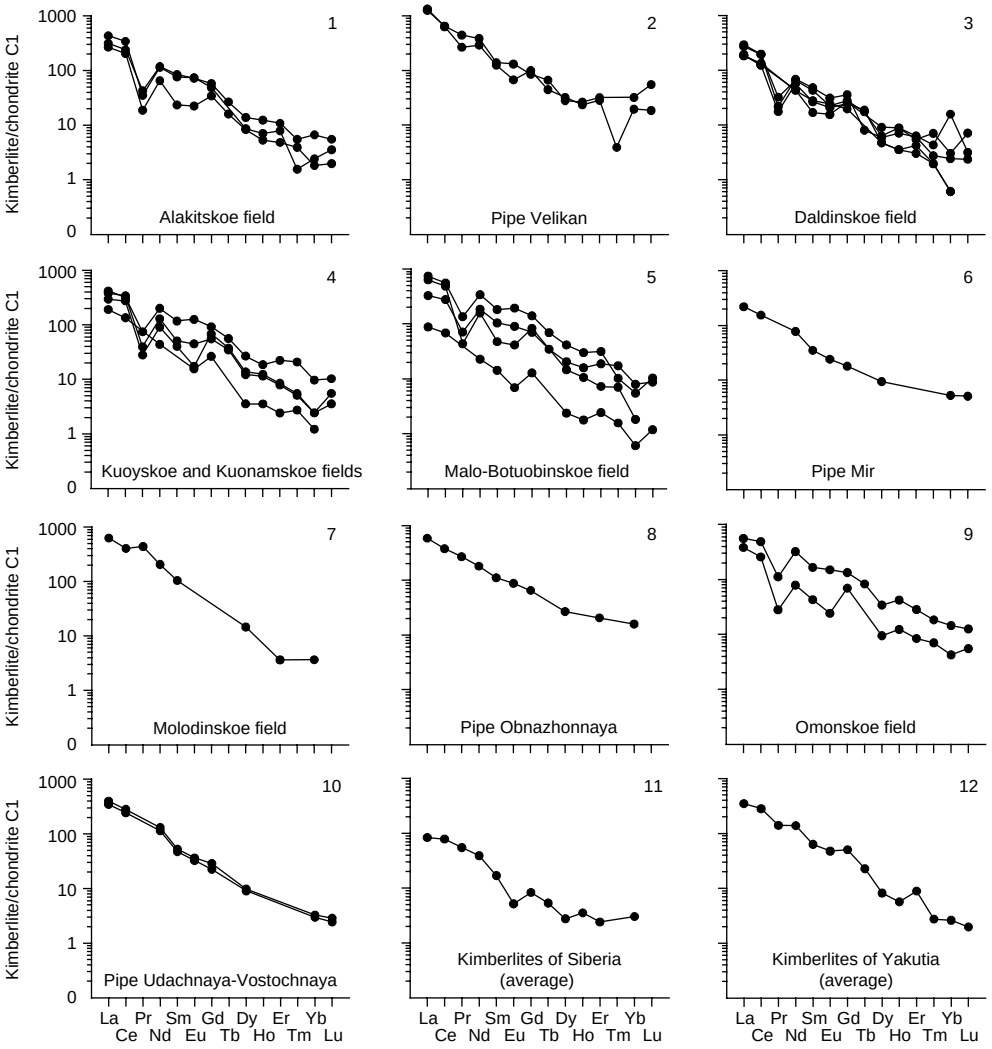

Figure 3.2 Chondrite-normalized REE patterns for kimberlites from some pipes and manifestations of Yakutian province (data Table 3.2).

The REE patterns of the vast majority of the studied kimberlites have a shape close to a straight line with a steep negative slope (see Fig. 3.1), some of them showing negative Eu anomalies of very low intensity. Such anomalies were observed earlier in kimberlites from the provinces of South Africa and Yakutia (Dawson, 1983). Within most provinces, kimberlites are characterized by a comparatively uniform rare earth composition as evidenced by compact arrangement and conformity of their patterns (see Fig. 3.1) as well as by relatively small standard deviations (see Table 3.3, Fig. 3.3).

Table 3.2 Rare earth element composition of kimberlites from Yakutian province (ppm).

	Pipe (field)									
	Alakit field				Velikan pipe		Daldyn field			
	(Kaminsky *et al.*, 1978)				(Marshintsev 1986)		(Kaminsky *et al.*, 1978)			
Element	Sit-1	A-6	D-19	A-4	Mar-1	Mar-2	D-18	D13-14	D-3	D-2
La	74.5	77.0	65.5	106.0	308.0	325.3	47.4	66.6	45.7	71.8
Ce	178.5	154.5	131.0	219.0	413.0	402.7	78.5	124.9	80.2	125.5
Pr	19.6	4.1	1.8	3.4	42.8	25.6	1.7	2.1	N.d.	3.1
Nd	58.3	56.1	30.9	54.0	182.6	137.9	26.9	32.5	20.8	30.9
Sm	9.4	13.1	3.6	11.8	21.4	19.2	4.1	7.4	2.6	6.6
Eu	N.d.	4.2	1.3	4.3	7.6	3.9	1.2	1.8	0.9	1.3
Gd	N.d.	11.8	7.0	10.0	17.4	20.4	5.0	7.3	5.4	5.7
Tb	N.d.	1.0	0.6	N.d.	2.5	1.67	0.7	0.3	N.d.	0.65
Dy	0.8	3.5	2.1	2.2	7.1	8.17	1.2	1.5	2.3	1.6
Ho	N.d.	0.7	0.3	0.4	1.5	1.33	0.2	0.4	0.5	0.5
Er	0.4	1.8	0.8	1.3	5.3	4.73	0.5	1.0	0.9	1.05
Tm	N.d.	0.14	0.10	0.04	N.d.	0.10	0.05	0.07	0.18	0.11
Yb	0.4	1.1	0.3	0.4	5.3	3.23	0.10	0.4	0.5	2.6
Lu	N.d.	0.14	0.05	0.09	1.4	0.47	N.d.	0.06	0.18	0.08

	Pipe (field)									
	Kuoyskoe field		Kuonamskoe field		Malo-Botuobinskoe field				Omonskoe field	
	(Kaminsky *et al.*, 1978)									
Element	K-10	K-3	Km-3	Km-13	B-7	B-1	B-4	B-6	O-4	O-5
La	46.7	102.5	93.5	72.3	80.5	21.5	182.0	155.0	93.6	136.6
Ce	85.9	205.0	217.0	175.5	176.0	43.4	356.0	311.0	164.0	312.0
Pr	N.d.	7.2	3.8	2.7	6.8	N.d.	13.0	4.2	2.7	10.8
Nd	20.8	95.0	61.4	42.8	88.0	10.7	160.5	75.0	37.4	152.5
Sm	N.d.	18.1	7.8	6.2	16.1	2.2	28.2	7.3	6.6	25.6
Eu	0.9	7.3	2.6	1.0	5.2	0.4	11.2	2.4	1.4	8.7
Gd	5.4	18.8	11.3	13.9	14.3	2.6	28.6	17.0	14.2	27.3
Tb	N.d.	2.1	1.3	1.4	1.3	N.d.	2.6	N.d.	N.d.	3.1
Dy	0.9	6.8	3.1	3.5	5.2	0.6	10.5	3.7	2.4	8.7
Ho	0.2	1.05	0.65	0.7	0.9	0.10	1.7	0.6	0.7	2.4
Er	0.4	3.7	1.3	1.4	3.1	0.4	5.2	1.2	1.4	4.7
Tm	0.07	0.53	0.13	0.14	0.44	0.04	0.26	0.18	0.18	0.47
Yb	0.2	1.6	0.4	0.4	1.3	0.10	0.9	0.3	0.7	2.4
Lu	N.d.	0.26	0.09	0.14	0.22	0.03	0.26	N.d.	0.14	0.32

(*Continued*)

3.1.3 Correlation of REE and other components in kimberlites

As shown by complex petrochemical and geochemical investigations on kimberlites, correlations differing in sign and intensity exist between the contents of their main

Table 3.2 Continued

	Pipe (field)							
	Udachnaya-Vostochnaya pipe		Mir pipe	Molodiozhnoe field	Ogon'kovskoe field	Obnazhennaya pipe	Udachnaya pipe	Internatsional'naya pipe
	(Laz'ko, 1988a)				(Ilupin) *et al.*, 1978)	(Balashov, 1976)		(Burkov, 1990)
Element	Laz-2	Laz-3	Laz-1	Ung-1	Aer-1	Bal-1	Bal-2	Bur-1
La	85.0	98.0	54.0	154.0	70.5	143.0	64.0	245.0
Ce	155.0	180.0	99.0	259.5	127.0	240.0	120.0	555.0
Pr	N.d.	N.d.	N.d.	42.6	9.9	26.0	13.0	49.0
Nd	54.0	62.0	37.0	97.0	46.0	85.0	45.0	150.0
Sm	7.3	8.1	5.4	16.1	5.6	17.1	8.2	22.0
Eu	1.9	2.1	1.4	N.d.	N.d.	5.1	1.90	2.6
Gd	4.6	5.9	3.7	N.d.	N.d.	13.3	6.5	13.0
Dy	2.3	2.5	2.4	3.7	0.8	6.8	4.1	5.2
Er	N.d.	N.d.	N.d.	0.6	N.d.	3.4	2.5	N.d.
Yb	0.49	0.54	0.87	0.6	N.d.	2.6	1.8	N.d.
Lu	0.06	0.07	0.13	N.d.	N.d.	N.d.	N.d.	N.d.

chemical components and REE, and estimates of these correlations are reliable only if use is made of the analysis selections that have statistically uniform contents of petrogenic elements (Vasilenko *et al.*, 1997, 2003a,b; Lesnov, 2002d, 2003b). These correlations were revealed after sorting through a special selection of analyses. Within the limits of this working selection, the content of each REE was found to vary over a wide range, usually with a polymodal empirical distribution. This selection appeared to represent several genetically independent types of kimberlites. In the course of further procedures, the primary selection of analyses was divided into several uniform subselections, and for each of these subselections coefficients of correlation between petrogenic elements were calculated. As a result, several correlation complexes, that is, groups of petrogenic components, were isolated in which there were strong positive correlations between the oxides. These complexes are: (1) "pyroxene complex" (SiO_2–Al_2O_3–Na_2O); (2) "calcite complex" (CaO–loss of ignition (LOI)); (3) "phlogopite complex" (MgO–K_2O); and (4) "ilmenite complex" (TiO_2–FeO_{tot}).

Further calculations of the coefficients of pair correlation between petrogenic oxides and REE on the basis of the these prepared selections of analyses have shown that all the light REE have a negative correlation with pyroxene complex components, stronger with SiO_2, and weaker with Na_2O and Al_2O_3 (Fig. 3.4), and all the heavy REE have a strong positive correlation with oxides of the ilmenite complex TiO_2 and FeO_{tot}. Distinct from the other light elements, La and Pr revealed a strong positive correlation with components of the calcite complex, that is, with CaO, and with LOI. In contrast to the other heavy REE, Yb and Lu manifested a strong positive correlation with oxides of the ilmenite complex and at the same time a strong negative dependence on calcite complex components. These calculations also showed that with increasing degree of REE fractionation, estimated from the values of the parameter $\sum(La + \ldots + Eu)/\sum(Tb + \ldots + Yb)$, in kimberlites, the content of CaO increases, and that of MgO decreases. The trend in the changes of correlation coefficient

Table 3.3 Average REE composition (x) and standard deviation (σ) of kimberlites from some provinces (ppm).

	Provinces											
	Australia (2)		China (22)		Canada (5)		India (15)		Finland (8)		USA (34)	
Element	x	σ	x	σ	x	σ	x	σ	x	σ	x	σ
La	251	17	197	109	173	29.0	117	54.2	150	32.3	181	82.8
Ce	387	46.5	317	149	265	51.4	259	152	249	48.2	301	136
Pr	N.d.	N.d.	35.8	14.0	25.4	5.36	12.3	8.4	24.3	4.35	N.d.	N.d.
Nd	92.5	10.5	103	37.7	80.2	16.7	115	74.9	76.7	12.4	86.2	34.7
Sm	9.27	0.68	13.5	4.99	9.52	1.78	22.1	11.9	8.90	1.47	12.7	5.00
Eu	2	0.09	3.31	1.17	2.31	0.38	4.32	2.42	1.89	0.40	3.20	1.31
Gd	N.d.	N.d.	N.d.	N.d.	6.26	1.07	9.48	5.13	6.09	1.00	7.27	3.96
Tb	0.5	N.d.	1.04	0.34	0.47	0.06	1.49	0.70	0.69	0.13	0.86	0.22
Dy	N.d.	N.d.	3.62	1.28	2.34	0.29	N.d.	N.d.	2.55	0.68	3.58	2.19
Ho	0.93	0.015	0.455	0.15	0.34	0.04	0.41	0.13	0.42	0.12	N.d.	N.d.
Er	N.d.	N.d.	N.d.	N.d.	0.72	0.09	1.70	0.50	1.03	0.35	1.31	0.75
Tm	N.d.	N.d.	0.12	0.04	0.08	0.01	0.23	0.09	0.13	0.04	N.d.	N.d.
Yb	1.07	0.03	0.96	0.42	0.44	0.06	1.45	0.80	0.78	0.30	0.96	0.40
Lu	0.16	0.01	0.16	0.07	0.06	0.01	0.17	0.13	0.10	0.06	0.20	0.07
Total	744	75.0	676	306	565	105	544	295	522	97.4	508	214
$(La/Yb)_n$	160	14.5	160	90.8	269	44.7	65.2	33.6	148	64.9	124	43.9

(*Continued*)

Table 3.3 Continued

	Provinces													
	Africa (28)		Timan (14)		Kola Peninsula (18)		Angola (22)		Arkhangelsk (33)		Yakutia (102)		Brazil (10)	
Element	*x*	σ	*x*	σ	*x*	σ	*x*	σ	*x*	σ	*x*	σ	*x*	σ
La	122	55.8	71.6	26.5	81.6	54.0	65.9	47.1	60.8	44.0	66.3	44.7	19.1	5.58
Ce	232	116	117	44.6	124	73.7	112	79.4	112	85.0	109	69.6	34.8	10.6
Pr	N.d.	N.d.	14.8	5.55	N.d.	N.d.	12.3	9.07	10.5	7.55	6.28	5.03	3.85	1.18
Nd	81.3	40.6	57.4	21.6	52.9	31.1	44.0	33.7	43.6	32.0	39.67	24.08	14.1	4.33
Sm	10.2	4.88	9.55	2.92	6.90	4.15	6.98	5.21	6.39	4.49	6.12	3.60	2.25	0.68
Eu	2.49	1.16	2.61	0.87	1.80	0.77	1.83	1.26	1.63	1.02	1.51	0.89	0.58	0.14
Gd	N.d.	N.d.	6.66	1.75	5.40	1.34	7.68	6.44	4.64	3.07	3.78	2.01	1.94	0.53
Tb	0.61	0.26	0.92	0.27	0.59	0.23	0.92	0.63	0.57	0.27	0.51	0.25	0.26	0.08
Dy	N.d.	N.d.	6.32	0.96	2.99	0.47	2.50	1.46	2.65	1.49	2.05	0.40	1.41	0.43
Ho	0.44	0.10	0.93	0.19	N.d.	N.d.	0.41	0.22	0.44	0.18	0.35	0.05	0.27	0.08
Er	N.d.	N.d.	2.01	0.27	1.06	0.10	1.56	0.86	1.00	0.48	0.83	0.10	0.74	0.22
Tm	N.d.	N.d.	0.27	0.04	N.d.	N.d.	0.14	0.07	0.13	0.06	0.11	0.04	0.11	0.03
Yb	0.58	0.19	1.50	0.28	1.58	1.21	0.91	0.51	0.97	0.84	0.61	0.24	0.67	0.18
Lu	0.08	0.02	0.23	0.07	0.12	0.05	0.12	0.06	0.12	0.04	0.08	0.07	0.10	0.03
Total	450	217	291	101	279	162	257	181	235	168	229	143	80.2	23.3
$(La/Yb)_n$	148	61.0	34.2	15.1	41.2	30.8	47.5	14.8	46.4	31.5	72.7	34.7	19.6	5.92

Data Table 3.1. Provinces are disposed according to decrease of average total contents REE in represented kimberlites in the brackets—quantity of analyses.

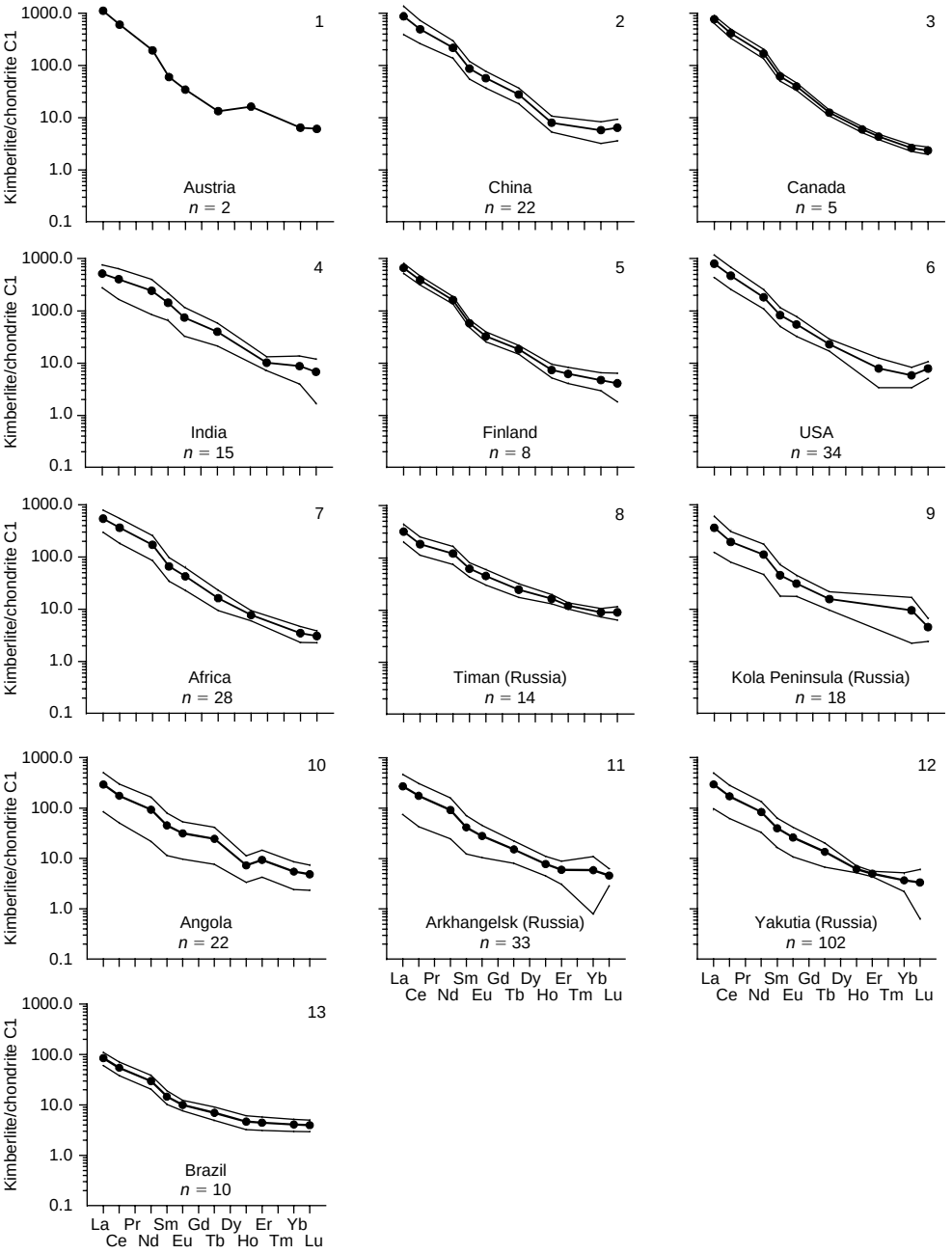

Figure 3.3 Chondrite-normalized patterns for average REE composition of kimberlites (data Table 3.3). Narrow lines mark limits of REE content variations on basis of standard deviations.

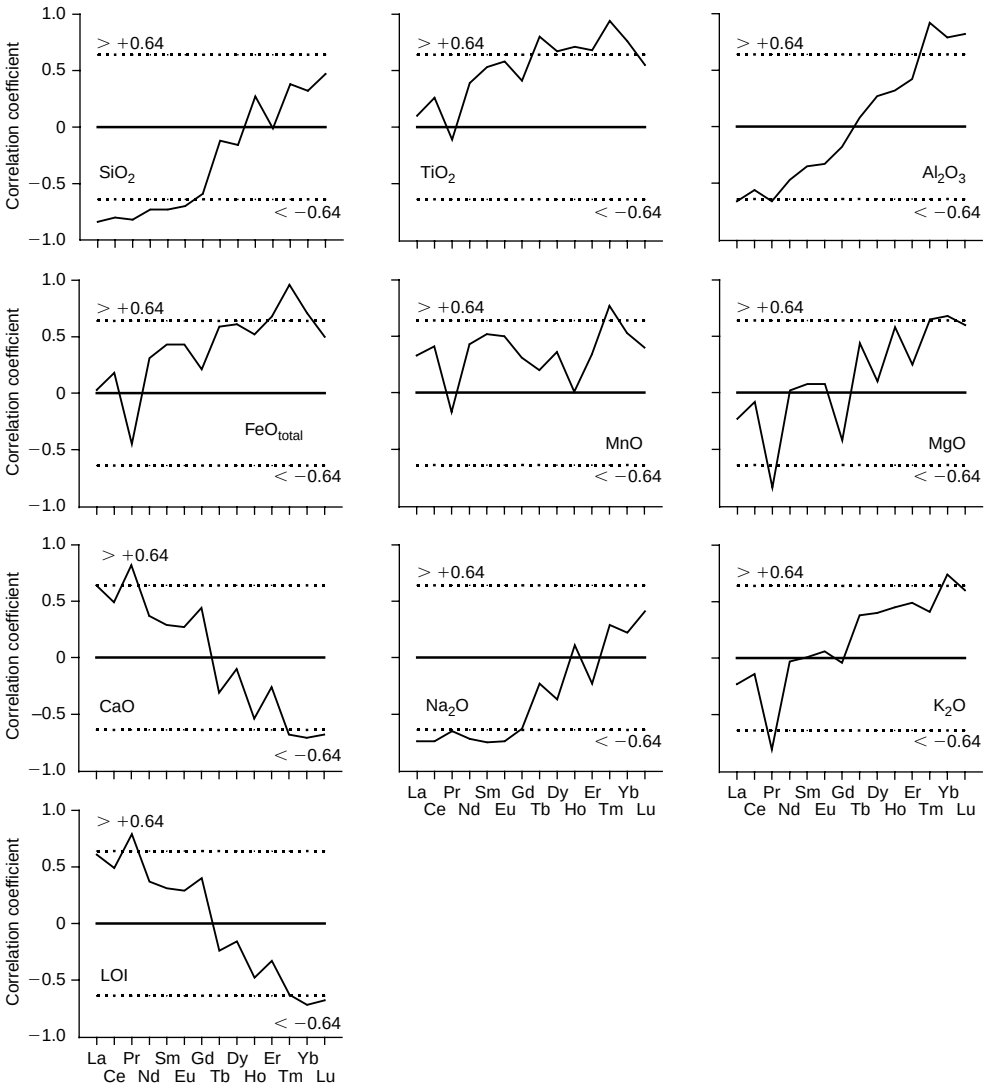

Figure 3.4 Changing of coefficients of correlation (r_{01}) between REE composition and composition of petrochemical components in kimberlites ($n = 15$, $r_{01} = 0.64$).

values for the majority of petrogenic components of kimberlites (SiO_2, TiO_2, Al_2O_3, FeO_{tot}, MgO, K_2O, Na_2O) have a positive slope (see Fig. 3.4), which can testify that the intensity of correlation between these components and REE increases from light elements toward heavy ones. The trend in the coefficients of correlations of REE with CaO and LOI is characterized by a negative slope, that is, the correlation intensity of these petrochemical components decreases from light REE to heavy ones. Certain tendencies in the correlations between the contents of REE and those of petrogenic components in kimberlites can also be judged from the two-dimensional diagrams

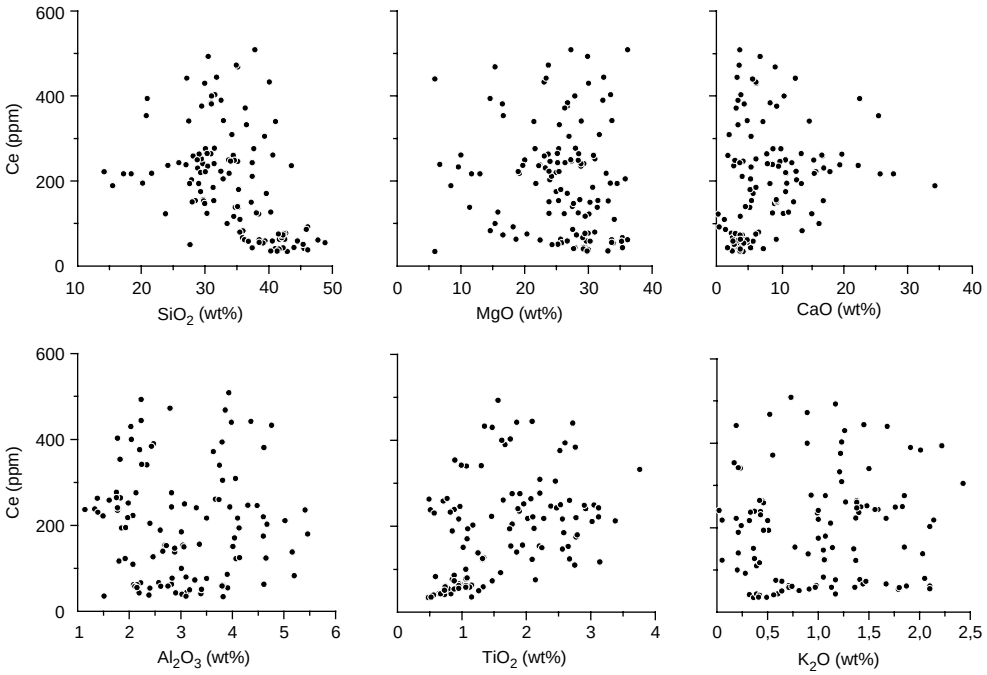

Figure 3.5 Correlation between content of Ce and contents of SiO_2, MgO, CaO, Al_2O_3, TiO_2, and K_2O in kimberlites.

reflecting the correlations between the contents of Ce and such components (Fig. 3.5). From the graph it follows that even at a significant scatter of figurative points, one can assume a sufficiently strong dependence of Ce on Si and at the same time a positive bond of Ce with Ti, while this rare earth component does not reveal distinct bonds with the other petrogenic components.

In many cases during geochemical investigations on kimberlites, besides REE, analyses were also made of other admixture elements. The largest number of these complex analyses has by now been made of kimberlites from the South African and Arkhangelsk provinces. Most of the admixtures were found to be distributed in kimberlites rather heterogeneously, which is predetermined by their petrochemical and mineralogical variety. Nevertheless, within separately taken kimberlite manifestations and provinces, the proportions between most admixture elements vary within relatively narrow ranges. According to their accumulation level, the whole series of studied admixture elements in kimberlites can be conventionally divided into three groups. The first group includes BA, Th, U, Nb, and Ta, which contents in kimberlites are two or more orders of multitude higher than those in chondrite Cl. The second group comprises Rb, Sr, Zr, Hf, Li, and Y, which are represented in amounts exceeding those in chondrite by no more than one and a half orders of magnitude. And, finally, the third group embraces V, Co, Ni, Cr, and Pb, which are represented in amounts close to, or even smaller than, their contents in chondrite.

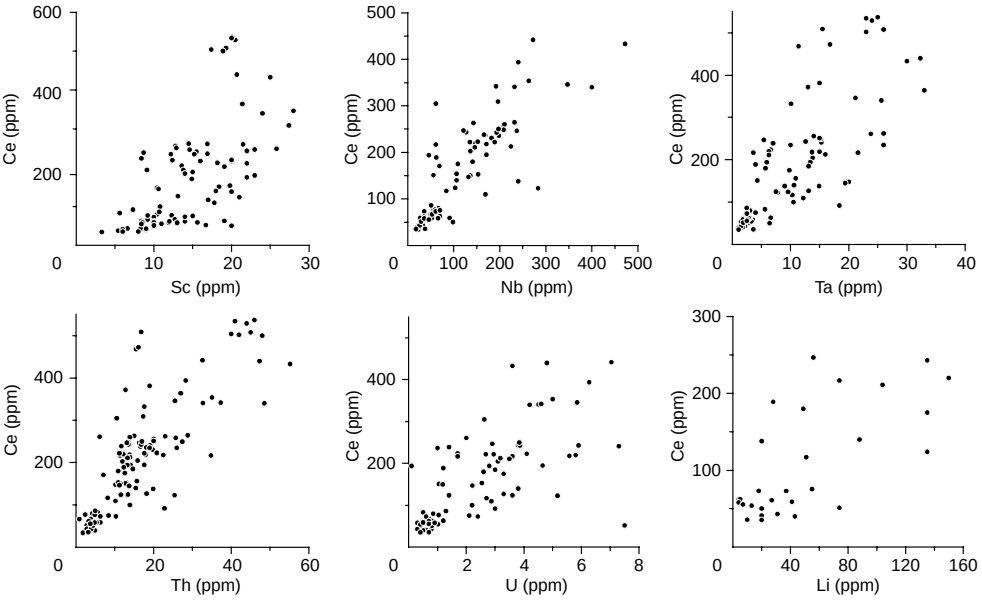

Figure 3.6 Correlation between content of Ce and contents of Sc, Nb, Ta, Th, U, and Li in kimberlites.

Some peculiarities of correlations between REE and the other admixture elements can be illustrated by the example of Ce and Yb. The content of Ce is more or less dependent on that of such elements as Sc, Nb, Ta, Th, U, and Li (Fig. 3.6). The content of Yb, in its turn, demonstrates a distinct and direct dependence on that of Sc, Y, Li, and a less explicit one on that of Zr, Hf, Sr (Fig. 3.7). On the basis of these data, Sc, Nb, Ta, Th, U, and possibly Li, just as Ce and other light REE, can be assumed to participate in isomorphous replacement of mesh-forming elements in the main minerals of kimberlites, and Y, Zr, Hf, and some amounts of Sc and Li take part in similar substitution jointly with heavy REE.

3.1.4 General regularities of REE distribution in kimberlites

The materials considered above show that kimberlites are characterized by significant heterogeneity of REE distribution, which reflects their general chemical heterogeneity caused by different geodynamic and petrogenetic factors. By example of the kimberlite provinces that have now been studied in sufficient detail, and what is more, by means of up-to-date analytic techniques, it has been shown that these rocks are always essentially enriched with light REE. Their content in kimberlites is 200–1100 times as large as that in chondrite Cl. It has also been found that REE content steadily decreases from light REE toward heavy ones down to a level of 2–20 chondrite normalization (t. ch.). The rocks most enriched with lanthanides are kimberlites from the Australian province, while the least enriched ones are those from the Arkhangelsk province (Lesnov, 2003b).

The analysis of the relationship between the contents of light REE and those of petrogenic components has revealed a very negative correlation with pyroxene correlation

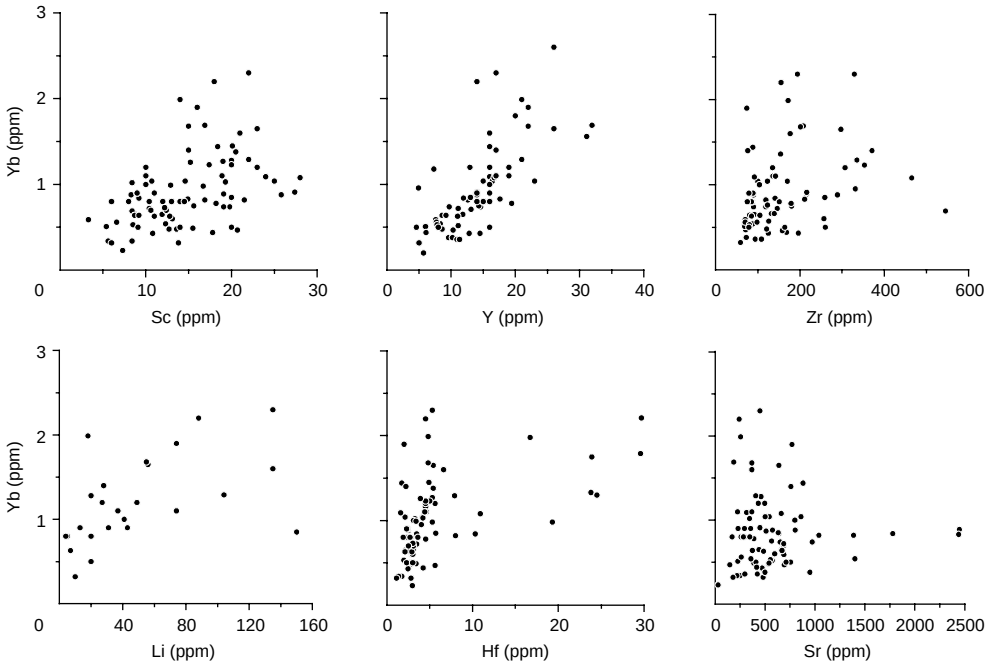

Figure 3.7 Correlation between content of Yb and contents of Sc, Y, Zr, Li, Hf, and Sr in kimberlites.

complexes, that is, with the contents of SiO_2, Al_2O_3, and Na_2O. The said bonds seem to have been caused by depleting kimberlite melts of REE since the rocks were contaminated by materials with lower REE content. This assumption is supported by the results of petrochemical investigations on the diamondiferous kimberlites in Yakutian province exemplified by the Mir pipe breaking through the carbonaceous-terrigenous and halogenic-carbonaceous formations of the Cambrian system (Vasilenko *et al.*, 1997, 2003a,b). An earlier hypothesis existed that the increased contents of Na_2O and Al_2O_3 observed in kimberlites from this pipe resulted from their contamination by halogen formations or from the action of buried salt brines (Pavlov *et al.*, 1985). However, the above participation of Na_2O in the correlation complexes with Al_2O_3 and SiO_2 does not agree with this assumption. According to the available data, high sodic kimberlites are distinguished by decreased contents of diamonds as well as by a smaller degree of iron oxidation. This peculiarity in the composition of kimberlites has made it possible to assume that their abnormal richness in sodium and their simultaneous decreased diamond content are conditioned by the same endogenous factors. To determine the possible reasons for the enrichment of kimberlites with Na_2O, study was made of the dependence between the contents of this component and mantle xenoliths of different composition (Vasilenko *et al.*, 1997, 2003a,b). As a result, the enrichment of kimberlites with sodium was found to be directly dependent on the volume amounts of magnesian eclogite xenoliths contained in them. This process has been shown to be the main reason for the abnormally high content of Na in kimberlites as well as the most important factor in weakening the correlation between light REE and

CaO. One of the main concentrators of lanthanides in mantle peridotites is known to be clinopyroxene, in which the overwhelming part of their trivalent ions replaces the Ca^{2+} ions according to the diagram of heterovalent isomorphism. It is not improbable that a similar diagram of isomorphism of REE is also realized in other silicate minerals from ultramafic rocks as well as in calcite. The considerable scatter of liquidus temperatures and pressures to which the kimberlite melts were subjected might have been one of the main factors in providing wide variations of light REE content in calcites present in kimberlites.

The available values of pair correlation coefficients testify that heavy REE have a sufficiently strong positive correlation with the components of an ilmenite correlation complex, while for light REE, such a correlation is not obvious. At the same time, the contents of light elements, for example, La (7–70 ppm), in ilmenites are much higher than those of heavy ones, for example, Lu (0.25–10 ppm) (Fesq *et al.*, 1975; Rikhvanov *et al.*, 2001). An essential predominance of light REE over heavy ones is also observed in another titaniferous mineral present in kimberlites, that is, perovskite. The reason for this lack of correspondence obviously consists in that ilmenite, which content in kimberlites may amount to about 2–4%, along with perovskite, concentrates an essential part of heavy REE while an overwhelming amount of light REE is contained in calcite, which modal amount essentially exceeds the content of the mentioned Ti minerals. It is this circumstance that evidently accounts for the observed strong positive bond between the contents of heavy REE and those of the components of the ilmenite correlation complexes, as well as for the absence of such a bond between these components and light REE. Probably, ilmenite, as a more widespread mineral in kimberlites compared with perovskite, concentrates essential amounts of heavy REE, which are contained in the kimberlites and which are also often concentrated in pyrope xenocrystals. The accumulation level of heavy REE in kimberlites can be used as one of the criteria for reconstructing the conditions of kimberlite formation, just as the content of TiO_2 is used to estimate the relative formation depth of various populations of these rocks (Vasilenko *et al.*, 1997).

Note that according to experimental data, the content of TiO_2 in clinopyroxene and garnet present in peridotites decreases with increasing equilibrium pressure in this system (Akella & Boyd, 1972; Ringwood, 1975). Hence, as the pressure and the depth of the melt generation increased, so did the content of TiO_2 in selective meltings on the basis of these minerals. According to observations, the content of TiO_2 in kimberlites varies within a sufficiently wide range (0.48–2.92 wt%), which is also one of the factors predetermining the significant fluctuations of REE content in these rocks. It appears topical to study in more detail the regularities of REE distribution in ilmenites, which, among other things, will contribute to solving the problem of kimberlite petrogenesis and to estimating the prospect of their diamond content. Data presented on the peculiarities of the REE distribution in kimberlites from different provinces and separate diatremes, along with evidence on the chemical and rare earth composition of the minerals composing them, can broaden to a certain degree the prospect of revealing additional geochemical criteria for investigating the genesis of kimberlites.

With reference to the above bonds between REE and some other admixture elements in kimberlites, it is necessary to call attention to the following correlations. There is reason to believe that as kimberlites were formed and their minerals were

crystallized, admixture elements such as Ba, Th, U, Nb, and Ta participated in isomorphic replacement of mesh-forming elements jointly with light and middle REE, while the isomorphism of heavy REE probably proceeded with the participation of the ions of Sc, Li, Y, Zr, Hf, and Sr. It is self-evident that the above geochemical bonds between REE and the other chemical elements in kimberlites are far from exhausting all their diversity. As kimberlites were formed, their rock-forming and accessory minerals, depending on their crystalline and chemical properties and crystallization conditions, selectively accumulated certain associations and amounts of REE in accordance with the mechanism of heterovalent isomorphism. At the same time it should be considered that smaller or larger amounts of REE may be present in these rocks outside the structures of minerals, that is, as non-structural impurities in the form of soluble compounds in the microcracks of mineral grains and in the intergranular space of the rocks.

* * *

According to their REE composition, kimberlites essentially differ from most of other rocks of magmatic origin. The available analytical data on the geochemistry of REE in kimberlites have made it possible to determine a number of new parameters of their material constitution. These parameters can be used to systematize both the rocks proper and the diatremes and provinces, as well as to solve the problems of the genesis of these rocks and of their diamond content. So far, however, far from all the known kimberlite manifestations and provinces formed by them, including those situated in Russia, have been explored in this respect more or less comprehensively.

According to data on the general level of REE accumulation in kimberlites, their provinces can be somewhat conventionally arranged in a sequence from the Australian province, in which the rocks are characterized by the highest level of REE accumulation, to the Archangel province, in which rocks the REE level turns out to be the lowest. Conceivably, the kimberlites from the said provinces might in a certain sense represent the range of physical and chemical conditions under which these rocks were formed. At the same time, within the limits of separate pipes and the provinces formed by them, the samples of kimberlites are characterized by a relatively uniform REE distribution. In all cases, the kimberlites manifest rather intensive REE fractionation, conditioned by sharply increased contents of the light elements (200–1100 t. ch.) compared to heavy ones (2–20 t. ch.). Judging by values of the parameter $(La/Yb)_n$, the most intensive REE fractionation is typical of kimberlites from the Canadian and Australian provinces, and the least intensive is typical of those from the Archangel and Timan provinces.

The rare earth patterns of kimberlites usually have the form of a line close to a straight one, but sometimes weak negative Eu anomalies occur due to some peculiarities of mineral composition. The overwhelming amount of REE in kimberlites are contained in the form of a structural admixture in their rock-forming and accessory minerals: clinopyroxenes, calcites, perovskites, apatites, ilmenites, phlogopites, as well as in xenogenous garnets. Light REE have positive correlations with CaO and at the same time negative bonds with SiO_2, Na_2O, and Al_2O_3, which implies that a significant amount of light REE enters into the structure of calcites and other carbonates. Heavy REE reveal positive bonds with TiO_2 and FeO_{tot}, which may indicate that an essential

amount of these REE enter into titanium minerals: perovskite and picroilmenite. The accumulation level and the peculiarities of REE distribution in kimberlites are assumed to be first of all due to the generation conditions of their parent melts. According to the suggested models, kimberlite melts were generated at very great depths and at very low melting degrees of the mantle sources (on the order of a few tenths of a percent). This process is assumed to have run at a pressure on the order of 6 GPa in the presence of very high concentrations of CO_2. The diversity of kimberlites with respect to the intensity of REE fractionation was above all due to the degree of the partial melting of mantle sources, which was in all cases very low. At the same time, the differences observed in kimberlites from different provinces as to the general level of REE accumulation are mainly dependent on the specificity of the material constitution of the mantle sources of their parent melts.

Further complex geochemical investigations on kimberlites from reference diatremes (pipes) and their provinces, including studies on the distribution of REE and other indicated admixture elements and on petrochemical and mineralogical characteristics, will contribute to the improvement of systematic classification of these rocks and to the creation of less contradictory models of the origin of these unique magmatic formations. This will also aid in obtaining additional information for discussing the conditions under which the diamond deposits linked with kimberlites were formed.

3.2 KOMATIITES

Komatiites represent rather a specific type of magmatic rocks. By a number of structural and microstructural features they can be identified as volcanogenic formations, however they differ considerably from the majority of other effusive rocks by an unusually high content of MgO, which makes it possible to regard them as effusive analogues of ultramafites. Most komatiite manifestations are concentrated on the shields within Archean greenstone belts, and more rarely they enter into the composition of younger volcanogenic complexes.

Komatiites were first discovered and described in the area of the Komati River in South Africa, they are located within the Archean greenstone belt Barberton (Viljoen & Viljoen, 1969). The volcanogenic rock masses contained in this belt were isolated as the Swaziland complex, which includes the provinces Onverwacht, Fig Try, and Modis. The age of the komatiites from the Onverwacht province was determined by the Sm–Nd method and amounted to 3.56 ± 0.24 million years (Jahn *et al.*, 1982). Somewhat later, komatiites were discovered in Australia (Kambalda province), Canada (Abitibi province, Monro Township manifestation), India (Holenarasipur and Sargur provinces), Columbia (Gorgona Island province), Finland, Russia (Kola Peninsula, Karelia, Aldan), and Vietnam. In most of these provinces, komatiites form distorted interbeds of insignificant thickness and extension alternating with thicker basalt levels. In the diagnostics of komatiites, use is made of a complex of structural and petrographical, petrochemical, and geochemical criteria. An especially important structural feature of these rocks consists in that the crystals of olivine and clinopyroxene have skeletal forms ("spinifex" structure) pointing to very high mineral crystallization rates due to quick cooling of high-magnesium and high-temperature melts. The petrographical criteria for the diagnostics of komatiites include their inherently high content of MgO,

which is uncommonly high for effusive rocks, as well as increased values of the parameters CaO/Al_2O_3 and Al_2O_3/TiO_2. According to their MgO content (wt%), it is the practice to divide komatiites into peridotitic (MgO > 20), pyroxenitic (MgO = 12–20), and basaltic (12 > MgO > 9) classifications.

In the geochemical diagnostics and systematic classification of komatiites as well as in solving the problem of their genesis, ever-widening use is now made of data on the distribution of REE and other admixture elements (Cullers & Graf, 1984). In recent decades, representative analytical evidence on REE in komatiites was obtained in the provinces of Onverwacht, Barberton, Kambalda, Abitibi, Monro Township, Gorgona Island, India, Karelia, Kola Peninsula, and other districts of the Baltic shield (Table 3.4, Fig. 3.8). According to these data, the total content of REE in komatiites varies within the range of 3–70 ppm, and at the same time is inversely proportional to the content of MgO in the rocks. Values of the parameter $(La/Yb)_n$ in different types of komatiites vary from less than unity to greater than unity. The rare earth patterns of some komatiites show negative or positive Eu anomalies of insignificant intensity.

In classifying komatiites according to their REE composition, it is proposed to use the values of the two main geochemical parameters: $(La/Sm)_n$ and $(Gd/Yb)_n$ (Jahn *et al.*, 1982). According to these criteria, three geochemical groups of komatiites have been isolated, which were, in their turn, divided into classes, represented in each province at different frequencies (Table 3.5).

Group I. Heavy REE, unfractionated,
$(Gd/Yb)_n \sim 1.0$.
Class 1. Light REE, unfractionated,
$(La/Sm)_n \sim 1.0$.
Class 2. Light REE, depleted,
$(La/Sm)_n < 1.0$.
Class 3. Light REE, enriched,
$(La/Sm)_n > 1.0$.
Group II. Heavy REE, depleted,
$(Gd/Yb)_n > 1.0$.
Class 4. Light REE, depleted,
$(La/Sm)_n < 1.0$.
Class 5. Light REE, enriched,
$(La/Sm)_n > 1.0$.
Group III. Class 6. Heavy REE, enriched,
$(Gd/Yb)_n < 1$

Consider further some peculiarities of REE distribution in komatiites from the best studied provinces (Table 3.6, Fig. 3.9).

The Province of the Baltic shield unites numerous areas of REE distribution within Archean greenstone belts located on the territory of Karelia and Kola peninsula. A number of large structures have been isolated there, in which stratigraphic section the bodies of komatiites alternating with those of basalts amounts to about 10–15% of the volume of volcanogenic rock masses (Smol'kin, 1992; Vrevsky *et al.*, 2003). Komatiites from this province were discovered to frequently contain relics of the "spinifex" structure. Petrochemical and geochemical data testify to a great diversity and lateral

Table 3.4 Rare earth element composition of komatiites (ppm).

	Provinces													
	Baltic shield, Russia													
	(Vrevsky *et al.*, 2003), ICP-MS													
Element	427-2	427-5	427-7	576-4	575-2	224	224/1	1	350-1b	41-1/2	547-10	737-2	746	c-197B
La	1.5	2.16	1.58	0.53	N.d.	0.42	0.51	0.38	0.67	0.45	N.d.	N.d.	N.d.	1.6
Ce	2.96	4.62	3.65	1.58	0.56	1.5	1.82	1.3	2.6	1.52	0.97	1.32	1.84	3.5
Pr	0.4	0.72	0.45	0.21	0.11	0.21	0.38	0.26	0.4	0.3	0.12	0.26	0.22	0.6
Nd	1.99	3.29	2.37	1.01	0.6	1.37	2.17	1.5	2	1.76	0.78	1.04	1.03	2.8
Sm	0.58	0.82	0.75	0.38	0.27	0.49	0.72	0.59	0.65	0.69	0.32	0.43	0.43	1.03
Eu	0.18	0.3	0.19	0.1	0.05	0.18	0.27	0.22	0.21	0.26	0.08	0.02	0.02	0.31
Gd	0.92	1.22	0.85	0.55	0.5	0.68	0.82	0.96	0.7	1.13	0.28	0.96	0.39	1.07
Tb	N.d.	N.d.	N.d.	N.d.	N.d.	0.15	0.17	0.16	0.11	0.19	0.05	0.13	0.1	0.21
Dy	0.87	1.12	0.93	0.53	0.44	0.81	1.02	1.16	0.94	1.17	0.32	0.82	1.02	1.64
Ho	N.d.	N.d.	N.d.	N.d.	N.d.	0.18	0.25	0.23	0.2	0.27	0.08	0.19	0.2	0.36
Er	0.58	0.67	0.55	0.39	0.29	0.45	0.71	0.68	0.59	0.8	0.26	0.5	0.61	0.94
Tm	N.d.	N.d.	N.d.	N.d.	N.d.	0.07	0.11	0.1	0.09	N.d.	0.04	0.06	N.d.	0.15
Yb	0.68	0.87	0.7	0.35	0.35	0.42	0.69	0.56	0.52	0.66	0.27	0.58	0.68	0.93
Lu	0.1	0.14	0.1	0.05	0.05	0.07	0.12	0.1	0.08	0.12	0.03	0.09	0.07	0.14
Total	N.d.	N.d.	N.d.	N.d.	N.d.	7.0	9.8	8.2	9.8	9.3	N.d.	N.d.	N.d.	15.3
$(La/Yb)_n$	1.5	1.7	1.5	1.0	N.d.	0.68	0.50	0.46	0.87	0.46	N.d.	N.d.	N.d.	1.2

	Provinces													
	Baltic shield, Russia													
	(Vrevsky *et al.*, 2003), ICP-MS													
Element	275-10	275-2b	9m01	05-2b	08-3b	19/92	235-a/5	753/7	723/7	185-a	194	200	200-a	202
La	1.3	1.2	N.d.	N.d.	N.d.	1.61	0.22	0.47	0.87	1.29	0.17	0.16	0.58	0.37
Ce	2.8	2.1	2.32	2.3	2.6	3.55	0.82	1.15	2.48	2.36	0.69	0.45	1.57	1.1
Pr	0.35	0.3	0.35	0.38	0.4	N.d.	N.d.	N.d.	N.d.	0.33	N.d.	N.d.	N.d.	N.d.
Nd	1.91	1.3	1.53	1.8	1.9	3.27	0.87	0.75	1.81	1.34	0.51	0.35	0.94	0.71
Sm	0.53	0.4	0.53	0.62	0.61	0.97	0.21	0.3	0.54	0.38	0.16	0.11	0.3	0.26
Eu	0.12	0.09	0.18	0.21	0.24	0.26	0.09	0.09	0.18	0.08	0.08	0.04	0.15	0.08
Gd	N.d.	0.48	0.54	0.79	0.83	N.d.	N.d.	N.d.	N.d.	0.29	N.d.	N.d.	N.d.	N.d.
Tb	N.d.	0.1	0.1	0.14	0.15	0.19	0.06	0.11	0.14	0.06	0.06	0.02	0.1	0.06
Dy	N.d.	0.7	0.8	1.1	1.05	N.d.	N.d.	N.d.	N.d.	0.4	N.d.	N.d.	N.d.	N.d.
Ho	N.d.	0.15	0.18	0.26	0.22	N.d.	N.d.	N.d.	N.d.	N.d.	N.d.	N.d.	N.d.	N.d.
Er	N.d.	0.46	0.53	0.74	0.62	N.d.	N.d.	N.d.	N.d.	0.25	N.d.	N.d.	N.d.	N.d.
Tm	0.1	0.07	N.d.	N.d.	N.d.	N.d.	N.d.	N.d.	N.d.	0.03	N.d.	N.d.	N.d.	N.d.
Yb	0.6	0.43	0.6	0.67	0.59	0.4	0.19	0.37	0.47	0.23	0.22	0.07	0.31	0.26
Lu	0.1	0.07	0.1	0.11	0.1	0.04	0.03	0.05	0.07	0.04	0.04	0.01	0.04	0.03
Total	N.d.	7.9	N.d.	N.d.	N.d.	N.d.	N.d.	N.d.	N.d.	7.1	N.d.	N.d.	N.d.	N.d.
$(La/Yb)_n$	1.5	1.9	N.d.	N.d.	N.d.	2.7	0.78	0.86	1.2	3.8	0.52	1.5	1.3	0.96

(*Continued*)

Table 3.4 Continued

	Provinces													
	Baltic shield					Onverwaht, South Africa								
	(Vrevsky *et al.*, 2003), ICP-MS					(Jahn *et al.*, 1982), IDMS								
Element	9019r	9016	9014/1	9014a/2	9014a	J5046	J5049	J5052	J5019	J5031	J5067	J5077	J5080	J5084
La	0.7	0.75	1.25	0.81	1.04	6.740	4.636	3.541	1.938	3.380	16.060	3.780	5.503	2.872
Ce	1.83	1.9	3	2.11	2.57	16.904	12.632	11.070	N.d.	N.d.	31.180	10.470	14.090	7.784
Pr	0.26	N.d.	N.d.	N.d.	0.38	N.d.	N.d.	N.d.	N.d.	N.d.	N.d.	N.d.	N.d.	N.d.
Nd	1.04	1.43	1.9	1.52	1.88	11.312	9.416	8.966	2.498	3.569	12.329	7.465	7.866	5.972
Sm	0.32	0.53	0.56	0.49	0.59	3.980	2.987	2.978	0.658	0.945	2.317	2.122	2.255	1.857
Eu	0.08	0.18	0.16	0.14	0.19	1.189	1.251	1.020	0.245	0.358	0.573	0.712	0.712	0.664
Gd	0.27	N.d.	N.d.	N.d.	0.62	4.168	3.810	3.900	0.832	1.210	2.180	2.732	2.825	2.351
Tb	0.05	0.13	0.11	0.09	0.11	N.d.	N.d.	N.d.	N.d.	N.d.	N.d.	N.d.	N.d.	N.d.
Dy	0.39	N.d.	N.d.	N.d.	0.63	4.485	4.157	5.216	0.880	1.078	2.494	2.843	3.083	2.709
Ho	0.08	N.d.	N.d.	N.d.	0.13	N.d.	N.d.	N.d.	N.d.	N.d.	N.d.	N.d.	N.d.	N.d.
Er	0.23	N.d.	N.d.	N.d.	0.34	2.499	2.110	2.400	0.548	0.599	1.678	1.710	1.767	1.557
Tm	0.03	N.d.	N.d.	N.d.	0.05	N.d.	N.d.	N.d.	N.d.	N.d.	N.d.	N.d.	N.d.	N.d.
Yb	0.18	0.52	0.49	0.35	0.32	2.229	2.065	2.110	0.465	0.568	1.742	1.652	1.614	1.450
Lu	0.03	0.08	0.08	0.05	0.05	0.338	N.d.	0.325	0.080	0.084	0.287	0.263	0.251	0.207
Total	5.5	N.d.	N.d.	N.d.	8.9	53.8	N.d.	N.d.	N.d.	N.d.	N.d.	N.d.	N.d.	N.d.
$(La/Yb)_n$	2.6	0.97	1.7	1.6	2.2	2.1	1.5	1.1	2.8	4.0	6.3	1.6	2.3	1.3

	Provinces													
	Onverwaht, South Africa					Barberton, South Africa								
	(Jahn *et al.*, 1982)	(Sun & Nesbitt, 1978), IDMS										(Herrmann *et al.*, 1976), RNAA		
Element	J5092	SuNes-3	SuNes-4	SuNes-5	49Ja	49Jb	331/78a	331/78a	87J	VB1	AB9	A-27	BK-2	BK-3
La	6.095	N.d.	0.730	2.200	0.776	N.d.	N.d.	1.62	2.23	2.36	3.71	0.82	3.5	2.6
Ce	13.780	4.700	N.d.	6.200	1.87	1.73	4.69	4.31	6.15	6.39	10.2	2.3	8.7	8
Pr	N.d.	N.d.	N.d.	N.d.	N.d.	N.d.	N.d.	N.d.	N.d.	N.d.	N.d.	N.d.	N.d.	N.d.
Nd	5.791	3.400	1.700	5.300	1.39	1.23	3.38	3.11	5.29	5.10	7.40	2.1	6.9	4.5
Sm	1.241	0.990	0.500	1.700	0.434	0.386	0.988	0.906	1.72	1.61	2.13	0.58	1.9	1.4
Eu	0.413	0.340	0.160	0.600	0.17	0.149	0.338	0.311	0.605	0.549	0.674	0.21	0.59	0.48
Gd	1.461	1.200	0.630	2.200	0.592	N.d.	1.17	1.06	2.21	N.d.	2.70	0.7	2.3	1.8
Tb	N.d.	N.d.	N.d.	N.d.	N.d.	N.d.	N.d.	N.d.	N.d.	N.d.	N.d.	0.14	0.44	0.32
Dy	1.987	1.300	0.700	2.400	0.721	0.606	1.26	1.16	2.39	2.25	3.01	0.89	2.8	2.0
Ho	N.d.	N.d.	N.d.	N.d.	N.d.	N.d.	N.d.	N.d.	N.d.	N.d.	N.d.	0.2	0.64	0.45
Er	1.759	0.760	0.410	1.400	0.462	0.402	0.755	0.663	1.39	1.36	1.85	0.5	1.6	1.0
Tm	N.d.	N.d.	N.d.	N.d.	N.d.	N.d.	N.d.	N.d.	N.d.	N.d.	N.d.	N.d.	N.d.	N.d.
Yb	1.700	0.680	0.370	1.200	0.446	0.371	0.681	0.597	1.24	1.21	1.73	0.49	1.56	1.19
Lu	0.284	N.d.	N.d.	N.d.	N.d.	N.d.	N.d.	N.d.	N.d.	N.d.	N.d.	0.08	0.24	0.18
Total	34.5	13.4	5.2	23.2	6.9	N.d.	N.d.	13.7	23.2	20.8	33.4	9.0	31.2	23.9
$(La/Yb)_n$	2.4	N.d.	1.3	1.2	1.2	N.d.	N.d.	1.8	1.2	1.3	1.5	N.d.	N.d.	N.d.

(*Continued*)

Table 3.4 Continued

	Provinces													
	Kambalda (Tripod Hill), Australia					Kambalda (Silver Lake), Australia								
	(Lesher & Arndt, 1995), LCHR													
Element	90741	90742	90745	90746	90749	90753	90699	90266	90700	90702	90704	90705	90707	90272
La	0.80	1.07	1.01	0.85	0.94	0.59	0.58	0.58	0.48	0.70	0.52	0.86	0.18	0.08
Ce	2.00	2.9	2.97	2.5	2.74	2.10	1.81	1.86	1.61	2.13	1.89	2.75	0.52	0.25
Pr	0.31	0.44	0.47	0.42	0.44	0.38	N.d.	N.d.	N.d.	N.d.	N.d.	N.d.	N.d.	N.d.
Nd	1.74	2.38	2.6	2.46	2.36	2.34	1.76	1.87	1.79	2.10	2.15	2.90	0.49	0.26
Sm	0.72	0.84	0.87	0.95	0.83	0.95	0.66	0.71	0.7	0.79	0.87	1.13	0.18	0.11
Eu	0.21	0.41	0.38	0.37	0.23	0.48	0.20	0.25	0.18	0.30	0.29	0.34	0.02	0.04
Gd	1.23	1.33	1.24	1.43	1.22	1.45	0.95	1.04	0.96	1.15	N.d.	1.62	0.26	0.17
Tb	0.24	0.25	0.22	0.27	0.22	0.27	N.d.	N.d.	N.d.	N.d.	N.d.	N.d.	N.d.	N.d.
Dy	1.74	1.81	1.51	1.81	1.51	1.8	1.16	1.27	1.24	1.42	N.d.	2.05	0.31	0.22
Ho	0.38	0.39	0.32	0.39	0.32	0.39	N.d.	N.d.	N.d.	N.d.	N.d.	N.d.	N.d.	N.d.
Er	1.17	1.18	0.98	1.18	0.98	1.19	0.72	0.81	0.78	0.90	N.d.	1.31	0.20	0.15
Tm	0.17	0.18	0.15	0.17	0.15	0.17	N.d.	N.d.	N.d.	N.d.	N.d.	N.d.	N.d.	N.d.
Yb	1.13	1.19	0.98	1.17	0.97	1.15	0.70	0.78	0.74	0.87	N.d.	1.25	0.21	0.16
Lu	0.17	0.18	0.14	0.17	0.15	0.17	0.11	0.12	0.12	0.14	N.d.	0.19	0.04	N.d.
Total	12.0	14.6	13.8	14.1	13.1	13.4	N.d.	N.d.	N.d.	N.d.	N.d.	14.4	2.4	1.4
$(La/Yb)_n$	0.48	0.61	0.70	0.49	0.65	0.35	0.56	0.50	0.44	0.54	N.d.	0.46	0.58	0.34

	Provinces													
	Kambalda (Silver Lake), Australia													
	(Lesher & Arndt, 1995), LCHR													
Element	90710	90273	90711	90695	90712	90718	90720	91726	91785	91789	91794	91819	91863	91975
La	0.16	0.29	0.55	0.84	0.36	0.23	0.12	0.26	0.66	1.01	0.23	0.92	1.88	1.39
Ce	0.48	0.83	1.76	2.59	1.03	0.64	0.37	0.75	1.81	2.72	0.99	2.88	4.92	3.44
Pr	N.d.	N.d.	N.d.	0.44	N.d.	N.d.	N.d.	N.d.	0.29	0.45	N.d.	0.43	0.73	0.56
Nd	0.45	0.76	1.82	2.56	0.93	0.58	0.39	0.74	1.92	2.55	1.49	2.51	4.02	3.01
Sm	0.16	0.27	0.68	0.94	0.34	0.21	0.15	0.28	0.69	0.89	0.83	0.82	1.36	1.10
Eu	0.06	0.08	0.26	0.38	0.05	0.03	0.05	0.04	0.13	0.2	0.05	0.40	0.85	0.42
Gd	0.23	0.40	1.00	1.40	0.49	0.31	0.23	0.42	1.03	1.27	1.49	1.10	1.94	1.63
Tb	N.d.	N.d.	N.d.	N.d.	N.d.	N.d.	N.d.	N.d.	0.19	0.24	N.d.	0.20	0.35	0.3
Dy	0.29	0.51	1.24	1.73	N.d.	0.39	0.29	0.53	1.39	1.76	2.02	1.44	2.55	2.15
Ho	N.d.	N.d.	N.d.	N.d.	N.d.	N.d.	N.d.	N.d.	N.d.	0.35	N.d.	0.28	0.50	0.46
Er	0.19	0.34	0.81	1.13	N.d.	0.25	0.19	0.34	0.81	1.00	1.19	0.79	1.47	1.28
Tm	N.d.	N.d.	N.d.	N.d.	N.d.	N.d.	N.d.	N.d.	N.d.	0.14	N.d.	0.11	0.19	0.18
Yb	0.20	0.35	0.80	1.04	N.d.	0.25	0.19	0.34	0.76	0.96	1.04	0.72	1.18	1.18
Lu	N.d.	0.12	0.15	N.d.	N.d.	N.d.	N.d.	N.d.	N.d.	0.19	N.d.	0.12	0.27	0.17
Total	N.d.	N.d.	N.d.	N.d.	N.d.	N.d.	N.d.	N.d.	N.d.	13.7	N.d.	12.7	22.2	17.3
$(La/Yb)_n$	0.54	0.56	0.46	0.55	N.d.	0.62	0.43	0.52	0.59	0.71	0.15	0.86	1.08	0.80

(*Continued*)

Table 3.4 Continued

	Province													
	Kambalda (Silver Lake), Australia						Abitibi, Canada							
	(Lesher & Arndt, 1995), LCHR						(Arndt, 1977)				(Beswick, 1983)			(Whitford & Arndt, 1978)
Element	91976	91977	91978	91980	91966	91968	Arn-1	Arn-2	Arn-3	Arn-4	Bes-5	Bes-6	Bes-7	P9-111
La	1.14	1.58	1.42	0.66	0.68	0.76	N.d.	N.d.	N.d.	N.d.	1.0	1.4	0.96	N.d.
Ce	2.99	3.94	3.63	2.06	1.74	2.08	0.68	0.94	0.46	1.4	2.6	2.6	1.4	2.79
Pr	0.47	0.57	0.57	0.37	0.29	0.34	N.d.	N.d.	N.d.	N.d.	N.d.	N.d.	N.d.	N.d.
Nd	2.67	3.15	2.98	2.01	1.99	1.92	0.84	1.1	0.5	1.6	3.4	3.9	3.0	2.77
Sm	0.98	1.05	0.98	0.76	0.80	0.77	0.36	0.48	0.22	0.74	1.0	0.95	0.63	1.05
Eu	0.44	0.43	0.42	0.30	0.34	0.41	0.17	0.21	0.1	0.32	0.34	0.24	0.36	0.41
Gd	1.44	1.54	1.43	1.11	1.28	1.17	N.d.	0.88	0.38	1.3	N.d.	N.d.	N.d.	1.55
Tb	0.27	0.3	0.27	0.20	0.25	0.22	N.d.	N.d.	N.d.	N.d.	N.d.	N.d.	N.d.	N.d.
Dy	1.87	2.27	1.86	1.48	1.96	1.54	0.78	1.1	0.5	1.7	1.7	1.8	1.3	1.89
Ho	0.42	0.47	0.47	0.28	0.65	0.33	N.d.	N.d.	N.d.	N.d.	N.d.	N.d.	N.d.	N.d.
Er	1.16	1.33	1.10	0.90	1.15	0.90	0.48	0.7	0.32	1.1	N.d.	N.d.	N.d.	1.2
Tm	0.18	0.21	0.16	0.13	0.17	0.13	N.d.	N.d.	N.d.	N.d.	N.d.	N.d.	N.d.	N.d.
Yb	1.14	1.27	1.00	0.85	1.08	0.85	0.49	0.72	0.34	1.0	0.9	0.96	0.65	1.13
Lu	0.25	0.24	0.16	0.12	0.20	0.13	0.084	N.d.	N.d.	N.d.	0.09	0.14	0.09	N.d.
Total	15.4	18.4	16.5	11.2	12.6	11.6	N.d.	N.d.	N.d.	N.d.	N.d.	N.d.	N.d.	N.d.
$(La/Yb)_n$	0.68	0.84	0.96	0.52	0.43	0.89	N.d.	N.d.	N.d.	0.30	0.75	0.99	1.0	N.d.

	Provinces													
	Abitibi, Canada						India			Gorgona islands, Columbia				
	(Whitford & Arndt, 1978), IDMS						(Naqvi *et al.*, 1978)			(Revillon *et al.*, 2000), ICP-MS				
Element	P9-155	P9-167	P9-107	P9-153	P9-106	S36	S1011	S53	GOR 501	GOR 502	GOR 519	GOR 521	GOR 525	GOR 537
La	N.d.	N.d.	N.d.	N.d.	N.d.	1.696	2.441	6.256	0.490	0.660	0.330	0.310	0.530	0.630
Ce	3.51	3.62	3.64	3.96	5.00	4.875	7.210	15.131	1.850	2.320	1.050	1.060	1.920	2.190
Pr	N.d.	N.d.	N.d.	N.d.	N.d.	N.d.	N.d.	N.d.	0.360	0.480	0.220	0.220	0.390	0.450
Nd	3.18	3.31	3.36	3.49	4.48	3.791	5.657	10.046	2.390	3.090	1.520	1.520	2.520	2.870
Sm	1.22	1.27	1.32	1.33	1.68	1.231	1.976	2.842	1.080	1.400	0.840	0.840	1.150	1.320
Eu	0.442	0.497	0.512	0.526	0.631	0.371	0.945	0.894	0.500	0.650	0.350	0.390	0.530	0.600
Gd	N.d.	N.d.	1.98	N.d.	2.76	1.585	2.688	3.216	1.770	2.340	1.810	1.690	1.860	2.140
Tb	N.d.	N.d.	N.d.	N.d.	N.d.	N.d.	N.d.	N.d.	0.320	0.430	0.330	0.330	0.340	0.390
Dy	2.31	2.58	2.67	2.67	3.28	1.753	3.135	3.222	2.240	3.010	2.520	2.460	2.370	2.730
Ho	N.d.	N.d.	N.d.	N.d.	N.d.	N.d.	N.d.	N.d.	0.470	0.620	0.560	0.550	0.490	0.560
Er	1.48	1.56	1.6	1.6	2.05	1.020	1.805	1.080	1.290	1.740	1.570	1.560	1.360	1.570
Tm	N.d.	N.d.	N.d.	N.d.	N.d.	N.d.	N.d.	N.d.	0.180	0.240	0.230	0.220	0.190	0.220
Yb	1.42	1.39	1.53	1.53	1.94	0.953	1.611	1.650	1.130	1.490	1.500	1.470	1.190	1.350
Lu	N.d.	N.d.	N.d.	N.d.	N.d.	0.153	0.247	0.254	0.180	0.240	0.230	0.230	0.190	0.210
Total	N.d.	N.d.	N.d.	N.d.	N.d.	17.4	27.7	44.6	14.3	18.7	13.1	12.9	15.0	17.2
$(La/Yb)_n$	N.d.	N.d.	N.d.	N.d.	N.d.	1.2	1.0	2.6	0.29	0.30	0.15	0.14	0.30	0.32

(*Continued*)

Table 3.4 Continued

	Provinces												
	Gorgona islands, Columbia												
	(Revillon *et al.*, 2000)		(Aitken & Echeverria, 1984), IDMS										
Element	GOR 538	GOR 539	1P	2P	3P	G-5	G-6	G-38	G-47	G-71	G-156	G-160	4P	G-167
La	0.430	0.520	N.d.	N.d.	N.d.	N.d.	N.d.	N.d.	N.d.	N.d.	N.d.	N.d.	N.d.	N.d.
Ce	1.490	1.940	1.950	2.190	2.140	2.620	2.720	1.770	0.880	2.150	1.720	2.010	2.520	2.920
Pr	0.310	0.390	N.d.	N.d.	N.d.	N.d.	N.d.	N.d.	N.d.	N.d.	N.d.	N.d.	N.d.	N.d.
Nd	1.980	2.540	2.560	2.870	2.770	2.790	2.920	2.600	1.440	2.830	2.300	2.730	3.460	3.500
Sm	0.910	1.160	1.220	1.350	1.290	1.320	1.380	1.300	0.740	1.330	1.110	1.290	1.610	1.660
Eu	0.410	0.510	0.560	0.620	0.590	0.610	0.630	0.630	0.410	0.620	0.470	0.550	0.690	0.710
Gd	1.510	1.860	N.d.	N.d.	N.d.	N.d.	2.710	2.350	1.610	2.800	1.730	2.100	2.610	2.500
Tb	0.280	0.330	N.d.	N.d.	N.d.	N.d.	N.d.	N.d.	N.d.	N.d.	N.d.	N.d.	N.d.	N.d.
Dy	1.920	2.300	2.320	3.270	N.d.	N.d.	3.230	2.870	2.270	3.600	2.150	2.540	3.200	2.970
Ho	0.400	0.480	N.d.	N.d.	N.d.	N.d.	N.d.	N.d.	N.d.	N.d.	N.d.	N.d.	N.d.	N.d.
Er	1.130	1.310	1.390	1.750	1.740	2.220	1.670	1.770	1.480	1.660	1.280	1.490	1.910	N.d.
Tm	0.160	0.180	N.d.	N.d.	N.d.	N.d.	N.d.	N.d.	N.d.	N.d.	N.d.	N.d.	N.d.	N.d.
Yb	0.960	1.140	1.350	1.530	1.460	1.810	1.460	1.610	1.380	1.380	1.150	1.320	1.700	1.580
Lu	0.160	0.180	N.d.	N.d.	N.d.	N.d.	N.d.	N.d.	N.d.	N.d.	N.d.	N.d.	N.d.	N.d.
Total	12.1	14.8	N.d.	N.d.	N.d.	N.d.	N.d.	N.d.	N.d.	N.d.	N.d.	N.d.	N.d.	N.d.
$(La/Yb)_n$	0.304	0.310	N.d.	N.d.	N.d.	N.d.	N.d.	N.d.	N.d.	N.d.	N.d.	N.d.	N.d.	N.d.

	Provinces													
	Song Da, Vietnam												Perseverance, W. Austr.	
	(Hanski *et al.*, 2004), ICP-MS												(Barnes *et al.*, 1995)	
Element	G1456	B6889	B6885	B6859	B6891	B6892	P12/86	P46/89	P8/86	P9/86	G946	G1448	P-249.2	P-433
La	0.7	0.64	0.36	0.49	1.24	0.68	0.8	0.89	0.66	1	0.77	0.91	1.5	0.42
Ce	2.08	2.05	1.18	1.12	3.2	2.03	1.57	2	2.05	2.39	2.3	2.9	4.2	1.66
Pr	0.33	0.39	0.22	0.2	0.5	0.38	0.27	0.31	0.4	0.35	N.d.	N.d.	0.62	0.31
Nd	2.25	2.37	1.36	1.34	2.7	2.34	1.61	1.69	2.45	1.82	2.5	2.8	3.2	1.55
Sm	0.99	1.11	0.35	0.51	1.08	1.07	0.71	0.72	1.01	0.71	1	1.1	1.2	0.59
Eu	0.38	0.48	0.3	0.22	0.47	0.45	0.32	0.32	0.49	0.33	0.42	0.47	1.5	0.19
Gd	1.78	1.84	1.12	1.03	1.79	1.93	1.32	1.46	1.74	1.25	1.5	1.7	1.6	0.83
Tb	0.31	0.36	0.23	0.19	0.33	0.36	0.25	0.24	0.32	0.24	0.28	0.3	N.d.	N.d.
Dy	2.39	2.33	1.58	1.37	2.23	2.35	1.77	1.79	2.17	1.67	N.d.	N.d.	N.d.	N.d.
Ho	0.49	0.53	0.37	0.31	0.51	0.51	0.41	0.4	0.45	0.37	N.d.	N.d.	N.d.	N.d.
Er	1.48	1.55	1.14	0.9	1.44	1.5	1.27	1.3	1.29	1.01	N.d.	N.d.	1.3	0.59
Tm	0.2	0.22	0.17	0.15	0.19	0.22	0.19	0.19	0.19	0.16	N.d.	N.d.	N.d.	N.d.
Yb	1.43	1.41	1.07	0.93	1.36	1.42	1.38	1.26	1.23	1.02	1.49	1.31	1.2	0.59
Lu	0.23	0.21	0.17	0.15	0.19	0.2	0.21	0.21	0.19	0.16	0.24	0.2	N.d.	N.d.
Total	15.0	15.5	9.62	8.91	17.2	15.4	12.1	12.8	14.6	12.5	10.5	11.7	16.3	6.73
$(La/Yb)_n$	0.33	0.31	0.23	0.36	0.62	0.32	0.39	0.48	0.36	0.66	0.35	0.47	0.84	0.48

(*Continued*)

Table 3.4 Continued

	Provinces													
	Perseverance, West Australia													
	(Barnes *et al.*, 1995), ICP-MS, LCHR													
Element	P-249-2	P-433	P-435-3	P-438-5	P-441	P-452	P-456	P-478-02	P-491-14	P-491	P-509	P-91-2	P-95-6	P-141-2
La	1.5	0.42	0.54	0.65	0.53	0.45	0.45	0.25	0.52	0.14	0.37	1.04	3.66	2.1
Ce	4.2	1.66	1.91	2	1.77	1.46	1.58	0.69	1.7	0.55	1.26	4.31	11.16	4.62
Pr	0.62	0.31	0.29	0.28	0.28	0.25	0.23	0.11	0.3	0.12	0.24	0.73	1.58	0.57
Nd	3.2	1.55	1.67	1.76	1.88	1.35	1.47	0.63	1.8	0.81	1.49	3.43	7.58	2.41
Sm	1.2	0.59	0.6	0.7	0.59	0.45	0.56	0.23	0.74	0.43	0.63	0.83	1.71	0.53
Eu	1.5	0.19	0.21	0.26	0.14	0.09	0.14	0.09	0.14	0.09	0.15	0.28	0.13	0.44
Gd	1.6	0.83	0.95	1.06	0.82	0.79	0.68	0.35	1.11	0.75	0.96	0.85	1.73	0.68
Tb	N.d.	N.d.	N.d.	N.d.	N.d.	N.d.	N.d.	0.06	0.21	0.15	0.17	0.13	0.27	0.11
Dy	N.d.	N.d.	N.d.	N.d.	N.d.	N.d.	N.d.	N.d.	N.d.	N.d.	N.d.	N.d.	N.d.	N.d.
Ho	N.d.	N.d.	N.d.	N.d.	N.d.	N.d.	N.d.	0.1	0.31	0.24	0.24	0.16	0.34	0.17
Er	1.3	0.59	0.54	0.7	0.59	0.62	0.56	0.36	0.92	0.72	0.72	0.46	0.96	0.51
Tm	N.d.	N.d.	N.d.	N.d.	N.d.	N.d.	N.d.	0.06	0.14	0.11	0.1	0.07	0.13	0.07
Yb	1.2	0.59	0.71	0.59	0.59	0.67	0.58	0.41	0.91	0.72	0.66	0.43	0.84	0.51
Lu	N.d.	N.d.	N.d.	N.d.	N.d.	N.d.	N.d.	0.06	N.d.	0.1	0.1	0.06	0.11	0.08
Total	N.d.	N.d.	N.d.	N.d.	N.d.	N.d.	N.d.	N.d.	N.d.	4.93	7.09	12.78	30.2	12.8
$(La/Yb)_n$	0.84	0.48	0.51	0.74	0.61	0.45	0.52	0.41	0.39	0.13	0.38	1.63	2.94	2.78

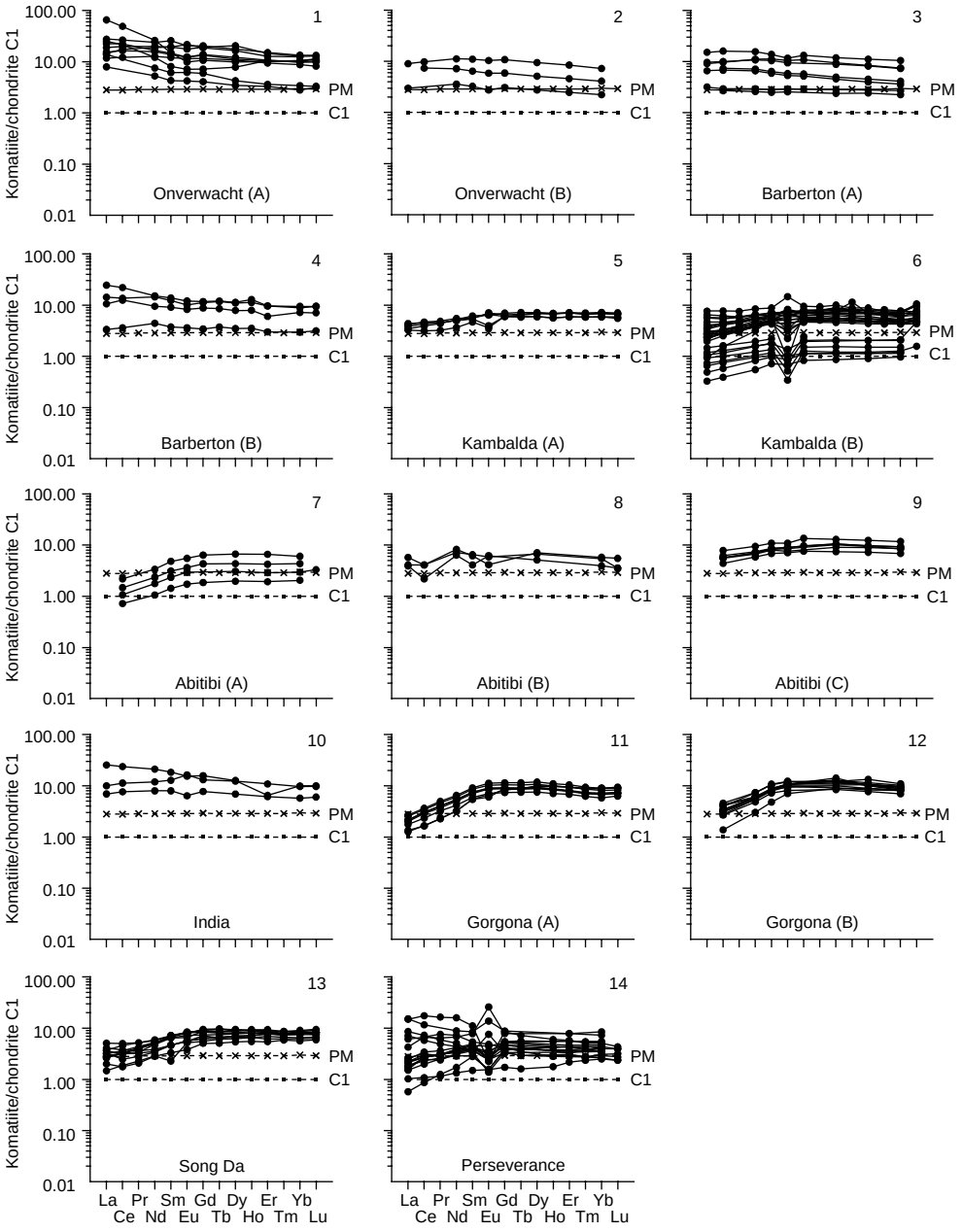

Figure 3.8 Chondrite-normalised REE patterns for komatiites from some provinces (data Table 3.4). Patterns on the plots 1 and 2, 3 and 4, 5 and 6, 7, 8 and 9, 15 and 16 are characterized the general totality of sample analysis from corresponding provinces.

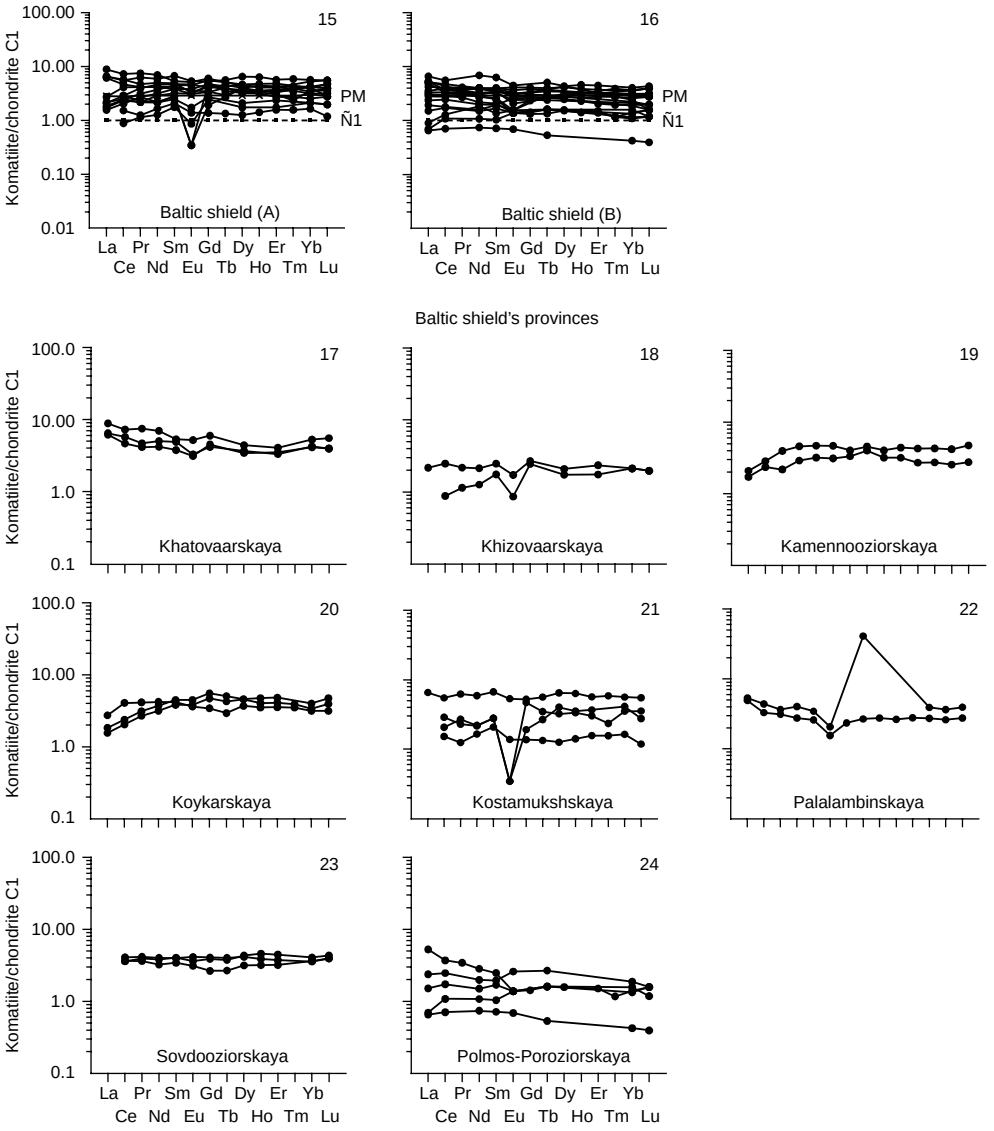

Figure 3.8 Continued

zonality of material composition of the komatiites. Thus, the MgO content in them varies in the range of 23–35 wt%, and the total level of REE accumulation fluctuates in the range of 1–10 t. ch. The average total REE content (~5.2 ppm) of the komatiites of the Baltic shield is less than that from many other provinces; the average accumulation level for light REE amounts to about 3 t. ch. and that for heavy REE is about 2 t. ch. The average value of the parameter $(La/Yb)_n$ is about 1.6. The REE patterns of the vast majority of komatiite samples from the Baltic shield have a gentle negative slope, and some patterns are complicated by negative Eu anomalies (see Figs. 3.8, 3.9). There are

Table 3.5 Density occurring komatiites geochemical types in some provinces ($n = 82$).

		Provinces									
Group	Class	Baltic shield	Onverwacht	Barberton	Kambalda	Abitibi	India	Gorgona islands	Song Da	Perseverance	All provinces
I	1	No	No	No	No	No	No	No	No	No	No
	2	1	No	No	25	5	No	No	8	7	46
	3	2	1	1	No	No	No	No	No	2	6
II	4	4	5	3	6	No	2	6	No	5	31
	5	3	5	5	No	No	1	No	No	2	16
III	6	6	1	No	3	2	No	2	4	2	20

For typing of komatiites was used classification in virtue of correlations parameters $(La/Sm)_n$ and $(Gd/Yb)_n$, by Jahn *et al.* (1982). No—komatiites of this class were absent.

four geochemical types of komatiites singled out within the province (Vrevsky *et al.*, 2003). Based on the average estimates of the parameters $(La/Sm)_n$ (1.1) and $(Gd/Yb)_n$ (1.0), and on the above geochemical classification, most komatiites of the Baltic shield are assigned to Class 6 (Group III).

The Onverwacht province consists of several subprovinces: Komatii, Sandspruit, Zeespruit, and others (Sun & Nesbitt, 1978; Jahn *et al.*, 1982). The volcanogenic rock masses widespread there contain peridotitic (MgO > 18 wt%) and basaltic (MgO = 10–18 wt%) komatiites as well as tholeiites (MgO < 10 wt%). The total REE content in komatiites varies in the range of 5–70 ppm, amounting to an average of about 30 ppm. This is the highest value of REE content in komatiites of all the provinces that have been explored. The average total content of heavy REE (8 ppm) is also one of the highest. The accumulation level of middle and heavy elements in komatiites usually exceeds the level of these admixtures in the primitive mantle (~2 t. ch.). In some samples, the accumulation level of light REE is somewhat higher than 30 t. ch. Values of the parameter $(La/Yb)_n$ vary in the range of 1.1–6.3, amounting to an average of about 2.6. The REE patterns of nearly all komatiites from the Onverwacht province have a sufficiently gentle negative slope (see Fig. 3.8, 1, 2). On the basis of the average values of the parameters $(La/Sm)_n$ (~1.6) and $(Gd/Yb)_n$ (~1.3), these komatiites are mostly assigned to Class 5 (Group II).

The Barberton province. Singled out here according to petrochemical features are three types of komatiites: (1) peridotitic komatiites, which are enriched with magnesium (MgO 27–32 wt%), usually possessing a "spinifex" structure; (2) peridotitic komatiites, which are more depleted with MgO (on average ~23 wt%), in which no "spinifex" structure is observed; and (3) basaltic komatiites (MgO 11–16 wt%) (Herrmann *et al.*, 1976; Sun & Nesbitt, 1978). The total REE content in all the three varieties varies within the range of 5–40 ppm, amounting to an average of about 20 ppm. By their average total heavy REE content (~6.6 ppm), komatiites from the Barberton province are comparable to samples from the Onverwacht province. Values of the parameter $(La/Yb)_n$ vary in the range of 1.2–2.7 with an average indicator on the order of 1.5. Most of the REE patterns of komatiites have a very gentle negative slope (see Figs. 3.4, 3.8) with weak negative Eu anomalies on some patterns. On the basis of the average values of the parameters $(La/Sm)_n$ (~1.3) and $(Gd/Yb)_n$ (~1.3), the

Table 3.6 Average REE composition (x) and standard deviation (σ) of komatiites from some provinces (ppm).

	Provinces									
	Onverwacht (13)		India (3)		Barberton (10)		Gorgona island (19)		Song Da (12)	
Element	x	σ	x	σ	x	σ	x	σ	x	σ
La	4.79	3.96	3.46	2.45	2.20	1.10	0.49	0.13	0.76	0.23
Ce	12.88	7.45	9.07	5.38	5.43	2.97	1.97	0.55	2.07	0.61
Pr	N.d.	N.d.	N.d.	N.d.	N.d.	N.d.	0.35	0.10	0.34	0.09
Nd	6.58	3.34	6.50	3.21	4.04	2.17	2.56	0.58	2.10	0.51
Sm	1.89	1.03	2.02	0.81	1.21	0.63	1.22	0.24	0.86	0.26
Eu	0.63	0.35	0.74	0.32	0.41	0.20	0.55	0.10	0.39	0.09
Gd	2.27	1.19	2.50	0.83	1.57	0.79	2.09	0.42	1.54	0.30
Tb	N.d.	N.d.	N.d.	N.d.	0.30	0.15	0.34	0.05	0.28	0.05
Dy	2.56	1.42	2.70	0.82	1.71	0.89	2.67	0.47	1.97	0.37
Ho	N.d.	N.d.	N.d.	N.d.	0.43	0.22	0.52	0.07	0.44	0.07
Er	1.48	0.70	1.30	0.44	1.00	0.52	1.57	0.26	1.29	0.22
Tm	N.d.	N.d.	N.d.	N.d.	N.d.	N.d.	0.20	0.03	0.19	0.02
Yb	1.37	0.65	1.40	0.39	0.95	0.49	1.40	0.21	1.28	0.18
Lu	0.24	0.10	0.22	0.06	0.17	0.08	0.20	0.03	0.20	0.03
Total	31.3	19.2	29.9	13.7	18.0	10.0	14.1	2.5	13.0	2.6
$(La/Yb)_n$	2.3	1.5	1.6	0.87	1.4	0.25	0.26	0.07	0.41	0.13

	Provinces							
	Abitibi (13)		Kambalda (34)		Perseverance (16)		Baltic shield (33)	
Element	x	σ	x	σ	x	σ	x	σ
La	1.12	0.24	0.72	0.43	0.91	0.91	0.87	0.53
Ce	2.51	1.43	2.05	1.10	2.80	2.59	2.04	0.98
Pr	N.d.	N.d.	0.44	0.11	0.43	0.36	0.34	0.14
Nd	2.69	1.26	1.93	0.91	2.24	1.64	1.53	0.73
Sm	0.94	0.43	0.72	0.32	0.72	0.36	0.50	0.22
Eu	0.37	0.16	0.27	0.18	0.35	0.46	0.15	0.08
Gd	1.48	0.84	1.06	0.48	0.97	0.37	0.71	0.28
Tb	N.d.	N.d.	0.25	0.04	0.16	0.07	0.11	0.05
Dy	1.87	0.82	1.41	0.64	N.d.	N.d.	0.85	0.32
Ho	N.d.	N.d.	0.40	0.10	0.22	0.09	0.20	0.07
Er	1.21	0.56	0.87	0.39	0.72	0.27	0.53	0.19
Tm	N.d.	N.d.	0.16	0.03	0.10	0.03	0.08	0.04
Yb	1.08	0.47	0.83	0.35	0.70	0.23	0.47	0.21
Lu	0.10	0.03	0.16	0.05	0.09	0.02	0.07	0.03
Total	11.4	5.3	10.4	5.3	10.1	6.6	7.2	3.5
$(La/Yb)_n$	0.76	0.33	0.59	0.19	0.88	0.84	1.38	0.79

Data Table 3.4.

komatiites from the Barberton province, just as those from the Onverwacht province, are assigned to Class 5 (Group II).

The Kambalda province is one of the least explored komatiites provinces. Within its bounds are singled out two subprovinces: Silver Lake and Tripod Hill (Lesher & Arndt, 1995). The komatiites that are widespread there are heterogeneous both in their

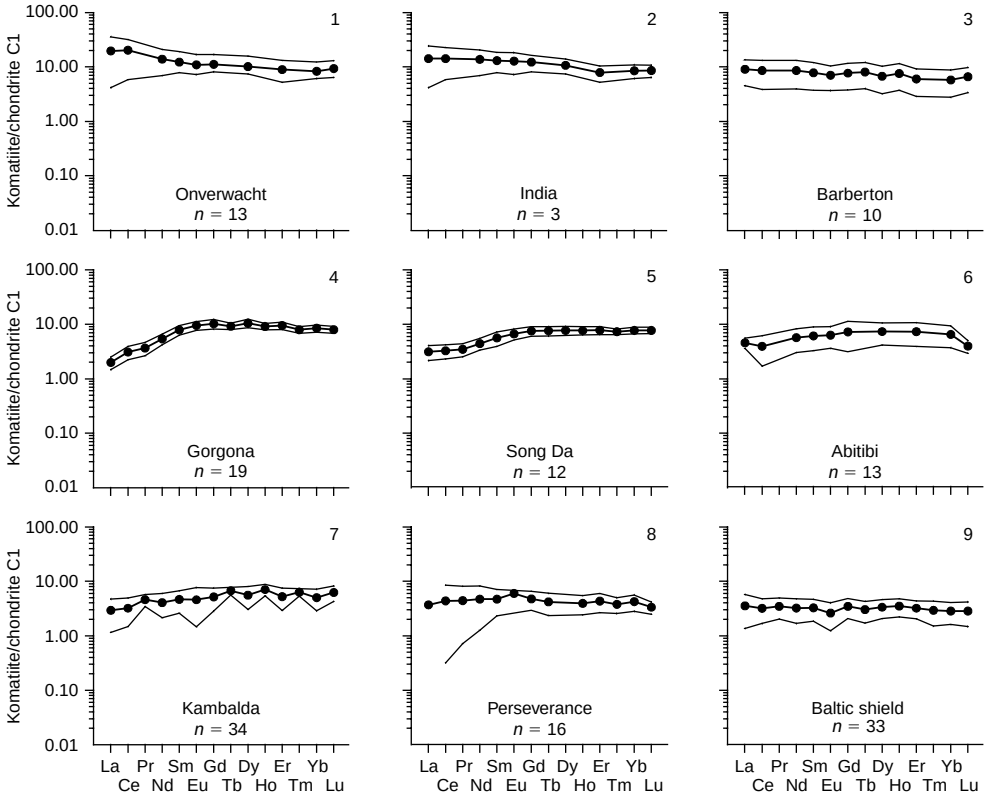

Figure 3.9 Chondrite-normalized patterns for average REE composition of komatiites from some provinces (data Table 3.6). Narrow lines mark limits of REE content variations on the basis of standard deviations.

structural features and material composition. They often reveal a "spinifex" structure, characterized by the presence of skeletal crystals of olivine and clinopyroxene. The content of MgO in komatiites from both subprovinces varies in a wide range of 11–47 wt%, amounting to an average of about 26 wt%. The level of REE accumulation naturally decreases with increasing MgO content. According to the said authors' observations, the komatiites, which are characterized by their cumulative structures, are distinguished by their lower level of REE accumulation compared to other varieties possessing the "spinifex" structure. On the whole, the komatiites from the Kambalda province are somewhat depleted of light REE; the average value of the parameter $(La/Yb)_n$ amounts to 0.59 and that of $(La/Sm)_n$ is 0.64. Their REE patterns have a very gentle positive slope (see Fig. 3.8, 5). Many patterns, particularly those constructed from samples from the Silver Lake province, display either negative or positive Eu anomalies (see Fig. 3.8, 6). Due to their average values of the parameters $(La/Sm)_n$ and $(La/Yb)_n$, the komatiites of the province in question are assigned to Class 2 (Group I).

The Abitibi province is structurally within the greenstone belt of the same name. It is one of the largest districts by the area of komatiite distribution, and komatiites are

the most widely represented type of rock within the manifestation (subprovince Monro Township) (Arndt, 1977; Whitford & Arndt, 1978; Beswick, 1983). In this territory, the flows of komatiites vary in thickness from 1 to 20 m with a visible extension of up to several hundred meters. In a flow, one can usually single out the low horizon with a cumulative structure of the rock and the upper horizon with the rock of a characteristically "spinifex" structure. In the uppermost part of the flows the komatiites with the "spinifex" structure are replaced by fractured aphanitic varieties.

The komatiites of this province are represented by peridotitic (MgO = 22–35 wt%), pyroxenitic (MgO < 20 wt%), and basaltic (MgO ~8 wt%) varieties. For all the three varieties of komatiites, the total REE content varies in the range 3–26 ppm with an average value of about 12 ppm. The accumulation level of separate elements in individual samples varies in the range 1–14 ppm. Also, in most cases the accumulation level of light REE is somewhat lower than that of heavy ones, so the REE patterns of these rocks have a very gentle positive slope (see Fig. 3.8, 7–9) By the average values of the parameters $(La/Sm)_n$ and $(Gd/Yb)_n$, the komatiites of the Abitibi province are similar to those from the Kambalda province and have also been assigned to Class 2 (Group 1).

The province of Gorgona Island is distinct from the above provinces and is within the Archean greenstone belts. The komatiites of Gorgona Island enter into the composition of a complicated volcano-plutonic structure which is assigned a Mesozoic-Tertiary age. Within its bounds, the ultramafic rocks are represented both by volcanic and by plutonic facies (Echeverria, 1980; Aitken & Echeverria, 1984; Revillon *et al.*, 2000). The komatiites in it form horizons of different thickness, often possess a "spinifex" structure, and vary from microgranular to macrogranular. Some varieties of komatiites, along with impregnations of olivine and clinopyroxene, contain manifestations of plagioclase as admixtures, and in some cases volcanic glass occurs in them.

MgO content in the komatiites of Gorgona Island varies in the range of 11–24 wt%. The total REE content varies from 10 to 19 ppm amounting to an average of about 14 ppm; the accumulation level of heavy and middle REE is increased relatively to the light ones, which makes these rocks similar to the komatiites from the Onverwacht and Barberton provinces. Distinct from most of the Archean komatiites, rocks from Gorgona Island rocks have more intensive REE fractionation. The accumulation level of light REE in these rocks amounts to 2–7 t. ch., while that of the heavy ones is higher at 8–10 t. ch. Komatiites of Gorgona Island feature low values of the parameter $(La/Yb)_n$, which amount to an average of about 0.24. Their geochemical peculiarity also manifests itself in the average values of the parameters $(La/Sm)_n$ (0.3) and $(Gd/Yb)_n$ (1.2). The rare earth patterns of most samples are drawn strictly parallel to one another, which testifies to stable correlations between separate elements (see Fig. 3.8, 11, 12). With allowance for the average values of the parameters $(La/Sm)_n$ and $(Gd/Yb)_n$, the Gorgona Island komatiites have been assigned to the rarest Class 4 (Group II), which once again emphasizes their geochemical specificity.

The Song Da province is located in northwest Vietnam, and according to available data, komatiites of this province interband with low-titanium olivine basalts by breaking through late Permian carbonate deposits (Hanski *et al.*, 2004). These rocks often include varieties with "spinifex" structures characterized by the presence of clinopyroxene skeletal crystals as well as varieties with phenocrysts of high-magnesium olivine. The contents of the main components in the komatiites of this province vary

in the following ranges (wt%): MgO (11.4–27.4), Al_2O_3 (7.1–11.0), CaO (6.6–15.3), and Na_2O (0.1–1.0). The total REE content in these komatiites varies from 8.9 to 17.2 ppm with an average value of about 13.0 ppm. By their petrochemical and geochemical characteristics, the komatiites of Song Da are similar to the rocks from the province of Gorgona Island. Similar to the latter, they are somewhat depleted of light REE, in which region their REE patterns have a positive slope, while in the region of the middle and heavy REE, its form is almost "flat" (see Fig. 3.8, 13). The geochemical parameters of the komatiites from the Song Da province have the following average values: $(La/Yb)_n$ (0.40), $(La/Sm)_n$ (0.58), and $(Gd/Yb)_n$ (0.97). Singled out among them by these criteria are two geochemical types: the prevailing varieties, assigned to Class 2 (Group I), and the less common varieties, assigned to Class 6 (Group III). According to the investigators, the fact that komatiites from the province in question are relatively depleted of light REE shows that the mantle source of their parent melts was subjected to preliminary depletion, and the nearly "flat" shape of their REE patterns gives grounds to conclude that in the course of the parent melt segregation their source contained no garnet (Hanski *et al.*, 2004).

The Perseverance province is situated in eastern Australia and is associated with the ultramafic complex and the sulfide–nickel deposit, both of which carry the same name as that of the province (Barnes *et al.*, 1995). Within the province, the komatiites form numerous flows are underlaid by felsic tuffs. In separate parts of the province, komatiites possess the "spinifex" structure. In zones of sulfide–nickel mineralization, the rocks are considerably metamorphozed. The REE composition of the province's komatiites is characterized by a noticeable heterogeneity, as can be seen both from the variations of the total element accumulation level and from the differences in their correlations (see Table 3.4, Fig. 3.8, 14). With allowance made for the peculiarities of REE distribution, komatiites of this province are divided into two types. Samples assigned to the first type are represented by weakly changed varieties, which often have the "spinifex" structure. They demonstrate a moderate accumulation level of most REE (on the order of 0.5–3 t. ch.), but for all that they are somewhat depleted of light elements, similar to the komatiites from the provinces of Gorgona Island, Song Da, and Abitibi. Values of the parameter $(La/Yb)_n$ in these komatiites vary in the range of 0.13–0.84. The second type is represented by significantly metamorphozed varieties of komatiites that are distributed in the zones of sulfide–nickel mineralization and are distinguished by a higher accumulation level of REE (7–15 t. ch.), especially the light ones. Due to this accumulation, the rocks are noted for having higher values of the parameter $(La/Yb)_n$ from 1.8 to 2.9. The REE patterns of the komatiites of both types often contain either negative or positive Eu anomalies of variable intensity. The investigators believe that the increased level of REE accumulation observed in the metamorphozed komatiites of this province as well as the changeable sign of the Eu anomalies are due to epigenetic redistribution of elements, which occurred during their metamorphism (Barnes *et al.*, 1995).

Thus, in classifying komatiites, use is made of geochemical approaches, along with others, including data on the parameters of REE distribution. According to the available analytical data, the total REE content in komatiites varies in the range of 3–70 ppm with an inverse dependence on MgO content. Most rare earth patterns of komatiites have gentle positive, sometimes negative, slopes pointing to relatively weak fractionation of elements. Some patterns are complicated by negative or positive Eu

anomalies of low intensity. In each province there is one or two geochemical types of rock that dominate over the others. For example, in the Baltic shield, komatiites assigned to Class 6 (Group III) and to Class 4 (Group II) occur most frequently. In the provinces of Onverwacht and Barberton as well as in India and on Gorgona Island, the predominant komatiites belong to Class 4 and Class 5 (Group II), and in the provinces of Kambalda and Abitibi the predominant komatiites belong to Class 2 (Group I).

The average values of the geochemical parameter Sm/Nd increase from the Archean komatiites represented in the Barberton to the Mesozoic-Tertiary komatiites of Gorgona Island. The average values of the parameter Th/U, on the contrary, decrease from the komatiites in the ancient provinces to the rocks in the young provinces. The correlation between the values of the parameters Sm/Nd and Th/U in the komatiites from provinces of different ages is inversely proportional (Campbell, 2002).

The genesis of komatiites, including the generation conditions of their parent melts, remains the subject of ongoing discussions (Laz'ko *et al.*, 1988; Pukhtel' & Simon, 1988). According to one hypothesis, these melts resulted from "advanced" melting (40–70%) of mantle protoliths at very great depths (~400 km) at a temperature of about 1800°C, their temperature at the moment of outflow being no lower than 1600°C, which is much higher than the outflow temperature of typical basalts (<1200°C) (Jochum *et al.*, 1991). According to other investigators, as komatiites from the subprovince of Monro Township (Abitibi province) were formed, the prevalent processes were those of the fractional crystallization of olivine proceeding at low pressures as well as the subsequent crystallization of clinopyroxene and plagioclase proceeding at lower temperatures (Whitford & Arndt, 1978). These authors came to the conclusion that the correspondence between the observed and calculated contents of REE (excluding Eu) in komatiites from the subprovince of Monro Township eliminates the need to resort to any other models in solving the problem of their genesis including the mechanism of REE redistribution in the course of rock diagenesis and metamorphism. In their opinion the differences between the rare earth element patterns of komatiites and ultramafic rocks of other types are due either to the peculiarities of the partial melting of mantle sources of like composition or to certain differences in the composition of the sources themselves.

The exploration of geochemical peculiarities of Archean ultramafic and mafic vulcanites from the provinces of Australia, South Africa, Canada and Greenland shows that some differences among komatiites, with respect to the distribution of REE, mainly the light ones, and Eu, may be connected with the metamorphic transformations of rocks (Sun & Nesbitt, 1978). At the same time, the concordance of the rare earth patterns of komatiites from within individual provinces as well as the differences observed between samples from different provinces make it possible to regard these patterns as an adequate reflection of primary REE distribution in the parent melts of komatiites. The said authors concluded that the crystallizing fractionation cannot be considered as one of the main mechanisms of komatiite melt formation.

The results of the research into the komatiites from the Kambalda province make it possible to state that a number of their features, including the high contents of compatible elements, REE among them, as well as the circumchondrite correlations between incompatible elements, indicate that the parent melts of these komatiites were generated at high degrees of the partial melting of a depleted source, in which the main phase was olivine (Lesher & Arndt, 1995). This viewpoint is also shared by other explorers,

who believe that since a large part of Archean komatiites was depleted of light REE relative to heavy ones, one can conclude that the peridotite mantle source of komatiite melts had been preliminarily depleted of these elements (Cullers & Graf, 1984a).

* * *

Komatiites are a relatively rare type of volcanic rocks that are characterized by a high content of MgO and by very low contents of incompatible elements, REE among them. The high content of MgO makes it possible to regard komatiites as volcanogenic analogues of ultramafic rocks occurring in plutonic facies. They feature a specific structure, "spinifex," indicating high rates of cooling and crystallization of the parent melts. The most widespread komatiites are those spatially associated with Archean greenstone belts located within ancient shields. Of much rarer occurrence are younger komatiites, which can be exemplified by the rocks from the provinces of Gorgona Island and Song Da. It is commonly supposed that the parent melts of komatiites resulted from the "advanced" partial melting of depleted mantle protoliths, proceeding at high rates, at great depths, and at very high temperatures. Further geochemical investigations of komatiites involving more-detailed analytical databases on REE will promote the development of more-constructive models of the genesis of these rocks.

3.3 MEIMECHITES

Meimechites are a still more rarely occurring variety of high-magnesium rocks, which, much like picrites, described below, and komatiites, are represented in subvolcanic and volcanic facies. These rocks were first discovered and described in the Meimecha–Kotuy alkaline ultrabasic province in the north of the Siberian Platform where they form numerous tabular bodies, flows, and dikes (Vasil'ev, 1988). They are also well-known in Kamchatka. In many cases, meimechites possess a magnophyric structure. Amygdaloidal, banded, and tuffaceous varieties also occur. Porphyric phenocrysts in meimechites are usually represented by different-sized isolations of olivine, which quantity sometimes amounts to 40–50% of the rock volume. These phenocrysts are immersed into weakly devitrified, sometimes glassy, groundmass consisting of fine crystals of the dominant clinopyroxene and auxiliary fine grains of olivine. In the groundmass, fine grains of phlogopites occur as well as chrome-spinel and titanomagnetite as admixtures. The petrogenic components are represented in meimechites in the following quantities (wt%): SiO_2 (40–42), Al_2O_3, (1.6–3.9), FeO_{tot} (8.9–13.3), MgO (28.7–43.3), and CaO (2.5–8.8) (Kogarko & Ryabchikov, 1995).

Data on the REE composition of meimechites published thus far are rather limited (Vasil'ev, 1988; Arndt *et al.*, 1995). They are presented in Table 3.7 and reflected in Figure 3.10. Meimechites are characterized by a sufficiently high general level of REE accumulation. Thus, according to the results of incomplete analyses, the total REE content in these rocks amounts to 83–210 ppm, the chondrite-normalized contents of light REE are much greater than those of the heavy ones, which testifies to intensive fractionation of impurities. In some samples of meimechites, values of the parameter $(La/Lu)_n$ amount to 200 and more. The great majority of REE in meimechites is concentrated in the groundmass, above all in the fine crystals of clinopyroxene forming

Table 3.7 Rare earth element composition of meimechites from Meimecha-Kotuy province (ppm).

	Specimen's numbers						
	(Vasil'ev, 1988)				(Arndt *et al.*, 1995)		
Element	Mai-1	Mai-2	Mai-3	Mai-4	26-6	29-1	1985/5
La	41.6	29.3	24.8	31.5	21.5	56.1	20.5
Ce	97.4	68.3	50.3	70.0	40.7	119.9	44.5
Pr	N.d.	N.d.	N.d.	N.d.	5.4	14.3	5.7
Nd	51.3	37.4	N.d.	N.d.	23.0	55.5	23.8
Sm	9.15	7.33	5.0	5.6	4.7	9.5	N.d.
Eu	2.21	2.02	1.7	1.8	1.4	2.8	N.d.
Gd	6.07	5.20	N.d.	N.d.	4.1	6.5	2.6
Tb	0.82	0.76	0.66	0.61	N.d.	0.7	0.3
Dy	N.d.	N.d.	N.d.	N.d.	3.3	N.d.	N.d.
Ho	N.d.	N.d.	N.d.	N.d.	0.5	0.5	0.3
Er	N.d.	N.d.	N.d.	N.d.	1.3	1.3	0.6
Tm	N.d.	N.d.	N.d.	N.d.	N.d.	N.d.	N.d.
Yb	0.92	0.88	N.d.	N.d.	N.d.	N.d.	N.d.
Lu	0.12	0.11	0.088	0.19	N.d.	0.1	0.01
Total	N.d.	N.d.	N.d.	N.d.	106	267	98.3
$(La/Lu)_n$	36.0	27.6	29.3	17.2	N.d.	58.2	213

	Specimen's numbers						
	(Arndt *et al.*, 1995)					(Zolotukhin & Vasil'ev, 2003)	
Element	26-4	37-6	113D	125	1985/3	1990/1	3009/6
La	18.0	32.5	26.0	32.8	17.8	26.0	26.0
Ce	39.7	71.7	57.4	71.5	39.2	57	60
Pr	4.8	8.2	6.5	9.4	4.6	N.d.	N.d.
Nd	19.9	32.8	26.6	38.5	18.5	29	33
Sm	3.7	6.1	5.0	7.7	3.4	5.9	6.6
Eu	1.0	1.7	1.4	2.3	1.0	1.57	1.79
Gd	2.7	4.7	3.8	5.6	2.5	4.6	4.4
Tb	N.d.	N.d.	N.d.	N.d.	N.d.	0.63	0.56
Dy	1.8	3.0	2.3	N.d.	1.6	N.d.	N.d.
Ho	0.3	0.5	0.4	0.6	0.2	N.d.	N.d.
Er	0.6	1.0	0.7	1.3	0.5	N.d.	N.d.
Tm	N.d.	N.d.	N.d.	N.d.	N.d.	N.d.	N.d.
Yb	N.d.	N.d.	N.d.	N.d.	N.d.	0.60	0.69
Lu	N.d.	N.d.	0.5	0.2	N.d.	0.07	0.10
Total	92.5	162	131	170	89.3	N.d.	N.d.
$(La/Lu)_n$	N.d.	N.d.	N.d.	N.d.	N.d.	38.6	27.0

this mass. Besides, rather insignificant amounts of REE, mostly heavy ones, may be contained as structural admixtures in the porphyric phenocrysts of olivine.

* * *

Although meimechites are high in magnesium content, they concentrate within them significant amounts of REE, above all light ones, which are mainly concentrated

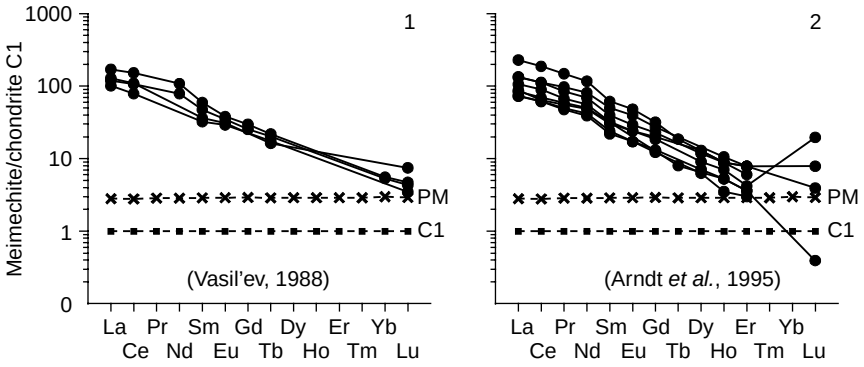

Figure 3.10 Chondrite-normalized REE composition patterns of meimechites from the Meimecha–Kotuy provinces (data Table 3.7).

in the groundmass. Initially, Kogarko *et al.* (1988) believed that meimechites were genetically connected with the formation of alkaline magmatic rocks, and the source of their parent melts was the long-lived depleted mantle reservoir subjected to active metasomatic reworking with addition of matter. Later on, Kogarko and Ryabchikov (1995) came to the opinion that the meimechite magmas were most probably generated as a result of melting lithosphere harzburgites, which had been preliminarily enriched with incompatible elements due to the infiltration of diapiric melts formed at low degrees of partial melting.

3.4 PICRITES

Picrites enter together with komatiites and meimechites into the family of hypabyssal and effusive rocks high in magnesium content. Picrites are more widespread than the other rocks, and they occur on platforms and within oceanic islands, as well as in folded regions. In the varieties of picrites represented in the folded regions, the content of MgO varies in the range of 23–36 wt%, and the value of $(Na_2O + K_2O)$ is less than 1.0 wt%. Platform picrites are characterized by about the same content of MgO (on an average, ~23% in lavas, ~25% in dikes), but differ by somewhat increased contents of alkalines with a value of $(Na_2O + K_2O)$ less than 1.0 wt% (Bogatikov *et al.*, 1981). The picrites that are widespread in folded regions enter mainly into the composition of volcanogenic-terrigenous complexes that were formed at early stages of the formation of folded structures (Markovsky, 1988). The picrites represented on the platforms and associating spatially with meimechites enter in most cases into the composition of alkaline ultrabasic volcano-plutonic complexes, which according their formation time preceded the plutonic facies of ultramafic rocks (Vasil'ev, 1988). In lavas and dikes, picrites frequently have a porphyric structure characterized by the presence of olivine and clinopyroxene phenocrysts immersed into the fine-crystalline groundmass.

The regularities of the REE distribution in picrites have been considered by generalizing the analytical data of samples from rocks widespread in the Chukotka, Kamchatka, Cyprus, Gorgona, Meimecha–Kotuy, and Noril'sk provinces, as well as the Hawaiian Islands (Table 3.8). Judging by these materials, picrites from

Table 3.8 Rare earth element composition of picrites (ppm).

	Provinces									
	East Kamchatka, Russia								Pekul'ney ridge, Russia	
	(Markovsky, 1988), INAA									
Element	Mark-1	Mark-2	Mark-3	Mark-4	Mark-5	Mark-6	Mark-7	Mark-8	Mark-9	Mark-10
La	3	2.3	2.7	3.5	2.5	2.7	2.2	0.72	0.53	0.49
Ce	6.8	5.4	6.4	8.2	6.6	6.5	5.3	2	1.8	1.3
Pr	N.d.	N.d.	N.d.	N.d.	N.d.	N.d.	N.d.	N.d.	N.d.	N.d.
Nd	N.d.	N.d.	N.d.	N.d.	N.d.	N.d.	N.d.	N.d.	N.d.	N.d.
Sm	1.6	1.2	1.4	1.8	1.3	1.3	1.1	0.58	0.83	0.73
Eu	0.52	0.39	0.48	0.67	0.46	0.46	0.39	0.26	0.35	0.31
Gd	N.d.	N.d.	N.d.	N.d.	N.d.	N.d.	N.d.	N.d.	N.d.	N.d.
Tb	0.25	0.21	0.24	0.31	0.23	0.21	0.17	0.17	0.24	0.24
Dy	N.d.	N.d.	N.d.	N.d.	N.d.	N.d.	N.d.	N.d.	N.d.	N.d.
Ho	N.d.	N.d.	N.d.	N.d.	N.d.	N.d.	N.d.	N.d.	N.d.	N.d.
Er	N.d.	N.d.	N.d.	N.d.	N.d.	N.d.	N.d.	N.d.	N.d.	N.d.
Tm	N.d.	N.d.	N.d.	N.d.	N.d.	N.d.	N.d.	N.d.	N.d.	N.d.
Yb	0.61	0.49	0.57	0.69	0.43	0.51	0.33	0.33	0.87	0.68
Lu	0.09	0.068	0.083	0.098	0.063	0.072	0.055	0.055	0.13	0.1
Total	N.d.	N.d.	N.d.	N.d.	N.d.	N.d.	N.d.	N.d.	N.d.	N.d.
$(La/Yb)_n$	3.3	3.2	3.2	3.4	3.9	3.6	4.5	1.5	0.41	0.49

	Provinces									
	Pekul'ney province, Russia		Troodos, Cyprus							
	(Markovsky, 1988), INAA		(Sobolev *et al.*, 1996), IPMA							
Element	Mark-11	Mark-12	T-133 /15	T-135/ 1	T-135/3	T-191/ 13	T-191/9	T-200/16	T-200/19	T-200/20
La	1.1	0.83	1.13	0.66	0.66	1.76	0.63	0.98	1.08	0.88
Ce	2.1	1.8	3.12	1.82	1.72	4.66	1.89	2.28	2.57	2.28
Pr	N.d.	N.d.	N.d.	N.d.	N.d.	N.d.	N.d.	N.d.	N.d.	N.d.
Nd	N.d.	N.d.	2.92	1.67	1.61	3.75	1.82	1.61	2.04	1.77
Sm	0.85	0.93	1.17	0.7	0.72	1.3	0.69	0.55	0.71	0.77
Eu	0.24	0.45	N.d.	N.d.	N.d.	N.d.	N.d.	N.d.	N.d.	N.d.
Gd	N.d.	N.d.	N.d.	N.d.	N.d.	N.d.	N.d.	N.d.	N.d.	N.d.
Tb	0.29	0.3	N.d.	N.d.	N.d.	N.d.	N.d.	N.d.	N.d.	N.d.
Dy	N.d.	N.d.	1.77	1.28	1.46	2.52	1.5	1.03	1.27	1.36
Ho	N.d.	N.d.	N.d.	N.d.	N.d.	N.d.	N.d.	N.d.	N.d.	N.d.
Er	N.d.	N.d.	1.11	0.78	0.77	1.53	0.81	0.59	0.75	0.79
Tm	N.d.	N.d.	N.d.	N.d.	N.d.	N.d.	N.d.	N.d.	N.d.	N.d.
Yb	0.87	1.1	1.16	1.02	0.96	1.69	1.04	0.69	0.81	0.95
Lu	0.13	0.16	N.d.	N.d.	N.d.	N.d.	N.d.	N.d.	N.d.	N.d.
Total	N.d.	N.d.	N.d.	N.d.	N.d.	N.d.	N.d.	N.d.	N.d.	N.d.
$(La/Yb)_n$	0.85	0.51	0.66	0.44	0.46	0.70	0.41	0.96	0.90	0.63

(*Continued*)

Table 3.8 Continued

	Provinces									
	Gorgona island, Columdia				Meimecha-Kotuy, Russia		Noril'sk region, Russia		Hawaii, USA	
	(Revillon *et al.*, 2000), ICP-MS				(Vasil'ev, 1988)		(Lul'ko *et al.*, 1994)		(Norman & Garcia, 1999), ICP-MS	
Element	GOR 512	GOR 513	GOR 514	GOR 515	Pik-5	Pik-6	SG-32	1F-30	LO-02-01	LO-02-02
La	0.08	0.12	0.15	0.15	46	120	6.21	4.54	7.22	7.73
Ce	0.33	0.42	0.55	0.46	105	220	16.90	10.34	16.6	18.1
Pr	0.08	0.11	0.13	0.11	N.d.	N.d.	N.d.	N.d.	2.15	2.37
Nd	0.67	0.81	0.91	0.77	N.d.	N.d.	11.10	6.28	10.2	11.1
Sm	0.48	0.57	0.55	0.45	9.2	14	2.96	1.85	2.44	2.69
Eu	0.27	0.3	0.28	0.23	3.2	3.3	0.946	0.71	0.82	0.88
Gd	1.14	1.3	1.2	1	N.d.	N.d.	3.33	2.02	2.68	2.93
Tb	0.24	0.27	0.25	0.21	1.0	0.82	0.502	0.32	0.43	0.47
Dy	1.91	2.09	1.98	1.69	N.d.	N.d.	N.d.	N.d.	2.3	2.47
Ho	0.43	0.48	0.46	0.39	N.d.	N.d.	0.635	0.46	0.45	0.49
Er	1.28	1.37	1.35	1.18	N.d.	N.d.	N.d.	N.d.	1.12	1.24
Tm	0.19	0.2	0.21	0.18	N.d.	N.d.	0.22	0.18	N.d.	N.d.
Yb	1.18	1.28	1.32	1.12	N.d.	N.d.	1.28	1.17	0.93	1.03
Lu	0.19	0.21	0.22	0.19	0.15	0.33	0.174	0.18	0.13	0.14
Total	8.47	9.53	9.56	8.13	N.d.	N.d.	44.3	28.1	47.5	51.6
$(La/Yb)_n$	0.05	0.06	0.08	0.09	N.d.	N.d.	3.28	2.62	128	129

	Provinces									
	Hawaii, USA									
	(Norman & Garcia, 1999), ICP-MS									
Element	LO-02-04F	LO-02-04C	KIL-1-7	KIL-1-10	KIL-1-18	KIL-2-1	KIL-1840	NK-1-6	H-5	H-11
La	8.43	6.49	9.05	8.59	9.94	8.27	9.68	10.32	6.88	7.19
Ce	19.7	14.5	22.4	21.03	25	20.3	24.2	26.2	17.3	18.1
Pr	2.55	1.95	3.09	2.98	3.43	2.82	3.36	3.7	2.43	2.53
Nd	11.9	9.1	15.6	14.5	17.2	14.1	17	18.1	12.1	12.6
Sm	2.94	2.19	4.02	3.76	4.43	3.77	4.52	4.92	3.42	3.52
Eu	0.97	0.72	1.4	1.31	1.52	1.26	1.57	1.61	1.21	1.25
Gd	3.16	2.36	4.36	4.14	4.94	4.07	5.01	5.53	3.96	4.12
Tb	0.51	0.37	0.72	0.67	0.77	0.65	0.79	0.9	0.65	0.67
Dy	2.73	2.06	3.93	3.71	4.34	3.59	4.4	4.91	3.72	3.87
Ho	0.52	0.39	0.77	0.72	0.84	0.69	0.85	0.97	0.73	0.76
Er	1.33	1	1.91	1.81	2.14	1.74	2.09	2.43	1.89	1.96
Tm	N.d.	N.d.	N.d.	N.d.	N.d.	N.d.	N.d.	N.d.	N.d.	N.d.
Yb	1.08	0.82	1.58	1.49	1.71	1.41	1.71	1.99	1.56	1.65
Lu	0.15	0.11	0.22	0.21	0.23	0.2	0.24	0.28	0.22	0.23
Total	56.0	42.1	69.1	64.9	76.5	62.9	75.4	81.9	56.1	58.5
$(La/Yb)_n$	131	132	102	100	109	102	101	93.6	78.6	78.7

(*Continued*)

Table 3.8 Continued

	Provinces									
	Hawaii, USA									
	(Norman & Garcia, 1999), ICP-MS									
Element	H-23	ML-2-50	ML-KAH-1	ML-KAH-2	ML-KAH-3	ML-1868	KOH-1-28	KW-25	KOO-CF	KOO-17a
La	4.33	5.45	6.42	6.02	6.04	6.02	6.26	7.49	10.08	8.03
Ce	10.9	14.1	16.6	16	15.6	15.4	15.7	17.7	23.8	20
Pr	1.54	2.03	2.31	2.36	2.25	2.19	2.21	2.53	3.36	2.81
Nd	7.7	10.4	11.7	11.9	11.7	11	11	12.8	16.8	14
Sm	2.16	3.01	3.3	3.48	3.39	3.05	3	3.58	4.35	3.44
Eu	0.77	1.06	1.13	1.2	1.2	1.05	1.03	1.31	1.48	1.17
Gd	2.61	3.53	3.88	3.86	3.97	3.4	3.47	3.87	4.49	3.67
Tb	0.43	0.58	0.62	0.66	0.65	0.55	0.56	0.62	0.68	0.57
Dy	2.45	3.32	3.54	3.74	3.65	3.1	3.21	3.56	3.7	3.18
Ho	0.48	0.65	0.7	0.74	0.72	0.61	0.62	0.74	0.69	0.61
Er	1.25	1.7	1.79	1.88	1.83	1.56	1.6	1.98	1.71	1.55
Tm	N.d.	N.d.	N.d.	N.d.	N.d.	N.d.	N.d.	N.d.	N.d.	N.d.
Yb	1.04	1.41	1.46	1.55	1.53	1.26	1.35	1.56	1.31	1.28
Lu	0.15	0.2	0.21	0.21	0.22	0.18	0.19	0.23	0.19	0.18
Total	35.8	47.4	53.7	53.6	52.8	49.4	50.2	58.0	72.6	60.5
$(La/Yb)_n$	72.7	70.5	79.1	76.2	70.9	85.6	82.6	77.0	125	111

	Provinces									
	Emeishan, China									
	(Zhang *et al.*, 2006), ICP-MS									
Element	DJ-2	DJ-3	DJ-25	DJ-34-1	DJ-31	DJ-26	DJ-35	SM-15	SM-14	SM-17
La	28.40	19.40	33.80	10.30	6.64	13.90	20.00	11.70	13.10	32.20
Ce	60.50	44.80	66.90	25.80	17.30	32.90	47.00	27.30	32.20	65.30
Pr	7.6	5.91	7.97	3.67	2.5	4.46	5.92	3.61	4.47	7.79
Nd	30.20	25.60	30.00	16.20	11.20	19.20	24.40	15.40	19.20	29.50
Sm	5.95	5.23	5.84	3.37	2.54	3.98	5.24	3.27	4.05	6.03
Eu	1.76	1.43	1.55	1.15	0.83	1.25	1.31	0.95	1.33	1.68
Gd	4.88	4.82	5.26	3.17	2.45	3.69	4.17	2.96	3.25	5.02
Tb	0.84	0.77	0.77	0.48	0.38	0.56	0.67	0.52	0.58	0.67
Dy	4.11	3.80	3.89	2.58	2.16	3.09	3.37	2.82	3.30	3.68
Ho	0.79	0.63	0.73	0.48	0.41	0.59	0.58	0.53	0.62	0.66
Er	1.96	1.47	1.81	1.27	1.06	1.56	1.32	1.30	1.59	1.63
Tm	0.28	0.20	0.26	0.18	0.15	0.23	0.18	0.19	0.23	0.23
Yb	1.71	1.16	1.58	1.05	0.91	1.40	1.09	1.28	1.34	1.41
Lu	0.25	0.16	0.24	0.16	0.14	0.20	0.15	0.18	0.21	0.21
Total	149	115	161	69.9	48.7	87.0	115	72.0	85.5	156
$(La/Yb)_n$	11.2	11.3	14.4	6.6	4.9	6.7	12.4	6.2	6.6	15.4

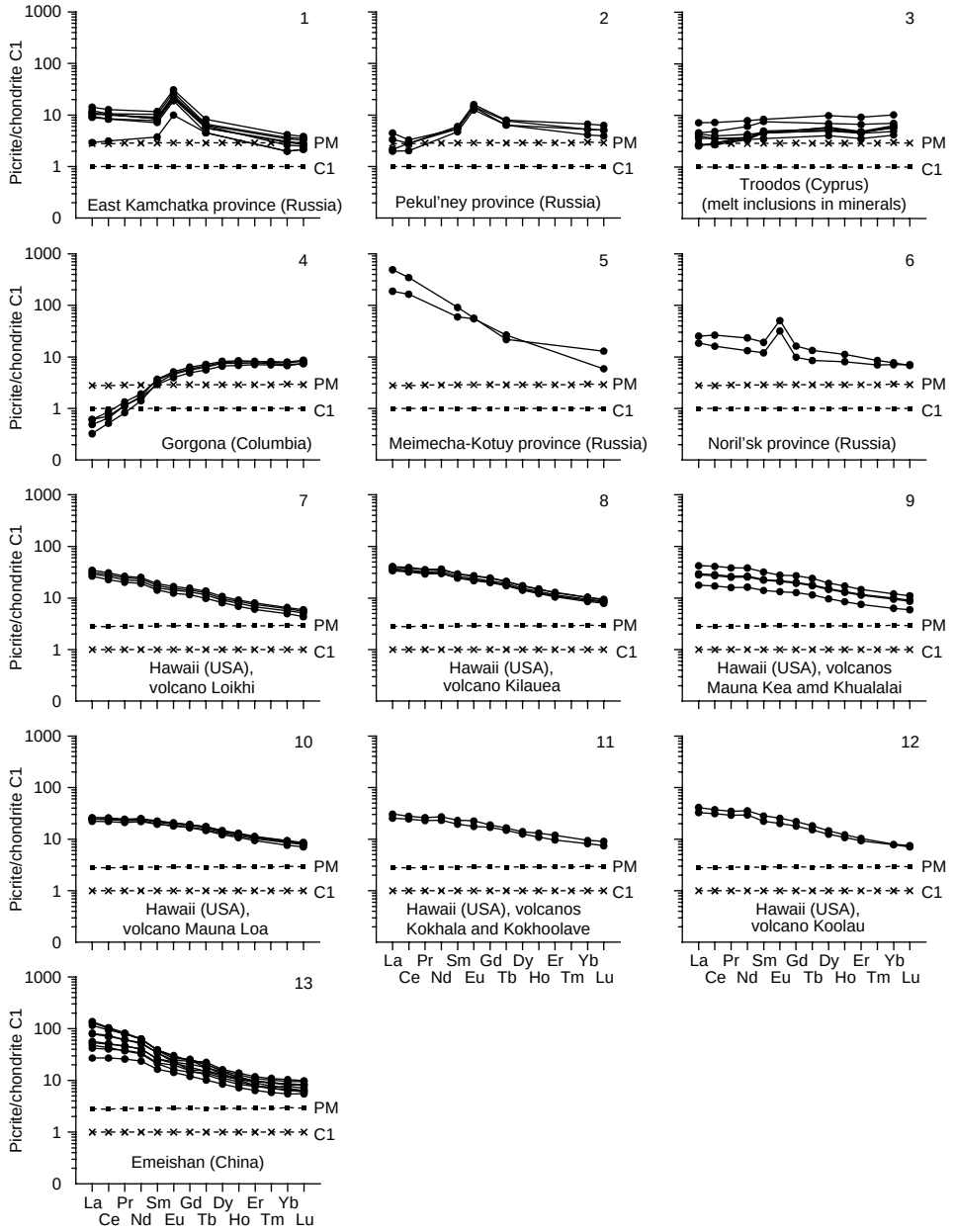

Figure 3.11 Chondrite-normalized REE composition patterns of picrites (data Table 3.8).

different provinces demonstrate a significant diversity of REE composition. Rocks from the volcanogenic-terrigenous and volcano-plutonic complexes of the folded regions (eastern Kamchatka, Chukotka, Cyprus) have, on average, lower total REE content (4–13 ppm) compared to the varieties entering into the composition of the platform

structures (Meimecha–Kotuy province, the Noril'sk district). The total REE content in the platform structures amounts to 20–360 ppm. Closely approaching them are the picrites from the Hawaiian Islands, in which the total REE content varies in the range of 36–82 ppm. The REE patterns of picrites differ in some provincial peculiarities (Fig. 3.11). Picrites from the eastern Kamchatka province are characterized by comparatively weak fractionation of REE, and at the same time they are insignificantly enriched with La and Ce (~10 t. ch.), and their level of Yb and Lu accumulation is comparable with the primitive mantle (~2 t. ch.). Values of the parameter $(La/Yb)_n$ in the eastern Kamchatka picrites vary in the range of 1.5–4.5. A distinctive feature of the REE composition of these picrites is also a significant excess of Eu, which is probably connected with the fractionation of plagioclase (see Fig. 3.11). In the picrites of the Pekul'ney mountain ridge (Chukotka), the accumulation level of the light (1–4 t.ch.) and heavy (3–5 t. ch.) elements is somewhat higher than in the primitive mantle. At the same time, they are markedly enriched with the middle elements, particularly with Eu, which brings them closer to the picrites from the eastern Kamchatka province (see Fig. 3.11, 2).

The REE composition of picrites from the volcano-plutonic complex Troodos on the island of Cyprus has been characterized on the basis of analytical materials on the melt inclusions from pyroxenes contained in them (Sobolev *et al.*, 1996). The REE accumulation level in these inclusions is somewhat higher compared to the primitive mantle, and the element fractionation degree is very low. Their patterns have an almost "flat" shape, and the values of $(La/Yb)_n$ vary in the range of 0.41–0.96 (see Fig. 3.11, 3). The picrites from the volcano-plutonic complex Gorgona Island are noted for being markedly depleted of light REE. Thus, the accumulation level of La and Ce in them is lower than that of these elements in chondrite C1, while that of the heavy elements in the series from Gd to Lu is much higher than their level in the primitive mantle (see Fig. 3.11, 4). These properties of the picrites of Gorgona Island bring them closer to the komatiites represented in the same province (see Fig. 3.8, 11, 12) (Revillon *et al.*, 2000). The picrites from the Noril'sk province, both by the level of REE accumulation and by the configuration of rare earth patterns, have much in common with the picrites of western Kamchatka. The level of REE accumulation in these rocks decreases from La (~20 t. ch.) to Lu (~8 t. ch.). The negatively inclined patterns are described by increased values of the parameter $(La/Yb)_2$ (2.6–3.3), and, in addition, show intensive positive Eu anomalies (see Fig. 3.11, 6). Subalkali picrites from the Meimecha–Kotuy province differ from the above varieties by a higher level of accumulation of both light (200–500 t. ch.) and heavy REE (6–15 t. ch.). Their rare earth patterns have a very steep slope, and the values of the parameter $(La/Lu)_n$ vary in the range of 32–38 (see Fig. 3.11, 5). There are representative analytical data on the REE composition of picrites widespread in the areas of active volcanoes on the Hawaiian Islands (Norman & Garcia, 1999). From these data follows the conclusion that, in spite of the sufficiently wide variation in MgO content (17–30 wt%), the accumulation level of both light (17–40 t. ch.) and heavy REE (4–11 t. ch.) as well as the values of the parameter $(La/Yb)_n$ (2.6–5.3) in these picrites vary in relatively narrow ranges.

A recent publication reported the results of research on the distribution of REE in the picrites from the western part of the late Permian basalt province Emeishan in South China (Zhang *et al.*, 2006). The content of MgO in these picrites varies in the range of 12.3–27.0 wt%, and, at the same time, olivine from porphyric phenocrystals

Table 3.9 Average REE composition of picrites from some provinces (ppm).

Element	Provinces								Average content in picrites from all provinces (except Emeishan)
	Gorgona (4)	Chukotka (4)	Troodos (8)	East Kamchatka (8)	Noril'sk (2)	Hawaii (22)	Meimecha-Kotuy (2)	Emeishan (10)	
La	0.13	0.74	0.97	2.45	5.38	7.52	83	7.47	18.9
Ce	0.44	1.75	2.54	5.90	13.62	18.60	16.35	16.76	42.0
Pr	0.11	N.d.	N.d.	N.d.	N.d.	2.59	N.d.	2.21	5.39
Nd	0.79	N.d.	2.15	N.d.	8.69	12.85	N.d.	8.90	22.09
Sm	0.51	0.84	0.83	1.29	2.41	3.44	11.6	2.51	4.55
Eu	0.27	0.34	Í. ä.	0.45	0.83	1.18	3.25	0.80	1.32
Gd	1.16	N.d.	N.d.	N.d.	2.68	3.83	N.d.	2.61	3.97
Tb	0.24	0.27	N.d.	0.22	0.41	0.62	0.91	0.40	0.62
Dy	1.92	N.d.	1.52	N.d.	N.d.	3.44	N.d.	2.80	3.28
Ho	0.44	N.d.	N.d.	N.d.	0.55	0.67	N.d.	0.49	0.60
Er	1.30	N.d.	0.89	N.d.	N.d.	1.71	N.d.	1.47	1.50
Tm	0.20	N.d.	N.d.	N.d.	0.20	N.d.	N.d.	0.08	0.21
Yb	1.23	0.88	1.04	0.50	1.23	1.40	N.d.	1.12	1.29
Lu	0.20	0.13	N.d.	0.07	0.18	0.20	0.24	0.14	0.19
Total	8.92	N.d.	N.d.	N.d.	36.2	58.1	N.d.	41.9	106
$(La/Y)_n$	0.07	0.57	0.64	3.32	2.95	3.64	N.d.	2.56	9.58

Data Table 3.8.

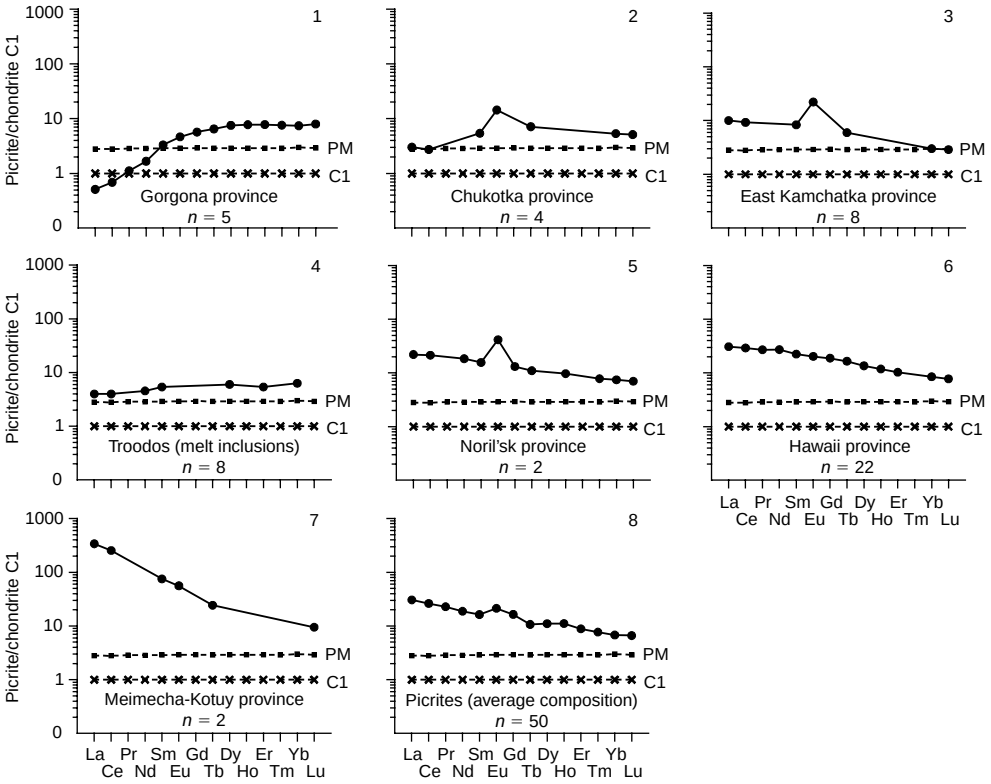

Figure 3.12 Chondrite-normalized patterns for the average REE composition of picrites (data Table 3.9).

features a high content of forsterite component (85.0–91.6) and an increased content of admixture CaO (0.25–0.45 wt%). The picrites from this province differ from most others by an increased accumulation level of REE, which total content amounts to 70–161 ppm. Compared to picrites from the Hawaiian Islands, the rocks from China demonstrate far higher values of the parameter $(La/Yb)_n$, which vary in the range of 4.9–15.4 (the average value is 9.6). Their REE patterns contain no Eu anomalies (see Fig. 3.11, 13), which brings these picrites close to those of the Hawaiian Islands.

The generalization of the available geochemical data makes it possible to assume that the parent melts of picrites from the Gorgona Island province were the derivations of a preliminarily depleted mantle source. Distinct from them, the sources in which melts were generated, that were responsible for the formation of picrites from the vast majority of the other provinces, were evidently subjected to no preliminary depletion. The results of geochemical investigations of the picrites from the Hawaiian province, including the obtained estimates of such pairs of parameters as Sm/Nd–La/Yb and Lu/Hf–La/Yb, show that their parent melts resulted from partial melting of garnet-spinel mantle peridotites in the range of 4–10%. Possibly, in cases when a source enriched with more garnet was subjected to partial melting, the rare earth composition of the generated melts did not always correspond to the composition of picrites

(Norman & Garcia, 1999). Picrites from the Emeishan province are assumed to have been formed from melts with an MgO content of about 22 wt%, at a temperature of about 1630–1690°C, and formed at a relatively low degree of the partial melting of the garnet-bearing mantle source (Zhang *et al.*, 2006).

In conclusion, it should be noted that picrites from different provinces scarcely differ in their average contents of heavy REE, while those of the light elements differ rather appreciably, which appears to reflect the differences in the degree of the partial melting of mantle sources (Table 3.9, Fig. 3.12).

* * *

Picrites represent one of the most widespread varieties of shallow magmatic rocks high in magnesium content. They are characterized by a significant diversity of REE composition. The geochemical systematic classification of picrites makes it possible to isolate from among them a successive series of varieties from significantly depleted of light REE (Gorgona Island) to subalkaline varieties significantly enriched with these elements (Hawaiian Islands, Meimecha–Kotuy province). Picrites from different provinces usually differ in the average contents of light REE, but in most cases they are comparable to the average contents of heavy elements. The picrites of the eastern Kamchatka, Chukotka, and the Noril'sk provinces, are distinct from those of other provinces in that they reveal an appreciable excess of Eu. The diversity in REE composition of picrites is likely to be due to the variation in the composition of the mantle sources of their parent melts as well to the differences in the degrees of the partial melting of protoliths, which varied from comparatively low to moderate.

3.5 LAMPROITES

Lamproites are shallow high-potassium rocks and are frequently high in magnesium content (Mitchell, 1988; Bogatikov *et al.*, 1991; Mitchell & Bergman, 1991). They differ from kimberlites both in the chemical and the mineral composition, but for all that they are comparable to them with respect to their high accumulation level of light elements and the fractionation intensity of REE as a whole. Lamproites more often form relatively small hypabyssal intrusives, stocks, sills, dikes, necks as well as pipes, and sometimes isolated layers within potassium-alkali stratified complexes. The geology, petrology, and geochemistry of lamproites have been studied in varying detail in the provinces and manifestations located in the territory of Australia (Western and Eastern Kimberley, Argyle, Ellendale), in the USA (Prairie Creek, Arkansas; Leucite Hills, Wyoming; Smoky Butte, Montana), in Spain (Murcia–Almeria), in Russia (Murunsky, Khany, Tomtor, and other massifs on the Aldan shield), as well as in southern and eastern India. Appreciable concentrations of diamonds were discovered in some lamproite volcanic pipes (Argyle, Ellendale).

In accordance with the systematic classification based on modal mineral composition, lamproites are divided into the following varieties: olivine lamproites, leucite lamproites and leucite-bearing, sanidine lamproites, phlogopite lamproites, olivine-diopside lamproites, and others. There are also lamproites with a porphyraceous

and rarer massive structure. The porphyry phenocrysts in lamproites can be represented by olivine, phlogopite, diopside, common potash feldspar, alkali amphiboles. Not infrequently, lamproites may contain chrome-spinel, magnetite, apatite, and sulfide as accessories. Sometimes lamproites contain deep xenoliths of lherzolites and harzburgites. In some provinces lamproites were to different extents subjected to carbonatization. Chemically, two varieties of lamproites are distinguished: (1) ultramafic lamproites in which the content of MgO varies in the range of 20–33 wt% and (2) mafic lamproites in which the content of this component is much lower (6–10 wt%).

The main peculiarities of the rare earth composition of lamproites were considered on the basis of results obtained by studying them in the territory of several best known provinces (Table 3.10).

The Aldan shield. Within this province, study was made of numerous manifestations of lamproites located close to the rock massifs of increased alkalinity. In these massifs, lamproites form dikes, sills, or layers of various mineral composition (Vladykin, 1997). Located there are olivine-phlogopite-pyroxenic, olivine-phlogopite-leucitic, K-richterite-phlogopite-leucitic, leucitic, olivine-leucitic, and olivinic lamproites. Most of these have a porphyraceous structure. All the studied lamproites from this province are characterized by comparatively low contents of REE, the olivine lamproites from the Khany and Murunsky massifs are noted for the lowest level of REE accumulation. The accumulation level of light REE in the lamproites of the Aldan shield varies in the range of 20–200 t. ch. and that of the heavy ones range from 2 to 30 t. ch. The rare earth patterns of these lamproites have a relatively gentle negative slope (Fig. 3.13). Weak Eu and Sm anomalies are observed in some of them. Values of the parameter $(La/Yb)_n$ in the lamproites of the Aldan shield vary from 5.4 (K-richterite-phlogopite-leucitic lavas) to 47 (K-richterite-phlogopite-sanidinic varieties forming xenolith in charoitic rock).

West and East Kimberley, Argyle, Ellendale, Prairie Creek, Leucite Hills, Smoky Butte, Murcia–Almeria. All the lamproites from the said provinces show a very high total accumulation level of light REE, with a rather low accumulation level of the heavy elements (Jaques *et al.*, 1984; Mitchel & Bergman, 1991). The content of La in these rocks varies in the range of 87–368 ppm, and that of Ce varies in the range of 242–805 ppm. The average total content of REE in the lamproites of each of the said provinces is about 5 times as high as that in the rocks of the Aldan shield province. This is also true for the average values of the parameter $(La/Yb)_n$. The rare earth patterns built from the average contents of the elements in lamproites from the entire series of the provinces have the form of nearly straight lines with a very steep negative slope. The rare earth patterns of olivinic and leucitic lamproites partially overlap, although on average, the REE accumulation level in the leucitic varieties is somewhat higher than that in the olivinic ones. Values of the parameter $(La/Yb)_n$ in their olivine-bearing varieties range from 128 to 316 (the average value is 227); in the phlogopites-bearing varieties, its values are somewhat lower, with a range of 92–238 and an average value of 160. In the whole set of the samples of lamproites from the manifestation Smoky Butte the accumulation level decreases from very high for light REE (1000–1400 t. ch.) to much lower for the heavy elements. The values of the parameter $(La/Yb)_n$ in lamproites from Smoky Butte vary in the range of 184–281 and amount to an average of 226, which makes it possible to compare them to the same kind of rocks from West Kimberley. Phlogopites-bearing and olivine-bearing lamproites from the Murcia–Almeria province have rare earth patterns of nearly identical configuration.

Table 3.10 Rare earth element composition of lamproites (ppm).

	Provinces									
	Aldan shield, Russia									
	(Vladykin, 1997), OES									
Element	Vlad-1	Vlad-2	Vlad-6	Vlad-7	Vlad-9	Vlad-10	Vlad-13	Vlad-15	Vlad-18	Vlad-22
La	50	29	44	72	37	5.5	18	27	23	30
Ce	68	53	74	130	74	19	55	44	36	53
Pr	N.d.	N.d.	N.d.	N.d.	N.d.	N.d.	N.d.	N.d.	N.d.	N.d.
Nd	31	31	32	68	34	14	25	29	26	21
Sm	6.8	7.9	6.1	19	7	3.5	6.1	6.8	4.7	4.7
Eu	1.9	3	1.3	5.1	2.4	0.7	1.4	1.5	0.83	1
Gd	5.1	6.1	3.7	42	8.5	2.3	5.3	3.3	3.1	4.7
Tb	N.d.	N.d.	N.d.	N.d.	N.d.	N.d.	N.d.	N.d.	N.d.	N.d.
Dy	3.8	3.8	2.2	20	4.3	1	2.9	3.5	2.7	2.5
Ho	0.52	0.81	0.31	3	0.92	0.2	0.58	0.45	0.54	0.6
Er	1.5	2	0.86	7	2.2	0.4	1.7	1.3	1	1.5
Tm	N.d.	N.d.	N.d.	N.d.	N.d.	N.d.	N.d.	N.d.	N.d.	N.d.
Yb	1.6	1.4	0.63	9	2	0.38	1.4	1.1	1.3	1.4
Lu	0.14	0.18	0.11	1	0.14	0.04	0.2	0.09	0.2	0.2
Total	170	138	165	376	172	47.0	118	118	99.4	121
$(La/Yb)_n$	21.1	14.0	47.1	5.40	12.5	9.8	8.7	16.6	11.9	14.5

	Provinces										
	Aldan shield, Russia							West Kimberly		Argyle	Frencis
	(Vladykin, 1997), OES							(Mitchell & Bergman, 1991), Australia			
Element	Vlad-23	Vlad-25	Vlad-26	Vlad-30	Vlad-31	Vlad-33	Vlad-35	Mitch.1 (aver.12)	Mitch.2 (aver.16)	Mitch.3 (aver.4)	Mitch.4 (aver.5)
La	52	21	40	41	26	35	27	348	242	129	133
Ce	87	43	50	86	42	59	57	629	414	269	275
Pr	N.d.	N.d.	N.d.	N.d.	N.d.	N.d.	N.d.	49	33	N.d.	33
Nd	44	25	36	50	20	48	40	212	146	104	128
Sm	8.1	5.2	5	10	4.7	11	11	25	18	15	17
Eu	1.9	1.8	1.8	1.6	1.3	1.8	1.5	5.8	4.3	3.4	3.7
Gd	6.8	5	6.8	11	4.7	5	8.9	9.5	8.4	8.7	9.5
Tb	N.d.	N.d.	N.d.	N.d.	N.d.	N.d.	N.d.	1.8	1.4	1.1	0.9
Dy	4.9	3.9	3.8	7	2.7	3.6	7	4.8	4.2	N.d.	4.8
Ho	1.1	0.68	0.62	1.2	0.56	0.55	1	0.9	1	0.9	N.d.
Er	2.2	2	1.8	3.4	1.5	1.6	2.4	1.8	1.9	N.d.	N.d.
Tm	N.d.	N.d.	N.d.	N.d.	N.d.	N.d.	N.d.	N.d.	N.d.	N.d.	N.d.
Yb	2.2	1.5	1.8	2.7	1.3	0.82	1.9	1.6	1.5	1.4	1.3
Lu	0.3	0.16	0.16	0.41	0.14	0.11	0.2	0.19	0.17	0.17	0.16
Total	211	109	148	214	105	166	158	1289	876	N.d.	N.d.
$(La/Yb)_n$	16.0	9.5	15.0	10.3	13.5	28.8	9.6	147	109	62.2	69.1

(*Continued*)

Table 3.10 Continued

	Provinces									
	Murcia-Almeria		Gaussberg	Smoky Butte	Leucite Hills		Sysco	Hills Pond	Prairie Creek	Priestly Peak
	(Mitchell & Bergman, 1991), Spain, USA									
Element	Mitch.5 (aver.11)	Mitch.6 (aver.4)	Mitch.7 (aver.13)	Mitch.8 (aver.15)	Mitch.9 (aver.10)	Mitch.10 (aver.3)	Mitch.11 (aver.5)	Mitch.12 (aver.5)	Mitch.13 (aver. 6)	Mitch. 14 (aver.4)
La	87	155	215	368	148	297	183	116	144	159
Ce	242	401	398	805	273	597	344	312	277	319
Pr	31	46	45	N.d.	N.d.	N.d.	N.d.	N.d.	N.d.	N.d.
Nd	149	224	134	N.d.	117	228	138	N.d.	107	149
Sm	27	40	16	33	15	27	20	14	13	27
Eu	4.5	6.9	4.1	8.1	3.6	6.2	3.1	3.1	3.1	7
Gd	14	21	11	N.d.	N.d.	N.d.	N.d.	N.d.	N.d.	N.d.
Tb	N.d.	N.d.	N.d.	2.1	1.1	1.6	1.1	0.6	0.9	N.d.
Dy	6.4	9.6	6.9	N.d.	N.d.	N.d.	N.d.	N.d.	N.d.	N.d.
Ho	1.1	1.6	0.6	N.d.	N.d.	N.d.	N.d.	N.d.	N.d.	N.d.
Er	2.6	3.7	1.5	N.d.	N.d.	N.d.	N.d.	N.d.	N.d.	N.d.
Tm	N.d.	N.d.	N.d.	N.d.	N.d.	N.d.	N.d.	N.d.	N.d.	N.d.
Yb	1.9	2.6	0.8	1.6	1.3	1.4	1.2	0.8	0.9	0.9
Lu	0.27	0.36	N.d.	N.d.	0.14	0.18	N.d.	0.16	0.12	N.d.
Total	567	912	833	N.d.	N.d.	N.d.	N.d.	N.d.	N.d.	N.d.
$(La/Yb)_n$	30.9	40.2	181	155	76.8	143	103	97.9	108	119

	Provinces										
	Bayliss	Tomtor, Russia									
	(Mitchell & Bergman, 1991)	(Kravchenko, 2002), INAA									
Element	Mitch.15 (aver.2)	115/158	1625/61.7	1625/70.1	1625/78	118/117	118/195	1625/91	1625/113	2425/134	2425/136
La	151	170	76.5	156	175	172	521	301	735	91	1370
Ce	309	325	161	361	341	247	534	447	1380	302	1750
Pr	N.d.	N.d.	N.d.	N.d.	N.d.	N.d.	N.d.	N.d.	N.d.	N.d.	N.d.
Nd	117	137	79.1	149	147	90.7	148	161	483	134	75
Sm	18	20.8	15.1	23.9	23.8	15.7	22.9	23.5	63.2	21.5	12.1
Eu	5.1	4.99	3.96	6.1	5.9	4.39	6.23	5.95	16.1	5.26	2.88
Gd	N.d.	14.5	11.1	15.8	14.1	12.6	16.6	16.3	41.7	13.2	7.32
Tb	N.d.	1.73	1.45	1.97	1.91	1.65	1.99	1.92	4.61	1.7	0.99
Dy	N.d.	N.d.	N.d.	N.d.	N.d.	N.d.	N.d.	N.d.	N.d.	N.d.	N.d.
Ho	N.d.	1.83	1.89	1.9	1.53	1.49	1.81	2.08	3.58	1.6	1.06
Er	N.d.	N.d.	N.d.	N.d.	N.d.	N.d.	N.d.	N.d.	N.d.	N.d.	N.d.
Tm	N.d.	0.6	N.d.	0.39	0.41	0.34	0.31	0.49	0.85	0.5	0.44
Yb	1.4	3.69	2.15	2.44	2.05	1.97	1.49	2.99	4.12	2.88	2.31
Lu	N.d.	0.53	0.26	0.32	0.28	0.22	0.18	0.37	0.51	0.39	0.33
Total	N.d.	681	353	719	713	549	1255	963	2733	574	3222
$(La/Yb)_n$	72.8	31.1	24.0	43.2	57.6	58.9	236	68.0	120	21.3	400

(*Continued*)

Table 3.10 Continued

	Provinces									
	Tomtor, Russia						West Kimberley, Australia			
	(Kravchenko, 2002), INAA						(Jaques *et al.*, 1984)			
Element	2425/138	6409/93	6409/155	7265/25	7265/48	7265/64	Jaq-1	Jaq-2	Jaq-3	Jaq-4
La	145	231	142	165	177	88.2	185	344	232	237
Ce	284	394	185	290	325	151	261	415	270	346
Pr	N.d.	N.d.	N.d.	N.d.	N.d.	N.d.	N.d.	N.d.	N.d.	N.d.
Nd	120	149	64.2	119	149	79	N.d.	N.d.	N.d.	N.d.
Sm	20.1	26	15.7	20.8	26.7	14.9	N.d.	N.d.	N.d.	N.d.
Eu	4.98	7.99	5.05	5.72	6.95	4.19	N.d.	N.d.	N.d.	N.d.
Gd	14.1	24.2	17.7	16.2	20.4	13.3	N.d.	N.d.	N.d.	N.d.
Tb	1.62	3.97	2.56	2.08	2.33	1.62	N.d.	N.d.	N.d.	N.d.
Dy	N.d.	N.d.	N.d.	N.d.	N.d.	N.d.	N.d.	N.d.	N.d.	N.d.
Ho	1.45	3.73	2.99	2.02	2.25	1.7	N.d.	N.d.	N.d.	N.d.
Er	N.d.	N.d.	N.d.	N.d.	N.d.	N.d.	N.d.	N.d.	N.d.	N.d.
Tm	0.34	0.95	0.83	0.64	0.56	0.59	N.d.	N.d.	N.d.	N.d.
Yb	2.1	4.75	4.82	3.67	2.81	3.33	N.d.	N.d.	N.d.	N.d.
Lu	0.31	0.62	0.63	0.49	0.39	0.46	N.d.	N.d.	N.d.	N.d.
Total	594	846	441	626	713	358	N.d.	N.d.	N.d.	N.d.
$(La/Yb)_n$	46.6	32.8	19.9	30.4	42.5	17.9	N.d.	N.d.	N.d.	N.d.

	Provinces										
	West Kimberley, Australia				Kuddapah, South India						
	(Jaques *et al.*, 1984)				(Chalapathi Rao *et al.*, 2004), ICP-MS						
Element	Jaq-5	Jaq-6	Jaq-7	Jaq-8	RU1	NR/1	NR/7	C5	C1-A	C1-C	ZP
La	412	158	436	519	106	124	120	388	240	207	254
Ce	673	210	619	788	234	237	231	709	473	417	493
Pr	N.d.	N.d.	N.d.	N.d.	26.77	25.7	26.5	76.9	56.7	45.8	55.3
Nd	N.d.	N.d.	N.d.	N.d.	96.3	92.2	95.7	263	197	163	196
Sm	N.d.	N.d.	N.d.	N.d.	15.03	13.6	15.1	32.4	25.4	21.9	27
Eu	N.d.	N.d.	N.d.	N.d.	4.22	3.48	4.17	8.17	6.1	5.59	7.02
Gd	N.d.	N.d.	N.d.	N.d.	13.93	13.57	13.62	30.27	26.1	19.4	23.2
Tb	N.d.	N.d.	N.d.	N.d.	1.38	1.27	1.31	2.54	1.53	1.68	1.98
Dy	N.d.	N.d.	N.d.	N.d.	5.98	5.74	5.73	10.13	6.03	7.07	7.98
Ho	N.d.	N.d.	N.d.	N.d.	0.96	0.95	0.91	1.85	0.9	1.08	1.22
Er	N.d.	N.d.	N.d.	N.d.	2.21	2.23	2.08	4.05	2.06	2.46	3.11
Tm	N.d.	N.d.	N.d.	N.d.	0.26	0.26	0.26	0.55	0.26	0.3	0.34
Yb	N.d.	N.d.	N.d.	N.d.	1.59	1.77	1.6	3.15	1.48	1.66	2.04
Lu	N.d.	N.d.	N.d.	N.d.	0.19	0.22	0.2	0.4	0.19	0.18	0.26
Total	N.d.	N.d.	N.d.	N.d.	509	522	518	1530	1037	894	1072
$(La/Yb)_n$	N.d.	N.d.	N.d.	N.d.	45.0	47.3	50.6	83.1	110	84.2	84.0

(*Continued*)

Table 3.10 Continued

	Provinces									
	Kuddapah, South India	Damodar valley, East India								
	(Chalapathi Rao *et al.*, 2004), ICP-MS	(Jia *et al.*, 2003), ICP-MS								
Element	ZP-1	M2/1	M2/2	SD-1	SD-2	P-1	P-2	CP60/93	B4	R839A
La	250	337	334	627	827	864	1059	1097	219	297
Ce	491	687	671	1337	1765	1812	2259	2440	461	597
Pr	54.1	79.2	79.6	155	201	207	263	291	53.6	65.5
Nd	194	330	318	564	729	746	1008	1241	217	249
Sm	26.3	45.5	47.7	78.6	102	97.1	126	156	27	29.91
Eu	7.01	11.7	12.2	19.2	24.3	23.4	30.5	35.1	6.4	7.18
Gd	22.7	29.4	29.7	49	59.5	59.1	76.8	87.5	18.2	19.74
Tb	2.01	2.73	2.94	4.52	5.05	5.15	7.13	7.4	1.8	1.86
Dy	7.91	13.2	14.4	20.9	20.6	21.7	33.4	32.2	8.35	8.77
Ho	1.21	2.05	2.21	3.17	2.83	3.13	4.86	4.39	1.29	1.36
Er	3.09	4.64	5.07	7.28	6.19	7.03	11.1	8.56	3.04	3.21
Tm	0.32	0.54	0.64	0.9	0.81	0.91	1.3	0.84	0.37	0.42
Yb	2.01	3.09	3.35	5.06	4.75	5.19	6.9	3.97	2.03	2.34
Lu	0.26	0.4	0.46	0.69	0.57	0.67	0.9	0.45	0.29	0.31
Total	1062	1546	1521	2872	3749	3852	4888	5405	1019	1284
$(La/Yb)_n$	84.0	73.6	67.3	83.6	118	112	104	187	72.8	85.7

Analysis from Mitch.1–to Mitch.15 characterizes averages REE compositions of lamproites from different manifestations (see Fig. 3.15).

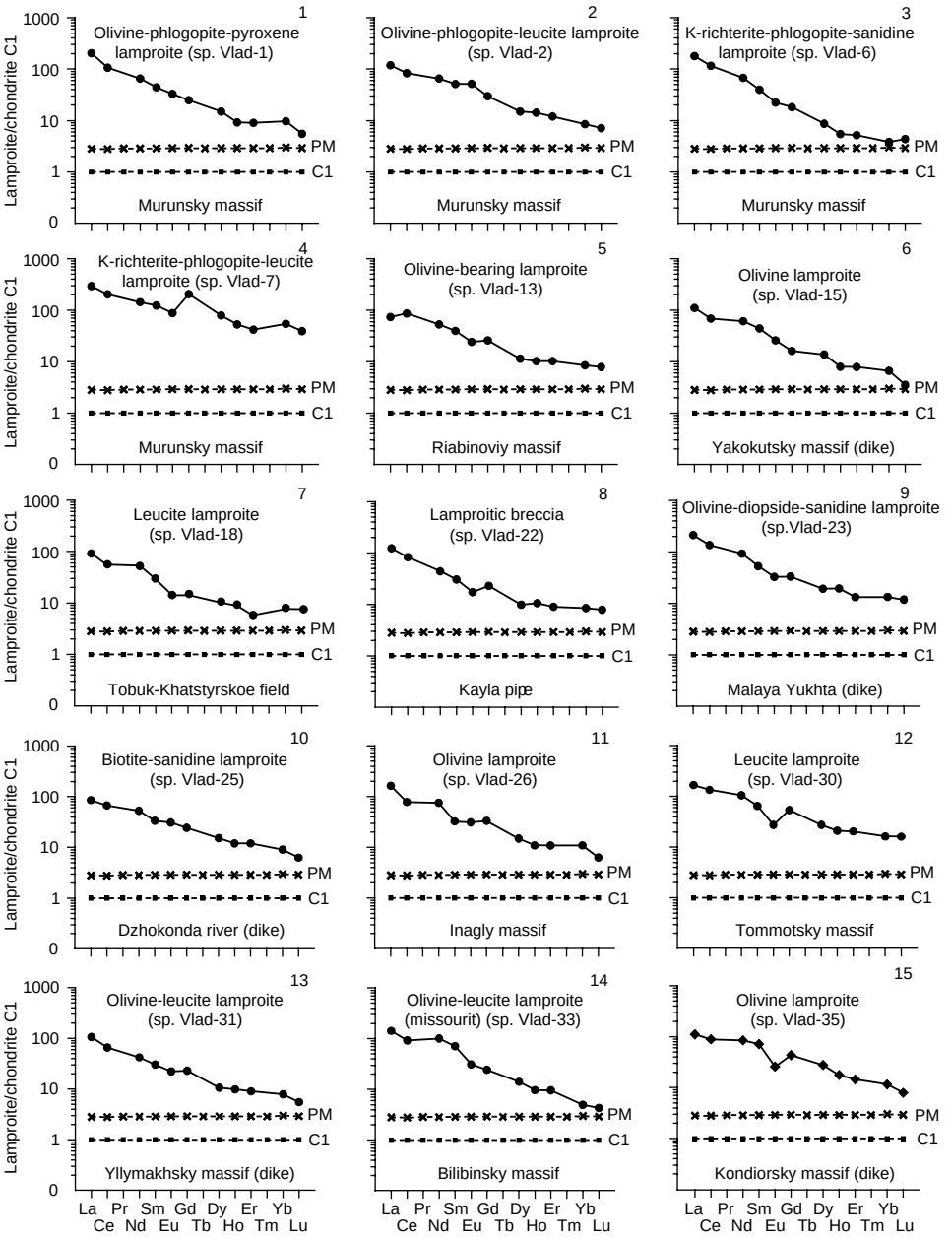

Figure 3.13 Chondrite-normalized REE patterns for lamproites from the Aldan shield (data Table 3.10).

These lamproites differ from the samples from most other provinces by their decreased values of the parameter $(La/Nd)_n$.

The Tomtor alkaline-ultramafic massif situated in the northern part of the Siberian Platform represents a complicated circular structure. Lamproites were discovered in

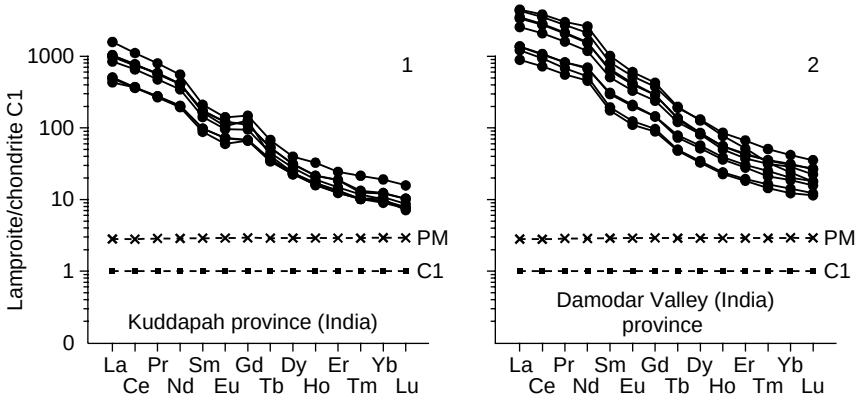

Figure 3.14 Chondrite-normalized REE patterns for lamproites from the Indian provinces (data Table 3.10).

it during well drilling. In most cases, these rocks are intensively carbonatized. From the exploration data, it has been found that the carbonatization of lamproites and their other metasomatic changes were accompanied by a significant addition of REE to them, particularly of light ones, as well as of other admixture elements (Kravchenko, 2002). As a result, these lamproites show an extremely high total accumulation level of light REE (300–2000 t. ch. or more) with a significantly lower accumulation level of the heavy ones (7–20 t. ch.). Correspondingly, the values of the parameter $(La/Yb)_n$ are also very high (20–400).

India. The rare earth composition of lamproites has been characterized using, by way of example, their samples from the manifestations situated in the eastern (Jia *et al.*, 2003) and southern districts of the country (Chalapathi Rao *et al.*, 2004). In south India, in the region of Kuddapah, there are several manifestations of lamproites forming numerous dikes. The rocks are known to contain significant amounts of phenocrysts of phlogopite as well as olivine, completely replaced by carbonate and serpentine, and in the groundmass occurs richterite and apatite. The content of MgO in these lamproites varies in the range of 9–15 wt%, that of TiO_2 varies from 3 to 5.6, and that of K_2O varies from 1 to 5 wt%. The total content of REE in them ranges from 1019 to 5405 ppm. The average accumulation levels of La (1717 t. ch.) and Ce (1370 t. ch.) are higher than those in the lamproites from most other provinces. The REE patterns of the rocks from south India have the same configuration and are located close to one another (Fig. 3.14, 1). They are characterized by very intensive fractionation of elements, which is also expressed in very high values of the parameter $(La/Yb)_n$ (67–187). They show very weak negative Eu and Sm anomalies.

Lamproites from eastern India (Karanapura, Bokaro, Rummgarkh, Jharia, and Ranyjang manifestations) contain high-titanium phlogopite, aegirine, amphibole, apatite, carbonate, chrome-spinel, fluorite, perovskite, titanomagnetite, as well as pseudomorphs of serpentine replacing olivine. The content of MgO in them varies in the range of 8–20 wt%, that of TiO_2 varies from 3.60 to 10.1 wt%, and that of K_2O varies from 2.9 to 7.3 wt%. Lamproites from these manifestations are noted for high contents not only of REE, but also of Ba, Th, and U. The total content of REE in these

Table 3.11 Average REE composition (x) and standard deviation (σ) of lamproites from some provinces (ppm).

	Provinces							
	East India (9)		Tomtor (16)		South India (8)		Aldan (17)	
Element	x	σ	x	σ	x	σ	x	σ
La	629	344	295	334	211	94.4	34.0	15.4
Ce	1337	763	467	445	411	169	60.6	25.1
Pr	155	89.9	N.d.	N.d.	46.0	18.5	N.d.	N.d.
Nd	600	360.4	143	96.3	162	62.3	33.8	13.2
Sm	78.9	45.0	22.92	11.6	22.1	6.87	7.51	3.71
Eu	18.9	10.2	6.04	2.95	5.72	1.66	1.81	1.01
Gd	47.7	25.0	16.82	7.64	20.3	6.31	7.78	9.10
Tb	4.29	2.11	2.13	0.92	1.71	0.44	N.d.	N.d.
Dy	19.3	9.13	N.d.	N.d.	7.07	1.55	4.68	4.23
Ho	2.81	1.24	2.06	0.75	1.14	0.32	0.80	0.63
Er	6.24	2.60	N.d.	N.d.	2.66	0.70	2.02	1.45
Tm	0.75	0.29	0.55	0.20	0.32	0.10	N.d.	N.d.
Yb	4.08	1.56	2.97	1.01	1.91	0.54	1.91	1.91
Lu	0.53	0.20	0.39	0.14	0.24	0.07	0.22	0.22
Total	2904	1648	959	824	893	361	155	70.6
$(La/Yb)_n$	100	37.1	78.1	101	73.5	23.2	15.5	9.73

Data Table 3.10.

rocks varies in the range of 1020–5400 ppm, the values of the parameter $(La/Yb)_n$ varies from 47 to 109. The REE patterns of lamproites from eastern India are very close to one another in their configuration (see Fig. 3.14, 2).

Geochemical investigations of lamproites have shown that, similar to kimberlites, nearly all of them are characterized by a sharply increased total REE accumulation level and by their exceptionally intensive fractionation. At the same time, their samples from different provinces and manifestations differ more or less from one another both in the average contents of REE and in the degree of their fractionation (see Figs. 3.15, 3.16, Table 3.11). Within the entire body of the selected analytical data, the accumulation level of light REE varies in the range of 500–2000 t. ch., while that of heavy elements is substantially lower (from 3 to 6 t. ch.). In addition, the average accumulation levels of La (~1000 t. ch.) and Lu (~10 t. ch.) differ by two orders of magnitude. The calculated average content of REE in lamproites from the entire selection of analytical data amounts to about 950 ppm, which is almost 3 times as much as that in kimberlites (~330 ppm).

The forms in which REE are contained in lamproites as well as the reasons why these rocks are so highly enriched with light REE are not yet fully elucidated and continue to be studied. Most of the REE represented in these rocks is assumed to be concentrated in the form of a structural impurity in perovskite and apatite, which contents in lamproites can vary over wide limits. In addition, more or less significant amounts of REE are contained in the structure of clinopyroxene, amphibole (K-richterite), phlogopite, leucite, and feldspars, as well as in that of some minerals formed by the REE themselves.

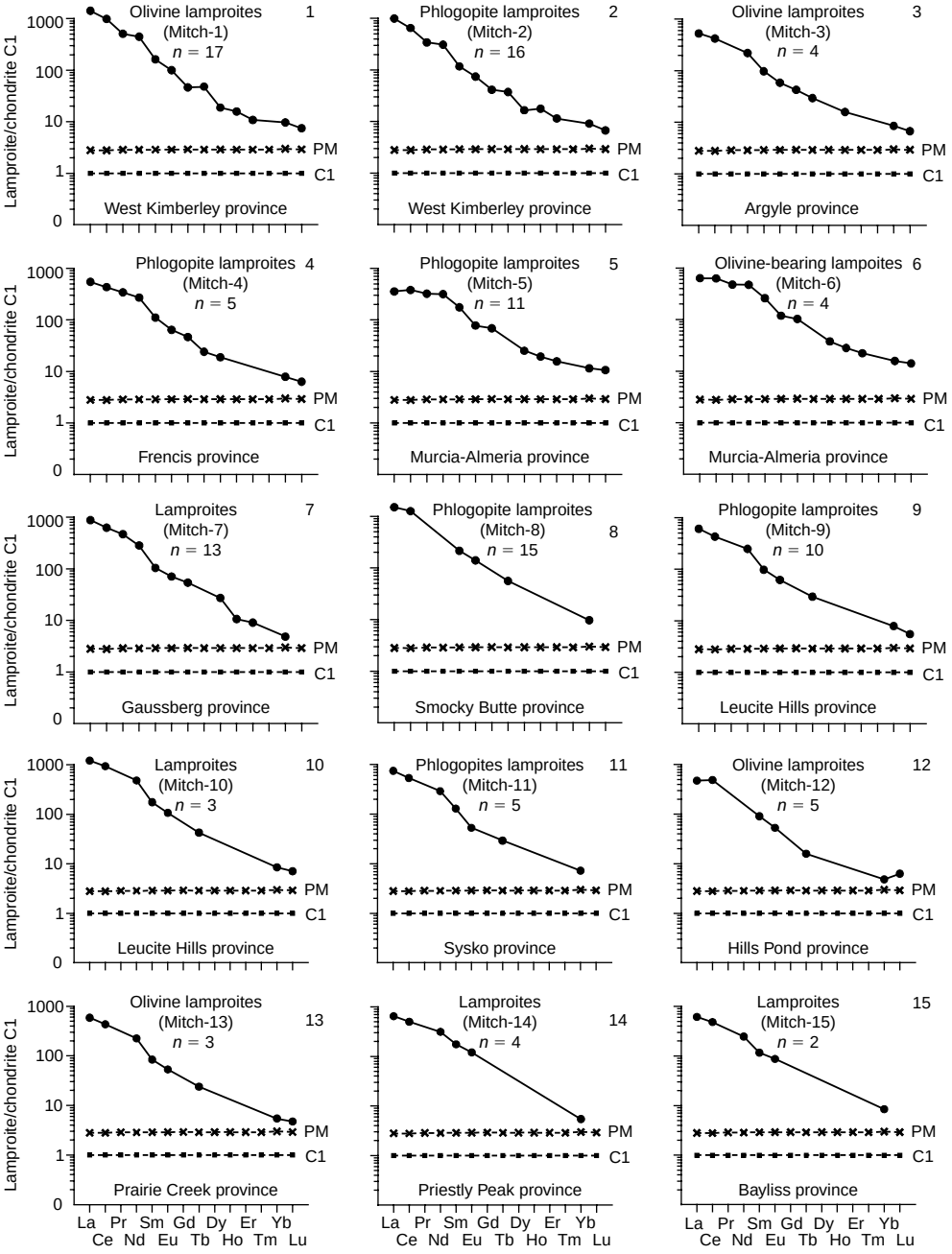

Figure 3.15 Chondrite-normalized patterns for average REE composition of lamproites from the provinces of Australia, Spain, the USA, and others (data Table 3.10).

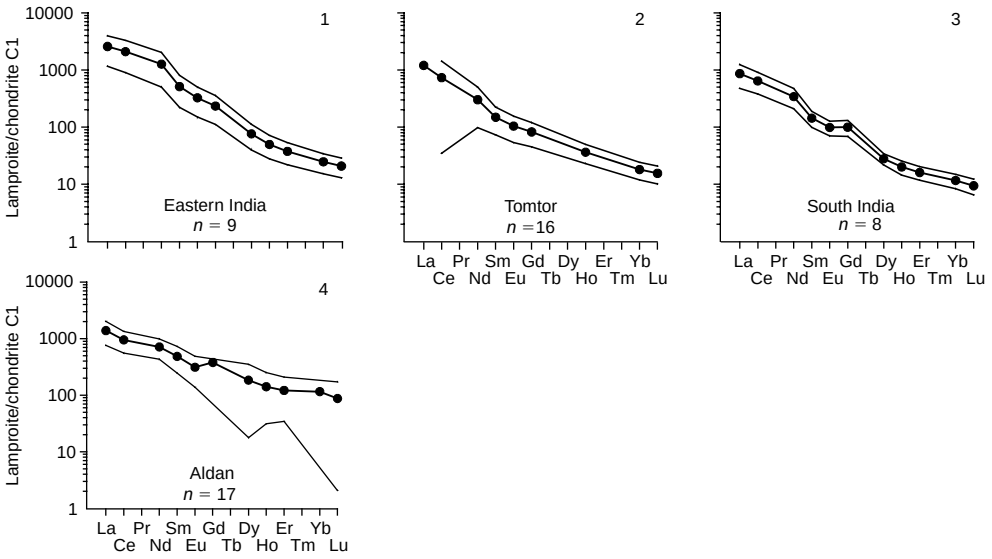

Figure 3.16 Chondrite-normalized patterns for average REE composition of lamproites from some provinces of eastern and southern India, and Russia (data Table 3.11). Narrow lines mark limits of REE content variations on basis of standard deviations.

Investigators name different reasons for the enrichment of lamproites with light REE, admitting its indubitable connection with the genesis of these rocks. Thus, there exists a hypothesis that the formation of lamproites is connected with the crystallization of abyssal melts resulting from the partial melting of metasomatized lherzolite–harzburgite mantle source enriched with phlogopite and depleted of garnet and diopside, and that the concentration of water and fluorine in this source was high while that of CO_2 was sufficiently low (Jaques *et al.*, 1984). According to other views, lamproites might have formed during intrachambered differentiation of parent melts from which there also effloresced all the other varieties of rocks that form the K-alkali complexes starting with ultramafites and finishing with granites. Such a model has been suggested, in particular, to explain the origin of lamproites of the Aldan shield (Vladykin, 1997). A hypothesis has been made that the sharp enrichment of lamproites with light REE is genetically connected with an extremely low degree of melting the mantle source (<1%), which composition supposedly corresponded to that of phlogopite-garnet lherzolite (Mitchell & Bergman, 1991). It is not improbable, however, that the mantle source was preliminarily enriched with REEa as a result of metasomatic transformations.

* * *

By now, lamproites have been discovered and studied to different degrees of detail within many cratons. Great interest in them is due to both an unusual chemical and mineral composition of these rocks, including abnormally high contents of REE, and their potential diamond content. Lamproites differ from kimberlites by having lower contents of MgO, higher contents of SiO_2, high contents of phlogopite, as well as,

on average, a higher accumulation level of light REE. Their samples from different provinces and manifestations differ to a greater or lesser extent in the general level of REE accumulation as well as in the intensity of their fractionation. The highest average level of REE accumulation is characteristic of the lamproites from the southern Indian provinces, and the lowest average level of REE is found in those from the Aldan shield. The great bulk of REE contained in lamproites is concentrated in the form of a structural admixture in their rock-forming and accessory minerals: clinopyroxene, amphiboles, perovskite, apatite, and others. The abnormal enrichment of lamproites with light REE is assumed to have been caused by an extremely low extent of the partial melting of the mantle source, which by its composition corresponded to phlogopite-garnet lherzolite preliminarily enriched with REE as a result of metasomatic transformations. It should be noted in conclusion that lamproites from diamond-bearing bodies, say, from the diatreme of Argyle, are noted for relatively increased concentrations of REE. On the whole, however, the problem of the dependence between the REE composition of lamproites and their diamond content remains unsolved.

3.6 SUMMARY

The above materials on the rare earth composition of kimberlites, komatiites, meimechites, picrites, and lamproites, which are considered subvolcanic and hypabyssal varieties of magmatic rocks high in magnesium content, testify that, apart from a number of specific petrographical, petrochemical, and mineralogical features, they differ from most of the other rocks of magmatic origin in the parameters of REE distribution.

Kimberlites are characterized by a sharply increased level of light REE accumulation with relatively low contents of middle and heavy elements. In the average total REE content, their varieties constitute a sequence from the rocks most enriched with these admixtures, located in the Australian provinces, to those most depleted of them, contained in the Arkhangelsk manifestations. In the kimberlites from each province, the REE content, just as their general chemical composition, varies in relatively narrow ranges. The rare earth patterns of kimberlites, represent, as a rule, nearly straight lines with sharp negative slopes. A particularly intensive fractionation of REE is typical of the varieties widespread in Canada and Australia, and the least intensive is typical of samples from the Arkhangelsk and Timan provinces. The principal minerals that concentrate REE in kimberlites are calcite, clinopyroxene, phlogopite, perovskite, apatite, ilmenite, monazite, as well as xenogeny garnet. The contents of light REE in these rocks have been found to be directly proportional to the content of CaO and inversely proportional to those of SiO_2, Na_2O, and Al_2O_3. In their turn, the contents of heavy REE are directly proportional to those of TiO_2 and FeO_{tot}. In addition, the content of Yb also has a positive connection with the contents of MgO and K_2O.

The specific REE composition of kimberlites may be due to the fact that their parent melts were generated at very low degrees of partial melting of mantle protoliths and at very high pressures.

Komatiites represent a special type of volcanogenic rocks with a very high content of magnesium. In many cases, they possess a "spinifex" structure testifying to high melt crystallization rates, which has led to the formation of skeletal crystals of olivine and

clinopyroxene. A majority of the komatiite provinces are located within the Archean greenstone belts. The younger provinces of southwest Vietnam and of Gorgona Island represent an exception. Most komatiites are significantly depleted of incompatible admixture elements, including REE. The total content of REE varies in the range of 3–70 ppm and are inversely proportional to the content of MgO. The values of the parameter $(La/Yb)_n$ vary from less than unity to greater than unity. The rare earth patterns of some komatiites show negative or positive Eu anomalies of low intensity. For the purposes of the geochemical systematic classification of komatiites, use has been made of the values of the parameters $(La/Sm)_n$ and $(Gd/Yb)_n$. The parent melts of komatiites appear to have generated at increased degrees of partial melting of mantle sources. Their rise to the crust's upper layers as well as their crystallization proceeded at high rates.

Meimechites represent a variety of subvolcanic rocks of high-magnesium content and differ from picrites, which are closely related to them, by having a higher REE content. These rocks are distributed within limited bounds and have so far been found mainly on the Siberian Platform. There is few available data on the REE composition of meimechites. The total REE content in them ranges from 83 to 210 ppm, and, in addition, they are noted for having rather intensive fractionation. In some varieties of meimechites, the values of the parameter $(La/Lu)_n$ is greater than 200. The greatest amount of REE in meimechites is concentrated in their groundmass, first of all in microcrystals of clinopyroxene. Also, insignificant amounts of REE may be contained in the structure of olivine phenocrysts. The high-magnesium content of meimechites and their significant enrichment with light REE are assumed to be due to the specific conditions of the regeneration of their parent melts, that is, to the high rate and low degree of the partial melting of the nondepleted mantle source at great depths.

Picrites represent the most widely distributed type of shallow rocks with high and moderate magnesium content and very heterogeneous REE composition. They form a sufficiently long series of varieties from rocks of normal alkalinity, depleted of light REE and distributed in eastern Kamchatka, Chukotka, and on the islands of Cyprus and Gorgona, to low-alkaline varieties significantly enriched with these elements and distributed on the Hawaiian Islands, plus subalkaline varieties from the Meimecha–Kotuy province. Picrites from different provinces are comparable in their contents of REE, but they differ significantly in the contents of light elements. Picrites from the eastern Kamchatka, Chukotka, and the Noril'sk provinces show a certain excess of Eu. The diversity of rare earth composition of these rocks may be due to both the heterogeneity of the material composition of the mantle sources of their parent melts and the differences in the extent of partial melting of the latter, from sufficiently low to moderate extents.

Lamproites represent a specific type of subvolcanic rocks high in magnesium content which possess a high, essentially potassic alkalinity and at the same time are highly enriched with REE, especially light ones. Like kimberlites, they are distributed exceptionally within the ancient cratons. They differ from kimberlites by having higher contents of SiO_2 and K_2O, lower contents of MgO, higher contents of phlogopite, as well as, on average, a higher accumulation level of light REE, which varies in the range of 500–2000 t. ch., whereas the level of heavy REEa amounts to only 3–6 t. ch. The average total content of REE in lamproites is about 950 ppm, which is nearly 3 times as much as in kimberlites (~330 ppm). The highest average level of REE accumulation is

characteristic of lamproites from the South Indian province, and the lowest is characteristic of those from the Aldan province. The great bulk of the structural admixture of REE in lamproites is concentrated in clinopyroxene, amphiboles, perovskite, apatite, and in some minerals formed by the REE themselves. The abnormally high enrichment of lamproites with light REE is assumed to have been caused by extremely low degrees of the partial melting of the mantle source, which composition might correspond to phlogopite-garnet lherzolite. It is not improbable that these sources had been preliminarily enriched with REE due to metasomatic transformations.

Chapter 4

Rare earth elements in plutonic mafic rocks

Magmatic rocks of mafic composition are widespread in all types of tectonic structures and geodynamic settings, including folded belts, mid-oceanic ridges, oceanic islands, cratons, as well as the moon. Rocks related to this voluminous group have been formed throughout geological history of the earth's crust until the present time. Parent melts of mafic rocks have been intruded and crystallized as plutonic massifs at abyssal, mesoabyssal, and hypabyssal depths, and as subvolcanic and volcanic formations under subsurface and surface conditions. Significant variations in chemical and mineral compositions of mafic rocks are caused by a wide range of physical and chemical conditions, at which generation, fractionation, contamination, and crystallization of their parent melts took place. The same processes have predetermined the wide variations in rare element contents of rocks, including rare earth contents in mafic rocks.

In this chapter we generalize data on REE distributions in mafic rocks, mainly in intrusive rocks of normal or slightly elevated alkalinity. According to the accepted recent nomenclature, the most widespread varieties of these rocks are the following: gabbros, gabbro-norites, norites, olivine gabbros, olivine gabbro-norites, troctolites, anorthosites, as well as transitional varieties between them. All these mafic rocks differ to some extent in mineral paragenesis and/or modal composition. In addition to the above-named rocks, in this chapter we discuss the peculiarities of REE geochemistry in eclogites, which can be considered high-pressure analogs of abyssal plutonic mafic rocks.

The below-described varieties of plutonic mafic rocks usually consist of various ultramafic–mafic and mafic–ultramafic massifs and magmatic complexes, which differ in age of formation, structural and tectonic position, formation type, mode of occurrence, size, morphology, internal structure, and other individual features. Many more ancient mafic–ultramafic massifs occurring in folded structures of the continents and oceans are regarded as components of ophiolite associations. A voluminous group of complicate massifs formed by interleaved bodies of mafic and less abundant ultramafic rocks is considered by many petrologists to be so-called differentiated or stratified plutons.

The main rock-forming minerals of plutonic mafic rocks are olivine, orthopyroxene, clinopyroxene, plagioclase, amphiboles, and less often garnet; the modal proportions between these minerals vary over a wide range. Based on the results of detailed geological, structural, and petrographical investigations of many mafic–ultramafic massifs located in various folded areas, we distinguish two main rock

types among the complex plutonic mafic rocks: (1) orthomagmatic mafic rocks, which crystallized from non-contaminated basic melts generated in the upper mantle; and (2) paramagmatic (hybrid) mafic rocks, crystallized from mantle mafic melts, which were preliminarily contaminated by substances of more-ancient ultramafites or terrigenous-volcanogenic and metamorphic rocks (Lesnov, 1984, 1986).

Normal gabbros, gabbro-norites, norites, as well as some olivine-bearing gabbros and gabbro-norites are related to orthomagmatic mafites. These rocks are usually medium- to thin-grained and have an equigranular texture and a massive structure. It has been proposed that two types of paramagmatic mafic rocks can be distinguished: A and B. Type A includes olivine gabbros and olivine gabbro-norites, troctolites, and some anorthosites, considerably varying in structure, texture, and modal composition. The majority of these paramagmatic mafites is characterized by taxitic structures, either banded or spotty. In complex mafic–ultramafic massifs usually related to ophiolite associations, paramagmatic mafic rocks of type A together with pyroxenites, wehrlites, plagioclase-bearing dunites, and plagioclase-bearing lherzolites compose so-called "banded" complexes, which are also known as "cumulative" complexes.

Paramagmatic mafic rocks related to type B are represented by the varieties contained in endocontact zones of abyssal and mesoabyssal mafic bodies, located along contacts of these bodies with enclosing volcanogenic, volcanogenic-terrigenous, and metamorphic rocks. This type of mafic rock includes hornblende gabbro, quartz-bearing and biotite-bearing gabbro, gabbro-diorite, and diorite, all of which are less abundant in the composition of such massifs. As noted above, the formation of this type of rock was connected with more or less intensive contamination of deep-seated basic melts by substances of different enclosing rocks. Such contamination resulting in the formation of type B mafic rocks could proceed most actively at prolonged cooling and crystallization of basic melts at abyssal depths. The results of the generalization of up-to-date information on REE geochemistry in plutonic mafic rocks from a great quantity of separate massifs, as stated in this chapter, have allowed researchers to reveal some general regularities of distribution of these elements in rocks related to this group, to consider probable causes of observable variations in their contents, to discuss possible ways of using these data for a more-detailed geochemical classification of massifs and their composing rocks to construct regional schemes of magmatism, as well as to solve some actual problems of the petrology of plutonic mafic rocks.

4.1 GABBROS

Common gabbro is the most widespread variety of orthomagmatic mafic rocks. Together with other varieties of mafites and ultramafites, they compose many mafic–ultramafic massifs that are different in their characteristics. Gabbro consists of two main minerals: clinopyroxene (35–65 vol%) and plagioclase (35–65 vol%). Sometimes minor minerals (<5%) occur: olivine, amphibole, and less often biotite. Accessory minerals in gabbros are represented by magnetite, titanomagnetite, ilmenite, apatite, zircon, sphene, and sulfide phases. The contents of major chemical components in gabbros vary in the following ranges (wt%): SiO_2 (42–52), Al_2O_3 (8–24), FeO_{tot} (3–20), MgO (5–17), CaO (11–17), Na_2O (0.5–3), K_2O (0.05–2.0). Values of the parameter $100 \cdot FeO_{tot}/(FeO_{tot} + MgO)$ vary in a wider range (45–52%) than do values of

the parameters CaO/Al_2O_3 (0.6–0.7), MgO/CaO (0.7–1.3), Al_2O_3/MgO (1.8–2.4) (Lesnov, 1986).

Some aspects of REE distribution in gabbros were discussed earlier (Lesnov, 2005b). Here, this question is regarded in more detail, on the basis of generalization of more than 100 analyses of these rock samples from many mafic–ultramafic massifs located in continental folded areas, island arcs, as well as in mid-oceanic ridges. The REE composition of gabbros varies over a wide range that is manifested not only when comparing samples from different massifs, but also frequently from the same massif (Table 4.1, Fig. 4.1). In the diagrams, the REE spectra of tholeiite basalts of mid-oceanic ridges (N-MORB) and basalts of oceanic islands (OIB) (Sun & McDonough, 1989) are shown for comparison.

The geochemical inhomogeneity of gabbros is visible most distinctly when comparing the total REE content or, best of all, total light REE content, in the samples. In the used dataset of analyses, the total REE content in gabbros varies over the range of 0.65–250 ppm, averaging about 46 ppm. The level of La accumulation changes over a wider interval (0.26–313 t. ch.) than does the level of Yb accumulation (0.24–83 t. ch.). The studied gabbros often differ in intensity of REE fractionation that is reflected in wide variations of values of the parameter $(La/Yb)_n$ (0.13–15). As a rule, rare earth spectra of the overwhelming majority of gabbro samples, especially those that are considerably depleted of REE, demonstrate positive Eu anomalies of various intensities. It should be noted also that in many mafic–ultramafic massifs, the dominant gabbro varieties are those in which the total REE concentration level is lower than the level in N-MORBs. Only in rare cases do gabbro varieties have total REE contents that are comparable with their concentrations in OIBs.

Gabbros from the massifs that are part of ophiolite associations, in particular those from the Bay of Islands, Pindos, Samail, Troödos, Mount Orford, Annieopsquotch, Hegenshan, Venezuela, and the bodies exposed in the Mid-Atlantic Ridge, have been subjected to more-detailed geochemical study. Most of these samples are depleted of REE, especially light ones, and the total REE content in them does not usually exceed 10 ppm. For example, the total REE content in gabbros from the Bay of Islands is 1.6–1.9 ppm, from Samail this value is 6.4–8.9 ppm, from Troödos this value is 1.0–12.1, and from Hegenshan this value is 5.0–9.4. These gabbros are also depleted of light REE. In addition, they are characterized by rather low values of the parameter $(La/Yb)_n$: Bay of Islands (0.31–0.57), Samail (0.18–0.46), Troödos (0.15–0.49), Mount Orford (0.34–0.71), Hegenshan (0.19–0.52), some samples from the Mid-Atlantic Ridge (0.27–0.82), Annieopsquotch, and Newfoundland (0.20–0.42). In REE patterns of the majority of gabbro samples from these massifs, positive Eu anomalies of variable intensity are observed. Values of the parameter $(Eu/Eu^*)_n$ vary over the following ranges: Bay of Islands (2.0–4.4), Pindos (1.3–4.7), Samail (1.04–1.41), Troödos (1.0–3.5), Venezuela (1.0–1.7), Hegenshan (1.4–2.1), and the Mid-Atlantic Ridge (1.3–1.9). The intensity of positive Eu anomalies usually increases with reducing total REE content in gabbros. In some massifs, alongside gabbros depleted of REE, gabbro varieties with higher REE contents are found, as, for example, in massifs of Pindos (see Fig. 4.1, 2), Mount Orford (see Fig. 4.1, 6), Venezuela (see Fig. 4.1, 7), and in the Mid-Atlantic Ridge (see Fig. 4.1, 15). Gabbros from massifs that are not related to ophiolite associations are characterized by an extremely high total REE content (ppm): Salt Chak (93–100), Union Bay (72–79), Skaergaard (21–118), Sept Iles (20–133),

Table 4.1 Rare earth element composition of gabbros from some massifs (ppm).

	Massifs													
	Bay of Islands, Canada			Pindos, Greece			Samail, Oman			Skaergaard, Greenland				
	(Suen *et al.*, 1979), INAA			(Montigny *et al.*, 1973), IDMS			(Pallister & Knight, 1981), RNAA			(Haskin & Haskin, 1968), NAA				(Paster *et al.*, 1974)
Element	201	203	205	A34	A40	A42	Kf-11-1	Kf-16-1	Kf-18-1	4427	4507	5086	4330	4312
La	0.120	0.150	0.320	N.d.	N.d.	N.d.	0.460	0.230	0.180	2.800	5.600	7.600	76.5	13.4
Ce	N.d.	N.d.	N.d.	0.690	2.340	13.8	1.300	0.830	1.300	6.500	12.10	14.10	171	41
Pr	N.d.	N.d.	N.d.	N.d.	N.d.	N.d.	N.d.	N.d.	N.d.	0.950	1.880	1.960	26	N.d.
Nd	0.650	N.d.	N.d.	0.610	2.070	13.4	2.300	1.600	1.800	4.500	9.200	8.400	113	33
Sm	0.320	0.310	0.410	0.250	0.810	4.42	0.780	0.560	0.730	1.370	2.510	2.090	35	9.9
Eu	0.310	0.310	0.340	0.220	0.440	1.6	0.370	0.330	0.320	0.730	1.040	0.910	14	2.9
Gd	N.d.	0.680	N.d.	N.d.	1.320	N.d.	1.200	0.900	1.200	1.740	2.880	2.160	35.5	12
Tb	0.080	0.120	0.140	N.d.	N.d.	N.d.	0.220	0.170	0.230	0.300	0.440	0.310	5.8	1.65
Dy	N.d.	N.d.	N.d.	0.600	1.850	7.05	1.400	1.100	1.600	N.d.	N.d.	N.d.	N.d.	N.d.
Ho	N.d.	N.d.	N.d.	N.d.	N.d.	N.d.	N.d.	N.d.	N.d.	0.390	0.540	0.440	6.2	1.63
Er	N.d.	N.d.	N.d.	0.360	N.d.	4.05	N.d.	N.d.	N.d.	1.010	1.450	1.250	15.4	N.d.
Tm	N.d.	N.d.	N.d.	N.d.	N.d.	N.d.	0.110	0.091	0.110	0.168	0.200	0.191	2.4	N.d.
Yb	0.260	0.310	0.380	0.420	1.130	N.d.	0.670	0.530	0.690	0.980	1.200	1.060	13.7	2.4
Lu	0.060	0.060	0.050	0.058	0.150	0.48	0.094	0.075	0.095	0.138	0.190	0.173	2.7	N.d.
Total	N.d.	N.d.	N.d.	N.d.	N.d.	N.d.	N.d.	N.d.	N.d.	21.6	39.2	40.6	N.d.	N.d.
$(La/Yb)_n$	0.31	0.33	0.57	N.d.	N.d.	N.d.	0.46	0.29	0.18	1.93	3.15	4.84	3.77	3.77

Element	Massifs Troodos, Cyprus				Mount Orford, Canada					Venezuela				
	(Kay & Seneshal, 1976), IDMS				(Harnois & Morency, 1989), RNAA					(Giunta *et al.*, 2002), ICP-MS				
	78B	CY10	CY3	CY4	E-12	E-38	E-5	E-8	E-9	VNZ152	VNZ159	VNZ162	VNZ231	VNZ232
La	0.063	0.066	0.785	0.100	0.084	1.090	1.180	7.140	6.590	0.710	4.030	7.590	4.090	0.660
Ce	0.210	0.097	2.350	0.361	0.248	3.520	3.360	24.520	22.550	1.960	9.320	16.40	9.090	1.860
Pr	N.d.	N.d.	N.d.	N.d.	N.d.	N.d.	N.d.	N.d.	N.d.	0.350	1.360	2.490	1.410	0.340
Nd	0.225	0.142	2.270	0.450	0.254	3.480	3.530	24.53	20.90	1.990	7.530	11.90	7.120	1.810
Sm	0.118	0.074	0.874	0.247	0.113	1.300	1.480	8.370	8.330	0.600	2.190	3.400	2.000	0.570
Eu	0.057	0.060	0.365	0.164	0.073	0.393	0.585	2.600	2.810	0.380	0.810	1.120	1.020	0.580
Gd	N.d.	0.144	1.380	N.d.	0.152	1.480	1.800	9.700	8.730	0.740	2.400	3.200	2.480	0.690
Tb	N.d.	N.d.	N.d.	N.d.	0.021	0.280	0.306	1.710	1.430	0.120	0.440	0.530	0.380	0.110
Dy	0.330	0.195	1.720	0.670	N.d.	N.d.	N.d.	N.d.	N.d.	0.680	2.740	3.680	2.310	0.560
Ho	N.d.	N.d.	N.d.	N.d.	N.d.	N.d.	N.d.	N.d.	N.d.	0.140	0.590	0.840	0.500	0.110
Er	0.251	0.132	1.100	0.425	N.d.	N.d.	N.d.	N.d.	N.d.	0.410	1.460	2.060	1.240	0.280
Tm	N.d.	N.d.	N.d.	N.d.	N.d.	N.d.	N.d.	N.d.	N.d.	0.070	0.220	0.360	0.200	0.040
Yb	0.277	0.125	1.090	0.399	0.165	1.400	1.570	6.790	6.570	0.410	1.320	2.600	1.230	0.320
Lu	0.051	N.d.	0.163	0.067	0.026	0.221	0.241	1.020	0.932	0.060	0.180	0.420	0.210	0.060
Total	N.d.	N.d.	N.d.	N.d.	N.d.	N.d.	N.d.	N.d.	N.d.	8.62	34.6	56.6	33.3	7.99
$(La/Yb)_n$	0.15	0.36	0.49	0.17	0.34	0.53	0.51	0.71	0.68	1.17	2.06	1.97	2.24	1.39

(*Continued*)

Table 4.1 Continued

	Massifs													
	Venezuela						Hegenshan, China					Band Ziarat, Iran		
	(Giunta *et al.*, 2002), ICP-MS						(Nozaka & Liu, 2002), ICP-MS					(Hassanipak *et al.*, 1996), ICP-MS		
Element	VNZ65	VNZ197	VNZ206	VNZ203	VNZ181	VNZ184	No1206	No2810	No2803	No2807	No2705	HP-16	HP-34	HP-35
La	0.260	2.340	0.280	0.330	1.050	1.590	0.700	0.300	0.200	0.200	0.200	0.9	1.0	1.4
Ce	0.900	5.330	1.110	1.240	2.920	4.270	1.200	0.500	0.700	0.400	0.800	3.56	2.8	3.78
Pr	0.150	0.780	0.200	0.240	0.480	0.680	0.300	0.100	0.200	0.100	0.200	N.d.	N.d.	N.d.
Nd	0.830	3.440	1.330	1.640	2.590	3.460	1.400	0.800	1.100	0.600	1.100	2.41	2.7	3.33
Sm	0.390	1.270	0.680	0.640	0.860	1.370	0.600	0.400	0.500	0.300	0.500	0.64	0.55	1.1
Eu	0.270	0.630	0.300	0.350	0.350	0.560	0.500	0.300	0.300	0.300	0.400	0.66	0.59	0.52
Gd	0.570	1.990	0.840	1.070	1.140	1.690	0.900	0.600	0.900	0.600	0.900	1.06	1.05	1.63
Tb	0.090	0.350	0.170	0.190	0.220	0.280	0.200	0.100	0.200	0.100	0.200	N.d.	N.d.	N.d.
Dy	0.700	2.360	1.620	1.260	1.280	2.270	1.300	0.900	1.100	0.900	1.200	1.24	1.8	2.1
Ho	0.150	0.550	0.260	0.270	0.280	0.450	0.300	0.200	0.300	0.200	0.300	N.d.	N.d.	N.d.
Er	0.370	1.480	0.680	0.640	0.850	1.300	0.900	0.500	0.700	0.600	0.800	0.26	0.57	0.83
Tm	0.050	0.230	0.100	0.120	0.130	0.210	0.100	0.100	0.100	0.100	0.100	N.d.	N.d.	N.d.
Yb	0.350	1.470	0.680	0.660	0.950	1.450	0.900	0.600	0.700	0.500	0.700	0.51	0.73	0.86
Lu	0.050	0.220	0.100	0.100	0.150	0.200	0.100	0.100	0.100	0.100	0.100	0.16	0.13	0.14
Total	5.13	22.4	8.35	8.75	13.3	19.8	9.40	5.50	7.10	5.00	7.50	N.d.	N.d.	N.d.
$(La/Yb)_n$	0.50	1.07	0.28	0.34	0.75	0.74	0.53	0.34	0.19	0.27	0.19	1.19	0.93	1.10

	Massifs													
	Band Ziarat, Iran			Bou Azzer, Morocco		Gorgona, Columbia			Balmuccia, Italy		Salt Chak, USA		Union Bay, USA	
	(Hassanipak *et al.*, 1996), ICP-MS			(Bodinier *et al.*, 1984)		(Revillon *et al.*, 2000), ICP-MS			(Rivalenti *et al.*, 1995), ICP-MS		(Himmelberg & Loney, 1995)			
Element	HP-19	HP-33	HP-31	1200	569	GOR 510	GOR 511	GOR 541	TS-4	MO383	86GH3B	86GH7A	87GH37A	87GH44A
La	1.44	2.46	2.01	1.540	1.100	0.940	1.000	0.860	2.8	0.51	18.1	14	15	13.7
Ce	5.32	6.97	6.26	5.120	2.570	3.060	3.100	3.090	13.47	3.03	40.9	34.4	31.9	29.9
Pr	N.d.	N.d.	N.d.	N.d.	N.d.	0.590	0.580	0.610	N.d.	N.d.	N.d.	N.d.	N.d.	N.d.
Nd	4.82	5.32	5.16	4.390	2.120	3.830	3.620	3.990	16.14	5.2	24.4	25.8	19.4	16.3
Sm	1.76	1.54	1.71	1.610	1.200	1.750	1.620	1.790	5.66	2.47	5.93	6.67	4.74	3.97
Eu	0.58	0.74	0.69	0.600	0.470	0.790	0.760	0.810	2.33	1.06	1.75	2.05	1.62	1.84
Gd	2.58	0.74	0.69	N.d.	N.d.	2.860	2.570	2.900	7.22	3.72	5.1	6.73	4.29	3.74
Tb	N.d.	N.d.	N.d.	0.470	0.360	0.520	0.470	0.520	N.d.	N.d.	0.743	0.902	0.601	0.543
Dy	3.06	1.08	3.55	N.d.	N.d.	3.620	3.220	3.660	8.32	4.27	N.d.	N.d.	N.d.	N.d.
Ho	N.d.	N.d.	N.d.	N.d.	N.d.	0.750	0.670	0.760	N.d.	N.d.	N.d.	N.d.	N.d.	N.d.
Er	0.82	0.57	1.36	N.d.	N.d.	2.050	1.860	2.060	4.71	2.22	N.d.	N.d.	N.d.	N.d.
Tm	N.d.	N.d.	N.d.	N.d.	N.d.	0.290	0.260	0.290	N.d.	N.d.	0.339	0.373	0.3	0.264
Yb	1.86	0.73	1.9	1.810	1.570	1.810	1.650	1.810	4.53	2.07	2.15	2.2	1.8	1.56
Lu	0.04	0.13	0.24	0.310	0.230	0.280	0.260	0.280	N.d.	N.d.	0.291	0.291	0.251	0.224
Total	N.d.	N.d.	N.d.	N.d.	N.d.	23.1	21.6	23.4	N.d.	N.d.	N.d.	N.d.	N.d.	N.d.
$(La/Yb)_n$	0.52	2.28	0.71	0.57	0.47	0.35	0.41	0.32	0.42	0.17	5.68	4.30	5.63	5.93

(*Continued*)

Table 4.1 Continued

	Massifs													
	Mid-Atlantic ridge									Kerguelen Islands, Indian Ocean				Mid.-Atl. ridge
	(Simonov *et al.*, 1999), INAA									(Mattielli *et al.*, 1996)				(Dostal & Muecke, 1978)
Element	15-17/3	15-17/12	15-28/21	15-31/19	15-31/36	15-35/37	15-35/52	15-35/62	15-38/89	RC-835	92-406	91-116	92-419	21-1
La	0.9	2.2	0.8	0.3	0.6	7.3	29	19	5.2	0.5	1.01	0.34	2.08	0.18
Ce	2.7	7	2.1	1.2	1.5	21	67	44	12.6	1.05	1.72	0.79	5.62	N.d.
Pr	N.d.	N.d.	N.d.	N.d.	N.d.	N.d.	N.d.	N.d.	N.d.	0.16	0.29	0.1	1.05	N.d.
Nd	2.6	6	1.6	1.5	1.3	16	44	25	8.8	0.72	1.4	0.34	5.5	0.47
Sm	1.1	2.1	0.57	0.66	0.51	4.8	13	6.1	2.7	0.23	0.5	0.07	2.01	0.19
Eu	0.74	0.99	0.47	0.43	0.39	1.29	4.3	1.9	0.71	0.25	0.32	0.08	0.79	0.135
Gd	1.5	2.8	1	1.2	1	5.7	14	6	3.5	0.3	0.71	0.08	2.84	0.37
Tb	0.28	0.51	0.15	0.25	0.14	0.95	2.3	1.05	0.63	N.d.	N.d.	N.d.	N.d.	0.08
Dy	N.d.	N.d.	N.d.	N.d.	N.d.	N.d.	N.d.	N.d.	N.d.	0.36	0.89	0.07	3.34	N.d.
Ho	N.d.	N.d.	N.d.	N.d.	N.d.	N.d.	N.d.	N.d.	N.d.	0.08	0.19	0.02	0.69	N.d.
Er	N.d.	N.d.	N.d.	N.d.	N.d.	N.d.	N.d.	N.d.	N.d.	0.2	0.53	0.04	1.84	N.d.
Tm	N.d.	N.d.	N.d.	N.d.	N.d.	N.d.	N.d.	N.d.	N.d.	N.d.	N.d.	N.d.	N.d.	N.d.
Yb	0.96	1.8	0.78	0.75	0.78	3.1	5.1	3.9	2.4	0.19	0.51	0.04	1.74	0.52
Lu	0.14	0.27	0.12	0.11	0.12	0.46	0.69	0.58	0.35	N.d.	N.d.	N.d.	N.d.	0.083
Total	N.d.	N.d.	N.d.	N.d.	N.d.	N.d.	N.d.	N.d.	N.d.	4.04	8.07	1.97	27.5	N.d.
$(La/Yb)_n$	0.63	0.83	0.69	0.27	0.52	1.59	3.84	3.29	1.46	1.78	1.34	5.74	0.81	0.23

	Massifs													
	Mid-Atlantic ridge									Sept Iles, Canada				
	(Dostal & Muecke, 1978)				(Masuda & Jibiki, 1973)					(Higgins & Doig, 1986), NAA				
Element	23-1	24-1	24-3	24-4	20AM11	20AM30	20AM33	RD6AM8	D6AM11	H10b	H114	H11b	H151	H65
La	0.23	0.16	0.095	N.d.	0.341	0.464	0.906	1.35	0.927	23.60	3.800	17.90	28.30	21.70
Ce	N.d.	0.41	0.25	0.12	1.08	1.94	3.25	4.71	3.61	59.30	10.90	44.40	83.70	51.30
Pr	N.d.	N.d.	N.d.	N.d.	N.d.	N.d.	N.d.	N.d.	N.d.	N.d.	N.d.	N.d.	N.d.	N.d.
Nd	0.6	0.45	0.28	0.17	8.64	2.45	4.02	4.37	4.21	N.d.	N.d.	N.d.	N.d.	N.d.
Sm	0.23	0.18	0.11	0.099	0.919	1.09	1.89	1.7	1.89	12.30	2.310	7.830	11.300	5.610
Eu	0.17	0.12	0.068	0.07	0.4	0.592	1.08	1	1.04	2.650	1.590	2.980	3.210	2.580
Gd	0.45	0.31	0.23	0.2	1.64	1.82	3.11	2.58	3.08	N.d.	N.d.	N.d.	N.d.	N.d.
Tb	0.1	0.067	0.052	0.045	N.d.	N.d.	N.d.	N.d.	N.d.	1.830	N.d.	1.410	1.640	1.280
Dy	N.d.	N.d.	N.d.	N.d.	2.3	2.53	4.19	3.15	4.16	10.35	N.d.	N.d.	N.d.	6.910
Ho	N.d.	N.d.	N.d.	N.d.	N.d.	N.d.	N.d.	N.d.	N.d.	N.d.	N.d.	N.d.	N.d.	N.d.
Er	N.d.	N.d.	N.d.	N.d.	1.51	1.64	2.62	1.97	2.58	N.d.	N.d.	N.d.	N.d.	N.d.
Tm	N.d.	N.d.	N.d.	N.d.	N.d.	N.d.	N.d.	N.d.	N.d.	N.d.	N.d.	N.d.	N.d.	N.d.
Yb	0.675	0.43	0.34	0.3	1.48	1.59	2.42	1.71	2.46	5.750	0.720	2.950	3.960	2.810
Lu	0.1	0.068	0.053	0.048	0.22	0.239	0.351	0.252	0.383	0.690	0.220	N.d.	0.510	0.390
Total	N.d.	N.d.	N.d.	N.d.	18.5	14.4	23.8	22.8	24.3	N.d.	N.d.	N.d.	N.d.	N.d.
$(La/Yb)_n$	0.23	0.25	0.19	N.d.	0.16	0.20	0.25	0.53	0.25	2.77	3.56	4.10	4.82	5.21

(*Continued*)

Table 4.1 Continued

	Massifs													
	Sept Iles, Canada			Japan	Ural, Russia	Tuva, Russia, INAA		Kurtushibinsky, Russia		Dugdinsky, Russia		Mongolia	Kamchatka, Russia	
	(Higgins & Doig, 1986), NAA			(Itoh *et al.*, 1993)	(Fershtater *et al.*, 1998)	(Lesnov *et al.*, 2001)	(Pfander *et al.*, 2001)	(Dobretsov *et al.*, 1985), INAA		Mekhonoshin *et al.*, 1986), INAA		(Izokh *et al.*, 1998)	(Bekhtold *et al.*, 1986), NAA	
Element	H72	H8b	H93	JGb-1	F4	Ma30-4	T97A55	80091	9064	Mekh-5	Mekh-6	I-2798	800b	805a
La	12.60	29.10	28.30	3.740	1.720	1.300	0.64	1.2	5.2	2.3	2.4	1.4	1.620	1.630
Ce	30.00	61.30	74.20	7.860	3.200	4.200	0.65	0.1	16.1	9.1	6.8	3.2	3.540	4.520
Pr	N.d.	N.d.	N.d.	1.140	0.580	N.d.	0.07	N.d.	2.5	N.d.	N.d.	N.d.	N.d.	N.d.
Nd	N.d.	N.d.	N.d.	5.650	2.940	4.100	0.5	1.3	10.5	13.5	7.1	2	N.d.	N.d.
Sm	5.110	7.230	7.600	1.490	0.970	1.310	0.2	0.75	3.3	3.7	3.2	0.7	1.600	2.420
Eu	1.730	3.420	2.990	0.630	0.340	0.480	0.09	0.27	0.8	1.18	1.03	0.46	0.950	N.d.
Gd	N.d.	N.d.	N.d.	1.630	1.030	1.600	0.28	N.d.	3.3	N.d.	N.d.	0.9	N.d.	N.d.
Tb	0.690	0.960	1.300	0.310	0.160	0.200	N.d.	N.d.	N.d.	0.48	0.37	0.15	N.d.	N.d.
Dy	3.370	N.d.	N.d.	1.530	0.930	N.d.	N.d.	N.d.	4.3	N.d.	N.d.	N.d.	N.d.	N.d.
Ho	N.d.	N.d.	N.d.	0.320	0.180	N.d.	0.08	N.d.	0.67	N.d.	N.d.	N.d.	N.d.	N.d.
Er	N.d.	N.d.	N.d.	1.070	0.460	N.d.	N.d.	N.d.	2.8	N.d.	N.d.	N.d.	N.d.	N.d.
Tm	N.d.	N.d.	N.d.	0.150	N.d.	0.120	N.d.	N.d.	N.d.	N.d.	N.d.	N.d.	N.d.	N.d.
Yb	1.480	2.250	2.700	0.970	0.460	0.680	0.19	0.6	0.23	0.95	0.76	0.71	1.910	3.790
Lu	0.390	0.350	0.370	0.150	0.040	0.100	0.03	N.d.	0.28	N.d.	N.d.	0.11	N.d.	N.d.
Total	N.d.	N.d.	N.d.	26.6	13.0	N.d.	N.d.	N.d.	N.d.	N.d.	N.d.	N.d.	N.d.	N.d.
$(La/Yb)_n$	5.75	8.73	7.08	2.60	2.52	1.29	21.7	1.35	15.3	1.63	1.63	1.33	0.57	0.29

	Massifs													
	Zapevalikhinsky, Russia		Zaoblachny, Russia		Gornaya Shoria, Russia			Patinsky, Russia				Chernosopkinsky, Russia		
	(Izokh *et al.*, 1998), INAA				(Babin, 2003), INAA							(Lavrenchuk, 2003), INAA		
Element	B6681	B6728	B3561	B3738-1	6055	6085/1	93-9/1	5470/2	5471a	5472/1	605	I-11-00	00A-24	I-6-00
La	4.9	3.3	6.3	1.1	0.33	1.52	14	3.77	2.25	2.85	35	47.4	39.8	47.3
Ce	12	10	16	2.5	0.77	2.51	28	7.5	5.4	6.6	67	104.5	85	101
Pr	N.d.	N.d.	N.d.	N.d.	0.1	0.4	N.d.	1.56	1.2	1.48	N.d.	12.95	10.6	11.3
Nd	7.9	8	10	1.6	0.36	0.87	14	8.1	7.6	8.4	25	49.0	39.0	47.0
Sm	2.3	2.7	2.9	0.47	0.05	0.26	4.0	2.9	2.6	2.53	4.1	9.15	7.6	9.85
Eu	0.8	0.96	0.94	0.27	0.18	0.11	1.75	1.23	1.02	1.04	0.85	2.74	2.24	3.10
Gd	2.5	3.2	3.1	0.5	0.1	0.29	2.35	2.71	2.4	2.69	3.3	7.9	6.1	7.7
Tb	0.42	0.55	0.53	0.2	0.01	0.06	0.62	0.5	0.48	0.47	N.d.	1.12	0.92	1.18
Dy	N.d.	N.d.	N.d.	N.d.	0.11	0.68	3.0	3.29	3.13	3.24	N.d.	6.1	4.55	5.5
Ho	N.d.	N.d.	N.d.	N.d.	N.d.	0.1	N.d.	0.83	0.68	0.8	N.d.	1.1	0.9	1.05
Er	N.d.	N.d.	N.d.	N.d.	0.06	0.34	N.d.	1.99	1.64	1.94	N.d.	3.4	2.55	3.15
Tm	N.d.	N.d.	N.d.	N.d.	0.01	0.04	N.d.	0.34	0.26	0.3	N.d.	0.5	0.4	0.5
Yb	1.13	1.7	1.6	0.33	0.04	0.31	1.15	1.88	1.34	1.72	1.72	3.20	2.35	2.8
Lu	0.16	0.26	0.23	0.05	0.01	0.05	0.23	0.24	0.21	0.23	0.26	0.46	0.36	0.44
Total	N.d.	N.d.	N.d.	N.d.	2.13	7.54	N.d.	36.8	30.2	34.3	N.d.	250	202	242
$(La/Yb)_n$	2.93	1.31	2.66	2.25	5.57	3.31	8.22	1.35	1.13	1.12	13.7	227	236	230

(*Continued*)

Table 4.1 Continued

	Massifs											
	Mallina, Australia					Veselkinsky, Russia				Kenguraksky, Russia		
	(Smithies *et al.*, 2004)					(Buchko *et al.*, 2007), ICP-MS				(Buchko *et al.*, 2006), ICP-MS		
Element	Mall-16	Mall-17	Mall-18	Mall-19	Mall-20	I-420	I-421	I-431	I-433	Ke-68	69/40	69/24
La	10.9	11.7	10.1	8.7	12.6	49.31	46.71	13.29	5.02	6.84	7.08	8.18
Ce	20.4	22.4	20.2	17.5	24.6	101.9	132.8	34.4	10.63	21.31	17.14	16.84
Pr	2.4	2.6	2.4	2	2.8	10.07	15.71	4.25	1.53	3	2.03	2.13
Nd	9.8	10.5	9.5	8.1	11	44.12	79.17	24.71	7.14	13.38	8.66	8.97
Sm	2.2	2.3	2	1.8	2.3	6.65	13.28	5.4	1.67	3.17	1.91	1.83
Eu	0.7	0.7	0.6	0.58	0.72	1.85	3.25	1.83	0.68	1.15	1.23	1.13
Gd	2.6	2.7	2.3	2.14	3.71	4.24	8.37	4.53	1.6	3.54	1.8	1.77
Tb	0.4	0.4	0.4	0.37	0.44	0.49	0.95	0.59	0.21	0.59	0.28	0.31
Dy	2.5	2.8	2.3	2.28	2.93	2.41	4.51	3.31	1.16	3.18	1.46	1.53
Ho	0.5	0.6	0.5	0.53	0.63	0.38	0.73	0.56	0.21	0.63	0.32	0.32
Er	1.6	1.7	1.5	1.47	1.73	0.95	1.82	1.4	0.54	1.69	0.74	0.82
Tm	N.d.	N.d.	N.d.	0.23	0.27	0.11	0.22	0.18	0.07	0.26	0.14	0.16
Yb	1.6	1.7	1.5	1.65	1.9	0.77	1.28	0.99	0.46	1.38	0.77	0.66
Lu	0.2	0.2	0.2	0.24	0.28	0.1	0.16	0.13	0.06	0.22	0.11	0.13
Total	55.8	60.3	53.5	47.6	65.9	223	309	95.6	31.0	60.3	43.7	44.8
$(La/Yb)_n$	4.60	4.65	4.54	3.56	4.48	43.2	24.6	9.06	7.37	3.35	6.21	8.37

	Massifs											
	Annieopsquotch, Canada											
	(Lissenberg *et al.*, 2004), ICP-MS											
Element	A196	A480	A933	A1228	A1352	A1628	A1737	A1795	A1795a	A2050	A2059	A2256
La	0.18	0.36	0.38	0.51	1.14	0.37	0.27	0.75	0.65	0.76	0.41	1.75
Ce	0.55	1.27	1.36	1.83	4.01	1.34	0.87	2.64	2.08	2.53	1.37	5.74
Pr	0.12	0.28	0.29	0.42	0.8	0.29	0.19	0.51	0.41	0.49	0.29	1.06
Nd	0.87	1.97	1.87	2.42	4.76	1.84	1.24	2.84	2.35	3.04	1.74	6.26
Sm	0.43	0.84	0.93	1.14	1.77	0.83	0.58	1.25	1.11	1.2	0.84	2.45
Eu	0.26	0.47	0.54	0.57	0.78	0.41	0.46	0.58	0.55	0.64	0.42	0.97
Gd	0.73	1.49	1.61	1.97	2.82	1.39	1.01	1.9	1.81	1.8	1.23	3.78
Tb	0.16	0.29	0.29	0.37	0.54	0.26	0.19	0.38	0.37	0.34	0.25	0.7
Dy	1.02	2.02	2.01	2.45	3.38	1.74	1.38	2.44	2.29	2.34	1.63	4.56
Ho	0.22	0.43	0.48	0.55	0.76	0.4	0.31	0.55	0.53	0.55	0.35	1.02
Er	0.65	1.26	1.38	1.58	2.25	1.08	0.94	1.63	1.5	1.68	1	2.89
Tm	0.1	0.2	0.21	0.25	0.33	0.16	0.14	0.25	0.24	0.22	0.15	0.44
Yb	0.55	1.23	1.26	1.49	2.04	1.08	0.76	1.45	1.35	1.49	0.95	2.78
Lu	0.09	0.19	0.2	0.21	0.34	0.16	0.12	0.25	0.22	0.23	0.15	0.45
Total	5.93	12.3	12.81	15.76	25.72	11.35	8.46	17.42	15.46	17.31	10.78	34.85
$(La/Yb)_n$	0.22	0.20	0.20	0.23	0.38	0.23	0.24	0.35	0.32	0.34	0.29	0.42

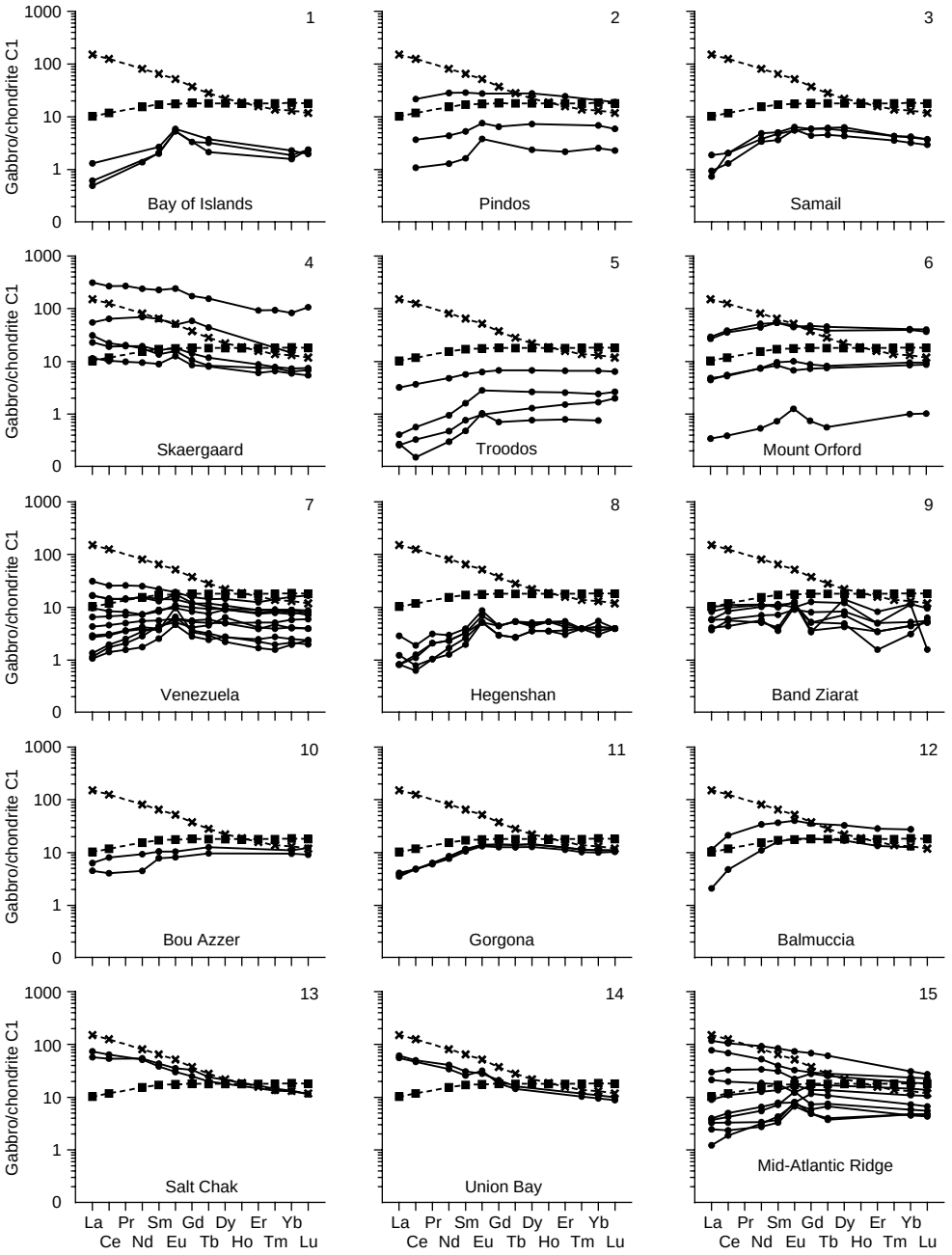

Figure 4.1 Chondrite-normalized REE patterns for gabbros from some massifs (data Table 4.1).

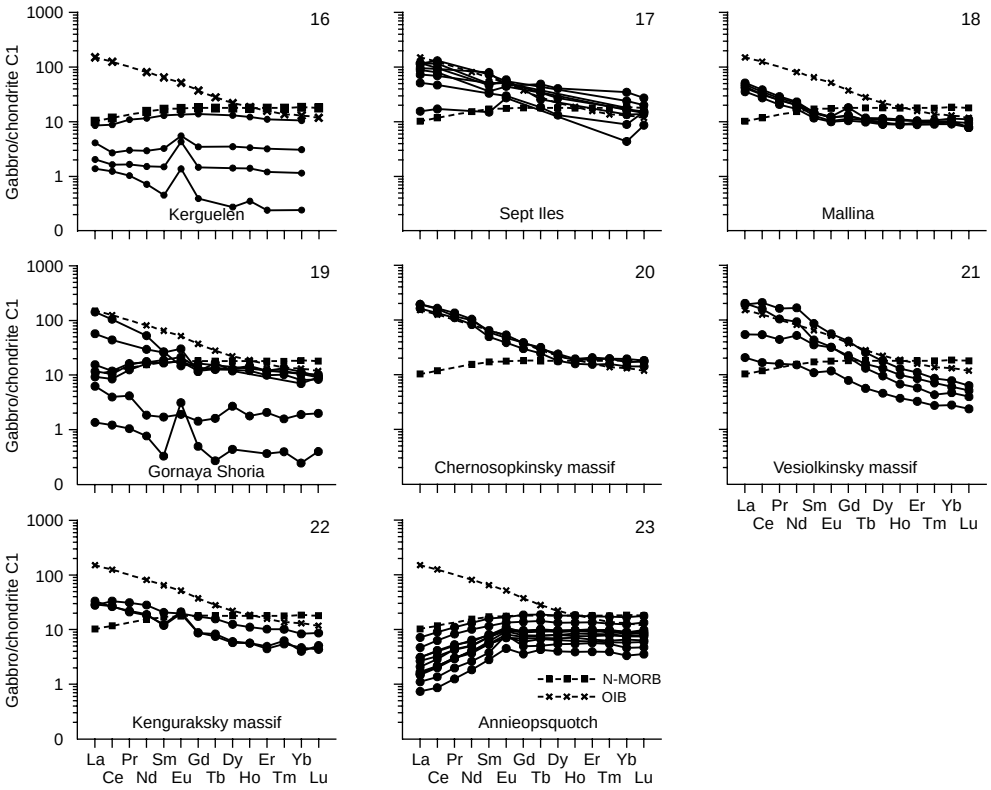

Figure 4.1 Continued

Mallina province (48–66), Dugdinsky (22–31), Zapevalikhinsky (31–32), Patynsky (30–137), Chernosopkinsky (180–250), Veselkinsky (31–309), and Kenguraksky (44–60) massifs. Differences in the REE composition of gabbros from separate massifs and their types are easily visible when comparing average REE content (Table 4.2, Fig. 4.2).

Concluding our consideration of REE distribution features in gabbros, it should be noted that when Coleman (1979) described gabbros of various types from mafic–ultramafic massifs entering into ophiolite associations, he distinguished their two geochemical types: (1) basic cumulates, or "bottom" gabbros, which are more-depleted of REE; and (2) "top" gabbros, represented by REE-enriched varieties (see Table 4.3, Fig. 4.3).

* * *

The observable variations in REE composition of gabbros from massifs, differing in composition and genesis, as well as differences in REE patterns in the limits of each gabbro occurrence, are directly connected with the inhomogeneity of the chemical and modal composition of the rocks. This inhomogeneity is seen first of all with differences in the modal quantities of plagioclase and clinopyroxene, since the overwhelming

Table 4.2 Average REE composition (x) and standard deviation (σ) of gabbros from some massifs (ppm).

	Massifs									
	Chernosopskinsky (3)		Sept Iles (8)		Mallina (5)		Mount Orford (5)		Skaergaard (5)	
Element	x	σ	x	σ	x	σ	x	σ	x	σ
La	44.8	4.36	20.7	8.90	10.8	1.50	3.22	3.36	21.2	31.2
Ce	96.8	10.4	51.9	23.5	21.0	2.65	10.8	11.7	48.9	69.5
Pr	11.6	1.21	N.d.	N.d.	2.44	0.30	N.d.	N.d.	7.70	12.2
Nd	45.0	5.29	N.d.	N.d.	9.78	1.11	10.5	11.3	33.6	45.8
Sm	8.87	1.15	7.41	3.25	2.12	0.22	3.92	4.08	10.2	14.3
Eu	2.69	0.43	2.64	0.67	0.66	0.06	1.29	1.30	3.92	5.70
Gd	7.23	0.99	N.d.	N.d.	2.69	0.61	4.37	4.48	10.9	14.4
Tb	1.07	0.14	1.30	0.39	0.40	0.02	0.75	0.76	1.70	2.36
Dy	5.38	0.78	6.88	3.49	2.56	0.29	N.d.	N.d.	N.d.	N.d.
Ho	1.02	0.10	N.d.	N.d.	0.55	0.06	N.d.	N.d.	1.84	2.49
Er	3.03	0.44	N.d.	N.d.	1.60	0.12	N.d.	N.d.	4.78	7.08
Tm	0.47	0.06	N.d.	N.d.	0.25	0.03	N.d.	N.d.	0.74	1.11
Yb	2.78	0.43	2.83	1.53	1.67	0.15	3.30	3.13	3.87	5.53
Lu	0.42	0.05	0.42	0.15	0.22	0.04	0.49	0.45	0.80	1.27
Total	231	25.7	94.0	N.d.	56.6	6.92	38.7	N.d.	33.8	10.6
$(La/Yb)_n$	231	4.58	5.25	1.94	4.37	0.46	0.55	0.15	3.49	1.06

	Gorgona (3)		Gornaya Shoria (7)		Pindos (3)		Mid-Atlantic ridge (19)		Venezuela (11)	
Element	x	σ	x	σ	x	σ	x	σ	x	σ
La	0.93	0.07	8.53	12.53	N.d.	N.d.	3.89	7.75	2.08	2.30
Ce	3.08	0.02	16.83	23.90	5.61	7.14	10.3	18.3	4.95	4.85
Pr	0.59	0.02	0.95	0.66	N.d.	N.d.	N.d.	N.d.	0.77	0.72
Nd	3.81	0.19	9.19	8.41	5.36	7.00	6.97	10.9	3.97	3.45
Sm	1.72	0.09	2.35	1.62	1.83	2.26	2.10	3.09	1.27	0.92
Eu	0.79	0.03	0.88	0.58	0.75	0.74	0.84	0.97	0.58	0.29
Gd	2.78	0.18	1.98	1.26	1.32	N.d.	2.66	3.24	1.53	0.88
Tb	0.50	0.03	0.36	0.26	N.d.	N.d.	0.47	0.62	0.26	0.15
Dy	3.50	0.24	2.24	1.45	3.17	3.42	3.27	0.89	1.77	0.99
Ho	0.73	0.05	0.60	0.34	N.d.	N.d.	N.d.	N.d.	0.38	0.23
Er	1.99	0.11	1.19	0.92	2.21	2.61	2.06	0.52	0.98	0.57
Tm	0.28	0.02	0.19	0.15	N.d.	N.d.	N.d.	N.d.	0.16	0.10
Yb	1.76	0.09	1.17	0.73	0.78	0.50	1.66	1.31	1.04	0.68
Lu	0.27	0.01	0.18	0.10	0.23	0.22	0.24	0.18	0.16	0.11
Total	22.7	0.96	22.2	16.13	21.3	N.d.	20.8	4.23	19.9	15.93
$(La/Yb)_n$	0.36	0.05	4.91	4.70	N.d.	N.d.	0.86	1.07	1.14	0.70

Table 4.2 Continued

	Massifs											
	Band Ziarat (6)		Kerguelen (4)		Samail (3)		Hegenshan (5)		Troodos (4)		Bay of Islands (3)	
Element	*x*	σ	*x*	σ	*x*	σ	*x*	σ	*x*	σ	*x*	σ
La	1.54	0.60	0.98	0.79	0.29	0.15	0.32	0.22	0.25	0.35	0.20	0.11
Ce	4.78	1.65	2.30	2.25	1.14	0.27	0.72	0.31	0.75	1.07	N.d.	N.d.
Pr	N.d.	N.d.	0.40	0.44	N.d.	N.d.	0.18	0.08	N.d.	N.d.	N.d.	N.d.
Nd	3.96	1.30	1.99	2.38	1.90	0.36	1.00	0.31	0.77	1.01	0.65	N.d.
Sm	1.22	0.54	0.70	0.89	0.69	0.12	0.46	0.11	0.33	0.37	0.35	0.06
Eu	0.63	0.08	0.36	0.30	0.34	0.03	0.36	0.09	0.16	0.14	0.32	0.02
Gd	1.29	0.71	0.98	1.27	1.10	0.17	0.78	0.16	0.76	0.87	0.68	N.d.
Tb	N.d.	N.d.	N.d.	N.d.	0.21	0.03	0.16	0.05	N.d.	N.d.	0.11	0.03
Dy	2.14	0.99	1.17	1.49	1.37	0.25	1.08	0.18	0.73	0.69	N.d.	N.d.
Ho	N.d.	N.d.	0.25	0.30	N.d.	N.d.	0.26	0.05	N.d.	N.d.	N.d.	N.d.
Er	0.74	0.37	0.65	0.82	N.d.	N.d.	0.70	0.16	0.48	0.43	N.d.	N.d.
Tm	N.d.	N.d.	N.d.	N.d.	0.10	0.01	0.10	N.d.	N.d.	N.d.	N.d.	N.d.
Yb	1.10	0.62	0.62	0.77	0.63	0.09	0.68	0.15	0.47	0.43	0.32	0.06
Lu	0.14	0.06	N.d.	N.d.	0.09	0.01	0.10	N.d.	0.09	0.06	0.06	0.01
Total	17.5	N.d.	10.4	11.7	7.86	N.d.	6.90	1.75	4.80	N.d.	2.68	N.d.
$(La/Yb)_n$	1.12	0.62	2.42	2.25	0.31	0.14	0.30	0.14	0.29	0.16	0.40	0.14

	Vesiolkinsky (4)		Kenguraksky (3)		Annieopsquotch (12)	
Element	*x*	σ	*x*	σ	*x*	σ
La	28.6	22.7	7.37	0.71	0.63	0.44
Ce	69.9	57.0	18.4	2.50	2.13	1.47
Pr	7.89	6.31	2.39	0.53	0.43	0.27
Nd	38.8	30.9	10.3	2.64	2.60	1.52
Sm	6.75	4.84	2.30	0.75	1.11	0.54
Eu	1.90	1.05	1.17	0.05	0.55	0.18
Gd	4.69	2.79	2.37	1.01	1.80	0.82
Tb	0.56	0.31	0.39	0.17	0.35	0.15
Dy	2.85	1.42	2.06	0.97	2.27	0.94
Ho	0.47	0.22	0.42	0.18	0.51	0.21
Er	1.18	0.55	1.08	0.53	1.49	0.61
Tm	0.15	0.07	0.19	0.06	0.22	0.09
Yb	0.88	0.35	0.94	0.39	1.37	0.59
Lu	0.11	0.04	0.15	0.06	0.22	0.10
Total	165	125	49.6	9.32	15.7	7.88
$(La/Yb)_n$	22.0	16.7	5.31	2.52	0.46	0.08

Data Table 4.1.

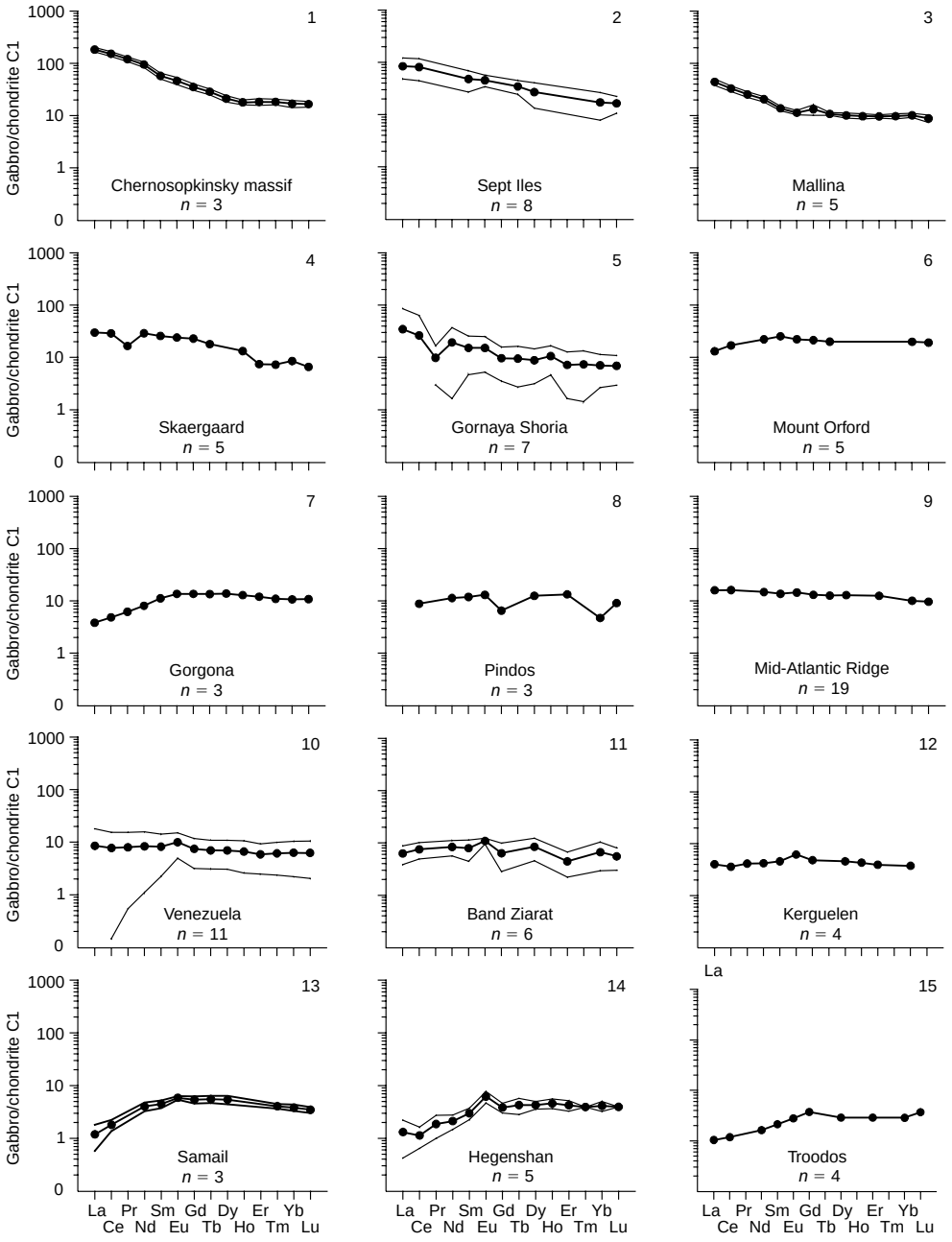

Figure 4.2 Chondrite-normalized patterns of average REE composition of gabbros (data Table 4.2). Narrow lines mark limits of REE content variations on basis of standard deviations.

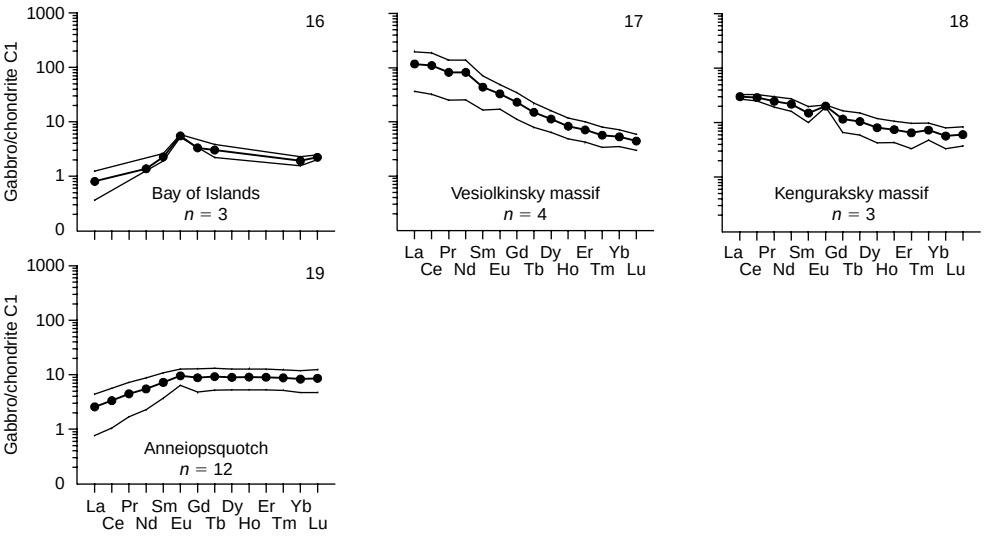

Figure 4.2 Continued

Table 4.3 Average REE composition of gabbros from ophiolite mafic–ultramafic massifs (ppm).

	Elements															
Rock	La	Ce	Pr	Nd	Sm	Eu	Gd	Tb	Dy	Ho	Er	Tm	Yb	Lu	Total	$(La/Yb)_n$
"Lower" gabbros	0.443	1.68	N.d.	1.6	0.644	0.323	1.38	N.d.	1.41	N.d.	0.763	N.d.	0.74	0.126	9.11	0.40
"Upper" gabbros	0.065	0.316	N.d.	0.384	0.173	0.119	0.297	N.d.	0.424	N.d.	0.275	N.d.	0.306	0.053	2.41	0.14

Data Coleman (1979).

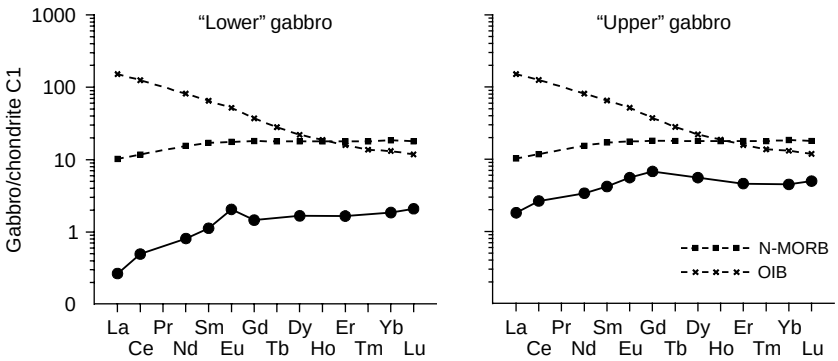

Figure 4.3 Chondrite-normalized patterns of average REE composition of gabbros from ophiolite associations (data Table 4.3).

amount of medium and heavy REE, and a lesser amount of light REE, is usually concentrated in only the clinopyroxene structure. In its turn, a characteristic feature of plagioclase structure is its ability to concentrate an essential amount of light REE, especially Eu. In addition, some quantities of REE usually enter into the compositions of minor minerals (amphibole) and accessories (apatite, zircon, and sphene). Those gabbro varieties, which are characterized by unusually high light REE contents, are most likely to contain the REE as non-structural impurities concentrated in various quantities in microcracks of the rocks and in fluid inclusions. The presence of such impurities distorts the information on original rare earth composition of the rocks.

To consider the reasons for the wide variation in rare earth composition of gabbros from a position of the model of partial melting of mantle sources, which was accompanied by generation of the parent melts, it is possible to make the following assumption. Apparently, those gabbro varieties that are considerably depleted of REE and usually occur in massifs from ophiolite associations were crystallized from mantle melts that originated at increased extents of protoliths melting. The gabbro varieties that are more essentially enriched with light REE, apparently, crystallized from mantle melts that originated at lowered extents of partial melting of mantle protoliths. Changes in the intensity of the positive Eu anomalies observed in spectra of many gabbroid samples from ophiolite associations are obviously caused by variously scaled fractionation of plagioclase crystals that resulted in changes in the modal proportions of plagioclase and coexisting clinopyroxene in the rocks.

4.2 GABBRO-NORITES

Gabbro-norites are a somewhat less widespread variety of plutonic mafic rocks of orthomagmatic type than gabbros, together with which they usually compose many mafic–ultramafic massifs located in folded areas, including massifs that are related to ophiolite associations. In the study of many such complexes, evidence of intrusive relationships of gabbros and gabbro-norites with closely spaced protrusions of ultramafites (Lesnov, 1984, 1986) was obtained.

Gabbro-norites consist of three main minerals, modal amounts of which in different massifs vary over a wide range: orthopyroxene (5–60%), plagioclase (35–65%), and clinopyroxene (5–60%). Sometimes the rocks contain olivine, amphibole, and in rare cases garnet, as minor phases. Accessory minerals of gabbro-norites are represented by apatite, zircon, sphene (titanite), sulphide phases, magnetite, titanomagnetite, and ilmenite. Most gabbro-norites are medium-grained and have an equigranular texture and a massive structure. Sometimes trachytoid signs are observed in them. Contents of the major chemical components in gabbro-norites vary within the following limits (wt%): SiO_2 (43–52), Al_2O_3 (12–19), CaO (5–14), FeO_{tot} (3.5–18), MgO (4.5–12), Na_2O (1.5–2.5), and K_2O (0.1–1.0). As with gabbro, these rocks are characterized by rather narrow ranges of some petrochemical parameters: CaO/Al_2O_3 (0.6–0.8), MgO/CaO (0.7–1), and Al_2O_3/MgO (1.8–2.4). The parameter $100 \cdot FeO_{tot}/(FeO_{tot} + MgO)$ varies from 46 to 52 (Lesnov, 1986).

Before consideration of the major peculiarities of REE distribution in gabbro-norites, we shall note that some aspects of this question in a more brief form were discussed in one of our recent publications (Lesnov, 2005a). To study the regularities

of distribution of REE in gabbro-norites, the dataset of analyses of these rocks from massifs located in Sakhalin Island, Transbaikalia, Tuva, Mongolia, Urals, Alaska, and other regions (Table 4.4) were used. Within the dataset, the total REE content varied from 0.46 to 88 ppm, averaging about 25 ppm. This geochemical parameter in gabbro-norites is almost twice as less than in basalts of the N-MORB type. The level of accumulation of light REE in the majority of the studied gabbro-norites does not fall outside the range of 1–10 t. ch., and the level of accumulation of heavy REE is 2–10 t. ch. (Fig. 4.4). Gabbro-norites from massifs related to ophiolite associations, for example, those from the Berezovsky (Sakhalin Island), Naransky (Mongolia), and Karashatsky (Tuva) massifs, are comparable in their rare earth composition to so-called "bottom" gabbros (basic cumulates) as recognized by Coleman (1979) (see Section 4.1).

Because of the relative enrichment with light REE, the rare earth spectra of some gabbro-norites have a general negative slope. Values of parameter $(La/Yb)_n$ range from 1.2 to 5.6. In other groups of samples, values of this parameter are less (from 0.2 to 1.0), and their spectra have a gentle positive slope. Gabbro-norites from massifs that are not related to ophiolite associations (Dovyrensky, Chaysky, Niurundukansky, Irokinda, Zapevalikhinsky, Rybinsk, Ostiurensky, Burakovsky, Salt Chak, Union Bay, Stillwater) are comparable to N-MORBs in total level of REE content, as well as in patterns of average contents of REE. Gabbro-norites that are part of massifs that enter into ophiolite associations are characterized, as a whole, by lower rare earth concentrations, that is well visible, for example, when comparing average REE content and total REE content (Table 4.5). From the spectra of average REE content on schedules, it is possible to conclude that gabbro-norites from ophiolite massifs (Berezovsky, Naransky, Karashatsky) have considerably lower REE contents than N-MORBs and differ from them by the presence of positive Eu anomalies (Fig. 4.5).

* * *

The level of accumulation and character of distribution of REE in gabbro-norites are connected to their bulk composition, as well as to the crystallization conditions of parent melts, and, as a consequence, to the modal composition of the rocks. The main concentrators of REE in these rocks are clinopyroxene and plagioclase. Orthopyroxene, amphiboles, as well as accessory apatite, sphene and zircon are minor contributors to the overall balance of REE in gabbro-norites. Most the gabbro-norites demonstrate rather moderate fractionation of REE, and in samples from ophiolite massifs there is usually an insignificant excess of Eu. Enrichment of some gabbro-norites with light REE and a corresponding negative slope in the REE spectra can be caused by the fact that their parent melts were generated at rather low extents of partial melting of undepleted mantle protoliths. The marked anomalously higher La contents in some samples of gabbro-norites from the Naransky and Berezovsky massifs is supposed to be connected to the presence of variable amounts of non-structural impurities concentrated in microcracks of mineral grains.

4.3 NORITES

Norites occur much less often in composition of mafic–ultramafic massifs than gabbros and gabbro-norites, to which they are spatially and genetically connected.

Table 4.4 Rare earth element composition of gabbro-norites (ppm).

	Massif													
	Alaska, USA		Stillwater, USA					Dovyrensky, Russia					Irokinda, Russia	
	(Himmelberg & Loney, 1995)		(Helz, 1985), INAA					(Amelin *et al.*, 1996)	(Kislov, 1998)				(Tsigankov & Konnikov 1995), INAA	
Element	80B149	87GH28	NB1/286	NB18/378	370-316	386/5032	373-322	D2	Do104/4	Do110/6	245/85	213a/85	Ir-22	Ir-24/2
La	3.22	5.58	1.28	11	6	7	9.1	12.85	17	10	18	6.7	5.6	12
Ce	7.87	12	8	22	13	16	20.8	26.69	43	32	47	13	12.6	25
Pr	N.d.	N.d.	N.d.	N.d.	N.d.	N.d.	N.d.	N.d.	2	2	5.3	1.3	N.d.	N.d.
Nd	8.02	8.17	8.9	17	8	14	13	12.78	N.d.	N.d.	N.d.	N.d.	4.8	10
Sm	2.53	2.44	1.29	3.7	3.2	3.6	3.4	2.675	2.8	2.4	2.5	1.7	1.3	2.4
Eu	0.958	1.05	0.58	1.1	1.21	1.23	1.27	0.802	1	1.1	1.1	0.5	0.85	1.1
Gd	3.26	2.51	N.d.	3.4	3.9	2.5	N.d.	2.656	4.3	3.9	4.5	1.6	3.4	N.d.
Tb	0.556	0.388	0.29	0.5	0.75	0.7	0.7	N.d.	N.d.	N.d.	N.d.	N.d.	N.d.	N.d.
Dy	N.d.	N.d.	N.d.	N.d.	N.d.	N.d.	N.d.	2.784	3.6	3.2	4.3	1.8	3.1	N.d.
Ho	N.d.	N.d.	0.4	N.d.	N.d.	0.8	N.d.	N.d.	N.d.	N.d.	N.d.	N.d.	0.47	N.d.
Er	N.d.	N.d.	N.d.	N.d.	N.d.	N.d.	N.d.	1.706	1.9	2.2	2	1.4	0.47	1.2
Tm	0.308	0.228	N.d.	N.d.	0.4	0.42	0.38	N.d.	N.d.	N.d.	N.d.	N.d.	N.d.	N.d.
Yb	1.82	1.39	1.29	1.6	2.7	2.7	2.86	1.591	2.6	2.2	2.7	1.1	1.4	1.5
Lu	0.257	0.209	0.2	0.24	0.4	0.44	0.44	N.d.	0.39	0.35	0.38	0.35	0.2	0.17
Total	N.d.	N.d.	N.d.	N.d.	N.d.	N.d.	N.d.	64.5	N.d.	N.d.	N.d.	N.d.	N.d.	N.d.
$(La/Yb)_n$	1.19	2.71	0.67	4.64	1.50	1.75	2.15	5.45	4.41	3.07	4.50	4.11	2.70	5.40

	Massif													
	Chaysky, Russia					Niurundukan, Russia			Zapevalikh., Rus.	Lukinda, Rus.	Rybin. Rus.	Ostiur., Rus.	Maysk., Rus.	Kalbagdag., Ru.
	(Amelin *et al.*, 1997), IDMS				(Data Konnikov)	(Tsigankov *et al.*, 2002), INAA			(Izokh *et al.*, 1998)	(Data Krivenko)	(Author's data), INAA		(Lesnov & Oydup, 2002), INAA	
Element	7MH	Ch-4	Ch-14	Ch-16	Chay-2	Nr-14/2	Nr-21/21	Nr-20/99	B-6681	B-1456	88	429	2150	Kal-12-4
La	3.7	0.794	1.24	1.28	3.7	1.4	4.8	5.9	4.9	0.96	10.7	8	5	0.7
Ce	6.8	2.44	3.05	4.85	6.8	2.6	11	13	12	4.5	18.5	19	10.6	1.2
Pr	N.d.	N.d.	N.d.	N.d.	N.d.	N.d.	N.d.	N.d.	N.d.	N.d.	N.d.	N.d.	N.d.	N.d.
Nd	4.3	2.48	2.3	5.26	4.3	2.1	8.4	8.6	7.9	3.9	8.7	11.5	6.6	0.9
Sm	1.5	0.83	0.674	1.77	1.5	0.64	2.7	2.2	2.3	1.1	2.3	2.6	1.85	0.34
Eu	0.4	0.313	N.d.	0.587	0.4	0.58	0.92	1.15	0.8	0.8	1	1.6	0.84	0.19
Gd	1.7	1.05	0.805	2.2	1.7	N.d.	N.d.	2.5	2.5	0.92	N.d.	N.d.	1.6	0.4
Tb	N.d.	N.d.	N.d.	N.d.	N.d.	0.14	0.49	N.d.	0.42	0.2	0.32	0.36	0.29	0.06
Dy	1.7	1.2	0.87	2.37	1.7	N.d.	N.d.	2.2	N.d.	N.d.	N.d.	N.d.	N.d.	N.d.
Ho	N.d.	N.d.	N.d.	N.d.	N.d.	N.d.	N.d.	0.38	N.d.	N.d.	N.d.	N.d.	N.d.	N.d.
Er	0.8	0.735	0.518	1.35	0.8	N.d.	N.d.	1.2	N.d.	N.d.	N.d.	N.d.	N.d.	N.d.
Tm	N.d.	N.d.	N.d.	N.d.	N.d.	N.d.	N.d.	N.d.	N.d.	0.13	N.d.	N.d.	0.18	0.04
Yb	0.8	0.69	0.478	1.16	0.8	0.49	1.3	1	1.13	0.64	1.3	1.15	1.14	0.32
Lu	0.1	N.d.	N.d.	N.d.	0.1	0.08	0.22	0.18	0.16	0.09	0.2	0.26	0.17	0.06
Total	21.8	10.5	10.3	20.8	21.8	N.d.	N.d.	N.d.	N.d.	N.d.	N.d.	N.d.	N.d.	N.d.
$(La/Yb)_n$	3.12	0.78	1.75	0.75	3.12	1.93	2.49	3.98	2.93	1.01	5.56	4.70	2.96	1.48

(*Continued*)

Table 4.4 Continued

	Massifs													
	Karaoss., Ru	Karashatsky, Russia		Naransky, Mongolia		Bayantsagan.	Nomgon.	Burakovsky	Beriozovsky, Russia					
	(Lesnov & Oydup, 2002), INAA					(Izokh *et al.*, 1998), INAA		(Chistyakov *et al.*, 1997)	(Lesnov *et al.*, 1998a), INAA					
Element	M-36-98	L-44	L-45	269	278	I-2798	I-4674	28a/218	131	132a	138a	141	144	147
La	1.6	0.3	0.2	N.d.	0.48	1.4	0.7	17	0.28	0.2	0.3	0.21	0.3	0.28
Ce	5	0.9	0.6	0.42	0.6	3.2	1.8	25	0.8	1.6	1.5	1.1	1.7	3
Pr	N.d.	N.d.	N.d.	N.d.	N.d.	N.d.	N.d.	N.d.	N.d.	N.d.	N.d.	N.d.	N.d.	N.d.
Nd	4.5	0.6	0.7	0.28	0.3	2	1.2	12	1.2	N.d.	N.d.	1.2	N.d.	N.d.
Sm	1.34	0.25	0.3	0.1	0.13	0.7	0.4	2.5	0.12	0.05	0.067	0.076	0.17	0.103
Eu	0.47	0.24	0.14	0.1	0.1	0.46	0.21	0.96	0.076	0.039	0.038	0.053	0.18	0.05
Gd	1.6	0.43	0.67	0.24	0.27	0.9	0.5	N.d.	N.d.	N.d.	N.d.	N.d.	N.d.	N.d.
Tb	0.21	0.08	0.1	0.042	0.05	0.15	0.09	0.42	0.034	N.d.	N.d.	0.1	N.d.	N.d.
Dy	N.d.	N.d.	N.d.	N.d.	N.d.	N.d.	N.d.	N.d.	N.d.	N.d.	N.d.	N.d.	N.d.	N.d.
Ho	N.d.	N.d.	N.d.	N.d.	N.d.	N.d.	N.d.	N.d.	N.d.	N.d.	N.d.	N.d.	N.d.	N.d.
Er	N.d.	N.d.	N.d.	N.d.	N.d.	N.d.	N.d.	N.d.	N.d.	N.d.	N.d.	N.d.	N.d.	N.d.
Tm	0.12	0.08	0.09	0.039	0.046	N.d.	N.d.	N.d.	N.d.	N.d.	N.d.	N.d.	N.d.	N.d.
Yb	0.78	0.51	0.61	0.25	0.29	0.71	0.4	0.92	0.22	0.14	0.34	0.2	0.3	0.17
Lu	0.12	0.1	0.1	0.037	0.045	0.11	0.06	0.15	0.038	0.05	N.d.	0.017	0.047	0.022
Total	15.74	3.49	3.51	1.51	2.31	N.d.	N.d.	N.d.	N.d.	N.d.	N.d.	N.d.	N.d.	N.d.
$(La/Yb)_n$	1.39	0.40	0.22	N.d.	1.12	1.33	1.18	12.5	0.86	0.96	0.60	0.71	0.68	1.11

	Massifs										
	Beriozovsky, Russia					Ural, Russia			Maysky, Rus.	Kalbagdag., Rus.	Karaoss., Rus.
	(Lesnov *et al.*, 1998a), RNAA					(Fershtater *et al.*, 1998), ICP-MS			(Lesnov *et al.*, 2005b), ICP-MS		
Element	132ab	r131	r132a	r138a	r144	F3	F5	F8	2150	1-2	M-29-98
La	0.33	0.28	N.d.	N.d.	0.25	8.53	3.68	0.84	3.391	0.729	2.893
Ce	0.23	0.44	0.1	0.58	N.d.	20.8	10.1	2.82	7.714	2.054	5.705
Pr	N.d.	N.d.	N.d.	N.d.	N.d.	2.76	1.73	0.59	1.225	0.386	0.848
Nd	0.17	0.48	0.18	0.9	N.d.	13.3	8.42	4.28	5.255	2.050	3.618
Sm	0.06	0.16	N.d.	0.067	0.23	3.04	2.51	1.74	1.350	0.772	0.872
Eu	0.038	0.075	0.038	0.03	N.d.	1.1	1.01	0.68	0.680	0.312	0.448
Gd	0.092	N.d.	N.d.	N.d.	N.d.	2.69	3.06	2.45	1.451	1.068	0.872
Tb	0.017	0.045	0.033	0.025	N.d.	0.47	0.49	0.5	0.259	0.195	0.143
Dy	N.d.	N.d.	N.d.	N.d.	N.d.	2.72	3.11	3.58	1.643	1.316	0.863
Ho	N.d.	N.d.	N.d.	N.d.	N.d.	0.58	0.61	0.82	0.346	0.276	0.172
Er	N.d.	N.d.	N.d.	N.d.	N.d.	1.55	1.89	2.01	1.028	0.748	0.462
Tm	0.019	N.d.	N.d.	N.d.	N.d.	0.27	0.28	0.28	0.168	0.114	0.076
Yb	0.11	0.245	0.104	0.156	0.197	1.65	1.93	1.66	1.052	0.715	0.439
Lu	0.02	0.03	N.d.	N.d.	N.d.	0.3	0.27	0.29	0.154	0.100	0.067
Total	N.d.	N.d.	N.d.	N.d.	N.d.	59.76	39.09	22.54	25.71	10.84	17.48
$(La/Yb)_n$	2.03	0.77	N.d.	N.d.	0.86	3.49	1.29	0.34	2.09	0.69	4.45

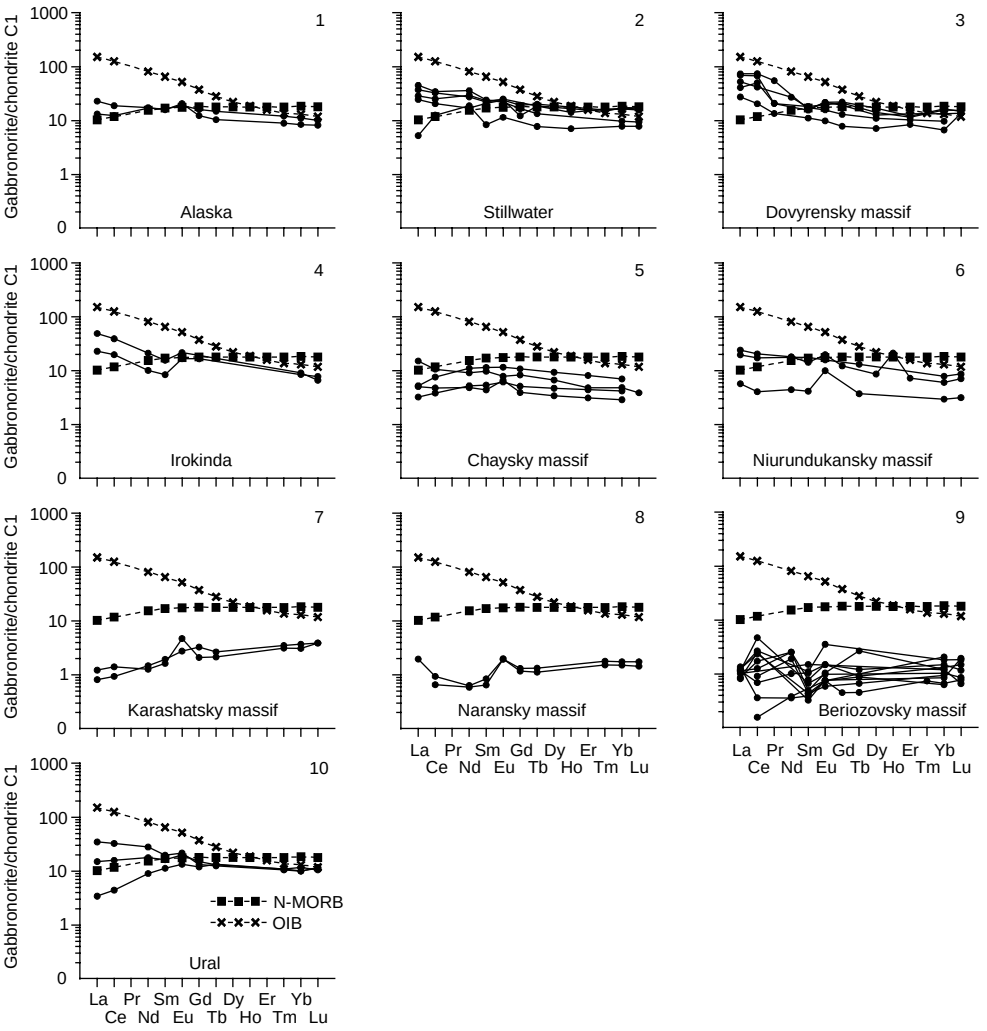

Figure 4.4 Chondrite-normalized REE patterns for gabbro-norites from some massifs (data Table 4.4).

These plutonic mafic rocks often occur in the dykes in peridotite massifs (Mazzucchelli *et al.*, 1999) and are medium-grained and have a massive texture; thin- or coarse-grained varieties are less common. Modal contents of their main minerals (orthopyroxene and plagioclase) vary over wide limits (from 35 to 65%). Some norites contain minor quantities of clinopyroxene, amphibole, or olivine. The contents of major chemical components in these rocks vary approximately over the same ranges as in gabbros and gabbro-norites (wt%): SiO_2 (47–53), Al_2O_3 (10–20), CaO (6–11), MgO (4–15), FeO_{tot} (4–14), Na_2O (0.05–3.0), and K_2O (0.2–1.0).

The rare earth composition of norites is still insufficiently studied. For its description we used the limited number of samples from the Voykar-Syn'insky mafic–ultramafic massif that enters into the ophiolite association of the Polar Urals,

Table 4.5 Average REE composition (x) and standard deviation (σ) of gabbro-norites from some massifs (ppm).

	Massifs							
Element	Beriozovsky (11)	Naransky (2)	Karashatsky (2)	Chaysky (3)	Niurundukansky (3)	Irokinda (2)	Stillwater (5)	Dovyrensky (5)
La	0.290	0.480	0.250	1.105	4.033	8.800	6.876	12.91
Ce	0.230	0.510	0.750	3.447	8.867	18.80	15.96	32.34
Pr	N.d.	N.d.	N.d.	N.d.	N.d.	N.d.	N.d.	2.650
Nd	0.170	0.290	0.650	3.347	6.367	7.400	12.18	12.78
Sm	0.145	0.115	0.275	1.091	1.847	1.850	3.038	2.415
Eu	0.038	0.100	0.190	0.412	0.883	0.975	1.078	0.900
Gd	0.092	0.255	0.550	1.352	2.500	3.400	3.267	3.391
Tb	0.017	0.046	0.090	N.d.	0.315	N.d.	0.588	N.d.
Dy	N.d.	N.d.	N.d.	1.480	2.200	3.100	N.d.	3.137
Ho	N.d.	N.d.	N.d.	N.d.	0.380	0.470	0.600	N.d.
Er	N.d.	N.d.	N.d.	0.868	1.200	0.835	N.d.	1.841
Tm	0.019	0.043	0.085	N.d.	N.d.	N.d.	0.400	N.d.
Yb	0.154	0.270	0.560	0.776	0.930	1.450	2.230	2.038
Lu	0.020	0.041	0.100	N.d.	0.160	0.185	0.344	0.368
Total	N.d.	N.d.	N.d.	13.9	25.4	43.8	44.7	63.9
$(La/Yb)_n$	1.44	1.12	0.31	1.09	2.80	4.05	2.14	4.31

Data Table 4.4.

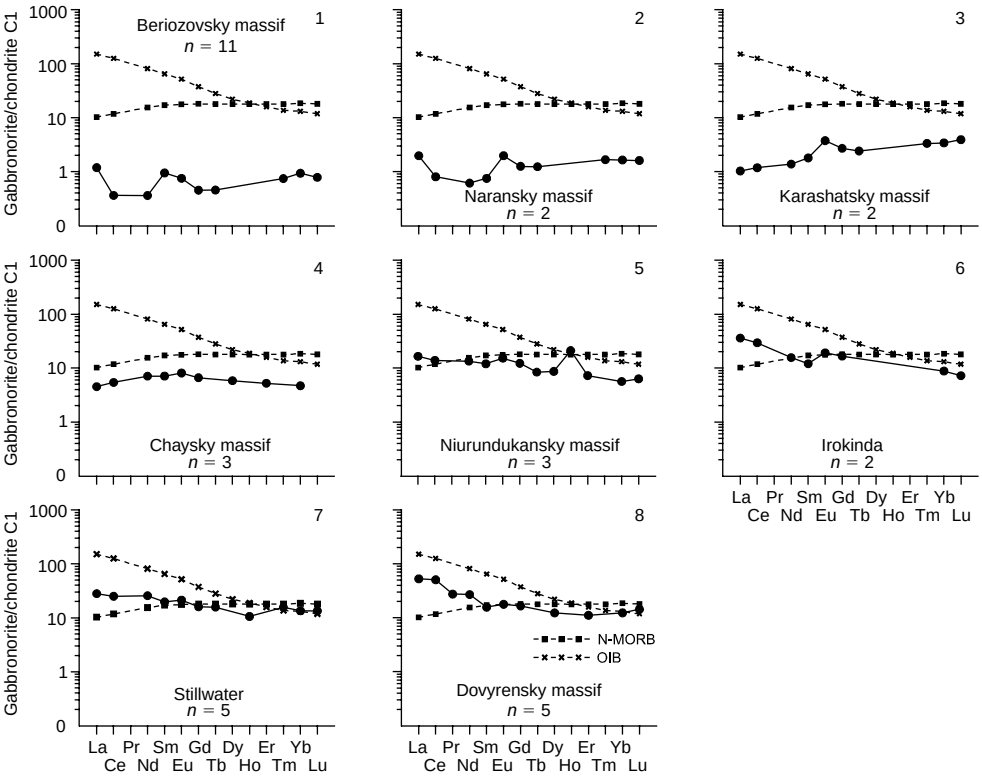

Figure 4.5 Chondrite-normalized patterns of average REE composition of gabbro-norites from some massifs (data Table 4.5).

as well as analyses of samples from the Stillwater massif, which is not related to ophiolite associations (Table 4.6). The total REE content in samples from the Voykar-Syn'insky massif is rather low, only several parts per million. The norites are depleted of light REE compared with heavy REE, and their spectra have a total positive slope, as noted from the values of the parameter $(La/Yb)_n$ (0.05–0.36). Norites from this massif are characterized by lower total REE contents than N-MORBs (Fig. 4.6). In their spectra, positive Eu anomalies are usually observed, with values of the parameter $(Eu/Eu^*)_n$ increasing from 1.3 to 6.2 as the total REE content decreases from 5.7 to 0.6 ppm. A similar trend was noted above in the description of REE composition of gabbros in massifs from Pindos, Skaergaard, Troödos, Kerguelen, and Venezuela, from magmatic bodies of the Mid-Atlantic Ridge (see Fig. 4.1), and in gabbro-norites from the Chaysky and Niurundukansky massifs (see Fig. 4.4). The presented geochemical data allow one to assume that parent melts of norites from the Voykar-Syn'insky massif were generated at an elevated extent of partial melting of mantle source that was probably preliminarily depleted.

In the Stillwater massif, norites compose numerous dikes; they are enriched with all REE, especially light ones (see Table 4.6). The level of La accumulation in them ranges from 6 to 150 t. ch., and the level of Yb accumulation is lower (3.6–18.6 t. ch.). Rare earth spectra of the norites show a rather steep negative slope; and values of the parameter $(La/Yb)_n$ vary over the range 1.8–7.9. These norites occupy an intermediate position between N-MORBs and E-MORBs in the average level of light REE accumulation. The peculiarities of rare earth composition of norites from the Stillwater massif suggest that the rocks crystallized from melts generated at rather low extents of partial melting of mantle source, which was not preliminarily subjected to depletion. Essential geochemical distinctions between considerably REE-depleted norites from the Voykar-Syn'insky massif that enters into ophiolite associations, and norites from the Stillwater massif which are not related to ophiolite, can be estimated by their average rare earth composition (Table 4.7, Fig. 4.7). In summary, it is necessary to emphasize that the rare earth composition of norites is appreciably stipulated by modal plagioclase as the main concentrator of REE in these rocks.

4.4 OLIVINE GABBROS

Olivine gabbros most often occur in those mafic–ultramafic massifs that, by indirect evidence, were formed at mesoabyssal or abyssal levels of the earth's crust. In the majority of such massifs, these rocks are present in subordinated amounts in relation to olivine-free gabbros and gabbro-norites. Massifs in which olivine gabbros are the predominant rock are less common, and autonomous intrusions, composed exclusively of olivine gabbros, are not described anywhere. In complex massifs that are related to ophiolite associations, olivine gabbros usually enter into the structure of layered complexes (transitional zones) located along the boundaries of ultramafic and gabbroid bodies. In these zones, olivine gabbros form stripe-shaped and lens-like bodies of variable thickness and extent. The bodies interleave with bodies of olivine-free gabbros and gabbro-norites, as well as troctolites, plagioclase-bearing pyroxenites, pyroxenites, plagioclase-bearing wehrlites, and wehrlites (Lesnov, 1984, 1986).

Table 4.6 Rare earth element composition of norites (ppm).

	Massifs											
	Voykar-Sin'insky, Russia						Stillwater, USA					
	(Savel'ev *et al.*, 1999)						(Helz, 1985), INAA					
Element	556-2	558	558-1	567-13	578-2	801-2	803-2	803-14	83/526.5	70/578	70/764	87/478
La	0.02	0.01	0.02	0.34	0.11	0.02	0.01	0.02	1.62	6.00	15.00	36.00
Ce	0.08	0.05	0.06	0.46	0.38	0.08	0.05	0.06	4.40	10.00	27.00	77.00
Pr	0.02	0.01	0.01	0.07	0.07	0.02	0.01	0.01	N.d.	N.d.	N.d.	N.d.
Nd	0.12	0.12	0.06	0.54	0.56	0.12	0.12	0.06	N.d.	6.00	17.00	51.00
Sm	0.07	0.08	0.02	0.32	0.32	0.07	0.08	0.02	0.45	9.00	3.80	12.70
Eu	0.06	0.08	0.05	0.22	0.20	0.06	0.08	0.05	0.31	1.26	1.63	3.64
Gd	0.15	0.14	0.03	0.76	0.66	0.15	0.14	0.03	N.d.	N.d.	3.80	13.00
Tb	0.04	0.03	0.01	0.15	0.11	0.04	0.03	0.01	N.d.	0.16	0.57	1.58
Dy	0.25	0.21	0.06	1.05	0.77	0.25	0.21	0.06	N.d.	N.d.	N.d.	N.d.
Ho	0.06	0.05	0.02	0.24	0.17	0.06	0.05	0.02	N.d.	N.d.	0.65	N.d.
Er	0.19	0.15	0.05	0.72	0.48	0.19	0.15	0.05	N.d.	N.d.	N.d.	N.d.
Tm	0.03	0.02	0.01	0.10	0.07	0.03	0.02	0.01	N.d.	0.23	0.31	0.36
Yb	0.25	0.13	0.07	0.64	0.45	0.25	0.13	0.07	0.60	1.20	1.90	3.07
Lu	0.04	0.02	0.01	0.10	0.06	0.04	0.02	0.01	0.10	0.25	0.32	0.42
Total	1.38	1.10	0.57	5.71	4.41	1.38	1.10	0.57	N.d.	N.d.	N.d.	N.d.
$(La/Yb)_n$	0.05	0.05	0.19	0.36	0.17	0.05	0.05	0.19	1.82	3.37	5.33	7.92
$(Eu/Eu^*)_n$	1.74	2.29	6.23	1.31	1.30	1.28	2.67	3.36	3.66	0.74	1.30	0.86

	Kuvalorogsky, Russia		
	(Konnikov *et al.*, 2009)		
Element	S5-436	S2-29	R1-1
La	4.8	7.8	7.7
Ce	14.6	18.8	19.1
Pr	2.3	2.7	2.3
Nd	10.6	12.0	10.0
Sm	2.9	2.7	1.9
Eu	0.6	1.1	1.0
Gd	2.7	2.4	2.0
Tb	0.5	0.4	0.3
Dy	2.7	2.4	2.0
Ho	0.6	0.4	0.3
Er	<2	<2	<1
Tm	0.2	0.1	0.2
Yb	1.5	1.0	1.10
Lu	0.2	0.2	0.2
Total	~46	~54	~49
$(La/Yb)_n$	2.16	5.26	4.72
$(Eu/Eu^*)_n$	0.65	1.30	1.56

Sample S5-436 (melanocratic amphibole-bearing norite); sample S2-29 (amphibole-bearing norite); sample R1-1 (biotite amphibole-bearing norite).

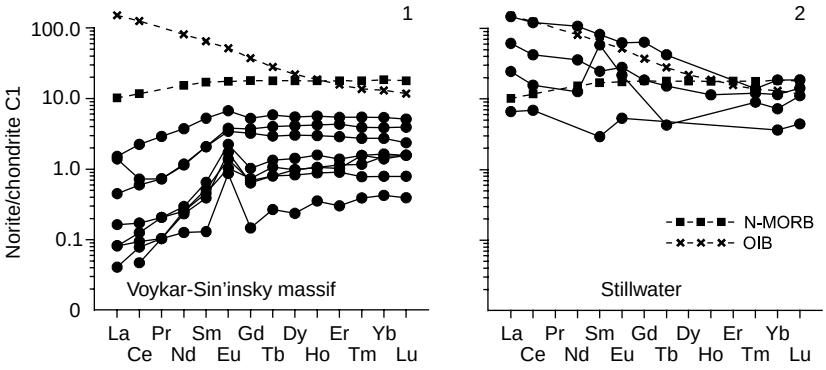

Figure 4.6 Chondrite-normalized REE patterns for norites from some massifs (data Table 4.6).

Table 4.7 Average REE composition (x) and standard deviation (σ) of norites from some massifs (ppm).

	Massifs			
	Voykar-Sin'insky (8)		Stillwater (4)	
Element	x	σ	x	σ
La	0.130	0.157	14.7	15.3
Ce	0.325	0.475	29.6	33.0
Pr	0.061	0.092	N.d.	N.d.
Nd	0.428	0.578	24.7	23.5
Sm	0.223	0.265	6.49	5.43
Eu	0.154	0.114	1.710	1.40
Gd	0.394	0.382	8.40	6.51
Tb	0.080	0.073	0.770	0.73
Dy	0.544	0.477	N.d.	N.d.
Ho	0.126	0.107	0.650	N.d.
Er	0.361	0.307	N.d.	N.d.
Tm	0.056	0.044	0.300	0.07
Yb	0.366	0.278	1.63	1.06
Lu	0.055	0.041	0.273	0.13
Total	3.30	3.29	89.2	N.d.
$(La/Yb)_n$	0.17	0.12	4.61	2.63
$(Eu/Eu^*)_n$	2.52	0.16	1.64	1.37

Data Table 4.6.

In most cases, olivine gabbros are characterized by a heterogeneous structure. Many of them have a taxitic texture, caused by a non-uniform, including banded, distribution of rock-forming minerals, modal quantities of which vary within significant limits: clinopyroxene (10–60%), plagioclase (35–65%), and olivine (5–35%). Sometimes olivine gabbros contain orthopyroxene and/or amphibole as minor phases, and such accessory minerals, as magnetite, titanomagnetite, ilmenite, apatite, sphene, zircon, and sulfide phases. The contents of major chemical components in the rocks also considerably vary (wt%): SiO_2 (42–49), Al_2O_3 (11–24), CaO (5–18), MgO (6–20), FeO_{tot} (5–12), Na_2O (0.5–2.0), and K_2O (0.5–1.0). Values of the parameter

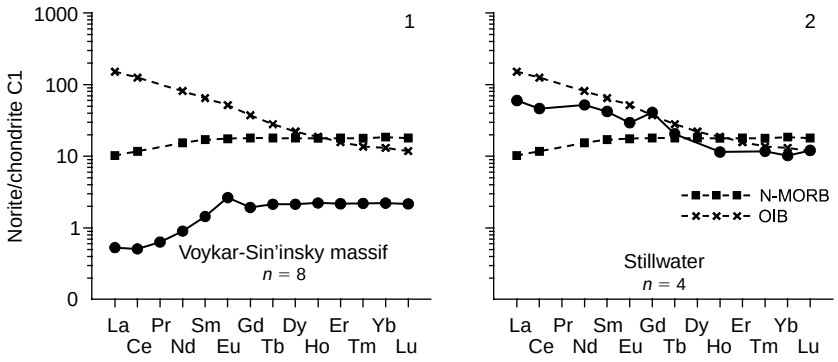

Figure 4.7 Chondrite-normalized patterns of average composition of REE for norites (data Table 4.7).

$100 \cdot FeO_{tot}/(FeO_{tot} + MgO)$ varies from 36 to 42 and the parameter CaO/Al_2O_3 varies from 0.67 to 0.85 (Lesnov, 1986).

The rare earth composition of olivine gabbros was studied in many massifs. For REE geochemical characteristics of the rocks, we used analyses of samples from the Kalbagdagsky, Mazhalyksky, Bulkinsky, Maysky, Irbiteisky, Karashatsky, Samail, Gorgona Island, Marinkin, Shildyrkheysky, Annieopsquotch, and other massifs (Table 4.8). REE patterns of olivine gabbros are usually characterized by the presence of positive Eu anomalies of various intensities (Fig. 4.8). By these analyses, the total REE content in olivine gabbros vary over a rather wide range. The average La content in samples from individual massifs ranges from 0.1 (the Mid-Atlantic Ridge) to 3.56 ppm (Marinkin), and the average Yb content ranges from 0.25 (Nomgonsky) to 1.2 ppm (Annieopsquotch). Mean values of the parameter $(La/Yb)_n$ vary from 0.19 (the Mid-Atlantic Ridge) to 4.6 (Nomgonsky). In olivine gabbros from all the massifs, the mean value of parameter $(Eu/Eu^*)_n$ is greater than unity (Table 4.9).

Let's consider some peculiarities of REE distribution in olivine gabbros by studying the examples of separate massifs. Among the mafic–ultramafic massifs of Tuva, olivine gabbros were studied in the Karashatsky massif that is related to ophiolite association, as well as in the Kalbagdagsky, Mazhalyksky, Bulkinsky, Maysky, and Irbiteisky massifs that are not related to ophiolites. The rocks from the Karashatsky and Kalbagdagsky massifs are more-depleted in all REE in comparison with olivine gabbros from the other massifs, however all of these rocks have a lower level of accumulation of these elements in comparison with N-MORBs. Rare earth spectra of many olivine gabbro samples look as almost straight lines with a gentle negative slope; some of them are complicated with weak positive Eu anomalies. Olivine gabbros from the Nomgonsky and Ortsog–Ula massifs, as well as the Marinkin and Lukinda massifs have similar REE compositions.

Olivine gabbros from the ophiolite massifs Samail and Annieopsquotch have been investigated in more detail. The total REE content in samples from the Sumail massif varies from 4.3 to 17.6 ppm, and averages to about 7.4 ppm. These samples are depleted of light REE (La content is 0.25–5.3 t. ch.) in comparison with heavy REE (Yb content is 1.2–7.9 t. ch.). Therefore, their rare earth spectra have an overall positive slope, and many of them display positive Eu anomalies of insignificant intensity

Table 4.8 Rare earth element composition of olivine gabbros (ppm).

	Massifs													
	Samail, Oman										Lukinda, Russia		Marinkin, Russia	
	(Pallister & Knight, 1981), RNAA										(Data Krivenko), INAA		(Izokh *et al.*, 1998), INAA	
Element	Kf-12-1	Kf-15-1	Kf-17-1	Kf-20-1	Kf-4-1	Kf-5-1	Kf-6-1	Kf-7-1	Kf-8-1	Kf-10-1	P-1597	B-1471	B-2685	B-3561
La	0.46	0.23	0.18	0.061	1.3	0.2	0.3	0.18	0.18	0.22	0.58	3.62	0.82	6.3
Ce	0.73	0.97	0.51	0.4	3.5	0.67	0.87	1.2	1.3	0.61	1.91	7.3	1.9	16
Pr	N.d.	N.d.	N.d.	N.d.	N.d.	N.d.	N.d.	N.d.	N.d.	N.d.	N.d.	N.d.	N.d.	N.d.
Nd	1.4	1.5	1.9	0.68	4	1.3	1.8	1.1	2.8	1.3	1.37	4.55	1.2	10
Sm	0.64	0.51	0.64	0.12	1.4	0.46	0.48	0.35	0.81	0.61	0.44	1.05	0.34	2.9
Eu	0.37	0.29	0.42	0.14	0.63	0.28	0.26	0.25	0.44	0.31	0.39	0.85	0.23	0.94
Gd	1.2	1	0.94	0.3	2	0.57	0.72	0.37	1.3	1.1	0.6	1.48	0.4	3.1
Tb	0.21	0.16	0.22	0.053	0.35	0.16	0.16	0.066	0.25	0.18	0.09	0.22	0.1	0.53
Dy	1.6	1.1	N.d.	2.6	2.7	0.97	0.96	0.48	1.5	1.3	N.d.	N.d.	N.d.	N.d.
Ho	N.d.	N.d.	N.d.	N.d.	N.d.	N.d.	N.d.	N.d.	N.d.	N.d.	N.d.	N.d.	N.d.	N.d.
Er	N.d.	N.d.	N.d.	N.d.	N.d.	N.d.	N.d.	N.d.	N.d.	N.d.	N.d.	N.d.	N.d.	N.d.
Tm	0.11	0.091	0.11	0.033	0.2	0.087	0.083	0.046	0.13	0.096	0.08	0.12	N.d.	N.d.
Yb	0.75	0.57	0.68	0.2	1.3	0.49	0.48	0.23	0.77	0.55	0.44	0.7	0.21	1.6
Lu	0.11	0.093	0.09	0.03	0.19	0.075	0.07	0.034	0.13	0.078	N.d.	0.07	0.031	0.23
Total	7.58	6.51	5.69	4.62	17.6	5.26	6.18	4.31	9.61	6.35	N.d.	N.d.	N.d.	N.d.
$(La/Yb)_n$	0.41	0.27	0.18	0.21	0.68	0.28	0.42	0.53	0.16	0.27	N.d.	N.d.	N.d.	N.d.
$(Eu/Eu^*)_n$	1.27	1.22	1.65	2.15	1.15	1.67	1.35	2.11	1.30	1.14	2.32	2.08	1.90	0.95

	Massifs													
	Shildyrkhey, Russia		Kalbagdagsky, Russia	Maysky, Russia	Nomgon., Mongolia		Ortsog Ula, Mongolia		Bayantsag., Mongolia	Tsentral'ny, Mongolia			Karashatsky, Russia	Skaergaard, Greenland
	(Izokh *et al.*, 1998), INAA		(Lesnov & Oydup, 2002)		(Izokh *et al.*, 1998), INAA								(Pfander *et al.*, 2001)	(Haskin & Haskin, 1968)
Element	6373	6375	Kal-10-3	2530	I-4652	I-4664	I-1553	I-1544	I-2221	I-1989	I-2038	I-2045	T97A54	5181
La	0.73	0.9	0.5	3.8	1.1	1.4	0.2	0.64	0.13	1.4	1.5	1	0.32	2.8
Ce	1.8	2.7	1.1	9	2	3.6	0.5	2.2	0.4	3.8	3.7	2.5	0.58	7.2
Pr	N.d.	N.d.	N.d.	N.d.	N.d.	N.d.	N.d.	N.d.	N.d.	N.d.	N.d.	N.d.	0.08	1.1
Nd	1.1	2.2	0.7	5.2	1	2.5	0.3	2.3	0.3	3	2.4	2	0.3	6
Sm	0.32	0.8	0.38	1.48	0.2	0.8	0.08	0.95	0.13	0.95	0.7	0.73	0.14	1.88
Eu	0.19	0.53	0.18	0.7	0.19	0.29	0.11	0.32	0.1	0.39	0.3	0.27	0.08	1.59
Gd	0.4	1	0.5	1.6	0.4	0.9	0.2	1.5	0.5	1.1	0.9	0.9	0.24	2.27
Tb	0.1	0.18	0.08	0.26	0.04	0.16	0.02	0.28	0.03	0.18	0.2	0.3	N.d.	0.32
Dy	N.d.	N.d.	N.d.	N.d.	N.d.	N.d.	N.d.	N.d.	N.d.	N.d.	N.d.	N.d.	N.d.	N.d.
Ho	N.d.	N.d.	N.d.	N.d.	N.d.	N.d.	N.d.	N.d.	N.d.	N.d.	N.d.	N.d.	0.11	0.4
Er	N.d.	N.d.	N.d.	N.d.	N.d.	N.d.	N.d.	N.d.	N.d.	N.d.	N.d.	N.d.	N.d.	1.1
Tm	N.d.	N.d.	0.06	0.12	N.d.	N.d.	N.d.	N.d.	N.d.	N.d.	N.d.	N.d.	N.d.	0.173
Yb	0.24	0.86	0.4	0.74	0.11	0.38	0.03	0.68	0.13	0.59	0.53	0.42	0.23	0.96
Lu	0.035	0.15	0.07	0.11	0.02	0.05	0.01	0.09	0.02	0.09	0.08	0.06	0.04	0.159
Total	N.d.	N.d.	N.d.	N.d.	N.d.	N.d.	N.d.	N.d.	N.d.	N.d.	N.d.	N.d.	N.d.	26.0
$(La/Yb)_n$	2.05	0.71	0.84	3.47	6.75	2.49	4.50	0.64	0.68	1.60	1.91	1.61	0.94	1.97
$(Eu/Eu^*)_n$	1.62	1.81	1.26	1.38	2.01	1.04	2.53	0.82	1.05	1.16	1.16	1.02	1.32	2.35

(*Continued*)

Table 4.8 Continued

	Massifs													
	Niurundukansky, Russia			Chaysky, Russia	Irbiteisky, Russia		Gorgona, Columbia				Ural, Russia	Mid-Atlantic ridge		Bulkinsky, Russia
	(Tsigankov *et al.*, 2002)			(Data Konnikov)	(Lesnov & Oydup, 2002)		(Revillon *et al.*, 2000), ICP-MS				(Fershtater *et al.*, 1998)	(Dostal & Muecke, 1978)		(Lesnov, 2005b)
Element	Nr-11/2	N-231	N-23m	Chay-1	L-66	L-68	GOR 508	GOR 509	GOR 534	GOR 535	F1	24-3	24-4	Bl-4
La	0.78	0.64	2.1	1.9	0.98	0.74	0.45	0.21	2.14	1.32	0.13	0.095	N.d.	0.98
Ce	2.1	1.8	4.4	3.3	2.50	1.90	1.42	0.63	5.57	3.52	0.77	0.25	0.12	3.06
Pr	N.d.	N.d.	N.d.	N.d.	N.d.	N.d.	0.29	0.12	0.83	0.54	0.06	N.d.	N.d.	N.d.
Nd	2	1.5	3	1.9	1.90	1.80	1.88	0.76	4.24	2.97	0.93	0.28	0.17	3.44
Sm	0.68	0.51	N.d.	0.9	0.67	0.64	0.87	0.39	1.5	1.1	0.19	0.11	0.099	1.19
Eu	0.38	0.2	0.28	0.3	0.32	0.32	0.43	0.21	0.65	0.46	0.18	0.068	0.07	0.67
Gd	N.d.	0.66	1	0.9	0.91	1.30	1.46	0.78	2.16	1.64	0.38	0.23	0.2	1.56
Tb	0.14	N.d.	N.d.	N.d.	0.16	0.15	0.27	0.16	0.38	0.29	0.06	0.052	0.045	0.29
Dy	N.d.	0.87	N.d.	1.3	N.d.	N.d.	1.91	1.25	2.59	1.98	0.83	N.d.	N.d.	1.78
Ho	N.d.	N.d.	N.d.	N.d.	N.d.	N.d.	0.4	0.29	0.53	0.41	0.13	N.d.	N.d.	0.34
Er	N.d.	0.4	0.43	0.5	N.d.	N.d.	1.09	0.88	1.43	1.09	0.49	N.d.	N.d.	0.92
Tm	N.d.	N.d.	N.d.	N.d.	0.09	0.10	0.16	0.13	0.2	0.16	0.08	N.d.	N.d.	0.13
Yb	0.43	0.42	0.36	0.5	0.58	0.54	0.88	0.88	1.24	0.98	0.51	0.34	0.3	0.76
Lu	0.07	0.07	N.d.	0.1	0.09	0.09	0.15	0.15	0.19	0.16	0.03	0.053	0.048	0.10
Total	N.d.	7.1	N.d.	N.d.	N.d.	N.d.	11.7	6.8	23.7	16.6	4.8	N.d.	N.d.	N.d.
$(La/Yb)_n$	1.22	1.03	3.94	2.57	1.14	0.93	0.35	0.16	1.17	0.91	0.17	0.19	N.d.	0.87
$(Eu/Eu^*)_n$	2.97	1.05	N.d.	1.01	1.25	1.05	1.16	1.14	1.10	1.05	2.01	1.27	1.49	1.48

	Massifs											
	Maysky, Russia			Kalbagdagsky, Russia			Mazhalyksky, Russia			Annieopsquotch, Canada		
	(Lesnov *et al.*, 2005b), ICP-MS									(Lissenberg *et al.*, 2004), ICP-MS		
Element	2530	2530–1	9-3	30-6	A153	A196	A933	A1228	A1228a	A1352	A1628	A2050
La	3.11	14.12	1.11	1.99	0.25	0.17	0.18	0.4	0.23	0.81	0.5	1.21
Ce	7.89	28.82	2.42	4.94	0.94	0.65	0.71	1.41	0.79	2.66	1.71	4.4
Pr	1.29	4.10	0.39	0.84	0.21	0.17	0.17	0.29	0.16	0.53	0.34	0.9
Nd	5.47	15.68	1.81	3.98	1.38	1.2	1.22	1.69	1.02	3.17	2.17	5.19
Sm	1.38	3.02	0.58	1.16	0.68	0.65	0.65	0.76	0.47	1.31	0.94	2.26
Eu	0.60	0.97	0.24	0.43	0.39	0.31	0.42	0.44	0.36	0.58	0.55	0.87
Gd	1.47	2.71	0.72	1.21	1.2	1.04	1.25	1.2	0.78	2.09	1.51	3.37
Tb	0.25	0.41	0.14	0.21	0.22	0.2	0.23	0.25	0.14	0.38	0.31	0.65
Dy	1.52	2.23	0.94	1.30	1.55	1.31	1.51	1.59	0.88	2.53	2.05	4.3
Ho	0.30	0.41	0.20	0.25	0.35	0.29	0.35	0.35	0.21	0.58	0.46	0.97
Er	0.83	1.11	0.59	0.68	1.05	0.89	1.02	1.06	0.62	1.62	1.36	2.81
Tm	0.12	0.16	0.09	0.10	0.15	0.13	0.14	0.15	0.09	0.25	0.2	0.45
Yb	0.77	0.97	0.50	0.58	0.89	0.82	0.94	0.95	0.55	1.52	1.27	2.73
Lu	0.11	0.14	0.07	0.08	0.15	0.12	0.15	0.16	0.1	0.24	0.2	0.42
Total	25.1	74.9	9.8	17.7	9.41	7.95	8.94	10.7	6.40	18.3	13.6	30.5
$(La/Yb)_n$	2.72	9.81	1.48	2.33	0.21	0.15	0.14	0.31	0.31	0.39	0.29	0.32
$(Eu/Eu^*)_n$	1.30	1.02	1.13	1.08	1.31	1.15	1.40	1.40	1.81	1.07	1.40	0.96

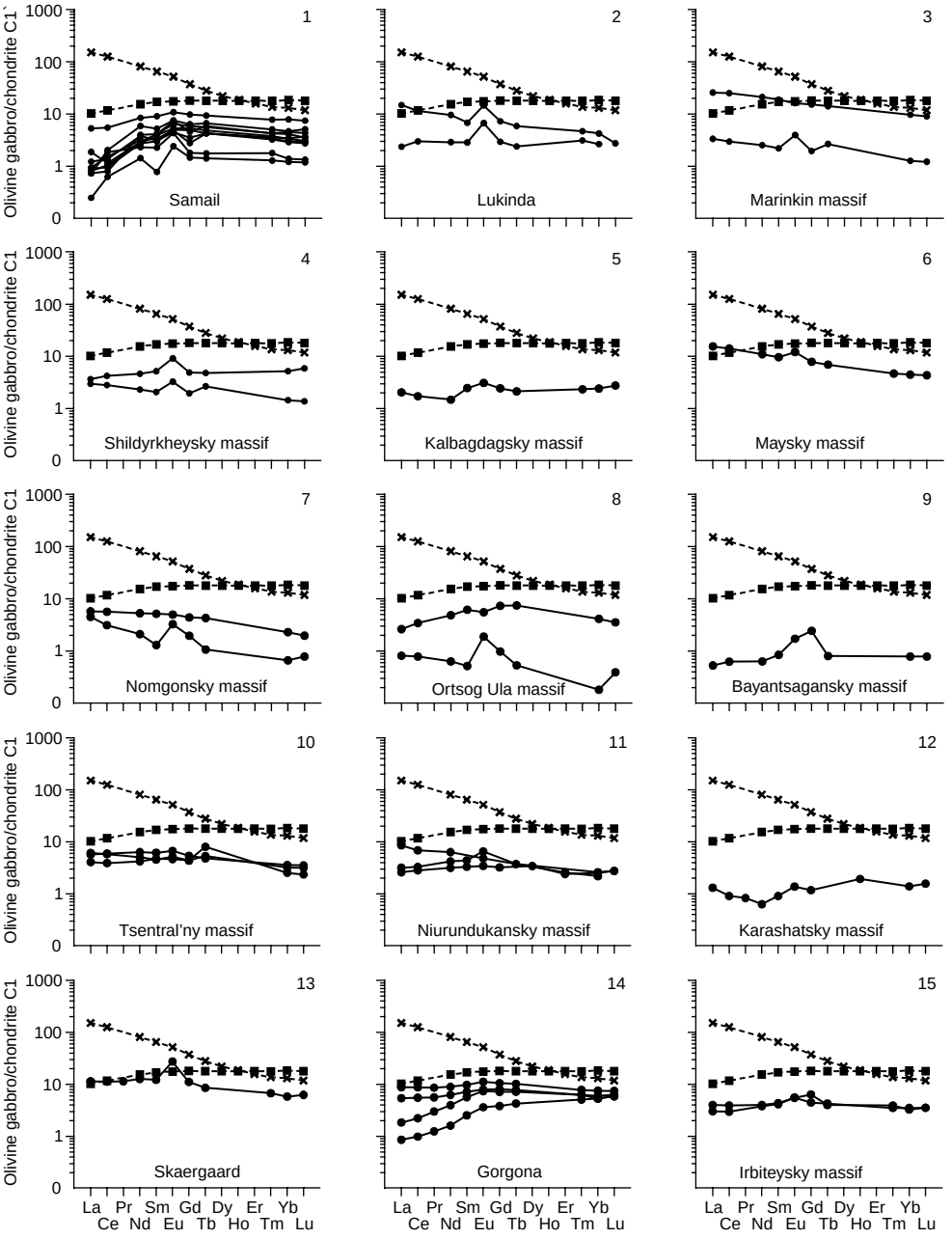

Figure 4.8 Chondrite-normalized REE patterns for olivine gabbros from some massifs (data Table 4.8).

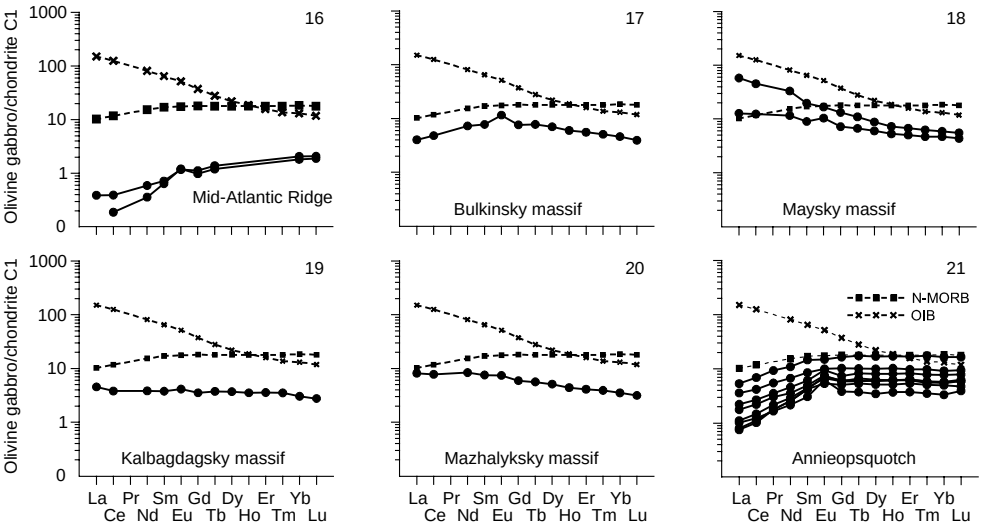

Figure 4.8 Continued

(see Fig. 4.8, 1). Olivine gabbros from the Annieopsquotch massif that enters into ophiolite association in Newfoundland, contain less REE than N-MORBs. The concentrations of separate elements, and also the total REE content (6.4–30.5 ppm), varies appreciably. The rare earth spectra of the rocks, being concordant to each other, have a positive slope in the field of light REE and an almost "flat" pattern in the interval from Gd to Lu (see Fig. 4.8, 21). Values of the parameter $(Eu/Eu^*)_n$ range from 1.07 to 1.8; with the intensity of positive Eu anomalies on the spectra consistently decreasing, up to an almost complete disappearance, as the total REE content increases. As noted above, this analogous regularity was observed in gabbroids from some other massifs. Apparently, it is caused by changes in modal amounts of plagioclase and clinopyroxene; the more modal plagioclase and the less modal clinopyroxene in gabbroids, the lower the overall level of accumulation of REE and the higher the intensity of Eu anomalies.

The total REE content in olivine gabbros from the massif of Gorgona Island range from 6.8 to 23.6 ppm and average to about 15 ppm. The rocks contain less REE than N-MORBs (see Fig. 4.8, 14). Two of four analyzed samples are characterized by decreased contents of light REE; as a result, their spectra display a positive slope in the field of light REE and a "flat" pattern in the other fields. These features resemble spectra of olivine gabbros from the Samail and Annieopsquotch ophiolite massifs. Two other samples from this massif are slightly enriched with light REE, and their spectra have an almost "flat" form.

* * *

The study of olivine gabbros from mafic–ultramafic massifs that differ in structure and composition and are located in various regions, suggests that the contents and character of distribution of REE in them vary within significant limits, and in most

Table 4.9 Average REE composition (x) and standard deviation (σ) of olivine gabbros from some massifs (ppm).

	Massifs											
Element	Mid-Atlantic Ridge (2)	Ortsog Ula (2)	Shildyrkheysky (2)	Samail (10)	Nomgon (2)	Irbitey (2)	Niurundukansky (3)	Tsentral'ny (3)	Lukinda (2)	Gorgona (4)	Marinkin (2)	Newfoundland (8)
La	0.095	0.42	0.815	0.331	1.25	0.86	1.173	1.300	2.100	1.030	3.560	0.469
Ce	0.185	1.35	2.250	1.076	2.8	2.2	2.767	3.333	4.605	2.785	8.950	1.659
Pr	N.d.	N.d.	N.d.	N.d.	N.d.	N.d.	N.d.	N.d.	N.d.	0.445	N.d.	0.346
Nd	0.225	1.3	1.650	1.778	1.75	1.85	2.167	2.467	2.960	2.463	5.600	2.130
Sm	0.105	0.515	0.560	0.602	0.5	0.655	0.595	0.793	0.745	0.965	1.620	0.965
Eu	0.069	0.215	0.360	0.339	0.24	0.32	0.287	0.320	0.620	0.438	0.585	0.490
Gd	0.215	0.85	0.700	0.950	0.65	1.105	0.830	0.967	1.040	1.510	1.750	1.555
Tb	0.049	0.15	0.140	0.181	0.1	0.155	0.140	0.227	0.155	0.275	0.315	0.298
Dy	N.d.	N.d.	N.d.	1.468	N.d.	N.d.	0.870	N.d.	N.d.	1.933	N.d.	1.965
Ho	N.d.	N.d.	N.d.	N.d.	N.d.	N.d.	N.d.	N.d.	N.d.	0.408	N.d.	0.445
Er	N.d.	N.d.	N.d.	N.d.	N.d.	N.d.	0.415	N.d.	N.d.	1.123	N.d.	1.304
Tm	N.d.	N.d.	N.d.	0.099	N.d.	0.095	N.d.	N.d.	0.100	0.163	N.d.	0.195
Yb	0.320	0.355	0.550	0.602	0.245	0.56	0.403	0.513	0.570	0.995	0.905	1.209
Lu	0.051	0.05	0.093	0.090	0.035	0.09	0.070	0.077	0.070	0.163	0.131	0.193
Total	N.d.	N.d.	N.d.	7.37	N.d.	N.d.	N.d.	N.d.	N.d.	14.7	N.d.	13.2
$(La/Yb)_n$	0.19	2.57	1.38	0.34	4.62	1.03	2.06	1.71	2.19	0.65	2.65	0.26
$(Eu/Eu^*)_n$	1.38	1.67	1.72	1.50	1.53	1.15	2.01	1.11	2.20	1.11	1.43	1.22

Data Table 4.8.

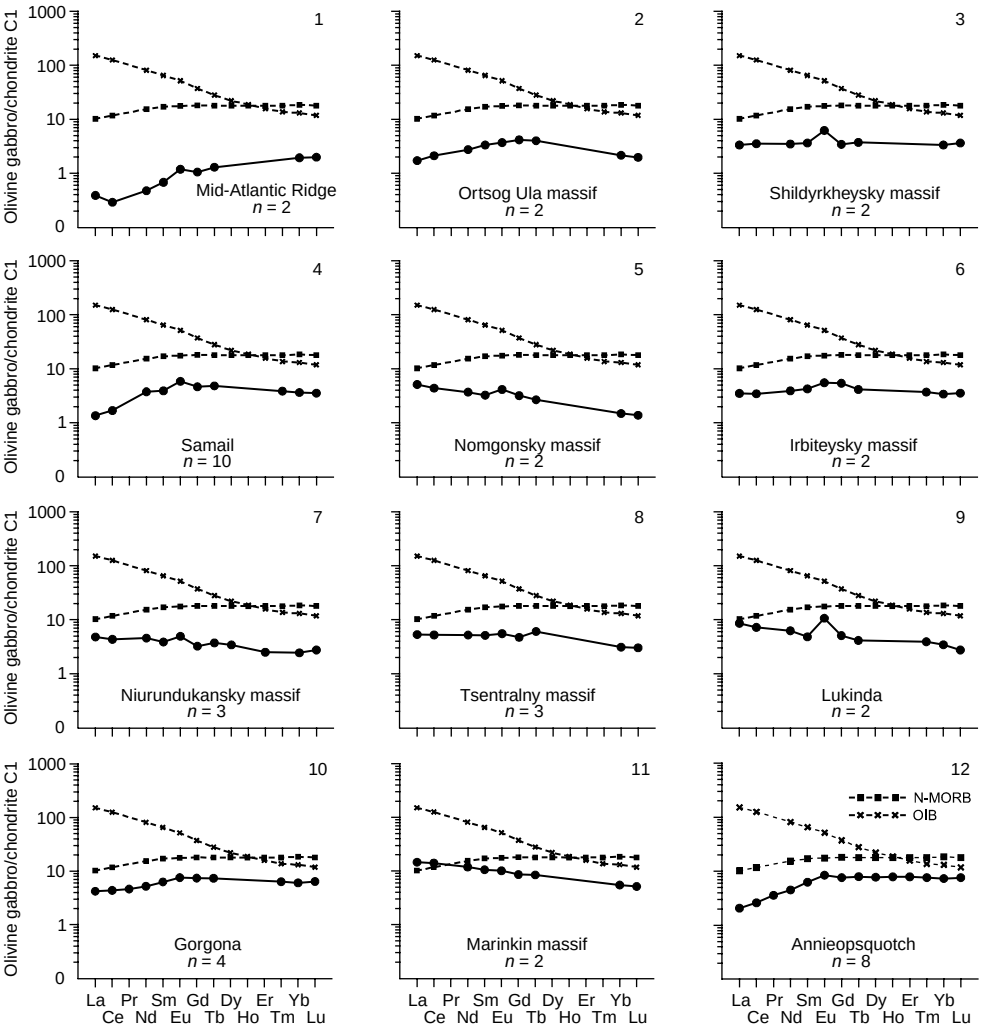

Figure 4.9 Chondrite-normalized patterns for average REE composition of olivine gabbros from some massifs (data Table 4.9).

cases the level of accumulation of REE in these gabbros is lower than in N-MORBs. The inhomogeneity of rare earth composition of olivine gabbros is caused by differences in the composition, and conditions of crystallization, of the parent melts, which predetermined variations in the modal and bulk compositions of the rocks. The majority of REE in these rocks is concentrated as an isomorphous impurity in clinopyroxene and plagioclase, modal quantities of which are changeable. Sometimes, amphibole is a minor contributor to the overall balance of REE in olivine gabbros, and apatite, zircon, and sphene are accessory minerals. On the whole, these rocks are characterized by weak fractionation of REE; many of their analyses demonstrate insignificant excess of Eu (Fig. 4.9).

Geological and petrographical observations allow one to assume that olivine gabbros could be of two-fold origin. Some of them are apparently orthomagmatic rocks that crystallized from uncontaminated mantle melts with and increased Mg/Fe ratio owing to generation at elevated extents of partial melting of mantle sources. Such olivine gabbro is characterized by rather homogeneous chemical, modal, and REE compositions. Samples from the Skaergaard and Bulkinsky massifs are related to this type.

The other variety of olivine gabbro is probably of hybrid origin. Such rocks differ by more or less significant inhomogeneity of structure and composition that is expressed in taxitic textures and in essential variations in chemical and modal compositions. This type is usually spatially associated with troctolites, pyroxenites, and plagioclase-bearing peridotites within the banded complexes of mafic–ultramafic massifs that enter in ophiolite associations. We consider such olivine gabbros as paramagmatic or magmatic and metasomatic rocks that were formed at crystallization of mantle tholeiite melts, contaminated to a variable degree by ultramafic restites, which were injected by the melts. Their spread is usually restricted by more or less thick contact zones of ultramafic restite protrusions with injected intrusions of gabbros and gabbro-norites (Lesnov, 1984, 1986, 1988). Examples of olivine gabbros of this type can be seen in samples from ophiolite massifs from Samail, Annieopsquotch, Karashatsky, Niurundukansky, as well as the Mid-Atlantic Ridge. Evidently, in view of the proposed heterogeneity of olivine gabbros, special investigations should be conducted with the purpose of revealing reliable geological, structural, petrographical, and geochemical criteria for their discrimination.

4.5 TROCTOLITES

Troctolites are much less abundant in all mafic–ultramafic massifs in comparison with associating gabbros and gabbro-norites. They mainly occur in those massifs that located in deeply eroded folded structures of the Precambrian era. Together with olivine gabbros, pyroxenites, and wehrlites, these rocks often compose structures of layered complexes (or contact-reactionary zones) in massifs that are related to ophiolite associations. The Kokpektinsky massif that enters into the Kempirsay ophiolite association (southern Ural), as well as the Samail and Pindos massifs, can serve as examples. Troctolites are also present in some massifs that are not related to ophiolites, for example, in the Dovyrensky, Rum, Marinkin, Lukinda, and Luchansky massifs. Plutonic rocks of troctolite composition are discovered on the moon (Magmatic rocks, 1985; Ariskin, 2007). A characteristic feature of troctolites is that they usually occur together with other varieties of gabbro, and also with plagioclase-bearing peridotites, while plutonic bodies that consist exclusively of troctolites have not been described yet anywhere.

In structures of ophiolite mafic–ultramafic massifs, troctolites compose stripe-shaped, usually wedging, bodies of various extent and thickness, as well as bodies of irregular shape, which interleave without apparent regularity with similar bodies of olivine gabbros, olivine gabbro-norites, wehrlites, and plagioclase-bearing wehrlites, pyroxenites, and plagioclase-bearing dunites. In the Dovyrensky massif, troctolites compose not less than three "horizons" (about 100–200 m in thickness), among which

lens-like, variously thickened bodies of dunites and plagiodunites are located. It is remarkable that plagioclase from troctolites of this massif is characterized by higher contents of anorthite component (82–84%) than plagioclase from adjacent "strips" of plagioclase-bearing dunites (60–70% anorthite component); this fact does not agree with the cumulative model of formation of this massif that is accepted by many researchers (Magmatic rocks, 1988). The troctolite texture varies from medium- to thin-grained. In most cases, troctolites are characterized by a taxitic texture, due to a non-uniform, including banded or spotty, distribution of plagioclase and olivine. The modal composition of troctolites varies from leucocratic varieties that contain 65% plagioclase to melanocratic varieties that contain up to 60% olivine; sometimes the melanocratic troctolites grade into plagioclase-bearing dunites. Sometimes troctolites contain clinopyroxene, amphibole, and rarely orthopyroxene as minor minerals. In the some troctolites, along the grain boundaries of olivine and plagioclase, there are narrow kelyphitic rims in which orthopyroxene, clinopyroxene, and amphibole have been observed. Accessory minerals in these rocks are presented by chrome-spinel, magnetite, and less often by sulfides (pyrrhotite, chalcopyrite). The irregularity of distribution of rock-forming minerals and taxitic texture of troctolites indicate significant variations in the contents of major elements, which have the following ranges of average values (wt%): SiO_2 (38–49), Al_2O_3 (8–26), CaO (8–15), MgO (8.5–25.0), FeO_{tot} (2–11), Na_2O (0.1–2.0), and K_2O (0.01–0.70). The average values of petrochemical parameters of troctolites are the following: $100 \cdot FeO_{tot}/(FeO_{tot} + MgO)$ (~36); MgO/CaO (~3.2); Al_2O_3/MgO (~1.5); and CaO/Al_2O_3 (~0.6) (Lesnov, 1986).

To characterize the rare earth composition of troctolites, the limited quantity of analyses of their samples from several different massifs (Table 4.10) has been used. The level of La accumulation in these troctolites varies over the range of 0.5–8.2 t. ch. and average to about 3.7 t. ch.. The level of Ce accumulation is slightly lower (0.4–6.3 t. ch.) and average to 2.7 t. ch.; and the level of Yb is even lower (0.1–4.4 t. ch.) and average to about 0.9 t. ch. Values of parameter $(La/Yb)_n$ in the studied troctolites vary over rather wide interval and are mainly greater than unity. The relative enrichment of troctolites with light REE, as well as the overall negative slope of their REE spectra are observed in a majority of samples (Fig. 4.10). Their spectra almost always show positive Eu anomalies of moderate or low intensities. Values of the parameter $(Eu/Eu^*)_n$ in investigated samples of troctolites vary over the interval 1.1–7.8.

In troctolites from the Dovyrensky massif, which have been the most analyzed samples, the total level of REE accumulation is essentially lower than that in N-MORB basalts. In all the samples from the Dovyrensky massif, the chondrite-normalized contents of light REE are appreciably higher than heavy REE, and the values of parameter $(La/Yb)_n$ ranges from 3.6 to 42.8. Their spectra show positive Eu anomalies, the intensity of which decreases as the total REE content in the samples increases (Fig. 4.10, 1; Fig. 4.11). A lower level of light REE accumulation is observed in troctolites from the Marinkin massif, for which the REE spectra are comparable to those of samples from the Dovyrensky massif (see Fig. 4.10, 2).

Undoubtedly, the available analytical data are not enough for full representation of the regularities of REE distribution in troctolites. Obviously, a major part of these trace elements is concentrated in plagioclase, on which the modal quantity of both the total REE content and the intensity of positive Eu anomalies observable on their spectra are considerably depended.

Table 4.10 Rare earth element composition of troctolites (ppm).

	Massifs									
	Dovyrensky, Russia									
	(Author's data), INAA									
Element	d-301	d-302	d-332	d-333	d-335	d-345	d-384	d-385	d-402	d-403
La	0.8	0.4	1.06	0.9	2	1.14	1.5	1.7	1.2	1.1
Ce	1.22	0.26	1.5	1.6	4.02	1.76	3.3	3.2	2.9	1.73
Pr	N.d.	N.d.	N.d.	N.d.	N.d.	N.d.	N.d.	N.d.	N.d.	N.d.
Nd	0.48	0.24	1.2	0.62	2.33	0.91	1.54	1.2	0.93	0.63
Sm	0.12	0.064	0.4	0.19	0.67	0.27	0.45	0.26	0.17	0.14
Eu	0.15	0.17	0.21	0.15	0.31	0.14	0.16	0.28	0.28	0.27
Gd	0.16	0.068	0.46	0.21	0.75	0.32	0.46	0.26	0.18	0.19
Tb	0.03	0.013	0.07	0.033	0.12	0.056	0.073	0.03	0.03	0.075
Dy	N.d.	N.d.	N.d.	N.d.	N.d.	N.d.	N.d.	N.d.	N.d.	N.d.
Ho	N.d.	N.d.	N.d.	N.d.	N.d.	N.d.	N.d.	N.d.	N.d.	N.d.
Er	N.d.	N.d.	N.d.	N.d.	N.d.	N.d.	N.d.	N.d.	N.d.	N.d.
Tm	N.d.	N.d.	N.d.	N.d.	N.d.	N.d.	N.d.	N.d.	N.d.	N.d.
Yb	0.12	0.039	0.2	0.13	0.27	0.018	0.22	0.064	0.06	0.17
Lu	0.015	0.005	0.028	0.015	0.039	0.021	0.028	0.006	0.008	0.014
Total	N.d.	N.d.	N.d.	N.d.	N.d.	N.d.	N.d.	N.d.	N.d.	N.d.
$(La/Yb)_n$	4.50	6.92	3.58	4.67	5.00	42.8	4.60	17.9	13.5	4.37
$(Eu/Eu^*)_n$	3.27	7.68	1.62	2.44	1.41	1.49	1.13	3.88	5.07	3.20

	Massifs								
	Marinkin, Russia			Zaoblachny, Ru.	Shildyrkheysky, Rus.	Lukinda, Russia	Nomgon., Mong.	Bayantsag., Mon.	Kokpektinsky, Russia
	(Izokh *et al.*, 1998), INAA					(Data Krivenko), INAA	(Izokh *et al.*, 1998), INAA		(Fershtater & Bea, 1996), ICP-MS
Element	B-2667	B-2668	B-2721	B-3660	6404	B-1432	I-4668	I-2261	hb-343
La	0.31	0.68	0.63	0.54	1.3	1.37	0.4	0.14	0.13
Ce	0.6	1.3	1.1	1.3	3.2	2.05	0.75	0.4	0.86
Pr	N.d.	N.d.	N.d.	N.d.	N.d.	N.d.	N.d.	N.d.	0.13
Nd	0.3	0.7	0.5	0.8	2.4	1.77	0.4	0.5	0.74
Sm	0.07	0.17	0.09	0.22	0.81	0.29	0.11	0.13	N.d.
Eu	0.1	0.12	0.17	0.17	0.48	0.35	0.11	0.09	0.15
Gd	0.08	0.18	0.2	0.2	1	0.25	0.3	0.2	0.38
Tb	0.1	0.03	0.1	0.08	0.18	0.04	0.02	0.03	N.d.
Dy	N.d.	N.d.	N.d.	N.d.	N.d.	N.d.	N.d.	N.d.	0.48
Ho	N.d.	N.d.	N.d.	N.d.	N.d.	N.d.	N.d.	N.d.	0.09
Er	N.d.	N.d.	N.d.	N.d.	N.d.	N.d.	N.d.	N.d.	0.26
Tm	N.d.	N.d.	N.d.	N.d.	N.d.	0.02	N.d.	N.d.	N.d.
Yb	0.05	0.1	0.05	0.12	0.73	0.1	0.07	0.12	0.28
Lu	0.0075	0.015	0.007	0.016	0.11	0.02	0.01	0.019	N.d.
Total	N.d.	N.d.	N.d.	N.d.	N.d.	N.d.	N.d.	N.d.	3.50
$(La/Yb)_n$	4.19	4.59	8.51	3.04	1.20	9.25	3.86	0.79	0.31
$(Eu/Eu^*)_n$	1.10	2.17	1.80	1.64	1.64	4.09	3.04	1.89	N.d.

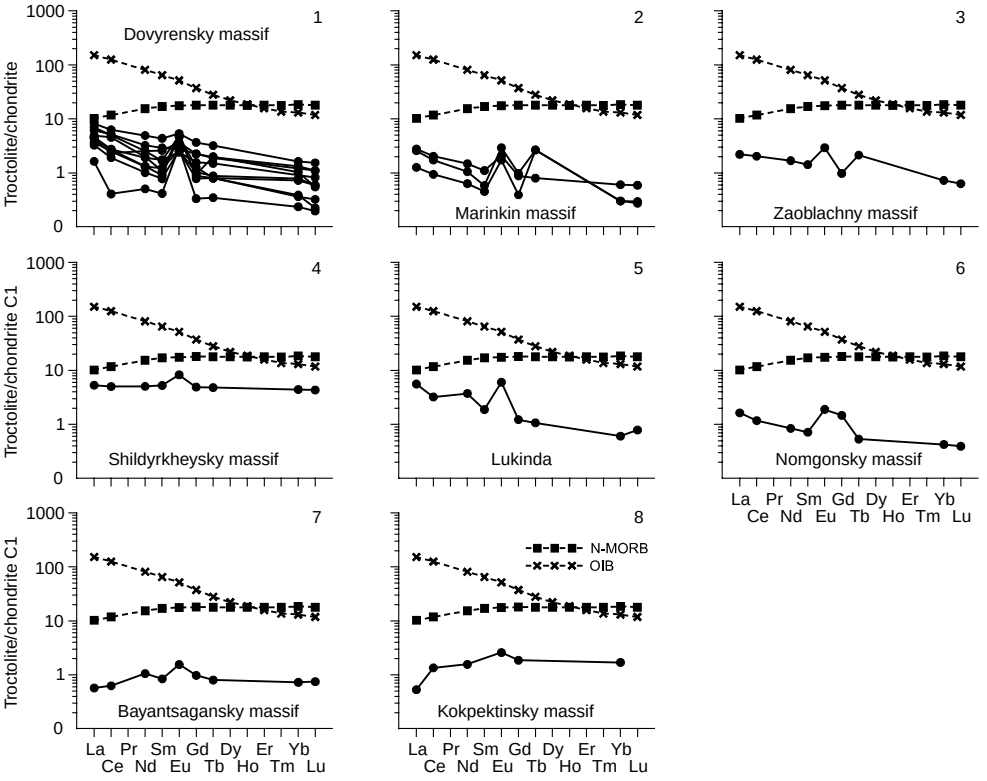

Figure 4.10 Chondrite-normalized REE patterns for troctolites from some massifs (data Table 4.10).

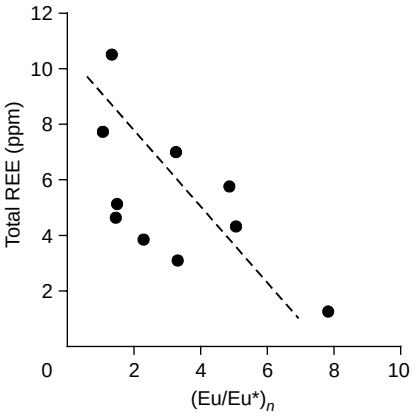

Figure 4.11 Correlation between the parameter $(Eu/Eu^*)_n$ and total REE composition of troctolites from Dovyrensky massif (data Table 4.10).

Troctolites are usually regarded as the products of crystallization and gravitational fractionation of basic melts. At the same time, the geological, structural, and petrographical investigations of troctolites from banded complexes of some polygenetic mafic–ultramafic massifs that enter into ophiolite associations, have allowed us to assume that some varieties of troctolites are of a hybrid nature, similar to the above-described olivine gabbros (see Section 4.4). Rocks from the banded complexes could be generated as a result of crystallization of basic melts contaminated to some extent by substances from ultramafic restites, in which the melts intruded. This process evidently proceeded in conditions of mesoabyssal and abyssal depths for a long time (Lesnov, 1984, 1986, 1988). At similar magmatic and metasomatic interactions with restites, the initial basic melts should be enriched with refractory components, in particular Mg, and simultaneously depleted of low-melting components, including REE. The assumption that some troctolites are of hybrid nature is confirmed by the recently obtained results of numerical modeling of troctolite formation processes on the basis of data on chemical compositions of these rocks occurring in the upper shell of the moon (Ariskin, 2007).

For a fuller representation about the peculiarities of REE distribution in troctolites, and also for an estimation of physical and chemical conditions of formation of this specific variety of mafic rock, further complex investigations with use of more-representative collections of samples from polytypic ultramafic–mafic massifs are necessary.

4.6 ANORTHOSITES

Anorthosites take part in structures of the majority of mafic–ultramafic massifs located in folded areas as one of the less common varieties of rock. In most cases, they form individual sheet bodies of small thickness and various extents, which are interleaved with bodies of troctolites, olivine gabbros, and plagioclase-bearing peridotites. Sometimes these rocks form the more or less clearly expressed, often branching, small-thickened veins, which inject ultramafic rocks. Anorthosites are represented in much greater volumes in large autonomous massifs, which are exposed in deeply eroded folded structures of the Precambrian era. In these cases, they associate with less abundant gabbroids, as well as plagioclase-bearing peridotites. Anorthosites have also been found among lunar magmatic rocks. The minor phases of some anorthosites can be clinopyroxene, orthopyroxene, olivine, amphibole, and garnet. The structure of the rocks varies from medium- to coarse-grained, and they are sometimes non-uniform; frequently anorthosites have a banded structure. These rocks are characterized by the following ranges of average contents of the major chemical components (wt%): SiO_2 (47–51.3), Al_2O_3 (24–30), CaO (11.7–15), MgO (0.85–4.5), and Na_2O (2.2–4.1). Rather narrow ranges of the mean of petrochemical parameters CaO/Al_2O_3 (0.47–0.53) and MgO/CaO (0.04–0.34) and wide intervals of values of the parameters Al_2O_3/MgO (5.8–56) and $100 \cdot FeO_{tot}$ ($FeO_{tot} + MgO$) (53–76) are characteristic of these rocks (Lesnov, 1986).

The major factor controlling REE distribution in anorthosites is the REE content in plagioclase (Duchesne *et al.*, 1974). From the available limited data, the total REE content in these rocks vary over the range of 2.7–82 ppm (Table 4.11), increasing from

Table 4.11 Rare earth element composition of anorthosites (ppm).

	Massifs											
	Glavny khrebet, Russia							Tsentral'ny, Russia		Kalarsky, Russia		Shildyrkheysky, Russia
	(Sukhanov *et al.*, 1990), RNAA											(Izokh *et al.*, 1998), INAA
Element	Sukh-1	Sukh-2	Sukh-4	Sukh-5	Sukh-6	Sukh-10	Sukh-12	Sukh-13	Sukh-14	Sukh-25	Sukh-26	6390
La	0.67	1.1	1.9	2.6	3	14	18	1.2	1.7	6	1.9	1.07
Ce	1.2	2.4	3.6	5.1	7.1	19	26	1.9	3	11	3.4	2.18
Pr	N.d.	N.d.	N.d.	N.d.	N.d.	N.d.	N.d.	N.d.	N.d.	N.d.	N.d.	N.d.
Nd	N.d.	N.d.	N.d.	N.d.	N.d.	N.d.	N.d.	N.d.	N.d.	N.d.	N.d.	1.2
Sm	0.27	0.04	0.58	0.86	1.2	0.67	1.2	0.27	0.23	1.3	0.19	0.32
Eu	0.15	0.24	0.43	0.47	0.74	1.2	2.8	0.29	0.49	1	0.62	0.44
Gd	N.d.	N.d.	N.d.	N.d.	N.d.	N.d.	N.d.	N.d.	N.d.	N.d.	N.d.	0.29
Tb	0.084	0.1	0.12	0.16	0.25	0.069	0.09	0.04	0.047	0.15	0.042	0.05
Dy	N.d.	N.d.	N.d.	N.d.	N.d.	N.d.	N.d.	N.d.	N.d.	N.d.	N.d.	N.d.
Ho	N.d.	N.d.	N.d.	N.d.	N.d.	N.d.	N.d.	N.d.	N.d.	N.d.	N.d.	N.d.
Er	N.d.	N.d.	N.d.	N.d.	N.d.	N.d.	N.d.	N.d.	N.d.	N.d.	N.d.	N.d.
Tm	N.d.	N.d.	N.d.	N.d.	N.d.	N.d.	N.d.	N.d.	N.d.	N.d.	N.d.	N.d.
Yb	0.25	0.37	0.41	0.68	0.9	0.43	0.19	0.21	0.12	0.67	0.79	0.12
Lu	0.049	0.06	0.071	0.12	0.14	0.098	0.03	0.18	0.36	0.11	0.068	0.018
Total	N.d.	N.d.	N.d.	N.d.	N.d.	N.d.	N.d.	N.d.	N.d.	N.d.	N.d.	N.d.
$(La/Yb)_n$	1.81	2.01	3.13	2.58	2.25	21.98	63.95	3.86	9.56	6.05	1.62	6.02
$(Eu/Eu^{**})_n$	1.29	2.82	2.13	1.64	1.76	6.68	9.47	3.54	6.15	2.77	9.07	4.44

	Massifs											
	Nomgon, Russia	Dugdinsky, Russia		Sept Iles, Canada								
	(Izokh *et al.*, 1998)	(Mekhonoshin *et al.*, 1986)		(Higgins & Doig, 1986), NAA								
Element	I-4640	Mekh-7	Mekh-8	H120	H125	H140	H148	H41	H60	H68	H77	H86
La	1.5	1.9	1.9	3.1	5	3.58	3.45	7.6	12.8	19.5	19.1	10.8
Ce	3.4	5.1	7.2	7.43	11.3	8.9	8.76	17.4	31.6	43.5	43.6	23.6
Pr	N.d.	N.d.	N.d.	N.d.	N.d.	N.d.	N.d.	N.d.	N.d.	N.d.	N.d.	N.d.
Nd	2.5	2	7.4	N.d.	N.d.	N.d.	N.d.	N.d.	N.d.	N.d.	N.d.	N.d.
Sm	0.74	0.65	1	0.85	1.74	1.15	0.76	2.78	3.43	8	4.76	2.72
Eu	0.35	0.51	0.75	1.02	1.06	0.99	0.98	1.31	1.94	2.7	2.28	1.68
Gd	0.9	N.d.	N.d.	N.d..	N.d.	N.d.	N.d.	N.d.	N.d.	N.d.	N.d.	N.d.
Tb	0.14	0.08	0.13	0.11	0.13	0.1	0.12	N.d.	0.56	0.93	0.89	0.53
Dy	N.d.	N.d.	N.d.	0.67	0.92	N.d.	0.64	1.73	3.29	5.3	5.57	3.15
Ho	N.d.	N.d.	N.d.	N.d.	N.d.	N.d.	N.d.	N.d.	N.d..	N.d.	N.d.	N.d.
Er	N.d.	N.d.	N.d.	N.d.	N.d.	N.d.	N.d.	N.d.	N.d.	N.d.	N.d.	N.d.
Tm	N.d.	N.d..	N.d.	N.d.	N.d.	N.d.	N.d.	N.d.	N.d.	N.d.	N.d.	N.d.
Yb	0.4	0.17	0.26	0.28	0.5	0.34	0.29	0.73	1.45	2.26	2.45	1.18
Lu	0.06	N.d.	N.d.	0.04	0.04	0.05	0.03	0.11	0.19	0.28	0.28	0.17
Total	N.d.	N.d.	N.d.	N.d.	N.d.	N.d.	N.d.	N.d.	N.d.	N.d.	N.d.	N.d.
$(La/Yb)_n$	2.53	7.54	4.93	7.47	6.75	7.12	8.03	7.03	5.96	5.82	5.26	6.18
$(Eu/Eu^{**})_n$	1.41	4.16	2.47	3.37	4.15	2.50	1.80	1.21	1.44	1.82	1.41	4.16

$(Eu^{**})_n = (Sm + Tb)_n/2$.

Table 4.12 Average REE composition of anorthosites from some massifs (ppm).

	Massifs				
Element	Tsentral'ny (2)	Kalarsky (2)	Dugdinsky (2)	Glavny khrebet (7)	Sent Iles (9)
La	1.450	3.950	1.900	5.896	9.437
Ce	2.450	7.200	6.150	9.200	21.79
Pr	N.d.	N.d.	N.d.	N.d.	N.d.
Nd	N.d.	N.d.	4.700	N.d.	N.d.
Sm	0.250	0.745	0.825	0.689	2.910
Eu	0.390	0.810	0.630	0.861	1.551
Gd	N.d.	N.d.	N.d.	N.d.	N.d.
Tb	0.044	0.096	0.105	0.125	0.421
Dy	N.d.	N.d.	N.d.	N.d.	2.659
Ho	N.d.	N.d.	N.d.	N.d.	N.d.
Er	N.d.	N.d.	N.d.	N.d.	N.d.
Tm	N.d.	N.d.	N.d.	N.d.	N.d.
Yb	0.165	0.730	0.215	0.461	1.053
Lu	0.270	0.089	N.d.	0.081	0.132
Total	N.d.	N.d.	N.d.	N.d.	N.d.
$(La/Yb)_n$	6.71	3.83	6.24	14.0	6.62
$(Eu/Eu^{**})_n$	4.84	5.92	2.68	3.69	2.55

Data Table 4.11. $(Eu/Eu^{**})_n = 2Eu_n/(Sm + Tb)_n$.

samples of the Central'ny massif to samples from the Sept Iles massif. The samples from the Sept Iles massif contain more light REE than those from basalts of the N-MORB type, but they contain less than OIBs. In the majority of the studied anorthosites, the level of La accumulation is much higher than the level of Yb. Values of the parameter $(La/Yb)_n$ in them vary over the interval 1.6–64; its mean values decrease from samples from the Glavny khrebet massif (14) to samples from the Kalarsky massif (3.8) (see Table 4.12). In REE spectra of anorthosites, intensive positive Eu anomalies (Fig. 4.12) are usually observed. Values of the parameter $(Eu/Eu^*)_n$ in the limits of the used dataset of analyses vary over the interval 1.2–9.5. The example of anorthosites from the massifs of Sept Iles and the Kalarsky Ridge confirms the above-mentioned regularity of a progressive rise in intensity of positive Eu anomalies with decreasing total level of REE accumulation in the rocks (see Fig. 4.12, 1, 4). In anorthosites from the Glavny Khrebet massif, the opposite trend (see Fig. 4.12, 2) is observed, which can be a sign of certain differences in formation conditions of the rocks in the above-noted massifs.

4.7 ECLOGITES

Most often, eclogites occur in deep-seated xenoliths from kimberlites and alkaline basaltic rocks, as well as in structures of tectonic blocks among ancient metamorphic belts. One such extended high-pressure belt is traced from the central regions of China to Kirghizia, and further to other regions of central Asia and polar Ural (Marakushev *et al.*, 2003). These rocks are characterized by a variety of mineral parageneses, which usually include garnet of pyrope-almandine-grossular composition, clinopyroxene (mainly omphacite), as well as various amphiboles: glaucophane,

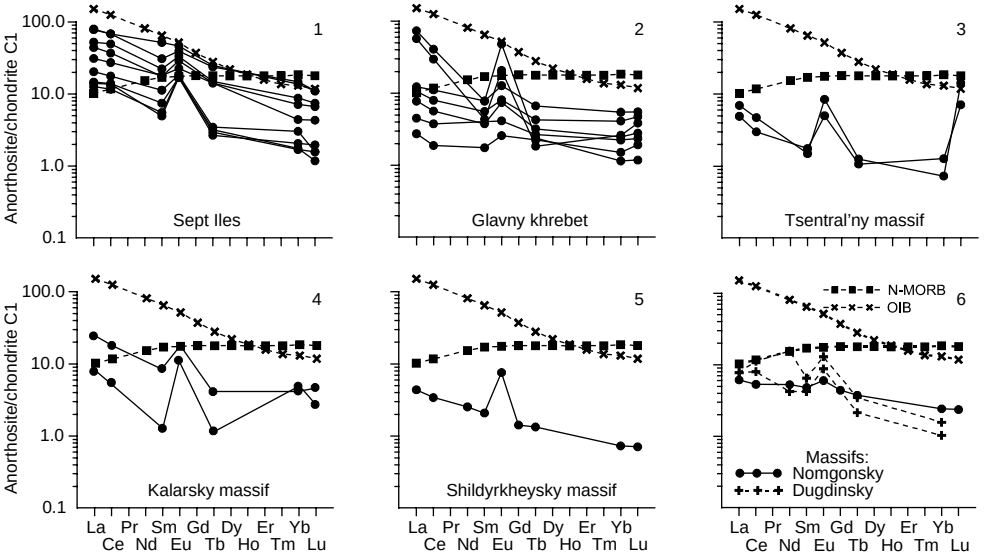

Figure 4.12 Chondrite-normalized REE patterns for anorthosites from some massifs (data Table 4.11).

actinolite, ferropargasite, barroisite, and winchite. Some eclogites contain quartz, phengite, plagioclase, epidote, zoisite, paragonite, talc, rutile, and others as minor minerals. The major element contents in these rocks vary in the following limits (wt%): SiO_2 (42.4–53.5), TiO_2 (0.2–5.0), Al_2O_3 (6.8–28.8), FeO_{tot} (5.5–17.5), MgO (3.4–1.6), CaO (6.2–14.0), Na_2O (0.4–6.0), and K_2O (0.02–1.2). The values of petrochemical parameters vary over the following ranges: MgO/CaO (0.2–0.9); Ca/Al_2O_3(0.3–1.3); Al_2O_3/MgO (0.7–6.3); and $100 \cdot FeO_{tot}/(FeO_{tot} + MgO)$ (37–77). In the opinion of the majority of researchers, eclogites were formed at high-pressure metamorphism of mafic rocks of various compositions (Miller *et al.*, 1988; Dobretsov *et al.*, 1989; Shatsky, 1990; Marakushev *et al.*, 2003; Lesnov *et al.*, 2004a). According to petrochemical and geochemical data, protoliths of eclogites were often various types of basalt and gabbro: tholeiite, alkaline, and calc-alkaline. In those samples of eclogites for which the rare earth composition is known, we present their chemical composition (Table 4.13).

The first data on the rare earth composition of eclogites were obtained by samples from deep-seated xenoliths, collected in kimberlite and alkaline basalt diatremes (Philpotts *et al.*, 1972). Later, eclogites that presented in metamorphic complexes of Norway (Gebauer *et al.*, 1985; Griffin & Brueckner, 1985), Austria (Miller *et al.*, 1988), Kirghizia and Kazakhstan (Dobretsov *et al.*, 1989; Shatsky, 1990), and some other regions (Table 4.14) were studied in this respect in more detail. The total REE content in studied eclogites varies over the interval 10–95 ppm and averages to about 38 ppm, which is comparable to the total REE content in N-MORBs (40 ppm). The average level of La accumulation in eclogites is 25 t. ch., and the average level of Yb is 17 t. ch. In most cases, the rare earth spectra display an overall negative slope (Fig. 4.13), with a mean of the parameter $(La/Yb)_n$ at 1.5. The rare earth spectra of some eclogite varieties have negative or positive Eu anomalies of insignificant intensity.

Table 4.13 Chemical composition of eclogites from some metamorphic complexes (wt %).

	Complexes											
	Atbashi, Kirgizia				Kumdy Kol', Kazakhstan				Kulet, Kazakhstan			
	(Lesnov *et al.*, 2005)		(Shatsky, 1990)									
Component	L-12	L-13	83-4	82-01	82-03	86-465	83-12	83-18	83-6	84-27	86-54	87-9
SiO_2	47.69	44.40	49.69	52.27	48.90	49.87	47.07	51.79	47.12	49.72	49.16	50.44
TiO_2	1.66	1.75	0.70	0.73	1.81	1.72	1.00	1.22	0.97	0.82	2.53	2.48
Al_2O_3	10.54	13.98	13.41	10.53	13.29	13.42	15.11	13.65	15.34	13.18	11.99	12.58
FeO_{tot}	11.54	15.17	9.47	13.39	13.42	12.96	12.31	12.11	12.89	13.28	15.77	11.09
MnO	0.19	0.26	0.17	0.16	0.19	0.22	0.18	0.18	0.19	0.20	0.26	0.20
MgO	7.93	7.10	7.33	9.19	7.11	7.56	7.96	6.32	7.82	7.66	5.26	5.84
CaO	13.32	9.17	11.29	12.52	11.04	9.66	11.41	11.00	12.26	10.26	9.85	12.58
Na_2O	4.64	2.97	2.56	3.05	2.36	1.62	1.74	1.92	2.39	2.48	2.16	2.59
K_2O	0.11	0.14	0.86	0.34	0.15	0.12	0.40	0.23	0.17	0.14	0.10	0.17
P_2O_5	0.04	0.02	0.14	0.17	0.27	0.13	0.17	0.23	0.16	0.17	0.22	0.26
CaO/Al_2O_3	1.26	0.66	0.84	1.19	0.83	0.72	0.76	0.81	0.80	0.78	0.82	1.00
MgO/CaO	0.60	0.77	0.65	0.73	0.64	0.78	0.70	0.57	0.64	0.75	0.53	0.46
Al_2O_3/MgO	1.33	1.97	1.83	1.15	1.87	1.78	1.90	2.16	1.96	1.72	2.28	2.15
Fe#	59.3	68.1	57.8	50.8	65.3	63.2	60.7	65.7	62.2	63.4	75.0	65.5

	Complexes											
	Aktiuz, Kirgizia		Chiglinka, Kazakhstan			Sulu Tube, Kazakhstan			Enbek Berlyk, Kaz.		Makbal	Austria
	(Shatsky, 1990)											(Miller *et al.*, 1988)
Component	83-17	81-1	84-12	84-3a	84-8	81-5	82-42	84-6	83-57	83-69	82-261	H8
SiO_2	43.88	47.44	48.64	48.93	50.82	47.86	48.78	47.85	49.81	48.42	52.35	50.93
TiO_2	3.85	5.01	1.34	2.07	3.22	1.63	1.82	1.15	0.76	1.00	0.32	0.63
Al_2O_3	15.06	12.19	14.47	13.52	12.67	13.75	12.91	14.10	14.27	14.73	6.80	16.18
FeO_{tot}	17.54	12.90	12.15	13.91	15.39	11.80	15.44	10.43	11.35	13.66	11.39	7.16
MnO	0.19	0.19	0.18	0.18	0.19	0.19	0.19	0.17	0.18	0.19	0.33	0.14
MgO	5.90	4.96	7.73	6.23	4.67	7.29	5.92	7.38	7.88	7.61	10.05	8.66
CaO	7.97	10.30	12.00	11.18	9.16	11.30	10.71	12.83	12.16	10.22	10.82	12.98
Na_2O	2.84	4.37	1.77	1.89	1.52	3.41	2.11	2.19	1.54	1.97	0.86	1.69
K_2O	0.57	0.25	0.14	0.26	0.19	0.29	0.16	0.20	0.28	0.33	0.11	0.02
P_2O_5	0.25	0.34	0.22	0.29	0.45	0.29	0.23	0.26	0.19	0.19	0.02	0.06
CaO/Al_2O_3	0.53	0.84	0.83	0.83	0.72	0.82	0.83	0.91	0.85	0.69	1.59	0.80
MgO/CaO	0.74	0.48	0.64	0.56	0.51	0.65	0.55	0.58	0.65	0.74	0.93	0.67
Al_2O_3/MgO	2.55	2.46	1.87	2.17	2.71	1.89	2.18	1.91	1.81	1.94	0.68	1.87
Fe#	74.8	72.2	61.1	69.1	76.7	61.8	72.3	58.6	59.0	64.2	53.1	45.3

(*Continued*)

Table 4.13 Continued

	Complexes											
	Austria											
	(Miller *et al.*, 1988)											
Component	SKP9	SK1	H12	KM10	KK1	KP2	KGR5	FYK236	SWR	SK17	GE2	SG4
SiO_2	48.92	42.40	49.09	48.29	50.30	49.39	44.70	46.45	47.66	48.67	46.67	48.74
TiO_2	0.58	0.42	1.60	1.87	1.72	1.74	2.70	1.32	1.51	1.45	2.08	2.54
Al_2O_3	16.72	28.78	14.67	14.39	14.94	14.97	14.20	14.89	16.97	15.56	15.26	14.55
FeO_{tot}	7.01	6.72	10.80	12.26	10.57	10.65	15.16	8.51	8.22	10.52	12.26	10.44
MnO	0.11	0.09	0.18	0.19	0.17	0.18	0.25	0.17	0.16	0.19	0.23	0.18
MgO	9.17	4.59	7.59	7.49	7.17	6.79	5.59	8.25	7.79	8.08	6.37	8.13
CaO	14.07	15.10	11.81	11.89	11.02	11.55	11.62	15.45	14.10	12.80	12.10	12.10
Na_2O	2.40	1.10	2.50	2.68	2.62	2.37	3.45	2.05	1.91	2.02	2.88	2.93
K_2O	0.02	0.06	0.02	0.04	0.09	0.11	0.09	0.21	0.07	0.03	0.09	0.02
P_2O_5	0.04	0.05	0.16	0.18	0.17	0.23	0.23	0.18	0.18	0.13	0.18	0.12
CaO/Al_2O_3	0.84	0.52	0.81	0.83	0.74	0.77	0.82	1.04	0.83	0.82	0.79	0.83
MgO/CaO	0.65	0.30	0.64	0.63	0.65	0.59	0.48	0.53	0.55	0.63	0.53	0.67
Al_2O_3/MgO	1.82	6.27	1.93	1.92	2.08	2.20	2.54	1.80	2.18	1.93	2.40	1.79
Fe#	43.3	59.4	58.3	62.1	59.6	61.1	73.1	50.8	51.3	56.6	65.8	56.2

Chemical composition tacked only for samples, which have data about their REE composition (see Table 4.14). $Fe\# = 100 \cdot FeO_{tot}/(FeO_{tot} + MgO)$.

Table 4.14 Rare earth element composition of eclogites from some metamorphic complexes and provinces of alkali basalts and kimberlites (ppm).

	Complexes (provinces)													
	Atbashi, Kirgizia									Aktiuz, Kirgizia		Makbal, Kirgizia		
	(Lesnov *et al.*, 2005a), ICP-MS		(Shatsky, 1990), INAA											
Element	L-12[a]	L-13[a]	11	28	83-4[a]	83-7	83-22	83-5	83-17a[a]	83-17[a]	81-1[a]	82-284	82-261[a]	16-192
La	3.752	8.262	2.6	4	2.1	9.4	3.6	2.4	2.2	9	13	9.3	9.7	4.8
Ce	6.488	15.84	4	16.5	N.d.	42	10	7	6	28	30	20	31.5	15
Pr	1.251	2.142	N.d.	N.d.	N.d.	N.d.	N.d.	N.d.	N.d.	N.d.	N.d.	N.d.	N.d.	N.d.
Nd	6.722	9.103		10	2.1	14.2	8	5	4	13	18.8	9	12.1	7.6
Sm	2.032	2.448	1.7	4	2.2	4.9	2.9	1.8	1.5	N.d.	4.5	2.2	4.1	3.8
Eu	0.625	0.800	0.7	1.5	0.9	0.96	1	0.7	0.58	N.d.	1.2	0.81	N.d.	0.95
Gd	3.361	4.131	N.d.	N.d.	N.d.	N.d.	N.d.	N.d.	N.d.	N.d.	N.d.	N.d.	N.d.	N.d.
Tb	0.703	0.994	N.d.	N.d.	N.d.	N.d.	N.d.	0.46	0.41	N.d.	N.d.	0.5	4	4
Dy	5.550	7.650	N.d.	N.d.	N.d.	N.d.	N.d.	N.d.	N.d.	N.d.	N.d.	N.d.	N.d.	N.d.
Ho	1.329	1.836	N.d.	N.d.	N.d.	N.d.	N.d.	N.d.	N.d.	N.d.	N.d.	N.d.	N.d.	N.d.
Er	3.908	5.508	N.d.	N.d.	N.d.	N.d.	N.d.	N.d.	N.d.	N.d.	N.d.	N.d.	N.d.	N.d.
Tm	0.625	0.918	1.8	1.1	0.7	0.8	0.7	N.d.	N.d.	N.d.	0.5	N.d.	0.8	0.6
Yb	4.143	5.737	1.8	5.3	2.2	5.2	4	2.5	2.3	2.3	1.8	1.8	4.7	5.6
Lu	0.625	0.841	0.2	N.d.	N.d.	N.d.	N.d.	0.37	0.31	N.d.	N.d.	0.3	1	0.76
Total	41.1	66.2	N.d.	N.d.	N.d.	N.d.	N.d.	N.d.	N.d.	N.d.	N.d.	N.d.	N.d.	N.d.
$(La/Yb)_n$	0.61	0.97	0.97	0.51	0.64	1.21	0.60	0.64	0.64	2.63	4.85	3.47	1.39	0.58

(*Continued*)

Table 4.14 Continued

	Complexes (provinces)											
	Kulet, Kazakhstan									Kumdy Kol', Kazakhstan		
	(Shatsky, 1990), INAA											
Element	83-18[a]	83-6[a]	83-12[a]	Ku-83-53	Ku-83-3	86-54[a]	84-27[a]	87-9[a]	Ku-16-79	82-01[a]	82-03[a]	86-465[a]
La	10.6	7.8	8.1	5.54	8	6.61	1.68	14.8	4.4	1.8	8.3	4.16
Ce	N.d.	19	11.3	12.4	14.2	13.9	21.7	32	10	5.7	20.1	5.46
Pr	N.d.	N.d.	N.d.	N.d.	N.d.	N.d.	N.d.	N.d.	N.d.	N.d.	N.d.	N.d.
Nd	13.3	12	21.2	N.d.	N.d.	N.d.	N.d.	20	20	N.d.	14.2	N.d.
Sm	3.7	2.7	2.9	3.78	4.2	5.06	4.46	3.9	2	1.3	4.6	3.9
Eu	1.8	1.2	1	0.85	1.1	1.39	1.08	2.3	1.5	0.5	1.6	0.61
Gd	N.d.	N.d.	N.d.	N.d.	N.d.	N.d.	N.d.	N.d.	N.d.	N.d.	N.d.	N.d.
Tb	0.63	0.5	0.77	0.81	0.7	1.52	0.56	0.61	0.87	0.24	0.75	0.44
Dy	N.d.	N.d.	N.d.	N.d.	N.d.	N.d.	N.d.	N.d.	N.d.	N.d.	N.d.	N.d.
Ho	N.d.	N.d.	N.d.	N.d.	N.d.	N.d.	N.d.	N.d.	N.d.	N.d.	N.d.	N.d.
Er	N.d.	N.d.	N.d.	N.d.	N.d.	N.d.	N.d.	N.d.	N.d.	N.d.	N.d.	N.d.
Tm	N.d.	N.d.	N.d.	N.d.	N.d.	N.d.	N.d.	0.29	N.d.	N.d.	0.75	N.d.
Yb	2.6	1.8	2.3	3.55	1.06	6.13	2	1.5	3.6	1	4.1	1.94
Lu	N.d.	0.28	N.d.	0.5	0.1	0.74	0.21	0.3	N.d.	N.d.	0.73	0.43
Total	N.d.	N.d.	N.d.	N.d.	N.d.	N.d.	N.d.	N.d.	N.d.	N.d.	N.d.	N.d.
$(La/Yb)_n$	2.74	2.91	2.36	1.05	5.07	0.72	0.56	6.62	0.82	1.21	1.36	1.44

	Complexes (provinces)													
	Chiglinka, Kazakhstan			Sulu Tube, Kazakhstan			Enbek Berlyk, Kazakhstan		Norway					
	(Shatsky, 1990), INAA								(Griffin & Brueckner, 1985)					
Element	84-12[a]	84-3a[a]	84-8[a]	81-5[a]	82-42[a]	84-6[a]	83-57[a]	83-69[a]	K-6	182	1428	U-19	N-16	S-19
La	3.7	4.9	18.8	5.8	7.45	3.54	2.7	3.5	5.1	13.6	6.1	1.3	2.6	1.1
Ce	5.6	10.4	40.1	15	15.22	8.36	6.5	8.5	20.8	37.5	25.7	3.7	11.8	4
Pr	N.d.	N.d.	N.d.	N.d.	N.d.	N.d.	N.d.	N.d.	N.d.	N.d.	N.d.	N.d.	N.d.	N.d.
Nd	14.9	N.d.	22.2	10	24.5	N.d.	3.3	6	18.9	51.1	41.1	N.d.	8.6	4
Sm	2.2	2.7	N.d.	3.5	4.83	3.97	1.3	1.86	4.7	9.5	10.4	13	3.4	1.4
Eu	0.78	0.8	2.5	1.29	N.d.	1.06	0.65	0.73	2	6.8	3.9	0.6	1.4	0.6
Gd	N.d.	N.d.	N.d.	N.d.	N.d.	N.d.	N.d.	N.d.	7.4	6.8	10.2	3	N.d.	N.d.
Tb	0.7	0.56	1.6	0.57	1.19	0.85	0.53	0.33	0.7	0.9	1.9	0.4	0.6	0.4
Dy	N.d.	N.d.	N.d.	N.d.	N.d.	N.d.	N.d.	N.d.	N.d.	N.d.	N.d.	N.d.	N.d.	N.d.
Ho	N.d.	N.d.	N.d.	N.d.	N.d.	N.d.	N.d.	N.d.	0.8	1.1	2.2	0.5	N.d.	N.d.
Er	N.d.	N.d.	N.d.	N.d.	N.d.	N.d.	N.d.	N.d.	N.d.	N.d.	N.d.	N.d.	N.d.	N.d.
Tm	N.d.	N.d.	N.d.	N.d.	N.d.	N.d.	0.35	0.21	0.4	0.5	1	0.2	N.d.	N.d.
Yb	4	3.2	9.3	3.9	6.05	2.36	3	2.8	2.8	4.2	6.7	1.3	2.6	2
Lu	N.d.	N.d.	N.d.	0.57	N.d.	0.22	0.38	0.39	0.3	0.3	0.4	0.2	0.4	0.3
Total	N.d.	N.d.	N.d.	N.d.	N.d.	N.d.	N.d.	N.d.	63.9	132	110	N.d.	N.d.	N.d.
$(La/Yb)_n$	0.62	1.03	1.36	1.00	0.83	1.01	0.60	0.84	1.23	2.19	0.61	0.67	0.67	0.37

(*Continued*)

Table 4.14 Continued

	Complexes (provinces)													
	Norway						Austria							
	(Griffin & Brueckner, 1985)				(Gebauer *et al.*, 1985)		(Miller *et al.*, 1988)							
Element	S-53a	5/79A	IB-51	IB-1	68/87	SEL-1	H8[a]	SKP9	SK1[a]	H12[a]	KM10[a]	KK1[a]	KP2[a]	KGR5[a]
La	16	1	6.3	5.1	N.d.	6.01	0.93	0.86	1.39	3.55	4.27	3.7	5.56	5.88
Ce	36.7	7	19.1	12.6	5.31	15.1	2.77	3.04	3.41	11.7	13	11.06	14.5	16.6
Pr	N.d.	N.d.	N.d.	N.d.	N.d.	N.d.	N.d.	N.d.	N.d.	N.d.	N.d.	N.d.	N.d.	N.d.
Nd	20.6	3.1	20.2	9.1	N.d.	N.d.	2.8	3.8	2.65	10.5	12	10.3	15.1	14.1
Sm	4.7	2.1	4.4	2.8	1.2	3.34	1.27	1.28	1.18	3.76	4.07	3.71	5.07	5.25
Eu	1.6	1.4	1.2	1.6	0.48	1.17	0.63	0.64	0.69	1.36	1.37	1.31	1.76	1.73
Gd	N.d.	6.9	N.d.	N.d.	N.d.	N.d.	2	1.9	1.6	N.d.	5.6	N.d.	6.4	6.7
Tb	0.9	1	0.7	0.5	0.26	0.73	0.33	0.35	0.29	0.93	0.96	0.91	1.02	1.27
Dy	N.d.	N.d.	N.d.	N.d.	N.d.	N.d.	N.d.	N.d.	N.d.	N.d.	N.d.	N.d.	N.d.	N.d.
Ho	N.d.	1.6	0.9	N.d.	N.d.	N.d.	0.53	0.61	0.41	N.d.	N.d.	N.d.	1.56	N.d.
Er	N.d.	N.d.	N.d.	N.d.	N.d.	N.d.	N.d.	N.d.	N.d.	N.d.	N.d.	N.d.	N.d.	N.d.
Tm	N.d.	0.6	0.4	N.d.	N.d.	N.d.	0.23	N.d.	N.d.	N.d.	0.76	N.d.	N.d.	N.d.
Yb	6.2	4.4	2.8	1.4	0.94	3	1.5	1.39	0.85	4.11	4.07	3.58	3.59	5.04
Lu	1.3	0.4	0.4	0.3	0.15	0.47	0.25	0.22	0.154	0.64	0.67	0.61	0.54	0.77
Tota	N.d.	29.5	56.4	N.d.	N.d.	N.d.	13.2	14.1	12.6	N.d.	N.d.	N.d.	55.1	N.d.
$(La/Yb)_n$	1.74	0.15	1.52	2.46	N.d.	0.91	0.42	0.42	1.10	0.58	0.71	0.70	1.05	0.79

	Complexes (provinces)													
	Austria					Sierra Leone, Africa								
	(Miller *et al.*, 1988)					(Barth *et al.*, 2002), ICP-MS								
Element	FYK236[a]	SWR[a]	SKP17[a]	GE2[a]	SG4[a]	K 81-2[b]	K 81-11[b]	K 86-15[b]	K 86-19[b]	K 86-58[b]	K 86-73A[b]	K 86-73B[b]	K 86-90[b]	K 86-107[b]
La	9.14	8.47	2.42	4.94	3.42	27.4	26.7	7.71	6.28	16.7	7.85	16.3	3.47	5.08
Ce	19.7	20.4	7.65	14.2	9.8	55.2	68.6	15.6	16.3	37.6	17.2	43.2	7.47	14.1
Pr	N.d.	N.d.	N.d.	N.d.	N.d.	6.33	8.6	1.86	2.43	4.33	2.18	6.17	0.93	2.1
Nd	12	12	7	11.8	10.2	23.6	33.2	7.1	10.7	14.6	8.86	24.5	3.84	9.34
Sm	3.19	3.37	2.64	4.58	3.25	4.07	5.72	1.58	2.53	2.23	2.33	4.38	1.19	2.3
Eu	1.09	1.31	1	1.57	1.15	1.2	1.65	0.65	0.91	0.63	0.8	1.38	0.48	0.72
Gd	N.d.	3.6	3.8	N.d.	4.6	3.85	5.19	2.07	3.34	1.68	3.06	3.77	1.97	2.24
Tb	0.53	0.71	0.69	1.06	0.82	0.57	0.78	0.39	0.73	0.42	0.55	0.6	0.37	0.36
Dy	N.d.	N.d.	N.d.	N.d.	N.d.	3.28	4.75	2.48	5.65	3.04	3.79	3.59	2.54	2.34
Ho	0.99	N.d.	1	N.d.	N.d.	0.69	1.02	0.58	1.64	0.74	0.89	0.74	0.6	0.55
Er	N.d.	N.d.	N.d.	N.d.	N.d.	1.98	3.02	1.78	5.86	2.4	2.72	2.14	1.56	1.63
Tm	0.26	0.27	N.d.	N.d.	0.63	N.d.	N.d.	N.d.	N.d.	N.d.	N.d.	N.d.	N.d.	N.d.
Yb	2.03	2.36	3.11	4.6	3.81	1.94	3.01	1.54	6.95	2.43	2.8	1.95	1.29	1.46
Lu	0.31	0.35	0.53	0.74	0.61	0.3	0.47	0.23	1.1	0.37	0.46	0.3	0.17	0.23
Total	49.2	N.d.	N.d.	N.d.	N.d.	130	163	43.6	64.4	87.2	53.5	109	25.9	42.5
$(La/Yb)_n$	3.04	2.42	0.53	0.72	0.61	9.53	5.99	3.38	0.61	4.64	1.89	5.64	1.82	2.35

(*Continued*)

Table 4.14 Continued

	Complexes (provinces)										
	Kakanui	Bessi, Japan	Datoitspan	Delegate	Obnazhennaya pipe[b]	Roberts Victor, Ghana			Salt Lake	Jagersfontane	Japan
	(Philpotts *et al.*, 1972)		(Balashov, 1976)						(Philpotts *et al.*, 1972)		(Balashov, 1976)
Element	21a[b]	202[b]	bal 26[b]	bal 24[b]	bal 28[b]	bal 25[b]	bal 19[b]	bal 20[b]	42[b]	152[b]	bal 27
La	N.d.	N.d.	7.4	3.6	6.1	4.2	N.d.	N.d.	N.d.	N.d.	1.8
Ce	10.7	14.1	37	14.1	14	9.7	7.73	8.13	6.25	10.9	9.5
Pr	7.73	N.d.	5.4	2.5	2.1	1.6	N.d.	N.d.	N.d.	N.d.	0.7
Nd	2.6	8.13	20	11.7	7.7	5.6	5.19	4.76	4.18	6.37	3.4
Sm	1.17	2.17	4.9	3.8	1.96	1.49	1.11	1.17	1.22	1.08	1.45
Eu	4.6	0.827	1.44	1.25	0.53	0.46	0.417	0.425	0.475	0.353	0.7
Gd	N.d.	2.41	4.7	5.2	2.1	1.7	1.22	1.56	1.61	0.893	2.1
Tb	N.d.	N.d.	0.75	0.75	0.3	0.25	N.d.	N.d.	N.d.	N.d.	0.32
Dy	7.18	1.97	N.d.	5.7	1.4	N.d.	1.66	1.95	1.82	0.568	3.1
Ho	N.d.	N.d.	1.33	1	N.d.	0.45	N.d.	N.d.	N.d.	N.d.	0.39
Er	5.14	0.808	2.9	2.8	1.05	1.6	1.5	1.33	0.955	0.256	1.11
Tm	N.d.	N.d.	0.46	0.41	N.d.	0.22	N.d.	N.d.	N.d.	N.d.	0.14
Yb	5.08	0.721	2.3	2	1.1	1.6	1.95	1.31	0.885	0.193	1.13
Lu	44.2	0.101	N.d.	0.32	N.d.	0.26	0.363	N.d.	N.d.	0.031	0.16
Total	N.d.	31.2	88.6	55.1	38.3	29.1	N.d.	N.d.	N.d.	N.d.	26.0
$(La/Yb)_n$	N.d.	N.d.	2.17	1.21	3.74	1.77	N.d.	N.d.	N.d.	N.d.	1.08

[a] Chemical composition of these samples see in Table 4.13.

[b] These samples tacked from deep xenoliths.

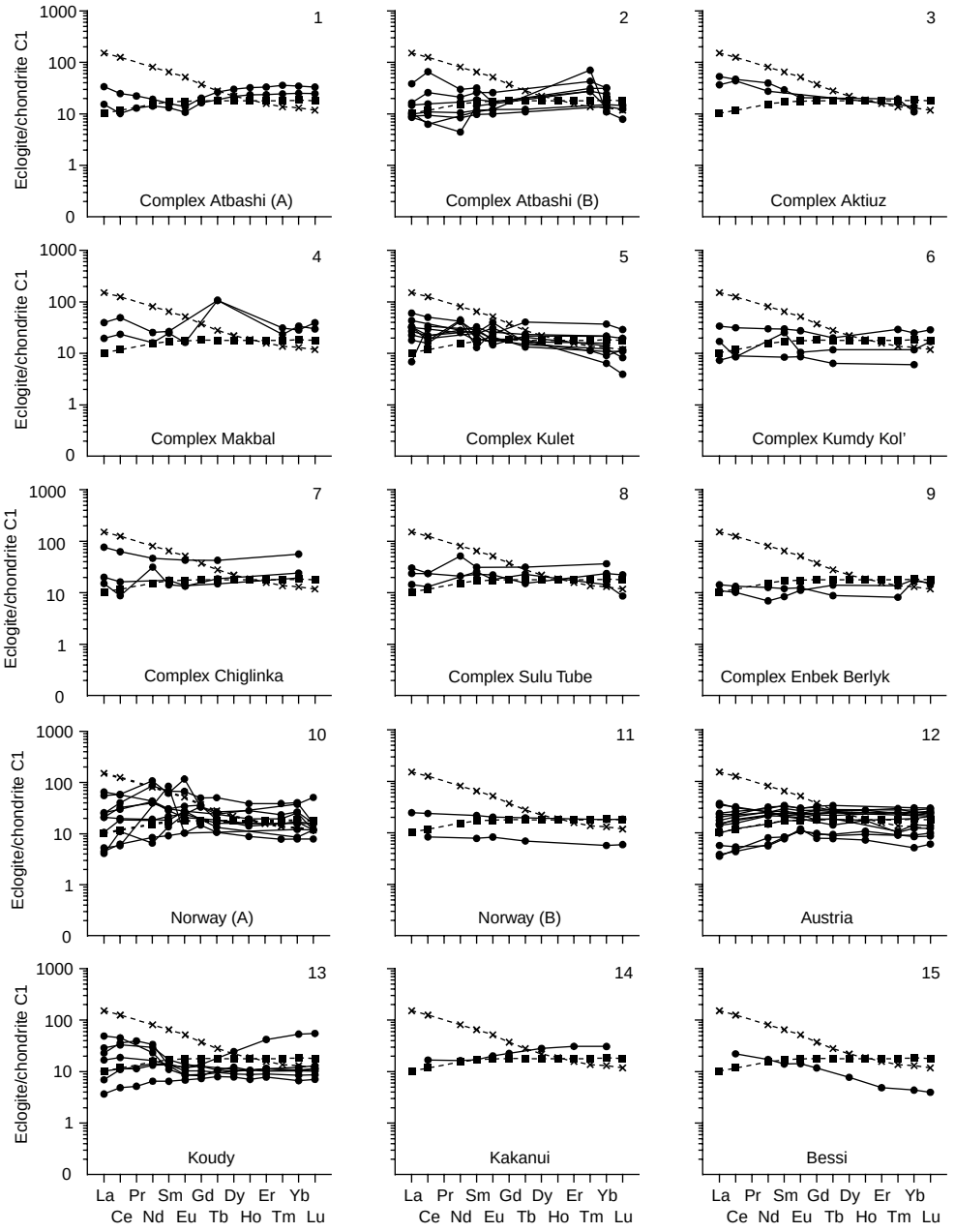

Figure 4.13 Chondrite-normalized REE patterns for eclogites from some metamorphic complexes and kimberlitic pipes (data Table 4.14).

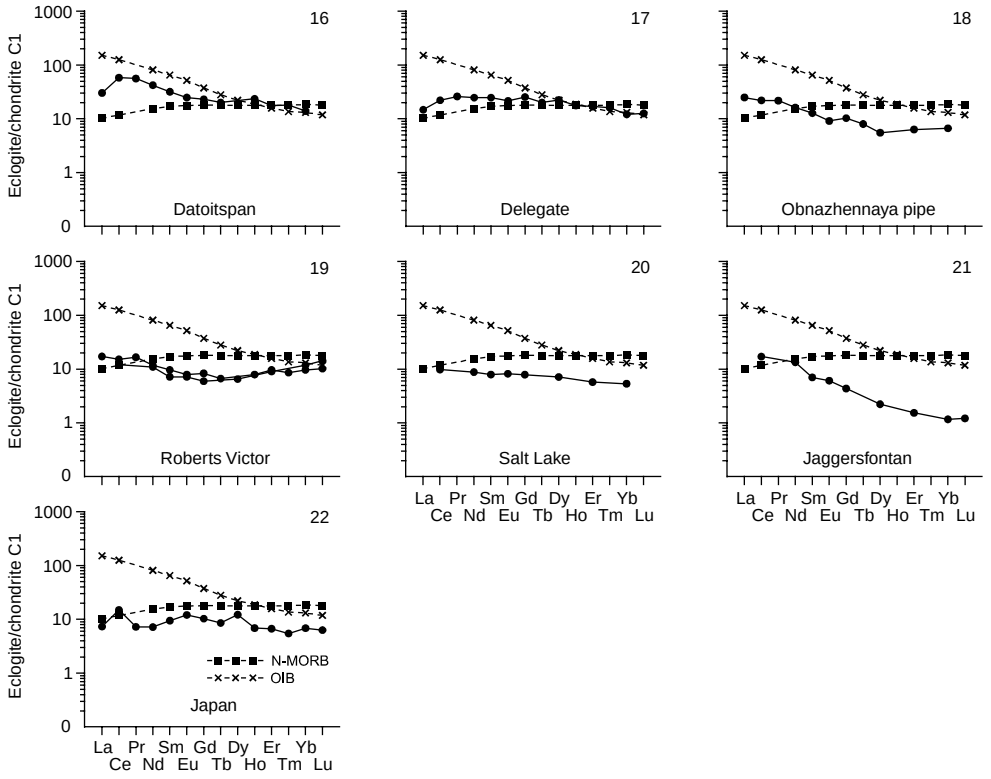

Figure 4.13 Continued

When studying regularities of REE geochemistry in eclogites, the basic question is whether these elements were exposed to fractionation during high-pressure metamorphism of their protoliths. Based on the results of studying eclogites from metamorphic complexes of Norway, the assumption has been stated that formation of these rocks was accompanied by intensive fractionation of REE (Griffin & Brueckner, 1985). Other data on eclogites from the same region showed that REE remained inert during eclogite formation (Gebauer *et al.*, 1985).

Shatsky (1990) considered this problem in more detail by studying the REE distribution in eclogites from metamorphic complexes of Kazakhstan and Kirghizia. According to his observations, during eclogite formation proceeding under high-pressure/low-temperature conditions of eclogite metamorphic facies, the behavior of REE could be complex. When the eclogitization process was accompanied by dehydration of their protoliths, escaped fluids were capable of extracting and removing certain quantities of mobile elements, including REE, from the rocks. In these conditions, eclogites depleted in REE in comparison with their protoliths were formed. In other situations, when eclogitization was accompanied by inflow of fluids in the protoliths, the process could result in supply of some quantities of mobile components, including REE. As a result, the eclogites became enriched in these trace elements in comparison

with their protoliths. Thus, processes of eclogite formation could be accompanied by both an enrichment and a depletion of their protoliths in REE. In some cases, these trace elements could be inert, that is, the level of their accumulation and character of distribution in eclogites remained the same as in the protoliths. Moreover, during eclogite formation, an isomorphous impurity of REE is redistributed between coexisting phases according to their crystallochemical properties and P–T conditions of their crystallization. The major part of REE was accumulated in structures of clinopyroxene and garnet, and a minor part entered in amphiboles and some other phases.

The obtained data on the rare earth composition of eclogites from the Atbashi metamorphic complex, Kirghizia, testify that omphacite, glaucophane, and epidote are characterized by higher levels of accumulation of light REE in comparison with medium and heavy REE. In turn, the internal zones of garnet porphyroblasts are characterized by higher chondrite-normalized concentrations of heavy and light REE than medium REE (Lesnov *et al.*, 2005). It is important to note that the "bulk" REE composition of eclogites quite often includes not only the part that enters into the structure of minerals, but also the amount of their non-structural impurities that, in the form of readily soluble compounds, is concentrated in intergrain and intragrain microcracks of rocks, owing to circulation of epigenetic fluids. So, Shatsky (1990) established that when the crushed samples of eclogites were subjected to a preliminary leaching in a dilute solution of hydrochloric acid, the La contents in them was lowered by 30–60% in comparison with the same samples that were not treated in a similar way.

* * *

The REE contents in eclogites vary over significant ranges; many eclogites are comparable in this feature to N-MORBs. As in the majority of mafic rocks of magmatic origin, the chondrite-normalized contents of light REE in eclogites are usually slightly higher than heavy REE; accordingly, their rare earth spectra have an overall negative slope. Sometimes positive or negative Eu anomalies of low intensity are observed in the spectra. When the eclogite formation proceeded under conditions of dehydration of their protoliths, some quantities of REE together with fluids could be removed from the rocks, which resulted in decreasing of the overall level of REE accumulation in comparison with the eclogite protoliths. At high-pressure metamorphism that proceeded in conditions of fluid supply, eclogites could be enriched to some extent in REE and other mobile elements compared with their protoliths.

4.8 SUMMARY

The generalization of available analytical data on REE distribution in various petrographical types of plutonic mafic rocks differing in modal and chemical compositions, as well as in formation conditions, from polytypic mafic–ultramafic massifs, testifies to the wide diversity of these elements, both in the level of accumulation of these trace elements and in the relationships between separate elements. Along with widespread varieties of essentially REE-depleted gabbroid rocks, which are characterized by appreciably lower total levels of accumulation in comparison to N-MORBs, in some massifs, gabbroids are variously enriched with REE, especially light REE. Such gabbro varieties can be compared to OIBs with regard to REE concentration. In the overwhelming

majority of gabbroids, the level of light REE accumulation exceeds to some extent the level of heavy REE accumulation; and their rare earth spectra have an overall negative slope. Almost always, these spectra are complicated by positive Eu anomalies of various intensities; and an inverse relationship between intensity of positive Eu anomalies and a total level of REE accumulation is observed in samples from some massifs. The major part of REE in mafic rocks is concentrated as an isomorphous impurity in clinopyroxenes, plagioclases, and amphiboles, and in some cases in garnets. The minor contributors to REE geochemistry in mafic rocks are accessory minerals (apatite, sphene, zircon), and orthopyroxenes and olivines contain extremely insignificant amounts REE.

The diversity of plutonic mafic rocks in relation to concentration and character of REE distribution is caused by many reasons, including inhomogeneity of composition of the upper mantle sources from which their parent melts were generated, the extent of melting of these sources, fractionation processes of crystallizing melts, as well as contamination of primary melts by substance of enclosed more-ancient rocks (ultramafic restites, volcanogenic-terrigenous, and metamorphic rocks). Relative REE-depletion of those orthomagmatic gabbroid rocks that usually compose massifs in ophiolite mafic–ultramafic complexes, allows one to assume that they crystallized from mantle melts that were generated at elevated extents of partial melting of mantle sources. Mafic rocks that compose contact-reactionary layered complexes of ophiolites, which we named as paramagmatic, also show significant depletion in REE. It is supposed that an initially low total level of REE accumulation in parent melts of these gabbroids became lower owing to their contamination by material of ultramafic restites, into which they intruded and with which they actively interacted, especially in deep-seated conditions. In contrast to REE-depleted gabbro rocks that enter into ophiolite mafic–ultramafic complexes, the gabbros that compose many other types of massifs are characterized by an increased overall level of REE accumulation. Most likely, they crystallized from primary melts, which generation proceeded at rather low extents of partial melting of undepleted mantle sources. In addition, the increased REE contents are peculiar to the hybrid gabbro rocks that crystallized from mantle basalt melts that were contaminated by material of enclosed volcanogenic, terrigenous, and metamorphic rocks. The positive Eu anomalies observable on the spectra of many samples of mafic rocks are often caused by rather high contents of modal plagioclase, which is capable to concentrate this element in increased quantities.

It is necessary to emphasize that along with the isomorphous impurity of REE entering into structures of the major, minor, and accessory minerals of mafic rocks, the rocks can contain different amounts of non-structural impurities of these elements, which was accumulated as readily soluble compounds in intergrain and intragrain microcracks at seepage of epigenetic fluids. Despite that in most cases, the contribution of such non-structural impurities of REE to the "bulk" REE composition of the rocks is rather insignificant, this circumstance is necessary to take into account when interpreting the results of geochemical investigations, because such impurities, not having a direct relation to endogenous processes of formation of mafic rocks, introduces certain errors to obtained results of analyses. In order to decrease the effect of such errors, the analyzed samples should be preliminarily subjected to leaching by very dilute solutions of hydrochloric acid; this procedure will allow the removal of almost all non-structural impurities of REE from rocks.

Chapter 5

Rare earth elements in rock-forming minerals from ultramafic and mafic rocks

In dealing with science examples are more useful than rules.

Isaac Newton

An important direction is the study of empiric laws in the distribution of chemical elements between coexisting minerals.

V.A. Zharikov & A.A. Yaroshevsky

Geochemical studies of REE in minerals from ultramafic and mafic rocks started in the late 1960s. Very low REE concentrations in minerals from ultramafic and mafic rocks and a lack of analytical techniques capable of detecting these elements made this work difficult. Owing to the development of techniques sensitive enough to determine REE content, the first analyses were made in minerals from ultramafic and lunar rocks. Later on, REE content was determined in small sample collections of olivines, orthopyroxenes, clinopyroxenes, plagioclases, amphiboles, and garnets. The first summaries on the REE geochemistry in igneous rocks and their minerals appeared approximately at that time (Balashov, 1976; Rare Earth Element Geochemistry, 1984; McKay, 1986; Rollinson, 1993). A great progress in this field of geochemistry was achieved after 1985, when a great number of REE analyses were made, though works summarizing these data were not published.

The data presented in this chapter, though probably not complete, must fill the gap in our knowledge of minerals from ultramafic and mafic rocks. We hope they will be useful both for specialists dealing with common problems of mafic–ultramafic magmatism and for geologists involved in mapping and prospecting surveys within particular mafic–ultramafic massifs and their complexes. A similar summary paper on minerals from metamorphic rocks has been recently written by Skublov (2005).

5.1 OLIVINES

Among minerals making up ultramafic, mafic and some other rocks, olivines are distinguished by their extremely low concentrations of REE and many other incompatible elements, which made their determination in this mineral impossible for a long time. The first determinations of REE in olivines were carried out in the late 1970s, using several kimberlite samples from Yakutia (Nekrasova & Gamyanina, 1968) and lherzolites sampled from deep xenoliths of the Salt Lake Crater (Nagasawa *et al.*, 1969). For the first time, these works showed that olivines are capable of accumulating a

very small amount of REE in their structure. Later, it was supported by data from the study of olivines of the Lost Coti meteorite (Schnetzler & Bottino, 1971) and from a number of other ultramafic xenoliths (Philpotts *et al.*, 1972; Ottonello *et al.*, 1978; Ottonello, 1980; Tanaka & Aoki, 1981). Later, olivines from ultramafic xenoliths found in the alkaline-basalt provinces of Germany were explored in more detail (Stosch & Seck, 1980; Stosch, 1982). Further studies of olivines from peridotite xenoliths showed that the level of accumulation of light REE in them is usually one or two orders of magnitude lower than that in chondrite C1, whereas their high REE content is often comparable to that in chondrite (McDonough *et al.*, 1992). Then the first estimated coefficients of REE distribution between olivines and coexisting minerals (K_d)—orthopyroxenes, clinopyroxenes, plagioclases, and garnets (McKay, 1986; Kennedy *et al.*, 1993; Dunn & Sen, 1994)—were obtained. Experimental studies showed that K_d(olivine/melt) values for Ce, Sm, and Tm increase proportionally with the degree of partial melting of lherzolites (Harrison, 1981). The study of ultramafic restites from the Shamansky massif (Transbaikalia) showed that dynamometamorphic recrystallization of olivines is accompanied by their essential depletion of REE (Lesnov, 1999, 2000a; Lesnov *et al.*, 1995, 2005d). Data on REE distribution in olivines from ultramafic xenoliths found in alkali basalts of Spitsbergen Island (Shubina *et al.*, 1997) and from lunar rocks (Floss *et al.*, 1998) were also published. Based on the study of REE distribution in olivines from mafic rocks of the Norilsk region, using the SIMS and LA ICP-MS techniques, Krivolutskaya *et al.* (2006) showed that there is an inverse relationship between heavy REE and forsterite contents in olivines, which they interpreted as direct evidence of isomorphic incorporation of heavy REE in the olivine structure.

5.1.1 REE composition of olivines

Let us consider some features of REE distribution in olivines in their samples from meteorites, dunites, harzburgites, lherzolites, wehrlites, troctolites, olivine-bearing anorthosites, and basalts (Table 5.1). Reported analyses were mainly made by the RNAA, INAA, and IPMA techniques, and only few of them were made by the LA ICP-MS method. In some cases, we failed to determine the content of the light elements. The overall REE content varies from about 0.1 to about 4.5 ppm in the whole collection of olivines. The majority of samples accumulate heavy REE in the range of 0.02–0.80 t. ch. and light REE in the range of 0.005–3 t. ch.

Meteorites. In most olivines from the Chessigny, Lafayette, and Valadares meteorites, the content of light REE was below the detection limit. The REE patterns of these olivines in the field of heavy elements exhibit a steep positive slope corresponding to very low values of the $(Dy/Yb)_n$ parameter. One sample from the Nakhla meteorites revealed an abnormally high content of light REE, which might result from the presence of minor nonstructural impurities introduced under terrestrial conditions (Fig. 5.1, 1).

Olivine-bearing anorthosites (the moon). The study of the rare earth composition of olivines from these lunar rocks is of special interest. Similar to olivines from meteorites, the level of accumulation of heavy REE in these rocks is comparable to that of chondrite C1 (see Table 5.1 and Fig. 5.1, 4). At the same time, an extremely low content of light REE did not allow us to determine them using the IPMA technique.

Table 5.1 Rare earth element composition of olivines from ultramafic, mafic and some different rocks (ppm).

	Manifestations									Massifs (manifestations)			
	Nakhla		Chessigny	Valadares	Lafayette	Experiment data				Kapfenstein, Austria	West Germany		
	(Nakamura *et al.*, 1982)	(Wadhwa & Crozaz, 1995), IPMA				(Harrison, 1981), ARG				(Kurat *et al.*, 1980)	(Stosch, 1982), RNAA		
	NmetB	M-1	M-2	M-3	M-4	16112.29	161120	161137.7	16118	Ka168[a]	D-42[a]	D-50[a]	D-58[a]
Element	*Meteorites*					*Garnet lherzolites*				*Spinel lherzolites*			
La	0.240	0.003	N.d.	N.d.	N.d.	N.d.	N.d.	N.d.	N.d.	0.030	0.0008	0.0022	0.0013
Ce	N.d.	0.012	N.d.	N.d.	N.d.	1.550	0.518	0.311	0.621	N.d.	N.d.	0.0043	0.0037
Pr	N.d.	N.d.	N.d.	N.d.	N.d.	N.d.	N.d.	N.d.	N.d.	N.d.	N.d.	N.d.	N.d.
Nd	N.d.	0.016	N.d.	N.d.	N.d.	N.d.	N.d.	N.d.	N.d.	N.d.	N.d.	N.d.	N.d.
Sm	0.251	0.009	N.d.	N.d.	N.d.	0.479	0.294	0.222	0.384	0.003	0.0005	0.0008	0.0009
Eu	0.048	0.004	N.d.	N.d.	N.d.	N.d.	N.d.	N.d.	N.d.	0.005	0.0002	0.0004	0.0005
Gd	0.013	0.016	N.d.	N.d.	0.017	N.d.	N.d.	N.d.	N.d.	N.d.	N.d.	N.d.	N.d.
Tb	0.075	0.003	0.002	N.d.	0.006	N.d.	N.d.	N.d.	N.d.	N.d.	N.d.	0.0004	0.0008
Dy	N.d.	0.036	0.025	0.042	0.081	N.d.	N.d.	N.d.	N.d.	N.d.	0.0022	0.0040	0.0076
Ho	N.d.	0.015	0.009	0.012	0.027	N.d.	N.d.	N.d.	N.d.	N.d.	0.0011	0.0012	0.0026
Er	0.081	0.055	0.048	0.048	0.136	N.d.	N.d.	N.d.	N.d.	N.d.	N.d.	0.0061	0.0100
Tm	N.d.	0.010	0.009	0.007	0.032	0.050	0.037	0.036	0.045	N.d.	0.0017	0.0013	0.0030
Yb	N.d.	0.073	0.073	0.090	0.284	N.d.	N.d.	N.d.	N.d.	0.047	0.0149	0.0140	0.0310
Lu	0.086	N.d.	N.d.	N.d.	N.d.	N.d.	N.d.	N.d.	N.d.	0.015	0.0040	0.0033	0.0073
Total	N.d.	0.166	N.d.	N.d.	N.d.	N.d.	N.d.	N.d.	N.d.	N.d.	0.028	0.042	0.072
$(La/Yb)_n$	1.28	0.04	N.d.	N.d.	0.03	N.d.	N.d.	N.d.	N.d.	0.12	0.003	0.009	0.005

(*Continued*)

Table 5.1 Continued

	Massifs (manifestations)												
	West Germany			New Mexico, USA	Shavaryn Tsaram, Mongolia			Yakutia, Ru.	Lherz, France		Kapfenstein, Aust.	East Germany	
	(Stosch, 1982), RNAA					(Erkushev, 1985), RNAA		RNAA	(Bodinier *et al.*, 1988), RNAA		(Kurat *et al.*, 1980)	(Stosch & Seck, 1980), RNAA	
	Ib/3[a]	Ib/5[a]	Ib/K1[a]	KH-K8[a]	Mo22[a]	200-81[a]	Sh-21[a]	O-ET[a]	70-367[a]	71-321[a]	Ka111[a]	Ia/105[a]	Ia/171[a]
Element	*Spinel lherzolites*												
La	0.230	0.0120	0.0108	0.0156	0.0008	0.180	0.150	0.820	0.020	0.022	0.0320	0.560	0.280
Ce	0.390	N.d.	0.024	0.0192	0.0013	0.450	0.470	2.000	0.037	0.090	N.d.	N.d.	N.d.
Pr	0.039	N.d.	N.d.	N.d.	N.d.	0.043	0.034	N.d.	N.d.	N.d.	N.d.	N.d.	N.d.
Nd	0.145	N.d.	0.011	0.007	0.0005	0.090	0.082	1.500	N.d.	N.d.	N.d.	N.d.	N.d.
Sm	0.022	0.0025	0.003	0.0012	0.0004	0.025	0.029	0.460	0.006	0.005	0.0063	0.059	0.042
Eu	0.0057	N.d.	0.0011	0.0006	0.0003	0.015	0.047	0.080	0.002	N.d.	N.d.	0.022	N.d.
Gd	0.019	N.d.	N.d.	N.d.	0.001	0.050	0.050	N.d.	N.d.	N.d.	N.d.	N.d.	N.d.
Tb	0.0025	N.d.	0.0012	0.0006	0.0004	0.010	0.085	0.090	N.d.	N.d.	N.d.	0.0081	0.0058
Dy	0.015	0.0076	0.013	0.0066	0.0042	0.045	0.050	N.d.	N.d.	N.d.	N.d.	N.d.	N.d.
Ho	0.0035	0.0024	0.0041	0.0017	0.0015	0.018	0.016	N.d.	N.d.	N.d.	N.d.	N.d.	N.d.
Er	N.d.	N.d.	N.d.	N.d.	N.d.	0.075	0.070	N.d.	N.d.	N.d.	N.d.	N.d.	N.d.
Tm	0.0031	N.d.	0.0037	0.002	0.0023	0.012	0.040	0.060	N.d.	N.d.	N.d.	N.d.	N.d.
Yb	0.024	0.0260	0.042	0.022	0.022	0.069	0.130	0.410	0.010	0.020	0.043	0.028	0.0162
Lu	0.0052	0.0062	0.0093	0.006	0.0053	0.028	0.040	0.060	N.d.	N.d.	0.0062	0.0069	0.0041
Total	0.904	N.d.	0.12	0.083	0.040	1.11	1.29	N.d.	N.d.	N.d.	N.d.	N.d.	N.d.
$(La/Yb)_n$	6.47	0.31	0.17	0.48	0.02	1.76	0.78	1.35	1.35	0.74	0.50	13.5	11.7

	Massifs (manifestations)												
	East Germany					Lizard, England		France	Otris, Greece	Kamperdown	West Eifel, Germ.	British Columbia, Canada	
	(Stosch & Seck, 1980), RNAA					(Frey, 1969), NAA		(Menzies, 1976), NAA		(Philpotts *et al.*, 1972), IPMA		(Sun & Kerrich, 1995), ICP-MS	
	Ia/236[a]	Ia/249[a]	Ib/2[a]	Ib/6[a]	Ib/8[a]	90681o	90683o	M4	O2	20[a]	57[a]	BM-11[a]	JL-14[a]
Element	*Spinel lherzolites*					*Lherzolites*							
La	0.165	0.580	0.026	0.024	0.184	0.078	0.045	0.060	0.900	N.d.	N.d.	0.106	0.080
Ce	0.140	1.220	0.046	N.d.	0.430	0.260	0.110	0.130	0.860	0.241	0.197	0.207	0.160
Pr	N.d.	0.129	N.d.	N.d.	N.d.	0.0194	0.0109	N.d.	N.d.	N.d.	N.d.	0.024	0.020
Nd	N.d.	N.d.	N.d.	N.d.	N.d.	0.112	0.048	N.d.	0.540	0.077	0.061	0.090	0.080
Sm	0.0064	0.047	0.0079	0.0052	0.025	0.0136	0.0132	0.010	N.d.	0.016	0.017	0.019	0.020
Eu	0.0024	0.017	N.d.	N.d.	0.0104	0.0011	0.0041	N.d.	0.050	0.005	N.d.	0.005	N.d.
Gd	N.d.	N.d.	N.d.	N.d.	N.d.	N.d.	0.0216	N.d.	0.300	N.d.	0.016	0.014	0.010
Tb	0.0018	N.d.	0.0022	N.d.	0.0063	0.0025	0.0043	0.010	0.050	N.d.	N.d.	0.003	N.d.
Dy	0.015	0.026	N.d.	0.0168	N.d.	N.d.	N.d.	N.d.	N.d.	0.014	0.021	0.018	0.020
Ho	0.0048	N.d.	N.d.	N.d.	N.d.	0.0027	0.0094	0.030	N.d.	N.d.	N.d.	0.004	N.d.
Er	N.d.	N.d.	0.014	N.d.	N.d.	0.011	0.034	N.d.	N.d.	N.d.	0.013	0.012	0.020
Tm	N.d.	N.d.	N.d.	N.d.	N.d.	0.002	0.0055	N.d.	N.d.	N.d.	N.d.	0.003	N.d.
Yb	0.021	0.017	0.023	0.037	0.048	0.012	0.045	N.d.	0.490	N.d.	0.028	0.018	0.030
Lu	0.0045	0.0038	0.0057	0.0091	0.0093	0.0044	0.0105	0.020	0.090	N.d.	0.006	0.003	0.010
Total	0.361	N.d.	N.d.	N.d.	N.d.	0.519	0.362	N.d.	N.d.	N.d.	N.d.	0.526	0.450
$(La/Yb)_n$	5.30	23.0	0.76	0.44	2.59	4.39	0.68	N.d.	1.24	N.d.	N.d.	3.98	1.80

(*Continued*)

Table 5.1 Continued

	Massifs (manifestations)												
	British Columbia, Canada							Itinome-Gata, Japan		Spitsbergen			
	(Sun & Kerrich, 1995), ICP-MS							(Tanaka & Aoki, 1981), IDMS		(Shubina *et al.*, 1997), INAA			
	JL-15[a]	JL-18[a]	KR-1[a]	KR-2[a]	KR-35[a]	LL-1[a]	LL-14[a]	2L[a]	3L[a]	12sv[a]	13sv[a]	4sv[a]	5ha[a]
Element	*Lherzolites*												
La	0.056	0.100	0.070	0.280	0.030	0.080	0.014	0.145	0.101	0.940	0.980	0.108	0.100
Ce	0.125	0.200	0.130	0.580	0.060	0.160	0.029	0.223	0.309	0.310	0.280	0.280	0.320
Pr	0.014	0.020	0.010	0.070	0.010	0.020	0.003	N.d.	N.d.	N.d.	N.d.	N.d.	N.d.
Nd	0.060	0.090	0.050	0.220	0.030	0.070	0.020	0.0901	0.095	N.d.	N.d.	N.d.	N.d.
Sm	0.008	0.020	0.010	0.040	0.010	0.010	0.002	0.0192	0.0235	0.054	0.080	0.050	0.060
Eu	0.005	0.010	N.d.	0.010	N.d.	N.d.	0.001	0.0035	0.004	0.022	0.025	0.027	0.030
Gd	0.008	0.020	0.010	0.060	0.010	0.020	0.001	0.0183	0.0261	N.d.	N.d.	N.d.	N.d.
Tb	0.002	N.d.	N.d.	N.d.	N.d.	N.d.	0.001	N.d.	N.d.	0.290	N.d.	0.019	0.020
Dy	0.020	0.020	0.010	0.030	0.010	0.020	0.004	0.0204	0.0323	N.d.	N.d.	N.d.	N.d.
Ho	0.006	N.d.	N.d.	0.010	N.d.	0.010	0.001	N.d.	N.d.	N.d.	N.d.	N.d.	N.d.
Er	0.014	0.020	0.010	0.020	0.010	0.030	0.003	0.0167	0.0253	N.d.	N.d.	N.d.	N.d.
Tm	0.003	N.d.	N.d.	N.d.	N.d.	0.010	0.001	N.d.	N.d.	N.d.	N.d.	N.d.	N.d.
Yb	0.033	0.020	0.010	0.030	0.030	0.050	0.009	0.0257	0.0431	0.065	0.070	0.062	0.100
Lu	0.007	0.010	N.d.	N.d.	0.010	0.010	0.002	0.0052	0.0083	0.010	0.009	0.010	0.018
Total	0.361	0.530	N.d.	N.d.	0.210	0.490	0.091	N.d.	N.d.	N.d.	N.d.	N.d.	N.d.
$(La/Yb)_n$	1.15	3.38	4.73	6.30	0.68	1.08	1.05	3.81	1.58	9.76	9.45	1.18	0.68

	Massifs (manifestations)												
	Spitsbergen	Erdeny, Mongolia	Naransky, Mongolia		Kapfenstein, Austr.	Shamansky, Russia					Spitsbergen	Dovyrensky, Russia	
	(Shubina *et al.*, 1997)	(Author's data), RNAA			(Kurat *et al.*, 1980)	(Lesnov *et al.*, 1995), RNAA					(Shubina *et al.*, 1997)	(Author's data), RNAA	
	9sv[a]	1133v	705b	N-4-4	Ka167[a]	Sh-16/6	Sh-5/4	Sh-7	Sh-2/2	Sh-26/1	11si[a]	L-36	L-62
Element	*Lherzolites*				*Harzburgites*				*Dunites*		*Wehrlites*		
La	0.085	0.0168	0.024	0.100	0.040	0.032	0.530	0.400	0.026	0.036	0.175	1.300	0.870
Ce	0.150	0.0308	0.063	0.120	N.d.	0.100	1.070	0.740	0.140	0.140	0.380	0.900	1.840
Pr	N.d.	0.0028	0.010	N.d.	N.d.	N.d.	N.d.	N.d.	N.d.	N.d.	N.d.	N.d.	N.d.
Nd	N.d.	0.0108	0.050	0.040	N.d.	0.070	0.580	0.270	0.088	0.060	N.d.	0.430	0.900
Sm	0.040	0.0025	0.016	0.004	0.006	0.014	0.170	0.070	0.011	0.008	0.100	0.060	0.170
Eu	0.0130	0.0009	0.0068	0.025	N.d.	0.002	0.055	0.090	0.012	0.002	0.036	0.012	0.015
Gd	N.d.	0.0034	0.043	0.100	N.d.	0.040	0.160	0.080	0.011	0.020	N.d.	0.210	0.230
Tb	0.180	0.0006	0.0080	0.013	N.d.	0.006	0.030	0.020	0.002	0.003	0.025	0.040	0.045
Dy	N.d.	0.0044	0.0623	N.d.	N.d.	N.d.	N.d.	N.d.	N.d.	N.d.	N.d.	N.d.	N.d.
Ho	N.d.	0.001	0.0016	N.d.	N.d.	N.d.	N.d.	N.d.	N.d.	N.d.	N.d.	N.d.	N.d.
Er	N.d.	0.0032	0.033	N.d.	N.d.	N.d.	N.d.	N.d.	N.d.	N.d.	N.d.	N.d.	N.d.
Tm	N.d.	0.0005	0.0075	0.007	N.d.	0.003	0.022	0.006	0.001	0.002	N.d.	0.030	0.040
Yb	0.077	0.0033	0.051	0.025	0.025	0.016	0.120	0.023	0.009	0.012	0.108	0.300	0.300
Lu	0.011	0.0005	0.010	0.004	0.013	0.004	0.023	0.005	0.001	0.002	0.015	0.060	0.070
Total	N.d.	0.082	0.386	N.d.	N.d.	N.d.	N.d.	N.d.	N.d.	N.d.	N.d.	3.34	4.48
$(La/Yb)_n$	0.75	3.44	0.32	2.70	1.08	1.35	2.98	11.7	1.95	2.03	1.09	2.92	1.96

(*Continued*)

Table 5.1 Continued

	Massifs (manifestations)												
	Dzhargalant., Mong.	Naransky	Dovyrensky, R.	Skaergaard, Greenland	The Moon			Mount Adams, USA			Japan	Hawaii	Mount Adams, USA
	(Author's data), RNAA			(Paster, 1974)	(Floss *et al.*, 1998), IPMA			(Dunn & Sen, 1994), IPMA			(Higuchi & Nagasawa, 1969)	(Nagasawa *et al.*, 1969)	(Dunn & Sen, 1994)
	N-155	N-8-302a	L-68	5181	67215	64435	60025	87-1	87-32	87-34	HN4	1a[a]	87-41
Element	*Wehrlites*		*Troctolite*	*Olivine gabbro*	*Olivine anorthosites*			*Basalts*					*Andesite*
La	0.180	0.350	0.350	0.280	N.d.	N.d.	N.d.	N.d.	N.d.	N.d.	0.009	N.d.	N.d.
Ce	0.240	0.920	1.440	0.760	N.d.	N.d.	N.d.	0.200	0.009	0.480	N.d.	0.010	0.470
Pr	N.d.	N.d.	N.d.	N.d.	N.d.	N.d.	N.d.	0.062	0.016	0.073	N.d.	N.d.	0.066
Nd	0.300	0.750	0.600	0.440	N.d.	N.d.	N.d.	0.330	0.082	0.290	N.d.	N.d.	0.300
Sm	0.057	0.220	0.180	0.100	N.d.	N.d.	N.d.	0.170	0.041	0.076	0.0089	N.d.	0.085
Eu	0.031	0.580	0.027	0.026	N.d.	N.d.	N.d.	0.039	0.011	0.013	0.0061	0.0011	0.027
Gd	0.120	0.250	0.220	0.140	0.053	0.004	N.d.	0.200	0.028	0.027	N.d.	N.d.	0.085
Tb	0.012	0.050	0.037	0.030	0.015	0.002	N.d.	0.029	0.006	0.010	0.0038	0.0012	0.018
Dy	N.d.	N.d.	N.d.	N.d.	0.180	0.014	0.002	0.190	0.061	0.072	N.d.	N.d.	0.140
Ho	N.d.	N.d.	N.d.	0.140	0.090	0.011	0.002	0.041	0.015	0.015	N.d.	N.d.	0.033
Er	N.d.	N.d.	N.d.	N.d.	0.510	0.063	0.012	0.140	0.065	0.058	N.d.	N.d.	0.110
Tm	0.011	0.025	0.026	N.d.	0.110	0.021	0.005	0.026	0.009	0.012	N.d.	N.d.	0.024
Yb	0.054	0.170	0.050	1.400	1.090	0.200	0.056	0.160	0.084	0.088	0.027	0.027	0.160
Lu	0.008	0.025	0.013	N.d.	0.200	0.059	0.014	N.d.	N.d.	0.041	0.0069	0.0065	0.032
Total	N.d.	N.d.	N.d.	N.d.	N.d.	N.d.	N.d.	N.d.	N.d.	N.d.	N.d.	N.d.	N.d.
$(La/Yb)_n$	0.24	0.92	1.44	0.76	N.d.	N.d.	N.d.	N.d.	N.d.	N.d.	0.33	N.d.	N.d.

[a]Samples from deep xenoliths

This suggests that nonstructural light REE impurities in lunar anorthosites are most unlikely but, as was mentioned above, it is quite common in olivines from terrestrial rocks.

Garnet lherzolites. Ce, Sm, and Tm in olivines from these rocks were determined by the X-ray technique (Harrison, 1981). According to the reported data, REE content in these minerals is somewhat higher than that in chondrite C1, while Ce concentration is lower than that of Sm and Tm (Fig. 5.1, 5).

Spinel lherzolites in xenoliths from the alkaline-basalt provinces of Germany. REE distribution in olivines from these rocks was studied by the RNAA technique (Stosch, 1982). According to the data obtained, olivines from different xenoliths vary in REE content, with light REE being the most variable. In many cases, their concentration level is higher (0.8–2.5 t. ch.) than that of middle (0.004–0.500 t. ch.) and heavy (~0.1–0.3 t. ch.) elements, so that their REE patterns have a U-like shape (Fig. 5.1, 7, 8). Stosch observed numerous fluid microinclusions under a binocular microscope in olivine grains which demonstrate this type of pattern. After some olivine samples were separated from grains richest in fluid microinclusions, they were repeatedly analyzed for REE. It was established that the light element content decreased considerably. Based on this result, Stosch concluded that the observed abnormal enrichment of olivines with light REE is due to the presence of these impurities in fluid microinclusions, that is, as nonstructural impurities. A similar abnormal enrichment with light REE was established in olivines from lherzolite xenoliths that were found in alkali basalts of New Mexico (USA) (Fig. 5.1, 6) and in olivines from ultramafic rocks in some other complexes (Fig. 5.1, 11, 12). In this respect, the data obtained by Khisina and Virt (2005) are of great interest. They analyzed olivines from ultramafic xenoliths in kimberlites using the IR spectroscopy and TEM techniques. It was shown that the olivines under study contained water-bearing nanoinclusions that were arranged as chains and confined to flat strain-induced microdefects within host olivine crystals. Apparently, these water-bearing nanoinclusions, which are nondetectable under the usual optical microscopes, are quite abundant in natural olivine crystals and, probably, possess some properties of, mainly, light REE, which show positive anomalies on the REE patterns of such samples.

Spinel lherzolites from xenoliths in alkali basalts of the Shavaryn Tsaram paleovolcano (Mongolia). The quaternary Shavaryn Tsaram paleovolcano located in the Tariat depression in the north of Mongolia (48°12′N, 100°E) is well-known to many petrologists. Alkali basalts that make up the eroded vent of the volcano contain numerous small and, less often, large xenoliths of spinel and garnet-spinel lherzolites. Some works on the geology, petrology, mineralogy, and partly on the geochemistry of ultramafic xenoliths from this manifestation were published earlier (Agafonov *et al.*, 1975, 1977; Lesnov *et al.*, 1976; Stosch, 1982; Stosch *et al.*, 1986; Ryabchikov *et al.*, 1988; Kovalenko *et al.*, 1989; Ionov *et al.*, 1994). Recently, we published new data on the REE geochemistry of ultramafic xenoliths from this paleovolcano and their minerals (Lesnov *et al.*, 2007). Their brief description is given below. We studied REE distribution in olivines from these ultramafic rocks by the example of a large (12 × 22 × 30 cm) spinel lherzolite xenolith. This xenolith has an undisturbed ("welded") contact with the host alkali basalt (Fig. 5.2). During microscopic study of the xenolith and hosting basalt, no indications of epigenetic alteration were found. The groundmass of basalt with a coarse-pored structure is weakly devitrified near the xenolith. The

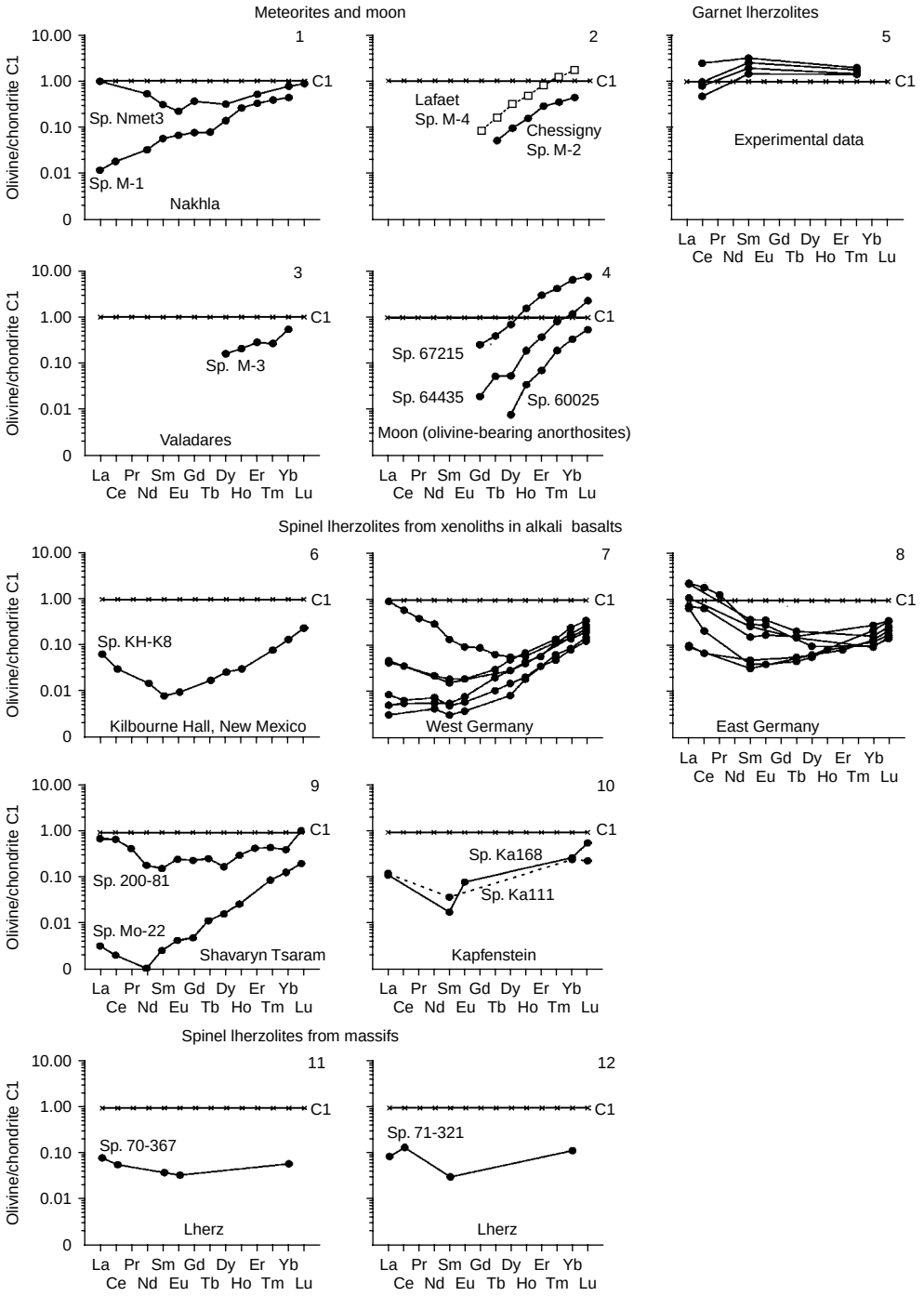

Figure 5.1 Chondrite-normalized REE patterns for olivines from meteorites, the moon's anorthosites, garnet, and spinel lherzolites (data Table 5.1).

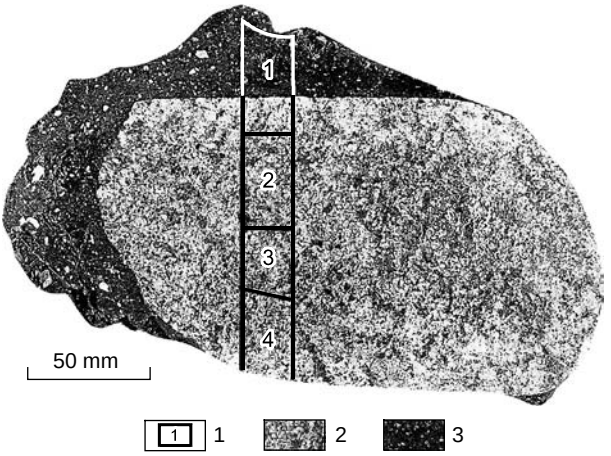

Figure 5.2 A general view of a xenolith of spinel lherzolite in an alkaline basalt (sp. M-699-27, paleovolcano Shavaryn Tsaram, Mongolia). 1—places of thin sections, in which analyses were carried out of REE by the LA ICP-MS method; 2—spinel lherzolite; 3—alkaline basalt (basanite).

groundmass contains rare olivine and clinopyroxene xenocrysts and small leucite phenocrysts. In composition, this basalt corresponds to nepheline-leucite basanite (Agafonov & Erkushev, 1984). Medium-grained spinel lherzolites from this xenolith consists of predominant subisometric olivine crystals, subordinate prismatic crystals of orthopyroxene and clinopyroxene, and rare small isometric grains of reddish-brown low-chromium spinel. The majority of grains of rock-forming minerals are dissected by numerous microcracks in various directions, which intensity increases toward the margin of the xenolith. We prepared four transparent slide specimens for the geochemical investigation of lherzolite and its minerals from this xenolith, which covers the profile of 160 mm total length passing through its opposite contacts and slightly extending into the host basalt (see Fig. 5.2). Analyses of the chemical and microelement compositions for a series of olivine, orthopyroxene, clinopyroxene, and spinel grains were performed along this profile, using X-ray pattern and LA ICP-MS techniques. REE content was determined at some points of concentration of intergranular and intragranular microcracks along this profile, as well as in the devitrified groundmass of the host basalt near its contact with the xenolith, and in olivine and clinopyroxene xenocrysts in the basalt. The layout of points in which analyses were performed is shown in Figure 5.3.

In the immediate vicinity of contact with the xenolith, the host basalt is highly enriched with REE, especially light REE, which is a specific feature of all alkali basalts (Table 5.2, Fig. 5.4). The concentration level of La in the basalt is 315–330 t. ch., while that of Yb is considerably lower (12–13 t. ch.), and, consequently, the $(La/Yb)_n$ values are very high (24–27). In REE concentrations and pattern features, alkali basalt from the Shavaryn Tsaram paleovolcano is similar to oceanic island basalts (OIBs).

According to the X-ray spectrum data, the content of forsterite end member in olivine from the lherzolite under investigation varies in a very narrow range (89.2–89.6%) (Table 5.3). Olivine xenocrystals in the basalt near its contact with the xenolith have the same content of forsterite end member (88.5–89.5%). Furthermore, olivine

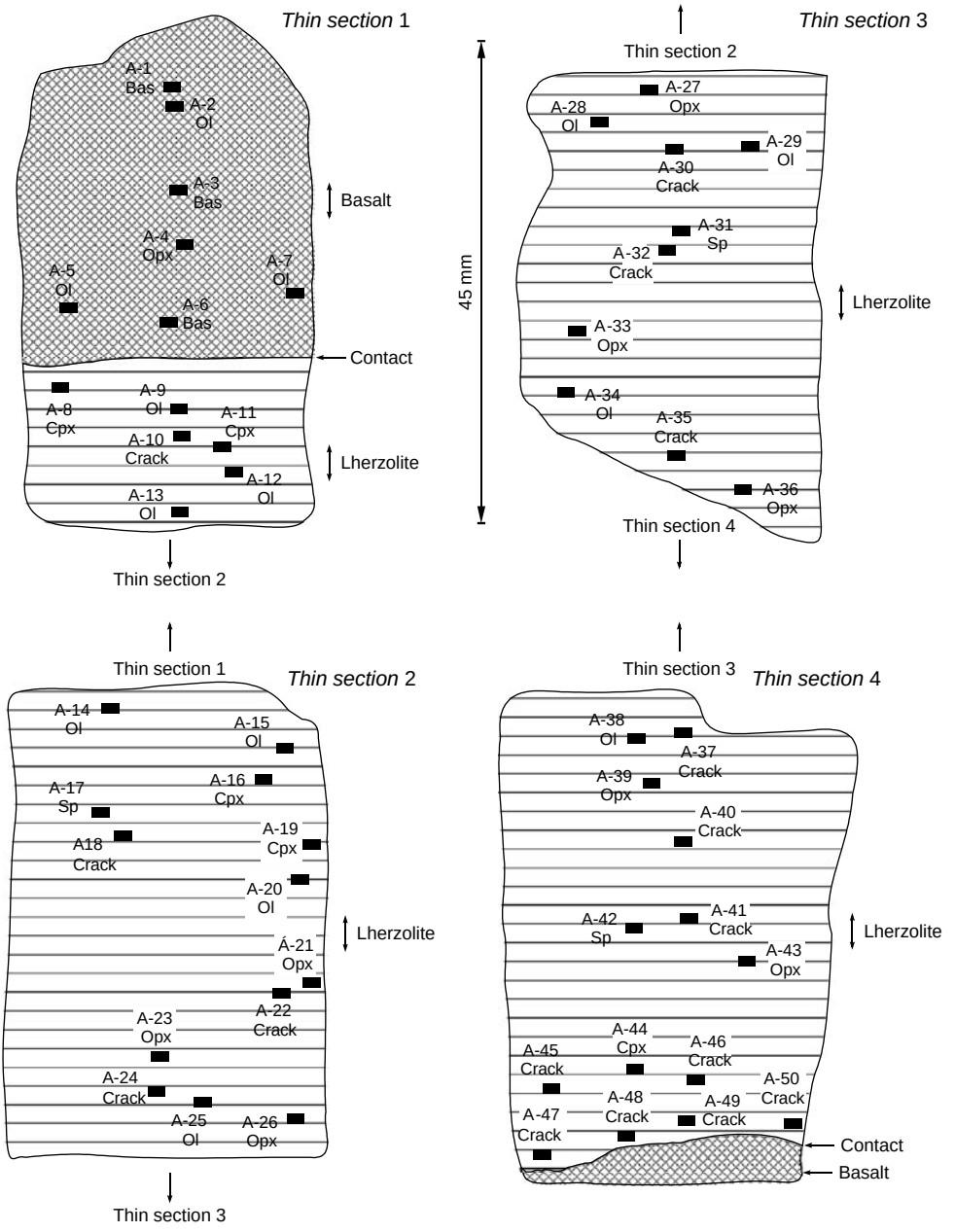

Figure 5.3 The scheme of disposition and numbers of points in which the analysis of chemical composition (microprobe method, see Table 5.3) and REE composition (LA ICP-MS method, see Table 5.4) of olivines, pyroxenes, chrome-spinels, and intergrain space in a xenolith of lherzolite and basalt (see Table 5.2) from the paleovolcano Shavaryn Tsaram. Ol—olivine, Opx—orthopyroxene, Cpx—clinopyroxene, Csp—chrome-spinel, Bas—basalt, Crack—intergrain and intragrain microcrack "contaminant".

Table 5.2 Rare earth element composition of alkali basalt near contact with xenolith of spinel lherzolites (ppm) (sp. M-699-27, paleovolcano Shavaryn Tsaram, Mongolia).

	Analysis number			
	A-1	A-3	A-6	
	Distance from point of analysis to contact of xenolith with basalt			
Element	−30.7 mm	−18.9 mm	−4.0 mm	Average
La	77.1	81.1	77.9	78.7
Ce	103.5	111.9	106.2	107.2
Pr	14.4	16.2	14.9	15.1
Nd	65.8	73.6	67.0	68.8
Sm	13.2	14.8	13.5	13.9
Eu	3.6	3.9	3.7	3.8
Gd	12.1	12.6	12.3	12.3
Tb	1.5	1.5	1.4	1.5
Dy	7.7	7.9	7.4	7.9
Ho	1.4	1.3	1.2	1.3
Er	3.2	3.1	2.9	3.1
Tm	0.37	0.35	0.34	0.35
Yb	2.1	2.1	2.0	2.1
Lu	0.27	0.25	0.24	0.26
Total	306	331	311	316
$(La/Yb)_n$	24.3	26.4	26.6	25.8

Analysis carried out by LA ICP-MS method (analysts S.V. Palessky and A.M. Kuchkin).

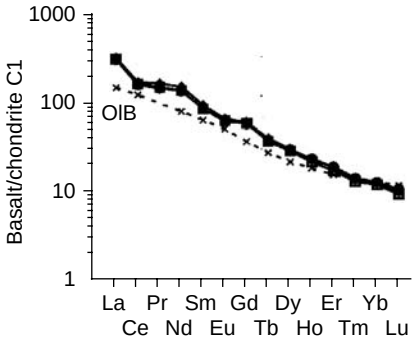

Figure 5.4 Chondrite-normalized REE patterns for alkaline basalts from the paleovolcano Shavaryn Tsaram (data Table 5.2, sp. A-1, A-3, A-6).

grains from the inner zone of the xenolith (samples A–28, A–29, and A–34) have a higher content of CaO impurity (0.60–0.63 wt%) than do grains from its marginal zone and olivine xenocrystals occurring in the host basalt (0.18–0.32 wt%). Most likely, this effect is the result of the irregular intensity of thermal recrystallization of olivine grains during the annealing of both the external and internal zones of the xenolith under influence of the basalt melt. This type of recrystallization seems to be accompanied by irregular diffusive refining of the mineral crystal lattice with respect to the same microdefects that were produced by the impurity of Ca ions.

Table 5.3 Chemical composition of olivines from spinel lherzolite from xenolith (wt%) (sp. M-699-27, paleovolcano Shavaryn Tsaram, Mongolia).

	Analysis number							
Component	A-2	A-7	A-9	A-12	A-15	A-20	A-25	A-25a
SiO_2	40.60	40.67	40.73	41.12	40.45	39.85	40.47	40.48
FeO	10.80	11.02	10.27	10.24	10.29	10.26	10.15	10.19
MgO	47.68	47.60	48.06	48.37	47.91	48.63	48.37	47.70
MnO	0.144	0.145	0.153	0.132	0.141	0.135	0.136	0.131
CaO	0.320	0.307	0.301	0.289	0.476	0.470	0.485	0.498
Total	99.40	99.74	99.51	100.15	99.27	99.35	99.61	99.00
Mg#	88.7	88.5	89.5	89.4	89.2	89.4	89.5	89.3
	A-28	A-29	A-34	A-34a	A-34b	A-38	A-38a	A-38b
SiO_2	41.01	40.75	41.16	40.75	41.09	40.55	40.71	40.65
FeO	10.38	10.30	10.26	10.13	10.28	10.30	10.35	10.09
MgO	48.17	48.47	48.63	47.08	47.50	48.68	48.83	48.69
MnO	0.132	0.130	0.131	0.139	0.134	0.132	0.153	0.143
CaO	0.600	0.631	0.600	0.176	0.178	0.247	0.238	0.261
Total	100.29	100.28	100.78	98.28	99.18	99.91	100.28	99.83
Mg#	89.2	89.4	89.4	89.2	89.2	89.4	89.4	89.6

Analysis carried out by X-ray spectrometry method on apparatus "Camebax-Micro" (analyst V.N. Koroliuk). $Mg\# = 100 \cdot Mg/(Mg + Fe)$ (formula coefficients). Analysis in samples A-34 and A-38, marked by indexes "a" and "b," carried out in two adjacent grains of minerals. Results of analysis of REE in olivines from this table are presented in Table 5.4 with right numbers.

The results obtained by the LA ICP-MS technique show that olivine crystals from various zones of the xenolith under investigation and from its xenocrystals in the basalt differ in REE content, especially light REE (Table 5.4, Fig. 5.5). For example, the total REE content in olivine from xenocrystals (samples A-2, A-5, and A-7) varies from 3.2 to 19.0 ppm, which is much higher than in its grains in the xenolith and the maximum total REE content was found in olivine xenocrystals most remote from contact with the xenolith. In xenocrystals localized nearer to the contact (samples A-5 and A-7), the total REE content is somewhat lower. The REE patterns of olivine xenocrystals show either positive or negative Eu anomalies of minor intensity (see Fig. 5.5, 1). In the olivine grain from lherzolite located at a distance of 5.5 mm from contact with the basalt (sample A-9), we also observed a markedly increased light REE content (see Fig. 5.5, 2), but it is still much lower than that in olivine xenocrystals from the basalt. Olivine grains within the xenolith located at still greater distance from the contact with the basalt (sample A-12 and A-13) have a slightly lower total REE content (0.53 and 0.77 ppm). The total REE content in olivine grains decreases gradually from the margin to the central zone of the xenolith (samples A-14, A-20, A-25, A-28, and A-34), though it was established that light REE concentrations were below their detection limit. Approaching nearer to the opposite xenolith–basalt contact, the light REE content in olivine grains increases again up to a level exceeding the detection limit (sample A-38). The data obtained indicate that the "bulk" REE composition of olivine from the lherzolite xenolith depends on the position of its grains with respect to contact with the basalt, while that of olivine xenocrystals in the basalt depends on the distance from contact with the lherzolite xenolith.

Table 5.4 Rare earth element composition of olivines from alkali basalt and spinel lherzolite from xenolith (ppm) (sp. M-699-27, paleovolcano Shavaryn Tsaram, Mongolia).

	Analysis number													
	A-2	A-5	A-7	A-9	A-12	A-13	A-14	A-15	A-20	A-25	A-28	A-29	A-34	A-38
	Basalt			*Spinel lherzolite*										
	Distance from grains of olivines to contact of xenolith with basalt (mm)													
Element	−28.3	−6.3	−7	+5.5	+12.9	+17.1	+22.4	+26.6	+41.9	+70.4	+82.7	+85.6	+112.8	+134.4
La	2.782	0.781	1.215	0.270	0.005	0.003	N.dis.	0.040	N.dis.	N.dis.	N.dis.	0.015	N.dis.	0.070
Ce	7.729	1.531	1.036	0.424	0.015	0.016	N.dis.	0.086	N.dis.	N.d.	N.dis.	0.022	N.dis.	0.100
Pr	0.750	0.178	0.153	0.042	0.001	0.004	N.dis.	0.008	N.dis.	N.d.	N.dis.	0.003	N.dis.	0.100
Nd	3.500	0.641	0.405	0.208	0.012	0.028	N.dis.	0.028	N.dis.	N.d.	N.dis.	0.014	0.001	0.080
Sm	0.773	0.126	0.081	0.032	0.006	0.012	N.dis.	0.004	N.dis.	0.001	0.001	0.005	0.001	0.010
Eu	0.141	0.016	0.145	0.011	0.003	0.006	N.dis.	0.001	N.dis.	0.001	N.dis.	N.dis.	N.dis.	0.001
Gd	0.737	0.102	0.060	0.029	0.025	0.043	N.dis.	0.004	0.001	0.003	0.002	0.001	N.dis.	0.010
Tb	0.089	0.016	0.008	0.007	0.007	0.01	N.dis.	N.dis.	N.dis.	N.dis.	N.dis.	0.001	N.dis.	N.dis.
Dy	0.688	0.146	0.053	0.052	0.075	0.092	0.001	0.002	N.dis.	0.001	0.001	0.005	N.dis.	0.045
Ho	0.168	0.030	0.009	0.011	0.025	0.026	0.001	0.001	N.dis.	N.d.	0.001	N.dis.	0.002	0.002
Er	0.601	0.108	0.027	0.037	0.106	0.117	0.004	0.001	0.003	0.005	0.004	0.005	0.004	0.005
Tm	0.102	0.015	0.005	0.007	0.022	0.021	0.001	0.001	N.dis.	0.001	0.001	0.001	0.001	0.001
Yb	0.809	0.106	0.022	0.071	0.187	0.36	0.012	0.010	0.008	0.016	0.005	0.017	0.005	0.010
Lu	0.132	0.016	0.004	0.011	0.036	0.034	0.002	0.021	0.002	0.001	0.002	0.002	0.003	0.002
Total	19.0	3.81	3.22	1.21	0.53	0.77	N.d.	0.208	N.d.	N.d.	N.d.	0.093	N.d.	0.44
$(La/Yb)_n$	2.3	5.0	37	2.57	0.02	0.01	N.d.	2.7	N.d.	N.d.	N.d.	0.59	N.d.	4.7

Analysis carried out by method LA ICP-MS on mass-spectrometry "Element" and UV Laser Probe (firm "Finnigan," Germany) (analysts S.V. Palessky and A.M. Kuchkin). Signs (−) mark distance from olivine's xenocrystals to contact xenolith with basalt; signs (+) mark distances from olivine's crystals in xenolith to its contact with basalt. Dispose of olivine's grains, which were analyzed, are shown in Figure 5.3. N.dis.—element wasn't discovered. N.d.—no data.

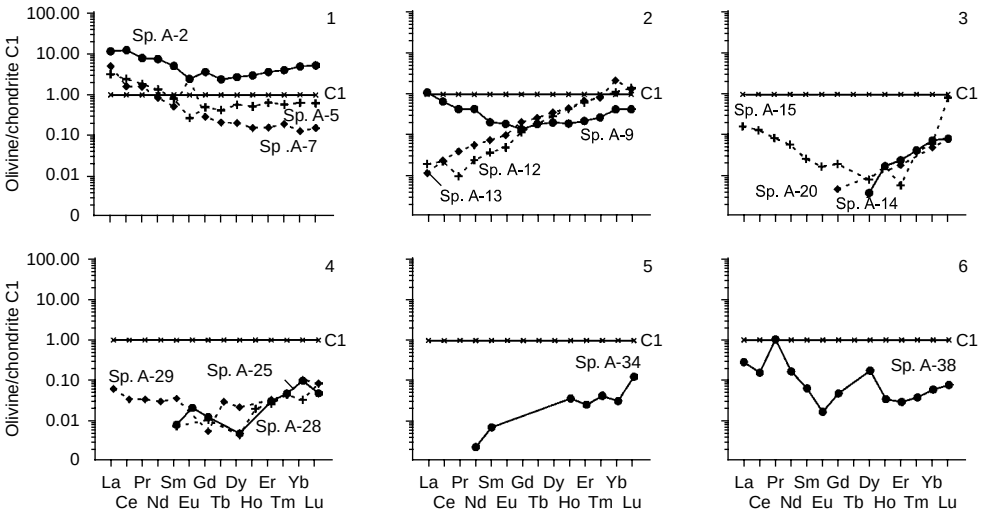

Figure 5.5 Chondrite-normalized REE patterns for olivines from spinel lherzolites in a deep xenolith from an alkaline basalt of the paleovolcano Shavaryn Tsaram (Mongolia), and from xenocrystals in the basalt in the immediate vicinity of the contact with this xenolith (data Table 5.4).

The same lherzolite slide specimens were used to determine REE content in the sites of concentration of microcracks dissecting the rock and mineral grains, including olivine grains. (Table 5.5). In all the points of concentration of microcracks, REE content was found to be essentially higher than that in adjacent mineral grains that are virtually free of microcracks. This fact may be explained by the presence of a considerable amount of nonstructural REE impurities in the microcracks, which was called a "contaminant" by Kovalenko *et al.*, (1989). The nonstructural REE impurity introduced by fluids liberated from basaltic melts has a zonal distribution throughout the xenolith volume as evidenced by a decrease in their concentration from the outer zone of the xenolith adjacent to contact with the basalt (samples A-10, A-40, A-41, and A-47) to its inner zone (samples A-30, A-35, A-37, etc.). In all cases, the level of light REE concentration in the microcrack "contaminant" is considerably higher than that of heavy REE and middle REE, and, as a result, the REE "contaminant" patterns have a U-like shape (Fig. 5.6).

Most likely, the ascending basaltic melt significantly changed the "bulk" REE composition of ultramafic xenoliths (in the melt) by means of percolated REE-enriched fluids. The introduced nonstructural REE impurity might have been distributed rather uniformly within small xenoliths, while in large xenoliths the external zones were more REE-enriched compared to the inner zones. It is also essential that the fluid-introduced nonstructural REE impurity could be accumulated not only in microcracks but also in gas–liquid micro- and nanoinclusions. The reported data on REE distribution in olivines from a large xenolith of spinel lherzolites agree well with previously published data from many provinces on REE distribution in ultramafic restites from deep xenoliths, which are generally abnormally enriched with nonstructural light REE impurities (Lesnov, 2003a).

Table 5.5 Rare earth element composition in the microcracks of spinel lherzolite from xenolith in alkali basalt (ppm) (sp. M-699-27, paleovolcano Shavaryn Tsaram, Mongolia).

	Analysis number							
	A-10	A-18	A-22	A-24	A-30	A-32	A-35	A-37
	Distance from point of analysis to contact of xenolith with basalt (mm)							
Element	+8.5	+36.7	+57.6	+69.1	+86.0	+97.4	+119.8	+136.4
La	5.316	0.077	0.872	1.250	0.067	0.394	5.303	0.070
Ce	11.54	0.093	1.318	2.351	0.128	0.334	6.160	0.100
Pr	1.748	0.015	0.161	0.251	0.012	0.066	0.906	0.007
Nd	9.050	0.075	0.620	0.922	0.067	0.249	3.481	0.004
Sm	2.610	0.016	0.118	0.164	0.009	0.035	0.577	N.d.
Eu	0.848	0.004	0.031	0.043	0.004	0.016	0.164	N.d.
Gd	2.862	N.dis.	0.057	0.076	N.d.	0.041	0.453	N.d.
Tb	0.459	0.001	0.008	0.016	0.001	0.005	0.058	N.d.
Dy	3.010	0.010	0.050	0.093	0.004	0.022	0.304	0.003
Ho	0.634	0.003	0.010	0.017	0.001	0.004	0.051	0.001
Er	1.827	0.009	0.025	0.063	0.004	0.012	0.132	0.005
Tm	0.245	0.001	0.004	0.007	0.001	0.003	0.017	0.001
Yb	1.698	0.015	0.029	0.075	0.010	0.013	0.154	0.003
Lu	0.232	0.004	0.004	0.015	0.003	0.001	0.017	0.001
Total	42.1	0.321	3.31	5.34	0.310	1.20	17.8	N.d.
$(La/Yb)_n$	2.12	3.49	20.3	11.3	4.57	20.8	23.3	15.8
	A-40	A-41	A-45	A-46	A-47	A-48	A-49	A-50
	+148.8	+157.5	+176.0	+174.9	+184.5	+183.1	+179.9	180.0
La	5.800	3.200	1.100	0.200	4.500	0.800	1.100	1.600
Ce	10.70	6.000	2.000	0.400	2.600	0.800	1.300	2.800
Pr	1.100	0.800	0.200	0.040	0.700	0.130	0.200	0.250
Nd	4.300	4.300	0.900	0.100	4.000	0.550	0.900	1.000
Sm	0.800	1.100	0.100	N.d.	0.660	0.060	0.150	0.100
Eu	0.250	0.400	0.060	0.004	0.150	0.025	0.050	0.040
Gd	0.800	1.600	0.200	0.020	0.600	0.080	0.170	0.100
Tb	0.100	0.250	0.020	0.005	0.060	0.008	0.020	0.015
Dy	0.700	1.700	0.100	0.050	0.400	0.070	0.100	0.100
Ho	0.150	0.400	0.030	0.009	0.070	0.010	0.020	0.020
Er	0.400	1.100	0.080	0.045	0.200	0.030	0.060	0.070
Tm	0.050	0.150	0.010	0.008	0.020	0.004	0.010	0.010
Yb	0.350	1.100	0.070	0.060	0.100	0.030	0.090	0.100
Lu	0.040	0.100	0.010	0.010	0.020	0.006	0.010	0.015
Total	25.5	22.2	4.88	0.95	14.1	2.60	4.18	6.22
$(La/Yb)_n$	11.2	1.96	10.6	2.25	30.4	18.0	8.25	10.8

Analysis carried out by method LA ICP-MS (analysts S.V. Palessky and A.M. Kuchkin). Dispose of olivine's grains, which were analyzed, show on Figure 5.3. N.dis.—element wasn't discovered. N.d.—no data.

Ultramafic rocks of the Shamansky massif (Transbaikalia). REE distribution in olivines from harzburgites and dunites of this massif was studied using the RNAA technique (see Table 5.1 and Fig. 5.7. 1, 2). The Shaman massif is one of the largest bodies of ultramafic restites not only within the Baikal–Muya ophiolitic belt but in the whole Altai–Sayan folded region (Lesnov *et al.*, 1995, 2005d). The rock samples from

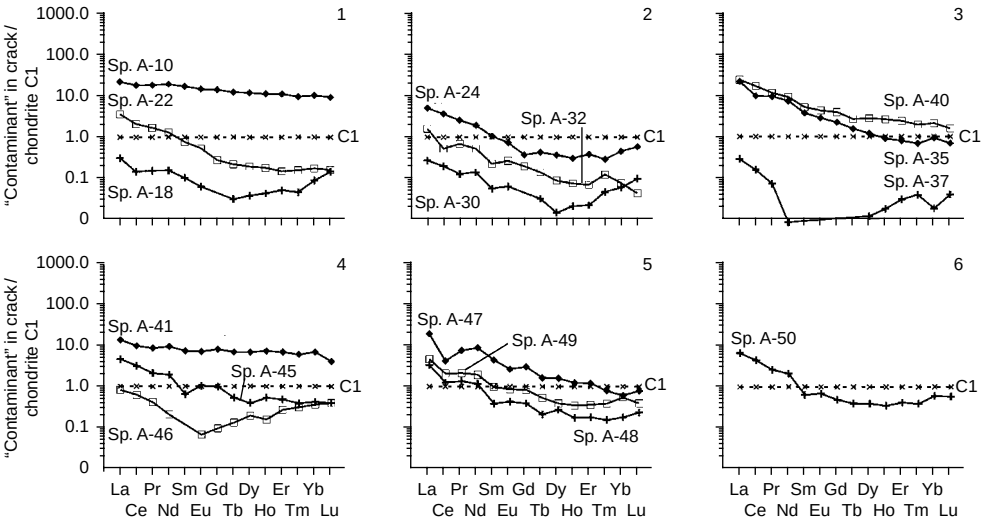

Figure 5.6 Chondrite-normalized REE patterns for "contaminant" from intergranular and intragranular microcracks in spinel lherzolites from a xenolith in an alkali basalt (sp. M-699-27, paleovolcano Shavaryn Tsaram, Mongolia). Numbers of patterns correspond to numbers of analysis in Table 5.5 and numbers of points on Figure 5.3.

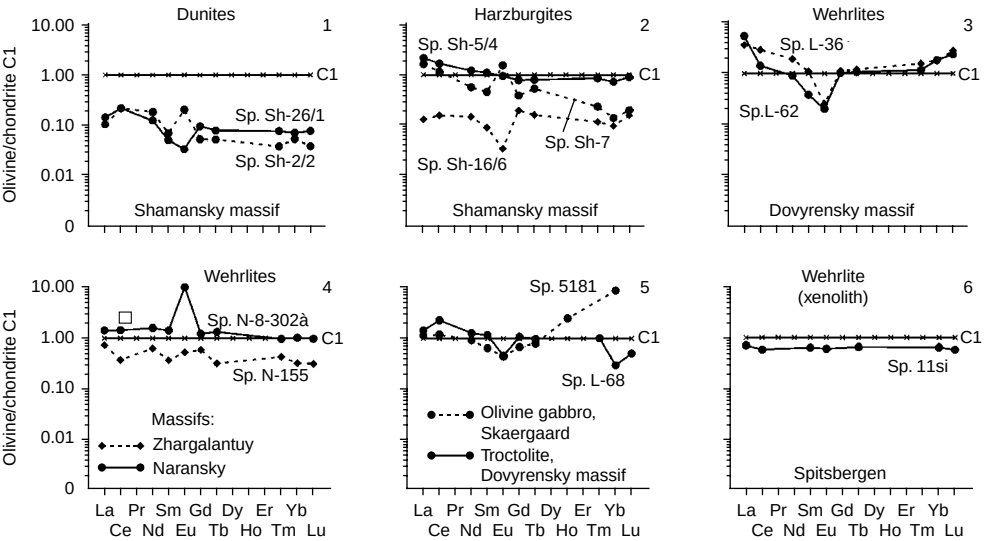

Figure 5.7 Chondrite-normalized REE composition patterns of olivines from dunites, harzburgites, and wehrlites (data Table 5.1).

which olivines were analyzed for REE were preliminary studied using the microstructural method (Goncharenko, 1989). Structural mapping of this massif conducted by Goncharenko and Chernyshov showed that there are relatively small rock blocks in its central part that experienced virtually no dynamometamorphic transformations under

the Earth's crust conditions. Olivines from the rocks composing these relic blocks have a protogranular microstructure that could have formed during plastic strain at upper mantle P–T conditions. Our observations show that the content of forsterite end member in olivines from harzburgites composing the relics blocks is 90.4%. The REE concentration in them and the features of rare earth patterns are similar to those of chondrite C1, as can be seen from sample Sh-5/4 (see Table 5.1, Fig. 5.7, 2). Olivines from harzburgites and dunites, which compose the major part of the Shaman massif, are highly altered and recrystallized especially near transcurrent faults and tectonic contacts with host rocks. Generally, olivines from such rocks have porphyroclastic and porphyroblade microstructures which are assumed to be formed during brittle-plastic strains under specific P–T conditions in the Earth's crust. These olivines have relatively increased contents of forsterite minal (91–92%) compared to olivines from the samples with protogranular microstructure. The REE concentration in olivines from the rocks with porphyroclastic and porphyroblade microstructures is about an order of magnitude lower than that observed in olivines from the samples with protogranular microstructure (see Table 5.1, samples sh-16/6, sh-26/1, sh-7, sh-2/2), while some REE patterns show negative or positive Eu anomalies of varying intensity (see Fig. 5.7, 1, 2).

Ultramafic rocks with porphyroclastic and porphyroblade microstructures, most likely, initially also had a protogranular microstructure, but during the intrusion of the Shaman massif and deformation of its blocks these rocks were recrystallized in the course of brittle-plastic strains under specific P–T conditions of the Earth's crust. Obviously, dynamometamorphism of ultramafic rocks took place under increased oxygen fugacity that promoted partial conversion of iron occurring in olivine structure from silicate to the oxide form and, as a result, led to an increase in forsterite end member content and a concurrent decrease in the concentration of structural REE impurities. This type of subsolidus compositional changes of olivines from ultramafic restites may result from diffusive purification of crystalline structure of this mineral during its re-equilibration under new physicochemical conditions.

The above data on olivines from ultramafic restites of the Shaman massif, which deformed under various conditions, suggest that the inner zones in the largest and deeply eroded ultramafic protrusions may have preserved relatively small blocks of these rocks that stayed "armored" during emplacement, that is, they did not undergo intense brittle-plastic strains and the accompanying olivine recrystallization. Therefore, olivines from such remnant ultramafic blocks might preserve their primary macro- and microelemental composition that they acquired at solidus after termination of partial melting of mantle protolith. Thus, ultramafic restites from similar relic blocks are the most favorable objects for geochemical studies of both the mantle restites and constituent minerals including olivines.

Wehrlites, troctolites, and olivine gabbros. Olivines from these rocks are characterized from the examples of several specimens from the Dovyrensky, Naransky, Dzhargalantuysky, and Skaergaard massifs as well as from xenoliths in the alkali basalts of Spitsbergen Island. (see Table 5.1). The similar patterns of two samples from the Dovyrensky massif indicate that olivine is abnormally rich in light REE and poor in Eu, while Gd, Tb, and Tm contents correspond to those of chondrite, and Yb and Lu contents are 2–3 times higher than those in chondrite (see Fig 5.7, 3). Olivine from troctolites of this massif has a similar REE composition (see Fig. 5.7, 5, sample L-68). A direct relationship between light REE content and amount of volatile components

in microinclusions determined by the method of gas chromatography was established for olivines from wehrlites of the Dovyrensky massif. In olivine from wehrlites of the Naransky massif, REE content is comparable with the content in chondrite, except for the abnormally high Eu content that may be related to sample contamination by plagioclase grains (see Fig. 5.7, 4, sample H-8-302a). Olivines from wehrlites represented in the Dzhargalantuysky massif (see Fig. 5.7, 4, sample H-155) and in xenoliths from the basalts of Spitsbergen Island (see Fig. 5.7, 6) show lower REE content than that in chondrite and a nearly flat shape in their patterns. Finally, olivine from olivine gabbros of the Skaergaard massif exhibits increased Ho and Yb contents, while other elements, except Eu, approximately correspond to chondrite content (see Fig. 5.7, 5, sample 5181).

Thus, a conclusion can be made that: (1) olivines are poor in REE, which content is often lower than that in chondrite C1; (2) many olivine samples from ultramafic and mafic rocks with varying composition and different conditions of formation and transformation contain abnormally increased concentrations of light elements due to the presence of some amount of nonstructural impurity; and (3) REE patterns of olivines free of nonstructural REE impurities have a positive slope, which suggests preferable incorporation of heavy elements into olivine structure.

5.1.2 Coefficients of REE distribution between olivines and coexisting phases

According to existing concepts, the values of the distribution coefficient (K_d) of incompatible trace elements between parental melt and minerals crystallized from it depend on many factors, including melt composition, temperature, pressure and redox conditions, crystallochemical properties of minerals, and valences and sizes of substituting and substituted ions, among others. (Balashov, 1976; Balashov *et al.*, 1970; Harrison, 1981; McKay, 1986; Nielsen *et al.*, 1992; Kennedy *et al.*, 1993; Green, 1994).

Originally, K_d(olivine/melt) values were calculated based on REE content in olivine phenocrysts and in the groundmass of host basalts. Later, it became obvious that the results obtained were not fairly correct, since the required chemical equilibrium between the groundmass and olivine phenocrysts was not attained in all cases. Later, more precise K_d(olivine/melt) values were obtained on the basis of experimental studies in which the equilibrium conditions in the melt–mineral system were attained, but these estimates are scarce to date. Some of them are given in Table 5.6 and the trends of their change are shown in Figure 5.8. T. Green (1994), who summarized the results of nearly 30 experiments on the estimation of K_d(olivine/melt), conducted under different conditions, reports that the values of K_d increase approximately by three orders of magnitude in the series from La ($n \cdot 10^{-5}$) to Lu ($n \cdot 10^{-2}$) (Green, 1994). These data imply that: (1) K_d(olivine/melt) for all REE is far lower than unity, that is, all these elements are strongly incompatible with olivine structure; (2) K_d values increase markedly in the series from light to heavy REE; (3) K_d values obtained for compositionally identical melts but under different P–T conditions of experiments vary strongly, especially for light REE; (4) the considerably higher K_d values for heavy REE compared to light REE indicate that heavy elements are more compatible with the olivine structure; and (5) in the course of olivine crystallization, the partial melts were slightly depleted of heavy REE, but, at the same time, they were enriched with light elements.

Table 5.6 Coefficients of REE distribution between olivines and basaltic melt (experimental data).

	Experiment's numbers								
	BO-30	BO-34	PO-49	N-92	H-95	P-85	CO-82	A-76	FI
Element	(Kennedy *et al.*, 1993)			(Nielsen *et al.*, 1992)	(Halliday *et al.*, 1995)	(Prinzhofer & Allegre, 1985)	(Cox *et al.*, 1982)	(Arth, 1976)	(Fujimaki *et al.*, 1984)
La	0.0061	0.0012	0.000031	0.0001	0.0002	0.00044	N.d.	N.d.	0.0067
Ce	0.0059	0.0012	0.0001	N.d.	0.00007	0.00030	0.001	0.0069	0.0060
Pr	N.d.	N.d.	N.d.	N.d.	0.0003	N.d.	N.d.	N.d.	N.d.
Nd	0.0062	0.0013	0.0004	N.d.	0.0003	0.0002	N.d.	0.0066	0.0059
Sm	0.0082	0.0023	0.0011	0.0011	0.0009	0.00018	0.002	0.0066	0.0070
Eu	0.0110	0.0020	0.0008	N.d.	0.0005	0.0002	0.002	0.0068	0.0074
Gd	0.0092	0.0029	0.0012	0.0029	0.0011	0.00025	N.d.	0.0077	0.0100
Tb	N.d.	N.d.	N.d.	N.d.	N.d.	0.000475	N.d.	N.d.	N.d.
Dy	0.0100	0.0056	0.0014	N.d.	0.0027	0.0007	N.d.	0.0096	0.0130
Ho	N.d.	N.d.	N.d.	0.0130	0.0100	0.00122	N.d.	N.d.	N.d.
Er	0.0150	0.0110	0.0130	N.d.	0.0109	0.00174	N.d.	0.0110	0.0256
Tm	N.d.	N.d.	N.d.	N.d.	N.d.	0.00348	N.d.	N.d.	N.d.
Yb	0.0230	0.0220	0.0300	N.d.	0.0240	0.00522	0.002	0.0140	0.0491
Lu	0.0290	0.0280	0.0390	N.d.	0.0500	0.00852	N.d.	0.0160	0.0454

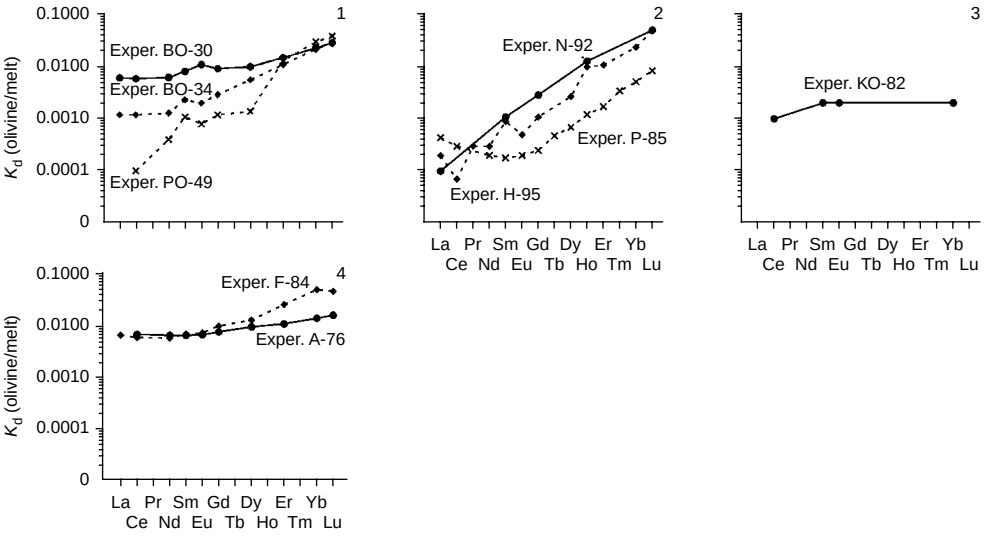

Figure 5.8 The trend coefficients of REE distribution between olivine and melt on the results of experiment studies (data Table 5.6).

The values of K_d(olivine/melt) for REE obtained from experimental data and fairly correct estimations of their contents in olivines can be used in calculations of rare earth contents of the melts from which these minerals most likely crystallized. The content of each of these elements in the model melt is calculated by the formula

$$C_i(\text{melt}) = C_i(\text{Ol})/K_{d_i}$$

where C_i(melt) is the unknown quantity of i rare earth element in the model, C_i(Ol) is the content of i element in olivine under study, and K_{d_i} is the accepted value of distribution coefficient of i element in the system olivine–melt, which was obtained from experimental data. As an example, this kind of calculation was made for olivines from the Dovyrensky mafic–ultramafic massif (northern Prebaikalia), which formation is assumed to result from the crystallization of mafic melts (Kislov, 1998). The calculations were based on the analyses of olivines from wehrlites (samples L-36 and L-62) and troctolites (sample L-68) (see Table 5.1 and Fig. 5.7) as well as K_{d_i} values obtained from the experiment (see Table 5.6, run VO-30). Undoubtedly, these are rather rough calculations, but still, if the applied values of K_d(olivine/melt) are correct for olivines from the Dovyrensky massif and if the results of estimation of REE in them have but minor errors due to the presence of nonstructural impurities of REE, the model REE composition of the parental melt can be assumed to be comparable with the REE composition of OIBs. At the same time, unlike the latter, the parental melt for these olivines had a higher accumulation level of REE and was depleted of Eu, which probably resulted from fractionation of plagioclase.

* * *

As was mentioned above, data on the content of isomorphous impurities of REE in the structure of olivines from ultramafic and mafic rocks are scarce and the regularities of their distribution in this mineral have not been adequately studied so far. The majority of analyses of REE in olivines were performed using the INAA and RNAA techniques, whereas local methods, including ICP-MS, were used in single cases. Most analyzed samples were olivines from ultramafic rocks in deep xenoliths; fewer analyses were carried out for olivines from the rocks of mafic–ultramafic massifs. Observations show that olivines can accumulate extremely low amounts of isomorphous REE impurities in their structure, with a predominance of heavy elements. In most studied samples, the accumulation level of REE is comparable or somewhat lower than that in chondrite C1.

Olivines from ultramafic rocks reveal an inverse relationship between the contents of heavy REE and the amount of forsterite end member, as well as a direct relationship between the contents of these elements and impurity of Ca. This type of relationship has not been found for light REE. These data confirm the assumption that the olivine structure is more favorable for the incorporation of minor amounts of heavy REE ions, which can isomorphically replace Ca ions with similar radius sizes in silicate minerals (Pyatenko & Ugryumova, 1988).

It was established that olivines from many rocks, with the exception of lunar and meteorite samples, often have elevated contents of light REE. According to the ratios of light REE and heavy REE, olivines can be divided into two types. The first type is scarce and includes samples characterized by virtually "flat" or gently sloping positive patterns. The second type is more widespread and includes olivines with concave downward patterns of a U-shape resulting from the enrichment of these samples with light REE. Taking into account that the olivine structure is unfavorable for the incorporation of considerable amounts of isomorphous impurities of light REE, it can be assumed that the elevated contents of light REE in this case depend not on the isomorphous impurity of these elements but on the presence of some amount of

nonstructural impurity called a "contaminant". Most likely, this kind of nonstructural impurity of light REE was concentrated in intergranular and intracranial microcracks as well as in micro- and nanoinclusions as a result of percolation of epigenetic fluids, which is most clearly seen in the examples of olivines from ultramafic xenoliths in alkali basalts. This assumption is also supported by the established direct relationship (in some olivine samples) between the contents of light REE and a number of fluid components conserved in microinclusions.

It is worth noting, however, that the obtained analytical data on the REE distribution in olivines are not sufficient to understand the mechanisms that could provide for their accumulation in olivine crystals both in the form of isomorphic (structural) impurities and in the form of a nonstructural "contaminant". This "contaminant" often provides a wrong idea of the primary rare earth composition of olivine, which resulted from crystallization in endogenic conditions. It is necessary to investigate the whole complex of cause-and-effect relationship between the character of REE distribution in olivines, on the one hand, and their crystallochemical properties and crystallization and recrystallization conditions, on the other, using a specially selected representative collections of natural and synthetic olivine samples, with application of the most sensitive techniques for determining REE as well as high-resolution electron microscopy and IR spectroscopy.

5.2 ORTHOPYROXENES

Orthopyroxene, along with olivine, clinopyroxene, and plagioclase, is one of the main rock-forming minerals of some varieties of ultramafic and mafic rocks and is an accessory mineral of some other rocks. It enters into the composition of harzburgites, lherzolites, websterites, orthopyroxenites, gabbro-norites, olivine gabbro-norites, and norites. The chemical composition of orthopyroxenes in the mentioned series of rock varieties changes from highly magnesian enstatite to moderately magnesian bronzite. Within the collection of orthopyroxene samples, which were studied with respect to their rare earth composition, the Mg# of the mineral changes from 85% (ferrous enstatite) to 37% (ferrous hyperstene). The content of refractory components (MgO, Cr_2O_3) in orthopyroxenes decreases in the following sequence: harzburgite → lherzolite → spinel peridotites → websterites → bronzitites → gabbro-norites → norites → basalts → andesites → rhyolites. In the same sequence of rocks, the mineral is enriched with TiO_2, FeO_{tot}, and Na_2O. Orthopyroxenes from mafic rocks formed under high pressures, and from some websterites, enstatitites, and basalts, have high contents of Al_2O_3. Many orthopyroxenes under a microscope show exsolution structures, which appear as a system of subparallel lamellae with clinopyroxene composition. Upon hydration of rocks, orthopyroxenes are often partly or completely replaced by the minerals of serpentine group.

The first data on the content of REE in orthopyroxenes were obtained when studying their ferric varieties represented in basalts, andesites, dacites, and rhyolites (Onuma *et al.*, 1968; Nagasawa *et al.*, 1969; Schnetzler & Philpotts, 1970). Some samples of the orthopyroxene from lherzolites (Frey, 1969; Philpotts *et al.*, 1972; Stosch, 1982; Ottonello *et al.*, 1978) from some varieties of mafic and ultramafic rocks from the Stillwater massifs (Lambert & Simmons, 1987), Zabargad Island (Vannucci *et al.*,

1993a), Mongolia, and many other regions (Erkushev, 1985; Lesnov & Gora, 1998; Lesnov *et al.*, 1998a,b,c), were also analyzed. Studies were also performed for the collections of orthopyroxene samples from ultramafic restites in deep xenoliths from alkali basalts (Ionov *et al.*, 1993a; Sun & Kerrich, 1995; Shubina *et al.*, 1997; Litasov, 1998), meteorites (Zipfel *et al.*, 1995), lunar rocks (Floss *et al.*, 1998), and some metamorphic formations (Reitan *et al.*, 1980; Pride & Muecke, 1981; Skublov, 2005). A brief survey of the available works on the distribution of REE in orthopyroxenes from different types of rock was made in 2001 (Lesnov, 2001b).

This chapter provides a summary of the materials on the geochemistry of REE in orthopyroxenes, based on analytical data including about 300 analyses of their samples from the majority of petrographic varieties of ultramafic, mafic, and some other rocks in which this mineral occurs as the main or minor phase. The analyses were performed using different techniques, including INNA, RNAA, IPMA, IDMS, SIMS, and ICP-MS. Most samples analyzed for REE are minerals from plutonic types of rocks, whereas mineral samples from volcanogenic and metamorphic formations and synthetic orthopyroxenes are far less used. The most thorough analyses were performed for orthopyroxenes in lherzolites from deep xenoliths in alkali basalts.

5.2.1 REE composition of orthopyroxenes

Orthopyroxenes from all varieties of rocks, in which they typically occur, are characterized by a low degree of REE accumulation, slightly higher than in olivines but considerably lower than in clinopyroxenes. The total content of REE increases from the varieties of orthopyroxenes represented in meteorites to the varieties from ultramafic and mafic rocks, with their maximum values in orthopyroxene from rhyolites in which they are an exotic phase. By the average content of REE, orthopyroxenes from ultramafic restites and from some varieties of mafic rocks are close to chondrite C1. The degree of accumulation of light REE in them is, typically, somewhat lower than in chondrite, whereas that of heavy REE is, on the contrary, slightly higher. The REE patterns of orthopyroxenes in most cases have a positive slope in conformity with $(La/Yb)_n$ values greater than unity. Occasionally these patterns display low-intensity, negative or positive Eu anomalies. Some orthopyroxene samples, especially from ultramafic rocks, were found to have abnormally high light REE contents, owing to which their patterns have a concave downward shape. As will be shown below, such enrichment typically results from the presence of different amounts of nonstructural light REE impurities. Let us consider some features of REE distribution in orthopyroxenes from the example of samples from some varieties of rock that have been studied so far (Table 5.7, Fig. 5.9).

Meteorites. Orthopyroxenes from meteorites were studied in single samples from the Acapulco occurrence using the SIMS technique (Zipfel *et al.*, 1995). All these samples were drastically depleted of REE, particularly light REE. The total content of analyzed REE varies in the range of 0.14–0.31 ppm, with La content of only about 0.002 ppm. These orthopyroxenes have extremely low $(La/Yb)_n$ values, owing to which their REE patterns have a positive slope (see Fig. 5.9, 1). It is reasonable to assume that all analyzed REE in orthopyroxenes from these meteorites occur purely as an isomorphous impurity.

Table 5.7 Rare earth element composition of orthopyroxenes from ultramafic, mafic and some other type of rocks (ppm).

	Manifestations								Provinces					
	Acapulco				Experiments				Roberts Victor	Shavaryn Tsaram, Mongolia		Dreiser Weiher, West Germany		
	(Zipfel *et al.*, 1995), SIMS				(Harrison, 1981), ARG				(Philpotts *et al.*, 1972)	(Erkushev, 1985), RNAA		(Stosch, 1982), RNAA		
	A1	A2	A10	A14	16112.29	161120	161137.7	16118	187[a]	200-81[a]	Sh-21[a]	D-42[a]	D-45[a]	D-50[a]
Element	*Meteorites*				*Garnet lherzolites*					*Spinel lherzolites*				
La	0.002	0.002	0.002	0.002	N.d.	N.d.	N.d.	N.d.	N.d.	0.200	0.270	0.016	0.011	0.020
Ce	0.008	0.007	0.003	0.004	2.797	0.826	N.d.	1.092	1.390	0.410	1.510	0.049	0.030	0.055
Pr	0.002	0.002	0.002	0.002	N.d.	N.d.	N.d.	N.d.	N.d.	0.125	0.210	N.d.	N.d.	0.011
Nd	0.003	0.008	0.004	0.011	N.d.	N.d.	N.d.	N.d.	0.646	0.650	0.290	0.063	0.028	0.069
Sm	0.002	0.003	0.002	0.002	0.672	0.452	0.314	0.636	0.117	0.380	0.190	0.034	0.023	0.037
Eu	0.002	0.002	0.002	0.002	N.d.	N.d.	N.d.	N.d.	0.029	0.013	0.040	0.013	0.012	0.014
Gd	0.007	0.003	0.009	0.003	N.d.	N.d.	N.d.	N.d.	N.d.	0.300	0.180	0.051	0.065	0.056
Tb	0.003	0.003	0.002	0.003	N.d.	N.d.	N.d.	N.d.	N.d.	0.028	0.086	0.010	0.017	0.013
Dy	0.015	0.038	0.042	0.029	N.d.	N.d.	N.d.	N.d.	0.052	0.170	0.210	0.098	0.170	0.107
Ho	0.004	0.015	0.015	0.014	N.d.	N.d.	N.d.	N.d.	N.d.	0.060	0.026	0.023	0.052	0.028
Er	0.026	0.060	0.067	0.063	N.d.	N.d.	N.d.	N.d.	0.023	0.200	0.240	N.d.	0.220	0.095
Tm	0.006	0.014	0.017	0.016	0.068	0.052	0.046	0.061	N.d.	0.032	0.040	0.018	0.036	0.018
Yb	0.054	0.129	0.097	0.098	N.d.	N.d.	N.d.	N.d.	N.d.	0.370	0.210	0.161	0.325	0.157
Lu	0.008	0.028	0.018	0.010	N.d.	N.d.	N.d.	N.d.	N.d.	0.055	0.036	0.033	0.060	0.029
Total	0.14	0.31	0.28	0.26	N.d.	N.d.	N.d.	N.d.	N.d.	2.99	3.54	0.57	1.05	0.71
$(La/Yb)_n$	0.03	0.01	0.01	0.01	N.d.	N.d.	N.d.	N.d.	N.d.	0.36	0.87	0.07	0.02	0.09

(*Continued*)

Table 5.7 Continued

	Massifs, provinces, manifestations													
	Dreiser Weiher, West Germany											New Mexico, USA	Arizona, USA	Mongolia
	(Stosch, 1982), RNAA						(Stosch & Seck, 1980), RNAA					(Stosch, 1982), RNAA		
	D-58[a]	Ib/24[a]	Ib/3[a]	Ib/5[a]	Ib/8[a]	Ib/K1[a]	Ia/105[a]	Ia/171[a]	Ia/236[a]	Ia/249[a]	Ib/6[a]	KH-K8[a]	SC-K2[a]	Mo22[a]
Element	*Spinel lherzolites*													
La	0.012	0.023	0.510	0.025	0.069	0.022	0.790	0.380	0.260	0.670	0.048	0.010	0.002	0.012
Ce	0.035	0.092	1.020	N.d.	0.163	0.086	2.100	1.100	0.290	1.730	N.d.	0.013	0.004	0.043
Pr	0.009	N.d.	0.115	N.d.	0.029	N.d.	0.300	0.135	N.d.	0.185	N.d.	N.d.	N.d.	N.d.
Nd	0.061	0.082	0.420	N.d.	0.128	0.107	1.300	N.d.	N.d.	N.d.	N.d.	0.019	0.015	0.063
Sm	0.043	0.036	0.076	0.024	0.074	0.059	0.161	0.128	0.015	0.110	0.072	0.023	0.021	0.040
Eu	0.021	0.013	0.024	0.010	0.030	0.027	0.048	0.049	0.005	0.023	0.028	0.012	0.013	0.021
Gd	0.101	0.056	0.076	N.d.	0.127	0.180	0.155	0.125	N.d.	N.d.	0.135	0.064	0.055	0.090
Tb	0.023	0.010	0.015	0.016	0.029	0.027	0.020	0.020	0.014	0.021	0.028	0.016	0.015	0.018
Dy	0.210	0.095	0.119	N.d.	0.250	0.250	N.d.	N.d.	0.100	0.130	N.d.	0.167	0.125	0.180
Ho	0.059	0.031	0.034	0.054	0.067	0.076	0.025	0.029	N.d.	N.d.	0.083	0.045	0.041	0.042
Er	N.d.	N.d.	N.d.	0.220	N.d.	N.d.	0.110	0.090	N.d.	N.d.	0.300	0.190	0.190	N.d.
Tm	0.039	0.022	0.027	N.d.	0.041	0.049	N.d.	N.d.	0.030	N.d.	N.d.	0.037	0.031	0.031
Yb	0.340	0.210	0.230	0.160	0.350	0.420	0.148	0.121	0.210	0.127	0.330	0.335	0.265	0.260
Lu	0.063	0.040	0.045	0.047	0.063	0.075	0.031	0.025	0.039	0.026	0.066	0.067	0.055	0.047
Total	1.02	0.71	2.71	N.d.	1.42	1.38	5.19	2.20	N.d.	N.d.	N.d.	1.00	0.83	0.85
$(La/Yb)_n$	0.02	0.07	1.5	0.11	0.13	0.04	3.6	2.1	0.84	3.6	0.10	0.02	0.004	0.03

	Massifs, provinces, manifestations													
	Assab, Ethiopia								Kapfenstein, Austria	Lherz, France		Naransky, Mongolia	Beriozovsky, Russia	Yuzhno-Shmidtovsky, Rus.
	(Ottonello *et al.*, 1978), RNAA								(Kurat *et al.*, 1980)	(Bodinier *et al.*, 1988)		(Lesnov, 1988; Lesnov & Gora, 1998), RNAA		
	3G12[a]	3G15[a]	3G17[a]	3G18[a]	3G19[a]	3G28[a]	3G51[a]	3G9[a]	Ka168[a]	70-367	71-321	1133v	154	160
Element	*Spinel lherzolites*									*Lherzolites*				
La	0.047	0.055	0.138	0.181	0.110	0.042	0.115	0.081	0.120	0.040	0.050	0.048	0.130	0.120
Ce	0.094	0.149	0.240	0.320	0.220	0.094	0.140	N.d.	N.d.	N.d.	N.d.	0.102	0.310	0.290
Pr	N.d.	N.d.	N.d.	N.d.	N.d.	N.d.	N.d.	N.d.	N.d.	N.d.	N.d.	0.020	N.d.	N.d.
Nd	N.d.	N.d.	N.d.	N.d.	N.d.	N.d.	N.d.	N.d.	N.d.	N.d.	N.d.	0.090	0.150	0.170
Sm	0.032	0.074	0.064	0.032	0.037	0.021	0.029	0.040	0.050	N.d.	0.064	0.047	0.030	0.039
Eu	0.015	0.037	0.030	0.015	0.017	0.009	0.012	0.018	0.030	0.029	N.d.	0.022	0.120	0.040
Gd	N.d.	0.155	N.d.	N.d.	N.d.	N.d.	N.d.	N.d.	N.d.	N.d.	N.d.	0.102	0.040	0.170
Tb	N.d.	N.d.	N.d.	N.d.	N.d.	N.d.	N.d.	N.d.	N.d.	N.d.	0.035	0.023	0.008	0.034
Dy	N.d.	N.d.	N.d.	N.d.	N.d.	N.d.	N.d.	N.d.	N.d.	N.d.	N.d.	0.183	N.d.	N.d.
Ho	N.d.	N.d.	N.d.	N.d.	N.d.	N.d.	N.d.	N.d.	N.d.	N.d.	N.d.	0.056	N.d.	N.d.
Er	N.d.	N.d.	N.d.	N.d.	N.d.	N.d.	N.d.	N.d.	N.d.	N.d.	N.d.	0.170	N.d.	N.d.
Tm	N.d.	0.046	0.033	N.d.	N.d.	N.d.	N.d.	N.d.	N.d.	N.d.	N.d.	0.028	0.005	0.029
Yb	0.110	0.255	0.222	0.219	0.091	0.107	0.104	0.149	0.290	0.190	0.210	0.260	0.048	0.250
Lu	0.024	0.055	0.052	0.074	0.023	0.028	0.022	0.039	0.046	0.047	0.045	0.055	0.008	0.041
Total	N.d.	N.d.	N.d.	N.d.	N.d.	N.d.	N.d.	N.d.	N.d.	N.d.	N.d.	1.21	N.d.	N.d.
$(La/Yb)_n$	0.29	0.15	0.42	0.56	0.82	0.26	0.75	0.37	0.28	0.14	0.16	0.12	1.83	0.32

(*Continued*)

Table 5.7 Continued

	Massifs, provinces, manifestations													
	Naransky, Mongolia, RNAA			Spitsbergen				Otago	Kempirsaysky	Kakanui	Efel, Germany	Salt Lake, USA	Bogemia	Carolina
	(Lesnov & Gora, 1998)		(Erkushev, 1985)	(Shubina *et al.*, 1997), INAA				(Philpotts *et al.*, 1972), IPMA						
	272	705b	727b	4sv[a]	5ha[a]	9sv[a]	12sv[a]	137[a]	20[a]	26[a]	57[a]	58[a]	59[a]	DR3[a]
Element	*Lherzolites*													
La	0.200	0.069	0.026	0.120	0.120	0.100	0.079	N.d.	N.d.	N.d.	N.d.	N.d.	N.d.	N.d.
Ce	1.000	0.133	0.073	0.370	0.360	0.230	0.270	0.021	0.828	0.074	0.201	0.408	2.320	0.046
Pr	N.d.	0.031	0.012	N.d.	N.d.	N.d.	N.d.	N.d.	N.d.	N.d.	N.d.	N.d.	N.d.	N.d.
Nd	0.220	0.138	0.062	N.d.	N.d.	N.d.	N.d.	N.d.	0.478	0.067	0.119	0.219	0.630	N.d.
Sm	0.140	0.070	0.020	0.072	0.070	0.055	0.072	N.d.	0.125	0.030	0.041	0.055	0.079	N.d.
Eu	0.003	0.022	0.010	0.031	0.023	0.024	0.032	0.003	0.048	0.013	0.015	N.d.	0.025	N.d.
Gd	0.100	0.122	0.036	N.d.	N.d.	N.d.	N.d.	N.d.	0.163	0.059	0.086	N.d.	N.d.	N.d.
Tb	0.020	0.033	0.007	0.020	0.250	0.171	0.390	N.d.	N.d.	N.d.	N.d.	N.d.	N.d.	N.d.
Dy	N.d.	0.269	0.053	N.d.	N.d.	N.d.	N.d.	0.068	0.227	0.130	0.184	N.d.	0.080	N.d.
Ho	N.d.	0.063	0.013	N.d.	N.d.	N.d.	N.d.	N.d.	N.d.	N.d.	N.d.	N.d.	N.d.	N.d.
Er	N.d.	0.124	0.050	N.d.	N.d.	N.d.	N.d.	0.100	0.175	0.121	0.175	0.074	0.072	0.016
Tm	0.009	0.040	0.008	N.d.	N.d.	N.d.	N.d.	N.d..	N.d.	N.d.	N.d.	N.d.	N.d.	N.d.
Yb	0.050	0.330	0.066	0.012	0.074	0.064	0.117	0.187	0.265	0.237	0.239	0.115	0.123	0.042
Lu	0.007	0.061	0.012	0.011	0.011	0.010	0.015	N.d.	N.d.	N.d.	N.d.	N.d.	0.026	0.012
Total	N.d.	1.51	0.45	N.d.	N.d.	N.d.	N.d.	N.d.	N.d.	N.d.	N.d.	N.d.	N.d.	N.d.
$(La/Yb)_n$	2.70	0.14	0.27	6.75	1.09	1.05	0.46	N.d.	N.d.	N.d.	N.d.	N.d.	N.d.	N.d.

	Massifs, provinces, manifestations													
	South Australia		Itinome-Gata, Japan		Lizard, England			West Alps, Italy					Liguria, Italy	
	(Frey & Green, 1974)		(Tanaka Aoki, 1981), IDMS		(Frey, 1969), NAA			(Ottonello *et al.*, 1984), RNAA					(Rampone *et al.*, 1991)	
	2604[a]	2640[a]	2L[a]	3L[a]	90681e	90683e	90684e	B-3C[a]	F-59b[a]	F-61b[a]	F-64[a]	F-66[a]	N1/4	R3/3
Element	*Lherzolites*													
La	0.686	0.034	0.129	0.059	0.004	0.003	0.012	0.024	N.d.	N.d.	0.024	0.023	N.d.	N.d.
Ce	1.130	0.100	0.378	0.177	0.015	0.022	N.d.	N.d.	0.412	0.526	0.754	1.050	0.086	0.020
Pr	0.176	0.019	N.d.	N.d.	0.002	0.005	0.006	N.d.	N.d.	N.d.	N.d.	N.d.	N.d.	N.d.
Nd	0.790	0.120	0.352	0.147	0.031	0.062	0.048	N.d.	0.768	N.d.	N.d.	N.d.	0.150	0.049
Sm	0.146	0.047	0.123	0.064	0.026	0.063	0.062	0.013	0.019	0.024	0.037	0.024	0.068	0.025
Eu	0.044	0.020	0.044	0.026	0.015	0.038	0.029	0.008	0.007	0.012	0.023	0.019	0.025	0.014
Gd	0.130	0.077	0.160	0.114	0.099	0.180	0.150	N.d.	N.d.	N.d.	N.d.	N.d.	N.d.	N.d.
Tb	0.020	0.017	N.d.	N.d.	0.028	0.047	0.051	N.d.	N.d.	0.029	0.066	N.d.	N.d.	N.d.
Dy	N.d.	N.d.	0.196	0.208	N.d.	N.d.	N.d.	N.d.	N.d.	N.d.	N.d.	N.d.	0.260	0.090
Ho	0.019	0.030	N.d.	N.d.	0.075	0.109	0.147	N.d.	0.032	0.028	N.d.	N.d.	N.d.	N.d.
Er	0.052	0.014	0.143	0.201	0.280	0.330	0.500	N.d.	N.d.	N.d.	N.d.	N.d.	0.260	0.100
Tm	0.009	0.023	N.d.	N.d.	0.052	0.077	0.088	N.d.	N.d.	N.d.	N.d.	N.d.	N.d.	N.d.
Yb	0.068	0.157	0.184	0.303	0.440	0.500	0.620	0.120	0.183	0.206	0.262	0.178	0.330	0.120
Lu	0.012	0.028	0.032	0.054	0.069	0.098	N.d.	0.041	0.044	0.066	0.069	0.035	N.d.	N.d.
Total	3.28	0.69	1.74	1.35	1.14	1.53	1.71	N.d.	N.d.	N.d.	N.d.	N.d.	N.d.	N.d.
$(La/Yb)_n$	6.81	0.14	0.47	0.13	0.01	0.004	0.01	0.13	N.d.	N.d.	0.06	0.09	N.d.	N.d.

(*Continued*)

Table 5.7 Continued

	Massifs, provinces, manifestations													
	British Columbia, Canada										France	Otris, Greece	France	Austria
	(Sun & Kerrich, 1995), ICP-MS										(Menzies, 1976), NAA		(Bodinier *et al.*, 1988)	(Kurat *et al.*, 1980)
	BM-11[a]	BM-16[a]	BM-55[a]	JL-15[a]	JL-18[a]	KR-1[a]	KR-2[a]	KR-35[a]	LL-1[a]	LL-14[a]	M4	O2	73-1	Ka167
Element	*Lherzolites*													*Harzburgite*
La	0.523	0.030	0.130	0.107	0.260	0.030	0.070	0.060	0.160	0.058	N.d.	N.d.	0.240	0.090
Ce	0.962	0.070	0.280	0.222	0.580	0.070	0.150	0.110	0.360	0.126	N.d.	0.880	0.450	N.d.
Pr	0.105	0.010	0.030	0.030	0.080	0.010	0.020	0.010	0.040	0.018	N.d.	N.d.	N.d.	N.d.
Nd	0.350	0.040	0.140	0.120	0.290	0.020	0.070	0.060	0.160	0.070	0.210	N.d.	N.d.	N.d.
Sm	0.066	0.020	0.040	0.040	0.080	0.010	0.020	0.030	0.050	0.017	0.080	0.100	0.140	0.021
Eu	0.028	0.010	0.020	0.020	0.030	N.d.	N.d.	0.010	0.020	0.006	0.020	0.080	0.053	N.d.
Gd	0.082	0.050	0.080	0.064	0.110	0.010	0.020	0.050	0.070	0.028	N.d.	0.340	N.d.	N.d.
Tb	0.017	0.010	0.020	0.016	0.020	N.d.	N.d.	0.010	0.020	0.004	N.d.	0.080	0.030	N.d.
Dy	0.161	0.130	0.170	0.158	0.180	0.050	0.040	0.140	0.150	0.028	N.d.	N.d.	N.d.	N.d.
Ho	0.041	0.040	0.050	0.046	0.050	0.010	0.020	0.040	0.040	0.007	0.240	0.340	N.d.	N.d.
Er	0.152	0.160	0.190	0.183	0.180	0.060	0.070	0.150	0.170	0.035	N.d.	N.d.	N.d.	N.d.
Tm	0.032	0.030	0.040	0.034	0.030	0.010	0.020	0.030	0.030	0.009	N.d.	N.d.	N.d.	N.d.
Yb	0.260	0.280	0.290	0.284	0.290	0.130	0.170	0.260	0.280	0.075	0.340	0.900	0.180	0.210
Lu	0.051	0.050	0.050	0.051	0.050	0.020	0.030	0.050	0.050	0.017	N.d.	0.100	0.040	0.032
Total	2.83	0.93	1.53	1.38	2.23	0.43	0.70	1.01	1.60	0.50	N.d.	N.d.	N.d.	N.d.
$(La/Yb)_n$	1.36	0.07	0.30	0.25	0.61	0.16	0.28	0.16	0.39	0.52	N.d.	N.d.	0.90	0.29

	Massifs, provinces, manifestations													
	Stillwater, USA						Naransky, Mongolia						Beriozovsky, Russia	
	(Lambert & Simmons, 1988), IDMS					(Philpotts *et al.*, 1972)	(Lesnov, 1988; Lesnov & Gora, 1998), RNAA							
	10-4-26	pp19	pp24	pp26	pp30	244	266	N-311	N-4-5	N-6-88a	N-8-310	280-3	134	137
Element	*Harzburgites*						*Websterites*							
La	N.d.	0.1080	0.076	0.060	0.045	N.d.	0.028	0.096	0.530	0.200	0.210	0.060	0.100	0.050
Ce	0.282	0.295	0.206	0.171	0.116	0.309	0.080	0.210	0.490	0.520	0.630	0.210	0.270	0.520
Pr	N.d.	N.d.	N.d.	N.d.	N.d.	N.d.	N.d.	N.d.	N.d.	N.d.	N.d.	N.d.	N.d.	N.d.
Nd	0.303	0.220	0.189	0.146	0.098	0.214	0.053	0.080	0.340	0.310	0.500	0.120	0.140	0.830
Sm	0.134	0.076	0.079	0.058	0.044	0.069	0.013	0.024	0.016	0.080	0.150	0.032	0.040	0.330
Eu	0.023	0.019	0.028	0.019	0.017	0.020	0.007	0.005	0.014	0.014	0.032	0.018	0.0470	0.020
Gd	0.222	0.103	0.122	0.090	0.072	0.124	0.028	0.260	0.120	0.100	0.220	0.060	0.100	0.160
Tb	N.d.	N.d.	N.d.	N.d.	N.d.	N.d.	0.006	0.004	0.015	0.016	0.035	0.012	0.025	0.032
Dy	0.390	0.179	0.236	0.176	0.148	0.207	N.d.	N.d.	N.d.	N.d.	N.d.	N.d.	N.d.	N.d.
Ho	N.d.	N.d.	N.d.	N.d.	N.d.	N.d.	N.d.	N.d.	N.d.	N.d.	N.d.	N.d.	N.d.	N.d.
Er	0.312	0.136	0.192	0.146	0.120	0.180	N.d.	N.d.	N.d.	N.d.	N.d.	N.d.	N.d.	N.d.
Tm	N.d.	N.d.	N.d.	N.d.	N.d.	N.d.	0.004	0.004	0.017	0.014	0.019	0.024	0.023	0.047
Yb	0.386	0.161	0.240	0.187	0.147	0.259	0.030	0.038	0.110	0.110	0.110	0.210	0.200	0.330
Lu	N.d.	N.d.	N.d.	N.d.	N.d.	0.046	0.007	0.005	0.017	0.022	0.021	0.035	0.032	0.063
Total	N.d.	1.30	1.37	1.05	0.81	1.43	N.d.	N.d.	N.d.	N.d.	N.d.	N.d.	0.98	2.38
$(La/Yb)_n$	N.d.	0.45	0.21	0.22	0.21	N.d.	0.63	1.71	3.25	1.23	1.29	0.19	0.50	0.15

(*Continued*)

Table 5.7 Continued

	Massifs, provinces, manifestations													
	Yuzhno-Shmidt., Rus.	Lherz, France		Frachinede, France		Beni Bousera, Morocco	Stillwater, USA							
	(Lesnov, 1988)	(Bodinier *et al.*, 1987), RNAA				(Pearson *et al.*, 1993)	(Papike *et al.*, 1995), SIMS							
	162	70-379b	70-379d	70-357	72-226	GP101a	374core	374rim	428core	428rim	432core	432rim	437bcore	437Brim
Element	*Websterites*						*Bronzitites*							
La	0.022	0.350	0.140	0.051	0.043	0.028	N.d.	N.d.	N.d.	N.d.	N.d.	N.d.	N.d.	N.d.
Ce	0.080	0.300	0.150	0.070	0.100	N.d.	0.043	0.011	0.162	0.046	0.084	0.018	0.078	0.024
Pr	N.d.	N.d.	N.d.	N.d.	N.d.	N.d.	N.d.	N.d.	N.d.	N.d.	N.d.	N.d.	N.d.	N.d.
Nd	0.050	N.d.	N.d.	N.d.	N.d.	0.041	N.d.	N.d.	N.d.	N.d.	N.d.	N.d.	N.d.	N.d.
Sm	0.012	0.068	0.046	0.010	0.012	0.017	N.d.	N.d.	N.d.	N.d.	N.d.	N.d.	N.d.	N.d.
Eu	0.008	0.031	0.019	0.007	0.008	0.010	N.d.	N.d.	N.d.	N.d.	N.d.	N.d.	N.d.	N.d.
Gd	0.024	N.d.	N.d.	N.d.	N.d.	0.065	N.d.	N.d.	N.d.	N.d.	N.d.	N.d.	N.d.	N.d.
Tb	0.006	0.032	0.028	0.010	0.012	N.d.	N.d.	N.d.	N.d.	N.d.	N.d.	N.d.	N.d.	N.d.
Dy	N.d.	N.d.	N.d.	N.d.	N.d.	N.d.	0.183	0.096	0.215	0.137	0.160	0.101	0.136	0.128
Ho	N.d.	N.d.	N.d.	N.d.	N.d.	N.d.	N.d.	N.d.	N.d.	N.d.	N.d.	N.d.	N.d.	N.d.
Er	N.d.	N.d.	N.d.	N.d.	N.d.	N.d.	0.216	0.093	0.215	0.126	0.139	0.087	0.134	0.124
Tm	0.004	N.d.	N.d.	N.d.	N.d.	N.d.	N.d.	N.d.	N.d.	N.d.	N.d.	N.d.	N.d.	N.d.
Yb	0.036	0.350	0.350	0.030	0.310	0.072	0.304	0.221	0.261	0.193	0.187	0.187	0.173	0.198
Lu	0.004	0.068	0.056	0.004	0.061	N.d.	N.d.	N.d.	N.d.	N.d.	N.d.	N.d.	N.d.	N.d.
Total	0.25	N.d.	N.d.	N.d.	N.d.	N.d.	N.d.	N.d.	N.d.	N.d.	N.d.	N.d.	N.d.	N.d.
$(La/Yb)_n$	0.41	0.67	0.27	1.15	0.09	0.26	N.d.	N.d.	N.d.	N.d.	N.d.	N.d.	N.d.	N.d.

	Massifs, provinces, manifestations													
	Stillwater, USA													
	(Papike *et al.*, 1995), SIMS			(Lambert & Simmons, 1987), IDMS										
	907	908	909	CM04	LM04	LM05	LM06	LM07	LM08	LM09	LM10	pp13	pp14	pp15
Element	*Bronzitites*													
La	0.039	0.044	0.020	0.036	0.095	0.094	0.057	0.130	0.091	0.077	0.099	0.092	0.057	0.067
Ce	0.156	0.212	0.066	0.099	0.304	0.329	0.155	0.292	0.236	0.214	0.209	0.213	0.149	0.192
Pr	N.d.	N.d.	N.d.	N.d.	N.d.	N.d.	N.d.	N.d.	N.d.	N.d.	N.d.	N.d.	N.d.	N.d.
Nd	0.201	0.256	0.097	0.087	0.345	0.354	0.129	0.209	0.196	0.192	0.136	0.148	0.122	0.155
Sm	0.088	0.146	0.071	0.036	0.117	0.148	0.053	0.088	0.083	0.082	0.054	0.054	0.046	0.059
Eu	0.0220	0.039	0.015	0.010	0.025	0.030	0.016	0.021	0.021	0.022	0.017	0.015	0.014	0.017
Gd	N.d.	N.d.	N.d.	0.056	0.186	0.223	0.085	0.119	0.124	0.123	0.081	0.077	0.070	0.086
Tb	N.d.	N.d.	N.d.	N.d.	N.d.	N.d.	N.d.	N.d.	N.d.	N.d.	N.d.	N.d.	N.d.	N.d.
Dy	0.374	0.373	0.155	0.110	0.323	0.348	0.152	0.210	0.224	0.229	0.153	0.153	0.141	0.167
Ho	N.d.	N.d.	N.d.	N.d.	N.d.	N.d.	N.d.	N.d.	N.d.	N.d.	N.d.	N.d.	N.d.	N.d.
Er	0.305	0.372	0.163	0.091	0.257	0.254	0.118	0.161	0.171	0.179	0.125	0.126	0.155	0.133
Tm	N.d.	N.d.	N.d.	N.d.	N.d.	N.d.	N.d.	N.d.	N.d.	N.d.	N.d.	N.d.	N.d.	N.d.
Yb	0.430	0.442	0.210	0.115	0.316	0.286	0.130	0.190	0.199	0.213	0.155	0.158	0.143	0.162
Lu	N.d.	N.d.	N.d.	N.d.	N.d.	N.d.	N.d.	N.d.	N.d.	N.d.	N.d.	N.d.	N.d.	N.d.
Total	1.62	1.88	0.80	0.64	1.97	2.07	0.90	1.42	1.35	1.33	1.03	1.04	0.90	1.04
$(La/Yb)_n$	0.06	0.07	0.06	0.21	0.20	0.22	0.28	0.46	0.31	0.24	0.43	0.39	0.27	0.28

(*Continued*)

Table 5.7 Continued

	Massifs, provinces, manifestations													
	Stillwater, USA		Zabargad, Red Sea											
	(Lambert & Simmons, 1987), IDMS		(Vannucci *et al.*, 1993b), IPMA											
	pp35	pp36	036\12\c	036\12\r	036\2\c	036\3\c	036\9\c	036A\1\r	036A\2\c	036A\3\c	036A\3\r	036B\12\	036B\2\c	036B\8\c
Element	*Bronzitites*		*Pyroxenites*											
La	0.120	0.057	N.d.	N.d.	N.d.	N.d.	N.d.	N.d.	N.d.	N.d.	N.d.	N.d.	N.d.	N.d.
Ce	0.291	0.147	0.010	0.020	0.050	0.070	0.050	0.080	0.010	0.010	0.010	0.060	0.010	0.060
Pr	N.d.	N.d.	N.d.	N.d.	N.d.	N.d.	N.d.	N.d.	N.d.	N.d.	N.d.	N.d.	N.d.	N.d.
Nd	0.218	0.134	0.040	0.070	0.220	0.180	0.190	0.210	0.050	0.060	0.020	0.070	0.020	0.060
Sm	0.080	0.059	0.120	0.120	0.270	0.260	0.330	0.060	0.020	0.070	0.040	0.080	0.030	0.040
Eu	0.021	0.016	0.010	0.030	0.040	0.040	0.100	0.020	0.040	0.030	0.010	0.020	0.010	0.020
Gd	0.117	0.087	N.d.	N.d.	N.d.	N.d.	N.d.	N.d.	N.d.	N.d.	N.d.	0.410	0.170	0.140
Tb	N.d.	N.d.	N.d.	N.d.	N.d.	N.d.	N.d.	N.d.	N.d.	N.d.	N.d.	N.d.	N.d.	N.d.
Dy	0.213	0.164	3.750	4.700	4.210	5.880	5.880	2.630	1.800	3.760	3.310	2.110	0.890	1.070
Ho	N.d.	N.d.	N.d.	N.d.	N.d.	N.d.	N.d.	N.d.	N.d.	N.d.	N.d.	N.d.	N.d.	N.d.
Er	0.170	0.128	6.960	8.320	6.240	8.700	10.300	4.240	3.230	5.800	5.190	3.690	1.590	2.190
Tm	N.d.	N.d.	N.d.	N.d.	N.d.	N.d.	N.d.	N.d.	N.d.	N.d.	N.d.	N.d.	N.d.	N.d.
Yb	0.212	0.152	12.19	13.51	12.12	16.41	19.20	7.890	7.240	10.39	9.670	7.050	3.970	5.140
Lu	N.d.	N.d.	N.d.	N.d.	N.d.	N.d.	N.d.	N.d.	N.d.	N.d.	N.d.	N.d.	N.d.	N.d.
Total	1.44	0.94	23.1	26.8	23.2	31.5	36.1	15.1	12.4	20.1	18.3	13.5	6.69	8.72
$(La/Yb)_n$	0.38	0.25	N.d.	N.d.	N.d.	N.d.	N.d.	N.d.	N.d.	N.d.	N.d.	N.d.	N.d.	N.d.

	Massifs, provinces, manifestations													
	Zabargad, Red Sea											Naransky, Mongolia		
	(Vannucci *et al.*, 1993b), IPMA											(Lesnov, 1988; Lesnov & Gora, 1998)		
	036C\17g	036C\8\c	036Cexs	096\12\c	145\1\c	145\6\c	145B\1\c	145B\1\r	146\2\c	146\8\c	146\8\r	269	270	278
Element	*Pyroxenites*											*Gabbro-norites*		
La	N.d.	N.d.	N.d.	N.d.	N.d.	N.d.	N.d.	N.d.	N.d.	N.d.	N.d.	0.200	0.210	2.960
Ce	0.010	0.010	0.090	0.010	0.070	0.060	0.050	0.080	0.050	0.030	0.090	0.850	0.460	6.900
Pr	N.d.	N.d.	N.d.	N.d.	N.d.	N.d.	N.d.	N.d.	N.d.	N.d.	N.d.	N.d.	N.d.	N.d.
Nd	0.020	0.030	0.070	0.020	0.140	0.100	0.190	0.130	0.090	0.100	0.060	0.900	0.350	2.370
Sm	0.020	0.040	0.040	0.010	0.230	0.240	0.180	0.060	0.070	0.070	0.030	0.400	0.085	0.390
Eu	0.010	0.020	0.030	0.010	0.050	0.050	0.040	0.060	0.030	0.030	0.0200	0.130	0.014	0.064
Gd	N.d.	0.180	N.d.	0.030	N.d.	N.d.	N.d.	N.d.	0.140	N.d.	N.d.	0.600	0.084	0.390
Tb	N.d.	N.d.	N.d.	N.d.	N.d.	N.d.	N.d.	N.d.	N.d.	N.d.	N.d.	0.100	0.020	0.069
Dy	0.190	1.070	0.970	0.140	1.600	2.160	1.920	1.160	0.300	0.280	0.320	N.d.	N.d.	N.d.
Ho	N.d.	N.d.	N.d.	N.d.	N.d.	N.d.	N.d.	N.d.	N.d.	N.d.	N.d.	N.d.	N.d.	N.d.
Er	0.390	2.180	1.820	0.180	1.870	2.370	2.210	2.160	0.330	0.260	0.340	N.d.	N.d.	N.d.
Tm	N.d.	N.d.	N.d.	N.d.	N.d.	N.d.	N.d.	N.d.	N.d.	N.d.	N.d.	0.070	0.010	0.034
Yb	0.900	4.540	4.080	0.340	2.920	3.760	3.180	2.650	0.500	0.450	0.450	0.500	0.100	0.190
Lu	N.d.	N.d.	N.d.	N.d.	N.d.	N.d.	N.d.	N.d.	N.d.	N.d.	N.d.	0.060	0.015	0.025
Total	1.54	8.07	7.10	0.74	6.88	8.74	7.77	6.30	1.51	1.22	1.31	3.81	1.35	13.4
$(La/Yb)_n$	N.d.	N.d.	N.d.	N.d.	N.d.	N.d.	N.d.	N.d.	N.d.	N.d.	N.d.	0.27	1.42	10.5

(*Continued*)

Table 5.7 Continued

	Massifs, provinces, manifestations													
	Beriozovsky, Russia						Shikotansky, Russia		Sheltingsky, Russia		Komsomol'sky Russia	Tamvatney., Rus.	Kuyul., Rus.	Valizhgen., Rus.
	(Lesnov, 1988; Lesnov & Gora, 1998), RNAA													
	131	132a	138a	141	144	147	186	187	173	183	190	114	115	115-11a
Element	*Gabbro-norites*													
La	0.110	0.060	0.040	0.150	0.570	0.060	0.066	0.200	0.120	0.090	0.140	0.120	0.160	0.220
Ce	0.310	0.130	0.130	0.250	1.460	0.490	0.360	0.880	0.600	0.420	0.340	0.220	0.420	0.430
Pr	N.d.	N.d.	N.d.	N.d.	N.d.	N.d.	N.d.	N.d.	N.d.	N.d.	N.d.	N.d.	N.d.	N.d.
Nd	0.160	0.150	0.100	0.200	0.930	0.460	0.490	1.070	0.760	0.500	0.190	0.240	0.280	0.370
Sm	0.060	0.040	0.027	0.050	0.240	0.180	0.330	0.780	0.320	0.180	0.044	0.065	0.070	0.090
Eu	0.013	0.020	0.015	0.013	0.044	0.060	0.150	0.230	0.110	0.070	0.010	0.040	0.020	0.050
Gd	0.070	0.100	0.110	0.070	0.300	0.250	0.660	2.200	0.510	0.310	0.066	0.160	0.100	0.095
Tb	0.015	0.025	0.009	0.017	0.050	0.050	0.170	0.460	0.130	0.060	0.014	0.023	0.030	0.032
Dy	N.d.	N.d.	N.d.	N.d.	N.d.	N.d.	N.d.	N.d.	N.d.	N.d.	N.d.	N.d.	N.d.	0.400
Ho	N.d.	N.d.	N.d.	N.d.	N.d.	N.d.	N.d.	N.d.	N.d.	N.d.	N.d.	N.d.	N.d.	N.d.
Er	N.d.	N.d.	N.d.	N.d.	N.d.	N.d.	N.d.	N.d.	N.d.	N.d.	N.d.	N.d.	N.d.	N.d.
Tm	0.020	0.015	0.012	0.015	0.040	0.033	0.160	0.600	0.094	0.031	0.020	0.015	0.060	0.080
Yb	0.090	0.095	0.090	0.170	0.240	0.360	1.220	5.620	0.680	0.260	0.170	0.060	0.330	0.280
Lu	0.028	0.020	0.014	0.023	0.034	0.055	0.200	0.580	0.100	0.040	0.033	0.017	0.060	0.080
Total	0.88	0.66	0.55	0.96	3.91	2.00	3.81	12.6	3.42	1.96	1.03	0.96	1.53	2.13
$(La/Yb)_n$	0.82	0.43	0.30	0.60	1.60	0.11	0.04	0.02	0.12	0.23	0.56	1.35	0.33	0.53

	Massifs, provinces, manifestations													
	Karaginsky, Russia		Lukinda, Russia	Voykar-Sin'in., Rus.	Chaysky, Russia	Monchegorsky, Russia	Rybinsky, Russia			Ostiurensky, Russia		Nizhnederbinsky, Rus.	Beriozovsky, Russia	Stillwater, USA
	(Lesnov, 1988; Lesnov & Gora, 1998), RNAA													(Lambert & Simmons, 1987)
	96	98	168	252	27	71	88	89	93	428	429	94	148	7W206
Element	*Gabbro-norites*													
La	0.060	0.270	2.580	0.590	0.260	0.260	0.990	1.940	0.270	2.500	0.550	0.700	0.040	0.034
Ce	0.240	1.000	8.100	2.040	0.820	1.100	3.400	5.750	1.690	11.200	2.380	2.000	0.150	0.099
Pr	N.d.	N.d.	N.d.	N.d.	N.d.	N.d.	N.d.	N.d.	N.d.	N.d.	N.d.	N.d.	N.d.	N.d.
Nd	0.100	0.700	6.000	1.900	0.800	0.930	3.100	5.500	1.730	10.800	2.810	1.840	0.150	0.087
Sm	0.060	0.210	2.150	0.850	0.240	0.240	1.210	2.010	0.740	4.370	1.230	1.030	0.150	0.047
Eu	0.048	0.180	0.740	0.130	0.110	0.110	0.240	0.490	0.260	1.960	0.410	0.270	0.026	0.010
Gd	0.230	0.590	0.800	1.050	0.380	0.430	2.300	2.210	1.240	4.200	1.000	1.320	0.120	N.d.
Tb	0.038	0.140	0.200	0.150	0.066	0.086	0.410	0.430	0.190	0.960	0.240	0.280	0.025	N.d.
Dy	0.200	N.d.	N.d.	N.d.	N.d.	N.d.	N.d.	N.d.	N.d.	N.d.	N.d.	1.700	N.d.	0.202
Ho	N.d.	N.d.	N.d.	N.d.	N.d.	N.d.	N.d.	N.d.	N.d.	N.d.	N.d.	N.d.	N.d.	N.d.
Er	N.d.	N.d.	N.d.	N.d.	N.d.	N.d.	N.d.	N.d.	N.d.	N.d.	N.d.	N.d.	N.d.	0.185
Tm	0.031	0.100	0.100	0.130	0.070	0.068	0.400	0.260	0.300	0.600	0.250	0.240	0.020	N.d.
Yb	0.200	0.540	0.590	0.990	0.640	0.500	2.880	1.490	1.960	4.770	1.300	1.630	0.130	0.251
Lu	0.039	0.100	0.090	0.100	0.100	0.100	0.360	0.260	0.290	0.510	0.230	0.270	0.022	N.d.
Total	1.25	3.83	21.4	7.93	3.49	3.82	15.3	20.3	8.67	41.9	10.4	11.3	0.83	0.92
$(La/Yb)_n$	0.20	0.34	2.95	0.40	0.27	0.35	0.23	0.88	0.09	0.35	0.29	0.29	0.21	0.09

(*Continued*)

Table 5.7 Continued

	Massifs, provinces, manifestations													
	Stillwater, USA									Elan		Alpine	Vilcha	Anakies
	(Lambert, Simmons, 1987), IDMS					(Papike *et al.*, 1995), SIMS				(Irving & Frey, 1984), NAA				
	7W-239.8	7W-65.8	LM01	LM02	LM11	903	904	905	906	Al-1	Al-3	ALP7	WA-1	2115b
Element	*Norites*									*Basalts*				
La	0.024	0.044	0.190	0.151	0.055	0.006	0.021	0.018	0.016	0.500	0.136	0.037	0.072	0.219
Ce	N.d.	0.140	0.471	0.381	0.219	0.035	0.120	0.118	0.095	1.640	0.488	N.d.	N.d.	0.610
Pr	N.d.	N.d.	N.d.	N.d.	N.d.	N.d.	N.d.	N.d.	N.d.	0.153	0.069	N.d.	N.d.	N.d.
Nd	0.056	0.133	0.353	0.350	0.269	0.051	0.185	0.227	0.123	0.674	0.363	N.d.	N.d.	N.d.
Sm	0.028	0.070	0.142	0.152	0.127	0.037	0.123	0.146	0.068	0.227	0.150	0.159	0.081	0.120
Eu	0.007	0.019	0.020	0.025	0.021	0.009	0.015	0.023	0.014	0.072	0.063	0.071	0.036	0.051
Gd	N.d.	N.d.	0.213	0.238	0.201	N.d.	N.d.	N.d.	N.d.	0.342	0.271	N.d.	N.d.	N.d.
Tb	N.d.	N.d.	N.d.	N.d.	N.d.	N.d.	N.d.	N.d.	N.d.	0.094	0.051	N.d.	N.d.	N.d.
Dy	0.115	0.307	0.360	0.405	0.346	0.222	0.474	0.661	0.290	N.d.	N.d.	N.d.	N.d.	N.d.
Ho	N.d.	N.d.	N.d.	N.d.	N.d.	N.d.	N.d.	N.d.	N.d.	0.106	0.088	N.d.	N.d.	N.d.
Er	0.104	0.286	0.264	0.307	0.260	0.227	0.415	0.499	0.306	0.358	0.264	N.d.	N.d.	N.d.
Tm	N.d.	N.d.	N.d.	N.d.	N.d.	N.d.	N.d.	N.d.	N.d.	0.059	0.049	N.d.	N.d.	N.d.
Yb	0.144	0.392	0.300	0.356	0.300	0.346	0.530	0.600	0.365	0.347	0.280	0.500	0.210	0.150
Lu	N.d.	N.d.	N.d.	N.d.	N.d.	N.d.	N.d.	N.d.	N.d.	0.067	0.047	0.096	0.040	0.032
Total	0.48	1.39	2.31	2.37	1.80	0.93	1.88	2.29	1.28	4.64	2.32	N.d.	N.d.	N.d.
$(La/Yb)_n$	0.11	0.08	0.43	0.29	0.12	0.01	0.03	0.02	0.03	0.97	0.33	0.05	0.23	0.99

	Massifs, provinces, manifestations									
	Mount Adams, USA			Japan	Saipan	Honshu, Japan				
	(Dunn & Sen, 1994), IPMA			(Schnetzler & Philpotts, 1970)		(Nagasawa *et al.*, 1969), IDMS				
	87-14	87-49	87-7	GSFC184	GSFC271	NC-1	NC-2	NC-3	NC-4	NC-6
Element	*Andesites*					*Dacites*				
La	4.100	18.000	N.d.	N.d.	N.d.	N.d.	N.d.	N.d.	N.d.	N.d.
Ce	7.700	N.d.	2.000	0.264	0.442	7.200	5.100	7.700	4.370	4.370
Pr	1.100	1.800	0.290	N.d.	N.d.	N.d.	N.d.	N.d.	N.d.	N.d.
Nd	4.800	8.200	1.400	0.322	0.645	3.920	3.130	4.460	2.550	3.290
Sm	1.400	2.000	0.630	0.147	0.347	0.900	0.750	1.010	0.700	1.050
Eu	0.230	0.310	0.072	N.d.	0.064	0.085	0.105	0.185	0.064	0.191
Gd	1.700	2.800	0.640	N.d.	N.d.	N.d.	0.910	1.180	0.930	N.d.
Tb	0.290	0.420	0.079	N.d.	N.d.	N.d.	N.d.	N.d.	N.d.	N.d.
Dy	2.400	3.200	0.560	0.503	1.350	1.230	1.370	1.280	1.440	2.380
Ho	0.580	0.710	0.140	N.d.	N.d.	N.d.	N.d.	N.d.	N.d.	N.d.
Er	2.100	2.500	0.560	0.451	1.400	1.290	1.360	1.080	1.340	2.160
Tm	0.330	0.410	0.071	N.d.	N.d.	N.d.	N.d.	N.d.	N.d.	N.d.
Yb	2.100	3.200	0.410	0.662	2.100	1.550	2.320	1.880	2.030	3.110
Lu	0.400	0.590	0.220	N.d.	0.414	0.305	0.480	0.361	0.421	0.570
Total	29.2	44.1	7.07	N.d.	N.d.	16.5	15.5	19.1	13.9	17.1
$(La/Yb)_n$	1.32	3.80	N.d.	N.d.	N.d.	N.d.	N.d.	N.d.	N.d.	N.d.

(*Continued*)

Table 5.7 Continued

	Massifs, provinces, manifestations									
	Twin Peaks, USA		Norway		The Moon					
	(Nash & Crecraft, 1985), NAA		(Reitan *et al.*, 1980)		(Floss *et al.*, 1998), IPMA					
	12	15	15/25	16/26	603	601MF	602MF	60025.699	64435.270	64435.27
Element	*Rhyolites*		*Granulites*		*Ferriferous mafic rocks*			*Magnesioferous mafic rocks*		
La	59.00	67.00	2.100	2.300	0.770	0.870	0.530	0.003	0.016	0.009
Ce	151.0	166.0	5.800	6.400	2.280	3.680	1.740	0.019	0.062	0.027
Pr	N.d.	N.d.	N.d.	N.d.	0.330	0.770	0.280	0.006	0.014	0.007
Nd	86.00	90.00	3.600	4.600	1.680	4.450	1.430	0.056	0.096	0.067
Sm	15.20	15.90	0.770	0.800	0.660	1.910	0.650	0.052	0.076	0.084
Eu	0.900	0.810	0.200	0.120	0.028	0.016	0.012	0.001	0.004	N.d.
Gd	N.d.	N.d.	0.900	0.390	0.970	2.950	1.123	0.150	0.240	0.240
Tb	2.100	2.180	0.090	0.150	0.290	0.620	0.250	0.052	0.089	0.100
Dy	14.00	13.00	N.d.	N.d.	2.150	4.850	2.390	0.490	0.830	0.920
Ho	N.d.	N.d.	N.d.	N.d.	0.640	1.040	0.670	0.130	0.230	0.290
Er	N.d.	N.d.	N.d.	N.d.	2.100	3.650	2.200	0.540	1.110	1.2200
Tm	N.d.	N.d.	N.d.	N.d.	0.350	0.490	0.380	0.091	0.170	0.240
Yb	10.00	10.80	0.630	1.600	2.870	3.770	3.220	0.800	1.590	1.940
Lu	1.510	1.600	0.110	0.300	0.470	0.560	0.450	0.130	0.290	0.340
Total	N.d.	N.d.	N.d.	N.d.	15.6	29.6	15.3	2.52	4.82	5.48
$(La/Yb)_n$	3.98	4.19	2.25	0.97	0.18	0.16	0.11	0.003	0.007	0.003

[aa] Samples from deep xenoliths.

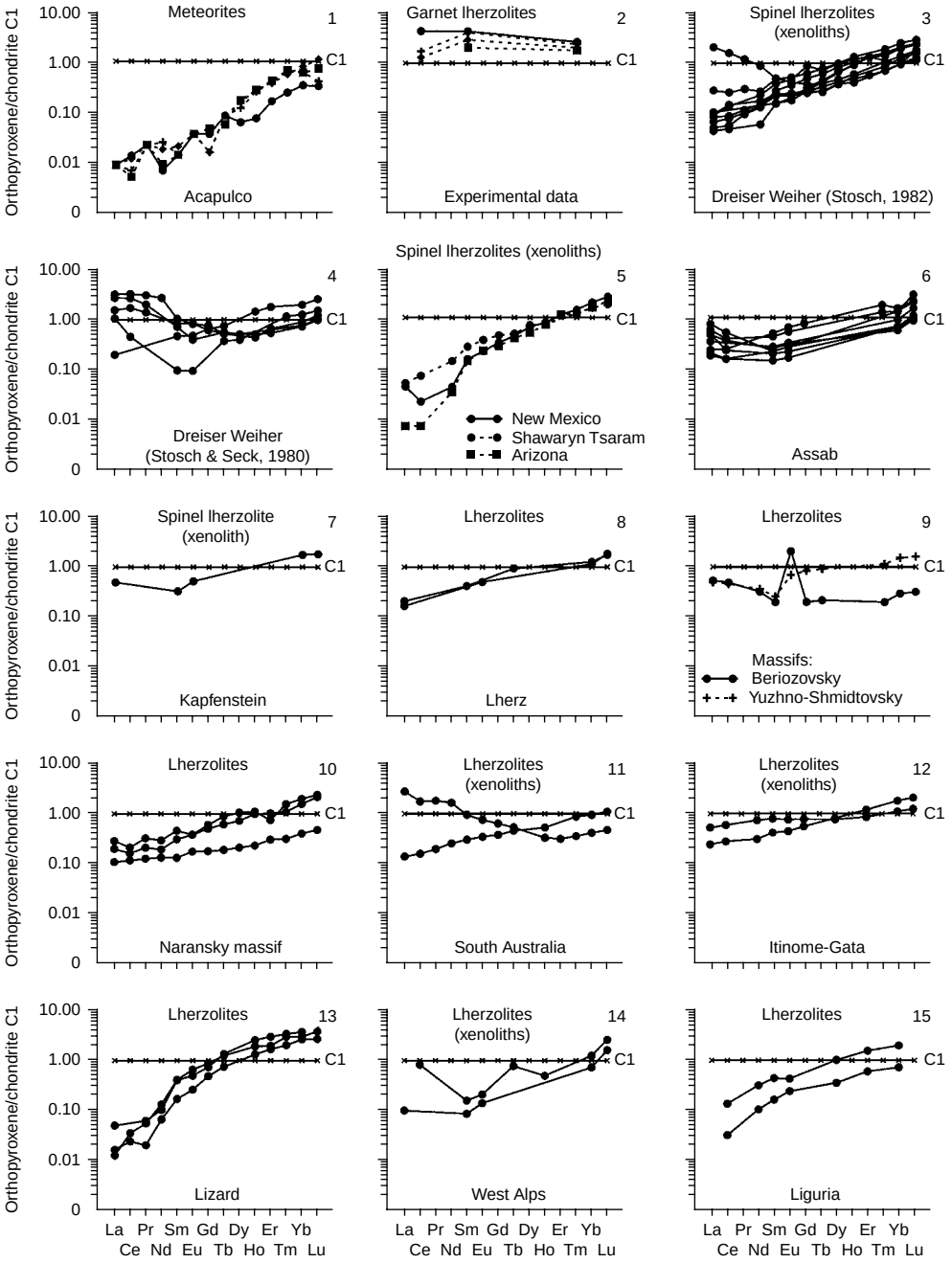

Figure 5.9 Chondrite-normalized REE patterns for orthopyroxenes from some types of rock (data Table 5.7).

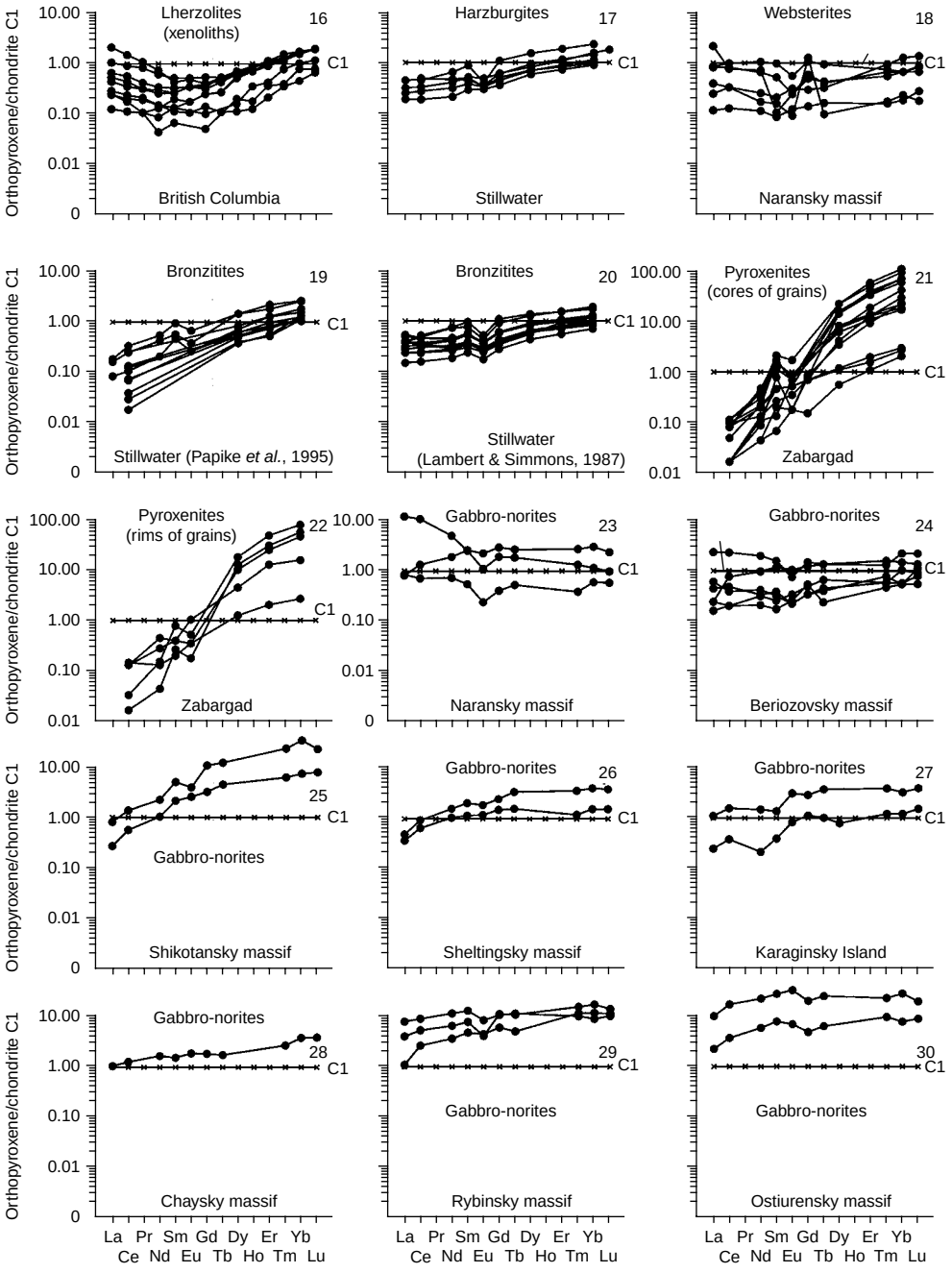

Figure 5.9 Continued

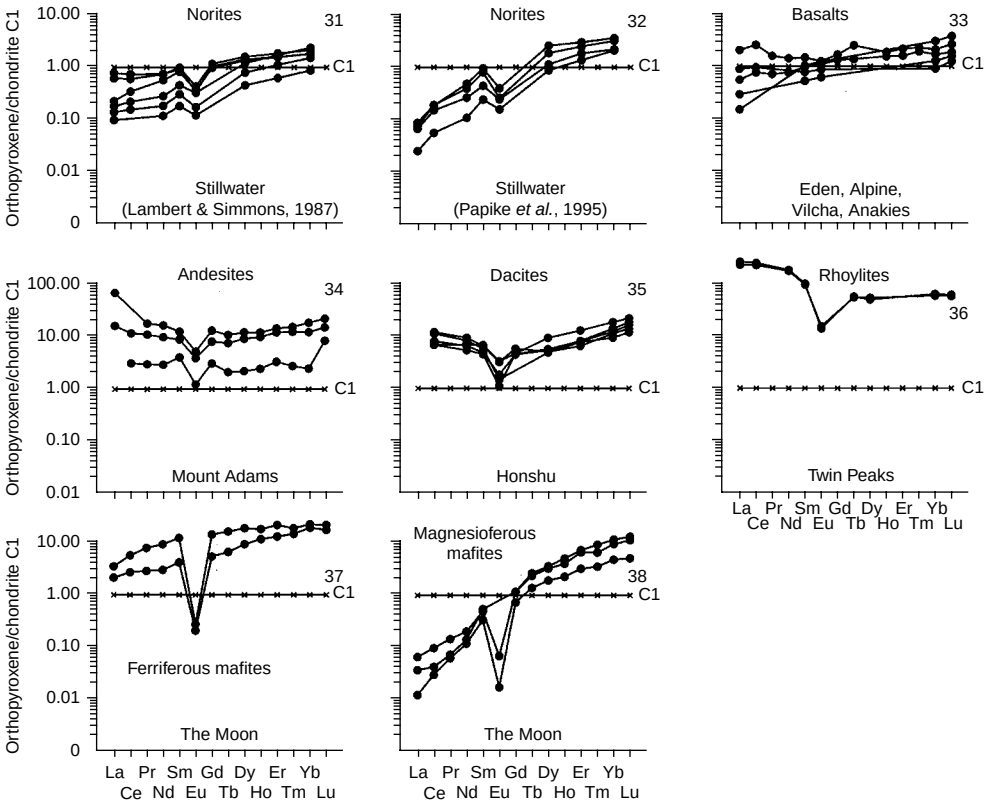

Figure 5.9 Continued

Mafic rocks of the Moon. Orthopyroxenes from these rocks were also characterized from examples of individual samples (Floss *et al.*, 1998). Differences in the level of accumulation of REE and in the ratios between light and heavy elements allow them to be divided into two groups. The first, represented by the samples of high-Fe rocks, is characterized by a higher total content of REE (15.3–29.6 ppm), which is due to increased concentrations of light and, partly, middle elements (Fig. 5.9, 37). The second group of orthopyroxenes from the rocks with a high Mg content has a lower total content of REE (2.5–5.5 ppm), owing to the considerable depletion of light REE (see Fig. 5.9, 38). One can observe that the REE patterns of both varieties have rather steep positive slopes and are complicated by very intensely negative Eu anomalies. Most likely, the deficit of Eu in these orthopyroxenes was due to the fact that, on crystallization of their parental basalt melts under strongly reduced conditions of the moon, virtually all Eu was in a bivalent state. As a result of this, Eu ions accumulated mainly in the structure of coexisting plagioclases and, in very small doses, in the structure of orthopyroxenes.

Spinel lherzolites from deep xenoliths. Orthopyroxenes from these rocks were studied from examples of xenoliths from the Dreiser Weiher province (Stosch, 1982; Stosch & Seck, 1980), Assab (Ottonello *et al.*, 1978), Spitsbergen Island (Shubina *et al.*,

1997), and British Columbia (Sun & Kerrich, 1995). Single samples of the mineral from xenoliths from some other provinces (Southern Australia, Itinome–Gata, and Western Alps) were analyzed as well. The total content of REE in these orthopyroxenes ranges from about 0.5 to 5.2 ppm, with an abnormal enrichment with light elements (Fig. 5.9, 3, 4–7, 11, 12), owing to which most REE patterns are U-shaped. These data suggest that orthopyroxenes contain various amounts of nonstructural impurities of light elements that were supplied during the percolation of fluids separated from basalt melts which carried xenoliths.

Lherzolites from mafic–ultramafic massifs. The rare earth composition of orthopyroxenes from this variety of ultramafic rocks was characterized from examples of individual samples from the Lherz (Bodinier *et al.*, 1988), Naransky (Lesnov, 1988; Lesnov & Gora, 1998), Lizard (Frey, 1969), and Liguria (Rampone *et al.*, 1991) massifs. In the majority of these samples, the total content of REE ranges from 0.2 to 2.8 ppm. In some samples, the level of accumulation of heavy REE is somewhat higher than that of light REE, owing to which their patterns have a positive slope (Fig. 5.9, 8, 10, 15). Orthopyroxenes from the Lizard massif are considerably depleted of light REE, which results in a steeper positive slope (Fig. 5.9, 13) and low values of $(La/Yb)_n$ (0.004–0.01).

Harzburgites. These orthopyroxenes are characterized from examples of samples from the Stillwater massif (Lambert & Simmons, 1987). The total content of analyzed elements in these orthopyroxenes ranged from 0.8 to 14 ppm. The level of accumulation of light REE in them is somewhat lower than that of heavy REE, owing to which their patterns have a gentle positive slope. The values of the $(La/Yb)_n$ parameter in these samples range from 0.20 to 0.45 (Fig. 5.9, 17). Some REE patterns display low-intensity, negative Eu anomalies. Similar Eu anomalies are observed in the patterns of orthopyroxenes from bronzitites of this massif (Fig. 5.9, 19, 20).

Pyroxenites. The REE composition of the studied orthopyroxene samples from Zabargad Island is unusual for this mineral (Vannucci *et al.*, 1993a,b); they have very low concentrations of light REE and very high concentrations of heavy REE (Fig. 5.9, 21, 22). R. Vannucci and coauthors think that this was due to the fact that orthopyroxenes formed during the decompressive metamorphism of high-pressure garnet pyroxenites by way of replacement of earlier garnets rich in heavy REE and poor in light REE.

Gabbro-norites. Orthopyroxenes from these rocks were studied in samples from several ophiolite mafic–ultramafic massifs (Lesnov & Gora, 1998). Samples from the rocks of the Sheltingsky massif (Sakhalin Island) have a rather low total level of accumulation of all REE, which increases from La (0.4–0.5 t. ch.) to Yb (1.6–3.9 t. ch.). Their patterns display very weakly positive Eu anomalies (Fig. 5.9, 26). Orthopyroxenes from gabbro-norites of the Beriozovsky massif (Sakhalin Island) are represented by two varieties. One of them is depleted of all REE, and the other is enriched with light REE. The patterns of both varieties display weakly negative Eu anomalies (Fig. 5.9, 24). The patterns of orthopyroxenes from gabbro-norites of the Naransky massif (Mongolia) have the same configuration. Some of them are abnormally enriched with light REE, which seems to be due to the presence of nonstructural impurities of these elements (Fig. 5.9, 23).

A somewhat different rare earth composition is observed in orthopyroxenes from gabbro-norites which make up mafic–ultramafic massifs unrelated to ophiolitic associations, such as the Ostiurensky, Rybinsky, Nizhnederbinsky, and Shikotansky massifs.

They have higher total contents of REE (4–42 ppm) and a positive slope in their patterns (Fig. 5.9, 25, 29, 30). We think that parental melts, from which gabbro-norites of these massifs crystallized, were richer in REE compared to the melts that resulted in gabbro-norites from the massifs pertaining to ophiolitic association, as their generation proceeded at lower degrees of partial melting of undepleted mantle sources.

Norites. Orthopyroxenes from these gabbros are characterized from examples of some samples of the Stillwater massif (Lambert & Simmons, 1987). These demonstrate depletion of all REE, which total content ranges within 0.5–2.4 ppm. In the level of accumulation of light REE, these orthopyroxenes can be divided into two groups: relatively enriched and relatively depleted of these elements. The REE patterns of samples of both groups have a positive slope and are complicated by negative Eu anomalies, the slope of patterns for the first group is gentler than that for the second (Fig. 5.9, 31, 32).

Basalts, andesites, dacites, and rhyolites. The REE composition of orthopyroxenes from these effusive rocks is characterized from examples of single samples. Orthopyroxenes from phenocrysts in basalts have a higher level of REE accumulation compared to chondrite C1 (Fig. 5.9, 33). Compared to the previous samples, the mineral samples from andesites, dacites, and rhyolites have a higher level of REE accumulation. Most of their patterns have negative Eu anomalies of varying intensity (Fig. 5.9, 34–36).

The availability of chemical analyses for some orthopyroxene samples in which REE were determined allowed us to establish the relationship between the contents of trace elements and major components. In particular, it was found that the contents of Gd, Tb, Tm, Yb, and Lu in orthopyroxenes increase with increasing Fe content and decreasing Mg content. Moreover, the contents of Sm, Nd, and all heavy REE in the mineral increase with increasing contents of Ca and Ti, and the contents of La and Ce have a direct relationship with Ti content.

At the end of characterization of orthopyroxene composition from various petrographic types of rocks and occurrences, we want to note that experimental data show a positive correlation between the contents of heavy REE and Al and a negative correlation between the contents of Mg and Fe and heavy REE in enstatite (Schwandt & McKey, 1998).

5.2.2 On the relationship between the REE composition and content of fluid components in orthopyroxenes

Fluid components (CO, H_2, N_2, CH_4, CO_2, H_2O, for example) are known to play an important role in the crystallization of minerals from magmatic melts, including the fractionation of REE between melts and solid phases (Balashov, 1976; Redder, 1987; Mysen, 1983; Green, 1994; Neruchev *et al.*, 1997). We analyzed the relationship between the contents of REE and fluid components in orthopyroxenes from samples from gabbro-norites, websterites, and lherzolites (Lesnov *et al.*, 1998b,c). The contents of REE in single-fraction mineral samples were determined by the RNAA method, and the content of fluid components separated from high- and low-temperature microinclusions in orthopyroxene grains was analyzed by the decrepitation procedure with further application of gas chromatography. The analyses showed that the concentration of heavy REE in orthopyroxenes increases with increasing content of reduced CO

Table 5.8 Chemical composition of orthopyroxenes from spinel lherzolite (wt%) (sp. M-699-27, xenolith from paleovolcano Shavaryn Tsaram, Mongolia).

Component	Analysis number						
	A-8[a]	A-12[a]	A-14[a]	A-21	A-27	A-33	A-39
SiO_2	55.27	55.32	54.44	53.86	55.17	54.76	53.64
TiO_2	0.123	0.128	0.149	0.165	0.132	0.147	0.140
Al_2O_3	4.30	4.61	4.67	5.28	4.27	4.86	4.33
Cr_2O_3	0.268	0.321	0.342	0.435	0.231	0.365	0.258
FeO	6.41	6.45	6.51	6.50	6.33	6.46	6.52
MgO	32.86	32.07	32.46	31.96	32.79	32.14	33.38
MnO	0.164	0.162	0.179	0.144	0.155	0.137	0.148
CaO	0.732	0.714	0.889	1.14	0.995	1.02	1.03
Na_2O	0.152	0.133	0.095	0.150	0.092	0.091	0.086
Total	100.29	99.93	99.74	99.64	100.17	99.99	99.54
Mg#	90.1	89.3	89.9	89.8	90.2	89.9	90.1

Analysis carried out by X-ray spectrographic method on apparatus "Camebax-Micro" (analysts V.N. Koroliuk). Mg# = 100·Mg/(Mg + Fe) (formula's coefficients). Dispose of orthopyroxene grains, which were analyzed, show on Figure 5.3. Results of analysis of REE in some orthopyroxenes from this table are presented in Table 5.9 with the right numbers.

[a] Analysis numbers of grain orthopyroxenes, which disposed near grain olivines with right analysis numbers.

gas. Moreover, the content of REE in the samples increases with increasing value of the reduction index of fluid components, which was calculated as the following ratio

$$(CO + H_2 + CH_4)/(CO + H_2 + CH_4 + CO_2 + H_2O)$$

At the same time, the total content of REE in orthopyroxene samples decreases with increasing total content of all fluid components separated from the samples during their decrepitation on heating to 900°C.

We obtained data on the dependence of REE and fluid components when studying the rare earth composition of orthopyroxenes from spinel lherzolite in a large xenolith from alkali basalts of Shavaryn Tsaram paleovolcano, which was mentioned in the characterization of rare earth composition of olivines (Chapter 5.1). One of the orthopyroxene grains analyzed by the LA ICP-MS technique (see Fig. sample A-4) is represented by a xenocrystal occurring in the host alkali basalt close to its contact with an ultramafic xenolith. The obtained data show that the analyzed orthopyroxene crystals, both in the xenolith and in xenocrystals, have the same chemical composition (Table 5.8). To determine REE content by the LA ICP-MS technique, we selected the orthopyroxene grains that had the minimum microcracks observable under a microscope. The contents of REE in the studied orthopyroxene grains from the xenolith, as well as from xenocrystals, depend on their distance from contact of the xenolith with the host basalt. On the other hand, no relationship was established between the contents of heavy REE in orthopyroxene grains and their distance from contact of the xenolith with the basalt (Table 5.9). These relations were reflected in changes of light REE content in orthopyroxene grains and in the configuration of their rare earth patterns (Fig. 5.10). One can see from Table 5.9 that an orthopyroxene xenocrystal, which occurs in the basalt at a distance of 13 mm from the contact with the xenolith (sample A-4), has the highest concentration of light REE, providing the highest total content

Table 5.9 Rare earth element composition of orthopyroxenes from alkali basalt and xenolith of spinel lherzolite (ppm) (sp. M-699-27, paleovolcano Shavaryn Tsaram, Mongolia).

	Analysis number							
	A-4	A-21	A-26	A-27	A-33	A-36	A-39	A-43
	Distance from grains of orthopyroxenes to contact of xenolith with basalt, mm							
	−13	+54	+72	+79	+106	+124	+142	+161
Element	*Basalt*	*Spinel lherzolite*						
La	0.784	0.092	0.008	0.001	0.002	0.003	0.005	0.030
Ce	1.514	0.188	0.021	0.003	0.003	0.012	0.010	0.090
Pr	0.171	0.019	0.003	0.001	0.001	0.003	0.002	0.008
Nd	0.757	0.087	0.024	0.006	0.015	0.024	N.d.	0.030
Sm	0.194	0.032	0.018	0.008	0.010	0.012	0.001	0.005
Eu	0.055	0.008	0.007	0.002	0.004	0.007	0.002	0.002
Gd	0.090	0.023	0.026	0.016	0.022	0.016	0.020	0.020
Tb	0.020	0.007	0.010	0.004	0.004	0.008	0.003	0.004
Dy	0.159	0.061	0.081	0.038	0.032	0.061	0.030	0.030
Ho	0.036	0.021	0.018	0.011	0.017	0.018	0.008	0.010
Er	0.138	0.085	0.087	0.051	0.076	0.087	0.030	0.040
Tm	0.022	0.012	0.018	0.009	0.015	0.018	0.006	0.010
Yb	0.179	0.125	0.150	0.101	0.132	0.154	0.060	0.080
Lu	0.034	0.026	0.026	0.019	0.025	0.029	0.010	0.020
Total	4.15	0.786	0.496	0.269	0.359	0.450	0.187	0.379
$(La/Yb)_n$	2.96	0.50	0.04	0.01	0.01	0.01	0.06	0.25

Analysis carried out by method LA ICP-MS on mass-spectrometry "Element" and UV Laser Probe (firma "Finnigan", Germany) (analysts S.V. Palessky and A.M. Kuchkin). Sign (−) mark distance from orthopyroxene's xenocrystal to contact basalt with xenolith; signs (+) mark distances from orthopyroxene's crystals in xenolith to its contact with basalt. Dispose of orthopyroxene grains, which were analyzed, show on Figure 5.3.

compared to all crystals entering into the xenolith composition. At a lower level of accumulation of light REE, a similar distribution is also observed in an orthopyroxene crystal that occurs in the xenolith at a distance of 54 mm from its contact with the basalt (sample A-21). Less considerable enrichment with light REE was established in the orthopyroxene grain localized at a distance of 72 mm from contact with the basalt, that is, virtually in the central zone of the xenolith (sample A-26). In the series of orthopyroxene grains remote from contact with the basalt (sample A-27, A-33, and A-36), the level of accumulation of light REE decreases to a minimum (0.004–0.01 t. ch.). Closer to the opposite contact of the xenolith with the basalt, the contents of light REE in orthopyroxene grains successively increase again (sample A-39 and A-43). Though the contents of light REE change as described above, the contents of heavy REE in the whole sequence of orthopyroxene grains between opposite contacts of xenolith with basalt do not vary (Fig. 5.10), and Lu, in particular, remains at the level of 1 t. ch.

The described variations in the contents of REE in orthopyroxene grains suggest that the zoning in analyzed ultramafic xenolith results from the fact that both orthopyroxene and olivine grains, along with isomorphous impurities of REE, contain variable amounts of nonstructural impurities represented mainly by light elements. These impurities are, most likely, localized in microcracks, which cleave the mineral grains, and in

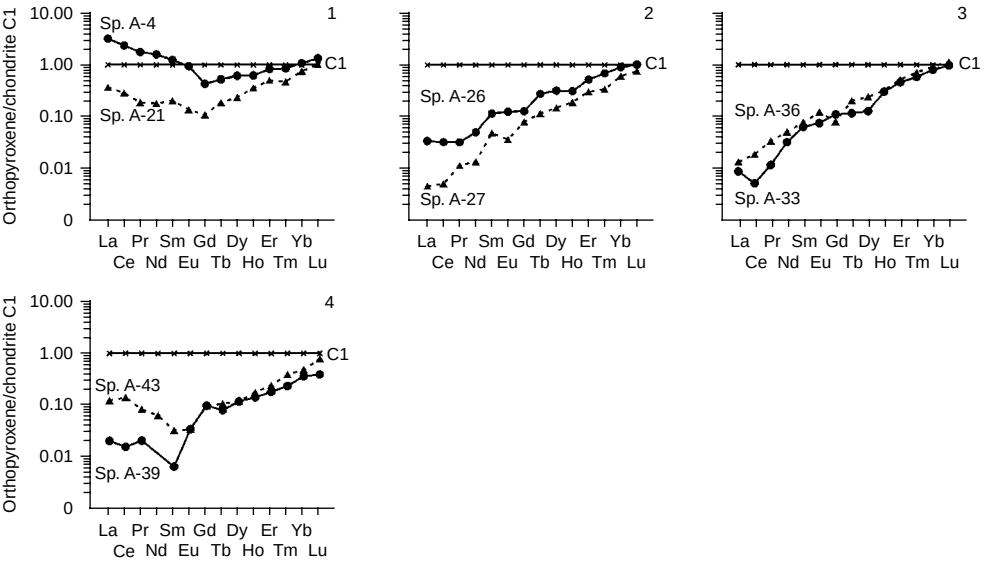

Figure 5.10 Chondrite-normalized REE patterns for orthopyroxenes from spinel lherzolites in a xenolith, represented in an alkaline basalt, and from the xenocrystals in the basalt (sp. M-699-27, paleovolcano Shavaryn Tsaram, Mongolia) (data Table 5.9).

mineral grains of fluid micro- and nanoinclusions. The accumulation of nonstructural impurities of REE in orthopyroxene grains as well as in olivine grains is assumed to be related to the percolation of fluids (separated from basalt melts) enriched with these impurities within the xenolith. Most likely, basalt melts with contained xenoliths of ultramafic rocks migrated along the volcanic channel to the surface at a rather high rate. For a relatively short period of time, during which xenoliths were in contact with basalt melts, the fluid components that separated from the melts percolated through microcracks into small xenoliths throughout all their volume and geochemical zoning of light REE distribution was not exhibited. For the same period of time, fluid components in large ultramafic xenoliths could penetrate only into their peripheral zones by a few centimeters.

5.2.3 Coefficients of REE distribution between orthopyroxenes and coexisting phases

Variations in REE concentrations in orthopyroxenes depend mainly on the coefficient of their distribution (K_d) between this mineral and coexisting phases, including melts. The calculations of available values of K_d(orthopyroxene/coexisting phase) are based on the analyses of both natural and experimental systems. These values vary over a wide range owing to many reasons, including different chemical compositions of coexisting phase, different physical and chemical conditions in which these phases crystallized, and more. Let us consider this problem in more details from the following examples.

Table 5.10 Coefficients of REE distribution between orthopyroxenes and basaltic melt (experimental data).

	Experiment's number							
	En/gl 1	En/gl 2	En/gl 3	En/gl 4	En/gl 5	opxRP31	opxRP40	opxRP45
Element	*(Schwandt & McKey, 1998)*					*(Kennedy et al., 1993)*		
La	0.0004	0.0003	0.0003	0.0006	0.0005	0.0001	0.0001	N.d.
Ce	0.0011	0.0009	0.0008	0.0041	0.0049	0.0004	0.0002	0.0001
Pr	N.d.	N.d.	N.d.	N.d.	N.d.	0.0008	0.0004	0.0003
Nd	0.0043	0.0037	0.0029	0.0041	0.0049	0.0017	0.0005	0.0005
Sm	0.0123	0.0112	0.0083	0.0119	0.0136	0.0038	0.0016	0.0016
Eu	0.0046	0.0045	0.0033	0.0046	0.0042	0.0023	0.0008	0.0006
Gd	N.d.	N.d.	N.d.	N.d.	N.d.	0.0037	0.0016	0.0047
Tb	N.d.	N.d.	N.d.	N.d.	N.d.	0.008	0.0044	0.0063
Dy	0.052	0.054	0.037	0.053	0.054	0.016	0.007	0.0084
Ho	N.d.	N.d.	N.d.	N.d.	N.d.	0.022	0.010	0.012
Er	0.092	0.097	0.069	0.098	0.096	0.028	0.016	0.017
Tm	N.d.	N.d.	N.d.	N.d.	N.d.	0.036	0.023	0.023
Yb	0.104	0.112	0.080	0.114	0.107	0.051	0.036	0.033
Lu	0.103	0.114	0.082	0.114	0.108	0.065	0.053	0.046

K_d(orthopyroxene/basalt melt). An experimental summary on the K_d(orthopyroxene/basalt melt) values for REE and some other trace elements was reported in 1994 (Green, 1994). These data were presented in a graphic form, whereas numeric values of K_d in the work were absent. Summarizing Green's data, it is worth noting that in the series of elements from La to Lu, K_d(orthopyroxene/basalt melt) values increase from about 10^{-4} to about 10^{-1}. The trend of changes in these K_d, which has a generally positive slope, is complicated by the minimum for Eu.

Some of the calculated absolute values of K_d(orthopyroxene/basalt melt) are reported in Table 5.10. Trends of their changes are shown in Figure 5.11, from which one can see that the trends of changes for K_d(orthopyroxene/basalt melt) in their configuration are comparable with the trends observed for K_d(olivine/basaltic melt) (Fig. 5.8), but in the case of orthopyroxenes, the absolute values of K_d are much higher. Based on the presented values of K_d(orthopyroxene/basaltic melt), which are less than unity in all cases, we can infer that all REE, when incorporated in the orthopyroxene structure, possesses the properties of incompatible elements. The degree of their incompatibility increases in the series from Lu, with the smallest size of ionic radius, to La, having the largest ionic radius among REE. Eu ions have a lower degree of incompatibility with the orthopyroxene structure compared to Sm and Gd, resulting in the minimums on the trends (Fig. 5.11). The described features of K_d(orthopyroxene/basaltic melt) suggest that during crystallization of orthopyroxenes from basaltic melts, the residual portions of the latter became slightly enriched with light REE, including Eu, and simultaneously became somewhat depleted of heavy elements.

K_d(orthopyroxene/olivine). These coefficients were calculated on the basis of analytical data on the rare earth compositions of coexisting orthopyroxenes and olivines from some varieties of rock. The average values of K_d(orthopyroxene/olivine) for all elements are greater than unity (Table 5.11), increasing successively from light REE to

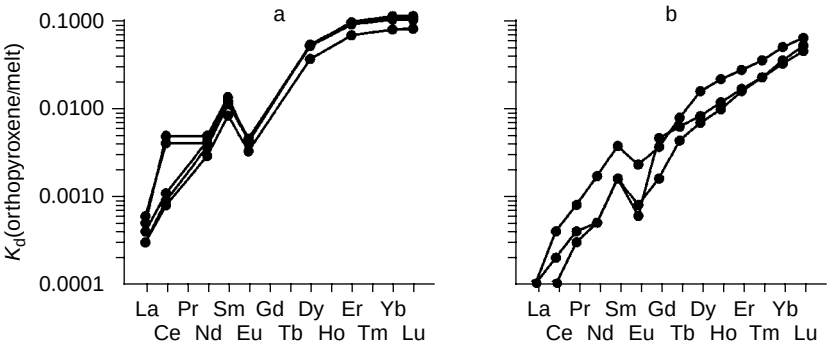

Figure 5.11 The trend coefficients of REE distribution between orthopyroxene and basalt melt, calculated on results of experiments (data Table 5.10). a—by (Schwandt and McKey, 1998); b—by (Kennedy *et al.*, 1993).

heavy REE. Therefore, on cocrystallization of these minerals from melts, all REE were more preferably accumulated in the orthopyroxene structure.

K_d(orthopyroxene/clinopyroxene). Compared to the previously mentioned parameters, these coefficients have a greater number of estimates calculated from paragenesis of these minerals in lherzolites, websterites, and gabbro-norites. The average values of K_d(orthopyroxene/clinopyroxene) (see Table 5.11) show that, firstly, for all REE, K_d is less than unity; secondly, in all the series of rare earth elements they change within a very narrow range (on average from ~0.1 to 0.3); thirdly, on cocrystallization of orthopyroxenes and clinopyroxenes, the latter can accumulate about 3–10 times more REE than orthopyroxenes can. The K_d(orthopyroxene/clinopyroxene) for lherzolites in deep xenoliths has higher values than the K_d for other two-pyroxene rocks. This suggests that on crystallization under higher pressures, the fractionation of REE between coexisting orthopyroxenes and clinopyroxenes is more variable. Obviously, the increased pressure, high temperature, and low gradients of their variations have a negative influence on the isomorphous incorporation of REE in the structure of orthopyroxene and, especially, elements with large ionic radii, that is, La, Ce, Nd, and Sm.

In the experimental studies of generation of basaltic melts in different P–T conditions and different degrees of partial melting of garnet peridotite, Harrison (1981) obtained K_d(orthopyroxene/clinopyroxene) values for Sm and Tm in crystallization products generated by basalt melts. We used these values for obtaining comparative estimates of partial melting of mantle protolites during formation of basalt melts from which gabbro-norites, occurring in different types of mafic–ultramafic massifs, crystallized (Lesnov & Gora, 1998; Lesnov *et al.*, 1998a). Our calculations suggest that the melts of gabbro-norites in mafic–ultramafic massifs from ophiolitic associations (for example, the Beriozovsky massif) in general were generated at higher degrees of partial melting of mantle protolites than the basalt melts from which gabbro-norites from non-ophiolite massifs (e.g., Rybinsky, Kuznetsky Alatau) crystallized. It is also worth noting that Eggins *et al.*, (1998) experimentally established that the K_d(orthopyroxene/clinopyroxene) values for Ce and Yb have a directly proportional dependence on temperature at which these minerals achieved the state of chemical equilibrium.

Table 5.11 Average values of coefficients REE distribution between orthopyroxenes and coexistent phases.

	Varieties of distribution coefficients												
Element	1 (21)	2 (26)	3 (16)	4 (143)	5 (34)	6 (17)	7 (25)	8 (10)	9 (26)	10 (4)	11 (9)	12 (32)	13 (9)
La	0.015	1.90	1.83	0.22	0.17	0.06	N.d.	0.43	0.33	2.35	8.12	N.d.	0.04
Ce	0.020	3.05	1.94	0.16	0.14	0.09	0.01	0.45	0.31	0.62	6.87	0.02	0.07
Pr	0.017	2.91	2.64	0.08	0.07	0.04	N.d.	N.d.	N.d.	2.02	N.d.	N.d.	0.15
Nd	0.012	2.91	2.74	0.15	0.09	0.06	0.01	N.d.	N.d.	1.93	8.21	0.52	0.27
Sm	0.022	5.43	4.98	0.10	0.05	0.06	0.03	0.16	0.28	3.88	8.04	0.22	0.79
Eu	0.015	6.84	8.12	0.09	0.05	0.05	0.03	0.18	0.20	0.14	0.79	0.05	0.002
Gd	0.025	7.90	8.35	0.16	0.08	0.05	N.d.	0.38	0.27	6.71	3.33	1.20	2.59
Tb	0.024	9.62	11.5	0.16	0.13	0.08	N.d.	0.22	0.25	22.58	7.24	N.d.	4.97
Dy	0.040	9.71	10.5	0.09	0.09	0.08	0.08	N.d.	0.20	6.87	N.d.	5.57	14.0
Ho	0.050	15.4	18.3	0.12	0.13	0.09	N.d.	N.d.	N.d.	N.d.	N.d.	N.d.	17.9
Er	0.059	12.1	13.3	0.14	0.12	0.11	0.14	N.d.	N.d.	8.60	N.d.	20.2	39.9
Tm	0.061	9.69	16.9	0.27	0.18	0.16	N.d.	0.30	0.42	N.d.	18.61	N.d.	N.d.
Yb	0.080	12.5	15.6	0.25	0.19	0.18	0.20	0.29	0.41	15.3	32.6	60.8	59.7
Lu	0.107	11.4	15.6	0.32	0.22	0.25	N.d.	0.31	0.45	24.4	1.50	N.d.	N.d.

1—orthopyroxenes/melt; 2—orthopyroxenes/olivines (common selection); 3—orthopyroxenes/olivines (lherzolites); 4—orthopyroxenes/clinopyroxenes (common selection); 5—orthopyroxenes/clinopyroxenes (lherzolites); 6—orthopyroxenes/clinopyroxenes (spinel lherzolites); 7—orthopyroxenes/clinopyroxenes (pyroxenites from Zabargad massif); 8—orthopyroxenes/clinopyroxenes (websterites); 9—orthopyroxenes/clinopyroxenes (gabbro-norites); 10—orthopyroxenes/plagioclases (andesites); 11—orthopyroxenes/plagioclases (gabbro-norites); 12—orthopyroxenes/plagioclases (pyroxenites from Zabargad massif); 13—orthopyroxenes/plagioclases (anorthosites, Moon).

K_d(orthopyroxene/plagioclase). The values of these coefficients were calculated based on analytical data on the content of REE in these coexisting minerals from gabbro-norites, plagioclase-bearing pyroxenites, plagioclase-bearing lherzolites, andesites, and lunar rocks (Table 5.11). The obtained estimates show that for most REE, K_d values vary over a wide range, revealing specific dependence on the type of rock, with a successive increase in the series from La to Yb. An exception is the K_d values for Eu, which are typically lower than those for the rest of the elements. This seems to be the result of selective accumulation of Eu in the plagioclase structure. Judging by the changes in the values of K_d(orthopyroxene/plagioclase) under strongly reducing conditions at great depths (high-pressure proximities from Zabargad Island) and on the moon (orthopyroxene-bearing anorthosites), heavy REE, namely Dy, Ho, Er, and Yb, must have been subjected to especially intense fractionation with the tendency to predominant accumulation in the orthopyroxene structure.

5.2.4 Isomorphism of REE in orthopyroxenes

As was mentioned above, the accumulation and character of distribution of REE in orthopyroxenes depend on their chemical composition and crystallochemical properties, the composition of melts from which they crystallized, temperature, pressure and redox conditions of crystallization, REE properties, including the sizes of ionic radii, and more. It is assumed that the most probable mechanism of isomorphous incorporation of REE in the structure of orthopyroxene and other silicates is their heterovalent replacement by ions of one or several net-forming elements (Pyatenko & Ugryumova, 1988). The most likely candidate for this replacement by REE ions is the Ca^{2+} ion, which radius (1.12 Å) is closest to the size of trivalent ions of REE, which vary from 1.16 Å for La^{3+} to 0.977 Å for Lu^{3+} (Voytkevich *et al.*, 1970; Shannon, 1976). The sizes of ionic radii of other net-forming elements of orthopyroxenes (Mg^{2+}, Fe^{2+}) do not fit this interval and are less favorable for such replacement. In Pyatenko & Ugryumova's (1988) opinion, during crystallization of silicate melts from melts including orthopyroxenes, realization of the following scheme of isomorphous replacement is probable: $3Ca^{2+} \rightarrow 2REE^{3+} +$ vacancy. However, the researchers assumed that owing to the appearance of vacancies in the mineral structure, its physical strength will decrease, which, in turn, will restrict the incorporation of REE in the mineral in case of high-pressure crystallization. The structure of orthopyroxenes can accumulate very limited amounts of REE as it also contains minor concentrations of Ca. The ions of the heavy REE are more preferably incorporated in the structure of orthopyroxenes as the sizes of their ions are more similar to that of the ionic radius of Ca^{2+} compared to the ionic radii of heavy REE.

* * *

The available analytical data on the contents of REE in orthopyroxenes are dominated by information about the samples from ultramafic restites in deep xenoliths. The studied samples of other varieties of orthopyroxene-bearing ultramafic, mafic, and some other rocks are far fewer in number. Orthopyroxenes represented in all natural parageneses are rather poor in their structural REE impurity. Total contents of REE in the majority of studied samples range within 0.01–3.5 ppm. The minimum level of

accumulation of REE was established in orthopyroxenes from meteorites. Compared to samples from other rocks, somewhat increased contents of REE were observed in orthopyroxenes represented in some varieties of pyroxenites and gabbro-norites, as well as in andesites and dacites. The crystal structure of orthopyroxenes was more favorable for isomorphous incorporation of ions of heavy and, partly, medium REE compared to light REE. In most studied orthopyroxenes, $(La/Yb)_n$ is less than unity, with a positive slope of REE patterns. Some of them display low-intensity negative and positive Eu anomalies.

Results of the estimations of REE concentrations in orthopyroxenes and the configuration features of their REE patterns can be used for geochemical systematization of both the mineral and the rocks it composes. The level of REE accumulation in orthopyroxene depends on some factors, beginning from the chemical composition of melts and its crystallization conditions and ending with the crystallochemical properties of mineral and chemical features of REE. The available data suggest that accumulation of structural REE impurities in orthopyroxenes was realized by heterovalent replacement of Ca^{2+} ions by trivalent ions of REE. It was established that the content of heavy elements in orthopyroxenes is in direct relationship with the contents of Ca, Fe, and Ti and in inverse relationship with the content of Mg. There is a tendency of a direct relationship between the contents of heavy REE in orthopyroxenes and the degree of reduction of fluids that occur in mineral grains in the composition of micro- and nanoinclusions. This relationship is supported by studies of the rare earth composition of orthopyroxenes from lunar rocks which crystallized under strongly reducing conditions. The revealed differences in the values of K_d(orthopyroxene/basalt melt) seem to be due to specific fractionation of REE during the growth of crystals from melts with different compositions and different P–T conditions. The relative stability of K_d(orthopyroxene/coexisting mineral) values for rocks from one magmatic body might serve as a criterion for the chemical equilibrium of these phases. As known, Ca in crystals of rock-forming orthopyroxenes is distributed nonuniformly, since most of it is normally concentrated in thin clinopyroxene lamellae resulting from exsolution. For this reason the ions of REE, which replace Ca^{2+} ions, must also be distributed in the crystals of this mineral nonuniformly, being concentrated mainly in these lamellae.

The abnormally high contents of low REE in some orthopyroxene samples suggest the presence of some amount of nonstructural impurity concentrated in the microcracks of grains as well as in fluid micro- and nanoinclusions. This impurity has no direct relationship with the crystallization of orthopyroxenes under endogenous conditions and introduces specific inaccuracies into the results of analyses. Therefore, to obtain more accurate values of the distribution of isomorphic impurity of REE in orthopyroxene samples, it is necessary to preliminarily remove a considerable part of this nonstructural impurity by short-time leaching of samples in a diluted solution of hydrochloric acid.

5.3 CLINOPYROXENES

Clinopyroxene is one of the most common phases not only in nearly all petrographical varieties of ultramafic and mafic rocks but also in some other types of magmatic and metamorphic formations. This mineral is the most important concentrator of REE in

most rocks. Participation of clinopyroxenes in numerous genetically different mineral parageneses suggests that they can crystallize in a wide range of physicochemical conditions. Results of generalization of available representative data on the distribution of REE in clinopyroxenes must promote extensive use of this rock-forming mineral as an effective indicator in solving various problems of the petrology of ultramafic, mafic, and related rocks.

Studies of the geochemistry of REE in clinopyroxenes started in the mid-1970s on single samples from lherzolites represented in deep ultramafic xenoliths from alkali basalts, meteorites, and some other rocks (Schnetzler & Philpotts, 1968, 1970; Nagasawa *et al.*,1969; Onuma *et al.*, 1968; Frey, 1969; Philpotts & Schnetzler, 1970a,b; Nagasawa & Schnetzler, 1971; Varne & Graham, 1971; Philpotts *et al.*, 1972). Later, greater volumes of analytical data were obtained on the distribution of REE in clinopyroxenes from most varieties of ultramafic, mafic, and other types of rock (Shimizu, 1975; Ottonello *et al.*, 1978; Ottonello, 1980, 1984; Pallister & Knight, 1981; Rass, 1982; Stosch, 1982; Irving & Frey, 1984; Downes & Dupuy, 1987; Liotard *et al.*, 1988; Bodinier *et al.*, 1987, 1988). The studies carried out during the recent decades are not on a smaller scale, often using much larger quantities of sample collections (Johnson & Dick, 1992; Sen *et al.*, 1993; Vannucci *et al.*, 1993a,b; Pearson *et al.*, 1993; Blusztajn & Shimizu, 1994; Ionov *et al.*, 1994; Ozawa & Shimizu, 1995; Rivalenti *et al.*, 1995, 1996; Sobolev & Batanova, 1995; Sobolev *et al.*, 1996; Andre & Ashchepkov, 1996; Shimizu *et al.*, 1997; Floss *et al.*, 1998; Shi *et al.*, 1998; Lesnov & Gora, 1998; Jolliff *et al.*, 1999; Simonov *et al.*, 2000; Lesnov, 2001c; Pertsev, 2004; Piccardo *et al.*, 2005). According to the amount of accumulated analytical data on the geochemistry of REE, clinopyroxenes are predominant among rock-forming minerals. These studies were earlier performed with a wide application of the NAA, INAA, and RNAA techniques, which were later replaced by more efficient techniques for analysis of low REE concentrations, such as IPMA, SIMS, LA ICP-MS, and some others.

The initial analytical database, which was created with the aim to generalize and genetically interpret the material on the geochemistry of REE in clinopyroxenes, included a few thousand analyses in the samples from the overwhelming majority of varieties of ultramafic and mafic rocks, and others. A part of these analyses on sorting for one reason or another was excluded from consideration. By now, the most thoroughly studied is the rare earth composition of those clinopyroxenes that are represented in ultramafic rocks from deep xenoliths, from individual mafic–ultramafic massifs, and from the samples dredged from within mid-oceanic ridges. Less thoroughly analyzed are clinopyroxenes from gabbroid rocks that compose different types of mafic and mafic–ultramafic massifs occurring within folded and platform regions and from effusive rocks. Clinopyroxenes analyzed for REE were mainly represented by diopsides, and to a lesser degree by augites, salites, endiopsides, omphacites, and some scarcer varieties.

5.3.1 REE composition of clinopyroxenes

Consider some features of REE distribution in clinopyroxenes from different mineral parageneses, including those from meteorites, mafic rocks, the moon, ultramafic rocks represented in deep xenoliths and in massifs, websterites, clinopyroxenites, various rocks of gabbroid composition, as well as from basalts and some other effusive rocks.

Meteorites. The total contents of REE determined in clinopyroxenes from plagioclase-bearing meteorites from the Acapulco range from 14 to 20 ppm (Zipfel *et al.*, 1995). The values of the $(La/Yb)_n$ parameter in them vary in a rather narrow range (0.18–0.34). In all of these pyroxenes, $(La/Sm)_n$ is greater than unity and $(Gd/Yb)_n$ is about 1 (Table 5.12). Their REE patterns are complicated by intensely negative Eu anomalies, which seem to be due to advanced crystallization of plagioclases under highly reducing conditions (Fig. 5.12, 1). In contrast to them, clinopyroxenes from plagioclase-free meteorites from Nakhla (Nakamura, *et al.*, 1982), Chessigny, Lafayette, and Valadares (Wadhwa & Crozaz, 1995) are characterized by a lower level of accumulation of REE, which total contents are no more than 10 ppm, and by a considerably lower intensity of negative Eu anomalies (Fig. 5.12, 2). The values of the $(La/Yb)_n$ parameter in this case vary in a wider range (0.20–2.78), though $(La/Sm)_n$ is less than unity. The decreased intensity of negative Eu anomalies in these clinopyroxenes is related to the fact that they formed without participation of the plagioclase phase.

Mafic rocks of the moon. Clinopyroxenes from lunar anorthosites and monzogabbros are characterized by a rather high level of REE accumulation (see Table 5.12). Their patterns also display intensely negative Eu anomalies, which also seems to be related to the prior crystallization of plagioclase (Fig. 5.12, 3–6). Clinopyroxenes from lunar anorthosites can be divided into two varieties according to their rare earth composition. The samples of the first variety (see Fig. 5.12, 3) have low total contents of REE (12–72 ppm), and their patterns in many respects are similar to those of clinopyroxenes from meteorites of the Acapulco occurrence, though compared to the latter they reveal a considerable deficiency in Eu. All samples have very low values of the $(La/Yb)_n$ and $(La/Sm)_n$ parameters. The second variety of clinopyroxenes from lunar anorthosites is characterized by high total contents of REE (84–323 ppm) and a slightly lower intensity of negative Eu anomalies on the patterns (Fig. 5.12, 4). Clinopyroxenes from lunar monzogabbros are also divided into two varieties: (1) those with a rather low total content of elements (21–42 ppm) and intensely negative Eu anomalies (Fig. 5.12, 5); and (2) those with an elevated total content of elements (123–129 ppm) and less intensely negative Eu anomalies (Fig. 5.12, 6). Moreover, the first variety differs from the second in lower values of the $(La/Yb)_n$ parameter (0.03–0.04 and 0.10–0.15, respectively).

Garnet and garnet-spinel lherzolites from deep xenoliths. The mineral from these high-pressure rocks was characterized from examples of samples from xenoliths occurring in alkali basalt (Ottonello *et al.*, 1978; Erkushev, 1985; Ionov *et al.*, 1993a; Litasov, 1998) and kimberlite provinces (Shimizu *et al.*, 1997) (Table 5.13). The total REE content in many of them is no more than 20 ppm. The level of accumulation of light and middle elements is an order of magnitude higher than that in chondrite C1, while the level of heavy elements is normally lower than that in chondrite. Many REE patterns of these clinopyroxenes have a gentle negative slope and smoothed maxima in the region of middle elements (Fig. 5.13). Two varieties were established among the samples of garnet peridotites in xenoliths from the Udachnaya kimberlite pipe. The first, more abundant, variety is represented by the samples in which the level of accumulation of light REE is about 10 t. ch., while that of heavy REE is about 1 t. ch. These clinopyroxenes are characterized by virtually linear patterns with a rather gentle slope (Fig. 5.13, 5). The second variety has a lower level of accumulation of

Table 5.12 Rare earth element composition of clinopyroxenes from meteorites and Moon's rocks (ppm).

	Meteorites												
	Acapulco							Nakhla			Chessigny		Valadares
	(Zipfel *et al.*, 1995), SIMS							(Nakamura *et al.*, 1982)			(Wadhwa & Crozaz, 1995), IPMA		
Element	A1	A12	A2	A3	A5	A7	AS	NmetA	NmetB	NmetB	Chess-1	Chess-2	Valad-1
La	0.390	0.750	0.700	0.410	0.620	0.740	0.500	1.080	0.386	0.588	0.420	0.060	0.100
Ce	1.900	3.300	3.200	1.700	2.500	2.900	2.100	N.d.	1.569	N.d.	2.170	0.190	0.560
Pr	0.360	0.600	0.560	0.350	0.500	0.530	N.d.	N.d.	N.d.	N.d.	N.d.	N.d.	N.d.
Nd	2.260	3.620	3.520	1.600	2.650	2.660	2.100	1.740	1.887	1.683	2.760	0.260	0.550
Sm	1.040	1.300	1.400	0.620	0.920	1.030	0.830	0.506	0.601	0.460	0.770	0.120	0.130
Eu	0.040	0.050	0.060	0.030	0.060	0.040	0.090	0.149	0.186	0.134	0.220	0.030	0.040
Gd	1.300	1.900	1.400	1.700	1.900	0.900	N.d.	0.520	0.676	0.534	1.090	0.160	0.210
Tb	0.300	0.400	0.300	0.400	0.300	0.200	0.200	N.d.	N.d.	N.d.	0.170	0.040	0.040
Dy	2.500	2.900	2.400	2.600	2.700	2.400	1.200	0.540	0.584	0.542	1.130	0.300	0.250
Ho	0.500	0.600	0.500	0.500	0.600	0.500	0.400	N.d.	N.d.	N.d.	0.190	0.050	0.050
Er	1.700	1.800	1.800	1.700	2.100	1.700	N.d.	0.304	0.322	0.305	0.570	0.210	0.120
Tm	0.300	0.300	0.300	0.300	0.300	0.300	N.d.	N.d.	N.d.	N.d.	0.070	0.030	0.020
Yb	1.500	1.900	1.600	1.400	1.900	1.800	1.000	0.262	0.269	0.256	0.600	0.200	0.120
Lu	0.200	0.200	0.200	0.300	0.200	0.300	0.200	0.036	0.037	N.d.	N.d.	N.d.	N.d.
Total	14.3	19.6	17.9	13.6	17.3	16.0	N.d.	N.d.	N.d.	N.d.	10.2	1.65	2.19
$(La/Yb)_n$	0.18	0.27	0.30	0.20	0.22	0.28	0.34	2.78	0.97	1.55	0.47	0.20	0.56

	Meteorites		The Moon										
	Lafayette	Nakhla	(Floss *et al.*, 1998), IPMA										
	(Wadhwa & Crozaz, 1995), IPMA		60055.5	62255.5	64435.268	64435.268	60025.702	60025.70	60025.699	64435.270	64435.270	67635.8	67215.63
Element	Laf-1	Nakhla-1	*Anorthosites*										
La	0.120	0.180	0.15	0.370	0.140	0.140	0.330	0.310	0.370	0.640	0.720	0.430	2.870
Ce	0.600	0.660	0.980	2.090	0.830	0.850	2.500	1.960	1.970	3.560	4.600	2.420	11.70
Pr	N.d.	N.d.	0.220	0.520	0.140	0.190	0.640	0.450	0.470	1.040	1.200	0.750	2.320
Nd	0.700	1.020	1.510	3.350	1.420	1.510	4.160	2.940	3.380	5.660	7.870	4.180	12.70
Sm	0.200	0.330	0.870	1.800	0.820	0.980	2.610	1.550	2.000	2.800	3.610	2.300	5.140
Eu	0.060	0.080	0.037	0.055	0.030	0.050	0.059	0.048	0.053	0.022	0.040	0.060	0.110
Gd	0.210	0.310	1.360	3.320	1.000	1.400	4.840	2.220	1.180	5.040	6.390	3.740	8.120
Tb	0.040	0.050	0.270	0.740	0.280	0.330	0.920	0.530	0.460	0.990	1.480	0.770	1.690
Dy	0.260	0.300	2.180	5.770	2.340	2.430	8.270	3.720	3.890	7.100	9.930	5.380	11.30
Ho	0.050	0.060	0.480	1.100	0.510	0.610	1.430	0.800	0.720	1.490	1.940	1.200	2.210
Er	0.150	0.170	1.420	3.910	1.460	1.650	4.020	2.390	2.060	4.700	5.760	2.680	6.490
Tm	0.150	0.030	0.190	0.560	0.170	0.210	0.500	0.300	0.310	0.580	0.740	0.360	0.920
Yb	0.140	0.160	1.350	3.140	1.950	1.620	2.680	2.210	2.070	3.910	4.270	2.360	5.690
Lu	N.d.	N.d.	0.180	0.450	0.270	0.230	0.360	0.250	0.230	0.530	0.560	0.220	0.870
Total	N.d.	N.d.	11.3	27.2	11.4	12.2	33.3	19.7	19.2	38.1	49.1	26.9	72.1
$(La/Yb)_n$	0.58	0.76	0.07	0.08	0.05	0.06	0.08	0.09	0.12	0.11	0.11	0.12	0.34

(*Continued*)

Table 5.12 Continued

	The Moon									
	(Jolliff *et al.*, 1999), IPMA						(Shervais & McGree, 1999), IPMA			
	Pig 1	Pig 2	Pig 3	Aug 1	Aug 2	Aug 3	118AugSp	118AugS	108AugS	412AugSp
Element	*Monzogabbro*						*Alkaline anorthosites*			
La	0.560	0.530	0.430	3.170	3.090	4.230	2.370	6.600	5.980	35.28
Ce	1.990	1.260	1.240	12.50	13.50	19.20	10.25	22.29	28.85	93.14
Pr	0.420	0.220	0.220	2.890	2.810	4.340	N.d.	N.d.	N.d.	N.d.
Nd	2.480	1.230	1.140	14.80	18.10	20.30	14.27	22.64	34.93	66.62
Sm	1.510	0.660	0.610	8.300	8.870	8.100	6.940	9.940	14.38	25.02
Eu	0.030	0.017	0.008	0.200	0.290	0.110	0.420	0.580	0.560	0.760
Gd	2.200	1.300	0.800	10.30	9.600	7.700	11.51	15.42	19.83	29.44
Tb	0.750	0.460	0.290	2.990	2.380	2.340	N.d.	N.d.	N.d.	N.d.
Dy	7.200	4.480	3.180	23.60	23.30	17.70	16.08	20.90	25.28	33.860
Ho	1.880	1.220	0.950	5.220	4.960	4.410	N.d.	N.d.	N.d.	N.d.
Er	7.010	5.100	3.710	17.20	16.60	11.50	10.05	11.29	13.070	18.48
Tm	1.060	0.960	0.760	2.850	2.480	2.000	N.d.	N.d.	N.d.	N.d.
Yb	12.60	8.100	6.500	21.80	20.10	19.40	11.71	14.79	16.17	20.08
Lu	1.910	1.460	1.200	3.290	3.350	2.050	N.d.	N.d.	N.d.	N.d.
Total	41.6	27.0	21.0	129	129	123	N.d.	N.d.	N.d.	N.d.
$(La/Yb)_n$	0.03	0.04	0.04	0.10	0.10	0.15	0.14	0.30	0.25	1.19

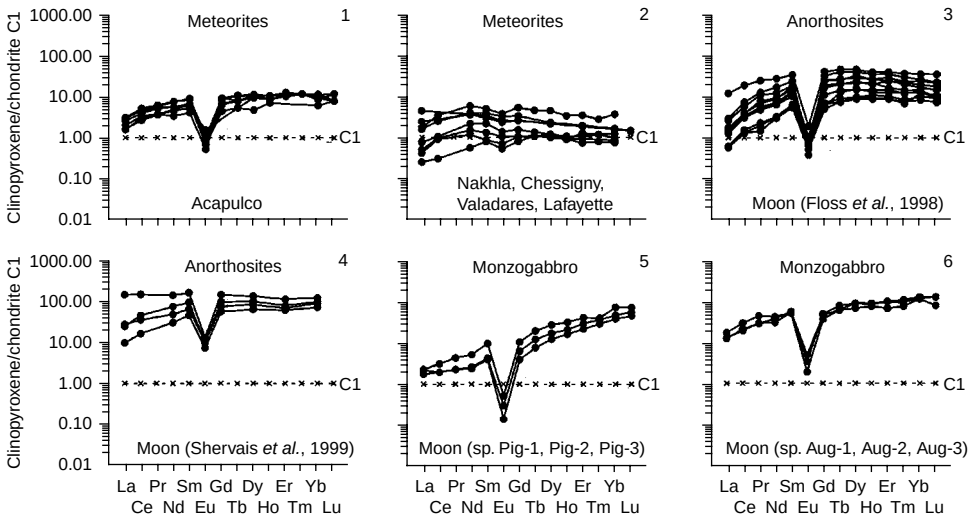

Figure 5.12 Chondrite-normalized REE patterns for clinopyroxenes from meteorites and from rocks of moon (data Table 5.12).

middle REE (0.2–0.7 t. ch.) and an irregular distribution of light elements, which level changes from abnormally high to very low (Fig. 5.13, 6).

Spinel peridotites from deep xenoliths. A considerable body of analytical data on clinopyroxenes from these rocks was obtained from samples of xenoliths occurring in alkaline-basalt provinces in Poland (Blusztajn & Shimizu, 1994), the Central massif in France (Downes & Dupuy, 1987), Hawaii (Sen *et al.*, 1993), Germany (Stosch, 1982), and Canada (Shi *et al.*, 1998) (Table 5.14). On average, the level of REE accumulation in them is higher than in chondrite C1, the level of light elements in many cases is higher than that of heavy REE (Fig. 5.14). Clinopyroxenes from xenoliths occurring in alkali basalts from the provinces of Poland, systematically reveal elevated, often abnormally high, contents of light REE, which level of accumulation at times exceeds 100 t. ch. (Fig. 5.14, 3). The values of the $(Ce/Yb)_n$ parameter are extremely high. Many clinopyroxenes from xenoliths of Central massif province are also abnormally enriched with light REE, with $(La/Yb)_n$ values ranging from 3 to 27 (Fig. 5.14, 4). Particularly high values of this parameter were established in clinopyroxenes from some lherzolite xenoliths occurring in the province of Canadian Cordillera (80–190) (see Fig. 5.14, 8). Samples from xenoliths in the provinces of Dariganga (Fig. 5.14, 2), Dreiser Weiher (Fig. 5.14, 5), the Hawaiian Islands (Fig. 5.14, 6), and some other places, have lower $(La/Yb)_n$ values.

Spinel lherzolites from xenoliths in basalts of the Shavaryn Tsaram paleovolcano. This large xenolith was mentioned when describing the results of analyses of the REE composition for olivines (Chapter 5.1) and orthopyroxene (Chapter 5.2). The scheme of arrangement of clinopyroxene grains, for which REE were determined, is shown in Figure 5.3. The content of enstatite end member in these clinopyroxenes is 91% (Table 5.15). Clinopyroxene grains, arranged in xenoliths at distances of 3 mm (sample A-8), 11 mm (sample A-11), 30 mm (sample A-16), and 38 mm (sample A-19) from

Table 5.13 Rare earth element composition of clinopyroxenes from garnet-, and garnet-spinel lherzolites, and peridotites from deep xenoliths (ppm).

	Provinces												
	Vitim, Russia												
	(Ionov *et al.*, 1993a), INAA												
	313-1	313-114	313-3	313-4	313-5	313-54	313-6	313-8	313-37	313113G	313113S	313113SG	314-580
Element	*Garnet lherzolites*								*Garnet-spinel lherzolites*				
La	0.640	1.270	0.870	1.290	1.350	1.490	1.210	1.470	0.850	1.670	1.360	1.320	2.210
Ce	2.800	7.450	4.550	5.400	4.500	4.850	5.150	4.450	2.450	5.030	6.250	4.360	6.750
Pr	N.d.	N.d.	N.d.	N.d.	N.d.	N.d.	N.d.	N.d.	N.d.	N.d.	N.d.	N.d.	N.d.
Nd	3.500	7.400	4.050	5.700	5.450	5.250	4.500	5.900	4.500	5.350	5.200	3.550	7.600
Sm	1.500	2.860	1.620	2.210	1.790	1.630	1.690	1.910	1.280	1.830	1.820	1.850	2.080
Eu	0.520	0.890	0.560	0.750	0.610	0.570	0.570	0.600	0.450	0.610	0.590	0.570	0.680
Gd	N.d.	N.d.	N.d.	N.d.	N.d.	N.d.	N.d.	N.d.	N.d.	1.770	1.900	2.600	2.410
Tb	0.260	0.450	0.245	0.308	0.247	0.240	0.262	0.262	0.320	0.292	0.324	0.245	0.372
Dy	N.d.	N.d.	N.d.	N.d.	N.d.	N.d.	N.d.	N.d.	N.d.	N.d.	N.d.	N.d.	N.d.
Ho	N.d.	N.d.	N.d.	N.d.	N.d.	N.d.	N.d.	N.d.	N.d.	N.d.	N.d.	N.d.	N.d.
Er	N.d.	N.d.	N.d.	N.d.	N.d.	N.d.	N.d.	N.d.	N.d.	N.d.	N.d.	N.d.	N.d.
Tm	N.d.	N.d.	N.d.	N.d.	N.d.	N.d.	N.d.	N.d.	N.d.	N.d.	N.d.	N.d.	N.d.
Yb	N.d.	N.d.	N.d.	0.190	0.180	0.165	N.d.	0.190	N.d.	N.d.	0.207	N.d.	N.d.
Lu	N.d.	N.d.	N.d.	0.024	0.027	0.034	0.048	N.d.	0.024	0.020	0.031	0.038	0.059
Total	N.d.	N.d.	N.d.	N.d.	N.d.	N.d.	N.d.	N.d.	N.d.	N.d.	N.d.	N.d.	N.d.
$(La/Yb)_n$	N.d.	N.d.	N.d.	4.58	5.06	6.10	N.d.	5.22	N.d.	N.d.	4.43	N.d.	N.d.

	Provinces												
	Vitim, Russia	Vitim, Russia				Ethiopia							
	(Ionov *et al.*, 1993a)	(Litasov, 1998), SIMS				(Ottonello *et al.*, 1978), RNAA							
	314-74	V-462a	V-462b	V-446	V-428	3G12	3G15	3G16	3G17	3G18	3G19	3G28	3G51
Element	*Garnet-spinel lherzolites*					*Garnet lherzolites*				*Garnet peridotites*			
La	0.990	3.534	2.805	1.334	1.349	1.450	3.260	0.930	5.510	0.650	3.640	1.100	1.070
Ce	3.580	13.21	9.552	5.617	5.076	3.620	14.86	2.420	10.30	1.640	9.500	2.730	2.360
Pr	N.d.	N.d.	N.d.	N.d.	N.d.	N.d.	N.d.	N.d.	N.d.	N.d.	N.d.	N.d.	N.d.
Nd	3.020	13.21	9.552	5.617	5.076	2.940	13.80	2.040	6.920	1.130	6.060	1.820	1.800
Sm	1.080	4.552	2.574	2.642	1.735	0.874	4.460	0.697	1.810	0.280	1.400	0.463	0.508
Eu	0.388	1.242	0.776	0.986	0.572	0.349	1.310	0.284	0.670	0.105	0.470	0.193	0.192
Gd	1.340	N.d.	N.d.	N.d.	N.d.	N.d.	3.770	N.d.	2.280	0.340	1.300	0.690	N.d.
Tb	0.279	N.d.	N.d.	N.d.	N.d.	0.230	0.610	0.180	0.370	0.050	0.210	N.d.	0.120
Dy	N.d.	3.102	1.671	2.180	1.116	N.d.	N.d.	N.d.	N.d.	N.d.	N.d.	N.d.	N.d.
Ho	N.d.	N.d.	N.d.	N.d.	N.d.	N.d.	N.d.	N.d.	N.d.	N.d.	N.d.	N.d.	N.d.
Er	N.d.	1.153	0.591	0.719	0.421	N.d.	N.d.	N.d.	N.d.	N.d.	N.d.	N.d.	N.d.
Tm	N.d.	N.d.	N.d.	N.d.	N.d.	0.165	0.230	0.100	0.170	0.036	0.092	0.100	0.081
Yb	0.640	0.972	0.589	0.590	0.320	0.970	0.930	0.440	1.030	0.240	0.500	0.590	0.470
Lu	0.088	N.d.	N.d.	N.d.	N.d.	0.175	0.162	0.078	0.190	0.046	0.097	0.101	0.082
Total	N.d.	41.0	28.1	19.7	15.7	N.d.	43.4	N.d.	29.3	4.52	23.3	7.79	N.d.
$(La/Yb)_n$	1.04	2.45	3.22	1.53	2.85	1.01	2.37	1.43	3.61	1.83	4.91	1.26	1.54

(*Continued*)

Table 5.13 Continued

	Provinces											
	Ethiopia	Yakutia (pipe Udachnaya), Russia										
	(Ottonello *et al.*, 1978)	(Shimizu *et al.*, 1997), IPMA										
	3G9	V306/89	V100/91	V107/89	V115/89	V121/91	V228/89	V239/89	U246/89	U25/91	U267/89	U417/89	U424/89
Element	*Garnet peridotites*												
La	1.060	1.170	0.014	1.830	1.750	2.840	2.760	2.530	3.330	15.200	2.700	3.520	1.940
Ce	2.700	0.305	0.026	5.020	6.420	9.430	9.690	8.650	11.400	39.000	8.740	7.830	6.810
Pr	N.d.	N.d.	N.d.	N.d.	N.d.	N.d.	N.d.	N.d.	N.d.	N.d.	N.d.	N.d.	N.d.
Nd	2.200	0.137	0.033	3.080	5.330	7.440	6.440	5.730	7.340	3.320	6.800	5.490	4.900
Sm	0.750	0.114	N.d.	0.678	1.140	1.900	1.820	1.210	1.610	0.113	1.560	1.380	0.810
Eu	0.310	0.073	0.017	0.179	0.470	0.455	0.530	0.278	0.588	0.027	0.389	0.540	0.240
Gd	N.d.	N.d.	N.d.	N.d.	N.d.	N.d.	N.d.	N.d.	N.d.	N.d.	N.d.	N.d.	N.d.
Tb	0.180	N.d.	N.d.	N.d.	N.d.	N.d.	N.d.	N.d.	N.d.	N.d.	N.d.	N.d.	N.d.
Dy	N.d.	0.096	0.037	0.212	0.660	0.632	0.773	0.358	1.020	0.062	0.902	0.760	0.200
Ho	N.d.	N.d.	N.d.	N.d.	N.d.	N.d.	N.d.	N.d.	N.d.	N.d.	N.d.	N.d.	N.d.
Er	N.d.	0.118	0.041	0.118	0.270	0.311	0.300	0.116	0.349	0.088	0.514	0.290	0.060
Tm	N.d.	N.d.	N.d.	N.d.	N.d.	N.d.	N.d.	N.d.	N.d.	N.d.	N.d.	N.d.	N.d.
Yb	0.490	0.093	0.042	0.063	0.190	0.184	0.288	0.099	0.241	0.048	0.282	0.220	0.070
Lu	0.090	N.d.	N.d.	N.d.	N.d.	N.d.	N.d.	N.d.	N.d.	N.d.	N.d.	N.d.	N.d.
Total	N.d.	1.99	0.21	11.2	16.2	23.2	22.6	19.0	25.9	57.9	21.9	20.0	15.0
$(La/Yb)_n$	1.46	8.48	0.22	19.5	6.22	10.4	6.47	17.2	9.33	215	6.46	10.8	18.7

	Provinces										
	Yakutia (pipe Udachnaya), Russia										
	(Shimizu *et al.*, 1997), IPMA										
	U51/92	U52/76	U61/91-1	U70/92	U74/89	U76/92	U80/92	U191/89	U564/89	U565/89	U65/92
Element	*Garnet peridotites*										
La	2.840	2.390	1.890	2.600	2.560	1.030	2.770	4.260	1.120	0.906	3.670
Ce	10.20	8.440	7.000	8.930	8.660	3.590	9.460	12.30	2.300	1.940	14.60
Pr	N.d.	N.d.	N.d.	N.d.	N.d.	N.d.	N.d.	N.d.	N.d.	N.d.	N.d.
Nd	7.440	5.660	6.620	5.840	4.580	0.336	7.190	9.560	0.875	1.090	10.70
Sm	2.000	1.360	1.830	1.500	1.140	0.079	1.810	1.280	0.247	0.246	2.090
Eu	0.599	0.403	0.465	0.478	0.299	0.008	0.522	0.364	0.105	0.088	0.477
Gd	N.d.	N.d.	N.d.	N.d.	N.d.	N.d.	N.d.	N.d.	N.d.	N.d.	N.d.
Tb	N.d.	N.d.	N.d.	N.d.	N.d.	N.d.	N.d.	N.d.	N.d.	N.d.	N.d.
Dy	0.850	0.642	0.701	0.696	0.513	0.051	0.852	0.427	N.d.	0.479	0.595
Ho	N.d.	N.d.	N.d.	N.d.	N.d.	N.d.	N.d.	N.d.	N.d.	N.d.	N.d.
Er	0.375	0.370	0.285	0.332	0.179	0.048	0.233	0.186	0.470	0.417	0.340
Tm	N.d.	N.d.	N.d.	N.d.	N.d.	N.d.	N.d.	N.d.	N.d.	N.d.	N.d.
Yb	0.236	0.200	0.228	0.220	0.192	0.031	0.286	0.147	0.488	0.448	0.293
Lu	N.d.	N.d.	N.d.	N.d.	N.d.	N.d.	N.d.	N.d.	N.d.	N.d.	N.d.
Total	24.5	19.5	19.0	20.6	18.1	5.17	23.1	28.5	6.07	5.61	32.8
$(La/Yb)_n$	8.12	8.07	5.60	7.98	9.00	22.6	6.54	19.6	1.55	1.37	8.45

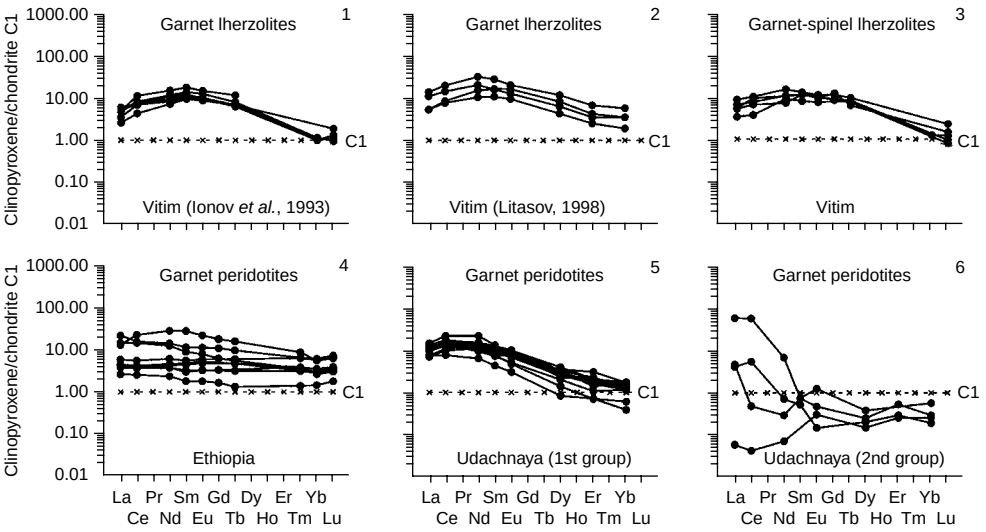

Figure 5.13 Chondrite-normalized REE patterns for clinopyroxenes from garnet-, garnet-spinel lherzolites, and garnet peridotites from deep xenoliths (data Table 5.13).

contact with the host basalt, are very similar in the level of REE accumulation and in the configuration of patterns (Table 5.16, Fig. 5.15). All of them are slightly depleted of light REE relative to heavy REE and have low $(La/Yb)_n$ values. Unlike clinopyroxenes from many other deep xenoliths and some grains of olivine (Fig. 5.5) and orthopyroxene (Fig. 5.10) from this xenolith, clinopyroxene grains do not contain high concentrations of light REE close to contact of the xenolith with the host basalt. Most likely, this is related to the fact that the clinopyroxene grains under study, unlike olivine and pyroxene grains, were not penetrated by microcracks, into which basalt melts with considerable amounts of nonstructural impurities of light REE could percolate. This question will be discussed in more details below.

Spinel lherzolites from massifs. Clinopyroxenes from these rocks were studied in samples from the Troodos (Sobolev & Batanova, 1995) and Lherz (Bodinier *et al.*, 1988) massifs and in samples dredged from the Indian Mid-Oceanic Ridge (Johnson & Dick, 1992) (Table 5.17). Minerals from the Troodos massif were appreciably depleted of La, Ce, and Nd, which levels do not exceed 0.3 t. ch., while the level of accumulation of other elements was much higher (from 2 to 6 t. ch.). The REE patterns of these clinopyroxenes have a general positive slope and are complicated by the minimum in the region of light REE (Fig. 5.16, 1). Samples from the Lherz massif have a somewhat higher level of accumulation of REE (8–10 t. ch.) (Fig. 5.16, 2).

Representative analytical data were obtained for clinopyroxenes from spinel lherzolites, which samples were dredged from the Indian Mid-Oceanic Ridge. Their REE patterns, similar in configuration, show depletion of minerals in light REE (see Fig. 5.16, 3, 4). The whole collection of these clinopyroxenes, by the degree of their depletion of light REE and by the values of $(Nd/Sm)_n$, can be divided into two varieties: the first variety predominantly includes samples that have values of the parameter that are considerably higher (0.27–0.42) than those in the second one (0.08–0.22).

Table 5.14 Rare earth element composition of clinopyroxenes from spinel lherzolites, and peridotites from deep xenoliths (ppm).

	Provinces											
	Vitim, Russia					Dariganga, Mongolia						
	(Ionov *et al.*, 1993a), INAA					(Wiechert *et al.*, 1997), INAA						
	314-56	314-58	314-59	314-6	86-1	8520-07	8520-09	8520-11	8520-12	8520-15	8520-17	8520-22
Element	*Spinel lherzolites*											
La	0.800	0.480	0.970	0.290	1.150	0.750	1.000	2.030	2.300	0.790	17.70	1.280
Ce	3.600	2.310	3.440	N.d.	2.600	3.000	4.000	6.500	3.800	4.100	31.10	4.400
Pr	N.d.	N.d.	N.d.	N.d.	N.d.	N.d.	N.d.	N.d.	N.d.	N.d.	N.d.	N.d.
Nd	4.350	3.870	N.d.	N.d.	4.800	N.d.	N.d.	N.d.	N.d.	N.d.	N.d.	N.d.
Sm	2.010	1.950	1.460	0.625	1.570	1.150	1.450	1.770	0.900	1.520	2.150	1.760
Eu	0.785	0.750	0.560	0.270	0.630	0.460	0.620	0.700	0.300	0.640	0.720	0.720
Gd	2.930	3.240	2.740	N.d.	N.d.	N.d.	N.d.	N.d.	N.d.	N.d.	N.d.	N.d.
Tb	0.710	0.580	0.438	0.250	0.535	0.310	0.400	0.470	0.200	0.470	0.310	0.440
Dy	N.d.	N.d.	N.d.	N.d.	N.d.	N.d.	N.d.	N.d.	N.d.	N.d.	N.d.	N.d.
Ho	N.d.	N.d.	N.d.	N.d.	N.d.	N.d.	N.d.	N.d.	N.d.	N.d.	N.d.	N.d.
Er	N.d.	N.d.	N.d.	N.d.	N.d.	N.d.	N.d.	N.d.	N.d.	N.d.	N.d.	N.d.
Tm	N.d.	N.d.	N.d.	N.d.	N.d.	N.d.	N.d.	N.d.	N.d.	N.d.	N.d.	N.d.
Yb	2.220	2.170	1.510	0.690	1.700	1.710	2.090	2.060	1.100	2.090	1.250	2.040
Lu	0.339	0.382	0.218	0.117	0.273	0.310	0.300	0.360	0.200	0.300	0.210	0.340
Total	N.d.	N.d.	N.d.	N.d.	N.d.	N.d.	N.d.	N.d.	N.d.	N.d.	N.d.	N.d.
$(La/Yb)_n$	0.24	0.15	0.43	0.28	0.46	0.30	0.32	0.67	1.41	0.26	9.56	0.42

(*Continued*)

Table 5.14 Continued

	Provinces											
	Dariganga, Mongolia	Poland										
	(Wiechert *et al.*, 1997), INAA	(Blusztajn & Shimizu, 1994), IPMA										
	8520-28	KS2-1	KS2-2	KS20	KS6	LA31	LA38	LA56-1	LA56-2	LA58	LA62	LA74
Element	*Spinel lherzolites*											
La	4.800	N.d.	N.d.	N.d.	N.d.	N.d.	N.d.	N.d.	N.d.	N.d.	N.d.	N.d.
Ce	11.30	13.40	33.00	36.30	38.80	32.90	4.590	24.30	82.80	55.30	60.20	65.30
Pr	N.d.	N.d.	N.d.	N.d.	N.d.	N.d.	N.d.	N.d.	N.d.	N.d.	N.d.	N.d.
Nd	N.d.	13.70	28.10	32.00	33.50	3.910	0.690	2.870	13.60	21.90	15.90	16.40
Sm	2.400	4.450	7.750	7.860	8.270	0.280	0.180	0.800	2.120	4.150	2.660	1.740
Eu	0.800	1.470	2.530	2.610	2.630	0.090	0.060	0.210	0.540	1.260	0.600	0.460
Gd	N.d.	N.d.	N.d.	N.d.	N.d.	N.d.	N.d.	N.d.	N.d.	N.d.	N.d.	N.d.
Tb	0.400	N.d.	N.d.	N.d.	N.d.	N.d.	N.d.	N.d.	N.d.	N.d.	N.d.	N.d.
Dy	N.d.	3.300	5.170	4.500	4.880	1.010	0.250	1.160	1.220	2.260	1.260	1.330
Ho	N.d.	N.d.	N.d.	N.d.	N.d.	N.d.	N.d.	N.d.	N.d.	N.d.	N.d.	N.d.
Er	N.d.	1.610	2.530	2.210	2.380	0.730	0.110	0.900	0.860	1.020	0.720	0.970
Tm	N.d.	N.d.	N.d.	N.d.	N.d.	N.d.	N.d.	N.d.	N.d.	N.d.	N.d.	N.d.
Yb	1.300	0.940	1.710	2.190	1.680	0.770	0.150	0.660	0.560	1.010	0.490	0.770
Lu	0.200	N.d.	N.d.	N.d.	N.d.	N.d.	N.d.	N.d.	N.d.	N.d.	N.d.	N.d.
Total	N.d.	N.d.	N.d.	N.d.	N.d.	N.d.	N.d.	N.d.	N.d.	N.d.	N.d.	N.d.
$(La/Yb)_n$	2.49	N.d.	N.d.	N.d.	N.d.	N.d.	N.d.	N.d.	N.d.	N.d.	N.d.	N.d.

	Provinces											
	Poland											
	(Blusztajn & Shimizu, 1994), IPMA											
	LA81	LA83	LA85	LA93	LU13-1	LU13-2	LU23	LU28	LU41	LU44	LU45	LU49
Element	*Spinel lherzolites*											
La	N.d.	N.d.	N.d.	N.d.	N.d.	N.d.	N.d.	N.d.	N.d.	N.d.	N.d.	N.d.
Ce	51.90	15.30	28.30	7.640	50.70	39.90	26.90	45.00	14.20	18.30	41.60	18.30
Pr	N.d.	N.d.	N.d.	N.d.	N.d.	N.d.	N.d.	N.d.	N.d.	N.d.	N.d.	N.d.
Nd	10.50	3.040	5.250	0.660	32.00	21.80	10.70	18.10	3.230	7.580	25.90	10.90
Sm	2.010	0.430	0.520	0.260	8.010	4.740	1.830	4.160	0.850	1.560	6.180	2.95
Eu	0.660	0.150	0.180	0.100	2.790	1.660	0.570	1.290	0.300	0.500	2.090	0.960
Gd	N.d.	N.d.	N.d.	N.d.	N.d.	N.d.	N.d.	N.d.	N.d.	N.d.	N.d.	N.d.
Tb	N.d.	N.d.	N.d.	N.d.	N.d.	N.d.	N.d.	N.d.	N.d.	N.d.	N.d.	N.d.
Dy	1.650	1.130	0.870	0.990	5.610	3.060	1.350	2.420	1.460	1.360	3.850	1.890
Ho	N.d.	N.d.	N.d.	N.d.	N.d.	N.d.	N.d.	N.d.	N.d.	N.d.	N.d.	N.d.
Er	0.750	0.980	0.760	0.870	2.850	1.660	0.930	1.050	1.090	0.650	2.000	0.840
Tm	N.d.	N.d.	N.d.	N.d.	N.d.	N.d.	N.d.	N.d.	N.d.	N.d.	N.d.	N.d.
Yb	0.790	0.930	0.680	0.550	2.600	1.270	0.720	1.060	0.910	0.610	1.760	0.770
Lu	N.d.	N.d.	N.d.	N.d.	N.d.	N.d.	N.d.	N.d.	N.d.	N.d.	N.d.	N.d.
Total	N.d.	N.d.	N.d.	N.d.	N.d.	N.d.	N.d.	N.d.	N.d.	N.d.	N.d.	N.d.
$(La/Yb)_n$	N.d.	N.d.	N.d.	N.d.	N.d.	N.d.	N.d.	N.d.	N.d.	N.d.	N.d.	N.d.

(*Continued*)

Table 5.14 Continued

	Provinces											
	Poland						Massif Central, France					
	(Blusztajn & Shimizu, 1994), IPMA						(Downes & Dupuy, 1987), INAA					
	LU5	LU50	LU53	LU8	PL29	WG31	Bo73	Bo73L	Bo74	BR11	BR12	BT1L
Element	*Spinel lherzolites*											
La	N.d.	N.d.	N.d.	N.d.	N.d.	N.d.	10.30	10.30	1.200	1.300	0.800	3.200
Ce	50.40	31.30	11.90	43.20	54.50	19.80	15.20	15.40	4.600	3.600	2.900	9.800
Pr	N.d.	N.d.	N.d.	N.d.	N.d.	N.d.	N.d.	N.d.	N.d.	N.d.	N.d.	N.d.
Nd	26.20	18.30	4.410	15.50	44.60	15.85	N.d.	N.d.	N.d.	N.d.	N.d.	N.d.
Sm	6.170	4.550	1.290	2.600	10.80	3.830	1.200	1.890	1.800	1.670	1.590	1.070
Eu	2.040	1.440	0.460	0.750	3.220	1.300	0.720	0.720	0.720	0.700	0.680	0.350
Gd	N.d.	N.d.	N.d.	N.d.	N.d.	N.d.	N.d.	N.d.	N.d.	N.d.	N.d.	N.d.
Tb	N.d.	N.d.	N.d.	N.d.	N.d.	N.d.	0.450	0.410	0.530	0.520	0.540	0.160
Dy	3.870	2.790	1.860	1.190	5.340	2.520	N.d.	N.d.	N.d.	N.d.	N.d.	N.d.
Ho	N.d.	N.d.	N.d.	N.d.	N.d.	N.d.	0.660	0.590	0.680	N.d.	N.d.	0.170
Er	1.730	1.180	1.130	0.470	2.180	1.310	N.d.	N.d.	N.d.	N.d.	N.d.	N.d.
Tm	N.d.	N.d.	N.d.	N.d.	N.d.	N.d.	N.d.	N.d.	N.d.	N.d.	N.d.	N.d.
Yb	1.760	1.250	0.940	0.520	2.080	0.980	1.710	1.640	1.890	1.830	1.900	0.530
Lu	N.d.	N.d.	N.d.	N.d.	N.d.	N.d.	0.200	0.270	0.300	0.280	0.290	0.080
Total	N.d.	N.d.	N.d.	N.d.	N.d.	N.d.	N.d.	N.d.	N.d.	N.d.	N.d.	N.d.
$(La/Yb)_n$	N.d.	N.d.	N.d.	N.d.	N.d.	N.d.	4.07	4.24	0.43	0.48	0.28	4.08

	Provinces											
	Massif Central, France											
	(Downes & Dupuy, 1987), INAA											
	BT2	Bt2L	Bt36L	Bt39A	Bt39B	Bt40	BT81507	Ms17	RP67	RP70	RP71	Ta19
Element	*Spinel lherzolites*											
La	2.600	1.930	22.75	5.800	6.000	4.300	3.200	2.800	23.60	10.40	16.60	12.90
Ce	5.200	4.500	75.55	15.50	15.10	10.10	4.400	6.400	54.10	18.00	17.10	24.20
Pr	N.d.	N.d.	N.d.	N.d.	N.d.	N.d.	N.d.	N.d.	N.d.	N.d.	N.d.	N.d.
Nd	N.d.	1.780	47.05	N.d.	N.d.	N.d.	N.d.	N.d.	N.d.	N.d.	N.d.	N.d.
Sm	0.420	0.350	9.290	1.450	1.510	2.080	0.280	2.270	4.700	2.200	1.190	2.250
Eu	0.130	0.130	1.810	0.490	0.490	0.750	0.100	0.820	1.340	0.790	0.430	0.750
Gd	N.d.	0.410	7.520	N.d.	N.d.	N.d.	N.d.	N.d.	N.d.	N.d.	N.d.	N.d.
Tb	0.070	N.d.	N.d.	0.300	0.310	0.500	N.d.	0.590	0.530	0.510	0.310	0.370
Dy	N.d.	0.550	5.720	N.d.	N.d.	N.d.	N.d.	N.d.	N.d.	N.d.	N.d.	N.d.
Ho	N.d.	N.d.	N.d.	0.420	0.420	0.580	N.d.	N.d.	N.d.	N.d.	N.d.	0.490
Er	N.d.	0.390	2.860	N.d.	N.d.	N.d.	N.d.	N.d.	N.d.	N.d.	N.d.	N.d.
Tm	N.d.	N.d.	N.d.	N.d.	N.d.	N.d.	N.d.	N.d.	N.d.	N.d.	N.d.	N.d.
Yb	0.410	0.410	2.190	1.140	1.120	1.550	0.190	2.090	1.120	1.810	1.410	1.330
Lu	0.070	N.d.	N.d.	0.190	0.190	0.250	0.040	0.330	0.170	0.270	0.230	0.220
Total	N.d.	N.d.	N.d.	N.d.	N.d.	N.d.	N.d.	N.d.	N.d.	N.d.	N.d.	N.d.
$(La/Yb)_n$	4.28	3.18	7.01	3.43	3.62	1.87	11.37	0.90	14.22	3.88	7.95	6.55

(*Continued*)

Table 5.14 Continued

	Provinces											
	Massif Central, France					Dreiser Weiher, West Germany						
	(Downes & Dupuy, 1987), INAA					(Stosch, 1982), RNAA						
	Ta39	Ta39L	Ta7	Tal3L	Z7	D-42	D-45	D-50	D-58	Ib/2	Ib/24	Ib/3
Element	*Spinel lherzolites*											
La	3.200	3.100	5.200	1.900	25.60	2.120	1.640	2.650	1.610	3.650	2.120	4.600
Ce	7.100	7.000	6.700	4.700	40.30	4.850	3.350	5.600	4.400	8.600	5.700	11.400
Pr	N.d.	N.d.	N.d.	N.d.	N.d.	0.680	0.480	0.750	0.680	1.320	0.710	1.440
Nd	N.d.	N.d.	N.d.	N.d.	N.d.	3.550	2.350	4.100	4.300	6.100	4.300	5.400
Sm	1.410	1.410	1.540	1.840	1.020	1.180	0.800	1.090	1.560	2.050	0.930	0.860
Eu	0.590	0.570	0.600	0.710	0.340	0.300	0.330	0.375	0.670	0.750	0.310	0.280
Gd	N.d.	N.d.	N.d.	N.d.	N.d.	1.030	1.410	1.200	2.450	N.d.	0.940	0.850
Tb	0.510	0.470	0.450	0.540	0.180	0.147	0.275	0.184	0.440	0.300	0.163	0.145
Dy	N.d.	N.d.	N.d.	N.d.	N.d.	0.940	N.d.	1.070	2.900	2.200	1.010	1.030
Ho	N.d.	0.670	N.d.	N.d.	N.d.	0.200	0.400	0.225	0.560	N.d.	0.270	0.260
Er	N.d.	N.d.	N.d.	N.d.	N.d.	N.d.	N.d.	0.680	N.d.	N.d.	N.d.	N.d.
Tm	N.d.	N.d.	N.d.	N.d.	N.d.	0.086	0.215	0.091	0.2700	N.d.	0.1130	0.1120
Yb	1.690	1.650	1.850	2.080	0.620	0.650	1.430	0.630	1.800	1.040	0.770	0.760
Lu	0.290	0.290	0.290	0.320	0.120	0.105	0.225	0.102	0.270	0.155	0.177	0.123
Total	N.d.	N.d.	N.d.	N.d.	N.d.	15.8	12.9	18.8	21.9	N.d.	17.5	27.3
$(La/Yb)_n$	1.28	1.27	1.90	0.62	27.87	2.20	0.77	2.84	0.60	2.37	1.86	4.09

	Provinces												
	Dreiser Weiher, West Germany			New Mexico, USA	Kapfenstein, Austria		Hawaii, USA						
	(Stosch, 1982), RNAA				(Kurat *et al.*, 1989)		(Sen *et al.*, 1993), IPMA						
	Ib/5	Ib/8	Ib/K1	KH-K8	Ka111	Ka168	20-BGr2	L211B-1	211B-2	I-10-1	LI-10-2	LI-5(Cc)	LI-5(Cr)
Element	*Spinel lherzolites*												
La	0.630	1.810	1.320	0.920	1.300	0.800	N.d.	N.d.	N.d.	6.850	4.880	2.530	9.780
Ce	2.200	6.200	5.100	1.920	N.d.	N.d.	9.770	16.43	12.86	15.10	11.18	4.940	23.82
Pr	N.d.	N.d.	0.920	0.380	N.d.	N.d.	N.d.	N.d.	N.d.	N.d.	N.d.	N.d.	N.d.
Nd	N.d.	6.200	5.100	2.730	N.d.	N.d.	7.355	12.54	11.11	8.270	6.310	3.830	16.970
Sm	0.750	2.050	2.130	1.480	1.600	1.750	2.710	4.040	3.580	2.480	1.830	2.040	4.570
Eu	0.310	0.720	0.800	0.640	0.670	0.690	0.930	1.290	1.160	1.100	0.640	0.840	1.670
Gd	1.450	2.600	2.900	2.500	N.d.	N.d.	N.d.	N.d.	N.d.	N.d.	N.d.	N.d.	N.d.
Tb	0.280	0.510	0.500	0.450	N.d.	N.d.	N.d.	N.d.	N.d.	N.d.	N.d.	N.d.	N.d.
Dy	2.400	N.d.	3.300	3.500	N.d.	N.d.	1.380	2.320	1.060	4.940	2.980	4.440	6.200
Ho	0.570	N.d.	0.840	0.770	N.d.	N.d.	N.d.	N.d.	N.d.	N.d.	N.d.	N.d.	N.d.
Er	1.620	N.d.	N.d.	2.250	N.d.	N.d.	0.380	1.080	0.880	3.150	1.910	2.690	3.690
Tm	N.d.	0.300	0.300	0.300	N.d.	N.d.	N.d.	N.d.	N.d.	N.d.	N.d.	N.d.	N.d.
Yb	1.400	1.850	2.130	2.100	2.110	2.000	0.390	0.980	0.900	2.560	1.550	2.110	2.990
Lu	0.230	0.250	0.320	0.330	0.340	0.320	N.d.	N.d.	N.d.	N.d.	N.d.	N.d.	N.d.
Total	N.d.	N.d.	25.7	20.3	N.d.	N.d.	N.d.	N.d.	N.d.	N.d.	N.d.	N.d.	N.d.
$(La/Yb)_n$	0.30	0.66	0.42	0.30	0.42	0.27	N.d.	N.d.	N.d.	1.81	2.13	0.81	2.21

(*Continued*)

Table 5.14 Continued

	Provinces												
	Hawaii, USA												
	(Sen *et al.*, 1993), IPMA												
	LI-5(sm)	LI-7	APS-17	APS-20-1	APS-20-2	APS-26	APS-29-1	APS-29-2	APS-3-1	APS-3-2	APS-4	APS-8	A-10II-1
Element	*Spinel lherzolites*												
La	17.34	4.550	6.990	3.550	1.520	N.d.	N.d.	N.d.	12.58	N.d.	N.d.	0.310	19.69
Ce	30.25	6.640	12.73	8.380	4.200	1.970	30.11	24.41	13.96	9.690	2.050	2.130	9.120
Pr	N.d.	N.d.	N.d.	N.d.	N.d.	N.d.	N.d.	N.d.	N.d.	N.d.	N.d.	N.d.	N.d.
Nd	22.090	5.490	8.010	5.390	4.140	2.400	11.90	9.630	7.900	5.780	2.130	4.240	6.720
Sm	5.530	2.320	2.810	1.820	1.770	1.250	2.900	2.220	2.820	1.850	1.130	2.210	9.620
Eu	2.170	1.080	1.230	0.660	0.900	0.620	0.970	0.770	1.320	0.610	0.510	0.550	14.48
Gd	N.d.	N.d.	N.d.	N.d.	N.d.	N.d.	N.d.	N.d.	N.d.	N.d.	N.d.	N.d.	N.d.
Tb	N.d.	N.d.	N.d.	N.d.	N.d.	N.d.	N.d.	N.d.	N.d.	N.d.	N.d.	N.d.	N.d.
Dy	7.000	4.820	4.740	3.320	3.780	2.730	2.190	1.760	5.410	1.610	2.230	4.370	14.790
Ho	N.d.	N.d.	N.d.	N.d.	N.d.	N.d.	N.d.	N.d.	N.d.	N.d.	N.d.	N.d.	N.d.
Er	4.400	2.950	2.940	1.990	2.280	1.700	1.020	0.980	3.290	0.850	1.300	2.880	14.92
Tm	N.d.	N.d.	N.d.	N.d.	N.d.	N.d.	N.d.	N.d.	N.d.	N.d.	N.d.	N.d.	N.d.
Yb	3.550	2.490	2.270	1.510	1.810	1.770	1.070	0.910	2.500	0.800	1.380	2.120	12.49
Lu	N.d.	N.d.	N.d.	N.d.	N.d.	N.d.	N.d.	N.d.	N.d.	N.d.	N.d.	N.d.	N.d.
Total	N.d.	N.d.	N.d.	N.d.	20.40	N.d.	50.2	40.7	49.8	21.2	10.7	18.8	102
$(La/Yb)_n$	3.30	1.23	2.08	1.59	0.57	N.d.	N.d.	N.d.	3.40	N.d.	N.d.	0.10	1.06

	Provinces												
	Hawaii, USA												
	(Sen *et al.*, 1993), IPMA												
	PA-10II-2	PA-2	PA-21-1	PA-21-2	PA-31A	PA-39-1	PA-39-2	PAII-1A-1	PAII-2	PAII-8	SL-10	77SL-13	77SL-2(X)
Element	*Spinel lherzolites*												
La	1.220	2.820	7.340	3.630	1.810	0.170	0.050	N.d.	4.260	5.770	N.d.	N.d.	N.d.
Ce	0.970	4.170	16.60	5.450	3.910	0.420	0.350	1.210	10.45	14.41	4.610	12.30	9.160
Pr	N.d.	N.d.	N.d.	N.d.	N.d.	N.d.	N.d.	N.d.	N.d.	N.d.	N.d.	N.d.	N.d.
Nd	3.780	2.700	7.330	2.740	3.190	2.370	1.770	2.220	6.530	9.890	4.020	6.840	10.60
Sm	8.650	1.470	1.930	1.390	1.580	1.540	1.220	1.550	1.860	3.380	1.490	1.390	3.300
Eu	6.330	0.750	0.740	0.660	0.650	0.540	0.770	0.650	0.570	1.180	0.620	0.470	1.190
Gd	N.d.	N.d.	N.d.	N.d.	N.d.	N.d.	N.d.	N.d.	N.d.	N.d.	N.d.	N.d.	N.d.
Tb	N.d.	N.d.	N.d.	N.d.	N.d.	N.d.	N.d.	N.d.	N.d.	N.d.	N.d.	N.d.	N.d.
Dy	10.96	3.030	3.480	3.070	3.400	3.650	2.950	2.780	2.270	5.320	1.960	1.150	2.320
Ho	N.d.	N.d.	N.d.	N.d.	N.d.	N.d.	N.d.	N.d.	N.d.	N.d.	N.d.	N.d.	N.d.
Er	11.27	2.010	2.190	1.900	2.140	2.360	1.810	1.710	1.370	3.120	0.990	0.570	1.000
Tm	N.d.	N.d.	N.d.	N.d.	N.d.	N.d.	N.d.	N.d.	N.d.	N.d.	N.d.	N.d.	N.d.
Yb	7.680	1.590	1.760	1.530	1.690	1.830	1.610	1.720	0.990	2.520	0.680	0.530	1.010
Lu	N.d.	N.d.	N.d.	N.d.	N.d.	N.d.	N.d.	N.d.	N.d.	N.d.	N.d.	N.d.	N.d.
Total	50.9	18.5	41.4	20.4	18.4	12.9	10.5	N.d.	28.3	45.6	N.d.	N.d.	N.d.
$(La/Yb)_n$	0.11	1.20	2.82	1.60	0.72	0.06	0.02	N.d.	2.90	1.55	N.d.	N.d.	N.d.

(*Continued*)

Table 5.14 Continued

	Provinces												
	Hawaii, USA					Yakutia, pipe Udach., Rus.	Wangquing, China						
	(Sen *et al.*, 1993), IPMA					(Data Kozmenko)	(Xu *et al.*, 1998)						
	77SL-5	77SL-6(X)	77SL-8(X)	Pal-3	SL-4	O-ET	Q91-1	Q91-37	Q91-6	Q91-11	Q91-77	Q91-20	Q91-21
Element	*Spinel lherzolites*												
La	N.d.	N.d.	N.d.	N.d.	N.d.	2.100	0.770	2.010	2.580	0.960	1.320	4.470	0.430
Ce	21.52	14.40	12.58	1.050	8.610	4.500	2.660	4.340	5.350	2.010	2.420	8.460	1.100
Pr	N.d.	N.d.	N.d.	N.d.	N.d.	N.d.	N.d.	N.d.	N.d.	N.d.	N.d.	N.d.	N.d.
Nd	15.08	7.570	10.86	2.150	6.850	2.600	3.110	4.190	3.980	1.330	2.550	4.400	1.090
Sm	4.170	2.050	3.750	1.330	1.710	0.760	1.290	1.660	1.510	0.450	1.150	1.230	0.470
Eu	1.510	0.830	1.380	0.640	0.640	0.270	0.540	0.680	0.610	0.210	0.500	0.450	0.200
Gd	N.d.	N.d.	N.d.	N.d.	N.d.	N.d.	2.070	2.550	N.d.	0.970	N.d.	1.530	0.850
Tb	N.d.	N.d.	N.d.	N.d.	N.d.	0.330	N.d.	N.d.	N.d.	N.d.	N.d.	N.d.	N.d.
Dy	3.350	2.800	2.550	2.450	1.570	N.d.	3.060	3.640	3.400	1.870	2.950	2.170	1.490
Ho	N.d.	N.d.	N.d.	N.d.	N.d.	N.d.	N.d.	N.d.	N.d.	N.d.	N.d.	N.d.	N.d.
Er	1.840	1.680	1.090	1.440	0.890	N.d.	2.100	2.290	2.220	1.370	2.010	1.420	1.150
Tm	N.d.	N.d.	N.d.	N.d.	N.d.	0.280	N.d.	N.d.	N.d.	N.d.	N.d.	N.d.	N.d.
Yb	1.700	1.710	1.070	1.590	0.760	2.000	1.910	2.080	2.020	1.290	1.880	1.230	1.070
Lu	N.d.	N.d.	N.d.	N.d.	N.d.	0.290	0.270	0.300	N.d.	0.190	N.d.	0.185	N.d.
Total	N.d.	N.d.	N.d.	N.d.	N.d.	13.1	17.8	23.7	N.d.	10.7	N.d.	25.6	7.85
$(La/Yb)_n$	N.d.	N.d.	N.d.	N.d.	N.d.	0.71	0.27	0.65	0.86	0.50	0.47	2.45	0.27

	Provinces											
	Cordillera, Canada											
	(Shi *et al.*, 1998), ICP-MS											
	Q91-5	Q91-13	Q91-22	AL-47	AL-88	AL-30	LG-36	HF-2	HF-24	FS-10	FS-15	WD-12
Element	*Spinel lherzolites*											
La	11.19	6.860	12.38	1.600	1.200	N.d.	N.d.	0.180	1.400	0.100	0.020	0.490
Ce	26.74	15.03	28.04	2.600	1.100	0.050	0.300	1.200	2.900	1.200	0.270	0.350
Pr	N.d.	N.d.	N.d.	0.350	0.180	0.030	0.140	0.320	0.380	0.380	0.190	0.050
Nd	10.19	6.310	14.05	1.900	1.700	0.470	1.500	2.600	1.900	2.700	1.700	0.690
Sm	1.320	1.250	3.160	1.500	1.000	0.470	1.950	1.500	1.000	2.000	1.500	0.710
Eu	0.390	0.460	1.040	0.480	0.510	0.280	0.490	0.640	0.440	0.610	0.530	0.380
Gd	0.800	N.d.	3.150	2.000	2.200	1.500	2.100	2.500	1.900	2.700	2.400	1.700
Tb	N.d.	N.d.	N.d.	0.400	0.410	0.290	0.400	0.480	0.360	0.480	0.470	0.340
Dy	0.580	1.150	3.100	2.800	2.900	2.500	2.900	3.300	2.800	3.500	2.900	2.600
Ho	N.d.	N.d.	N.d.	0.630	0.650	0.580	0.680	0.780	0.630	0.760	0.730	0.620
Er	0.330	0.680	1.550	1.900	1.900	1.900	2.100	2.400	2.000	2.100	2.300	1.900
Tm	N.d.	N.d.	N.d.	0.280	0.290	0.260	0.310	0.340	0.300	0.300	0.310	0.250
Yb	0.370	0.640	1.160	1.600	1.800	1.700	1.900	2.200	1.900	1.800	2.100	1.800
Lu	0.058	N.d.	0.150	0.230	0.250	0.260	0.280	0.320	0.280	0.290	0.290	0.230
Total	52.0	N.d.	67.8	18.3	16.1	10.3	N.d.	18.8	18.2	18.9	15.7	12.1
$(La/Yb)_n$	20.4	7.23	7.20	0.68	0.45	N.d.	N.d.	0.06	0.50	0.04	0.01	0.18

(*Continued*)

Table 5.14 Continued

	Provinces											
	Cordillera, Canada					Shavaryn Tsaram, Mongolia		Dreiser Weiher, West Germany				
	(Shi *et al.*, 1998), ICP-MS					(Erkushev, 1985)	(Ionov *et al.*, 1994)	(Stosch & Seck, 1980), RNAA				
	WD-14	AL-41	AL-49	AL-52	AL-53	W-21	Mo-99	Ia/105	Ia/171	Ia/236	Ia/249	Ib/6
Element	*Spinel lherzolites*							*Spinel peridotites*				
La	4.700	79.00	40.00	59.00	45.00	1.520	1.330	21.50	25.00	14.60	40.00	1.620
Ce	9.500	162.0	60.00	92.00	73.00	2.680	4.350	54.00	62.00	14.40	106.0	6.300
Pr	0.660	16.00	5.300	9.800	7.800	0.340	N.d.	8.300	9.000	0.950	14.20	1.130
Nd	3.100	51.00	23.00	36.00	28.00	1.460	4.180	30.00	41.00	3.000	47.00	6.000
Sm	1.000	5.200	4.300	5.700	3.700	1.340	1.610	3.400	6.100	0.560	7.600	2.000
Eu	0.450	1.300	1.300	1.300	1.300	1.000	0.700	0.900	1.780	0.195	2.300	0.780
Gd	1.900	2.700	3.000	2.900	2.800	2.410	N.d.	N.d.	4.600	0.790	N.d.	N.d.
Tb	0.370	0.310	0.320	0.290	0.360	0.360	N.d.	0.260	0.480	0.163	0.600	0.440
Dy	2.300	1.300	1.200	1.000	1.600	2.460	2.580	N.d.	N.d.	N.d.	4.700	N.d.
Ho	0.540	0.190	0.190	0.120	0.260	0.510	N.d.	N.d.	0.330	0.380	N.d.	0.620
Er	1.800	0.390	0.430	0.300	0.550	2.960	1.710	0.980	0.690	N.d.	1.900	1.710
Tm	0.270	0.040	0.050	0.030	0.060	0.600	N.d.	N.d.	N.d.	0.170	N.d.	N.d.
Yb	1.800	0.280	0.280	0.210	0.380	1.970	1.600	0.670	0.630	1.100	1.090	1.390
Lu	0.240	0.030	0.040	0.040	0.020	0.062	N.d.	0.114	0.097	0.168	0.163	0.230
Total	28.6	320	139	209	165	19.7	N.d.	120	152	36.5	226	22.2
$(La/Yb)_n$	1.76	190	96.4	190	79.9	0.52	0.56	N.d.	26.8	8.96	24.8	0.79

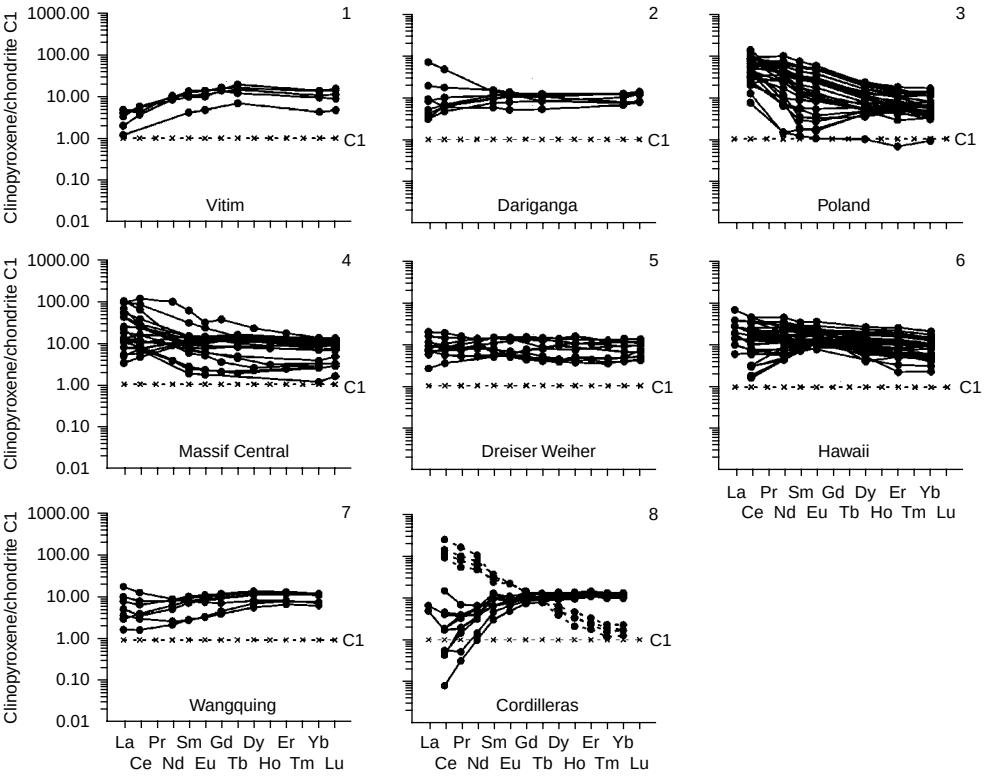

Figure 5.14 Chondrite-normalized REE patterns for clinopyroxenes from spinel lherzolites from deep xenoliths, represented in alkaline basalts (data Table 5.14).

Table 5.15 Chemical composition of clinopyroxenes from spinel lherzolites xenolith in alkali basalt (wt%) (sp. M-699-27, paleovolcano Shavaryn Tsaram, Mongolia).

	Analysis number		
Component	A-11	A-38	A-38a
SiO_2	51.42	51.50	51.35
TiO_2	0.69	0.74	0.69
Al_2O_3	6.99	7.10	7.24
Cr_2O_3	0.68	0.76	0.72
FeO	2.57	2.73	2.59
MgO	14.27	14.70	14.55
MnO	0.10	0.09	0.09
CaO	20.47	20.30	20.59
Na_2O	2.10	2.00	2.07
K_2O	0.02	0.04	0.03
Total	99.30	99.95	99.91
Mg#	90.9	90.5	90.9

Analysis carried out in Analytical center IGM SB RAS by X-ray spectrographic method on apparatus "Camebax-Micro" (analyst V.N. Koroliuk). $Mg\# = 100 \cdot Mg/(Mg + Fe)$ (formula coefficients). Dispose of orthopyroxene's grains, which were analyzed, show on Figure 5.3. Results of analysis of REE in some orthopyroxenes from this table are presented in Table 5.9 with the right numbers.

(*)—Analysis numbers of grain orthopyroxenes, which disposed near grain olivines with right analysis numbers.

Table 5.16 Rare earth element composition of clinopyroxenes from basalt, and spinel lherzolite xenolith in alkali basalt (ppm) (sp. M-699-27, paleovolcano Shavaryn Tsaram, Mongolia).

	Analysis number			
	A-8	A-11	A-16	A-19
	Distance from grains of clinopyroxenes to contact of xenolith with basalt (mm)			
Element	+3	+11	+30	+38
La	1.482	1.133	0.859	1.331
Ce	4.885	3.764	2.885	3.582
Pr	1.091	0.818	0.614	0.763
Nd	6.89	5.76	4.231	4.841
Sm	3.048	2.576	1.683	1.872
Eu	1.068	0.944	0.650	0.723
Gd	4.342	3.877	2.483	2.958
Tb	0.775	0.614	0.443	0.500
Dy	5.525	4.449	3.172	3.508
Ho	1.218	1.028	0.704	0.819
Er	3.855	3.168	2.173	2.404
Tm	0.514	0.435	0.295	0.309
Yb	3.512	3.007	2.089	2.324
Lu	0.492	0.388	0.271	0.308
Total	38.7	32.0	22.6	26.2
$(La/Yb)_n$	0.28	0.25	0.28	0.39

Analysis carried out in Analytical center IGM SB RAS by method LA ICP-MS on mass-spectrometry "Element" and UV Laser Probe (firma "Finnigan", Germany) (analysts S.V. Palessky and A.M. Kuchkin). Sign (+) mark distances from clinopyroxene's grains to contact xenolith with basalt. Dispose of clinopyroxene's grains, which were analyzed, show on Figure 5.3.

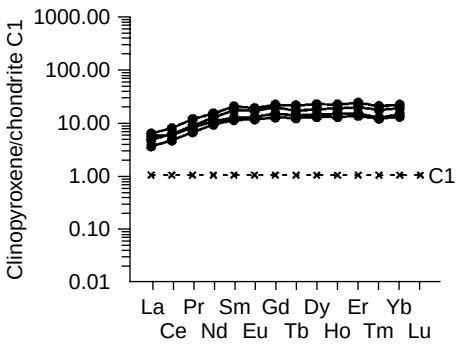

Figure 5.15 Chondrite-normalized REE patterns for clinopyroxenes from spinel lherzolites (sp. M-699-27, xenolith from alkaline basalt of paleovolcano Shavaryn Tsaram, Mongolia) (data Table 5.16).

Plagioclase-bearing lherzolites from deep xenoliths and massifs. Clinopyroxenes of this type were studied in ultramafic xenoliths from the alkaline-basalt province of the Khamar–Daban Ridge (southern Prebaikalia) and in the mafic–ultramafic massifs of Horoman, Lanzo, and Troodos. Their total REE content is an order of magnitude higher than that in chondrite C1 and values of the $(La/Yb)_n$ parameter vary from 0.3 to 0.9 (Table 5.18). In clinopyroxenes from plagioclase-bearing lherzolites from

Table 5.17 Rare earth element composition of clinopyroxenes from spinel lherzolites from massifs (ppm).

	Massifs												
	Troodos, Ciprus						Lherz, France			Indian Ocean			
	(Sobolev & Batanova, 1995), IPMA						(Bodinier *et al.*, 1988), RNAA			(Johnson & Dick, 1992), IPMA			
	TV-2	TV-24	TV-27	TV-28	TV-29	TV-5	70-367	71-107	71-321	18-23-1	18-23-2	18-45-2	18-45-6
Element	*Spinel lherzolites*												
La	0.030	0.050	0.060	0.050	0.060	0.040	0.750	3.420	0.770	N.d.	N.d.	N.d.	N.d.
Ce	0.060	0.070	0.150	0.060	0.140	0.050	2.800	5.620	3.300	0.084	0.040	0.038	0.064
Pr	N.d.	N.d.	N.d.	N.d.	N.d.	N.d.	N.d.	N.d.	N.d.	N.d.	N.d.	N.d.	N.d.
Nd	0.070	0.060	0.050	0.040	0.040	0.050	3.200	2.610	4.500	0.820	0.670	0.500	0.740
Sm	0.140	0.090	0.070	0.090	0.070	0.140	1.400	0.920	1.730	0.890	0.710	0.590	0.840
Eu	0.080	0.080	0.040	0.040	0.080	0.090	0.590	0.330	0.720	0.440	0.340	0.300	0.370
Gd	N.d.	N.d.	N.d.	N.d.	N.d.	N.d.	N.d.	N.d.	N.d.	N.d.	N.d.	N.d.	N.d.
Tb	N.d.	N.d.	N.d.	N.d.	N.d.	N.d.	0.440	0.240	0.480	N.d.	N.d.	N.d.	N.d.
Dy	0.850	0.990	0.790	0.680	0.670	1.210	N.d.	N.d.	N.d.	2.320	2.110	2.000	2.360
Ho	N.d.	N.d.	N.d.	N.d.	N.d.	N.d.	N.d.	0.380	0.640	N.d.	N.d.	N.d.	N.d.
Er	0.600	0.790	0.610	0.470	0.470	0.930	N.d.	N.d.	N.d.	1.470	1.180	1.160	1.410
Tm	N.d.	N.d.	N.d.	N.d.	N.d.	N.d.	N.d.	N.d.	N.d.	N.d.	N.d.	N.d.	N.d.
Yb	0.610	0.780	0.650	0.550	0.560	0.920	2.010	0.170	1.790	1.420	1.350	1.280	1.440
Lu	N.d.	N.d.	N.d.	N.d.	N.d.	N.d.	0.330	0.200	0.260	N.d.	N.d.	N.d.	N.d.
Total	2.44	2.91	2.42	1.98	2.09	3.43	N.d.	13.9	14.2	N.d.	N.d.	N.d.	N.d.
$(La/Yb)_n$	0.03	0.04	0.06	0.06	0.07	0.03	0.25	13.6	0.29	N.d.	N.d.	N.d.	N.d.

(*Continued*)

Table 5.17 Continued

	Massifs												
	Indian Ocean												
	(Johnson & Dick, 1992), IPMA												
	23-1-1	23-1-2	23-1-3	25-138-1	25-138-2	25-138-3	25-138-4	25-142-1	25-142-2	25-142-3	25-142-4	25-142-5	25-142-6
Element	*Spinel lherzolites*												
La	N.d.	N.d.	N.d.	N.d.	N.d.	N.d.	N.d.	N.d.	N.d.	N.d.	N.d.	N.d.	N.d.
Ce	0.350	0.078	0.147	0.139	0.133	0.125	0.102	0.120	0.094	0.109	0.125	0.125	0.066
Pr	N.d.	N.d.	N.d.	N.d.	N.d.	N.d.	N.d.	N.d.	N.d.	N.d.	N.d.	N.d.	N.d.
Nd	0.720	0.770	1.090	0.970	0.960	0.990	0.990	1.120	0.810	0.890	0.930	0.940	0.750
Sm	0.720	0.770	1.020	0.910	0.920	0.910	0.770	1.010	0.940	0.880	1.130	0.990	0.600
Eu	0.420	0.370	0.440	0.410	0.400	0.410	0.380	0.520	0.470	0.440	0.470	0.550	0.370
Gd	N.d.	N.d.	N.d.	N.d.	N.d.	N.d.	N.d.	N.d.	N.d.	N.d.	N.d.	N.d.	N.d.
Tb	N.d.	N.d.	N.d.	N.d.	N.d.	N.d.	N.d.	N.d.	N.d.	N.d.	N.d.	N.d.	N.d.
Dy	2.000	2.230	2.960	2.230	2.240	2.920	1.970	2.530	2.390	2.440	2.300	2.670	2.040
Ho	N.d.	N.d.	N.d.	N.d.	N.d.	N.d.	N.d.	N.d.	N.d.	N.d.	N.d.	N.d.	N.d.
Er	1.210	1.400	1.960	1.370	1.260	1.340	1.180	1.580	1.480	1.570	1.430	1.680	1.270
Tm	N.d.	N.d.	N.d.	N.d.	N.d.	N.d.	N.d.	N.d.	N.d.	N.d.	N.d.	N.d.	N.d.
Yb	1.370	1.420	1.800	1.360	1.340	1.440	1.240	1.700	1.600	1.630	1.580	1.870	1.420
Lu	N.d.	N.d.	N.d.	N.d.	N.d.	N.d.	N.d.	N.d.	N.d.	N.d.	N.d.	N.d.	N.d.
Total	N.d.	N.d.	N.d.	N.d.	N.d.	N.d.	N.d.	N.d.	N.d.	N.d.	N.d.	N.d.	N.d.
$(La/Yb)_n$	N.d.	N.d.	N.d.	N.d.	N.d.	N.d.	N.d.	N.d.	N.d.	N.d.	N.d.	N.d.	N.d.

	Massifs												
	Indian Ocean												
	(Johnson & Dick, 1992), IPMA												
	30-32-1	30-32-2	30-32-3	30-40-1	30-40-2	30-40-3	34-58-1	34-58-2	34-58-3	34-63-1	34-63-2	35-49-1	35-49-2
Element	*Spinel lherzolites*												
La	N.d.	N.d.	N.d.	N.d.	N.d.	N.d.	N.d.	N.d.	N.d.	N.d.	N.d.	N.d.	N.d.
Ce	0.166	0.237	0.197	0.097	0.077	0.139	0.015	0.013	0.018	0.010	0.016	0.019	0.014
Pr	N.d.	N.d.	N.d.	N.d.	N.d.	N.d.	N.d.	N.d.	N.d.	N.d.	N.d.	N.d.	N.d.
Nd	1.030	1.150	0.940	0.730	0.910	1.280	0.030	0.048	0.052	0.077	0.062	0.103	0.081
Sm	0.840	0.970	0.810	0.720	0.760	1.230	0.130	0.130	0.120	0.180	0.120	0.150	0.120
Eu	0.410	0.450	0.390	0.380	0.400	0.520	0.070	0.065	0.058	0.088	0.079	0.088	0.063
Gd	N.d.	N.d.	N.d.	N.d.	N.d.	N.d.	N.d.	N.d.	N.d.	N.d.	N.d.	N.d.	N.d.
Tb	N.d.	N.d.	N.d.	N.d.	N.d.	N.d.	N.d.	N.d.	N.d.	N.d.	N.d.	N.d.	N.d.
Dy	2.010	2.230	2.260	2.110	2.260	3.490	0.770	0.910	0.900	1.240	0.860	1.290	0.880
Ho	N.d.	N.d.	N.d.	N.d.	N.d.	N.d.	N.d.	N.d.	N.d.	N.d.	N.d.	N.d.	N.d.
Er	1.330	1.510	1.310	1.430	1.350	2.310	0.560	0.690	0.580	0.790	0.550	0.810	0.620
Tm	N.d.	N.d.	N.d.	N.d.	N.d.	N.d.	N.d.	N.d.	N.d.	N.d.	N.d.	N.d.	N.d.
Yb	1.200	1.460	1.210	1.200	1.280	2.280	0.610	0.660	0.640	0.860	0.590	1.030	0.610
Lu	N.d.	N.d.	N.d.	N.d.	N.d.	N.d.	N.d.	N.d.	N.d.	N.d.	N.d.	N.d.	N.d.
Total	N.d.	N.d.	N.d.	N.d.	N.d.	N.d.	N.d.	N.d.	N.d.	N.d.	N.d.	N.d.	N.d.
$(La/Yb)_n$	N.d.	N.d.	N.d.	N.d.	N.d.	N.d.	N.d.	N.d.	N.d.	N.d.	N.d.	N.d.	N.d.

(*Continued*)

Table 5.17 Continued

	Massifs												
	Indian Ocean												
	(Johnson & Dick, 1992), IPMA												
	35-49-4	35-80-1	35-80-2	35-80-3	44-1-1	44-1-2	46-1-1	46-1-3	46-2-1	46-2-2	6-3-1	6-3-2	6-3-4
Element	*Spinel lherzolites*												
La	N.d.	N.d.	N.d.	N.d.	N.d.	N.d.	N.d.	N.d.	N.d.	N.d.	N.d.	N.d.	N.d.
Ce	0.012	0.014	0.011	0.017	0.035	0.023	0.026	0.028	0.041	0.021	0.023	0.052	0.036
Pr	N.d.	N.d.	N.d.	N.d.	N.d.	N.d.	N.d.	N.d.	N.d.	N.d.	N.d.	N.d.	N.d.
Nd	0.029	0.054	0.046	0.052	0.170	0.160	0.420	0.440	0.400	0.330	0.360	0.500	0.550
Sm	0.120	0.090	0.110	0.130	0.280	0.340	0.680	0.650	0.540	0.450	0.520	0.570	0.760
Eu	0.077	0.072	0.060	0.068	0.160	0.160	0.300	0.300	0.270	0.200	0.310	0.340	0.350
Gd	N.d.	N.d.	N.d.	N.d.	N.d.	N.d.	N.d.	N.d.	N.d.	N.d.	N.d.	N.d.	N.d.
Tb	N.d.	N.d.	N.d.	N.d.	N.d.	N.d.	N.d.	N.d.	N.d.	N.d.	N.d.	N.d.	N.d.
Dy	0.800	1.040	0.800	0.950	1.500	1.650	2.170	2.520	2.120	1.620	1.870	1.880	2.030
Ho	N.d.	N.d.	N.d.	N.d.	N.d.	N.d.	N.d.	N.d.	N.d.	N.d.	N.d.	N.d.	N.d.
Er	0.560	0.750	0.580	0.580	0.880	0.980	1.310	1.630	1.300	1.010	1.170	1.070	1.290
Tm	N.d.	N.d.	N.d.	N.d.	N.d.	N.d.	N.d.	N.d.	N.d.	N.d.	N.d.	N.d.	N.d.
Yb	0.600	0.680	0.630	0.660	0.900	1.010	1.400	1.670	1.290	1.010	N.d.	0.820	1.250
Lu	N.d.	N.d.	N.d.	N.d.	N.d.	N.d.	N.d.	N.d.	N.d.	N.d.	N.d.	N.d.	N.d.
Total	N.d.	N.d.	N.d.	N.d.	N.d.	N.d.	N.d.	N.d.	N.d.	N.d.	N.d.	N.d.	N.d.
$(La/Yb)_n$	N.d.	N.d.	N.d.	N.d.	N.d.	N.d.	N.d.	N.d.	N.d.	N.d.	N.d.	N.d.	N.d.

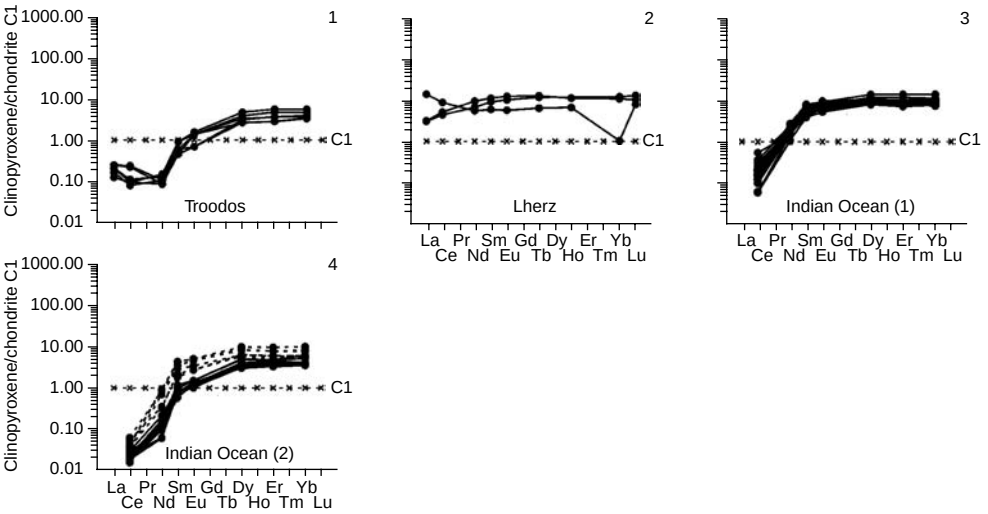

Figure 5.16 Chondrite-normalized REE patterns for clinopyroxenes from spinel lherzolites (data Table 5.17). Diagram 3 – less depleted of Ce, Nd, Sm, Eu, and heavy REE varieties; diagram 4—more depleted of Ce, Nd, Sm, Eu, and heavy REE varieties. Dotted lines—patterns of intermediate varieties.

Table 5.18 Rare earth element composition of clinopyroxenes from plagioclase-bearing lherzolites from massifs, and from deep xenoliths (ppm).

	Xenoliths				Massifs					
	Khamar–Daban, Russia				Horoman, Japan					Troodos, Cyprus
	(Ionov *et al.*, 1995a), INAA				(Frey *et al.*, 1991), RNAA					(Batanova *et al.*, 1996)
Element	83-36	83-50	83-69	98-13	62210a	62210b	62210c	62212	62213	TV-143
La	1.260	1.010	1.040	2.850	0.950	1.280	1.270	1.060	1.990	0.050
Ce	4.310	3.460	3.700	6.780	4.470	5.840	5.380	4.980	8.590	0.240
Pr	0.837	N.d.	N.d.	1.050	N.d.	N.d.	N.d.	N.d.	N.d.	N.d.
Nd	4.890	3.740	3.560	5.380	4.850	5.250	5.740	5.750	7.890	0.590
Sm	1.910	1.910	1.980	1.890	2.010	2.280	2.240	2.420	3.270	0.490
Eu	0.801	0.770	0.710	0.771	0.740	0.780	0.740	0.900	1.100	0.220
Gd	2.930	N.d.	N.d.	2.850	N.d.	N.d.	N.d.	N.d.	N.d.	N.d.
Tb	0.542	0.520	0.570	0.528	N.d.	N.d.	N.d.	N.d.	N.d.	N.d.
Dy	3.730	N.d.	N.d.	3.650	2.670	2.190	3.240	3.140	3.450	1.690
Ho	0.828	N.d.	N.d.	0.813	N.d.	N.d.	N.d.	N.d.	N.d.	N.d.
Er	2.330	N.d.	N.d.	2.320	1.760	1.210	2.110	1.890	1.980	1.070
Tm	0.339	0.400	0.310	0.337	N.d.	N.d.	N.d.	N.d.	N.d.	N.d.
Yb	2.090	2.340	2.000	2.070	1.660	1.180	1.880	1.800	2.140	1.170
Lu	0.328	0.330	0.300	0.326	N.d.	N.d.	N.d.	N.d.	N.d.	N.d.
Total	27.1	N.d.	N.d.	31.6	N.d.	N.d.	N.d.	N.d.	N.d.	N.d.
$(La/Yb)_n$	0.41	0.29	0.35	0.93	0.39	0.73	0.46	0.40	0.63	0.03

the Troodos massif, the total level of accumulation of REE is relatively low, mainly owing to their depletion of light REE. A similar depletion of light REE was also observed in clinopyroxenes in the majority of other mineral parageneses studied in the Troodos massif.

Detailed studies were performed for clinopyroxenes from plagioclase-bearing peridotites of the Lanzo massif in the western Alps (Piccardo *et al.*, 2005). These authors think that plagioclase-bearing peridotites in the Lanzo massif formed during feldspathization and clinopyroxenization of ultramafic restites under the influence of intruded mafic melts and percolation of their fluids. As a result, ultramafic restites were transformed into hybrid ultramafic rocks with a nonuniform structure, texture, and quantitative-mineral composition. Clinopyroxenes from these rocks are characterized by a nonuniform distribution of REE. Newly formed clinopyroxenes of this type are observed in the contact zones of protrusions of ultramafic restites and intruding gabbroid intrusions in ophiolitic associations (Lesnov, 1981a,b, 1984, 1988).

Lherzolites from deep xenoliths. The rare earth composition of clinopyroxenes from lherzolite xenoliths were studied in samples from many alkaline-basalt provinces. The most abundant data were obtained for samples from the British Columbia, Canadian Cordillera, Hawaiian Islands, Hannuoba, and Victoria provinces (Table 5.19, Fig. 5.17). The total REE content in these clinopyroxenes ranges from 5–20 ppm in depleted varieties to 50–150 ppm in enriched varieties. Judging from the REE patterns, most clinopyroxenes from xenoliths in the Victoria, Hawaiian Islands, and Hannuoba provinces are depleted of REE, with samples abnormally enriched with them are less abundant. On the basis of a special sampling of analyses, it was established that clinopyroxenes from lherzolite xenoliths from the above provinces of clinopyroxenes have a polymodal static distribution of light REE and a polymodal distribution of $(La/Yb)_n$ values. Considering this parameter, three varieties were established among clinopyroxenes from the British Columbia province: (1) those with low values (0.03–0.20); (2) those with moderate values (0.28–0.56); and (3) those with high values (1.08–3.68). Clinopyroxenes from lherzolite xenoliths of Hannuoba were, in turn, divided into two varieties: (1) those depleted of light REE; and (2) those enriched with these elements. Abnormal enrichment with light REE was also found in the majority of clinopyroxenes from lherzolite xenoliths in alkali basalts of the Hawaii, Vogelsberg, and Vitim provinces as well as from kimberlites of South Africa (Fig. 5.17, 7–10). We think that accumulation of abnormally increased amounts of light REE in clinopyroxenes from peridotite xenoliths in alkali basalts and kimberlites provinces is a widespread phenomenon and is related to their supply of fluid components that separated from surrounding melts (Lesnov, 2003a). When studying peridotite xenoliths from basalts of the Vitim and Udokan volcanic fields, Litasov *et al.* (1999) established features of percolation of basalt melts in them.

Peridotites from deep xenoliths. A similar rare earth composition was established for clinopyroxenes from ultramafic xenoliths in the provinces of Dariganga, Dzhilinda, Udokan, and Nunivak Island, which are described under a joint name of "peridotites" (Table 5.20). Most of these clinopyroxenes were found to have a moderate general level of accumulation of REE at about 10 t. ch. However, some of them were found to have an abnormally high level of accumulation of REE, less often, of middle elements, reaching 80–100 t. ch. Clinopyroxenes from xenoliths in the Dariganga and Dzhilinda provinces display a bimodal distribution of La, Ce, Pr, Nd, suggesting two varieties

Table 5.19 Rare earth element composition of clinopyroxenes from lherzolites from deep xenoliths (ppm).

	Provinces												
	Spitsbergen				Victoria, Australia						Hawaii, USA		
	(Shubina *et al.*, 1997), INAA				(Frey & Green, 1974), RNAA						(Sen *et al.*, 1993)		
	12sv	13sv	9sv	5ha	2604	2640	2642	2669	27008	2728	20-BGr1	PA-12-1	PA-12-2
Element	*Lherzolites*												
La	19.60	1.760	2.600	14.60	26.60	5.490	3.730	23.40	13.00	1.070	N.d.	3.260	2.670
Ce	32.00	5.260	5.400	11.80	64.50	15.30	6.600	61.00	17.60	3.000	13.42	10.77	8.100
Pr	N.d.	N.d.	N.d.	N.d.	8.430	2.380	1.120	9.840	2.550	0.680	N.d.	N.d.	N.d.
Nd	N.d.	N.d.	N.d.	N.d.	33.30	11.10	5.210	39.40	10.50	4.100	10.36	10.74	7.810
Sm	1.920	1.160	0.700	1.060	5.780	2.730	1.570	6.310	1.980	1.430	3.710	3.160	2.310
Eu	0.615	0.460	0.260	0.390	1.580	0.880	0.620	1.865	0.700	0.620	1.350	1.130	1.000
Gd	N.d.	N.d.	N.d.	N.d.	4.000	2.700	2.300	5.000	2.000	2.400	N.d.	N.d.	N.d.
Tb	0.016	0.017	0.714	0.013	0.460	0.450	0.440	0.580	0.290	0.420	N.d.	N.d.	N.d.
Dy	N.d.	N.d.	N.d.	N.d.	N.d.	N.d.	N.d.	N.d.	N.d.	N.d.	2.020	2.410	2.010
Ho	N.d.	N.d.	N.d.	N.d.	0.340	0.510	0.680	0.640	0.270	0.620	N.d.	N.d.	N.d.
Er	N.d.	N.d.	N.d.	N.d.	0.880	1.440	1.640	1.450	0.780	1.750	0.660	0.890	0.780
Tm	N.d.	N.d.	N.d.	N.d.	0.097	0.180	0.250	0.200	0.110	0.250	N.d.	N.d.	N.d.
Yb	1.240	1.480	0.675	1.090	0.470	1.020	1.730	1.200	0.530	1.430	0.570	0.560	0.410
Lu	0.169	0.226	0.126	0.160	0.095	0.183	0.280	0.169	0.100	0.260	N.d.	N.d.	N.d.
Total	N.d.	N.d.	N.d.	N.d.	148	44.4	26.2	151	50.4	18.0	N.d.	N.d.	N.d.
$(La/Yb)_n$	10.7	0.80	2.60	9.04	38.2	3.63	1.45	13.2	16.6	0.51	N.d.	3.93	4.40

(*Continued*)

Table 5.19 Continued

	Provinces												
	Hawaii, USA						Hannuoba, China						
	(Sen *et al.*, 1993), IPMA						(Song & Frey, 1989), IPMA						
	SL-2(Y)	SL-28A	SL-28B	SL-6(Y)	77SL-7	77SL-8Y	DM1-2	DM1-3H	DM1-3V	DM1-4	DM1-5H	DM1-5V	DM1-7V
Element	*Lherzolites*												
La	N.d.	N.d.	N.d.	N.d.	N.d.	N.d.	0.810	2.020	10.11	0.440	2.000	2.070	6.260
Ce	23.94	10.10	8.770	13.79	21.11	12.22	2.070	2.840	13.68	1.320	5.050	6.860	11.75
Pr	N.d.	N.d.	N.d.	N.d.	N.d.	N.d.	0.470	0.500	1.480	0.270	0.960	1.220	1.950
Nd	18.55	6.520	5.900	9.240	21.43	9.690	3.620	2.910	6.520	2.180	5.420	7.360	9.560
Sm	5.780	2.000	2.010	2.860	6.990	3.070	1.490	1.180	1.190	0.980	2.350	3.030	2.100
Eu	2.240	0.730	0.670	1.090	2.560	1.190	0.650	0.470	0.450	0.420	1.030	1.100	0.730
Gd	N.d.	N.d.	N.d.	N.d.	N.d.	N.d.	N.d.	N.d.	N.d.	N.d.	N.d.	N.d.	N.d.
Tb	N.d.	N.d.	N.d.	N.d.	N.d.	N.d.	N.d.	N.d.	N.d.	N.d.	N.d.	N.d.	N.d.
Dy	3.800	1.020	0.810	2.710	4.170	3.050	2.290	1.840	1.700	1.990	3.740	2.6900	1.150
Ho	N.d.	N.d.	N.d.	N.d.	N.d.	N.d.	N.d.	N.d.	N.d.	N.d.	N.d.	N.d.	N.d.
Er	1.510	0.390	0.350	1.290	1.520	1.580	1.600	1.170	1.400	1.390	2.440	1.590	0.960
Tm	N.d.	N.d.	N.d.	N.d.	N.d.	N.d.	N.d.	N.d.	N.d.	N.d.	N.d.	N.d.	N.d.
Yb	1.530	0.270	0.250	1.390	1.880	1.590	N.d.	N.d.	N.d.	N.d.	N.d.	N.d.	N.d.
Lu	N.d.	N.d.	N.d.	N.d.	N.d.	N.d.	N.d.	N.d.	N.d.	N.d.	N.d.	N.d.	N.d.
Total	57.4	21.0	18.8	32.4	59.7	32.4	N.d.	N.d.	N.d.	N.d.	N.d.	N.d.	N.d.
$(La/Yb)_n$	N.d.	N.d.	N.d.	N.d.	N.d.	N.d.	N.d.	N.d.	N.d.	N.d.	N.d.	N.d.	N.d.

	Provinces												
	Hannuoba, China	British Columbia, Canada											Ataq, Yemen
	(Song & Frey, 1989), IPMA	(Sun & Kerrich, 1995), ICP-MS											(Varne & Graham, 1971)
	DM1-9	BM-11	BM-16	BM-55	JL-14	JL-15	JL-18	KR-1	KR-2	KR-35	LL-1	LL-14	VG
Element	*Lherzolites*												
La	0.560	1.760	0.090	0.340	0.300	0.795	12.00	1.180	0.750	0.680	4.000	0.690	20.00
Ce	1.660	4.140	0.400	1.300	1.430	2.653	32.60	1.930	1.270	2.990	9.540	1.260	21.00
Pr	0.390	0.612	0.150	0.310	0.400	0.540	4.540	0.250	0.120	0.652	1.340	0.160	3.100
Nd	2.690	3.400	1.490	2.260	2.760	3.590	19.30	1.050	0.440	4.460	6.300	0.770	10.00
Sm	1.370	1.400	1.050	1.280	1.490	1.520	4.370	0.390	0.150	1.830	1.820	0.200	2.500
Eu	0.640	0.636	0.490	0.550	0.640	0.647	1.480	0.180	0.080	0.736	0.630	0.070	0.660
Gd	N.d.	2.600	2.090	2.230	2.490	2.410	4.350	0.760	0.470	2.930	2.460	0.230	2.400
Tb	N.d.	0.472	0.410	0.420	0.470	0.449	0.640	0.140	0.120	0.524	0.420	0.050	0.470
Dy	2.570	3.600	3.050	3.230	3.440	3.270	4.240	1.080	1.090	3.930	3.080	0.350	1.700
Ho	N.d.	0.786	0.700	0.690	0.730	0.701	0.820	0.240	0.290	0.814	0.630	0.080	0.450
Er	1.680	2.300	2.150	2.100	2.140	2.100	2.290	0.790	0.970	2.460	1.940	0.300	1.500
Tm	N.d.	0.342	0.320	0.320	0.330	0.302	0.350	0.120	0.170	0.366	0.290	0.050	0.180
Yb	N.d.	2.140	2.190	1.990	1.980	1.900	2.200	0.740	1.050	2.300	1.770	0.410	0.930
Lu	N.d.	0.320	0.310	0.290	0.290	0.285	0.310	0.120	0.160	0.331	0.260	0.060	0.150
Total	11.6	24.5	14.9	17.3	18.9	21.2	89.5	9.0	7.13	25.0	34.5	4.68	65.0
$(La/Yb)_n$	N.d.	0.56	0.03	0.12	0.10	0.28	3.68	1.08	0.48	0.20	1.53	1.14	14.5

(*Continued*)

Table 5.19 Continued

	Provinces												
	Itinome-Gata, Japan		Vogelsberg, Germany			Vitim, Russia			Bulfontan		Tuba Putsoa	Motae	Likhobo
	(Tanaka & Aoki, 1981), IDMS		(Witt-Eickschen, 1993), INAA			(Litasov, 1998), SIMS			(Shimizu, 1975), IDMS				
	2L	3L	DH1127	DH1128	DH1137	V-439	V-706	V-857v	BUL6	JJG352	PHN1566	PHN1925	PHN2302
Element	*Lherzolites*												
La	0.616	0.243	17.90	10.30	16.50	1.569	8.437	1.553	N.d.	N.d.	N.d.	N.d.	N.d.
Ce	2.290	0.945	10.50	22.70	12.20	5.879	23.66	5.720	21.30	18.70	6.010	3.020	24.30
Pr	N.d.	N.d.	N.d.	N.d.	N.d.	N.d.	N.d.	N.d.	N.d.	N.d.	N.d.	N.d.	N.d.
Nd	2.900	2.230	2.840	6.280	3.560	5.871	23.66	5.720	21.60	19.70	5.900	6.020	15.20
Sm	1.220	1.320	0.720	0.600	0.710	2.221	4.323	2.315	5.330	2.660	1.640	1.510	3.700
Eu	0.483	0.512	0.350	0.290	0.330	0.745	1.396	0.747	1.470	0.563	0.610	0.533	1.060
Gd	1.990	2.320	N.d.	N.d.	N.d.	N.d.	N.d.	N.d.	2.780	0.930	1.640	1.690	1.890
Tb	N.d.	N.d.	0.280	0.180	0.240	N.d.	N.d.	N.d.	N.d.	N.d.	N.d.	N.d.	N.d.
Dy	2.760	3.240	N.d.	N.d.	N.d.	1.849	3.840	1.485	0.694	0.459	1.060	1.330	0.545
Ho	N.d.	N.d.	N.d.	N.d.	N.d.	N.d.	N.d.	N.d.	N.d.	N.d.	N.d.	N.d.	N.d.
Er	1.600	2.080	N.d.	N.d.	N.d.	0.651	2.313	0.452	0.101	0.091	0.390	0.365	0.0718
Tm	N.d.	N.d.	0.310	0.130	0.260	N.d.	N.d.	N.d.	N.d.	N.d.	N.d.	N.d.	N.d.
Yb	1.360	1.750	1.920	0.850	1.960	0.560	2.725	0.513	0.068	0.026	0.255	0.195	0.024
Lu	0.190	0.250	0.290	0.120	0.350	N.d.	N.d.	N.d.	N.d.	N.d.	N.d.	N.d.	N.d.
Total	15.4	14.9	N.d.	N.d.	N.d.	19.3	70.4	18.5	53.3	43.1	17.5	14.7	46.8
$(La/Yb)_n$	0.31	0.09	6.29	8.18	5.68	1.89	2.09	2.04	N.d.	N.d.	N.d.	N.d.	N.d.

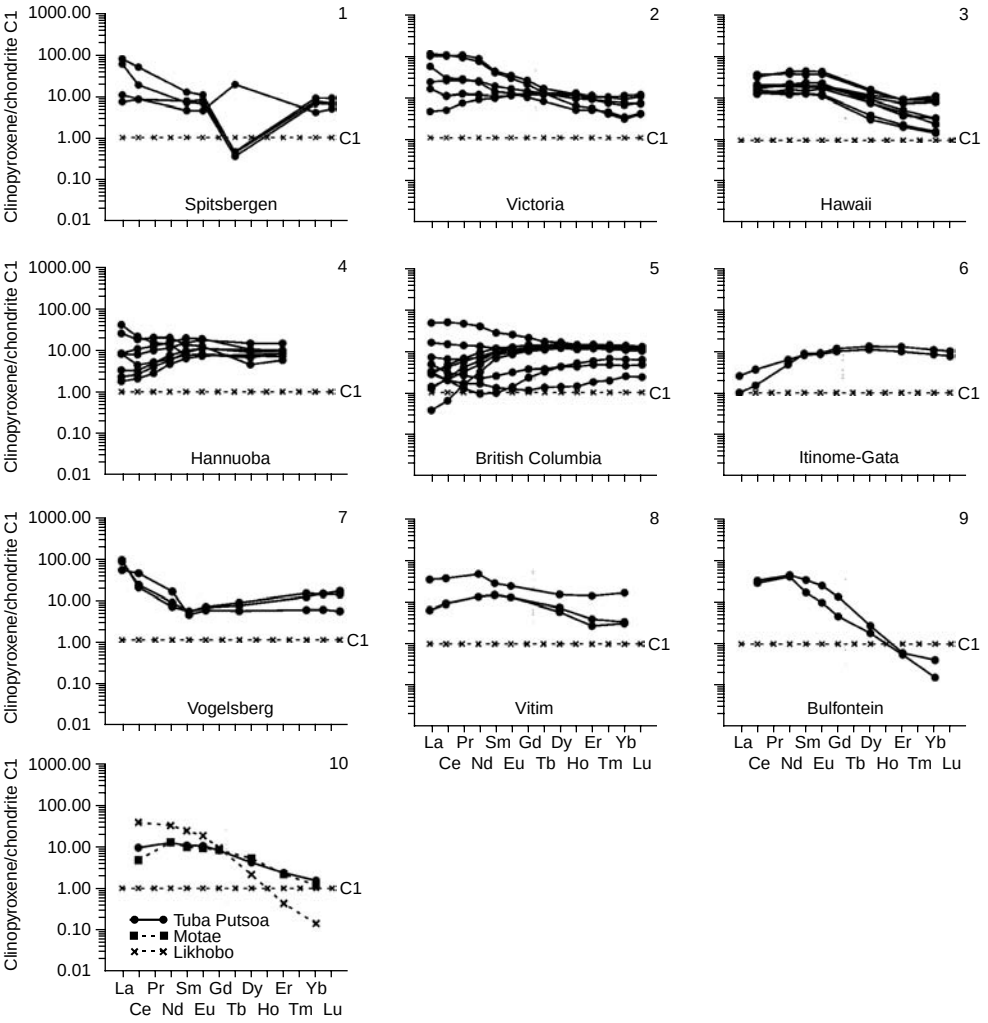

Figure 5.17 Chondrite-normalized REE patterns for clinopyroxenes from lherzolites, represented in deep xenoliths (data Table 5.19).

among them: (1) those relatively depleted of light REE; and (2) those abnormally enriched with them.

Lherzolites and peridotites from massifs. Data on clinopyroxenes from these rocks are scarcer than those on samples from deep xenoliths (Table 5.21, Fig. 5.18). The data are also rather heterogeneous with respect to REE content and configuration of REE patterns. In samples from the Lizard, Newfoundland, and Balmuccia massifs, REE are intensely fractionated, and the $(La/Yb)_n$ parameter has lower values. In clinopyroxenes from the Balmuccia massif, the concentrations of La and Ce vary in a narrower range compared to the mineral from other massifs. Unlike most others, clinopyroxenes from lherzolites in the Otris, Naransky, Freychinede, and Caussou massifs display less pronounced fractionation of elements (Fig. 5.18, 5, 6).

Table 5.20 Rare earth element composition of clinopyroxenes from peridotites from deep xenoliths (ppm).

	Provinces												
	Dariganga, Mongolia						Shavaryn Tsaram, Mongolia						
	(Ionov *et al.*, 1994), IPMA												
	5c-1	8520-41	8520-6Br	8520-6co	8520-6ri	8525-1	5a-1	aMo8530	5a-5alt	5pheno	Mo8530	5b-4	5b5phen
Element	*Peridotites*												
La	3.250	18.40	16.70	2.150	10.10	7.830	4.470	5.520	9.350	8.010	3.860	9.450	14.80
Ce	5.260	58.40	42.60	8.320	28.00	26.80	7.890	12.10	32.20	31.80	7.350	28.60	40.20
Pr	N.d.	N.d.	N.d.	N.d.	N.d.	N.d.	N.d.	1.280	N.d.	N.d.	0.700	N.d.	N.d.
Nd	1.700	48.80	27.40	8.990	20.30	15.50	2.190	4.360	25.10	29.90	2.400	14.80	28.50
Sm	0.750	13.30	9.370	3.730	7.130	3.520	0.900	0.950	7.000	9.460	0.720	3.490	8.460
Eu	0.360	3.030	3.420	1.370	2.550	1.620	0.360	0.390	2.130	2.830	0.320	1.160	2.810
Gd	N.d.	N.d.	N.d.	N.d.	N.d.	N.d.	N.d.	1.390	N.d.	N.d.	1.230	N.d.	N.d.
Tb	N.d.	N.d.	N.d.	N.d.	N.d.	N.d.	N.d.	0.272	N.d.	N.d.	0.244	N.d.	N.d.
Dy	1.620	10.30	5.750	2.910	4.600	2.850	1.620	1.940	4.610	6.390	1.780	2.260	5.460
Ho	N.d.	N.d.	N.d.	N.d.	N.d.	N.d.	N.d.	0.438	N.d.	N.d.	0.405	N.d.	N.d.
Er	1.000	3.110	2.320	1.130	1.770	1.870	1.080	1.280	2.200	3.010	1.170	1.390	2.850
Tm	N.d.	N.d.	N.d.	N.d.	N.d.	N.d.	N.d.	0.184	N.d.	N.d.	0.170	N.d.	N.d.
Yb	1.030	2.150	1.450	0.770	1.330	1.510	1.050	1.140	1.490	2.190	1.060	1.070	2.160
Lu	N.d.	N.d.	N.d.	N.d.	N.d.	N.d.	N.d.	0.180	N.d.	N.d.	0.167	N.d.	N.d.
Total	N.d.	N.d.	N.d.	N.d.	N.d.	N.d.	N.d.	31.4	N.d.	N.d.	21.6	N.d.	N.d.
$(La/Yb)_n$	2.1	5.8	7.8	1.9	5.1	3.5	2.9	3.3	4.2	2.5	2.5	6.0	4.6

	Provinces												
	Shavaryn Tsaram, Mongolia		Nunivak islands, USA					Dzhilinda, Russia					
	(Ionov *et al.*, 1994)		(Roden *et al.*, 1984), RNAA					(Litasov, 1998), SIMS					
	5b-5rel	M8531-40	10002	10004	10051	10056	10067	D-160	D-82	D-871	D-9	D-122	D-19
Element	*Peridotites*												
La	8.050	14.40	18.80	9.260	13.50	25.10	12.10	0.763	1.672	2.503	0.407	8.243	1.263
Ce	31.60	43.80	42.10	25.00	47.20	48.30	43.90	2.864	4.742	4.667	1.995	23.01	5.390
Pr	N.d.	N.d.	N.d.	N.d.	N.d.	N.d.	N.d.	N.d.	N.d.	N.d.	N.d.	N.d.	N.d.
Nd	21.10	28.10	15.00	12.60	40.70	17.00	23.00	3.869	4.793	4.658	3.365	13.89	7.571
Sm	6.080	7.720	1.800	2.360	10.30	3.150	5.220	1.454	1.961	1.798	1.335	3.450	3.051
Eu	1.930	2.240	0.628	0.815	3.440	1.010	1.770	0.543	0.739	0.638	0.457	1.068	1.072
Gd	N.d.	N.d.	N.d.	N.d.	N.d.	N.d.	N.d.	N.d.	N.d.	N.d.	N.d.	N.d.	N.d.
Tb	N.d.	N.d.	0.190	0.362	1.420	0.364	0.730	N.d.	N.d.	N.d.	N.d.	N.d.	N.d.
Dy	3.950	4.040	N.d.	N.d.	N.d.	N.d.	N.d.	1.607	3.838	2.103	1.814	3.526	4.229
Ho	N.d.	N.d.	N.d.	N.d.	N.d.	N.d.	N.d.	N.d.	N.d.	N.d.	N.d.	N.d.	N.d.
Er	1.950	2.100	N.d.	N.d.	N.d.	N.d.	N.d.	0.857	2.499	1.208	1.081	2.140	2.630
Tm	N.d.	N.d.	N.d.	N.d.	N.d.	N.d.	N.d.	N.d.	N.d.	N.d.	N.d.	N.d.	N.d.
Yb	1.280	1.420	1.110	1.340	3.150	1.510	2.160	0.625	2.400	0.861	1.063	1.966	2.478
Lu	N.d.	N.d.	0.190	0.210	0.480	0.220	0.330	N.d.	N.d.	N.d.	N.d.	N.d.	N.d.
Total	75.9	104	N.d.	N.d.	N.d.	N.d.	N.d.	12.6	22.7	18.4	11.5	57.3	27.7
$(La/Yb)_n$	4.3	6.8	11.4	4.7	2.9	11.2	3.8	0.8	0.47	2.0	0.26	2.8	0.34

(*Continued*)

Table 5.20 Continued

	Provinces												
	Dzhilinda, Russia								Udokan, Russia				
	(Litasov, 1998), SIMS												
	D-24	D-133	D-55	D-63x	D-35	D-37	D-32	D-40	95/74-4	95/74-DU	95/74-42	95/74-42r	95/74-24
Element	*Peridotites*												
La	0.755	0.732	1.733	4.636	1.229	1.014	0.283	0.291	25.98	25.98	15.56	24.24	8.348
Ce	2.918	1.782	4.918	10.16	4.401	4.378	1.487	1.500	54.936	67.33	37.90	70.85	34.55
Pr	N.d.	N.d.	N.d.	N.d.	N.d.	N.d.	N.d.	N.d.	N.d.	N.d.	N.d.	N.d.	N.d.
Nd	3.902	1.865	2.988	4.263	4.565	4.139	3.041	3.249	22.99	37.19	23.86	49.07	28.44
Sm	1.756	0.727	0.723	0.743	1.773	2.042	1.583	1.657	3.791	7.359	4.770	10.82	7.409
Eu	0.659	0.256	0.232	0.280	0.757	0.677	0.636	0.671	1.158	1.987	1.565	3.003	2.046
Gd	N.d.	N.d.	N.d.	N.d.	N.d.	N.d.	N.d.	N.d.	N.d.	N.d.	N.d.	N.d.	N.d.
Tb	N.d.	N.d.	N.d.	N.d.	N.d.	N.d.	N.d.	N.d.	N.d.	N.d.	N.d.	N.d.	N.d.
Dy	3.903	0.996	1.155	1.257	3.824	3.325	3.982	3.912	2.313	3.661	2.917	7.414	3.959
Ho	N.d.	N.d.	N.d.	N.d.	N.d.	N.d.	N.d.	N.d.	N.d.	N.d.	N.d.	N.d.	N.d.
Er	2.455	0.661	0.927	0.824	2.402	2.418	2.587	2.472	1.242	1.504	1.403	3.102	1.587
Tm	N.d.	N.d.	N.d.	N.d.	N.d.	N.d.	N.d.	N.d.	N.d.	N.d.	N.d.	N.d.	N.d.
Yb	2.383	0.664	0.964	1.000	2.340	2.217	2.658	2.609	1.196	1.369	1.477	3.028	1.380
Lu	N.d.	N.d.	N.d.	N.d.	N.d.	N.d.	N.d.	N.d.	N.d.	N.d.	N.d.	N.d.	N.d.
Total	18.7	7.68	13.6	23.2	21.3	20.2	16.3	16.4	114	146	89.4	172	87.7
$(La/Yb)_n$	0.21	0.74	1.2	3.1	0.35	0.31	0.07	0.08	14.7	12.8	7.1	5.4	4.1

Table 5.21 Rare earth element composition of clinopyroxenes from lherzolites, and peridotites from massifs (ppm).

	Massifs											
	Horoman, Japan				Lizard, England			Balmuccia, Italy			Baldissero, Italy	
	(Frey *et al.*, 1991), RNAA				(Frey, 1969), NAA			(Ottonello *et al.*, 1984), RNAA				
	62131a	62130	62131b	62131c	90681d	90683d	90684d	B-3C	F-59b	F-61b	F-64	F-66
Element	*Lherzolites*											
La	0.890	0.580	1.280	0.720	0.018	0.007	0.088	0.237	0.113	0.102	N.d.	0.081
Ce	2.980	3.130	5.460	3.140	0.063	0.210	N.d.	2.100	2.410	7.990	1.690	2.670
Pr	N.d.	N.d.	N.d.	N.d.	0.016	0.126	0.095	N.d.	N.d.	N.d.	N.d.	N.d.
Nd	2.380	5.120	5.530	3.180	0.290	1.700	0.900	2.350	2.110	N.d.	1.590	2.540
Sm	1.090	2.330	2.560	1.440	0.430	1.320	0.970	0.919	0.864	0.729	0.822	1.220
Eu	0.350	0.900	0.790	0.490	0.191	0.645	0.388	0.414	0.363	0.332	0.407	0.538
Gd	N.d.	N.d.	N.d.	N.d.	1.230	2.800	2.100	N.d.	N.d.	N.d.	N.d.	N.d.
Tb	N.d.	N.d.	N.d.	N.d.	0.255	0.600	0.460	0.302	0.347	0.326	0.345	0.454
Dy	0.830	3.980	3.400	1.950	N.d.	N.d.	N.d.	N.d.	N.d.	N.d.	N.d.	N.d.
Ho	N.d.	N.d.	N.d.	N.d.	0.471	0.855	0.813	N.d.	N.d.	N.d.	N.d.	N.d.
Er	0.510	2.400	1.930	1.140	1.490	2.300	2.700	N.d.	N.d.	N.d.	N.d.	N.d.
Tm	N.d.	N.d.	N.d.	N.d.	0.220	0.350	0.400	N.d.	N.d.	N.d.	N.d.	N.d.
Yb	0.600	2.130	1.920	0.910	1.280	2.100	1.790	1.400	1.420	1.500	1.490	1.560
Lu	N.d.	N.d.	N.d.	N.d.	0.200	0.340	0.350	0.226	0.301	0.366	0.287	0.275
Total	9.63	20.6	22.9	13.0	6.15	13.4	11.1	N.d.	N.d.	N.d.	N.d.	N.d.
$(La/Yb)_n$	1.0	0.18	0.45	0.53	0.01	0.01	0.03	0.11	0.05	0.05	N.d.	0.04

(*Continued*)

Table 5.21 Continued

	Massifs										
	Otris, Greece	Freychinede, Fr.	Caussou, Fr.	Naransky, Mongolia, RNAA			Erdeny, Mongolia	Beriozovsky, Russia	Balmuccia, Italy		
	(Menzies, 1976)	(Bodinier *et al.*, 1988), RNAA		(Lesnov & Gora, 1998)		(Erkushev, 1985)	(Lesnov & Gora, 1998), RNAA		(Rivalenti *et al.*, 1995), SIMS		
	O2	73-1	CAU-2	272	705b	727b	1133v	154	BM5	BM7	M90-11B
Element	*Lherzolites*								*Peridotites*		
La	1.160	5.100	2.400	0.350	0.940	0.970	2.200	0.070	0.110	0.130	0.780
Ce	2.000	15.80	9.600	1.300	0.646	2.670	4.140	0.280	0.400	0.520	2.730
Pr	N.d.	N.d.	N.d.	N.d.	0.180	0.380	0.830	N.d.	N.d.	N.d.	N.d.
Nd	4.440	14.10	14.00	0.900	1.280	2.070	4.970	0.260	1.130	1.220	2.820
Sm	1.720	4.230	4.800	0.100	1.810	0.690	2.100	0.110	0.800	0.840	1.120
Eu	0.580	1.460	1.400	0.014	0.610	0.270	1.160	0.070	0.370	0.330	0.490
Gd	1.630	N.d.	N.d.	0.120	1.410	1.010	1.700	0.250	1.410	1.710	1.780
Tb	0.420	0.790	0.810	0.023	0.280	0.220	0.050	0.047	N.d.	N.d.	N.d.
Dy	N.d.	N.d.	N.d.	N.d.	1.220	1.420	0.330	N.d.	2.120	1.900	2.310
Ho	0.850	N.d.	N.d.	N.d.	0.260	0.280	0.073	N.d.	N.d.	N.d.	N.d.
Er	N.d.	N.d.	N.d.	N.d.	1.000	0.790	0.180	N.d.	1.260	1.270	1.470
Tm	N.d.	N.d.	N.d.	0.010	0.153	0.100	0.025	0.025	N.d.	N.d.	N.d.
Yb	1.820	1.760	1.530	0.100	1.140	0.690	0.500	0.190	1.340	1.280	1.500
Lu	0.310	0.280	0.210	0.013	0.128	0.097	0.120	0.028	N.d.	N.d.	N.d.
Total	14.9	N.d.	N.d.	N.d.	11.1	11.7	18.4	N.d.	8.94	9.20	15.0
$(La/Yb)_n$	0.43	2.0	1.1	2.4	0.56	0.95	3.0	0.25	0.06	0.07	0.35

	Massifs											
	Balmuccia, Italy											
	(Rivalenti *et al.*, 1995), SIMS											
	M90-11L	M90-12L	BM90-14	B90-15	B90-16	B90-20	B90-21	B90-22	B90-23	B90-25	B90-30	B90-36PD
Element	*Peridotites*											
La	0.240	0.100	1.900	0.240	0.520	0.410	0.020	0.250	1.890	0.040	0.310	0.540
Ce	0.670	0.320	5.020	1.000	1.790	1.370	0.310	0.790	5.570	0.290	0.930	2.000
Pr	N.d.	N.d.	N.d.	N.d.	N.d.	N.d.	N.d.	N.d.	N.d.	N.d.	N.d.	N.d.
Nd	1.330	1.230	3.770	1.840	2.160	1.580	1.570	1.530	4.290	1.300	1.020	2.440
Sm	0.980	0.880	1.430	1.100	0.950	0.720	1.040	1.020	1.050	0.790	0.410	0.990
Eu	0.460	0.420	0.560	0.470	0.410	0.230	0.450	0.440	0.400	0.340	0.180	0.450
Gd	1.950	1.600	2.270	1.910	1.640	1.000	2.050	1.670	1.230	1.740	0.680	1.600
Tb	N.d.	N.d.	N.d.	N.d.	N.d.	N.d.	N.d.	N.d.	N.d.	N.d.	N.d.	N.d.
Dy	2.750	2.100	2.990	2.530	2.270	1.180	2.560	2.310	1.420	1.970	0.860	2.050
Ho	N.d.	N.d.	N.d.	N.d.	N.d.	N.d.	N.d.	N.d.	N.d.	N.d.	N.d.	N.d.
Er	1.820	1.430	1.970	1.520	1.490	0.810	1.540	1.470	0.860	1.160	0.610	1.320
Tm	N.d.	N.d.	N.d.	N.d.	N.d.	N.d.	N.d.	N.d.	N.d.	N.d.	N.d.	N.d.
Yb	1.640	1.360	1.910	1.520	1.460	0.720	1.570	1.300	0.740	1.250	0.570	1.290
Lu	N.d.	N.d.	N.d.	N.d.	N.d.	N.d.	N.d.	N.d.	N.d.	N.d.	N.d.	N.d.
Total	11.8	9.44	21.8	12.1	12.7	8.02	11.1	10.8	17.5	8.88	5.57	12.7
$(La/Yb)_n$	0.10	0.05	0.67	0.11	0.24	0.38	0.01	0.13	1.7	0.02	0.37	0.28

(*Continued*)

Table 5.21 Continued

	Massifs										
	Balmuccia, Italy						Newfoundland, Canada				
	(Rivalenti *et al.*, 1995), SIMS						(Batanova *et al.*, 1998), IPMA				
	B90-41	B90-4PD	B90-5	B90-6	TFA	TS9	tv5D	TM 1062	TM 613	TM 922	TM 599
Element	*Peridotites*						*Lherzolites*				
La	0.100	0.100	0.100	0.030	1.380	0.580	0.009	0.006	0.003	0.003	0.040
Ce	0.260	0.370	0.380	0.140	5.230	1.770	0.010	0.030	0.010	0.005	0.110
Pr	N.d.	N.d.	N.d.	N.d.	N.d.	N.d.	N.d.	N.d.	N.d.	N.d.	N.d.
Nd	0.770	1.160	1.240	0.990	5.310	2.440	0.040	0.450	0.030	0.060	0.130
Sm	0.720	0.850	0.900	0.710	1.930	1.410	0.120	0.580	0.090	0.160	0.090
Eu	0.380	0.420	0.360	0.330	0.770	0.590	0.060	0.250	0.070	0.090	0.040
Gd	1.620	1.680	1.810	1.360	2.410	2.230	N.d.	N.d.	N.d.	N.d.	N.d.
Tb	N.d.	N.d.	N.d.	N.d.	N.d.	N.d.	N.d.	N.d.	N.d.	N.d.	N.d.
Dy	2.030	2.270	2.440	2.120	3.040	3.110	0.970	2.040	0.840	1.230	0.580
Ho	N.d.	N.d.	N.d.	N.d.	N.d.	N.d.	N.d.	N.d.	N.d.	N.d.	N.d.
Er	1.440	1.400	1.490	1.270	1.830	1.950	0.063	1.310	0.700	0.860	0.510
Tm	N.d.	N.d.	N.d.	N.d.	N.d.	N.d.	N.d.	N.d.	N.d.	N.d.	N.d.
Yb	1.330	1.380	1.500	1.310	1.870	1.950	0.710	1.350	0.720	0.880	0.550
Lu	N.d.	N.d.	N.d.	N.d.	N.d.	N.d.	N.d.	N.d.	N.d.	N.d.	N.d.
Total	8.65	9.63	10.2	8.26	N.d.	N.d.	N.d.	N.d.	N.d.	N.d.	N.d.
$(La/Yb)_n$	0.05	0.05	0.05	0.02	0.50	0.20	0.01	0.003	0.003	0.002	0.05

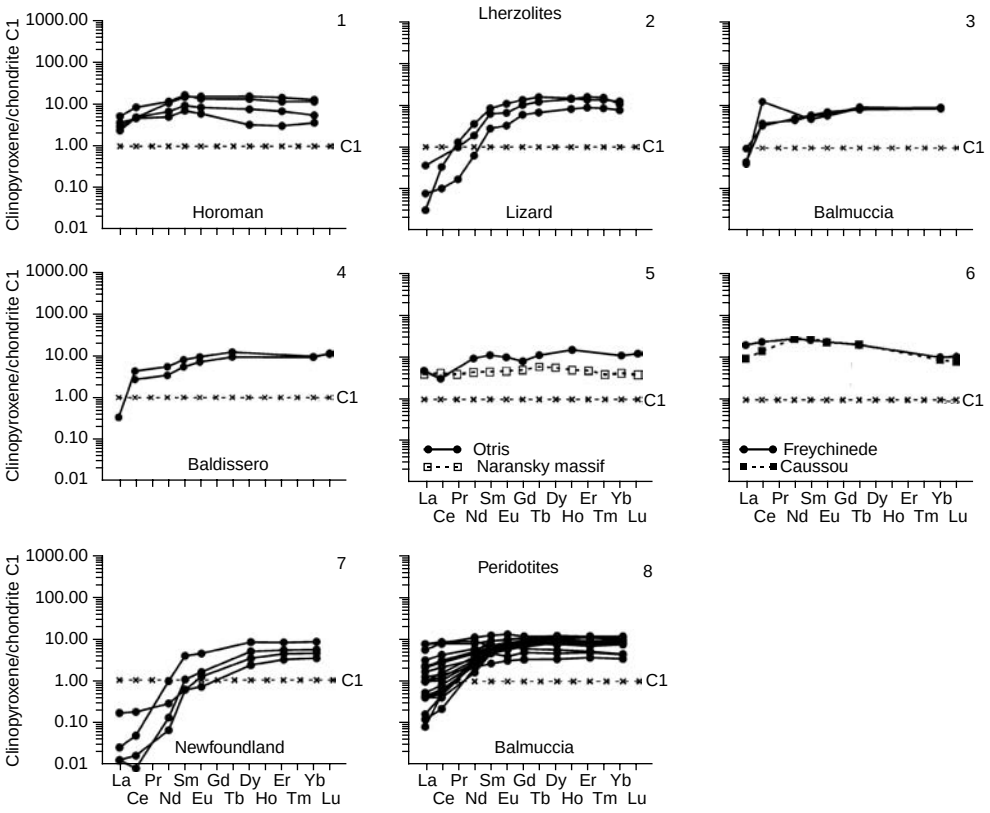

Figure 5.18 Chondrite-normalized REE composition patterns of clinopyroxenes from lherzolites and peridotites, represented in some massifs (data Table 5.21).

Harzburgites from massifs and xenoliths. Clinopyroxenes in these rocks are represented as a secondary phase. Their rare earth composition was studied in the Troodos, Horoman, and Newfoundland massifs and the provinces of Cordillera, Hannuoba, Vogelsberg, and Kerguelen and Madeira Islands (Table 5.22). The samples in xenoliths typically have a slightly increased level of REE accumulation compared to the samples of harzburgites from the massifs. The level of accumulation of heavy REE in clinopyroxenes from the Troodos and Newfoundland massifs is comparable with that in chondrite C1, and the level of light REE is far lower (~0.1 t. ch.), with respectively low values of the $(La/Yb)_n$ parameter (0.003–0.4). The contents of heavy REE in clinopyroxenes from the rocks of the Horoman massif are also comparable with their contents in chondrite C1, but these rocks are somewhat enriched with light REE, making them comparable with clinopyroxenes from harzburgite xenoliths. In the mineral from harzburgites that compose xenoliths in the provinces of Hannuoba, Vogelsberg, and Madeira Island, the level of accumulation of light REE is about 10 t. ch., and in some samples from the province of Kerguelen Island, it is much higher (~100 t. ch.), which suggests that they contain variable amounts of nonstructural impurities of these elements.

Table 5.22 Rare earth element composition of clinopyroxenes from harzburgites from massifs, and from deep xenoliths (ppm).

	Massifs (provinces)										
	Kerguelen islands, Indian ocean			Madeira islands		Hannuoba, Cin.	Vogelsberg, Germany	Troodos, Cyprus			
	(Mattielli *et al.*, 1996), ICP-MS			(Munha *et al.*, 1990), IPMA		(Song & Frey, 1989)	(Witt-Eickschen, 1993)	(Sobolev & Batanova, 1995), IPMA			
	G-92-509[a]	G-91-38[a]	G-91-42[a]	PM-3A1[a]	PM-7[a]	DM1-7H[a]	DH1182[a]	trd-101	trd-114	trd-116	trd-117
Element	*Harzburgites*										
La	16.40	1.800	4.550	1.730	1.380	6.610	2.570	0.030	0.090	0.040	0.010
Ce	47.60	2.100	4.710	6.050	5.050	12.23	N.d.	0.030	0.110	0.070	0.020
Pr	N.d.	N.d.	N.d.	N.d.	N.d.	1.920	N.d.	N.d.	N.d.	N.d.	N.d.
Nd	25.30	0.450	0.890	6.210	5.810	9.690	5.10	0.010	0.030	0.010	0.020
Sm	5.330	0.150	0.430	2.590	2.480	2.190	1.720	N.d.	N.d.	N.d.	N.d.
Eu	1.650	0.030	0.140	0.520	0.450	0.690	0.770	0.010	0.010	0.010	0.010
Gd	N.d.	N.d.	N.d.	2.400	2.310	N.d.	N.d.	N.d.	N.d.	N.d.	N.d.
Tb	N.d.	N.d.	N.d.	N.d.	N.d.	N.d.	N.d.	N.d.	N.d.	N.d.	N.d.
Dy	2.490	0.110	0.570	1.730	2.070	1.360	N.d.	0.050	0.060	0.040	0.080
Ho	N.d.	N.d.	N.d.	N.d.	N.d.	N.d.	N.d.	N.d.	N.d.	N.d.	N.d.
Er	0.950	0.180	0.410	1.020	1.040	1.020	N.d.	0.070	0.050	0.090	0.130
Tm	N.d.	N.d.	N.d.	N.d.	N.d.	N.d.	N.d.	N.d.	N.d.	N.d.	N.d.
Yb	0.980	0.190	0.500	0.900	1.120	N.d.	1.510	0.100	0.110	0.150	0.220
Lu	N.d.	N.d.	N.d.	N.d.	N.d.	N.d.	0.260	N.d.	N.d.	N.d.	N.d.
Total	101	5.01	12.2	23.2	21.7	35.7	N.d.	0.30	0.46	0.41	0.49
$(La/Yb)_n$	11.30	6.39	6.14	1.30	0.83	N.d.	1.15	0.20	0.55	0.18	0.03

	Massifs (provinces)										
	Troodos, Cyprus					Horoman, Japan		Newfoundland, Canada			
	(Sobolev & Batanova, 1995), IPMA					(Frey *et al.*, 1991), RNAA		(Batanova *et al.*, 1998), IPMA			
	TV-19	TV-21	TV-25	TV-34	TV-7	62127	62128	TM 827	TM 1141	TM 1274	TM 1232
Element	*Harzburgites*										
La	0.060	0.050	0.020	0.080	0.050	2.410	0.800	0.003	0.160	0.007	0.010
Ce	0.120	0.080	0.040	0.100	0.070	7.280	2.100	0.010	0.380	0.020	0.030
Pr	N.d.	N.d.	N.d.	N.d.	N.d.	N.d.	N.d.	N.d.	N.d.	N.d.	N.d.
Nd	0.020	0.050	0.040	0.040	0.060	4.150	1.450	0.030	0.220	0.015	0.020
Sm	0.010	0.060	0.070	0.030	0.010	1.050	0.385	0.070	0.090	0.015	0.020
Eu	0.010	0.060	0.060	0.030	0.010	0.330	0.150	0.040	0.030	0.006	0.007
Gd	N.d.	N.d.	N.d.	N.d.	N.d.	N.d.	N.d.	N.d.	N.d.	N.d.	N.d.
Tb	N.d.	N.d.	N.d.	N.d.	N.d.	N.d.	N.d.	N.d.	N.d.	N.d.	N.d.
Dy	0.130	1.020	0.530	0.360	0.090	0.650	0.310	0.650	0.340	0.120	0.120
Ho	N.d.	N.d.	N.d.	N.d.	N.d.	N.d.	N.d.	N.d.	N.d.	N.d.	N.d.
Er	0.150	0.600	0.350	0.320	0.140	0.310	0.230	0.540	0.300	0.180	0.011
Tm	N.d.	N.d.	N.d.	N.d.	N.d.	N.d.	N.d.	N.d.	N.d.	N.d.	N.d.
Yb	0.230	0.500	0.350	0.370	0.220	0.370	0.300	0.580	0.300	0.280	0.017
Lu	N.d.	N.d.	N.d.	N.d.	N.d.	N.d.	N.d.	N.d.	N.d.	N.d.	N.d.
Total	0.73	2.42	1.46	1.33	0.65	16.6	5.73	1.92	1.82	0.643	0.235
$(La/Yb)_n$	0.18	0.07	0.04	0.15	0.15	4.40	1.80	0.003	0.36	0.02	0.40

(*Continued*)

Table 5.22 Continued

	Massifs (provinces)									
	Newfoundland, Canada		Miyamori, Japan						Hayachine, Japan	
	(Batanova *et al.*, 1998), IPMA		(Ozawa & Shimizu, 1995)							
	TM 1454	TM 1531	MY-1	MY-2	MY-3	MY-4	MY-8	MY-9	HY-1	HY-2
Element	*Harzburgites*									
La	0.020	0.017	1.8	1.6	1.5	2.4	0.23	0.17	0.06	0.16
Ce	0.050	0.070	5.2	6.5	6.2	7.9	0.68	0.46	0.35	0.47
Pr	N.d.	N.d.	N.d.	N.d.	N.d.	N.d.	N.d.	N.d.	N.d.	N.d.
Nd	0.140	0.060	4.8	6.1	6.4	6.9	0.38	0.20	1.5	0.81
Sm	0.130	0.070	1.6	2.1	2.5	1.8	0.11	0.06	1.3	0.69
Eu	0.050	0.035	0.45	0.60	0.74	0.58	0.04	0.02	0.55	0.24
Gd	N.d.	N.d.	N.d.	N.d.	N.d.	N.d.	N.d.	N.d.	N.d.	N.d.
Tb	N.d.	N.d.	N.d.	N.d.	N.d.	N.d.	N.d.	N.d.	N.d.	N.d.
Dy	0.630	0.380	0.59	0.83	1.1	0.65	0.32	0.22	3.0	1.4
Ho	N.d.	N.d.	N.d.	N.d.	N.d.	N.d.	N.d.	N.d.	N.d.	N.d.
Er	0.490	0.230	0.36	0.40	0.41	0.51	0.18	0.21	1.9	0.79
Tm	N.d.	N.d.	N.d.	N.d.	N.d.	N.d.	N.d.	N.d.	N.d.	N.d.
Yb	0.530	0.210	0.23	0.24	0.35	0.30	0.24	0.27	1.9	0.83
Lu	N.d.	N.d.	N.d.	N.d.	N.d.	N.d.	N.d.	N.d.	N.d.	N.d.
Total	2.04	1.07	N.d.	N.d.	N.d.	N.d.	N.d.	N.d.	N.d.	N.d.
$(La/Yb)_n$	0.025	0.055	5.29	4.51	2.89	5.39	0.02	0.13	0.65	0.42

[a] Samples from deep xenoliths.

Dunites, wehrlites, and plagioclase-bearing wehrlites from massifs and deep xenoliths. These paragenetic types of clinopyroxenes were studied in samples from the Troodos, Voykar-Syn'insky, and Gal'moenansky massifs, and from some xenoliths (Table 5.23, Fig. 5.19). In the mineral from dunites of the Troodos massif, the contents of heavy REE are similar to those in chondrite C1, whereas the concentrations of light REE are lower. Depletion of light elements is also observed in samples from wehrlites and plagioclase-bearing wehrlites in the Voykar-Syn'insky massif. In the mineral from wehrlites of the Dovyrensky and Kytlymsky massifs and from xenoliths of Madeira Island province, the level of accumulation of all REE is an order of magnitude higher than that in the previous samples from dunites, which are virtually not fractionated.

Websterites from some massifs and deep xenoliths. Data on these clinopyroxenes were obtained when studying the Balmuccia, Beni Bousera, Naransky, Beriozovsky, and some other massifs, as well as several xenoliths in basalts (Table 5.24). In each of these objects, clinopyroxenes are characterized by approximately identical ratios of some REE, which is suggested by the similar configuration of their REE patterns with a gentle positive slope. In the absolute content of elements, these samples differ from each other (Fig. 5.20). Within the collection of the most thoroughly studied clinopyroxenes from the Balmuccia massif, the levels of accumulation of some elements vary from 3 to 30 t. ch. Such considerable variation in the level of accumulation of REE in websterites, to our opinion, is related to the differences in quantitative ratios of the substance supplied from the mafic melt and ultramafic restite, the metasomatic interaction of which resulted in these rocks. In the mineral from websterites of the Naransky and Beriozovsky massifs, the level of accumulation of middle and heavy REE is comparable to that in chondrite C1, while for light REE, it varies considerably. In the Stillwater and Lherz massifs, the contents of REE in clinopyroxenes of these rocks are at a level of 10 t. ch., with a minor depletion of La and Ce. The mineral from garnet websterites of the Beni Bouchera massif revealed wide variations of Yb and Lu contents, compared to light REE, and clinopyroxenes from websterites xenoliths of the Vitim province are considerably enriched with light REE relative to heavy REE (Fig. 5.20, 6).

Clinopyroxenites, including garnet-bearing, from some massifs and deep xenoliths. Clinopyroxenes from these rocks were studied in samples from the Beni Bouchera and Zabargad Island massifs, and in fewer samples from the Gal'moenansky and Kytlymsky massifs (Table 5.25). Clinopyroxenes from pyroxenites of Zabargad Island have a unique REE composition. Some clinopyroxenites contain drastically subordinate amounts of orthopyroxene, which REE composition was discussed above (see Chapter 5.2). In spite of the presence of orthopyroxene, these rocks are not referred to as websterites, as the orthopyroxene in them is regarded as a later phase formed during the replacement of garnet grains (Vannucci *et al.*, 1993b). Clinopyroxenes under study are moderately enriched with light REE (2–10 t. ch.) but are extremely rich in heavy REE, which level of accumulation at times reaches 300 t. ch. (Fig. 5.21, 4).

The REE patterns of clinopyroxenes from garnet pyroxenites from the Beni Bouchera massif show a uniform distribution of both light and heavy REE with a rather stable content of middle elements (Fig. 5.21, 3). In garnet pyroxenites from the Lherz massif, the level of accumulation of middle REE is higher than that of light and heavy REE (Fig. 5.21, 2). The same REE distribution was found in the mineral from olivine and olivine-free clinopyroxenites from the Gal'moenansky and Kytlymsky massifs (Fig. 5.21, 7, 8). Clinopyroxene grains from plagioclase-olivine clinopyroxenes of

Table 5.23 Rare earth element composition of clinopyroxenes from dunites, wehrlites, and plagioclase-bearing wehrlites from massifs, and from deep xenoliths (ppm).

	Massifs (provinces)													
	Troodos, Cyprus		Gal'moenansky, Rus.	Voykar-Sin'insky, Russia	Dovirensky, Russia			Spitsbergen	Madeira islands		Kytlymsky, Russia	Voykar-Sin'insky, Russia		
	(Batanova *et al.*, 1996), IPMA		(Pertsev, 2004)		(Author's data), RNAA			(Shubina *et al.*, 1997), INAA	(Munha *et al.*, 1990), IPMA		(Pertsev, 2004)			
	TV-111a	TV-111b	G14-5	V804-1	L-26	L-36	L-62	11si[a]	PM-1[a]	PM-8B[a]	KT-19-2	V803-11	V591-4	V803-3
Element	*Dunites*				*Wehrlites*								*Plag.-bearing wehrlites*	
La	0.020	0.010	0.390	0.049	9.740	8.130	6.800	16.50	1.41	1.280	2.600	0.019	0.110	0.016
Ce	0.070	0.030	1.200	0.310	18.82	12.20	10.10	40.20	4.64	4.710	8.000	0.064	0.530	0.100
Pr	N.d.	N.d.	N.d.	N.d.	N.d.	N.d.	N.d.	N.d.	N.d.	N.d.	N.d.	N.d.	N.d.	N.d.
Nd	0.140	0.090	1.300	0.790	14.73	11.60	7.400	N.d.	5.140	4.990	8.300	0.100	1.100	0.140
Sm	0.100	0.080	0.390	0.490	3.760	2.300	2.100	4.090	2.350	2.010	2.400	0.100	0.670	0.100
Eu	0.060	0.030	0.140	0.240	1.240	0.700	0.610	1.370	0.450	0.470	0.800	0.054	0.280	0.062
Gd	N.d.	N.d.	N.d.	N.d.	5.070	3.000	3.200	N.d.	2.290	2.020	N.d.	N.d.	N.d.	N.d.
Tb	N.d.	N.d.	N.d.	N.d.	0.980	0.550	0.620	0.023	N.d.	N.d.	N.d.	N.d.	N.d.	N.d.
Dy	0.490	0.230	0.460	1.300	N.d.	N.d.	N.d.	N.d.	2.120	2.060	2.500	0.300	1.400	0.340
Ho	N.d.	N.d.	N.d.	N.d.	N.d.	N.d.	N.d.	N.d.	N.d.	N.d.	N.d.	N.d.	N.d.	N.d.
Er	0.420	0.190	0.380	0.800	N.d.	N.d.	N.d.	N.d.	0.980	0.860	1.200	0.210	1.000	0.280
Tm	N.d.	N.d.	N.d.	N.d.	0.470	0.300	0.250	N.d.	N.d.	N.d.	N.d.	N.d.	N.d.	N.d.
Yb	0.360	0.230	0.280	0.760	2.780	1.800	1.800	1.770	1.040	1.070	1.100	0.190	0.910	0.250
Lu	N.d.	N.d.	N.d.	N.d.	0.410	0.240	0.280	0.280	N.d.	N.d.	N.d.	N.d.	N.d.	N.d.
Total	1.66	0.89	4.54	4.74	N.d.	N.d.	N.d.	N.d.	20.4	19.4	N.d.	N.d.	N.d.	N.d.
$(La/Yb)_n$	0.04	0.03	0.94	0.04	2.36	3.05	2.55	6.29	0.92	0.81	1.60	0.07	0.08	0.04

[a] Samples from deep xenoliths.

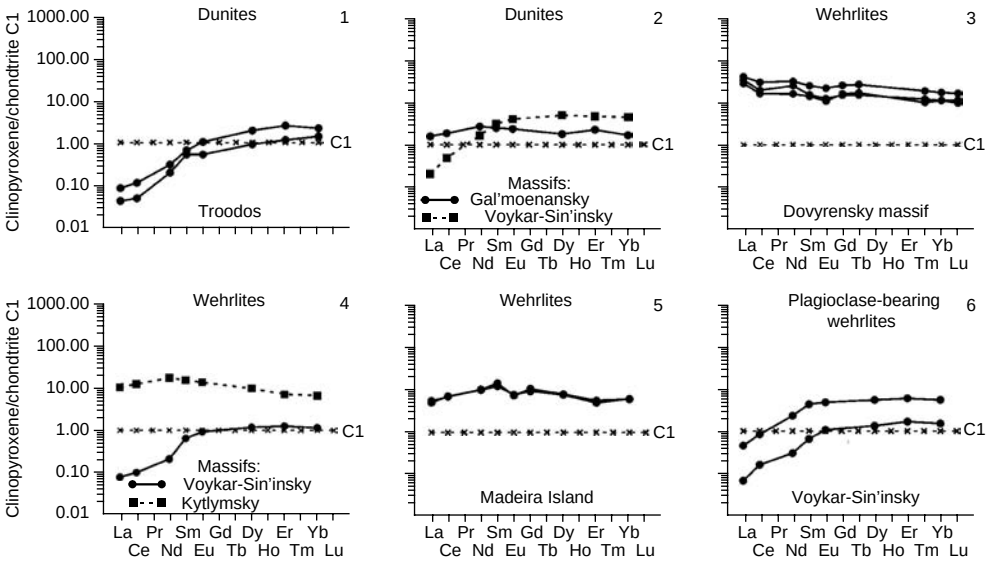

Figure 5.19 Chondrite-normalized REE patterns for clinopyroxenes from dunites, wehrlites, and plagioclase-bearing wehrlites, represented in some massifs and deep xenoliths (data Table 5.23).

the Gal'moenansky massif exhibit zonal REE distribution; in outer zones, the content of all REE is 3–5 times higher than in the cores (Pertsev, 2004). At the same time, the relationships between the contents of some elements in the inner and outer zones do not change, which is suggested by the same configuration of their patterns (Fig. 5.21, 12). It is worth noting that all clinopyroxenes from clinopyroxenites in xenoliths from basalts of Vitim province are characterized by a rather nonuniform distribution of both light and heavy REE in them (Fig. 5.21, 5).

Olivine gabbros, gabbro-norites, and picrites. The REE composition of clinopyroxenes of these rocks were studied in samples from the Troodos and Kytlymsky massifs, and in fewer samples from the Samail, Gal'moenansky, and Riparbello massifs (Table 5.26). In the rocks of each massif, clinopyroxenes demonstrate rather stable relationships between some elements, which are inferred from the same configuration of their REE patterns (Fig. 5.22). Samples from the Troodos massif are, compared to others, depleted of all REE, particularly light REE. They have low $(La/Sm)_n$ values, and in the field of middle and heavy elements their patterns have a "flat" shape. Compared to others, all clinopyroxenes are considerably enriched with light REE, but in content of middle and heavy elements, they are comparable to the samples from other massifs. As in the case with the mineral from clinopyroxenites, Pertsev (2004) established the zonal distribution of REE in clinopyroxenes from gabbros of the Gal'moenansky massif, which appears as a systematic increase in the content of elements from inner zones toward the periphery.

Gabbro-norites. Despite the wide occurrence of these mafic rocks, clinopyroxenes in them are poorly studied with respect to REE distribution (Table 5.27). Judging by the

Table 5.24 Rare earth element composition of clinopyroxenes from websterites from massifs and from deep xenoliths (ppm).

	Massifs (provinces)												
	Beriozovsky, Russia		Yuzhno-Shmidtovsky	Naransky, Mongolia					Frachinede, France		Stillwater, USA		Balmuccia, Italy
	(Lesnov & Gora, 1998), RNAA								(Bodinier *et al.*, 1987), RNAA		(Papike *et al.*, 1995)		(Rivalenti *et al.*, 1995)
	134	137	162	266	N-8-310	N-311	N-4-5	N-6-88a	70-357	72-226	428	432	90-11CR
Element	*Websterites*												
La	0.110	0.110	0.062	0.033	0.500	0.200	0.760	0.360	0.120	1.520	1.900	0.554	0.390
Ce	0.360	0.500	0.130	0.170	0.990	0.350	1.390	0.710	0.450	2.800	7.100	2.480	3.420
Pr	N.d.	N.d.	N.d.	N.d.	N.d.	N.d.	N.d.	N.d.	N.d.	N.d.	N.d.	N.d.	N.d.
Nd	0.290	0.590	0.055	0.140	0.650	0.210	0.910	0.400	1.260	2.300	5.700	2.450	3.670
Sm	0.100	0.260	0.008	0.066	0.400	0.110	0.260	0.170	1.110	1.630	2.200	0.856	1.190
Eu	0.070	0.096	0.011	0.073	0.100	0.056	0.053	0.098	0.510	0.770	0.600	0.317	0.470
Gd	0.300	0.340	0.052	0.230	0.430	0.220	0.280	0.260	N.d.	N.d.	N.d.	N.d.	1.340
Tb	0.058	0.1000	0.010	0.040	0.1100	0.048	0.060	0.052	0.210	0.630	N.d.	N.d.	N.d.
Dy	N.d.	N.d.	N.d.	N.d.	N.d.	N.d.	N.d.	N.d.	N.d.	N.d.	3.400	1.600	1.470
Ho	N.d.	N.d.	N.d.	N.d.	N.d.	N.d.	N.d.	N.d.	N.d.	N.d.	N.d.	N.d.	N.d.
Er	N.d.	N.d.	N.d.	N.d.	N.d.	N.d.	N.d.	N.d.	N.d.	N.d.	1.800	0.835	0.830
Tm	0.045	0.120	0.009	0.026	0.056	0.033	0.047	0.037	N.d.	N.d.	N.d.	N.d.	N.d.
Yb	0.330	0.830	0.064	0.150	0.330	0.210	0.340	0.230	0.130	2.700	1.500	0.791	0.780
Lu	0.046	0.140	0.011	0.018	0.055	0.029	0.053	0.040	0.017	0.560	N.d.	N.d.	N.d.
Total	1.71	3.09	0.41	0.95	3.62	1.47	4.15	2.36	3.81	12.9	24.2	9.88	13.6
$(La/Yb)_n$	0.22	0.09	0.65	0.15	1.02	0.64	1.51	1.06	0.62	0.38	0.85	0.47	0.34

	Massifs (provinces)												
	Balmuccia, Italy												Vitim, Russia
	(Rivalenti *et al.*, 1995)												(Andre & Ashchepkov, 1996)
	BM90-13	BM90-17	BM90-19C	BM90-36CR	BM90-37	BM90-39	BM90-7	MO383	TS2	TS32A	TS4	TS5	302-202 (spinel)[a]
Element	*Websterites*												
La	0.390	1.650	0.600	0.630	N.d.	1.640	2.300	2.490	0.510	1.010	0.890	2.800	3.590
Ce	3.420	5.980	1.510	1.960	2.310	7.070	10.40	8.050	3.030	3.700	4.760	13.470	12.66
Pr	N.d.	N.d.	N.d.	N.d.	N.d.	N.d.	N.d.	N.d.	N.d.	N.d.	N.d.	N.d.	2.260
Nd	3.670	6.370	1.970	2.910	2.710	7.510	11.03	8.340	5.200	5.010	5.290	16.140	12.26
Sm	1.190	2.710	0.820	1.020	1.020	2.470	3.850	2.720	2.470	1.850	1.740	5.660	3.530
Eu	0.470	0.790	0.320	0.370	0.440	0.920	1.340	0.980	1.060	0.780	0.560	2.330	1.270
Gd	1.340	4.380	1.030	1.220	1.320	3.020	4.670	3.280	3.720	2.770	1.710	7.220	3.790
Tb	N.d.	N.d.	N.d.	N.d.	N.d.	N.d.	N.d.	N.d.	N.d.	N.d.	N.d.	N.d.	N.d.
Dy	1.470	6.390	1.230	1.270	1.620	3.310	4.730	3.260	4.270	3.440	1.580	8.320	2.870
Ho	N.d.	N.d.	N.d.	N.d.	N.d.	N.d.	N.d.	N.d.	N.d.	N.d.	N.d.	N.d.	0.477
Er	0.830	4.020	0.710	0.750	0.870	1.830	2.470	1.930	2.220	2.230	0.810	4.710	1.060
Tm	N.d.	N.d.	N.d.	N.d.	N.d.	N.d.	N.d.	N.d.	N.d.	N.d.	N.d.	N.d.	N.d.
Yb	0.780	3.870	0.730	0.740	0.940	1.680	2.280	1.760	2.070	1.880	0.910	4.530	0.704
Lu	N.d.	N.d.	N.d.	N.d.	N.d.	N.d.	N.d.	N.d.	N.d.	N.d.	N.d.	N.d.	0.091
Total	13.6	36.2	8.92	10.9	11.2	29.5	43.1	32.8	24.6	22.7	18.3	65.2	44.6
$(La/Yb)_n$	0.34	0.29	0.55	0.57	N.d.	0.66	0.68	0.95	0.17	0.36	0.66	0.42	3.44

(*Continued*)

Table 5.24 Continued

	Massifs (provinces)									
	Vitim, Russia	Carolina, USA	Lherz, France		Beni Bousera, Morocco					Frachinede, France
	(Andre & Ashchepkov, 1996)	(Philpotts *et al.*, 1972)	(Bodinier *et al.*, 1987), RNAA		(Pearson *et al.*, 1993), IDMS					(Bodinier *et al.*, 1987)
	315-252[a]	174[a]	70-379b	70-379d	GP101a	GP132(1)	GP188	GP236	GP30	70-385c
Element	*Websterites*		*Garnet websrerites*							
La	1.790	N.d.	1.500	0.210	2.171	1.803	1.158	0.629	1.085	0.480
Ce	5.870	0.376	4.800	1.010	3.135	4.006	3.665	2.400	3.288	2.030
Pr	1.020	N.d.	N.d.	N.d.	N.d.	N.d.	N.d.	N.d.	N.d.	N.d.
Nd	5.240	0.436	4.900	3.800	4.251	2.247	3.209	2.621	3.984	3.200
Sm	1.600	0.168	2.020	1.660	1.256	0.867	1.062	0.907	1.705	1.530
Eu	0.610	0.063	0.750	0.550	0.330	0.455	0.288	0.349	0.760	0.620
Gd	1.730	N.d.	N.d.	N.d.	N.d.	1.572	0.993	1.235	N.d.	N.d.
Tb	N.d.	N.d.	0.800	0.570	N.d.	N.d.	N.d.	N.d.	N.d.	0.500
Dy	1.100	0.309	N.d.	N.d.	0.962	1.920	0.979	N.d.	N.d.	N.d.
Ho	0.183	N.d.	N.d.	N.d.	N.d.	N.d.	N.d.	N.d.	N.d.	N.d.
Er	0.351	0.173	N.d.	N.d.	0.575	1.280	0.588	N.d.	N.d.	N.d.
Tm	N.d.	N.d.	N.d.	N.d.	N.d.	N.d.	N.d.	N.d.	N.d.	N.d.
Yb	0.192	0.186	2.170	1.270	0.500	1.108	0.504	0.299	2.529	1.420
Lu	0.023	N.d.	0.340	0.200	N.d.	N.d.	N.d.	N.d.	N.d.	0.210
Total	19.7	N.d.	N.d.	N.d.	13.2	15.3	12.5	N.d.	N.d.	N.d.
$(La/Yb)_n$	6.29	N.d.	0.47	0.11	2.93	1.10	1.55	1.42	0.29	0.23

[a] Samples from deep xenoliths.

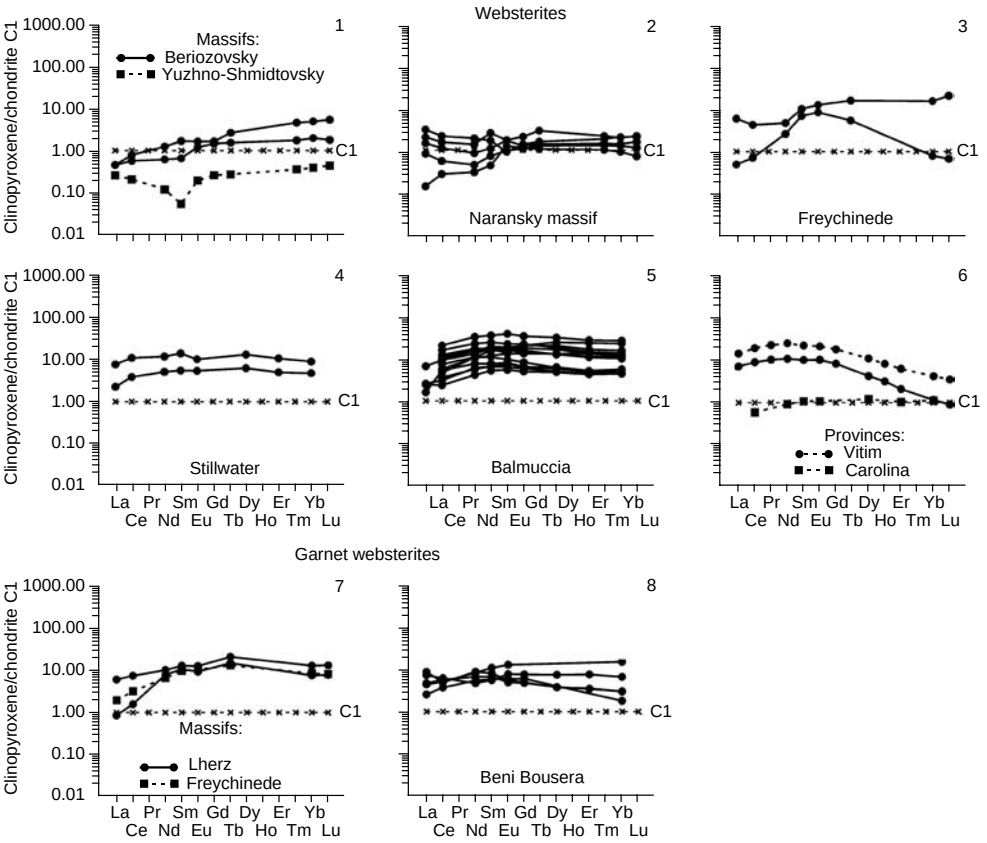

Figure 5.20 Chondrite-normalized REE patterns for clinopyroxenes from websterites, represented in some massifs and deep xenoliths (data Table 5.24).

available data, clinopyroxene from gabbro-norites in mafic–ultramafic massifs from ophiolitic associations (Karaginsky, Valizhgensky, Kuyul'sky, Beriozovsky, Sheltingsky, Naransky, Voykar-Syn'insky, and others) are characterized by lower REE contents compared to the samples from the massifs unrelated to ophiolitic associations (Rybinsky, Nizhnederbinsky, Shikotansky, Ostiurensky) (Lesnov & Gora, 1998; Lesnov, 2001c). The REE patterns of most studied clinopyroxenes from gabbro-norites have a gentle positive slope (Fig. 5.23, 1–9).The exception is the samples from the Voykar-Syn'insky massif, which have a steeper positive slope of patterns owing to a significant depletion of light REE (Fig. 5.23, 10). At times, patterns of clinopyroxenes from gabbro-norites exhibit positive and negative Eu anomalies of low intensity (Fig. 5.23, 2, 4, 7). The rather low level of REE accumulation in clinopyroxenes from gabbro-norites in the massifs that form ophiolitic associations can be due to the higher level of partial melting of mantle sources during generation of their parental melts or to preliminary depletion of these sources.

Table 5.25 Rare earth element composition of clinopyroxenes from pyroxenites massifs, and deep xenoliths (ppm).

	Massifs (provinces)											
	Vitim, Russia		Lherz, France		Beni Bousera, Morocco							
	(Andre & Ashchepkov, 1996), ICP-MS		(Bodinier *et al.*, 1988), RNAA		(Pearson *et al.*, 1993), IDMS							
	315-302[a]	315-305[a]	70-291	70-358	GP139	GP194m	GP33	GP37	GP87b	GP87m	GP147	GP81
Element	*Garnet pyroxenites*											
La	1.870	1.960	0.100	0.510	0.014	0.237	2.290	0.143	0.953	0.451	0.015	0.018
Ce	6.200	4.640	0.510	2.260	0.126	0.937	9.526	0.788	3.693	1.773	0.085	0.073
Pr	1.090	0.680	N.d.	N.d.	N.d.	N.d.	N.d.	N.d.	N.d.	N.d.	N.d.	N.d.
Nd	5.900	3.500	N.d.	3.100	1.199	1.586	9.439	2.537	4.726	2.535	0.411	0.698
Sm	1.560	1.230	0.270	1.030	2.494	0.793	2.828	1.580	1.819	1.120	0.374	1.066
Eu	0.560	0.450	N.d.	0.370	0.521	0.308	0.948	0.643	0.680	0.447	0.159	0.422
Gd	1.640	1.710	N.d.	N.d.	2.963	0.618	2.840	1.963	1.899	1.323	0.951	1.833
Tb	N.d.	N.d.	0.043	0.150	N.d.	N.d.	N.d.	N.d.	N.d.	N.d.	N.d.	N.d.
Dy	0.910	1.150	N.d.	N.d.	2.974	N.d.	2.810	1.139	N.d.	0.856	0.378	2.421
Ho	0.136	1.171	N.d.	N.d.	N.d.	N.d.	N.d.	N.d.	N.d.	N.d.	N.d.	N.d.
Er	0.253	0.323	N.d.	N.d.	1.146	0.333	1.510	0.273	0.430	0.234	0.810	1.191
Tm	N.d.	N.d.	N.d.	N.d.	N.d.	N.d.	N.d.	N.d.	N.d.	N.d.	N.d.	N.d.
Yb	0.139	0.178	0.043	0.190	0.657	0.105	1.289	0.110	0.216	0.108	0.680	0.859
Lu	0.017	0.021	0.004	0.026	N.d.	N.d.	N.d.	N.d.	N.d.	N.d.	N.d.	N.d.
Total	20.3	17.0	N.d.	N.d.	12.1	N.d.	33.5	9.18	N.d.	8.85	3.86	8.58
$(La/Yb)_n$	9.08	7.43	1.57	1.81	0.014	1.52	1.20	0.88	2.98	2.82	0.02	0.014

	Massifs (provinces)											
	Beni Bousera, Morocco	Zabargad Island, Red Sea										
	(Pearson *et al.*, 1993), IDMS	(Vannucci *et al.*, 1993a), IPMA										
	PHN5730	2096\7\1	2036B\3c	2036B\3r	2036Bc	2036Br	2036C1c	2036C\17g	2036C\2c	2036C\2r	2036C\3\r	2036C4c
Element	*Pyroxenites*											
La	0.016	N.d.	N.d.	N.d.	N.d.	N.d.	N.d.	N.d.	N.d.	N.d.	N.d.	N.d.
Ce	0.017	3.380	7.000	5.700	6.200	5.630	5.340	5.450	4.800	4.800	4.050	5.410
Pr	N.d.	N.d.	N.d.	N.d.	N.d.	N.d.	N.d.	N.d.	N.d.	N.d.	N.d.	N.d.
Nd	0.214	3.740	10.85	11.14	9.310	11.20	7.490	6.840	5.450	6.380	7.450	10.26
Sm	0.544	2.020	4.070	4.900	3.600	4.730	3.670	3.040	2.780	3.150	4.330	5.83
Eu	0.226	0.890	1.770	1.770	1.740	1.790	1.200	1.220	1.080	1.140	1.170	1.750
Gd	2.596	N.d.	N.d.	N.d.	N.d.	N.d.	N.d.	6.120	N.d.	N.d.	N.d.	N.d.
Tb	N.d.	N.d.	N.d.	N.d.	N.d.	N.d.	N.d.	N.d.	N.d.	N.d.	N.d.	N.d.
Dy	8.270	4.520	24.52	36.94	25.68	34.91	12.43	9.800	11.03	14.40	21.51	27.07
Ho	N.d.	N.d.	N.d.	N.d.	N.d.	N.d.	N.d.	N.d.	N.d.	N.d.	N.d.	N.d.
Er	5.960	2.660	25.53	34.73	26.13	32.09	12.71	8.830	12.59	14.65	21.96	27.81
Tm	N.d.	N.d.	N.d.	N.d.	N.d.	N.d.	N.d.	N.d.	N.d.	N.d.	N.d.	N.d.
Yb	5.080	3.000	37.14	42.74	36.68	38.07	15.36	11.60	16.86	18.41	27.99	35.17
Lu	N.d.	N.d.	N.d.	N.d.	N.d.	N.d.	N.d.	N.d.	N.d.	N.d.	N.d.	N.d.
Total	22.9	20.2	111	138	109	128	58.2	52.9	54.9	62.9	88.5	113
$(La/Yb)_n$	0.002	N.d.	N.d.	N.d.	N.d.	N.d.	N.d.	N.d.	N.d.	N.d.	N.d.	N.d.

(*Continued*)

Table 5.25 Continued

	Massifs (provinces)										
	Zabargad Island, Red Sea										
	(Vannucci *et al.*, 1993a), IPMA										
	2036C7g	2096	2096\7\r	2096\8i	2145\10c	2145\12\c	2145B6gc	2145B\6gr	2146\1\i	2146\3\c	2146\7\c
Element	*Pyroxenites*										
La	N.d.	N.d.	N.d.	N.d.	N.d.	N.d.	N.d.	N.d.	N.d.	N.d.	N.d.
Ce	1.980	2.380	3.660	4.080	2.350	2.570	2.430	2.710	2.950	1.760	1.990
Pr	N.d.	N.d.	N.d.	N.d.	N.d.	N.d.	N.d.	N.d.	N.d.	N.d.	N.d.
Nd	3.150	2.930	4.770	4.610	4.280	5.180	3.990	5.420	3.810	3.740	3.240
Sm	1.210	1.350	2.080	1.940	2.770	2.860	1.630	2.920	1.610	1.980	1.630
Eu	0.460	0.690	0.980	0.950	0.930	1.130	0.950	1.200	0.510	0.810	0.690
Gd	N.d.	N.d.	N.d.	N.d.	N.d.	N.d.	N.d.	N.d.	N.d.	N.d.	N.d.
Tb	N.d.	N.d.	N.d.	N.d.	N.d.	N.d.	N.d.	N.d.	N.d.	N.d.	N.d.
Dy	6.270	3.340	4.360	4.730	13.04	12.95	6.740	9.740	3.640	4.510	3.940
Ho	N.d.	N.d.	N.d.	N.d.	N.d.	N.d.	N.d.	N.d.	N.d.	N.d.	N.d.
Er		2.110	2.870	3.300	9.930	9.670	5.620	7.390	2.230	2.470	2.290
Tm	N.d.	N.d.	N.d.	N.d.	N.d.	N.d.	N.d.	N.d.	N.d.	N.d.	N.d.
Yb	5.290	2.430	2.740	3.260	11.18	12.24	6.320	7.840	2.200	2.640	2.570
Lu	N.d.	N.d.	N.d.	N.d.	N.d.	N.d.	N.d.	N.d.	N.d.	N.d.	N.d.
Total	24.2	15.2	21.5	22.9	44.5	46.6	27.7	37.2	17.0	17.9	16.4
$(La/Yb)_n$	N.d.	N.d.	N.d.	N.d.	N.d.	N.d.	N.d.	N.d.	N.d.	N.d.	N.d.

	Massifs (provinces)											
	Vitim, Russia				Nunivak, USA	Troodos, Cyprus		Vitim, Russia	Gal'moenansky, Russia			
	(Andre & Ashchepkov, 1996), ICP-MS				(Roden *et al.*, 1984)	(Batanova *et al.*, 1996)		(Andre & Ashchepkov, 1996)	(Pertsev, 2004)			
	315-167[a]	315-254[a]	327-2[a]	327-3[a]	10056[a]	TV-102	TV-103	327-5[a]	G9-2	G14-8	G14-10	G14-13
Element	*Pyroxenites*					*Olivine pyroxenites*		*Plagiocl.-bearing pyroxenites*	*Olivine clinopyroxenites*			
La	1.730	1.150	8.550	11.02	2.990	0.060	0.040	6.430	0.092	0.120	0.150	0.140
Ce	6.760	4.220	45.75	48.70	3.700	0.170	0.230	28.95	0.410	0.450	0.610	0.560
Pr	1.370	0.860	10.05	8.93	N.d.	N.d.	N.d.	5.440	N.d.	N.d.	N.d.	N.d.
Nd	7.920	4.950	58.22	41.60	0.990	0.350	0.490	27.54	0.690	0.590	0.890	1.100
Sm	2.700	1.720	15.04	6.770	0.264	0.260	0.300	5.720	0.320	0.270	0.370	0.460
Eu	1.030	0.660	3.600	1.860	0.171	0.090	0.150	1.470	0.110	0.100	0.160	0.210
Gd	3.120	2.100	13.09	3.490	N.d.	N.d.	N.d.	3.790	N.d.	N.d.	N.d.	N.d.
Tb	N.d.	N.d.	N.d.	N.d.	0.130	N.d.	N.d.	N.d.	N.d.	N.d.	N.d.	N.d.
Dy	2.180	1.770	8.880	1.100	N.d.	0.640	0.780	1.750	0.390	0.270	0.470	0.580
Ho	0.352	0.334	1.520	0.159	N.d.	N.d.	N.d.	0.249	N.d.	N.d.	N.d.	N.d.
Er	0.646	0.713	3.640	0.278	N.d.	0.430	0.570	0.486	0.210	0.130	0.300	0.360
Tm	N.d.	N.d.	N.d.	N.d.	N.d.	N.d.	N.d.	N.d.	N.d.	N.d.	N.d.	N.d.
Yb	0.288	0.391	2.740	0.144	0.735	0.430	0.470	0.275	0.160	0.130	0.270	0.270
Lu	0.031	0.058	0.380	0.018	0.120	N.d.	N.d.	0.034	N.d.	N.d.	N.d.	N.d.
Total	28.1	18.9	172	124	N.d.	2.43	3.03	82.1	2.38	2.06	3.22	3.68
$(La/Yb)_n$	4.05	1.99	2.11	51.7	N.d.	0.094	0.057	15.8	0.39	0.62	0.37	0.35

(*Continued*)

Table 5.25 Continued

	Kytlymsky, Russia		Nuralinsky, Russia			Gal'moenansky, Russia						Voykar-Sin'insky, Russia
	(Pertsev, 2004)											
	KT-8	KT-13	N1809	N1809b	N1808	G320a	G320b	G12-6	G12-2a c	G12-2b r	G12-2s mat	V588
Element	*Olivine clinopyroxenites*					*Clinopyroxenites*		*Plagioclase-olivine-bearing clinopyroxenites*				*Clinopyroxenite*
La	0.700	0.300	0.140	0.620	0.260	0.150	0.990	0.380	0.310	0.950	0.740	0.012
Ce	2.500	1.100	0.720	1.800	1.000	0.530	2.800	1.500	1.200	4.900	3.600	0.089
Pr	N.d.	N.d.	N.d.	N.d.	N.d.	N.d.	N.d.	N.d.	N.d.	N.d.	N.d.	N.d.
Nd	2.400	1.400	1.400	1.600	1.200	0.740	2.700	2.100	1.500	7.700	6.200	0.170
Sm	0.800	0.620	0.670	0.550	0.530	0.350	0.820	0.920	0.690	3.400	2.400	0.095
Eu	0.280	0.190	0.260	0.200	0.160	0.140	0.290	0.320	0.240	1.000	0.820	0.054
Gd	N.d.	N.d.	N.d.	N.d.	N.d.	N.d.	N.d.	N.d.	N.d.	N.d.	N.d.	N.d.
Tb	N.d.	N.d.	N.d.	N.d.	N.d.	N.d.	N.d.	N.d.	N.d.	N.d.	N.d.	N.d.
Dy	0.690	0.570	1.200	0.730	0.740	0.350	0.740	1.100	0.820	4.200	3.400	0.340
Ho	N.d.	N.d.	N.d.	N.d.	N.d.	N.d.	N.d.	N.d.	N.d.	N.d.	N.d.	N.d.
Er	0.390	0.330	0.740	0.500	0.470	0.250	0.420	0.680	0.500	2.400	1.800	0.170
Tm	N.d.	N.d.	N.d.	N.d.	N.d.	N.d.	N.d.	N.d.	N.d.	N.d.	N.d.	N.d.
Yb	0.310	0.320	0.580	0.420	0.360	0.220	0.340	0.550	0.420	2.200	1.700	0.190
Lu	N.d.	N.d.	N.d.	N.d.	N.d.	N.d.	N.d.	N.d.	N.d.	N.d.	N.d.	N.d.
Total	8.07	4.83	5.71	6.42	4.72	2.73	9.10	7.55	5.68	26.8	20.7	1.12
$(La/Yb)_n$	1.52	0.63	0.16	1.00	0.49	0.46	1.97	0.47	0.50	0.29	0.29	0.04

[a] Samples from deep xenoliths.

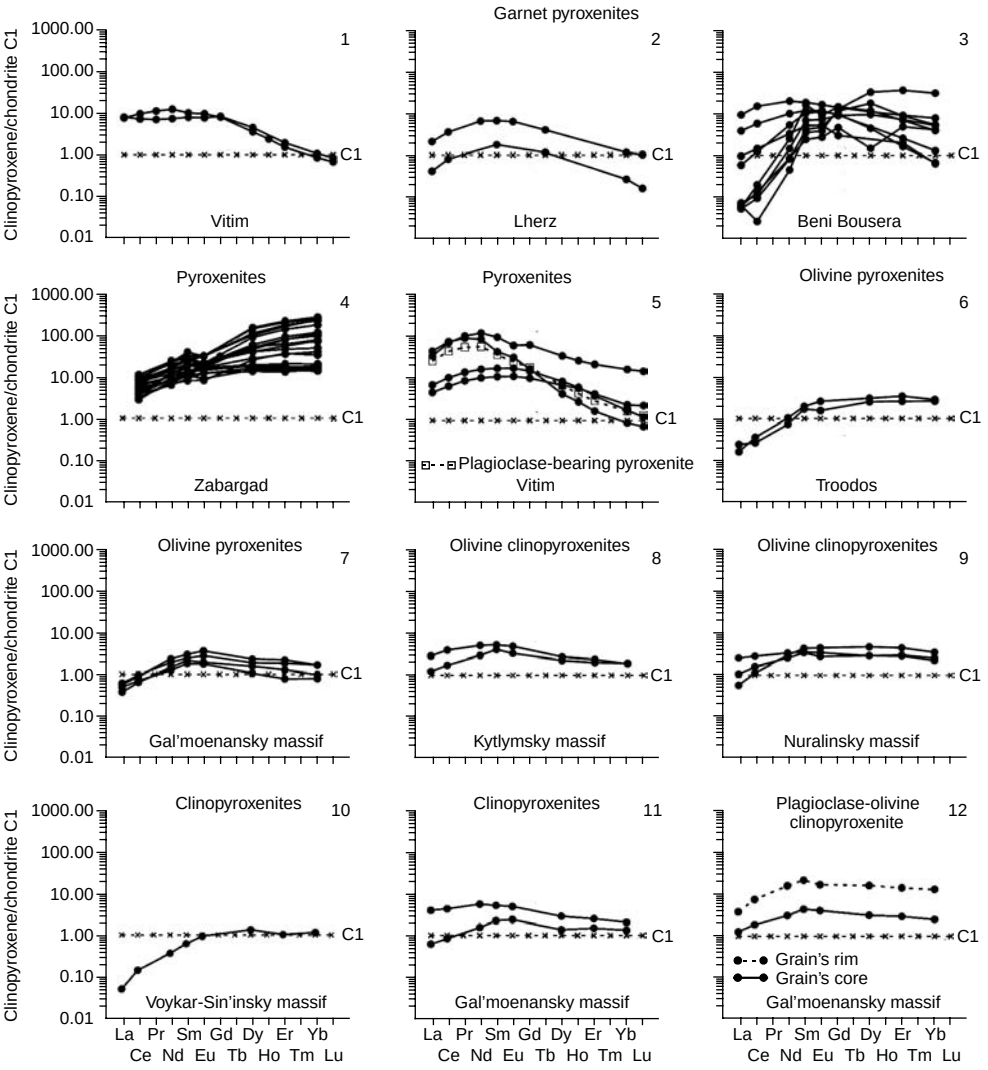

Figure 5.21 Chondrite-normalized REE patterns for clinopyroxenes from pyroxenites, represented in some massifs and deep xenoliths (data Table 5.25).

Gabbros. Data on the REE composition of clinopyroxenes from these widely spread rocks are also scarce (Table 5.26). It was established that gabbro samples from the Ivrea Verbano massif have an uncommonly high level of accumulation of light REE compared to heavy REE (Mazzucchelli *et al.*, 1992a). They also exhibit a significant excess of Eu ($(Eu/Eu^*)_n$ ~3–14) (Fig. 5.23, 11). Mazzucchelli and coauthors believe that these specific features of the rare earth composition of gabbros from the Ivrea Verbano massif are due to their formation from hybrid melts resulting from

Table 5.26 Rare earth element composition of clinopyroxenes from olivine gabbros, olivine gabbro-norites, and picrites (ppm).

	Massifs												
	Troodos, Cyprus											Samail, Oman	
	(Batanova *et al.*, 1996), IPMA											(Pallister & Knight, 1981), RNAA	
	TV-129a	TV-129b	TV-58	TV-69	TV-73	TV-73	TV-73	TV-73	TV-73	TV-73	TV-73	Kf-12-1	Kf-17-1C
Element	*Olivine gabbros*												
La	0.120	0.050	0.040	0.030	0.040	0.040	0.030	0.030	0.050	0.070	0.040	0.270	0.260
Ce	0.370	0.150	0.120	0.210	0.270	0.200	0.200	0.200	0.240	0.340	0.210	1.800	2.300
Pr	N.d.	N.d.	N.d.	N.d.	N.d.	N.d.	N.d.	N.d.	N.d.	N.d.	N.d.	N.d.	N.d.
Nd	0.560	0.150	0.280	0.480	0.660	0.430	0.380	0.370	0.460	0.700	0.360	2.500	2.600
Sm	0.380	0.150	0.220	0.390	0.440	0.240	0.280	0.340	0.340	0.420	0.200	1.200	1.500
Eu	0.150	0.080	0.100	0.150	0.190	0.130	0.110	0.160	0.130	0.170	0.110	0.450	0.620
Gd	N.d.	N.d.	N.d.	N.d.	N.d.	N.d.	N.d.	N.d.	N.d.	N.d.	N.d.	1.900	2.200
Tb	N.d.	N.d.	N.d.	N.d.	N.d.	N.d.	N.d.	N.d.	N.d.	N.d.	N.d.	0.400	0.480
Dy	1.330	0.490	0.660	1.070	1.310	0.930	0.500	0.950	1.040	1.300	0.670	2.600	3.300
Ho	N.d.	N.d.	N.d.	N.d.	N.d.	N.d.	N.d.	N.d.	N.d.	N.d.	N.d.	N.d.	N.d.
Er	0.890	0.420	0.410	0.770	0.790	0.560	0.290	0.530	0.670	0.750	0.430	N.d.	N.d.
Tm	N.d.	N.d.	N.d.	N.d.	N.d.	N.d.	N.d.	N.d.	N.d.	N.d.	N.d.	0.230	0.290
Yb	0.800	0.330	0.430	0.750	0.840	0.590	0.360	0.640	0.690	0.720	0.520	1.400	1.600
Lu	N.d.	N.d.	N.d.	N.d.	N.d.	N.d.	N.d.	N.d.	N.d.	N.d.	N.d.	0.200	0.230
Total	4.60	1.82	2.26	3.85	4.54	3.12	2.15	3.22	3.62	4.47	2.54	13.0	15.4
$(La/Yb)_n$	0.10	0.10	0.06	0.03	0.03	0.05	0.06	0.03	0.05	0.07	0.05	0.13	0.11

	Massifs											
	Samail, Oman		Kytlymsky, Russia							Riparbello, Italy		Komsomol'sky, Russia
	(Pallister & Knight, 1981), RNAA		(Pertsev, 2004)							(Tiepolo *et al.*, 1997)		(Lesnov & Gora, 1998)
	Kf-20-1C	Kf-7-1	KT-10b-4a	KT-10b-4b	KT-10b-5	KT-10b-5a	KT-86a	KT-86ab	KT-86ab	CBC3b	CBC3a	190
Element	*Olivine gabbros*											*Olivine gabbro-norite*
La	0.110	0.270	4.00	1.700	1.400	3.000	1.900	5.100	2.700	0.320	0.180	0.290
Ce	1.100	1.800	7.500	5.200	4.00	6.500	6.800	11.000	7.700	1.560	1.150	0.800
Pr	N.d.	N.d.	N.d.	N.d.	N.d.	N.d.	N.d.	N.d.	N.d.	N.d.	N.d.	N.d.
Nd	1.000	1.800	7.300	5.700	4.200	4.800	6.100	6.800	6.600	2.610	1.950	0.610
Sm	0.580	0.970	2.400	2.100	1.500	1.800	2.000	2.200	2.100	1.490	1.120	0.220
Eu	0.260	0.350	0.840	0.690	0.560	0.740	0.760	0.790	0.750	0.510	0.430	0.100
Gd	1.100	1.400	N.d.	N.d.	N.d.	N.d.	N.d.	N.d.	N.d.	1.890	2.130	0.440
Tb	0.260	0.310	N.d.	N.d.	N.d.	N.d.	N.d.	N.d.	N.d.	N.d.	N.d.	0.045
Dy	1.900	2.200	2.500	2.400	1.600	2.000	2.000	2.400	2.200	2.520	2.560	N.d.
Ho	N.d.	N.d.	N.d.	N.d.	N.d.	N.d.	N.d.	N.d.	N.d.	N.d.	N.d.	N.d.
Er	N.d.	N.d.	1.200	1.100	0.920	1.100	1.200	1.400	1.300	1.550	1.550	N.d.
Tm	0.180	0.180	N.d.	N.d.	N.d.	N.d.	N.d.	N.d.	N.d.	N.d.	N.d.	0.100
Yb	1.100	1.100	1.100	1.100	0.800	1.000	1.000	1.100	1.000	1.630	1.540	0.680
Lu	0.170	0.160	N.d.	N.d.	N.d.	N.d.	N.d.	N.d.	N.d.	N.d.	N.d.	0.120
Total	7.76	10.5	N.d.	N.d.	N.d.	N.d.	N.d.	N.d.	N.d.	14.1	12.6	N.d.
$(La/Yb)_n$	0.07	0.17	2.45	1.04	1.18	2.02	1.28	3.13	1.82	0.13	0.08	0.29

(*Continued*)

Table 5.26 Continued

	Massifs										
	Gal'moenansky, Russia			Troodos, Cyprus							
	(Pertsev, 2004)			(Sobolev *et al.*, 1996), IPMA							
	G12-10a core	G12-10b	G12-10c rim	T-133/15	T-135/1	T-135/3	T-191/13	T-191/9	T-200/16	T-200/19	T-200/20
Element	*Olivine gabbro-norites*			*Picrites*							
La	0.440	1.700	3.600	0.032	0.018	0.025	0.048	0.031	0.015	0.032	0.036
Ce	1.500	6.200	13.00	0.182	0.096	0.093	0.266	0.152	0.075	0.113	0.171
Pr	N.d.	N.d.	N.d.	N.d.	N.d.	N.d.	N.d.	N.d.	N.d.	N.d.	N.d.
Nd	1.800	6.600	11.00	0.373	0.167	0.148	0.550	0.366	0.125	0.181	0.350
Sm	0.800	2.400	3.700	0.124	0.118	0.091	0.321	0.241	0.089	0.129	0.267
Eu	0.280	0.780	1.200	N.d.	N.d.	N.d.	N.d.	N.d.	N.d.	N.d.	N.d.
Gd	N.d.	N.d.	N.d.	N.d.	N.d.	N.d.	N.d.	N.d.	N.d.	N.d.	N.d.
Tb	N.d.	N.d.	N.d.	N.d.	N.d.	N.d.	N.d.	N.d.	N.d.	N.d.	N.d.
Dy	0.850	3.100	4.100	0.418	0.253	0.246	0.861	0.560	0.132	0.261	0.543
Ho	N.d.	N.d.	N.d.	N.d.	N.d.	N.d.	N.d.	N.d.	N.d.	N.d.	N.d.
Er	0.520	1.900	2.600	0.235	0.147	0.152	0.462	0.322	0.077	0.165	0.332
Tm	N.d.	N.d.	N.d.	N.d.	N.d.	N.d.	N.d.	N.d.	N.d.	N.d.	N.d.
Yb	0.450	1.500	2.200	0.197	0.154	0.160	0.467	0.312	0.082	0.157	0.325
Lu	N.d.	N.d.	N.d.	N.d.	N.d.	N.d.	N.d.	N.d.	N.d.	N.d.	N.d.
Total	6.64	24.2	41.4	N.d.	N.d.	N.d.	N.d.	N.d.	N.d.	N.d.	N.d.
$(La/Yb)_n$	0.66	0.76	1.10	0.11	0.08	0.11	0.07	0.07	0.12	0.14	0.07

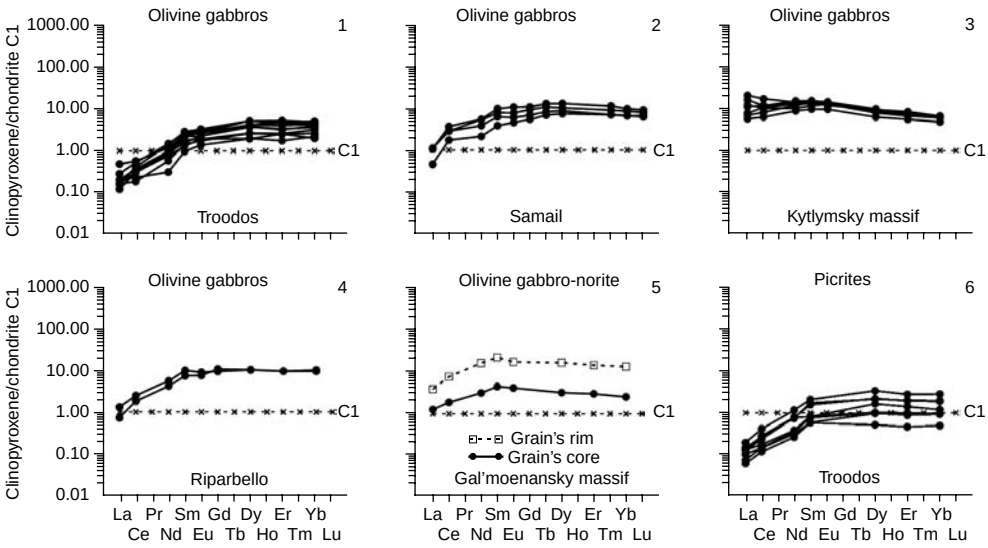

Figure 5.22 Chondrite-normalized REE patterns for clinopyroxenes from olivine gabbros, olivine gabbro-norites, and picrites (data Table 5.26).

intense contamination of initial mantle-derived magmas during assimilation of host sedimentary rocks enriched with REE. Analyses of clinopyroxenes from gabbros of the Skaergaard massif also show a rather high level of accumulation of REE, weak fractionation, and a minor deficit of Eu (Fig. 5.23, 12). The samples from the Skaergaard massif are similar to clinopyroxenes from diorites of the Bracco massif (Fig. 5.23, 13, 14).

Basalts, andesites, dacites, and rhyolites. The REE composition of clinopyroxenes from these effusive rocks was studied on individual phenocrysts from Liguria, Central massif (France), Gorny Altay, and some other provinces (Table 5.28).

The total contents of REE in phenocrysts from basalts of normal alkalinity, occurring in Liguria, range from 13 to 100 ppm, and their REE patterns have a shape of slightly upwardly bent lines with a very gentle slope (Fig. 5.24, 1). Most likely, these basalts crystallized from primitive mantle melts generated at moderate levels of partial melting of undepleted mantle source. Clinopyroxenes from basalts of the Central massif, having increased alkalinity, are characterized by approximately the same level of REE accumulation: La (14–52 t. ch.), Ce (16–60 t. ch.), and Yb (6–14 t. ch.). The patterns of these clinopyroxenes have a steeper negative slope ($(La/Yb)_n$ ~2.3–4.6) (Fig. 5.24, 2). The elevated alkalinity of basalts from the Central massif and rather high level of REE accumulation in contained clinopyroxene phenocrysts suggest that the parental melts of these basalts were generated at a rather low degree of melting of undepleted mantle source. Unlike the previous samples, clinopyroxene phenocrysts from basalts of Gorny Altay are essentially depleted of light REE, which suggests that they crystallized from melts generated during partial melting of preliminarily depleted mantle source (Fig. 5.24, 5). Clinopyroxene from phenocrysts in andesites of the Mount Adams

Table 5.27 Rare earth element composition of clinopyroxenes from gabbros, gabbro-norites, and diorites from massifs (ppm).

	Massifs											
	Beriozovsky, Russia						Kuyul'sky, Russia	Valizhgen, Russia	Sheltingsky, Russia		Shikotansky, Russia	
	(Lesnov, 1988; Lesnov & Gora, 1998), RNAA											
	131	132a	138a	141	144	147	115	115-11a	173	183	186	187
Element	*Gabbro-norites*											
La	0.240	0.330	0.110	0.310	0.320	0.960	0.380	0.610	0.380	0.098	1.400	1.850
Ce	0.530	0.570	0.370	0.750	1.280	1.410	0.980	2.600	1.370	0.240	5.980	13.20
Pr	N.d.	N.d.	N.d.	N.d.	N.d.	N.d.	N.d.	N.d.	N.d.	N.d.	N.d.	N.d.
Nd	0.960	0.460	0.360	0.500	1.440	0.880	0.650	1.700	1.610	0.120	6.880	9.200
Sm	0.270	0.160	0.180	0.140	0.620	0.220	0.120	0.680	0.810	0.025	3.700	4.060
Eu	0.160	0.150	0.090	0.060	0.450	0.140	0.320	0.520	0.660	0.020	1.710	2.130
Gd	0.370	0.420	0.330	0.200	2.160	0.260	0.740	1.620	3.160	0.130	4.290	7.000
Tb	0.080	0.080	0.060	0.044	0.310	0.048	0.140	0.320	0.710	0.033	1.170	1.800
Dy	0.700	0.430	N.d.	N.d.	N.d.	N.d.	1.000	N.d.	N.d.	N.d.	N.d.	N.d.
Ho	N.d.	N.d.	N.d.	N.d.	N.d.	N.d.	N.d.	N.d.	N.d.	N.d.	N.d.	N.d.
Er	N.d.	N.d.	N.d.	N.d.	N.d.	N.d.	N.d.	N.d.	N.d.	N.d.	N.d.	N.d.
Tm	0.070	0.050	0.050	0.039	0.100	0.035	0.170	0.200	0.400	0.025	1.070	0.700
Yb	0.500	0.220	0.430	N.d.	0.600	0.230	0.800	1.430	2.340	0.300	9.150	8.450
Lu	0.100	0.040	0.060	0.040	0.100	0.025	0.290	0.160	0.360	0.037	1.330	0.690
Total	3.98	2.91	N.d.	N.d.	N.d.	N.d.	5.59	N.d.	11.8	1.03	36.7	49.1
$(La/Yb)_n$	0.32	1.01	0.17	N.d.	0.36	2.82	0.32	0.29	0.11	0.22	0.10	0.15

	Massifs											
	Voykar-Sin'insky, Russia	Naransky, Mongolia		Chaysky, Russia	Ostiurensky, Russia	Monchegorsky	Rybinsky, Russia			Nizhnederbinsky, Russia	Karaginsky, Russia	
	(Lesnov, 1988; Lesnov & Gora, 1998), RNAA											
	252	269	270	27	429	71	88	89	93	94	96	98
Element	*Gabbro-norites*											
La	0.150	0.350	1.490	0.700	4.400	1.060	10.70	9.170	2.460	2.000	0.110	0.720
Ce	1.560	1.600	2.500	2.900	22.25	4.000	36.00	29.30	10.90	15.00	0.380	3.320
Pr	N.d.	N.d.	N.d.	N.d.	N.d.	N.d.	N.d.	N.d.	N.d.	N.d.	N.d.	N.d.
Nd	1.820	1.800	1.400	3.070	21.30	3.100	35.60	25.50	12.50	6.900	0.550	2.100
Sm	0.740	0.750	0.400	1.280	8.300	1.650	12.90	11.20	6.900	3.900	0.360	1.140
Eu	0.360	0.410	0.190	1.070	4.200	0.480	3.710	2.700	2.830	1.900	0.260	0.660
Gd	1.490	2.020	0.700	2.200	10.60	1.460	15.70	10.60	9.000	9.200	0.900	2.020
Tb	0.280	0.330	0.110	0.220	1.640	0.280	3.000	2.180	1.700	1.600	0.170	0.360
Dy	N.d.	N.d.	N.d.	N.d.	N.d.	1.620	N.d.	N.d.	N.d.	8.510	1.000	1.980
Ho	N.d.	N.d.	N.d.	N.d.	N.d.	N.d.	N.d.	N.d.	N.d.	N.d.	N.d.	N.d.
Er	N.d.	N.d.	N.d.	N.d.	N.d.	N.d.	N.d.	N.d.	N.d.	N.d.	N.d.	N.d.
Tm	0.180	0.150	0.060	0.100	0.570	0.170	1.500	0.800	0.700	0.800	0.110	0.230
Yb	1.140	0.850	0.500	0.690	4.200	1.060	10.600	3.900	4.750	4.960	0.530	1.350
Lu	0.200	0.110	0.070	0.100	0.480	0.160	1.280	0.560	0.610	0.760	0.140	0.180
Total	7.92	8.37	7.42	12.3	77.9	15.0	131	95.9	52.4	55.5	4.51	14.1
$(La/Yb)_n$	0.09	0.28	2.01	0.69	0.71	0.68	0.68	1.59	0.35	0.27	0.14	0.36

(*Continued*)

Table 5.27 Continued

	Massifs										
	Lukinda, Russia	Troodos, Cyprus	Gal'moenansky, Russia				Voykar-Syn'insky, Russia			Ivrea Verbano, Italy	
	(Lesnov, 1988; Lesnov & Gora, 1998), RNAA	(Batanova *et al.*, 1996)	(Pertsev, 2004)							(Mazzucchelli *et al.*, 1992a,b), IPMA	
	168	TV-56	G12-10d	G12-3a	G12-3b	G12-3c	V803-1	V803-14a	V803-14b	FE19	FE31
Element	*Gabbro-norites*									*Gabbro*	
La	4.760	0.020	3.300	1.200	2.800	2.200	0.043	0.026	0.022	N.d.	N.d.
Ce	19.10	0.210	11.00	3.600	12.00	10.00	0.250	0.160	0.150	12.99	5.900
Pr	N.d.	N.d.	N.d.	N.d.	N.d.	N.d.	N.d.	N.d.	N.d.	N.d.	N.d.
Nd	15.80	0.550	10.00	3.300	15.00	14.00	0.790	0.440	0.360	19.31	8.900
Sm	4.850	0.320	3.200	1.200	5.700	5.200	0.600	0.380	0.390	7.040	4.020
Eu	1.500	0.180	1.100	0.430	1.600	1.400	0.300	0.210	0.250	1.810	1.500
Gd	3.200	N.d.	N.d.	N.d.	N.d.	N.d.	N.d.	N.d.	N.d.	N.d.	N.d.
Tb	0.560	N.d.	N.d.	N.d.	N.d.	N.d.	N.d.	N.d.	N.d.	N.d.	N.d.
Dy	N.d.	1.200	3.800	1.300	6.000	5.800	1.900	1.100	1.300	9.120	6.770
Ho	N.d.	N.d.	N.d.	N.d.	N.d.	N.d.	N.d.	N.d.	N.d.	N.d.	N.d.
Er	N.d.	0.840	2.500	0.870	3.400	3.500	1.200	0.940	1.100	4.850	3.830
Tm	0.240	N.d.	N.d.	N.d.	N.d.	N.d.	N.d.	N.d.	N.d.	N.d.	N.d.
Yb	1.590	0.760	2.200	0.620	3.300	3.100	1.100	0.820	0.890	4.920	3.810
Lu	0.190	N.d.	N.d.	N.d.	N.d.	N.d.	N.d.	N.d.	N.d.	N.d.	N.d.
Total	51.8	N.d.	37.1	12.5	49.8	45.2	6.18	4.08	4.46	60.0	34.7
$(La/Yb)_n$	2.02	0.02	1.01	1.31	0.57	0.48	0.03	0.02	0.02	N.d.	N.d.

	Massifs										
	Ivrea Verbano, Italy										
	(Mazzucchelli *et al.*, 1992a,b), IPMA										
	FE51	MO95	MP12	MP13	MP18	MP6	MP9	MZ132	MZ145	MP1c	MP1r
Element	*Gabbro*										
La	N.d.	N.d.	N.d.	N.d.	N.d.	N.d.	N.d.	N.d.	N.d.	N.d.	N.d.
Ce	69.02	40.73	14.59	36.00	22.49	44.22	69.39	47.97	28.89	13.41	12.70
Pr	N.d.	N.d.	N.d.	N.d.	N.d.	N.d.	N.d.	N.d.	N.d.	N.d.	N.d.
Nd	76.00	32.36	23.69	47.23	36.36	29.33	59.51	42.34	11.48	17.23	15.50
Sm	23.87	6.500	8.740	13.59	12.33	4.300	10.66	8.590	1.110	6.790	6.200
Eu	3.030	4.230	1.920	2.330	2.460	5.670	6.840	8.240	2.440	2.890	2.520
Gd	N.d.	N.d.	N.d.	N.d.	N.d.	N.d.	N.d.	N.d.	N.d.	N.d.	N.d.
Tb	N.d.	N.d.	N.d.	N.d.	N.d.	N.d.	N.d.	N.d.	N.d.	N.d.	N.d.
Dy	28.420	1.730	2.450	2.520	3.990	0.530	1.120	6.410	0.160	12.440	8.640
Ho	N.d.	N.d.	N.d.	N.d.	N.d.	N.d.	N.d.	N.d.	N.d.	N.d.	N.d.
Er	14.61	0.630	0.610	0.510	1.070	0.200	0.470	4.140	0.070	7.230	3.360
Tm	N.d.	N.d.	N.d.	N.d.	N.d.	N.d.	N.d.	N.d.	N.d.	N.d.	N.d.
Yb	14.560	0.460	0.250	0.290	0.540	0.080	0.330	3.630	0.040	7.260	2.980
Lu	N.d.	N.d.	N.d.	N.d.	N.d.	N.d.	N.d.	N.d.	N.d.	N.d.	N.d.
Total	230	86.6	52.3	102	79.2	84.3	148	121	44.2	67.3	51.9
$(La/Yb)_n$	N.d.	N.d.	N.d.	N.d.	N.d.	N.d.	N.d.	N.d.	N.d.	N.d.	N.d.

(*Continued*)

Table 5.27 Continued

	Massifs											
	Ivrea Verbano, Italy		Samail, Oman	Skaergaard, Greenland			Liguria, Italy				Bracco, Italy	
	(Mazzucchelli *et al.*, 1992a,b), IPMA		(Pallister & Knight, 1981)	(Paster *et al.*, 1974), NAA			(Tribuzio *et al.*, 1995), SIMS				(Tiepolo *et al.*, 1997)	
	MP3	MP5	Kf-16-1	4312	4427	5086	AP3/3-2	AP3/3-1	AP3/3-1	AP3/3-2	N1Aa	N1Ab
Element	*Gabbro*									*Diorites*		
La	N.d.	6.830	0.200	2.300	5.500	6.800	0.480	0.340	0.440	0.340	2.660	2.710
Ce	16.89	32.80	2.300	23.00	19.00	26.00	3.250	1.820	3.040	1.990	13.10	13.12
Pr	N.d.	N.d.	N.d.	N.d.	N.d.	N.d.	N.d.	N.d.	N.d.	N.d.	N.d.	N.d.
Nd	32.59	38.93	2.100	18.00	19.00	25.00	5.800	3.360	5.510	3.640	22.70	23.68
Sm	10.26	10.70	0.950	6.100	5.400	7.600	2.840	1.830	2.760	1.970	10.90	10.30
Eu	2.190	2.440	0.370	1.830	1.210	1.240	0.920	0.720	0.790	0.680	2.890	3.070
Gd	N.d.	10.730	1.800	8.500	6.200	9.000	4.870	2.640	4.080	2.810	15.60	15.86
Tb	N.d.	N.d.	0.310	1.320	1.060	1.550	N.d.	N.d.	N.d.	N.d.	N.d.	N.d.
Dy	3.050	3.460	2.100	N.d.	N.d.	N.d.	5.490	3.500	4.830	3.470	18.80	18.24
Ho	N.d.	N.d.	N.d.	1.440	1.260	1.900	N.d.	N.d.	N.d.	N.d.	N.d.	N.d.
Er	0.570	0.730	N.d.	N.d.	N.d.	N.d.	2.900	1.980	2.730	1.860	11.10	10.19
Tm	N.d.	N.d.	0.160	N.d.	N.d.	N.d.	N.d.	N.d.	N.d.	N.d.	N.d.	N.d.
Yb	0.270	0.200	1.100	3.100	2.500	3.600	2.810	1.730	2.450	1.830	10.60	10.57
Lu	N.d.	N.d.	0.150	N.d.	N.d.	N.d.	N.d.	N.d.	N.d.	N.d.	N.d.	N.d.
Total	65.8	107	11.5	65.6	61.1	82.7	29.4	17.9	26.6	18.6	108	108
$(La/Yb)_n$	N.d.	N.d.	0.12	0.50	1.49	1.28	0.12	0.13	0.12	0.13	0.17	0.17

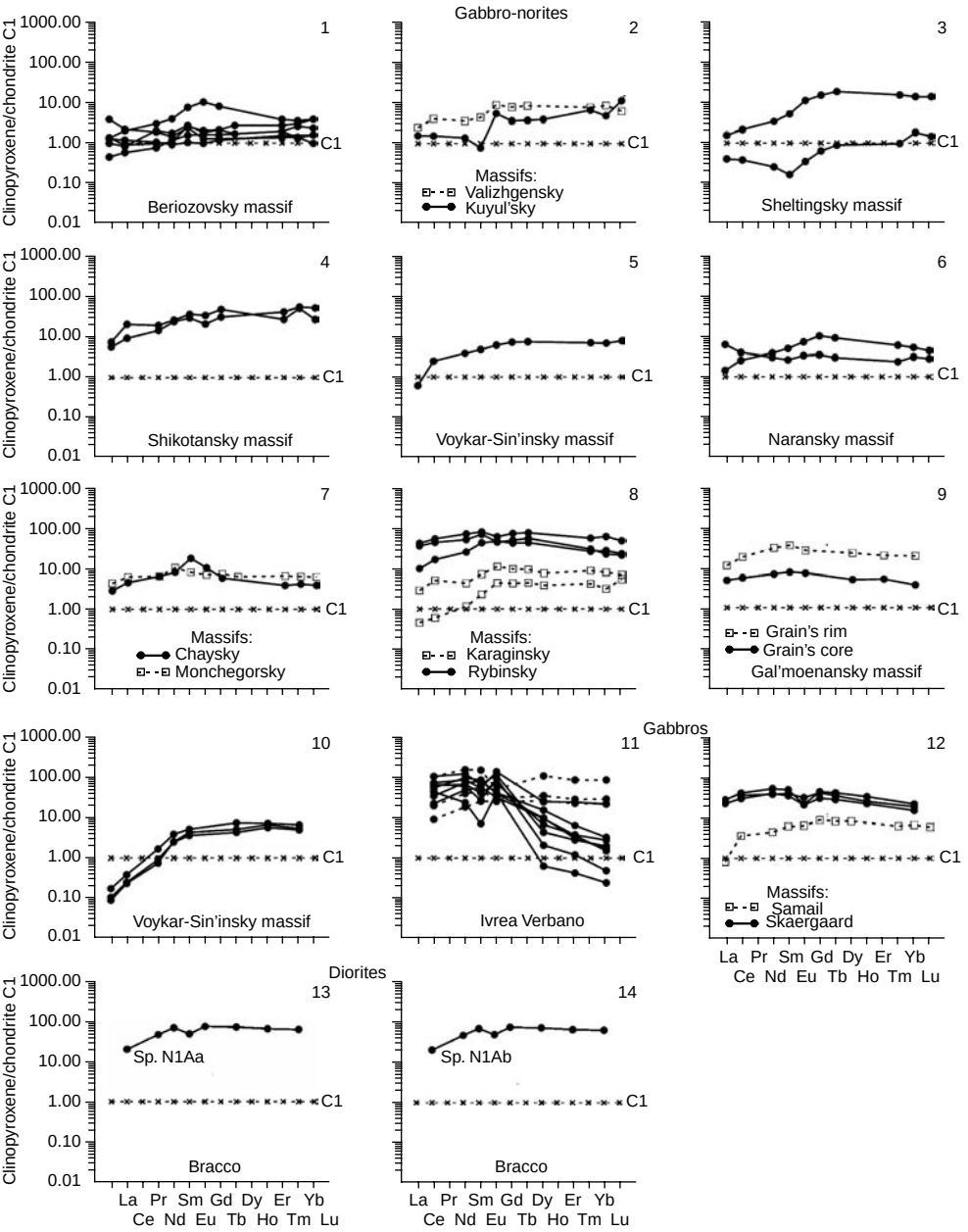

Figure 5.23 Chondrite-normalized REE patterns for clinopyroxenes from gabbro-norites, gabbros, and diorites from some massifs (data Table 5.27).

Table 5.28 Rare earth element composition of clinopyroxenes from normal, and alkali basalts, andesites, dacites, and rhyolites (ppm).

	Provinces												
	Liguria, Italy												
	(Vannucci *et al.*, 1993b), IPMA												
	L9-1/e/c	L9-2/e/c	S1A-1/m/c	S1A-2/i	Li51-1/i	Li51-2/i	Li56-1/i	Li56-2/i	R1/15-11/i	R1/15-2/i	R1/15-5/i	R1/18-1mc	R1/18-1mr
Element	*Basalts*												
La	N.d.	N.d.	N.d.	N.d.	N.d.	N.d.	N.d.	N.d.	N.d.	N.d.	N.d.	N.d.	N.d.
Ce	2.340	2.340	1.740	6.850	5.040	4.770	6.680	6.200	9.850	6.910	7.110	4.510	4.800
Pr	N.d.	N.d.	N.d.	N.d.	N.d.	N.d.	N.d.	N.d.	N.d.	N.d.	N.d.	N.d.	N.d.
Nd	3.670	3.230	2.370	6.950	7.050	6.440	10.45	8.980	12.87	9.820	9.400	6.790	6.910
Sm	2.010	2.170	1.220	2.850	2.760	2.880	4.110	3.630	4.940	4.320	3.680	2.300	2.950
Eu	0.740	0.690	0.480	1.060	1.020	0.920	1.600	1.220	1.830	1.510	1.270	1.070	1.100
Gd	3.980	3.210	2.020	4.600	3.970	3.990	5.600	4.680	N.d.	N.d.	5.740	N.d.	N.d.
Tb	N.d.	N.d.	N.d.	N.d.	N.d.	N.d.	N.d.	N.d.	N.d.	N.d.	N.d.	N.d.	N.d.
Dy	4.900	4.200	2.380	5.300	4.610	4.610	6.590	5.390	7.300	6.510	6.200	4.310	4.590
Ho	N.d.	N.d.	N.d.	N.d.	N.d.	N.d.	N.d.	N.d.	N.d.	N.d.	N.d.	N.d.	N.d.
Er	2.920	2.560	1.370	3.030	2.550	2.560	3.830	3.160	3.860	3.410	3.430	2.380	2.230
Tm	N.d.	N.d.	N.d.	N.d.	N.d.	N.d.	N.d.	N.d.	N.d.	N.d.	N.d.	N.d.	N.d.
Yb	2.970	2.630	1.350	3.070	2.690	2.410	3.980	2.780	3.720	3.500	3.310	2.170	2.150
Lu	N.d.	N.d.	N.d.	N.d.	N.d.	N.d.	N.d.	N.d.	N.d.	N.d.	N.d.	N.d.	N.d.
Total	23.5	21.0	12.9	33.7	29.7	28.6	42.8	36.0	N.d.	N.d.	40.1	N.d.	N.d.
$(La/Yb)_n$	N.d.	N.d.	N.d.	N.d.	N.d.	N.d.	N.d.	N.d.	N.d.	N.d.	N.d.	N.d.	N.d.

	Provinces												
	Liguria, Italy												
	(Vannucci *et al.*, 1993b), IPMA												
	R1/18-2/i	R1/18-3mc	R1/18-3mr	R1/18-7mc	R4/12-3/i	R4/12-5/i	R4/12-6/i	R4/23-11/i	R4/23-12/i	R4/23-13/i	R9/5-1/i	R9/5-4/i	R9/5-5/i
Element	*Basalts*												
La	N.d.	N.d.	N.d.	N.d.	N.d.	N.d.	N.d.	N.d.	N.d.	N.d.	N.d.	N.d.	N.d.
Ce	6.410	4.740	6.480	4.890	17.34	25.39	11.60	6.230	12.47	5.460	8.600	6.410	6.150
Pr	N.d.	N.d.	N.d.	N.d.	N.d.	N.d.	N.d.	N.d.	N.d.	N.d.	N.d.	N.d.	N.d.
Nd	9.600	6.850	8.810	6.570	21.07	30.13	14.39	8.120	16.63	7.790	10.73	8.140	8.190
Sm	3.700	2.890	3.900	2.630	8.180	10.27	5.040	3.290	6.230	3.170	4.230	3.330	3.250
Eu	1.280	1.100	1.530	0.960	2.840	3.210	2.060	1.250	2.300	1.140	1.720	1.360	1.160
Gd	5.810	N.d.	N.d.	4.100	N.d.	N.d.	N.d.	N.d.	N.d.	4.650	N.d.	N.d.	4.870
Tb	N.d.	N.d.	N.d.	N.d.	N.d.	N.d.	N.d.	N.d.	N.d.	N.d.	N.d.	N.d.	N.d.
Dy	5.810	4.810	6.150	4.490	11.55	14.83	7.760	5.110	9.750	4.820	6.880	5.470	5.040
Ho	N.d.	N.d.	N.d.	N.d.	N.d.	N.d.	N.d.	N.d.	N.d.	N.d.	N.d.	N.d.	N.d.
Er	3.270	2.440	3.500	2.290	6.180	8.040	4.020	2.620	5.190	2.650	3.630	3.140	2.920
Tm	N.d.	N.d.	N.d.	N.d.	N.d.	N.d.	N.d.	N.d.	N.d.	N.d.	N.d.	N.d.	N.d.
Yb	2.890	2.350	3.540	2.260	5.950	8.640	3.870	2.750	5.520	2.510	3.460	2.860	2.750
Lu	N.d.	N.d.	N.d.	N.d.	N.d.	N.d.	N.d.	N.d.	N.d.	N.d.	N.d.	N.d.	N.d.
Total	38.8	25.2	33.9	28.2	73.1	101	48.7	29.4	58.1	32.2	39.3	30.7	34.3
$(La/Yb)_n$	N.d.	N.d.	N.d.	N.d.	N.d.	N.d.	N.d.	N.d.	N.d.	N.d.	N.d.	N.d.	N.d.

(*Continued*)

Table 5.28 Continued

	Provinces												
	Liguria, Italy	Eden	Porndom	Gabier	Duts. Dush.	Franklin	Firmerikh	Hardt	Kilbourne Hall, USA			Hawaii, USA	Japan
	(Vannucci *et al.*, 1993a)	(Irving & Frey, 1984), NAA										(Nagasawa & Schnetzler, 1971)	
	R9/5-9/i	19594	2133a	2182a	DD-2	F4	I/7ad	II/1ad	KH-1	KH-1a	KH-1E	1a	6e
Element	*Basalts*												
La	N.d.	0.750	2.850	3.250	1.670	2.640	7.200	6.900	1.250	1.240	1.240	1.000	1.500
Ce	7.420	2.910	8.800	11.10	5.100	9.300	21.00	21.80	5.400	5.100	5.300	30.00	4.900
Pr	N.d.	0.518	N.d.	N.d.	N.d.	N.d.	3.700	3.700	N.d.	N.d.	N.d.	N.d.	N.d.
Nd	10.03	3.540	7.800	10.00	6.000	9.700	15.00	18.00	5.400	5.500	5.800	N.d.	N.d.
Sm	4.160	1.130	2.860	3.490	2.010	3.880	3.500	3.800	1.800	1.800	1.880	3.800	2.100
Eu	1.380	0.387	1.070	1.360	0.690	1.460	1.120	1.300	0.720	0.710	0.730	0.980	0.820
Gd	6.030	1.810	N.d.	N.d.	N.d.	N.d.	N.d.	N.d.	N.d.	N.d.	N.d.	4.000	3.700
Tb	N.d.	0.260	0.510	0.600	0.340	0.640	0.410	0.440	0.370	0.340	0.420	0.430	0.570
Dy	6.600	N.d.	N.d.	N.d.	N.d.	N.d.	2.350	2.400	N.d.	N.d.	N.d.	N.d.	N.d.
Ho	N.d.	0.280	N.d.	0.600	N.d.	N.d.	N.d.	N.d.	0.370	0.400	0.450	N.d.	N.d.
Er	3.360	1.060	N.d.	N.d.	N.d.	N.d.	0.910	0.890	N.d.	N.d.	N.d.	N.d.	N.d.
Tm	N.d.	N.d.	N.d.	N.d.	N.d.	N.d.	N.d.	N.d.	N.d.	N.d.	N.d.	N.d.	N.d.
Yb	3.260	0.502	0.800	1.340	0.510	0.460	0.580	0.640	1.130	1.030	1.160	0.880	1.700
Lu	N.d.	0.098	0.093	0.180	0.071	0.043	0.084	0.090	0.190	0.190	0.220	0.140	0.250
Total	42.2	13.3	N.d.	31.9	N.d.	N.d.	55.9	60.0	16.6	16.3	17.2	N.d.	N.d.
$(La/Yb)_n$	N.d.	1.01	2.40	1.64	2.21	3.87	8.38	7.28	0.75	0.81	0.72	0.77	0.60

	Provinces												
	Massif Central, France												Alaska, USA
	(Liotard *et al.*, 1988), INAA												(Nagasawa & Schnetzler, 1971)
	f-10	f-11	f-12	f-5	f-6	f-7	f-8	f-9	f-1	f-2	f-3	f-4	5
Element	*Alkaline basalts*												
La	7.600	7.100	6.700	5.300	3.300	11.00	12.70	5.500	6.000	8.900	11.00	7.400	0.750
Ce	22.60	19.20	22.30	17.70	10.00	32.40	38.70	20.30	19.80	32.20	38.60	20.80	4.100
Pr	N.d.	N.d.	N.d.	N.d.	N.d.	N.d.	N.d.	N.d.	N.d.	N.d.	N.d.	N.d.	N.d.
Nd	20.40	15.30	22.00	16.70	8.000	28.50	32.10	20.40	N.d.	N.d.	N.d.	17.20	N.d.
Sm	6.100	4.500	5.800	5.400	3.200	7.300	8.700	6.900	5.700	8.100	9.300	4.800	2.800
Eu	1.980	1.520	1.970	1.900	1.210	2.400	2.780	2.360	1.750	2.670	2.730	1.640	1.200
Gd	N.d.	N.d.	N.d.	N.d.	N.d.	N.d.	N.d.	N.d.	N.d.	N.d.	N.d.	N.d.	4.200
Tb	0.840	0.650	0.830	0.930	0.750	1.070	1.150	1.030	0.600	0.910	0.950	0.820	0.850
Dy	N.d.	N.d.	N.d.	N.d.	N.d.	N.d.	N.d.	N.d.	N.d.	N.d.	N.d.	N.d.	N.d.
Ho	N.d.	N.d.	N.d.	N.d.	N.d.	N.d.	N.d.	N.d.	N.d.	N.d.	N.d.	N.d.	N.d.
Er	N.d.	N.d.	N.d.	N.d.	N.d.	N.d.	N.d.	N.d.	N.d.	N.d.	N.d.	N.d.	N.d.
Tm	N.d.	N.d.	N.d.	N.d.	N.d.	N.d.	N.d.	N.d.	N.d.	N.d.	N.d.	N.d.	N.d.
Yb	1.280	1.270	1.230	1.470	1.050	1.630	2.050	1.610	1.390	2.030	2.280	1.320	2.700
Lu	0.210	0.210	0.190	0.220	0.160	0.280	0.390	0.260	0.220	0.290	0.330	0.200	0.440
Total	61.0	49.8	61.0	49.6	27.7	84.6	98.6	58.4	35.5	55.1	65.2	54.2	17.0
$(La/Yb)_n$	4.01	3.77	3.68	2.43	2.12	4.56	4.18	2.31	2.91	2.96	3.26	3.78	0.19

(*Continued*)

Table 5.28 Continued

	Provinces									
	Gorny Altay, Russia			Mount Adams, USA			Honshu, Japan	Twin Peaks, USA		
	(Safonova, 2005)			(Dunn & Sen, 1994), IPMA			(Nagasawa & Schnetzier, 1971), IDMS	(Nash & Crecraft, 1985), INAA		
	S-1	S-2	S-3	87-7	87-14	87-41	NC-6	12	15	6
Element	*Basalts*			*Andesites*			*Dacites*	*Rhyolites*		
La	0.2	0.3	0.5	15.00	12.00	9.40	N.d.	62.00	68.00	103.0
Ce	1.2	1.5	2.6	38.00	28.00	26.00	19.20	202.0	235.0	331.0
Pr	N.d.	N.d.	N.d.	6.30	4.30	4.60	N.d.	N.d.	N.d.	N.d.
Nd	2.2	3.0	3.9	33.00	25.00	27.00	25.90	157.0	164.0	224.0
Sm	1.4	1.9	3.4	9.60	8.10	8.90	9.90	36.00	36.00	47.00
Eu	0.5	0.7	0.8	1.50	0.96	1.50	1.67	3.38	3.30	3.16
Gd	1.4	2.8	3.0	10.00	13.00	10.00	N.d.	N.d.	N.d.	N.d.
Tb	N.d.	N.d.	N.d.	1.60	1.60	1.50	N.d.	5.30	5.70	7.60
Dy	2.4	3.6	4.2	11.00	11.00	11.00	18.20	34.00	36.00	49.00
Ho	N.d.	N.d.	N.d.	2.20	2.10	2.10	N.d.	N.d.	N.d.	N.d.
Er	1.9	2.6	3.2	6.20	6.50	6.00	9.20	N.d.	N.d.	N.d.
Tm	N.d.	N.d.	N.d.	0.89	0.89	0.80	N.d.	N.d.	N.d.	N.d.
Yb	1.6	2.3	3.3	5.40	5.60	5.00	8.60	17.90	18.30	33.60
Lu	N.d.	N.d.	N.d.	0.86	1.00	0.72	1.34	2.40	2.50	4.90
Total	12.8	18.7	24.9	142	120	115	N.d.	N.d.	N.d.	N.d.
$(La/Yb)_n$	0.08	0.09	0.10	1.87	1.45	1.27	N.d.	2.34	2.51	2.07

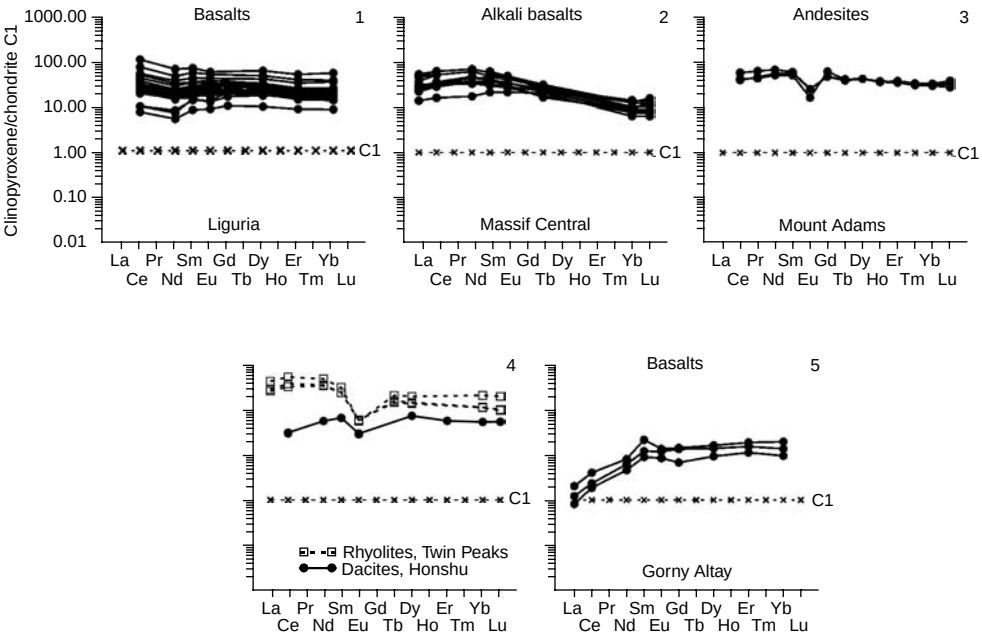

Figure 5.24 Chondrite-normalized REE patterns for clinopyroxenes from basalts, dacites, and rhyolites, represented in some volcanic complexes (data Table 5.28).

complex differs from samples of this mineral from basalts by having a higher level of REE accumulation and a deficit of Eu (Fig. 5.24, 3). Clinopyroxene from dacites of the Honshu Island complex, by the level of REE accumulation and intensity of the negative Eu anomaly, is similar to the mineral from andesite of the Mount Adams complex, but the level of Yb accumulation in it is higher than that of Ce (Fig. 5.24, 4). Having studied clinopyroxenes from trachydolerites, tholeiites, and porphyritic melanephelinites from the Krestovsky massif (Meimecha-Kotuy province, Russia) and presented in them melt inclusions, Panina & Usol'tseva (2009) have shown that these clinopyroxenes are essentially enriched with incompatible elements, especially light and middle REE concerning heavy elements. It is supposed that these rocks crystallized, at least, from three types of the magmas generated on the various depths. Finally, clinopyroxene from porphyry phenocrysts of the Twin Peaks complex was found to have the highest level of REE accumulation among the samples of this mineral from all parageneses characterized above (Fig. 5.24, 4).

Results of analyses of clinopyroxenes (Tables 5.12–5.28) were used in the calculations of average REE content in clinopyroxenes from the varieties of ultramafic, mafic, and some other plutonic and volcanogenic rocks that compose various massifs and complexes (Table 5.29). These average values must be regarded as approximations because, firstly, many of the particular samplings are limited in volume and, secondly, within more representative samplings of analyses, the static distribution of the contents of elements do not always meet the criteria of normal law. Nevertheless, the obtained

Table 5.29 Average rare earth element composition of clinopyroxenes from various type of rocks (ppm).

	Massifs (provinces)										
Element	1 (6)	2 (3)	3 (5)	4 (4)	5 (4)	6 (3)	7 (2)	8 (21)	9 (2)	10 (9)	11 (2)
La	0.05	1.65	1.31	0.87	0.04	0.15	0.08	0.47	0.02	0.05	1.61
Ce	0.09	3.91	5.85	3.68	0.09	4.17	2.18	1.52	0.05	0.07	4.69
Pr	N.d.	N.d.	N.d.	N.d.	0.079	N.d.	N.d.	N.d.	N.d.	N.d.	N.d.
Nd	0.05	3.44	5.90	4.05	0.96	2.23	2.07	1.96	0.12	0.03	2.80
Sm	0.10	1.35	2.44	1.86	0.91	0.84	1.02	0.983	0.09	0.02	0.72
Eu	0.07	0.55	0.85	0.63	0.41	0.37	0.47	0.42	0.05	0.02	0.24
Gd	N.d.	N.d.	N.d.	N.d.	2.043	N.d.	N.d.	1.683	N.d.	N.d.	N.d.
Tb	N.d.	0.387	N.d.	N.d.	0.438	0.325	0.400	N.d.	N.d.	N.d.	N.d.
Dy	0.87	N.d.	2.94	2.54	N.d.	N.d.	N.d.	2.21	0.36	0.26	0.48
Ho	N.d.	0.510	N.d.	N.d.	0.713	N.d.	N.d.	N.d.	N.d.	N.d.	N.d.
Er	0.65	N.d.	1.79	1.50	2.16	N.d.	N.d.	1.40	0.31	0.21	0.27
Tm	N.d.	N.d.	N.d.	N.d.	0.323	N.d.	N.d.	N.d.	N.d.	N.d.	N.d.
Yb	0.68	1.32	1.73	1.39	1.72	1.44	1.53	1.37	0.30	0.25	0.34
Lu	N.d.	0.26	N.d.	N.d.	0.30	0.30	0.28	N.d.	N.d.	N.d.	N.d.
Total	N.d.	N.d.	N.d.	N.d.	10.2	N.d.	N.d.	N.d.	N.d.	N.d.	N.d.
$(La/Yb)_n$	0.05	4.71	0.52	0.54	0.02	0.07	0.04	0.26	0.03	0.17	3.10
	12 (2)	13 (2)	14 (5)	15 (2)	16 (2)	17 (5)	18 (13)	19 (2)	20 (10)	21 (22)	22 (2)
La	0.86	0.11	0.37	0.82	1.23	1.37	1.37	0.31	0.42	N.d.	0.05
Ce	2.91	0.43	0.72	1.63	4.79	3.30	5.53	1.39	1.71	3.94	0.20
Pr	N.d.	N.d.	N.d.	N.d.	N.d.	N.d.	N.d.	N.d.	N.d.	N.d.	N.d.
Nd	4.35	0.44	0.46	1.78	4.08	3.26	6.43	3.10	2.37	6.15	0.42
Sm	1.84	0.18	0.20	1.37	1.53	1.16	2.35	0.65	1.33	2.91	0.28
Eu	0.65	0.08	0.08	0.64	0.46	0.44	0.88	0.37	0.46	1.13	0.12
Gd	N.d.	0.32	0.28	N.d.	N.d.	1.28	3.08	N.d.	1.93	6.12	N.d.
Tb	0.69	0.08	0.06	0.42	N.d.	N.d.	N.d.	0.10	N.d.	N.d.	N.d.
Dy	N.d.	N.d.	N.d.	N.d.	2.50	1.29	3.55	N.d.	2.91	13.46	0.71
Ho	N.d.	N.d.	N.d.	N.d.	N.d.	N.d.	N.d.	N.d.	N.d.	N.d.	N.d.
Er	N.d.	N.d.	N.d.	N.d.	1.32	0.81	2.02	N.d.	1.34	12.43	0.50
Tm	N.d.	0.08	0.04	N.d.	N.d.	N.d.	N.d.	N.d.	N.d.	N.d.	N.d.
Yb	1.72	0.58	0.25	1.42	1.15	0.99	1.91	0.12	1.00	15.53	0.45
Lu	0.27	0.09	0.04	0.29	N.d.	N.d.	N.d.	0.02	N.d.	N.d.	N.d.
Total	N.d.	N.d.	N.d.	N.d.	17.0	12.5	27.0	N.d.	12.9	55.8	2.7
$(La/Yb)_n$	0.29	0.16	0.88	0.50	0.66	1.46	0.50	1.69	0.95	N.d.	0.08
	23 (3)	24 (8)	25 (5)	26 (11)	27 (4)	28 (2)	29 (6)	30 (2)	31 (2)	32 (3)	33 (3)
La	8.22	0.03	3.14	0.05	0.23	0.25	0.38	0.24	1.63	7.44	0.42
Ce	13.71	0.14	14.80	0.23	1.75	1.36	0.82	0.81	9.59	25.40	1.85
Pr	N.d.	N.d.	2.28	N.d.	N.d.	N.d.	N.d.	N.d.	N.d.	N.d.	N.d.
Nd	11.24	0.28	12.18	0.44	1.98	2.28	0.77	0.87	8.04	24.53	1.33
Sm	2.72	0.17	3.66	0.31	1.06	1.31	0.27	0.42	3.88	10.33	0.75
Eu	0.85	N.d.	1.13	0.14	0.42	0.47	0.18	0.34	1.92	3.08	0.46
Gd	3.76	N.d.	3.10	N.d.	1.65	2.01	0.62	1.65	5.65	11.77	1.46
Tb	0.72	N.d.	0.31	N.d.	0.36	N.d.	0.10	0.37	1.49	2.29	0.27
Dy	N.d.	0.41	2.06	0.93	2.50	2.54	0.57	N.d.	N.d.	N.d.	1.49
Ho	N.d.	N.d.	0.30	N.d.	N.d.	N.d.	N.d.	N.d.	N.d.	N.d.	N.d.
Er	N.d.	0.24	0.87	0.59	N.d.	1.55	N.d.	N.d.	N.d.	N.d.	N.d.
Tm	0.34	N.d.	0.09	N.d.	0.22	N.d.	0.06	0.21	0.89	1.00	0.17
Yb	2.13	0.23	0.69	0.61	1.30	1.59	0.40	1.32	8.80	6.42	0.94
Lu	0.31	N.d.	0.07	N.d.	0.19	N.d.	0.06	0.20	1.01	0.82	0.16
Total	N.d.	N.d.	44.4	N.d.	11.7	13.5	3.77	N.d.	N.d.	N.d.	9.29
$(La/Yb)_n$	2.65	0.09	3.05	0.05	0.12	0.11	0.64	0.12	0.12	0.78	0.30

Table 5.29 Continued

	Massifs (provinces)												
Element	34 (11)	35 (3)	36 (4)	37 (6)	38 (2)	39 (11)	40 (3)	41 (2)	42 (2)	43 (27)	44 (3)	45 (3)	46 (48)
La	N.d.	4.867	0.400	6.830	2.685	7.736	1.243	1.050	N.d.	N.d.	0.3	12.1	N.d.
Ce	35.65	22.67	2.53	17.55	13.11	24.89	5.27	3.80	23.15	7.36	1.8	30.7	0.072
Pr	N.d.	N.d.	N.d.	N.d.	N.d.	N.d.	N.d.	N.d.	N.d.	N.d.	N.d.	5.07	N.d.
Nd	35.14	20.67	4.58	22.98	23.19	20.43	5.57	4.50	20.10	9.70	3.0	28.3	0.569
Sm	9.16	6.37	2.35	7.79	10.60	6.46	1.87	1.59	10.16	3.76	2.2	8.87	0.613
Eu	3.68	1.43	0.78	2.41	2.98	2.12	0.72	0.61	0.85	1.40	0.7	1.32	0.305
Gd	N.d.	7.90	3.60	10.73	15.73	N.d.	N.d.	N.d.	13.15	4.52	2.4	11.0	N.d.
Tb	N.d.	1.31	N.d.	N.d.	N.d.	0.88	0.38	0.32	N.d.	N.d.	N.d.	1.57	N.d.
Dy	5.75	N.d.	4.32	8.21	18.52	N.d.	N.d.	N.d.	17.55	6.15	3.4	11.0	1.992
Ho	N.d.	1.533	N.d.	N.d.	N.d.	N.d.	0.407	N.d.	N.d.	N.d.	N.d.	2.13	N.d.
Er	2.82	N.d.	2.37	4.04	10.65	N.d.	N.d.	N.d.	10.42	3.35	2.6	6.23	1.223
Tm	N.d.	N.d.	N.d.	N.d.	N.d.	N.d.	N.d.	N.d.	N.d.	N.d.	N.d.	0.86	N.d.
Yb	2.63	3.07	2.21	4.01	10.59	1.57	1.11	0.50	9.59	3.31	2.4	5.33	1.248
Lu	N.d.	N.d.	N.d.	N.d.	N.d.	0.25	0.20	0.07	1.52	N.d.	N.d.	0.86	N.d.
Total	N.d.	69.8	23.1	69.9	108	N.d.	16.7	N.d.	106	37.4	18.8	125	5.93
$(La/Yb)_n$	N.d.	1.07	0.12	1.13	0.17	3.32	0.76	1.42	N.d.	N.d.	0.10	1.54	N.d.

Data Tables 5.12–5.28. 1—spinel lherzolites, Troodos (Cyprus) (Sobolev & Batanova, 1995); 2—spinel lherzolites, Lherz (France) (Bodinier *et al.*, 1988); 3—plagioclase-bearing lherzolites, Horoman (Japan) (Frey *et al.*, 1991); 4—lherzolites, Horoman (Japan) (Frey *et al.*, 1991); 5—lherzolites, Lizard (England) (Frey, 1969); 6—lherzolites, Balmuccia (Italy) (Ottonello *et al.*, 1984); 7—lherzolites, Baldissero (Italy) (Ottonello *et al.*, 1984); 8—peridotites, Balmuccia (Italy) (Rivalenti *et al.*, 1995); 9—clinopyroxenes-bearing dunites, Troodos (Cyprus) (Batanova *et al.*, 1996); 10—clinopyroxenes-bearing harzburgites, Troodos (Cyprus) (Sobolev & Batanova, 1995); 11—clinopyroxenes-bearing harzburgites, Horoman (Japan) (Frey *et al.*, 1991); 12—garnet-bearing websterites, Lherz, (France) (Bodinier *et al.*, 1987); 13—websterites, Beriozovsky, Sakhalin Island (Russia) (Lesnov & Gora, 1998); 14—websterites, Naransky (Mongolia) (Lesnov & Gora, 1998); 15—websterites, Freychinede (France) (Bodinier *et al.*, 1987); 16—websterites, Stillwater, Montana (USA) (Papike *et al.*, 1995); 17—websterites, Beni Bousera (Morocco) (Pearson *et al.*, 1993); 18—websterites, Balmuccia (Italy) (Rivalenti *et al.*, 1995); 19—garnet-bearing pyroxenites, Lherz (France) (Bodinier *et al.*, 1988); 20—garnet-bearing pyroxenites, Beni Bousera (Morocco) (Pearson *et al.*, 1993); 21—pyroxenites, Zabargad Island (Red sea) (Vannucci *et al.*, 1993a,b); 22—olivine-bearing pyroxenites, Troodos (Cyprus) (Batanova *et al.*, 1996); 23—wehrlites, Dovyrensky, North Transbaikalia (Russia) (author's data); 24—picrites, Troodos (Cypros) (Sobolev *et al.*, 1996); 25—lamprofyres, Budgel Har, Newfoundland (Foley *et al.*, 1996); 26—olivine gabbros, Troodos (Cyprus) (Batanova *et al.*, 1996); 27—olivine gabbros, Samail (Oman) (Pallister & Knight, 1981); 28—olivine gabbros, Riparbello (Italy) (Tiepolo *et al.*, 1997); 29—gabbro-norites, Beriozovsky, Sakhalin Island (Russia) (Lesnov & Gora, 1998); 30—gabbronorites, Sheltingsky, Sakhalin Island (Russia) (Lesnov & Gora, 1998); 31—gabbro-norites, Shikotansky, Kuril Islands (Russia) (Lesnov & Gora, 1998); 32—gabbro-norites, Rybinsky, Kuznetsky Altay (Russia) (Lesnov & Gora, 1998); 33—gabbro-norites, Karaginsky Island, Kamchatka (Russia) (Lesnov & Gora, 1998); 34—gabbro, Ivrea Verbano (Italy) (Mazzucchelli *et al.*, 1992a,b); 35—gabbro, Skaergaard (Greenlandia) (Paster *et al.*, 1974); 36—gabbro, Liguria (Italy) (Tribuzio *et al.*, 1995); 37—gabbro, Ivrea Verbano (Italy) (Mazzucchelli *et al.*, 1992a,b); 38—diorites, Bracco (Italy) (Tiepolo *et al.*, 1997); 39—alkaline basalts, Massif Central (France) (Liotard *et al.*, 1988); 40—basalts, Kilbourne Hall (USA) (Irving & Frey, 1984); 41—basalts, Vilcha (Irving & Frey, 1984); 42—basalts, Moon (Philpotts & Schnetzler, 1970); 43—basalts, Liguria (Italy) (Vannucci *et al.*, 1993a,b); 44—basalts, Kuray zone, Gorny Altay (Russia) (Safonova, 2005); 45—andesites, Mount Adams (USA) (Dunn & Sen, 1994); 46—lherzolites, Indian Ocean (Johnson & Dick, 1992).

average values of the rare earth compositions of clinopyroxenes from rocks with different compositions and genesis suggest that among the diversity of paragenetic types of clinopyroxenes there are three major types: (1) REE enriched; (2) moderately enriched; and (3) depleted. Obviously the three groups of clinopyroxenes crystallized from melts with substantially different chemical and rare earth compositions and under a very wide range of P–T conditions.

The REE patterns reflecting the distribution of average contents of the elements in the corresponding paragenetic types of clinopyroxenes provide an idea of the most significant differences in the REE composition of pyroxenes that are exhibited in samples from most magmatic rocks they compose (Fig. 5.25). Within the whole series of characterized paragenetic types of clinopyroxenes, the total contents of REE range from 10 to 125 ppm. The patterns of distribution of average contents of elements in most of them have a positive slope, that is, $(La/Yb)_n$ is greater than unity. In very few clinopyroxene samples, this parameter has increased values with a maximum of 4.7. The paragenetic types of clinopyroxenes enriched with REE includes, for example, their samples from pyroxenites from the massif of Zabargad Island, wehrlites from the Dovyrensky massif, lamprophyres from the Budgel Har complex, gabbro-norites from the Shikotansky and Rybinsky massifs, gabbros from the Ivrea Verbano and Skaergaard massifs, diorites from the Bracco complex, basalts from the Central massif (France), lunar basalts, andesites from the Mount Adams complex, and rhyolites from the Twin Peaks complex. REE-depleted clinopyroxenes occur in dunites, harzburgites, lherzolites, pyroxenites, and gabbros of the Troodos massif, in harzburgites of the Horoman massif, and in websterites of the Beriozovsky and Naransky massifs. Especially depleted of light REE are clinopyroxenes from ultramafic rocks in the Troodos and Lizard massifs and from the samples dredged from the Indian Mid-Oceanic Ridge, which suggests their crystallization from extremely depleted melts, which could generate on repeated melting of preliminarily depleted sources.

5.3.2 Coefficients of REE distribution between clinopyroxenes and coexisting phases

Studies on the estimation of coefficients of REE distribution between coexisting phases have always been given special attention because they provide a possibility for solving many important problems of the petrology of magmatic rocks, including determination of generation conditions for different types of rocks and minerals, modeling of generation and crystallization processes of magmatic melts, and more. (Zharikov & Yaroshevskii, 2003). Of primary importance are data on the distribution coefficients from clinopyroxenes, as this mineral occurs in a wide range of natural magmatic formations and in many crystallization products of melts in physical experiments.

Clinopyroxene crystals at different stages of formation of rocks were in intimate contact with their parental melts and with coexisting solid phases, mainly crystals of olivine, orthopyroxene, plagioclase, amphibole, garnet, and chrome-spinel. During long-term crystallization of melts owing to redistribution of major and trace elements, the system "clinopyroxene–coexisting phase" reached a state close to chemical equilibrium. At rather high cooling rates of melts and, hence, at shorter periods of crystallization of mineral phases and initial-melt assimilation of xenogeny material of different origin, no complete chemical equilibrium was attained between the phases. The chemical equilibrium between clinopyroxene crystals and melts, as well as coexisting minerals, and the absence of subsolidus redistribution of elements, caused by different reasons, is an important prerequisite for obtaining correct estimates of K_d(clinopyroxene/coexisting phase) for trace elements. Let us focus on a brief consideration of some data and concepts of K_d(REE) with the participation of clinopyroxenes.

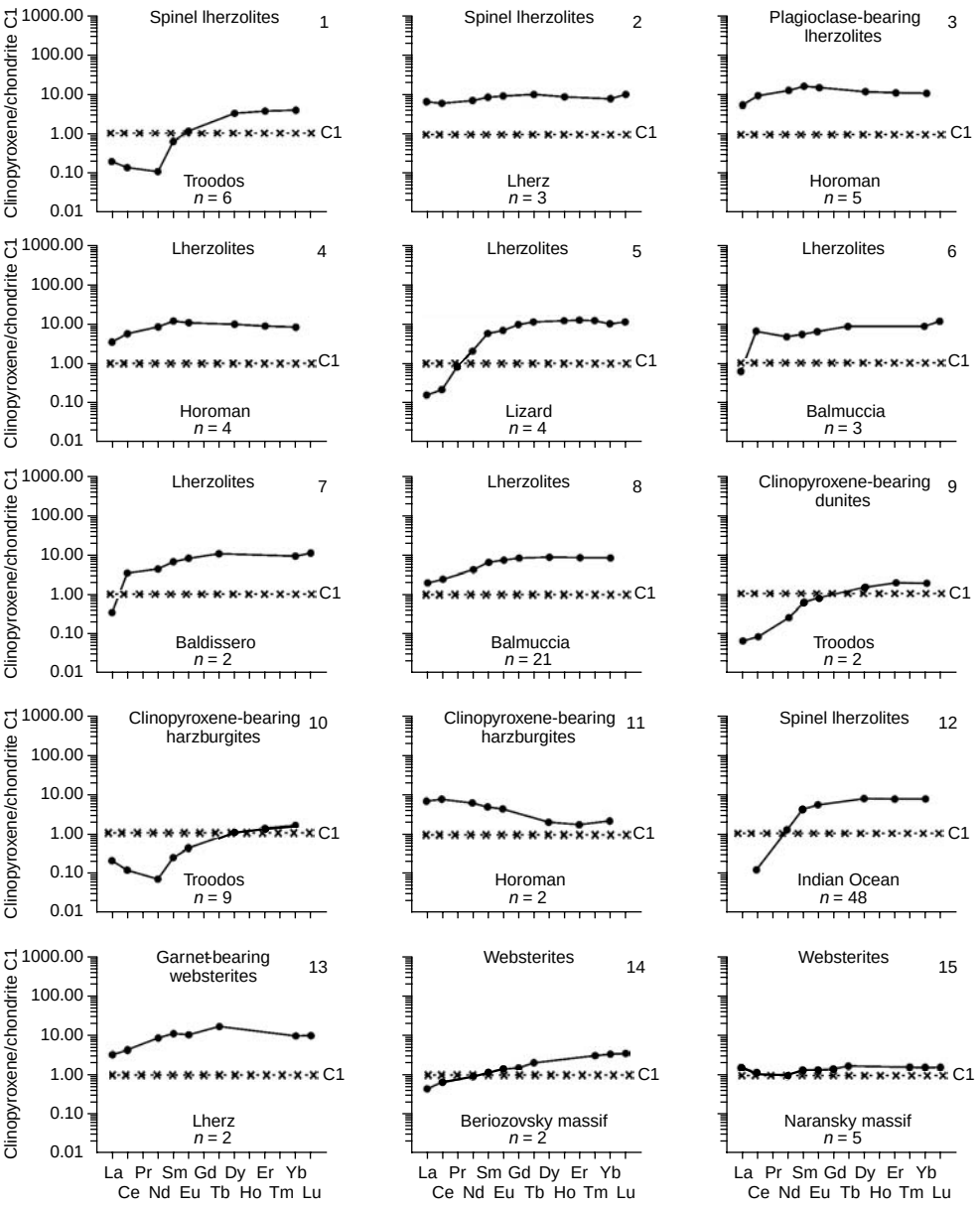

Figure 5.25 Chondrite-normalized patterns for average REE composition of clinopyroxenes from some types of rock (data Table 5.29).

K_d*(clinopyroxene/melt)*. The first estimates of these coefficients were obtained in the studies of REE distribution between porphyry inclusions of clinopyroxene and the groundmass of effusive rocks containing them. However, with further improvement in techniques for determination of REE, for these purposes, more and more

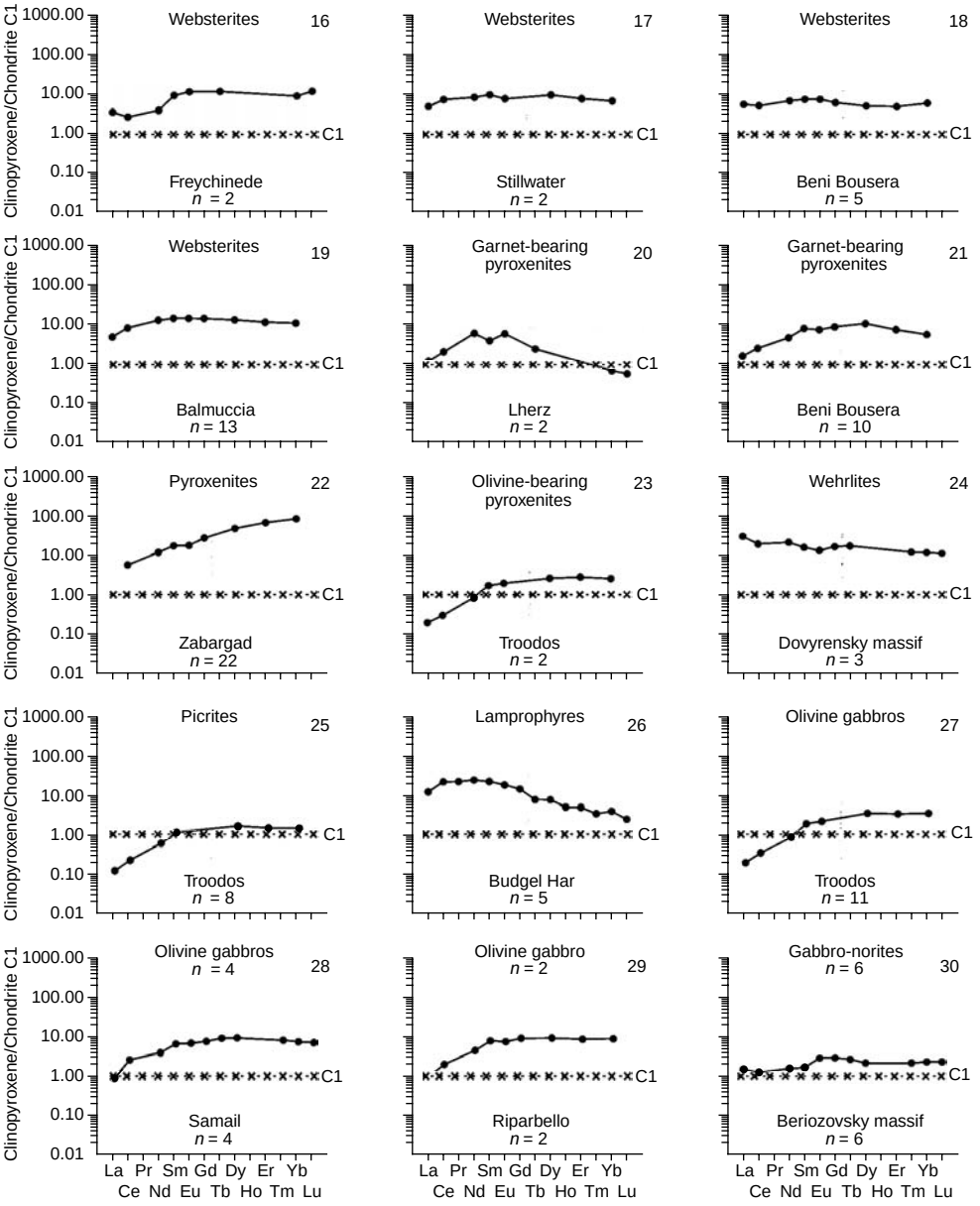

Figure 5.25 Continued

frequently the results of physical experiments with crystallization of melts at different compositions and different P–T conditions are used (Green, 1994). It has already been emphasized that clinopyroxenes are the most important REE concentrators in ultramafic, mafic, and some other igneous rocks. According to existing concepts, the value

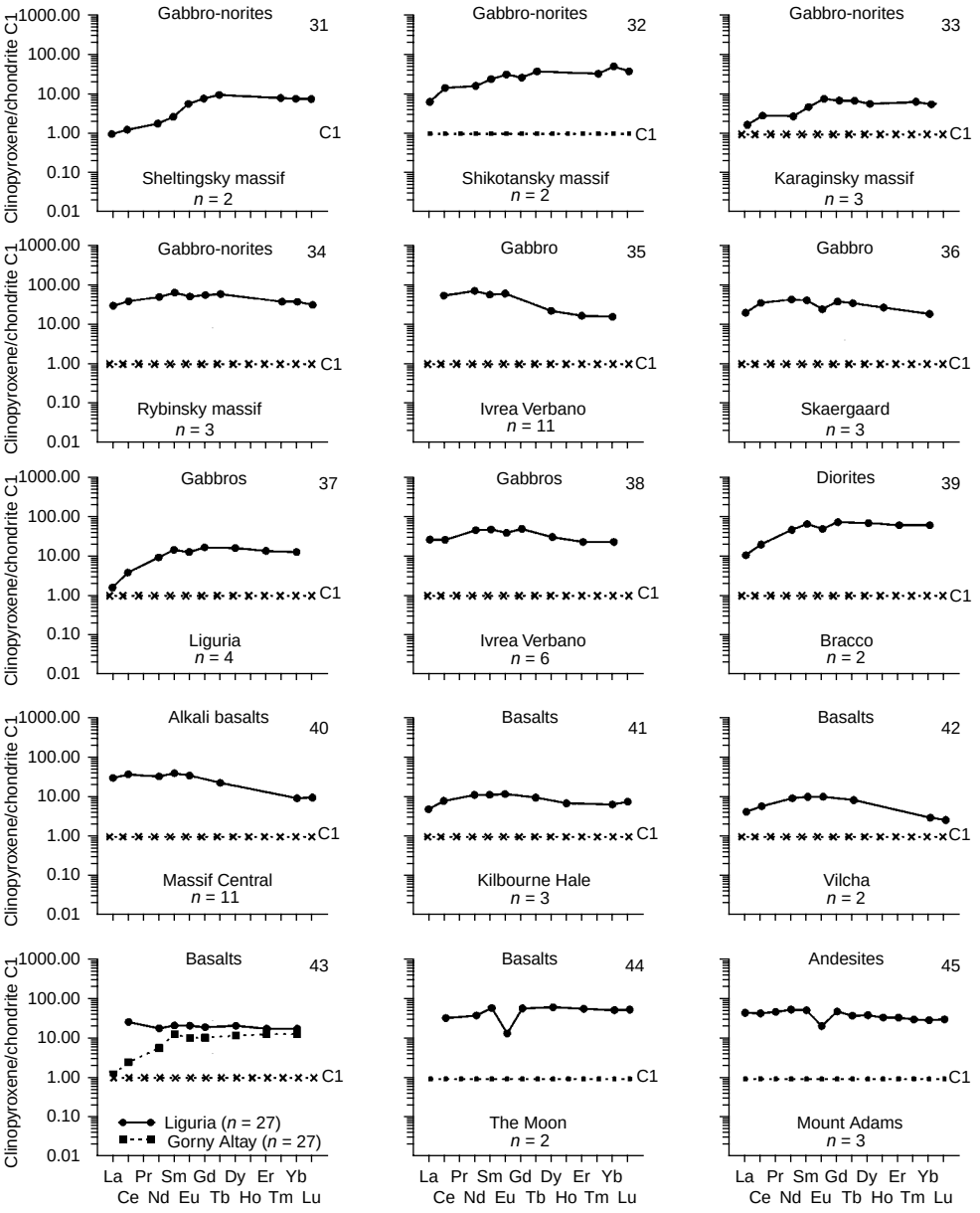

Figure 5.25 Continued

of K_d(clinopyroxene/melt) to some extent depends on a number of factors. The most important of them are: (1) the crystallochemical properties of clinopyroxenes; (2) the degree of oxidation (redox conditions) and the ratio of sizes of ionic radii of replacing REE and replaced ions of net-forming elements; (3) the chemical composition of

parental melts, including, their contents of alkalis; (4) temperature; (5) crystallization pressure; and (6) the sequence of separation of coexisting phases (Balashov, 1976).

Some values of K_d(clinopyroxene/melt) for picrite, basalt, and andesite melts obtained in physical experiments with fixed P–T conditions are reported in Table 5.30. Some of them were obtained on the basis of the REE compositions of clinopyroxene phenocrysts and contained melt microinclusions (Sobolev *et al.*, 1996; Safonova, 2005). The representative experimental summary on these K_d was published by Green (1994), but the data are presented only in a graphic form. Judging from these data, the values of K_d(clinopyroxene/melt) for heavy REE are higher (~0.15–0.8) than the K_d for light REE (~0.02–0.15). For all REE, the K_d for clinopyroxenes is higher than the respective values of K_d for olivines, orthopyroxenes, and plagioclases (except Eu). On the plots presented in the works by Green, the generalized trend of changes in K_d(clinopyroxene/melt) has a positive slope, steeper on the segment from La to Sm and rather gentle on the segment from Sm to Lu. Green points out that the values of K_d(clinopyroxene/melt) have an inversely proportional dependence on crystallization temperature but a directly proportional dependence on SiO_2 content in the melt and on the amount of wollastonite end member in clinopyroxene. Referring to McKay *et al.* (1986), he notes that κd(La) values have a stronger positive dependence on the amount of wollastonite end member than do K_d(Lu) values. His observations show that for silica-rich melts, the values of K_d(clinopyroxene/melt) somewhat increase with increasing temperature, whereas basalt melts have an inverse dependence; K_d values slightly decrease with increasing pressure.

In picrites, basalts, and andesites melts, all REE, have K_d values less than unity, whereas in dacite melts the elements from Sm to Lu, K_d values are greater than unity (Table 5.30). Hence, on crystallization of clinopyroxenes from picrites, basalts, and andesites melts, all REE display the properties of incompatible impurities, and in dacites systems, the elements from Sm to Lu have features typical of trace elements. It is worth noting that in numerical modeling of REE compositions of those melts, from which clinopyroxene-bearing rocks could crystallize, selection of the best values of K_d(clinopyroxene/melt) is the most significant operation.

Let us consider some data on the values of K_d(clinopyroxene/coexisting phase) that were calculated using associated analyses of these minerals from different rocks.

K_d(clinopyroxene/olivine). The level of accumulation of all REE in clinopyroxenes is always much higher than that in coexisting olivines, so in all cases the values of these K_d are greater than unity. The trends of changes in distribution coefficients for different types of rocks and their massifs normally to some extent differ in configuration and location on the plots (Table 5.31). For garnet lherzolites, the K_d of all elements have rather low values (6–10). In spinel lherzolites, the values of K_d(Sm) and K_d(Eu) are much higher than those for La and Ce. On the trends of K_d for lherzolites from deep xenoliths of the provinces Itinome–Gata and British Columbia, one can observe maximums in the region of middle REE. Rather high values of K_d(clinopyroxene/olivine) for light elements in lherzolites from deep xenoliths are due to the fact that both of these minerals contain nearly the same amounts of these trace elements, which are presented not in isomorphous form but in nonstructural form.

K_d(clinopyroxene/orthopyroxene). Owing to the clinopyroxene property to accumulate greater amounts of impurity elements in its structure, compared to orthopyroxene, their typical values of κd are greater than unity. Some features of REE

Table 5.30 Coefficients of REE distribution between clinopyroxenes and coexisting melts.

	Melts										
	Picrites[a]								Basalts[a]		
	(Sobolev *et al.*, 1996)								Calculated by data (Safonova, 2005)		
Element	135/1	135/3	191/9	191/13	133/15	6200/16	200/19	200/20	C-80A-04-1	C-80A-04-2	C-80A-04-3
La	0.027	0.039	0.049	0.027	0.028	0.015	0.030	0.041	0.057	0.085	0.142
Ce	0.053	0.054	0.081	0.057	0.058	0.033	0.044	0.075	0.100	0.125	0.216
Pr	N.d.	N.d.	N.d.	N.d.	N.d.	N.d.	N.d.	N.d.	N.d.	N.d.	N.d.
Nd	0.100	0.092	0.201	0.147	0.128	0.078	0.089	0.197	0.198	0.270	0.351
Sm	0.167	0.127	0.351	0.246	0.107	0.162	0.181	0.345	0.318	0.432	0.773
Eu	N.d.	N.d.	N.d.	N.d.	N.d.	N.d.	N.d.	N.d.	0.349	0.488	0.558
Gd	N.d.	N.d.	N.d.	N.d.	N.d.	N.d.	N.d.	N.d.	0.301	0.602	0.645
Tb	N.d.	N.d.	N.d.	N.d.	N.d.	N.d.	N.d.	N.d.	N.d.	N.d.	N.d.
Dy	0.197	0.169	0.374	0.342	0.236	0.128	0.206	0.399	0.393	0.590	0.689
Ho	N.d.	N.d.	N.d.	N.d.	N.d.	N.d.	N.d.	N.d.	N.d.	N.d.	N.d.
Er	0.188	0.198	0.399	0.302	0.212	0.131	0.220	0.421	0.386	0.529	0.651
Tm	N.d.	N.d.	N.d.	N.d.	N.d.	N.d.	N.d.	N.d.	N.d.	N.d.	N.d.
Yb	0.151	0.167	0.299	0.276	0.169	0.118	0.195	0.341	0.336	0.483	0.692
Lu	N.d.	N.d.	N.d.	N.d.	N.d.	N.d.	N.d.	N.d.	N.d.	N.d.	N.d.

(*Continued*)

Table 5.30 Continued

	Melts						
	Basalts[b]						
	(Kuechner *et al.*, 1989)		(Johnson, 1998)	(Cox *et al.*, 1982)	(Mysen, 1978)		(Dostal & Muecke, 1978)
Element	Dmin1	Drim1	Jcpx	cpx/m	cpx1/max	cpx1/min	Dcpx
La	0.084	0.130	0.050	N.d.	N.d.	N.d.	0.035
Ce	N.d.	N.d.	0.072	0.100	0.296	0.296	0.043
Pr	N.d.	N.d.	N.d.	N.d.	N.d.	N.d.	N.d.
Nd	N.d.	N.d.	0.177	N.d.	N.d.	N.d.	N.d.
Sm	0.340	0.530	0.281	0.260	0.700	0.490	0.090
Eu	N.d.	N.d.	N.d.	0.200	N.d.	N.d.	0.091
Gd	N.d.	N.d.	N.d.	N.d.	N.d.	N.d.	0.095
Tb	N.d.	N.d.	N.d.	N.d.	N.d.	N.d.	N.d.
Dy	N.d.	N.d.	0.420	N.d.	N.d.	N.d.	0.105
Ho	N.d.	N.d.	N.d.	N.d.	N.d.	N.d.	N.d.
Er	N.d.	N.d.	0.360	N.d.	N.d.	N.d.	0.107
Tm	N.d.	N.d.	N.d.	N.d.	0.414	0.414	N.d.
Yb	0.340	0.530	0.432	0.280	N.d.	N.d.	0.092
Lu	N.d.	N.d.	0.439	N.d.	N.d.	N.d.	0.071

	Melts						
	Basaltic[b]					Andesitic[b]	Dacitic[b]
	(Grutzeck *et al.*, 1974)	(Lundstrom *et al.*, 1998)		(Harrison, 1981)		(Grutzeck *et al.*, 1974)	(Nagasawa & Schnetzler, 1971)
Element	Adil	Di65	Di55	cp2ma	cpx2mi	DbDi/L	NC-6
La	0.069	0.063	0.056	N.d.	N.d.	0.095	N.d.
Ce	0.098	N.d.	N.d.	0.510	0.206	0.120	0.362
Pr	N.d.	N.d.	N.d.	N.d.	N.d.	N.d.	N.d.
Nd	0.210	0.180	0.160	N.d.	N.d.	0.240	0.940
Sm	0.260	0.270	0.220	0.513	0.250	0.320	1.520
Eu	0.310	N.d.	N.d.	N.d.	N.d.	0.360	1.110
Gd	0.300	0.280	0.250	N.d.	N.d.	0.380	N.d.
Tb	N.d.	N.d.	N.d.	N.d.	N.d.	N.d.	N.d.
Dy	0.330	N.d.	N.d.	N.d.	N.d.	0.370	2.630
Ho	N.d.	N.d.	N.d.	N.d.	N.d.	N.d.	N.d.
Er	0.300	N.d.	N.d.	N.d.	N.d.	0.370	2.250
Tm	N.d.	N.d.	N.d.	0.310	0.216	N.d.	N.d.
Yb	N.d.	0.230	0.220	N.d.	N.d.	N.d.	2.010
Lu	0.280	N.d.	N.d.	N.d.	N.d.	0.420	1.810

[a] According to studied results of melting inclusions in clinopyroxenes.
[b] Data of physical experiments.

Table 5.31 Coefficients of REE distribution between clinopyroxenes and coexisting olivines.

	Massifs (provinces)													
	Kapfenstein, Austria		Shavaryn Tsaram, Mongolia	Pipe Udachnaya, Russia	Lherz, France		Shavaryn Tsaram, Mon.	Data of physical experiments				Erdeny, Mongolia	Naransky, Mongolia	Lizard, England
	Ka111	Ka168	Sh-21	O-ET	70-367	71-321	200-81	16112.29	161120	161137.7	16118	1133v	705b	90681d
Element	*Spinel lherzolites*						*Garnet lherzolites*					*Lherzolites*		
La	41	27	10	2.6	38	35	3.4	N.d.	N.d.	N.d.	N.d.	131	39	0.23
Ce	N.d.	N.d.	5.7	2.3	76	37	7.8	7.3	7.0	10	7.58	134	10	0.24
Pr	N.d.	N.d.	10	N.d.	N.d.	N.d.	14	N.d.	N.d.	N.d.	N.d.	296	18	0.82
Nd	N.d.	N.d.	10	1.7	N.d.	N.d.	41	N.d.	N.d.	N.d.	N.d.	460	26	2.6
Sm	254	583	46	1.7	233	346	82	8.4	8.4	7.4	9.29	840	113	32
Eu	N.d.	138	21	3.4	295	N.d.	56	N.d.	N.d.	N.d.	N.d.	1261	90	174
Gd	N.d.	N.d.	48	N.d.	N.d.	N.d.	68	N.d.	N.d.	N.d.	N.d.	500	33	N.d.
Tb	N.d.	N.d.	4.2	3.7	N.d.	N.d.	57	N.d.	N.d.	N.d.	N.d.	79	35	N.d.
Dy	N.d.	N.d.	49	N.d.	N.d.	N.d.	74	N.d.	N.d.	N.d.	N.d.	74	20	N.d.
Ho	N.d.	N.d.	32	N.d.	N.d.	N.d.	47	N.d.	N.d.	N.d.	N.d.	71	164	174
Er	N.d.	N.d.	42	N.d.	N.d.	N.d.	6.4	N.d.	N.d.	N.d.	N.d.	57	30	135
Tm	N.d.	N.d.	15	4.7	N.d.	N.d.	30	5.9	7.0	6.8	6.42	50	20	110
Yb	49	43	15	4.9	201	90	23	N.d.	N.d.	N.d.	N.d.	152	22	107
Lu	55	21	1.6	4.8	N.d.	N.d.	7.5	N.d.	N.d.	N.d.	N.d.	226	13	45

	Massifs (provinces)												
	Lizard, England	British Columbia, Canada								Itinome–Gata, Japan		Kamperdaun	Eifel, Germany
	90683d	BM-11	JL-14	JL-15	JL-18	KR-1	KR-2	KR-35	LL-1	LL-14	2L	3L	20	57
Element	*Lherzolites*													
La	0.16	17	3.8	14	120	17	2.7	23	50	49	4.3	2.4	N.d.	N.d.
Ce	1.9	20	8.9	21	163	15	2.2	50	60	43	10	3.1	114	29
Pr	12	26	20	39	227	25	1.7	65	67	53	N.d.	N.d.	N.d.	N.d.
Nd	35	38	35	60	214	21	2.0	149	90	38	32	23	192	61
Sm	100	74	75	190	219	39	3.8	183	182	100	64	56	206	62
Eu	157	127	N.d.	129	148	N.d.	N.d.	N.d.	N.d.	70	139	127	230	0.39
Gd	130	186	249	301	218	76	7.8	293	123	230	109	89	N.d.	96
Tb	140	157	N.d.	225	N.d.	N.d.	N.d.	N.d.	N.d.	50	N.d.	N.d.	N.d.	N.d.
Dy	N.d.	200	172	164	212	108	36	393	154	88	135	100	239	88
Ho	11	197	N.d.	117	N.d.	N.d.	29	N.d.	63	80	N.d.	N.d.	N.d.	N.d.
Er	68	192	107	150	115	79	49	246	65	100	96	82	N.d.	89
Tm	64	114	N.d.	101	N.d.	N.d.	N.d.	N.d.	29	50	N.d.	N.d.	N.d.	N.d.
Yb	47	119	66	58	110	74	35	77	35	46	53	41	N.d.	36
Lu	32	107	29	41	31	N.d.	N.d.	33	26	30	37	30	N.d.	31

Data Tables 5.1 and 5.12–5.28.

distribution between these phases were discussed earlier in the example of individual varieties of ultramafic and mafic rocks from different massifs (Rampone *et al.*, 1991; Sun & Kerrich, 1995; Dobosi *et al.*, 1998; Lesnov & Gora, 1998). The values of K_d(clinopyroxene/orthopyroxene) vary within a wide range, exhibiting a certain relationship between the rock composition and their suggested genesis (Table 5.32). For example, for spinel lherzolites from deep xenoliths of provinces Dreiser Weiher and Ethiopia and for high-pressure pyroxenites of Zabargad Island, the widest variations were established for the K_d of light REE, which are on the average much higher than the K_d of light and, especially, of heavy REE. Therefore, the trends of changes in the values of K_d(clinopyroxene/orthopyroxene) have a steep negative slope (Fig. 5.26, 1–3). According to the values of K_d(clinopyroxene/orthopyroxene), pyroxenites of Zabargad Island can be divided into two varieties: (1) those with lower K_d(30–120); and (2) those with higher K_d(200–700) values.

A different tendency in the variations of K_d(clinopyroxene/orthopyroxene) is observed in websterites and gabbro-norites from mafic–ultramafic massifs; K_d values for light and heavy REE are rather low, whereas those for Eu and Sm are much higher than those observed on the trends for websterites from the Lherz and Freychinede massifs (Fig. 5.26, 4). It is worth noting that gabbro-norites from the Beriozovsky massif have less intensive maximums for K_d(Eu) than do gabbro-norites from the Komsomol'sky (sample 190), Kuyul'sky (sample 115), and Valizhgensky (sample 115-11a) massifs (Fig. 5.26, 5, 6). The abnormal values of K_d for Eu suggest particularly variable distribution of this element between coexisting clino- and orthopyroxenes in websterites and gabbro-norites. The above data suggest that formation of bipyroxene ultramafic restites, which compose deep xenoliths and high-pressure pyroxenites, was marked by more variable fractionation of light REE between coexisting clinopyroxenes and orthopyroxenes compared to websterites and gabbro-norites that crystallized at lower pressures. Most likely, syncrystallization of these phases at higher pressures promotes more efficient accumulation of REE, particularly Eu, in the clinopyroxene structure and less efficient accumulation in the orthopyroxene structure.

K_d(clinopyroxene/plagioclase). Paragenesis of clinopyroxenes and plagioclases is represented in many plutonic and volcanogenic rocks, less often it is observed in ultramafic rocks, diorites, and some other formations. The calculations of these K_d values are based on the analyses of minerals from pyroxenites of Zabargad Island, olivine gabbros from the Samail and Skaergaard massifs, gabbro-norites from the Beriozovsky massif, gabbros from the Ivrea Verbano complex, as well as basalts and andesites from the Mount Adams complex (Table 5.33, Fig. 5.27). The values of K_d for light elements are much lower compared to those for middle and, especially, heavy REE. Therefore, their trends have a generally positive slope and are typically complicated by minimums for Eu. All clinopyroxene–plagioclase rocks exhibit wide variations in K_d values for heavy REE, which was most distinctly revealed in pyroxenites from Zabargad Island (Fig. 5.27, 1).

Data on the coefficients of REE distribution between clinopyroxenes and coexisting phases may be of interest in respect to conditions under which their rocks formed. Thus, the great spread of values of K_d(clinopyroxene/coexisting mineral) for most REE within the studied magmatic body suggests that the parental melts crystallized under different conditions, or no state of chemical equilibrium was attained between clinopyroxene and coexisting phases, or, finally, it was attained but then disturbed in

Table 5.32 Coefficients of REE distribution between clinopyroxenes, and coexisting orthopyroxenes.

	Massifs (provinces)												
	Kapfenstein, Austria	Dreiser Weiher, Germany								New Mexico, USA	Shavaryn Tsaram, Mo.	Arizona, USA	British Columbia, Can.
	Ka168	D-42	D-45	D-50	D-58	Ib/24	Ib/3	Ib/5	Ib/8	Ib/K1	KH-K8	Mo22	SC-K2	BM-11
Element	*Spinel lherzolites*													
La	6.7	131	155	133	131	92	9.0	25	26	60	92	222	169	3.4
Ce	N.d.	99	112	102	126	62	11	N.d.	38	59	148	170	364	4.3
Pr	N.d.	N.d.	N.d.	68	76	N.d.	13	N.d.	N.d.	N.d.	N.d.	N.d.	N.d.	5.8
Nd	N.d.	56	85	59	70	52	13	N.d.	48	48	144	99	183	9.7
Sm	35	35	34	29	36	26	11	31	28	36	66	54	70	21
Eu	23.0	23	28	26	32	23	12	30	24	30	52	38	48	23
Gd	N.d.	20	22	21	24	17	11	N.d.	20	16	39	29	46	32
Tb	N.d.	14.41	16	15	19	17	9.7	18	18	19	28	26	29	28
Dy	N.d.	9.6	N.d.	10	12	11	8.7	N.d.	N.d.	13	21	18	25	22
Ho	N.d.	8.7	7.7	8.2	9.5	8.7	7.7	11	N.d.	11	17	17	17	19
Er	N.d.	N.d.	N.d.	7.2	N.d.	N.d.	N.d.	7.4	N.d.	N.d.	12	N.d.	11	15
Tm	N.d.	4.8	6.0	5.1	6.9	5.1	4.1	N.d.	7.3	6.1	8.1	8.2	8.7	11
Yb	6.9	4.0	4.4	4.0	5.3	3.7	3.3	8.8	5.3	5.1	6.3	7.5	7.1	8.2
Lu	7.0	3.2	3.8	3.5	4.3	4.4	2.7	4.9	4.0	4.3	4.9	5.7	5.5	6.3

(*Continued*)

Table 5.32 Continued

	Massifs (provinces)													
	British Columbia, Canada									Erdeny, Mongolia	Berioz., Ru.	Naransky, Mongolia		
	BM-16	BM-55	JL-15	JL-18	KR-1	KR-2	KR-35	LL-1	LL-14	1133v	154	272	705b	727v
Element	*Spinel lherzolites*									*Lherzolites*				
La	3.0	2.6	7.4	46	39	11	11	25	12	46	N.d.	1.8	14	37
Ce	5.7	4.6	12	56	28	8.5	27	27	10	41	N.d.	1.3	4.9	37
Pr	15	10	18	57	25	6.0	65	34	8.9	42	N.d.	N.d.	5.8	32
Nd	37	16	30	67	53	6.3	74	39	11	55	1.7	4.1	9.3	33
Sm	53	32	30	55	39	7.5	61	36	12	45	3.7	N.d.	26	35
Eu	49	28	32	49	N.d.	N.d.	74	32	12	53	N.d.	4.7	28	27
Gd	42	28	38	40	76	24	59	35	8.2	17	6.3	1.2	12	28
Tb	41	21	28	32	N.d.	N.d.	52	21	13	2.2	5.9	1.2	8.5	31
Dy	23	19	21	24	22	27	28	21	13	1.8	N.d.	N.d.	4.5	27
Ho	18	14	15	16	24	15	20	16	11	1.3	N.d.	N.d.	4.1	22
Er	13	11	11	13	13	14	16	11	8.6	1.1	N.d.	N.d.	8.1	16
Tm	11	8.0	8.9	12	12	8.5	12	9.7	5.6	N.d.	5.0	1.1	3.8	13
Yb	7.8	6.9	6.7	7.6	5.7	6.2	8.9	6.3	5.5	1.9	4.0	2.0	3.5	10
Lu	6.2	5.8	5.6	6.2	6.0	5.3	6.6	5.2	3.5	2.2	3.5	1.9	2.1	8.1

	Massifs (provinces)												
	Lizard, England			Victoria, Australia		Balmuccia, Italy			Baldissero, Italy		Otago, USA	Kamperdaun	Kakanui	Eifel, Germany
	90681d	90683d	90684d	2604	2640	B-3C	F-59b	F-61b	F-64	F-66	137	20	26	57
Element	*Lherzolites*													
La	4.7	2.4	7.3	39	163	9.9	N.d.	N.d.	N.d.	3.5	N.d.	N.d.	N.d.	N.d.
Ce	4.2	9.6	N.d.	57	153	N.d.	5.9	15	2.2	2.5	22	33	25	26
Pr	8.4	24	16	48	127	N.d.	N.d.	N.d.	N.d.	N.d.	N.d.	N.d.	N.d.	N.d.
Nd	9.4	27	19	42	93	N.d.	2.8	N.d.	N.d.	N.d.	N.d.	31	44	31
Sm	17	21	16	40	59	71	45	30	22	51	N.d.	26	49	26
Eu	13	17	13	36	44	52	52	28	18	28	N.d.	24	46	26
Gd	12	16	14	31	35	N.d.	N.d.	N.d.	N.d.	N.d.	N.d.	N.d.	48	18
Tb	9.1	13	9	23	26	N.d.	N.d.	11	5.2	N.d.	N.d.	N.d.	N.d.	N.d.
Dy	N.d.	N.d.	N.d.	N.d.	N.d.	N.d.	N.d.	N.d.	N.d.	N.d.	31	15	25	10
Ho	6.3	7.8	5.5	18	17	N.d.	N.d.	N.d.	N.d.	N.d.	N.d.	N.d.	N.d.	N.d.
Er	5.3	7.0	5.4	17	103	N.d.	N.d.	N.d.	N.d.	N.d.	15	10	17	6.6
Tm	4.2	4.6	4.6	11	8.0	N.d.	N.d.	N.d.	N.d.	N.d.	N.d.	N.d.	N.d.	N.d.
Yb	2.9	4.2	2.9	6.9	6.5	12	7.8	7.3	5.7	8.8	7.6	5.9	7.8	4.3
Lu	2.9	3.5	N.d.	7.9	6.5	5.5	6.8	5.6	4.2	7.9	N.d.	N.d.	N.d.	4.2

(*Continued*)

Table 5.32 Continued

	Massifs (provinces)													
	Salt Lake, USA	Bogemia	Carolina, USA	Itinome-Gata, Japan		Zabargad Island, Red Sea								
	58	59	DR3	2L	3L	2036B\1\12	2036B\1\2	2036B\1\8	2036B\3\12	2036B\3\2	2036C\17g17	2036C\1\e	2036C\2\8	2036C\2\e
Element	*Lherzolites*					*Pyroxenites*								
La	N.d.	N.d.	N.d.	4.8	4.1	N.d.	N.d.	N.d.	N.d.	N.d.	N.d.	N.d.	N.d.	N.d.
Ce	36	22	5.5	6.1	5.3	103	620	103	117	700	545	59	480	53
Pr	N.d.	N.d.	N.d.	N.d.	N.d.	N.d.	N.d.	N.d.	N.d.	N.d.	N.d.	N.d.	N.d.	N.d.
Nd	53	11	N.d.	8.2	15	133	466	155	155	543	342	107	182	78
Sm	52	4.9	N.d.	9.9	21	45	120	90	51	136	152	92	70	70
Eu	N.d.	4.7	N.d.	10.9	20	87	174	87	89	177	122	40	54	36
Gd	N.d.	N.d.	N.d.	12.4	20	N.d.	N.d.	N.d.	N.d.	N.d.	N.d.	N.d.	N.d.	N.d.
Tb	N.d.	N.d.	N.d.	N.d.	N.d.	N.d.	N.d.	N.d.	N.d.	N.d.	N.d.	N.d.	N.d.	N.d.
Dy	N.d.	7.8	N.d.	14.1	16	12	29	24	11.62	28	52	13	10	11
Ho	N.d.	N.d.	N.d.	N.d.	N.d.	N.d.	N.d.	N.d.	N.d.	N.d.	N.d.	N.d.	N.d.	N.d.
Er	14	7.7	19	11.2	10	7.1	16	12	6.92	16	23	7.0	5.8	6.9
Tm	N.d.	N.d.	N.d.	N.d.	N.d.	N.d.	N.d.	N.d.	N.d.	N.d.	N.d.	N.d.	N.d.	N.d.
Yb	7.4	4.8	115	7.4	5.8	5.2	9.2	7.1	5.27	9.4	13	3.8	3.7	4.1
Lu	N.d.	N.d.	8.0	5.9	4.6	N.d.	N.d.	N.d.	N.d.	N.d.	N.d.	N.d.	N.d.	N.d.

	Massifs (provinces)													
	Zabargad Island, Red sea													
	2036C\4\8	2036C\4\e	2036C\7g17	2096\3\1	2096\7\1	2145B\6\1	2145\10\1	2145\10\6	2145\12\1	2146\3\2	2146\3\8	2146\7\2	2146\7\8	2036B
Element	*Pyroxenites*													
La	N.d.	N.d.	N.d.	N.d.	N.d.	N.d.	N.d.	N.d.	N.d.	N.d.	N.d.	N.d.	N.d.	N.d.
Ce	541	60	198	238	338	49	34	39	37	35	59	40	66	117
Pr	N.d.	N.d.	N.d.	N.d.	N.d.	N.d.	N.d.	N.d.	N.d.	N.d.	N.d.	N.d.	N.d.	N.d.
Nd	342	147	158	147	187	21	31	43	37	42	37	36	32	181
Sm	146	146	61	135	202	9.1	12	12	12	28	28	23	23	102
Eu	88	58	46	69	89	24	19	19	23	27	27	23	23	89
Gd	N.d.	N.d.	N.d.	N.d.	N.d.	N.d.	N.d.	N.d.	N.d.	N.d.	N.d.	N.d.	N.d.	N.d.
Tb	N.d.	N.d.	N.d.	N.d.	N.d.	N.d.	N.d.	N.d.	N.d.	N.d.	N.d.	N.d.	N.d.	N.d.
Dy	25	28	33	24	32	3.5	8.2	6.0	8.1	15	16	13	14	23
Ho	N.d.	N.d.	N.d.	N.d.	N.d.	N.d.	N.d.	N.d.	N.d.	N.d.	N.d.	N.d.	N.d.	N.d.
Er	13	15	15	12	15	2.5	5.3	4.2	5.2	7.5	9.5	6. 4	8.8	12
Tm	N.d.	N.d.	N.d.	N.d.	N.d.	N.d.	N.d.	N.d.	N.d.	N.d.	N.d.	N.d.	N.d.	N.d.
Yb	7.8	8.6	5.9	7.2	8.8	2.0	3.8	3.0	4.2	5.3	5.9	5.1	5.7	7.2
Lu	N.d.	N.d.	N.d.	N.d.	N.d.	N.d.	N.d.	N.d.	N.d.	N.d.	N.d.	N.d.	N.d.	N.d.

(*Continued*)

Table 5.32 Continued

	Massifs (provinces)													
	Lherz, France		Beriozovsky, Russia		Yuzhno-Shmidtovsky, Rus.	Naransky, Mongolia						Freychinede, France		Beni Bousera, Morocco
	70-379b	70-379d	134	137	162	266	280-3	H-8-310	H-311	H-4-5	H-6-88a	70-357	72-226	GP101a
Element	*Websterites*													
La	4.3	1.5	1.1	2.2	2.8	1.2	2.3	2.4	2.1	1.4	1.8	2.4	35	77.5
Ce	16	6.7	1.3	N.d.	1.6	2.1	3.3	1.6	1.7	2.8	1.4	6.4	28	N.d.
Pr	N.d.	N.d.	N.d.	N.d.	N.d.	N.d.	N.d.	N.d.	N.d.	N.d.	N.d.	N.d.	N.d.	N.d.
Nd	N.d.	N.d.	2.1	N.d.	1.1	2.6	11	1.3	2.6	2.7	1.3	N.d.	N.d.	103
Sm	30	36	2.5	N.d.	N.d.	5.1	19	2.7	4.6	16	2.1	111	136	76
Eu	24	29	1.5	4. 0	1.4	10	17	3.3	11	3.8	7.0	73	96	33
Gd	N.d.	N.d.	3.0	2.1	2.2	8.2	12	2.0	N.d.	2.3	2.6	N.d.	N.d.	N.d.
Tb	25	20	2.3	3.1	1.7	6.7	13	3.1	12	4.0	3.3	21	53	N.d.
Dy	N.d.	N.d.	N.d.	N.d.	N.d.	N.d.	N.d.	N.d.	N.d.	N.d.	N.d.	N.d.	N.d.	N.d.
Ho	N.d.	N.d.	N.d.	N.d.	N.d.	N.d.	N.d.	N.d.	N.d.	N.d.	N.d.	N.d.	N.d.	N.d.
Er	N.d.	N.d.	N.d.	N.d.	N.d.	N.d.	N.d.	N.d.	N.d.	N.d.	N.d.	N.d.	N.d.	N.d.
Tm	N.d.	N.d.	2.0	2.6	2.3	6.5	5.0	3.0	8.3	2.8	2.6	N.d.	N.d.	N.d.
Yb	6.2	3.6	1.7	2.5	1.8	5.0	3.4	3.0	5.5	3.1	2.1	4.3	8.7	6.9
Lu	5.0	3.6	1.4	2.2	2.8	2.6	2.8	2.6	7.3	3.1	1.8	4.3	9.2	N.d.

	Massifs (provinces)													
	Komsomol'sky	Kuyul., Rus.	Valizhgen., Rus.	Beriozovsky, Russia						Lukinda, R.	Sheltingsky, Russia		Shikotansky, Russia	
	190	115	115-11a	131	132a	138a	141	144	147	168	173	183	186	187
Element	*Gabbro-norites*													
La	2.1	2.4	2.8	2.2	5.5	2.8	2.1	N.d.	16	1.9	3.2	1.1	21	9.3
Ce	2.4	2.3	6.1	1.7	4.4	2.9	3.0	N.d.	2.9	2.4	2.3	0.57	17	15
Pr	N.d.	N.d.	N.d.	N.d.	N.d.	N.d.	N.d.	N.d.	N.d.	N.d.	N.d.	N.d.	N.d.	N.d.
Nd	3.2	2.3	4.6	6.0	3.1	3.6	2.5	1.6	1.9	2.6	2.1	0.24	14	8.6
Sm	5.0	1.7	7.6	4.5	4.0	6.7	2.8	2.6	1.2	2.3	2.5	0.14	11	5.2
Eu	10	16	10	12	7.5	6.0	4.6	10	2.3	2.0	6.0	0.29	11	9.3
Gd	6.7	7.4	17	5.3	4.2	3.0	2.9	7.2	1.0	4.0	6.2	0.42	6.5	3.2
Tb	3.2	4.7	10	5.3	3.2	6.7	2.6	6.2	N.d.	2.8	5.5	0.55	6.9	3.9
Dy	N.d.	N.d.	N.d.	N.d.	N.d.	N.d.	N.d.	N.d.	N.d.	N.d.	N.d.	N.d.	N.d.	N.d.
Ho	N.d.	N.d.	N.d.	N.d.	N.d.	N.d.	N.d.	N.d.	N.d.	N.d.	N.d.	N.d.	N.d.	N.d.
Er	N.d.	N.d.	N.d.	N.d.	N.d.	N.d.	N.d.	N.d.	N.d.	N.d.	N.d.	N.d.	N.d.	N.d.
Tm	5.0	2.8	2.5	3.5	3.3	4.2	2.6	2.5	1.1	2.4	4.3	0.81	6.7	1.2
Yb	4.0	2.4	5.1	5.6	2.3	4.8	N.d.	2.5	N.d.	2.7	3.4	1.2	7.5	1.5
Lu	3.6	4.8	2.0	3.6	2.0	4.3	1.74	2.9	N.d.	2.1	3.6	0.93	6.7	1.2

(*Continued*)

Table 5.32 Continued

	Massifs (provinces)											
	Voykar-Sin'insky, Rus.	Naransky, Mongolia		Chaysky, Russia	Ostiurensky, Russia	Monchegorsky, Russia	Rybinsky, Russia			Nizhne-Derbinsky, Rus.	Karaginsky, Russia	
	252	269	270	27	429	71	88	89	93	94	96	98
Element	*Gabbro-norites*											
La	N.d.	1.8	7.1	2.7	8.0	4.1	11	4.7	9.1	2.9	1.8	2.7
Ce	N.d.	1.9	5.4	3.5	9.4	3.6	11	5.1	6.5	7.5	1.6	3.2
Pr	N.d.	N.d.	N.d.	N.d.	N.d.	N.d.	N.d.	N.d.	N.d.	N.d.	N.d.	N.d.
Nd	N.d.	2.0	4.0	3.8	7.6	3.3	11	4.6	7.2	3.8	5.5	3.0
Sm	N.d.	1.9	4.7	5.3	6.8	6.9	11	5.6	9.3	3.8	6.0	5.4
Eu	2.8	3.2	14	9.7	10	4.4	15	5.5	11	7.0	5.4	3.7
Gd	1.4	3.4	8.3	5.8	11	3.4	6.8	4.8	7.3	7.0	3.9	3.4
Tb	1.9	3.3	5.5	3.3	6.8	3.3	7.3	5.1	9.0	5.7	4.5	2.6
Dy	N.d.	N.d.	N.d.	N.d.	N.d.	N.d.	N.d.	N.d.	N.d.	5.0	5.0	N.d.
Ho	N.d.	N.d.	N.d.	N.d.	N.d.	N.d.	N.d.	N.d.	N.d.	N.d.	N.d.	N.d.
Er	N.d.	N.d.	N.d.	N.d.	N.d.	N.d.	N.d.	N.d.	N.d.	N.d.	N.d.	N.d.
Tm	1.4	2.1	6.0	1.4	2.3	2.5	3.8	3.1	2.3	3.3	3.6	2.3
Yb	1.2	1.7	5.0	1.1	3.2	2.1	3.7	2.6	2.4	3.0	2.7	2.5
Lu	2.0	1.8	4.7	1.0	2.1	1.6	3.6	2.2	2.1	2.8	3.6	1.8

Note: Data Tables 5.12–5.28 and 5.7.

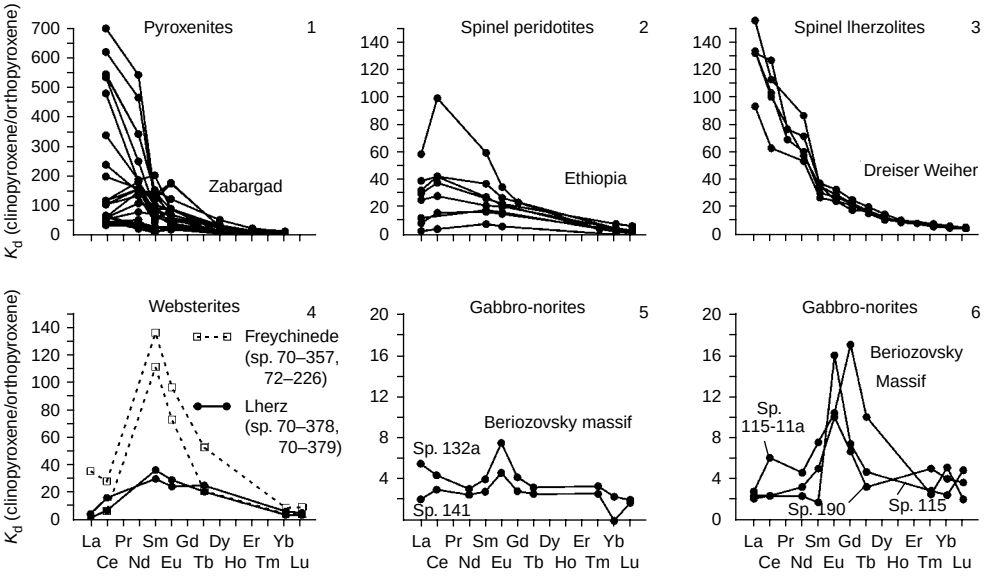

Figure 5.26 The trend coefficients of REE distribution between clinopyroxenes and coexisting orthopyroxenes (data Table 5.32).

subsolidus processes. In the cases with minor variations in the values of these K_d and a similar configuration of their trends, the equilibrium REE distribution during crystallization of the melts was, most likely, attained between clinopyroxenes and coexisting minerals and was not disturbed in subsolidus processes

5.3.3 Isomorphism of REE in clinopyroxenes

As was already emphasized, clinopyroxenes are an important accumulator of structural REE impurities in ultramafic, mafic, and some other magmatic rocks. Investigation in the possible mechanisms of REE accumulation in the structure of this widespread mineral is one of important elements providing insight into the genesis of rocks composed by them.

Accumulation of structural impurities of REE in clinopyroxenes was controlled by different influences of a number of physicochemical parameters including: (1) the composition of parental melts, especially their alkalinity and fluid regime; (2) the composition of clinopyroxenes and their crystallochemical properties; (3) the relationship between the ionic radii of REE ions and ions of net-forming elements replaced by them; (4) temperature and pressure; and (5) redox conditions (Balashov *et al.*, 1970; Balashov, 1976; Pyatenko & Ugryumova, 1988). Nowadays, we cannot determine the real contributions of these factors into the final results, that is, levels of accumulation and types of REE distribution observed in clinopyroxene crystals. Therefore, the mechanisms and influence of each of these factors on REE isomorphism in clinopyroxenes in many respects remain the subject for investigation, mainly, with the help of physical

Table 5.33 Coefficients of REE distribution between clinopyroxenes and coexisting plagioclases.

	Massifs (provinces)													
	Zabargad Island, Red sea													
	036B\3\c1	036B\3\r1	036Bc1	036Br1	036C\17g1	036C\1\c1	036C\2\c1	036C\2\r1	036C\3\r1	036C\4\c1	036C\7\g1	036B\3\c2	036B\3\r2	036Bc2
Element	*Plagioclase-bearing pyroxenites*													
La	N.d.	N.d.	N.d.	N.d.	N.d.	N.d.	N.d.	N.d.	N.d.	N.d.	N.d.	N.d.	N.d.	N.d.
Ce	3.6	2.9	3.2	2.9	2.6	2.5	2.3	2.3	1.9	2.6	0.94	4.4	3.6	3.9
Pr	N.d.	N.d.	N.d.	N.d.	N.d.	N.d.	N.d.	N.d.	N.d.	N.d.	N.d.	N.d.	N.d.	N.d.
Nd	7.4	7.6	6.3	7.6	7.2	7.9	5.7	6.7	7.8	11	3.3	15	15	13
Sm	13	16	12	15	17	20	15	18	24	32	6.7	25	31	23
Eu	2.5	2.5	2.5	2.6	2.7	2.7	2.4	2.5	2.6	3.9	1.0	3.7	3.7	3.6
Gd	N.d.	N.d.	N.d.	N.d.	N.d.	N.d.	N.d.	N.d.	N.d.	N.d.	N.d.	N.d.	N.d.	N.d.
Tb	N.d.	N.d.	N.d.	N.d.	N.d.	N.d.	N.d.	N.d.	N.d.	N.d.	N.d.	N.d.	N.d.	N.d.
Dy	68	103	71	97	45	57	50	66	98	123	29	153	231	161
Ho	N.d.	N.d.	N.d.	N.d.	N.d.	N.d.	N.d.	N.d.	N.d.	N.d.	N.d.	N.d.	N.d.	N.d.
Er	128	174	131	160	88	127	126	147	220	278	59	365	496	373
Tm	N.d.	N.d.	N.d.	N.d.	N.d.	N.d.	N.d.	N.d.	N.d.	N.d.	N.d.	N.d.	N.d.	N.d.
Yb	338	389	333	346	129	171	187	205	311	391	59	1238	1425	1223
Lu	N.d.	N.d.	N.d.	N.d.	N.d.	N.d.	N.d.	N.d.	N.d.	N.d.	N.d.	N.d.	N.d.	N.d.

	Massifs (provinces)													
	Zabargad Island, Red Sea													
	036Br2	036C\17g2	036C\1\c2	036C\2\c2	036C\2\r2	036C\3\r2	036C\4\c2	036C\7\g2	036C\17g3	036C\1\c3	036C\2\c3	036C\2\r3	036C\3\r3	036C\4\c3
Element	*Plagioclase-bearing pyroxenites*													
La	N.d.	N.d.	N.d.	N.d.	N.d.	N.d.	N.d.	N.d.	N.d.	N.d.	N.d.	N.d.	N.d.	N.d.
Ce	3.5	2.6	2.5	2.3	2.3	1.9	2.6	0.94	3.6	3.6	3.2	3.2	2.7	3.6
Pr	N.d.	N.d.	N.d.	N.d.	N.d.	N.d.	N.d.	N.d.	N.d.	N.d.	N.d.	N.d.	N.d.	N.d.
Nd	15	8.1	8.9	6.5	7.6	8.9	12	3.8	9.1	10	7.3	8.5	9.9	14
Sm	30	20	24	19	21	29	39	8.1	22	26	20	23	31	42
Eu	3.7	3.2	3.2	2.8	3.0	3.1	4.6	1.2	3.0	2.9	2.6	2.8	2.9	4.3
Gd	N.d.	N.d.	N.d.	N.d.	N.d.	N.d.	N.d.	N.d.	51	N.d.	N.d.	N.d.	N.d.	N.d.
Tb	N.d.	N.d.	N.d.	N.d.	N.d.	N.d.	N.d.	N.d.	N.d.	N.d.	N.d.	N.d.	N.d.	N.d.
Dy	218	98	124	110	144	215	271	63	98	124	110	144	215	271
Ho	N.d.	N.d.	N.d.	N.d.	N.d.	N.d.	N.d.	N.d.	N.d.	N.d.	N.d.	N.d.	N.d.	N.d.
Er	458	147	212	210	244	366	464	98	126	182	180	209	314	397
Tm	N.d.	N.d.	N.d.	N.d.	N.d.	N.d.	N.d.	N.d.	N.d.	N.d.	N.d.	N.d.	N.d.	N.d.
Yb	1269	232	307	337	368	560	703	106	193	256	281	307	467	586
Lu	N.d.	N.d.	N.d.	N.d.	N.d.	N.d.	N.d.	N.d.	N.d.	N.d.	N.d.	N.d.	N.d.	N.d.

(*Continued*)

Table 5.33 Continued

	Massifs (provinces)													
	Zabargad Island, Red Sea									Samail, Oman				
	036C\7\g3	036C\17g4	036C\1\c4	036C\2\c4	036C\2\r4	036C\3\r4	036C\4\c4	036C\7\g4	036C\7\g3	Kf-12-1	Kf-17-1C	Kf-20-1C	Kf-7-1	Kf-12-1
Element	*Plagioclase-bearing pyroxenites*									*Olivine gabbros*				
La	N.d.	N.d.	N.d.	N.d.	N.d.	N.d.	N.d.	N.d.	N.d.	0.66	1.2	0.46	0.51	0.66
Ce	1.3	3.8	3.8	3.4	3.4	2.9	3.8	1.4	1.3	1.2	2.1	0.9	1.0	1.2
Pr	N.d.	N.d.	N.d.	N.d.	N.d.	N.d.	N.d.	N.d.	N.d.	N.d.	N.d.	N.d.	N.d.	N.d.
Nd	4.2	15	17	12	14	17	23	7.0	4.2	3.7	4.5	2.3	1.8	3.7
Sm	8.6	61	73	56	63	87	117	24	8.6	10	20	9.8	5.1	10
Eu	1.1	4.7	4.6	4.2	4.4	4.5	6.7	1.8	1.1	1.4	2.2	1.5	1.2	1.4
Gd	N.d.	N.d.	N.d.	N.d.	N.d.	N.d.	N.d.	N.d.	N.d.	17	25	22	7.0	17
Tb	N.d.	N.d.	N.d.	N.d.	N.d.	N.d.	N.d.	N.d.	N.d.	24	37	34	10	24
Dy	63	245	311	276	360	538	677	157	63	N.d.	N.d.	N.d.	N.d.	N.d.
Ho	N.d.	N.d.	N.d.	N.d.	N.d.	N.d.	N.d.	N.d.	N.d.	N.d.	N.d.	N.d.	N.d.	N.d.
Er	84	442	636	630	733	1098	1391	293	84	N.d.	N.d.	N.d.	N.d.	N.d.
Tm	N.d.	N.d.	N.d.	N.d.	N.d.	N.d.	N.d.	N.d.	N.d.	N.d.	N.d.	N.d.	N.d.	N.d.
Yb	88	580	768	843	921	1400	1759	265	88	36	31	79	19	36
Lu	N.d.	N.d.	N.d.	N.d.	N.d.	N.d.	N.d.	N.d.	N.d.	33	26	68	15	33

	Massifs (provinces)													
	Skaergaard, Green.	Beriozovsky, Russia						Ivrea Verbano, Italy						
	5181	269	131	132a	138a	141	144	FE31	MO95	MP12	MZ145	FE51	MP13	MP5
Element	*Olivine gabbros*	*Gabbro-norites*						*Gabbro*						
La	1.2	2.2	5.5	N.d.	2.7	16	11	N.d.	N.d.	N.d.	N.d.	N.d.	N.d.	1.3
Ce	2.6	3.1	N.d.	5.7	N.d.	5.4	N.d.	2.8	2.9	2.8	1.2	5.9	5.6	4.3
Pr	N.d.	N.d.	N.d.	N.d.	N.d.	N.d.	N.d.	N.d.	N.d.	N.d.	N.d.	N.d.	N.d.	N.d.
Nd	8.4	9.0	13	5.8	6.0	7.1	36	11	9.8	10	3.2	29	21	17
Sm	17	24	23	5.3	12.0	5.2	36	30	33	32	6.5	77	61	57
Eu	0.34	4.3	2.8	8.3	5.6	1.9	9.0	2.1	3.0	1.8	2.0	4.0	3.3	1.9
Gd	24	N.d.	N.d.	N.d.	N.d.	N.d.	N.d.	N.d.	N.d.	N.d.	N.d.	N.d.	N.d.	26
Tb	31	47.1	16	N.d.	N.d.	10	N.d.	N.d.	N.d.	N.d.	N.d.	N.d.	N.d.	N.d.
Dy	N.d.	N.d.	N.d.	N.d.	N.d.	N.d.	N.d.	117	12	56	2.3	195	54	75
Ho	44	N.d.	N.d.	N.d.	N.d.	N.d.	N.d.	N.d.	N.d.	N.d.	N.d.	N.d.	N.d.	N.d.
Er	N.d.	N.d.	N.d.	N.d.	N.d.	N.d.	N.d.	174	26	55	3.2	170	19	43
Tm	N.d.	50	47	N.d.	N.d.	N.d.	100	N.d.	N.d.	N.d.	N.d.	N.d.	N.d.	N.d.
Yb	67	71	50	N.d.	N.d.	N.d.	60	346	77	83	3.6	404	24	22
Lu	N.d.	N.d.	N.d.	N.d.	N.d.	N.d.	N.d.	N.d.	N.d.	N.d.	N.d.	N.d.	N.d.	N.d.

(*Continued*)

Table 5.33 Continued

	Massifs (provinces)										
	Ivrea Verbano, Italy			Samail, Oman	Mount Adams, USA				Spain	Japan	
	MP6	MP9	MZ132	Kf-16-1	1	14	41	7	GSFC271	GSFC204	GSFC204
Element	*Gabbros*				*Basalt*	*Andesites*				*Andesite-basalt*	
La	N.d.	N.d.	N.d.	0.95	1.5	4.0	1.8	3.8	N.d.	N.d.	N.d.
Ce	3.8	5.3	4.4	3.2	4.0	5.3	3.2	6.1	2.5	0.15	0.75
Pr	N.d.	N.d.	N.d.	N.d.	8.2	12	5.5	10	N.d.	N.d.	N.d.
Nd	15	20	15	4.3	14	23	8.5	15	4.6	0.33	2.2
Sm	35	55	41	14	25	54	19	32	8.9	0.54	4.1
Eu	5.4	3.3	4.1	1.7	1.2	0.69	1.1	1.5	0.94	0.21	1.5
Gd	N.d.	N.d.	N.d.	33	14	52	18	33	N.d.	0.45	4.1
Tb	N.d.	N.d.	N.d.	34	47	N.d.	35	64	N.d.	N.d.	N.d.
Dy	5.6	7.0	105	29	109	N.d.	79	220	27	0.53	4.9
Ho	N.d.	N.d.	N.d.	N.d.	460	N.d.	191	N.d.	N.d.	N.d.	N.d.
Er	5.7	8.0	166	N.d.	N.d.	N.d.	N.d.	N.d.	32	0.44	3.9
Tm	N.d.	N.d.	N.d.	N.d.	N.d.	N.d.	N.d.	N.d.	N.d.	N.d.	N.d.
Yb	13.3	55	79	41	N.d.	N.d.	N.d.	N.d.	N.d.	0.31	3.00
Lu	N.d.	N.d.	N.d.	N.d.	N.d.	N.d.	N.d.	N.d.	N.d.	0.29	2.9

Data Tables 5.12–5.28 and 5.34.

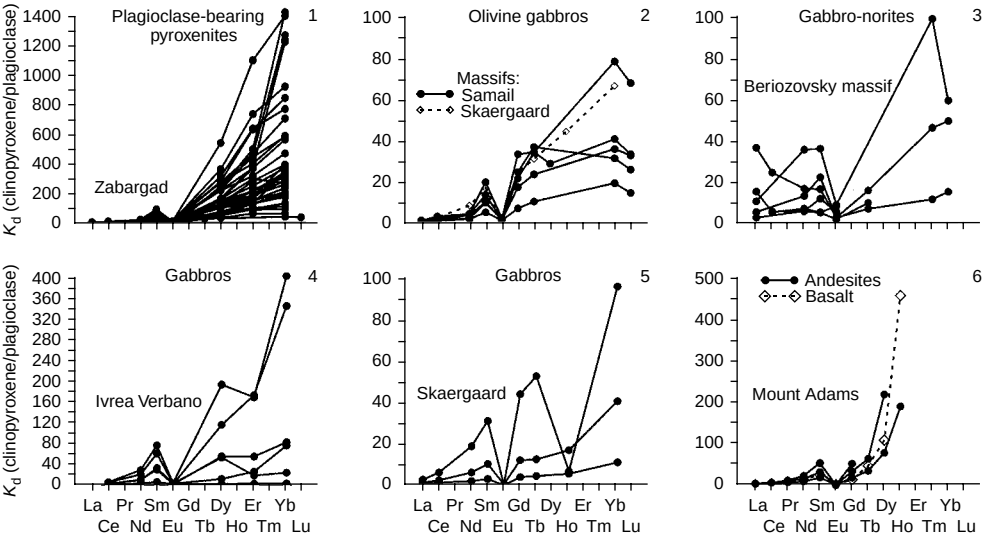

Figure 5.27 The trend coefficients of REE distribution between clinopyroxenes and coexisting plagioclases (data Table 5.33).

experiments. The fact that net-forming elements, the same as the REE ions replacing them, might occupy different positions in the silicate structure must be taken into account when considering the probable schemes of REE isomorphism in clinopyroxenes. It is known that Ca^{2+} and Na^{+} ions in their structure are normally localized in the M2 position, whereas Mg^{2+} ions may occur in the M2 and M1 positions. In turn, Al^{3+} and Fe^{3+} ions might occupy M1 and T positions, and Ti^{4+} ions enter exclusively in Ì1 positions (Morimoto *et al.*, 1988).

The available data suggest that the crystal structure of clinopyroxenes is an extremely favorable matrix for the accumulation not only of REE but of many other compatible elements as well. This property of clinopyroxenes seems to be due to the fact that their crystal structure is a multivariant set of cations of various sizes and charges, it can easily transform to provide a high probability of compensative heterovalent distribution of ions of different elements (Balashov, 1976). From the crystallochemical viewpoint, the most favorable net-forming components for replacement by REE ions, especially middle elements, are bivalent Ca^{2+} ions. As mentioned above, for Ca-bearing silicates the following hypothetic scheme for the isomorphism of REE was proposed: $3Ca^{2+} \rightarrow 2REE^{3+} +$ vacancy (Pyatenko & Ugryumova, 1988).

Probable tendencies of REE isomorphism in clinopyroxenes can be considered on the basis of the correlation relationship established between their contents and the contents of net-forming elements. For example, some of these relationships were revealed by us during the statistical analysis of the working base of related analytical data on the chemical composition of clinopyroxenes and their REE composition. A direct relationship was found between the contents of REE and the concentrations of

such net-forming elements as Fe, Ti, and Na, with the strongest relations for Tm, Yb, and Lu. A tendency of inverse relationship was established between the contents of Eu and some other REE with the contents of Mg and Ca. Some data show a direct relationship between the amount of enstatite end member and Mg# and content of Al_2O_3, on the one hand, and concentrations of Ce and Yb, on the other (Batanova *et al.*, 1998; Johnson, 1998).

Taking into account the above correlation relationships between the contents of REE and net-forming elements in natural clinopyroxene crystals, and considering the optimal balances of ion charges and sizes of their radii on distribution of these elements, it can be assumed that not only can the above scheme of heterovalent isomorphism be applied for this mineral, but some others can as well. These also include those isomorphous replacements in which Fe^{3+} and Na^{+} ions play the part of charge compensators. Based on this assumption, two more schemes of isomorphous incorporation of REE into clinopyroxene structure are proposed

$$3Ca^{2+} \rightarrow REE^{3+} + Fe^{3+} \tag{5.1}$$

$$2Ca^{2+} \rightarrow REE^{3+} + Na^{+} \tag{5.2}$$

The second scheme seems to be of greater priority for the isomorphism of middle REE, including Eu^{3+}, as in this case, the total sizes of ionic radii in the left ($1.12\,Å \cdot 2 = 2.240\,Å$) and right ($1.066\,Å + 1.180\,Å = 2.246\,Å$) parts are almost equal. The above-mentioned direct relationship between the contents of Eu and Ti and the inverse relationship between Eu and Mg do not rule out the probability of realization of isomorphic replacement in clinopyroxenes by another hypothetical scheme in which Mg^{2+} ions play the role of replaced ions, Eu^{2+} ions are replacing ions, and Ti^{4+} ions are charge compensators

$$3Mg^{2+} \rightarrow Eu^{2+} + Ti^{4+} \tag{5.3}$$

It is worth noting that all the above-mentioned schemes of REE isomorphism in clinopyroxenes are regarded by us as strictly hypothetical, requiring special study and crystallochemical proof.

Among other factors influencing the character and intensity of isomorphic replacements of REE in clinopyroxenes is, most likely, the sequence of crystallization of phases from melts, which is, in turn, predetermined by the conditions of the process. In those cases when at appropriate P–T conditions clinopyroxenes began to crystallize only after the termination of crystallization of plagioclase, which selectively extracted light and partly middle REE, especially Eu, the residual portions of melts and, respectively, crystallized clinopyroxenes must be depleted of these REE. The illustration of this phenomenon is the rare earth composition of clinopyroxenes from meteorites and from lunar mafic rocks that were considerably depleted of Eu, probably, as a result of advance crystallization of plagioclases under drastically reducing conditions. Another example is that at high-pressure conditions, the crystallization of clinopyroxenes should have preceded crystallization of garnet and orthopyroxene, which would preferably extract heavy REE from the melt. In this case, the residual portions of the

melt, the same as clinopyroxenes crystallized from them, must be depleted of heavy REE relative to light elements.

* * *

Clinopyroxenes are normally the most important concentrator of REE in ultramafic, mafic, and some other rocks, as their crystallochemical properties are favorable for the intense accumulation of these trace elements. Investigations into the geochemistry of REE in this mineral were paid more attention than the studies of other rock-forming minerals. Nowadays the paragenetic types of clinopyroxenes in this respect were studied to a greater or lesser extent. These paragenetic types vary in the concentrations of REE and the ratios between some elements, which is the result of many factors. The total contents of structural impurities of REE in them increase from the varieties of mineral from meteorites and mantle ultramafic restites to the samples from basic, intermediate, acid, and alkali rocks. Heavy REE in clinopyroxenes are distributed more uniformly than are middle and light elements. Clinopyroxenes from some types of rocks and their massifs display considerable depletion of light elements compared to middle and heavy REE and have a generally positive slope of REE patterns. Clinopyroxenes from some other mafic rocks display a deficit of Eu, resulting from advanced crystallization of coexisting plagioclases, but the rocks formed under the conditions of fractionation of plagioclase typically have excess Eu. In hybrid varieties of gabbros, clinopyroxenes might be abnormally enriched with light REE, whereas their samples from high-pressure mafic and ultramafic rocks are abnormally enriched with heavy elements. The values of K_d(clinopyroxene/melt) for all REE increase from picrite to basalt, andesite, and dacite melts and their trends of changes normally have a generally positive slope. Particular changes in the values of these K_d might result from variations in temperature and pressure on crystallization of melts. Most likely, accumulation of REE in clinopyroxene structure is normally realized by way of heterovalent isomorphic replacement by trivalent ions of net-forming Ca^{2+} ions with participation of some net-forming elements, which play the role of charge compensators.

Further thorough analytical and crystallochemical studies of the regularities of REE distribution in clinopyroxene, establishment of new typomorphic features of this mineral as well as wide generalization of rapidly accumulating data and their genetic interpretation are urgent problems for the nearest future.

5.4 PLAGIOCLASES

Plagioclases in varying quantitative ratios with other minerals occur in many varieties of magmatic, metamorphic, and metasomatic rocks, concentrating a considerable part of structural REE impurities, mainly light REE. The neutron activation analysis of REE in this mineral from meteorites in the late 1970s for the first time showed that the plagioclase structure can accumulate abnormally increased amounts of Eu (Honda & Shima, 1967). Later, the rare earth composition of plagioclases was studied in lunar rocks and some phenocrysts from basalts, andesites, dacites, and rhyolites (Higuchi & Nagasawa, 1969; Philpotts & Schnetzler, 1970a,b; Schnetzler & Philpotts, 1970; Dudas *et al.*, 1971; Nagasawa & Schnetzler, 1971; Schnetzler & Bottino,

1971). Schnetzler & Bottino (1971) showed that, as a result of crystallization under low oxygen volatility in plagioclase from meteorites, Eu occurs mainly in a bivalent form. Moreover, studies of plagioclases from porphyry inclusions in effusive rocks yielded first tentative values of coefficients of REE distribution between this mineral and its parental melts. It was also established that the values of K_d(plagioclase/melt) for Eu depend on its valence state and with decreasing oxygen volatility in melt, the $Eu^{2+}/(Eu^{2+} + Eu^{3+})$ value approaches unity (Drake & Weill, 1975). More representative analytical data were obtained on REE distribution in plagioclases from mafic rocks of the Skaergaard (Paster *et al.*, 1974), Samail (Pallister & Knight, 1981), Stillwater (Lambert & Simmons, 1988), and Ivrea Verbano (Mazzucchelli *et al.*, 1992a,b) massifs, from lunar rocks (Floss *et al.*, 1998; Shervais & McGree, 1999), from the rocks of the Beriozovsky and Naransky massifs (Lesnov *et al.*, 1987, 1998a), and from basalts of the Kuril Islands (Bindeman & Bailey, 1999). Some published works were devoted to the general problems of REE geochemistry in rock-forming plagioclases (Lesnov, 1991, 2000b,c,d, 2001a,b, 2005). Among plagioclases analyzed up to date, about 19% are from gabbros, about 17% from anorthosites, about 13% from gabbro-norites and norites, and about 9% from basalts. The predominant part of these analyses was performed using the following techniques: IPMA (~45%), IDMS (~19%), INAA (~18%), and RNAA (~7%), among others. In the majority of cases, the contents of Ce, Sm, and Eu were determined; fewer analyses were performed for La, Nd, and Yb, and the fewest for Pr, Ho, and Tm.

5.4.1 REE composition of plagioclases

Let us consider some features of REE distribution in plagioclases from several varieties of rocks.

Meteorites and lunar rocks. REE distribution in plagioclases from meteorites can be inferred from the results of scarce analyses of their samples from the occurrences of Chessigny, Valadares, Lafayette, Nakhla, "Mars" (Wadhwa & Crozaz, 1995), and Acapulco (Zipfel *et al.*, 1995) (Table 5.34, Fig. 5.28). In general, these samples have decreased amounts of these impurities, rather intense fractionation, and a considerable excess of Eu. Acapulco meteorites have the lowest level of accumulation of La compared to the samples from other meteorites. More representative data obtained for plagioclases from mafic rocks of the moon show a rather wide interval in their rare earth composition (see Table 5.34). Average total contents of the elements increase from the samples from ferriferous anorthosites to the samples from magnesioferous and ferriferous mafic rocks and further to the samples from monzogabbros, alkali anorthosites, and alkali gabbro-norites. Plagioclases from the mentioned varieties of lunar rocks differ also in the average values of the $(Ce/Yb)_n$ parameter. At the same time, all these samples are comparable in the configuration of negatively sloping spectra complicated by very intensely negative Eu anomalies (Fig. 5.28). Plagioclases from lunar basalts have a slightly higher level of REE accumulation than do plutonic lunar rocks; however, they have a lower intensity of positive Eu anomalies, which suggests their crystallization under higher volatility of oxygen compared to plagioclases from plutonic mafic rocks of the moon (Fig. 5.28, 18).

Table 5.34 Rare earth element composition of plagioclases from meteorites, and from mafic rocks of Moon (ppm).

	Meteorites									
	Chessigny	Valadares	Lafayette	Nakhla	"Mars"		Acapulco			
	(Wadhwa & Crozaz, 1995), IPMA						(Zipfel *et al.*, 1995), SIMS			
Element	Chess-1	Valad-1	Laf-1	Nakhla-1	PL 1	PL 2	A1	A2	A3	A9
La	1.990	1.300	1.890	1.630	0.833	0.880	0.254	0.242	0.265	0.268
Ce	3.080	2.620	3.390	3.520	1.166	1.525	0.347	0.268	0.391	0.389
Pr	N.d.	N.d.	N.d.	N.d.	0.129	0.128	0.027	0.020	0.026	0.028
Nd	0.630	1.080	1.050	1.300	0.361	0.396	0.103	0.072	0.093	0.100
Sm	0.100	0.160	0.120	0.210	0.026	0.052	0.032	0.024	0.013	0.013
Eu	0.990	1.020	1.170	1.250	1.435	1.220	0.547	0.727	0.811	0.894
Gd	N.d.	N.d.	0.060	0.080	0.047	0.048	0.021	0.010	0.009	0.018
Tb	N.d.	N.d.	N.d.	N.d.	0.007	0.007	0.004	0.003	0.002	0.002
Dy	N.d.	N.d.	N.d.	N.d.	N.d.	N.d.	0.057	0.037	0.014	0.017
Ho	N.d.	N.d.	N.d.	N.d.	N.d.	N.d.	0.003	0.003	0.003	0.003
Er	N.d.	N.d.	N.d.	N.d.	N.d.	N.d.	0.003	0.003	0.003	0.003
Tm	N.d.	N.d.	N.d.	N.d.	N.d.	N.d.	0.003	0.003	0.003	0.003
Yb	N.d.	N.d.	N.d.	N.d.	N.d.	N.d.	0.003	0.003	0.005	0.003
Lu	N.d.	N.d.	N.d.	N.d.	N.d.	N.d.	0.005	0.005	0.005	0.005
Total	N.d.	N.d.	N.d.	N.d.	N.d.	N.d.	1.41	1.42	1.64	1.75
$(Ce/Yb)_n$	N.d.	N.d.	N.d.	N.d.	N.d.	N.d.	29.9	23.1	20.2	33.6
$(Eu/Eu^*)_n$	N.d.	N.d.	38	25	125	73	61	122	218	179

(*Continued*)

Table 5.34 Continued

	The Moon													
	(Floss *et al.*, 1998), IPMA									(Shervais & McGree, 1999), IPMA				
	699MCI	699MM	270MMC	270MCD	600(MF)	601(MF)	602(MF)	603(MF)	604(MF)	2PlcSp4	2PlcSp5	2PlcSp6	2PlcSp8	9PlcSp3
Element	*Magnesioferous mafites*				*Ferriferous mafites*					*Alkali gabbro-norites*				*Alkal. norites*
La	0.33	0.28	0.51	0.71	1.670	1.980	2.540	1.910	1.710	5.000	13.11	4.160	11.97	4.410
Ce	0.82	0.77	1.37	1.65	3.530	3.830	5.280	4.140	3.840	10.83	29.81	7.970	27.13	7.880
Pr	0.087	0.094	0.2	0.21	0.330	0.410	0.550	0.530	0.430	N.d.	N.d.	N.d.	N.d.	N.d.
Nd	0.43	0.43	0.72	0.73	1.290	1.600	1.990	1.630	1.580	3.830	12.78	3.680	14.79	3.020
Sm	0.06	0.095	0.14	0.13	0.200	0.350	0.350	0.310	0.340	0.990	3.060	0.650	3.490	0.480
Eu	1.05	1.06	0.95	1.01	1.120	1.010	1.200	1.000	1.000	6.980	10.90	6.090	5.460	3.550
Gd	0.071	0.081	0.14	0.12	0.170	0.250	0.250	0.270	0.250	0.800	2.090	0.490	2.600	0.610
Tb	0.008	0.012	0.022	0.024	0.017	0.028	0.037	0.031	0.033	N.d.	N.d.	N.d.	N.d.	N.d.
Dy	0.039	0.031	0.097	0.061	0.083	0.220	0.190	0.170	0.180	0.600	1.130	0.320	1.710	0.740
Ho	0.012	0.009	0.02	0.019	0.026	0.046	0.038	0.048	0.041	N.d.	N.d.	N.d.	N.d.	N.d.
Er	0.018	0.015	0.045	0.025	0.059	0.130	0.086	0.081	0.082	N.d.	N.d.	N.d.	N.d.	N.d.
Tm	N.d.	N.d.	N.d.	N.d.	N.d.	N.d.	N.d.	N.d.	N.d.	N.d.	N.d.	N.d.	N.d.	N.d.
Yb	0.022	0.006	0.038	0.041	0.079	0.130	0.082	0.110	0.120	0.184	0.238	0.133	0.590	0.688
Lu	N.d.	N.d.	N.d.	N.d.	N.d.	N.d.	N.d.	N.d.	N.d.	N.d.	N.d.	N.d.	N.d.	N.d.
Total	2.95	2.88	4.25	4.73	8.57	9.98	12.6	10.2	9.61	N.d.	N.d.	N.d.	N.d.	N.d.
$(Ce/Yb)_n$	9.65	33.21	9.33	10.4	11.6	7.63	16.7	9.74	8.28	15.2	32.4	15.5	11.9	2.96
$(Eu/Eu^*)_n$	49.1	36.1	20.5	24.3	18.1	10.0	11.8	10.3	10.0	23.3	12.5	31.7	5.3	20.1

	The Moon													
	(Shervais & McGree, 1999)	(Jolliff *et al.*, 1999), IPMA				(Floss *et al.*, 1998), IPMA								
	9PlcSp7	Plg 1	Plg 2a	Plg 2b	Plg 3	55.42AFcl	55.42AFmt	15.82AF	35.268AFcl S	35.268AFcl L	35.268AFmt	25.702AFcl	25.702AFmt	35.8AS
Element	*Alkali norites*	*Monzogabbros*				*Ferriferous anorthosites*								
La	5.210	4.790	4.970	6.120	3.330	0.300	0.340	0.130	0.140	0.140	0.130	0.240	0.260	0.450
Ce	10.88	9.010	9.590	11.80	5.310	0.760	0.890	0.310	0.320	0.350	0.360	0.670	0.750	1.050
Pr	N.d.	0.900	0.820	1.110	0.480	0.089	0.094	0.034	0.039	0.042	0.042	0.089	0.085	0.130
Nd	4.430	2.940	3.390	4.180	1.690	0.330	0.410	0.160	0.160	0.150	0.180	0.390	0.390	0.510
Sm	0.590	0.380	0.360	0.520	0.150	0.069	0.100	0.041	0.049	0.031	0.032	0.094	0.100	0.100
Eu	3.950	3.400	3.290	3.290	3.710	0.990	0.910	0.660	0.760	0.800	0.780	1.030	0.970	1.330
Gd	0.550	0.360	0.480	0.570	0.230	0.070	0.110	0.043	0.038	0.041	0.038	0.093	0.085	0.087
Tb	N.d.	0.070	0.080	0.080	0.040	0.011	0.014	0.008	0.013	0.006	0.008	0.016	0.015	0.014
Dy	0.520	0.380	0.450	0.500	0.240	0.053	0.065	0.029	0.030	0.023	0.028	0.055	0.061	0.075
Ho	N.d.	0.070	0.090	0.090	0.070	0.013	0.012	0.007	0.004	0.050	0.009	0.013	0.012	0.017
Er	N.d.	0.170	0.300	0.260	0.270	0.019	0.032	0.011	0.008	0.013	0.014	0.025	0.029	0.034
Tm	N.d.	0.030	0.020	0.030	0.020	N.d.	N.d.	N.d.	N.d.	N.d.	N.d.	N.d.	N.d.	N.d.
Yb	0.582	0.230	0.520	0.150	0.170	0.021	0.032	0.019	0.013	0.015	0.010	0.031	0.028	0.042
Lu	N.d.	0.020	0.019	0.017	0.014	N.d.	N.d.	N.d.	N.d.	N.d.	N.d.	N.d.	N.d.	N.d.
Total	N.d.	22.8	24.4	28.7	15.7	N.d.	N.d.	N.d.	N.d.	N.d.	N.d.	N.d.	N.d.	N.d.
$(Ce/Yb)_n$	4.84	10.1	4.77	20.4	8.08	9.37	7.20	4.22	6.37	6.04	9.32	5.59	6.93	6.47
$(Eu/Eu^*)_n$	20.9	27.7	24.2	18.4	60.9	43.2	26.4	47.7	52.0	68.6	68.3	33.3	31.4	42.6

(*Continued*)

Table 5.34 Continued

	The Moon													
	(Floss *et al.*, 1998)	(Shervais & McGree, 1999), IPMA												
	55.5AF	5PlAcSp1	5PlArSp2	5PlBcSp3	5PlCcSp4	5PlcSp1	8PlcSp2	8PlrSp3	8PlcSp4	8PlrSp7	8PlAcSp1	8PlArSp2	8PBcSp3	8PlBrSp4
Element	*Ferri. anorthosites*	*Alkaline anorthosites*												
La	0.150	5.750	5.000	7.720	6.140	7.400	7.380	2.720	5.690	2.220	9.320	9.300	10.510	9.170
Ce	0.370	13.34	10.83	16.48	12.40	14.78	14.61	4.840	13.08	3.950	20.28	18.87	22.49	18.81
Pr	0.047	N.d.	N.d.	N.d.	N.d.	N.d.	N.d.	N.d.	N.d.	N.d.	N.d.	N.d.	N.d.	N.d.
Nd	0.200	5.770	4.070	6.530	4.250	5.870	6.840	2.400	6.100	2.150	6.140	7.200	6.770	6.740
Sm	0.060	1.200	1.710	1.250	0.940	1.430	1.890	0.950	1.360	0.870	0.810	1.020	1.630	1.340
Eu	0.850	5.530	5.310	6.090	6.670	7.310	9.320	7.410	7.520	6.260	5.620	5.980	6.170	5.740
Gd	0.058	0.750	0.990	0.810	0.680	1.150	1.190	0.600	1.050	0.610	0.580	0.700	1.040	0.790
Tb	0.090	N.d.	N.d.	N.d.	N.d.	N.d.	N.d.	N.d.	N.d.	N.d.	N.d.	N.d.	N.d.	N.d.
Dy	0.035	0.300	0.270	0.360	0.430	0.870	0.480	0.260	0.730	0.360	0.350	0.390	0.450	0.240
Ho	0.008	N.d.	N.d.	N.d.	N.d.	N.d.	N.d.	N.d.	N.d.	N.d.	N.d.	N.d.	N.d.	N.d.
Er	0.022	N.d.	N.d.	N.d.	N.d.	N.d.	N.d.	N.d.	N.d.	N.d.	N.d.	N.d.	N.d.	N.d.
Tm	N.d.	N.d.	N.d.	N.d.	N.d.	N.d.	N.d.	N.d.	N.d.	N.d.	N.d.	N.d.	N.d.	N.d.
Yb	0.026	0.073	0.169	0.107	0.100	0.281	0.162	0.095	0.191	0.206	0.109	0.079	0.147	0.124
Lu	N.d.	N.d.	N.d.	N.d.	N.d.	N.d.	N.d.	N.d.	N.d.	N.d.	N.d.	N.d.	N.d.	N.d.
Total	1.92	32.7	28.3	39.3	31.6	39.1	41.9	19.3	35.7	16.6	43.2	43.5	49.2	43.0
$(Ce/Yb)_n$	3.68	47.3	16.6	39.9	32.1	13.6	23.3	13.2	17.7	4.96	48.2	61.8	39.6	39.3
$(Eu/Eu^*)_n$	43.5	16.6	11.5	17.4	24.4	16.9	17.8	28.1	18.6	25.0	23.9	20.5	13.6	15.7

	The Moon												
	(Shervais & McGree, 1999), IPMA											(Philpotts & Schnetzler, 1970a,b), IDMS	
	8PlCcSp6	2PlAcSp1	2PlAhSp2	2PlArSp3	2PlArSp5	2PlBcSp4	2PlCcSp8	2PlCrSp9	2PlDcSp10	2PlDrSp11	3PlcSp	10044-24	10062-29
Element	*Alkaline anorthosites*											*Basalts*	
La	8.970	8.050	5.850	5.750	4.560	4.970	9.340	8.950	8.800	7.900	7.900	N.d.	N.d.
Ce	19.17	17.11	12.14	11.31	9.780	12.24	19.60	19.54	18.85	17.60	20.59	18.50	9.190
Pr	N.d.	N.d.	N.d.	N.d.	N.d.	N.d.	N.d.	N.d.	N.d.	N.d.	N.d.	N.d.	N.d.
Nd	5.020	7.590	5.740	5.560	3.990	5.720	7.110	7.380	8.340	6.290	5.920	15.00	6.750
Sm	1.220	2.810	0.830	0.450	1.200	0.950	1.060	1.430	1.790	1.380	1.130	4.340	2.000
Eu	5.950	7.390	6.180	6.700	6.440	5.610	6.830	6.840	6.610	6.780	9.700	4.790	2.750
Gd	0.730	1.730	0.630	0.410	0.750	0.690	0.740	0.960	1.100	1.040	0.800	N.d.	N.d.
Tb	N.d.	N.d.	N.d.	N.d.	N.d.	N.d.	N.d.	N.d.	N.d.	N.d.	N.d.	N.d.	N.d.
Dy	0.250	0.640	0.430	0.380	0.300	0.420	0.410	0.490	0.420	0.700	0.480	4.430	2.560
Ho	N.d.	N.d.	N.d.	N.d.	N.d.	N.d.	N.d.	N.d.	N.d.	N.d.	N.d.	N.d.	N.d.
Er	N.d.	N.d.	N.d.	N.d.	N.d.	N.d.	N.d.	N.d.	N.d.	N.d.	N.d.	3.040	1.320
Tm	N.d.	N.d.	N.d.	N.d.	N.d.	N.d.	N.d.	N.d.	N.d.	N.d.	N.d.	N.d.	N.d.
Yb	0.121	0.222	0.145	0.147	0.097	0.089	0.113	0.153	0.084	0.109	0.160	2.540	1.290
Lu	N.d.	N.d.	N.d.	N.d.	N.d.	N.d.	N.d.	N.d.	N.d.	N.d.	N.d.	0.401	0.200
Total	41.4	45.5	32.0	30.7	27.1	30.7	45.2	45.7	46.0	41.8	46.7	53.0	26.1
$(Ce/Yb)_n$	41.0	20.0	21.7	19.9	26.1	35.6	44.9	33.1	58.1	41.8	33.3	1.89	1.84
$(Eu/Eu^*)_n$	17.8	9.5	25.1	46.9	19.4	20.3	22.4	16.9	13.4	16.6	29.7	N.d.	N.d.

(*Continued*)

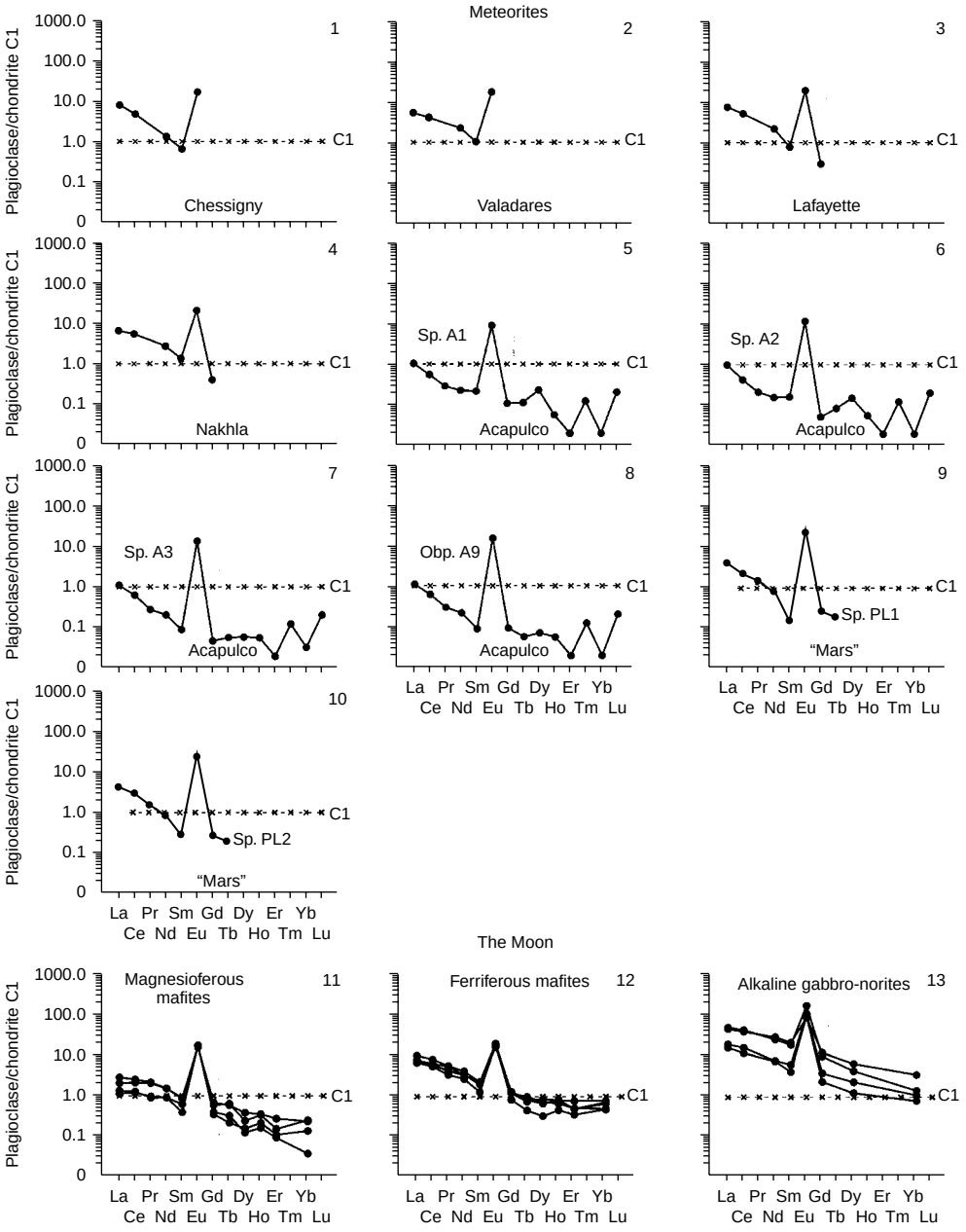

Figure 5.28 Chondrite-normalized REE patterns for plagioclases from meteorites and the moon's mafic rocks (data Table 5.34).

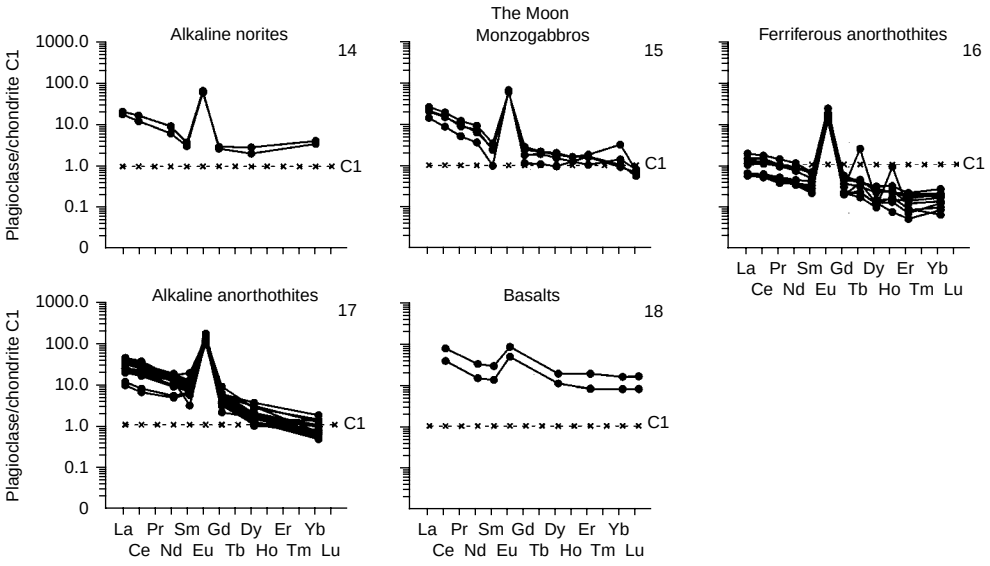

Figure 5.28 Continued

Lherzolites, dunites, and pyroxenites. The rare earth composition of plagioclases from the mentioned varieties of rocks was characterized by their samples from the Liguria, Stillwater, Dovyrensky, and Naransky massifs (Table 5.35). For the mineral from the Liguria massifs, we obtained data for only light REE, which level of accumulation is uncommonly low: Ce (0.06–0.30 t. ch.), Nd (0.18–1.10 t. ch.), Sm (0.21–1.30 t. ch.), and Eu (2.4–5.3 t. ch.) (Fig. 5.29, 1). Plagioclases from pyroxenites of Zabargad Island exhibit a very nonuniform REE distribution, especially heavy REE (Fig. 5.29, 6). The intensity of positive Eu anomalies on their spectra decreases with increasing total level of REE accumulation in the samples. The abnormal enrichment of these plagioclases with heavy REE is assumed to result from the fact that pyroxenites from Zabargad Island formed under decompression metamorphism of garnet-bearing mafic rocks (Vannucci *et al.*, 1993a). Plagioclase-bearing dunites and plagioclase-bearing bronzitites from the Stillwater massif, plagioclase-bearing wehrlites from the Dovyrensky massif, and plagioclase-bearing websterites from the Naransky massif plagioclases show a rather low level of REE accumulation. In the Stillwater samples, the fractionation of REE is more intense (see Fig. 5.29, 2, 5), and, in addition, they have higher values of the $(Eu/Eu^*)_n$ (see Fig. 5.29, 6–11) parameter compared to plagioclases from the Dovyrensky and Naransky massifs (see Fig. 5.29, 3, 4), which can be due to the crystallization of the latter under higher volatility of oxygen.

Troctolites and olivine gabbros. Characterization of plagioclases from these rocks is based on their studies in the Stillwater, Samail, Skaergaard, and Troodos massifs (Table 5.36). The position and configuration of REE patterns and the intensity of Eu anomaly suggest that plagioclases from olivine gabbros from the Samail massif have a similar REE distribution (Fig. 5.30, 2) and the samples from the Stillwater

Table 5.35 Rare earth element composition of plagioclases from plagioclase-bearing lherzolites, dunites, wehrlites, and pyroxenites (ppm).

	Massifs												
	Liguria, Italy										Stillwater, USA		Dovyrensky, Rus.
	(Rampone *et al.*, 1991), IPMA										(Lambert & Simmons, 1988), IDMS		(Lesnov, 2001a)
	ER-F1/6	ER-F1/9	ER-F1/9a	C36	C2/5A	C2/5B	C223/3	C222/3	C2/9	C2/9A	18W-137.0	7W-24.0	L-25-89
Element	*Plagioclase-bearing lherzolites*										*Plagioclase-bearing dunites*		*Plag.-bear. wherl.*
La	N.d.	N.d.	N.d.	N.d.	N.d.	N.d.	N.d.	N.d.	N.d.	N.d.	0.696	0.629	3.860
Ce	0.069	0.049	0.077	0.038	0.071	0.057	0.160	0.072	0.110	0.170	1.490	1.040	5.130
Pr	N.d.	N.d.	N.d.	N.d.	N.d.	N.d.	N.d.	N.d.	N.d.	N.d.	N.d.	N.d.	N.d.
Nd	0.130	0.130	0.140	0.130	0.150	0.086	0.480	0.280	0.210	0.460	0.652	0.390	2.200
Sm	0.048	0.033	0.041	0.053	0.033	0.035	0.200	0.130	0.100	0.160	0.130	0.065	0.260
Eu	0.170	0.190	0.250	0.210	0.150	0.140	0.310	0.200	0.170	0.220	0.229	0.195	0.230
Gd	N.d.	N.d.	N.d.	N.d.	N.d.	N.d.	N.d.	N.d.	N.d.	N.d.	0.095	0.042	0.200
Tb	N.d.	N.d.	N.d.	N.d.	N.d.	N.d.	N.d.	N.d.	N.d.	N.d.	N.d.	N.d.	0.030
Dy	N.d.	N.d.	N.d.	N.d.	N.d.	N.d.	N.d.	N.d.	N.d.	N.d.	0.067	0.037	N.d.
Ho	N.d.	N.d.	N.d.	N.d.	N.d.	N.d.	N.d.	N.d.	N.d.	N.d.	N.d.	N.d.	N.d.
Er	N.d.	N.d.	N.d.	N.d.	N.d.	N.d.	N.d.	N.d.	N.d.	N.d.	0.026	0.019	N.d.
Tm	N.d.	N.d.	N.d.	N.d.	N.d.	N.d.	N.d.	N.d.	N.d.	N.d.	N.d.	N.d.	0.110
Yb	N.d.	N.d.	N.d.	N.d.	N.d.	N.d.	N.d.	N.d.	N.d.	N.d.	0.087	0.014	0.060
Lu	N.d.	N.d.	N.d.	N.d.	N.d.	N.d.	N.d.	N.d.	N.d.	N.d.	N.d.	N.d.	0.009
Total	N.d.	N.d.	N.d.	N.d.	N.d.	N.d.	N.d.	N.d.	N.d.	N.d.	3.47	2.43	12.1
$(Ce/Yb)_n$	N.d.	N.d.	N.d.	N.d.	N.d.	N.d.	N.d.	N.d.	N.d.	N.d.	4.43	19.2	N.d.
$(Eu/Eu^*)_n$	N.d.	N.d.	N.d.	N.d.	N.d.	N.d.	N.d.	N.d.	N.d.	N.d.	6.0	10.7	3.0

	Massifs												
	Dovyrensky, Russia		Naransky, Mongolia	Zabargad Island, Red Sea									Stillwater, USA
	(Lesnov, 2001a), RNAA			(Vannucci *et al.*, 1993a,b), IPMA									(Lambert & Simmons, 1988), IDMS
	L-73-89	L-76-89	N-5-4	2036\7	2036A\1	2036A\2	2036B\3	2036B\4	2036C\1	2036C\2	2036C\6	2036C\71	LM04
Element	*Plag.-bear. wehrlites*		*Plag.-bear. websterite*	*Plagioclase-bearing pyroxenites*									*Plagioclase-bearing bronzitite*
La	5.700	2.900	0.080	N.d.	N.d.	N.d.	N.d.	N.d.	N.d.	N.d.	N.d.	N.d.	2.020
Ce	8.100	4.700	0.190	3.390	1.950	1.610	1.970	1.600	2.100	2.100	1.500	1.420	3.160
Pr	N.d.	N.d.	N.d.	N.d.	N.d.	N.d.	N.d.	N.d.	N.d.	N.d.	N.d.	N.d.	N.d.
Nd	2.900	1.900	0.170	2.770	1.810	1.890	1.470	0.740	0.950	0.840	0.750	0.450	1.040
Sm	0.330	0.200	0.050	1.480	0.640	0.570	0.310	0.160	0.180	0.150	0.140	0.050	0.144
Eu	0.200	0.200	0.067	0.810	0.440	0.590	0.700	0.480	0.450	0.380	0.410	0.260	0.315
Gd	0.190	0.210	0.060	N.d.	N.d.	N.d.	N.d.	0.230	0.260	0.140	0.120	0.100	0.082
Tb	0.030	0.033	0.010	N.d.	N.d.	N.d.	N.d.	N.d.	N.d.	N.d.	N.d.	N.d.	N.d.
Dy	N.d.	N.d.	N.d.	2.580	1.840	1.170	0.360	0.160	0.220	0.100	0.100	0.040	0.055
Ho	N.d.	N.d.	N.d.	N.d.	N.d.	N.d.	N.d.	N.d.	N.d.	N.d.	N.d.	N.d.	N.d.
Er	N.d.	N.d.	N.d.	1.310	0.870	0.600	0.200	0.070	0.100	0.060	0.070	0.020	0.019
Tm	0.010	0.024	0.006	N.d.	N.d.	N.d.	N.d.	N.d.	N.d.	N.d.	N.d.	N.d.	N.d.
Yb	0.065	0.130	0.030	1.020	0.320	0.410	0.110	0.030	0.090	0.050	0.060	0.020	0.010
Lu	0.008	0.018	0.004	N.d.	N.d.	N.d.	N.d.	N.d.	N.d.	N.d.	N.d.	N.d.	N.d.
Total	17.5	10.3	0.67	13.4	7.87	6.84	5.12	3.47	4.35	3.82	3.15	2.36	6.85
$(Ce/Yb)_n$	32.3	9.36	1.64	0.86	1.58	1.02	4.64	13.8	6.04	10.9	6.47	18.4	81.8
$(Eu/Eu^*)_n$	2.2	3.0	3.7	2.9	3.7	5.5	12.0	7.6	6.4	7.9	9.4	11.0	8.1

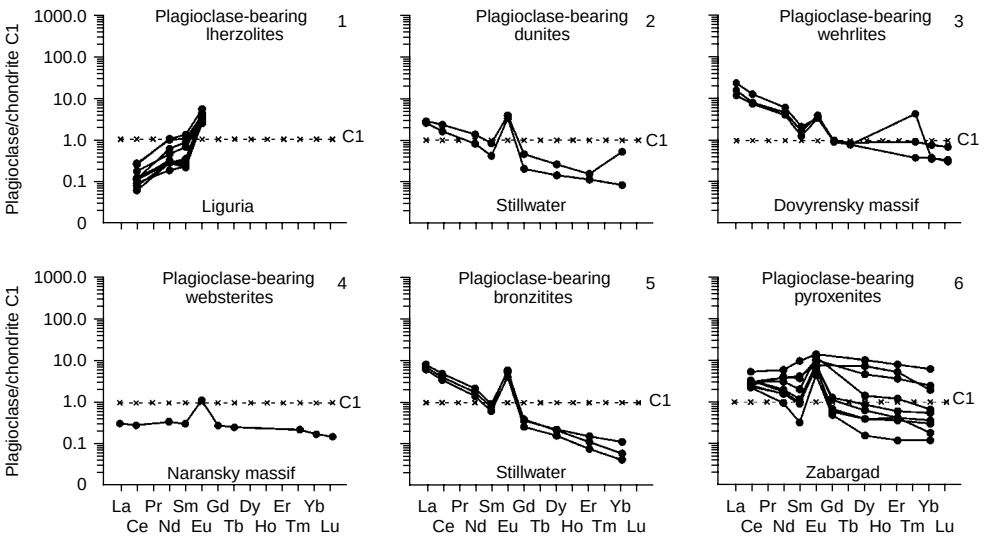

Figure 5.29 Chondrite-normalized REE patterns for plagioclases from plagioclase-bearing lherzolites, plagioclase-bearing wehrlites, and plagioclase-bearing pyroxenites (data Table 5.35).

Table 5.36 Rare earth element composition of plagioclases from troctolites and olivine gabbros (ppm).

	Massifs						
	Stillwater, USA		Samail, Oman				
	(Lambert & Simmons, 1988), IDMS		(Pallister & Knight, 1981), RNAA				
	7W-11.5	7W-19.0	Kf-17-1p	Kf-12-1p	Kf-15-1p	Kf-8-1pl	Kf-10-1p
Element	*Troctolites*		*Olivine gabbros*				
La	0.947	0.816	0.220	0.410	0.230	0.720	0.350
Ce	1.710	1.470	1.100	1.500	1.300	2.000	1.200
Pr	N.d.	N.d.	N.d.	N.d.	N.d.	N.d.	N.d.
Nd	0.722	0.605	0.580	0.670	0.740	1.100	0.540
Sm	0.134	0.108	0.076	0.120	0.085	0.180	0.120
Eu	0.225	0.240	0.280	0.320	0.240	0.430	0.240
Gd	0.105	0.080	0.089	0.110	0.097	0.230	0.130
Tb	N.d.	N.d.	0.013	0.017	0.016	0.041	0.021
Dy	0.080	0.057	N.d.	N.d.	N.d.	N.d.	N.d.
Ho	N.d.	N.d.	N.d.	N.d.	N.d.	N.d.	N.d.
Er	0.036	0.024	N.d.	N.d.	N.d.	N.d.	N.d.
Tm	N.d.	N.d.	N.d.	N.d.	N.d.	N.d.	N.d.
Yb	0.025	0.015	0.051	0.039	0.042	0.049	0.053
Lu	N.d.	N.d.	0.009	0.006	0.006	0.009	0.009
Total	3.98	3.42	N.d.	N.d.	N.d.	N.d.	N.d.
$(Ce/Yb)_n$	17.7	25.4	5.58	9.95	8.01	10.6	5.86
$(Eu/Eu^*)_n$	5.6	7.6	10.4	8.4	8.1	6.5	5.8

Table 5.36 Continued

	Massifs						
	Samail, Oman				Skaergaard, Greenland	Troodos, Cyprus	Beriozovsky, Russia
	(Pallister & Knight, 1981), RNAA				(Paster *et al.*, 1974), NAA	(Batanova *et al.*, 1996), IPMA	(Lesnov, 2001a–c), RNAA
	Kf-5-1pl	Kf-7-1pl	Kf-20-1p	Kf-6-1pl	5181	TV-73	132
Element	*Olivine gabbros*						
La	0.260	0.530	0.240	0.290	2.310	0.160	0.036
Ce	0.660	1.800	1.200	1.000	4.490	0.220	0.020
Pr	N.d.	N.d.	N.d.	N.d.	N.d.	N.d.	N.d.
Nd	0.730	1.000	0.440	0.800	1.620	0.160	0.051
Sm	0.094	0.190	0.059	0.093	0.300	0.050	0.010
Eu	0.220	0.300	0.170	0.210	3.000	0.090	0.017
Gd	0.089	0.200	0.051	0.120	0.250	N.d.	N.d.
Tb	0.013	0.030	0.008	0.020	0.036	N.d.	N.d.
Dy	N.d.	N.d.	N.d.	N.d.	N.d.	0.020	N.d.
Ho	N.d.	N.d.	N.d.	N.d.	0.032	N.d.	N.d.
Er	N.d.	N.d.	N.d.	N.d.	N.d.	0.020	N.d.
Tm	N.d.	N.d.	N.d.	N.d.	N.d.	N.d.	N.d.
Yb	0.034	0.057	0.014	0.048	0.045	0.020	N.d.
Lu	0.007	0.011	0.003	0.008	N.d.	N.d.	N.d.
Total	N.d.	N.d.	N.d.	N.d.	12.1	0.74	N.d.
$(Ce/Yb)_n$	5.02	8.17	22.2	5.39	25.8	2.85	N.d.
$(Eu/Eu^*)_n$	7.3	4.7	9.3	6.1	32.6	9.6	N.d.

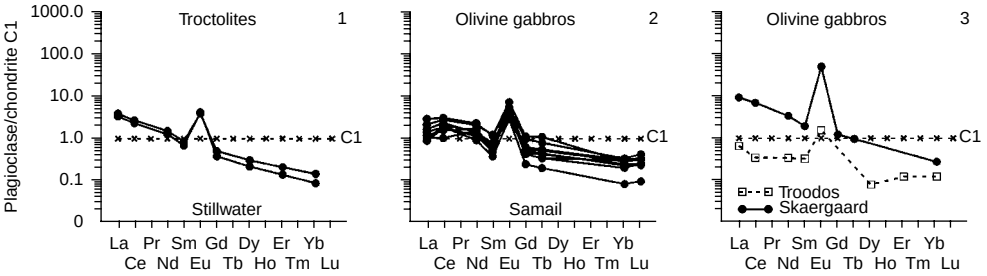

Figure 5.30 Chondrite-normalized REE patterns for plagioclases from troctolites and olivine gabbros (data Table 5.36).

and Skaergaard massifs REE are more fractionated (Fig. 5.30, 1, 3). Plagioclases from olivine gabbros of the Skaergaard massif have a considerable excess of Eu, whereas the Troodos sample has a very low level of REE accumulation (Fig. 5.30, 3).

Gabbro-norites, gabbros, and norites. Plagioclases from gabbro-norites were studied in the Beriozovsky and Naransky mafic–ultramafic massifs, which belong to ophiolitic associations (Lesnov, 2001). The minerals in both massifs reveal a depletion of REE, poor REE fractionation, and a considerable excess of Eu (Table 5.37,

Table 5.37 Rare earth element composition of plagioclases from gabbro-norites, norites, and gabbros (ppm).

	Massifs											
	Beriozovsky, Russia											
	(Lesnov, 2001), RNAA											
	128	130	131	131a	132a	138a	141	144	146	147	148	151
Element	*Gabbro-norites*											
La	0.180	0.060	0.044	0.075	N.d.	0.041	0.020	0.030	N.d.	0.026	0.018	0.024
Ce	0.350	0.140	N.d.	0.120	0.100	N.d.	0.140	N.d.	0.050	0.057	0.061	0.081
Pr	N.d.	N.d.	N.d.	N.d.	N.d.	N.d.	N.d.	N.d.	N.d.	N.d.	N.d.	N.d.
Nd	0.140	0.110	0.072	N.d.	0.080	0.060	0.070	0.040	0.030	0.052	0.050	0.065
Sm	0.025	0.020	0.012	0.018	0.030	0.015	0.027	0.017	0.010	0.013	0.020	0.015
Eu	0.075	0.050	0.058	0.056	0.018	0.016	0.031	0.050	0.047	0.050	0.040	0.056
Gd	N.d.	N.d.	N.d.	N.d.	N.d.	N.d.	N.d.	N.d.	N.d.	N.d.	N.d.	N.d.
Tb	0.002	0.003	0.005	0.002	N.d.	N.d.	0.004	N.d.	0.004	0.007	0.005	0.005
Dy	N.d.	N.d.	N.d.	N.d.	N.d.	N.d.	N.d.	N.d.	N.d.	N.d.	N.d.	N.d.
Ho	N.d.	N.d.	N.d.	N.d.	N.d.	N.d.	N.d.	N.d.	N.d.	N.d.	N.d.	N.d.
Er	N.d.	N.d.	N.d.	N.d.	N.d.	N.d.	N.d.	N.d.	N.d.	N.d.	N.d.	N.d.
Tm	0.001	0.002	0.002	0.002	N.d.	N.d.	N.d.	0.001	0.002	0.003	0.002	0.040
Yb	0.006	0.009	0.010	0.009	N.d.	N.d.	0.002	0.010	0.013	0.015	0.018	0.020
Lu	N.d.	N.d.	N.d.	N.d.	N.d.	N.d.	N.d.	N.d.	N.d.	N.d.	N.d.	N.d.
Total	N.d.	N.d.	N.d.	N.d.	N.d.	N.d.	N.d.	N.d.	N.d.	N.d.	N.d.	N.d.
$(Ce/Yb)_n$	14.2	4.03	N.d.	N.d.	N.d.	N.d.	N.d.	N.d.	N.d.	N.d.	N.d.	N.d.
$(Eu/Eu^*)_n$	N.d.	N.d.	N.d.	N.d.	N.d.	N.d.	N.d.	N.d.	N.d.	N.d.	N.d.	N.d.

	Massifs											
	Naransky, Mongolia			Samail, Oman			Skaergaard, Greenland			Stillwater, USA		
	(Lesnov, 2001), RNAA			(Pallister & Knight, 1981), RNAA			(Paster *et al.*, 1974), NAA			(Lambert & Simmons, 1988), IDMS		
	269	269r	278	Kf-11-1p	Kf-16-1p	Kf-18-1p	4312	4427	5086	7W-226.0	7W-47.6	7W-53.5
Element	*Gabbro-norites*			*Gabbros*								
La	0.130	0.130	0.100	0.440	0.210	0.230	3.000	1.750	4.300	0.332	0.636	0.362
Ce	0.510	0.210	0.290	1.500	0.730	0.830	14.10	2.900	9.200	5.280	0.905	0.546
Pr	N.d.	N.d.	N.d.	N.d.	N.d.	N.d.	N.d.	N.d.	N.d.	N.d.	N.d.	N.d.
Nd	0.200	0.180	0.100	0.820	0.490	0.440	7.400	0.990	3.800	0.185	0.274	0.185
Sm	0.031	0.100	0.022	0.140	0.070	0.069	1.760	0.172	0.710	0.030	0.040	0.028
Eu	0.096	0.440	0.088	0.300	0.220	0.200	4.300	1.550	1.450	0.070	0.118	0.098
Gd	N.d.	0.180	N.d.	0.110	0.054	0.082	1.940	0.140	0.720	0.021	0.026	N.d.
Tb	0.007	0.070	0.005	0.017	0.009	0.013	0.270	0.020	0.120	N.d.	N.d.	N.d.
Dy	N.d.	N.d.	N.d.	0.150	0.073	N.d.	N.d.	N.d.	N.d.	0.020	0.021	0.017
Ho	N.d.	N.d.	N.d.	N.d.	N.d.	N.d.	0.240	0.175	0.110	N.d.	N.d.	N.d.
Er	N.d.	N.d.	N.d.	N.d.	N.d.	N.d.	N.d.	N.d.	N.d.	0.010	0.010	0.009
Tm	0.003	0.010	0.002	N.d.	N.d.	N.d.	N.d.	N.d.	N.d.	N.d.	N.d.	N.d.
Yb	0.012	0.200	0.009	0.041	0.027	0.029	0.270	0.026	0.088	0.010	0.007	0.007
Lu	N.d.	0.040	N.d.	0.011	0.005	0.005	N.d.	N.d.	N.d.	N.d.	N.d.	N.d.
Total	0.99	1.56	0.62	N.d.	N.d.	N.d.	33.3	7.72	20.5	5.96	2.04	1.25
$(Ce/Yb)_n$	N.d.	0.27	N.d.	9.47	7.00	7.41	13.5	28.9	27.1	137	33.6	20.2
$(Eu/Eu^*)_n$	N.d.	9.91	N.d.	7.14	10.6	8.12	7.08	29.7	6.14	8.11	10.5	18.6

(*Continued*)

Table 5.37 Continued

	Massifs											
	Ivrea Verbano, Italy											
	(Mazzucchelli *et al.*, 1992a,b), IPMA											
	FE31-1	FE31-2	FE51	MO95-2	MO95-5	MP12-1	MP12-2	MP13	MP5	MP6	MP9	MZ132
Element	*Gabbros*											
La	1.280	1.510	7.890	11.30	11.20	2.610	2.500	3.470	5.360	9.830	9.090	7.470
Ce	2.120	2.190	11.70	14.20	14.50	5.190	4.750	6.420	7.640	11.60	13.10	10.80
Pr	N.d.	N.d.	N.d.	N.d.	N.d.	N.d.	N.d.	N.d.	N.d.	N.d.	N.d.	N.d.
Nd	0.830	1.010	2.590	3.300	3.430	2.260	2.030	2.270	2.280	1.960	3.020	2.760
Sm	0.133	0.120	0.309	0.197	0.202	0.270	0.220	0.221	0.189	0.124	0.194	0.210
Eu	0.730	0.515	0.755	1.410	1.310	1.100	0.955	0.700	1.300	1.050	2.090	2.000
Gd	0.124	0.087	0.321	0.125	0.090	0.122	0.105	0.120	0.407	0.089	0.133	0.138
Tb	N.d.	N.d.	N.d.	N.d.	N.d.	N.d.	N.d.	N.d.	N.d.	N.d.	N.d.	N.d.
Dy	0.058	0.048	0.146	0.140	0.119	0.044	0.034	0.047	0.046	0.095	0.161	0.061
Ho	N.d.	N.d.	N.d.	N.d.	N.d.	N.d.	N.d.	N.d.	N.d.	N.d.	N.d.	N.d.
Er	0.022	0.018	0.086	0.024	0.019	0.011	0.008	0.027	0.017	0.035	0.059	0.025
Tm	N.d.	N.d.	N.d.	N.d.	N.d.	N.d.	N.d.	N.d.	N.d.	N.d.	N.d.	N.d.
Yb	0.011	0.014	0.036	0.006	0.010	0.003	0.007	0.012	0.009	0.006	0.006	0.046
Lu	N.d.	N.d.	N.d.	N.d.	N.d.	N.d.	N.d.	N.d.	N.d.	N.d.	N.d.	N.d.
Total	5.31	5.51	23.8	30.7	30.9	11.6	10.6	13.3	17.3	24.8	27.9	23.5
$(Ce/Yb)_n$	49.9	40.5	84. 2	613	375	448	176	138	220	500	565	60.8
$(Eu/Eu^*)_n$	17.1	14.7	7.27	25.7	25.8	16.1	17.0	11.9	13.9	29.2	37.7	33.8

	Massifs											
	Ivrea Verbano, Italy		East Sayan, Russia			Mid-Atlantic Ridge				Stillwater, USA		
	(Mazzucchelli *et al.*, 1992a,b), IPMA		(Mekhonoshin *et al.*, 1993), RNAA			(Balashov, 1976)				(Lambert & Simmons, 1988), IDMS		
	MZ145-2	MZ145-3	V2-84	V20-84	V9-84	T52	T14	T7	7W-206.6	7W-239.7	7W-65.8	LM01	LM11
Element	*Gabbros*									*Norites*			
La	22.73	21.40	4.800	5.600	4.500	N.d.	0.538	N.d.	0.568	0.336	0.728	1.340	0.761
Ce	24.65	22.60	10.20	12.50	7.900	1.700	1.060	1.140	1.020	5.850	1.260	2.450	1.260
Pr	N.d.	N.d.	N.d.	N.d.	N.d.	N.d.	N.d.	N.d.	N.d.	N.d.	N.d.	N.d.	N.d.
Nd	3.560	2.970	6.100	7.900	3.800	1.120	0.627	0.652	0.423	0.232	0.537	1.050	0.500
Sm	0.170	0.144	1.700	2.200	0.890	0.263	0.145	0.151	0.077	0.040	0.098	0.185	0.086
Eu	1.250	1.490	1.890	1.640	1.500	0.480	0.429	0.294	0.111	0.069	0.227	0.276	0.161
Gd	0.175	0.091	1.220	1.580	0.920	0.285	0.154	0.165	0.054	0.027	0.070	0.140	0.060
Tb	N.d.	N.d.	0.160	0.200	0.110	N.d.	N.d.	N.d.	N.d.	N.d.	N.d.	N.d.	N.d.
Dy	0.070	0.050	N.d.	N.d.	N.d.	0.205	0.101	0.133	0.039	0.023	0.053	0.088	0.047
Ho	N.d.	N.d.	N.d.	N.d.	N.d.	N.d.	N.d.	N.d.	N.d.	N.d.	N.d.	N.d.	N.d.
Er	0.022	0.018	N.d.	N.d.	N.d.	0.101	0.045	0.072	0.014	0.011	0.021	0.032	0.020
Tm	N.d.	N.d.	N.d.	N.d.	N.d.	N.d.	N.d.	N.d.	N.d.	N.d.	N.d.	N.d.	N.d.
Yb	0.011	0.006	0.180	0.170	0.090	0.065	0.033	0.053	0.006	0.009	0.015	0.017	0.015
Lu	N.d.	N.d.	0.020	0.020	0.010	0.008	0.005	0.001	N.d.	N.d.	N.d.	N.d.	N.d.
Total	52.6	48.8	N.d.	N.d.	N.d.	4.23	3.14	2.66	2.31	6.60	3.01	5.58	2.91
$(Ce/Yb)_n$	580	975	14.7	19.0	22.7	6.8	8.3	5.6	44	17	22	37	22
$(Eu/Eu^*)_n$	22.0	37.2	3.83	2.57	5.03	5.3	8.7	5.7	5.0	6.1	8.0	5.0	6.5

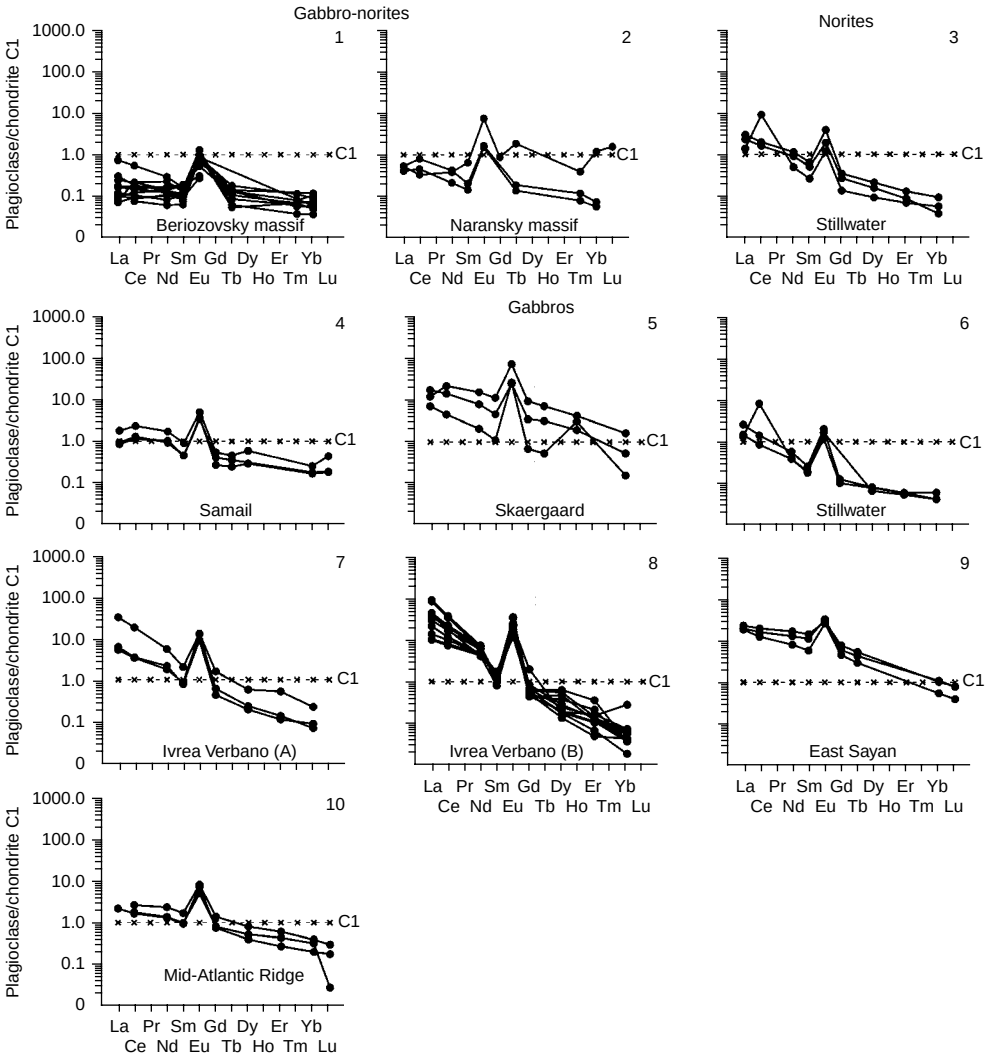

Figure 5.31 Chondrite-normalized REE patterns for plagioclases from gabbro-norites, norites, and gabbros (data Table 5.37).

Fig. 5.31). Plagioclases from gabbro were studied in the samples from the Samail, Skaergaard, and Stillwater massifs, from the Ivrea Verbano complex, the Eastern Sayan massifs, and the Mid-Atlantic Ridge (Table 5.37, Fig. 5.31). In the average total contents of elements, plagioclases from the Samail and Stillwater complexes and from the Mid-Atlantic Ridge are similar to chondrite C1, with very poor fractionation of REE in the samples from the Samail massif and the Mid-Atlantic Ridge (Fig. 5.31, 4, 10). They are more fractionated in the samples from the Skaergaard

and Eastern Sayan massifs (Fig. 5.31, 5, 9), but most considerably, in the samples from the Ivrea Verbano complex (Fig. 5.31, 7). The researchers suggest that the REE enrichment of the latter is the result of their crystallization from melts contaminated by sedimentary rock material (Mazzucchelli *et al.*, 1992a,b). Data on plagioclases from norites are available only for the Stillwater massif (see Table 5.37). They are depleted both in heavy REE (<0.1 t. ch.) and in light REE, which level of accumulation is comparable to chondrite C1 (Fig. 5.31, 6). The REE patterns of plagioclases from norites are similar to those of their samples from gabbros of the Mid-Atlantic Ridge.

Monzonorites and anorthosites. Data on plagioclases from these rocks were obtained from the studies of some mafic massifs on the territories of Norway and Iceland, and from the Stillwater massif (Table 5.38). The mineral from monzonorites and anorthosites, which compose the Norwegian massifs, is enriched with all REE, but especially light REE, compared to samples from the Iceland and Stillwater massifs. But all these plagioclases are comparable in their intensity of positive Eu anomalies (Fig. 5.32). Plagioclases from anorthosites are most thoroughly studied in the Stillwater massif. They demonstrate a tendency of an inverse relationship between the general level of REE accumulation and intensity of positive Eu anomalies (see Fig. 5.32, 2). The observed concordance of REE patterns implies the stability of inter-element relationships in these plagioclases, which, in turn, suggests their equilibrium crystallization from melts.

Basalts. The REE composition of plagioclases from terrestrial basalts was studied on a few samples from volcanogenic complexes of Canada, USA, Japan, and Greenland (Table 5.39). These plagioclases reveal a varying but moderate level of REE accumulation. The mineral from basalts of Mount Adams and Japan provinces (Fig. 5.33, 1, 2) is characterized by a somewhat elevated level of Ce accumulation compared to samples from the basalts of Greenland and Canada provinces (see Fig. 5.33, 3, 4). At the same time, all plagioclases from basalts of different provinces to some degree differ in the intensity of fractionation of the elements.

Andesites, dacites, and rhyolites. The total level of REE accumulation in plagioclases increases from andesites to dacites and rhyolites, that is, with increasing amount of anorthite end member (Table 5.40). In most of them, REE are intensely fractionated, particularly in the samples from andesites of the Mount Adams complex (Fig. 5.34). The REE patterns of most samples demonstrate rather intensely positive Eu anomalies. The patterns of all plagioclase samples from dacite of Honshu Island and from rhyolites of the Twin Peaks complex are similar in the position on the plots and their configuration, which suggests that phenocrysts of these plagioclases were in equilibrium state with their parental melts (see Fig. 5.34, 5, 6).

Metamorphic rocks and products of experiments. Data on the REE composition of plagioclases from these formations are scarce (Table 5.41). The data show that REE in the mineral from mafic gneisses and granulites are distributed more uniformly than in the samples from garnet amphibolites. In plagioclases from amphibolites and granulites, Eu content is somewhat higher than in samples from mafic gneisses, with stronger fractionation of the elements in the latter. In plagioclases synthesized in the experiments under atmospheric conditions, no positive Eu anomalies were observed, most likely, owing to the very high volatility of oxygen during their crystallization.

Table 5.38 Rare earth element composition of plagioclases from monzonorites, and anorthosites (ppm).

	Massifs										
	Hidra, Norway				Stillwater, USA						
	(Duchesne *et al.*, 1974), NAA				(Lambert & Simmons, 1988), IDMS						
	P7020	P251-2/1	P200-2/2	P199-2/1	18W-105.5	18W-112.5	18W-120.5	18W-142.0	18W-99.5	7W-29.0	7W-34.0
Element	*Monzonorites*				*Anorthosites*						
La	37.20	19.80	52.30	15.10	0.941	2.100	1.590	0.937	1.300	0.770	0.556
Ce	18.30	35.50	26.30	23.10	1.790	3.840	2.890	1.560	2.160	1.450	0.915
Pr	N.d.	N.d.	N.d.	N.d.	N.d.	N.d.	N.d.	N.d.	N.d.	N.d.	N.d.
Nd	7.100	15.20	9.600	8.600	0.724	1.690	1.220	0.614	0.834	0.591	0.351
Sm	1.490	2.420	1.270	1.04	0.126	0.340	0.225	0.100	0.139	0.108	0.061
Eu	2.860	4.230	3.030	2.33	0.256	0.308	0.309	0.249	0.285	0.228	0.179
Gd	N.d.	1.570	0.900	0.81	0.093	0.301	0.193	0.018	0.107	0.077	0.043
Tb	0.160	0.260	0.120	0.08	N.d.	N.d.	N.d.	N.d.	N.d.	N.d.	N.d.
Dy	N.d.	N.d.	N.d.	N.d.	0.072	0.252	0.139	0.055	0.072	0.057	0.043
Ho	N.d.	0.300	0.160	0.08	N.d.	N.d.	N.d.	N.d.	N.d.	N.d.	N.d.
Er	N.d.	N.d.	N.d.	N.d.	0.032	0.123	0.062	0.022	0.031	0.023	0.022
Tm	N.d.	0.130	N.d.	N.d.	N.d.	N.d.	N.d.	N.d.	N.d.	N.d.	N.d.
Yb	0.310	0.820	0.260	0.089	0.023	0.100	0.044	0.016	0.022	0.014	0.020
Lu	0.047	0.120	0.036	0.013	N.d.	N.d.	N.d.	N.d.	N.d.	N.d.	N.d.
Total	N.d.	80.4	94.0	51.2	4.06	9.05	6.67	3.57	4.95	3.32	2.19
$(Ce/Yb)_n$	15.3	11.2	26.2	67.2	20.1	9.9	17.0	25.2	25.4	26.8	11.8
$(Eu/Eu^*)_n$	N.d.	6.2	8.3	7.5	6.9	2.9	4.4	11.6	6.9	7.3	10.2

	Massifs										
	Stillwater, USA			Bierkreim, Norway					Egersund, Norway		
	(Lambert & Simmons, 1988), IDMS			(Griffin *et al.*, 1974), NAA							
	7W-45.8	7W-72.6	7W-91.0	66-187	66-71	64-23	64-58	58	45	48	64100
Element	*Anorthosites*										
La	3.100	0.684	N.d.	2.870	2.890	3.950	9.730	8.550	1.720	1.730	1.690
Ce	6.090	1.110	1.540	N.d.	N.d.	N.d.	N.d.	22.20	3.100	3.650	N.d.
Pr	N.d.	N.d.	N.d.	N.d.	N.d.	N.d.	N.d.	N.d.	N.d.	N.d.	N.d.
Nd	2.630	0.410	0.628	N.d.	N.d.	N.d.	N.d.	N.d.	N.d.	N.d.	N.d.
Sm	0.523	0.068	0.118	0.510	0.450	0.300	1.490	2.410	0.180	0.160	0.360
Eu	0.301	0.210	0.220	0.880	0.910	0.780	3.630	1.810	0.900	0.800	0.450
Gd	0.462	0.046	0.104	N.d.	N.d.	N.d.	N.d.	N.d.	N.d.	N.d.	N.d.
Tb	N.d.	N.d.	N.d.	0.084	0.070	0.030	0.150	0.360	0.021	0.020	0.060
Dy	0.368	0.039	0.087	N.d.	N.d.	N.d.	N.d.	N.d.	N.d.	N.d.	N.d.
Ho	N.d.	N.d.	N.d.	N.d.	N.d.	N.d.	N.d.	N.d.	N.d.	N.d.	N.d.
Er	0.158	0.019	0.042	N.d.	N.d.	N.d.	N.d.	N.d.	N.d.	N.d.	N.d.
Tm	N.d.	N.d.	N.d.	N.d.	N.d.	N.d.	N.d.	N.d.	N.d.	N.d.	N.d.
Yb	0.116	0.014	0.032	0.063	0.009	0.011	0.250	1.600	0.030	0.012	0.180
Lu	N.d.	N.d.	N.d.	N.d.	N.d.	N.d.	0.030	0.240	0.004	0.003	0.002
Total	13.8	2.60	2.77	N.d.	N.d.	N.d.	N.d.	N.d.	N.d.	N.d.	N.d.
$(Ce/Yb)_n$	13.6	20.5	12.5	N.d.	N.d.	N.d.	N.d.	3.59	26.7	78.7	N.d.
$(Eu/Eu^*)_n$	1.8	10.7	6.0	9.2	10.7	13.8	12.9	4.0	26.5	26.5	6.6

(*Continued*)

Table 5.38 Continued

	Massifs									
	Holand, Norway		Bergen, Norway	Sogn, Norway	Iceland					
	(Griffin *et al.*, 1974), NAA									
	69	77	2C	9A	IV-7	IV-17	V-7	V-13	H-6	H-13
Element	*Anorthosites*									
La	4.130	2.460	2.050	1.280	0.240	0.360	0.220	0.300	0.500	0.130
Ce	8.200	4.800	2.350	2.260	N.d.	N.d.	N.d.	N.d.	N.d.	N.d.
Pr	N.d.	N.d.	N.d.	N.d.	N.d.	N.d.	N.d.	N.d.	N.d.	N.d.
Nd	N.d.	N.d.	N.d.	N.d.	N.d.	N.d.	N.d.	N.d.	N.d.	N.d.
Sm	0.770	0.190	0.170	0.120	0.110	0.160	0.100	0.200	0.090	0.100
Eu	1.000	0.770	0.430	0.400	0.190	0.330	0.160	0.410	0.210	0.180
Gd	N.d.	N.d.	N.d.	N.d.	N.d.	N.d.	N.d.	N.d.	N.d.	N.d.
Tb	0.085	0.011	0.005	0.009	0.015	0.037	0.016	0.010	0.025	0.013
Dy	N.d.	N.d.	N.d.	N.d.	N.d.	N.d.	N.d.	N.d.	N.d.	N.d.
Ho	N.d.	N.d.	N.d.	N.d.	N.d.	N.d.	N.d.	N.d.	N.d.	N.d.
Er	N.d.	N.d.	N.d.	N.d.	N.d.	N.d.	N.d.	N.d.	N.d.	N.d.
Tm	N.d.	N.d.	N.d.	N.d.	N.d.	N.d.	N.d.	N.d.	N.d.	N.d.
Yb	0.140	0.013	0.014	0.015	0.020	0.008	0.077	0.066	0.009	0.056
Lu	0.022	N.d.	N.d.	N.d.	0.001	0.001	0.008	0.006	0.006	0.001
Total	N.d.	N.d.	N.d.	N.d.	N.d.	N.d.	N.d.	N.d.	N.d.	N.d.
$(La/Yb)_n$	15.2	95.6	43.4	39.0	8.1	30.4	1.9	3.1	37.5	1.6
$(Eu/Eu^*)_n$	6.9	21.5	13.4	17.7	9.2	11.1	8.5	10.9	12.4	9.6

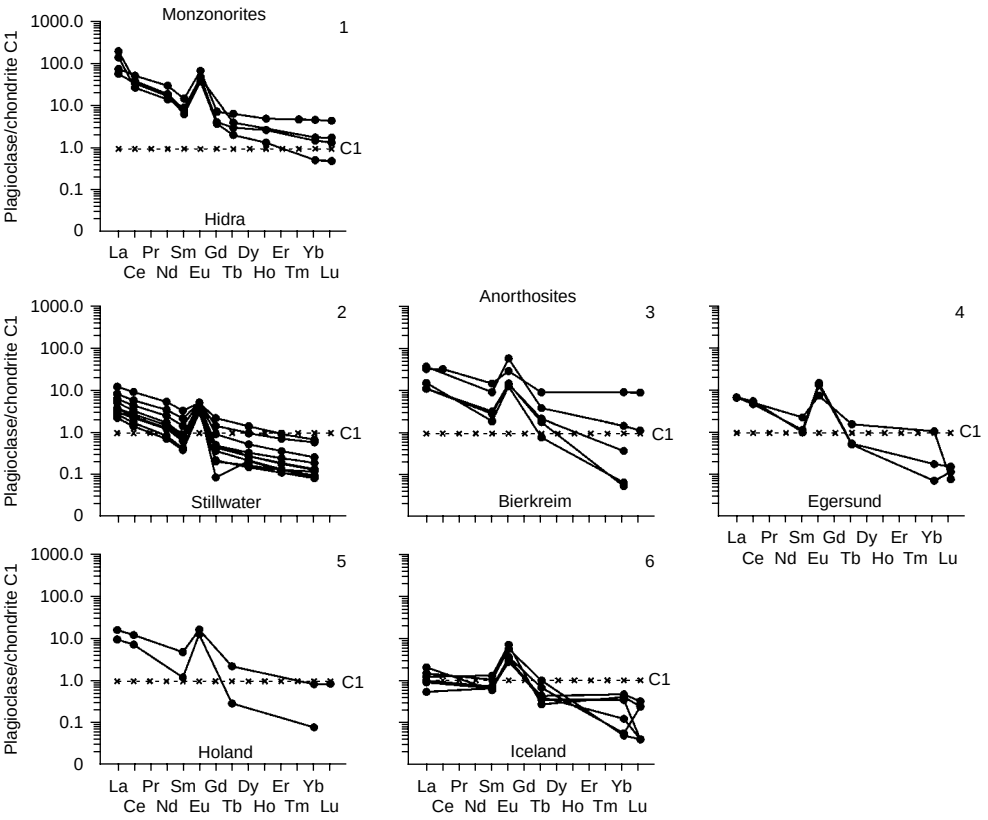

Figure 5.32 Chondrite-normalized REE patterns for plagioclases from monzonorites and anorthosites (data Table 5.38).

5.4.2 Experience of systematization of plagioclases on the basis of some parameters of REE distribution

The values of some parameters of REE distribution in plagioclases from different types of rocks, calculated from collection of 200 analyses, were used to determine the criteria for establishing geochemical types of this mineral. The following three criteria were chosen as the most efficient: (1) level of Ce accumulation, which varies in the range of 0.11–55 t. ch.; (2) intensity of positive Eu anomaly expressed in terms of $(Eu/Eu^*)_n$ values, which vary in the range of 2.7–143; and (3) degree of fractionation of the elements expressed in terms of $(Ce/Yb)_n$ values, which vary in the range of 6.5–365. Using these criteria, the total collection of analyzed plagioclase samples by their petrographic feature was divided into 30 subsamplings ranging from 2 to 24 analyses (Table 5.42). The distribution patterns of average contents of elements in plagioclases, calculated for each of them, are shown in Figure 5.35.

Table 5.39 Rare earth element composition of plagioclases from basalts (ppm).

	Provinces							
	Mount Adams, USA	Japan		Greenland	Manitoba, Canada			
	(Dunn & Sen, 1994), IPNA	(Higuchi & Nagasawa, 1969), NAA	(Philpotts & Schnetzler, 1970b), IDMS		(Phinney & Morrison, 1990), INAA			
	1	HN1	GSFC204	GSFC208	M41	BRN2A	AB11	BVL100A
Element	*Basalts*							
La	4.700	4.570	N.d.	N.d.	0.492	0.164	2.482	0.194
Ce	7.500	5.970	3.520	1.790	0.800	0.260	4.040	0.370
Pr	0.660	N.d.	N.d.	N.d.	N.d.	N.d.	N.d.	N.d.
Nd	2.200	1.200	2.040	1.080	N.d.	N.d.	N.d.	N.d.
Sm	0.370	0.230	0.467	0.224	0.063	0.043	0.161	0.052
Eu	1.200	0.686	0.401	0.621	N.d.	N.d.	N.d.	N.d.
Gd	0.810	0.240	0.627	N.d.	N.d.	N.d.	N.d.	N.d.
Tb	0.034	0.022	N.d.	N.d.	0.010	0.006	0.012	0.009
Dy	0.110	N.d.	0.573	0.094	N.d.	N.d.	N.d.	N.d.
Ho	0.005	N.d.	N.d.	N.d.	N.d.	N.d.	N.d.	N.d.
Er	N.d.	N.d.	0.420	0.044	N.d.	N.d.	N.d.	N.d.
Tm	N.d.	N.d.	N.d.	N.d.	N.d.	N.d.	N.d.	N.d.
Yb	N.d.	0.037	0.489	0.054	0.016	0.022	0.027	0.028
Lu	N.d.	N.d.	0.085	0.008	0.002	0.003	0.005	0.005
Total	N.d.	N.d.	8.62	3.92	N.d.	N.d.	N.d.	0.658
$(Ce/Yb)_n$	N.d.	N.d.	1.86	8.58	N.d.	N.d.	N.d.	N.d.
$(Eu/Eu^*)_n$	6.5	8.9	2.3	14.7	N.d.	N.d.	N.d.	N.d.

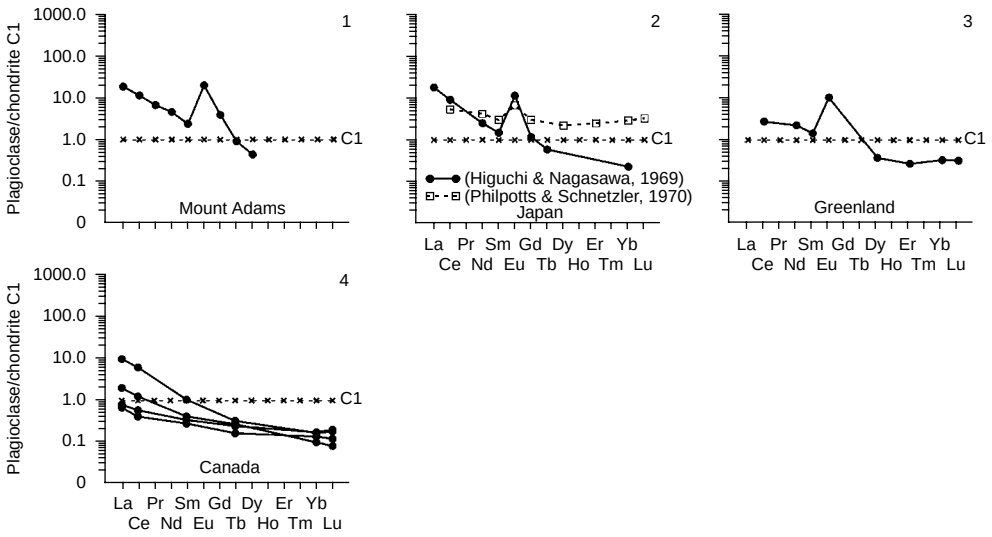

Figure 5.33 Chondrite-normalized REE patterns for plagioclases from basalts (data Table 5.39).

Level of Ce accumulation. By the average contents of this element, which occurs in great amounts in plagioclases and is detected with a fairly high accuracy, plagioclases are divided into four geochemical types:

1. Enriched (55–20 t. ch.). Represented by samples from rhyolites (Twin Peaks), monzonorites (Hidra), alkali gabbro-norites (the moon), and alkali anorthosites (the moon).
2. Moderately enriched (19–10 t. ch.). Represented by samples from dacites (Japan), gabbros (Ivrea Verbano), monzogabbros (the moon), gabbros (Eastern Sayan and Skaergaard), anorthosites (Norway), and andesites (Mount Adams).
3. Depleted (9–1 t. ch.). Represented by samples from wehrlites (Dovyrensky massif), ferriferous mafic rocks (the moon), anorthosites (Stillwater), meteorites (Chessigny, Valadares, and others), gabbros (Stillwater), pyroxenites (Zabargad), magnesian mafic rock (the moon), troctolites, plagioclase-bearing dunites and norites (Stillwater), olivine gabbros (Samail), basalts (Manitoba province), and gabbros (Mid-Atlantic Ridge and Samail).
4. Strongly depleted (0.9–0.1 t. ch.). Represented by samples from lherzolites (Liguria massifs), gabbro-norites (Beriozovsky massif), meteorites (Acapulco), and ferriferous anorthosites (the moon).

$(Eu/Eu^*)_n$ parameter. Based on the average values of this especially representative parameter for plagioclases, this mineral are divided into four geochemical types:

1. High values (143–99). Represented by samples from meteorites of Acapulco, Chessigny, and Valadares.

Table 5.40 Rare earth element composition of plagioclases from andesites, dacites, and rhyolites (ppm).

	Provinces														
	Mount Adams, USA			Japan				Saipan	Kuril islands, Russia						
	(Dunn & Sen, 1994), IPMA			(Higuchi & Nagasawa, 1970), NAA	(Philpotts & Schnetzler, 1970a), IDMS				(Bindeman & Bailey, 1999), IPMA						
	14	49	7	41	GSFC184	GSFC233	GSFC240	GSFC271	B25-24/3	B-540	B15-81/1	R135-1	B17-40/6	B17-41/4	92-223
Element	*Andesites*														
La	3.000	5.400	4.000	5.300	N.d.	N.d.	N.d.	N.d.	1.000	0.640	0.670	0.880	1.250	2.670	6.000
Ce	5.300	8.000	6.200	8.200	0.529	10.200	0.459	2.360	1.100	1.200	1.230	1.630	2.450	4.800	15.87
Pr	0.370	0.690	0.620	0.840	N.d.	N.d.	N.d.	N.d.	0.150	0.140	0.130	0.150	0.260	0.540	0.590
Nd	1.100	2.300	2.200	3.170	0.483	N.d.	0.156	1.570	0.780	0.640	0.560	0.650	0.970	1.730	1.280
Sm	0.150	0.340	0.300	0.480	0.127	0.827	0.063	0.369	0.180	0.180	0.120	0.160	0.190	0.240	0.270
Eu	1.400	1.500	1.000	1.400	0.202	0.238	0.053	0.588	0.200	0.180	0.220	0.160	0.320	0.600	0.310
Gd	N.d.	0.250	0.300	0.550	0.133	N.d.	N.d.	0.272	N.d.	N.d.	N.d.	N.d.	N.d.	N.d.	N.d.
Tb	N.d.	0.010	0.025	0.043	N.d.	N.d.	N.d.	N.d.	N.d.	N.d.	N.d.	N.d.	N.d.	N.d.	N.d.
Dy	N.d.	N.d.	0.050	0.140	0.126	0.863	0.035	0.254	N.d.	N.d.	N.d.	N.d.	N.d.	N.d.	N.d.
Ho	N.d.	N.d.	N.d.	0.011	N.d.	N.d.	N.d.	N.d.	N.d.	N.d.	N.d.	N.d.	N.d.	N.d.	N.d.
Er	N.d.	N.d.	N.d.	N.d.	0.074	N.d.	N.d.	0.126	N.d.	N.d.	N.d.	N.d.	N.d.	N.d.	N.d.
Tm	N.d.	N.d.	N.d.	N.d.	N.d.	N.d.	N.d.	N.d.	N.d.	N.d.	N.d.	N.d.	N.d.	N.d.	N.d.
Yb	N.d.	N.d.	N.d.	N.d.	0.066	N.d.	N.d.	0.102	N.d.	N.d.	N.d.	N.d.	N.d.	N.d.	N.d.
Lu	N.d.	N.d.	N.d.	N.d.	0.012	N.d.	N.d.	0.017	N.d.	N.d.	N.d.	N.d.	N.d.	N.d.	N.d.
Total	N.d.	N.d.	N.d.	N.d.	1.75	N.d.	N.d.	5.66	N.d.	N.d.	N.d.	N.d.	N.d.	N.d.	N.d.
$(Ce/Yb)_n$	N.d.	N.d.	N.d.	N.d.	2.07	N.d.	N.d.	5.99	N.d.	N.d.	N.d.	N.d.	N.d.	N.d.	N.d.
$(Eu/Eu^*)_n$	N.d.	15.1	10.1	8.3	4.7	N.d.	N.d.	5.4	N.d.	N.d.	N.d.	N.d.	N.d.	N.d.	N.d.

	Provinces										
	Honshu, Japan					Twin Peaks, USA					
	(Nagasawa & Schnetzler, 1971), IDMS					(Nash & Crecraft, 1985), INAA					
	NC-1	NC-2	NC-4	NC-6	NC-8	12	15	20	4	6	8
Element	*Dacites*					*Rhyolites*					
La	N.d.	N.d.	N.d.	N.d.	N.d.	35.00	35.00	18.00	20.00	28.00	9.000
Ce	11.40	6.800	12.70	N.d.	15.60	50.00	52.00	28.00	29.00	40.00	15.90
Pr	N.d.	N.d.	N.d.	N.d.	N.d.	N.d.	N.d.	N.d.	N.d.	N.d.	N.d.
Nd	2.870	1.690	3.600	3.330	4.650	15.00	14.00	8.100	7.700	12.00	5.400
Sm	0.327	0.280	0.480	0.550	0.590	1.760	1.720	0.870	0.830	1.330	0.740
Eu	0.970	0.770	1.690	1.440	2.450	5.550	5.120	2.280	2.570	3.390	1.450
Gd	N.d.	N.d.	0.435	N.d.	N.d.	N.d.	N.d.	N.d.	N.d.	N.d.	N.d.
Tb	N.d.	N.d.	N.d.	N.d.	N.d.	0.150	0.140	0.070	0.080	0.110	0.070
Dy	0.144	N.d.	0.255	0.313	0.308	0.700	0.700	0.500	0.400	0.700	0.500
Ho	N.d.	N.d.	N.d.	N.d.	N.d.	N.d.	N.d.	N.d.	N.d.	N.d.	N.d.
Er	0.079	0.092	0.136	0.160	N.d.	N.d.	N.d.	N.d.	N.d.	N.d.	N.d.
Tm	N.d.	N.d.	N.d.	N.d.	N.d.	N.d.	N.d.	N.d.	N.d.	N.d.	N.d.
Yb	0.085	0.069	0.123	0.129	0.194	0.340	0.360	0.350	0.250	0.360	0.420
Lu	0.015	0.012	0.020	0.022	0.025	0.040	0.050	0.060	0.040	0.050	0.070
Total	15.9	N.d.	19.4	N.d.	23.8	109	109	58.2	60.9	85.9	33.6
$(Ce/Yb)_n$	34.7	25.5	26.7	N.d.	20.8	38.1	37.4	20.7	30.0	28.8	9.8
$(Eu/Eu^*)_n$	N.d.	N.d.	11.1	N.d.	N.d.	N.d.	N.d.	N.d.	N.d.	N.d.	N.d.

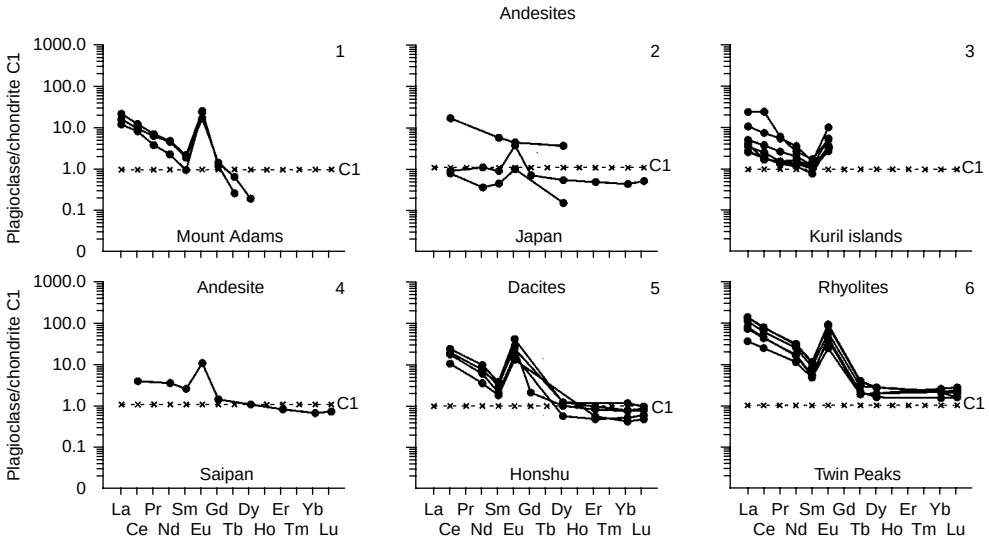

Figure 5.34 Chondrite-normalized REE patterns for plagioclases from andesites, dacites, and rhyolites (data Table 5.40).

2. Elevated values (50–18). Represented by samples from ferriferous anorthosites, monzogabbros, magnesioferous gabbros, alkali anorthosites, and alkali gabbro-norites (the moon), and gabbros (Ivrea Verbano).
3. Moderate values (17–5). Represented by samples from gabbro-norites (Beriozovsky massif), gabbros (Skaergaard, Samail, and Mid-Atlantic Ridge), magnesioferous mafic rocks (the moon), olivine gabbros (Samail), pyroxenites (Zabargad), and troctolites (Stillwater).
4. Low values (<4). Represented by samples of gabbros (massifs in Eastern Sayan) and wehrlites (Dovyrensky massif).

$(Ce/Yb)_n$ parameter. According to the average values of this parameter, plagioclases are divided into four geochemical types:

1. Very high values (365). Represented in gabbros (Ivrea Verbano).
2. High values (70–20). Represented in gabbros, norites, and troctolites (Stillwater), anorthosites (Norway), monzonorites (Hidra), anorthosites (the moon), dacites (Honshu Island), rhyolites (Twin Peaks), meteorites (Acapulco), gabbros (Skaergaard), and wehrlites (Dovyrensky massif).
3. Moderate values (19–10). Represented in anorthosites and plagioclase-bearing dunites (Stillwater), in gabbros (massifs in Eastern Sayan), ferriferous mafic rocks (the moon), basalts (Manitoba province), and monzogabbros (the moon).
4. Low values (<10). Represented in gabbros and olivine gabbros (Samail), pyroxenites (Zabargad Island), gabbros (Mid-Atlantic Ridge), and anorthosites (the moon).

Table 5.41 Rare earth element composition of plagioclases from metamorphic rocks and in synthetic plagioclase (ppm).

	Provinces											
	Scotland							Catalina Schist, California, USA				Dariganga, Mongolia
	(Pride & Muecke, 1981), INAA							(Sorensen & Grossman, 1989), INAA				(Stosch *et al.*, 1995), INAA
	67-109	64-12	65-165	65-33	65-41	66-11	67-30	712845	BCM	MIG	MM	8519/52
Element	*Gneisses*							*Garnet amphibolites*				
La	6.930	8.780	3.130	1.990	3.340	4.410	3.650	2.470	0.990	2.470	0.590	5.700
Ce	6.060	11.80	4.760	3.670	5.030	5.080	7.790	3.550	5.000	4.420	0.940	9.000
Pr	N.d.	N.d.	N.d.	N.d.	N.d.	N.d.	N.d.	N.d.	N.d.	N.d.	N.d.	N.d.
Nd	N.d.	N.d.	N.d.	N.d.	N.d.	N.d.	N.d.	1.260	12.00	2.030	0.440	2.800
Sm	0.200	0.540	0.360	0.350	0.300	0.610	0.510	0.176	0.172	0.490	0.098	0.354
Eu	0.230	0.560	0.620	0.430	0.460	0.400	1.210	1.190	0.540	0.400	1.220	1.090
Gd	N.d.	N.d.	N.d.	N.d.	N.d.	N.d.	N.d.	N.d.	N.d.	N.d.	N.d.	0.330
Tb	0.050	0.100	0.110	0.080	0.070	0.150	0.100	0.023	0.300	0.037	0.010	0.047
Dy	N.d.	N.d.	N.d.	N.d.	N.d.	N.d.	N.d.	N.d.	N.d.	N.d.	N.d.	N.d.
Ho	N.d.	N.d.	N.d.	N.d.	N.d.	N.d.	N.d.	N.d.	N.d.	N.d.	N.d.	N.d.
Er	N.d.	N.d.	N.d.	N.d.	N.d.	N.d.	N.d.	N.d.	N.d.	N.d.	N.d.	N.d.
Tm	N.d.	N.d.	N.d.	N.d.	N.d.	N.d.	N.d.	N.d.	N.d.	N.d.	N.d.	N.d.
Yb	0.080	0.120	0.100	0.120	0.050	0.150	0.040	0.070	0.500	0.058	0.030	0.160
Lu	0.008	0.020	0.010	0.020	0.007	0.020	0.007	0.007	0.100	0.010	0.004	0.021
Total	13.6	21.9	9.09	6.66	9.26	10.8	13.3	8.75	19.6	9.92	3.33	19.5
$(Ce/Yb)_n$	19.6	25.5	12.3	7.9	26.0	8.8	50.4	13.1	2.6	19.7	8.1	14.6
$(Eu/Eu^*)_n$	N.d.	N.d.	N.d.	N.d.	N.d.	N.d.	N.d.	N.d.	N.d.	N.d.	N.d.	9.6

(*Continued*)

Table 5.41 Continued

	Provinces		Experiment's numbers										
	Shavaryn Tsaram, Mongolia (Stosch *et al.*, 1995), INAA		(Bindeman *et al.*, 1998), IPMA										
	4399/17	4399/20	87-1	87-5	91-3	91-4	92-5	92-2	94-3	94-5	94-7	S2-2	S2-3
Elemen	*Granulites*							*Basalts*					
La	8.300	10.80	2.830	2.360	2.190	2.500	2.680	1.910	5.540	7.380	N.d.	0.630	1.000
Ce	11.10	14.20	5.230	3.810	4.190	4.690	5.060	3.400	8.470	7.480	10.80	1.660	2.100
Pr	N.d.	N.d.	0.600	0.600	0.500	0.500	0.600	0.400	1.100	1.100	1.100	0.200	0.200
Nd	2.350	2.800	2.480	2.010	2.600	1.780	2.860	2.860	4.990	4.040	3.510	1.120	1.000
Sm	0.239	0.240	0.470	0.260	0.290	0.350	0.490	0.560	1.060	0.890	0.520	0.960	0.350
Eu	0.709	0.667	0.090	0.070	0.120	0.190	0.070	0.040	0.470	2.080	0.500	0.050	0.060
Gd	0.390	0.600	N.d.	N.d.	N.d.	N.d.	N.d.	N.d.	N.d.	N.d.	N.d.	N.d.	N.d.
Tb	0.046	0.067	N.d.	N.d.	N.d.	N.d.	N.d.	N.d.	N.d.	N.d.	N.d.	N.d.	N.d.
Dy	N.d.	N.d.	N.d.	N.d.	N.d.	N.d.	N.d.	N.d.	N.d.	N.d.	N.d.	N.d.	N.d.
Ho	N.d.	N.d.	N.d.	N.d.	N.d.	N.d.	N.d.	N.d.	N.d.	N.d.	N.d.	N.d.	N.d.
Er	N.d.	N.d.	N.d.	N.d.	N.d.	N.d.	N.d.	N.d.	N.d.	N.d.	N.d.	N.d.	N.d.
Tm	N.d.	N.d.	N.d.	N.d.	N.d.	N.d.	N.d.	N.d.	N.d.	N.d.	N.d.	N.d.	N.d.
Yb	0.190	0.220	N.d.	N.d.	N.d.	N.d.	N.d.	N.d.	N.d.	N.d.	N.d.	N.d.	N.d.
Lu	0.026	0.030	N.d.	N.d.	N.d.	N.d.	N.d.	N.d.	N.d.	N.d.	N.d.	N.d.	N.d.
Total	23.35	29.62	N.d.	N.d.	N.d.	N.d.	N.d.	N.d.	N.d.	N.d.	N.d.	N.d.	N.d.
$(Ce/Yb)_n$	15.1	16.7	N.d.	N.d.	N.d.	N.d.	N.d.	N.d.	N.d.	N.d.	N.d.	N.d.	N.d.
$(Eu/Eu^*)_n$	7.1	5.1	N.d.	N.d.	N.d.	N.d.	N.d.	N.d.	N.d.	N.d.	N.d.	N.d.	N.d.

Table 5.42 Average rare earth element composition of plagioclases (ppm).

	Meteorites						The Moon								
	Chessigny, Valadares *et al.*, (6)			Acapulco (4)			Max.	Min.	Average	Max.	Min.	Average	Max.	Min.	Average
Element	Max.	Min.	Average	Max.	Min.	Average	*Magnesioferous mafites* (4)			*Ferriferous mafites* (5)			*Alkaline gabbro-norites* (4)		
La	1.990	0.833	1.418	0.268	0.242	0.257	0.710	0.280	0.470	2.540	1.670	2.003	13.11	4.160	8.585
Ce	3.520	1.166	2.498	0.391	0.268	0.342	1.650	0.770	1.172	5.280	3.530	4.204	29.81	7.970	18.92
Pr	0.129	0.128	0.129	0.028	0.020	0.025	0.210	0.087	0.148	0.550	0.330	0.447	N.d.	N.d.	N.d.
Nd	1.300	0.361	0.810	0.103	0.072	0.091	0.730	0.430	0.578	1.990	1.290	1.624	14.79	3.680	8.925
Sm	0.210	0.026	0.113	0.032	0.013	0.021	0.140	0.060	0.104	0.350	0.200	0.300	3.490	0.650	2.055
Eu	1.435	0.990	1.189	0.894	0.547	0.737	1.060	0.950	1.013	1.200	1.000	1.076	10.90	5.460	7.632
Gd	0.080	0.047	0.060	0.021	0.009	0.015	0.140	0.071	0.104	0.270	0.170	0.233	2.600	0.490	1.512
Tb	0.007	0.007	0.007	0.004	0.002	0.003	0.024	0.008	0.016	0.037	0.017	0.029	N.d.	N.d.	N.d.
Dy	N.d.	N.d.	N.d.	0.057	0.014	0.033	0.097	0.031	0.059	0.220	0.083	0.164	1.710	0.320	0.965
Ho	N.d.	N.d.	N.d.	0.003	0.003	0.003	0.020	0.009	0.015	0.048	0.026	0.039	N.d.	N.d.	N.d.
Er	N.d.	N.d.	N.d.	0.003	0.003	0.003	0.045	0.015	0.027	0.130	0.059	0.090	N.d.	N.d.	N.d.
Tm	N.d.	N.d.	N.d.	0.003	0.003	0.003	N.d.	N.d.	N.d.	N.d.	N.d.	N.d.	N.d.	N.d.	N.d.
Yb	N.d.	N.d.	N.d.	0.005	0.003	0.004	0.041	0.006	0.026	0.130	0.079	0.104	0.590	0.133	0.311
Lu	N.d.	N.d.	N.d.	0.005	0.005	0.005	N.d.	N.d.	N.d.	N.d.	N.d.	N.d.	N.d.	N.d.	N.d.
Total	N.d.	N.d.	N.d.	1.75	1.41	1.56	4.73	2.88	3.74	12.6	8.57	10.3	N.d.	N.d.	N.d.
$(Ce/Yb)_n$	N.d.	N.d.	N.d.	33.6	20.2	26.8	33.2	9.33	17.5	16.7	7.63	11.2	32.4	11.9	19.9
$(Eu/Eu^*)_n$	125	73.0	99.1	218	60.7	143	49.1	20.5	33.3	18.1	9.96	12.6	31.7	5.32	18.3

(*Continued*)

Table 5.42 Continued

	The Moon									Massifs (provinces)					
										Liguria, Italy			Stillwater, USA		
	Max.	Min.	Average	Max.	Min.	Average	Max.	Min.	Average	Max.	Min.	Average	Max.	Min.	Average
Element	*Monzogabbros* (4)			*Ferriferous anorthosites* (10)			*Alkaline anorthosites* (24)			*Plagioclase-bearing lherzolites* (10)			*Plagioclase-bearing dunites* (2)		
La	6.120	3.330	4.777	0.450	0.130	0.238	10.51	2.220	7.003	N.d.	N.d.	N.d.	0.696	0.629	0.663
Ce	11.800	5.310	8.803	1.050	0.310	0.599	22.49	3.950	14.97	0.170	0.038	0.090	1.490	1.040	1.265
Pr	1.110	0.480	0.817	0.130	0.034	0.071	N.d.	N.d.	N.d.	N.d.	N.d.	N.d.	N.d.	N.d.	N.d.
Nd	4.180	1.690	3.012	0.510	0.150	0.295	8.340	2.150	5.768	0.480	0.086	0.230	0.652	0.390	0.521
Sm	0.520	0.150	0.347	0.100	0.031	0.067	2.810	0.450	1.304	0.200	0.033	0.089	0.130	0.065	0.098
Eu	3.710	3.290	3.448	1.330	0.660	0.923	9.700	5.310	6.730	0.310	0.140	0.205	0.229	0.195	0.212
Gd	0.570	0.230	0.407	0.110	0.038	0.068	1.730	0.410	0.872	N.d.	N.d.	N.d.	0.095	0.042	0.069
Tb	0.080	0.040	0.065	0.090	0.006	0.024	N.d.	N.d.	N.d.	N.d.	N.d.	N.d.	N.d.	N.d.	N.d.
Dy	0.500	0.240	0.385	0.075	0.023	0.046	0.870	0.240	0.443	N.d.	N.d.	N.d.	0.067	0.037	0.052
Ho	0.090	0.070	0.080	0.050	0.004	0.017	N.d.	N.d.	N.d.	N.d.	N.d.	N.d.	N.d.	N.d.	N.d.
Er	0.300	0.170	0.245	0.034	0.008	0.021	N.d.	N.d.	N.d.	N.d.	N.d.	N.d.	0.026	0.019	0.023
Tm	0.030	0.020	0.025	N.d.	N.d.	N.d.	N.d.	N.d.	N.d.	N.d.	N.d.	N.d.	N.d.	N.d.	N.d.
Yb	0.520	0.150	0.290	0.042	0.010	0.024	0.281	0.073	0.140	N.d.	N.d.	N.d.	0.087	0.014	0.051
Lu	0.020	0.014	0.017	N.d.	N.d.	N.d.	N.d.	N.d.	N.d.	N.d.	N.d.	N.d.	N.d.	N.d.	N.d.
Total	28.7	15.7	22.7	3.84	1.45	2.39	N.d.	N.d.	N.d.	N.d.	N.d.	N.d.	N.d.	N.d.	N.d.
$(Ce/Yb)_n$	20.4	4.77	11.4	9.37	3.68	6.52	61.8	4.96	32.3	N.d.	N.d.	N.d.	19.2	4.43	11.8
$(Eu/Eu^*)_n$	60.9	18.4	35.1	68.6	26.4	46.0	46.9	9.5	20.9	N.d.	N.d.	N.d.	10.7	6.03	8.37

	Massifs (provinces)														
	Dovyrensky, Rus.			Zabargad Island, Red Sea			Stillwater, USA			Samail, Oman			Beriozovsky, Russia		
	Max.	Min.	Average	Max.	Min.	Average	Max.	Min.	Average	Max.	Min.	Average	Max.	Min.	Average
Element	*Plagioclase-bearing wehrlites* (3)			*Plagioclase-bearing pyroxenites* (9)			*Troctolites* (2)			*Olivine gabbros* (9)			*Gabbro-norites* (12)		
La	5.700	2.900	4.212	N.d.	N.d.	N.d.	0.947	0.816	0.882	0.720	0.220	0.381	0.026	0.018	0.022
Ce	8.100	4.700	6.146	3.390	1.420	2.041	1.710	1.470	1.590	2.000	0.660	1.311	0.081	0.057	0.067
Pr	N.d.	N.d.	N.d.	N.d.	N.d.	N.d.	N.d.	N.d.	N.d.	N.d.	N.d.	N.d.	N.d.	N.d.	N.d.
Nd	2.900	1.900	2.360	2.770	0.450	1.354	0.722	0.605	0.664	1.100	0.440	0.740	0.065	0.050	0.056
Sm	0.330	0.200	0.264	1.480	0.050	0.474	0.134	0.108	0.121	0.190	0.059	0.115	0.020	0.013	0.016
Eu	0.230	0.200	0.212	0.810	0.260	0.508	0.240	0.225	0.233	0.430	0.170	0.274	0.056	0.040	0.048
Gd	0.210	0.190	0.200	0.260	0.100	0.173	0.105	0.080	0.093	0.230	0.051	0.127	N.d.	N.d.	N.d.
Tb	0.033	0.030	0.031	N.d.	N.d.	N.d.	N.d.	N.d.	N.d.	0.041	0.008	0.021	0.007	0.005	0.006
Dy	N.d.	N.d.	N.d.	2.580	0.040	0.835	0.080	0.057	0.069	N.d.	N.d.	N.d.	N.d.	N.d.	N.d.
Ho	N.d.	N.d.	N.d.	N.d.	N.d.	N.d.	N.d.	N.d.	N.d.	N.d.	N.d.	N.d.	N.d.	N.d.	N.d.
Er	N.d.	N.d.	N.d.	1.310	0.020	0.421	0.036	0.024	0.030	N.d.	N.d.	N.d.	N.d.	N.d.	N.d.
Tm	0.110	0.010	0.053	N.d.	N.d.	N.d.	N.d.	N.d.	N.d.	N.d.	N.d.	N.d.	0.040	0.002	0.017
Yb	0.130	0.060	0.089	1.020	0.020	0.286	0.025	0.015	0.020	0.057	0.014	0.042	0.020	0.015	0.018
Lu	0.018	0.008	0.012	N.d.	N.d.	N.d.	N.d.	N.d.	N.d.	0.011	0.003	0.007	N.d.	N.d.	N.d.
Total	17.5	10.3	13. 6	13.4	2.36	6.01	3.98	3.42	3.70	N.d.	N.d.	N.d.	N.d.	N.d.	N.d.
$(Ce/Yb)_n$	32.3	9.36	21.1	18.4	0.86	7.53	25.4	17.7	21.5	22.2	5.02	9.81	1.05	0.88	0.97
$(Eu/Eu^*)_n$	2.97	2.24	2.68	12.0	2.91	7.39	7.57	5.60	6.59	10.4	4.67	7.40	20.1	10.6	16.3

(*Continued*)

Table 5.42 Continued

	Massifs (provinces)														
	Samail, Oman			Skaergaard, Greenland			Stillwater, USA			Ivrea Verbano, Italy			East Sayan, Russia		
	Max.	Min.	Average	Max.	Min.	Average	Max.	Min.	Average	Max.	Min.	Average	Max.	Min.	Average
Element	*Gabbros* (3)			*Gabbros* (3)			*Gabbros* (3)			*Gabbros* (14)			*Gabbros* (3)		
La	0.440	0.210	0.306	4.300	1.750	3.020	0.636	0.332	0.460	22.73	1.280	8.853	5.600	4.500	5.000
Ce	1.500	0.730	1.058	14.10	2.900	8.640	5.280	0.546	2.511	24.65	2.120	11.14	12.50	7.900	10.20
Pr	N.d.	N.d.	N.d.	N.d.	N.d.	N.d.	N.d.	N.d.	N.d.	N.d.	N.d.	N.d.	N.d.	N.d.	N.d.
Nd	0.820	0.440	0.602	7.400	0.990	4.116	0.274	0.185	0.221	3.560	0.830	2.416	7.900	3.800	5.900
Sm	0.140	0.069	0.098	1.760	0.172	0.915	0.040	0.028	0.033	0.309	0.120	0.196	2.200	0.890	1.576
Eu	0.300	0.200	0.244	4.300	1.450	2.610	0.118	0.070	0.095	2.090	0.515	1.204	1.890	1.500	1.684
Gd	0.110	0.054	0.082	1.940	0.140	0.976	0.026	N.d.	0.018	0.407	0.087	0.164	1.580	0.920	1.244
Tb	0.017	0.009	0.013	0.270	0.020	0.140	N.d.	N.d.	N.d.	N.d.	N.d.	N.d.	0.200	0.110	0.156
Dy	0.150	0.073	0.112	N.d.	N.d.	N.d.	0.021	0.017	0.019	0.161	0.034	0.082	N.d.	N.d.	N.d.
Ho	N.d.	N.d.	N.d.	0.240	0.110	0.175	N.d.	N.d.	N.d.	N.d.	N.d.	N.d.	N.d.	N.d.	N.d.
Er	N.d.	N.d.	N.d.	N.d.	N.d.	N.d.	0.010	0.009	0.010	0.086	0.008	0.030	N.d.	N.d.	N.d.
Tm	N.d.	N.d.	N.d.	N.d.	N.d.	N.d.	N.d.	N.d.	N.d.	N.d.	N.d.	N.d.	N.d.	N.d.	N.d.
Yb	0.041	0.027	0.033	0.270	0.026	0.136	0.010	0.007	0.008	0.046	0.003	0.015	0.180	0.090	0.142
Lu	0.011	0.005	0.007	N.d.	N.d.	N.d.	N.d.	N.d.	N.d.	N.d.	N.d.	N.d.	0.020	0.010	0.016
Total	N.d.	N.d.	N.d.	33.3	7.72	20.5	5.96	1.25	3.29	52.6	5.31	24.0	N.d.	N.d.	N.d.
$(Ce/Yb)_n$	9.47	7.00	8.07	28.9	13.5	22.4	137	20.2	69.4	975	40.5	365	22.7	14.7	18.8
$(Eu/Eu^*)_n$	10.6	7.14	8.70	29.7	6.14	15.7	18.6	8.11	12.8	37.7	7.27	22.2	5.03	2.57	3.80

	Massifs (provinces)														
	Mid-Atlantic Ridge			Stillwater, USA			Hidra, Norway			Stillwater, USA			Norway		
	Max.	Min.	Average	Max.	Min.	Average	Max.	Min.	Average	Max.	Min.	Average	Max.	Min.	Average
Element	*Gabbros* (3)			*Norites* (5)			*Monzonorites* (24)			*Anorthosites* (10)			*Anorthosites* (12)		
La	0.538	0.538	0.538	1.340	0.336	0.773	52.30	15.10	31.97	3.100	0.556	1.421	9.730	1.280	3.861
Ce	1.140	1.060	1.100	2.450	0.585	1.373	35.50	18.30	26.17	6.090	0.915	2.619	22.20	2.260	7.891
Pr	N.d.	N.d.	N.d.	N.d.	N.d.	N.d.	N.d.	N.d.	N.d.	N.d.	N.d.	N.d.	N.d.	N.d.	N.d.
Nd	0.652	0.627	0.640	1.050	0.232	0.575	15.20	7.100	10.47	2.630	0.351	1.095	N.d.	N.d.	N.d.
Sm	0.151	0.145	0.148	0.185	0.040	0.102	2.420	1.040	1.613	0.523	0.061	0.207	2.410	0.120	0.689
Eu	0.429	0.294	0.362	0.276	0.069	0.170	4.230	2.330	3.168	0.309	0.179	0.256	3.630	0.400	1.199
Gd	0.165	0.154	0.160	0.140	0.027	0.074	1.570	0.810	1.132	0.462	0.018	0.165	N.d.	N.d.	N.d.
Tb	N.d.	N.d.	N.d.	N.d.	N.d.	N.d.	0.260	0.080	0.160	N.d.	N.d.	N.d.	0.360	0.005	0.091
Dy	0.133	0.101	0.117	0.088	0.023	0.052	N.d.	N.d.	N.d.	0.368	0.039	0.137	N.d.	N.d.	N.d.
Ho	N.d.	N.d.	N.d.	N.d.	N.d.	N.d.	0.300	0.080	0.184	N.d.	N.d.	N.d.	N.d.	N.d.	N.d.
Er	0.072	0.045	0.059	0.032	0.011	0.020	N.d.	N.d.	N.d.	0.158	0.019	0.061	N.d.	N.d.	N.d.
Tm	N.d.	N.d.	N.d.	N.d.	N.d.	N.d.	0.130	0.130	0.130	N.d.	N.d.	N.d.	N.d.	N.d.	N.d.
Yb	0.053	0.033	0.043	0.017	0.006	0.012	0.820	0.089	0.398	0.116	0.014	0.045	1.600	0.009	0.282
Lu	0.005	0.001	0.003	N.d.	N.d.	N.d.	0.120	0.013	0.058	N.d.	N.d.	N.d.	0.240	0.002	0.068
Total	3.14	2.66	2.90	5.58	1.33	3.15	94.0	51.2	73.0	13.7	2.19	6.01	N.d.	N.d.	N.d.
$(Ce/Yb)_n$	8.3	5.6	7.0	44.0	16.8	28.9	67.2	11.2	33.0	26.8	9.9	18.8	95.6	3.6	44.6
$(Eu/Eu^*)_n$	8.7	5.7	7.2	8.0	5.0	6.2	8.3	6.2	7.3	11.6	1.8	7.0	N.d.	N.d.	N.d.

(*Continued*)

Table 5.42 Continued

	Massifs (provinces)														
	Iceland			Manitoba, Canada			Mount Adams, USA			Honshu, Japan			Twin Peaks, USA		
	Max.	Min.	Average	Max.	Min.	Average	Max.	Min.	Average	Max.	Min.	Average	Max.	Min.	Average
Element	*Anorthosites* (6)			*Basalts* (4)			*Andesites* (3)			*Dacites* (5)			*Rhyolites* (6)		
La	0.500	0.130	0.298	2.482	0.164	0.996	5.400	3.000	4.133	N.d.	N.d.	N.d.	35.00	9.000	23.63
Ce	N.d.	N.d.	N.d.	4.040	0.260	1.628	8.000	5.300	6.500	15.60	6.800	11.83	52.00	15.90	35.35
Pr	N.d.	N.d.	N.d.	N.d.	N.d.	N.d.	0.690	0.370	0.560	N.d.	N.d.	N.d.	N.d.	N.d.	N.d.
Nd	N.d.	N.d.	N.d.	N.d.	N.d.	N.d.	2.300	1.100	1.867	4.920	1.690	3.459	15.00	5.400	10.33
Sm	0.200	0.090	0.131	0.161	0.043	0.087	0.340	0.150	0.263	0.705	0.280	0.490	1.760	0.740	1.219
Eu	0.410	0.160	0.256	N.d.	N.d.	N.d.	1.500	1.000	1.300	2.450	0.770	1.568	5.550	1.450	3.420
Gd	N.d.	N.d.	N.d.	N.d.	N.d.	N.d.	0.300	0.250	0.267	0.462	0.435	0.449	N.d.	N.d.	N.d.
Tb	0.037	0.010	0.020	0.012	0.006	0.009	0.025	0.010	0.018	N.d.	N.d.	N.d.	0.150	0.070	0.105
Dy	N.d.	N.d.	N.d.	N.d.	N.d.	N.d.	0.050	0.050	0.050	0.313	0.144	0.246	0.700	0.400	0.575
Ho	N.d.	N.d.	N.d.	N.d.	N.d.	N.d.	N.d.	N.d.	N.d.	N.d.	N.d.	N.d.	N.d.	N.d.	N.d.
Er	N.d.	N.d.	N.d.	N.d.	N.d.	N.d.	N.d.	N.d.	N.d.	0.160	0.079	0.123	N.d.	N.d.	N.d.
Tm	N.d.	N.d.	N.d.	N.d.	N.d.	N.d.	N.d.	N.d.	N.d.	N.d.	N.d.	N.d.	N.d.	N.d.	N.d.
Yb	0.077	0.008	0.040	0.028	0.016	0.023	N.d.	N.d.	N.d.	0.194	0.069	0.125	0.420	0.250	0.344
Lu	0.008	0.001	0.004	0.005	0.002	0.004	N.d.	N.d.	N.d.	0.025	0.012	0.019	0.070	0.040	0.053
Total	N.d.	N.d.	N.d.	N.d.	N.d.	N.d.	N.d.	N.d.	N.d.	23.8	5.94	15.9	N.d.	N.d.	N.d.
$(Ce/Yb)_n$	N.d.	N.d.	N.d.	38.7	3.06	16.7	N.d.	N.d.	N.d.	34.7	20.8	27.1	38.1	9.8	26.6
$(Eu/Eu^*)_n$	N.d.	N.d.	N.d.	N.d.	N.d.	N.d.	22.0	10.1	15.7	22.04	10.1	15.0	N.d.	N.d.	N.d.

Data Tables 5.34–5.41.

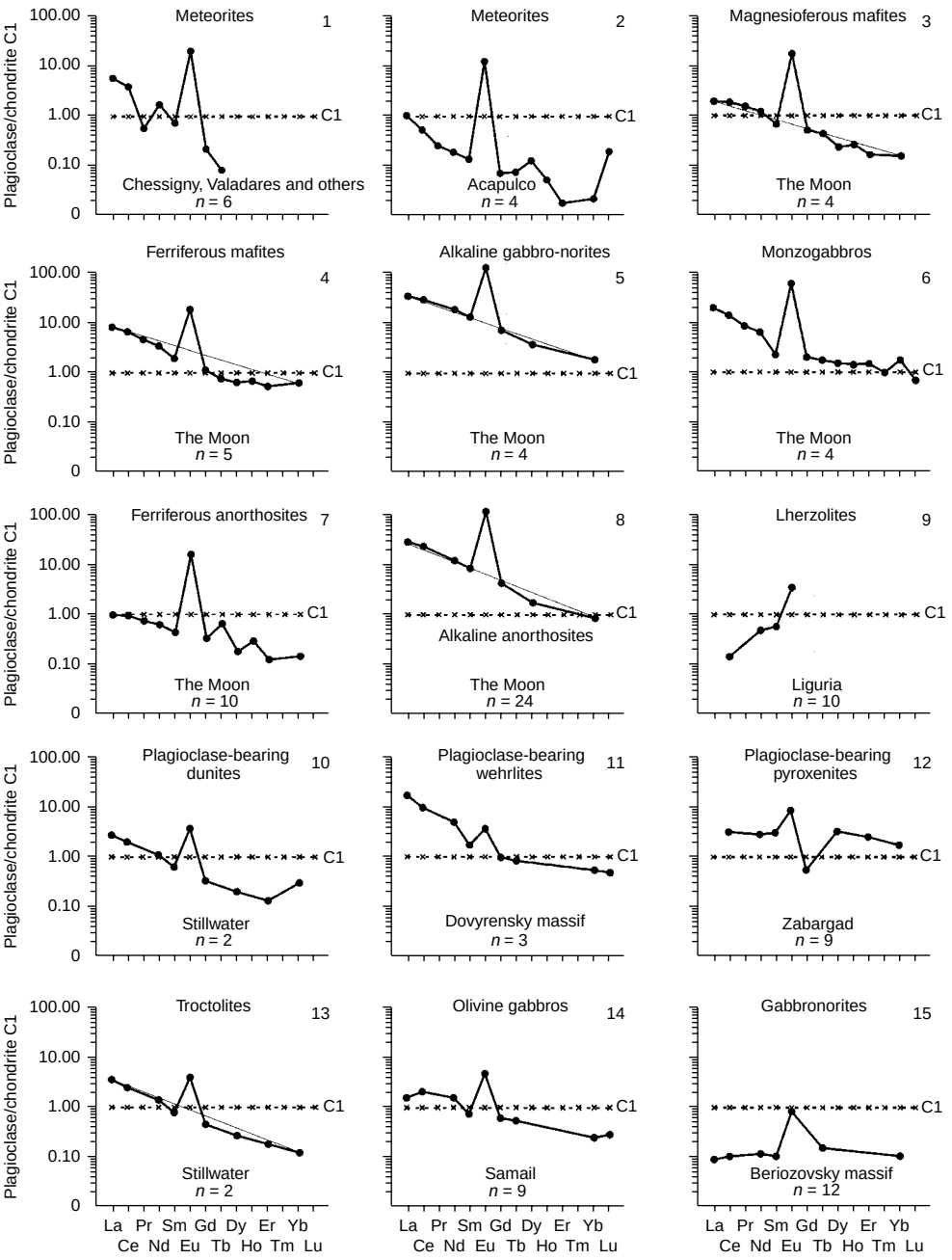

Figure 5.35 Chondrite-normalized patterns for average REE composition of plagioclases (data Table 5.42).

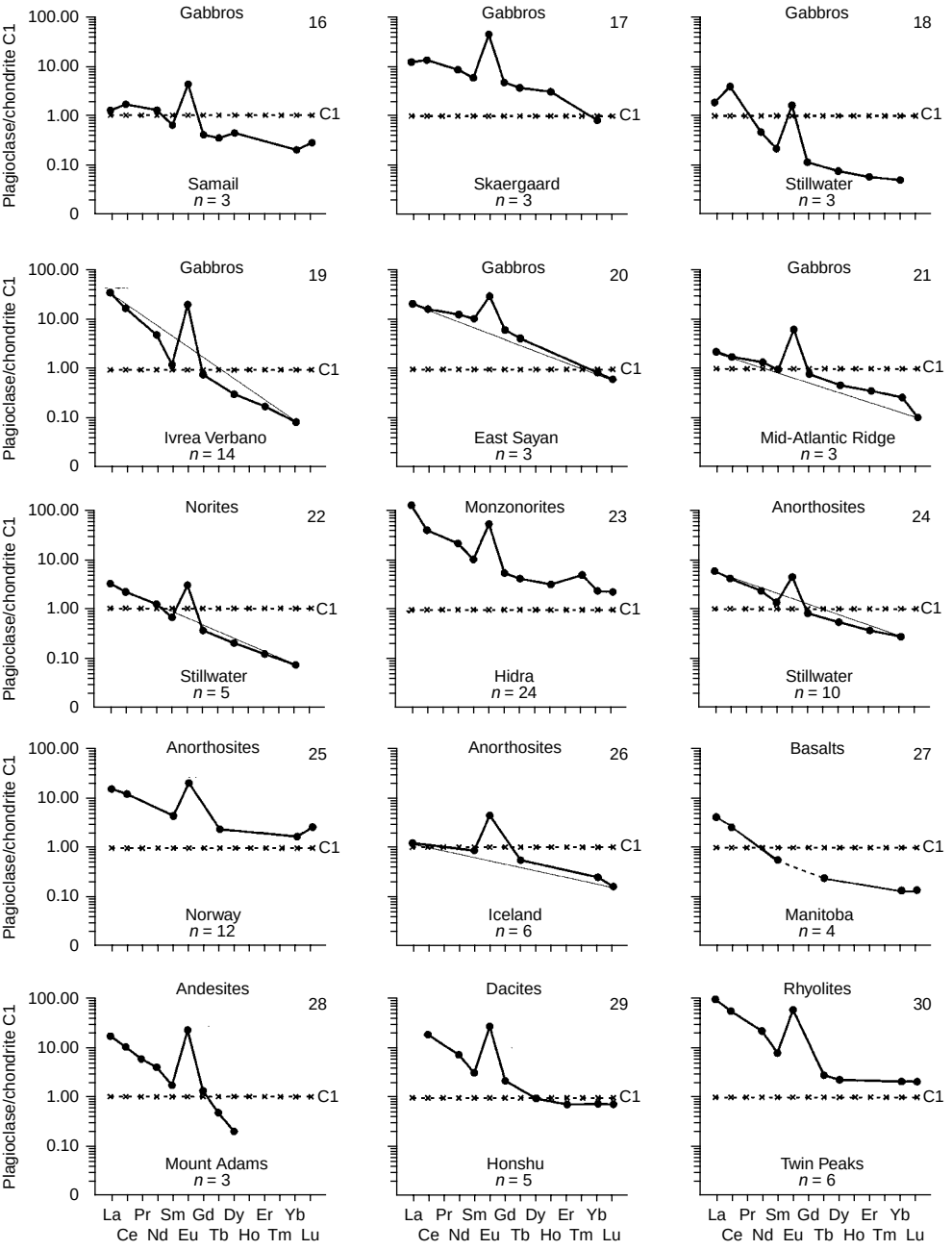

Figure 5.35 Continued

The proposed variant of geochemical systematization of plagioclases, based on the values of three parameters of REE distribution, requires to be made more precise with application of more complete analytical database. Nevertheless, this classification of plagioclases can be used in the comparative studies of mafic–ultramafic massifs and complexes at a regional scale as well as in the solution of some other problems.

5.4.3 Coefficients of REE distribution between plagioclases and coexisting phases

In this chapter we summarize the essential part of available data on the coefficients of REE distribution between plagioclases and parental melts with different compositions and between plagioclases and coexisting minerals.

K_d(plagioclase/melt). These K_d values were calculated based on the results of analysis of porphyric phenocrystals of plagioclase and groundmass of effusive rocks. The accuracy of these values was rather poor, as porphyric phenocrysts did not always attain a state of chemical equilibrium with surrounding melts. But the data on K_d(plagioclase/melt) values obtained in physical experiments are practically absent so far, which can be seen from the published experimental summary including the K_d values for many minerals (Green, 1994). Irrespective of melt composition, in all REE, including Eu, K_d(plagioclase/melt) is less than unity (Tables 5.43 and 5.44), being slightly higher for light REE than for heavy REE (Fig. 5.36). The K_d(Eu) values increase in the series from basalts (~1) to andesites, dacites (~2–3), and rhyolite melts (~10). A rather close position of trends of changes in K_d(plagioclase/melt) values, calculated on the basis of results of analyses for plagioclase phenocrysts from basalts (Fig. 5.36, 1) and especially from rhyolites (Fig. 5.36, 5) shows that these phenocrysts could achieve a state close to chemical equilibrium with melts. The K_d(plagioclase/basalt melt) values obtained in physical experiments under atmospheric pressure and only for light REE virtually do not change in the series from La to Eu.

K_d(plagioclase/clinopyroxene). Despite the wide occurrence of plagioclase–clinopyroxene paragenesis in nature, data on the coefficients of REE distribution between these minerals are scarce (Table 5.45). According to these data, their values successively decrease from light to heavy elements, and their trends have a negative slope. They normally have maximums of varying intensity for Eu. In pyroxenites from Zabargad Island (Fig. 5.37, 1), and in olivine gabbros from the Samail massif (Fig. 5.37, 2), the K_d values for some elements change in a rather narrow interval, and the trends for most samples have a similar configuration, which may show that these minerals achieved a state of chemical equilibrium. Wider variations in the values of these K_d were found in gabbros from the Ivrea Verbano complex and in gabbro-norites from the Naransky massif (Fig. 5.37, 3, 4). In the samples from Ivrea Verbano, the values of coefficients for La, Ce, and Eu vary less than the K_d for other elements. The most variable distribution of heavy REE between plagioclases and clinopyroxenes is typical of andesites and basalts from the Mount Adams complex and pyroxenites from Zabargad Island (Fig. 5.37, 1, 5, 6).

Table 5.43 Coefficients of REE distribution between phenocrysts of plagioclases and groundmass of basalts, andesites, dacites, and rhyolites.

	Sample's number											
	1	2	3	4	5	6	7	8	9	10	11	12
	(Schnetzler & Philpotts, 1970)	(Shearer *et al.*, 1989)	(Phinney & Morrison, 1990)			(McKay, 1986)	(Paster *et al.*, 1974)	(Arth, 1976)	(Morse & Nolan, 1985)	(Elton, 1984)	(Coogan *et al.*, 2000)	
Element	*Basalts*											
La	N.d.	N.d.	0.0358	0.0418	0.0415	0.041	0.069	0.143	0.174	0.230	0.12	0.14
Ce	0.023	0.035	0.0307	0.0302	0.0297	0.0357	0.062	0.130	0.094	0.140	0.10	0.12
Nd	0.023	N.d.	N.d.	N.d.	N.d.	N.d.	0.028	0.081	N.d.	N.d.	0.07	0.07
Sm	0.024	0.022	0.020	0.017	0.018	0.021	0.017	0.067	0.0177	0.080	N.d.	N.d.
Eu	0.232	1.200	0.236	0.166	0.168	N.d.	0.680	0.340	0.346	0.380	N.d.	N.d.
Gd	0.017	N.d.	0.016	N.d.	N.d.	0.015	0.014	0.063	N.d.	0.050	N.d.	N.d.
Tb	N.d.	N.d.	N.d.	0.0095	0.0096	0.0125	0.013	N.d.	0.014	N.d.	N.d.	N.d.
Dy	0.018	0.019	N.d.	N.d.	N.d.	N.d.	N.d.	0.055	N.d.	0.040	N.d.	N.d.
Ho	N.d.	N.d.	N.d.	N.d.	N.d.	N.d.	0.011	N.d.	N.d.	N.d.	N.d.	N.d.
Er	0.020	N.d.	N.d.	N.d.	N.d.	N.d.	N.d.	0.063	N.d.	N.d.	N.d.	N.d.
Yb	0.030	0.017	0.007	0.0065	0.0070	0.0049	0.009	0.067	0.011	N.d.	N.d.	N.d.
Lu	0.037	N.d.	N.d.	0.0068	0.0067	0.0041	N.d.	0.060	0.008	0.040	N.d.	N.d.

	Sample's number												
	13	14	15	16	17	18	19	20	21	22	23	24	25
	(Arth, 1976)	(Irving & Frey, 1984)	(Nagasawa & Schnetzler, 1971)					(Nash & Crecraft, 1985)					
Element	*Andesites*		*Dacites*					*Rhyolites*					
La	0.302	N.d.	N.d.	N.d.	N.d.	N.d.	N.d.	0.320	0.450	0.300	0.420	0.450	0.340
Ce	0.321	0.186	0.270	0.109	0.279	N.d.	0.347	0.210	0.340	0.210	0.290	0.310	0.240
Nd	N.d.	N.d.	0.191	0.061	0.290	0.121	0.237	0.140	0.290	0.170	0.220	0.210	0.190
Sm	0.149	0.143	0.125	0.050	0.144	0.084	0.153	0.110	0.230	0.140	0.180	0.180	0.150
Eu	0.102	0.117	2.350	0.820	2.490	0.960	2.810	3.800	6.200	4.200	5.200	5.200	7.900
Gd	1.214	0.376	N.d.	N.d.	0.129	N.d.	N.d.	N.d.	N.d.	N.d.	N.d.	N.d.	N.d.
Tb	0.067	N.d.	N.d.	N.d.	N.d.	N.d.	N.d.	0.090	0.190	0.100	0.130	0.120	0.120
Dy	N.d.	N.d.	0.059	N.d.	0.076	0.452	0.078	0.070	0.180	0.110	0.090	0.100	0.120
Er	0.05	0.126	0.045	0.029	0.065	0.380	N.d.	N.d.	N.d.	N.d.	N.d.	N.d.	N.d.
Yb	N.d.	N.d.	0.043	0.022	0.056	0.302	0.066	0.060	0.130	0.100	0.070	0.080	0.100
Lu	0.045	0.034	0.039	0.022	0.054	0.290	N.d.	0.060	0.110	0.120	0.060	0.070	0.130

Table 5.44 Coefficients of REE distribution between plagioclases and basalt melt (experimental data at atmospheric conditions; Bindeman *et al.*, 1998).

	Experiment's numbers					
Element	1	2	3	4	5	6
La	0.237	0.219	0.197	0.217	0.176	0.197
Ce	0.173	0.143	0.156	0.166	0.136	0.144
Pr	0.171	0.176	0.152	0.152	0.140	0.138
Nd	0.198	0.157	0.154	0.138	0.175	0.235
Sm	0.179	0.086	0.106	0.124	0.122	0.188
Eu	0.120	0.074	0.132	0.183	0.061	0.047

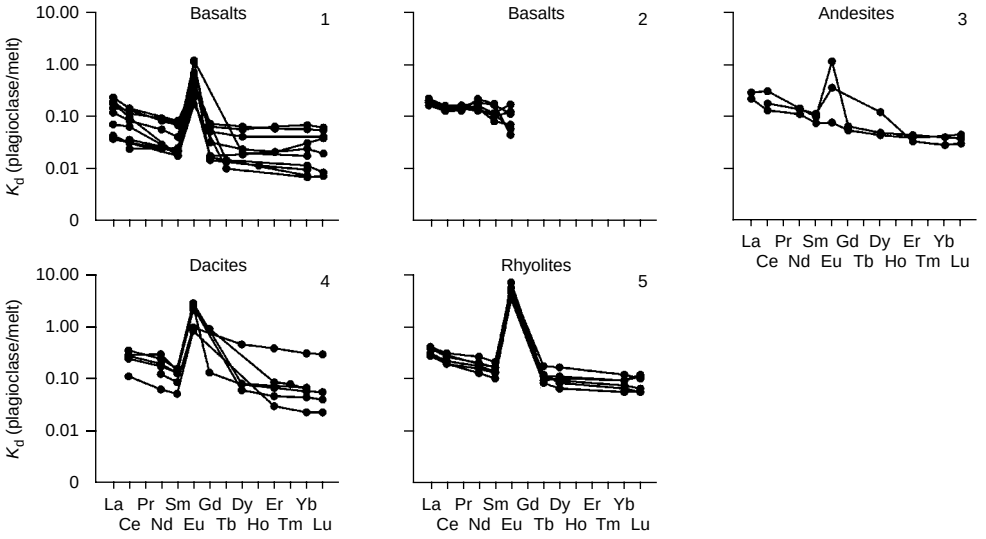

Figure 5.36 The trend coefficients of REE distribution between plagioclases and coexisting melts. Diagrams 1 and 3–5 were carried out on the results of phenocryst analyses (data Table 5.43); diagram 2—on the results of experiments at atmospheric pressures (data Table 5.44).

K_d(plagioclase/orthopyroxene). K_d values of greater than unity are common for light REE, reaching 100 in some rocks, whereas for heavy REE, K_d is less than 0.1 (Table 5.46). Their trends often have a very steep negative slope (Fig. 5.38). Judging by K_d, the contents of La and Ce in plagioclase from pyroxenites of Zabargad Island is 20–200 times higher, whereas the content of Yb is 10–50 times lower, than that in orthopyroxene. In lunar rocks, the distribution of light REE between plagioclase and orthopyroxene is less variable. The nearly identical configuration of trends of changes in these K_d and their close location suggest that in pyroxenites (Fig. 5.38, 1), in lunar anorthosites (Fig. 5.38, 3), and in ferruginous mafic rocks (see Fig. 5.38, 4), plagioclases and orthopyroxenes occur in a state close to chemical equilibrium. Gabbro-norites from the Beriozovsky and Naransky massifs and andesites from the

Table 5.45 Coefficients of REE distribution between plagioclases and coexisting clinopyroxenes.

	Massifs														
	Zabargad Island, Red Sea											Samail, Oman			
	(Vannucci *et al.*, 1993b)											(Pallister & Knight, 1981)			
	2036B\3\c1	2036B\3\r1	2036Bc1	2036Br1	2036C\17g1	2036C\1\c1	2036C\2\c1	2036C\2\r1	2036C\3\r1	2036C\4\c1	2036C\7\g1	Kf-12-1	Kf-17-1C	Kf-20-1C	Kf-7-1
Element	*Plagioclase-bearing pyroxenites*											*Olivine gabbros*			
La	N.d.	N.d.	N.d.	N.d.	N.d.	N.d.	N.d.	N.d.	N.d.	N.d.	N.d.	1.519	0.846	2.182	1.963
Ce	0.281	0.346	0.318	0.350	0.385	0.393	0.438	0.438	0.519	0.388	1.061	0.833	0.478	1.091	1.000
Pr	N.d.	N.d.	N.d.	N.d.	N.d.	N.d.	N.d.	N.d.	N.d.	N.d.	N.d.	N.d.	N.d.	N.d.	N.d.
Nd	0.135	0.132	0.158	0.131	0.139	0.127	0.174	0.149	0.128	0.093	0.302	0.268	0.223	0.440	0.556
Sm	0.076	0.063	0.086	0.066	0.059	0.049	0.065	0.057	0.042	0.031	0.149	0.100	0.051	0.102	0.196
Eu	0.395	0.395	0.402	0.391	0.369	0.375	0.417	0.395	0.385	0.257	0.978	0.711	0.452	0.654	0.857
Gd	N.d.	N.d.	N.d.	N.d.	N.d.	N.d.	N.d.	N.d.	N.d.	N.d.	N.d.	0.058	0.040	0.046	0.143
Tb	N.d.	N.d.	N.d.	N.d.	N.d.	N.d.	N.d.	N.d.	N.d.	N.d.	N.d.	0.043	0.027	0.029	0.097
Dy	0.015	0.010	0.014	0.010	0.022	0.018	0.020	0.015	0.010	0.008	0.035	N.d.	N.d.	N.d.	N.d.
Ho	N.d.	N.d.	N.d.	N.d.	N.d.	N.d.	N.d.	N.d.	N.d.	N.d.	N.d.	N.d.	N.d.	N.d.	N.d.
Er	0.008	0.006	0.008	0.006	0.011	0.008	0.008	0.007	0.005	0.004	0.017	N.d.	N.d.	N.d.	N.d.
Tm	N.d.	N.d.	N.d.	N.d.	N.d.	N.d.	N.d.	N.d.	N.d.	N.d.	N.d.	N.d.	N.d.	N.d.	N.d.
Yb	0.003	0.003	0.003	0.003	0.008	0.006	0.005	0.005	0.003	0.003	0.017	0.028	0.032	0.013	0.052
Lu	N.d.	N.d.	N.d.	N.d.	N.d.	N.d.	N.d.	N.d.	N.d.	N.d.	N.d.	0.030	0.039	0.015	0.069

(*Continued*)

Table 5.45 Continued

	Massifs														
	Skaergaard, Greenland				Samail, Oman	Ivrea Verbano, Italy									
	(Paster *et al.*, 1974)				(Pallister & Knight, 1981)	(Mazzucchelli *et al.*, 1992a,b)									
	5181	4312	4427	5086	Kf-16-1	FE31	MO95	MP12	MZ145	FE51	MP13	MP5	MP6	MP9	MZ132
Element	*Olivine gabbros*	*Gabbros*													
La	0.856	1.304	0.318	0.632	1.050	N.d.	N.d.	N.d.	N.d.	N.d.	N.d.	0.785	N.d.	N.d.	N.d.
Ce	0.387	0.613	0.153	0.354	0.317	0.359	0.349	0.356	0.853	0.170	0.178	0.233	0.262	0.189	0.225
Pr	N.d.	N.d.	N.d.	N.d.	N.d.	N.d.	N.d.	N.d.	N.d.	N.d.	N.d.	N.d.	N.d.	N.d.	N.d.
Nd	0.119	0.411	0.052	0.152	0.233	0.093	0.102	0.095	0.310	0.034	0.048	0.059	0.067	0.051	0.065
Sm	0.059	0.289	0.032	0.093	0.074	0.033	0.030	0.031	0.153	0.013	0.016	0.018	0.029	0.018	0.024
Eu	2.941	2.350	1.281	1.169	0.595	0.487	0.333	0.573	0.512	0.249	0.300	0.533	0.185	0.306	0.243
Gd	0.041	0.228	0.023	0.080	0.030	N.d.	N.d.	N.d.	N.d.	N.d.	N.d.	0.038	N.d.	N.d.	N.d.
Tb	0.032	0.205	0.019	0.077	0.029	N.d.	N.d.	N.d.	N.d.	N.d.	N.d.	N.d.	N.d.	N.d.	N.d.
Dy	N.d.	N.d.	N.d.	N.d.	0.035	0.009	0.081	0.018	0.438	0.005	0.019	0.013	0.179	0.144	0.010
Ho	0.023	0.167	0.139	0.058	N.d.	N.d.	N.d.	N.d.	N.d.	N.d.	N.d.	N.d.	N.d.	N.d.	N.d.
Er	N.d.	N.d.	N.d.	N.d.	N.d.	0.006	0.038	0.018	0.314	0.006	0.053	0.023	0.175	0.126	0.006
Tm	N.d.	N.d.	N.d.	N.d.	N.d.	N.d.	N.d.	N.d.	N.d.	N.d.	N.d.	N.d.	N.d.	N.d.	N.d.
Yb	0.015	0.087	0.010	0.024	0.025	0.003	0.013	0.012	0.275	0.002	0.041	0.045	0.075	0.018	0.013
Lu	N.d.	N.d.	N.d.	N.d.	0.030	N.d.	N.d.	N.d.	N.d.	N.d.	N.d.	N.d.	N.d.	N.d.	N.d.

	Massifs											
	Beriozovsky, Russia						Naransky, Mongolia	Mount Adams, USA				Spain
	(Lesnov, 2001)							(Dunn & Sen, 1994)				(Schnetzler & Philpotts, 1970b)
	131	132a	138a	141	144	147	269	1	14	41	7	cpGSFC271
Element	*Gabbro-norites*							*Basalts*	*Andesites*			
La	0.183	N.d.	0.373	0.065	0.094	0.027	0.371	0.671	0.250	0.564	0.267	N.d.
Ce	N.d.	0.175	N.d.	0.187	N.d.	0.040	0.319	0.250	0.189	0.315	0.163	0.397
Pr	N.d.	N.d.	N.d.	N.d.	N.d.	N.d.	N.d.	0.122	0.086	0.183	0.098	N.d.
Nd	0.075	0.174	0.167	0.140	0.028	0.059	0.111	0.073	0.044	0.117	0.067	0.217
Sm	0.044	0.188	0.083	0.193	0.027	0.060	0.041	0.039	0.019	0.054	0.031	0.112
Eu	0.363	0.120	0.178	0.517	0.111	0.357	0.234	0.857	1.458	0.933	0.667	1.061
Gd	N.d.	N.d.	N.d.	N.d.	N.d.	N.d.	N.d.	0.074	0.019	0.055	0.030	N.d.
Tb	0.063	N.d.	N.d.	0.100	N.d.	0.142	0.021	0.021	N.d.	0.029	0.016	N.d.
Dy	N.d.	N.d.	N.d.	N.d.	N.d.	N.d.	N.d.	0.009	N.d.	0.013	0.005	0.038
Ho	N.d.	N.d.	N.d.	N.d.	N.d.	N.d.	N.d.	0.002	N.d.	0.005	N.d.	N.d.
Er	N.d.	N.d.	N.d.	N.d.	N.d.	N.d.	N.d.	N.d.	N.d.	N.d.	N.d.	0.031
Tm	0.021	N.d.	N.d.	N.d.	0.010	0.086	0.020	N.d.	N.d.	N.d.	N.d.	N.d.
Yb	0.020	N.d.	N.d.	N.d.	0.017	0.065	0.014	N.d.	N.d.	N.d.	N.d.	N.d.
Lu	N.d.	N.d.	N.d.	N.d.	N.d.	N.d.	N.d.	N.d.	N.d.	N.d.	N.d.	N.d.

Data Tables 5.34–5.41 and 5.12–5.28.

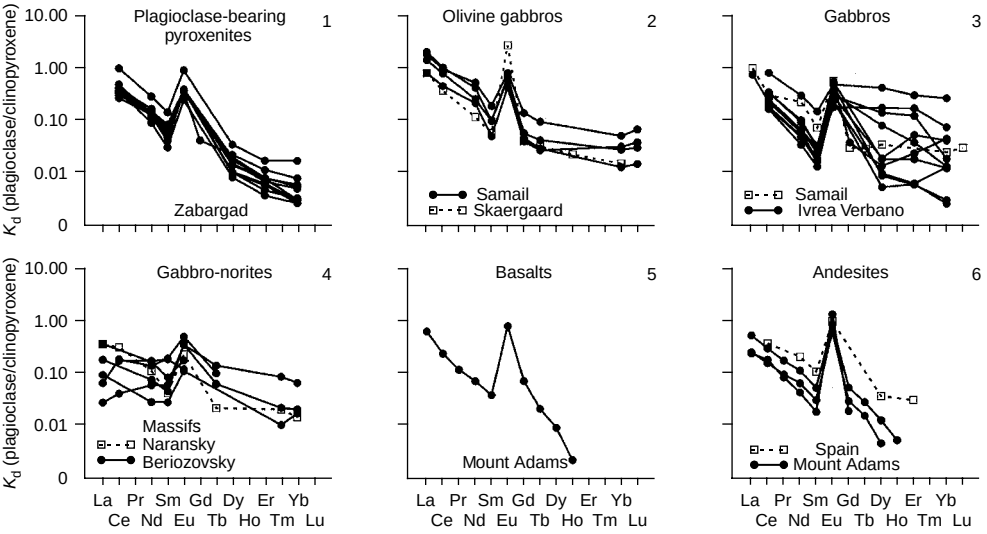

Figure 5.37 The trend coefficients of REE distribution between plagioclases and coexisting clinopyroxenes (data Table 5.45).

Mount Adams complex exhibit wide variations in the values of K_d(plagioclase/orthopyroxene), which might be regarded as evidence that during joint crystallization, these minerals either did not achieve chemical equilibrium or their equilibrium was disturbed later. On the trends of K_d(plagioclase/orthopyroxene) for all varieties of rocks, one can observe Eu maximums of different intensities. This suggests that plagioclases from lunar anorthosites and ferruginous mafic rocks concentrate two to three orders of magnitude more Eu than coexisting orthopyroxenes. In pyroxenites from Zabargad Island, the level of Eu accumulation in plagioclase is one to two orders of magnitude higher than in orthopyroxene and is one order of magnitude higher than in gabbro-norites from the Beriozovsky and Naransky massifs.

K_d(plagioclase/amphibole). Paragenesis of plagioclase and amphibole occurs in many varieties of mafic and some ultramafic rocks. It is most common in the rocks of intermediate and acidic compositions. In the thin sections of these rocks one can often observe that amphibole grains are xenomorphic with respect to plagioclase grains, which suggests prior crystallization of the latter. Moreover, many varieties of rock contain amphiboles that pseudomorphously replaced clinopyroxene grains. Gabbros often contain segregations of amphibole in the form of kelyphitic rims at the boundary of plagioclase grains with clinopyroxene, orthopyroxene, and olivine grains. Most likely, each of these parageneses formed its own relationship between REE contents in coexisting plagioclases and amphiboles, which makes calculation of K_d(plagioclase/amphibole) values difficult. The values calculated for single samples from troctolites, olivine gabbros, norites, and dacites are given in Table 5.47. Judging by them, the values of these K_d for all REE are much lower than unity. They successively decrease from light to heavy elements and their trends demonstrate intense maximums for Eu (Fig. 5.39).

Table 5.46 Coefficients of REE distribution between plagioclases and coexisting orthopyroxenes.

	Massifs														
	Zabargad Island, Red sea														
	(Vannucci *et al.*, 1993b)														
	36A\1\r2	36A\2\c2	36A\3\c2	36A\3\r2	36B\12\c2	36B\2\c2	36B\8\c2	36C\17g2	36C\8\c2	36Cexs2	36C\17g3	36C\8\c3	36Cexs3	36C\17g4	36C\8\c4
Element	*Plagioclase-bearing pyroxenites (websterites)*														
La	N.d.	N.d.	N.d.	N.d.	N.d.	N.d.	N.d.	N.d.	N.d.	N.d.	N.d.	N.d.	N.d.	N.d.	N.d.
Ce	20.12	161.3	161.3	161.3	26.67	161.3	26.67	208.3	208.3	23.31	149.3	149.3	16.67	142.9	142.9
Pr	N.d.	N.d.	N.d.	N.d.	N.d.	N.d.	N.d.	N.d.	N.d.	N.d.	N.d.	N.d.	N.d.	N.d.	N.d.
Nd	9.001	37.74	31.55	94.34	10.57	37.04	12.33	42.02	28.01	12.01	37.45	25.00	10.72	22.52	14.99
Sm	9.497	28.49	8.143	14.25	2.000	5.333	4.000	7.502	3.750	3.750	6.998	3.500	3.500	2.500	1.250
Eu	29.50	14.75	19.69	59.17	23.98	48.08	23.98	38.02	19.01	12.66	40.98	20.49	13.66	25.97	13.00
Gd	N.d.	N.d.	N.d.	N.d.	0.561	1.353	1.643	N.d.	0.778	N.d.	N.d.	0.667	N.d.	N.d.	0.556
Tb	N.d.	N.d.	N.d.	N.d.	N.d.	N.d.	N.d.	N.d.	N.d.	N.d.	N.d.	N.d.	N.d.	N.d.	N.d.
Dy	0.445	0.650	0.311	0.353	0.076	0.180	0.150	0.526	0.093	0.103	0.526	0.093	0.103	0.211	0.037
Ho	N.d.	N.d.	N.d.	N.d.	N.d.	N.d.	N.d.	N.d.	N.d.	N.d.	N.d.	N.d.	N.d.	N.d.	N.d.
Er	0.142	0.186	0.103	0.116	0.019	0.044	0.032	0.154	0.028	0.033	0.179	0.032	0.038	0.051	0.009
Tm	N.d.	N.d.	N.d.	N.d.	N.d.	N.d.	N.d.	N.d.	N.d.	N.d.	N.d.	N.d.	N.d.	N.d.	N.d.
Yb	0.052	0.057	0.039	0.042	0.004	0.008	0.006	0.056	0.011	0.012	0.067	0.013	0.015	0.022	0.004
Lu	N.d.	N.d.	N.d.	N.d.	N.d.	N.d.	N.d.	N.d.	N.d.	N.d.	N.d.	N.d.	N.d.	N.d.	N.d.

(*Continued*)

Table 5.46 Continued

	Massifs														
	Beriozovsky, Russia						Naransky, Mongolia		The Moon						
	(Lesnov, 2001)								(Floss *et al.*, 1998)						
	131	132a	138a	141	144	147	278	269	5.5AF	42AFCl	42AFMx	82AF	68AFCs	702AFCl	702AFMx
Element	*Gabbro-norites*								*Orthopyroxene-bearing anorthosites*						
La	0.400	N.d.	1.025	0.133	0.053	0.433	0.034	0.650	75.00	11.54	20.00	32.50	20.00	13.33	32.50
Ce	N.d.	0.769	N.d.	0.560	N.d.	0.116	0.042	0.600	33.64	5.846	9.674	11.92	13.91	17.18	15.63
Pr	N.d.	N.d.	N.d.	N.d.	N.d.	N.d.	N.d.	N.d.	N.d.	2.618	4.700	11.33	7.800	5.563	7.727
Nd	0.450	0.533	0.600	0.350	0.043	0.113	0.042	0.222	11.77	1.320	2.412	5.000	3.810	3.250	4.815
Sm	0.200	0.750	0.556	0.540	0.071	0.073	0.056	0.078	4.615	0.493	1.176	1.864	1.633	0.855	1.923
Eu	4.462	0.900	1.067	2.384	1.136	0.833	1.375	0.738	N.d.	990	910	330	380	258	970
Gd	N.d.	N.d.	N.d.	N.d.	N.d.	N.d.	N.d.	N.d.	N.d.	0.194	0.407	0.453	0.345	0.227	0.607
Tb	N.d.	N.d.	N.d.	0.259	N.d.	0.136	0.074	0.070	4.500	0.092	0.152	0.229	0.333	0.123	0.385
Dy	N.d.	N.d.	N.d.	N.d.	N.d.	N.d.	N.d.	N.d.	0.135	0.047	0.070	0.076	0.068	0.045	0.130
Ho	N.d.	N.d.	N.d.	N.d.	N.d.	N.d.	N.d.	N.d.	0.118	0.043	0.044	0.064	0.036	0.039	0.109
Er	N.d.	N.d.	N.d.	N.d.	N.d.	N.d.	N.d.	N.d.	0.067	0.015	0.031	0.024	0.014	0.020	0.055
Tm	0.075	N.d.	N.d.	N.d.	0.025	0.091	0.059	0.043	N.d.	N.d.	N.d.	N.d.	N.d.	N.d.	N.d.
Yb	0.111	N.d.	N.d.	0.009	0.042	0.042	0.048	0.024	0.045	0.013	0.022	0.023	0.013	0.020	0.029
Lu	N.d.	N.d.	N.d.	N.d.	N.d.	N.d.	N.d.	N.d.	N.d.	N.d.	N.d.	N.d.	N.d.	N.d.	N.d.

	Massifs										
	The Moon						Mount Adams, USA			Japan	Saipan, Japan
	(Floss *et al.*, 1998)						(Dunn & Sen, 1994)			(Schnetzler & Philpotts, 1970b)	
	99MMM	270MMCc	600MF	601MF	602MF	603MF	14	49	7	GSFC184	GSFC271
Element	*Magnesioferous mafites*		*Ferriferous mafites*				*Andesites*				
La	93.33	56.67	3.479	2.276	4.792	2.481	0.732	0.300	N.d.	N.d.	N.d.
Ce	40.53	50.74	1.801	1.041	3.034	1.816	0.688	N.d.	3.100	2.004	5.339
Pr	15.67	28.57	0.868	0.532	1.964	1.606	0.336	0.383	2.138	N.d.	N.d.
Nd	7.679	10.75	1.075	0.360	1.392	0.970	0.229	0.280	1.571	1.500	2.434
Sm	1.827	1.667	0.225	0.183	0.538	0.470	0.107	0.170	0.476	0.864	1.063
Eu	1.060	N.d.	46.7	63.1	100	35.7	6.09	4.84	13.9	N.d.	9.19
Gd	0.540	0.583	0.130	0.085	0.223	0.278	0.147	0.089	0.469	N.d.	N.d.
Tb	0.231	0.220	0.061	0.045	0.148	0.107	N.d.	0.024	0.316	N.d.	N.d.
Dy	0.063	0.105	0.032	0.045	0.079	0.079	N.d.	N.d.	0.089	0.250	0.188
Ho	0.069	0.069	0.041	0.044	0.057	0.075	N.d.	N.d.	N.d.	N.d.	N.d.
Er	0.028	0.037	0.028	0.036	0.039	0.039	N.d.	N.d.	N.d.	0.164	0.090
Tm	N.d.	N.d.	N.d.	N.d.	N.d.	N.d.	N.d.	N.d.	N.d.	N.d.	N.d.
Yb	0.008	0.020	0.031	0.034	0.025	0.038	N.d.	N.d.	N.d.	0.100	0.049
Lu	N.d.	N.d.	N.d.	N.d.	N.d.	N.d.	N.d.	N.d.	N.d.	N.d.	0.041

Data Tables 5.34–5.41 and 5.7.

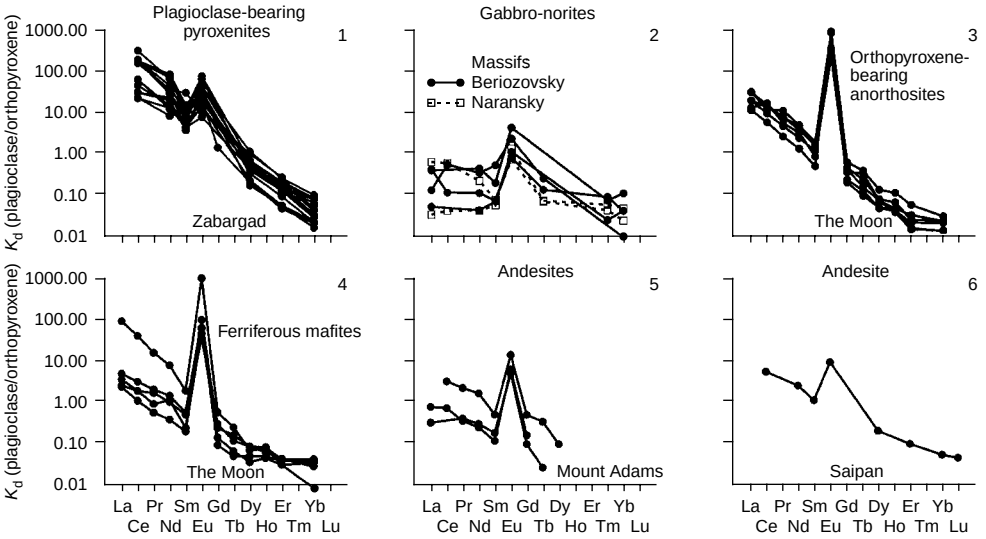

Figure 5.38 The trend coefficients of REE distribution between plagioclases and coexisting orthopyroxenes (data Table 5.46).

The reported data on the coefficients of REE distribution between plagioclase and coexisting phases, in spite of their scarcity, suggest that this feature is one of the most important criteria that can be used in solving problems of geochemical systematization of plagioclase-bearing rocks and in determining the crystallization conditions of minerals. More efficient application of these possibilities requires much more representative bases of analytical data on the contents of REE in plagioclases and coexisting phases.

5.4.4 Isomorphism of REE in plagioclases

According to existing concepts, the crystal structure of plagioclases is a framework of connected (Si, Al)–O tetrahedra, which big cavities are occupied by Ca^{2+} and Na^{+} ions (Deer *et al.*, 1966). In plagioclases and in other silicates, Ca is assumed to be the most favorable net-forming element, which can be replaced by REE. Its bivalent ions play an important part in plagioclase structure when it accumulates REE impurities. Taking into account the need for minimization of differences between the sizes of ionic radii in replacing and replaced ions and selection of optimal balances and charges, the following hypothetic schemes of REE isomorphism with participation of some charge-compensating ions can be proposed for plagioclases:

1. $[2Ca^{2+}] \rightarrow [La^{3+} + Na^{+}]$. Calculated total sizes of ionic radii in the left and right parts of replacement scheme are [1.04 Å + 1.04 Å] → [1.032 Å + 0.98 Å] and differ by 3.3%;
2. $[3Ca^{2+}] \rightarrow [La^{3+} + Na^{+} + Eu^{2+}]$. Calculated total sizes of ionic radii in the left and right parts of the replacement scheme are [1.04 Å + 1.04 Å + 1.04 Å] → [1.032 Å + 0.98 Å + 1.17 Å] and differ by 1.9%;

Table 5.47 Coefficients of REE distribution between plagioclases and coexisting amphiboles.

	Massifs (provinces)							
	Sondalo, Italy		Apennine, Italy		Liguria, Italy	Sondalo, Italy		New Mexico, USA
	(Tribuzio *et al.*, 1999a)		(Tribuzio *et al.*, 1999b)		(Tribuzio *et al.*, 1996)	(Tribuzio *et al.*, 1999a)		(Arth & Barker, 1976)
	SOX/1-1	SO5/1-1	CBC3-2	CB16-1	T-1	SO5/11-1	SO3/2-1	BP-1
Element	*Troctolites*		*Olivine gabbros*		*Ferriferous gabbro*	*Norites*		*Dacite*
La	0.373	0.119	0.131	0.234	0.108	0.512	0.243	N.d.
Ce	0.160	0.060	0.060	0.105	0.048	0.203	0.106	0.203
Pr	N.d.	N.d.	N.d.	N.d.	N.d.	N.d.	N.d.	N.d.
Nd	0.055	0.026	0.021	0.050	0.021	0.057	0.047	0.062
Sm	0.027	0.016	0.009	0.018	0.090	0.026	0.023	0.025
Eu	0.344	0.323	0.276	0.237	0.389	0.403	0.401	0.237
Gd	0.012	0.013	N.d.	N.d.	0.006	0.021	0.012	0.016
Tb	N.d.	N.d.	N.d.	N.d.	N.d.	N.d.	N.d.	N.d.
Dy	0.074	0.007	0.002	0.004	0.003	0.010	0.005	0.010
Ho	N.d.	N.d.	N.d.	N.d.	N.d.	N.d.	N.d.	N.d.
Er	N.d.	N.d.	N.d.	N.d.	0.001	N.d.	N.d.	0.009
Tm	N.d.	N.d.	N.d.	N.d.	N.d.	N.d.	N.d.	N.d.
Yb	N.d.	N.d.	N.d.	N.d.	0.001	N.d.	N.d.	0.011
Lu	N.d.	N.d.	N.d.	N.d.	N.d.	N.d.	N.d.	N.d.

Data Tables 5.34–5.41 and 5.50–5.52.

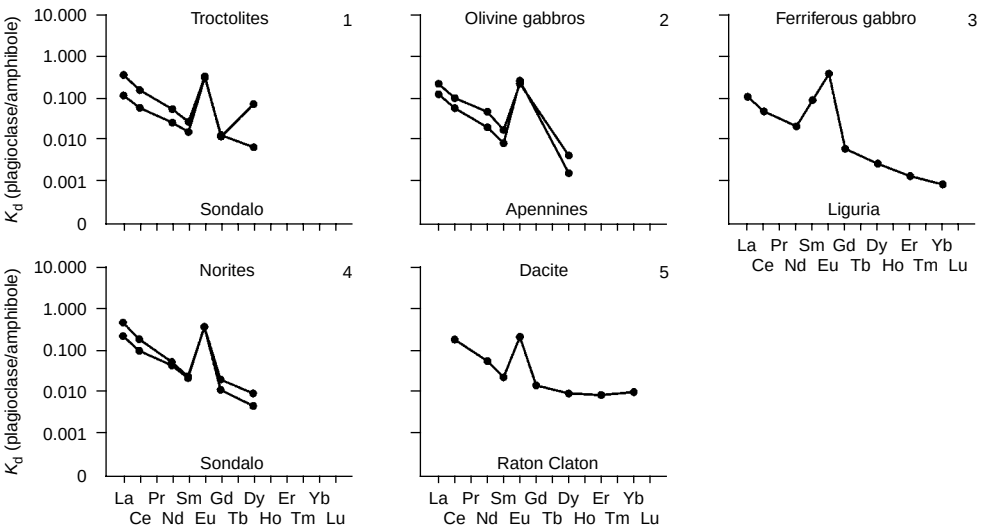

Figure 5.39 The trend coefficients of REE distribution between plagioclases and coexisting amphiboles (data Table 5.47).

3. $[3Ca^{2+}] \rightarrow [La^{3+} + Sr^{2+} + Na^{+}]$. Total sizes of ionic radii in the left and right parts of the replacement scheme are $[1.04\,Å + 1.04\,Å + 1.04\,Å] \rightarrow [1.032\,Å + 1.10\,Å + 0.98\,Å]$ and differ by only 0.3%. If only the balance between total sizes of ionic radii in the left and right parts of the scheme is taken into consideration, then only a third of them is optimal.

   We cannot rule out the probability of realization of isomorphous replacement in plagioclases by one more scheme proposed for the case of isomorphism of REE in clinopyroxenes (Dobosi *et al.*, 1998):

4. $[Ca^{2+} + Si^{4+}] \rightarrow [REE^{3+} + Al^{3+}]$. In this case, the total sizes of ionic radii in the left and right parts of the scheme are $[1.04\,Å + 0.39\,Å] \rightarrow [(1.032\,Å \ldots 0.861\,Å) + 0.57\,Å]$, that is, they must vary from very large (12%) for La to very small (0.06%) for Lu. This scheme of isomorphism is, probably, most plausible in the replacement of Ca^{2+} ions by heavy REE.

In conclusion, it is pertinent to emphasize that the proposed schemes of REE isomorphism in plagioclases should be treated as strictly hypothetical and, undoubtedly, as requiring special experimental and crystallochemical justification.

5.4.5 Examples of numerical experiments on modeling of the REE composition of parental melts based on data on plagioclases

Values of average REE contents in plagioclases from some varieties of rock (Table 5.42) and specially chosen values of coefficients of their distribution between this

Table 5.48 Average values of coefficients of REE distribution between plagioclases and basalt's melt, which was used for calculation of modeling melt's compositions.

	Sample's number			
Element	1	2	3	Average
La	0.0358	0.0418	0.0415	0.039
Ce	0.0307	0.0302	0.0297	0.030
Nd	N.d.	N.d.	N.d.	N.d.
Sm	0.0204	0.0170	0.0177	0.018
Eu	0.2360	0.1660	0.1680	0.190
Gd	0.0160	N.d.	N.d.	0.016
Tb	N.d.	0.0095	0.0096	0.010
Dy	N.d.	N.d.	N.d.	N.d.
Ho	N.d.	N.d.	N.d.	N.d.
Er	N.d.	N.d.	N.d.	N.d.
Yb	0.0070	0.0065	0.0070	0.007
Lu	N.d.	0.0068	0.0067	0.006

Data Table 5.43.

mineral and basalt melts (Table 5.43) can be used in numerical modeling of REE compositions of parental melts from corresponding rocks crystallized. We used the average values of K_d(plagioclase/melt) of REE calculated on the basis of the results of their determinations in plagioclases from the Archean anorthosites in Phinney and Morrison (1990) (Table 5.48) as the most appropriate for solving this problem. The contents of REE in plagioclases in model melts (Table 5.49, Fig. 5.40) was calculated by the formula

$$C_{melt} = C_{plagioclase}/K_d(\text{plagioclase/melt})$$

where $C_{plagioclase}$ is the average REE content in plagioclases (from data of Table 5.42) and K_d(plagioclase/melt) is the average value of coefficients of REE distribution between plagioclase and basalt melts (from data of Table 5.48). If the calculated REE contents in plagioclases from the varieties of rock used in the numeric experiment reflect their real REE composition rather accurately and the K_d(plagioclase/melt) values are chosen correctly, then the following assumption can be made from these calculations.

Firstly, the melts from which plagioclases from Chessigny and Valadares meteorites could have crystallized were richer in REE than the melts from which plagioclases from meteorites of the Acapulco occurrence crystallized. In both cases, the melts were characterized by intense fractionation of elements at a considerable excess of Eu (Fig. 5.40, 1, 2).

Secondly, the melts that generated plagioclases occurring in lunar magnesium and ferriferous mafic rocks, alkali gabbro-norites, monzogabbros, and alkali anorthosites have a very high level of REE accumulation (Fig. 5.40, 3–6, 8). Unlike them, the melts from which lunar ferriferous anorthosites could crystallize were REE depleted

Table 5.49 Average rare earth element composition of some modeling melts, calculated with using plagioclase's data (ppm).

	Meteorites		The Moon					
Element	Chessigny, Valadares, and others	Acapulco	Magnesioferous mafites	Ferriferous mafites	Alkaline gabbro-norites	Monzogabbros	Ferriferous anorthosites	Alkaline anorthosites
La	149	26.9	49.3	210	900	501	25.0	734
Ce	131	17.9	61.2	220	989	460	31.3	782
Pr	N.d.	N.d.	N.d.	N.d.	N.d.	N.d.	N.d.	N.d.
Nd	N.d.	N.d.	N.d.	N.d.	N.d.	N.d.	N.d.	N.d.
Sm	40.7	7.64	37.6	108	741	125	24.3	471
Eu	108	66.8	91.9	97.6	692	313	83.7	610
Gd	18.5	4.49	31.8	71.2	462	124	20.7	267
Tb	20.1	7.96	45.9	80.3	N.d.	183	68.2	N.d.
Dy	N.d.	N.d.	N.d.	N.d.	N.d.	N.d.	N.d.	N.d.
Ho	N.d.	N.d.	N.d.	N.d.	N.d.	N.d.	N.d.	N.d.
Er	N.d.	N.d.	N.d.	N.d.	N.d.	N.d.	N.d.	N.d.
Tm	N.d.	N.d.	N.d.	N.d.	N.d.	N.d.	N.d.	N.d.
Yb	N.d.	3.27	22.9	92.9	277	258	21.5	125
Lu	N.d.	33.4	N.d.	N.d.	N.d.	116	N.d.	N.d.

	Massifs							
	Stillwater, USA		Dovyrensky, Russia		Ivrea Verbano, Italy		Samail, Oman	
Element	Dunites	Troctolites	Norites	Anorthosites	Wehrlites	Gabbro	Olivine gabbro	Gabbro
La	69.5	92.4	81.0	149	442	928	39.9	32.1
Ce	66.1	83.1	71.7	137	321	582	68.5	55.3
Pr	N.d.	N.d.	N.d.	N.d.	N.d.	N.d.	N.d.	N.d.
Nd	N.d.	N.d.	N.d.	N.d.	N.d.	N.d.	N.d.	N.d.
Sm	35.2	43.7	36.6	74.6	95.2	70.6	41.5	35.2
Eu	19.2	21.1	15.4	23.2	19.2	109	24.8	22.1
Gd	21.0	28.3	22.6	50.6	61.2	50.1	38.9	25.1
Tb	N.d.	N.d.	N.d.	N.d.	87.7	N.d.	58.1	36.5
Dy	N.d.	N.d.	N.d.	N.d.	N.d.	N.d.	N.d.	N.d.
Ho	N.d.	N.d.	N.d.	N.d.	N.d.	N.d.	N.d.	N.d.
Er	N.d.	N.d.	N.d.	N.d.	N.d.	N.d.	N.d.	N.d.
Tm	N.d.	N.d.	N.d.	N.d.	N.d.	N.d.	N.d.	N.d.
Yb	45.0	17.8	10.8	40.4	79.3	12.9	37.1	29.4
Lu	N.d.	N.d.	N.d.	N.d.	81.4	N.d.	49.0	47.5

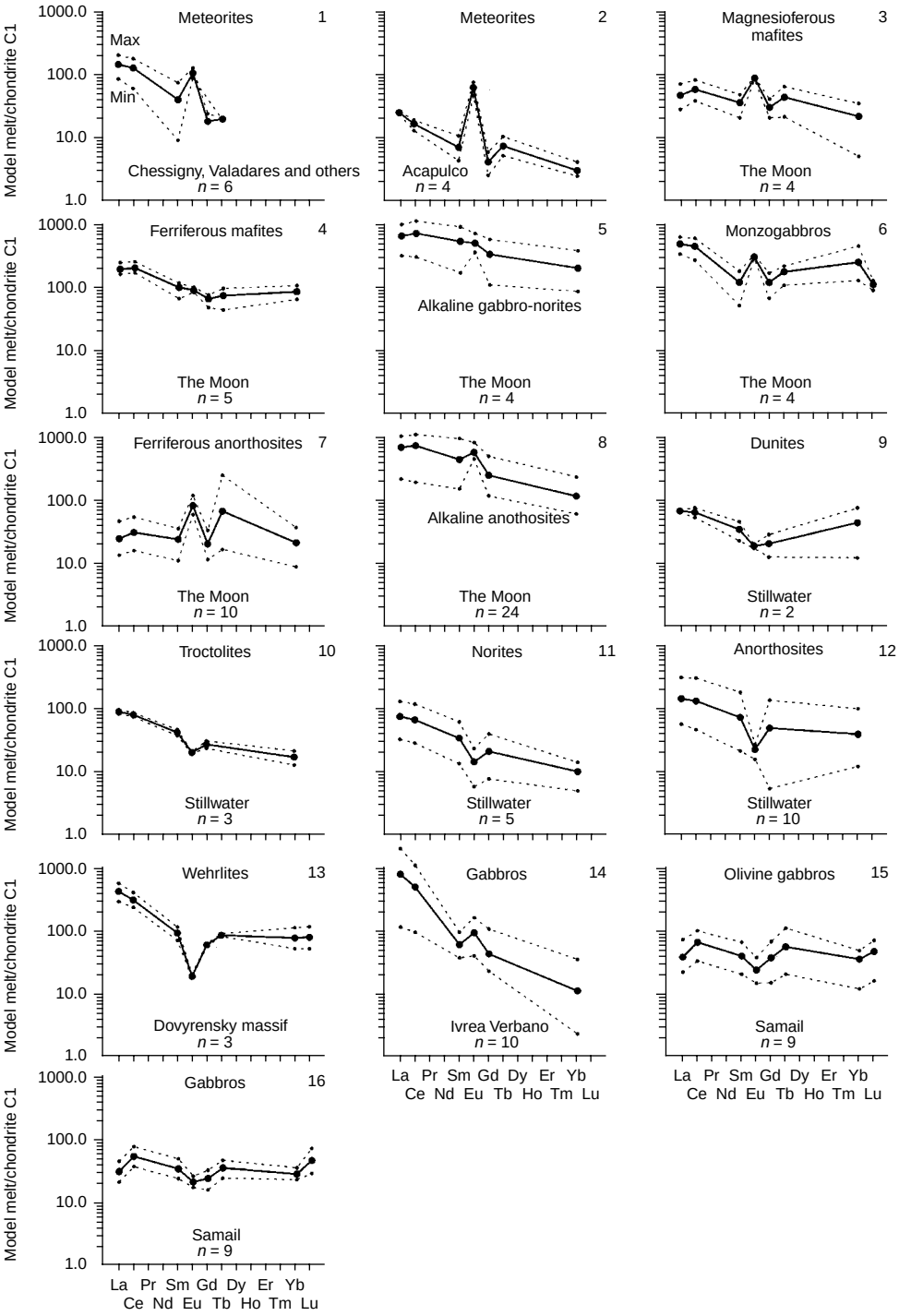

Figure 5.40 Chondrite-normalized REE patterns for model paternal melts for plagioclases (data Table 5.49). Dotted lines—chondrite-normalized patterns of maximal and minimal REE composition.

(Fig. 5.40, 7). Excess Eu content is likely found only in those lunar melts from which magnesium mafic rocks, monzogabbros, alkali, and ferriferous anorthosites crystallized. Considering the accepted assumptions, the parental melts of the above-listed rocks of the moon were, most likely, generated on melting of sources considerably enriched with REE.

Thirdly, the melts resulting in the crystallization of plagioclases from dunites, troctolites, norites, and anorthosites from the Stillwater massif also seem to be enriched with REE, which underwent fractionation and had a deficit of Eu (Fig. 5.40, 9–12). The REE compositions of model melts calculated using data on plagioclases from compositionally different rocks of the Stillwater massif showed comparable results. This implies that all plagioclases from the rocks of this massif crystallized from one parental melt, which was generated on partial melting of undepleted mantle source.

Fourthly, results of modeling using data on the REE composition of plagioclases from wehrlites of the Dovyrensky massif suggest that their parental melt was also characterized by an elevated level of REE concentrations, especially light REE, but was Eu deficient (Fig. 5.40, 13). The model melt, which generated plagioclase occurring in gabbros from the Ivrea Verbano complex, was strongly enriched with light REE but was rather depleted of heavy elements and had excess Eu (Fig. 5.40, 14). Mazzucchelli *et al.* (1992a) report that the parental melts of gabbroid from this complex were preliminarily contaminated by the matter of host rocks enriched with light REE. Unlike the previous melts, the parental melts from which gabbros of the ophiolite Samail massif crystallized were depleted of light REE. (see Fig. 5.40, 15, 16). This suggests that they were generated at a high level of partial melting of the source that was, probably, preliminarily depleted.

* * *

Plagioclases from all the varieties of mafic, ultramafic, and some other rocks are an important concentrator of light REE, especially Eu. The total REE contents in plagioclases from these rocks vary from a few to a few tens of ppm. The varieties of these rocks containing an increased amount of anorthite end member, including those occurring in different rocks from ophiolite mafic–ultramafic massifs as well as in meteorites and some other rocks, have a rather low general level of REE accumulation. Plagioclases with a low content of anorthite end member occurring in andesites, dacites, rhyolites, and mafic rocks with elevated alkalinity can accumulate more considerable amounts of REE in their structure. In plagioclases from rocks of ophiolite mafic–ultramafic massifs, REE demonstrate mainly poor fractionation of elements and rather low values of the $(Eu/Eu^*)_n$ parameter. The mineral from meteorites and lunar mafic rocks, which crystallized under strongly reducing conditions, displays especially intensely positive Eu anomalies. Abnormal enrichment with light REE, particularly Eu, was revealed in plagioclases from gabbroids that crystallized from melts contaminated by the matter of host sedimentary rocks enriched with these impurities. The parameters of REE distribution, such as absolute Ce contents and the $(Ce/Yb)_n$ and $(Eu/Eu^*)_n$ values can be efficiently used in the geochemical systematization of plagioclases.

Numerical experiments performed using the average REE compositions of plagioclases from different types of rock and available estimations of the K_d(plagioclase/melt) values allowed calculation of the model REE compositions of parental melts from

which these rocks could crystallize. The coefficients of REE distribution between plagioclases and coexisting minerals (clinopyroxene, orthopyroxene, and amphibole) calculated from the results of cross-spectrum analyses of these minerals for the rock samples of any one magmatic body and the character of trends of K_d changes reveal the degree of chemical equilibrium of plagioclases and coexisting minerals, which was attained at the end of crystallization of the parental melt. Thus, rather narrow ranges of variations in K_d and similar configurations of their trends may suggest that the existing phases attained equilibrium and it was disturbed by any epigenetic process. The data obtained up to date suggest that the structural REE impurity in plagioclases accumulated by way of realization of some schemes of their heterovalent isomorphous replacement by trivalent ions of net-forming ions of bivalent Ca^{2+}, with some other elements playing the auxiliary role. At the same time, Ca content is most likely not the single factor controlling the level of REE accumulation in plagioclases, as commonly this level decreases with increasing amount of anorthite end member.

5.5 AMPHIBOLES

Amphiboles are typically of minor significance in the composition of ultramafic and mafic rocks. Most commonly they crystallize at the late stages of formation of these rocks with participation of volatile components. Amphiboles are more abundant in quartz-bearing gabbros, diorites, granites, effusive of varying compositions, and in many metamorphic and metasomatic rocks. In the ability to accumulate REE in the form of isomorphous impurities, amphiboles surpass clinopyroxenes, orthopyroxenes, plagioclases, and, especially, olivines. Owing to this property, even at minor modal contents, amphiboles might concentrate a considerable part of the REE occurring in the rock sample. Unlike the previously mentioned rock-forming minerals, the amphibole structure contains a hydroxyl group (OH).

The first amphibole samples in which REE contents were determined are the phenocrysts from alkali basalts (Higuchi & Nagasawa, 1969) and grains from some peridotites (Frey, 1969). These data and the analytical data obtained later show that amphiboles can concentrate considerable amounts of structural REE impurities. At that time, the first estimates of REE distribution between amphiboles and coexisting phases were obtained. A brief summary of general regularities of REE distribution in amphiboles was reported in Lesnov's work. Most analyses performed for REE by now characterize their samples from ultramafic rocks from deep xenoliths and from some varieties of gabbroid rocks. Fewer analyses are available for amphiboles from basalts, andesites, and other amphibole-bearing rocks. In chemical composition, the amphiboles analyzed for REE belong mainly to their Ca varieties (pargasite and kaersutite). The studies of REE distribution in amphiboles were performed using the IPMA (50%), INAA (18%), and SIMS (15%) techniques.

5.5.1 REE composition of amphiboles

The characterization of REE composition of amphiboles is based on the results of studies of their samples from ultramafic rocks, occurring in deep xenoliths from

basalts, from ultramafic and mafic rocks that compose mafic–ultramafic massifs, and from some volcanogenic and metamorphic rocks.

Ultramafic rocks from deep xenoliths. More thoroughly studied are the amphiboles from lherzolite xenoliths in alkali basalts of the Eifel province (Germany) (Witt-Eickschen *et al.*, 1998). The authors divided them into three morphological types—tabular, interstitial, and pseudomorphs after clinopyroxene. However, the samples referred to these types did not reveal any evident differences either in the level of REE accumulation (Table 5.50) or in the configuration of REE patterns (Fig. 5.41). Total REE content in the whole series of amphibole samples vary from 107 to 227 ppm with an average content of 165 ppm. The level of accumulation of La (100 t. ch.) in them is an order of magnitude higher than that of Lu (10 t. ch.) and the average value of $(La/Yb)_n$ is 12. The configuration of negatively sloping patterns of these amphiboles is nearly straight lines that are compactly arranged on the plots (Fig. 5.41, 2). In the mineral grains that occur in ultramafic rocks at the exocontacts of cutting amphibole veins, the average total content of REE is much lower (132 ppm), but their patterns are described by the same average value of the $(La/Yb)_n$ parameter (11) as the patterns of other samples. A similar REE composition is typical of amphiboles that compose their monomaniacal veins that penetrate the xenoliths of lherzolites. Ashchepkov (2007) reported that kaersutite from amphibole–phlogopite veins that cut the xenoliths from spinel lherzolites of alkali basalts in southern Siberia have lower contents of REE. The level of accumulation of some elements in them increased from La (20–30 t. ch.) to Nd (26–50 t. ch.) and gradually decreased to Lu (1.5–3 t. ch.). Single analyses of REE were performed for amphiboles from lherzolite xenoliths occurring in alkaline-basalt provinces in Nunivak Island (Alaska) (Roden *et al.*, 1984), Ataq (South Yemen) (Varne & Graham, 1971), and Vitim (Russia) (Ionov *et al.*, 1993a; Litasov, 1998). The level of accumulation of elements in amphibole from Ataq province successively decreases from La (190 t. ch.) to Lu (4 t. ch.) (Fig. 5.41, 1). A similar REE pattern was observed in amphibole from Nunivak Island, in which the level of REE accumulation gradually decreases from La (70 t. ch.) to Lu (10 t. ch.) (Fig. 5.41, 7). A somewhat lower level of REE accumulation and their less significant fractionation was found in amphiboles from lherzolite xenoliths in the provinces of Leura, Dush Hill, and Itinome–Gata, and in the Caussou and Lizard massifs (Fig. 5.41, 3–6). Unlike others, amphibole from Itinome–Gata province demonstrates relative depletion of light REE.

Ultramafic rocks from ophiolite massifs. These amphiboles were characterized in samples from the ophiolite Miyamori and Hayachine massifs, in which ultramafic rocks are represented by harzburgites and subordinate lherzolites, with fewer dunites and wehrlites (Table 5.50). Most samples from the Miyamori massif demonstrate a higher level of accumulation of light and middle REE (20–100 t. ch.) than heavy REE (2–5 t. ch.) resulting in a negative slope of their patterns (Fig. 5.41, 11–13, 15, 16). Unlike the previous samples, amphiboles from the Hayachine massif are depleted of light REE (0.2–2 t. ch.), and, hence, their patterns have a positive slope (Fig. 5.41, 14).

Troctolites, gabbros, norites, diorites, and websterites. Data on the REE composition of amphiboles from the first four varieties of rock were obtained from samples of some massifs occurring on the territory of Italy—Sondalo, Castelly, Riparbello, and Graveglia (Tribuzio *et al.*, 1999à, 2000)—and from the massifs in Liguria (Tribuzio *et al.*, 1995). The total REE content in these amphiboles vary from 45 to 238 ppm and their REE patterns have a gentle slope and a flattened shape in the region of heavy

Table 5.50 Rare earth element composition of amphiboles from ultramafic rocks, represented in massifs, and deep xenoliths (ppm).

	Massifs (provinces)												
	Yemen[a]	West Eifel, Germany[a]								Itinome–Gata, Japan[a]	Caussou, France		Leura
	(Varne & Graham, 1971)	(Witt-Eickschen *et al.*, 1998), IPMA								(Tanaka & Aoki, 1981)	(Bodinier *et al.*, 1988)		(Frey & Green, 1974)
	VG-1	MM214P	MM248P	MM262P	MM262P	MM307P	MM310P	MM332P	MM333P	L3	CAU-1	CAU-2	2642
Element	*Lherzolites*												
La	39.00	12.32	29.80	32.30	33.10	24.40	20.50	30.90	14.50	0.822	4.400	5.200	8.330
Ce	32.00	42.30	91.20	85.50	79.30	78.80	53.60	85.60	41.60	2.740	17.10	17.10	20.30
Pr	3.900	6.660	13.40	10.10	9.390	10.70	6.560	11.60	5.860	N.d.	N.d.	N.d.	2.040
Nd	11.00	33.30	59.00	38.00	38.90	44.00	29.20	43.40	26.40	3.760	21.00	24.00	9.220
Sm	2.500	8.240	11.70	5.160	4.970	8.200	6.220	6.400	5.760	1.750	7.600	8.100	2.720
Eu	0.660	2.240	2.860	1.370	1.170	2.260	1.770	1.560	1.370	0.728	2.400	2.400	1.130
Gd	2.400	5.610	8.000	3.960	4.200	5.670	4.760	4.380	4.480	2.870	N.d.	N.d.	4.340
Tb	0.580	0.900	1.030	0.540	0.340	0.870	0.640	0.620	0.620	N.d.	1.210	1.160	0.760
Dy	2.000	4.560	5.270	2.850	2.620	4.560	3.500	3.460	3.030	3.820	N.d.	N.d.	N.d.
Ho	0.500	0.760	0.860	0.580	0.540	0.800	0.620	0.580	0.630	N.d.	1.140	1.200	1.380
Er	1.200	2.300	2.250	1.760	1.480	2.100	1.580	1.800	1.400	2.510	N.d.	N.d.	3.640
Tm	0.200	N.d.	N.d.	N.d.	N.d.	N.d.	N.d.	N.d.	N.d.	N.d.	N.d.	N.d.	0.510
Yb	0.900	1.730	1.340	1.420	1.350	1.610	1.460	1.090	1.270	2.140	1.850	1.920	3.430
Lu	0.100	0.180	0.250	0.180	0.140	0.200	0.110	0.160	0.120	0.309	0.240	0.250	0.520
Total	96.9	121	227	184	178	184	131	192	107	N.d.	N.d.	N.d.	58.3
$(La/Yb)_n$	29.4	4.81	15.0	15.4	16.6	10.2	9.48	19.1	7.71	0.26	1.61	1.83	1.64
$(Eu/Eu^*)_n$	0.81	0.95	0.86	0.89	0.76	0.96	0.96	0.85	0.80	0.99	N.d.	N.d.	1.00

	Massifs (provinces)											
	Lizard, England	Nunivak Island[a]	Vitim, Russia[a]				West Eifel, Germany[a]					
	(Frey, 1969)	(Roden *et al.*, 1984)	(Ionov *et al.*, 1993a)		(Litasov, 1998), SIMS		(Witt-Eickschen *et al.*,1998), IPMA					
	90691	10067	313-103	313-114	V-122	V-244	251Tc	262Tc1	262Tr1	262Tc2	262Tr2	307Tc
Element	*Lherzolites*		*Peridotites*								*Amphibole-bearing lherzolites from contact with amphibole's veins*	
La	2.200	16.10	2.080	2.750	12.97	16.38	44.80	31.50	20.700	22.10	16.80	21.90
Ce	6.100	41.90	9.500	9.900	41.53	58.51	93.30	80.80	55.400	58.90	42.90	88.90
Pr	0.900	N.d.	N.d.	N.d.	N.d.	N.d.	9.770	9.600	7.060	7.920	5.670	12.10
Nd	4.900	23.10	8.800	10.00	31.67	60.28	35.30	34.50	26.60	31.80	23.80	45.60
Sm	1.650	5.060	3.270	3.380	5.490	12.57	7.300	4.620	4.620	4.900	3.810	8.030
Eu	0.751	1.720	1.030	1.070	1.350	3.450	1.760	1.300	1.280	1.150	1.190	2.020
Gd	2.590	N.d.	3.310	3.900	N.d.	N.d.	6.100	3.660	3.980	3.700	3.290	5.770
Tb	0.460	0.685	0.530	0.500	N.d.	N.d.	0.940	0.560	0.510	0.510	0.480	1.030
Dy	N.d.	N.d.	N.d.	N.d.	2.740	9.350	5.270	2.100	2.740	3.190	2.360	4.650
Ho	0.708	N.d.	N.d.	N.d.	N.d.	N.d.	0.840	0.480	0.510	0.530	0.400	0.780
Er	2.000	N.d.	N.d.	N.d.	1.110	4.800	2.350	1.740	1.530	1.340	1.160	1.590
Tm	0.330	N.d.	N.d.	N.d.	N.d.	N.d.	N.d.	N.d.	N.d.	N.d.	N.d.	N.d.
Yb	1.900	1.740	N.d.	N.d.	1.080	5.140	1.700	1.310	1.100	1.220	1.100	1.640
Lu	0.340	0.270	0.038	0.056	N.d.	N.d.	0.150	0.230	0.230	0.150	0.160	0.160
Total	24.8	N.d.	N.d.	N.d.	N.d.	N.d.	210	172	126	137	103	194
$(La/Yb)_n$	0.78	6.25	N.d.	N.d.	8.11	2.15	17.8	16.2	12.7	12.2	10.3	9.01
$(Eu/Eu^*)_n$	1.11	N.d.	0.95	0.90	N.d.	N.d.	0.79	0.94	0.89	0.79	1.00	0.87

(*Continued*)

Table 5.50 Continued

	Massifs (provinces)											
	West Eifel, Germany[a]											
	(Witt-Eickschen *et al.*, 1998), IPMA											
	307Tr	313c1	313c2	326Tc	329Tc	MM214	MM251	MM248	MM262	MM307	MM310	MM313
Element	*Amphibole-bearing lherzolites near contact with veins of amphibole*					*Veins of amphibole in xenoliths of lherzolites*						
La	13.00	8.340	8.760	14.20	11.00	11.84	44.80	16.30	15.30	14.60	18.80	7.340
Ce	42.00	27.90	29.90	45.10	41.80	38.20	87.80	40.60	38.50	46.20	49.40	24.20
Pr	5.460	4.000	4.640	6.660	6.230	5.750	9.940	5.510	5.190	6.040	6.240	3.880
Nd	25.60	19.00	21.50	31.10	28.20	29.20	37.00	24.80	21.30	26.50	28.30	18.60
Sm	5.130	4.270	4.190	5.960	4.820	6.870	7.330	5.430	4.650	5.710	5.320	4.600
Eu	1.520	1.400	1.280	1.640	1.260	2.260	1.980	1.310	1.360	1.570	1.710	1.440
Gd	5.650	3.640	3.270	4.870	3.450	5.950	5.610	3.810	3.640	4.280	4.600	4.550
Tb	0.640	0.530	0.490	0.600	0.570	0.940	0.980	0.600	0.550	0.620	0.710	0.700
Dy	4.080	3.180	2.860	3.360	3.710	4.750	4.840	2.840	2.890	3.330	3.680	3.280
Ho	0.590	0.470	0.530	0.610	0.590	0.740	0.910	0.530	0.500	0.610	0.610	0.560
Er	1.260	1.240	0.970	1.450	1.720	1.880	2.450	1.390	0.950	1.430	1.420	1.410
Tm	N.d.	N.d.	N.d.	N.d.	N.d.	N.d.	N.d.	N.d.	N.d.	N.d.	N.d.	N.d.
Yb	0.830	0.960	0.730	1.170	1.460	1.490	2.080	1.110	0.780	1.070	1.230	1.010
Lu	0.170	0.120	0.090	0.130	0.160	0.200	0.250	0.140	0.110	0.100	0.150	0.120
Total	106	75.1	79.2	117	105	110	206	104	95.7	112	122	71.7
$(La/Yb)_n$	10.6	5.86	8.10	8.19	5.09	5.36	14.5	9.91	13.2	9.21	10.3	4.91
$(Eu/Eu^*)_n$	0.86	1.06	1.02	0.19	0.90	1.06	0.91	0.84	0.98	0.93	1.03	0.95

	Massifs (provinces)											
	West Eifel, Germany[a]					Dush Hill[a]		Miyamori, Japan				
	(Witt-Eickschen *et al.*, 1998), IPMA					(Irving & Frey, 1984), INAA		(Ozawa & Shimizu, 1995), IPMA				
	MM326	MM329	MM331	MM332	MM333	H-19	Ba172	MY-1	MY-2	MY-3	MY-4	MY-6
Element	*Veins of amphibole in xenoliths of lherzolites*							*Harzburgites*				
La	13.60	8.730	20.00	17.80	7.100	6.550	13.10	7.9	6.7	4.5	4.9	22.9
Ce	38.90	30.28	58.00	50.10	22.20	22.70	41.50	21.2	24.3	17.1	17.1	58.8
Pr	4.900	4.390	8.280	7.120	3.480	N.d.	N.d.	N.d.	N.d.	N.d.	N.d.	N.d.
Nd	22.00	20.60	35.30	30.40	18.30	N.d.	N.d.	22.2	26.4	16.3	19.3	35.1
Sm	4.620	4.510	6.550	5.850	5.460	5.600	8.600	6.2	7.8	6.2	4.8	6.7
Eu	1.280	1.270	1.740	1.590	1.410	1.950	2.770	1.8	2.8	1.7	1.6	2.2
Gd	4.500	3.740	5.720	4.220	4.300	N.d.	N.d.	N.d.	N.d.	N.d.	N.d.	N.d.
Tb	0.620	0.550	0.800	0.750	0.570	1.000	1.320	N.d.	N.d.	N.d.	N.d.	N.d.
Dy	3.120	2.680	4.000	3.340	2.900	N.d.	N.d.	2.2	2.7	2.3	1.4	1.7
Ho	0.510	0.500	0.650	0.660	0.510	N.d.	N.d.	N.d.	N.d.	N.d.	N.d.	N.d.
Er	1.160	1.110	1.550	1.690	1.140	N.d.	N.d.	0.79	0.94	1.1	0.54	0.73
Tm	N.d.	N.d.	N.d.	N.d.	N.d.	N.d.	N.d.	N.d.	N.d.	N.d.	N.d.	N.d.
Yb	0.810	0.930	1.140	1.290	0.690	1.570	2.200	0.48	0.50	0.83	0.32	0.30
Lu	0.110	0.100	0.130	0.140	0.080	0.250	0.300	N.d.	N.d.	N.d.	N.d.	N.d.
Total	96.1	79.4	144	125	68.1	N.d.	N.d.	62.8	72.1	50.0	50.0	128
$(La/Yb)_n$	11.3	6.34	11.8	9.31	6.95	2.82	4.02	11.1	9.04	3.66	10.3	51.5
$(Eu/Eu^*)_n$	0.85	0.92	0.85	0.93	0.86	N.d.	N.d.	N.d.	N.d.	N.d.	N.d.	N.d.

(*Continued*)

Table 5.50 Continued

	Massifs (provinces)												
	Miyamori, Japan											Hayachine, Japan	
	(Ozawa & Shimizu, 1995), IPMA												
	MY-7	MY-8	MY-9	ORM-25	ORM-39	ORM-26	ORM-M27U	ORM-31	ORM-M22	ORM-M9	ORM-M26D	HY-1	HY-2
Element	*Harzburgites*						*Lherzolites*		*Dunite*	*Wehrlites*		*Lherzolites*	
La	5.6	0.76	0.48	7.6	14.5	10.1	6.2	6.5	7.7	8.2	10.6	0.09	0.47
Ce	13.1	2.2	1.2	26.5	52	27	20.9	21.6	27.9	23.1	29	0.58	0.15
Pr	N.d.	N.d.	N.d.	N.d.	N.d.	N.d.	N.d.	N.d.	N.d.	N.d.	N.d.	N.d.	N.d.
Nd	5.4	1.5	0.69	30.3	52.9	23	23.7	24.6	33.6	19.9	23	1.9	2.3
Sm	1.2	0.40	0.14	8.5	13.8	5.4	7.4	7.1	10	4.8	5.6	1.5	1.5
Eu	0.39	0.18	0.02	2.9	4.3	2.2	2.5	2.3	3.2	1.7	2.0	0.64	0.70
Gd	N.d.	N.d.	N.d.	N.d.	N.d.	N.d.	N.d.	N.d.	N.d.	N.d.	N.d.	N.d.	N.d.
Tb	N.d.	N.d.	N.d.	N.d.	N.d.	N.d.	N.d.	N.d.	N.d.	N.d.	N.d.	N.d.	N.d.
Dy	0.53	1.0	0.65	3.1	4.8	1.7	3.1	2.4	3.3	1.5	2.0	3.7	3.7
Ho	N.d.	N.d.	N.d.	N.d.	N.d.	N.d.	N.d.	N.d.	N.d.	N.d.	N.d.	N.d.	N.d.
Er	0.26	0.65	0.51	1.0	1.7	0.64	0.92	0.91	0.96	0.74	0.75	2.6	2.4
Tm	N.d.	N.d.	N.d.	N.d.	N.d.	N.d.	N.d.	N.d.	N.d.	N.d.	N.d.	N.d.	N.d.
Yb	0.14	0.58	0.50	0.53	0.85	0.31	0.5	0.44	0.64	0.34	0.3	2.8	2.4
Lu	N.d.	N.d.	N.d.	N.d.	N.d.	N.d.	N.d.	N.d.	N.d.	N.d.	N.d.	N.d.	N.d.
Total	26.6	7.27	4.19	80.4	145	70.5	65.2	65.9	87.3	60.3	73.3	13.8	13.6
$(La/Yb)_n$	27.0	0.88	0.65	9.68	11.51	21.99	8.37	9.97	8.12	16.3	23.9	0.02	0.13
$(Eu/Eu^*)_n$	N.d.	N.d.	N.d.	N.d.	N.d.	N.d.	N.d.	N.d.	N.d.	N.d.	N.d.	N.d.	N.d.

[a] Samples from deep xenoliths.

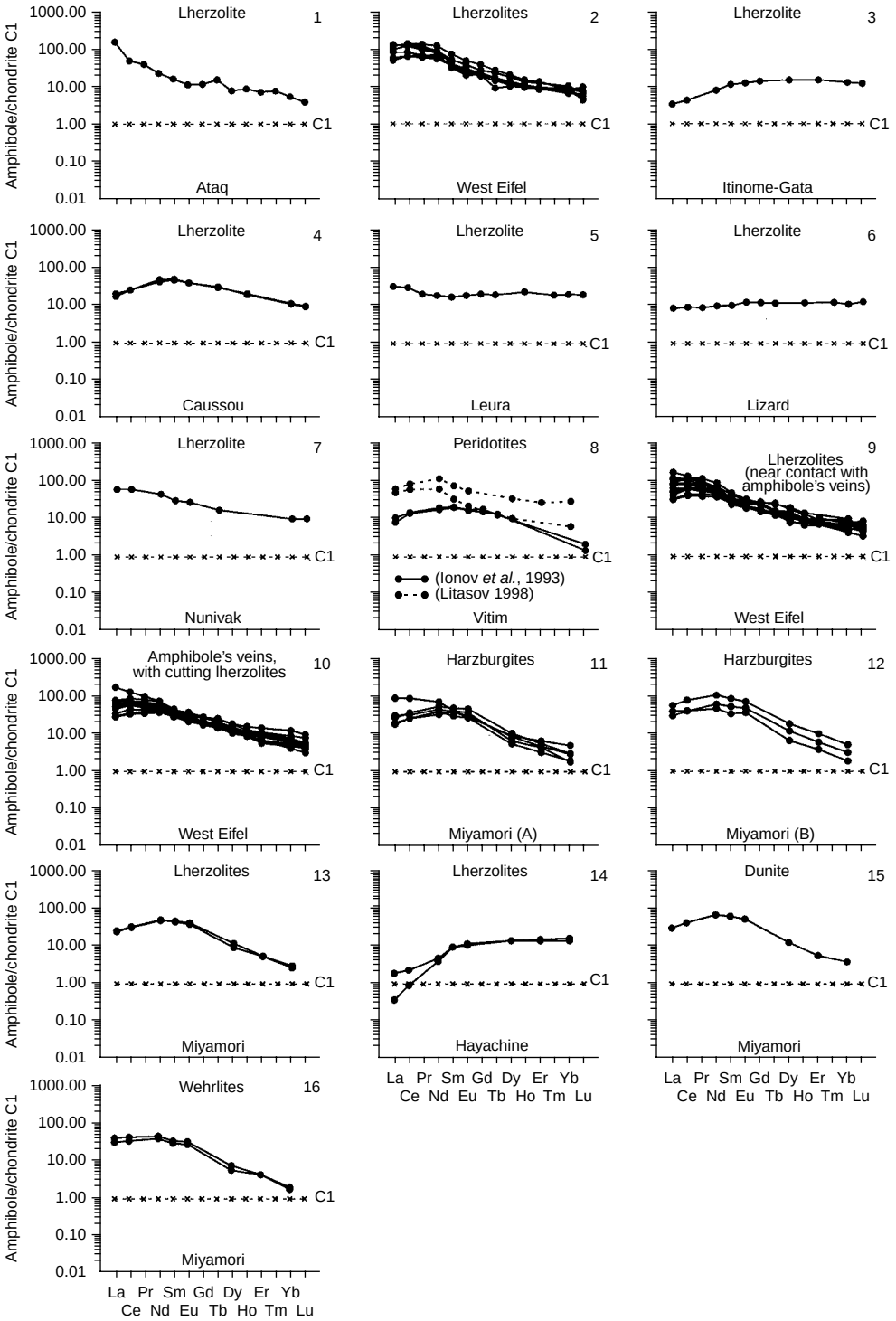

Figure 5.41 Chondrite-normalized REE patterns for amphiboles from ultramafic rocks, represented in some massifs and deep xenoliths (data Table 5.50).

elements (Table 5.51, Fig. 5.42, 1–7). Their patterns regularly display negative Eu anomalies of low intensity, which is probably due to the prior crystallization of plagioclases. In some amphiboles from Ti–Fe gabbros of the Graveglia massif and from websterites xenolith of Vitim province, such negative Eu anomalies are absent (Fig. 5.42).

Volcanogenic rocks and amphibolites. The level of accumulation of light REE in the majority of analyzed amphiboles from basalts and andesites is slightly higher than that of heavy REE (Table 5.52, Fig. 5.43). In their phenocrysts from basalts, alkali basalts, and basanites, the level of accumulation decreases from La and Ce (20–30 t. ch.) to Yb and Lu (10 t. ch.) resulting in a generally negative slope of the patterns (Fig. 5.43, 1, 2). A similar REE distribution was described by A. Basu (1978) in kaersutites from some other effusive rocks. In amphibole phenocrysts from dacites, the level of Ce accumulation varies in the range of 42–125 t. ch., with nearly the same variations in the level of Yb accumulation (37–133 t. ch.). One can see that amphiboles from phenocrysts in acid effusive rocks are much richer in REE than the mineral from phenocrysts in basalts and andesites. Note that the REE patterns of all amphiboles from dacites display negative Eu anomalies of moderate intensity (Fig. 5.43, 4). Approximately the same contents and configurations of patterns were observed in amphiboles from phenocrysts in basanites (Fig. 5.43, 2) and nepheline-bearing alkali basalts (Fig. 5.43, 5). Studies of potassic richterite from lamproites and their synthetic analogs showed that these amphiboles are depleted of REE compared to amphiboles of different chemical composition (Brumm *et al.*, 1998). Finally, it was noted that the level of REE accumulation in amphiboles from those that are widespread in the framing of the mafic–ultramafic Lizard massif is comparable with that in phenocrysts from normal and subalkali basalts (32–63 t. ch.) but the elements are virtually not fractionated (Fig. 5.43, 6).

5.5.2 Experience of systematization of amphiboles on the basis of some parameters of REE distribution

Based on the calculated average contents of REE in amphiboles from the above-described collection (Table 5.53), using the parameters of REE distribution, we divided them into two major geochemical types.

The first type includes varieties of amphibole in which the average level of accumulation of light REE and middle REE is considerably higher than that of heavy REE. This geochemical type includes mineral samples from ultramafic rocks occurring in deep xenoliths from alkali basalts and samples from ultramafic and mafic–ultramafic massifs. Their spectra have a general negative slope and typically lack Eu anomalies, as, for example, observed on the patterns of amphiboles from xenoliths of alkali basalts from the Eifel (Fig. 5.44, 1, 2; Fig. 5.41) and Vitim (Fig. 5.44, 3, 4) provinces and from the Miyamori massif (Fig. 5.44, 15–17). Tentatively, samples from ultramafic xenoliths of the provinces Ataq, Leura, and Nunivak Island (see Fig. 5.41, 1, 5, 7) and from lherzolites of the Caussou massif (Fig. 5.41, 4) can be also referred to the first type. Enrichment of the first type of amphiboles with light elements is, most likely, due to their crystallization during metasomatic transformations of ultramafic rocks caused by percolation of REE-enriched fluids. The latter were supplied from later mafic melts, with this type of percolation proceeding under the conditions of both plutonic and

Table 5.51 Rare earth element composition of amphiboles from troctolites, gabbros, norites, diorites, and websterites (ppm).

	Massifs (provinces)														
	Sondalo, Italy					Castelly, Italy				Riparbello, Italy				Liguria, Italy	
	(Tribuzio *et al.*, 1999a), SIMS					(Tribuzio *et al.*, 2000), IPMA								(Tribuzio *et al.*, 1995), SIMS	
	SOX/1-1	SOX/1-2	SO5/1-1	SO5/1-2	MF1-1	MF1-2	MF2-1	MF2-2	CBC3-1	CBC3-2	CB16-1	CB16-2	CB16-3	AP3/3-2	MC2-1
Element	*Troctolites*					*Olivine gabbros*					*Magnesioferous gabbros*				
La	4.910	4.920	7.630	5.720	1.360	1.610	2.260	2.450	7.450	6.780	4.140	4.090	3.340	1.250	10.10
Ce	20.70	20.70	30.40	24.60	6.840	8.820	12.60	12.40	37.50	31.60	20.30	20.80	15.90	6.510	39.50
Pr	N.d.	N.d.	N.d.	N.d.	N.d.	N.d.	N.d.	N.d.	N.d.	N.d.	N.d.	N.d.	N.d.	N.d.	N.d.
Nd	25.10	23.70	30.60	26.00	10.40	12.70	20.00	17.00	46.30	37.10	26.60	27.20	23.40	11.80	48.30
Sm	9.480	8.750	10.20	8.000	4.340	5.560	7.160	6.160	16.30	12.80	10.60	11.20	9.020	6.220	19.60
Eu	1.950	2.590	2.170	1.890	1.460	1.890	2.110	2.000	2.260	2.100	2.870	2.850	2.400	2.010	4.200
Gd	11.60	10.40	10.70	9.630	5.940	7.210	9.880	7.240	20.70	14.80	14.40	14.60	12.20	10.20	26.80
Tb	N.d.	N.d.	N.d.	N.d.	N.d.	N.d.	N.d.	N.d.	N.d.	N.d.	N.d.	N.d.	N.d.	N.d.	N.d.
Dy	12.20	10.70	12.00	9.990	6.760	7.980	10.90	9.280	23.80	18.40	16.10	17.10	13.80	11.50	31.80
Ho	N.d.	N.d.	N.d.	N.d.	N.d.	N.d.	N.d.	N.d.	N.d.	N.d.	N.d.	N.d.	N.d.	N.d.	N.d.
Er	6.200	5.510	7.390	5.920	4.000	4.530	6.140	5.570	13.90	11.10	9.350	9.780	8.370	6.490	19.90
Tm	N.d.	N.d.	N.d.	N.d.	N.d.	N.d.	N.d.	N.d.	N.d.	N.d.	N.d.	N.d.	N.d.	N.d.	N.d.
Yb	5.780	5.800	6.980	5.990	3.590	4.310	6.130	5.190	13.50	11.80	8.510	9.280	7.930	6.050	19.70
Lu	N.d.	N.d.	N.d.	N.d.	N.d.	N.d.	N.d.	N.d.	N.d.	N.d.	N.d.	N.d.	N.d.	N.d.	N.d.
Total	97.9	93.1	118	97.7	44.7	54.6	77.2	67.3	182	146	113	117	96.4	62.0	220
$(La/Yb)_n$	0.57	0.57	0.74	0.64	0.26	0.25	0.25	0.32	0.37	0.39	0.33	0.30	0.28	0.14	0.35
$(Eu/Eu^*)_n$	0.57	0.83	0.63	0.66	0.88	0.91	0.77	0.91	0.38	0.47	0.71	0.68	0.70	0.77	0.56
$(La/Sm)_n$	0.33	0.35	0.47	0.45	0.20	0.18	0.20	0.25	0.29	0.33	0.25	0.23	0.23	0.13	0.32

(*Continued*)

Table 5.51 Continued

	Massifs (provinces)														
	Liguria, Italy			Graveglia, Italy						Sondalo, Italy			Vitim, Rus.	Graveglia, Italy	
	(Tribuzio *et al.*, 1995)			(Tribuzio *et al.*, 2000), IPMA						(Tribuzio *et al.*, 1999a), SIMS			(Litasov, 1998)	(Tribuzio *et al.*, 2000), IPMA	
	MC2-2	AP3/3-1	T-1	N1A-1	N1A-2	MC2-1	MC2-2	AP1/2-1	AP1/2-2	SO5/11-1	SO5/11-2	SO3/2-1	V-462	MC0-1	MC0-2
Element	*Magnesioferous gabbros*		*Ferriferous and titan-ferriferous gabbros*							*Norites*			*Websterite*	*Diorites*	
La	13.10	1.150	7.950	8.440	6.800	10.10	12.30	4.010	4.940	5.080	6.290	12.40	3.230	23.30	15.90
Ce	52.10	6.280	36.80	39.10	34.60	42.50	50.30	14.90	17.90	24.10	27.90	49.90	10.89	112.0	83.90
Pr	N.d.	N.d.	N.d.	N.d.	N.d.	N.d.	N.d.	N.d.	N.d.	N.d.	N.d.	N.d.	N.d.	N.d.	N.d.
Nd	60.00	12.20	52.10	55.20	56.80	47.50	55.50	15.20	18.80	36.50	40.20	51.60	11.80	157.0	112.0
Sm	21.60	6.240	20.00	21.10	24.60	18.80	18.90	6.510	7.730	14.10	16.00	15.50	3.070	62.40	45.90
Eu	4.290	1.840	5.710	6.030	5.730	4.370	4.220	2.770	2.990	2.930	3.020	2.740	0.820	6.800	5.360
Gd	24.30	8.520	23.40	24.80	32.70	22.70	23.40	10.00	9.570	16.80	17.80	19.00	N.d.	77.90	55.20
Tb	N.d.	N.d.	N.d.	N.d.	N.d.	N.d.	N.d.	N.d.	N.d.	N.d.	N.d.	N.d.	N.d.	N.d.	N.d.
Dy	28.50	10.70	26.70	28.20	37.30	33.20	28.20	13.00	13.70	15.00	16.10	22.20	2.050	102.0	74.00
Ho	N.d.	N.d.	N.d.	N.d.	N.d.	N.d.	N.d.	N.d.	N.d.	N.d.	N.d.	N.d.	N.d.	N.d.	N.d.
Er	17.40	6.350	15.20	16.10	21.00	21.90	17.40	8.580	9.700	7.730	6.710	12.10	0.560	55.70	42.00
Tm	N.d.	N.d.	N.d.	N.d.	N.d.	N.d.	N.d.	N.d.	N.d.	N.d.	N.d.	N.d.	N.d.	N.d.	N.d.
Yb	16.90	6.120	14.10	15.00	18.60	22.10	18.40	9.710	10.70	6.660	6.520	11.10	0.580	54.50	43.60
Lu	N.d.	N.d.	N.d.	N.d.	N.d.	N.d.	N.d.	N.d.	N.d.	N.d.	N.d.	N.d.	N.d.	N.d.	N.d.
Total	238	59.4	202	214	238	223	229	84.7	96.0	129	141	197	33.0	652	478
$(La/Yb)_n$	0.52	0.13	0.38	0.38	0.25	0.31	0.45	0.28	0.31	0.51	0.65	0.75	3.76	0.29	0.25
$(Eu/Eu^*)_n$	0.57	0.77	0.81	0.80	0.62	0.65	0.61	1.05	1.06	0.58	0.54	0.49	N.d.	0.30	0.33
$(La/Sm)_n$	0.38	0.12	0.25	0.25	0.17	0.34	0.41	0.39	0.40	0.23	0.25	0.50	0.66	0.24	0.22

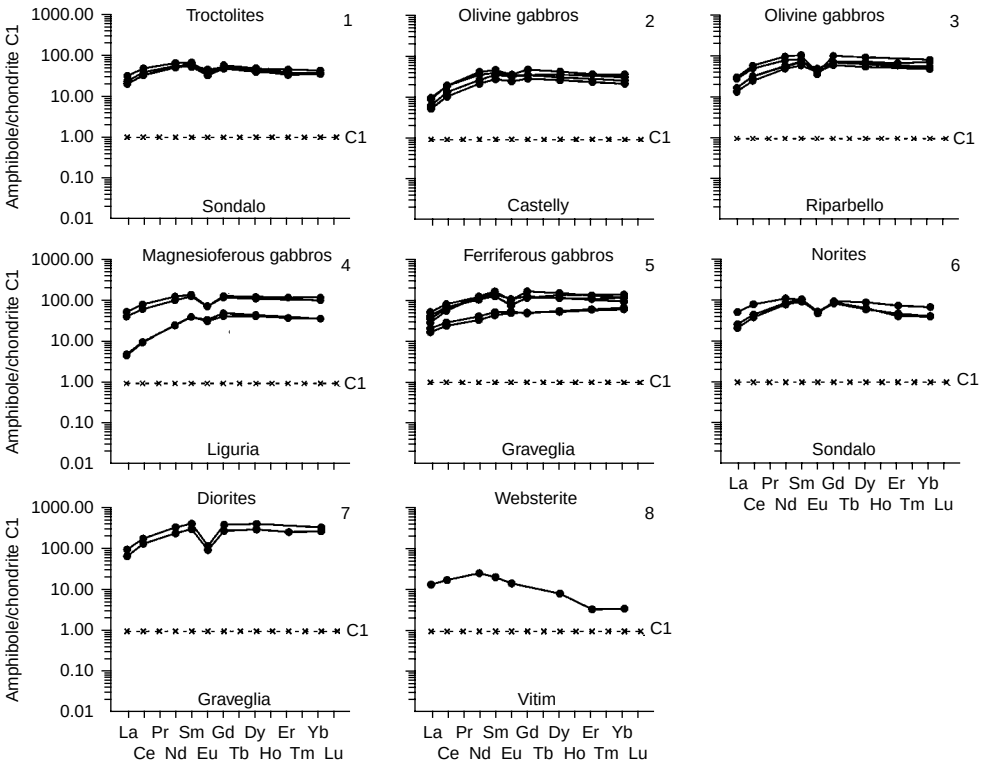

Figure 5.42 Chondrite-normalized REE composition patterns of amphiboles from troctolites, gabbros, norites, diorites, and websterites from some massifs (data Table 5.51).

volcanic processes. This interpretation of obtained data agrees well with the fact that all amphiboles from metasomatically altered ultramafic rocks occurring both in xenoliths and massifs are similar in the level and character of REE distribution to oceanic E-MORBs or OIBs.

Amphiboles referred to the second geochemical type differ from the first type mainly in some depletion of light REE and Eu (typical of most of them). Examples of these amphiboles are their samples from the rocks composed of gabbros from the Castelly, Riparbello, Sondalo, Graveglia massifs (Fig. 5.44, 5–9), from the Liguria massif (Fig. 5.44, 10, 11), and, somewhat tentatively, from lherzolites of the Hayachine massif (Fig. 5.44, 18). These amphiboles are assumed to crystallize directly from the residual portions of mafic melts depleted of light REE as a result of prior crystallization of clinopyroxenes and plagioclases, which structure incorporated most light and middle elements (including Eu) initially contained in mafic melts.

It is worth noting in conclusion that in studies of regularities of REE distribution in amphiboles and in other rock-forming minerals from ultramafic and mafic rocks, consideration must be given to the fact that, along with isomorphous REE impurities, their crystals may contain some amount of nonstructural impurities of light REE

Table 5.52 Rare earth element composition of amphiboles from basalts, andesites, dacites, and other rocks (ppm).

	Provinces										
	Japan	Guver Dam	Dutsen Dushovo	Kilbourne Hall	Riley Maar	Japan	New Mexico, USA	Honshu, Japan			
	(Higuchi & Nagasawa, 1969), INAA	(Irving & Frey, 1984), INAA				(Schnetzler & Philpotts, 1970), IDMS	(Arth & Barker, 1976), IDMS	(Nagasawa & Schnetzler, 1971), IDMS			
	HN-1	HD-1	DD-3	KH80A	WP-1	GSFC 233	BP-1	NC-1	NC-2	NC-3	NC-8
Element	*Basalts*		*Basanites*			*Andesite*	*Dacites*				
La	9.040	6.350	4.050	5.100	8.100	N.d.	N.d.	N.d.	N.d.	N.d.	N.d.
Ce	38.50	22.00	13.10	17.10	25.40	3.260	45.10	60.00	26.70	40.90	80.00
Pr	N.d.	N.d.	N.d.	N.d.	N.d.	N.d.	N.d.	N.d.	N.d.	N.d.	N.d.
Nd	N.d.	N.d.	N.d.	N.d.	N.d.	3.880	34.70	64.00	28.50	52.00	87.00
Sm	10.30	5.320	3.840	4.470	6.200	1.370	8.770	21.50	9.300	18.50	30.50
Eu	4.160	1.750	1.390	1.670	2.170	0.422	2.650	2.450	1.290	3.410	3.940
Gd	9.300	N.d.	N.d.	N.d.	N.d.	1.760	8.310	N.d.	11.00	N.d.	N.d.
Tb	1.680	0.890	0.530	0.710	1.030	N.d.	N.d.	N.d.	N.d.	N.d.	N.d.
Dy	N.d.	N.d.	N.d.	N.d.	N.d.	1.760	6.310	32.90	12.20	8.800	51.00
Ho	N.d.	N.d.	N.d.	N.d.	N.d.	N.d.	N.d.	N.d.	N.d.	N.d.	N.d.
Er	N.d.	N.d.	N.d.	N.d.	N.d.	0.806	2.920	19.10	7.500	17.40	33.00
Tm	N.d.	N.d.	N.d.	N.d.	N.d.	N.d.	N.d.	N.d.	N.d.	N.d.	N.d.
Yb	3.650	1.490	0.310	1.590	2.000	0.724	2.350	17.30	6.100	17.10	21.90
Lu	0.474	0.230	0.029	0.230	0.280	0.275	0.343	2.300	0.950	2.500	1.970
Total	N.d.	N.d.	N.d.	N.d.	N.d.	14.3	111	220	104	161	309
$(La/Yb)_n$	1.67	2.88	8.82	2.17	2.73	N.d.	N.d.	N.d.	N.d.	N.d.	N.d.
$(Eu/Eu^*)_n$	1.28	1.75	1.92	1.98	1.86	0.83	0.94	0.60	0.39	0.98	0.69

	Provinces										
	Rench	Montau	Hill 32	Anakies			Lizard, England		Kapfenstein, Austria	Scotland	
	(Irving & Frey, 1984), INAA						(Frey, 1969), INAA		(Kurat *et al.*, 1980)	(Pride & Muecke, 1981), INAA	
	188/5	SM8	32K1	28	9	2110x	90693	90695	Ka105	64-12	67-109
Element	*Hawaiite*	*Analcimite*	*Nephelinite*	*Nephelineferous mugearites*			*Amphibolites*		*Hornblendite*	*Mafic gneiss*	
La	13.80	4.750	7.350	5.700	13.10	11.60	3.800	11.90	11.30	15.60	12.50
Ce	47.30	16.30	24.50	19.10	43.00	37.00	27.00	36.00	N.d.	64.10	33.70
Pr	N.d.	N.d.	N.d.	N.d.	N.d.	N.d.	2.710	7.700	N.d.	N.d.	N.d.
Nd	N.d.	N.d.	N.d.	N.d.	N.d.	33.40	13.10	34.50	N.d.	N.d.	N.d.
Sm	10.10	4.890	5.570	6.200	10.80	9.700	5.280	12.50	5.380	12.20	3.870
Eu	3.540	1.770	1.840	2.160	3.600	3.300	2.000	3.760	1.790	2.560	0.990
Gd	N.d.	N.d.	N.d.	N.d.	N.d.	N.d.	5.830	11.90	N.d.	N.d.	N.d.
Tb	1.440	0.920	0.860	1.010	1.440	0.890	1.150	2.580	N.d.	2.530	0.560
Dy	N.d.	N.d.	N.d.	N.d.	N.d.	N.d.	N.d.	N.d.	N.d.	N.d.	N.d.
Ho	N.d.	N.d.	N.d.	N.d.	N.d.	N.d.	1.700	3.470	N.d.	N.d.	N.d.
Er	N.d.	N.d.	N.d.	N.d.	N.d.	N.d.	4.670	10.50	N.d.	N.d.	N.d.
Tm	N.d.	N.d.	N.d.	N.d.	N.d.	N.d.	0.686	1.370	N.d.	N.d.	N.d.
Yb	2.480	1.200	0.880	0.870	0.500	0.560	4.340	8.500	1.210	9.600	1.100
Lu	0.370	0.160	0.130	0.130	0.049	0.066	0.530	1.150	0.180	1.100	0.130
Total	N.d.	N.d.	N.d.	N.d.	N.d.	N.d.	72.8	146	N.d.	N.d.	N.d.
$(La/Yb)_n$	3.76	2.67	5.64	4.42	17.7	14.0	0.59	0.94	6.30	1.10	7.67
$(Eu/Eu^*)_n$	1.86	1.92	1.75	N.d.	N.d.	N.d.	1.10	0.93	1.77	1.11	1.36

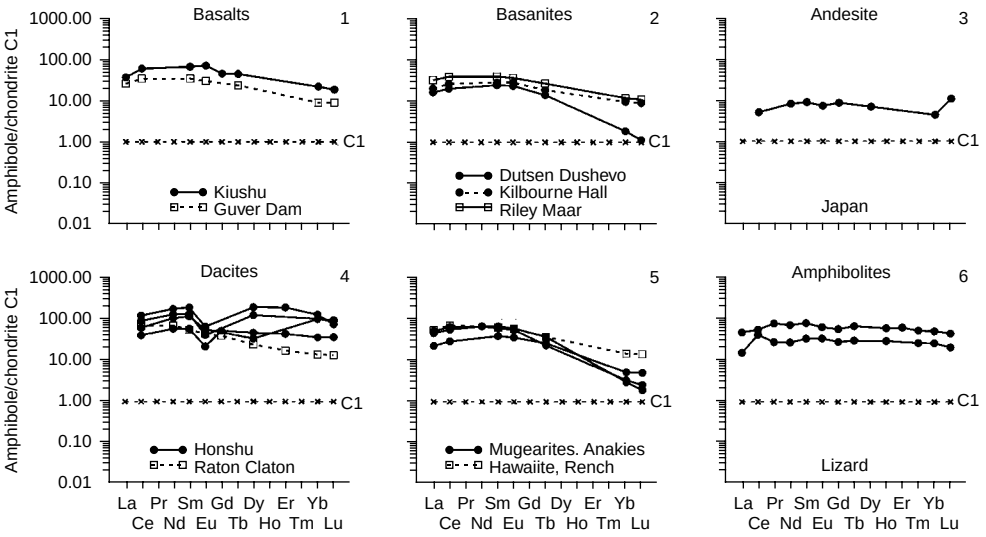

Figure 5.43 Chondrite-normalized REE patterns for amphiboles from basalts, basanites, andesites, dacites, mugearites, and amphibolites from some manifestations (data Table 5.52).

accumulated as a result of epigenetic processes in microcracks of these crystals and in fluid micro- and nanoinclusions.

5.5.3 Coefficients of REE distribution between amphiboles and coexisting phases

In this chapter we discuss some of the available data on the features of REE distribution between amphiboles and coexisting minerals.

K_d*(amphibole/melt)*. The values of these K_d were calculated from the results of determination of REE in phenocrysts of amphiboles and their groundmass from some varieties of effusive rock and from studies of synthetic amphibole crystals grown at different temperatures and pressures. The estimations of values of these coefficients, which are scarce, were reported in some summary reviews and publications (Irving, 1978; Green & Pearson, 1985, Green, 1994). Some of these values are given in Table 5.54. Irrespective of the composition of parental melts, the predominant values of K_d(amphibole/melt) are less than unity, slightly changing from La to Gd and remaining nearly the same for Lu (Fig. 5.45).

Some authors report results of experimental studies of the dependence of K_d(amphibole/melt) values on the composition of melts and on their crystallization temperature and pressure. It was established that on crystallization of amphiboles from andesite melt at 900°C and 12 kbar, the K_d value for Sm was 2.0, and on crystallization at higher temperature (925°C) and lower pressure (5 kbar), the K_d(amphibole/melt) decreased to 1.8 (Drake & Holloway, 1977). In experiments on the synthesis of

Table 5.53 Average rare earth element composition of amphiboles (ppm).

	Varieties of rocks, massifs, and provinces						
Element	1 (8)	2 (12)	3 (2)	4 (3)	5 (4)	6 (5)	7 (4)
La	24.73	20.18	2.415	6.638	1.920	5.160	5.795
Ce	69.74	56.36	9.700	23.34	10.17	25.22	24.10
Pr	9.28	7.306	N.d.	N.d.	N.d.	N.d.	N.d.
Nd	39.03	29.73	9.400	21.99	15.03	32.12	26.35
Sm	7.081	5.286	3.325	5.184	5.805	11.98	9.108
Eu	1.825	1.443	1.050	1.462	1.865	2.496	2.150
Gd	5.133	4.377	3.605	3.605	7.568	15.34	10.58
Tb	0.695	0.619	0.515	0.515	N.d.	N.d.	N.d.
Dy	3.731	3.403	N.d.	4.713	8.730	17.84	11.22
Ho	0.671	0.574	N.d.	N.d.	N.d.	N.d.	N.d.
Er	1.834	1.511	N.d.	2.157	5.060	10.50	6.255
Tm	N.d.	N.d.	N.d.	N.d.	N.d.	N.d.	N.d.
Yb	1.409	1.211	N.d.	2.267	4.805	10.20	6.138
Lu	0.168	0.161	0.047	0.047	N.d.	N.d.	N.d.
Total	165	132	N.d.	65.3	60.9	131	102
$(La/Yb)_n$	11.9	11.3	2.42	1.98	0.27	0.34	0.64
	8 (3)	9 (4)	10 (2)	11 (4)	12 (4)	13 (2)	14 (2)
La	7.923	6.048	1.200	15.600	N.d.	9.825	7.850
Ce	33.97	26.63	6.395	71.88	51.90	32.10	31.50
Pr	N.d.	N.d.	N.d.	N.d.	N.d.	N.d.	5.205
Nd	42.77	36.50	12.00	94.33	57.88	N.d.	23.80
Sm	15.20	14.99	6.230	37.38	19.95	7.100	8.890
Eu	2.897	4.380	1.925	5.163	2.773	2.360	2.880
Gd	17.87	19.27	9.360	46.05	11.00	N.d.	8.865
Tb	N.d.	N.d.	N.d.	N.d.	N.d.	1.160	1.865
Dy	17.77	23.05	11.10	59.08	26.23	N.d.	N.d.
Ho	N.d.	N.d.	N.d.	N.d.	N.d.	N.d.	2.585
Er	8.847	13.85	6.420	33.75	19.25	N.d.	7.585
Tm	N.d.	N.d.	N.d.	N.d.	N.d.	N.d.	1.028
Yb	8.093	13.50	6.085	33.68	15.60	1.885	6.420
Lu	N.d.	N.d.	N.d.	N.d.	1.930	0.275	0.840
Total	155	158	60.7	397	198	N.d.	109
$(La/Yb)_n$	0.66	0.30	0.13	0.31	N.d.	3.52	0.83

kaersutite from tholeiite basalt melts at 1000°C and 5 kbar, the K_d values for middle REE were about 0.2, and were about 1 for heavy elements (Irving, 1978). In another experiment with basalt melts at 1000°C and 15 kbar, the K_d values for Ce, Sm, and Tm were much higher, averaging to 0.07 (Mysen, 1978). In the synthesis of Ti pargasite from basanite melts at 1150°C and 1.5 GPa, the K_d values were 0.055 for La, 0.62 for Ho, and 0.43 for Lu (La Tourrette *et al.*, 1995). Brenan *et al.* (1995) synthesized amphibole at 1200°C and 1.5 GPa and obtained the following K_d values: 0.22 for Ce, 0.62 for Nd, 0.66 for Sm, and 1.25 for Yb. Nicholls and Harris (1980), using the results of experiments conducted at similar P–T parameters, determined that

Table 5.53 Continued

	15 (9)	16 (2)	17 (2)	18 (2)
La	7.88	6.35	9.4	0.28
Ce	23.65	21.25	26.05	0.365
Pr	N.d.	N.d.	N.d.	N.d.
Nd	22.80	24.15	21.45	2.1
Sm	6.23	7.25	5.2	1.5
Eu	2.13	2.4	1.85	0.67
Gd	N.d.	N.d.	N.d.	N.d.
Tb	N.d.	N.d.	N.d.	N.d.
Dy	2.25	2.75	1.75	3.7
Ho	N.d.	N.d.	N.d.	N.d.
Er	0.83	0.915	0.745	2.5
Tm	N.d.	N.d.	N.d.	N.d.
Yb	0.40	0.47	0.32	2.6
Lu	N.d.	N.d.	N.d.	N.d.
Total	66.2	65.5	66.8	13.7
$(La/Yb)_n$	13.4	9.12	19.8	0.07

Data Tables 5.50–5.52. 1—lherzolites from xenoliths in basalts, West Eifel (Germany) (Witt-Eickschen *et al.*, 1998); 2—lherzolites from xenoliths in basalts, near contacts with amphibole's veins, West Eifel (Germany) (Witt-Eickschen *et al.*, 1998); 3—peridotites from xenoliths in basalts, Vitim, Transbaykalia (Russia) (Ionov *et al.*, 1993a,b); 4—peridotites from xenoliths in basalts, Vitim, Transbaykalia (Russia) (Litasov, 1998); 5—olivine gabbros, Castelly (Italy) (Tribuzio *et al.*, 2000); 6—olivine gabbros, Riparbello (Italy) (Tribuzio *et al.*, 2000); 7—troctolites, Sondalo (Italy) (Tribuzio *et al.*, 1999a,b); 8—norites, Sondalo (Italy) (Tribuzio *et al.*, 1999a,b); 9—ferriferous and titan-ferriferous gabbros, Graveglia (Italy) (Tribuzio *et al.*, 2000); 10—Magnesioferous gabbros, Liguria (Italy) (Tribuzio *et al.*, 1995); 11—diorites, Liguria and Graveglia (Italy) (Tribuzio *et al.*, 1995, 2000); 12—dacites, Honshu (Japan) (Nagasawa & Schnetzler, 1971); 13—veins of amphibole in xenoliths of lherzolites, Dush Hill (Irving & Frey, 1984); 14—amphibolites, Lizard (England) (Frey, 1969); 15—harzburgites, Miyamori (Japan) (Ozawa & Shimizu, 1995); 16—lherzolites, Miyamori (Japan) (Ozawa & Shimizu, 1995); 17—wehrlites, Miyamori (Japan) (Ozawa & Shimizu, 1995); 18—lherzolites, Hayachine (Japan) (Ozawa & Shimizu, 1995).

the K_d(amphibole/andesite melt) for La, Sm, Ho, and Yb have higher values than K_d(amphibole/basalt melt). These data suggest that, as crystallization temperature decreases from 1020 to 900°C, the K_d(amphibole/melt) values for all REE increase, the maximum K_d value being 3.5 for Ho and 2.0 for Yb. A regular increase in K_d values from melts with a lower silica content to melts with a higher silica content was also supported in the results of experiments on the synthesis of amphiboles from rhyolites melts, in which these values for middle REE were about 10 (Hanson, 1980). Green (1994) summarized the available data on K_d(amphibole/melt) values obtained in experimental studies using andesite, basanite, and basalt melts in the temperature range from 900 to 1050°C and pressures from 0.75 to 2 kbar both for REE and other trace elements. The major tendencies in the changes of K_d(amphibole/melt) values are shown in Figure 5.46.

The available estimates of the K_d(amphibole/melt) values suggest that during crystallization of amphiboles their parental melts of various compositions must have been more intensely depleted of middle and heavy REE than light elements. On crystallization of amphiboles, the K_d values for all REE regularly increase from basalt melts

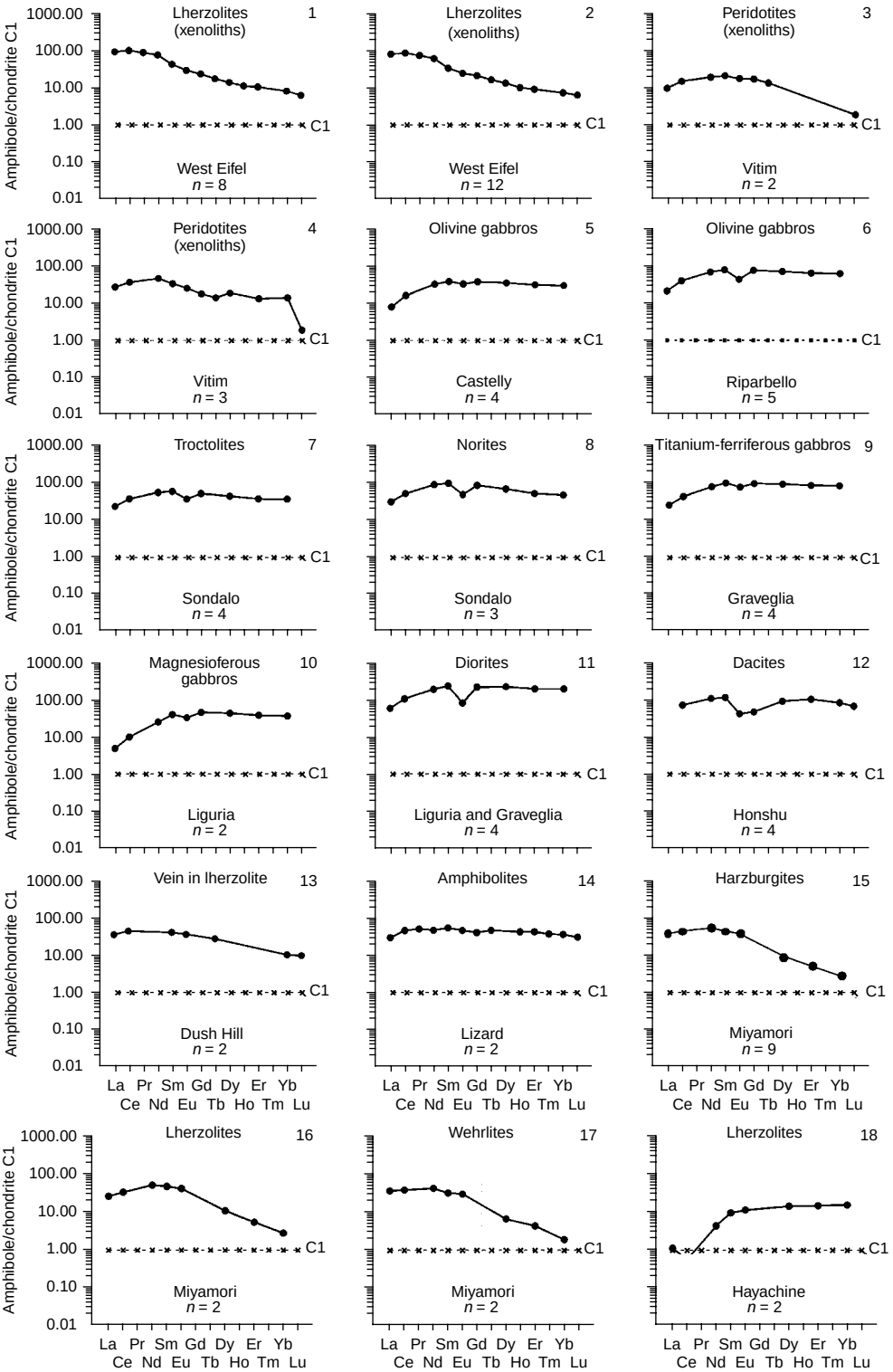

Figure 5.44 Chondrite-normalized patterns for average REE composition of some amphiboles (data

Table 5.54 Coefficients of REE distribution between amphiboles and coexisting melts.

	Variety of melts												
	Basalts			Trachybasalt	Andesites			Basanites		Phonolite	Olivine basalts	Lamproites	
	(Higuchi & Nagasawa, 1969)	(Hanson, 1980)	(Mysen, 1977, 1978)	(Nagasawa, 1973)	(Nicholls & Harris, 1980)	(Brenan *et al.*, 1995)	(Schnetzler & Philpotts, 1970)	(La Tourette *et al.*, 1995)	(Dalpe & Baker, 1994)	(Irving & Price, 1981)	(Bottazzi *et al.*, 1999)		
Element	HN-3[a]	HAN-9[a]	My-1[b]	Nag-3[a]	4095[b]	B-1[b]	G233[a]	3048[b]	DB-1[b]	IP-1[b]	4722[b]	RB-52[b]	RB-31[b]
La	0.167	N.d.	N.d.	N.d.	0.26	N.d.	N.d.	0.055	0.039	0.14	0.116	0.0437	0.0274
Ce	0.338	0.899	0.038	N.d.	N.d.	0.22	0.094	0.096	0.067	0.25	0.185	0.0709	0.293
Pr	N.d.	N.d.	N.d.	N.d.	N.d.	N.d.	N.d.	0.17	0.105	N.d.	0.277	N.d.	N.d.
Nd	N.d.	2.8	N.d.	0.63	N.d.	0.62	0.189	0.25	0.142	0.51	0.396	0.123	0.0325
Sm	0.93	3.99	0.072	0.94	1.8	0.66	0.336	N.d.	0.188	0.80	0.651	0.158	0.024
Eu	1.11	3.44	N.d.	1.02	N.d.	N.d.	0.358	N.d.	0.351	0.90	0.657	0.175	0.0498
Gd	1.08	5.48	N.d.	N.d.	N.d.	N.d.	0.509	0.32	0.368	N.d.	0.933	0.188	0.018
Tb	1.02	N.d.	N.d.	N.d.	N.d.	N.d.	N.d.	N.d.	0.385	0.87	1.000	N.d.	N.d.
Dy	N.d.	6.2	N.d.	1.19	3.7	N.d.	0.636	N.d.	0.406	N.d.	0.967	0.165	0.0136
Ho	N.d.	N.d.	N.d.	N.d.	N.d.	N.d.	N.d.	0.62	0.350	N.d.	1.030	N.d.	N.d.
Er	N.d.	5.94	N.d.	1.05	N.d.	N.d.	0.483	0.57	0.362	N.d.	0.851	0.175	0.0318
Tm	N.d.	N.d.	0.063	N.d.	N.d.	N.d.	N.d.	0.51	0.281	N.d.	0.816	N.d.	N.d.
Yb	0.98	4.89	N.d.	0.88	2.1	1.25	0.462	N.d.	0.349	0.57	0.787	0.177	0.102
Lu	0.82	N.d.	N.d.	0.89	N.d.	N.d.	0.436	0.43	0.246	0.47	0.698	N.d.	N.d.
$(K_dYb)/K_dLa)$	5.87	N.d.	N.d.	N.d.	8.08	N.d.	N.d.	N.d.	8.95	4.07	6.78	4.05	3.72
Mineral	Kaersutite	N.d.	N.d.	Kaersutite	N.d.	N.d.	N.d.	N.d.	Pargasite	Kaersutites		Pargasite	Richterite

[a] Natural systems.
[b] Experimental systems.

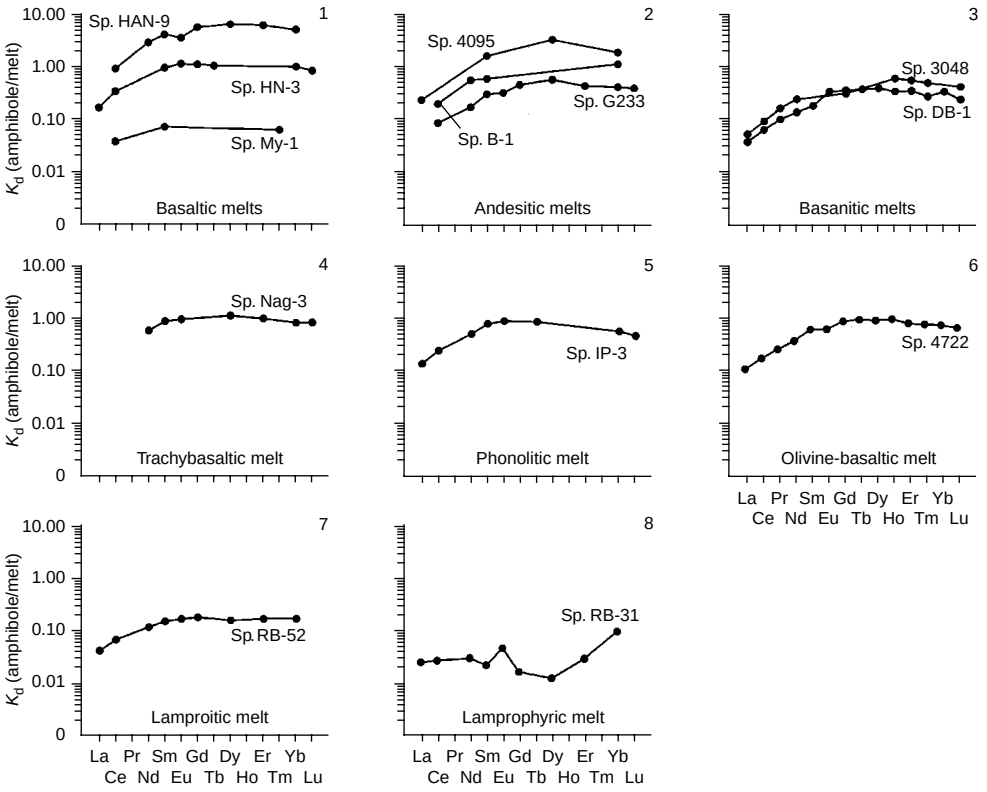

Figure 5.45 The trend coefficients of REE distribution between amphiboles and melts with different composition (data Table 5.54).

to basanite, andesite and rhyolite melts. The comparison of K_d(amphibole/melt) values obtained in studies of porphyrous phenocrysts from effusive rocks with the values obtained for melts with similar compositions shows that they are comparable only in single cases (Irving & Frey, 1984).

K_d(amphibole/clinopyroxene). Paragenesis of amphiboles and clinopyroxenes is widespread in mafic and ultramafic rocks. According to petrographical data, crystallization of clinopyroxenes always preceded crystallization of amphiboles. Clinopyroxene-bearing ultramafic rocks from massifs and deep xenoliths along with amphiboles, which pseudomorphously replace clinopyroxene grains occasionally, contain cutting veinlets and veins complicated by amphiboles. As was shown, the level of REE accumulation in amphiboles is somewhat higher than in coexisting clinopyroxenes and, hence, K_d(amphibole/clinopyroxene) is greater than unit (Table 5.55). Tribuzio *et al.* (1999b) report that the higher level of REE accumulation, compared to associated clinopyroxenes, in amphiboles from gabbroid rocks suggests that these amphiboles crystallized directly from melts, but not by pseudomorphous replacement

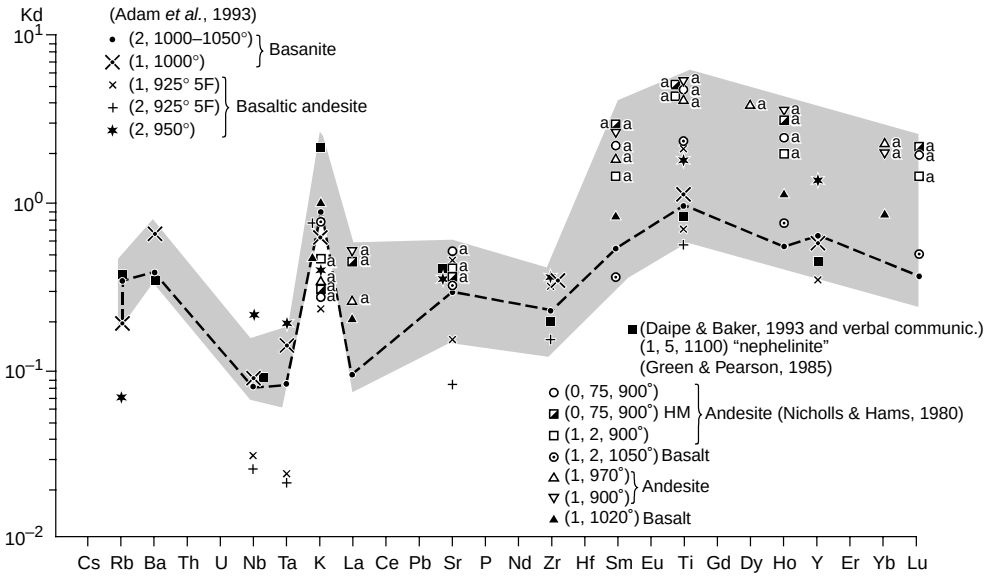

Figure 5.46 The generalized trend distribution coefficients of REE and other impurity elements between amphiboles (pargasite and pargasite hornblende) and melts with different compositions (darkened field) on the basis of experimental studies (data Green, 1994). Dotted lines—trend K_d, calculated on the basis of experiments with basanite melts at temperatures of 1000–1050°C and a pressure of 2 kbar.

of clinopyroxene crystals, which would have resulted in higher depletion of amphiboles in these impurities.

The data reported in Table 5.55 and in Figure 5.47 show that in all studied amphibole–clinopyroxene rocks, the values of K_d(amphibole/clinopyroxene) for the whole series of REE vary in a narrow range. For example, in harzburgites, lherzolites, wehrlites, and dunites from the Miyamori and Hayachine massifs, these values range from 1.2 to 4.6. In the samples from the Miyamori massif, the K_d(La)/K_d(Yb) ratios vary in the range of 1.3–2.4 and in the samples from the Hayachine massif these ratios are close to unit. Very often the REE spectra of coexisting amphiboles and clinopyroxenes have a similar configuration, though their positions on the plots differ. Some researchers point out that the crystal structures of both minerals have many equal or similar motives (Higuch & Nagasawa, 1969; Roden *et al.*, 1984; Tiepolo *et al.*, 1997; Herrmann & Muntener, 1999; Laurora *et al.*, 1999). In the rocks from some massifs, the trends of K_d(amphibole/clinopyroxene) are not only similar in configuration but are also located rather compactly on the trend, which suggests that both of these phases are close to chemical equilibrium (Herrmann & Muntener, 1999). In the cases when the trends of coexisting amphiboles and clinopyroxenes have different configurations and are separated from each other on the plot, their state is assumed not to be close to chemical equilibrium.

Table 5.55 Coefficients of REE distribution between amphiboles and coexisting clinopyroxenes.

	1	2	3	4	5	6	7	8	9	10
Element	VG-1	V-462	M310	M307	M332	3L	1-Gar	2642	T-1	3/3-2
La	1.95	1.15	1.13	1.38	1.79	0.77	1.30	2.23	3.00	2.60
Ce	1.52	1.14	0.90	1.31	1.65	0.79	1.200	3.08	2.81	2.00
Pr	1.26	N.d.	0.71	1.23	1.52	N.d.	N.d.	1.82	N.d.	N.d.
Nd	1.10	1.16	0.69	1.18	1.37	0.86	1.10	1.77	2.25	2.03
Sm	1.00	1.20	0.76	1.14	1.02	1.12	1.10	1.73	1.89	2.19
Eu	1.00	1.05	0.69	1.32	0.95	1.39	1.10	1.82	1.92	2.19
Gd	1.00	N.d.	0.81	1.06	1.14	0.93	0.90	1.89	1.49	2.09
Tb	1.23	N.d.	0.74	1.24	1.02	N.d.	1.10	1.73	N.d.	N.d.
Dy	1.18	1.23	0.77	1.14	1.05	1.09	1.00	N.d.	1.44	2.10
Ho	1.11	N.d.	0.84	1.18	1.07	N.d.	1.00	2.03	N.d.	N.d.
Er	0.80	0.95	0.78	1.19	1.14	1.04	1.00	2.22	1.43	2.24
Tm	1.11	N.d.	N.d.	N.d.	N.d.	N.d.	1.00	2.04	N.d.	N.d.
Yb	0.97	0.98	0.79	0.93	0.79	1.18	1.00	1.98	1.33	2.15
Lu	0.67	N.d.	0.48	N.d.	0.84	N.d.	1.00	1.86	N.d.	N.d.
K_d(La)/K_d(Yb)	2.02	1.17	1.43	1.48	2.26	0.66	1.30	1.13	2.25	1.21

	11	12	13	14	15	16	17	18	19
	3/3-1	CB16	CBC3-2	S5/11-1	S3/2-1	S5/11-2	SX/1-1	S5/1-1	10067
La	2.61	3.39	5.14	2.75	2.98	3.36	4.55	7.71	1.33
Ce	2.09	3.10	4.69	2.81	2.82	3.10	4.77	7.33	1.20
Nd	2.21	2.50	N.d.	2.24	2.42	2.74	3.88	6.34	1.00
Sm	2.26	2.42	2.61	2.39	1.75	2.61	3.35	4.30	0.97
Eu	2.33	2.43	2.08	2.59	2.25	2.67	2.38	2.86	0.97
Gd	2.09	2.89	2.26	2.40	1.93	2.81	3.05	3.82	N.d.
Tb	N.d.	N.d.	N.d.	N.d.	N.d.	N.d.	N.d.	N.d.	0.94
Dy	2.22	2.31	2.41	2.49	1.93	2.67	2.68	3.40	N.d.
Er	2.33	2.01	2.55	2.56	2.08	2.17	2.37	3.42	N.d.
Yb	2.50	2.16	2.71	2.51	1.94	2.17	2.23	3.14	0.81
Lu	N.d.	N.d.	N.d.	N.d.	N.d.	N.d.	N.d.	N.d.	0.82
K_d(La)/K_d(Yb)	1.05	1.57	1.89	1.09	1.53	1.55	2.04	2.45	1.64

	20	21	22	23	24	25	26	27	28	29	30	31	32
	MY-1	MY-2	MY-3	MY-4	MY-8	MY-9	ORM-22	ORM-27	ORM-31	ORM-9	ORM-26	HY-1	HY-2
La	4.39	4.19	3.00	2.04	3.30	2.82	2.41	2.30	2.83	2.93	2.00	1.50	2.94
Ce	4.08	3.74	2.76	2.16	3.24	2.61	2.29	2.22	2.37	2.78	2.15	1.66	3.19
Nd	4.63	4.33	2.55	2.80	3.95	3.45	2.65	2.75	2.80	3.32	3.07	1.27	2.84
Sm	3.88	3.71	2.48	2.67	3.64	2.33	2.56	2.47	2.84	3.20	3.11	1.15	2.17
Eu	4.00	4.67	2.30	2.76	4.50	1.00	2.67	2.81	2.77	3.78	3.08	1.16	2.92
Gd	N.d.	N.d.	N.d.	N.d.	N.d.	N.d.	N.d.	N.d.	N.d.	N.d.	N.d.	N.d.	N.d.
Tb	N.d.	N.d.	N.d.	N.d.	N.d.	N.d.	N.d.	N.d.	N.d.	N.d.	N.d.	N.d.	N.d.
Dy	3.73	3.25	2.09	2.15	3.13	2.95	2.20	2.38	2.61	2.73	2.78	1.23	2.64
Er	2.19	2.35	2.68	1.06	3.61	2.43	1.30	1.84	1.86	2.85	1.56	1.37	3.04
Yb	2.09	2.08	2.37	1.07	2.42	1.85	1.16	1.02	1.19	1.36	0.91	1.47	2.89
Lu	N.d.	N.d.	N.d.	N.d.	N.d.	N.d.	N.d.	N.d.	N.d.	N.d.	N.d.	N.d.	N.d.
K_d(La)/K_d(Yb)	2.10	2.01	1.27	1.91	1.37	1.52	2.07	2.25	2.38	2.15	2.20	1.02	1.02

1—Lherzolites from xenolith in basalt, Ataq (Yemen) (Varne & Graham, 1971); 2—peridotite from xenolith in basalt, Vitim (Russia) (Litasov, 1998); 3–5—peridotites from xenoliths in basalt, Eifel (Germany) (Witt-Eickschen *et al.*, 1998); 6—lherzolite from xenolith in basalt, Itinome–Gata (Japan) (Tanaka & Aoki, 1981); 7—peridotite, Caussou massif (France) (Garrido *et al.*, 2000); 8—lherzolite from xenolith in basalt, Leura (Australia) (Frey & Green, 1974); 9—ferriferous gabbro, Liguria (Italy) (Tribuzio *et al.*, 1996); 10 and 11—magnesioferous gabbro, Liguria (Italy) (Tribuzio *et al.*, 1995); 12 and 13—olivine-bearing gabbro, North Apennine (Italy) (Tribuzio *et al.*, 1999b); 14–16—norites, Sondalo (Italy) (Tribuzio *et al.*, 1999a); 17 and 18—troctolites, Sondalo (Italy) (Tribuzio *et al.*, 1999a); 19—peridotite from xenolith in basalt, Nunivak Island, Alaska (USA) (Roden *et al.*, 1984); 20–30—Miyamori (Japan) (Ozawa & Shimizu, 1995): 20–25—harzburgites; 26—dunite; 27 and 28—lherzolite; 29 and 30—wehrlites; 31 and 32—lherzolites, Hayachine (Japan) (Ozawa & Shimizu, 1995).

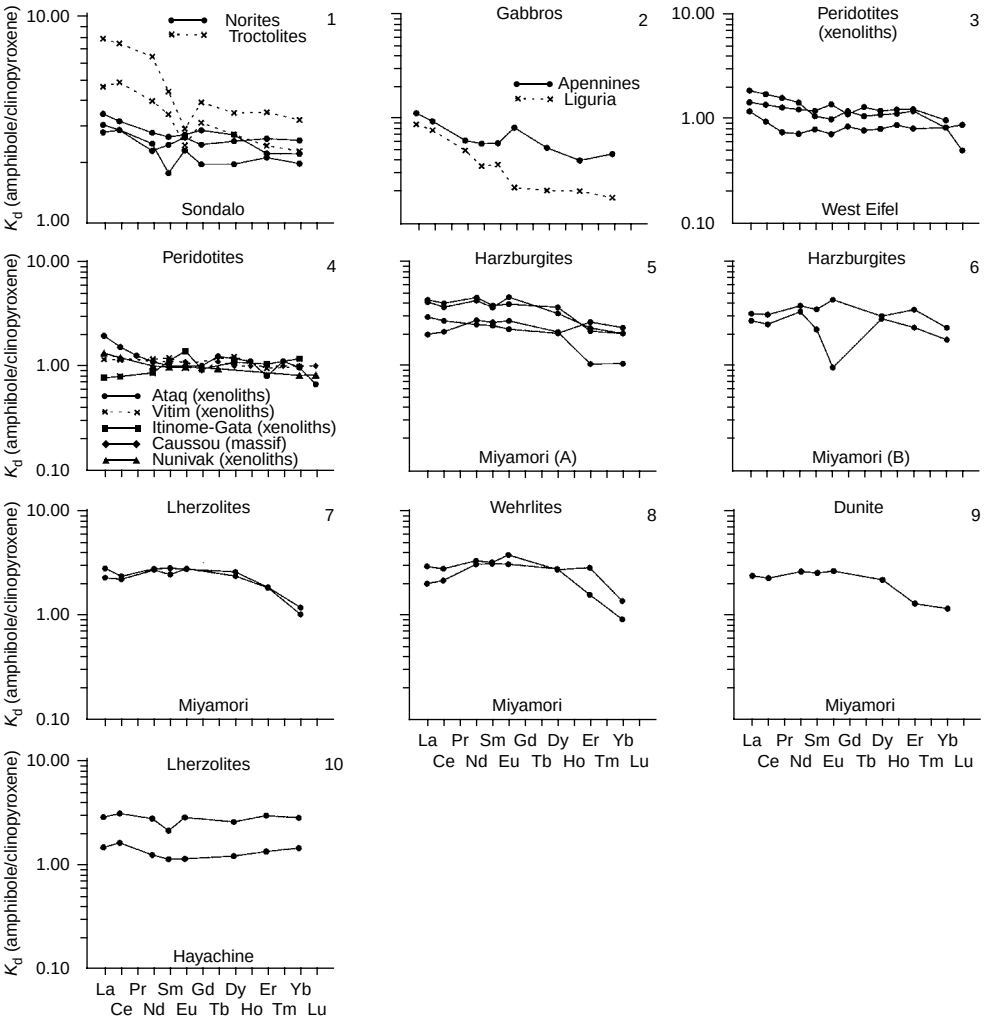

Figure 5.47 The trend of REE distribution coefficients between amphiboles and coexistent clinopyroxenes (data Table 5.55).

K_d(amphibole/plagioclase). Coexisting amphiboles and plagioclases often occur in plagioclase-bearing ultramafic rocks, gabbros, effusive rocks, and hornblendites. The relationships between grains under a microscope show that plagioclase crystallized somewhat earlier than coexisting amphibole. According to calculated values, the level of REE accumulation in amphibole to one degree or another exceeds their level in coexisting plagioclase, and, hence, the values of K_d(amphibole/plagioclase) are greater than unity, being lower for light REE than for heavy REE. In gabbros from the Apennines and Liguria, the K_d for La varies from 2 to 10, whereas for Dy they are much higher (98–613) (Table 5.56). The values of K_d are normally lower than the K_d for Sm

Table 5.56 Coefficients of REE distribution between amphiboles and coexisting plagioclases.

	Massif							
	Apennine, Italy		Liguria, Italy	Raton Claton, USA	Sondalo, Italy			
	(Tribuzio *et al.*, 1999b)		(Tribuzio *et al.*, 1996)	(Arth & Barker, 1976)	(Tribuzio *et al.*, 1999a)			
	CBC3-2	CB16-1	T-1	BP-1	SOX/1-1	SO5/1-1	SO5/11-1	SO3/2-1
Element	*Olivine gabbros*		*Ferriferous gabbro*	*Dacite*	*Troctolites*		*Norites*	
La	7.62	4.27	9.24	N.d.	2.68	8.38	1.95	4.12
Ce	16.54	9.49	20.79	4.92	6.23	16.70	4.93	9.40
Nd	48.18	20.15	47.80	16.21	18.06	38.25	17.46	21.23
Sm	116	55.79	11.11	39.86	36.46	63.75	39.17	43.06
Eu	3.62	4.22	2.57	4.23	2.91	3.10	2.48	2.49
Gd	N.d.	N.d.	167	62.48	82.86	76.43	46.67	82.61
Dy	613	230	381	98.0	136	150	100	202
Er	N.d.	N.d.	760	107	N.d.	N.d.	N.d.	N.d.
Yb	N.d.	N.d.	1200	90.7	N.d.	N.d.	N.d.	N.d.

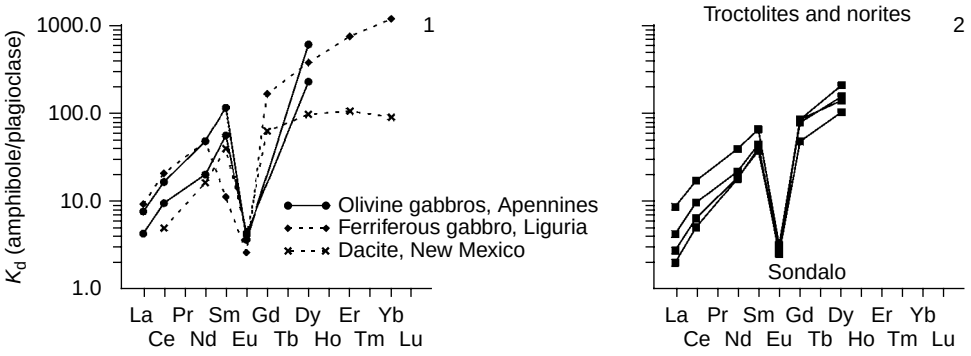

Figure 5.48 The trend of REE distribution coefficients between amphiboles and coexistent plagioclases (data Table 5.56).

and Gd, and, therefore, their trends have a general steep positive slope and typically demonstrate intense minimums for Eu (Fig. 5.48). The above data suggest that during joint crystallization of plagioclases and amphiboles, REE were significantly fractionated, owing to which most light REE accumulated in the structure of plagioclases. Therefore, the residual portions of melts from which amphiboles crystallized were fairly enriched with heavy REE compared to the primary melt.

The trends of K_d(amphibole/plagioclase) for gabbros from the Sondalo massif are located compactly on the plot and have the same configuration (see Fig. 5.48). This suggests that, by the moment of termination of crystallization of mafic melt and

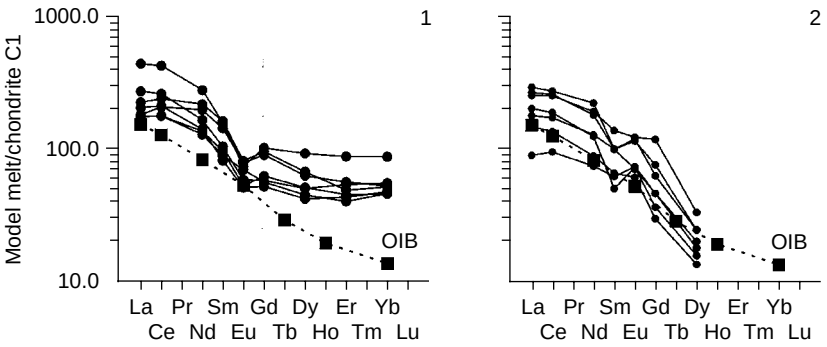

Figure 5.49 Chondrite-normalized REE patterns for model paternal melts for troctolites (sp. SOX/1-1, SO5/1-1) and norites (sp. SO5/11-1, SO3/2-1) from the Sondalo massif (Italy), calculated on the basis of REE composition of coexistent amphibole (1) and plagioclase (2) (data Tribuzio *et al.*, 1999a). Values K_d(amphibole/olivine basalt) (data Bottazzi *et al.*, 1999) and value K_d(plagioclase/basalt) (data Phinney & Morrison, 1990; Schnetzler & Philpotts, 1970) were used for the calculation.

formation of these gabbros, plagioclase, and amphibole attained the state close to a chemical equilibrium, which was not disturbed by epigenetic processes.

Taking this circumstance into consideration, we made an attempt to numerically model the REE compositions of parental melts from which troctolites and norites of the Sondalo massif crystallized. For this purpose, we used two independent procedures of calculations: (1) a calculation based in the REE composition of amphiboles; and (2) a similar calculation based on the REE composition of coexisting plagioclases. On the assumption that calculations did not have gross errors, the obtained values reflected on corresponding patterns (Fig. 5.49) show that troctolites and norites from the Sondalo massif had parental melts with a similar REE composition. We assume that these melts were considerably richer in light REE compared to heavy REE and they have many similar features with the parental melts of OIB.

5.5.4 Isomorphism of REE in amphiboles

As mentioned above, the multicomponent crystal structure of amphiboles has many similar features with the clinopyroxene structure and is also a favorable matrix for the isomorphous incorporation of REE. According to Leake (1978), the structure of amphiboles includes several crystallochemical positions, including position A in which Na^+ and K^+ ions are located, position M4 with Fe^{2+}, Mn^{2+}, Mg^{2+}, Ca^{2+}, and Na^+ ions, position M1 with Al^{3+}, Cr^{3+}, Ti^{4+}, Fe^{3+}, Mg^{2+}, Fe^{2+}, and Mn^{2+} ions, and position M2 in which Si^{4+}, Al^{3+}, Cr^{3+}, Fe^{3+}, and Ti^{4+} ions are located. The multicomponent chemical composition and multivariant structural motives of crystal lattice of amphiboles significantly complicate the solution of the question: what ions in which positions can be isomorphously replaced by ions of REE? At the same time, by the analogy with other Ca-bearing silicates, it can be assumed that in this mineral the majority

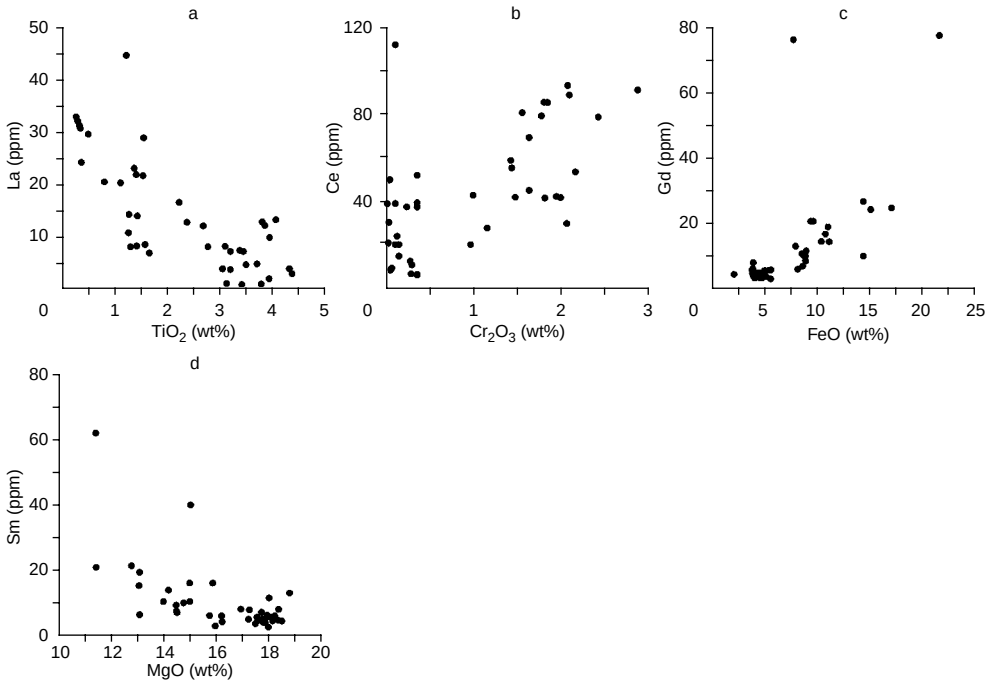

Figure 5.50 Correlation of REE and some net-forming elements in the amphiboles from different rock types: a—(La–TiO_2); b—(Ce – Cr_2O_3); c—(Gd–FeO); d—(Sm–MgO).

of REE ions isomorphously replaces Ca^{2+} ions, that is, the replacement predominantly occurs in position M4.

Scarce complex data on the chemical and REE compositions of amphiboles would allow, at least to a first approximation, discussion of the question on probable correlation relationships between net-forming components and REE. For example, they display features of an inverse relationship between the content of La and the content of TiO_2(Fig. 5.50, a) and a tendency of a direct relationship between Ce and Cr_2O_3 contents (see Fig. 5.50, b). Features of direct relationship were observed between the contents of Gd, Nd, Sm, and Dy, on the one hand, and content of FeO on the other (see Fig. 5.50, c). Finally, an inverse relationship is probable between the contents of Sm and MgO (see Fig. 5.50, d).

It is most likely that the above-listed cases of correlation relationships between the contents of some REE and net-forming elements in amphiboles may be indicative of corresponding tendencies of their heterovalent isomorphous replacement in real crystals of this mineral. As an example of probable schemes of this replacement, two hypothetic variants can be considered in which Ca^{2+} ions play the part of replaced ions and Fe^{2+} and Na^{+} ions occurring together with Ca^{2+} ion in position M4 are charge compensators: (1) $3Ca^{+} \rightarrow REE^{3+} + Fe^{2+} +$ vacancy; and (2) $2Ca^{2+} \rightarrow REE^{3+} + Na^{+}$. Most

likely, the second of these schemes is most probable in case of the isomorphism of middle REE because the difference between the total sizes of ionic radii in the left and right parts are smaller: $1.120\,Å \cdot 2 = 2.240\,Å$ (left part); and $1.066\,Å + 1.180\,Å = 2.246\,Å$ (right part). Note that the reported schemes of isomorphous incorporation of REE into the structure of amphiboles are by no means the only schemes to be assumed and must be regarded as more or less probable variants of replacements in real amphibole crystals. The problem of REE isomorphism in amphibole structure is very actual and requires special studies using more representative material.

* * *

In spite of the fact that the modal amounts of amphiboles are rather low in most mafic and ultramafic rocks, this mineral can be assumed to play an important part in the distribution of REE impurities in them. As was mentioned above, the amphibole structure is very favorable for concentrating increased amounts of isomorphous REE impurities. Depending on the chemical and REE composition of parental melts and on P–T conditions of crystallization of the melts, the total REE content in amphiboles may vary in a rather wide range, from a few tens of ppm in ultramafic rocks to 240 ppm in rocks with high silica contents.

It was established that the total REE content in amphiboles typically exceeds the summary contents in coexisting plagioclases and pyroxenes. Based on the parameters of REE distribution, the amphiboles studied can be tentatively divided into two major geochemical types. The first includes the majority of amphibole samples analyzed for REE. These amphiboles enter in the composition of metasomatically altered ultramafic rocks occurring mainly in deep xenoliths from alkali basalts. These amphiboles are relatively enriched with light and, partly, middle REE, and their patterns normally have a steep negative slope. The enrichment of amphiboles from ultramafic xenoliths with light elements is assumed to be due to the metasomatic transformation of these rocks resulting from percolation of light REE-enriched fluids that were supplied from alkali-basalt melts carrying these xenoliths. This type also includes amphiboles from ultramafic rocks of the massifs that are also fairly enriched with light REE and middle REE compared to heavy REE. Their negatively sloping patterns display smoothed maximums in the region of middle elements. The relative enrichment of these amphiboles with light and especially middle REE seems to be the result of percolation of middle REE-enriched fluids supplied from mafic melts that intruded into earlier bodies of ultramafic restates.

The second includes amphiboles occurring in gabbroid rocks of normal alkalinity. Unlike the samples of the first geochemical type, these samples are characterized by a more moderate or even decreased level of light REE accumulation. Their patterns typically have the shape of negatively inclined lines complicated by negative Eu anomalies of minor intensity. The depletion of this type of amphiboles in light REE is, most likely, the result of their crystallization from residual portions of mafic melts depleted of these impurities due to preceding prior crystallization of clinopyroxenes and plagioclases. It is worth noting that along with isomorphous REE impurities, the microcracks and fluid inclusions of real amphibole crystals may contain various amounts of nonstructural impurities of light REE, which, though bearing no direct relation to endogenic processes, might introduce errors into analytical data and their interpretation.

Scarce data on the estimation of the K_d(amphibole/melt) values show that for most REE they successively increase from basalt melts to alkali basalt, andesite, dacite, and rhyolite melts. The trends of changes of these K_d have the shape of somewhat curved upward lines with a generally positive slope. The values of K_d(amphibole/clinopyroxene) for all REE in most studied couples of these minerals is basically more than unit and vary in a rather narrow range, slightly decreasing from light to heavy elements. The values of K_d(amphibole/plagioclase), on the contrary, increase from light to heavy REE, with intense minimums for Eu on their trends. In gabbros from some more carefully studied massifs, the trends of K_d(amphibole/plagioclase) for all samples were found to have nearly identical configuration with a close location to each other on the plots. These features suggest that in such gabbros, amphiboles and plagioclases are in the state close to chemical equilibrium. The accumulation of REE in the structure of amphiboles, as seen from scarce observations, is the result of their heterovalent isomorphous replacement by trivalent ions of bivalent Ca^{2+} ions. The ions of net-forming components (Na, Fe, Ti, Cr, and others) most likely acted as charge compensators.

Chapter 6

Indicator properties of rare earth elements and their role in studies of genesis of rocks and minerals from mafic–ultramafic complexes

It is necessary that the hypotheses of the origin and relationships of magmas, based on the results of experimental investigations and studies of major elements, would agree with the results of geochemical studies of distribution of trace elements.

D.H. Green & A.E. Ringwood

In spite of the fact that ultramafic and mafic plutonic rocks are of subordinate importance in the Earth's crust structure, they are a very important source of information about the structure, properties, and material composition of the upper mantle and the Earth's crust. These specific magmatic rocks allow reconstruction of the evolution of practically unobservable deep processes that have occurred for many hundreds of millions years in the upper Earth's covers. These global processes and their products are studied using modern procedures for analysis of the trace-element composition of ultramafic and mafic rocks and the minerals composing them, including the studies of distribution regularities of REE in them. Data on the distribution of REE in ultramafic and mafic rocks collected in the last half of the century gave rise to the origin and development of many concepts and models of mantle magma formation, evolution of the upper mantle substrate and formation of various magmatic rocks, their massifs and complexes and ore mineralization occurring on the upper levels of the Earth's crust available for direct observation. At the same time, despite achieved success in the geochemical study of ultramafic and mafic rocks and their minerals, and the rather wide application of new developed parameters and criteria for solving different problems in the systematization, metallogeny, and petrology of these formations, the information potential of rare earth and other trace elements is far from being exhausted.

In the previous chapters we discussed many aspects of the geochemistry and REE in ultramafic and mafic rocks and their minerals, and cause and effect relations between the rare earth composition of rocks and minerals and their features and conditions of formation. Below, we will focus on some indicator properties of REE that require introduction of some restrictions in petrological reconstructions and constructions of petrogenetic models relevant to ultramafic and mafic magmatism.

6.1 REE AS INDICATORS OF FORMATION AND TRANSFORMATION CONDITIONS OF ULTRAMAFIC ROCKS

Over the whole history of studies of ultramafic rocks, different classifications and principles of their construction were proposed. Particular attention to this problem

was paid by petrologists and other researchers in the second half of the twentieth century. In 1967, collected articles on ultramafic and related rocks were published and edited by P. Willy (*Ultramafic and Related Rocks*, 1967). In these collected works, nine associations with participation of ultramafic rocks are singled out: (1) layered large gabbro-norite–peridotite intrusions; (2) ultramafic rocks in differentiated basic sills and small intrusions; (3) associations of concentrically zoned dunite-peridotite massifs; (4) associations of alpine-type peridotites and serpentites; (5) small occurrences of ultrabasic rocks in acid batholites; (6) alkaline ultrabasic rocks in ring complexes; (7) kimberlites; (8) ultrabasic lavas; and (9) nodules of ultrabasic rocks (Coleman, 1979). The mineralogical and petrochemical classification of ultramafic rocks proposed by Bogatikov *et al.*, (1981) includes four large categories: (1) ultrabasic volcanic rocks of a normal series; (2) ultrabasic plutonic rocks of a normal series; (3) ultrabasic volcanic rocks of an alkaline series; and (4) ultrabasic plutonic rocks of an alkaline series. Somewhat later, using geological, structural, petrochemical, mineralogical, and petrographical criteria, Frey (1984) proposed the following classification of ultramafic rocks, which also includes four types: (1) alpine-type ultramafic rocks from isolated massifs; (2) ultramafic rocks composing basal components of ophiolitic associations; (3) ultramafic rocks occurring within the bottoms of oceans; and (4) ultramafic rocks from inclusions (deep xenoliths) in alkaline basalts and kimberlites.

The types of ultramafic rock distinguished by Frey include their three main petrographical varieties: lherzolites, harzburgites, and dunites. Geochemical data suggest that the general level of accumulation of REE in these varieties of ultramafic rock is typically lower than or comparable with that in chondrite C1. The average contents of these trace elements slightly increase in the series from dunites to harzburgites to lherzolites, which agrees with the concept of a gradual decrease in depletion with decreasing degrees of partial melting of mantle substrate. Typically, the chondrite-normalized patterns of these rocks have a positive general slope due to a slight increase in the level of accumulation of light to middle to heavy REE.

Petrochemical and geochemical investigations show that all ultramafic rocks to a certain degree are enriched with refractory components (Mg, Cr, Ni, Co, Fe, platinum group elements) and are considerably depleted in less-refractory elements (Si, Ca, Al, Ti, Na, K, REE, and some other trace elements). All these chemical and geochemical properties of ultramafic rocks were later consistently interpreted within the model of their formation as refractory residuals (restites) resulting from partial melting of the upper mantle pyrolite sources, which chemical and mineral composition was similar to lherzolite (Green & Ringwood, 1968) or, according to other data, pyroxenite (Kutolin, 1972; Andersen, 1981; Gorbachov *et al.*, 2006b).

Ultramafic restites from massifs. Within the folded regions, these rocks occur as rare autonomous massifs or as part of complex mafic–ultramafic massifs in ophiolitic associations, in which they often predominate. Comparative studies of the regularities of REE distribution in lherzolites, harzburgites, and dunites from massifs of different locations, inner structures, and petrographical compositions allow a more detailed geochemical systematization of such restites. Ultramafic restites from small blocks in the inner zones of the largest massifs that underwent minimum dynamometamorphic transformations and serpentization are the most appropriate objects for obtaining more exact information on the distribution regularities of REE impurities, which are

isomorphously incorporated into the structure of their minerals. When studying virtually nonserpentinized harzburgites with a protogranular microstructure from weakly deformed boudine-like blocks in the Shamansky ultramafic massif (eastern Transbaikalia), it was established that these ultramafic rocks were not contaminated by nonstructural impurities of light REE. Such nonserpentinized harzburgites were also found in small boudine-like bodies among dynamometamorphic and serpentinized ultramafic rocks of the Voykar-Syn'insky massif in the polar Urals (Vakhrusheva, 2007). These rocks are regarded as virtually unaltered restites of the upper mantle, favorable for detailed mineralogical and geochemical studies.

The observed differences in the levels of REE accumulation among similar petrographical varieties of ultramafic rock from different massifs are mainly due to their different contents of modal clinopyroxene as the major concentrator of these impurities. The content of clinopyroxene in these rocks is, in turn, predetermined by variations in the degree of partial melting of mantle sources, which is related to certain differences in P–T parameters, including the heat flows in some parts of the asthenosphere. A representative example of this is dunites and harzburgites from the Samail massif and lherzolites from the Baldissero, Balmuccia, Lherz, Lanzo, and Lizard massifs, which are most intensely depleted of light REE. Considerable depletion of light REE relative to heavy REE was also established for dunites from the Gorgona massif, but the general level of REE accumulation in these rocks is higher than that in dunites from the above-mentioned massifs located in folded regions.

The models of formation of ultramafic rocks as restites suggest that the varieties for which the qualitative mineral composition corresponds to harzburgites formed at moderate or slightly increased degrees of partial melting of mantle sources—lower than during formation of dunites but higher than during formation of lherzolites. On the assumption that the initial quantitative mineral composition of mantle protoliths corresponded to lherzolite, in which the amount of modal clinopyroxene ranges from 50 to 10%, then on its partial melting and depletion with formation of restites similar in composition to harzburgites lacking clinopyroxene, REE content must have decreased proportionally, that is, from 50 to 10%. The fact that many harzburgites contain up to 5% clinopyroxene suggests that this mineral, as an important REE concentrator in the upper mantle substrate, did not always pass into melts and, hence, the degree of partial melting of mantle sources in the general case could not amount to 50%. Some researchers believe that the formation of harzburgites as restites most likely took place at degrees of partial melting of mantle sources in the range of 10–30% (Menzies, 1976; Prinzhofer & Allegre, 1985; Godard *et al.*, 2000).

In the above-mentioned ultramafic massifs, and some others, along with harzburgites and dunites, which typically have a lower level of accumulation of light REE than medium and heavy REE, there are samples that have the same quantitative mineral composition yet reveal uncommonly high contents of light elements. This type of dunite enriched with light REE is found in the Paramsky, Twin Sisters, Tetford Mines, Lukinda, New Caledonia, and New Guinea massifs. Abnormally light-REE-enriched harzburgites were found in the Lherz, Ivrea Verbano, Sud, Tiebugy, Paramsky, Tetford Mines, and Trinity massifs, whereas considerably light-REE-enriched lherzolites occur in the Caussou, Bay of Islands, Peak Couder, and Beni Bouchera massifs. Abnormal enrichment in light REE is also observed in some ultramafic restites from mid-oceanic ridges, for example in San Paulu Island. Moreover, abnormally enriched

contents of light REE are typical of some geochemical standards, including DTS-1 dunite and PCC-1 serpentinized harzburgite (Frey, 1984). Such ultramafic rocks usually have U-shaped REE patterns. Less often, they display patterns of a flattened shape, for example, in dunites dredged from the Romanche trough (Nikol'skaya & Kogarko, 1995). Ultramafic restites that are uncommonly enriched with light REE, which patterns are nearly straight lines with a negative slope, also occur.

It is quite probable that such anomalous enrichment of ultramafic restites from massifs with light REE is at odds with the model of partial melting of mantle sources, because as a result of this melting, the level of light REE accumulation must be lower than that of middle and heavy REE. The reasons for this phenomenon have often been discussed in the literature, but opinions on this subject still differ. There is a viewpoint that the observed enrichment of some restites with light REE is their primary property, as it results from the specific conditions of depleted mantle sources. According to other data, the nature of this phenomenon is related to mantle magma generation processes with participation of fluids or melts that separated from subducting oceanic lithosphere. Some researchers think that the abnormal enrichment of ultramafic restites with light REE could have taken place after termination of the melting process of mantle sources. Here are some more hypothetical interpretations: (1) interaction of ultramafic restites with melts enriched with light REE; (2) differential transport rates of some REE during the interaction of later melts with ultramafic restites; (3) selective removal of medium REE from ultramafic restites during their serpentization; and (4) low-temperature enrichment of ultramafic restites with light REE during their serpentization under the influence of oceanic or meteoric water.

It is worth noting that the abnormal light REE enrichment of ultramafic restites occurring in ophiolite massifs is indeed very often observed in those varieties that underwent intense serpentization or amphibolization. There is evidence in favor of the opinion that the enrichment of ultramafic restites with light REE is related to the infiltration of fluids that were supplied from later basaltic or more acidic melts. The most representative in this respect are ultramafic restites making up deep xenoliths from alkaline basalts, which will be discussed below.

As was emphasized, one and the same petrographical variety of ultramafic restite from different massifs or even within one massif might differ in the contents of light, medium, and heavy REE. These differences can be due to two main reasons: (1) variations in the quantitative mineral composition, especially in the modal amount of clinopyroxene; and (2) different intensities of epigenetic enrichment of these rocks with nonstructural REE impurities. This can be illustrated by the example of some harzburgites that are abnormally enriched with light REE. As harzburgites consist mainly of olivine and orthopyroxene, which structures cannot concentrate any significant amount of REE, then in the case of increased amounts of light REE, it is most likely that these elements are concentrated not in the form of isomorphous impurities but in the form nonstructural impurities occurring either in intragrain or in intergrain microcracks. The reason for abnormal enrichment of ultramafic restites in nonstructural impurities of light REE involve both endogenic and exogenic fluids. We discussed the probable mechanism of enrichment of ultramafic restites in exogenic processes based on the results of a numerical experiment with a supply of REE during infiltration of oceanic water of mid-oceanic ridges into ultramafic rocks (see Chapter 1.2). The probable mechanisms of abnormal enrichment of

ultramafic restites with light REE under the influence of endogenic processes will be described below.

Ultramafic restites from deep xenoliths. Xenoliths of ultramafic restites were found virtually in all alkali-basaltoid and kimberlite provinces. The mineralogical and geochemical properties of these xenoliths always attract the attention of petrologists and geochemists as these xenoliths are considered important carriers of information on the material composition of deep upper mantle shells that are unavailable for direct observations. In their petrographical, petrochemical, mineralogical, and other properties, most ultramafic restites from deep xenoliths are comparable with alpine-type ultramafic restites that compose mafic–ultramafic complexes of different ages and compositions occurring in mobile belts of continents and mid-oceanic ridges. At the same time, unlike the latter, ultramafic rocks from deep xenoliths often display mineralogical and geochemical evidence that these rocks formed under higher pressures and temperatures, for example, the presence of pyrope garnets, diamonds, and clinopyroxenes with elevated K content.

As scientists have always focused considerable attention on ultramafic restites from deep xenoliths, they created the most representative basis of analytical information for these rocks. These rocks were one of the first to be studied with respect to REE distribution. At the very beginning of geochemical studies of ultramafic rocks from deep xenoliths, they were assumed to be similar to rocks composing various mafic–ultramafic massifs exposed on the continents. But with time, it became obvious that, though in the level of heavy REE accumulation both groups of ultramafic rocks have much in common, in the level of accumulation of light and heavy elements the samples of ultramafic rocks from deep xenoliths, typically, have some specific features, including significant irregularities in light REE distribution, not only between xenoliths from different provinces or individual diatremes but within individual xenoliths as well. Xenoliths in which ultramafic rocks, in the level of light REE accumulation and distribution of other elements, are comparable with rocks from mafic–ultramafic massifs exposed on the continents, are scarce. In many provinces, more widespread are xenoliths in which ultramafic rocks are abnormally enriched with light REE. This abnormal enrichment with light REE is equally specific of lherzolites, harzburgites, and dunites. Detailed study of one of the largest xenoliths of spinel lherzolites from alkali basalts of the Shavaryn Tsaram paleovolcano (Mongolia) showed its geochemical zonation with respect to light REE distribution. This concentric zoning is manifested as a gradual increase in the contents of light REE in the direction from the outer zone of the xenolith, which is in intimate contact with the host basalt, to its inner zone.

Therefore, the observations of the regularities of light REE distribution in ultramafic restites from deep xenoliths suggest that a considerable part of these elements occurs in ultramafic rocks not as isomorphous impurities in its minerals, but in the form of a nonstructural admixture, which is the form of different easily soluble compounds concentrated in intergrain and intragrain microcracks, as well as in fluid and nanoinclusions. We think that accumulation of nonstructural impurities of light REE in ultramafic rocks from xenoliths and in their minerals was the result of infiltration of light-REE-enriched epigenetic fluids. The source of these elements was alkaline basalts that transported fragments of mantle restites from the level of their formation in the upper mantle to the day surface. Therefore, in standard procedures of sampling of ultramafic rocks from deep xenoliths, true data on their primary rare earth

composition can be obtained only for heavy and, partly, medium REE. More or less reliable data on the content of light REE in the form of isomorphous impurities in ultramafic rocks from deep xenoliths can, most likely, be obtained only after special treatment of samples, for example, by leaching nonstructural impurities from them with the help of diluted hydrochloric acid.

Subvolcanic rocks with increased magnesium content. The specific features of REE distribution in these formations were considered based on the materials of different analytical data on kimberlites, tomtits, meimechites, picrites, and lamproites. Results of geological, structural, and experimental studies suggest that these rocks formed in near-to-surface conditions during crystallization of melts with different chemical compositions. These melts are also assumed to form mainly at considerable depths of the upper mantle on partial melting of its substrates with different compositions. The level of partial melting, according to researchers, varied from low and very low (kimberlites, lamproites) to significant (picrites, komatiites, meimechites).

A specific geochemical feature of kimberlites is their particularly high general level of REE accumulation, which is also intensely fractionated as a result of generation of their melts at rather low levels of melting of mantle sources. For example, the average $(La/Yb)_n$ parameter calculated from 313 analyses of kimberlite samples from different provinces is 85. Results of numerical modeling show that parental melts of kimberlites could have been generated at very low melting degrees of magnesite-bearing peridotites at pressures equal to 6–16 GPa (Girnis & Ryabchikov, 2005). The rise of kimberlite melts to the surface is assumed to have been accompanied by considerable amounts of CO_2, which provided high rates of migration and high explosive activity during formation of kimberlite pipes. These researchers also think that the conditions of intrusion of kimberlite melts promoted the preservation of high-pressure minerals, including diamonds, in them. The available data show that the largest amounts of REE in kimberlites are concentrated in clinopyroxenes, calcites, perovskites, xenogenic garnets, and in a drastically altered cementing mass. It is worth noting that kimberlite provinces, similarly to the pipes occurring in them, are studied nonuniformly with respect to REE geochemistry. Nevertheless, the obtained data can be efficiently used in the geochemical systematization of kimberlites and kimberlite pipes and provinces, as well as in the discussion of the models of their genesis.

Observations show that the total contents of REE in komatiites vary in the range of 3–70 ppm and have an inverse dependence on MgO content in these rocks. The $(La/Yb)_n$ values in different types of komatiites range from <1 to >1, and their rare earth patterns occasionally display both negative and positive Eu anomalies of minor intensity. The formation conditions of parental melts of komatiites and their crystallization conditions are still the subject of discussions in which one of the most important criteria are the features of REE distribution. According to one of the models of the origin of komatiites, their parental melts could have been generated at a depth of 400 km at about 1800°C with a very high degree of partial melting of mantle source (from 40 to 70%). By the moment of outpouring on the surface, komatiite melts must have been at a temperature no lower than 1600°C, that is, much higher than the temperature assumed for basalt melts (<1200°C) (Jochum *et al.*, 1991). Another proposed model of the origin of komatiites is based on three main arguments: (1) uncommonly high contents of compatible elements; (2) low contents of incompatible trace elements, including REE; and (3) near-to-chondrite distribution of incompatible trace elements.

The parental melts of komatiites could have been generated at high degrees of partial melting of previously depleted mantle sources with olivine as the main residual phase in it (Lesher & Arndt, 1995). A model similar to the previous one was proposed by Cullers and Graf (1984b). As the Achaean peridotite komatiites are mostly markedly depleted of light REE, the researchers suggested that the peridotite mantle source of their parental melts was previously depleted of these elements to the same degree as the source of tholeiite melts from contemporary mid-oceanic ridges. Hanski *et al.*, (2004), based on studies of komatiites from northwestern Vietnam, believe that during segregation of komatiite melts, their mantle source did not contain residual garnet. According to available data, most structural REE impurities are concentrated in skeleton crystals of clinopyroxene as well as in its microliths composing the groundmass of these rocks. We want to emphasize once more that the parameters of REE distribution are regarded as the most important criteria in the present day geochemical systematization and models of genesis of komatiites (Jahn *et al.*, 1982).

Meimechites are characterized by higher total contents of REE (83–210 ppm), with the level of accumulation of light REE considerably higher than that of heavy REE ($(La/Lu)_n > 200$). Most REE occurring in meimechites are, most likely, concentrated in the groundmass of these rocks and in the contained microliths of clinopyroxene. Such enrichment of these rocks with light REE at a rather high Mg content was initially interpreted as the result of particular generation conditions of their parental melts, which took place at great depths but at rather low degrees of rapid melting of undepleted mantle sources. According to the model proposed later, meimechites are genetically related to formations of alkaline rocks, and the source for their parental melts was a long-living depleted mantle reservoir that underwent active metasomatic treatment shortly before the generation of meimechite melts (Kogarko *et al.*, 1988). Later, Kogarko and Ryabchikov (1995) made this model more precise by suggesting that meimechite magmas formed from the melting of lithospheric harzburgites that were enriched in incompatible elements as a result of infiltration of diapiric melts generated at low degrees of partial melting. It is worth noting that the uneven distribution of porphyrous olivine inclusions that are virtually free of REE and the related geochemical inhomogeneity of meimechites hampers obtaining correct data on the distribution of REE in these rocks.

Picrites, widely spread in various geologic structures, have inhomogeneous chemical compositions, including the contents of Mg and alkalines. These rocks occur both in subvolcanic and in alkaline varieties. The total contents of REE in picrites vary significantly; in the rocks from volcanic–terrigenous complexes of folded regions, the total contents of REE are considerably lower (4–13 ppm) than the varieties occurring in oceanic islands (36–82 ppm) in alkali–ultrabasic complexes of platforms (28–360 ppm). The largest quantity of structural REE impurities in picrites is concentrated in clinopyroxene phenorysts and in their groundmass, lesser amounts occur in amphiboles, plagioclases, and micas. The differences in the level of REE accumulation are suggested to be due to the variations in the composition of mantle sources of their parental melts and different degrees of partial melting of these sources.

The observations of Ryabchikov (2005) suggest that alkaline picrites that are widespread on the Siberian platform, similar to meimechites and picrite basalts, crystallized from near-solidus melts of deep origin, which had very high contents of incompatible elements, including REE. Ryabchikov thinks that the steep negative

slopes of REE patterns of picrites in the region of heavy elements indicate the significant role of garnet in crystal restite, that is, they suggest that picrite melts generated at high pressures. Picrite rocks are also assumed to be more promising as a source of information about thermal conditions of the mantle substrate, which participated in magma formation, than are platobasalts.

Lamproites are a unique type of subvolcanic rock in which an increased Mg content combines with a particularly high alkalinity from K-type trace elements and a very high level of REE accumulation, typically exceeding their level in kimberlites. They differ from kimberlites also in higher contents of SiO_2 and modal phlogopite but in a slightly lower content of MgO. Similarly to kimberlites, the level of accumulation of light REE in lamproites is considerably higher than that of heavy elements. It is assumed that the most considerable amount of REE in lamproites occur as isomorphous impurities in clinopyroxenes, amphiboles, perovskites, and apatites. Most likely, lamproites crystallized from especially deep melts that generated at low degrees of partial melting of metasomatically altered mantle sources of lherzolite–harzburgite composition enriched with phlogopite but depleted of garnet and diopside. These melts should have contained elevated amounts of water and fluorine and practically no CO_2 (Jaques *et al.*, 1984). According to the model of Mitchell and Bergman (1991), the abnormal enrichment of lamproites with light REE was promoted by a very low (<1%) degree of partial melting of mantle sources, which composition was similar to phlogopite–garnet lherzolites. These authors do not rule out the probability that these sources were preliminarily enriched with REE as a result of transformations at depths, which are often called mantle metasomatism. There is a hypothesis that lamproites might have formed during intrachamber differentiation of the same parental melts from which all other varieties composing K-alkaline concentrically zoned complexes crystallized, ranging from ultramafic rocks to alkaline syenites (Vladykin, 1997).

High-magnesium rocks from the contact zones of protrusions of ultramafic restites with breaking mafic intrusives. When studying the structural, petrographical, and petrochemical features of mafic–ultramafic massifs occurring in many folded regions, which are assumed to belong to ophiolitic associations, abundant evidence was established that these massifs are polychronic and polygenic bodies (Pinus *et al.*, 1973, 1984; Lesnov, 1976, 1981a,b, 1982, 1983, 1984, 1986, 1988, 2006, 2009b; Piccardo *et al.*, 2005). Their texture, along with "orthomagmatic" ultramafic restites composing protrusions of various sizes, includes intermediate ultramafic rocks with inhomogeneous quantitative mineral composition and texture: wehrlites, websterites, clinopyroxenites, and their olivine- and plagioclase-bearing varieties. We place all these varieties of rocks into the category of "paramagmatic" ultramafic rocks (Lesnov, 1984, 1986, 1988). These rocks compose "transitional" zones with varying thickness and length permanently occurring along the contacts of ultramafic protrusions, which are known as "banded" or "layered" complexes of ophiolitic associations. The rocks referred to as paramagmatic ultramafic rocks are characterized by textural, structural, and quantitative mineral nonuniformity and by a banded and schlieren distribution of olivine, pyroxene, and plagioclase. This fact is also responsible for the rather considerable nonuniform distribution of macrocomponents and microcomponents.

The level of REE accumulation in paramagnetic ultramafic rocks depends mainly on the relationship between the modal amounts of olivine, orthopyroxene, clinopyroxene, and plagioclase, as most of the structural impurities of these elements are concentrated in clinopyroxene. Some wehrlites, clinopyroxenites, and websterites

contain accessory amphibole, which can also accumulate some amount of REE. Wehrlites contain a rather low total amount of REE, which ranges from a few to 10 ppm. Somewhat higher amounts of REE are found in samples that contain amphibole, plagioclase, or garnet as secondary phases. REE in wehrlites are commonly fractionated, with the level of accumulation of La and Ce being somewhat lower than that of middle and heavy elements. The rare earth patterns of samples from some massifs display smoothed maximums in the region of Nd, Sm, and Eu. As already mentioned, most REE in wehrlites are concentrated in clinopyroxene, which model content is mainly responsible for their accumulation level and distribution pattern. Some samples of wehrlites are found to contain abnormally high contents of light REE, which are assumed to be due to the presence of nonstructural impurities of these elements.

The total contents of REE in studied clinopyroxenites are higher than in wehrlites and range from a few ppm to 100 ppm. As in wehrlites, the level of accumulation of light REE in them is lower than that of middle and heavy elements, which is well observed in samples from the Voykar-Syn'insky and Mount Orford massifs

In the level of accumulation and distribution pattern of REE, websterites are comparable with wehrlites, but in some samples, the total content of REE reach 20 ppm or more, which is related to the slightly increased fraction of clinopyroxene. At the same time, clinopyroxene-rich varieties of websterites, like clinopyroxenites, are poor in La and Ce with respect to middle and heavy elements, owing to which their spectra have a positive slope.

The considerable nonuniformity of the rare earth composition of wehrlites, clinopyroxenites, and websterites with respect to REE distribution as well as their quantitative mineral and petrochemical inhomogeneity are a common distinctive feature of these paramagmatic ultramafic rocks. We suggest that the formation of these rocks is related to magmatic and metasomatic interactions between mantle mafic melts and their fluids, on one hand, and earlier bodies of ultramafic restites, on the other, the latter differing in the intensity of dynamometamorphism and degree of serpentization. During this reaction process, mafic melts along with Si, Al, Ca, alkalines, Ti, and some other macrocomponents, supplied and uniformly dispersed additional contents of rare earth and other incompatible elements in ultramafic restites.

Here it is pertinent to mention Frey's (1984) observations of the Ronda massif. He showed that the mineral composition of rocks composing veined bodies, which occur among peridotites of these massif, ranges from garnet clinopyroxenite to olivine gabbro. The contents of REE in pyroxenites strongly vary but, in most cases, the ratio of contents of light and heavy elements in them is lower than that in the host peridotites. Frey emphasized that the role of pyroxenites in the upper mantle is still debatable, but the presence of their veins in olivine–peridotites is an important form of occurrence of mantle heterogeneity. Data on REE content in pyroxenites show that these rocks cannot be regarded as the source for MORBs, and, in their composition, they are nonequivalent to crystallized basalt magmas. Thus, Frey came to a conclusion that the presence of pyroxene-rich stratiform and veined bodies among alpine-type peridotites from the massifs similar to the Ronda massif and the presence of these rocks among ultramafic deep xenoliths reflect the magmatic processes that took part both in the upper mantle and within the crust. According to other researchers, the observed properties of the composition of pyroxenites could result from both fractionation crystallization of magmas and their interaction with the walls of host ultramafic rocks (Suen *et al.*, 1979; Obata, 1980).

The concept of the contact–reaction, that is, the hybrid, nature of wehrlites and pyroxenites, is supported not only by the numerous samples of their structural position, for example by their localization in the contact zones of protrusions of ultramafic restites with breaking bodies of gabbroids, but also by some experimental studies. Green and Ringwood (1968) showed that at a pressure of about 9 kbar, the following reactions are realized:

1. olivine + plagioclase → aluminiferous pyroxenes;
2. spinel + plagioclase → aluminiferous pyroxenes.

However, we must admit that nowadays there are no substantiated arguments in favor of the hypothesis that wehrlites and pyroxenites of varying composition are the products of direct crystallization of primary mantle melts. By contrast, many geological, petrographical, and geochemical data show that the formation of these rocks is the direct result of upper mantle and intracrustal interaction between mantle mafic melts and solid ultramafic restites, which in most cases were preliminarily subjected to dynamometamorphism, disintegration, and serpentization.

In connection to this, we think it is pertinent to cite principally important results of experiments on the study of the "peridotite–basalt-volatile components" system, obtained by Gorbachov *et al.*, (2006a): "Here two mechanisms of magma formation are realized: (1) 'reactional', related to the interaction of melt formed during melting of initial basalt with peridotite, producing 'reactional' melts; (2) 'filmy', resulting from partial melting of peridotites, yielding intragrain, 'filmy' melts. At T = 1250–1350°C and P = 1.5–2.5 GPa, depending on the composition of basalts, two petrochemical types of reactional types of 'reactional' melts formed. In the experiments with basalts, the complementary of the main correlation of partial melting of peridotite: lherzolite + harzburgite (dunite) + basalt (tholeiite, olivine) magnesian melts of picrite-basalt melts are formed. In the experiments with compositions, noncomplementary of the main mantle correlation (andesite) or with addition of alkalines, SiO_2-enriched magnesian melts of bonnite type or alkaline basalt are formed." As a result, the authors came to the following conclusion: "Most likely, the process of 'filmy' melting of peridotite with formation of intragrain above-solidus melts and their migration through the mineral framework of mantle peridotite to unification in rather large chambers is nonequilibrium." I hope that in the nearest future the products of such experiments will be studied with respect to distribution of both major and trace elements. This will give a better insight into REE behavior both at partial melting of ultramafic substrates of the upper mantle and in the processes of interaction of mafic melts and their fluids with ultramafic restites at a distance from the magma chamber, including the upper part of the Earth's crust.

6.2 REE AS INDICATORS OF FORMATION AND TRANSFORMATION CONDITIONS OF MAFIC ROCKS

As mentioned above (see Chapter 4), results of geological and petrographical studies of mafic–ultramafic massifs allowed us to establish two major substance genetic categories among mafic plutonic rocks—orthomagmatic and paramagmatic (Lesnov, 1984, 1986, 1988). The category of orthomagmatic mafic rocks includes the varieties

that crystallized directly from mantle basalt melts that did not undergo intense contamination by the substance of any wall rocks. To this category we include gabbros, gabbro-norites, norites, and some varieties of olivine gabbros and gabbro-norites with a homogeneous quantitative mineral composition and a massive structure. The category of paramagmatic mafic rocks is represented by the varieties that, as assumed, crystallized from the same mafic melts but were to a certain degree preliminarily contaminated by the substance of various wall rocks and have increased inhomogeneity of structure, texture, and mineral composition. Paramagnetic mafic rocks are divided into two types—A and B. Type A is represented by rocks that formed during crystallization of melts contaminated by the matter of earlier ultramafic restites, including their serpentinized varieties. This type includes rocks from leucocratic to melanocratic varieties of taxite olivine gabbros, olivine gabbro-norites, troctolites, and some varieties of anorthosites. Type B includes rocks that resulted from crystallization of deep mafic melts that were previously contaminated by material enriched with Si, Ca, Al, and alkaline terrigeneous, volcanogenic, and carbonate rocks or their metamorphic derivatives. Among the paramagnetic rocks of this type, the most widespread are amphibole, quartz-amphibole, and biotite-bearing gabbros, gabbro-diorites, and diorites.

The above-mentioned varieties of orthomagmatic mafic rocks of normal alkalinity are characterized by a moderate level of accumulation and a rather uniform distribution of REE, which are commonly weakly fractionated. Among these rocks there are varieties that are both slightly depleted in light elements, especially in ophiolite mafic–ultramafic massifs, and slightly enriched with these impurities. In turn, paramagmatic mafic rocks of type A typically have a decreased level of REE accumulation and a very nonuniform distribution from sample to sample within one magmatic body. Unlike the previous rocks, paramagmatic mafic rocks of type B display an increased level of REE accumulation, which are also distributed nonuniformly in different samples from one intrusive body.

In recent geochemical studies, the distribution of REE in different plutonic mafic rocks was given considerable attention, owing to which large volumes of analyses of their samples from many hundreds of mafic–ultramafic massifs were carried out, but all these data have not been systematized and generalized yet. For example, the fundamental report on the REE geochemistry of magmatic rocks and other natural formations, edited by Henderson (Rare Earth Element Geochemistry, 1984), actually lacks a specialized chapter concerning studies on the geochemistry of REE in plutonic mafic rocks.

Within separate intrusive bodies, gabbros typically have a rather uniform rare earth composition, but the comparison of the rare earth composition of their samples from different massifs show that they often differ significantly in the level of REE accumulation, at times by more than two orders of magnitude. Generalization of analyses of more than 100 gabbro samples showed that the average total content of REE in these rocks is about 46 ppm, the level of La accumulation in them is higher than the level of Yb. The $(La/Yb)_n$ values in these rocks range from 0.13 to 15. The patterns of gabbros, especially those depleted of REE, display positive Eu anomalies of varying intensity. Gabbros that compose different mafic–ultramafic massifs within continental folded regions normally have a lower level of REE accumulation than N-MORBs, and only some of their samples are comparable in this respect with OIBs. It is worth noting

that those gabbros that occur in mafic–ultramafic massifs are more depleted of REE than their analogs from the massifs not pertaining to ophiolitic associations. Coleman (1979), based on data of rare earth composition, suggested that gabbros belonging to ophiolite mafic–ultramafic massifs must be divided into two geochemical types: (1) rocks depleted of REE, called "lower" gabbros; and (2) rocks enriched with REE, called "upper" gabbros. Among the reasons responsible for the differences in the rare earth composition of gabbros from different mafic–ultramafic massifs the following three reasons are the most significant: (1) the composition of mantle protoliths; (2) the temperature and pressure on which the level of partial melting of protoliths depended; and (3) physicochemical parameters under which crystallization of melts and formation of mafic intrusives proceeded.

The most important REE concentrators in the composition of upper mantle substrate were, most likely, clinopyroxene and garnet on melting, during which these impurities were supplied into basalt melts. During crystallization of the latter, in the form of orthomagmatic and paramagmatic mafic rocks, the overwhelming quantity of REE again accumulated in clinopyroxenes and in plagioclases, partly in amphiboles and accessory minerals—apatite, sphene, zircon, ilmenite, and, occasionally, garnet. The established increased depletion of REE of the gabbros that occur in massifs from ophiolitic associations is, obviously, due to their crystallization from those portions of mantle melts that were generated at increased degrees of partial melting of mantle sources. The varieties of gabbro from the massifs that do not belong to ophiolitic associations enriched with light REE, most likely, crystallized from melts that were generated at somewhat lower degrees of partial melting of mantle sources. The positive Eu anomalies observed on gabbro patterns are assumed to be due to fractionation of plagioclases during crystallization of melts in intrusive chambers. Data on gabbro samples from some massifs suggest that such fractionation of plagioclase was intense on those melts that were generally depleted of REE.

The level of REE accumulation in gabbro-norites is slightly lower than that in gabbros. The average total content of REE in gabbro-norites is about 25 ppm, with weak fractionation of the elements. In the level of accumulation and distribution patterns of REE, gabbro-norites from ophiolite mafic–ultramafic massifs yield to N-MORBs and are comparable with the "lower gabbros" from the classification of Coleman (1979). Gabbro-norites from such massifs as Dovyrensky, Chaysky, Burakovsky, Salt-Chak, Union Bay, and Stillwater, which do not pertain to ophiolitic associations, in the level of REE accumulation are comparable with N-MORBs. Most REE in gabbro-norites, like in gabbros, are concentrated in clinopyroxene and plagioclase, with lesser quantities of them in secondary amphiboles and accessory phases—apatite, sphene, zircon, and ilmenite. Many of the analyzed gabbro-norites, judging by their patterns, have a slight excess of Eu.

The accumulation of REE in norites is lower than that in N-MORBs and their patterns have both positive (Voykar-Syn'insky massif) and negative (Stillwater massif) slopes. These spectra are complicated by positive anomalies of Eu, which is concentrated mainly in orthopyroxene, whereas heavy elements occur in orthopyroxene and, probably, in accessory zircon. The low contents of REE and the relative depletion of light elements observed in norites from the Voykar-Syn'insky massif are, most likely, a result of their generation from parental melts at elevated degrees of partial melting of mantle source. Unlike them, norites from the Stillwater massif that have a higher

level of REE accumulation and are enriched with light elements seem to be crystallized from melts generated at a lower degrees of partial melting of nondepleted source.

Continuing on to the consideration of the rare earth composition of paramagmatic mafic rocks, we want to emphasize that REE contents in olivine gabbros are characterized by rather wide variations, which is the result of variations in modal amounts of clinopyroxene, olivine, and plagioclase. The general level of accumulation of these impurities in olivine gabbro is lower than that in N-MORBs. These rocks are often depleted of light REE and have a positive slope of patterns virtually always complicated by positive Eu anomalies of varying intensity. Structural, geological, and petrographic observations suggest that olivine gabbros might have a double origin. The varieties having a constant quantitative mineral composition within the composed bodies, most likely, crystallized from primary melts with elevated Mg content, that is, these are orthomagmatic rocks. Those varieties of olivine gabbros that have a nonuniform quantitative mineral composition and taxitic, including eutaxitic, textures and make up layered and lenticular bodies within transitional contact zones (layered complexes) of polygenic mafic–ultramafic massifs were, likely, generated by crystallization of hybrid melts contaminated by the matter of ultramafic restites. A rather intense contamination of these melts could take place only under the conditions of their long-term cooling and crystallization in abyssal or mesoabyssal conditions of occurrence of intrusive chambers and with participation of fluid components.

Troctolites are a less widespread variety of rock participating in the structure of mafic–ultramafic massifs. Typically, they do not form autonomous intrusive bodies. These rocks have rather low total contents of REE, typically not exceeding 10 ppm. These impurities are mostly concentrated in plagioclase, which modal contents vary considerably, predetermining the inhomogeneity of rare earth composition of these rocks. The rare earth spectra of troctolites in most cases have a general negative slope and are complicated by positive Eu anomalies. In troctolites from some massifs, for example, the Dovyrensky massif, an inverse relationship was established between total REE contents and $(Eu/Eu^*)_n$ values. Our observations show that most troctolites, similar to olivine gabbros, are hybrid rocks that crystallized from mantle basaltoid melts substantially contaminated by the substance of ultramafic restites during their long-term interaction under the conditions of decreased oxygen volatility. Evidence for this comes, for example, from the rather wide occurrence of troctolites and olivine gabbros on the moon, which have higher Mg content than their Earth analogs (Magmatic rocks, 1985). The quantitative mineral nonuniformity and the rather low general level of REE accumulation in troctolites seem to result from mixing of different proportions of the substance of tholeiite melts and substantially REE-depleted nonserpentinized ultramafic restites. A numerical modeling based on data of the chemical compositions of lunar troctolites and their minerals also supports the concept that these are hybrid formations (Ariskin, 2007).

The total REE contents in anorthosites varies from 3 to 80 ppm, with their genera; the level of accumulation is higher than that in N-MORBs, but lower than that in OIBs. Most REE in anorthosites are concentrated in plagioclases and only minor amounts of them occur in secondary and accessory phases—clinopyroxene, orthopyroxene, potassium feldspar, amphibole, mica, apatite, and ilmenite. Anorthosites from the Central massif (Anabarsky shield) have a lower level of REE accumulation than samples of these rocks from the Sept Iles massifs and some others. Similar to their major mineral,

plagioclase, the level of accumulation of light elements in anorthosites is considerably higher than that of heavy elements The REE patterns of anorthosites have a general negative slope and constantly display positive Eu anomalies of varying intensity. The average values of the $(Eu/Eu^*)_n$ parameter from different massifs are mostly the same. An inverse relationship between the total contents of REE and $(Eu/Eu^*)_n$ values was revealed in anorthosite samples from the Sept Iles and Kalarsky massifs. Unlike the above-mentioned samples, this relationship was not observed in rock samples from the Glavny Khrebet massif. On the basis of geological, petrographical, and geochemical observations, including data on REE distribution, some petrologists believe that most anorthosites associated with other mafic and ultramafic rocks were generated under specific conditions of fractionation of basalt melts with tholeiite composition (Magmatic rocks, 1985).

When considering the specific features of REE distribution in eclogites, its worth noting that, according to existing concepts, these rocks were either produced by high-pressure crystallization of mafic rocks or formed during the recrystallization of different mafic rocks under very high pressures. The available data show that total REE contents in eclogites vary in a wide range and average 38 ppm, which is comparable with the average total REE content in N-MORBs. The level of accumulation of some elements in these rocks ranges within 14–27 t. ch., being slightly higher for light REE than for heavy REE. The rare earth patterns of some eclogites display positive or negative Eu anomalies of low intensity. In analyzing the regularities of REE distribution in eclogites, it is important to know whether REE distribution took place during the high-pressure recrystallization of those protoliths after which these rocks formed. Shatsky (1990) reports that in cases in which eclogite formation was accompanied by dehydration of protoliths, then together with fluids, some quantities of mobile elements, including REE, could have also been removed from the rocks. This implies that under these conditions, eclogites were depleted of the above-mentioned impurities compared to their protoliths. In other cases, when the formation of eclogites was accompanied by the supply of fluids, the level of REE accumulation could increase compared to that in protoliths. In addition, data reported by Shatsky show that many eclogites contain certain amounts of nonstructural REE impurities, which is easily leached when their ground samples are washed by a strongly diluted hydrochloric acid.

On the relationship between rare earth elements and platinum group elements in mafic and ultramafic rocks. Recent studies show that in systematizing and revealing the conditions of mafic and ultramafic rocks, not only are data on the distribution of REE of considerable interest, but so are the related data on the distribution of platinum group elements in these rocks (Lazarenkov *et al.*, 1989; Lesnov, 2003c,d; Lesnov *et al.*, 2001, 2004b, 2005b,c; Lesnov & Oydup, 2002; Lesnov, 2003c,d; Lesnov & Balykin, 2005). Rare observations show that between these group of elements, which differ substantially in their physical and chemical properties, there exists some geochemical "antagonism" that promotes their fractionation during the processes of generation, contamination, and crystallization of mafic melts.

Platinum group elements characterized by K_d(silicate mineral/melt) values less than unity, are incompatible with the major minerals of the upper mantle—olivine, orthopyroxene, clinopyroxene, and garnet (Borisov, 2005). This author thinks that at the level of partial melting of about 20%, the phases containing platinum group elements must melt completely. His calculations show that, in this case, the content of platinum group

elements in basalt melts will be (ppm): Os (17), Ir (16), Ru (25), Pt (35), and Pd (20). If these values are extrapolated to a melting degree of about 10%, then the contents of each of the mentioned platinum elements in melts will probably be 2 times lower. On the other hand, the model of partial melting of upper mantle substrate suggests that in the portions of melt that were generated at a 20% degree of partial melting, the contents of REE will be lower than that in the portions formed at a degree of melting of 10%. Hence, with the increasing degree of partial melting in each subsequent portion of basalt melt, the total REE content will be lower than in the previous portion, whereas the total platinum group element content, as refractory components, in later melts will, on the contrary, slightly increase. In other words, during the partial melting of undepleted upper mantle, a rather intense fractionation of REE and platinum group elements, most likely, took place between basalt melts and complementary ultramafic restites. As a result of this process, both in basalt melts and in ultramafic restites, lower REE concentrations must be associated with higher platinum group element concentrations and vice versa.

The signs of an inverse relationship between REE and platinum group element contents, which we established in mafic and ultramafic rocks from some massifs, are certain evidence supporting the existence of geochemical "antagonism" in the behavior of REE and platinum group elements during formation of these rocks, though we cannot rule out the probability that the opposite tendencies were caused by some other reasons. Further advanced search in this direction will help to obtain additional analytical data on this problem. This will provide insight into the physical and chemical mechanisms responsible for the fractionation of REE and platinum group elements during formation of ultramafic and mafic rocks and probably will help to determine geochemical parameters of joint distribution of elements of these two contrasting groups, which could be used as indicators in the systematization of these rocks and their massifs and in determination of their generation and crystallization conditions.

The problems of geochemical relationships between the REE and platinum group elements are discussed in more detail in a special section of the 2nd book of this monograph (Lesnov, 2009a).

6.3 INDICATOR PROPERTIES OF REE IN STUDY OF THE FORMATION AND TRANSFORMATION OF ROCK-FORMING MINERALS OF ULTRAMAFIC AND MAFIC ROCKS

In recent decades, new advanced analytical methods were used to obtain a large quantity of REE determinations in rock-forming and accessory minerals from ultramafic, mafic, many other magmatic, and some other metamorphic rocks, which together with other data obtained by other methods, has considerably improved our knowledge of the typomorphism of these minerals and promoted the appearance of new ideas and models of magma, rock, and mineral formation. New data has stimulated new studies on forms of occurrence and mechanisms of isomorphous replacement of net-forming elements by REE in mineral structures. Various viewpoints on this problem were summarized, for example, by Skublov (2005). He distinguishes three main forms of REE occurrence in minerals: (1) surface adsorption; (2) occlusion; and (3) formation of

solid melts. Like some other authors, for example, Suzuki (1987), Skublov interprets surface adsorption as the presence of foreign ions in a diffusion layer on the surface of mineral grains. It is worth noting that this form of occurrence of impurity elements in minerals is of particular interest in those cases in which we deal with the host mineral, which is an aggregate consisting of very many "small" blocks. Kovalenko *et al.*, (1989) interpret this form of occurrence as a so-called "contaminant," which concentrated in intragrain microcracks and on the surface of mineral grains during infiltration of later fluids. In turn, occlusion usually means the form of occurrence of impurity elements in the composition of crystal, glassy (melt), or fluid microinclusions that were "trapped" by the host mineral during its growth. However, the most significant process, in a quantitative sense, is the form of occurrence of impurity elements, including REE, in minerals that is represented by their ions being incorporated directly into the crystal structure during growth of the crystals by isomorphous replacement of net-forming elements. This form of occurrence of REE in rock-forming and other minerals is the most interesting in the studies of endogenic mineral formation.

We think that two most important forms of occurrence of REE in minerals are: (1) isomorphous, that is, structural impurities, by which we mean impurity elements that occur in the points or interstices of mineral crystal lattices in the positions where main (net-forming) elements) are located; and (2) nonstructural impurities, by which we mean impurity elements that are concentrated not directly in the mineral crystal lattice but in its different macro and micro defects, including those trapped (occluded) during the growth of crystals of melts and fluid microinclusions and nanoinclusions, as well as those adsorbed on the walls of microcracks of mineral grains and their outer surface. Figuratively, if information about the conditions of endogenic crystallization of minerals is "recorded" in the distribution of isomorphous REE impurities, then information about various later, including exogenic, processes is "recorded" in the distribution of their nonstructural impurities. This in no way minimizes the genetic significance of nonstructural forms of occurrence of impurity elements in crystallines, melts, and fluid inclusions, which are of interest as the source of information about the rare earth composition of those media from which mineral crystals could form.

As was shown in the previous chapters, some researchers think that the most important mechanism of accumulation of structural REE impurities in the lattice of silicate minerals is their isomorphous replacement of trivalent ions of net-forming Ca^{2+} ions. However, in certain conditions, some REE might have another valence. For example, under reducing conditions, most Eu ions can occur in a bivalent form, and Ce ions mainly occur in a tetravalent form under oxidizing conditions.

Isomorphism of REE in rock-forming minerals of ultramafic and mafic rocks in, most likely, all cases is heterovalent and was generally realized with participation of the ions of some additional elements, which played the part of charge compensators. With increasing general level of REE accumulation, the main minerals of ultramafic and mafic rocks form the following sequence: olivines → orthopyroxenes → plagioclases → clinopyroxenes → amphiboles. At the same time, depending on the composition of parental melts and rocks crystallized from them as well as on the crystallization conditions of minerals, the absolute contents of REE in each mineral species could range rather widely.

Olivine structure is the least favorable for the occurrence of structural impurities of REE, which can be accumulated in this mineral in minor amounts. This structure is

more favorable for the accumulation of heavy REE. Investigations show that olivines from ultramafic restites with a protogranular microstructure can reflect the character of primary REE distribution in this mineral more adequately than can the considerably deformed and recrystallized varieties of this mineral, which rare earth composition could be both depleted of structural impurities and enriched with nonstructural REE impurities owing to the infiltration of epigenetic fluids. Depletion of REE in olivines under deformation was a kind of "refinement" of their crystal lattices by way of diffusion removal of some amount of ions of these incompatible elements during its adaptation to changing P–T conditions of equilibrium.

The level of REE accumulation in orthopyroxenes is somewhat higher than that in olivines but at the same is 3–10 times lower than that in clinopyroxenes. The total REE content in most studied orthopyroxenes from ultramafic and mafic rocks are comparable or slightly higher than that in chondrite C1. The most REE-depleted orthopyroxenes are found in meteorites, and the most REE-enriched orthopyroxenes occur in acid effusives. Most of the structural REE impurities in orthopyroxenes that isomorphously replace Ca^{2+} ions are concentrated in clinopyroxene lamellas resulting from exsolution, providing a nonuniform distribution of these impurities within individual mineral grains. Orthopyroxenes from high-pressure ultramafic rocks reveal a more intense fractionation of REE due to a lower content of light elements. Moreover, there is evidence that in high-pressure lherzolites, the distribution of light REE between coexisting orthopyroxenes and clinopyroxenes is more variable than their distribution between these minerals from less deep varieties of rocks. This effect is probably due to the fact that at elevated pressures, larger ions of light REE are found to be less compatible with the orthopyroxene structure and, being accumulated in residual liquids, are incorporated in increased amounts into the structure of clinopyroxenes that crystallized later.

Clinopyroxenes are a more important source of geochemical information on the processes of formation of ultramafic and mafic rocks compared to other rock-forming minerals, as these minerals occur much more frequently in these rocks, and their structure can accumulate considerably greater amounts of REE than can the structure of other minerals. The total REE content in clinopyroxenes, similar to other parameters, varies widely, being dependent on rock composition and crystallization conditions of the mineral. For example, at simultaneous or later crystallization with respect to plagioclases, which selectively extracted light and middle REE, especially Eu, from melts, clinopyroxenes were depleted of these elements. This is well seen in the example of clinopyroxenes from meteorites and lunar mafic rocks that crystallized under drastically reducing conditions after formation of plagioclases. In turn, during crystallization of mafic melts under high pressures, the first to crystallize were garnets and orthopyroxenes, which selectively extracted heavy REE from these melts, depleted residual liquids in them. Therefore, clinopyroxenes that crystallized from these liquids somewhat later were substantially enriched with heavy elements. This can be seen in the example of clinopyroxenes from garnet peridotites occurring in deep xenoliths from the Udachnaya kimberlite pipe (Yakutia). Clinopyroxene crystals from plagioclase–olivine pyroxenites of the Gal'moenansky massif (Koryakia) are characterized by a zonal REE distribution; their outer zones contain considerably greater amounts of REE than do the inner zones, but the rare earth patterns of both inner and outer zones have the same configuration. This type of REE distribution in clinopyroxene crystals seems to

result from the fact that during their crystallization residual liquids were enriched uniformly with all REE. Clinopyroxenes from gabbros of the Ivrea Verbano massif are significantly enriched with light REE because, according to the researchers' interpretation, these rocks were crystallized from hybrid melts substantially contaminated by the substance of host terrigenous rocks (Mazzucchelli *et al.*, 1992a,b). Nevertheless, it is worth noting that Rivalenti *et al.*, (1996) report that representative analytical data on clinopyroxenes from peridotite characterizing both the subvolcanic and subcontinental mantle did not reveal any statistically important differences in REE distribution in these clinopyroxenes.

A very important geochemical feature of two-pyroxene rocks (lherzolites, websterites, and gabbro-norites) is the distribution coefficients of REE between coexisting clinopyroxenes and orthopyroxenes. As was mentioned above, the rather low variation of K_d(clinopyroxene/orthopyroxene) values and the corresponding close location of trends of changes with similar configuration in the samples selected within one and the same magmatic body may suggest that these two minerals under subfolder conditions reached a state of chemical equilibrium not disturbed by later processes. Finally, many clinopyroxenes might contain more or less significant amounts of nonstructural impurities of light REE. Most frequently, this structural impurity is observed in clinopyroxenes from deep ultramafic xenoliths, the evidence for which comes from the study of numerous samples of ultramafic samples in xenoliths from Polish alkaline-basaltoid provinces (Blusztajn & Shimizu, 1994).

Plagioclases and clinopyroxenes are known to widely occur in mafic and some ultramafic rocks, to say nothing of Mg-depleted magmatic rocks. Therefore, study of the regularities of REE in this mineral is of particular importance. As has already been reported, the total REE content in plagioclases ranges from a few ppm to a few tens of ppm. The level of accumulation of light elements in them, especially Eu, is much higher than that of heavy elements. The general level of REE accumulation in plagioclases increases in the series from their anorthite-rich varieties from ultramafic and mafic rocks, and from meteorites, to lower Ca varieties of mineral from alkaline gabbroid rocks, andesites, dacites, and rhyolites. In the geochemical systematization of plagioclases, rather efficient parameters are the level of Ce accumulation and the values of $(Eu/Eu^*)_n$ and $(Ce/Yb)_n$. Especially high $(Eu/Eu^*)_n$ values are typical of plagioclases from meteorites, lunar mafic rocks, and contaminated gabbroids. The lowest values of this parameter are found in the mineral from some varieties of gabbros and from plagiowehrlites. A particularly high intensity of positive Eu anomalies was established in plagioclases that crystallized under a very low oxygen volatility, for example in lunar mafic rocks and in meteorites. The $(Ce/Yb)_n$ values in plagioclases also vary in a wide range. Maximum values were established in plagioclases from contaminated gabbros of the Ivrea Verbano massif, and the lowest values are seen in the mineral from most gabbroids composing the massifs of ophiolitic associations and from lunar anorthosites. It is safe to say that during crystallization of plagioclases, the residual mafic liquids in all cases were significantly depleted in light REE, most of all Eu.

In spite of the secondary role of amphiboles in the composition of ultramafic and mafic rocks, this mineral might function as the main concentrator of structural REE impurities both in these and other genetic types of amphibole-bearing rocks. In the level of accumulation and character of REE distribution, two major types can be distinguished among amphiboles. The first type is amphiboles that are considerably enriched

with light and middle elements. Their patterns have a general negative slope and, as a rule, do not display Eu anomalies. These amphiboles mainly occur in metasomatically altered ultramafic restites from deep xenoliths and in rocks of some mafic–ultramafic massifs. It is assumed that the relative enrichment of these amphiboles with light and, partly, middle REE was promoted by their crystallization with active participation of light-REE- and middle-REE-enriched fluids separated from later mafic melts. The second geochemical type of amphiboles, which are more depleted of light REE and have a positive slope of patterns, at times complicated by negative Eu anomalies, is represented mainly in mafic–ultramafic massifs of varying composition. The negative Eu anomalies typical of these amphiboles are, most likely, due to the fact that they crystallized later than coexisting plagioclases and clinopyroxenes, which composition involves most of these element. The K_d(amphibole/melts) values for most REE successively increase in the series from basalt to andesite melts. In turn, the K_d(amphibole/clinopyroxene) values vary in a narrow range, slightly decreasing in the series from light to heavy REE. Those amphibole crystals that pseudomorphously replaced the crystals of earlier clinopyroxenes often inherit a considerable part of structural REE impurities of the latter, the quantitative ratios between separate elements being undisturbed. The trends of changes in K_d(amphibole/plagioclase) values often have a steep positive slope and are normally complicated by intense minimums for Eu. Those trends that are very compactly located on the plots can be used as evidence for the chemical equilibrium of co-existing amphiboles and plagioclases.

Afterword

Investigations into the geochemistry of REE in ultramafic and mafic rocks and in their minerals, which differ in scales, directions, and used procedures, have been carried out recently in various research institutes and laboratories of the world and have contributed, and are still contributing, significantly to the solution of many urgent petrological problems of magmatic formations. Active study of the distribution of decreased and very low concentrations of REE typical of most varieties of rock under consideration became possible owing to the development and introduction of a number of principally new analytical methods for REE analysis, providing the required detection limit of detectability of these elements. The available research data allowed, to some extent, the frames of discussions on some topical problems in the study of mafic–ultramafic magmatism to be restricted. They also preconditioned the development of new models of magma, mineral, and rock formation and the ability to gain better insight into the essence of processes and mechanisms responsible for the distribution and redistribution of REE as exceptionally informative geochemical indicators of magmatic processes. In this connection, noteworthy are the achievements in the study of interphase and intraphase distribution of REE in ultramafic and mafic rocks. It is obvious now that along with isomorphous, that is, structural, REE impurities, which replaces net-forming components in minerals, mainly Ca, and characterizes *endogenous processes* in rocks and minerals, very often but in various amounts there are *nonstructural* impurities of these elements concentrated in intergrain and intragrain microcracks as well as in various microinclusions, which is related to *exogenous processes*. Mainly represented by light REE, these nonstructural impurities can provide certain "disturbances" in interpreting analytical data and revealing the regularities of distribution of nonstructural REE impurities, which is the main source of related information on endogenic processes. In studying the geochemistry of mafic–ultramafic magmatism, such data as the general level of accumulation and character of REE distribution in ultramafic rocks and their minerals strongly depleted of these elements are very important because the present day models of melting processes of mantle sources and generation of compositionally different mantle sources are based on these data. Clinopyroxenes and garnets have been established as the most important REE concentrators in the upper mantle substrate, whereas orthopyroxenes, olivines, chrome-spinels, and other phases play a drastically subordinate role. Owing to the accumulated data on the distribution of REE in ultramafic restites from massifs and deep xenoliths, it is possible (at regional and interregional levels) to establish several types and subtypes among these rocks and their bodies. This helps to reveal and study the lateral heterogeneity of the upper mantle.

In addition, new geochemical data provides a possibility for discussing some problems related to the epigenetic changes in the trace element composition of ultramafic rocks, resulting from the infiltration of endogenic and exogenic fluids from different sources, with different time of occurrence and compositions. It is quite obvious that the U-shape of REE patterns typical of many ultramafic restites from massifs and deep xenoliths is a result of, mainly, an epigenetic supply of nonstructural light REE impurities.

Investigations into the geochemistry of REE in plutonic mafic rocks of various geological positions, material compositions, and formation conditions in subvolcanic rocks with increased Mg content, and in their major minerals, provide additional evidence that all these magmatic rocks formed as a result of multievent introduction, fractionation, contamination, and further crystallization of mantle melts with different chemical and rare earth compositions. These melts were generated at different degrees of partial melting of mantle sources, which also differ in material composition and depth of occurrence. On the basis of already available data and geochemical information obtained in the future, it will be possible to provide more detailed geochemical systematization of these magmatic rocks. Thorough studies of the nature of concentration and regularities of REE distribution within particular magmatic bodies will help to reveal geochemical heterogeneity of petrographically indistinguishable rocks and to provide additional possibility for the reconstruction of contamination of deep melts by the substance of surrounding rocks with varying compositions.

With further development of research in the field of REE geochemistry and the accompanying increase in the base of correct analytical data on all types and minerals of mafic–ultramafic complexes with different structures, substance compositions, and geodynamic history, their theoretical and petrogenetic interpretation, in our opinion, are topical problems of present day magmatic geology.

At the end of this book I want to cite a pertinent quotation from the famous French geochemist Show that "no research can be considered finished." Therefore, summing up the survey, I dare to formulate some of the most topical problems in studying the regularities of REE distribution in ultramafic and mafic rocks and their minerals, which solution will promote further progress in the research of mafic–ultramafic magmatism in its various manifestations:

- deepening of studies of regularities of endogenic distribution of REE in the whole series of petrographical varieties of rocks and minerals from multitype and standard mafic–ultramafic massifs and complexes;
- extension of ranges of experimental studies in the field of magmatogenic fractionation of REE with the aim to obtain more accurate values of distribution coefficients of REE in various "mineral/melt" and "mineral/mineral" systems for the most widespread mineral paragenesis and at a wide interval of P–T parameters;
- wider application of experimentally obtained values of K_d(mineral/melt) in modeling the rare earth compositions of parental melts for orthomagmatic mafic and ultramafic rocks and values of K_d(mineral/mineral) for diagnosing chemically equilibrium mineral paragenesis;
- conduction of complex studies in the field of geochemistry of REE and platinum group elements in ultramafic and mafic rocks for revealing the mechanisms responsible for their joint fractionation and "antagonism" both during partial melting of upper mantle sources and during crystallization of mantle melts;

- extension of ranges of investigations into the isomorphism and crystallochemistry of REE in rock-forming and accessory minerals from ultramafic and mafic rocks;
- conduction of special studies for revealing the features of distribution and mechanisms of concentration and scattering of nonstructural REE impurities (microcrack "contaminants," fluid microinclusions) in mafic and ultramafic rocks and their minerals; solutions of problems related to the validity of the results of analyses of isomorphous impurities of these elements, using various analytical methods, as only the level and character of distribution of these impurities of elements are a reflection of the real characteristics of endogenic processes of rock and mineral formation.

References

Agafonov, L.V. & Erkushev, Yu.A. (1984) Distribution of REE in the rocks of Shavaryn Tsaram volcano (Mongolia). *Geol Geofiz, 6*, 65–76 (in Rus.).

Agafonov, L.V. & Erkushev, Yu.A. (1985) *Connection of REE with Chemistry and Serpentinisation of Ultramafites. Geochemistry of REE in the Basalts and Ultramafites*. Novosibirsk: IGG SB AS USSR. pp. 86–98 (in Rus.).

Agafonov, L.V., Pinus, G.V., Lesnov F.P., *et al.* (1975) Deep nodules in the alkali basalts of pipe Shavaryn Tsaram. *Dokl AS USSR*, 224 (*5*), 1163–1165 (in Rus.).

Agafonov, L.V., Pinus, G.V., Lesnov, F.P., *et al.* (1977) Pyrope lherzolite xenoliths in the Cenozoic lavas of Central Hangay. General geological problems of Mongolia. Moscow: Nauka. 156–167 (in Rus.).

Agashev, A.M., Pohilenko, N.P. & Cherepanov, Yu.V. (2008) *Geochemical Evolution of Lithosphere Mantle Basis under the Kimberlitic Pipe Udachnaya according to Studying Xenoliths of Deformed Lherzolites. Petrologiya Lithosphery and a Diamond Origin*. Novosibirsk: Siberian Branch of the RAS. p. 7. (in Rus.).

Aitken, B.G. & Echeverria, L.M. (1984) Petrology and geochemistry of komatiites from Gorgona island, Columbia. *Contrib Mineral Petrol, 86*, 94–105.

Akella, J. & Boyd, F.R. (1972) *Partitioning of Ti and Al between Pyroxenes, Garnets and Oxides. Year Book 71*. Washington: Carnegie Institute. pp. 378–384.

Aleksiev, El. & Zheliazkova-Panayotova, M. (1971) REE in the ultramafites of Bulgaria. *Geokhimiya, 10*, 1254–1257 (in Rus.).

Alibert, C. & Albarede, F. (1988) Relationships between mineralogical, chemical and isotopic properties of some North American kimberlites. *J Geophys Res, 93* (B7), 7643–7671.

Amelin, Yu.V., Neymark, L.A., Ritsk, E.Yu. & Nemchin, A.A. (1996) Enriched Nd–Sr–Pb isotopic signature in the Dovyren layered intrusion (Eastern Siberia, Russia): Evidence for source contamination by ancient upper-crustal material. *Chem Geol, 129*, pp. 39–69.

Amelin, Yu.V., Ritsk, E.Yu. & Neymark, L.A. (1997) Effects of interaction between ultramafic tectonite and mafic magma on Nd–Pb–Sr isotopic systems in the neoproterozoic Chaya massif, Baykal-Muya ophiolite belt. *Earth Planet Sci Lett, 148*, 299–316.

Anders, E. & Grevesse, N. (1989) Abundances of the elements: Meteoritic and solar. *Geochim Cosmochim Acta, 53*, 197–214.

Andersen, D.L. (1981) Hotspots, basalts and evolution of the mantle. *Science, 213*, 125–133.

Andre, L. & Ashchepkov, I.V. (1996) *Acid Leaching Experiments on the Mantle Derived Vitim Clinopyroxenes: Implications for the Role of Clinopyroxenes in the Mantle Processes. Petrology and Geochemistry of Magmatic Suites of Rocks in the Continental and Oceanic Crust*. Tervuren: Royal Museum for Central Africa. pp. 321–336.

Ariskin, A.A. (2007) Paternal magmas of Moon's troctolites: Problems of genesis and valuation of primary composition. *Geokhimiya, 5*, 467–482 (in Rus.).

Arndt, N.T. (1977) Ultrabasic magma and high-degree malting of mantle. *Contrib Mineral Petrol, 64* (2), 205–221.

Arndt, N.T. (2003) Komatiites, kimberlites, and boninites. *J Geophys Res, 108* (B6), 2293.

Arndt, N., Lehnert, K. & Vasil'ev, Y. (1995) Meimechites: Highly magnesian lithosphere-contaminated alkali magmas from deep subcontinental mantle. *Lithos, 34* (1–3), 41–59.

Arth, J.G. (1976) Behavior of trace elements during magmatic processes—a summary of theoretical models and their applications. *J Res US Geol Serv, 4*, 41–47.

Arth, J.G. & Barker, F. (1976) Rare earth partitioning between hornblende and dacitic liquid and implication for the genesis of trondhjemitic-tonalitic magmas. *Geology, 4*, 534–536.

Ashchepkov, I.V. (2007) *Structure and Evolution of Lithospheric Mantle of Siberian Platform and Its Encirclement (Data of Termobarometry and Geochemistry of Depth including of Mantle Magmas). Abstract of Dissertation*. Novosibirsk: IGM SB RAS. 48 p. (in Rus.).

Babin, G.A. (2003) *Magmatism of Gornaya Shoria. Abstract of Dissertation*. Novosibirsk: UIGGM SB RAS. 24 p. (in Rus.).

Balashov, Yu.A. (1963) Differentiation of rare earth elements in magmatic processes. In: Vinogradov, A.P. (ed.) *Chemistry of the Earth's Crust*. Volume. 1. Moscow: Nauka. pp. 352–365 (in Rus.).

Balashov, Yu.A. (1976) Geochemistry of Rare Earth Elements. Moscow: Nauka. 268 p. (in Rus.).

Balashov, Yu.A., Frenkel, M.Ya. & Yaroshevsky, A.A. (1970) Influence of crystallochemical factor on the separation of rare earth elements in the processes of crystallize differentiation of silicates. *Geokhimiya*, 855–858 (in Rus.).

Barnes, S.J., Lesher, C.M. & Keays, R.R. (1995) Geochemistry of mineralised and barren komatiites from the Perseverance nickel deposit, Western Australia. *Lithos, 34*, 209–234.

Barth, M.G., Rudnick, R.L., Horn I., *et al.* (2002) Geochemistry of eclogites xenoliths from West Africa. Part 2: Origin of the high MgO eclogites. *Geochim Cosmochim Acta, 66* (24), 4325–4345.

Basu, A.R. (1978) Trace elements and Sr-isotopes in some mantle-derived hydrous minerals and their significance. *Geochim Cosmochim Acta, 42*, 659–668.

Batanova, V.G., Sobolev, A.V. & Sminke H.-U. (1996) Initial melts of intrusive cumulates of Troodos massif (Cyprus): Data of study clinopyroxenes and melt inclusions in plagioclases. *Petrologia, 4* (3), 272–282 (in Rus.).

Batanova, V.G., Suhr, G. & Sobolev, A.V. (1998) Origin of geochemical heterogeneity in the mantle peridotites from the Bay of Islands ophiolite, Newfoundland, Canada: Ion probe study of clinopyroxenes. *Geochim Cosmochim Acta*, 62 (5), 853–866.

Beard, A.D., Downes, H., Hegner, E., *et al.* (1998) Mineralogy and geochemistry of Devonian ultramafic minor intrusions of the southern Kola peninsula, Russia: Implications for the petrogenesis of kimberlites and melilites. *Contrib Mineral Petrol, 130*, 288–303.

Beard, A.D., Downes, H., Hegner, E. & Sablukov, S.M. (2000) Geochemistry and mineralogy of kimberlites from Arkhangelsk region, NW Russia: Evidence for transitional kimberlite magma types. *Lithos, 51* (1–2), 47–73.

Bekhtold, A.F., Kvasov, A.I. & Semionov, A.D. (1986) Geology, petrography and geochemistry of ophiolite of peninsula Kamchatsky point (West Kamchatka). *Tikh Geol, 6*, 78–84 (in Rus.).

Belousova, E.A., Griffin, W.L., O'Reilly, S.Y. & Fisher N.I. (2002) Apatite as indicator mineral for mineral exploration: Trace element compositions and their relationship to host rock type. *J Geochem Explor, 76*, 45–69.

Beswick, A.E. (1983) Praymery fractionation and secondary alteration within an archean ultramafic lava flow (Abitibi). *Contrib Mineral Petrol, 82* (2–3), 221–231.

Bindeman, I.N. & Bailey, J.C. (1999) Trace elements in anorthite megacrysts from the Kurile Island Arc: A window to across-arc geochemical variations in magma compositions. *Earth Planet Sci Lett, 169*, 209–226.

Bindeman, I.N., Davis, A.M. & Drake, M.J. (1998) Ion microprobe of plagioclase-basalt partition experiments natural concentration levels of trace elements. *Geochim Cosmochim Acta, 62* (7), 1175–1193.

Blusztajn, J. & Shimizu, N. (1994) The trace-element variations in clinopyroxenes from spinel peridotite xenoliths from southwest Poland. *Chem Geol, 111*, 227–243.

Bodinier, J.I., Dupuy, C. & Dostal, J. (1984) Geochemistry of Precambrian ophiolite from Bou Azzer, Morocco. *Contrib Mineral Petrol, 87*, 43–50.

Bodinier, J.L., Guiraud, M., Fabries, J., *et al.* (1987) Petrogenesis of layered pyroxenites from the Lherz, Freychinede and Prades ultramafic bodies (Ariege, French Pyrenees). *Geochim Cosmochim Acta, 51* (2), 279–291.

Bodinier, J.L., Dupuy, C. & Dostal, J. (1988) Geochemistry and petrogenesis of Eastern Pyrenean peridotites. *Geochim Cosmochim Acta, 52* (12), 2893–2907.

Bodinier, J.L., Vasseur, G., Vernieres, J., *et al.* (1990) Mechanisms of mantle metasomatism: Geochemical evidence from the Lherz orogenic peridotite. *J Petrol, 31* (Part 3), 597–628.

Bogatikov, O.A., Mikhailov, N.P. & Gon'shakova, V.I. (eds.) (1981) *Classification and Nomenclature of Magmatic Rocks*. Moscow: Nedra. 160 p. (in Rus.).

Bogatikov, O.A., Ryabchikov, I.D., Kononova, V.A., *et al.* (1991) *Lamproites*. Moscow: Nauka. 304 p. (in Rus.).

Bogatikov, O.A., Kononova, V.A., Pervov, V.A., *et al.* (2003) Perspective presence of diamond of the platform magmatic complexes of the West-European platform on result petrology–geochemistry analysis. Problem of prognostication, prospecting and study deposits minerals at threshold XXI century. Voronezh: Voronezh State University. pp. 356–365 (in Rus.).

Bogatikov, O.A., Kononova, V.A., Golubeva, Yu.Yu., *et al.* (2004) Petrochemistry and geochemistry variations of the composition of kimberlites of Yakutia and their causes. *Geokhimiya, 9*, 915–939 (in Rus.).

Borisov, A.A. (2005) Crystallization and stability of alloy of precious metals in magmatic processes. *Geol Rud Mest, 47* (6), 516–523 (in Rus.).

Bottazzi, P., Tiepolo, M., Vannucci, R., *et al.* (1999) Distinct site preference for heavy and light REE in amphibole and the prediction of $^{Amph/L}D_{REE}$. *Contrib Mineral Petrol, 137*, 36–45.

Boynton, W.V. (1984) Cosmochemistry of the rare earth elements: Meteorite studies. In: P. Henderson, P. (ed.) *Rare Earth Element Geochemistry*. Oxford: Elsevier. pp. 63–114.

Brenan, J.M., Shaw, H.F., Ryerson, F.J. & Phynney, D.L. (1995) Experimental determination of trace-element partitioning between pargasite and syntetic hydrous andesitic melt. *Earth Planet Sci Lett, 135*, 1–11.

Brookins, D.G. (1989) Aqueous geochemistry of rare earth elements. In: Lipin, B.R. & McKey, G.A. (eds.) *Geochemistry and Mineralogy of Rare Earth Elements. Reviews in Mineralogy*. Volume 21. Washington: Mineralogical Society of America. pp. 201–223.

Brumm, R.C., Foley, S., Tiepolo, M. & Vannucci R. (1998) Trace element distribution between richteritic amphiboles and silicate melts, and contrasts to their behaviour in calcic amphiboles. *Mineral Mag, 62a*, 250–251.

Buchko, I.V., Sal'nikova, E.B., Sorokin, A.A., *et al.* (2006) First data about age and geochemistry of rocks from Kengurak-Sergachinsky gabbro-anorthosites massif (south-west framing of Siberian craton). *Tikh Geol, 25* (2), 15–23 (in Rus.).

Buchko, I.V., Izokh, A.E., Sal'nikova, E.B., *et al.* (2007) Petrology of late Jurassic ultramafic-mafic Vesiolkinsky massif, south-west framing of Siberian craton. *Petrologia, 15* (3), 283–294 (in Rus.).

Burkov, V.V. (1990) Geochemistry same rare elements in kimberlitic crust of weathering. *Geochemical Methods of Prospecting of Non-metal Minerals*. Moscow: Publishing House of Institute Mineralogy and Geochemistry of Rare Elements of Academy of Sciences of USSR. pp. 16–21 (in Rus.).

Burkov, V.V. & Podporina, E.K. (1966) First data about rare earths in kimberlitic rocks. *Dokl AN USSR, 171* (4), 148–160 (in Rus.).

Campbell, I.H. (2002) Implications of Nb/U and Sm/Nd in plume magmas for the relationship between continental and oceanic crust formation and the development of the depleted mantle. *Geochim Cosmochim Acta, 66* (9), 1651–1661.

Chakhmouradian, A.R. & Mitchell, R.H. (1999) Niobian ilmenite, hydroxylapatite and sulfatian monazite: Alternative hosts for incompatible elements in calcite kimberlite from Internatsional'naya, Yakutia. *Can Mineral, 37* (5), 1177–1189.

Chalapathi Rao, N.V., Gibson, S.A., Pyle, D.M. & Dicken, A.P. (2004) Petrogenesis of proterozoic lamproites and kimberlites from Cuddapah Basin and Dharwar craton, Southern India. J Petrol, 45 (5), 907–948.

Chaschukhin, I.S., Ronkin, Yu.L. & Lepikhina, O.P. (2003) On influence early serpentinisation on the geochemistry of REE in harzburgites of Kempirsay massif. Annual-2002. Information collection. Ekaterinburg: IGG UrB RAS. pp. 243–249 (in Rus.).

Chistyakov, A.V., Sukhanov, M.K. & Bogatikov, O.A. (1997) The peculiarity of distribution rare and rare earth elements in the Burakovsky layered massif (South Karelia, Russia). *Dokl RAS, 356* (3), 376–381 (in Rus.).

Coleman, R.G. (ed.) (1979) *Ophiolites*. Moscow: Mir. 264 p. (in Rus.).

Coogan, L.A., Kempton, P.D., Saunders, A.D. & Norry, M.J. (2000) Melt aggregation within the crust beneath the Mid-Atlantic Ridge: Evidence from plagioclase and clinopyroxene major and trace element compositions. *Earth Planet Sci Lett, 176*, 245–257.

Coryell, C.D., Chase, J.W. & Winchester, J.W. (1963) A procedure for geochemical interpretation of terrestrial rare-earth abundance patterns. *J Geophys Res, 63* (2), 559–566.

Cox, C.G., Bell, J.D. & Pankherst, R.J. (1982) *Interpretation of Igneous Rocks*. Moscow: Nedra. 414 p. (in Rus.).

Cullers, R.L. & Graf, J.L. (1984a) Rare earth elements in igneous rocks of the continental crust: Predominantly basic and ultrabasic rocks. Chapter 7.2: Kimberlite. In: Henderson, P. (ed.) *Rare Earth Element Geochemistry*. Oxford: Elsevier. pp. 239–243.

Cullers, R.L. & Graf, J.L. (1984b) Rare earth elements in igneous rocks of the continental crust: Predominantly basic and ultrabasic rocks. Chapter 7.5: Komatiites and associated basic rocks. In: Henderson, P. (ed.) *Rare Earth Element Geochemistry*. Oxford: Elsevier. pp. 251–254.

Cullers, R.L., Mullenax, J., Dimarco, M.J. & Nordeng, S. (1982) The trace element content and petrogenesis of kimberlites in Riley county, Kansas, U.S.A. *Amer Mineral, 67* (3–4), pp. 223–233.

Dalpe, C. & Baker D.R. (1994) Partition coefficients for rare-earth elements between calcic amphibole and Ti-rich basanitic glass at 1,5 Gpa, 1100°C. *Abstract. V. M. Goldschmidt Conf.: Int. Conf. Adv. Geochem. Edinburgh*. pp. 207–210.

Dawson, J.B. (1962) Basutoland kimberlites. *Geol Soc Amer Bull, 73* (5), 545–560.

Dawson, J.B. (1983) *Kimberlites and Xenoliths in it*. Moscow: Mir. 300 p. (in Rus.).

Deer, W.A., Howie R.A. & Zussman, J. (1966) *Rock-forming Minerals*. Volume 4. Moscow: Mir. 482 p.

Dobretsov, N.L., Skliarov, E.V. & Ponomarchuk, V.A. (1985) Peculiarity of geochemistry of Lower Paleozoic ophiolites from south surrounding of Siberian platform. *Geochemistry of Rare Earth Elements in Mafic and Ultramafic Rocks*. Novosibirsk: Publishing House of Institute of Geology and Geophysics. Siberian Branch of Academy of Sciences of USSR. pp. 26–41 (in Rus.).

Dobretsov, N.L., Sobolev, N.V., Shatskiy, V.S., *et al.* (1989) *Eclogites and Glaucophane Schists in Folded Regions*. Novosibirsk: Nauka. 236 p. (in Rus.).

Dobosi, G., Jenner, G.A. & Embey-Isztin, A. (1998) Clinopyroxene/orthopyroxene trace element partition coefficients in spinel peridotite xenoliths. *Goldschmidt Conference* (Toulouse). pp. 393–394.

Dostal, J. & Muecke, G.K. (1978) Trace element geochemistry of the peridotite-gabbro-basalt suite from DSDP LEG 37. *Earth Planet Sci Lett, 40*, 415–422.

Downes, H. & Dupuy, C. (1987) Textural, isotopic and REE variations in spinel peridotite xenoliths, Massif Central, France. *Earth Planet Sci Lett, 82*, 121–135.

Downes, H., Upton, B.G.J., Handisyde, E. & Thirlwall, M.F. (2001) Geochemistry of mafic and ultramafic xenoliths from Fidra (Southern Uplands, Scotland): Implications for lithosphere processes in Permo-Carboniferous time. *Lithos, 58*, 105–124.

Drake, M.J. & Holloway, J.R. (1977) Partitioning Sm between plagioclase, clinopyroxene, amphibole, and hydrous silicate liquid at high pressure (Abstract). Papers Presented to the *International Conference on Experimental Trace Element Geochemistry*. pp. 21–23.

Drake, M.J. & Weill, D.F. (1975) Partition of Sr, Ba, Ca, Y, Eu^{3+}, Eu^{2+}, and other REE between plagioclase feldspar and magmatic liquid: An experimental study. *Geochim Cosmochim Acta, 39* (2), 689–712.

Dubinin, A.V. (2006) *Geochemistry of Rare Earth Elements in Ocean*. Moscow: Nauka. 360 p. (in Rus.).

Duchesne, J.C., Roelands, I., Demaiffe, D., *et al.* (1974) Rare earth data on monzonoritic rocks related to anorthosites and their bearing on the nature of the parental magma of the anorthosites series. *Earth Planet Sci Lett, 24* (2), 323–335.

Dudas, M.J., Schmitt, R.A. & Harward, M.E. (1971) Trace element partitioning between volcanic plagioclase and dacitic pyroclastic matrix. *Earth Planet Sci Lett, 11*, 440–446.

Dunn, T. & Sen C. (1994) Mineral/matrix partition coefficients for orthopyroxene, plagioclase and olivine in basaltic to andesitic systems: A combined analytical and experimental study. *Geochim Cosmochim Acta, 58* (2), 717–733.

Dupuy, C., Liotard, J.M. & Dostal, J. (1992) Zr/Hf fractionation in intraplate basaltic rocks: Carbonate metasomatism in the mantle source. *Geochim Cosmochim Acta, 56*, 2417–2423.

Echeverria, L.M. (1980) Tertiary or Mezozoic komatiites from Gorgona Island, Columbia: Field relations and geochemistry. *Contrib Mineral Petrol, 73*, 253–266.

Edwards, D., Rock, N.M.S., Taylor, W.R., *et al.* (1992) Mineralogy and petrology of the Aties diamondiferous kimberlite pipe, central Kimberley block, Western Australia. *J Petrol, 33* (5), 965–1005.

Eggins, S.M., Rudnick, R.L. & McDonough, W.F. (1998) The composition of peridotites and their minerals: A laserablation ICP-MS study. *Earth Planet Sci Lett, 154*, 53–71.

Egorov, K.N. (2006) Geochemistry (ICP-MS) and mantle source of kimberlites from north-east Angola. *Otech Geol, 2*, 20–28. (in Rus.).

Elton, D. (1984) Plagioclase buoyancy in oceanic basalts: Chemical effect. *Geochim Cosmochim Acta, 48* (2), 753–768.

Erkushev, Yu.A. (1985) *Geochemistry of Rare Earth Elements in Ophiolite of Mongolia (Data Neutron-Activation Analysis). Abstract of Dissertation*. Novosibirsk: IGG SB AS USSR. 18 p. (in Rus.).

Evensen, N.M., Hamilton, P.J. & O'Nions, R.K. (1978) Rare earth abundances in chondrite meteorites. *Geochim Cosmochim Acta, 42*, 1199–1212.

Fedorov, P.I., Koloskov, A.V. & Lyapunov, S.M. (1993) Deep xenoliths from alkali basalts of cape Navarin (east of Koryak highland). *Dokl RAS, 333* (2), 246–249 (in Rus.).

Fershtater, G.B. & Bea, F. (1996) Geochemical systematic of Ural ophiolite. *Geokhimiya, 3*, 195–218 (in Rus.).

Fershtater, G.B., Bea, F., Borodina, N.S. & Montero, P. (1998) Lateral zonation, evolution and geodynamic interpretation of Ural magmatism on the light of new petrological and geochemical data. *Petrologia, 6* (7), 451–477 (in Rus.).

Fershtater, G.B., Krasnobaev, A.A., Bea F., *et al.* (2009) Isotopic-geochemistry peculiarity and age of zircons from the dunites of Ural platinum-bearing massifs, petrogenetic consequences. *Petrologia, 17* (5), 539–558 (in Rus.).

Fesq, H.W., Kable, E.J. & Gurney, J.J. (1975) Aspects of geochemistry of kimberlites from the Premier Mine and other South Africa occurrences, with particular reference to the rare earth elements. *Phys Chem Earth, 9*, 687–707.

Fieremans, M., Hertogen, J. & Demaiffe, D. (1984) Petrography, geochemistry and strontium isotopic composition of the Mbuji-Mayi and Kundelungu kimberlites (Zaire). In: Kornprobst, J. (ed.) *Kimberlites. Part I: Kimberlites and Related Rocks*. Amsterdam: Elsevier. pp. 110–120.

Floss, C., James, O.B., McGee, J.J. & Crozaz, G. (1998) Lunar ferroan anorthosites petrogenesis: Clues from trace element distributions in FAN subgroup. *Geochim Cosmochim Acta, 62* (7), 1255–1283.

Foley, S.F., Jackson, S.E., Fryer, B.J., Greenough, J.D. & Jenner, G.A. (1996) Trace element partition coefficients for clinopyroxene and phlogopite in an alkaline lamprophyre from Newfoundland by LAM-ICP-MS. *Geochim Cosmochim Acta, 60* (4), 629–638.

Frey, F.A. (1966) Rare earth elements in basic and ultrabasic rocks. Ph.D. Dissertation. University of Wisconsin.

Frey, F.A. (1969) Rare earth abundances in a high-temperature peridotite intrusion. *Geochim Cosmochim Acta, 33* (11–12), 1429–1449.

Frey, F.A. (1984) Rare earth element abundances in upper mantle rocks. In: Henderson, P. (ed.) *Rare Earth Element Geochemistry*. Oxford: Elsevier. 153–203.

Frey, F.A. & Green, D.H. (1974) The mineralogy, geochemistry and origin of lherzolite inclusions in Victorian basanites. *Geochim Cosmochim Acta, 38* (7), 1023–1059.

Frey, F.A. & Prinz, M. (1978) Ultramafic inclusions from San Carlos, Arizona: Petrologic and geochemical data bearing on their petrogenesis. *Earth Planet Sci Lett, 38*, 129–176.

Frey, F.A., Haskin, L.A. & Haskin, M.A. (1971) Rare earth abundances in some ultramafic rocks. *J Geophys Res, 76* (8), 2057–2070.

Frey, F.A., Suen, C.J. & Stockman, H.W. (1985) The Ronda light temperature peridotite: Geochemistry and petrogenesis. *Geochim Cosmochim Acta, 49* (11), 2469–2491.

Frey, F.A., Shimizu, N., Leinbach, A., *et al.* (1991) Compositional variations within the lower layered zone of the Horoman peridotite, Hokkaido, Japan: Constraints on models for melt-solid segregation. *J Petrol (Special lherzolites issue)*, 211–227.

Fujimaki, H., Tatsumoto, M. & Aoki, K. (1984) Partition coefficients of Hf, Zr and REE between phenocrysts and groundmass. Proc. 14th Lunar Planet. Sci. Conf. Part 2. *J Geophys Res, 89* (Suppl.), B662–B672.

Garrido, C., Bodinier, J.-L. & Alard, O. (2000) Incompatible trace element partitioning and residence in anhydrous spinel peridotites and websterites from the Ronda orogenic peridotite. *Earth Planet Sci Lett, 181*, 341–358.

Garvella, F. & Remaidi, M. (1993) Field trip to Ronda ultramafic massif: An example of asthenosphere–lithosphere interaction? *Ofioliti, 18*, 21–35.

Gebauer, D., Lappin, M.A., Grunenfelder, M. & Wittenbrach, A. (1985) The age and origin of some Norwegian eclogites: A U-Pb zircon and REE study. *Chem Geol, 52* (2), 227–247.

Girnis, A.B. & Ryabchikov, I.D. (2005) Conditions and mechanism of generation kimberlitic magmas. *Geol Rud Mest, 47* (3), 524–536 (in Rus.).

Giunta, G., Beccaluva, L., Coltorti, M., *et al.* (2002) The southern margin of Caribbean Plate in Venezuela: Tectonomagmatic setting of the ophiolite units and kinematic evolution. *Lithos, 63* (1–2), 19–40.

Gladkikh, V.C., Gusev, G.S., Peskov, A.I., *et al.* (1998) Peridotites of Paramsky massif (Baykal-Patom region). *Sovet Geol, 5*, 89–96 (in Rus.).

Godard, M., Jousselin, D. & Bodinier, J.-L. (2000) Relationships between geochemistry and structure beneath a paleospreading centre: A study of mantle section in the Oman ophiolite. *Earth Planet Sci Lett, 180*, 133–148.

Goles, G.G. (1968) *Rare earth geochemistry of pre-Cambrian plutonic rocks*. International Geological Congress. Report of the Twenty-Third Session. Proceedings of 6. Geochemistry. pp. 237–249.

Golubeva, Yu.Yu., Ovchinnikova, G.V. & Levsky, L.K. (2004) Pb–Sr–Nd-isotopic characteristic of mantle sources Nankin field (Yakutia). *Dokl RAS, 394* (6), 796–800 (in Rus.).

Goncharenko, A.I. (1989) *Deformation and Structural Evolution of Alpinotype Ultramafites*. Tomsk: Tomsk State University. 400 p. (in Rus.).

Gorbachov, N.S., Kost'uk, A.V. & Nekrasov, A.N. (2006a) Mantle–crust interaction and generation of magmas. Annual seminar on experimental mineralogy, petrology and geochemistry (BSEMPG). Abstracts. Moscow: GEOKHI RAS. pp. 19–20 (in Rus.).

Gorbachov, N.S., Kost'uk, A.V., Nekrasov, A.N. (2006b) On unolivine source of magnesium mantle magmas. Annual seminar on experimental mineralogy, petrology and geochemistry (BSEMPG). Abstracts. Moscow: GEOKHI RAS. pp. 20–21 (in Rus.).

Green, T.H. (1994) Experimental studies of trace-element partitioning applicable to igneous petrogenesis—Sedona 16 years latter. *Chem Geol, 117*, 1–36.

Green, T.H. & Pearson, N.J. (1985) Experimental determination of REE partition coefficients between amphibole and basaltic to andesitic liquids at high pressure. *Geochim Cosmochim Acta, 49* (6), 1465–1468.

Green, D.H. & Ringwood, A.E. (1968) *Origin of Basaltic Magma. Petrology of Upper Mantle*. Moscow: Mir. pp. 132–227 (in Rus.).

Greenwood, J.C., Gibson, S.A., Thompson, R.N., *et al.* (1999) Cretaceous kimberlites from the Paranatinga-Batovi region, Central Brazil: Geochemical evidence for subcratonic lithosphere mantle heterogeneity. *Proc. 7th Int. Kimberlite Conference (Cape Town, 1999)*. Volume 1. pp. 291–298.

Griffin, W.L. & Brueckner, H.K. (1985) REE and Rb-Sr and Sm-Nd studies of Norwegian eclogites. *Chem Geol, 52* (2), 249–271.

Griffin, W.L., Sundvoll, B. & Kristmannsdottir, H. (1974) Trace element composition of anorthosites plagioclase. *Earth Planet Sci Lett, 24*, 213–223.

Gruau, G., Bernard-Griffiths, J. & Lecuyer, C. (1998) The origin of U-shaped rare earth patterns in ophiolite peridotites: Assessing the role of secondary alteration and melt/rock reaction. *Geochim Cosmochim Acta, 62*, 3545–3560.

Grutzeck, M., Kridelbaugh, S. & Weill, D. (1974) The distribution of Sr and REE between diopside and silicate liquid. *Geophys Res Lett, 1*, 273–275.

Halliday, A.N., Lee, D.-C., Tommasiny, S., *et al.* (1995) Incompatible trace elements in OIB and MORB and source enrichment in the sub-oceanic mantle. *Earth Planet Sci Lett, 133*, 379–395.

Hanski, E., Walker, R.J., Huhma, H., *et al.* (2004) Origin of Permian–Triassic kimberlites, northwestern Vietnam. *Contrib Mineral Petrol, 147*, 453–469.

Hanson, G.N. (1980) Rare earth elements in petrogenetic studies of igneous systems. *Annual Rev Earth Planet Sci, 8*, 371–406.

Harnois, L. & Morency, M. (1989) Geochemistry of Mount Orford ophiolite complex, Northern Appalachians, Canada. *Chem Geol, 77*, 133–147.

Harnois, L., Trottier, J. & Morency, M. (1990a) Rare earth element geochemistry of Thetford Mines ophiolite complex, Northern Appalachians, Canada. *Contrib Mineral Petrol, 105*, 433–445.

Harnois, L., Mineau, R. & Morency, M. (1990b) Rare element geochemistry of alnoitic Cretaceous rocks and ultramafic xenoliths from Ile Bizard (Quebec, Canada). *Chem Geol, 85*, pp. 135–145.

Harrison, W.J. (1981) Partitioning of REE between minerals and coexisting melts during partial melting of a garnet lherzolite. *Amer Mineral, 66*, pp. 242–259.

Hartmann, G. & Wedepohl, K.H. (1993) The composition of peridotite tectonites from the Ivrea Complex, northern Italy: Residues from melt extraction. *Geochim Cosmochim Acta, 57*, 1761–1782.

Haskin, L.A. & Frey, F.A. (1966) Dispersed and not-so-rare earths. *Science, 152*, p. 299.

Haskin, L.A. & Haskin, M.A. (1968) Rare-earth elements in Skaergaard intrusion. *Geochim Cosmochim Acta, 32*, pp. 433–447.

Haskin, L.A., Frey, F.A., Schmitt, R.A. & Smith, R.H. (1966) Meteoritic, solar and terrestrial rare-earth distributions. *Phys Chem Earth, 7*, pp. 169–321.

Haskin, L.A., Haskin, M.A., Frey, F.A. & Wildeman, T.R. (1968) Relative and absolute terrestrial abundances of the rare earths. In: Ahrens, L.H. (ed.) *Origin and Distribution Elements*. Oxford: Pergamon Press. pp. 889–912.

Hassanipak, A.A., Ghazi, A.M. & Wampler, J.M. (1996) Rare earth element characteristics and K-Ar ages of the Band Ziarat ofiolite complex, southeastern Iran. *Can J Earth Sci, 33*, 1534–1542.

Helz, R.T. (1985) Compositions of fine-grained mafic rocks from sills and dikes associated with the Stillwater complex. The Stillwater complex, Montana: Geology and guide. *Special Publication, 92*, 97–117.

Henderson, P. (ed.) (1984) *Rare Earth Element Geochemistry*. Oxford: Elsevier. Volume 2. 510 p.

Henderson, P. (1985) *Inorganic Geochemistry*. Moscow: Mir. 340 p. (in Rus.).

Herrmann, J. & Muntener, O. (1999) Differentiation of mafic magma in a continental crust-to-mantle transition zone (Val Malenco, Alps). *Ofioliti, 24* (1a), 108–109.

Herrmann, A.G., Blanhard, D.P., Haskin, L.A., *et al.* (1976) Major, minor and trace element compositions of peridotitic and basaltic komatiites from Precambrian crust of Southern Africa. *Contrib Mineral Petrol, 59* (1), 1–12.

Higgins, M.D. & Doig, R. (1986) Geochemical constraints on the differentiation processes that were active in the Sept Iles complex. *Can J Earth Sci, 23*, 670–681.

Higuchi, H. & Nagasawa, H. (1969) Partition of trace elements between rock-forming minerals and the host volcanic rocks. *Earth Planet Sci Lett, 7*, 281–287.

Himmelberg, G.R. & Loney, R.A. (1995) Characteristics and petrogenesis of Alaskan-type ultramafic-mafic intrusions, Southeastern Alaska. *J Res US Geol Surv Profes Paper, 1564*, 1–47.

Honda, M. & Shima, M. (1967) Distribution of rare earths among component minerals of Bruderheim chondrite. *Earth Planet Sci Lett, 2* (4), 344–348.

Humphris, S.E. (1984) The mobility of the rare earth elements in the crust. In: Henderson, P. (ed.) *Rare Earth Element Geochemistry*. Oxford: Elsevier. pp. 317–342.

Ilupin, I.P., Varshal, G.M., Pavlutskaya, V.I. & Kalenchuk, G.E. (1974) Rare earth elements in kimberlites of Yakutia. *Geochimiya, 1*, 126–131 (in Rus.).

Ilupin, I.P., Kaminsky, F.V. & Frantsesson, E.V. (1978) *Geochemistry of Kimberlites*. Moscow: Nedra. 352 p. (in Rus.).

Ionov, D.A. (1988a) Xenoliths in basalts of continents. In: Laz'ko, E.E. & Sharkov, E.V. (eds.) *Magmatic Rocks. Ultramafic Rocks*. Volume 5. Moscow: Nauka. pp. 311–332 (in Rus.).

Ionov, D.A. (1988b) Xenoliths in basalts of oceans. In: Laz'ko, E.E. & Sharkov, E.V. (eds.) *Magmatic Rocks. Ultramafic Rocks*. Volume 5. Moscow: Nauka. pp. 332–346 (in Rus.).

Ionov, D.A., Aschepkov, I.V., Stosch, H.-G., *et al.* (1993a) Garnet peridotite xenoliths from the Vitim volcanic field, Baikal region: The nature of the garnet-spinel peridotite transition zone in continental mantle. *J Petrol, 34*, 1141–1175.

Ionov, D.A., Dupuy, C., O'Reilly, S.Y., *et al.* (1993b) Carbonated peridotite xenoliths from Spitsbergen: Implication for trace element signature of mantle carbonate metasomatism. *Earth Planet Sci Lett, 119*, 283–297.

Ionov, D.A., Hofmann, A.W. & Shimizu, N. (1994) Metasomatism-induced melting in mantle xenoliths from Mongolia. *J Petrol, 35* (Part 3), 753–785.

Ionov, D.A., O'Reilly, S.Y. & Ashchepkov, I.V. (1995a) Feldspar-bearing lherzolite xenoliths in alkali basalts from Khamar-Daban, Southern Baikal region, Russia. *Contrib Mineral Petrol, 105*, 433–445.

Ionov, D.A., Prikhod'ko, V.S. & O'Reily, S.Y. (1995b) Peridotite xenoliths in alkali basalts from the Sikhote-Alin', Southeastern Siberia, Russia: Trace-element signature of mantle beneath a convergent continental margin. *Chem Geol, 120*, 275–294.

Irving, A.J. (1978) Review of experimental studies of crystal/liquid trace element partitioning. *Geochim Cosmochim Acta, 42a* (6a, Part 2), 743–770.

Irving, A.J. & Frey, F.A. (1984) Trace element abundance in megacrysts and their host basalts: Constraints on partition coefficients and megacryst genesis. *Geochim Cosmochim Acta, 48* (6), 1201–1221.

Irving, A.J. & Price, R.C. (1981) Geochemistry and evolution of lherzolite-bearing phonolitic lavas from Nigeria, Australia, East Germany and New Zealand. *Geochim Cosmochim Acta, 45* (8), 1309–1320.

Itoh, S., Terashima, S., Imai, N., *et al.* (1992) 1992 compilation of analytical data for rare earth elements, scandium, ytrium, zirconium and hafnium. *Bull Geol Surv Japan, 43* (11), 659–733.

Itoh, S., Terashima, S., Imai, N., *et al.* (1993) 1992 compilation of analytical data for rare earth elements, scandium, yttrium, zirconium and hafnium in twenty-six GSJ reference samples. *Geostand Newslett, 1*, 5–79.

Ivanov, O.K. (1997) *Cyrcum-Zonary Pyroxenites-Dunite Massifs of Ural*. Ekaterinburg: Ural State University. 488 p. (in Rus.).

Izokh, A.E., Polyakov, G.V., Gibsher, A.S., *et al.* (1998) High aluminiumferous layered gabbros of Central-Asia folded belt: Geochemical peculiarity, Sm-Nd isotopic age and geodynamic conditions of forming. *Geol Geofiz, 39* (11), 1565–1577 (in Rus.).

Jahn, B., Gruau, G. & Glikson, A.Y. (1982) Komatiites of the Onverwacht group, S. Africa: REE geochemistry, Sm/Nd age and mantle evolution. *Contrib Mineral Petrol, 80*, 25–40.

Jaques, A.L., Lewis, J.D., Smith, C.B., *et al.* (1984) The diamond ultrapototassic (lamproitic) rocks of the west Kimberley region, Western Australia. In: Kornprobst, J. (ed.) *Kimberlites. Part I: Kimberlites and Related Rocks*. Amsterdam: Elsevier. pp. 225–254.

Jedwab, J. (1953) Sur la définition des éléments typochimiques. *Bull Soc Geol Belg paleo et d'hydrol, 62*, 173–179.

Jia, Y., Kerrich, R., Gupta, A.K. & Fyfe, W.S. (2003) ^{15}N-enriched Gondwana lamproites, eastern India: Crustal N in the mantle source. *Earth Planet Sci Lett, 215*, 43–56.

Jochum, K.P., Arnd, N.T. & Hofman, A.W. (1991) Nb-Th-La in basalts: Constraints on komatiite petrogenesis and mantle evolution. *Earth Planet Sci Lett, 107*, 272–289.

Johnson, K.T.M. (1998) Experimental determination of partition coefficients for rare earth and high-field-strength elements between clinopyroxene, garnet, and basaltic melt at high pressures. *Contrib Mineral Petrol, 133*, 60–68.

Johnson, K.T.M. & Dick, H.J.B. (1992) Open system melting and spatial variation of peridotite and basalt at the Atlantis II fracture zone. *J Geophys Res, 97* (B6), 9219–9241.

Jolliff, B.L., Floss, C., McCallum, I.S. & Schwartz, J.M. (1999) Geochemistry, petrology, and cooling history of 14161, 7373: A plutonic lunar sample with textural evidence of granitic-fraction separation by silicate-liquid immiscibility. *Amer Mineral, 84* (5–6), 821–837.

Kaminsky, F.V., Sazonov, O.F. & Frantsesson, E.V. (1978) On contents of rare earth elements in kimberlites and nodules. *Geokhimiya, 7*, 1088–1094 (in Rus.).

Kargin, A.V., Golubeva, G.G, Bogatikov, O.A. & Kononkova, V.A. (2008) On the nature of rare earth elements heterogeneity in complicate constructed pipes of Daldyn-Alakit area (Yakutia). *Dokl RAS, 41* (4), 516–519 (in Rus.).

Kay, R.W. & Senechal, R.G. (1976) The rare earth geochemistry of Troodos ophiolite complex. *J Geophys Res, 81* (5), 964–970.

Kennedy, A.K., Lofgren, G.E. & Wasserburg, G.J. (1993) An experimental study of trace element partitioning between olivine, orthopyroxene and melt in chondrules: Equilibrium values and kinetic effects. *Earth Planet Sci Lett, 115*, 177–195.

Khisina, N.R. & Virt, R. (2005) Residence forms of OH^- and peculiarity of mantle olivine IR-patterns. *Spectroscopy, Rentgenology and Crystallochemistry of Minerals*. Kazan: Kazan State University. pp. 251–252 (in Rus.).

Kislov, E.V. (1998) Ioko-Dovirensky layered massif. Ulan-Ude: BNC SB RAS. 265 p. (in Rus.).

Kogarko, L.N. & Ryabchikov, I.D. (1995) Conditions of generation of mimechite magmas (Polar Siberia) on geochemical data. *Geokhimiya, 12*, 1699–1709 (in Rus.).

Kogarko, L.N., Karpenko, S.F., Lialikov, A.V. & Teplev, M.G. (1988) Isotopic criterion of meimechite magmatism's genesis. *Dokl SA USSR, 301* (4), 939–942 (in Rus.).

Konnikov, E.G., Nekrasov, A.N., Orsoev, D.A., Khantsuan', Ya. & Slaogou, Ch. (2009) Garnet-bearing basites of Kuvalorog massif, Kamchatka. *Geol Geofiz, 50* (5), 595–612 (in Rus.).

Kovalenko, V.I., Ryabchikov, I.D. & Stosch, H.G. (1989) Geochemistry of rare earth elements in nodules of lherzolites: Model of primitive mantle. *Geochimiya, 6*, 771–784 (in Rus.).

Kovaliova, V.A. & Anoshin, G.N. (1996) Radiochemical neutron-activation determination of the rare earth elements in the ultramafic rocks. Analitica of Siberia and Far East. *Proceeding of 5th Conference*. Novosibirsk. pp. 134–135.

Kravchenko, S.M. (2002) Lower ore-bearing horizon of Tomtor massif (Polar Siberia)—carbonaceoused volcanites—lamproites. *Dokl RAS, 386* (3), 362–367 (in Rus.).

Krivolutskaya, N.A., Sobolev, A.V. & Kuz'min, D.V. (2006) Peculiarity of olivine composition from ore-bearing and nonore-bearing massifs of Noril'sk region. *Actual Problems of Ore Formation and Metallogeny*. Novosibirsk: Academic Publishing House "GEO". pp. 121–122 (in Rus.).

Kuechner, S.M., Laughlin, J.R., Grossman, L., *et al.* (1989) Determination of trace element mineral/liquid partition coefficients in melilite and diopside by ion and electron microprobe techniques. *Geochim Cosmochim Acta, 53* (12), 3115–3130.

Kurat, G., Palme, H., Spettel, B., *et al.* (1980) Geochemistry of ultramafic xenoliths from Kapfenstein, Austria: Evidence for a variety of upper mantle processes. *Geochim Cosmochim Acta, 44*, 45–60.

Kutolin, V.A. (1972) *Problems of Petrochemistry and Petrology of Basalts*. Novosibirsk: Nauka. 200 p. (in Rus.).

Lambert, D.D. & Simmons, E.C. (1987) Magma evolution in the Stillwater complex, Montana. Part I: Rare-earth element evidence for the formation of the ultramafic series. *Amer J Sci, 287*, 1–32.

Lambert, D.D. & Simmons, E.C. (1988) Magma evolution in the Stillwater, Montana. Part II. Rare earth element evidence for the formation of the J-M reef. *Econ Geol, 83* (6), 1109–1126.

Larsen, L.M. & Rex, D.C. (1992) A review of the 2500 Ma span of alkaline-ultramafic, potassic and carbonatitic magmatism in West Greenland. *Lithos, 28* (3–6), 367–402.

La Tourrette, T., Herving, R.L. & Holloway, J.R. (1995) Trace element partitioning between amphibole, phlogopite, and basanite melt. *Earth Planet Sci Lett, 135*, 13–30.

Laurora, A., Rivalenti, G., Mazzucchelli M., *et al.* (1999) Carbonated peridotite xenoliths from mantle wedge: The Patagonia case. *Ofioliti, 24* (1a), 123–124.

Lavrenchuk, A.V. (2003) *Petrology of Chernosopkinsky Syenite—Alkali Gabbroic Complex (East Sayan). Abstract of Dissertation*. Novosibirsk: UIGGM SB RAS. 24 p. (in Rus.).

Lazarenkov, V.G., Balmasova, E.A., Vaganov, P.F. & Onischina Y.M. (1989) Distribution of precious metals an rare earth elements in chromitite of Burakovsko-Aganoziorsky massif. *Proceeding LSU, Series 7*, (4), 68–70 (in Rus.).

Laz'ko, E.E. (1988a) Kimberlites. In: Laz'ko, E.E. & Sharkov, E.V. (eds.) *Magmatic Rocks. Ultramafic Rocks*. Volume 5. Moscow: Nauka. pp. 196–217 (in Rus.).

Laz'ko, E.E. (1988b) Ultramafic rocks of ophiolite. In: Laz'ko, E.E. & Sharkov, E.V. (eds.) *Magmatic Rocks. Ultramafic Rocks*. Volume 5. Moscow: Nauka. pp. 8–96 (in Rus.).

Laz'ko, E.E., Sharkov, E.V. & Markovsky, B.A. (1988) The problems of genesis of ultramafic rocks. In: Laz'ko, E.E. & Sharkov, E.V. (eds.) *Magmatic Rocks. Ultramafic Rocks*. Volume 5. Moscow: Nauka. pp. 442–486 (in Rus.).

Leake, B.E. (1978) Nomenclature of amphiboles. *Mineral Mag, 42*, 533–563.

Ledniova, G.V. (2001) Geochemistry, conditions and mechanism of rock's origin layered dunite-clinopyroxenite-gabbros series (on example Seinavsky massif, Oliutor zona, Koryakia). *Petrology and Metallogeny of Basic-Ultrabasic Complexes of Kamchatka*. Moscow: Publishing House Nauchny Mir. pp. 32–63 (in Rus.).

Lesher, C.M. & Arndt, N.T. (1995) REE and Nd-isotope geochemistry, petrogenesis and volcanic evolution of contaminated komatiites at Kambalda, Western Australia. *Lithos, 34* (3–4), pp. 127–157.

Lesnov, F.P. (1976) On structure-texture criterion of effect of gabbros on ultramafites in the mafic-ultramafic plutons of folded regions. *Documents on Genetic and Experimental Mineralogy*. Volume 10. Novosibirsk: Nauka, pp. 75–80 (in Rus.).

Lesnov, F.P. (1981a) *Platy Cleavage in the Ultramafites and Problems of Genesis Banded Structures in Rocks of Polygenic Mafic-Ultramafic Plutons. Questions of Genetic Petrology.* Novosibirsk: Nauka. pp. 205–213 (in Rus.).

Lesnov, F.P. (1981b) *Structure-Genetically Relationship of Ultramafites and Gabbros in the Ophiolite Belts of Mongolia. Questions of Magmatism and Metallogeny MPR*. Novosibirsk: IGG SB AS USSR. pp. 62–72 (in Rus.).

Lesnov, F.P. (1982) *Naransky Polygenic Mafic-Ultramafic Pluton (West Mongolia). Ultramafic Associations of Folded Regions*. Issue 1. Novosibirsk: IGG. SB AS USSR. pp. 58–95 (in Rus.).

Lesnov, F.P. (1983) *The Xenoliths of Ultramafites and Gabbros and Questions of Genesis of Polygenic Mafic-Ultramafic Plutons. Mantle Xenoliths and Problems of Ultramafic Magmas*. Novosibirsk: Nauka. pp. 34–38 (in Rus.).

Lesnov, F.P. (1984) Petrology of polygenic mafic-ultramafic plutons. *Proceeding of AS USSR. Geol Series, 2*, 71–78 (in Rus.).

Lesnov, F.P. (1986) *Petrochemistry of Polygenic Mafic-Ultramafic Plutons of Folded Regions*. Novosibirsk: Nauka. 136 p. (in Rus.).

Lesnov, F.P. (1988) *Petrology of Polygenic Mafic-Ultramafic Plutons of Folded Regions. Abstract of Dissertation*. Novosibirsk: IGG SB AS USSR. 48 p. (in Rus.).

Lesnov, F.P. (1991) *The Plagioclases from Polygenic Mafic-Ultramafic Plutons*. Novosibirsk: Nauka. 112 p. (in Rus.).

Lesnov, F.P. (1999) *Geochemistry of Rare Earth Elements in Olivines (Short Survey). Questions of Petrology, Mineralogy, Geochemistry and Geology of Ophiolite*. Kyzil: IG SB RAS. pp. 95–114 (in Rus.).

Lesnov, F.P. (2000a) *The regularities of REE distribution in olivines*. Reports of Russian Mineralogy Society, 6, 88–103 (in Rus.).

Lesnov, F.P. (2000b) On REE geochemistry in plagioclases from gabbros of Beriozovsky mafic-ultramafic massif (Sakhalin island). *Petrology and Metallogeny of Kamchatka Mafic-Ultramafic Complexes*. Petropavlovsk-Kamchatsky: Publishing House Nauchny Mir. pp. 51–52 (in Rus.).

Lesnov, F.P. (2000c) On REE concentration in the plagioclases of different composition and genesis. *Petrology of Magmatic and Metamorphic Complexes*. Tomsk: Tomsk State University. pp. 38–42 (in Rus.).

Lesnov, F.P. (2000d) REE in plagioclases: Certain regularities. *Geologichna nauka ta osvita v Ukrainy na mezhi tysiacholit*. Lviv: Lviv National University. p. 67 (in Ukrainian).

Lesnov, F.P. (2001a) Geochemistry of rare earth elements in the plagioclases. *Geol Geofiz, 42* (6), 917–936 (in Rus.).

Lesnov, F.P. (2001b) *Regularities of REE distribution in orthopyroxenes*. Reports of Russian Mineralogy Society, 1, 3–20 (in Rus.).

Lesnov, F.P. (2001c) *The regularities of REE distribution in clinopyroxenes*. Reports of Russian Mineralogy Society, 4, pp. 78–97 (in Rus.).

Lesnov, F.P. (2002a) Geochemistry of REE in harzburgites from continental ultramafic and mafic-ultramafic massifs. *Mineral Sbir*, 52 (2), 172–177 (in Ukrainian).

Lesnov, F.P. (2002b) *The regularities of REE distribution in amphiboles*. Reports of Russian Mineralogy Society, 5, pp. 75–98 (in Rus.).

Lesnov, F.P. (2002c) Rare earth elements in the dunites: General regularities of distribution. *Petrology of Magmatic and Metamorphic Complexes*. Tomsk: Publishing House of Tomsk State University. pp. 120–125 (in Rus.).

Lesnov, F.P. (2002d) State and problems of researches in the domain of REE geochemistry in kimberlites. *Petrology of Magmatic and Metamorphic Complexes*. Tomsk: Publishing House of Tomsk State University. pp. 126–133 (in Rus.).

Lesnov, F.P. (2003a) Deep xenoliths of ultramafites in the alkaline basalt provinces: Some peculiarity of REE geochemistry. *Pac Geol, 2*, pp. 15–37 (in Rus.).

Lesnov, F.P. (2003b) The role of REE in researches of kimberlite genesis. New ideas in sciences about Earth. *Proceeding of 6th International conference*. Volume 2. Moscow: MGGRU. p. 32 (in Rus.).

Lesnov, F.P. (2003c) The role of REE and PGE in the problem of systematic of rocks of ultramafic-mafic formations. *Contemporary Problems of Formation Analysis, Petrology Ore-Bearing of Magmatic Formations*. Novosibirsk: SB RAS, Branch "GEO". pp. 195–196 (in Rus.).

Lesnov, F.P. (2003d) The correlation of platinum group elements and rare earth elements in the mafic-ultramafic rocks as possible criteria of their systematic. *Geochemistry of Magmatic Rocks*. Apatity: Publishing House of Geological Institute. Kola Science Center of Russian Academy of Sciences. pp. 101–102 (in Rus.).

Lesnov, F.P. (2005a) On the coefficients of distribution REE between plagioclase and coexistent fazes. Condition and mastering of natural resources of Tuva and adjacent regions of Central Asia. *Geoecology of Natural Environment*. Kizil: Publishing House of Tuvinian Institute of complexes mastering of natural resources. Siberian Branch of Russian Academy of Sciences. pp. 44–55 (in Rus.).

Lesnov, F.P. (2005b) Main regularities of distribution of REE in the principal types of mafic rocks from mafic-ultramafic massifs. State and development of natural resources of Tuva and adjacent regions of Central Asia. *Geoecology of Nature and Socium*. Issue 8. Kyzil: Tuvinian Institute of complexes mastering of natural resources, SB RAS. pp. 56–79 (in Rus.).

Lesnov, F.P. (2006) Spatial-temporary correlations between ultramafic and mafic rocks—main question in the problem of genesis of ophiolite mafic-ultramafic complexes. *Ophiolite: Geology, Petrology, Metallogeny and Geodynamic*. Ekaterinburg: IGG UrB RAS. pp. 32–35 (in Rus.).

Lesnov, F.P. (2009a) Rare Earth Elements in Ultramafic and Mafic Rocks and Their Minerals. Book 2. Minor and accessory minerals. Novosibirsk: Academic Publishing House "Geo". 195 p. (in Rus.).

Lesnov, F.P. (2009b) Structure and composition of mafic-ultramafic massifs as evidence of their polygenic formation. Ultramafic-mafic complexes of folded regions and connected deposits. Volume 2. Ekaterinburg: Institute of Geology and Geochemistry UrB RAS. pp. 20–23 (in Rus.).

Lesnov, F.P. & Balykin, P.A. (2005) On the supplementary evidences of "antagonism" between PGE and REE in the igneous rocks. *Noble and Rare Metals of Siberia and Far East*. Irkutsk: Publishing House of Institute of Geochemistry. Siberian Branch of Russian Academy of Sciences. pp. 17–19 (in Rus.).

Lesnov, F.P. & Gora, M.P. (1998) Geochemistry of REE in the coexisting pyroxenes from different types of mafic-ultramafic rocks. *Geochimiya, 9*, 899–918 (in Rus.).

Lesnov, F.P. & Oydup, Ch.K. (2002) On the "antagonism" between Pd and Pt and REE in rocks of mafic-ultramafic massifs. *Geology, Genesis and Questions of Mastering Complex Deposits of Noble Metals*. Moscow: Publishing House of Institute of Geology, Geochemistry and Ore Deposits of Russian Academy of Sciences. pp. 48–52 (in Rus.).

Lesnov, F.P., Agafonov, L.V., Pinus, G.V. & Lipovsky, Yu.O. (1976) On the first discovery of moissonite in Mongolia. *Geol Geofiz, 6*, 119–122 (in Rus.).

Lesnov, F.P., Ponomarchuk, V.A. & Pyaling, A.O. (1987) On the distribution of REE in the mineral of Naransky (Mongolia) and Beriozovsky (Sakhalin Island) polygenic mafic-ultramafic plutons. *Ultramafic Associations of Folded Regions*. Issue 4. Novosibirsk: IGG SB AS USSR. pp. 124–145 (in Rus.).

Lesnov, F.P., Lomonosova, E.B., Goncharenko, A.I., *et al.* (1995) Distribution of REE in the olivines from ultramafites of ophiolite associations. *Geol Geofiz, 36* (2), 50–60 (in Rus.).

Lesnov, F.P., Gora, M.P., Bobrov, V.A. & Kovaliova, V.A. (1998a) Distribution of REE and questions of genesis of Beriozovsky mafic-ultramafic massif (Sakhalin Islands). *Tikh Geol, 17* (4), 42–58 (in Rus.).

Lesnov, F.P., Gora, M.P., Koviazin, C.V. & Fomina, E.N. (1998b) Connection between volatiles components and REE in the orthopyroxenes from mafic-ultramafic rocks. *Materials of Scientific Conference Devoted to V.S. Sobolev*. Lviv: Lviv State University. pp. 40–45 (in Ukrainian.).

Lesnov, F.P., Gora, M.P., Koviazin, C.V. & Fomina, E.N. (1998c) Fluid components in the orthopyroxenes from bipyroxenes mafic-ultramafic rocks and their connection with REE composition of the mineral. *Problems of Petrology and Metallogeny of Mafic-Ultramafic Complexes of Siberia*. Issue 1. Tomsk: Publishing House of Tomsk State University. pp. 62–78 (in Rus.).

Lesnov, F.P., Mongush, A.A. & Oydup, Ch.K. (2001) Geochemical consanguinity PGE and REE in the mafic-ultramafic rocks of Tuva (first data). *Platinum in the Geological Formations of Siberia*. Krasnoyarsk: Publishing House of Kasnoyarsk Research Institute of Geology, Geophysics and Mineral Material. pp. 107–110. (in Rus.).

Lesnov, F.P., Volkova, N.I., Bakirov, A.B., *et al.* (2004a) New data on composition of minerals and origin conditions of eclogites of ridge Atbashi (South Tian' Shan'). *Petrology of Magmatic and Metamorphic Complexes*. Tomsk: Publishing House of Tomsk State University. pp. 255–263 (in Rus.).

Lesnov, F.P., Mongush, A.A. & Mel'gunov, M.S. (2004b) On some peculiarity of geochemistry PGE and REE in the rocks of ultramafic-mafic massifs (Tuva). State and development of natural resources of Tuva and adjacent regions of Central Asia. *Geoecology of Nature and Socium*. Kyzil: Tuvinian Institute of complexes mastering of natural resources, Siberian Branch of RAS. pp. 54–60 (in Rus.).

Lesnov, F.P., Kuchkin, A.M., Palessky, S.V. & Volkova, N.I. (2005a) REE in the garnets from eclogites of the Atbashi metamorphic complex (South Tian' Shan', Kirgizia). *Metallogeny of Ancient and Modern Oceans*. Miass: Publishing House of Institute of Mineralogy. Ural Branch of Russian Academy of Sciences. pp. 63–67 (in Rus.).

Lesnov, F.P., Mongush, A.A., Anoshin, G.N., *et al.* (2005b) Research of PGE and REE distribution in the rocks of mafic-ultramafic massifs of Tuva by ICP-MS method (first data). *Petrology of Magmatic and Metamorphic Complexes*. Tomsk: Tomsk State University. pp. 268–277 (in Rus.).

Lesnov, F.P., Mongush, A.A. & Palessky, S.V. (2005c) Correlation of PGE and REE in some rocks of the mafic-ultramafic massifs of Tuva (data ICP-MS method). *Noble and Rare Metals of Siberia and Far East: Ore-Bearing Systems of Deposits of Complex and Nontraditional Types of Ores*. Irkutsk: Institute of Geochemistry SB RAS. pp. 19–22 (in Rus.).

Lesnov, F.P., Chernyshov, A.I. & Istomin, V.E. (2005d) Geochemical properties and typomorphism of olivines from heterogenic ultramafic rocks. *Geokhimiya, 4*, 395–414 (in Rus.).

Lesnov, F.P., Palessky, S.V., Nikolaeva, I.V., *et al.* (2007) Peculiarity of distribution of impurity elements in the large spinel lherzolite xenolith in alkali basalt of Shavaryn Tsaram paleovolcano, Mongolia (data ICP-MS method). State and development of natural resources of Tuva and adjacent regions of Central Asia. *Geoecology of Nature and Socium*. Issue 8. Kizil: Publishing House of Tuvinian Institute of complexes mastering of natural resources. Siberian Branch of Russian Academy of Sciences. pp. 68–82 (in Rus.).

Lesnov, F.P., Kozmenko, O.A, Nikolaeva, I.V. & Palessky, S.V. (2008) Distribution of incompatible elements in spinel lherzolite from large xenolith in alkali basalt of paleovolcano Shavaryn Tsaram (Mongolia). *Petrology of Lithosphere and a Diamond Origin. Theses of Reports of the International Conference*. Novosibirsk: IGM SB RAS. p. 51 (in Rus.).

Lesnov, F.P., Palessky, S.V., Nikolaeva, I.V., *et al.* (2009a) Detailed mineralogical-geochemical study of large spinel lherzolite xenolith in alkali basalt of Shavaryn Tsaram paleovolcano (Mongolia). *Geokhimiya, 1*, 21–44 (in Rus.).

Lesnov, F.P., Palessky, S.V., Nikolaeva, I.V., *et al.* (2009b) Detailed mineralogical-geochemical study of large spinel lherzolite xenolith in alkali basalt of Shavaryn Tsaram paleovolcano, Mongolia. *Geochem Int, 47* (1), 21–44.

Lesnov, F.P., Koz'menko, O.A, Nikolaeva, I.V. & Palessky, S.V. (2009c) Residence of incompatible trace elements in a large spinel lherzolite xenolith from alkali basalt of Shavaryn Tsaram-1 paleovolcano (Western Mongolia). *Geol Geofiz, 50* (12), 1367–1380 (in Rus).

Lesnov, F.P., Koz'menko, O.A, Nikolaeva, I.V. & Palessky, S.V. (2009d) Residence of incompatible trace elements in a large spinel lherzolite xenolith from alkali basalt of Shavaryn Tsaram-1 paleovolcano (Western Mongolia). *Russ Geol Geophys, 50* (12), 1063–1072.

Liotard, J.M., Briot, D. & Boivin, P. (1988) Petrological and geochemical relationships between pyroxene megacrysts and associated alkali-basalts from Massif Central (France). *Contrib Mineral Petrol, 98*, 81–90.

Lipin, B.R. & McKey, G.A. (eds.) (1989) *Geochemistry and Mineralogy of Rare Earth Elements. Reviews in Mineralogy*. Volume 21. Washington: Mineralogical Society of America. 348 p.

Lissenberg, C.J., Bedard, J.H. & van Staal, C.R. (2004) The structure and geochemistry of the gabbro zone of the Annieopsquotch ofiolite, Newfoundland: Implications for low crystal accretion at spreading ridges. *Earth Planet Sci Lett, 229*, 105–123.

Litasov, K.D. (1998) *Geochemical Models of Development of the Mantle Magmatic Systems on Data of Study Deep Xenoliths of Vitim and Udokan Volcanic Fields. Abstract of Dissertation*. Novosibirsk: IGG SB RAS. 22 p. (in Rus.).

Litasov, K.D., Dobretsov, N.L. & Sobolev, A.V. (1999) Evidences of melt reaction percolation in the upper mantle on data study of peridotite xenoliths in the basalt of Vitim and Udokan volcanic fields, Transbaykalia. *Dokl RAS, 368* (4), 525–529. (in Rus.).

Loubet, M., Shimizu, N. & Allegre, C.J. (1975) Rare earth elements in alpine peridotites. *Contrib Mineral Petrol, 53* (1), 1–12.

Lul'ko, V.A., Fedorenko, V.A., Distler, V.V., *et al.* (1994) Geology and Ore deposits of the Noril'sk region. *VII International Platinum Symposium (Moskow–Noril'sk)*. Guidebook, 68 p.

Lundstrom, C.C., Show, H.F., Ryerson, F.J., *et al.* (1998) Crystal chemical control of clinopyroxene-melt partitioning in the Di–Ab–An system: Implications for elemental fractionations in the depleted mantle. *Geochim Cosmochim Acta, 62* (16), 2849–2862.

Lutts, B.G. (1975) Chemical composition of continental crust and upper mantle. Moscow: Nauka. 168 p. (in Rus.).

Lutts, B.G. & Frantsesson, E.V. (1976) Geochemical characteristic of kimberlites and their comparison with ultramafic and mafic rocks. *5th Session of International Geological Congress.*

Reports of Soviet Geologists. Geochemistry, Mineralogy, Petrology. Moscow: Nauka. pp. 170–180 (in Rus.).

Magmatic Rocks (1985) *Mafic Rocks*. Volume 4. Moscow: Nauka. 488 p. (in Rus.).

Magmatic Rocks (1988) *Mafic Rocks*. Volume 5. Moscow: Nauka. 508 p. (in Rus.).

Makhotkin, I.L., Gibson, S.A., Tompson, R.N., *et al.* (2000) Late devonian diamondiferous kimberlite and alkaline picrite (proto-kimberlite) magmatism in the Arkhangelsk region, NW Russia. *J Petrol, 41* (2), 201–227.

Malakhov, I.A. (1985) *Rare Earths—Indicators for Estimation of the Ore-Bearing Kimberlites of Middle Ural*. Annual-1984. Sverdlovsk: Institute Geology and Geochemistry UrSC USSR. pp. 66–67 (in Rus.).

Markovsky, B.A. (1988) Picrites. In: Laz'ko, E.E. & Sharkov, E.V. (eds.) *Magmatic Rocks. Ultramafic Rocks*. Volume 5. Moscow: Nauka. pp. 114–129 (in Rus.).

Marakushev, A.A., Lonkan, S., Bobrov, A.V., *et al.* (2003) Evolution of eclogites-ultramafites folded belt in East China. Herald Moscow State University, Series 4. *Geol, 6*, 27–36 (in Rus.).

Marshintsev, V.K. (1986) Vertical nonhomogeneous of kimberlitic bodies of Yakutia. Novosibirsk: Nauka, Siberian Branch. 240 p. (in Rus.).

Masuda, A. (1982) Regularities in variation of relative abundances of lanthanide elements and an attempt to analyse separation-index patterns of some minerals. *J Earth Sci Nagova University, 10* (1–2), 173–187.

Masuda, A. & Jibiki, H. (1973) Rare earth patterns of Mid-Atlantic Ridge gabbros: Continental nature? *Geochem J, 7*, 55–65.

Masuda, A., Nakamura, N. & Tanaka, T. (1973) Fine structures of mutually normalized rare-earth patterns of chondrites. *Geochim Cosmochim Acta, 37*, 239–248.

Mattielli, N., Weis, D., Gregoire, M., *et al.* (1996) Kerguelen basic and ultrabasic xenoliths: Evidence for long-lived Kerguelen hotspot activity. *Lithos, 37*, 261–280.

Mazzucchelli, M., Rivalenti, G., Vannucci, R., *et al.* (1992a) Primary positive Eu anomaly in clinopyroxenes of lowcrust gabbroic rocks. *Geochim Cosmochim Acta, 56*, 2363–2370.

Mazzucchelli, M., Rivalenti, G., Vannucci, R., *et al.* (1992b) Trace element distribution between clinopyroxene and garnet in gabbroic rocks of the deep crust: An ion microprobe study. *Geochim Cosmochim Acta, 56*, 2371–2385.

Mazzucchelli, M., Rivalenti, G., Zanetti, A., *et al.* (1999) Origin and significance of late noritic dykes in the Baldissero peridotite massif (Ivrea Verbano zone). *Ofioliti, 24* (1a), 129–130.

McDonough, W.F. & Frey, F.A. (1989) Rare earth elements in upper mantle rocks. In: Lipin, B.R. & McKey, G.A. (eds.) *Geochemistry and Mineralogy of Rare Earth Elements. Reviews in Mineralogy*. Volume 21. Washington: Mineralogical Society of America. Chapter 5, pp. 99–145.

McDonough, W.F., Stosch, H.-G. & Ware, N.G. (1992) Distribution of titanium and rare earth elements between peridotitic minerals. *Contrib Mineral Petrol, 110*, 321–328.

McKay, G.A. (1986) Crystal/liquid partitioning of REE in basaltic systems: Extreme fractionation of REE in olivine. Geochim Cosmochim Acta, 50, 69–79.

McKay, G.A. (1989) Partitioning of rare earth elements between major silicate minerals and basaltic melts. In: Lipin, B.R. & McKey, G.A. (eds.) *Geochemistry and Mineralogy of Rare Earth Elements. Reviews in Mineralogy*. Volume 21. Washington: Mineralogical Society of America. pp. 45–78.

McKay, G.A., Wagstaff, J. & Yang, S.R. (1986) Clinopyroxene REE distribution coefficients for shergotites: The REE content of the Shergitty melt. *Geochim Cosmochim Acta, 50*, 927–937.

Mekhonoshin, A.S., Plyusnin, G.S., Bognibov, V.I., *et al.* (1986) Isotopes of strontium and rare earth elements in the Dugdinsky peridotite-pyroxenite-gabbro massif. *Geol Geofiz, 8*, 3–9 (in Rus.).

Mekhonoshin, A.S., Bognibov, V.I. & Lomonosova, E.I. (1993) Rare earth elements and petrogenesis of ultramafic-mafic massifs in South Siberia. *Geol Geofiz, 2*, 43–49 (in Rus.).

Menzies, M. (1976) Rare earth geochemistry of fused ophiolitic and alpine lherzolites. Part I: Othris, Lanzo and Troodos. *Geochim Cosmochim Acta, 40*, 645–656.

Miller, Ch., Stosch, H.-G. & Hoernes, St. (1988) Geochemistry and origin eclogites from the type locality Koralpe and Saualpe, Eastern Alps, Austria. *Chem Geol, 67* (1–2), 103–118.

Mitchell, R.H. (1986) *Kimberlites: Mineralogy, Geochemistry and Petrology*. New York: Plenum Press. 442 p.

Mitchell, R.H., (1988) *Lamproites—family of alkali high magnesium rocks*. Reports of Russian Mineralogy Society, Part 117, Issue 5, pp. 575–586 (in Rus.).

Mitchell, R.H. & Bergman, S.C. (1991) *Petrology of Lamproites*. New York: Plenum Press. 448 p.

Montigny, R., Bougault, H., Bottinga, Y. & Allegre, C.J. (1973) Trace element geochemistry and genesis of the Pindos ophiolite suite. *Geochim Cosmochim Acta, 37* (9), 2135–2147.

Morimoto, N., Ferguson, A.K., Ginsburg, I.V., *et al.* (1988) Nomenclature of pyroxenes. *Amer Mineral, 73*, 1123–1133.

Morse, S.A. & Nolan, K.M. (1985) Kiglapait geochemistry VII: Yttrium and the rare earth elements. *Geochim Cosmochim Acta, 49* (7), 1621–1644.

Munha, J., Palacios, T., Macrae, N.D. & Mata, J. (1990) Petrology of ultramafic xenoliths from Madeira island. *Geol Mag, 127* (6), 543–566.

Mysen, B.O. (1977) *Partitioning of Cerium, Samarium and Thulium Between Pargasite, Garnet Peridotite Minerals and Hydrous Silicate Liquid at High Temperature and Pressure*. Washington: Carnegie Institute, Volume 76. pp. 588–594.

Mysen, B.O. (1978) Experimental determination of rare earth element partitioning between hydrous silicate melt, amphibole and garnet peridotite minerals at upper mantle pressure and temperatures. *Geochim Cosmochim Acta, 42*, 1253–1263

Mysen, B.O. (1983) Rare earth element partitioning between (H_2O + CO_2) vapor and upper mantle minerals: experimental data bearing on the conditions of formation of alkali basalt and kimberlite. *Neues Jarb Mineral Abh, 146*, 41–65.

Nagasawa, H. (1973) Rare-earth distribution in alkali rocks from Oki-Dogo Island, Japan. *Contrib Mineral Petrol, 39* (4), 301–308.

Nagasawa, H. & Schnetzler, C.C. (1971) Partitioning of rare earth, alkali and alkali earth elements between phenocrysts and acidic igneous magma. *Geochim Cosmochim Acta, 35* (9), 953–968.

Nagasawa, H., Wakita, H., Higuchi, H. & Onuma, N. (1969) Rare earths in peridotite nodules: An explanation of the genetic relationship between basalt and peridotite nodules. *Earth Planet Sci Lett, 5*, 377–381.

Nakamura, N. (1974) Determination of REE, Ba, Fe, Mg, Na and K in carbonaceous an ordinary chondrites. *Geochim Cosmochim Acta, 38*, 757–775.

Nakamura, N., Unruh, D.M., Tatsumoto, M. & Hutchison, R. (1982) Origin and evolution of the Nakhla meteorite inferred from the Sm-Nd and U-Pb systematics and REE, Ba, Sr, Rb and K abundances. *Geochim Cosmochim Acta, 46* (9), 1555–1573.

Naqvi, S.M., Viswanathan, S. & Visvanatma, M.N. (1978) Geology and geochemistry of the Holenarasipur schist belt and its place in the evolutionary history of the Indian peninsula. In: Windley, B.F. & Naqvi, S.M. (eds.) *Archean Geochemistry*. Amsterdam: Elsevier. pp. 109–126.

Nash, W.P. & Crecraft, H.R. (1985) Partition coefficients for trace elements in silicic magmas. *Geochim Cosmochim Acta, 49* (11), 2309–2322.

Nekrasova, R.A. & Gamyanina, V.V. (1968) Composition of rare earth elements in kimberlite minerals. *Dokl AS USSR, 182*, 449-452 (in Rus.).

Neruchev, S.S., Prasolov, E.M. & Stepanov, V.A. (1997) Fluid regime of basic and ultrabasic magmatism. *3th International Conference on New Ideas in Sciences on Earth, Moscow*. pp. 104–105 (in Rus.).

Nicholls, I.A. & Harris, K.L. (1980) Experimental rare earth element partition coefficients for garnet, clinopyroxene and amphibole coexisting with andesitic and basaltic liquids. *Geochim Cosmochim Acta, 44*, 287–308.

Nielsen, R.L., Gallahan, W.E. & Newberger, F. (1992) Experimentally determined mineral-melt partition coefficients for Sc, Y and REE for olivine, orthopyroxene, pigeonite and ilmenite. *Contrib Mineral Petrol, 110*, 488–499.

Nikol'skaya, N.E. & Kogarko, L.N. (1995) Geochemical peculiarity of Romansh fault ultramafites (Equatorial Atlantica). *Geokhimiya, 9*, 1280–1295 (in Rus.).

Niu, Y. (2004) Bulk-rock major and trace element compositions of abyssal peridotites: Implication for mantle melting, melt extraction and post-melting processes beneath mid-ocean ridges. *J Petrol, 45* (12), 2443–2458.

Norman, I., Kyle, P.R. & Baron, C. (1989) Analysis of trace elements including rare earth elements in fluid inclusion liquids. *Econ Geol, 84*, 162–166.

Norman, M.D. & Garcia, M.O. (1999) Primitive magmas and source of the Hawaiian plume: Petrology and geochemistry of shield picrites. *Earth Planet Sci Lett, 168*, 27–44.

Norman, M.D. & Leeman, W.P. (1990) Open-system magmatic evolution of andesite and basalts from Salmon Greek volcano, southwestern Idaho, U.S.A. *Chem Geol, 84*, 167–189.

Norman, M.D., Pearson, N.J., Sharma, A. & Griffin, W.L. (1996) Quantitative analysis of trace elements in geologic materials by laser ablation ICP-MS: instrumental operating conditions and calibration values of NIST glasses. *Geostand Newslett, 20* (2), 247–261.

Nozaka, T. & Liu Yan (2002) Petrology of the Hegenshan ophiolite and its implication for the tectonic evolution of northern China. *Earth Planet Sci Lett, 202* (1), 89–104.

Obata, M. (1980) The Ronda peridotite: Garnet-spinel- and plagioclase-lherzolite facies and P–T trajectories of high-temperature mantle intrusion. *J Petrol, 21* (3).

O'Brien, H.E. & Tyni, M. (1999) Mineralogy and geochemistry of kimberlites and related rocks from Finland. *Proc. 7th Int. Kimberlite Conference (Cape Town, 1999)*. Volume 2. pp. 625–636.

Onuma, N., Higuchi, H., Wakita, H. & Nagasawa, H. (1968) Trace element partition between two pyroxenes and the host lava. *Earth Planet Sci Lett, 5*, 47–51.

Ottonello, G. (1980) Rare earth abundances and distribution in some spinel peridotite xenoliths from Assab (Ethiopia). *Geochim Cosmochim Acta, 44*, 1885–1901.

Ottonello, G., Piccardo, A., Mazzukotelli, A. & Cimmino, F. (1978) Clinopyroxene-ortopyroxene major and rare earth elements partitioning in spinel peridotite xenoliths from Assab (Ethiopia). *Geochim Cosmochim Acta, 42*, 1817–1828.

Ottonello, G., Ernst, W.G. & Jordon, J.L. (1984) Rare earth and 3d transition element geochemistry of peridotitic rocks. Part I: Peridotites from the Western Alps. *J Petrol, 25* (Pt 2), 343–372.

Ozawa, K. & Shimizu, N. (1995) Open system melting in the upper mantle: Constrains from the Hayachine-Miyamori ophiolite, northeastern Japan. *J Geophys Res, 100* (B11), 22315–22335.

Pallister, J.S. & Knight, R.J. (1981) Rare earth element geochemistry of the Samail ophiolite near Ibrea, Oman. *J Geophys Res, 86* (B4), 2673–2697.

Panina, L.I. & Usol'tseva, L.M. (2009) Pyroxenites of the Krestovsky alcaline-ultramafic intrusive: Structure of parental magmas and their sources. *Geokhimiya, 4*, 378–392 (in Rus.).

Papike, J.J., Spild, M.N., Fowler, G.W. & McCallum, I.S. (1995) SIMS studies of planetary cumulates: Orthopyroxene from the Stillwater Complex, Montana. *Amer Mineral, 80* (11–12), 1208–1222.

Parsadanian, K.C., Kononova, V.A. & Bogatikov, O.A. (1996) Sources of heterogenic magmatism of Arkhangelsk diamond provinces. *Petrologia, 4* (5), 496–517 (in Rus.).

Paster, T.P., Schauwecker, D.S. & Haskin, L.A. (1974) The behavior of some trace elements during solidification of the Skaergaard layered series. *Geochim Cosmochim Acta, 38* (10), 1549–1579.

Pavlov, D.I., Ilupin, I.P. & Gorbachova, S.A. (1985) Buried salt brines as possible factor of transformation kimberlite primary composition. *Izvestia AS USSR, Series of Geology Sciences, 3*, 44–53 (in Rus.).

Paul, D.K., Potts, P.J., Gibson, I.L. & Harris, P.G. (1975) Rare-earth abundances in Indian kimberlite. *Earth Planet Sci Lett, 25*, 151–158.

Pearson, D.G., Davies, G.R. & Nixon, P.H. (1993) Geochemical constraints on the petrogenesis of diamond facies pyroxenites from Beni Bousera peridotite massif, North Morocco. *J Petrol, 34* (Part 1), 125–172.

Pertsev, A.N. (2004) *Petrology of Plutonic Mafic-Ultramafic Complexes of Active Regions of Transition Ocean-Continent. Abstract of Dissertation*. Moscow: IGEM RAS. 44 p. (in Rus.).

Pfander, J.A., Jochum, K.P., Oidup, Ch. & Kroner, A. (2001) *Ultramafic Cumulates and Gabbros from Boninitic Primary Melts and Lower Oceanic Crustal Evolution Agardag-Teschem Ophiolite (Tuva, Central Asia)—Petrological and Geochemical Constraints*. GFR. Mainz: Max Plank Institute.

Philpotts, J.A. & Schnetzler, C.C. (1970a) Apollo 11 lunar samples: K, Rb, Sr, Ba and rare-earth concentrations in some rocks and separated phases. *Proceedings of the Apollo 11 Lunar Science Conference*. Volume 2. pp. 1471–1486.

Philpotts, J.A. & Schnetzler, C.C. (1970b) Potassium, rubidium, strontium, barium and rare earth concentrations in lunar rocks and separated phases. *Science, 167* (3918), 493–495.

Philpotts, J.A., Schnetzler, C.C. & Thomas, H.H. (1972) Petrogenetic implications of some new geochemical data on eclogitic and ultrabasic inclusions. *Geochim Cosmochim Acta, 36* (10), 1131–1166.

Phinney, W.C. & Morrison, D.A. (1990) Partition coefficients for calcic plagioclase: Implications for Archean anorthosites. *Geochim Cosmochim Acta, 54*, 1639–1654.

Piccardo, G.B., Zanetti, A., Spagnolo, G. & Poggi, E. (2005) Recent researches on melt-rock interaction in the Lanzo south peridotite. *Ofioliti, 30* (2), 135–160.

Pinus, G.V., Velinsky, V.V., Lesnov, F.P., *et al.* (1973) *Alpinotype Ultramafites of Anadir-Koriakia Folded System*. Novosibirsk: Nauka, Siberian Branch. 350 p. (in Rus.).

Pinus, G.V., Agafonov, L.V. & Lesnov, F.P. (1984) *Alpinotype Ultramafites of Mongolia*. Moscow: Nauka. 250 p. (in Rus.).

Price, S.E., Russel, J.K. & Kopylova, M.G. (2000) Primitive magma from the Jericho pipe. N.W.T., Canada: Constraints on primary kimberlite melt chemistry. *J Petrol, 41* (6), 789–808.

Pride, C. & Muecke, G.K. (1981) Rare earth element distributions among coexisting granulite facies minerals, Scourian complex, NW Scotland. *Contrib Mineral Petrol, 76* (4), 463–471.

Prinzhofer, A. & Allegre, C.J. (1985) Residual peridotites and mechanisms of partial melting. *Earth Planet Sci Lett, 74* (2–3), 251–265.

Pukhtel', I.S. & Simon, A.K. (1988) Ultramafites of the greenstone belts. In: Laz'ko, E.E. & Sharkov, E.V. (eds.) *Magmatic Rocks. Ultramafic Rocks*. Moscow: Nauka. pp. 230–248 (in Rus.).

Pushkariov, Yu.D., Nikitina, L.P., Skiba, V.I., Sergeev, S.A. & Yurgina, E.K. (2004) Isotopic-petrochemical systematics of mantle xenoliths and nature of layer "D" at "core-mantle" margin. *XVII symposium on isotopes geochemistry name Academician A.P. Vinogradov*. Report's abstract. Moscow: GEOKHI. pp. 211–212 (in Rus.).

Pyatenko, Yu.A. & Ugryumova, N.G. (1988) Mineralogical crystallochemistry of rare earth elements. *Izvestia AS USSR. Geological Series, 11*, 75–86 (in Rus.).

Rampone, E., Bottazzi, P. & Ottolini, L. (1991) Complementary anomalies in orthopyroxene and clinopyroxene from mantle peridotites. *Nature, 354*, 518–520.

Rass, I.T. (1982) Rare-earth elements in the rock-forming minerals of melilitic rocks in alkali-ultrabasic complex. *Geochim Cosmochim Acta, 46* (9), 1477–1488.

Redder, E. (1987) *Fluid Inclusions in the Minerals*. Volume 1. Moscow: Mir. 557 p. (in Rus.).

Reid, J.B. & Frey, F.A. (1971) Rare earth distribution in lherzolite and garnet pyroxenites xenoliths and the constitution of the upper mantle. *J Geophys Res, 76* (5), 1184–1196.

Reitan, P.H., Roelandts, I. & Brunfelt, A.O. (1980) Optimum ionic size for substitution in the M(2)-site in metamorphic diopside. *N Jb Miner Mh H, 4*, 181–191.

Reverdatto, V.V., Kolmogorov, Yu.P. & Parkhomenko, V.S. (2000) Rare and rare earth elements in the mafic granulites of Kokchetav massif (Kazakhtan). *Dokl RAS, 372* (1), 95–98 (in Rus.).

Reverdatto, V.V. & Selyatitsky, A.Yu. (2004) Chloritic rocks and chloritised basalts as possible predecessors of metamorphic peridotites and pyroxenites in Kokchetav massis, Northern Kazakhtan. *Dokl RAS, 394* (4), 533–536 (in Rus.).

Revillon, S., Arndt, N.T., Chauvel, C. & Hallot, E. (2000) Geochemical study ultramafic volcanic and plutonic rocks from Gorgona Island, Colombia: The plumbing system of an oceanic plateau. *J Petrol, 41* (7), 1127–1153.

Rikhvanov, L.P., Kropanin, S.S., Babenko, S.A., *et al.* (2001) *Zircon-Ilmenite Placer Deposits as Potential Source of Development of West-Siberian Regions*. Kemerovo: Tomsk Polytechnic University. 200 p (in Rus.).

Ringwood, A.E. (1975) *Composition and Petrology of the Earth's Mantle*. New York: McGraw-Hill. 584 p.

Rivalenti, G., Mazzucchelli, M., Vannucci, R., *et al.* (1995) The relationship between websterite and peridotite in the Balmuccia peridotite massif (NW Italy) as revealed by trace element variations in clinopyroxene. *Contrib Mineral Petrol, 121* (3), 275–288.

Rivalenti, G., Vannucci, R., Rampone, E., *et al.* (1996) Peridotite clinopyroxene chemistry reflects mantle processes rather then continental versus oceanic setting. *Earth Planet Sci Lett, 139*, 423–437.

Roden, M.F., Frey, F.A. & Francis, D.M. (1984) An example of consequent mantle metasomatism in peridotite inclusions from Nunivak Island, Alaska. *J Petrol, 25* (Part 2), 546–577.

Rollinson, H.R. (1993) Using Geochemical Data: Evaluation, Presentation, Interpretation. Singapore: Longman. 352 p.

Ryabchikov, I.D. (2005) Mantle magmas—sensor of deep geospheres composition. *Rud Mest, 47* (6), 501–515 (in Rus.).

Ryabchikov, I.D., Kogarko, L.N., Kovalenko, *et al.* (1988) Rare earth elements as indicators of geochemical evolution of mantle substance (data of study of peridotite nodules). *Dokl AS USSR, 302* (2), 440–443 (in Rus.).

Saccani, E., Beccaluva, L., Coltorti, M. & Siena, F. (2004) Petrogenesis and tectonomagmatic significance of the Albanide-Hellenide subpelagonian ophiolites. *Ofioliti, 29* (1), 75–93.

Safonova, I.Yu. (2005) *Geodynamic Forming Conditions of Vend-Paleozoic Basalts in Paleoasian Ocean from Gorni Altay and East Kazakhstan. Abstract of Dissertation*. Novosibirsk: IGM SB RAS. 24 p. (in Rus.).

Sano, S., Oberhansli, R., Romer, R.L. & Vinx, R. (2002) Petrological, geochemical and isotopic constraints on the origin of Harzburg intrusion, Germany. *J Petrol, 43* (8), 1529–1549.

Savel'ev, A.A, Sharaskin, A.Ja. & Orazio, M.D. (1999) Plutonic to volcanic rocks of the Voykar ophiolite massif (Polar Urals): Structural and geochemical constraints on their origin. *Ofioliti, 24* (1), 21–30.

Savel'ev, D.E., Snachov, V.I., Savel'eva, E.N. & Romanovskaya, M.A. (2000) New data on geochemistry of rocks from banded complex of Sredny Kraka massif (South Ural). *Vestnik Moscow State University, Series 4, Geology, 6*, 32–40 (in Rus.).

Savel'ev, D.E., Snachov, V.I., Savel'eva, E.N. & Bazhin, E.A. (2008) *Geology, Petrochemistry and Chromite-Bearing of Gabbro-Ultramafic Massifs of the South Ural*. Ufa: Institute Geology Ufa Science Center RAS, 320 p. (in Rus.).

Schnetzler, C.C. & Bottino, M.L. (1971) Some alkali, alkali earths, and rare earth element concentrations and the Rb-Sr age of the Lost Coty meteorite and separated phases. *J Geophys Res, 76* (17), 4061–4066.

Schnetzler, C.C. & Philpotts, J.A. (1968) *Partition Coefficients of the Rare Earths and Barium Between Igneous Matrix Material and Rock-Forming Mineral Phenocrysts–I. Origin and Distribution of the Elements*. Oxford: Pergamon Press. pp. 929–947.

Schnetzler, C.C. & Philpotts, J.A. (1970) Partition coefficients of rare-earth elements between igneous matrix material and rock-forming mineral phenocrysts–II. *Geochim Cosmochim Acta, 34* (3), 331–341.

Schwandt, C.S. & McKey, G.A. (1998) Rare earth element partition coefficients from enstatite/melt synthesis experiments. *Geochim Cosmochim Acta, 62* (16), 2845–2848.

Sen, G., Frey, F.A., Shimizu, N. & Leeman, W.P. (1993) Evolution of the lithosphere beneath Oahu, Hawaii: Rare earth element abundances in mantle xenoliths. *Earth Planet Sci Lett, 119*, 53–69.

Serov, I.V., Garanin, V.K., Zinchuk, N.N. & Rotman, A.Ya. (2001) Mantle sources of kimberlitic volcanism of Siberian platform. *Petrologia, 9* (6), 657–670 (in Rus.).

Shannon, R.D. (1976) Reversed effective ionic radii and systematic studies of interatomic distances in halides and chalcogenides. *Acta Crystallogr, 32a*, 751–767.

Sharkov, E.V. & Bogatikov, O.A. (1985) The layered intrusions of mafic and ultramafic rocks. In: Laz'ko, E.E. & Sharkov, E.V. (eds.) *Magmatic Rocks. Mafic Rocks*. Volume 4. Moscow: Nauka. pp. 72–104 (in Rus.).

Sharkov, E.V., Snayder, G.A., Taylor, L.A., *et al.* (1996) The geochemical peculiarity of astenosphera under the Arabian plate on data study of mantle xenoliths from Quaternary volcano Tell-Danun, Syria–Jordan plateau, South Syria. *Geokhimiya, 9*, 819–835 (in Rus.).

Shatsky, V.S. (1990) *The High-Pressure Mineral Associations of Eclogites-Bearing Complexes of Ural–Mongol Folded Belt. Abstract of Dissertation*. Novosibirsk: IGM SB RAS. 24 p. (in Rus.).

Shaw, D.M. (1969) *Geochemistry Traces Elements of Crystalline Rocks*. Moscow: Nedra. 208 p. (in Rus.).

Shearer, C.K., Papike, J.J., Simon, S.B. & Shimizu, N. (1989) An ion microprobe study of the intra-crystalline behavior of REE and selected trace elements in pyroxene from mare basalts with different cooling and crystallization histories. *Geochim Cosmochim Acta, 53* (5), 1041–1054.

Shervais, J.W. & McGree, J.J. (1999) KREEP cumulates in the western lunar highlands: Ion and electron microprobe study of alkali-suite anorthosites and norites from Apollo 12 and 14. *Amer Mineral, 84* (5–6), 806–820.

Shi, L., Ludden, J., Frederiksen, A. & Bostok, M. (1998) Xenolith evidence for lithospheric melting above anomalously hot mantle under the Northern Cordillera. *Contrib Mineral Petrol, 131*, 39–53.

Shimizu, N. (1975) Rare earth elements in garnets and clinopyroxenes from garnet lherzolite nodules in kimberlites. *Earth Planet Sci Lett, 25*, 26–32.

Shimizu, N., Pokhilenko, N.P., Boyd, F.P. & Pirson, D.G. (1997) The geochemical characteristic of mantle xenoliths in the kimberlitic pipe Udachnaya. *Geol Geofiz, 38* (1), 194–205 (in Rus.).

Shubina, N.A., Ukhanov, A.V., Genshaft, Yu.S. & Kolesov, G.M. (1997) Rare and rock-forming elements in the peridotite nodules from basalts of north-west Spitsbergen: To problems of heterogeneity of upper mantle. *Geokhimiya, 1*, 21–36 (in Rus.).

Simon, N.S.C., Neumann, E.-R., Bonadiman, C., *et al.* (2008) Ultra-refractory domains in oceanic mantle lithosphere samples as mantle xenoliths from ocean islands. *J Petrol, 49* (6), 1223–1251.

Simonov, V.A., Kolobov, V.Yu. & Peyve, A.A. (1999) *Petrology and Geochemistry of Geodynamic Processes in the Central Atlantika*. Novosibirsk: SB RAS. 224 p. (in Rus.).

Simonov, V.A., Lesnov, F.P., Ganelin, A.V. & Stupakov, C.I. (2000) Geochemistry of REE in the clinopyroxenes from the rocks of Voykar-Sin'insky and Khadatinsky ophiolitic complexes (Polar Ural). Collision stage of active belts development. *4th Reading A.N. Zavaritsky*. Ekaterinburg: IGG UrB RAS. pp. 98–99 (in Rus.).

Sklyarov, E.V. (ed.) (2001) *Interpretation of Geochemical Data*. Moscow: Intermet Ingeniring. 288 p. (in Rus.).

Skublov, S.G. (2005) *Geochemistry of REE in Minerals of Metamorphic Rocks*. Sankt-Peterburg: Nauka. 147 p. (in Rus.).

Smithies, R.H., Champion, D.C. & Sun, S.-S. (2004) Evidence for early LREE-enriched mantle source regions: Diverse magmas from the c. 3,0 Ga Mallina Basin, Pilbara craton, NW Australia. *J Petrol, 45* (8), 1515–1537.

Smol'kin, V.F. (1992) *Komatiitic and Picritic Magmatism of Early Pre-Cambrian of Baltic Shield*. Sankt-Peterburg: Nauka. 273 p. (in Rus.).

Sobolev, A.V. & Batanova, V.G. (1995) Mantle lherzolites of Troodos complex, Cyprus Island: Geochemistry of clinopyroxene. *Petrologia, 3* (5), 487–495 (in Rus.).

Sobolev, A.V., Migdisov, A.A., Portniagin, M.V. (1996) Distribution of incompatible elements between clinopyroxene and basaltic melts on data study of melt inclusions in the minerals of Troodos massif, Cyprus Island. *Petrologia, 4* (3), 326–336 (in Rus.).

Solodov, N.A., Semionov, E.I. & Usova, T.Yu. (1998) *Mineral Products. Yttrium and Lantanoids*. Moscow: "Geoinformmark". 52 p. (in Rus.).

Song, Y. & Frey, F.A. (1989) Geochemistry of peridotite xenoliths in basalt from Hannuoba, Eastern China: Implications for subcontinental mantle heterogeneity. *Geochim Cosmochim Acta, 53* (1), 97–113.

Sorensen, S.S. & Grossman, J.N. (1989) Enrichment of trace elements in garnet amphibolites from a paleo-subduction zone: Catalina Schist, Southern California. *Geochim Cosmochim Acta, 53* (12), 3155–3177.

Stosch, H.-G. (1982) Rare earth partitioning between minerals from anhydrous peridotite xenoliths. *Geochim Cosmochim Acta, 46*, 793–811.

Stosch, H.-G. & Seck, H.A. (1980) Geochemistry and mineralogy of two spinel peridotite suites from Dreiser Weiher, West Germany. *Geochim Cosmochim Acta, 44*, 457–470.

Stosch, H.-G., Lungmair, G.W. & Kovalenko, V.I. (1986) Spinel peridotite xenoliths from Tariat depression, Mongolia. II: Geochemistry and Nd and Sr isotopic composition and their implications for the evolution of the subcontinental lithosphere. *Geochim Cosmochim Acta, 50*, 2601–2614.

Stosch, H.-G., Ionov, D.A., Puchtel, I.S., *et al.* (1995) Lever crustal xenoliths from Mongolia and their bearing on the nature of the deep crust beneath central Asia. *Lithos, 36*, 227–242.

Suen, C.J., Frey, F.A. & Malpas, J. (1979) Bay of islands ophiolite suite, Newfoundland: Petrologic and geochemical characteristics with emphasis on rare earth element geochemistry. *Earth Planet Sci Lett, 45*, 337–348.

Sukhanov, M.K., Bogdanova, N.G., Lyapunov, S.M. & Ermolaev, B.V. (1990) Geochemistry of REE in formation of autonomous anorthosites. *Geokhimiya, 2*, 184–194 (in Rus.).

Sun, M. & Kerrich, R. (1995) Rare earth element and high field strength element characteristics of whole rocks and mineral separates of ultramafic nodules in Cenozoic volcanic vents of southeastern British Columbia, Canada. *Geochim Cosmochim Acta, 59* (23), 4863–4879.

Sun, Sh.S. & McDonough, W.F. (1989) Chemical and isotopic systematics of oceanic basalt: Implications for mantle composition and processes. *Magmatism in Ocean Basins*. Saunders, A.D. & Norry, M.J. (eds.). *Geol Soc Spec Public, 42*, 313–345.

Sun, Sh.S. & Nesbitt, R.W. (1978) Petrogenesis of archean ultrabasic and basic volcanics: Evidence from rare earth elements. *Contrib Mineral Petrol, 65* (5), 301–325.

Suzuki, K. (1987) Grain-boundary enrichment of incompatible elements in some mantle peridotites. *Chem Geol, 63*, 319–334.

Tanaka, T. & Aoki, K.-I. (1981) Petrogenetic implication of REE and Ba data on mafic and ultramafic inclusions from Itinome-Gata, Japan. *J Geol, 89* (3), 369–390.

Taylor, S.R. & McLennan, S.M. (1985) *The Continental Crust. Its Composition and Evolution*. Oxford: Blackwell. 312 p.

Taylor, W.R., Tompkins, L.A. & Haggerty, S.E. (1994) Comparative geochemistry of West African kimberlites: Evidence for a micaceous kimberlite end member of sublithospheric origin. *Geochim Cosmochim Acta, 58* (19), 4017–4037.

Tiepolo, M., Tribuzio, R. & Vannucci, R. (1997) Mg- and Fe-gabbroids from northern Apennine ophiolites: Parental liquids and igneous differentiation process. *Ofioliti, 22* (1), 57–69.

Tompkins, L.A., Mayer, S.P., Han, Z., *et al.* (1999) Petrology and geochemistry of kimberlites from Shandong and Lioning provinces, China. Proc. 7th Int. Kimberlite Conference (Cope Town, 1999). Vol. 2. P. 872–887.

Tribuzio, R., Riccardi, M.P. & Ottolini, L. (1995) Trace element redistribution in high-temperature deformed gabbro from East Ligurian ophiolites (Northern Apennines, Italy): Constrains on the origin of sindeformation fluids. *J Metamorph Geol, 13*, 367–377.

Tribuzio, R., Messiga, B., Vannucci, R. & Bottazzi, P. (1996) Rare element redistribution during high-temperature metamorphism in ophiolite Fe-gabbros (Liguria, Northwestern Italy): Implications for light REE mobility in subduction zones. *Geology, 24* (8), 711–714.

Tribuzio, R., Thirwall, M.F. & Messiga, B. (1999a) Petrology, mineral and isotope geochemistry of the Sondalo gabbroic complex (Central Alps, Northern Italy): Implications for the origin of post-Variscan magmatism. *Contrib Mineral Petrol, 136*, 48–62.

Tribuzio, R., Tiepolo, M., Vannucci, R. & Bottazzi, P. (1999b) Trace element distribution within olivine-bearing gabbros from the Northern Apennine ophiolite (Italy): Evidence for post-cumulus crystallization in MOR-type gabbroic rocks. *Contrib Mineral Petrol, 134*, 123–133.

Tribuzio, R., Tiepolo, M. & Thirwall, M.F. (2000) Origin of titanian pargasite in gabbroic rocks from the Northern Apennine ophiolites (Italy): Insights into the late-magmatic evolution of a MOR-type intrusive sequence. *Earth Planet Sci Lett, 176*, 281–293.

Tsigankov, A.A. & Konnikov, E.G. (1995) Geochemical types and geodynamic conditions of formation of gabbroic complexes of east branch of Baykal-Muya ophiolitic belt. *Geol Geofiz, 36* (1), 19–30 (in Rus.).

Tsigankov, A.A., Filimonov, A.V., Vrublevskaya, T.T. & Travin, A.V. (2002) Genesis of Niurundukan ultramafic-mafic massif (Baikal mountain region). *Petrologia, 10* (1), 60–87 (in Rus.).

Vakhrusheva, Y.V. (2007) Non-serpentinized harzburgites and websterites in Voykar-Sin'insky massif: Mineralogy, geochemistry, Sm-Nd age. *Ultramafic-Mafic Complexes of Folded Regions*. Irkutsk: IGTU. pp. 293–296 (in Rus.).

Van der Wal D. & Bodinier, J.-L. (1996) Origin of the recrystallisation front in the Ronda peridotite by km-scale pervasive porous melt flow. *Contrib Mineral Petrol, 122*, 387–405.

Vannucci, R., Rampone, E., Piccardo, G.B., *et al.* (1993a) Ophiolitic magmatism in the Ligurian Tethys: An ion microprobe study of basaltic clinopyroxenes. *Contrib Mineral Petrol, 115*, 123–137.

Vannucci, R., Shimizu, N., Piccardo, G.B. & Bottazzi, P. (1993b) Distribution of trace elements during breakdown of mantle garnet: An example from Zabargad. *Contrib Mineral Petrol, 34* (1), 437–449.

Varne, R. & Graham, A.L. (1971) Rare earth abundances in hornblende and clinopyroxene of a hornblende lherzolite xenolith: Implications for upper mantle fractionation processes. *Earth Planet Sci Lett, 13*, 11–18.

Vasil'ev, Yu.R. (1988) Ultramafites from alkaline-ultramafic complexes. In: Laz'ko, E.E. & Sharkov, E.V. (eds.) *Magmatic Rocks. Ultramafic Rocks*. Moscow: Nauka. pp. 172–195 (in Rus.).

Vasilenko, V.B., Zinchuk, N.N. & Kuznetsova, L.G. (1997) *Petrochemical Modeless for Diamond Deposits of Yakutia*. Novosibirsk: Nauka. 574 p. (in Rus.).

Vasilenko, V.B., Lesnov, F.P., Zinchuk, N.N., *et al.* (2003a) On connection of distributions of rare earth elements and rock-forming oxides in the rocks of kimberlitic formation. *Problem of Prognostication, Prospecting and Study Deposits Minerals at Threshold XXI Century*. Voronezh: Voronezh State University. pp. 33–38 (in Rus.).

Vasilenko, V.B., Lesnov, F.P. & Kuznetsova, L.G. (2003b) Population approach to typification of rocks kimberlitic formations by rare earth element composition. *Modern Problems of Formation Analysis, Petrology and Ore-Bearing of Magmatic Making*. Novosibirsk: SB RAS, Branch "GEO". pp. 49–50 (in Rus.).

Viljoen, M.J. & Viljoen, R.P. (1969) The geology and geochemistry of the lower ultramafic unit the Onverwacht group and proposed new class of igneous rock. *Geol Soc S Afr Spec Publ, 2*, 55–86.

Vladimirov, B.M., Maslovskya, M.N., Dneprovskaya, L.V., *et al.* (1990) *Chemistry of Kimberlites and Kimberlitic Rocks. Kimberlites and Kimberlite-Similar Rocks*. Novosibirsk: Nauka. pp. 93–122 (in Rus.).

Vladykin, N.V. (1997) Geochemistry and genesis of lamproites from Aldan shield. *Geol Geofiz, 38* (1), 123–135 (in Rus.).

Voytkevich, G.V., Miroshnikov, A.E., Povarenikh, A.C. & Prokhorov, V.G. (1970) *Short Reference Book on Geochemistry*. Moscow: Nedra. 278 p. (in Rus.).

Vrevsky, A.B., Matrenichev, V.A. & Ruzh'eva, M.C. (2003) Petrology of komatiites of Baltic shield and isotopic-geochemical evolution of their mantle sources. *Petrologia, 11* (6), 587–617 (in Rus.).

Wadhwa, M. & Crozaz, G. (1995) Trace and minor elements in minerals of Nakhla and Chassigny meteorites: Clues to their petrogenesis. *Geochim Cosmochim Acta, 59* (17), 3629–3645.

Wager, L.P. & Brown, G. (1970) *Layered Igneous Rocks*. Moscow: Mir. 550 p. (in Rus.).

Wakita, H., Rey, P. & Schmidtt, R.A. (1971) Abundances of the 14 rare-earth elements and other trace elements in Apollo 12 samples: Five igneous and one breccia rocks and four soils. *Proc. 2nd Lunar Science Conf*. pp. 1319–1329.

Wedepohl, K.H. & Muramatsu, Y. (1979) The chemical composition of kimberlites compared with the average composition of three basaltic magma types. In: Boyd, F.R. & Meyer, H.O.A. (eds.) *Kimberlites, Diatremes and Diamonds: Their Geology, Petrology and Geochemistry*. Washington: AGU. pp. 300–312.

Whitford, D.J. & Arndt, N.T. (1978) Rare earth element abundances in thick, layered komatiite lava flow from Ontario, Canada. *Earth Planet Sci Lett, 41*, 188–196.

Wiechert, U., Ionov, D.A. & Wedepohl, K.H. (1997) Spinel peridotite xenoliths from Atsagin-Dush volcano, Dariganga lava plateau, Mongolia: A record of partial melting and cryptic metasomatism in the upper mantle. *Contrib Mineral Petrol, 126*, 345–364.

Willy, P.J. (ed.) (1967) *Ultramafic and Related Rocks*. New York: Wiley. 464 p.

Witt-Eickschen, G. (1993) Upper mantle xenoliths from alkali basalts of the Vogelsberg, Germany: Implications for mantle upwelling and metasomatism. *Eur J Mineral, 5*, 361–376.

Witt-Eickschen, G., Kaminsky, W., Kramm, U. & Harte, B. (1998) The natural of young vein metasomatism in the lithosphere of West Eifel (Germany): Geochemical and isotopic constraints from composite mantle xenoliths from the Meerfelder maar. *J Petrol, 39* (1), 155–185.

Xu, Y., Mensies, M.A., Vroon, P., *et al.* (1998) Texture-temperature-geochemistry relationships in the upper mantle as revealed from spinel peridotite xenoliths from Wangqing, NE China. *J Petrol, 39*, 469–493.

Yang, H.-J., Sen, G. & Shimizu, N. (1998) Mid-ocean ridge melting: Constraints from lithospheres' xenoliths at Oahu, Hawaii. *J Petrol, 39*, 277–295.

Zhang, Z., Mahony, J.J., Mao, J. & Wang, F. (2006) Geochemistry of picrites associated basalt flows of the western Emeishan flood basalt province, China. *J Petrol, 47* (10), 1997–2019.

Zharikov, V.A. & Yaroshevskiy, A.A. (2003) Geochemistry and their problems (to 50-years jubilee of geochemistry chair). J *Mosc Sta Univ, Series 4, Geology, 4*, 3–7 (in Rus.).

Zipfel, J., Palme, H., Kennedy, A.K. & Hutcheson, I.D. (1995) Chemical composition and origin of the Acapulco meteorite. *Geochim Cosmochim Acta, 59* (17), 3607–3627.

Zolotukhin, V.V. & Vasil'ev, Yu.R. (2003) On different composition of potassium un the sub-alkaline ultramafic lavas of north of Siberian platform and problems of their genesis. *Geol Geofiz, 44*, (11), 1145–1161 (in Rus.).